CONF-770331--

MASTER




university of new orleans

a member of the louisiana state university system

# PROCEEDINGS

## FOURTH ANNUAL CONFERENCE ON

# OCEAN THERMAL ENERGY CONVERSION

# OTEC

**UNIVERSITY OF NEW ORLEANS**

**NEW ORLEANS, LOUISIANA**

**March 22-24, 1977**

GEORGE E. IOUP, Editor

**Supported By:**

**THE DIVISION OF SOLAR ENERGY**

**U.S. ENERGY RESEARCH AND DEVELOPMENT ADMINISTRATION**

**July 1977**

DISTRIBUTION OF THIS DOCUMENT IS UNLIMITED

## DISCLAIMER

This report was prepared as an account of work sponsored by an agency of the United States Government. Neither the United States Government nor any agency Thereof, nor any of their employees, makes any warranty, express or implied, or assumes any legal liability or responsibility for the accuracy, completeness, or usefulness of any information, apparatus, product, or process disclosed, or represents that its use would not infringe privately owned rights. Reference herein to any specific commercial product, process, or service by trade name, trademark, manufacturer, or otherwise does not necessarily constitute or imply its endorsement, recommendation, or favoring by the United States Government or any agency thereof. The views and opinions of authors expressed herein do not necessarily state or reflect those of the United States Government or any agency thereof.

**DISCLAIMER**

**Portions of this document may be illegible in electronic image products. Images are produced from the best available original document.**

L9.n

# PROCEEDINGS

## FOURTH ANNUAL CONFERENCE ON

# OCEAN THERMAL ENERGY CONVERSION

# OTEC

## UNIVERSITY OF NEW ORLEANS

## NEW ORLEANS, LOUISIANA 70122

## March 22-24, 1977

GEORGE E. IOUP, Editor

**Supported By:**

**THE DIVISION OF SOLAR ENERGY**

**U.S. ENERGY RESEARCH AND DEVELOPMENT ADMINISTRATION**

**July 1977**

This work has been supported by the Energy Research and Development Administration, under Grant No. EG-77-G-05-5363, initiated February 1, 1977.

All conclusions, opinions, findings or recommendations expressed herein are those of the authors and do not necessarily reflect the views of the U. S. Government or the Energy Research and Development Administration.

NOTICE

This report was prepared as an account of work sponsored by the United States Government. Neither the United States nor the United States Department of Energy, nor any of their employees, nor any of their contractors, subcontractors, or their employees, makes any warranty, express or implied, or assumes any legal liability or responsibility for the accuracy, completeness or usefulness of any information, apparatus, product or process disclosed, or represents that its use would not infringe privately owned rights.

DISTRIBUTION OF THIS DOCUMENT IS UNLIMITED

THIS PAGE

WAS INTENTIONALLY

LEFT BLANK

# FOREWORD

The Fourth Conference on Ocean Thermal Energy Conversion (OTEC) was hosted by the University of New Orleans (UNO) on March 22-24, 1977, in New Orleans, Louisiana. It followed previous Conferences in Pittsburgh, Washington, D. C., and Houston, but it has grown substantially from the first Conference to have over 350 attendees. The conferees heard papers presented which revealed significant progress in OTEC technology and planning. They also participated in spirited discussions of these developments. Very encouraging to those involved with OTEC is the fact that the concept seems to be doing well under the close scrutiny it must continue to endure if it is to become a major new energy source for humankind.

All connected with the Conference were extremely gratified by the very distinguished guests OTEC attracted. The Honorable Lindy Boggs, Member of Congress, Second District, Louisiana, delivered the very well received keynote address at the banquet Wednesday evening. She emphasized her commitment and that of Congress. She was followed by a second invited speaker. Mr. Edwin Hartzman, President of Avondale Shipyards, largest industrial employer in Louisiana, communicated in an engaging manner the enthusiasm of shipyards to be a part of OTEC. In attendance at the banquet was Dr. Henry Marvin, Director, Division of Solar Energy, U. S. Energy Research and Development Administration (ERDA). Another highlight of the banquet was a special demonstration of Sea Solar Power's working OTEC model. The electricity produced was used to power a Teledyne Energy Systems electrolysis unit which generated hydrogen fuel. James Anderson, Jr. and George May of Sea Solar Power, Raymond Feldwick and Guy Linkous of Teledyne, and Dr. David Mayer and Roy Ponthier of UNO are to be commended for the success of this exhibit. In the Tuesday morning opening session, conferees were welcomed to the State by The Honorable William Huls, Secretary, Department of Natural Resources, State of Louisiana, and to the campus by Chancellor Homer Hitt of UNO. They heard an overview of ERDA's OTEC program by Mr. Sigmund Gronich, Chief, Ocean Systems Branch, Division of Solar Energy, ERDA.

In assembling the Proceedings, I found it better to collect all papers on a given subject into one section than to use a chronological ordering. The Proceedings therefore begin with the invited papers and proceed to the contributed papers, arranged by subject. Following some of the contributed papers is discussion or written comment with response by the authors. I thank the authors for preparing photo-ready copy and enduring pressing deadlines, as well as for their cooperation in so many aspects of the Conference and Proceedings. Session and Working Group Chairmen are due a special acknowledgment for their assistance. The papers are succeeded by the reports of the eight working groups which met on Thursday morning to discuss various aspects of OTEC. The volume ends with a list of attendees which includes all non-students who registered for and attended the Conference.

Finally I thank all those who contributed to the success of the Conference and the publication of these Proceedings. While it is not possible to name everyone, there are some who must be singled out. Dr. Abrahim Lavi, Program Director, Ocean Systems Branch, Division of Solar Energy, ERDA, spent an enormous amount of time and effort for which we are extremely grateful. In fact, to all of ERDA, for sponsoring the Conference and for their interest in OTEC we owe a debt of gratitude. Here at the University, Dr. David Mayer served with me as a Conference Coordinator. For all his enthusiastic devotion to the success of the Conference, which had to be prepared in little more than two months, I express heartfelt appreciation. Likewise the staffs of our departments and of the University Center, where the Conference was held, all performed admirably through some very trying times. Dr. Joseph Murphy, Assistant Vice Chancellor for Academic Affairs, was especially helpful in taking care of administrative matters. Richard Kaufmann, a student, handled many important details. So many members of the University community contributed, from the Chancellor to student workers, that there is no way to give them all the individual recognization they deserve. I cannot overlook the contributions of Mrs. Cala Bobo, Assistant to the Coordinators, however. She was the person who made the whole effort come together and work smoothly. I cannot envision that we would have yet finished preparation for the Conference without her. Nor can I see how the Proceedings would have come to be published in her absence. By her capable and dedicated work she has earned the respect and thanks of us all.

To all conferees I extend thanks for their earnestness and good will. It is truly a noble pursuit which seeks a solution to so pressing a world problem. These Proceedings are dedicated to that mission and its success.

George Ioup

THIS PAGE

WAS INTENTIONALLY

LEFT BLANK

# TABLE OF CONTENTS


Foreword . . . . . iii

I. INVITED PAPERS . . . . . I-1

Conference Introduction . . . . . I-3
Abrahim Lavi
Ocean Systems Branch
Division of Solar Energy, ERDA

ERDA INTRODUCTION: . . . . . I-4
ERDA's OTEC Program
Sigmund Gronich
Chief, Ocean Systems Branch
Division of Solar Energy, ERDA

KEYNOTE ADDRESS: . . . . . I-18
A Congressional View of OTEC
The Honorable Lindy Boggs
Member of Congress
Second District, Louisiana

INVITED PRESENTATION: . . . . . I-22
OTEC and the Louisiana Shipbuilding Industry
Edwin Hartzman
President, Avondale Shipyards, Inc.

II. TOTAL SYSTEMS . . . . . II-1

Early Ocean Test Platform Conversion,
L. K. Donovan and C. R. Odden . . . . . II-3

An Early Ocean Test Platform for Testing Cycle Components,
R.W. Falconer, F. A. Cohan, and M. J. Smith . . . . . II-6

A Comparison of Two Generic OTEC Systems and Missions,
Gay Heit Lavi and Clarence Zener . . . . . II-11

Cost Comparison of Selected OTEC Power Plant Designs,
Ralph Roberts . . . . . II-26

Influence of Design Factors on the Economy of Sea Thermal
Power Plants, J. Hilbert Anderson and James H. Anderson, Jr. . . . II-39

III. MISSION ANALYSIS . . . . . III-1

Economic Incentives for the Commercialization of OTEC,
Jack M. Nilles and Byron J. Washom . . . . . III-3

Legal, Political, and Environmental Aspects of Ocean Thermal
Energy Conversion: A Report on an ASIL/ERDA Study, H. Cary
Knight, Robert E. Stein, and J. Daniel Nyhart . . . . III-17

Potential Mariculture Yield of Sea Thermal Power Plants. Part
2--Food Chain Efficiency, S. Laurence and O. A. Roels . . . . III-21

Electrical Energy Transmission for OTEC Power Plants, B. Winer and J. Nicol . . . . . III-26

Ocean Energy Industrial Complexes, B. Lindal, C. D. Hornburg, and N. El-Ramly . . . . . III-34

Alternative Forms of Energy Transmission from OTEC Plants, A. Konopka, N. Biederman, A. Talib, and B. Yudow . . . III-47

Market Definition, Commercial Development Plan and OTEC Financing, E. J. Francis and J. Seelinger . . . . . III-58

A Methodology for OTEC Mission Analysis, Robert W. Reid, Jr. . . . . III-67

OTEC Implementation Problems for Specific Missions, E. Tschupp, B. Berkowitz, and W. Hausz . . . . . III-76

IV. ENVIRONMENTAL AND SITING CONSIDERATIONS . . . . . IV-1

Air-Sea Interaction Perturbations by Plant Operations, S. A. Piacsek, A. C. Warn-Varnas, and P. J. Martin . . . IV-3

Stratified Turbulence Modeling for the Near Field External Flow, Glyn O. Roberts . . . . . IV-7

An Estimate of the Impact of OTEC Operation on the Vertical Distribution of Heat in the Gulf of Mexico, P. J. Martin and G. O. Roberts . . . . . IV-26

Investigations of Mixing and Recirculation in the Vicinity of an Ocean Thermal Energy Conversion Plant, Gerhard H. Jirka, David J. Fry, R. Peter Johnson, and Donald R. F. Harleman . . . . . IV-35

The External Flow Induced by an Ocean Thermal Energy Conversion (OTEC) Power Plant, T. R. Sundaram, E. Sambuco, A. M. Sinnarwalla, and S. K. Kapur . . . . . IV-42

Development of a Numerical Ocean Model of the Gulf of Mexico for OTEC Environmental Impact and Resource Availability Studies, J. Dana Thompson, H. E. Hurlburt, and L. B. Lin . . . IV-50

Monthly Assessment of Temperature Resource for Three Potential OTEC Sites, Paul M. Wolff and Lloyd Lewis . . . . . IV-57

Operational Sea State and Design Wave Criteria: State-of-the-Art of Available Data for U.S.A. Coasts and the Equatorial Latitudes, Charles L. Bretschneider . . . . . IV-61

Resource Assessment of a High Potential OTEC Site Near Puerto Rico, Donald K. Atwood, C. Peter Duncan, Marvel C. Stalcup, and Michael J. Barcelona . . . . . IV-74

A Further Evaluation of the Oceanographic Conditions Found Off Keahole Point, Hawaii, and the Environmental Impact of Nearshore Ocean Thermal Energy Conversion Plants on Subtropical Hawaiian Waters, Karl H. Bathen . . . . . IV-79

V. OCEAN ENGINEERING . . . . . V-1

Dynamic Response of Moored Bodies to Wave Motion, C. J. Garrison . . . . . V-3

Some Factors Affecting the Selection of OTEC Plant Platform/Cold Water Pipe Designs, Roderick A. Barr and Pin Yu Chang . . . V-11

Hydrodynamic Loads on the Cold Water Pipe, D. T. Hove and W. C. L. Shih . . . . . V-23

Cold Water Transport, Cold Water Pipe, and Deep Water Mooring Line Analysis - - A Parametric Approach, Thomas E. Little . . . V-40

Anchor Systems, Philip J. Valent and J. Michael Atturio . . . V-49

Screens for OTEC Plants, John H. Nath, Julie W. Ambler, and Robert M. Hansen . . . . . V-56

Concrete OTEC Structures - Fabrication Methods, H. H. Haynes and R. D. Rail . . . . . V-70

VI. HEAT EXCHANGERS

SESSION 1 . . . . . VI-1

Compact Heat Exchangers for Sea Thermal Power Plants, J. Hilbert Anderson and James H. Anderson, Jr. . . . . VI-3

Analytical and Experimental Studies of OTEC Heat Transfer Problems at Oak Ridge National Laboratory, John W. Michel . . . VI-15

Accelerated Heat Exchanger Core Testing, Norman F. Sather . . VI-27

An Outline for Optimizing and Evaluating Proposed OTEC Systems, R. N. Lyon . . . . . VI-34

SESSION 2 . . . . . VI-39

Enhanced Single-Phase Heat Transfer for OTEC Systems, A. E. Bergles and M. K. Jensen . . . . . VI-41

The OTEC Program at Carnegie-Mellon University -- Heat Transfer Research and Power Cycle Transient Modeling, Robert R. Rothfus and Charles P. Neuman . . . . . VI-55

Enhanced Performance Heat Exchangers, A. M. Czikk, H. D. Fricke, and E. N. Ganić . . . . . VI-71

Heat Transfer Enhancement for Evaporators, C. M. Sabin and H. F. Poppendiek . . . . . VI-93

Comments on Sea Water Side Enhancement for OTEC Heat Exchangers, W. L. Owens . . . . . VI-105

Reply to Comments on Seawater Side Enhancement for OTEC Heat Exchangers, C. M. Sabin and H. F. Poppendiek . . . . VI-110

Experiments on and Design of Low-Cost Aluminum Heat Exchangers for OTEC Plant Ships, G. L. Dugger, H. L. Olsen, P. P. Pandolfini, and W. H. Avery . . . . . VI-111

A Design and Producibility Study of Heat Exchangers for Ocean Thermal Energy Conversion Systems, A. F. Manikowski and A. R. Pfluger . . . . . VI-124

VII. BIOFOULING AND CORROSION . . . . . VII-1

The OTEC Biofouling and Corrosion Program Lyle D. Perrigo and George A. Jensen . . . . . VII-3

Ultra Clean Heat Exchangers -- A Critical OTEC Requirement, Andrew F. Conn, Mark S. Rice, and Dahlia Hagel . . . . . VII-11

Studies of Biofouling in Ocean Thermal Energy Conversion Plants, J. G. Fetkovich, G. N. Grannemann, L. M. Mahalingam, D. L. Meier, and F. C. Munchmeyer . . . . . VII-15

Primary Biofouling Films and OTEC Heat Exchangers, E. C. Haderlie . . . . . VII-24

Cataloguing of Oceanographic Parameters of Interest to Biofouling and Corrosion, H. Lee Craig, Jr. and Robert S. C. Munier . . . . VII-26

Corrosion and Biofouling on an Ocean Thermal Energy Conversion Power Plant, V. J. Castelli . . . . . VII-34

Application of Aluminum Alloys, R. A. Bonewitz . . . . . VII-37

Corrosion Fatigue of 5086-H34 Aluminum in Sea Water, Steven P. Flodder and William H. Hartt . . . . . VII-41

Compatibility Studies for the Ammonia-Titanium-Seawater System as Related to Ocean Thermal Energy Conversion, E. W. Saaski and P. C. Owzarski . . . . . VII-46

Design Factors Influencing Biofouling and Corrosion of Ocean Thermal Energy Conversion Heat Exchangers, J. F. Jenkins . . . VII-54

Hydrodynamic Control of Biofouling in OTEC Heat Exchangers, J. S. Tennant and M. A. Wood . . . . . VII-56

Automatic Tube Cleaning System - Brush and Cage Principle, E. Dieter Nübel . . . . . VII-61

Increasing Heat Exchanger Efficiency Through Continuous Mechanical Tube Maintenance, W. I. Kern . . . . . VII-64

VIII. ALTERNATIVE POWER CYCLES . . . . . VIII-1

Potential of Open Cycle OTEC - A General Survey, Arthur D. Watt, Frank S. Mathews, and Robert E. Hathaway . . . . VIII-3

Sea Thermal Power Cycles, Ludo Van Hemelryck . . . . VIII-12

Steam Lift Cycle at Very Low Mist Densities, Earl J. Beck . . . VIII-18

The Foam OTEC System: A Proposed Alternative to the Closed Cycle OTEC System, Clarence Zener . . . . . VIII-27

Preliminary Analysis of the Effects of Sea Water Leakage on the Performance of the Ammonia Cycle, Hafez Hafezzadah, D. W. Johnson, and K. E. Starling . . . . . VIII-31

The Mist Flow OTEC Plant, Stuart L. Ridgway . . . . VIII-37

IX. WORKING GROUP REPORTS . . . . . IX-1

Total Systems
Abrahim Lavi, Chairman . . . . . IX-3

Mission Analysis
Robert Cohen, Chairman . . . . . IX-4

Environmental and Siting Considerations
Lloyd Lewis, Chairman . . . . . IX-6

Ocean Engineering
Eugene Silva, Chairman . . . . . IX-8

Heat Exchangers
Norman Sather, Chairman . . . . . IX-10

Biofouling and Corrosion
Lyle Perrigo, Chairman . . . . . IX-11

Modeling and Optimization
Richard Lyon, Chairman . . . . . IX-13

Reporting and Information Dissemination
Steve Griffith, Chairman . . . . . IX-15

LIST OF ATTENDEES . . . . . IX-16

THIS PAGE

WAS INTENTIONALLY

LEFT BLANK

# I. INVITED PAPERS

THIS PAGE

WAS INTENTIONALLY

LEFT BLANK

# CONFERENCE INTRODUCTION

ABRAHIM LAVI
*Ocean Systems Branch*
*Division of Solar Energy*
*Energy Research and Development Administration*

Good Morning. Welcome to the Fourth OTEC Workshop. I want to thank the University of New Orleans for their efforts in making this meeting possible. Thanks to Dr. David Mayer and Dr. George Ioup, the workship coordinators, for their dedication and energy, we can look forward to a successful workshop.

As I look at the attendees assembled here, I feel extremely encouraged by the enthusiasm of all participants. In 1973, I organized the first national workshop on OTEC at Carnègie Mellon University. I had trouble inducing 50 people to participate. Today, I am told we have more than 300 registrants. It is a consequence of the evolution of OTEC from an engineering curiosity into a potential energy resource for the United States and the rest of the world.

Credit is due to the early proponents of OTEC. I would like to recognize Mr. J. Hilbert Anderson of Sea Solar Power Incorporated who is not with us today. Jim Anderson is here. I would like to recognize Professor William Heronomus of the University of Massachusetts; his colleague Jon McGown is with us today. My colleague and dear friend, Clarence Zener of Carnegie Mellon University has done an outstanding job in advancing OTEC. Finally, I would like to recognize Dr. William Avery of the Applied Physics Lab of Johns Hopkins.

On the ERDA side, Dr. Robert Cohen deserves much praise for advancing OTEC from an insignificant program within NSF into a national effort of great potential. Dr. Cohen deserves the credit for moving OTEC from a small "r", for research, into a large "D", for demonstration. We are all aware of the handicap under which he had to function, limited manpower, insufficient resources and a skeptical technical world.

Last Fall, when I joined ERDA, a new thrust for OTEC has already been defined. As you will see, the OTEC program is rather ambitious. It is moving in the direction necessary to resolve all the critical issues. It is my pleasure to introduce to you Mr. Sigmund Gronich who will describe for you the program which he has successfully develped and won approval for within ERDA.

# ERDA'S OTEC PROGRAM

SIGMUND GRONICH
*Chief, Ocean Systems Branch*
*Division of Solar Energy*
*Energy Research and Development Administration*

I want to thank Dr. Abe Lavi for his introduction. I think everyone here knows the role he has played from the early days of OTEC until today. His contributions to OTEC are worthy of the same recognition he has accorded to other people who have played a key role in OTEC. I would like to express my appreciation to Abe for his past and present efforts.

As you can tell from the introduction, I am a new kid on the block. I came into ERDA as Projects Branch Chief under Dr. Richard Blieden. Part of my responsibility was to look at all solar electric options. In time, I became convinced that OTEC had great promise and should be considered the pre-eminent solar electric option.

A feature of OTEC is our ability to identify the technological advances necessary to achieve economic viability. Another advantage of OTEC is that, unlike other solar approaches, it does not require energy storage and it offers a base-load option. We are beginning to discern some recognition of that fact on the part of the Administration and Congress. The proposed total solar budget for FY 78 is approximately equal that for FY 77, yet the OTEC budget is roughly doubled. Thus, in relation to others, OTEC funding is on a rapid increase.

My experience with OTEC over the past 6 months has been a pleasant one. We have been presented many creative ideas. Our problem has not been the lack of good ideas but the implementation of those judged worthwhile. I feel that we shall need some time to understand the ramifications of all the proposals we have been receiving so that we can select those we must pursue. We feel that we have evolved a sound research and development program as Abe has indicated. We are indeed moving from little research, a small "r", into the capital "D" on our way to demonstration. We have several (about 8) approaches on heat exchangers that have been proposed by yourselves. We would like to evaluate them all. Until we get certain critical tests conducted and evaluated, we cannot advocate proceeding to a demonstration yet. On the other hand, we feel it is futile to linger interminably in an R&D mode. So while conducting these tests, concurrently, we are implementing large system acquisition requiring a few years to complete. Thus we are proceeding with the design activities that are required in the power cycle area, the determination of the platform specifications and the type of platform we shall need. In a short period of time this year, we have aggressively pursued all these tasks and have committed to an early ocean testing of a large prototype heat exchanger.

I want to take this opportunity to thank the many of you who have done your homework and given us the variety of approaches from which we may synthesize systems to achieve economic viability.

One of the tasks that we have is the building of a

etent team within the Government so that we can do an adequate job of assessing and implementing all of the ideas that come to us. Bob Cohen has certainly done a tremendous job considering it was really just Bob and Hal Skorubo for a while. It was an enormous task. So we have been trying to broaden our staff, to develop an expertise to do our half of the job.

I would like to indicate the progress that we have made. It has been significant in several areas. In addition to OTEC, the Oceans Systems Branch includes wave energy and salinity gradients. Dr. Mike McCormick of the U.S. Naval Academy has been shouldering this burden. By far the Branch's effort is primarily devoted to the ocean thermal system. We are supported by Gilbert and Harris who are architectural engineers; Gilbert in the power field and Harris in marine systems. Lloyd Lewis has come to us from the Navy and works in the Environmental and Resources Assessment Branch. He is a very important addition to our capability. Bob Cohen who has been introduced earlier is carrying the activity in evaluating the applications that OTEC can fulfill. We feel very fortunate to have Abe Lavi join our staff. We hope it is a long stay. He is being supported by the Argonne National Laboratory, who right now has the assignment of putting together the facility to test bench-scale size heat exchangers and Oak Ridge National Laboratory who has been supporting the program activity. Norm Sather at Argonne and John Michel at Oak Ridge are the team leaders.

I think it very fortunate that Bob had acquired, prior to my coming, a panel of 5-6 consultants with extensive background in the heat-exchanger area. They have been very instrumental in the formulation of the program and in its development.

We have brought into our organization a person with a materials background and previous experience with Combustion Engineering and Copper Development Associates, Gene Kinelski. He has been ably supported by Lyle Perrigo and his people from the Battelle Laboratories.

In ocean engineering we plan to add Bill Sherwood, a highly qualified individual, to our staff. Bill has recently completed assignments in converting two barges and is considered an expert in underwater cable installation. We feel very fortunate in having Bill join our staff.

I really have to take my hat off to Larry Donavan and Whitey Odden for their efforts especially in the barge program. They have really kept the program moving. I want to personally thank them both.

We plan to move ahead with NOAA. They have recruited people in the area of ocean engineering to support us in the activities associated with the cold water pipe and position control system. This activity is being headed by Joe Vadus. We are currently pursuing some tentative arrangements with the Maritime Administration and it is our hope that we can get support from them in the area of platform constructability and in applications analysis.

I also feel very happy that we were able to pick up Bill Howerton to support us as a construction representative out at San Francisco. Bill has had an extensive back-

ground with the barge and the Glomar Explorer. He has a great deal of background here and again we are very fortunate.

The San Francisco Operations Office has been just outstanding in supporting the program and Art Wilbur has led those activities. Lastly, in the area of the electric cable, we are being supported by Bill Smith of the conservation group at ERDA.

I think you begin to see that we have achieved increased technical and management competence on our staff. We do not yet have that much meat on the bones but we are at least functional. We have all of the areas basically covered at this time. I encourage you to establish direct communications with all the individuals listed as you see fit.

Where are we going? First, let us take a look at what the market demand is. We have a demand for electric energy in the Southeastern portion of the United States. This is represented by three Southern regional councils called SERC, SWPP and ERCOT. It includes Texas and Oklahoma and goes east to Florida. On the East Coast it goes as far north as Virginia. So obviously, OTEC cannot penetrate this entire market. If OTEC power penetrated just the Southern portion of these regional councils, then the figure would be something like 700 GW between 1975 and 2020. The three urban centers of Houston, New Orleans, and Miami would be about 30 percent or 40 percent of that figure. In addition, OTEC can serve in energy intensive markets such as aluminum production and ammonia production.

As shown in figure 1, we have organized several studies. I will not go through each of these but we have had two studies, one by GE-Tempo and the other by Aerospace. The GE-Tempo study is proceeding ahead into looking at the marketability. We have not yet addressed commercialization in a comprehensive manner. We shall begin soon to address the subject of commercialization. GE-Tempo and Aerospace are going to take a closer look at the market penetration of OTEC electricity and energy intensive products. We are going to look at the incentives that could be applied by the government to bring about this new industry.

In another task, we shall look at open sea mariculture to see if it can make the basic energy production more economical.

Aerospace is going to expand the computer models that they developed in the first part of the contract so that we as an organization have the capability to evaluate the many proposals before us and can also do the proper mission analyses and trade-off studies.

There will be several regional market assessment activities. These are broader than the OTEC program. They are being done for the solar division. The first one is being done for Paul Maycock and his group, and the second one is being done for Lloyd Herwig. They are comparing all of the solar options to one another. OTEC is getting to look very good in these comparisons.

Lastly, we will be investigating the implications of the law of the sea and policy in determining the needs of OTEC in this arena. At one point we felt we had to be further out from shore and into international zones. Now we are coming to the realization that we will prob-

ably be within 30 to 60 miles from shore for the continental United States and closer than that for Puerto Rico and Hawaii.

As I indicated, we have many alternative approaches. The early direction of the program was to move towards the closed-cycle ammonia system. We are continuing that. We think it is time that we went back and reevaluated the open cycle on a more systematic basis. We have had the Colorado School of Mines looking at it. They will be reporting on their activities at this workshop. They have some interesting results to report. We plan to follow that up with a solicitation to industry for preliminary designs of open and hybrid systems on an equivalent level to that of the closed-cycle system. In addition, there have been several very unique approaches proposed. In this area Earl Beck, Clarence Zener, and Stuart Ridgeway have different concepts. We currently have these under evaluation and will be considering those for possible future activities.

Let us examine the thermal resource next. From figure 2, we see the monthly temperature line for Puerto Rico. We have a resource potential there of something like 39° going up to 42°F. This kind of thermal resource exists in the Central Gulf region, Hawaii, and Brazil. When we move further north into areas like 30 miles out from New Orleans or 120 east of Brownsville, or off the Miami area, we see that we get the same high temperatures in the summer months but we have a drop off during the winter. We have to assure ourselves that we are able to operate during the winter. If we are able to do so, we would be generating about 40 percent of the power in the winter as we would be at say a temperature difference of 40°F. The important thing is that the average temperature difference for New Orleans and Brownsville is something like 37°F while for Puerto Rico it is 41.3°F. I will later show you the implications of that type of information on the economic viability as applied to the systems studies which were conducted by Lockheed and TRW.

In the environmental and resource areas, I have discussed the first line of figure 3, which was an initial thermal resource search conducted by Ocean Data Systems, Inc. (ODSI). We are now having ODSI look at additional zones. We feel that temperature information exists in the archives and we will be able to rely on these sources for data.

In conjunction with that activity we will be looking at some satellite data so that we can get an understanding of the horizontal variation of the warm water temperatures. We will be correlating the measurements that we get from the satellite (which will not be precise) with terrestrial measurements so that we can get the proper differentials.

The next three activities will be directed to specifying the test results which will be required in developing a national data center for everyone to use. The third activity is concerned with the implementation of tests and making the actual measurements. More than 80 percent of that money will go towards the actual measurements. We feel the greatest uncertainty in the program at this time is in the area of ocean currents. This does not appear to be well known presently.

The last three activities assess the overall

environmental impacts. The first is associated with looking at climatic and certain oceanographic effects. The Naval Research Lab, Hydronautics and Science Application, Inc., studies are directed to looking at the influx and effluent of OTEC. The MIT JACOR study is to look at the overall climatic impact in a macroscopic sense; like the impact of taking energy out of the Gulf or redistributing the energy in the Gulf Area on the weather. In addition, we will examine the effect of these activities on the marine biota and we will prepare impact assessments for the two test platforms which we are considering: OTEC-1 and OTEC-5.

When I first became involved with the program, the conclusion was made that for the best risk reward balance it was best to concentrate on the heat exchangers. In the original Lockheed and TRW studies, the heat exchangers represented something like 55 percent of the total cost of the system. So it was obvious that for economic viability, what we had to do was to concentrate on the heat exchangers. As such, we prepared what we considered a very aggressive program where we committed to running tests on shell and tube concepts by the end of this year. We hope to begin those tests in August and have them run through November. In addition, we wanted to test the plate type heat exchangers that have been proposed: the plate fin, the APL configuration and others. We are looking forward to testing those as quickly as we can.

We feel we are going to have biofouling. There is no question about it. The important point is, can we clean the surfaces? Can we clean efficiently and can we clean the surfaces in a manner that does not enhance corrosion? Hence, we have planned tests which we will be initiating in July of this year on about three mechanical and two chemical approaches. We will also look at a water jet approach to cleaning tubes.

The other decision which we made was the early 1 MW heat exchanger. We felt it important to test large scale hardware in an ocean environment. You will notice that we would like to go out with a 5 MW pilot plant test in 1980. And then depending on the success of those programs go into a demonstration test in 1984. We think this is a very accelerated schedule; we are putting out today many of the procurements necessary to implement these commitments.

While we are carrying these activities on in parallel with the R&D program we wanted the agency to have the ability to review the progress of the overall program. Thus, we have incorporated three programmatic decision points which represent times when we can accumulate data from our accelerated core tests, cleaning tests and the 1 MW program to allow the Administration and later Congress to make an evaluation of how fast the program should move ahead and in what direction. We should also recognize that there is a range of options to different commercialization strategies. We have proposed this as a total program through demonstration but there are many alternative paths which can be traveled.

In the accelerated core test program, we are planning to test three different shell and tube configurations. These are pool boiling and spray evaporation, where Union Carbide is developing specialized coatings to enhance the heat transfer, and vertical fluted tube exchangers that have been pioneered by Carnegie-Mellon University.

In heat exchangers, different plate type concepts are considered. One concept is really an inverse of the vertical fluted tube where the ammonia is sprayed on the inside and the water is on the outside. Oak Ridge is pursuing that one for us. Our philosophy in managing the program has been to keep the original creative people in the program so that they can make the most out of their efforts and still attract industry into the program. The originators are encouraged to participate in all the studies on a non-exclusive basis. We feel that this is our best approach to achieving the marriage by which we can utilize everyone's talents and contributions.

As I mentioned, we have committed to an early ocean test of the 1 MW heat exchanger. We did an evaluation in considering ocean versus land-based tests. On the basis of schedule and cost we selected an ocean test. We evaluated several different options and selected the Hughes Mining Barge as the platform. In the front end of the barge we will have storage for a cold water pipe, which will be something like 2500 to 3000 feet long. We will have provisions for several 1 MW heat exchangers. We have recently gone out for competition on the early 1 MW, but we have also put out a request for proposal to look at alternative heat exchanger approaches. Out of that will come additional 1 MW designs. We will also test 1 MW versions of the plate types. So we are evaluating the possibility of running several 1 MW's simultaneously or sequentially on the same platform.

In the solicitation for the early 1 MW heat exchanger, we have currently entered into negotiation with TRW and Southwest Engineering to provide us with that early test article. In the heat exchanger concept proposed, they will give us the capability to evaluate spray evaporation at high-range (deluge) as well as at low-range systems. The evaporator and condenser will have 10 special test sections of 15 tubes each. These tubes will be replaceable so that we can put in different configurations. In addition to the spray type configuration, we will be able to evaluate nucleate boiling and forced convection. In addition, it will really permit us to obtain a higher vapor velocity at the edge of the square configuration which is more indicative of the kind of module that will exist in a larger heat exchanger. We are hopeful that these features will result in a broad base program which will give us significant information leading to subsequent hardware.

In the platform area, many of you are aware of the different configurations that have been proposed to date. The spar buoy has come out of the Lockheed study, a disc barge of TRW, and a grazing ship concept of APL. We feel we have a whole range of options to look at, going from floating to semi-submersible to fully-submersible. These options have major implications considering construction location, cost, and the integration of the power plant to the platform. We have recently put out an RFP to have industry look at these particular issues. They will determine the best platform configuration, from there proceed to a conceptual design, and then present a demonstration plan. From this activity, we would hope to determine the specifications to which we would then move out to a demonstration system sometime in FY 1979. In addition, the other large contract shown in figure 4 is in the OTEC-1 system integration. The RFP will be out on the street around July and the work initiated in November to perform the design, construction and operation of the

OTEC-1 system.

I shall not go through any of the others. I think you can see that we have specialized studies which are being conducted on some of the major ocean system areas.

Lastly, in biofouling and corrosion, the questions which we are asking ourselves is can we qualify aluminum as an engineering material? Can we clean the enhanced surfaces and in addition how do we clean the configurations in which the water is flowing on the outside of the tubes? The program which has been generated (figure 5) includes studies at given sites to determine the biofouling rate. We feel that it is important to know what the biofouling rate is at each of these specific sites. It is going to effect how often we have to clean. And that can effect the solution to be used. It may mean for instance that too much chlorine may be required or it may mean that if we use a mechanical system for cleaning we may disturb the protective oxide coating that would exist on the tubes. This is particularly important for aluminum. So the choice of a cleaning approach does effect us in an engineering sense.

We are going to test three mechanical and two chemical systems down in Panama City, Florida. These tests are to start in July. We are going to be looking at tubes with enhancements on the water side of 50 and 100 percent. In 1978 we will be going to some multi-tube tests of the preferred cleaning methods. It should be recognized that one of the major purposes of the 1 MW program is that for the first time we will have something like 9000 tubes with which to evaluate cleaning approaches. This will be a very important portion of that total program. So in 1979 we really look for the biofouling and cleaning test program transiting into the 1 MW articles. We are particularly interested in corrosion studies on aluminum and titanium as well as the calcareous deposits from the cold water.

When the initial studies were done by Lockheed and TRW, both recommended the utilization of smooth tubed titanium heat exchangers as being state of art and one in which there was a good deal of assurance that it would work. In the Lockheed study they assumed a $\Delta T$ of $33.5^{\circ}F$. This resulted in a plant cost of \$3600/kilowatt for the first unit and \$2900 for the 25th unit. This was something like three times the cost necessary to be economically viable. So there was a lot of work that one had to put in to get from there down to about \$1000/kW. Lockheed was funded on a producability study in which they took a closer look as to how they would manufacture these titanium as well as aluminum heat exchangers. They found that they could reduce the price about 30 percent or about \$70 million. And, in addition, we now upgraded the design to be reflective of the $38^{\circ}F$ $\Delta T$ which I had indicated would represent a better average for the applications we are considering. This then brought us down to something like (\$1510-\$1760)/kilowatt, depending on the biofouling factor used. See figure 6. The next question is the qualification of aluminum as an engineering material. This is still smooth tube technology. With aluminum, the system cost will decrease to (\$1160-\$1350)/kilowatt. This is only 20 percent to 30 percent above what we considered economically viable.

Lastly, if we can achieve surface enhancement on the

waterside in particular and find the mechanism and the

is to clean it, and I think there will be some interesting papers along those lines at this workshop, then we can look towards costs of ($800-$1000)/kilowatt.

So we think we have a real goal to aim for and we feel that we have been very fortunate in that you have provided us with designs on the tubes, on the heat exchanger configurations, with which we feel we can achieve these performance levels. Beyond that we are very anxious to explore the two-phase flow heat exchangers where the ammonia is on the inside. We think they are very attractive. They are much easier to fabricate. They eliminate the shell which is 30 percent of the cost of the heat exchanger. We are very anxious to have the technology proved out. We feel that is the way to go provided we can achieve the predicted performance and effective cleaning.

I tried today to give you a capsule version of the program. I hope that you have acquired an overview of where we are today and where we hope to go. As Abe Lavi said "In the first conference that he held he was happy to see 50 people." Here I believe we have some 350 registrants and I think if the program moves and develops as we all hope it will, we will probably have our next conference with over 500 people. I thank you and appreciate your support. We hope to make OTEC happen as quickly as possible.

FIGURE 1

# OTEC MISSION ANALYSIS AND INSTITUTIONAL STUDIES

| STUDY | CONTRACTOR | COMPLETION DATE | ANTICIPATED RESULTS |
|---|---|---|---|
| MARKETABILITY | GE-TEMPO | 11/77 | • PROJECTIONS OF MARKET PENETRATION OF OTEC ELECTRICITY<br>• PROJECTIONS OF MARKET PENETRATION OF ENERGY-INTENSIVE PRODUCTS<br>• EVALUATION OF INCENTIVES<br>• DETERMINATION OF FEASIBILITY OF OPEN-OCEAN MARICULTURE FOR PRODUCING ENERGY CROPS AND FOOD AS OTEC BYPRODUCTS |
| SYSTEMS ANALYSIS | AEROSPACE | 11/77 | PREPARATION OF COMPUTER ANALYSES SUITABLE FOR MISSION ANALYSIS TRADE-OFF STUDIES |
| REGIONAL MARKET ASSESSMENT | RFP | 9/78 | COMPARATIVE U.S. ELECTRICAL UTILITY MARKET POTENTIAL FOR SOLAR-ELECTRIC OPTIONS IN VARIOUS REGIONS |
| MARKET PENETRABILITY | MITRE | 4/77 | PROJECTION OF COMPARATIVE MARKET-PENETRATION POTENTIALS OF SOLAR-ENERGY OPTIONS |
| LAW-OF-THE-SEA AND POLICY ANALYSIS | TO BE DETERMINED | 10/77 | CLARIFICATION OF THE NEEDS OF OTEC DEVELOPMENT AND COMMERCIALIZATION IN LAW-OF-THE-SEA AREA |

# MONTHLY THERMAL RESOURCES COMPARISON FOR SELECTED OTEC SITES

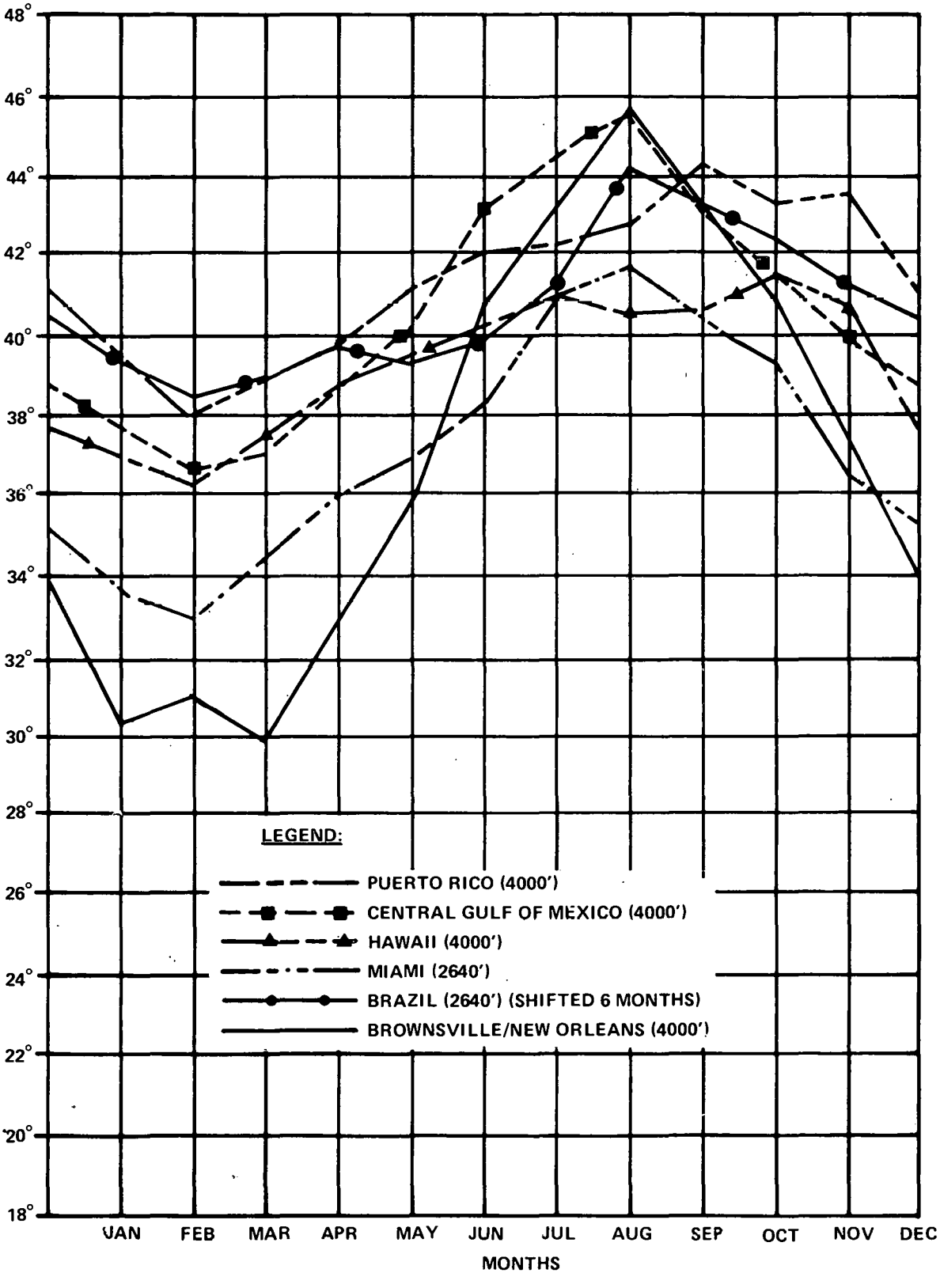



FIGURE 2

FIGURE 3

# ENVIRONMENTAL AND THERMAL RESOURCE ASSESSMENT

| ACTIVITY | CONTRACTOR | COMPLETION DATE | ANTICIPATED RESULTS |
|---|---|---|---|
| ORIGINAL THERMAL RESOURCE SEARCH | ODSI | COMPLETED | THERMAL RESOURCE FOR SELECTED SITES |
| THERMAL SURVEY | ODSI | 8/77 | DETAILED THERMAL RESOURCE |
| SEA SURFACE SATELLITE THERMAL DATA FOR OTEC | RES. TRIANGLE INST. | 4/78 | SYNOPTIC SEA SURFACE CIRCULATION & TEMPERATURE |
| OCEAN DATA FOR DESIGN | WHOI | 4/78 | DATA SPECIFICATION FOR TEST & DEMONSTRATION |
| OCEANOGRAPHIC DATA BASE FOR OTEC | NOAA/EDS | 10/77 | NATIONAL ARCHIVES FOR OTEC |
| OCEAN CURRENTS AND THERMAL OBSERVATION | NOAA/AOMC | 7/78 | SITE SPECIFIC WATER COLUMN CIRCULATION & TEMPERATURE |
| OCEANOGRAPHIC AND CLIMATIC IMPACTS | NRL/SAI/HYDRONAUTICS<br>MIT, JAYCOR<br>ANL (SUPPORT)<br>FOLLOW ON | 5/77<br>10/77<br>10/77 | OCEANOGRAPHIC AND CLIMATIC IMPACTS FOR SINGLE & MULTIPLE DEMONSTRATION PLANTS |
| MARINE BIOTA IMPACTS ASSESSMENT | RFP | 3/78 | BIOLOGICAL/ECOLOGICAL IMPACTS FOR SINGLE & MULTIPLE DEMONSTRATION PLANTS |
| ENVIRONMENTAL IMPACT ASSESSMENT – OCEAN TEST PLATFORM | RFP | 2/78 | SPECIFIC POTENTIAL IMPACTS FOR EOTP-1, EOTP-5 |

FIGURE 4

# OCEAN ENGINEERING

| ACTIVITY | CONTRACTOR | COMPLETION DATE | ANTICIPATED RESULTS |
|---|---|---|---|
| PLATFORM INTEGRATION AND CONFIGURATION | RFP | 7/78 | PLATFORM CONFIGURATION CONCEPTUAL DESIGN DEMONSTRATION PLAN |
| OTEC-1 SYSTEM INTEGRATION<br>• COLD WATER PIPE<br>• WARM AND COLD WATER SYSTEMS<br>• AMMONIA SYSTEM<br>• PIPE HANDLING | RFP | MULTI-YEAR | DESIGN, CONSTRUCT AND OPERATE OTEC-1 |
| ELECTRIC CABLE | RFP | 7/78 | DESIGN APPROACHES |
| COLD-WATER PIPE/PLATFORM STUDIES | HYDRONAUTICS | 9/77 | STRUCTURAL LOADS IN CWP<br>ALTERNATE PLATFORM CONFIGURATIONS |
| PUMP, MOORING, COLD-WATER PIPE | WESTINGHOUSE | 6/77 | DYNAMIC AND MOORING PARAMETRIC COST DATA<br>PUMP PARAMETRIC DATA |
| ANCHOR DESIGN | CEL | 5/78 | COMPARISON OF ANCHOR SYSTEMS |
| SCREENING STUDIES | OSU | 9/77 | DESIGN APPROACHES |
| HIGH REYNOLDS DATA | SAI | 4/77 | PRESSURE DISTRIBUTION ON COLD-WATER PIPE |
| SPHERICAL PLATFORM | TSI | 10/77 | STABILITY ANALYSIS AND FEASIBILITY |

FIGURE 5

# BIOFOULING AND CORROSION

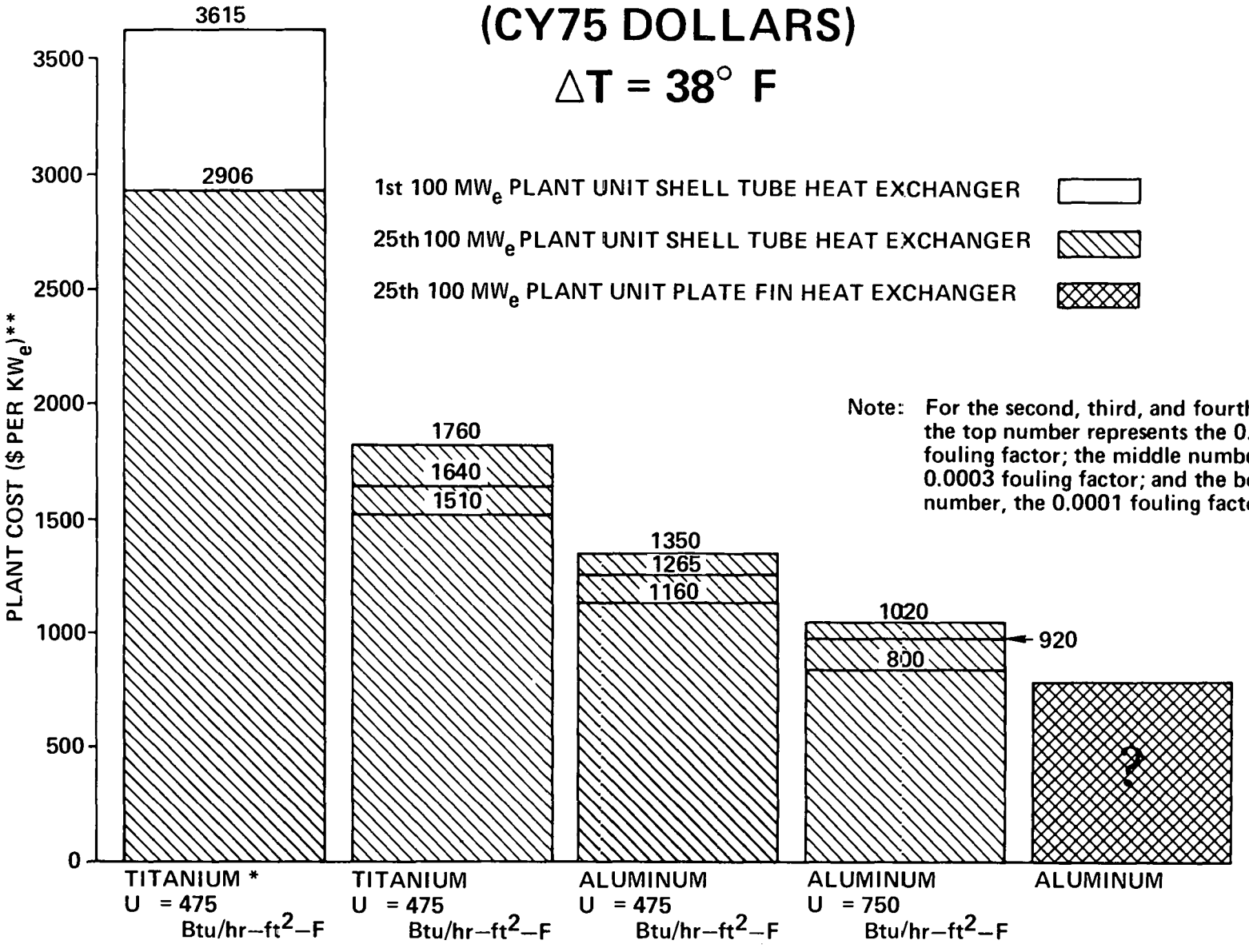
| PROJECT | COMPLETION DATE | ANTICIPATED RESULTS |
|---|---|---|
| SITE STUDIES – BIOFOULING, CORROSION, AND OCEAN DATA | | |
| • SITE 1 – HAWAII (WARM WATER) | 10/77 | BIOFOULING RATE DATA |
| • SITE 2 – ST. CROIX, V.I. (WARM AND COLD WATER) | 9/78 | BIOFOULING RATE DATA |
| • SITE 3 – GULF OF MEXICO (WARM WATER) | 9/78 | BIOFOULING RATE DATA |
| PREVENTION AND CONTROL OF FOULING ON HEAT EXCHANGER TUBES | 9/77 | DATA FROM THREE MECHANICAL AND TWO CHEMICAL TESTS |
| | 9/78 | • DATA FROM MULTITUBE TEST OF CLEANING METHODS |
| | | • SELECTION OF METHOD |
| CORROSION STUDIES ON ALUMINUM AND TITANIUM | 9/78 | • DATA FROM PITTING AND CORROSION FATIGUE TESTS |
| | | • ALLOY SELECTION |
| COLD-WATER CALCAREOUS DEPOSIT EVALUATION | 9/78 | • COLD-WATER TESTS |
| | | • SELECTION OF PROPER CLEANING METHOD |
| HULL PROTECTION AND CLEANING | 9/77 | SELECTION OF CLEANING METHOD FOR PLATFORM |

FIGURE 6

# PLANT COST—VS—HEAT EXCHANGER DESIGN

## (CY75 DOLLARS)

## $\Delta T = 38^\circ$ F




* LMSC BASELINE DESIGN ($\Delta T = 33.5^\circ$ F)

** EXCLUSIVE OF ELECTRIC POWER CABLING COST

# A CONGRESSIONAL VIEW OF OTEC

THE HONORABLE LINDY BOGGS
*Member of Congress, Second District, Louisiana*
*1524 Longworth Building*
*Washington, D. C.*

Thank you so much Dr. Hitt and thank all of you very much. I always feel, when looking around after a beautiful introduction from such a distinguished person, "will the real Lindy Boggs stand up?" I am so thrilled, not only to be here myself, but to have you in this place, in this University setting, because I think that UNO is one of the most exciting aspects of the whole scene of educational progress in this country. It is amazing to me each time I come to the campus to see new growth in the physical facilities (we would like to have more; we keep telling the Governor and the Legislature that) but also in the growth in the student body, and also in the growth of excellence. And I'm pleased to have you here in this lovely humanistic setting for your very scientific considerations. And I would like also to say that it gives honor to this University to have this very special conference here and we're extremely grateful to you for coming. We're also extremely grateful to Dr. Lavi, Dr. Ioup, Dr. Mayer, to Cala Bobo and all of you who have arranged this. Certainly we're pleased and delighted to have a distinguished business person such as Ed Hartzman here with us this evening and to have, of course, Dr. Marvin to grace us with his presence.

I said this the other day, Dr. Marvin, in committee hearings. (I'm on the appropriations committee this year and I'm on the sub-committee on public works.) I was sharing some of my feelings about that, saying that I felt a little intellectually stir crazy because I'm new to appropriations and I thought: "we're not really doing anything innovative, we're not really initiating any legislation, we're just hearing about everybody else's problems and everybody else's evaluations and everybody else's priorities and we simply have to choose among them and say which one of them has the best cost-benefit ratio." And then came the ERDA testimony and certainly life became exciting. And I must say to all of you here that you are now in the presence of a disciple of OTEC.

Having been last week in committee hearings with ERDA all week and then having the privilege of going out to the geopressure test facility outside of Lafayette on Saturday, I came back to hearings on Monday. I said to the assembled ERDA personnel at the witness table that I felt that I had spent the whole week with them, and especially the weekend, and the chairman suggested that we should strike that from the record.

It really is particularly appropriate that you gather here in New Orleans to study the problems associated with extracting the energy the sun puts into the waters of the oceans of the earth. You are, of course, on the banks of the mighty Mississippi River which the Indians in the past called the Father of Waters. This great river drains 41% of the forty-eight contiguous states and through the port of New Orleans it acts as a highway for commerce between our nation's interior and almost every nation in the world.

I would also like to note the strong and enthusiastic support the people of the state of Louisiana have historically given to the efforts to maximize development of our oil and gas resources, consistent with the conservation ethic based upon avoidance of both economic and resource waste and serious environmental damage. We have freely and unselfishly given of our resource treasure because we know that it is America's natural resources that have made her a great and powerful nation and that have contributed to the commonwealth of all her people. Just as an example of the magnitude of the contribution by Louisiana, I wonder how many of the people are aware of the fact that this state contributes approximately 44% of the interstate supply of natural gas. This is more than the aggregate contributions to that same market by the states of Texas, Oklahoma, New Mexico, and Kansas. If we did not recognize the importance of this extremely vital resource in the past, I think everyone experienced a vivid example of its importance this past winter.

Speaking of going out to the test drilling site near Lafayette, Louisiana, I think that one of the great aspects of having any type of testing facilities in this area is that you will meet an attitude of success. Everybody on that test facility was absolutely certain of success, whether he was simply using the wrench around the pipes that went down, or whether he was really in charge of the scientific data to be gathered from the area, or in charge of the whole project. It's within an area infused with this kind of attitude of success that we need to put the test facilities for these great new projects.

This Nation has recently experienced the second energy crisis in three years. The first, of course, was caused by the Arab oil embargo and the second by the frigid winter of 1977, and a shortage of natural gas. A recent study by the Library of Congress found that recurrent shortages are a real possibility during the next twenty-five years. The problem lies in the conflicting goals which energy policy makers must pursue. These goals include lessening the impact of higher energy prices, reducing dependence on foreign oil sources, protecting the environment, and shifting away from declining resources of domestic oil and gas.

In attempting to meet these goals, both Congress and the Executive Branch have been putting out inconsistent signals on the subject of price, end-use controls, import policy, and development of new energy sources. Policy uncertainties are reflected in the wide variations of projections of future energy consumption, as well as a lack of reliable estimates of energy supplies.

The elements that turn the confusion and indetern

nate character of the United States energy picture into sis are inadequate domestic supplies of oil and gas, unreliable foreign sources. Oil exporting nations, Library of Congress study concludes, are unlikely to supply the United States, or the industrial world as a whole, with all the petroleum it wants at a price it can afford. This is not because the reserves are not there, but because the exporting nations have adopted a policy of conserving their resources over an extended period of time in order to fund a long term economic development process. And they have developed a mechanism, the OPEC cartel, of enforcing that policy. Another embargo like the Arab action of 1973-74 does not appear likely at present. However, a limitation on the level of exports, either through a simple ceiling on production or through increased prices, seems almost certain as world oil demands tax the production capacity of even such large producers as Saudi Arabia.

There exists a great deal of uncertainty about what energy sources will substitute for oil and natural gas, but there is certainty that much substitution will have to take place, even if conservation measures can substantially reduce consumption of energy without severe economic penalties. These are some of the alternatives among the fossil fuels: enhanced recovery of petroleum and natural gas, improvements in coal technology, and the production of oil from shale deposits in the Rocky Mountain States with their high concentration of hydrocarbons. These are some of the alternatives from among the nonfossil fuels: nuclear fusion and fission, solar energy, bioconversion technology, geothermal energy, wind power, and, of course, the various ocean energy technologies.

Unfortunately, the lead times for developing alternatives to petroleum and natural gas are quite long, as you well know, and most alternative sources involve large amounts of capital investment. Energy suppliers will be faced with alternatives of either investing heavily in equipment or production capacity that may not be utilized, or would be unable to meet increased energy needs that arise within a year or less through restriction or cutoff of foreign oil supplies.

I would point out that, while it has been commonplace to say that the United States has no national energy policy, this has really not been the case. The United States has had an energy policy and has had one for at least a century! That policy has been to rely to the maximum extent possible on private enterprise to make the major investment, development and pricing decisions affecting energy supply. In effect, we have been deliberately delegating to the private sector authority and responsibility for determining and changing the direction and content of national energy policy as a whole. The issue is thus, not whether we should have an energy policy but if, or how, the one we have should be changed. The answer to this question will depend, at least in part, on the Nation's concensus on what the energy problem is. This is how we're attempting to address the problems associated with the various alternative sources of energy available in the future.

In the early twenty-first century, the annual American energy appetite may reach a staggering 200 quadrillion BTUs, or "quads". No longer will we, as Americans, be able to rely on any single resource for the bulk of our energy, as we have periodically throughout our history: first with wood, later with coal, and today with petroleum. By the year 2020, it is quite possible that six energy sources, none supplying more than 25% of the total, may power the Nation.

In the wake of this unparalled energy supply-demand dilemma, the members of Congress and the Executive branch have joined with the researchers in the United States in looking with renewed interest and a sense of urgency at the nontraditional alternative energy sources. We've been assured that six facets of solar energy technology, in particular, could help shoulder this demand: solar heated buildings, "biomass" fuels from sun-nourished organic crops, steam power from solar-thermal machines, electricity from solar cells, power produced by sun-driven winds, and energy generated by ocean temperature differences. Together, as estimated by the Energy Research and Development Administration, they can supply up to 7% of the Nation's power needs by the year 2000 and as much as 25% by the year 2020.

Your conference attests that innovative among solar application technologies is the Ocean Thermal Energy Conversion process. One of the last great sources of untapped raw energy is the ocean. Its tides, currents, waves, and temperature differences all have enormous potential --- aside from energy stored in oil and gas deposits beneath the seabed continental shelf. Until recently the ocean was being given less attention and research money than it deserved. In particular, the former situation is being remedied in the area of energy from ocean thermal differences.

The concept of producing energy by using these temperature differentials or thermal gradients has been with us, of course, since the French physicist, Jacque D'Arsonval, proposed it in 1881. In 1929, George Claude, another Frenchman, built a shore based ocean gradient power plant in Cuba that produced 22 kw of electricity. This operation proved the concept to be sound but was an economic failure due to the technical inferiority of the plant design. Recently this idea was rediscovered and many people in groups, such as yourselves, are conducting research on this process. Based on current technology we could produce a plant of this type. Practically everything that has been done to make mechanical cooling work applies directly to the ocean thermal power concept.

The principal applications of this process are the production of base load electricity and the manufacture of energy intensive products, such as ammonia, aluminum and even chlorine and methane. Such manufacturing could conceivably take place on plant ships on the ocean. As you know ammonia is vital to the production of fertilizers. Present processes require natural gas which could be freed by this process for other applications. For example, at present the equivalent of some 17,700 Mw of electrical capacity are utilized in the production of the 17,700,000 short tons of ammonia produced annually, requiring the use of 700,000,000,000 scf of methane. One of OTEC's greatest potentials is in meeting the needs created by the growth in demand for ammonia. It has been estimated by the year 2020 the annual incremental

increase in the demand for ammonia will be 1,150,000 short tons, requiring the equivalent of an additional electrical capacity of 1,150 Mw or 50,000,000,000 scf of methane each year. We could use OTEC to meet these increased demands. Another potential of ocean thermal energy conversion could be development of an aquaculture system to produce plant and/or animal life, such as shellfish and kelp, as Dr. Roels told you about today.

Ocean areas contiguous to the United States are quite suitable for commercial OTEC development and operations. These points include areas off the coast of Louisiana, Texas, Florida, Hawaii, the Virgin Islands, and Puerto Rico.

Although technological breakthroughs are not required for the development of ocean thermal systems, certain engineering improvements and adaptations of presently available power technologies, along with refinement and optimization within the existing body of technology, are needed to satisfy OTEC's specialized requirements. As Donald Beatte, Deputy Assistant Administrator for Solar, Geothermal, and Advanced Energy Systems, pointed out last week when he testified in support of ERDA's fiscal 1978 budget: "The critical issue in the development of ocean thermal systems is production of durable, low cost, and efficient heat exchangers. No major technical breakthroughs are required but significant engineering improvements are needed to make these systems economically attractive and to ensure their survival in the harsh ocean environment." In addition, he said, "Attention must be paid to the impact of the OTEC system on the ocean, as well as the effects that corrosion, scaling, and slime have on the equipment."

Other areas among the concerns are the ecological and environmental impacts, due to the large amount of water that is moved and altered thermally in the production of energy. Research must be done to determine how rapidly the thermally altered water will recover, as is expected, to more or less normal conditions. The fiscal year 1978 OTEC budget represents the tremendous increase over the past several years of real commitment by Congress to develop this technology. In fiscal '76 the budget called for $6,000,000, in fiscal '77 it was increased to $7,000,000, for fiscal '78 we're talking in terms of $17,000,000 or more, an increase of $10,000,000 over last year.

In fiscal '76, two individual teams from private industry evaluated OTEC and found in a base line commercial offshore power plant using existing technology could produce electrical power at about $2,000 per kwh or 56 to 50 mills per kwh. To be economically viable this cost must be brought down to somewhere around $1,000 per kwh. Of course, most energy generation requires fuel. In the final analyses, OTEC fuel costs are zero so there is only capital cost. In ten years, if the research you are pursuing is successful, OTEC technology improvements will decrease capital costs and increase efficiency. This coupled with increased fuel costs for other energy systems might well be the key to OTEC's contribution.

This year, ERDA has accorded OTEC a higher priority than in previous budget periods. The request at the authority level has doubled for OTEC while the overall solar budget has remained essentially fixed. This indicates the higher priority on OTEC, and all of you should take pride in that accomplishment.

One of the most significant increases in the ERDA budget for OTEC is in the area of engineering tests and evaluation. The amounts requested have risen from $1,570,000 for fiscal '77 to $7,300,000 for fiscal '78. This is in recognition of the sense of the Congress that ERDA must proceed with an early ocean test of a 1 Mw heat exchanger in an ocean environment.

ERDA has prepared a separate early solicitation to industry on the 1 Mw heat exchanger and has acquired and undertaken the conversion of the Hughes Mining Barge (formerly used by the CIA) to OTEC-1. ERDA intends to complete conceptual and preliminary designs for the barge conversion by the end of fiscal '77. It's presently in the California shipyard for removal of the dredge base in the superstructure. The contract has not yet been let for the actual refitting work which will be necessary. After the hull modifications and refitting of the barge is completed it is hoped that the first realistic testing of the 1 Mw facility can commence in September of '79. During the same period the decision will be made whether or not to further refit OTEC-1 for testing of a 5 Mw power cycle or to run the projects in parallel using another vessel. Further plans call for a 25 Mw power module, which could eventually be used in the 100 Mw plant, to be on line in 1983. It is hoped these activities could lead to the operation of a 100 Mw plant in 1984. I would point out that a 100 Mw power plant could probably handle the demands of a Louisiana city of some 10,000 households.

1977 is a major year for Ocean Thermal Energy Conversion. As Mr. Beatte pointed out to our subcommittee last week, "We will know much more about potential heat exchange efficiencies (by the end of calendar year 1977) and will re-evaluate our design objectives. It is possible that the efficiency will be so good that private industry will want to proceed with no further Federal technical involvement. Alternatively, the result might be so poor (that's Mr. Beatte saying that, not me) that the program would be reduced in scope until heat exchanger problems were solved." As he further pointed out, the current estimates of the program warrant continued commitment by ERDA and the Congress to move aggressively toward OTEC operations.

Our subcommittee members feel that federal support of projects such as this are easily justified in terms of the economic and social, as well as the educational contributions they make to society, and they are in the best American tradition. Scientific research is recognized as an expression of man's highest intellectual aspirations. In addition most economic theories link economic growth to technological innovation. Such innovation increasingly depends on basic science.

Benjamin Franklin and Thomas Jefferson were men of the eighteenth century enlightenment, in addition to being founders of our Nation. They were inheritors of Francis Bacon and Isaac Newton. Convinced of the power of the rational mind, they saw the intricacies of nature as complicated but solvable puzzles. Ultimately, natu

would be controlled for the use of mankind. In this
newerk, science became empirical rather than contem-
:ive, focused on facts rather than the essential nat-
l laws. Franklin is recognized as America's greatest scientist of the 18th century and Jefferson, though less well known, pursued botany and agricultural science with some competence. His talent for mechanical invention is preserved in his home at Monticello. Both of these men knew fully the pleasures in the abstract exercise of the rational mind. Yet both these men were convinced that genuine science must, in the end, yield useful results, and it was that utility which justified the enjoyment of the abstract. Franklin's electrical experiments dissatisfied him until he invented the lightening rod.

I think we in the Congress still endorse this sentiment. We fully recognize that understanding nature in a very basic way has always proved to be very profitable for society. Unlike the times of Franklin and Jefferson our scientific and political communities may not overlap significantly, but there has to develop some reasonable interface of values and concern such that the two communities will actively seek to work together for the benefit of all of our people. We in the Congress and you in the scientific, industrial, and technological communities must continue to commit ourselves to solve the Nation's energy problems.

Thank you so much for having me; thank you for being here.

# OTEC AND THE LOUISIANA SHIPBUILDING INDUSTRY

EDWIN HARTZMAN
*President, Avondale Shipyards, Inc.*
*P. O. Box 50280*
*New Orleans, Louisiana*

Thank you Chancellor Hitt. Honorable Lindy Boggs, Dr. Lavi, David Mayer, George Ioup and honored guests. I've met a lot of you and couldn't remember your names so if I didn't name you, you're one of the honored guests. Ladies and gentlemen, you know I'm really glad that Chancellor Hitt introduced Lindy as Congresswoman Boggs and as a woman because she is first a great woman, a great lady, and a great member of Congress, furthermore, she must have one hell of a research staff to make a speech like that. I think you folks ought to elect her chairman. Next, I would like to congratulate OTEC for a fine turnout. I didn't envision a group like this when I was invited to speak, since I seldom talk to this many people. Could it be that the attraction of New Orleans had something to do with the size of the group? And then let me congratulate UNO for inviting you and attracting you here.

Orginally I started my career as a mechanical engineer, as Chancellor Hitt mentioned, but I've now been involved in management so long I don't believe I can claim to be an engineer any longer, but I haven't resigned from the profession. And then that brings me to this little interchange between Dr. Lavi and Mr. Gronich about degrees. When I graduated from college it was with a bachelor's degree. That's all you needed to get a job, and I was some pumpkin with a bachelor's degree. Now I hire doctors.

Your interest is in a form of Solar Energy but I think a few general remarks on the energy situation are not out of order and in spite of Lindy's rundown on it I've got a few things to say about it myself. Despite the hard winter it appears to me that the American people and even some members of Congress, not Lindy, of course, and a lot of people do not believe that the shortage is real. They think it is contrived and will go away. Because Louisiana is the source of much of the oil and gas this country has and because of my long association with this industry I know that the shortage is real. The end of U.S. oil and gas is in sight. The end of oil and gas worldwide can also be figured out and it's not too far off. Energy is the basis of American life. The good life we Americans have is due to energy.

It goes back to Mr. Watts' steam engine. Ever since then there has been the industrial revolution and all of that and it's all based on energy. You know, people wouldn't ordinarily think about it but the food we eat is produced by American farmers. One farmer can feed a lot of people these days but he does it with energy; he has fertilizer that came from energy. There are many other endless examples but that's one: food. Everything we have and do is based on energy.

Information is given to the American people that conservation is the answer. This is certainly true for the short run. But you cannot live on your bank account forever, particularly if your bank account isn't any larger than ours is in energy. It's going to take more than conservation to get past the rough times ahead. The American system is based on free enterprise, capitalism, if you will. Our laws and government regulations are going to have to be such in the near future that producers of energy can make a profit so they can afford to produce from mariginal and high cost areas.

After this is done Americans have to learn another form of conservation. They're going to have to get used to spending a much larger part of their income for energy. If a man's house is heated by solar energy his heating system will cost very much more than just the simple system he now uses that probably burns gas. The energy may be free but the solar heating system is not. Nonetheless it could be a cost effective system and I certainly hope so. Then we go on to other things that are in the near future, gas is to be brought to this country as liquified gas, from places like Algeria. This gas is going to be tremendously costly. A one hundred and twenty five thousand cubic meter LNG ship costs $140,000,000 at today's prices and there are quite a few of them being built, twelve or fifteen in this country. If coal in the west is to be strip-mined and the face of the earth restored to its original condition this is going to be costly. Transportation is costly. Learning to burn this coal without polluting the atmosphere is going to be costly. Developing energy sources such as ocean thermal energy is going to be costly. Until the Arab oil crisis forced shortages and higher prices on us, sources of energy like ocean thermal energy were unthinkable from the cost standpoint. Now they are on the way to becoming feasible. Perhaps we owe the Arabs a vote of thanks. That's enough of my philosophy on energy; I'm so far over to the right that I guess I'm out of order.

It appears that an ocean thermal energy plant must be in a fairly deep part of the ocean to function. This would indicate that it must be on a floating platform, which brings shipbuilders such as Avondale Shipyards, into the picture. The relatively small contact we at Avondale have had with the problem indicates to us that the most suitable platform would be similar to the semi-submersible offshore drilling rigs that we've been building for the oil industry for many years. The model in the corner to my left, built by Sea Solar Power, Incorporated, looks much like one of the rigs we've built at Avondale. We on the Gulf Coast; oil companies, building contractors, service contractors, ship builders, have

been working on the problem of providing stable, safe, forms at sea for producing oil ever since the end of d War II. I'm sure that some of our technology is applicable to your problems. At Avondale Shipyards in the late forties we built the first pipe jacket drilling platform that was installed in the Gulf of Mexico. We built many of the first offshore drilling rigs for shallow water by today's standards. Later on, we helped a leading drilling contractor, here in New Orleans, Ocean Drilling and Exploration Company, develop and build the first semi-submersible rig. We've since built many more for them and many others. In the meantime, we've built many naval vessels with aluminum superstructures, complex machinery, and very complex electronics. We're now building some large LNG tankers: the 125,000 cubic meter ship that I previously referred to. The price of those ships at the time we took the job was $103,000,000, now another contract would be $140,000,000. With experience like this we feel that we are able to build an ocean thermal platform and install the machinery and plant when that stage of development is reached.

In the Gulf Coast area there are many engineers with offshore experience that may be applicable to the problem. I understand there is a plan to modify a part of the famous "Spy Ship" as a test platform for your work. Avondale has the largest dry dock in the U. S. and we can do the job if we get the chance.

Then if the Gulf of Mexico is the place where there is enough surface water temperature and enough cold water at depths to work one of your machines, New Orleans or the Louisiana Gulf Coast would make a wonderfully fine base of operations. We do have the surface equipment, we have the people, we have experience. Should the plant produce ammonia, we are used to handling it as cargo. And further we're not afraid of new things, we're not afraid to drill for oil off our shore like some of the people from the east. And in doing so we haven't ruined our state or the ocean. We've made a little mess a time or two but we've cleaned it up. And if anybody has a chance to fly over the coast of Louisiana I defy them to find where it has been hurt by the oil development. If you had been fishing in the Gulf twenty or thirty years ago then were to go fishing there again today, you'll find the fishing better today than it ever was. So where have we done the harm? It hasn't been done and the east coast and some of the others could take a leaf from our book of experience. I think it's their duty to do it. As Lindy pointed out, we've been providing 44% of the natural gas that the country has. It's time for someone else to get on the ball and do something else.

Well, I've reached the end of my page here and about all I can do is hope you fellows really get onto it because the shipyards need some work.

# II. TOTAL SYSTEMS

SIGMUND GRONICH, CHAIRMAN
*Ocean Systems Branch*
*Division of Solar Energy, ERDA*

THIS PAGE

WAS INTENTIONALLY

LEFT BLANK

# AN EARLY OCEAN TEST PLATFORM CONVERSION

L. K. DONOVAN AND C. R. ODDEN
*Naval Facilities Engineering Command*
*Alexandria, Virginia*

Abstract

This project will provide the first Ocean Thermal Energy Conversion (OTEC) test platform for testing scaled heat exchangers and condensers in the open ocean. The Hughes Mining Barge is being converted into this test platform OTEC-1 and is scheduled for sea trials in 1979.

## Introduction

The Ocean Thermal Energy Conversion (OTEC) Program is a development effort of the Energy Research and Development Administration (ERDA) to achieve an economically viable ocean thermal power system. The investigation of OTEC has progressed systematically from university feasibility studies, through baseline platform/plant conceptual design studies. Present efforts include design and fabrication of scaled subsystems and components to evaluate the criticality of existing design problems and the development of an ocean platform upon which these OTEC subsystems and components can be tested.

ERDA took temporary custody of the Hughes Mining Barge (HMB) and its associated underwater transfer platform for possible use in testing ocean thermal energy conversion equipment in April 1976 (see Figure 1). The barge was a support vessel for the federally-owned Hughes Glomar Explorer. It is 324 feet long with a 106 foot beam having displacement of about 6,000 light tons. Studies have shown that the HMB can be used effectively and economically for testing components to be used in an ocean thermal conversion power plant.

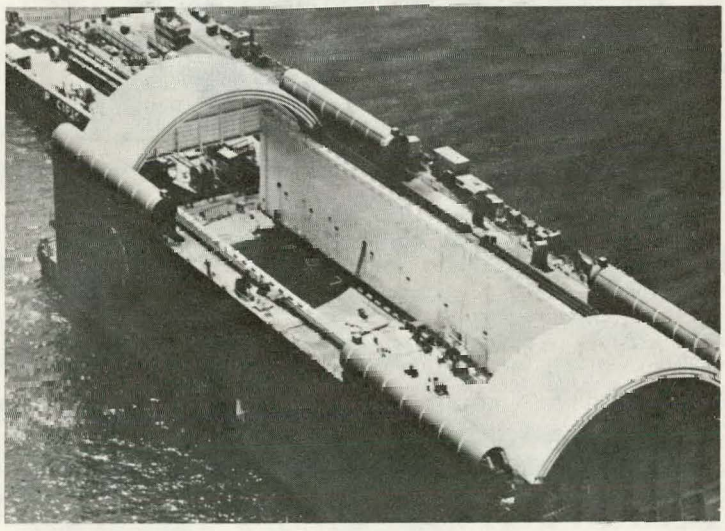


Figure 1

Presently the Hughes Mining Barge is being converted to serve as the first test platform. This platform, OTEC-1, will be the first major test vehicle to perform operational testing of power cycle components. In addition, it will serve to predict the performance of future full scale plants to operate under real world environmental conditions. The plant will be designed to test components which will produce approximately 1 MWe (gross). The components include heat exchangers, pumps, cold water pipe and ammonia system. Figure 2 is a conceptual design used to study the feasibility and economics of HMB use as a test platform. Actual HMB conversion may look substantially different than this design.

Depending upon prototype test results and supporting studies, a full scale 25 MWe (nominal) floating prototype OTEC plant module may be designed, constructed, deployed and tested in the 1980's.

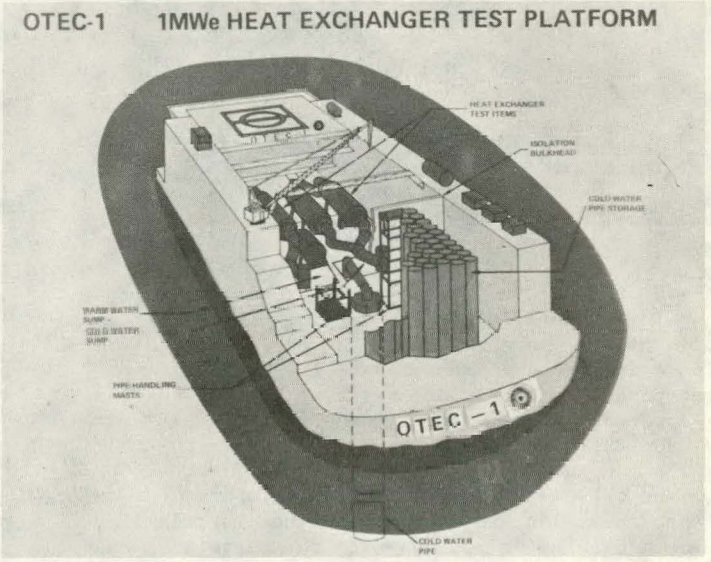



Figure 2

## HMB Conversion Project

A recent study (Mechanics Research Inc. (1)) described various technical, engineering and support aspects of converting the HMB to an OTEC test platform. While the study did not produce detail specifications or working plans, aspects of the conversion were brought to a detail which indicated the converted barge would be a viable test platform. The HMB Conversion Project results from this study.

The objective of the HMB-1 Conversion Project is to complete the conversion of, and deliver the Hughes Mining Barge (HMB) to serve as the testing platform for the 1 MWe (gross) prototype Ocean Thermal Energy Conversion Plant/Components by early 1979. Full uninterrupted test operation could begin in 1980.

The HMB Conversion Project is separated into three phases.

Phase I: Removal of Dredge Base - Figures 3 and 4 show the barge with the dredge base located inside. In this phase, the dredge base will be removed to permit location of OTEC subsystems and components. Disposition of the dredge base is also carried out in this phase.

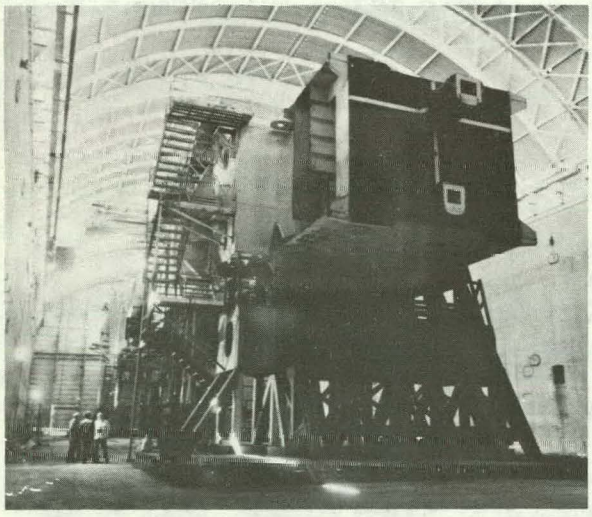


Figure 3

Phase II: HMB Drydock Work including installation of hull penetrations - In this phase, the barge will be drydocked to accommodate the cold and warm water pipe, seachests for auxiliary systems such as fire protection, and other access requirements which may include thrusters.

The cold water pipe subsystem is a critical aspect of the Conversion Project. Pipe size, material, dynamics and relative motions with the barge will bear directly upon the size of the cold water well in the hull, the design of the cold water pipe handling system, pipe storage and barge/pipe relative motion control. Therefore, Phase II includes critical subsystem and componer studies and designs which must occur before plans and specifications for the drydocking and hull penetration can be prepared.

It should be noted that the HMB Conversion Project does not include heat exchanger or power turbine development efforts. The heat exchangers for OTEC-1 will be Government Furnished Equipment. The initial thermal energy cycle for OTEC-1 will not include a power turbine, but instead will utilize a reducer/desuperheater to simulate turbine operation.

Phase III: HMB Conversion - In Phase III a solicitation will be prepared to select a System Contractor to execute the conversion. This contractor will be responsible for preparation of conceptual/preliminary/final designs for the conversion, identification of required equipments and components, preparation of equipment specifications, procurement of long lead time material, selection of a shipyard to perform actual conversion work, and possible continuation of testing, subsequent to the barge conversions.



Figure 4

Phases II and III overlap to an extent. During the process of awarding the Phase III System Contract, critical subsystem and component studies of Phase II are proceeding in order to improve the Project completion schedule. The overlap provides a further advantage in that the System Contractor will provide an independent assessment of Phase II studies/design work prior to hull penetration work.

Included in Phase III is the provision of vital Government Furnished Information for integration into this effort.

(1) "Feasibility of Using the Hughes Mining Barge as a Test Platform for Early Ocean Testing of Ocean Thermal Energy Conversion Components", Mechanics Research Inc., MR1 2906-01, 10 December 1976.

## Course of Action

To achieve the Project Objective, the following ons will be followed:

Phase I

- Complete the removal of the dredge base.
- Arrange for disposition of dredge base.

Phase II

- Prepare OTEC-1 Mission Profile requirements and design data book including plan for use, maintenance/test profile.
- Perform critical subsystem and component studies in parallel with selection of the System Contractor to maintain or improve completion schedule.
- Prepare designs, plans and specifications for drydocking and hull work.
- Perform drydocking and hull work.
- Perform other miscellaneous functions such as preservation and documentation.

Phase III

- Prepare a performance specification for acquiring a System Contractor. This specification will require the System Contractor to:
  - oo Prepare system/subsystem studies to improve reliability and maximize utilization of HMB as a test platform.
  - oo Prepare conceptual/preliminary/final designs.
  - oo Account for all subsystem/components including component identification specification preparation, and procurement of long lead time components.
  - oo Develop a support system.
  - oo Select a conversion shipyard.
  - oo Perform testing.
- o Prepare Government Furnished Information. This will include contract type barge system drawings, studies and other documentation previously performed or performed in parallel with the System Contractor acquisition effort.

## Project Schedule

Schedules for the HMB Conversion Project are presented in Figure 5. Phases I, II and III and significant events within each Phase are shown. At this time, the schedule is achievable, reflecting no known fiscal or technical impacts.

Detailed information for Phase I is not included since required actions are underway. The dredge base removal should be completed by summer.

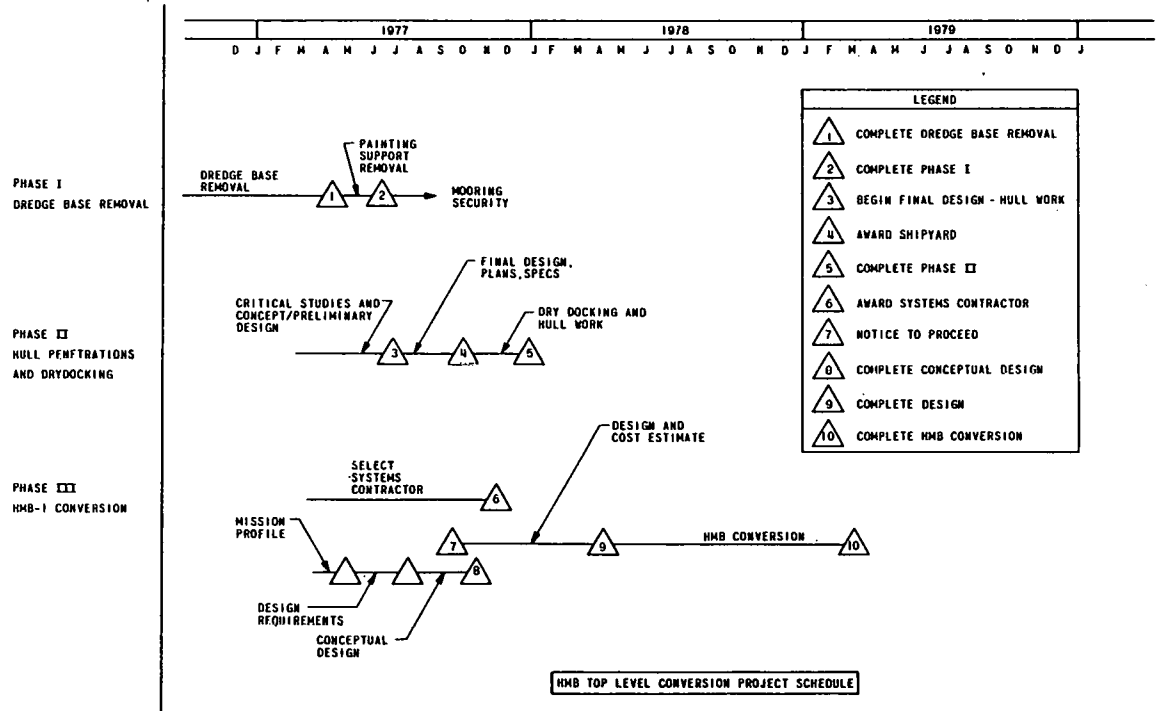



Figure 5.

# AN EARLY OCEAN TEST PLATFORM FOR TESTING CYCLE COMPONENTS

R. W. FALCONER, F. A. COHAN, AND M. J. SMITH
*Electro-Mechanical Systems Division*
*Mechanics Research Incorporated*
*2500 Colorado Boulevard*
*Santa Monica, California*

Abstract

The background data for this paper was assembled during a five-month study conducted by Mechanics Research, Inc. and L. R. Glosten and Associates, Inc. The study purpose was to evaluate the feasibility of using the Hughes Mining Barge (HMB) as an Early Ocean Test Platform (EOTP) for supporting the Ocean Thermal Energy Conversion (OTEC) developmental programs. The effort was conducted for the Energy Research and Development Administration (ERDA) under subcontract to Gilbert Associates, Inc.

The study results show that the HMB is well-suited for the EOTP tasks. This conclusion is based on several HMB physical characteristics. In addition, ERDA currently controls the HMB and it is readily available for conversion. The major HMB features which enhance its use for testing OTEC components are: (1) It has a large, unobstructed interior deck that is protected by wing walls. There is adequate room for locating moon pools for cold and warm water intake, crew quarters, the OTEC plant, the support shops, and for storing over 3000 feet of cold water pipe. (2) There is a 15-ton overhead crane that can move over the entire interior. This crane can support the pipe handling system, OTEC plant reconfiguration, and material logistics. (3) The HMB can be easily modified to allow large pipes to penetrate through the bottom of the hull between the wing walls. (4) The structural integrity of the main deck and wing walls will allow heavy equipment, additional decking, and cutouts to be located any place on the HMB where they can best support operational testing.

## 1.0 INTRODUCTION

Mechanics Research Incorporated and its major subcontractor, L. R. Glosten and Associates, conducted a five-month study to assess the feasibility of using the Hughes Mining Barge (HMB) as an Early Ocean Test Platform (EOTP) for testing OTEC components. This study, which was performed for the Energy Research and Development Administration's Ocean Systems Branch under subcontract to Gilbert Associates Incorporated, showed that the HMB was ideally suited as an EOTP using a 1MWe plant.

This paper summarizes the study findings and conclusions, and highlights the criteria used for judging feasibility of the HMB to perform the EOTP role. The general arrangement of the EOTP ocean systems and OTEC plant is presented, as well as a preliminary systems breakdown structure showing the allocation of systems and components to EOTP functions. The options considered for modifying the HMB are discussed and the resultant recommendations are described.

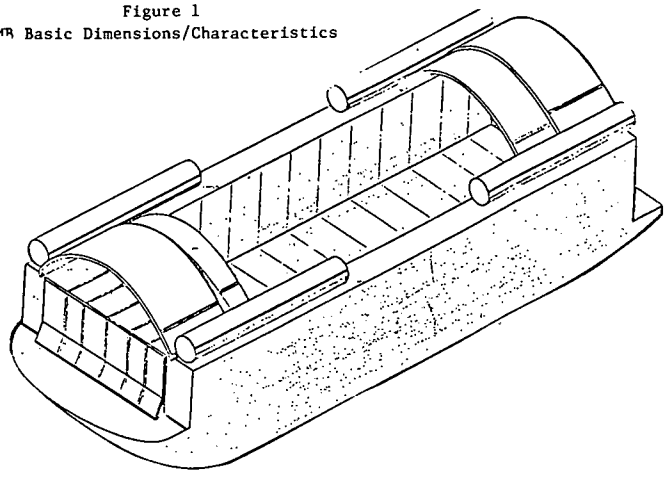
## 2.0 EOTP REQUIREMENTS AND CONSTRAINTS

The feasibility of using the HMB (Figures 1 and 2) as an EOTP was judged by its ability to meet a minimum set of mission needs established by ERDA. These requirements and constraints are shown in Table 1 and include: consideration of the EOTP's testing objectives, its ability to function for an acceptable duration of time (operability), the need to meet specified dates for test operations (operational need dates) at designated sites (siting conditions) while operating in acceptable modes and subjected to potential environmental conditions (EOTP operating modes and environments) and motion constraints. In addition, the HMB had to be capable of accepting major physical modifications and a predefined OTEC plant, and meeting required weights, loading conditions, reliability/maintainability goals and applicable codes and standards. The analysis and design evaluations performed in this study showed that the HMB could be modified at a cost of approximately 4.9 million dollars to meet these stringent requirements and constraints.

## 3.0 EOTP TRADEOFF OPTIONS AND SELECTION CRITERIA

The tradeoff areas considered for converting the HMB into an EOTP are shown in Table 2, along with the evaluation criteria used in making the selection of a preferred option in each area. These areas address modifications to both the vessel and the major systems and equipments which interface with the power plant (e.g. pipe handling system). A brief description of some of the major considerations and selection rationale used in evaluating several of the more significant areas is presented below. These tradeoffs relate to options available for the dredge base, cold water pump installation, cold water pipe design, and cold water pipe joint.

Figure 1
HMB Basic Dimensions/Characteristics



- BASIC DIMENSIONS
  - Length, Overall 324' - 0"
  - Breadth, Molded 106' - 8"
  - Height, Wing Wall Above Baseline 62' - 0"
  - Length Inside Wing Walls 276' - 0"
  - Width, Inside Wing Walls, Molded 76' - 8"
  - Rated Payload Capacity 2,500 LT
  - Width of Wing Walls 15' - 0"
  - Distributed Deck Loading 1,500 LB/SQ FT
- PRINCIPAL FEATURES
  - Control Rooms, P/S, Amidship, 02 Level
  - (24) Voids 02-03 Level
  - (4) Trim Tanks 01-02 Level
  - (22) Variable Ballast Tanks 01-02 Level
  - (22) Soft Tanks
  - Overhead Crane

## Dredge Base

Three options were considered for the dredge base: removal from the HMB, leaving it in its present elevated position (20 ft. above the main deck), or lowering it to near deck level. The main advantages of removing the dredge base were:

a) It permitted more equipment and expanded testing capability to be included on EOTP. Specifically, an additional set of 1MWe heat exchangers, 3 biofouling laboratories, 40 ft. rather than 30 ft. length cold water pipe sections, and expanded diver capability can be incorporated after dredge base removal.

b) More desirable moon pool locations at mid-ship are possible.

## Cold Water Pump Installation

Four concepts were considered for the cold water pump support arrangement: vertical, axial flow with the pump hard-mounted over the sump (the recommended arrangement); horizontal, inline axial flow; vertical, "soft-mounted" axial flow; and a dry-pit installation.

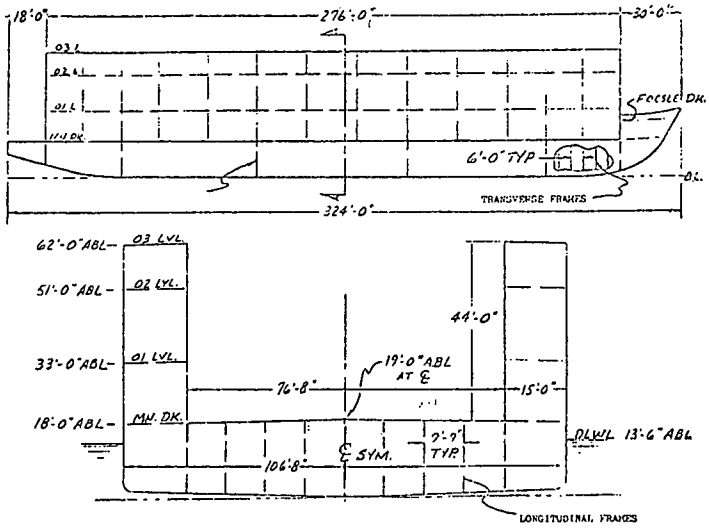



Figure 2 Basic Dimensions, HMB-1

PROGRAM OBJECTIVES

- Experimentally establish the viability of the OTEC power cycle at an early date.
- Assess the criticality of presently identified design problems.
- Perform early development testing of OTEC components, particularly heat exchangers, under real operating conditions.

OPERABILITY FIGURES OF MERIT

- Expected test platform downtime percentage due to equipment failure, maintenance, and repair.
- Expected number of hours per year that the test platform is available to conduct OTEC test operations.
- Probability that the test platform will operate reliably without shutdown given that test operations have started.
- Expected number of hours per year that the test platform can conduct test operations without standby or shutdown due to weather, equipment failure, scheduled maintenance, retrofit or relocation.

OPERATIONAL NEED DATES

- May 1978 - HMB available for installation of heat exchangers.
- November 1978 - Start test program, HMB on site with heat exchangers installed.
- September 1979 - Complete testing of state-of-practice heat exchangers, retrofit advanced design heat exchangers of same capacity.
- September 1980 - Complete testing of advanced design heat exchangers, retrofit second generation heat exchangers of same capacity.
- September 1981 - Complete testing of second generation heat exchangers, terminate program.

HEAT EXCHANGER TESTING

- Startup
- Overall Performance
- Component/Special

DESIGN CRITERIA

- Siting Conditions
  - Six geographical locations
  - Acceptable sites - 30°F ΔT for three consecutive months. Depth not to exceed 3280 ft.
  - Optimum sites - 30°F ΔT for nine consecutive months. Depth not to exceed 2000 ft.
- EOTP Operating Modes and Environments
  - Towing - Sea State 6 or less
  - Standby During Tow - Greater than sea state 6
  - Shelter Seeking - To be determined
  - Standby - Sea state 4 to sea state TBD
  - Testing - Sea state 4 or less
  - Cold Water Pipe Deployment and Recovery - To be defined
- Motion Constraints
  - Operational - Pitch, roll and heave in sea state 4
  - Survival - Pitch, roll and heave in sea state 9
- HMB Modifications
  - Cold and warm water moon pools and sump
  - Equipment foundations
  - $NH_3$ isolation bulkheads
  - Pedestal crane foundation
  - Heliport and crew decks
  - Wiring, piping, catwalks, ladders
  - Thruster Wells
- OTEC Plant
  - 1 MW gross (simulated)
  - Dual condensers - 68,500 $ft^2$
  - Dual evaporators - 68,000 $ft^2$
  - Cold water circulation - 79,000 gpm
  - Warm water circulation - 70,000 gpm
  - Ammonia circulation - 900 gpm, 200 psid
  - Ammonia recirculation
  - Electrical load - 1,000 KW connected
  - Instrumentation - 1,000 test points
- Allowable Weights and Loads

  (To be defined as final design progresses)
- Maintainability
  - Repair or Replace - To be defined
  - System Levels of Replacement - To be defined
- Reliability
  - Failure Rates - To be defined
  - Main-Time-to-Failure - To be defined
  - Reliability Budget Allocation - To be defined
- Applicable Codes and Standards

Table 1 EOTP Requirements

| Tradeoff Areas | Technical Risk | Reliability | Operations Time | Program Cost | Operational Ease | Public Relations | Safety | R&D Requirements | Life | Strength | Usability | Future Expansion | Maintenance |
|---|---|---|---|---|---|---|---|---|---|---|---|---|---|
| | Selection Criteria | | | | | | | | | | | | |
| Dredge Base Removal | | | | | X | | | | | | X | X | |
| Cold Water Pump | X | X | X | | X | | | X | | | | | X |
| Pipe Storage | | | | X | X | | | | | | | X | |
| Pipe Design | X | X | | X | | | | X | X | X | | | X |
| Joint Design | | | | X | | | | | | | | | |
| Heliport | | | | | X | | | | | | X | | |
| Generators | | X | | X | | | | | | | | | X |
| Fresh Water | | | | | X | X | | | | | | | X |
| Sewage | | | | X | X | X | | | | | | | |
| Station Keeping | X | X | X | X | | | X | | X | | | | X |
| Pipe Handling | | | | | | | | | | X | X | | |
| Crew Quarters | | | | X | | | | | | | | | |
| Roof Sections | | | | | X | X | | | | | X | | |
| Moon Pools | | | | | | | X | | | | X | | |
| Pipe Diameter | X | X | | | | | | X | | | | | |

Table 2 Primary EOTP Tradeoff Parameters

The recommended cold water pump arrangement is comprised of a 500 hp pump installed for vertical axial flow with the intake in a closed sump. The sump is fed through a flexible joint siphon line from the cold water pipe string. This configuration has the pump hard-mounted over the sump where it can be maintained in place. The sump has a controllable water level which can be used to tune the surge chamber for partially decoupling the cold water flow dynamics between the pipe string and condenser. An accessible, cleanable screen is installed in the sump to filter debris before it reaches the pump intake. The sump water level is controlled by the same automatically operated vacuum pump that primes the siphon line during operations.

The initial concept for both the cold and warm water pumps was to use horizontal, inline axial flow units. Pump system priming with this concept is accomplished by ballasting the HMB until the water line is approximately 8 feet above the main deck. Then, once system startup is completed, the vessel is deballasted to its working water line. This horizontal axis pump concept was dropped because the time to ballast/deballast substantially reduced the available operation time, and it limited the use of the existing main deck.

The concept of mounting a vertical axis, axial flow pump in the top section of the cold water pipe string appeared to offer the least cost/complex pumping arrangement. However, the major disadvantages were that the pump had to be handled before the pipe string could be retracted; the motion clearance envelope for the pump motor end of the assembly required the deployment system masts to be moved away from the string during hold condition, and any filter screen maintenance required pulling the pump to access the bell and screen.

Once the hard-mounted cold water pump concept was selected, a dry-pit arrangement was also evaluated. The principal reason for discarding the dry-pit arrangement was the direct hydrodynamic couple of the pump inlet to the cold water pipe string. Also, this concept includes an inline filter system which required pulling the pump for any bell-end maintenance.

## Cold Water Pipe Design

Three primary design options were considered for the cold water pipe: fiber reinforced plastic (FRP) cylinder sections with steel flanges and lifting surfaces (the selected configuration), all FRP pipe including FRP flanges and lifting surfaces, and an all-aluminum pipe.

FRP was selected because of: 1) its strength to weight properties, 2) its resistance to sea water corrosion, and 3) its least overall technical risk. The steel flanges and lifting surfaces were chosen for the

| Parameter | Options Considered | Baseline Design |
|---|---|---|
| Dredge Base | 1) Left on Stands<br>2) Lowered to Deck<br>3) Removed | 3 |
| Cold Water Pump | 1) "Soft" Mounted - Vertical<br>2) Hard Mounted - Dry Well<br>3) Hard Mounted Over Sump | 3 |
| CW Pipe Storage | 1) Vertical - Along Wingwalls<br>2) Vertical and Horizontal - Aft<br>3) Vertical - Forward | 3 |
| CW Pipe Design | 1) FRP<br>2) FRP With Steel Fitting<br>3) Aluminum | 2 |
| Cold Water Pipe Joint | 1) Bell and Spigot<br>2) Marman Clamp | 2 |
| Heliport Location | 1) Forward<br>2) Aft Over Crew Quarters<br>3) Elevated | 2 |
| Electric Generators | 1) Diesel Electric<br>2) Gas Turbine | 1 |
| Fresh Water | 1) Supplied<br>2) On-Board Purifier With Storage | 2 |
| Sewage Disposal | 1) Dump Overboard<br>2) Treatment/Incinerate Solids<br>3) Treatment/Convert Solids | 3 |
| Station Keeping | 1) Four-Point Mooring<br>2) One-Point Mooring<br>3) Thrusters | 3 |
| Pipe Handling System | 1) Cable Lift System<br>2) Conventional Drill Rig Type | 2 |
| Crew Quarters | 1) Industrial Vans<br>2) Facility Construction | 1 |
| Retention of Roof Sections | 1) Keep<br>2) Remove | 2 |
| Moon Pool Location | Various Locations | |
| Cold Water Pipe | Various Diameters | |
| Equipment Tradeoffs | Summarized in Section | |

Table 3 Primary EOTP Tradeoff Options

conceptual design since it is not known (without more detailed design and development effort) whether the pipe section can be made out of FRP. A development effort with a pipe vendor is recommended since substantial pipe weight reduction and cost savings appear possible if all-FRP pipe sections are feasible.

The all-aluminum pipe section weighs two-thirds as much and costs about half as much as the selected FRP design. However, the aluminum pipe was not recommended because of its potentially poor corrosion resistance in sea water and because many steel interfaces would have to be isolated from the pipe sections.

Cold Water Pipe Joint

Both a Marmon clamp and bell and spigot type joints were evaluated for joining the cold water pipe sections. The bell and spigot method was found to be technically superior. However, their estimated cost of $35,000 per pipe joint exceeded the total cost for pipe and was felt to be prohibitive. The Marmon clamp is by comparison reliable, cheaper, and technically acceptable.

A summary of the major options in each tradeoff area is shown in Table 3, along with the selected approaches used in developing the EOTP baseline.

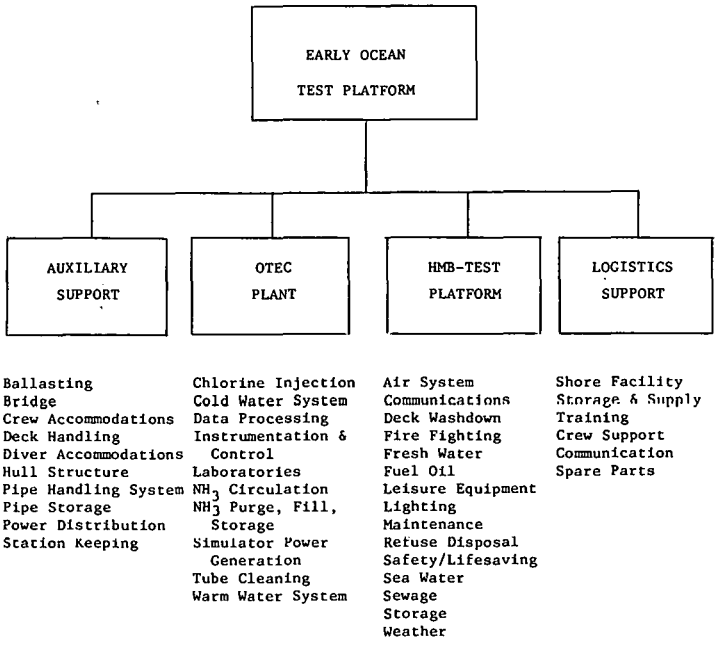



Figure 3

Level 1, 2, and 3 EOTP-1 Systems

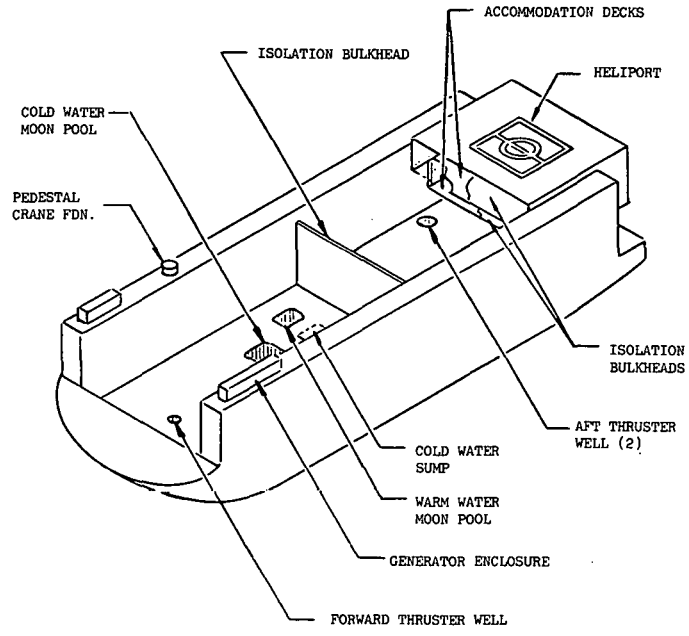



Figure 4 Hull Modifications

## 4.0 EOTP CONFIGURATION

The evaluation of the EOTP requirements and constraints, and the results of the tradeoff studies were used to define the EOTP systems and equipment and to identify the physical modifications required for the HMB. The systems and equipment are shown by functional area in Figure 3. The cutaway drawing in Figure 4 highlights the physical changes proposed for the HMB, and the general arrangement drawing (Figure 5) shows how all required personnel and equipment for the EOTP mission can be accommodated.

## 5.0 SUMMARY AND CONCLUSIONS

This study showed that the Hughes Mining Barge is ideally suited for use as the OTEC Early Ocean Test Platform using a 1MWe power plant. The general arrangement evolved from a systematic series of tradeoff analyses which considered the EOTP system requirements, operational suitability, technical feasibility/risk and cost-effectiveness. These analyses identified the necessary HMB physical modifications to accommodate the planned OTEC plant, crew accommodations and support equipment. In addition, it was determined that the only EOTP system having unique design requirements is the pipe handling system (i.e., all other systems can be comprised of off-the-shelf items). However, a design configuration was recommended based on the use of components and procedures proven on other large pipe handling systems. This configuration stresses simplicity of design and operation, and avoids use of elaborate hydraulic systems and control equipment.

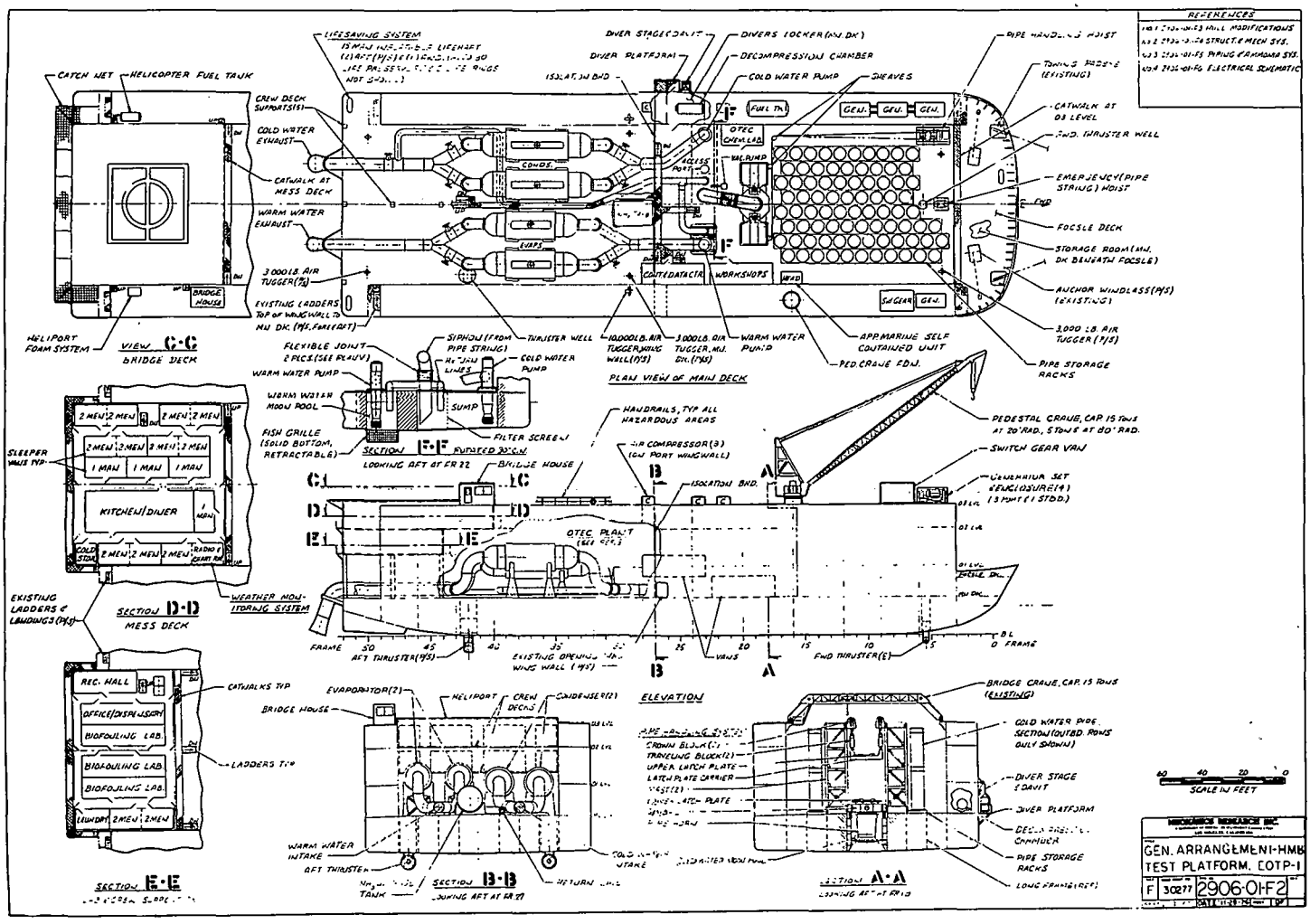



Figure 5. General Arrangement--HMB Test Platform

# A COMPARISON OF TWO GENERIC OTEC SYSTEMS AND MISSIONS

GAY HEIT LAVI AND CLARENCE ZENER
*Carnegie-Mellon University*
*Pittsburgh, Pennsylvania*

## Abstract

A number of OTEC plant design options and missions have been proposed. In this paper, comparisons are made between electrical versus chemical utilization, near shore versus open sea installation, shell and tube versus plate type heat exchangers. It is argued that the electric power mission for direct delivery to the U.S. mainland and its possessions is the most favored economically. If the busbar cost of OTEC power can be reduced, the first demonstration plant can more profitably utilize an over-designed vessel (semi-submersible type) located near the U.S. than it can a simpler vessel (barge type) located in the open seas. It is argued that even with the added cost of a sturdier hull to withstand possible disturbances from hurricane-prone sites and even with the added cost of transmission, a busbar cost of 20-30 mills/kwh projected for electric utilization off the U.S. shore is more achievable than a busbar cost of 10 mills/kwh projected for economic production of chemicals ( ammonia as proposed by APL) in the open seas. However, it is concluded that because of the potentially lower cost of the plate-type variety (as proposed by APL), continued development of the plate-type design and other shell-less heat exchangers (the plate-fin type with or without pressure balancing) is justified.

## Introduction

A highlight of the 1975 OTEC Workshop was the presentation of baseline system concepts evolved by Lockheed Missiles and Space Company (LMSC) (1) and TRW Systems, Inc. (TRW) (2). The Applied Physics Laboratory (APL) presented the concept of ammonia production using electricity from OTEC plants located off the coast of Brazil (3). In the same conference, Abrahim Lavi of Carnegie-Mellon University (CMU) (4) attempted to reconcile the different costs projected in the above three studies. Since, APL has completed a detailed study for the Maritime Administration (MARAD). The results were published in a comprehensive report issued in 1976 (5). Also LMSC has updated its cost figures for the 1975 baseline through an optimization of the design and an increase of the $\Delta T$ from 33.5° to 38°F. The Test Facility Requirements Study by TRW (6) and by LMSC (7), the Heat Exchanger Producibility Study by LMSC (8) and three major ERDA-funded studies have also been completed since the Workshop (9-11). Finally, ERDA in the Program Summary Document of 1976 (12) has indicated a readiness to move ahead to a demonstration of OTEC in the mid- or early 1980's. ERDA's task is complicated by a lack of consensus on how to proceed.

This paper aims to reconcile the divergent claims of proponents so as to clarify the direction ERDA and industry should take in implementing plans for OTEC demonstrations. At the outset, it must be noted that in the case of OTEC, the demonstration stage is perhaps the most critical phase of program development. More so than other solar schemes, OTEC is a capital-intensive project. Hence, considerable funding is required to build a working model at sea. The first demonstration must indicate OTEC's potential for impacting the U.S. energy market; and by impact, we mean an eventual market penetration of 10 to 15% of the total energy demand of the U.S. in the years 2000 and beyond.

However convincing we as proponents have been in presenting various proposals, the fact remains that capital resources are limited. Only one of the many available concepts is likely to be demonstrated now. Of necessity, ERDA must make a choice. It must decide which design to use, where to site the plant and what mission to adopt. Meanwhile, R & D must continue to explore a number of promising alternatives to the particular closed-cycle concept adopted for demonstration.

The literature gives decision-makers little help in their job of determining which of the many proposed system concepts should be used for demonstration. Mainly, the literature has advanced the technical and economic feasibility of this or that scheme without providing a methodology for settling on any one program plan in particular. As it is, the many different recommendations can conceivably justify a number of different design concepts and mission objectives. If ERDA is to evolve a meaningful scenario for OTEC development, a synthesis of the various published results is needed so that a generic model, incorporating the most promising features of the available design options, can be determined for demonstration of the OTEC concept. While many groups have made significant contributions to aspects of the program, APL, LMSC and TRW have presented the most detailed designs. Their work, adequately funded and professionally conducted, provides

a broad spectrum of ideas that may be used to define a possible approach to program development. In this paper, we aim to examine the major assumptions upon which these groups predicate their studies and pursuant claims.

## Siting as a Function of $\Delta T$

We begin with the obvious. The one assumption agreed upon by all is that the capital cost of an OTEC plant is largely dependent on the available $\Delta T$. If we consider only busbar cost, it seems logical to site plants in areas that offer the greatest possible $\Delta T$. The closer the plant is to equatorial regions, the more favorable are the temperatures. Site selection becomes problematic if we add the cost of energy delivery and if we consider ocean-site characteristics other than thermal, such as winds, waves and currents. The closer the plant is to shore, the easier it is to transmit power to mainland consumers. If the mission is to service mainland U.S. with electricity, it seems logical to site plants off the coast of southeastern states. However, as the economics of electric utilization is in part determined by temperature conditions, it may pay to deliver the energy in the intermediate form of energy intensive products. But then we must ask ourselves what is the magnitude of the market for such products? Further, we must consider the efficiency and the cost for conversion to electrical and other high demand energy forms.

## OTEC Cost and Market Competition

The speed with which OTEC may free us from fossil fuel dependency will depend upon the marketplace. The lower the cost of OTEC power, the larger will be its penetration of the energy market. The goal to obtain a significant share of the total energy market will put pressure on OTEC proponents to lower the cost of OTEC plants. Presently, OTEC is a government-sponsored project. ERDA has supported and is continuing to support much work aimed at cutting OTEC's cost. Eventually, it is hoped that industry will take over the commercialization of OTEC. However, industry, more so than government, has difficulty in financing a capital project with marginal return on investment. In industry, profit is the name of the game. Hence, commercialization of OTEC hinges on the profit potential of an OTEC industry. Where will industry look for OTEC's opening wedge into the energy market? The answer, of course, is wherever OTEC power will bring the greatest return on investment.

Our initial hunch is that OTEC power can better compete with power generated from fossil fuel plants than with chemical complexes using fossil fuel as a feedstock. An amplification of this is expressed in quantitative terms in Fig. 1. In constructing this figure, we assume that competitiveness in chemical complexes using fossil fuel and electric power implies an equality in cost of Btu's from fossil fuels and from electric power. Thus, an output of 1 million Btu/hr requires a 300 kw output. If this output is to cost \$2/hr, then

$$300 \text{ kw} \times \frac{\text{cost}}{\text{kw capacity}} \times 2 \times 10^{-5} = 2$$

$$\frac{\text{cost}}{\text{kw capacity}} = \$330/\text{kw} \quad .$$

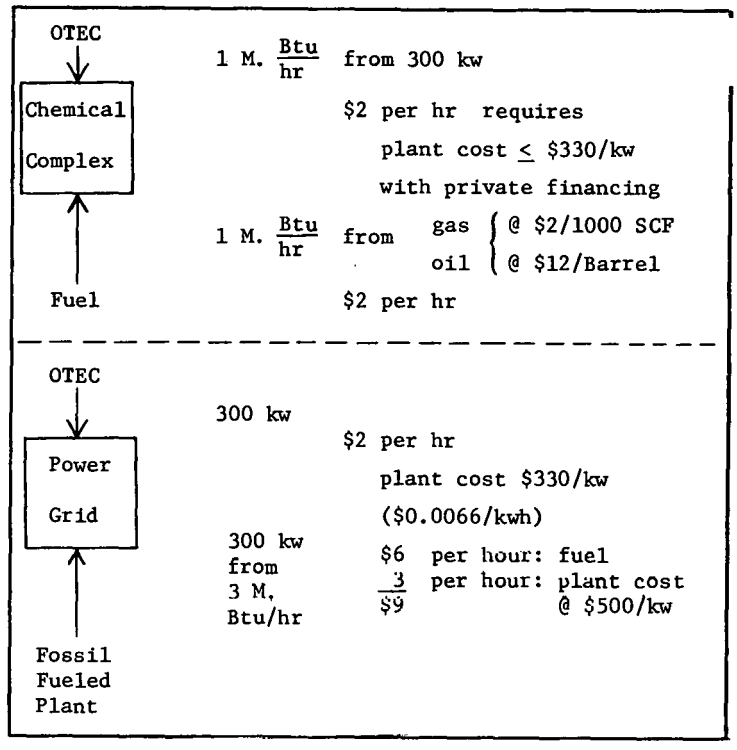



Fig. 1. Comparison of Chemical Complexes and Power Grids as Competitive Arenas.

The factor, $2 \times 10^{-5}$, converts initial capital costs into hourly capital charges using customary required return on capital. The upper part of the figure shows that whether the energy input to a chemical complex comes in the form of fossil fuel at current prices or from OTEC, the capital cost of the plant must be about \$330/kw (a figure corresponding to a busbar electricity cost of 7 mills/kwh) if the cost of energy input is to be the same for both fossil fuel and OTEC power. The lower part of the figure shows that the cost of feeding power generated from a fossil fuel plant into an electric grid is four to five times the cost of power generated from a \$330/kw OTEC plant. This figure suggests that an OTEC plant may receive a much greater return on investment by feeding its power into an electric grid than by using its power to produce chemical products. However, we do concede that factors other than those indicated may enter into an assessment of the economic potential of OTEC/chemical complexes.

## Two Generic Missions and System Concepts

APL has pointed out three advantages that chemical complexes operating in equatorial waters would have over plants transmitting power directly into a grid on the continental U.S.:

(1) Ocean temperatures near U.S. shores do not provide as high a $\Delta T$ as waters in the high seas near the equator;

(2) To feed power into an electric grid requires high transmission costs;

Equatorial regions are comparatively free of hurricanes and therefore require less costly structures.

Based on these assumptions, APL has opted for the 43° ΔT available off the coast of Brazil where it proposes to build ammonia plantships. By siting plants off Brazil with its environmental advantage, APL claims it is possible to bring down the capital cost to a point low enough to compensate for the added cost of producing alternate products.

The CMU OTEC team concedes the ΔT penalty imposed on near shore plants. In Fig. 2, we show the penalty for siting a plant 50 miles off the coast of Louisiana. We also concede that the additional investment in underwater transmission must be considered. In an Arthur D. Little Report (13), it has been estimated that based on a plant cost of $\leq$ \$1000/kw, the cost of a hundred mile transmission cable will run ~ \$200/kw. Finally, we must ask ourselves whether in spite of the ΔT penalty and the added cost of transmission, OTEC power can be competitive with power generated from fossil fuel plants.

$$\Delta T = \begin{cases} 43°F: & \text{Choice off-shore locations} \\ 37.7°F: & \text{50 miles off Louisiana} \end{cases}$$

$$\text{cost} \sim (1/\Delta T)^2$$

$$\left(\frac{43}{37.7}\right)^2 = 1.3$$

Fig. 2. The ΔT Penalty

In Fig. 3, we compare the cost of OTEC power produced 100 miles off the coast of Louisiana and OTEC power produced at an optimum site off the coast of Puerto Rico to the cost of power produced by fossil fuel plants. Although our figures for OTEC power production at these sites may be too low given current cost projections, they do compare with APL's busbar estimates to be given in detail in a subsequent section. The point is that even if the busbar cost of plants designed for electric utilization off the U.S. shore can be brought down to a point where OTEC becomes competitive with fossil fuel systems, the advantage of using OTEC electricity to power chemical complexes at sea must be questioned.

A question that must be decided is whether we should design the OTEC system for a particular mission. In determining the end product for the demonstration and early commercial stages, we must determine which of the available options appears most promising. Should OTEC produce electricity for direct transmission to shore and connection to mainland power grids? Should electricity be transmitted directly to shore for subsequent use in land-based production of energy intensive products? Should electricity be produced for industrial complexes at sea and then be transmitted to shore in the intermediate form of energy intensive products? These are the options. The CMU OTEC team has opted for the lower ΔT available off the U.S. shore where we propose electric utilization of OTEC power. We base our scenario on the assumption that the market for grid electricity is both larger and more profitable than the market for electricity used for ammonia production. We contend that if private industry is to become involved in the commercialization of OTEC, it should not be constrained in its search for the most lucrative OTEC market. To be fair, we note that APL has considered industrial incentives for the commercialization of OTEC. APL has suggested that a cruising chemical complex ship might qualify for a maritime government loan. Such a guaranteed loan would enable a company to receive 100% debt financing. Thereby, the company would avoid all income taxes. To this we reply that consideration of possible government subsidy under present rules should not influence the government's decision as to how OTEC power should be used. If the government really aims to subsidize OTEC power production, it must modify its own rules.

## The Problem of Cost Prediction

While it is possible to predict the cost of a given design if the variables that determine performance are known, comparative cost estimates are problematic because different designs assume different performance criteria and system attributes. While the APL design assumes an overall heat transfer coefficient $U < 400$ Btu/hr ft$^2$ °F, both the LMSC and TRW designs assume $U \sim 450$. While APL assumes a 5-MWe module, LMSC assumes 66-MWe and TRW assumes 25-MWe. While APL employs aluminum shell-less heat exchangers, both LMSC and TRW employ titanium shell and tube. Our job will be to equalize the variables

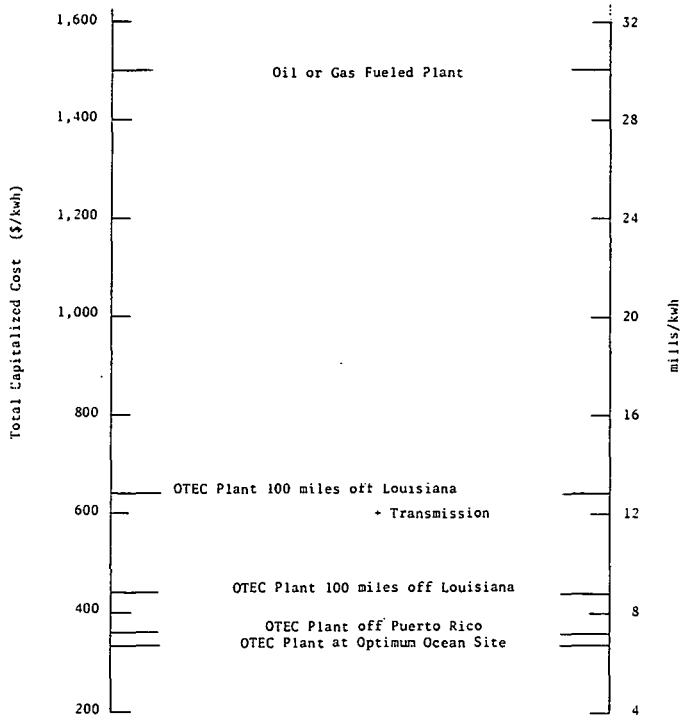



Fig 3. Competition of OTEC with Fossil Fuels

assumed for the different plant concepts so as to assess with reasonable accuracy the ultimate cost of energy to the consumer. To this end, we will establish methods whereby a systematic appraisal of the data may be made.

## Method for Equalizing the Variables

First we consider the $\Delta T$. In Table 1, we show the seasonal variations in temperature for a set of representative sites available to the United States. Then in Appendix 1, we calculate the net output of a given plant as $\Delta T$ varies.

Table 1. Seasonal Variations of Temperature, °F

| | Ocean Data by Month | | | | | |
|---|---|---|---|---|---|---|
| | Brazil | New Orleans Brownsville | Miami | Hawaii | Puerto Rico | Gulf of Mexico |
| Jan. | 40 | 32 | 34.75 | 37.25 | 40.25 | 38.5 |
| Feb. | 39 | 31 | 33.25 | 36.75 | 38.75 | 37 |
| Mar. | 39 | 30.5 | 35.75 | 37 | 38.5 | 36.75 |
| Apr. | 39.75 | 31.5 | 35.25 | 38 | 39 | 38 |
| May | 39.5 | 35.5 | 36.5 | 39 | 40.5 | 39.5 |
| Jun. | 39.5 | 40.2 | 37.5 | 40 | 41.5 | 41.75 |
| Jul. | 40.75 | 42 | 40.5 | 40.75 | 42 | 43.8 |
| Aug. | 42.5 | 44.5 | 41.25 | 41.25 | 42.5 | 45 |
| Sept. | 43.25 | 44.3 | 40.75 | 41 | 43.25 | 44.25 |
| Oct. | 43 | 42 | 41.25 | 40 | 43.75 | 42.75 |
| Nov. | 41.75 | 39 | 40.75 | 37.75 | 43.5 | 41.25 |
| Dec. | 40.75 | 35.5 | 39.5 | 37.75 | 42 | 39.25 |
| Average | 40.69 | 37.33 | 37.92 | 38.71 | 41.29 | 40.65 |
| RMS $\Delta T$ | 40.72 | 37.68 | 38.03 | 38.75 | 41.33 | 40.74 |

Assuming the water flow rate and hence the pumping losses remain constant, we find that

$$P_{net} = P^*_{gross}\left(\frac{\Delta T}{\Delta T^*}\right)^2 - P_{loss}$$

where the starred terms represent the design point. We use this formula to determine the annual average output as a function of the monthly average $(\Delta T)^2$ for a given design without redesigning or re-optimizing. The next step in our approach is to determine the respective annual output at the six representative sites for two representative systems, the shell-less design presented by APL and the shell and tube (s-t) design presented by LMSC and by TRW. To do this, we take the published cost figures which have been optimized by their proponents for specific sites and adjust these figures for each of the representative sites presented in Table 1.

Based on APL's energy balance sheet,

$$P^*_{gross} = 121 \text{ MWe}$$

$$P_{loss} = 16 \text{ MWe} \quad \text{and} \quad \Delta T^* = 43\ ^\circ\text{F}\ .$$

APL shows an additional 5 MWe loss which is a function of the load. Thus we derive

$$P_{net} = \frac{1}{1.05}\left(121\left(\frac{\Delta T}{43}\right)^2 - 16\right) \quad \text{MWe}\ .$$

In Table 2, we calculate the net output from APL's nominal 100 MWe baseline design for each of the six sites using the root mean square $\Delta T$. In column (1), we give the adjusted output based on the $\Delta T$ for each of the six sites. In column (2), we adjust for the pumping losses which we claim to have been underestimated by at least 75%.

Table 2. Nominal 100 MWe Baseline (APL & LMSC) Designs

| | | APL 100 MWe Nominal Based on $\Delta T^* = 43°F$ | | LMSC's Adjusted Output for Nominal 100 MWe Based on $\Delta T^* = 38°F$ |
|---|---|---|---|---|
| Site | RMS $\Delta T$ | Calculated (1) | True Net Output (2) | (3) |
| Brazil | 40.72 | 88.08 | 76.08 | 120 |
| New Orleans / Brownsville | 37.68 | 73.25 | 61.25 | 97.75 |
| Miami | 38.03 | 74.91 | 62.91 | 100.25 |
| Hawaii | 38.75 | 78.34 | 66.34 | 105.5 |
| Puerto Rico | 41.33 | 91.23 | 79.23 | 125. |
| Gulf of Mexico | 40.74 | 88.22 | 76.22 | 120.5 |

For the s-t system, we use LMSC's figures because LMSC has recently updated its 1975 baseline design as shown in Tables 3 and 4 reproduced from LMSC's Test Facility Study. Based on the data, we calculate in column (3) of Table 2 the net output for the LMSC design at each of the six sites using the equation given below (equalized for a 100 MWe plant):

Table 3. Baseline Power Cycle Changes (LMSC)
Module/Cycle Comparison

| | June 1976 | |
|---|---|---|
| Warm Water Inlet Temp (°F) | 79.75 | 38°F |
| Cold Water Inlet Temp (°F) | 41.76 | |
| Inlet Water Temp Delta (°F) | 37.98 | |
| Heat Exchanger LMTD (°F) | | |
| Evaporator | 7.56 | |
| Condenser | 7.68 | |
| Total Sea Water Flow/Module (CFS) | 28175. | |
| Ratio Water Flow Warm/Cold | 1.065 | |
| Overall Heat Transfer Coeff. (Btu/hr ft$^2$ °F) | | |
| Evaporator | 505 (540) | |
| Condenser | 441 (490) | |
| Fouling Resistance (hr ft$^2$ °F/Btu) | 0.0001 | |
| Tube Sea Water Velocity (FPS) | | |
| Evaporator | 6.46 | |
| Condenser | 6.00 | |
| Total Heat Flow Across (Btu/sec $10^6$) | | |
| Evaporator | 2.858 | |
| Condenser | 2.774 | |
| Gross Turbine Power, MW | 91.8 | |

Table 4. OTEC Plant Electric Power Output (LMSC) Four Modules

| Item | June 1976 Baseline (KW) |
|---|---|
| Generator Gross Output | 361,552 |
| Plant Cycle Auxiliaries | 84,664 |
| Module Support Systems | 2,832 |
| Core Support Systems | 854 |
| Losses-Internal Transmission | 3,336 |
| Step-up Transformer Input | 269,866 |
| Losses-Transformer/Rectifier | 5,397 |
| Plant Electric Output-Net | 264,469 |

$$P_{net} = 136.71 \left(\frac{\Delta T}{38}\right)^2 - 36.71 .$$

Table 5, reproduced from APL's Table 5-14 ( p. 5-24), shows APL's cost figures. As shown in column (1), APL's cost breakdown for its demo-plantship (100 MWe) excluding the ammonia plant is

| | |
|---|---|
| Total basic ship | $99.8 M. |
| 12% escalation | 12.0 |
| Deployment | 1.0 |
| | $112.8 M. or $1120/kw . |

As shown in column (2), APL's cost breakdown for its 6th plantship (500 MWe) also excluding the ammonia plant is

| | |
|---|---|
| Total basic ship | $250.90 M. |
| 12% escalation | 30.11 |
| Deployment | 2.00 |
| | $283.01 M. |

$$\$/kw = \frac{\$283 \times 10^6}{500{,}000 \text{ kw}} \text{ or } \$566/kw .$$

From Tables 5 and 2 (column 2), we calculate Table 6. Based on the results, the cost of APL's sixth plantship for all six sites roughly decreases about 50 percent from the 100 MWe demo.

We now examine the s-t design. In order to equalize the design to that of APL's, we adjust the material from titanium to aluminum. To do this, we use data from Table 25 on page 150 of LMSC's Producibility Study. Table 7, reproduced from LMSC's Test Facility Study, shows the cost of LMSC's 25th production unit with material adjustment. Based on titanium heat exchangers, the cost of the plant is $1700/kw. Calculating only the cost of the heat exchangers, the study shows the cost reduced from $835/kw for titanium, as shown in Table 7, to $355/kw for aluminum as obtained from the Producibility Study. With aluminum adjustment, the overall cost reduces to $1220/kw. We estimate further cost reductions are ble if the overall heat transfer coefficient is

Table 5. Plant Cost Breakdown Excluding Ammonia Plantship (all costs in Millions, 1975 Dollars)

| | APL'S COST Demo-Plantship 100 MWe (1) | APL'S COST 6th Ship 500 MWe (2) | *Audited Cost for Corrected L.C. (3) |
|---|---|---|---|
| Heat Exchangers | 34.5 (5-MWe) | 107.7 (5-MWe) | 107.7 |
| Ships' Platform | | | |
| Basic Hull | 13.5 | 44.3 | 104.0 |
| Other Platform Items | 15.5 | 26.8 | |
| Equipment | | | |
| Cold Water Pumps & Starters | 7.34 | 12.8 | 28.6 |
| Warm Water Pumps & Starters | 5.98 | 10.3 | 24.3 |
| Ammonia Pumps & Starters | 0.25 | 0.39 | 1.0 |
| Ammonia Turbines | 5.80 | 8.8 | 17.9 |
| Demisters | 0.33 | 0.50 | 1.0 |
| Control & Auxiliary Equipment | 5.00 | 11.0 | 16.2 |
| Generators, Transformers, Rectifiers, Auxiliary Transformers | 4.60 | 10.1 | 20.3 |
| Cleaning System | 0.05 | 0.12 | .2 |
| Ammonia Inventory | 0.78 | 3.1 | 3.9 |
| Cold Water Pipe | 6.25 | 15.0 | 20.7 |
| Total Basic Ship | 99.8 | 250.9 | 345.8 |
| Construction, Interest & Escalation (12%) | 12.0 | 30.11 | 41.5 |
| | 111.8 | 281.01 | 387.3 |
| Deployment | 1.0 | 2.0 | 2.0 |
| TOTAL PLANT INVESTMENT | 112.8 | 283.01 | 389.3 |

*for a "500 MWe" OTEC Plant, excluding Ammonia ($778.6/kw versus APL's $566/kw); .8 capacity factor

Table 6. APL's Adjusted Cost*

| | $/kw (100 MWe) (1) | APL's 6th Plantship ($566/kw) (2) | Corrected Learning C. ($778.6/kw) (3) |
|---|---|---|---|
| Brazil | 1483 | 745 | 985 |
| New Orleans / Brownsville | 1841 | 924 | 1223 |
| Miami | 1793 | 900 | 1191 |
| Hawaii | 1700 | 853 | 1130 |
| Puerto Rico | 1423 | 714 | 946 |
| Central Gulf | 1480 | 743 | 983 |

*APL's first 100 MWe = $1128/kw.

$1128 = [(99.8)(1 + .12) + 1][$10^6/10^5$] .

Table 7. Comparison of 25th Production Unit Cost (LMSC) Titanium Heat Exchangers, $M.

| Item | June 1976 Baseline |
|---|---|
| Modules - Shells | 24.8 |
| Modules - Heat Exchangers | 221.3 |
| Modules - Rotating Equipment | 49.7 |
| Modules - Other | 34.8 |
| Platform - Core | 42.0 |
| Platform - Other | 18.5 |
| Cold Water Pipe | 12.3 |
| Mooring System | 34.1 |
| Integration and Checkout | 5.6 |
| Facility Preparation | 7.2 |
| Total | 450.3 |
| Net Output | 264.5 |
| Dollars/kw | 1700. |

Table 8. Adjusted Cost Based on Shell and Tube Design, $/kw (LMSC Platform)

| | (1) $1700/kw + 12% = 1904 | (2) $1220/kw + 12% = 1365 | (3)* $1125/kw + 12% = 1260 |
|---|---|---|---|
| Brazil | 1588 | 1139 | 1050 |
| New Orleans / Brownsville | 1946 | 1397 | 1288 |
| Miami | 1899 | 1363 | 1257 |
| Hawaii | 1804 | 1295 | 1194 |
| Puerto Rico | 1523 | 1093 | 1008 |
| Gulf of Mexico | 1581 | 1134 | 1046 |

* Compare Col.(3) of Table 8 with (3) of Table 6 (APL's)

increased as will be shown subsequently. If we use ammonia side enhancement and keep the water side clean, the overall heat transfer coefficient can be increased from LMSC's 500 to 682 Btu/hr $ft^2$ °F, reducing the cost of the heat exchangers to $260/kw and the overall plant cost to $1125/kw. Reoptimization will further reduce cost. In Table 8 we calculate the effective capital cost for LMSC's adjusted plant output for each of the six representative sites.

We observe that APL's cost comes out to be lower than the s-t's cost even though the s-t's overall heat transfer coefficient is higher (500 ~ 700 versus 400). We have to ask ourselves what is the reason for this wide cost margin. The site conditions have been equalized. The material has been adjusted. The difference in hull, barge-type for APL and spar buoy for s-t, does not justify APL's comparatively low figures. To answer this question, we conducted an audit of APL's Table 5-14 in order to determine how APL arrived at such a low overall cost. It appears that by using learning curve techniques, APL has been able to project a 50% cost reduction from the demo-stage to the sixth generation plantship. In column 3 of Table 5, we present a cost breakdown of APL's 500 MWe plantship adjusted to our audited estimate. In column 3 of Table 6, we present APL's cost for each site based on our application of the learning curve. Based on these figures, APL's projected cost of $566/kw increases to $778.6/kw.

In our audit, we have disallowed much of the cost reduction projected on the basis of economy of scale and learning. We have limited economy of scale effects to the hull and cold water pipe because scale factor reduction is not always applicable, for example in the case of APL's power modules which remain 5-MWe for both the demo- and 6th plantships. APL's 100 MWe demo-plant has twenty 5-MWe modules and its 500 MWe 6th plantship has one hundred 5-MWe modules. Also we have disallowed cost reduction projected on the basis of learning applied to certain components because learning will not improve the cost of all equipment, i.e., such off-the-shelf items as generators, transformers and rectifiers. What we are saying in effect is that all the modules for a given plantship will have the same design and hence the same cost. This is so because as we go from one generation of manufacture to another, we do not change the basic design of the plant. To do so would be to violate the very principles of the learning curve approach. In our estimates of cost reduction based on learning, we change only the manufacturing cost. We apply learning only to labor and to a complete plant design.

One advantage of the APL design appears to be its low cost heat exchangers. If we estimate the material requirements of APL's exchangers and compare them to the s-t variety, we observe that the s-t requires less material than the plate-type by a ratio ranging from 2 to 3. APL's surface area is $(8.2 \times 10^6)/(40)$ $ft^2$ for a 5-MWe heat exchanger. The average thickness of the tubes is calculated to be about .152 inches. Hence, the material volume of APL's exchangers comes to about 2600 $ft^3$ for each of the 5-MWe modules. We then calculate the total material (all aluminum) needed for a 5-MWe s-t design using the same heat transfer coefficient as APL. We found the material volume of s-t exchangers to be about 1600 $ft^3$. Immediately, we observe that s-t requires less material than the plate-type by a ratio of 3:2. In App. B, we show this calculation in detail.

If we apply the learning curve correctly, that is, separate labor from material cost, we deduce that the APL concept, even if the initial labor cost were lower, would not drop in cost as much as the s-t concept. This is so because the APL design uses more material than the enhanced s-t design. We do not question APL's lower labor cost. The point is that if labor goes through the learning experience with the material remaining constant, it would seem better to start off with a lower material cost and a higher labor cost, as is the case with the s-t design, because material is not affected by learning, whereas labor is. Hence, learning techniques can bring down the cost of labor and so, also bring down the overall capital cost of the system.

The ultimate answer to heat exchanger design may very be neither the shell-less APL nor the s-t variety. er, the submerged plate-fin type of the compact variety similar to those proposed by the Andersons and the University of Massachusetts may prove to be the wave of the future. The advantage of plate-fin, with or without pressure balancing, is the considerable reduction in both heat exchanger and hull costs. However, plate-fin exchangers for OTEC application require a longer development time.

In Table 9, we present four typical cases that show how both water and ammonia side enhancement can improve the overall heat transfer coefficient. We calculate U

Table 9. Improved Heat Transfer Coefficient Using Ammonia Side Enhancement

| | $U_e$ | $U_c$ | Clean Smooth Water Side | $NH_3$/ Evap. | $NH_3$/ Cond. | Fouling ev/con |
|---|---|---|---|---|---|---|
| Water Side Smooth | | | | | | |
| Case 1. | 644 | 588 | 1000 | 4000 | 2000 | .0003/.0002 |
| Case 2. | 740 | 625 | 1000 | 4000 | 2000 | .0001/.0001 |
| Water Side Enhancement - 50% Improvement | | | | | | |
| | $U_e$ | $U_c$ | Clean Enhanced Water Side | $NH_3$/ Evap. | $NH_3$/ Cond. | Fouling ev/con |
| Case 3. | 822 | 732 | 1500 | 4000 | 2000 | .0003/.0002 |
| Case 4. | 984 | 790 | 1500 | 4000 | 2000 | .0001/.0001 |

based on a clean smooth water side, a clean enhanced water side, an enhanced ammonia side with vertical fluted tubes and various fouling factors. In Table 10, we proceed to give the average U for each of the four cases presented in Table 9. Then without changing the shell thickness as the shell diameter decreases, we give the total material volume of aluminum needed to build a 5-MWe s-t heat exchanger prorated on the surface requirements of s-t components and based on

Table 10. Design of 5-MWe Shell and Tube based on Different Overall Heat Transfer Coefficients (See App.B)

| Case | U | Area $ft^2$ | Number of Tubes | Shell Diam. | Shell Vol. | Tube Vol. | S-T Material ($ft^3$) Total |
|---|---|---|---|---|---|---|---|
| | 400 | $2.05 \times 10^5$ | 26100 | 19.04 | 449 | 1110 | 1559 |
| | 600 | 1.37 | 17400 | 15.55 | 366 | 745 | 1111 |
| 1 | 616.5 | 1.33 | 17000 | 15.34 | 362 | 715 | 1077 |
| 2 | 682.5 | 1.704 | 15300 | 14.58 | 344 | 646 | 990 |
| 3 | 777 | 1.06 | 13465 | 13.67 | 322 | 568 | 890 |
| | 877 | .933 | 11880 | 12.79 | 302 | 480 | 782 |

different average U values. Arbitrarily, we select case 2 as a realizable concept and find that with no water side enhancement and with cleaning to a .0001 fouling factor, we can reduce the cost of s-t exchangers from \$355/kw to \$260/kw, giving us an overall capital cost of \$1125/kw.

## Energy Cost

Using the methodology developed in this paper, we can calculate the busbar cost of electricity for both the APL and s-t designs at various sites. Table 11 summarizes the results. It appears that the cost of electric power

Table 11. Energy Cost at the Busbar
Mills/kwh = (.15 × \$/kw)(.8 / 8760) × 1000
Capacity factor = .8
Fixed charges = 15% per annum

| Site | Capital Cost \$/kw / $\Delta T°F$ RMS | APL (Sixth Plantship) 566† @ 43°F | APL (Sixth Plantship) 778.6†† @ 43°F | Shell-Tube 2100* @ 40°F | Shell-Tube 1700 @ 38°F | Shell-Tube 1220 @ 38°F | Shell-Tube 1125 @ 38°F |
|---|---|---|---|---|---|---|---|
| Brazil | 40.72 | 14 | 22 | 43 | 30 | 22 | 20 |
| New Orleans Brownsville | 37.68 | 17 | 27 | 52 | 38 | 27 | 25 |
| Miami | 38.03 | 16 | 26 | 50 | 36 | 26 | 24 |
| Hawaii | 38.75 | 16 | 25 | 48 | 35 | 25 | 23 |
| Puerto Rico | 41.33 | 13 | 21 | 42 | 29 | 21 | 19 |
| Gulf of Mexico | 40.74 | 14 | 21 | 43 | 30 | 22 | 20 |

† As reported by APL

†† Corrected for $\Delta T$ and losses

* TRW Baseline Cost (1975) based on 40°F

for the APL, LMSC, TRW and other improved s-t designs ranges from a low of 13 mills/kwh for the Puerto Rico and Brazil sites, using APL's optimistic figures, to a high of 52 mills/kwh for the New Orleans-Brownsville sites, using TRW's baseline (1975). Using the corrected APL figures and the improved s-t (aluminum) figures, we find the range narrows to between 19-27 mills/kwh. Adding the cost of underwater transmission, we conclude that busbar electricity transmitted to shore will cost about 25-30 mills/kwh. At this price range, OTEC may be able to compete with electricity produced from nuclear plants, the stand-by U.S. option today.

## Comparison with Nuclear

The rapidly rising cost of nuclear power plants is making them vulnerable to competition from OTEC plants. Yet, controversy continues between the "nukes" who persist in their optimistic claims for nuclear and the "solars"

who refute the claims on grounds of nuclear's questionable cost potential. Perhaps the answer to nuclear's real cost may be obtained from engineers who design the plants, from industries that build them and from utilities that pay for them. In Fig. 4, we give estimates that show how good the utility experts have been at projecting the final cost of nuclear power during this period of rapidly escalating costs. The bottom line (x) shows the average total $/kw spent for plants coming on line in a given year (14). The second line (•) shows the cost announced by utilities for plants to be built as a function of the year in which it was decided to build the plants (14). In the time of the Atomic Energy Commission (AEC), it was customary every two years to estimate the cost of plants planned in that year. The AEC estimates are plotted in the third line (□)(15). Finally, the top line (⊙) shows what the plants actually cost as a function of the year in which they were first planned (16). We can see that the actual costs have been consistently greater than the estimated costs by a factor of two. This diagram was constructed a year ago. The January 1977 ERDA Milestone Report gives an update of the two bottom curves. It appears that the factors that have caused this spectacular rise in nuclear cost in the past are still operating.

F.C. Olds, Senior Editor of Power Engineering, writes in the September 1975 issue that "the industry [utility] is looking at 1985 costs of $1500-$2000/kw for plants it is ordering today at the same time new plants are coming on line for $300-$400/kw." Note that the $1500-$2000/kw range referred to by Olds straddles the extrapolation of the actual cost plotted in Fig. 4 (⊙) and so jibes with unofficial utility cost estimates. We can only surmise that if these estimates of nuclear cost were publicized, approval to proceed with nuclear commercialization would not be given by Public Utility Commissions.

The worst news on the nuclear cost issue is the cost in dollars prorated by kw capacity. When buying a plant, a utility plans on a cummulative capacity factor of at least 80%. This is the ratio of total kilowatts produced divided by the number which would have been produced if the plant had operated full time at rated capacity. As of January 1977, the record for cummulative capacity for all plants over 750 MWe is shown in Fig. 5 (17). It appears that the capacity actually realized is about 54% which means that the effective cost of nuclear power plants coming on line in the mid-eighties is

$$\frac{.80}{.54} \quad \$1750/kw = \$2600/kw .$$

If we use the $1500/kw figure, the cost will run about $2200/kw ( ~46 mills/kwh). In comparison, the cost of first generation commercial plants designed by Lockheed and by TRW are well below this range, namely $1700/kw. Adoption of the enhanced heat transfer exchangers being developed by Rothfus at CMU would lower the $1700/kw estimate to the $1200/kw level.

## Conclusion

We conclude that if OTEC cost projections are valid, OTEC is in an extremely competitive position with nuclear and fossil fuel systems. It appears more realistic to aim for the 20 to 30 mills/kwh transmitted to shore than for the 10 mills/kwh produced at sea for the production of ammonia and other chemicals. In fairness to APL, they have been assuming a year round $\Delta T$ of 43°F by having

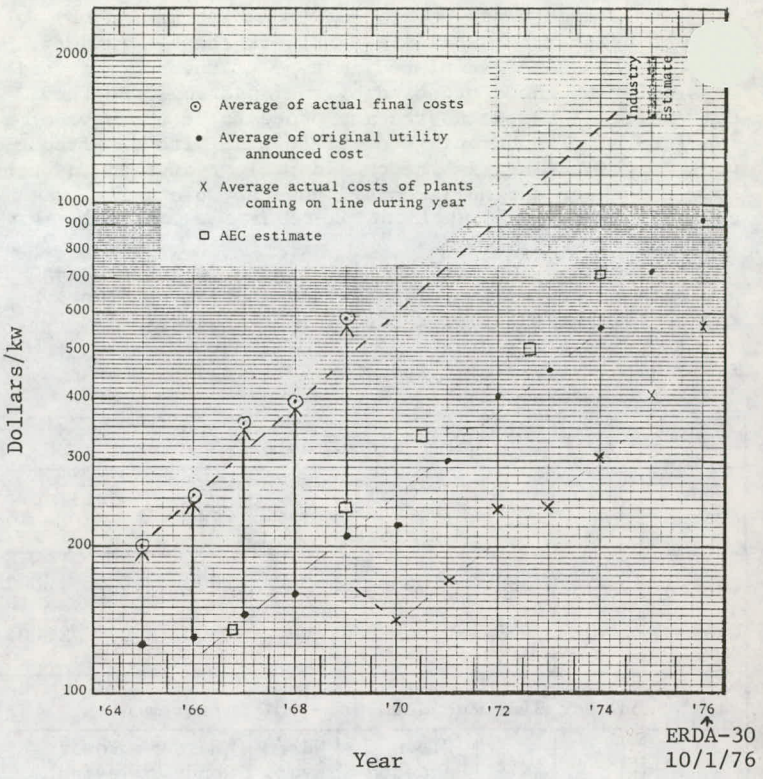
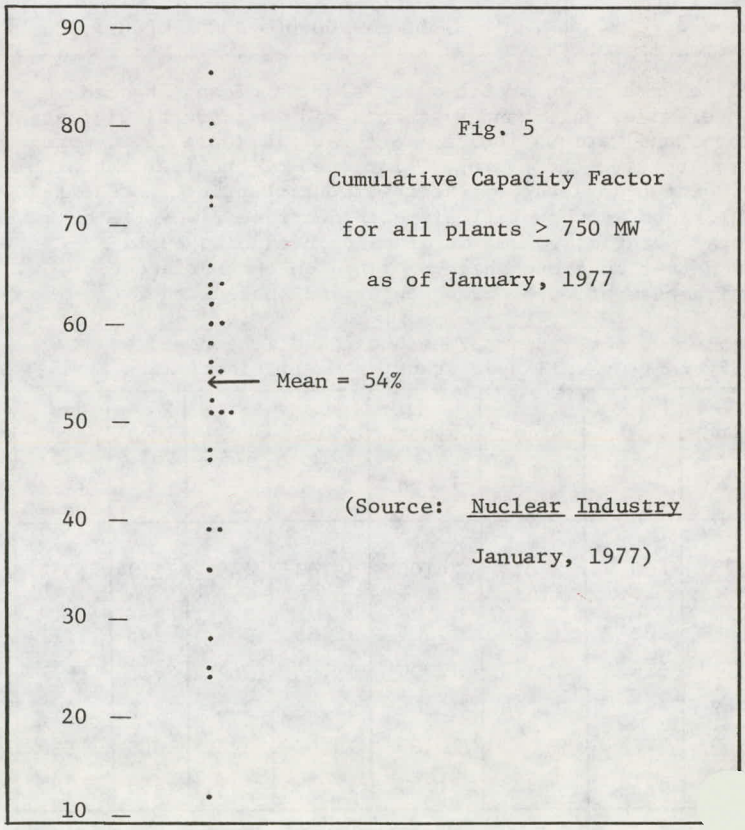



Fig. 4. Comparison of original utility announced costs with actual final costs and with costs of plants coming on line during year.



the plantship "graze" continuously while looking for "better pastures." If this approach turns out to be feasible, based on our audited cost figures ($778.6/kw) corrected for underestimated pumping losses (75% increase), APL's capital cost becomes in fact $778.6/kw ÷ .88 ≅ $880/kw , and their corresponding busbar cost rises to 20 mills/kwh.

A word of caution is in order here. It behooves OTEC proponents neither to underestimate OTEC's cost potential nor to be unduly optimistic. Nor should we be unduly committed to any one design or to any particular mission approach. Too many uncertainties remain. First, we must resolve the uncertainties by proving the OTEC concept at sea.

In our paper, we have concluded that it may be more profitable to produce electricity near shore and to feed that electricity into a grid than to produce chemical products at sea. The cost differential between the APL concept and the conventional shell and tube concept with the Lockheed platform is not great enough to justify the low capital cost projection of APL. There appears to be a potential merit in the APL heat exchanger concept. If the APL exchanger can be developed to function as has been analytically predicted, then there is a justification for pursuing this concept in an R & D program. Finally, if we were to exclude the "grazing" concept, there seems to be little advantage for the U.S. to locate OTEC plants in international or foreign waters.

References


1. Lloyd C. Trimble et al., "Ocean Thermal Energy Conversion System Study Report," Proceedings, Third Workshop on Ocean Thermal Energy Conversion, Houston, TX, May 8-10, 1975, G.L. Dugger, editor, APL/JHU SR 75-2, August 1975, pp. 3-21.

2. Robert H. Douglass, "Ocean Thermal Energy Conversion: An Engineering Evaluation," IBID., pp. 22-38.

3. G.L. Dugger et al., "Tropical Ocean Thermal Power Plants Producing Ammonia or Other Products," IBID., pp. 106-115.

4. Abrahim Lavi, "Solar Sea Power Plants, Costs and Economics," IBID., pp. 64-72.

5. W.H. Avery, R.W. Blevins, G.L. Dugger, E.J. Francis, Maritime and Construction Aspects of Ocean Thermal Energy Conversion (OTEC) Plant Ships. APL/JHU SR 76-1B, April 1976.

6. Test Facility Requirements Study by TRW, 1976.

7. Ocean System (LMSC) Ocean Thermal Energy Conversion (OTEC) Test Facilities Study Program, LMSC-D506781, 17 January 1977.

8. Lockheed Missiles and Space Company, OTEC Heat Exchanger Design and Producibility Study, LMSCD-507632, 28 October 1976.

9. P.M. Wolff and Lloyd Lewis (See paper 1, session 2A) "Monthly Assessment of Temperature Resources for Three Potential OTEC Sites," Proceedings Fourth OTEC Conference and Workshop, New Orleans, LA, March 22-24, 1977.

10. A. Konopka et al. (See paper 1, session 4A), "Alternate Forms of Chemical Fuel Transmission from OTEC Plants," IBID.

11. E.J. Tschupp et al. (See paper 4, session 4A), "Problems Associated with OTEC Missions," IBID.

12. Program Summary Document: Ocean Thermal Program Plan, ERDA, October 1976.

13. Energy Utilization Workshop, Arthur D. Little Report, Chicago, IL, June 17-18, 1976.

14. U.S. Central Station Nuclear Electric Generating Units: Significant Milestones , ERDA, Division of Nuclear Research and Applications.

15. WASH-1345 (October 1974), USAEC Division of Reactor Research and Development.

16. "Central Station Nuclear Plants" Quarterly, Industry Relations, ISL, ERDA.

17. Cumulative capacity factor for all nuclear plants is reported monthly in Nuclear Industry.

## Appendix A

### OTEC Plant Output Variations with ΔT

We are interested in the variations of the net output power of a given OTEC plant design when the ocean ΔT changes. Thus, once a plant is built, we wish to know how we can maximize the plant's net output power when the existing ΔT differs from the design ΔT*. Whatever the design point of an OTEC plant is, we assume that the flow rates of water are unchanged from their nominal values. The ammonia flow must be controlled to insure maximum output. For the time being, we do not consider the problem of generator frequency or plant stability. Previous analysis indicates that the system is self-adjusting (self-regulating).

### Definition of Symbols

| | | |
|---|---|---|
| $\delta_1$ | warm water temperature drop in evaporator | °F |
| $\delta_e$ | Thermal potential across evaporator | °F |
| $\delta_E$ | engine ΔT | °F |
| $\delta_c$ | thermal potential across condenser | °F |
| $\delta_2$ | cold water temperature rise in condenser | °F |
| $Q_e, Q_c$ | heat flux through evaporator/condenser, | Btu/sec |
| $A_e, A_c$ | surface area of evaporator/condenser | $ft^2$ |
| $\Omega_e, \Omega_c$ | water flux through evaporator/condenser, | $ft^3$/sec |
| $U_e, U_c$ | overall heat transfer coefficients, | Btu/sec $ft^2$°F |
| $\eta_{tg}$ | turbogenerator efficiency | |
| $\eta_c$ | Carnot efficiency | |
| $\eta_p$ | pump efficiency | |
| g | acceleration constant | |
| $C_p$ | specific heat | Btu/lb °F |
| Δ | total ΔT | °F |
| ρ | water density | $lb/ft^3$ |
| P | power | kw |

### The Model

1. Heat Flow

   Warm water: $C_p \rho \Omega_e \delta_1 \geq Q_e$ .

   Cold water: $C_p \rho \Omega_c \delta_2 \geq Q_c$ .

   Heat transfer: $U_e A_e \delta_e \geq Q_e$ .

   Heat transfer: $U_c A_c \delta_c \geq Q_c$ .

2. Engine

$$\eta_{tg} \eta_c Q_e \geq P_{gross} \quad \text{Btu/sec} .$$

3. Energy Balance

$$Q_e - Q_c \geq P_{gross}$$

$$P_{gross} \geq P_{net} + \frac{P_{pumps}}{\eta_p} .$$

4. Temperature allocation

$$\frac{1}{2}(\delta_1 + \delta_2) + \delta_e + \delta_E + \delta_c \leq \Delta .$$

5. Carnot efficiency

$$\eta_c \cong \frac{\delta_E}{T}$$

6. The relation between gross power, net power and power loss is given by

$$P_{gross} = P_{net} + P_{loss}$$

The problem we solve here is to find how the maximum value of $P_{net}$ depends upon Δ, the water flux through the evaporator and condenser being held fixed. Constant water fluxes essentially imply constant $P_{loss}$. Maximizing $P_{net}$ is therefore equivalent to maximizing $P_{gross}$ subject to the constraint expressed in item 4.

Our first step is to rewrite the heat flow equation as

$$\frac{1}{2}\delta_1 \geq Q/(2C_p \rho \Omega_e)$$

$$\frac{1}{2}\delta_2 \geq Q/(2C_p \rho \Omega_c)$$

$$\delta_e \geq Q/(U_e A_e)$$

$$\delta_c \geq Q/(U_c A_c) .$$

7. We next add these four inequalities, and substitute the left hand member into eq. 4, obtaining

$$Q/C \leq \Delta - \delta_E$$

with

$$\frac{1}{C} = \frac{1}{2C_p \rho \Omega_e} + \frac{1}{2C_p \rho \Omega_c} + \frac{1}{U_e A_e} + \frac{1}{U_c A_c} .$$

Substitution of items 5. and 7. into 2. gives

$$P_{gross} \leq \eta_{tg} C \frac{\delta_E}{T}(\Delta - \delta_E) .$$

The maximum $P_{gross}$ therefore occurs at

$$\delta_E = \frac{1}{2}\Delta ,$$

and is given by

$$\max P_{gross} = \eta_{tg} \frac{C}{4T} \Delta^2 .$$

## Appendix B

## Material Requirement Estimation

## of Heat Exchangers

1. APL's Shell-less Heat Exchangers

Based on APL design, 20 modules, 5 MWe each, the heat transfer area is

$$8.2 \times 10^6 \text{ ft}^2.$$

Based on 6" diameter pipe, the thickness varies between .141 and .188 inch.

$$\text{average thickness } \frac{.141 \times 69 + .188 \times 22}{69 + 22} = .152 \text{ in.}$$

Total heat transfer volume =

$$\frac{.152}{12} \times 8.2 \times 10^6 \text{ ft}^3 = 10.4 \times 10^4 \text{ ft}^3.$$

Material volume per heat exchanger module =

$$\frac{10.4 \times 10^4}{40} = 2.6 \times 10^3 \text{ ft}^3 .$$

2. Shell and Tube Design

Tubes

Assume an overall heat transfer coefficient U = 400 (slightly higher than APL's), the tube volume based on 65 mil thickness =

$$\frac{8.2 \times 10^6}{40} \text{ ft}^2 \times \frac{.065}{12} \text{ ft} = 1110 \text{ ft}^3/5 \text{ MW module.}$$

Shell

The tube length is taken as 30 ft, OD = 1". The intertube pitch is 1.25. Thus the void volume equals that of the tubes. Surface area/tube =

$$(30)\ \pi/12 = 2.5\ \pi \text{ ft}^2 .$$

$$\text{Number of tubes } N = \frac{\text{surface area of tubes}}{\text{area/tube}}$$

$$= \frac{\frac{8.2 \times 10^6}{40}}{2.5\ \pi} = 26100 \text{ tubes.}$$

$$\text{Tube sheet area} = 2\left[N \frac{\pi}{4} \left(\frac{1}{12}\right)^2\right] = 90.6\ \pi \text{ ft}^2 .$$

Shell Diameter D = 19 ft .

Shell thickness = 3 in.

$$\text{Shell volume} = 30\ \pi D \left(\frac{3}{12}\right) = 448.6 \text{ ft}^3 .$$

For U > 400, the area of the tubes is reduced by the ratio 400/U .

## COMMENTS

Written Comments by W.H. Avery, G.L. Dugger, and E.J. Francis (Applied Physics Lab., Johns Hopkins University):

We are delighted that the CMU team has been applying their talents to considerations for reducing the onboard power cost of OTEC from the very disheartening original industry baseline figure of 1975. However, we find many areas for criticism of the subject paper, and we question the statement on the first page that: "Only one of the many available concepts is likely to be demonstrated now. Of necessity, ERDA must make a choice." We would urge ERDA to evaluate objectively and in depth the two major OTEC mission possibilities, electricity-to-shore and onboard production of chemicals and metals. We believe that, if both have merit, ERDA should try to get both types of missions supported through pilot plant demonstrations as rapidly as possible. This view was supported by the National Planning Conference on Commercial Development of the Oceans in June 1976, which was sponsored by NOAA, MarAd, ERDA, and Department of Interior and had wide representation by industry and government, as well as by the Working Group on Mission Analysis at this Conference, which included 20 different organizations.

The energy resource is much greater in both the Atlantic and the Pacific Oceans (hundreds of thousands of square miles of suitable siting area) than it is at sites close enough to the U.S. mainland to deliver electricity to the utility grid. In terms of delivering electricity or heating and cooling capacity to the southeastern U.S., OTEC will also be competing with other solar energy options that warrant development. Not so on the high seas. Let us urge the parallel development. We certainly must if OTEC is to provide 10% to 15% of the total U.S. energy demand in the years beyond 2000 as the authors advocate. For example, provision of 20 $GW_e$ of electricity by direct transmission to the southeastern states in the year 2000 would represent about 1.3% of the total U.S. energy demand (based on a 34% energy conversion efficiency for the power plants) in the year 2000. To complement this, we suggest that 100 $GW_e$ in tropical grazing OTEC plants could supplant another 3% to 4% of the total U.S. energy requirements in the year 2000.

It is unfortunate that the authors use the word "True" at the head of column three in Table 2 and the word "optimistic" in references to APL's estimates. Figure 1 impugns the chemical plant mission without appropriate justification, which we will address later. Our immediate concerns will be addressed to Tables 2 and 5, upon which the authors' major conclusions are based.

1. Table 2 is seriously at fault in three respects:

   a. The r.m.s. $\Delta T$'s listed for the sites other than "Brazil" and Miami are for a 4000 ft depth. If the authors had used the depth for which the Lockheed plant is designed the r.m.s. $\Delta T$'s for offshore operation would be lowered by about 2°F.

b. The APL plant is designed to graze in the doldrums near the equator, to follow the maximum ΔT which does, in fact, average 43°F with a 3000 ft pipe. (See example in the paper by Francis and Seelinger in these Proceedings.) It optimized for minimum cost for use in Atlantic Site 1, which is a 360,000-square-n.mi. area of open ocean from 300 to 900 n.mi. east of Recife, Brazil. It is not designed for moored operation in the hurricane belt. (See also comment 3.)

c. The Lockheed plant design is heavier and more costly because it is designed to be moored in the hurricane belt; on the other hand, it cannot graze in Atlantic Site 1. (See also comment 2.)

Comparisons of outputs at multiple inapplicable sites using inappropriate ΔT's in Table 2 are irrelevant and will mislead the reader. We trust this is not the authors' intention.

2. Some of the sites mentioned, e.g., Puerto Rico and Hawaii, have very small power demands in relation to the total U.S. energy demand. Sites similar to the New Orleans/Brownsville sites, on the other hand, may represent an appreciable fraction of the total potential for delivering OTEC power to the U.S., and there the seasonal variations of ΔT are very large. The costs of delivering a guaranteed baseload would increase as a result.

3. The barge-type platform chosen by APL and the Sun Shipbuilding and Dry Dock Company is (a) suitable for grazing in equatorial waters, (b) readily buildable in several existing U.S. shipyards, with only 30-ft draft prior to installation of the CWP, and (c) similar to recent construction (e.g., the ARCO barge built by Concrete Technology of Tacoma, Washington). It requires only 40% as much material per 100 $MW_e$ and is lower in cost than submarine configurations designed to survive in hurricane belts (see Ralph Roberts' paper in these Proceedings).

4. We disagree with the statement that the APL costs are optimistic, whereas (it is implied that) Lockheed's are not. We disagree with the "audit" whereby the authors increased the APL cost by 37% in Table 5 but made no upward audit on Lockheed's for many reasons:

a. Lockheed's $1700/kW cost is based on an 0.0001 $ft^2$-hr-°R/Btu fouling coefficient whereas APL's is based on 0.0005; raising Lockheed's coefficient to the latter value would increase their total plant cost by approximately 17%.

b. Their CWP length would have to be increased by 75% to achieve the ΔT's for Puerto Rico, New Orleans/Brownsville, Gulf of Mexico, and Hawaii, in Table 1, which are based on a 4000-ft depth. The APL cold water pipe will have to be increased by 18% in order to achieve the 43°F ΔT.

c. The APL cost was based on $500/$yd^3$ for reinforced concrete whereas Lockheed's was based on $350/$yd^3$ (see paper by Roberts and comment 3 above).

d. Contrary to the statement on the authors' ratio ale for their "audit," APL has assumed that in going from a 100-$MW_e$ demonstration-size plant to 500-$MW_e$ commercial-size plants the size of heat exchanger modules would double and the size of power modules would quintuple, using 25-$MW_e$ turbines. Use of scale-up cost improvements for the OTEC machinery is appropriate.

e. Contrary to the authors' statement on the sixth page below Table 8, we contend that learning curve improvements can be applied to units of components purchased for installation on the ship without requiring design changes. Lockheed also has assumed learning curve improvements but employs smaller numbers of units and therefore has less to gain from learning. Some ratios of numbers of items on the APL commercial plant to those on a Lockheed plant are: 100 identical evaporator modules vs 4(500 MW/265 MW) = 8 for a 500-$MW_e$ plant; 100 ammonia pumps vs 8; 20 turbines vs 8, etc. The Lockheed costs are stated (Ref. 7) to be based on a 93% learning curve for the entire ship, which calculates to a 29% cost reduction from the first ship to the 25th ship cost quoted. Overall, APL's learning curve assumptions resulted in only a 25% reduction from the first 500-$MW_e$ ship to the sixth and subsequent plant-ships (Ref. 5) even though many more units of components are employed in the APL design.

f. The overall reduction in cost from Lockheed's 5-$MW_e$ aluminum prototype heat exchanger to their 25th production units of 25-$MW_e$ size was from $1252/kW to $353/kW, a factor of 3.5, per their producibility study (Ref. 8). The overall reduction from APL's 2.5-$MW_e$/module (2 each for a 5-$MW_e$ power module) demonstration unit to the 550th 5-$MW_e$ production module (5 each for a 25-$MW_e$ power module, which APL stated to be the average cost for 6th and subsequent plant-ships) was from $394/kW to $246/kW, a factor of only 1.6.

Furthermore, the APL plant capacity factor is assumed by APL to be 0.945, because of the basic simplicity and reliability of the system components and because there are so many modules. As a point of reference, concrete LNG tanker operations are based on 353 days/yr or 0.966 availability (DYTAM's Gastech Paper, "A Concrete Answer to LNG Transportation," Designers and Classification Society Panel Session, Oct. 1976). Lockheed's own assumption for their power costs is 0.9. The authors do not explain why they assume 0.8 for both types of plants in Table 11.

If we take the CMU "Brazil" value of 14 mills/kWh for APL in Table 11 and apply the ΔT and plant capacity corrections for the grazing plant, we get

$$14(40.72/43)^2(0.8/0.945) = 10.6 \text{ mills/kWh}$$

A grazing tropical plant could have lower fixed charges, too, because of lack of local taxes, bringing this down

to the 10 mills/kWh APL has quoted.

As the authors have correctly noted, one reason that APL design for heat exchangers (integrated with the simple concrete barge hull) is lower is that they require no shells per se. Other things being equal, including material choice (aluminum), this immediately saves approximately 1/3 of the heat exchanger cost.

6. The APL heat exchanger design also has the important advantage that fabrication of simple assemblies of folded tubes requires no complicated and expensive developments for setting up and welding huge, 3.5-in.-thick aluminum shells or for indexing and successfully joining tens of thousands of tubes into multiple tube sheets. The joining technique for the latter approach is stated by Lockheed to require development (as opposed to a simple orbital weld around a 3-in.-diam x 0.060-in. wall tube in the APL case). Since the APL approach also requires fewer joints, it seems likely that the APL heat exchangers will cost much less than the Lockheed aluminum shell-and-tube heat exchangers. It should be noted further (as Ralph Roberts noted at this Conference) that Lockheed's ratio of labor to material cost is lower than APL's allowing less learning curve improvement.

7. The authors' estimates of comparative material requirements are out of date. They overlooked the facts that (a) all costs in Ref. 5 were based on the use of 4-in.-diam tubes as detailed in App. B thereof, and in a paper published in the Proceedings of the ISES Sharing the Sun Conference, Vol. 5, Winnipeg, August 1976, and (b) in early 1977 the design was again updated to use of 3-in.-diam tubes after two errors in our computer code were discovered. By optimizing with a lower water velocity, we limited the increase in total power required to 9% (to net the same power output) but decreased the required hull depth by 17% and the heat exchanger tube wall thickness by 32% by going to the 3-in. tubes. The net result was that plant cost increased only 1% as reported in our paper (Dugger, Olsen, Pandolfini and Avery) at the Conference. An additional 1% must be added to cover the 18% increase in cold water pipe length. And, if we use the 93% learning curve to 25th ship used by Lockheed and reduce our fouling coefficient from 0.0005 to 0.0002 $ft^2$-hr-°F/Btu (Lockheed used 0.0001 as shown in Table 3), our estimated plant-ship cost (in 1975 dollars) is still lower than stated in Ref. 5.

8. The authors misread our original power summary. The 121 $MW_e$ was gross turbine shaft power. A 96% generator efficiency was assumed, giving 116 $MW_e$ gross power output. The equation on p. 4 should be corrected, as well as Table 2. Our parasitic power did go up from 16 MW to 26.6 MW, or 66%. Using the redesigned APL system as noted in 7. above, the correct equation becomes:

$$P_{net} = (132)(.96)(\Delta T/43)^2 - 26.6$$

Thus, all entries in column (2) of Table 2 are erroneously low and should be increased by about 10 MW.

9. In relation to a cost saving that could be achieved for the Lockheed plant by applying fluted tubes as indicated in Tables 9 to 11, the authors have not indicated that extruded tubing costs more per unit volume of material than the rolled-and-welded tubes proposed for use in the APL design by Kaiser Aluminum and Chemical Corp., and that fluted, extruded tubing will cost still more. Although the authors do not espouse cost reduction by surface enhancement on the water side, they fail to note that it may be impossible to clean such surfaces without destroying their enhancement qualities.

10. On page 3 the authors err in saying that APL assumes that investors in chemical plants would pay no income taxes. Our estimates of the time required to recover plant investment do allow for a first year investment tax credit but assume full 48% federal income tax rate on gross profit. (See Ref. 5 and the paper by Francis and Seelinger presented at the Conference.) The important point is that a lower plant investment can be recovered much faster for a given annual profit level per unit of net OTEC power.

11. The comparisons in Fig. 1 are subject to many important qualifications which must be taken into account in mission evaluations, including the following:

a. A chemical plant on shore may use a fossil fuel as feedstock and waste part of the energy content in processing.

b. An OTEC "chemical" plant may alternatively use electric power directly in aluminum, chromium, or nickel refining, gaining the same full benefit as onshore.

c. A tropical oceans OTEC plant requires no land (including land that may be needed for an environmental buffer zone) and pays no local taxes.

d. An offshore OTEC electric plant including transmission system and designed to withstand hurricanes will cost at least twice as much per unit of power delivered to customer (onshore grid or onboard plant) as a plant designed to graze in equatorial waters, based on any of the costs we have seen published and justified to date.

e. An industrial chemical user of onboard captive power has not paid for another industry's state and federal taxes and profit on that power.

f. For the OTEC vs fossil fuel comparison, comparable advances in technology (e.g., fluidized-bed combustion of coal) could raise onshore electric plant efficiency and reduce its relative cost.

12. An example of auditing another organization's cost estimate can also produce a disheartening conclusion for the electricity-to-shore mission. Let us consider Lockheed's $1700/kW onboard power cost. Let us increase their fouling coefficient from 0.0001 to the 0.0005 value used by APL. This reduces their U and power output by approximately 17%, so the onboard power cost becomes $2048/kW. Now let us add the $200/kW cost for the transmission system and say that the plant has to operate off Brownsville in winter and deliver a guaranteed base load to a utility grid while using a $\Delta T$ of

31°F vs the Lockheed ΔT* of 38°F, and that it has a 0.9 availability factor (value used by Lockheed) and that there is a 5% loss in transmission. The cost per guaranteed baseload kW might be deemed to be

$$\frac{\$2248}{0.9(0.95)} \left| \frac{38}{31} \right|^2 = \$3950/kW$$

or 70 mills/kWh (using 15% fixed charged and 2 mills/kWh for O&M). In fairness to the CMU team, the APL team concedes that this is an unlikely worst case, even though we believe the winter demand for electric power will indeed approach the summer demand as less and less natural gas and oil remain available for heating systems. It already has in Florida.

In constrast, we have been told by industry that even if the APL onboard power cost should double, to 18-20 mills/kWh, such a cost will be very attractive for many applications including ore smelting.

13. Finally on p. 9 the authors counsel against committing to one mission and yet conclude that they have already made a judgment favoring the electricity-to-shore mission. It is APL's view that both the electricity-to-shore and the chemicals-onboard approaches should be pursued in parallel to maximize the chances for OTEC program success and benefits to the nation from the vast ocean thermal resource.

Reply by Authors:

We welcome this opportunity to respond to criticism of our paper. We are pleased to have APL scrutinize our work so meticulously. Such criticism indicates that OTEC has advanced to a mature level where debate among research teams can be aired in public. The thrust of our paper was simply to compare system designs and missions proposed by various reputable teams. Our analysis is based on published works. We have no access to internal reports or last minute changes in data.

It is to APL's credit that they have proposed a complete system directed to a specific mission at a given site. As independent evaluators, we have to ask questions. Is the system design for the power plant proposed by APL superior to those proposed by other teams? Is the mission addressed as economical as has been claimed? If the APL power cycle is indeed superior to those of others, then it follows that it should prove superior at sites other than that site for which it was designed. Hence, we tabulate performance at various sites. The final question our paper raises has to do with the economics of the ammonia mission. If OTEC can produce electricity cheap enough to make OTEC-ammonia production competitive with ammonia production from fossil fuel feedstock, does it then follow that OTEC will be competitive to produce and transmit electricity to shore, in spite of the considerably lower ΔT's available at alternate sites?

These questions, if properly answered, will enable Congress, ERDA and most importantly, industry to select a design and a mission. Conceivably, the APL design is absolutely correct in all questioned aspects and therefore, ammonia plants sited near Brazil employing the APL power system, hull, etc., can be commercialized at an acceptable cost. However, when all of the data has been verified, industry may settle on APL's mission with somebody else's design. Equally possible, industry may end up with an electricity mission with APL's power cycle and somebody else's platform. The data at hand from various teams are not yet reliable enough to decide the ultimate design and mission at this stage of OTEC's development. Our hope is that Congress and ERDA will continue to pursue the various options without prematurely locking the OTEC concept into any one design and mission.

We respond next to each point raised in the discussion:

1. If the grazing approach can indeed achieve an average $\Delta T = 43°F$, then APL's cost figures can be reduced by a factor of $(\Delta T/43)^2$. According to our audit, the temperature advantage from grazing reduces APL's cost from 22 to 19 mills/kWh.

2. We concede that the island sites, e.g., Puerto Rico and Hawaii, have low demand. But if OTEC electricity transmitted to shore can be made cheap enough, various energy intensive products can be economically produced at island sites. We thus add a third mission option: an energy intensive island concept.

3. In our paper, we have not attempted to compare platforms. We do not know whether the weather conditions at the Brazil site postulated by APL are indeed so benign that a very low cost platform is practical. However, we point out that the difference in platform cost between plants designed for the Brazil site and those designed for hurricane-prone sites is not very substantial.

4. Presently, we see no reasons to conclude that a 65 or 25 $MW_e$ module is feasible for the shell and tube designs. Conceivably, a 5 $MW_e$ module is, as APL predicts, more practical. If this is the case, the cost reduction projections proposed by APL could be applied to other designs. The discussion appears to conclude that we consider the Lockheed design as presented in 1975 the final prototype. Our hope is that ERDA and industry will improve upon that design. In the use of scale up and learning curve factors, we feel that APL's figures are unduly optimistic.

5. Shell-less heat exchangers should cost less provided the heat transfer coefficients and the pressure drops are equal. Cost comparisons must be made on the basis of identical performance requirements.

6. We have not attempted to evaluate the labor requirements of APL's versus Lockheed's exchangers. We have accepted the published cost figures presented by each group.

7. Our estimate of the material requirements and the pressure drops are based on APL's published data. We attempted to correct for APL's errors and we suspect that by re-optimization the cost would turn out to be lower than our simplified calculations indicate. The 1% claimed by APL appears unduly optimistic.

8. The equation referred to on page 4 should be corrected to read:

$$P_{net} = (121)(.96)(T/43)^2 - 16.6$$

This change requires a correction of columns (1) and (2) of Table 2. The overall changes result in an insignificant decrease in all entries.

9. Fluting on the ammonia side would only add about 10% to the cost of the material while it would increase the heat coefficient by 30-40% without increasing the shell diameter.

10. We have no comment to make on this point of criticism because it would apply to any mission or to any design of OTEC. The key issue is capital cost.

11. We stand by our statement.

12. APL's point is well taken but the conclusions of our study remain valid. As already stated, we are not attempting to justify Lockheed's or any one else's design.

13. See opening statement.

Editor's Comments:

Based on the data presented in Appendix B of APL's MarAd study (5), the materials estimate is as follows:

For a 5 $MW_e$ module of APL

Ex. evaporator tube length = 2 x 799 x 132 = 210936 ft

condenser = 2 x 691 x 132 = 182424 ft

total = 393360 ft

average area/module = $(1/2)\pi(4/12)\ L_{total}$ = 205963 $ft^2$

volume/heat exchanger = $(1/2)(\pi D\ L_{total})(.088/12)\ ft^3$

$= (1/2)\pi(4/12)(393360)(.088/12)$

$= 1510\ ft^3$

This is considerably lower than the 2560 $ft^3$ calculated by the authors based on APL's earlier 6" tube. Further reduction of tube diameter and wall thickness would reduce the material requirement. However, the manufacturing cost might go up.

Part of the disagreement between the authors and the discussors stems from the emphasis on ammonia production espoused by APL's MarAd Study. The authors addressed that issue only. The APL discussion appears to highlight aluminum and other metals lumped under chemical utilization. Clearly the production of ammonia is a thermal process while that of aluminum is electrical and herein lies the difference.

# COST COMPARISON OF SELECTED OTEC POWER PLANT DESIGNS

RALPH ROBERTS
*Metrek Division*
*The Mitre Corporation*
*Westgate Research Park*
*McLean, Virginia*

Abstract

As part of The MITRE Corporation studies on solar energy systems and their engineering cost estimates, some of the proposed closed cycle OTEC systems have been reviewed (1). That effort included the review of the most recent engineering design estimates of the Applied Physics Laboratory (APL) (2), and the Lockheed Missiles and Space Co. (LMSC) (3). This paper compares the cost of the two designs on the basis of their missions, operating conditions and components. The major differences largely originate from the missions and operating conditions selected with a lesser contribution from the specific component technologies, other than the heat exchangers. It is also noted that assumptions regarding scale-up and the application of experience curves contribute much to the difference in the projected cost estimates for the production of these OTEC power plants. It is emphasized that the costs derived are based on those of the proponents and are not an independent verification of the published design cost estimates.

## Introduction

During the past year, detailed information on the Applied Physics Laboratory (APL) study on Ocean Thermal Energy Conversion (OTEC) Plant Ships (2) and a revised study of the Lockheed Missiles and Space Co. (LMSC) design of an OTEC power plant (3)(4) have become available. As shown in Table I, the cost per kWe net power produced for designs of the demonstration or prototype units was projected for the two systems. Based on these designs, cost of delivered power have been extrapolated for production plants. Both the demonstration and production plant costs for the APL design are lower than those for the LMSC design. In addition, as shown in Table I, the APL estimates show a much more marked decrease in cost per unit of power produced between the demonstration and production units. This is in spite of the APL production cost being based on the sixth unit and the LMSC one on the twenty-fifth unit. It should be noted that the APL demonstration unit is a 100 MWe (net) power plant and the production unit is a 500 MWe (net) plant. The LMSC demonstration or prototype power output is 264.5 MWe (net).

The following discusses these differences in cost in terms of the missions, technologies, and component cost estimates utilized in the two different designs. In view of this, the revised costs can not be construed as an independent verification of the cost estimates or the designs of the proponents.

TABLE I

COST COMPARISON OF APL AND LMSC SYSTEMS

| | APL | LMSC | APL / LMSC |
|---|---|---|---|
| DEMONSTRATION $/kWe (net)<br>APL - 100 MWe net<br>LMSC - 264 MWe net | 1128 | 1980 | .569 |
| PRODUCTION $/kWe (net)<br>APL - 500 MWe net<br>LMSC - 264 MWe net | 566 | 1394 | .408 |
| RATIO: DEMONSTRATION: PRODUCTION | 1.99 | 1.420 | - |

## Overall Plant Costs

Table II shows the comparative costs of the two stems distributed among the four major components as given in references 2 and 3. Both costs were estimated in FY '75 dollars and these have not been adjusted for changes in the cost index. Greater than 50 percent differences between the components of the APL and LMSC demonstration design estimates exist, except for the case of the cold water pipe. In both systems the highest cost items are the heat exchangers with the platform and power generation equipment being lower in cost. Their average cost for the two designs are within 10 percent of each other. In the case of LMSC, the mooring system is an additional high cost item which is not included in the APL design. This is due to their different missions and site selections as discussed in the next section.

Normalization of the costs of both designs to $\Delta T = 40°$ F, using the equation suggested by Lavi (5), reduces the cost differential, but this remains large for the demonstration units and increases for the production units.

## Missions and Site Selection for the APL and LMSC OTEC Systems

A major difference between the APL and LMSC systems is in the missions selected. The former has the objective of generating electric power to carry out the on-site production of selected energy intensive materials such as ammonia, aluminum and hydrogen. The LMSC system is designed to deliver power ashore where it can be used in the electric distribution system or for on-shore industry. The possibility of on-site utilization of the energy for processes similar to those discussed by APL has been included in the cited LMSC studies.

The differences in missions have led to the selection of ocean sites most compatible with the plant objectives, Table III. In the APL study, a site with a high year round ocean water temperature differential and relatively free of hurricanes and high seas was chosen. This enables the use of a barge-like platform with limited propulsion capability for station keeping. There is some question, however, as to the adequacy of the propulsive power estimated for station keeping. The estimate is based on a normal requirement of 0.5 knot and maximum of 1.0 knot. In Table IV (6) is given the relationship of the surface current to the sea state. At Beaufort 7, maximum wind - speed 33 knots, this is approximately one knot and is reported by APL as the maximum on-site wind. In addition, the platform has a large exposed area, roughly 196' x 50' in its narrowest dimension, which in the presence of this wind would further increase the drag on the OTEC platform. An estimate of this effect leads to the requirement of approximately 4.0 MW (7) of power to overcome the force on the platform. This does not include the additional power required to overcome the increase in surface currents. However, the latter has a steep gradient below the surface so that the net effect will

TABLE II

COMPARATIVE SYSTEM COSTS

$/kWe (net)

| COMPONENT | APL $\Delta T = 43°$ F | | LMSC $\Delta T = 37.8°$ F | |
|---|---|---|---|---|
| | DEMONSTRATION | PRODUCTION #6 | DEMONSTRATION | PRODUCTION #25 |
| PLATFORM | 290 | 143 | 427 | 334 |
| HEAT EXCHANGER | 344 | 215 | 590 | 418 |
| POWER GENERATION | 301 | 114 | 497 | 299 |
| COLD WATER PIPE | 63 | 30 | 56 | 45 |
| TOTAL | 998 | 502 | 1570 | 1096 |
| CONSTRUCTION, INTEREST, AND ESCALATION (12%) | 120 | 60 | 188 | 132 |
| DEPLOYMENT, MOORING | 10 | 64 | 222 | 166 |
| PLANT TOTAL | 1128 | 566 | 1980 | 1394 |
| NORMALIZED TO $\Delta T = 40°$ F | 1349 | 674 | 1748 | 1232 |

1975 DOLLARS

TABLE III

SITE CHARACTERISTICS

| | APL | LMSC |
|---|---|---|
| LOCATION | ATLANTIC, EQUATOR | GULF STREAM (2,500 FT)<br>DEEP OCEAN (20,000 FT) |
| ΔT | 43°F | 37.8°F |
| SEA STATE | FORCE 4 - PREDOMINANT<br>FORCE 6 - MEASURED<br>FORCE 7 - POSSIBLE | <br>FORCE 7<br>60' WAVE HEIGHT |
| WIND | 70 KNOT - TRANSIT<br>50 KNOT - ON-SITE | >64 KNOTS 4-6 DAYS<br>>34 KNOTS 27 DAYS<br>MAXIMUM 100=120 KNOTS |
| STATION KEEPING | 1 KNOT PROPULSION | MOORED<br>3 KNOT (GULF STREAM) |

TABLE IV

VELOCITY OF WIND CURRENTS

| BEAUFORT FORCE OF WIND | WIND SPEED, KNOTS | WIND CURRENT, MI/DAY | WIND CURRENT KNOTS |
|---|---|---|---|
| 1 | 1-3 | 2 | .07 |
| 2 | 4-6 | 4 | .14 |
| 3 | 7-10 | 7 | .25 |
| 4 | 11-16 | 11 | .40 |
| 5 | 17-21 | 16 | .56 |
| 6 | 22-27 | 21 | .75 |
| 7 | 28-33 | 26 | .94 |
| | 50 | ~45 | ~1.60 |

be less than the surface velocity increase. Thus, between 4 and 5 MW will be required for station keeping at the high end of the atmospheric conditions reported by APL. This increases the parasitic power requirement by between 3 and 4 MW. For the 50 knot maximum wind design point of APL, the propulsive power requirement would increase to 10 MW, increasing the parasitic power needed by approximately 9 MW. Although the platform design has been based on observed conditions, it is questionable that sufficient long term data has been obtained to rule out the chance of higher winds during the 10 to 20 years the OTEC plant will be on station.

The LMSC system is designed to deliver power to the southeastern United States and to withstand the high winds of hurricanes in the Gulf of Mexico, the Gulf Stream, and the Caribbean Islands. In these locations, winds reach 100-120 knots and individual waves of 60 feet have been recorded (8). In the Gulf Stream, a vertical shear of 4 knots between surface and bottom has been observed with a gradient of more than 1 knot in the first 100 feet. To meet these conditions, LMSC has opted for a moored spar type construction with a small exposed area above the surface and requires no propulsive power.

## Platform Costs

The differences in site selection and plant end- as shown in Table III have resulted in a much heavier platform and cold water pipe for the LMSC system than for the APL design, Table V. The estimated costs for the platform and cold water pipe for the LMSC design as given in Tables II and VI are low. They are based on a cost for installed reinforced concrete of approximately $350/yd^3$. A more realistic value (9) is $610/yd^3$. The APL cost is based on an estimate of $500/yd^3$ for low density reinforced concrete. Applying the higher cost of reinforced concrete on a proportional basis to the hull structure and cold water pipe of both designs leads to the adjusted costs shown in parenthesis. This increases the difference in the two platform cost estimates.

The hull equipment, auxiliary systems and controls have been detailed in the early LMSC report (3). These are listed in Table VII. These constitute equipment necessary for the overall plant operation and safety. They are based on known technology which must be adapted to the OTEC system. The APL study, also includes an overall cost item for auxiliaries and controls. Neither report details the costs of these components.

## Heat Exchanger

The heat exchanger is the other major cost item in the system. The APL and LMSC designs are compared in Table VIII. There are some major differences in the two designs. The nested tube design of APL with internal ammonia flow essentially uses a concrete section of the platform for the external sea water chambers of the heat exchangers. LMSC has selected a shell and tube design and the detailed analysis of an evaporator and condenser for a 25 MWe module has been published (10). The sea water flows internally to the tubes and the ammonia externally. The referenced APL design requires approximately 220 lbs of aluminum per kW for the 4" tube design (2) and 145 lbs per kw for the 3" tube design (12). The former includes a 30% contingency and the latter a 20% contingency. Based on a 25 MWe (net) heat exchanger design the LMSC design requires 158 lbs per kW with a 10% margin.

An additional factor in the cost differential results from material selection. The APL design is based on rolled and welded Alclad tubing at a quoted price of $0.72¢/lb.[11] The LMSC production design is based on an alloy with a cost of $1.00/lb and a tube fabrication cost of $0.25/lb, leading to an estimated tube cost of $1.25 per lb. This makes the comparative cost ratio for heat exchanger tubing materials of the

TABLE V

PLATFORM STRUCTURE

100 MW(e)

| | | APL | LMSC |
|---|---|---|---|
| TYPE | | SURFACE | SPAR |
| WEIGHT: | STRUCTURE | | |
| | CONCRETE | 39,000 LT* | |
| | STEEL | 1,500 LT | |
| | | 40,500 LT | 99,100 LT |
| | COLD WATER PIPE | | |
| | CONCRETE | 13,248 LT | |
| | STEEL | 207 LT | |
| | | 13,455 LT | 26,780 LT |
| | COST CONCRETE | $ 500/YD$^3$ | $ 610/YD$^3$ |
| | STEEL | $ 2,000/LT | |

*LT = Long ton, 2,240 lbs.

TABLE VI

PLATFORM COSTS

| | APL SURFACE TYPE | | LMSC SPAR TYPE WITH POWER MODULES | |
|---|---|---|---|---|
| | COMPONENT COSTS ($/kWe) | | | |
| | PROTOTYPE | PRODUCTION | PROTOTYPE | PRODUCTION |
| HULL STRUCTURE | 135 (165)* | 88 (107) | 192 (335) | 154 (268) |
| OTHER HULL | 23 | 54 | 25 | 18 |
| HULL EQUIPMENT | 132 | | 209 | 162 |
| COLD WATER PIPE | 63 (77) | 30 (37) | 56 (98) | 48 (84) |
| TOTAL PLATFORM | 353 (397) | 172 (198) | 482 (667) | 382 (532) |
| MOORING SYSTEM | | | 135 | 120 |
| DEPLOYMENT INTEGRATION | 10 | 4 | 28 | 20 |
| FACILITY PREPARATION | | | 60 | 26 |
| | | | 223 | 166 |

*Numbers in parentheses indicate modified costs based on installed reinforced concrete cost of $610/yd$^3$.

LMSC design to that in the APL design 1.73. Another factor contributing to the difference in cost is the ocean water temperature gradient used in the designs. For a $\Delta T$ of 40° F, the APL design would require approximately 7 percent more heat exchanger surface whereas the LMSC design would require a 6 percent decrease. This will also increase the parasitic loss in the APL design and decrease it in the LMSC one due to changes in the pressure drops. This would make a further change in heat exchanger cost which leads to a roughly estimated overall change of 10-15 percent in materials cost for APL and an equivalent reduction for LMSC. The effect of these changes on heat exchanger cost is shown in Table VIII. The most appropriate comparisons are between the APL prototype and the LMSC first production. The latter includes a high tooling cost, $200/kw, whereas APL includes only $14/kw for a welding rack.

The APL cost estimate for the demonstration heat exchanger gives a material:labor ratio of 1.52. In the case of the LMSC design, this ratio for the first production unit is 2.7 and for the twenty-fifth unit it is 3.1. This ratio for the LMSC prototype unit is not given as its cost estimate was based on an in-place constructed shell and the data does not enable the separation of these two costs. In addition to the cost for material and labor, the cost of tooling, as noted above, has been included in both designs and in the cost estimates of Table VIII. Both designs also include contingency and other costs. In the case of APL, these amount to 30 and 20 percent of the basic design cost for the 4" and 3" heat exchanger, respectively, and LMSC, 25 percent.

The APL 3" heat exchanger leads to a decrease in the depth of the vessel saving approximately 10% of the hull volume and 6% of the hull cost. This is reflected in summary Table XIV, column 3.

Pumps and Power Generation

The mechanical and electrical components make up the remaining one-third of the cost of the system. In the APL design, a number of small components operating in parallel were used, whereas in the LMSC design larger components have been selected. The higher design $\Delta T$ in the APL system requires less fluid transport, thus leading in general to lower requirements for pumping. This is illustrated in Table IX on water pumps. The water flows in the LMSC are double those in the APL design with the expected increase in pump costs. Since the enthalpy required in both systems for 100 MWe generation is the same--except for differences in parasitic loss-normalization of both plants to a $\Delta T$ of 40° C would lead to similar sea water flow rate requirements, or approximately 15,000 cu.ft./sec. This also would lead to essentially equivalent pump costs. Similar considerations apply to the ammonia systems.

TABLE VII

AUXILIARY SYSTEMS AND CONTROLS

AUXILIARY SYSTEMS

- Ammonia cleanup system
- Leak-detection and fluid-sampling system
- Heat exchanger tube-cleaning system
- Cooling water system
- Turbine oil purification system
- Fire-protection system
- Ammonia make up and storage system
- Compressed air system
- Emergency breathing system
- Standby power system
- Cathodic protection system
- Hydraulic pressure system
- Tubesheet and shell pressurizing system
- Nitrogen purge system
- Electrical system
- Sea water pump pod pressurizing system
- Communications system
- Control systems
- Equipment handling and removal system

CONTROL EQUIPMENT

- Critical power cycle alarms, readouts, and controls
- AC on-board grid system control
- DC rectifier control
- Power factor adjustment
- Operation of safety pressure doors in main access trunks
- Ammonia transfer control
- Screen cleaning control

The respective cost estimates for electrical generating equipment are shown in Table X. As in the case of the other equipment, APL has selected a number of small units operating in parallel whereas LMSC has selected fewer larger units. However, the difference in prototype cost can, in part, be attributed to the greater mass flow rate required in the Lockheed design. As in the case of the water pumps and the ammonia system these differences would markedly decrease if normalized for the same $\Delta T$.

The APL use of a number of small units operating in parallel can lead to larger control problems than in the case of LMSC. For example, 20 ammonia turbines are used to drive four generators which can lead to difficulties in coupling and control.

The redesign of the heat exchangers by APL (12) also has led to a calculated increase in the parasitic power required from 16.0 to 26.6 MW for the 100 MWe installation. This results in an estimated six percent increase in the machinery cost. When the estimated added propulsive power required for station keeping is included, 3.5 MW, parasitic power becomes 30.1 MW and increases the machinery cost by eight percent using the APL scale-up factor (12):

Power ratio to prior baseline: $\frac{130.1}{116} = 1.122$

Machinery cost scale-up factor: $1.122^{0.7} = 1.084$

The effect of these changes on system cost are included in the final summation of suggested cost revisions, Table XIV.

TABLE VIII

HEAT EXCHANGER COMPARISON

| | APL | LSMC |
|---|---|---|
| TYPE | NESTED TUBES | SHELL AND TUBE, 2 |
| FLOW | AMMONIA INTERNAL | AMMONIA EXTERNAL |
| | SEA WATER EXTERNAL | SEA WATER INTERNAL |
| CLEANING | CAVIJET$^{tm}$ | MOVING SPHERES |
| AMMONIA FLOW #/SEC per 100 MWe | 6760 | 8239 |
| U OVERALL, EVAP & COND. BTU/hr-ft$^2$-°F | 375 | 445, 365 |
| OVERALL COST, INSTALLED $/kWe | | |
| PROTOTYPE - 4" | 345 (370)* | 724 |
| 3" | 352 (375) | |
| FIRST PRODUCTION | 263 | 593 (564) |
| PRODUCTION | 216 (205-265) | 353 (324) |
| MATERIAL: LABOR | | |
| PROTOTYPE | 1.52 (1.08) | 2.17 |
| PRODUCTION | (2.63) | 3.19 |

*Numbers in parentheses indicate revised estimates.

TABLE IX

WATER PUMPS (100 MWe)

| | APL | | LMSC | |
|---|---|---|---|---|
| | PROTOTYPE | PRODUCTION #6 | PROTOTYPE | PRODUCTION |
| COLD WATER | | | | |
| CU. FT./SEC. | 9,899 | 9,899 | 20,633 | 20,633 |
| # PUMPS | 19 | 19 | 1.5 | 1.5 |
| POWER | 8.1 MWe | 8.1 MWe | | |
| COST $ X 10$^6$ | 7.34 | 2.56 | 8.39 | 4.95 |
| WARM WATER | | | | |
| CU. FT./SEC. | 10,300 | 10,300 | 21,976 | 21.976 |
| # PUMPS | 20 | 20 | 1.5 | 1.5 |
| POWER | 5.0 MWe | 5.0 MWe | | |
| COST $ X 10$^6$ | 5.98 | 2.06 | 9.83 | 5.78 |

TABLE X

ELECTRICAL GENERATION EQUIPMENT
(100 MWe)

| CHARACTERISTICS | TURBINES | | | | GENERATORS AND TRANSFORMERS | |
|---|---|---|---|---|---|---|
| | APL | | LMSC | | APL | LMSC |
| NUMBER OF UNITS | 20 | | 30 | | 4 | 1.5 |
| FLOW #/SEC. $NH_3$ | 6,750 | | 8,239 | | | |
| $T_{IN}$,$T_{OUT}$ °F | 69.0 | 49.6 | 70.2 | 51.6 | | |
| $P_{IN}$,$P_{OUT}$, PSIA | 126.5 | 88.4 | 129.2 | 91.9 | | |
| Δ ENTHALPY, BUT/lb | 19.3 | | 15.7 | | | |
| OUTPUT, MWe | 121 | | 139 | | 116 | 133* |
| COST ($/kWe) | | | | | | |
| PROTOTYPE | 58 | | | | 46.0 | |
| PRODUCTION | 17.6 | | | | 20.1 | |
| TOTAL, COST ($/kWe) | | | | | | |
| ELECTRICAL GENERATION | | | APL | | LSMC | |
| PROTOTYPE | | | 104 (110) | | 79 | |
| PRODUCTION (Estimated modified cost) | | | 38.0 (40.0) | | 47 | |

*95% Efficiency Assumed

Production Cost Projections

The production cost estimates cited for both OTEC configurations are derived from the detailed analyses of the prototype or demonstration designs. In the case of APL, the demonstration design was for an installation with 100 MWe net power and the first production unit was for a net power of 500 MWe. Various scaling factors were used in projecting the cost of the components of the system based on the demonstration unit costs. Selected scaling factors and experience curve slopes (ECS) used in the calculation of the first plant cost are shown in Table XI. The scaling factors used for estimating the cost of larger units was the capacity multiplier raised to the 0.7th power. This scale-up factor for rotating machinery is an accepted engineering practice. In reference 4 it is noted that testing of one-fifth scale models is considered to be adequate for developing prototype full-scale pump designs. Similarly, scaling factors for turbines are well established so that doubling the turbine output between the demonstration and production model presents no new engineering considerations. However, as noted in the APL studies, ammonia turbines of the size ired are not state-of-the-art and the cost used is based on estimates from various turbine manufacturers.

The experience curve slope was applied to obtain the average cost of the first plant components and for estimating the cost of the sixth plant. As can be noted by comparing the first and last columns of Table XI, this leads to a marked reduction in the estimated cost of rotating equipment between the demonstration and first production plant. This reduction results from treating the items as essentially the first of a kind, applying an experience curve slope to the first production lot, and averaging the cost over the number of units produced.

The experience curve slope has been applied by APL to the total cost of the first production units. This is consistent with its application in other studies on this subject (13). However, the LMSC study has applied an experience slope curve of 93 percent to the labor component and assumes no change in material cost resulting from experience. The APL procedure gives a more rapid decrease in cost with the number of units produced than does the latter. The effect of this difference in the application of the experience curve is illustrated in Table XII, which shows that the

TABLE XI

AMMONIA SYSTEM
NORMALIZED TO 100 MWe (NET)

| | APL | LMSC |
|---|---|---|
| AMMONIA FLOW #/SEC. | 6,760 | 8,239 |
| # PUMPS | 40 | 8 |
| PUMPING POWER | 2.3 MWe | |
| NO. DEMISTERS | 20 | 8 |

COST ESTIMATES $ X $10^6$

| | PROTOTYPE | PRODUCTION | PROTOTYPE | PRODUCTION |
|---|---|---|---|---|
| PUMPS | 0.25 | 0.08 | .87 | .45 |
| DEMISTERS | 0.33 | 0.10 | 13.83 | 8.20 |
| PIPING | (3.5)[A] | (2.1)[A] | | |
| INVENTORY | 0.78 | 0.62 | 0.5 | 0.5 |
| TOTAL | 1.36 | 0.8 | 15.2 | 9.15 |

(A) Also included in heat exchanger.

TABLE XII

COST RATIO
PRODUCTION: DEMONSTRATION

| | NUMBER OF UNITS DEMONSTRATION AND PRODUCTION | | TOTAL PRODUCTION: DEMONSTRATION | | TOTAL PRODUCTION: 1ST PRODUCTION |
|---|---|---|---|---|---|
| | APL | LMSC | APL | LMSC | APL |
| PRODUCTION NUMBER | 7 | 26 | 6 | 25 | 6 |
| TOTAL SYSTEM | 7 | 26 | .503 | .70 | .71 |
| PLATFORM | 7 | 26 | .49 | .78 | .62 |
| COLD WATER PIPES | 13 | 26 | .48 | .80 | .76 |
| HEAT EXCHANGERS | 1240 | 208 | .63 | .48 | .82 |
| WATER PUMPS | 627 | 104 | .34 | .59 | .66 |
| AMMONIA SYSTEMS | 140 | 104 | .58 | .60 | .67 |
| TURBINES | 140 | 104 | .45 | .59 | .76 |
| GENERATOR, ETC. | 74 | 104 | | | |

decrease in total production costs estimated by APL for six units is equal to that calculated by LMSC for nits. This also comes, in part, from the use by of a large number of small units so that the total er of units produced for six plants exceeds those produced for 25 LMSC plants.

A study by Gadsby (14) on experience curves is now in progress. The results of this study on the components and materials most closely related to OTEC are shown in Table XIII. These are not qualitatively inconsistent with those used by APL and indicate that, on the basis of this work, the LMSC estimates of cost reduction due to experience may be conservative.

## Discussion

The previous sections have discussed the variation in cost of the various component parts of the APL and LMSC designs. Table XIV summarizes the discussion in terms of the first demonstration units. Under the APL costs, the first column represents the original estimate for the demonstration unit. The next column includes the revised cost based on an increase in the concrete cost, see platform costs. The next column reflects the costs for the 3" heat exchanger, including the higher concrete costs, and the increase in parasitic losses to 26.6 MWe for a 100 MWe (net) installation, see section on heat exchangers and power generation. The fourth column is a further adjustment based on the additional estimated propulsion power requirements for a 33 knot wind, see mission discussion, but does not include the small additional parasitic loss for the required larger heat exchanger. In the case of the LMSC design, the revised costs are primarily due to the increase in concrete costs, shown in the last column. The LMSC heat exchanger cost is that of the first production unit, rather than the demonstration unit, as the former more closely reflects the method of construction proposed for the production units. In the APL case, these methods are the same.

To normalize the two systems to the same temperature, the Lavi correction was used. It was applied to the power plant cost prior to the addition of construction costs. In the case of the LMSC design, the mooring costs have been added as a separate item and include construction costs.

The net result of applying these cost adjustments leads to a difference in cost for the designed power plants, without construction costs and mooring for the LMSC system, of $574/kWe. When these plants are normalized for power generation, at the same ocean temperature differential (40° F), the cost differential for power production reduces to $109/kWe. With construction cost and mooring these cost differences increase to $370/kWe for the systems after all adjustments. Thus, the major differences in the normalized cost can be attributed to mooring and hull structure costs. Normalization to $\Delta T=40°$ F of heat exchanger and rotating machinery costs using the Lavi formulation lead to costs for these components which are essentially the same.

TABLE XIII

EXPERIENCE CURVE SLOPES

| CATEGORY OR COMMODITY | TIME FRAME | PRODUCTION VOLUME | EXPERIENCE CURVE SLOPE, % |
|---|---|---|---|
| CENTRIFUGAL PUMPS >4 in. outlet | 1970-75 | $46.6-84.7 \times 10^3$ | 68 |
| GENERATORS AC >400 kW | 1960-69 | $0.3-17.7 \times 10^3$ | 85 |
| CONCRETE REINFORCING BARS | 1965-75 | $3.5-45.2 \times 10^6$ s.t.* | 93 |
| OCEAN-GOING TANKERS 200,000-300,000 DWT | 1974-77 | 2-9 | 93 |

*s.t. - short ton.

TABLE XIV

SUMMARY OF COSTS

DEMONSTRATION UNITS

| | APL, ΔT = 43° F | | | | LSMC, ΔT = 37.8° F | |
|---|---|---|---|---|---|---|
| DESIGN ADJUSTMENT | ORIGINAL | ORIGINAL CONCRETE | 3" Ht. X CONCRETE | 3" Ht. X PARA. LOSS* | ORIGINAL | ORIGINAL CONCRETE |
| REFERENCE | (2) | (2) | (12) | (12) | (3) | (3) |
| PLATFORM: | | | | | | |
| HULL STRUCTURE | 135 | 165 | 155 | 173 | 192 | 335 |
| OTHER HULL | 23 | 23 | 23 | 23 | 25 | 25 |
| HULL EQUIPMENT | 132 | 132 | 132 | 132 | 209 | 209 |
| COLD WATER PIPE | 63 | 77 | 77 | 77 | 56 | 98 |
| TOTAL PLATFORM | 353 | 397 | 387 | 405 | 482 | 667 |
| HEAT EXCHANGER | 345 | 345 | 418 | 429 | 590 | 590 |
| ROTATING MACHINERY | 301 | 309 | 319 | 346 | 497 | 497 |
| TOTAL: DESIGN | 999 | 1051 | 1124 | 1180 | 1569 | 1754 |
| CONSTRUCTION, ESCALATION (12%) | 1118 | 1177 | 1259 | 1321 | 1757 | 1964 |
| MOORING (INCL. ESCALATION) | - | - | - | - | 248 | 248 |
| TOTAL: | 1118 | 1177 | 1259 | 1321 | 2005 | 2212 |
| ADJUSTMENT FOR 40° F | | | | | | |
| TOTAL: DESIGN | 1197 | 1259 | 1346 | 1413 | 1362 | 1522 |
| TOTAL WITH ESCALATION | 1340 | 1410 | 1508 | 1583 | 1525 | 1705 |
| TOTAL WITH MOORING | - | - | - | - | 1773 | 1953 |

*Parasitic Losses

## Conclusions

This review of the cost differential of the Applied Physics Laboratory and the Lockheed Missile and Space Division designs for the OTEC system shows that the differences in design cost estimates arise from the mission and the temperature differential selected. The less benign locations for the LMSC system lead to a heavier platform and additional costs for mooring.

The costs for heat exchangers and power plants, in spite of the differences in design, when normalized to the same temperature, are virtually identical. The large apparent difference in the published design cost estimates for these components are thus attributable to the difference in the ocean thermal gradients selected for the two studies.

The differences in the extrapolated cost for the production units can be attributed to the variation in the methodologies used in applying experience slopes to the cost estimates. However, both approaches have been used in the literature on the use of experience curves.

The cost adjustments presented are based on the original design estimates of the proponents and do not constitute an independent verification of either design.

Acknowledgement: The support of the Division of Solar Energy of ERDA, under Contract E(49-18)-2322, is gratefully acknowledged. The cooperation of representatives of APL and LMSC in providing information is greatly appreciated.

## References

1. R. Eldridge and R. Roberts, Systems Descriptions and Engineering Costs for Solar-Related Technologies, Volume VII Ocean Thermal Energy Conversion (OTEC) MITRE Technical Report MTR-7485, dated April 1977.

2. W. H. Avery, R. W. Blevins, G. L. Dugger and E. J. Francis, Maritime and Construction Aspects of Ocean Thermal Energy Conversion (OTEC) Plant Ships, APL/JHU SR 76-1B, dated April 1976.

3. R. J. Pont, Lockheed Ocean Systems presentation entitled, OTEC Cost Estimates, October 1976.

4. Ocean System (LMSC), Ocean Thermal Energy Conversion (OTEC) Test Facilities Study Program, LMSC-D506781, dated 17 January 1977.

5. A. Lavi, "Solar Sea Power Plants, Cost and Economics," in Proceedings, Third Workshop on Ocean Thermal Energy Conversion (OTEC), G. L. Dugger, Editor, APL/JHU SR 75-2, August 1975.

6. J. J. Myers, C. H. Holm, R. F. McAllister, Handbook of Ocean and Underwater Engineering, p 11-89, McGraw-Hill (1969).

.. R. Roddy, Private Communication.

8. P. M. Wolff and W. E. Hubert, Ocean Thermal Energy Conversion; Resource, Ecological and Environmental Studies, Ocean Data Systems Contract No. NSF-CH020, Monterey, California, March 1976.

9. R. J. Pont, Private Communication.

10. Lockheed Missile and Space Co., OTEC Heat Exchanger Design and Producibility Study, LMSCD-507632 dated October 28, 1976.

11. G. L. Dugger, Private Communication.

12. G. L. Dugger, Recalculation of OTEC Costs with HX Corrections for 7 Nested 3 in. Tubes, APL/JHU Memorandum GLD-77-54, dated March 15, 1977 (also this conference)

13. "Perspectives on Experience," by the Boston Consulting Group (1968), Boston, Massachusetts.

14. N. G. Gadsby, loc. cit. 1, Volume I, Appendix A.

## COMMENTS

Written Comments by G.L. Dugger, W.H. Avery, and E.J. Francis (Applied Physics Lab., Johns Hopkins University):

The author has undertaken a difficult task in trying to compare fairly the costs of OTEC plant designs from two different organizations addressing two different and distinct OTEC missions when the details of both cost estimates have been changing as each organization did further optimizations. Some of our comments on the paper by Lavi and Zener are also pertinent here, so we will mention only a few points here.

1. We concur with the author's conclusion that "the differences in design cost estimates arise from the mission and temperature differential selected. The less benign locations for the LMSC system lead to a heavier platform and additional costs of mooring."

2. The heat exchangers, which are the costliest components of an OTEC plant-ship, are greatly different in concept as Mr. Roberts has noted, and some interesting points are:

a) The heat exchanger cost ratios in Table XII from demonstration to production and from 1st ship to nth ship are more conservative for APL than for LMSC. This relative conservatism is reinforced by the facts that APL would be producing 6 times as many identical units to the nth ship, and the material-to-labor ratios are lower for APL as shown in Table VIII, so there is more room for improvement through learning. (See also our paper at this Conference: Dugger, Olsen, Padolfini and Avery.)

b) Tooling costs for the APL design are indeed much lower, because the fabrication and assembly requirements are much simpler (see our paper, Dugger et al.) than those for the LMSC concept for spherical-shell-and-tube heat exchangers (see the LMSC paper by Manakowski and Pfluger).

c) The fouling coefficient assumed by APL (0.0005 $ft^2$-hr-°F/Btu) is more conservative than that assumed by LMSC (0.0001, Ref. 4, or 0.0003, Ref. 10). Use of 0.0005 instead of 0.0001 would raise LMSC's plant cost (Ref. 4) by about 17%.

3. Regarding the APL demonstration-size plant-ship's propulsive capability and the effect of a 33-knot wind, the author overestimated the ship's exposed frontal area by a factor of 2.1. The actual area is 4730 $ft^2$, so that a 33 knot (56 ft/s) wind would impose a drag of 18,300 lb, requiring 2760 SHP (at 67% screw efficiency) or 2.3 $MW_e$ (at 90% electric drive motor efficiency). The plant-ship is already equipped with 4800 SHP capability (4 $MW_e$ maximum power draw) for just this reason, so it can cruise at 0.95 knot in the face of a 33-knot wind when the very rare occasion of necessity arises (no sea state 7 conditions measured in over 1000 observations at Atlantic Site 1; see Woods Hole data, Ref. 2, Fig. 3-29). However, under normal onsite conditions with a 10 knot wind, the wind load power requirement is down by a factor of $3.3^3 = 36$, and the underwater drag load power requirement for 1/2 knot cruise is down by a factor of $(0.95/0.5)^3 = 7$, so only 0.6 $MW_e$, the design case, is required. The component sizes and costs should not be increased to handle the very rare 33-knot wind. Our average annual plant capacity factor is assumed to be 0.945, so we could lose one pair of our 80 heat exchanger modules and cruise 0.95 knot in the face of a 33-knot wind without dropping below this value.

4. Our references (via Sun Shipbuilding and Dry Dock Co.) indicated that \$500/$yd^3$ in 1975 dollars for low density reinforced concrete is a reasonable number. For this reason and the previous one, we consider our estimates of \$1148/ W for a demonstration plant and \$804/kW for the first production plant (see our paper, Dugger et al.) to be more appropriate than those shown for APL in Table XIV.

5. We believe a slip also was made in applying the Lavi criterion for costs changing inversely with $(\Delta T)^2$. The reduction for LMSC in the last column of Table XIV near the bottom should be $(37.7/40)^2 \times 2212 =$ 1975, not 1522. There would still remain a sizable and justifiable cost difference between APL's grazing surface ship and LMSC's moored submarine vessel, which would be even larger percentagewise for the nth commercial unit.

Reply by Author:

The author is pleased that there is agreement that the major cause of cost differences in the two designs

primarily results from the mission and site selections of APL and LMSC. He also appreciates their noting of certain oversights. The following replies are numbered in accordance with the comments of Dugger et al:

2a. The remarks in the discussion section of the paper were on the overall use of experience curves by the two groups, not solely with respect to the heat exchangers. The LMSC estimates were based on the use of 0.93 slopes for the labor component only. The APL used various slopes for different components, 0.95 for the heat exchangers, and 0.8 to 0.95 for other components. The author also noted in Table XII the difference in the number of units involved in the application of the experience curves. The author still considers the LMSC the more conservative approach. Only time will prove which is the better approximation of actual experience.

2b. The author noted the difference in tooling costs for the two designs. This is a major contribution to the higher heat exchanger cost for the LMSC demonstration plant.

2c. The author used the global heat transfer coefficients of the two designs . He concurs that use of the same fouling resistance factor by both goups would increase the cost of the LMSC system vis-a-vis the APL one. This uncertainty in the magnitude of the fouling resistance emphasizes the importance of the experimental verification under operating conditions, fouling and cleaning, of the performance of the heat exchanger.

3. The author used the geometric area for lack of detail on the platform profile. Half the frontal area will decrease the wind drag as indicated in the comments and reduce the power requirements. However, it is the understanding of the author that the cube law proportionately between platform power requirements and speed is for well shaped hulls. For the large structure, as proposed, the power-velocity relationship probably will be given by an exponent greater than cubic.

4. The use of the larger value to normalize concrete cost recognized the difference in cost of the suggested use of different density concretes. In actuality, the OTEC system will utilize that type of concrete most compatible with the mission and cost. Thus, normalization of the concrete cost was, in the opinion of the author, proper.

5. The Lavi formulation, reference 5, for the change in cost with temperature uses the ratio of $(\Delta T_{new}: \Delta T_{old})^{2.5}$. This ratio is based on the change in plant cost for a fixed power output; the $(\Delta T)^2$ function applies to the change in power output for a given plant designed for another $\Delta T$.

Table X has been corrected as a result of errors noted by the reviewers.

# INFLUENCE OF DESIGN FACTORS ON THE ECONOMY OF SEA THERMAL POWER PLANTS

J. HILBERT ANDERSON AND JAMES H. ANDERSON, JR.
*Sea Solar Power, Inc.*
*2422 S. Queen Street*
*York, Pennsylvania*

ABSTRACT

At first thought, it seems that, because a sea thermal power plant is fuel-free, efficiency and losses don't really matter. Actually, nothing could be farther from the truth. The greatest costs in operating a low-temperature power plant such as this are those of getting heat to and from the working cycle. Therefore plant cost is almost inversely proportional to net plant efficiency. This paper examines the effects of efficiency losses on plant economics and shows how various design factors do affect overall feasibility.

When we consider the process of converting the thermal energy in the ocean into useful power, we immediately think of the ocean as a practically infinite fuel source. This also leads us to the conclusion that, since the energy is free, it really doesn't matter how efficient we make a power plant to convert this heat into electrical power. We are accustomed to thinking of fuel-fired power plants and also to thinking that less efficient plants are likely to cost less than more efficient plants. Therefore we automatically conclude that efficiency of a sea thermal power plant doesn't have much bearing on its cost. Nothing could be farther from the truth. In this paper, I will try to show, by simple examples, how the losses and plant efficiency can drastically affect the cost of a sea thermal power plant. All too often, these factors have been ignored in the studies that have thus far been made on the subject.

We can start by considering that every thermal power plant must have a heat input and a heat rejection part of the cycle. Figure 1 shows the fundamental relationship of the ratio of the heat rejected to the useful energy produced from the plant, plotted vs. plant efficiency. Looking at this curve, you will note that an ordinary nuclear power plant, with approximately 33% efficiency, must reject twice as much heat equivalent as the power that is produced from the plant. I am sure that you have recognized from many articles and discussions that the heat rejection from nuclear plants is a difficult and costly problem, and has caused much argument and litigation wherever nuclear plants were built.

Next, let us consider a plant with lower efficiency, such as a geothermal plant using hot water as a heat source. Note on Figure 1 that, in a geothermal power plant of approximately 10% efficiency, the ratio of heat rejection to plant output is 9 to 1. Therefore a geothermal plant is likely to have a heat rejection rate of approximately four and one-half times that of a nuclear plant. Many people speak of geothermal power as a cheap source of potential energy. Not so many people realize that the major cost of a geothermal plant is actually the cooling system. Figure 1 shows the reason for this.

Figure 2 shows the ratio of heat rejection and heat input to power production vs. plant efficiency plotted on a logarithmic scale. This makes it convenient to carry the plot to very low efficiencies, such as those that might be expected in a sea thermal power plant. The equation for ratio of heat rejection to power output is simply (1-e)/e, as shown on Figure 3. As an example, for a plant of 2% efficiency, the ratio is 49 to 1. If we merely drop the efficiency from 2% to 1.9%, the ratio increases to 51. In other words, by reducing the efficiency of a sea thermal plant by only 4%, we must immediately add as much cooling capacity as is required for an entire nuclear plant. This gives one some idea of the basic problem that we must face in a sea thermal power plant. This shows the fundamental reason why any losses in, or decrease in, efficiency of such a plant have a very important effect on the actual investment cost to build the plant.

Let us now list some of the potential losses in a sea thermal power plant, as shown in Figure 4. These are:

Temperature Losses - These are represented by loss of temperature in not obtaining the maximum possible temperature at the warm surface water, loss in temperature difference by not going deep enough in the ocean to get the coldest possible water, and loss in temperature difference due to design factors in the heat exchanger system.

Internal Friction Losses require power in order to overcome them. This power must be generated from the plant, and therefore the plant must be made with sufficient excess output to provide the power to overcome these losses.

Machinery Losses are direct losses in efficiency of the machinery itself.

Buoyancy Losses are losses caused by making the physical machinery larger than necessary, thereby causing the required supporting structure to be larger than necessary, which obviously costs more money. In addition to this,

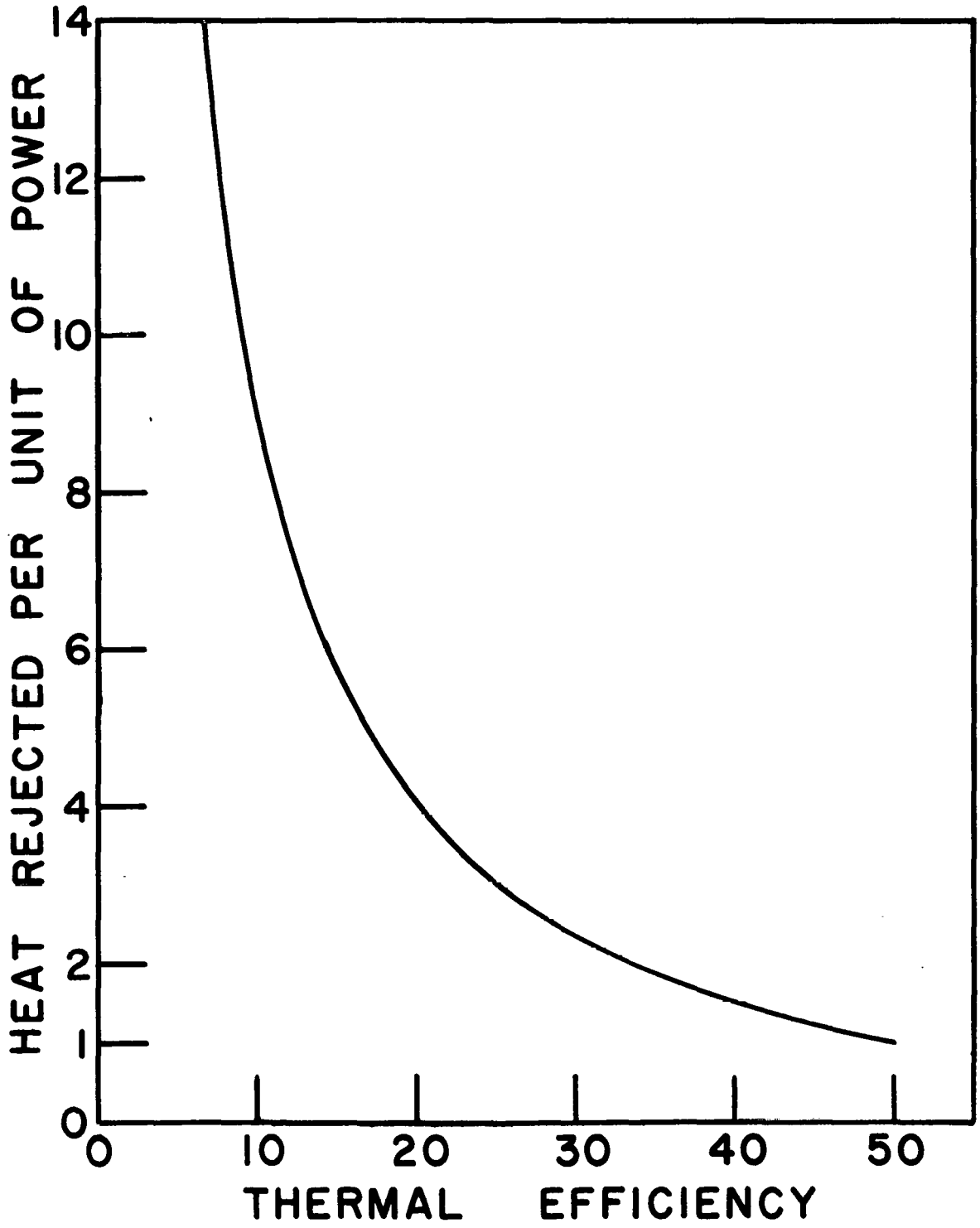

HEAT REJECTED PER UNIT OF POWER
14
12
10
8
6
4
2
1
0
0
10
20
30
40
50
THERMAL EFFICIENCY

FIG. 1

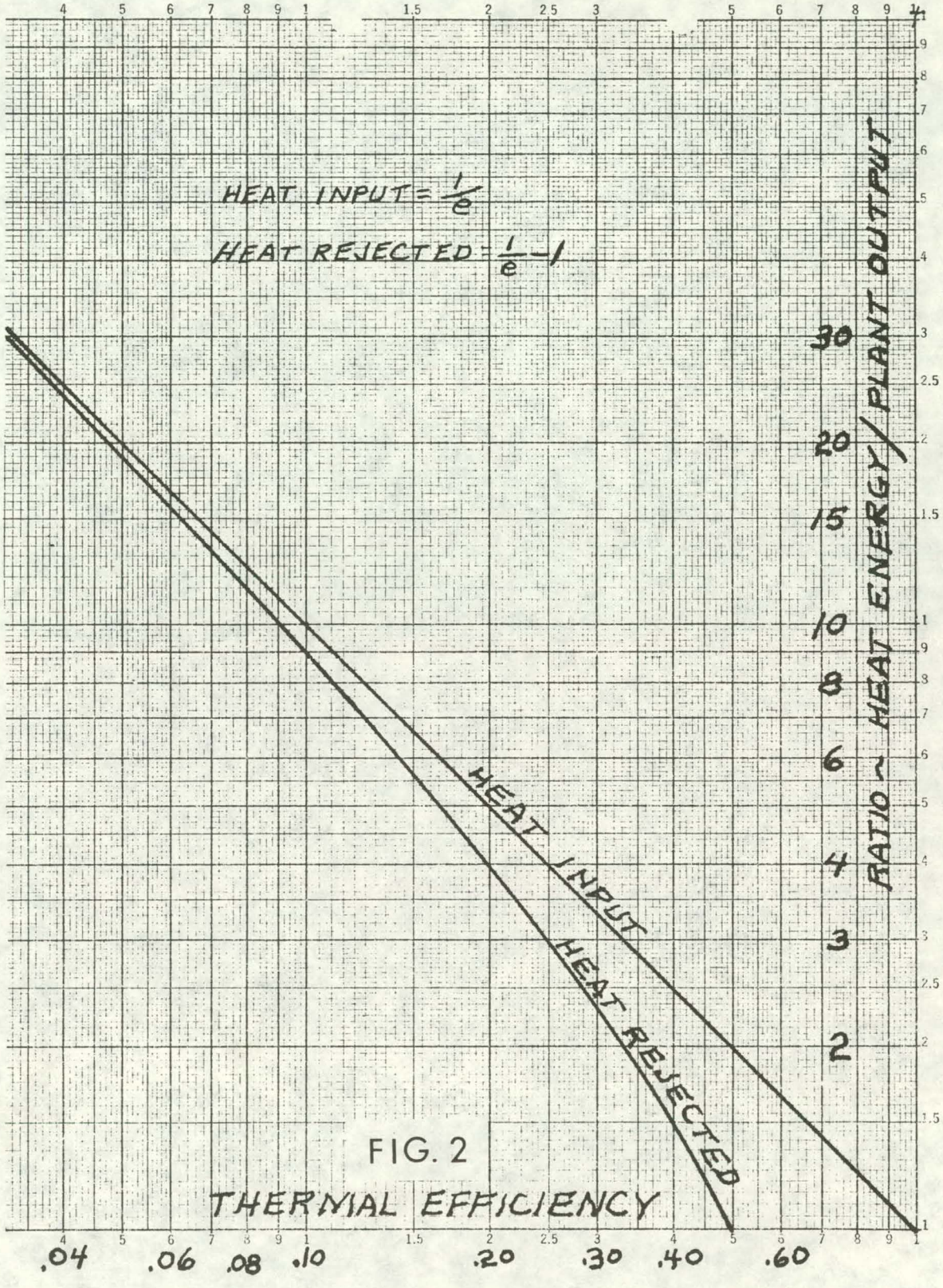



FIG. 2

THERMAL EFFICIENCY

# PLANT EFFICIENCY
## vs.
# HEAT REJECTION

$$\frac{Ho}{kw} = \frac{\text{HEAT REJECTED}}{\text{POWER OUTPUT}} = \frac{1 - e}{e}$$

WHERE e = PLANT EFFICIENCY

| e | Ho/kw. |
|---|---|
| .02 | 49.0 |
| .33 | 2.0 |
| .0192 | 51.0 |

$$.02/.0192 = 1.042$$

FIG. 3

LOSSES IN SEA POWER PLANTS

TEMPERATURE

INTERNAL FRICTION

MACHINERY LOSSES

BUOYANCY

EXTERNAL FRICTION

PIPE LOAD

FIG. 4

the larger sized structure required to support the vessel then, in turn, must resist greater forces created by storms or current, and this again requires either larger mooring lines and anchors or larger power units, in order to maintain the structure on location.

External Friction Losses apply to drag losses on the structure, and these are affected by the physical design of the structure, and also by its physical size. Any external friction losses must be overcome either by larger mooring systems or by power for positioning systems.

The cold water pipe is the most massive single element in the system. This must be supported by the floating structure above it. Therefore the load of the pipe on the structure determines again how large the structure must be, and the larger the force of the pipe is on the structure, the larger the structure must be and the more it will cost.

Let us now look at a simple diagram, which shows us what some of the fundamental loss problems are as far as the plant is concerned. Figure 5 shows power output plotted against temperature difference. The power output scale is put in the same units as temperature because basic power output from the plant is practically proportional to available temperature difference. The upper straight line represents the available power output in theory and varies from 40 at 40° temperature difference to 0 at 0° temperature difference.

It has generally been suggested that the most economic plant design will utilize approximately half of the available temperature difference to get the heat in and out of the heat exchangers. Therefore the line starting at 20 and coming to 0 at a $\Delta T$ of 20 represents the available power vs. $\Delta T$ remaining in the working fluid after the heat is transferred to the heat exchangers. This assumes a constant supply of water and a constant size of heat exchangers with the same temperature difference across them. Then the diagonal line from 20 down to 20 $\Delta T$ represents how much power is available from a plant with temperature differences of 40° down to 20°. Next, if we apply the cycle efficiency, which has been assumed at 90%, the line then drops to 18 at 40 and still goes to 0 at 20° $\Delta T$.

Next, we must subtract the parasitic losses, such as pumping power losses. In this case, we have subtracted an equivalent of 4 more degrees, so that the remaining available power line goes from 14 at 40 $\Delta T$ down to 0 at 24 $\Delta T$. If we double the losses, then the dash line would represent the available power output going from 10 at 40° $\Delta T$ down to 0 at 28° $\Delta T$. This is a very much simplified diagram, but still gives a general idea of how much power you can get from a given physical size plant vs. the overall $\Delta T$ available. The slope of the actual line is steeper than this because, as the available $\Delta T$ to a given size turbine drops, the physical size of the turbine to utilize that $\Delta T$ must go up. This is not taken into account on the lines shown.

Since this chart is represented by straight lines of power output vs. $\Delta T$, we can easily develop an approximate equation for the line, and that equation is shown on Figure 6.

From the equation shown, we can take several examples to show the effect on the plant output per degree change in $\Delta T$. If, for example, we go from 36 to 35, with the loss equal to 4 units and efficiency of 90%, t plant output, which would be inversely proportional to the plant cost per degree, changes 9-1/2% per degree Fahrenheit. If we have higher losses, at 8 units instead of 4, the percent change in cost per degree Fahrenheit is 16.4%. From this, it can be seen that a very, very tiny change in available temperature affects the cost of the plant quite drastically.

To corroborate the basic idea presented here, it might be useful to look at the actual net power output from a geothermal plant vs. the available temperature. A geothermal plant has similar operating principles to those of a sea thermal plant because the source of heat is warm water, and the waste heat is rejected to cold water. The basic difference is that the temperature difference is higher, and plant efficiency is higher. On Figure 7, we have shown the actual net plant output from a geothermal plant, plotted vs. the available cooling water temperature. Our firm has been given complete responsibility for designing and building America's first commercial geothermal hot water plant, which is now being constructed in the Imperial Valley of California. The basic design of this plant is complete, and all losses have been calculated, so that the performance curve shown should be very near to being factual for actual operating conditions. The available water temperature for the geothermal plant is 360 F., and the water temperature at the bottom of the cycle is shown on the chart. The temperature difference available for generation of power is much greater than that in the sea thermal plant. Despite this, the rate of change of power output per degree Fahrenheit change in water temperature is very high. As can be seen, the slope of the curve becomes steeper, the higher the temperature of the cooling water or the lower the overall $\Delta T$. At a water temperature of 80 F., for example, the percent change of power output per degree is 6.6% per degree Fahrenheit. Since the temperature difference available here is far greater than that in a sea thermal power plant, it suggests that, in an actual sea thermal power plant, the effect on efficiency or plant output per degree will probably be even greater than the figures calculated from the simple diagram shown on Figure 5.

Now, let us look at where some of the temperature losses can be in a sea thermal power plant. Figure 8 shows a more or less typical profile expected for temperature available in the tropical oceans. This particular figure was taken from the TRW report on feasibility of sea thermal power plants. Note that this curve shows no change in temperature through a range of about 100 ft. near the surface of the ocean. Note also that going from 1,500 feet to 4,000 feet shows a difference in temperature of 8°. This makes one realize how extremely import- and it is to get the cold water pipe as deep as possible in order to get maximum plant output.

Next, let us look at Figure 9, which shows a series of points actually measured in the ocean near Puerto Rico. You will note that, while the more or less theoretical curve previously shown indicates a constant temperature through the upper depths to about 100 ft., the actual curve shows that there is a continual variation much

# PLANT POWER OUTPUT
# vs.
# TEMPERATURE DIFFERENCE

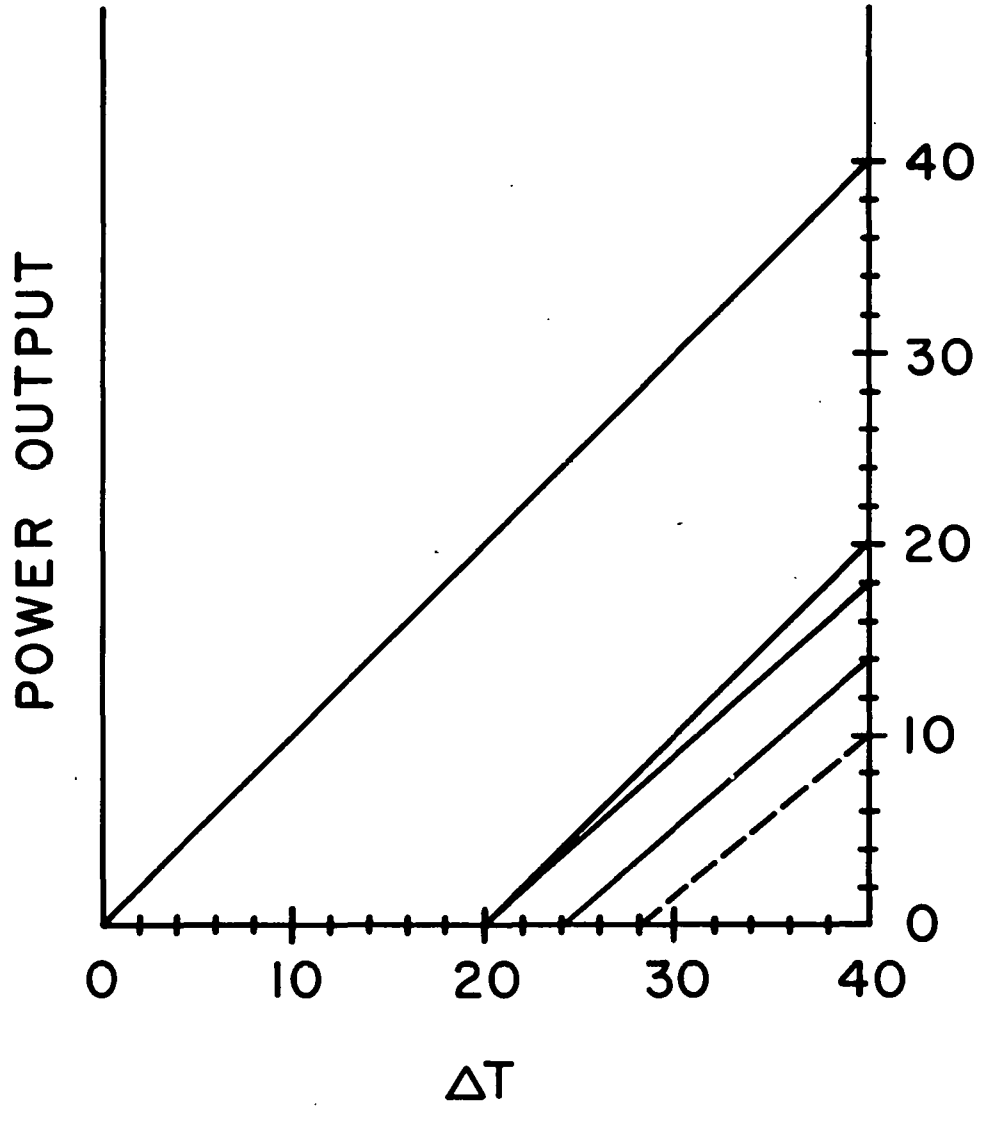



FIG. 5

$$\text{PLANT COST} \approx \text{CONST.}\left[(\Delta T - 20)e - L\right]$$

$\Delta T$ = OVERALL TEMPERATURE DIFFERENCE - °F

$e$ = GROSS EFFICIENCY RATIO

$L$ = PARASITIC LOSS IN °F

EXAMPLES

| $\Delta T$ | $e$ | $L$ | FACTOR | % COST/DEGREE |
|---|---|---|---|---|
| 36 | .90 | 4 | 10.4 | 9.5 |
| 35 | .90 | 4 | 9.5 | |
| 36 | .90 | 8 | 6.4 | 16.4 |
| 35 | .90 | 8 | 5.5 | |

FIG. 6

# ESTIMATED POWER PROFILE WITH SPRAY COOLING SYSTEM

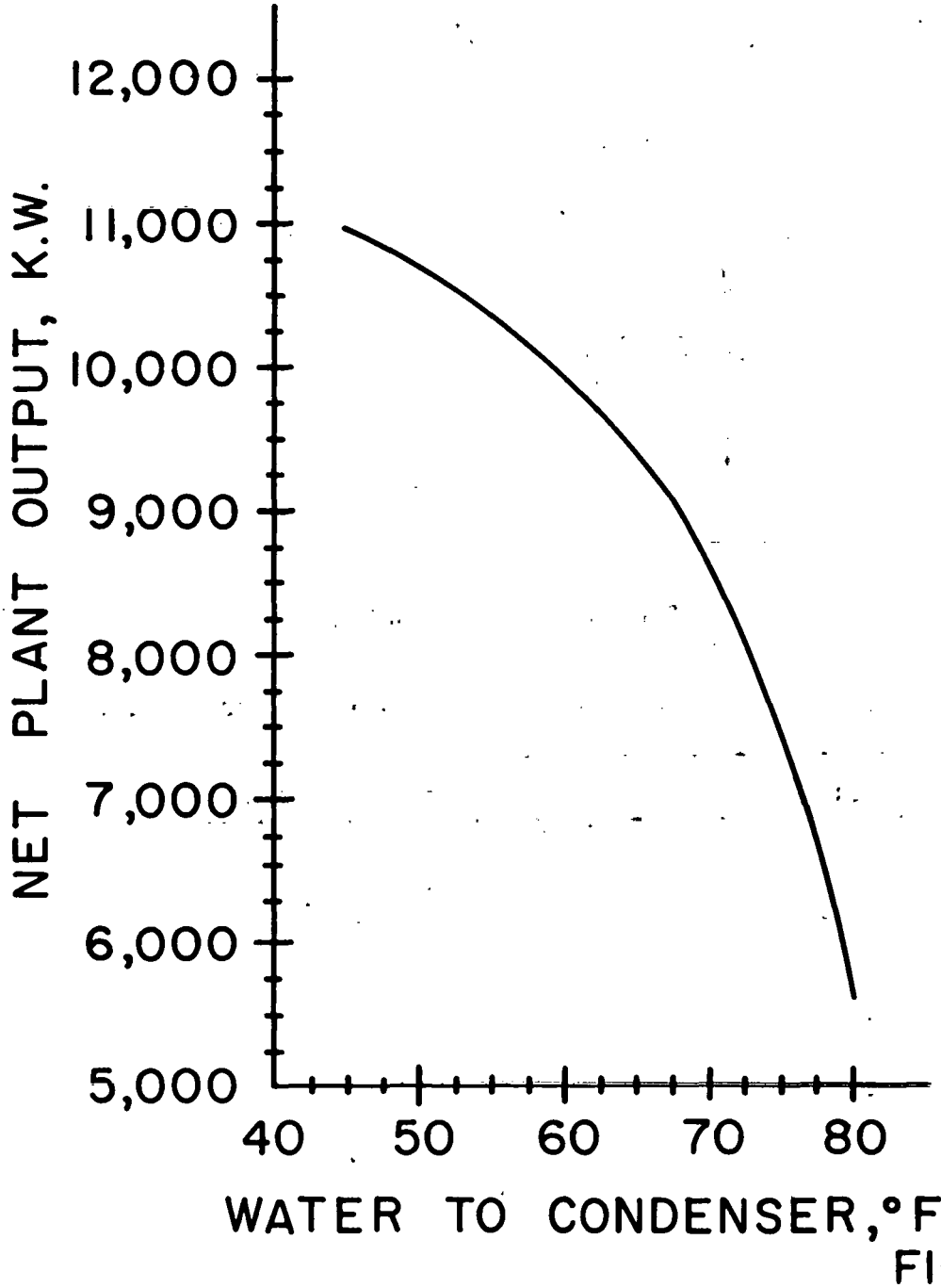
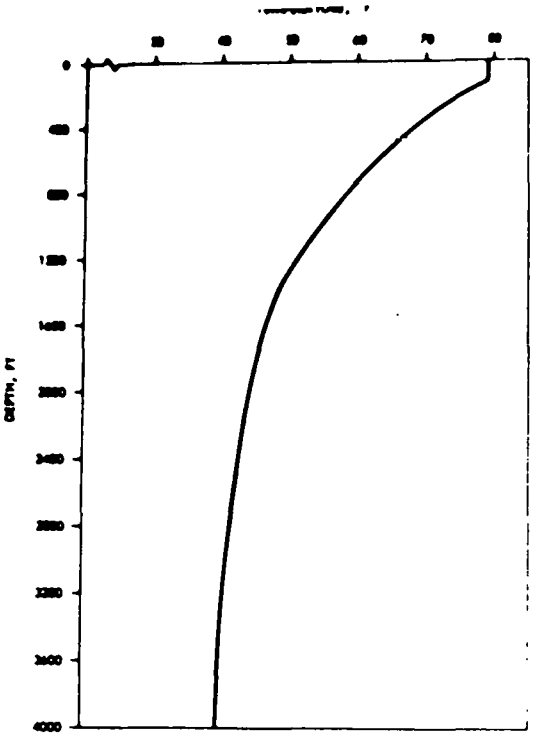



FIG. 7



OTEC Design Bathythermal Profile

'able 3-2. Available Temperature Difference for Specified Depths

| Depth, ft | $T_{surface} - T_{depth}$, $^{o}F$ |
|---|---|
| 0 | 0. |
| 1,500 | 31.3 |
| 2,000 | 34.8 |
| 2,500 | 36.4 |
| 3,000 | 38.5 |
| 3,500 | 39.0 |
| 4,000 | 39.3 |

FIG. 8

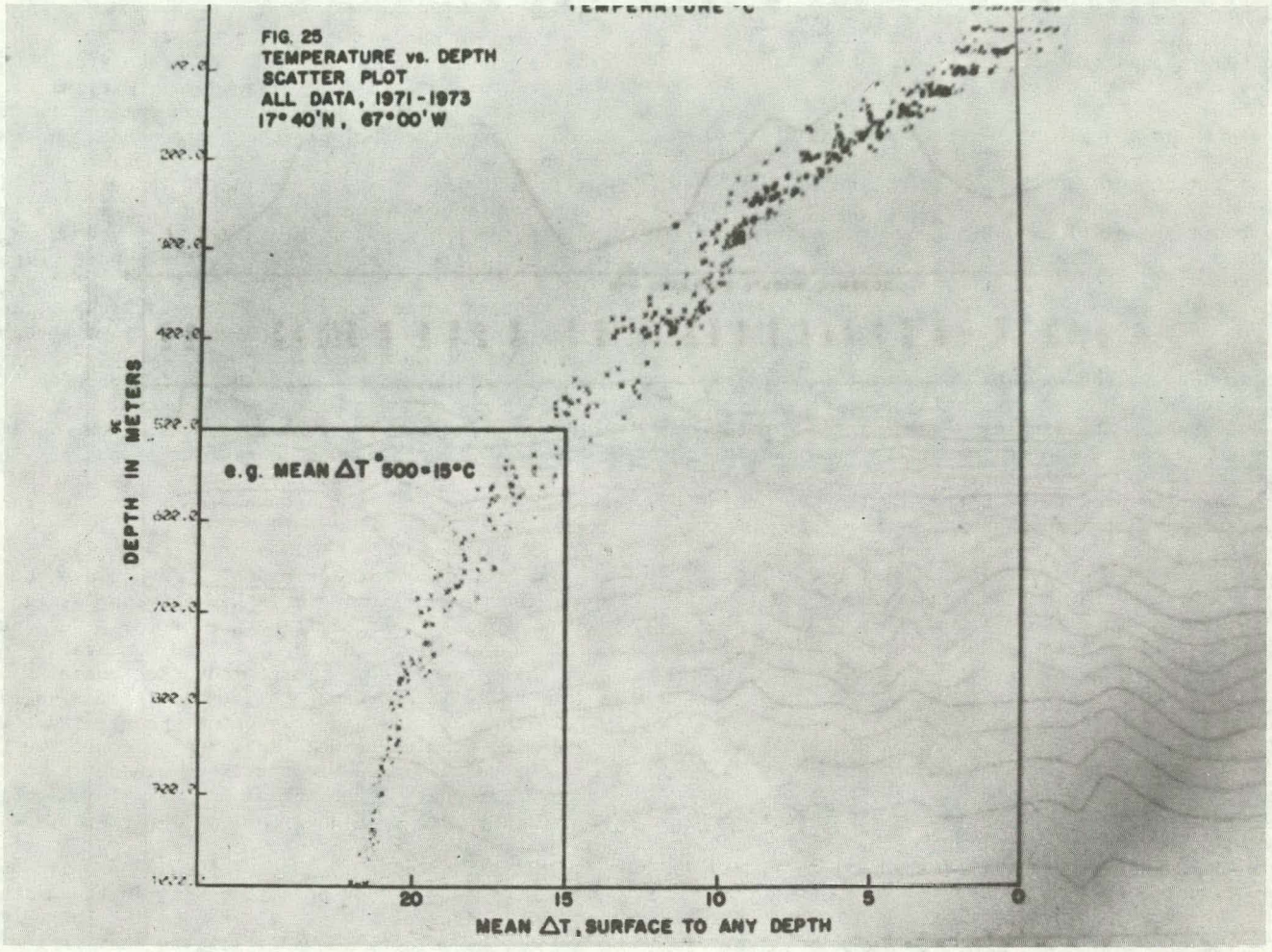

FIG. 25
TEMPERATURE vs. DEPTH
SCATTER PLOT
ALL DATA, 1971 - 1973
17° 40'N, 67° 00'W
DEPTH IN METERS
e.g. MEAN ΔT °500 = 15°C
20
15
10
5
0
MEAN ΔT, SURFACE TO ANY DEPTH

FIG. 9

nearer to the surface. Therefore it is important to get warm water from as close to the surface as possible.

Now, let us consider some problems with water pumping and pressure losses. Figure 10 shows a picture taken from the TRW report showing a cross-sectional view of the plant concept. Note that, in order to get in and out of the heat exchangers, the water must flow through pipes, then decelerate from the pipe outlet to enter the frontal surface of the evaporator, be accelerated into a pipe at the outlet of the evaporator, then turn two sharp elbows and pass through a tee, before being ejected through an additional series of pipes to act as positioning devices for the structure. The close connections of piping and the sharp elbows are made necessary because the evaporator and condensers are enclosed in the large buoyant structure, and utilization of better streamlining and elbows that have less pressure drop would have made necessary a much larger structure.

Figure 11 shows a picture with dimensions of the actual evaporators proposed by TRW. By actual calculation of the losses through these inlets, outlets, and piping elbows alone, the total pumping horsepower required caused by these restrictions and high velocity turns was calculated to be approximately 6,000 HP. This is a direct, and unnecessary, loss that is attributable to forcing a design that requires so many turns to get in and out of the heat exchangers.

When we look at the physical size of the evaporator and learn that this is a recirculating type of ammonia evaporator, in which the liquid is pumped from the bottom to the top as it boils, and the vapor and some liquid go out of the top of the evaporator, you then have a situation where the pressure at the bottom of the evaporator is considerably higher than that at the top. In refrigeration terminology, this difference in pressure is called "static head penalty." By actual calculation, in this particular case, the static head penalty is approximately 5.7° F. This means that the effective temperature difference across this exchanger is far less than that which has been assumed, and the evaporator cannot possibly produce the heat transfer that was calculated.

Next, let us look at some simple diagrams illustrating the effect of putting all machinery inside the hull of the vessel, vs. putting as much as possible machinery outside of the supporting buoyant hull. Some fundamental principles are shown on Figure 12. On the left, we show a diagram in which we have a cylinder of volume $V_1$ and mean density, $\rho_1$, supported from a separate supporting cylinder. The overall buoyancy of the entire structure is assumed to be neutral. On the right, we have the case where the same cylinder, volume $V_1$ and mean density, $\rho_1$, is supported inside a buoyant structure. The equation shows that the required volume of an enclosed buoyant structure divided by the volume of the separate buoyant structure is equal to $\rho_1 / (\rho_1 - \rho_w)$, where $\rho_w$ is the density of water. Taking two examples that might be more or less typical, the ratio for a mean density of 500 lbs./ft.$^3$ is 1.15, or at a perhaps more typical density of 100 lbs./ft.$^3$ is 2.78. From this, it can be seen that, for any given structure to be supported in the ocean, less amount of buoyant hull is requried if the structure is outside the hull than if it is inside the hull. This can have an important effect on the overall size and cost of the structure.

Let us now consider the problem of supporting the cold water pipe from the structure. The cold water pipe is the heaviest mass that must be supported by the structure. Since the hull near the surface of the ocean is subject to motion from external wave forces, then we must consider the interaction between the supporting hull and the cold water pipe, which extends for a long distance into the ocean. It is obvious that, whenever the hull moves, it will also try to move the cold water pipe, which tends to be stationary and have a large inertia as it hangs in the deep water. Therefore there are potentially large forces between the hull and the cold water pipe. It is interesting to note that, when Claude, years ago, tried to suspend a cold water pipe from a ship to produce power, the cold water pipe broke from the supporting structure within only a few days of trying to get it into operation. This should tell us something. If we calculate the theoretical forces produced by harmonic motions assumed from harmonic type waves, then one can easily calculate that the potential forces created by dynamic motion between the hull and the pipe are a small fraction of the pipe weight in air. If you assume this to be true, then theoretically the cold water pipe can simply be pivoted and supported from the hull and needs only to take large reactions in the horizontal, and rolling or pitching directions. However, it is probably safe to say that no ship was ever pounded to pieces by purely harmonic motion, and no ocean actually operated for very long in pure harmonic motion. The actual breakup of ships or structures at sea is caused, not so much by harmonic motion, but by motions which get out of phase with each other. These motions and forces are very difficult to calculate, but from actual experience, we know that they can be quite high.

As a simple, similar example, we can use the case of an ordinary induction motor. We have long designed induction motors to transmit torque at the power output level at the motor. However, if you momentarily disconnect the current from a large induction motor, and then a few cycles later reconnect it, the induced voltage within the rotor is probably out of phase with the voltage coming from the power line. As a result, we find that the torque, upon reconnection, can be as much as 14 to 20 times that of the normal torque. This is because the voltages are completely out of phase with each other.

Another example is that of pushing a child on a swing. As long as you push the swing in tune with the motion, the forces are very, very small compared with the amplitude of motion. However, if you step in the way of the swing at the wrong time, POW! We can very easily have the same sort of condition in a sea thermal power plant. Therefore it is only logical to think that we might have the situation where wave motion is not purely harmonic, and the motion of the hull can easily get completely out of phase with that of the pipe. In such a case, it is quite conceivable that pipe forces could be much more than the weight in air. For this reason, we have concluded that the safe way to design a support for the cold water pipe is to use a spring support that definitely eliminates the possibility of large transmission of forces between the hull and the pipe at any time.

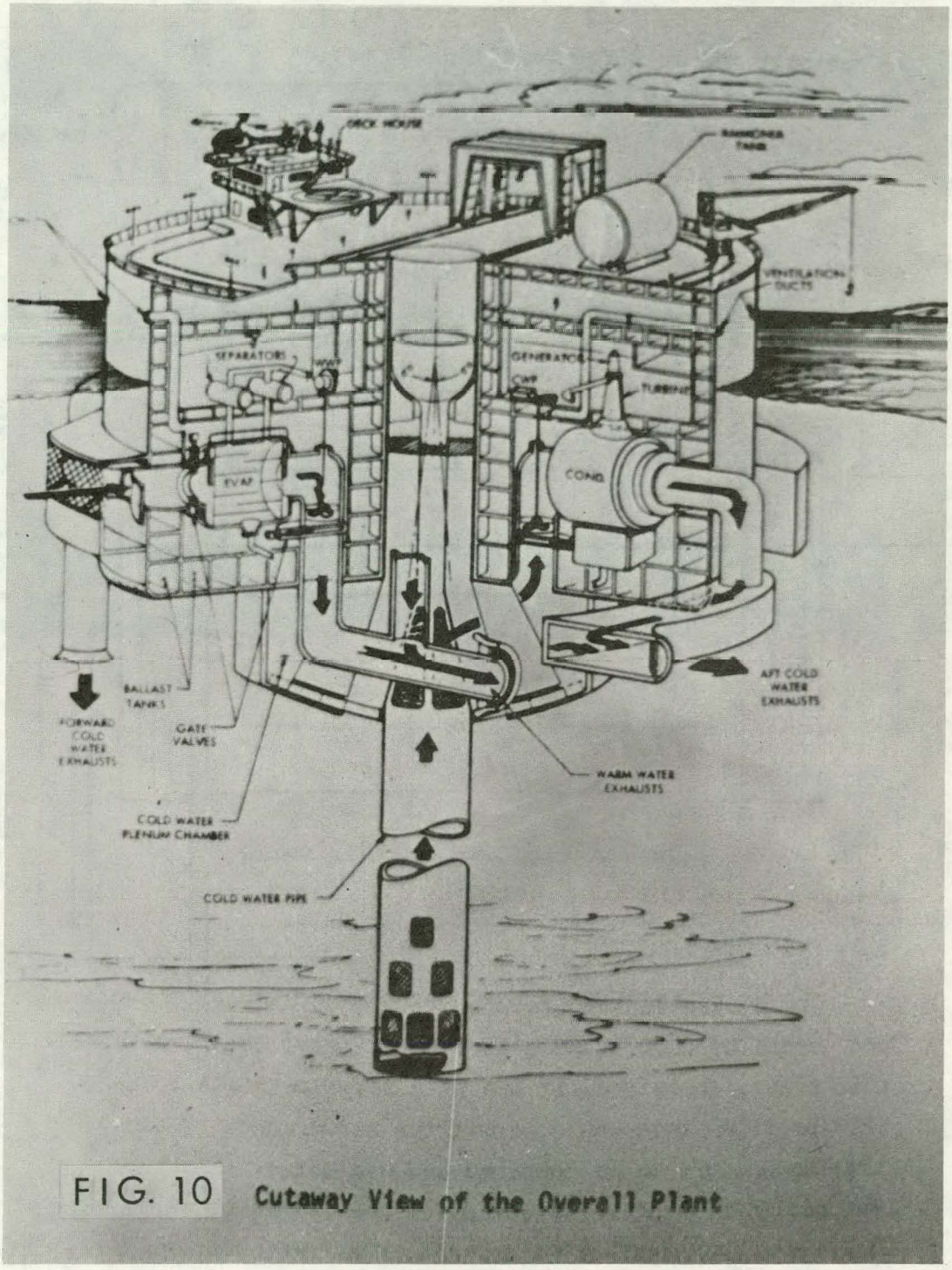
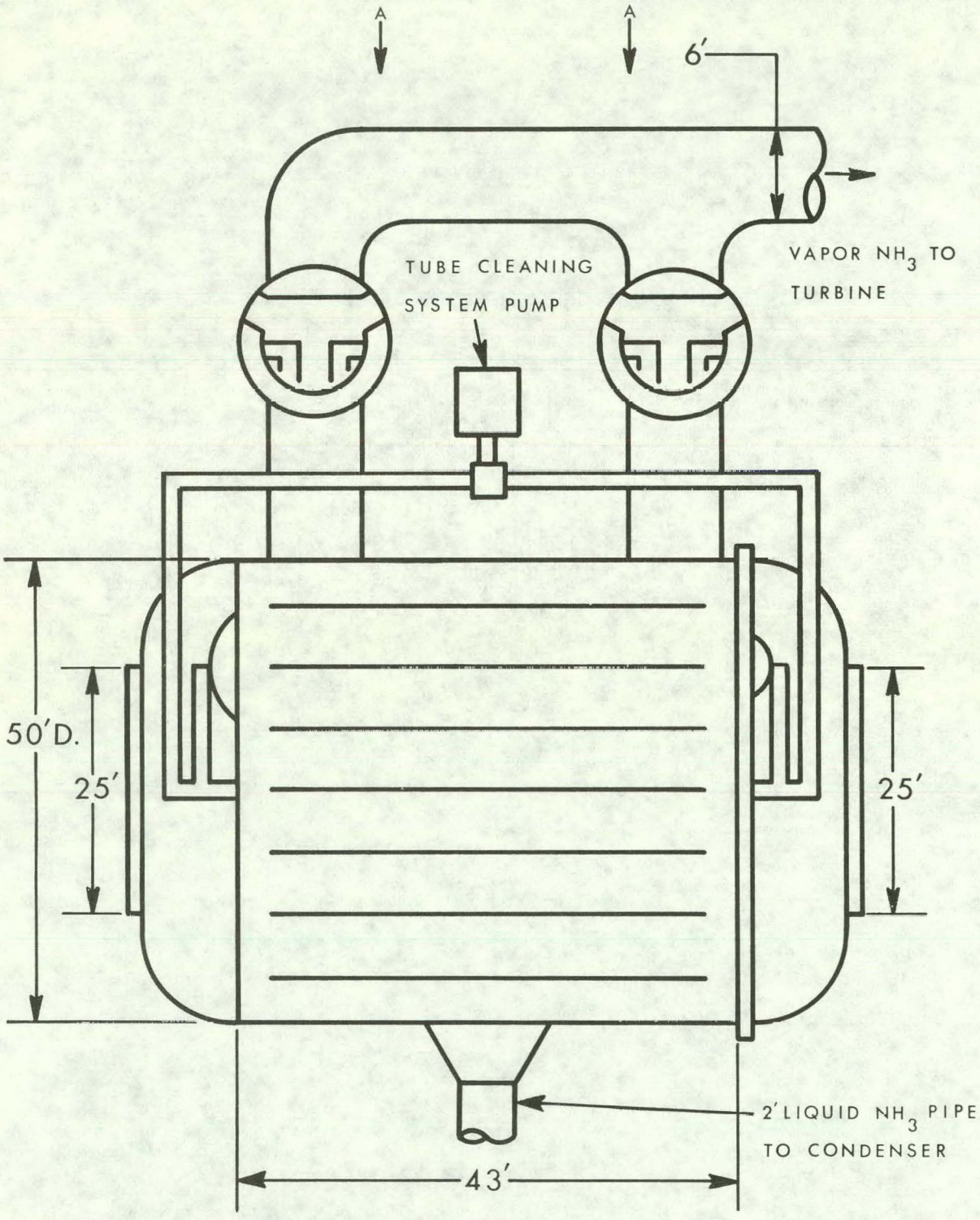
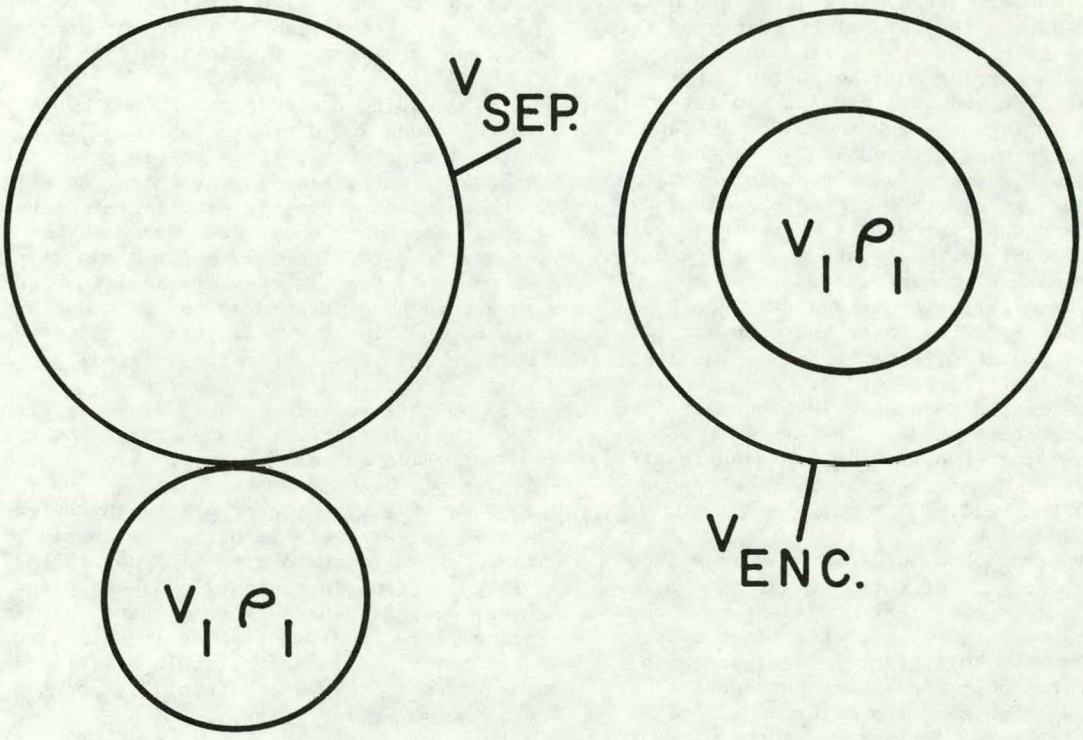



FIG. 10 Cutaway View of the Overall Plant




SIDE VIEW

FIG. 11




$$\frac{V_{ENCLOSED}}{V_{SEPARATE}} = \frac{\rho_1}{\rho_1 - \rho_W}$$

AT $\rho_1$ = 500 $\quad \frac{V_E}{V_S} = 1.15$

AT $\rho_1$ = 100 $\quad \frac{V_E}{V_S} = 2.78$

FIG. 12

Figure 13 illustrates such a spring mounting diagrammatically. In order to make sure that the spring effectively isolates forces from being transmitted from the hull to the pipe, we must design the natural frequency of the spring to be lower than that of any applied wave force. In order to do this, the spring must be sufficiently strong to support the pipe and must have sufficient energy storage to give a spring rate low enough to isolate the pipe from the platform. The equation shows the energy storage required in the spring as a function of natural frequency, the downward force P of the pipe, and the mass of the pipe. As can be noted, the energy storage in the spring is proportional to the square of the downward force divided by the mass of the pipe. Spring mass and spring cost are approximately proportional to energy storage capacity. Therefore the lower the downward force, or negative buoyancy, of the pipe can be made, the less the physical size and cost of the spring. Also, the lower the downward force can be made, the less buoyant force is required in the structure above. Therefore it becomes very important to introduce buoyancy in the pipe itself, because this reduces the net force that must be supported by the spring and the hull.

In order to illustrate how some of these loss problems can be overcome, and all of these losses can be reduced so as to make a more efficient and lower cost power plant, Figure 14 shows a diagram of the plant as proposed by Sea Solar Power. This plant is designed as a skeleton with all of the heat exchangers outside the buoyant structure. We also have the major amount of piping outside the structure. This reduces the size of buoyant structure required. To show how great this reduction can be, the approximate weight of the Sea Solar Power plant is probably less than 30,000 tons, vs. something of the order of 260,000 tons, as proposed for similar sized plants in which all of the machinery is enclosed. While it is too early to say that such estimates of weight are accurate, a ratio of 10 to 1 should be within the capability of ordinary estimating.

Our Sea Solar Power plant is designed so that the water inlet is right at the surface of the ocean, so as to reach the maximum possible upper surface temperature. It is also designed with a flexibly supported pipe, suspended from the center of the vessel so that the semi-buoyant pipe produces the minimum down-force on the vessel, and also can be constructed from the upper deck of the vessel, section by section, at sea, and can easily be made long enough to extend to great depths, thereby attaining the maximum possible available temperature difference.

In order to minimize the power losses due to pumping water, the cold water pipe has the pump installed at the top of the pipe, and discharges into a plenum chamber, from whence it flows directly through the condensers without any elbows or high-velocity turns. This permits the minimum possible pressure loss, requires the minimum possible pumping power, and thereby increases overall efficiency.

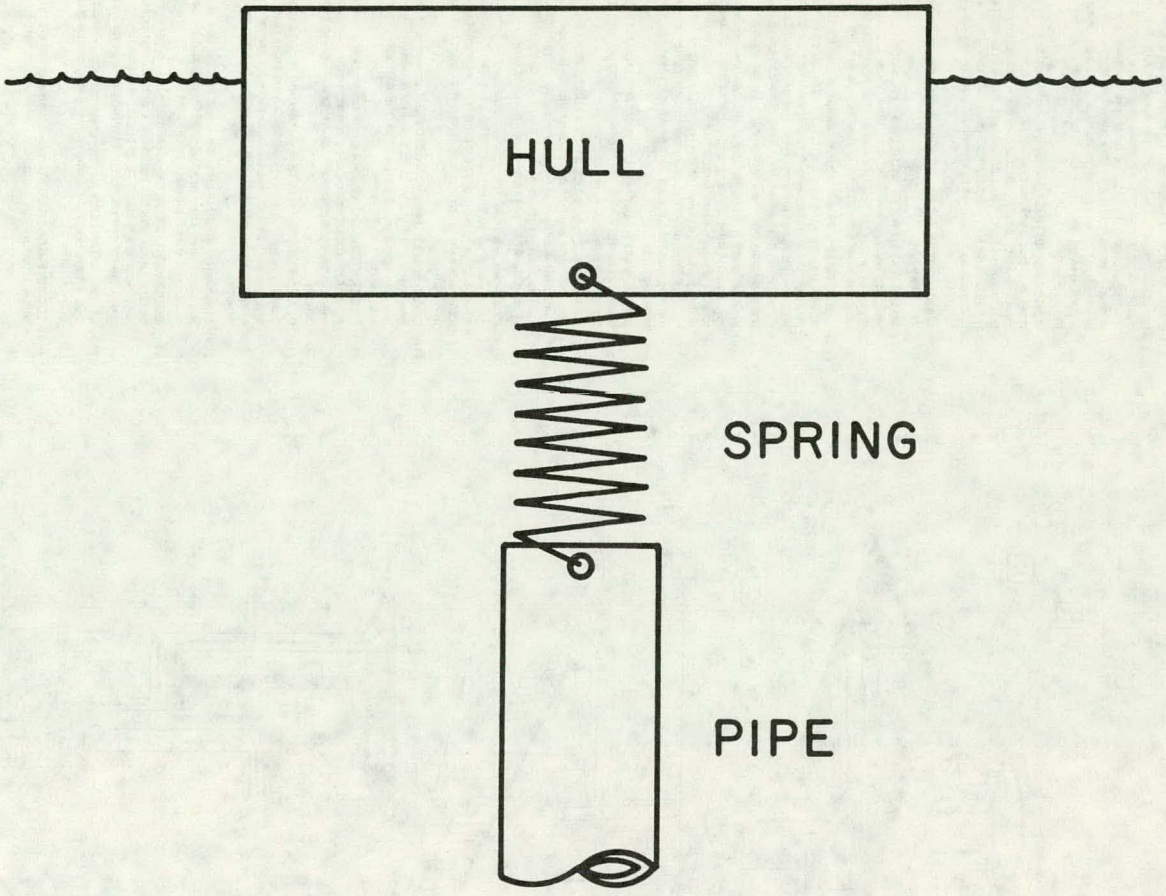
Similarly, the warm water comes into the largest possible screening area at very low velocities near the surface and is pumped straight down the pipes into the plenum chamber in front of the evaporators. Therefore there are no high-velocity turns of any kind in the entire system. This construction, in both the warm and cold water cases, also permits easy accessibility to the pumps, since they can be lifted straight up to the deck from the pipe through which they are installed.

By having the evaporators and condensers directly in the ocean and directly connected to eject the spent water into the sea, it is possible to install louvers at exchanger outlets as shown, which can direct the outgoing jets to produce dynamic positioning without any accessory power. In cases of storms, where larger than usual drag occurs, the turbine-driven pumps can simply be increased in speed to produce excess velocity and sufficient excess thrust to handle the drag forces under any conceivable storm conditions. These jets can also be used for propelling the vessel from its original manufacturing point to its final location in the ocean. The much smaller size of this vessel per unit of power also tends to reduce the amount of station-keeping power required while in operation at sea.

We have tried here to show, by a few simple examples, why it is extremely important to consider the many potential losses in the design of a sea thermal power plant. All too often, in the many proposed plans that we have seen, designers have ignored these most fundamental principles, and this has resulted in excessively large structures and in unattainable efficiencies, and much larger costs than are potentially necessary for building sea thermal power plants.

As an example of how careful design and paying attention to losses of all kinds can affect the cost of power plants, we can mention that the cost of America's first hot water geothermal power plant, for which we have total responsibility for design and construction, will be probably of the order of 60% or less of most projections of geothermal power plant costs. The reason, and the basic explanation, why these costs are so much lower than those projected by many feasibility studies is, purely and simply, that we have paid a great deal of attention to the losses in the plant, and how to design it so as to minimize those losses. The amount of efficiency to be gained in the design of a sea thermal power plant is potentially even greater than that which has been gained in geothermal power plants.

The development of ocean thermal energy is, by far, the most important energy project of this century. Its potential is almost beyond imagination. Therefore we cannot stress too highly that every effort be made to improve the design of such plants, and that the payoff for doing so can justify almost any effort that is made in this direction.




P = NET DOWNWARD FORCE OF PIPE

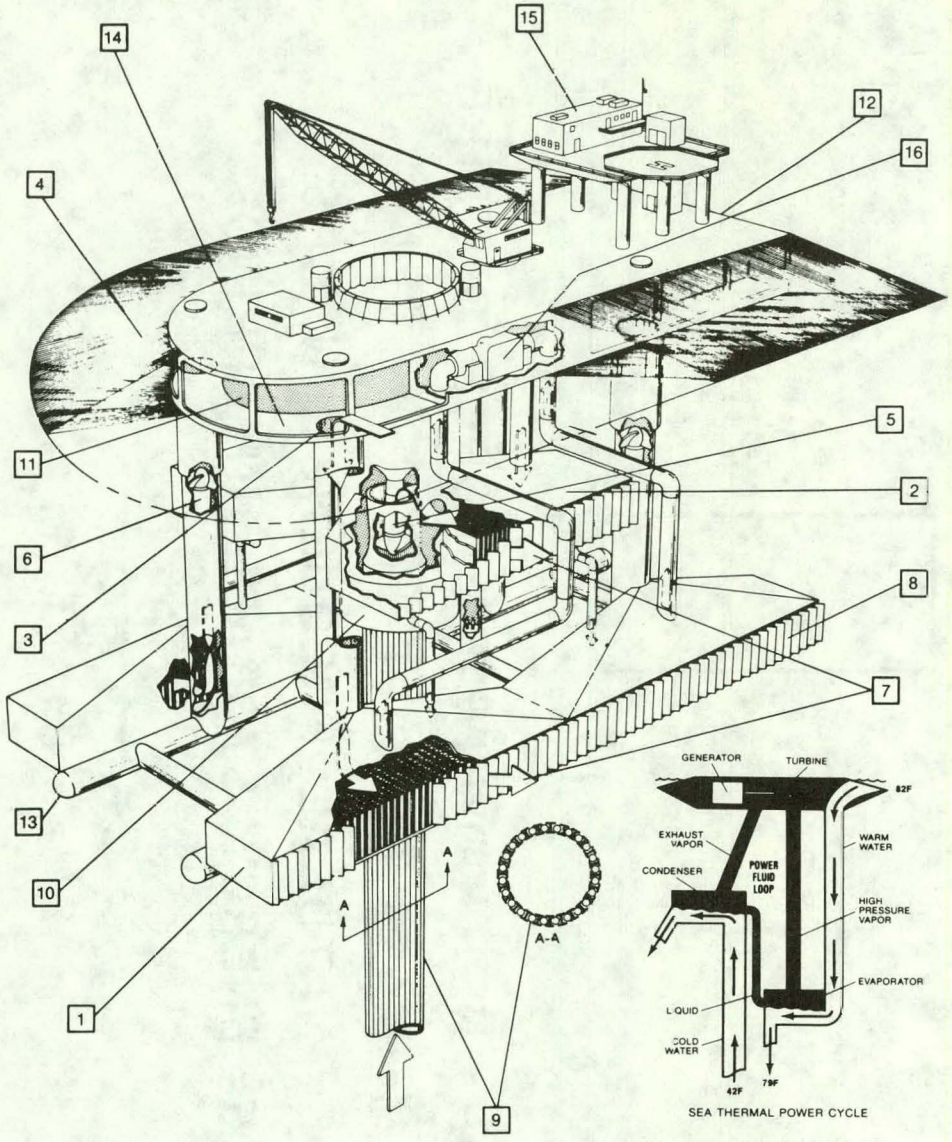
M = MASS OF PIPE

f = NATURAL FREQUENCY IN CPS.

E = ENERGY STORAGE IN SPRING

$$E = \frac{P^2}{8\pi^2 f^2 M}$$

FIG. 13




SEA THERMAL POWER CYCLE

FIG. 14

(1) **EVAPORATORS** (Heat Exchangers) convert the working fluid from a liquid to a vapor. In the evaporators, the heat from water coming from the warm water pumps is used to vaporize the working fluid. The heat exchangers are the most critical components from the standpoint of cost and plant efficiency. The evaporators have a patented pressure-balanced design and are modular for ease of service and replacement.

(2) **CONDENSERS** (Heat Exchangers) change the working fluid from a vapor back into a liquid. The condensers use the cooler water from the cold water pump to liquefy the vaporized working fluid. The condensers, like the evaporators, are modular and have a patented pressure design. A variety of materials can be used to construct condenser and evaporator.

(3) **WARM WATER INLET** utilizes maximum area to keep inlet velocities low.

(4) **WARM WATER INLET SCREENS** have sloped sides to provide for wave protection, and they allow the warmest top layer of water to be received. The gentle sloping inlet screens also protect fish and other marine life.

(5) **COLD WATER PUMP** draws cooler water from the lower ocean depths through the cold water pipe and pumps it through the condensers. It is a propeller-type pump with a submerged vapor turbine drive. The drive would be powered by the main system working fluid. The complete pump-drive package can be lifted to the deck for servicing.

(6) **WARM WATER PUMPS** draw the warmer surface water through the inlet screens and pump it through the evaporators. The warm water pumps are similar in design to the cold water pump. The use of the vapor turbine drive minimizes the pumping power requirements over other schemes, and permits variable speed to adjust for seasonal changes in temperatures.

(7) **WARM WATER AND COLD WATER EXHAUSTS** are positioned at levels which will prevent mixing of cold water with the warm surface layer.

(8) **ADJUSTABLE LOUVERS AT EXHAUST POINTS** are used to automatically control the positioning of the plant, like on a semi-submersible drill rig. Louvers can close each individual heat exchanger module for a cleaning cycle or for removal of module while plant remains in operation.

(9) **COLD WATER PIPE** transports colder water from the lower ocean depths to the plant. The pipe is of stockade construction for strength and stability. It is semi-buoyant and can be easily constructed at sea through the top of the platform.

(10) **COLD WATER PIPE CONNECTION** provides isolation between the cold water pipe and hull structure. It is used to isolate wave forces and allows the hull structure to move with respect to the pipe.

(11) **DEAERATORS** (not shown) condition the warm water to minimize heat exchanger biofouling and corrosion. They also provide valuable by-products, such as oxygen, nitrogen, and carbon dioxide.

(12) **PLANT STARTUP SYSTEM** (not shown) minimizes the size of auxiliary power system needed to start the entire plant. It permits a controlled, smooth startup and provides power for station-keeping when plant is not operating (during maintenance periods).

(13) **BUOYANCY CHAMBERS** are used to float the structure to the plant site. They are then flooded and provide dynamic control of plant submergence level.

(14) **EQUIPMENT DECK** houses the turbine-generator room, control room, electric substation, and other mechanical and electrical equipment. A product manufacturing space is available for production of alternate energy delivery means.

(15) **LIVING QUARTERS** for the crew include recreation facilities. All areas are air-conditioned, using cold water from the plant supply.

(16) **TURBINE-GENERATOR** utilizes a small high efficiency vapor turbine to turn an electrical generator to produce power.

# III. MISSION ANALYSIS

ROBERT COHEN, CHAIRMAN
*Ocean Systems Branch*
*Division of Solar Energy, ERDA*

THIS PAGE

WAS INTENTIONALLY

LEFT BLANK

# ECONOMIC INCENTIVES FOR THE COMMERCIALIZATION OF OTEC

JACK M. NILLES AND BYRON J. WASHOM
*Office of Interdisciplinary Program Development*
*University of Southern California*
*University Park*
*Los Angeles, California*

Abstract

This report examines the needs for, and the alternative means of, federal intervention in the market process through regulatory influence and through provision of various incentives to change the supply and the demand portions of the market process.* We are concerned with the reasons for preferential or other governmental support of OTEC, and with the policy options available to government agencies in this regard.

We are also concerned with anticipating the transition period between demonstration of technological feasibility and widespread commercial application of OTEC. In particular, if OTEC is to be depended upon to supply a portion of the nation's energy demand to replace fossil and fissile fuel use, then adequate economic and public policy environments must exist.

## Decision-Making Criteria

During our research, the three major potential markets found to be most relevant to OTEC technology were the U.S. public utilities, the ammonia and aluminum industries within the U.S., and the thermal gradient belt countries. Each market has its own particular decision-making criteria regarding capital investment and energy supply and demand. The separate decision-making criteria must be well understood by anyone in the process of analyzing the market feasibility of OTEC and recommending appropriate incentives for accelerating OTEC's market receptivity. Furthermore, we also postulated that the primary beneficiaries of the use of the technology must clearly be identified and considered worthy from a political point of view as a prerequisite for the development of economic incentives by the government.

## Public Utilities

We came to three conclusions as to the current attitude towards OTEC of the public utility industry. In general terms, two basic questions were considered: (1) In which technology, among an array of alternatives, should a public utility invest? and (2) Once an investment has been made, what levels of operations should be maintained? The analysis led to the conclusion that high capital costs, technological uncertainties (including transmission uncertainties), present (but possibly waning) dedication to nuclear power by utilities, limited site availability on a national basis, and possibly lengthy licensing time, would limit total investment in OTEC by U.S. utilities. However, should the above conditions be mitigated or eliminated, there are several factors that would cause a reevaluation of investment interests on a regional basis. The probability of having a substantially lower operating cost than any alternative "conventional" energy facility, as well as long-term availability of "fuel," low site costs and minimum environmental impact, would undoubtedly appeal to many public utilities and could cause them to operate OTEC on a continual baseload basis. The absence of any significant ability or desire within these utilities to engage in major OTEC research and the absence of any research plans at EPRI for OTEC leads to the conclusion that OTEC will not be developed by the public utilities and/or related public utility enterprises. The actual status of interconnections and current extent of dynamic baseload management in the Southeast United States need to be studied further in more detail as a next step in assessing the potential market.

## Ammonia Production

We then developed projections for ammonia production, using OTEC plant cost data supplied by Lockheed, and scaled the output to a 900 ST/day, 265 MWe plant. It is important to note that the nitrogenous fertilizer market is based on a derived demand; consequently a sensitive balance of fertilizer-to-crop price ratio is maintained by the consumers. In order for an OTEC plant to be considered feasible in this application, the resulting independence from national gas as a feedstock must have cost savings which outweigh, over the life of the project, the difference in initial capital investment. A $568 million, 900 ST/day OTEC/ammonia plant does not economically compete with an $80 million, 1500 ST/day onshore plant that is dependent on natural gas. Economic feasibility would increase substantially should OTEC/ammonia be available at less than $568 million ($2140/kw) and be able to produce quantities greater than 900 ST/day, or if curtailments of natural gas to the industry

*This paper summarizes the results of a research program at the University of Southern California which was partially supported by the National Science Foundation under Grant No. APR75-18279. The responsibility for the content of this paper rests solely with the authors and not with any organization which may have been associated ... the research.

become so intolerable that substitutes become essential.

Thermal Belt Countries

A third, and potentially the largest, market for OTEC exists in the thermal gradient belt countries lying roughly within 15° of the equator. This band includes the 40 nations possessing the greatest abundance of ocean thermal gradient areas for OTEC operations. The specific applications of OTEC technology in this region are similar to the previously discussed two types of markets; however, the unique characteristics of the foreign owner/operator warrant separate documentation of their decision-making criteria.

Our analysis included consideration of available foreign investment scenarios, geopolitical receptivity, individual LDC's energy posture and the international 15% rule. As a result nine countries were considered to be currently viable for OTEC operation. The high-potential countries are Puerto Rico, Singapore and Brazil, while those of moderate potential are Mexico, India, Philippines, Indonesia, Australia and Malaysia.

During the course of this analysis, some general patterns and trends emerged concerning the existence of foreign markets for OTEC. Demand for rural power, agricultural development, increased exportation of possible OTEC products, natural resource development, existence of economic incentives, and a stable government were the most common factors in identifying favorable countries. Conversely, prohibition of foreign public utility investment, government-owned public utilities, high home equity rules, high rates of inflation, economic stagnation, price controls, and lack of capital were the negative common factors.

## Economic Competitiveness

OTEC is best perceived as a future means of supplementing the national energy supply in helping to meet the energy demands of a specific group of industries and of public utilities. On the basis of their decision-making criteria, there presently appears to be no economic or technological information which indicates that OTEC possesses enough competitive advantages to displace any existing or actively proposed energy plants. Conceivably, OTEC can be utilized in the future if conventional fuels experience high cost escalation over the next two decades and learning curve benefits are experienced in the construction of OTECs.

The costs developed for this analysis were based on those projected by Lockheed, under their contract to ERDA. Our research derived two different sets of cost data, depending upon the material used for the heat exchanger -- titanium or aluminum.

The ERDA/EPRI Power Plant Economic Model was used as a basis for comparing the economic factors for OTEC with those for coal and nuclear energy. Appendix D of our final report to NSF* contains a copy of the model and of the relevant parameters employed in this economic analysis. The primary output of the model is a quantity called the levelized busbar energy cost (LBBEC). This the price per unit of energy (mills/kwh) which, if held constant through the life of the system, would provide enough revenue to exactly equal expenses. The approach taken was to compare units coming on-line in like years and to note their relative cost competitiveness. By cost competitiveness, we mean that the OTEC levelized busbar energy costs must be equal to or less than those of an alternative source.

The LBBEC difference area between the two curves represents the magnitude of the economic incentives that will have to be provided in order to make OTEC competitive (Figure 1).

A second level of comparing costs is concerned with the operating costs of each individual unit. In this context, operating costs include the variable costs of operations, maintenance and fuel. Primarily, this is of concern to public utilities which evaluate baseload units and decide which ones to operate during excess baseload supply periods. Clearly, OTEC, with a levelized operating cost of 2.9 mills/kwh on the 1986 unit, is extremely competitive with like-year nuclear and coal units. Due to fuel escalation, this operating cost advantage for OTEC increases over time (Figure 2).

The third level of comparison relates to the debt, common stock and preferred stock components of the energy sources.* (See Figure 3.)

These three levels of comparison are evaluated differently by each of the three user sectors identified previously. With respect to existing industrial standards and forecast markets, OTEC does not appear to offer distinctive cost advantages which provide substantial market penetration over conventional activities. However, none of the aforementioned costs are so prohibitive as to eliminate the technology from further consideration.

The high initial capital cost in each market analysis exists as the one discouraging economic factor when considering OTEC, for the savings from low operating cost are insufficient to offset the high capital costs on a net present value basis. The reduction of capital costs should be the single, most important goal when developing this technology. These aforementioned cost reductions can be achieved through technological development and with institutional incentives.

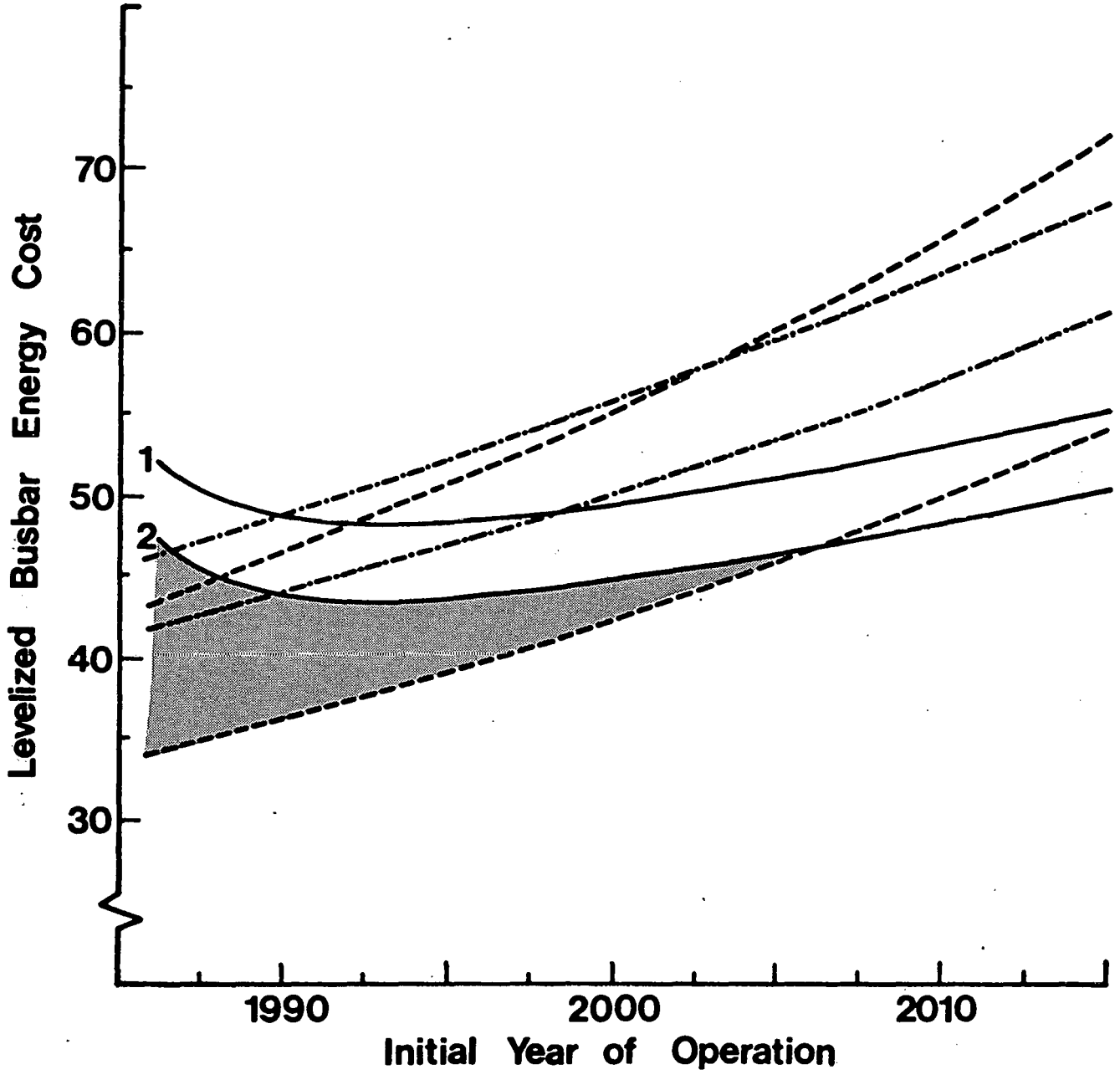
Public funding for the technological development and institutional incentives depends upon the justification for OTEC with respect to other energy options and upon societal demands. Therefore, the basic question is, "Are the national benefits worth the economic and societal costs necessary to provide incentives for the development of OTEC?"

*"Incentives for the Commercialization of Ocean Thermal Energy Conversion Technology (OTEC)"

*There are additional arguments that differential escalation of capital costs will play an important part. The cause of these differential rates is the varying difficulty of meeting environmental and safety standards. These factors were not considered in our analysis.

FIGURE 1

ECONOMIC COMPETITIVENESS OF OTEC,
NUCLEAR AND COAL ENERGY




—— OTEC: 1) Titanium, 2) Aluminum Heat Exchangers
—·— Coal
—— Nuclear
] Upper curves relate to maximum, lower curves to minimum anticipated fuel prices

FIGURE 2

THE VARIABLE COSTS OF ENERGY PRODUCTION

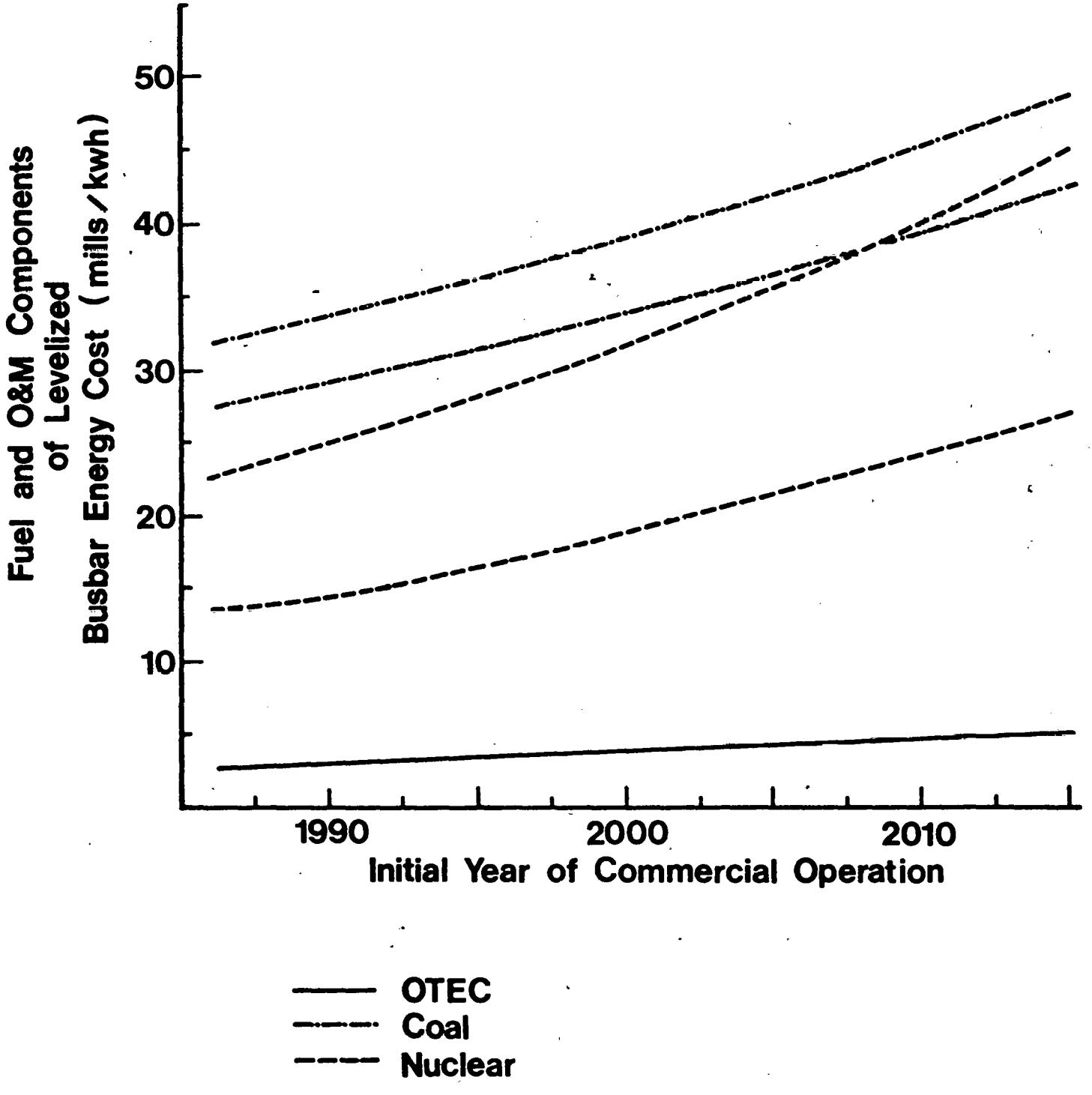
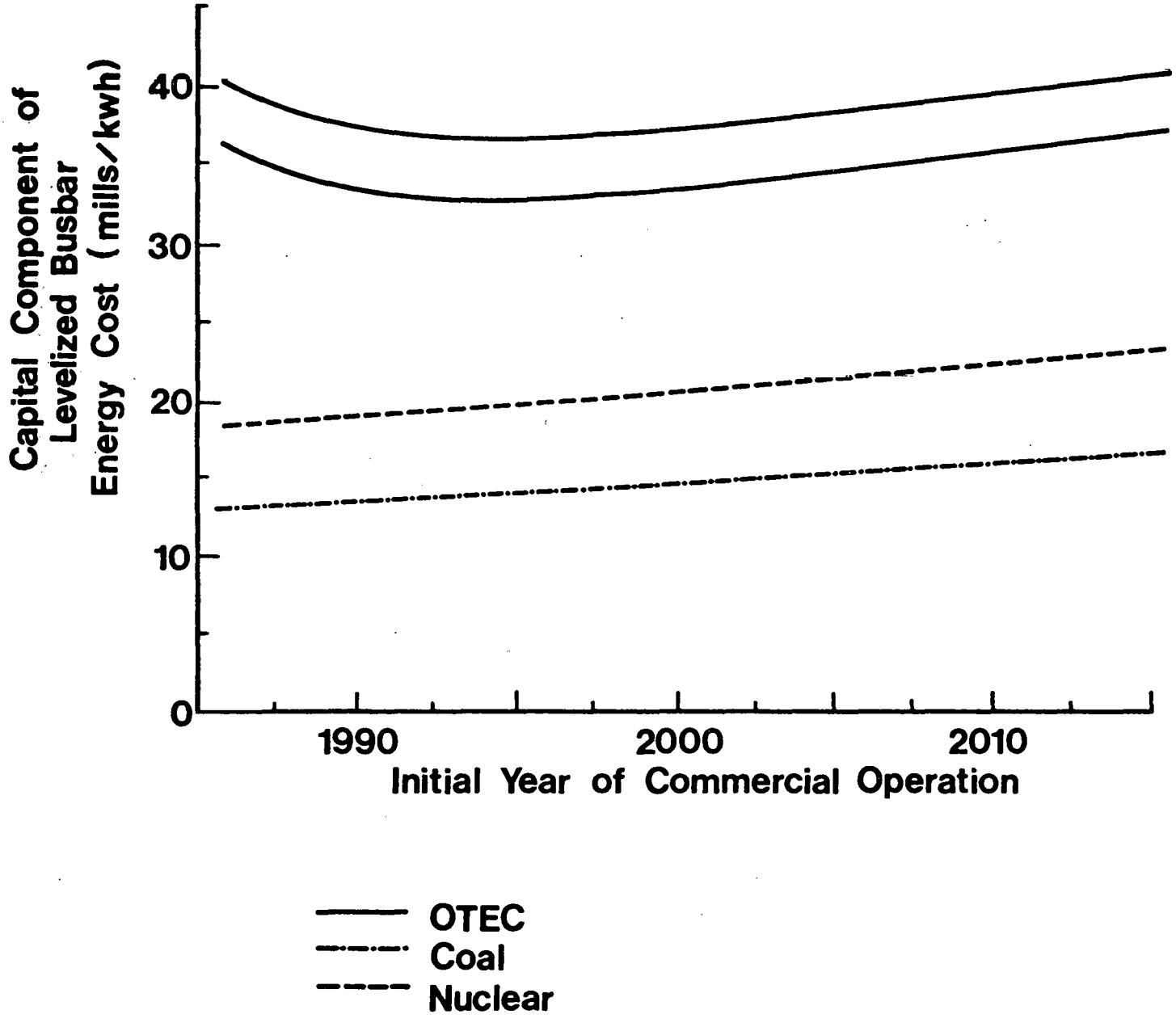


FIGURE 3

CAPITAL COSTS FOR ENERGY PRODUCTION



## Incentives

Potential public policy incentives can be divided into two basic categories. First, push incentives act to accelerate the rate of technological development, increasing the supply of technology, with the anticipation that the demand side of the marketplace will naturally respond. Second, pull incentives are designed to induce an artificial marketplace with the anticipation that technology will naturally respond to the market demands. Not uncommon are push and pull incentives programs to accelerate technology and to alter the marketplace.

In the case of OTEC, the pull incentives primarily should be oriented toward reducing the risk, uncertainties and conflict that will ultimately reduce the cost of debt service and the total capital required. Concurrently pull incentives are required to develop the actual technology. Aside from the purpose of the incentives, there are three primary forms of incentives: institutional, tax and expenditure.

### Institutional Incentives

Institutional incentives are primarily concerned with the formulation of public policy that encourages the development and use of a technology.

Federal legal definition of an OTEC plant as a vessel is probably the most essential institutional incentive involving the economic viability of OTEC (Table 1). Trivial as it may sound, this definition allows access to Maritime Administration subsidy support and associated leverage lease financing as well as guaranteeing the application of tax incentives such as Investment Tax Credit and Foreign Trade Credit.

Another critical institutional incentive involves clarification of the responsibilities and requirements of the Environmental Impact Statement process required by the National Environmental Policy Act.

### Tax Incentives

Although a variety of incentives (and disincentives) exist in the tax laws today, they are not equally applicable to all phases of development of a new technology. In general, the number of incentives available is a function of the maturity of the technology in question. That is, few incentives are available at the research and development phase, while most are available at the commercialization phase of technology innovation.

The incentives for OTEC were first examined in terms of their applicability at various phases of development of the technology. They are summarized in Table 2. Single X's denote some applicability while double X's denote major applicability of a particular incentive in the Table. It was found that the Investment Tax Credit and Accelerated Depreciation were the two most effective means for reducing capital costs for OTEC.

It is important to note that, in order to give OTEC or other unconventional energy technologies an advantage over conventional technologies, these tax incentives and the expenditure incentives must be applied preferentially, that is to the unconventional technologies and not to the others, in order to have maximum effect. Clearly, a decision for development of preferential incentives must considered carefully in terms of the broader scale effects of such policies on the economy. Tax policy does appear to be an effective method for expressing broad national policies in quantified form. However, the ability of tax incentives to have a detailed, specific effect on the particular energy technologies developed is limited. Direct expenditure incentives which offer the government more flexibility in technical supervision, cost controls, and reevaluation of national energy goals, have the potential for greater impact on the more particularized problems of developing (if not disseminating) an energy technology.

Of the panoply of available tax incentives, three points are quite important to make regarding OTEC:

1) Leverage Leasing will become an integral part of OTEC commercialization. In essence, it allows an owner/operator to lease an OTEC plant at a rate much less than it would cost him to own it directly.

2) Corporate structures capable of utilizing the full tax benefits would have to be permitted and available.

3) Accelerated Depreciation and Investment Tax Credit, as reflected in Table 2, are the major tax vehicles.

Only the largest of financial institutions will have the capital resources to extend the venture capital necessary for the initial seven OTECs, and only these institutions will be large enough to fully utilize the tax credits and deferrals. It is therefore recommended that further consideration be given to allowing formation of advantageous corporate structures to fully attract the private capital resources necessary. This will in turn reduce the dependency of OTEC development upon direct expenditures by the federal government.

### Expenditure Incentives

The history of federal government efforts to encourage and influence private-sector investment in certain preferred directions and endeavors is replete with examples of expenditure incentives. Although they have differed widely in focus and substance in the past, government programs have included such types of expenditures as:

1) Direct grants
2) Direct loan programs
3) Loan guarantee programs
4) Interest subsidies
5) Price supports
6) Product procurement

Each of these types of expenditures was examined during our research with respect to its effectiveness in accelerating the development of OTEC.

Potential incentives are evaluated on the basis of

TABLE 1

INSTITUTIONAL INCENTIVES RECOMMENDATIONS

| Recommendation | R&D | Advanced Development | Proof-of-Concept | Commercial-ization |
|---|---|---|---|---|
| Promulgate Coherent Federal Energy Policy | X | | | |
| Clarify EIR Requirements | X | X | X | X |
| Flexible Patent Policy | X | | | |
| Clarify State-Federal Jurisdictions | | | X | X |
| One-Stop Permit System | | | X | X |
| Clarify International Ocean Legal System | | | | X |
| Create Site Distribution System | | | | X |
| Treat OTEC Plants as Vessels | X | | | X |
| Regulate Public Utilities Equitably | X | | | X |

TABLE 2

SUMMARY OF EXISTING TAX INCENTIVES

| | I. R&D | II. Prototype | III. Demonstration | IV. Construction | V. Commercialization |
|---|---|---|---|---|---|
| EXISTING TAX INCENTIVES | | | | | |
| Expenses & Losses | | | | | |
| a. R&D Expenses | x | x | x | | |
| b. Losses | | x | x | x | x |
| c. Depreciation | | x | x | x | xx |
| d. Investment Credit | | x | xx | xx | xx |
| e. Interest | | | x | x | x |
| Corporate Structures | | | | | |
| a. Consolidated Returns | | x | x | x | x |
| b. Corporate Organizations & reorganizations | | x | x | x | x |
| c. Dividends | | | | x | x |
| d. Small business stock Losses | x | x | x | | |
| e. Interest | | | | x | x |
| Foreign Operations | | | | | |
| a. Foreign Tax Credit | | | | | x |
| b. Domestic International Sales Corporation | | | | | x |
| c. Possessions Corporation | | | | x | x |
| EXISTING TAX DISINCENTIVES | | | | | |
| a. Depreciation Recapture | | x | x | x | x |
| b. Investment Credit Recapture | | x | x | x | x |
| c. Foreign Personal Holding Company | | | | | x |
| d. Controlled Foreign Corporations | | | | | x |

1) Cost to Government
2) Effectiveness and Flexibility
3) Competitiveness and Breadth of Industry Involvement
4) Administrative Feasibility and Flexibility
5) Degree of Federal Involvement

The options are rather numerous, as Table 3 reflects.

## Recommendations

*In all of the cases where we list expenditure incentives, they refer to the highest cost case of OTEC design (i.e., plants with titanium heat exchangers) compared with the lowest cost LWR nuclear alternative. Hence, they are the "worst case" incentives under the assumptions we have used.*

### Research and Development Phase

The following are recommendations concerning the R&D phase:

1) Direct expenditures of grants and contracts by ERDA, and possibly by the Maritime Administration, represent the most significant and mandatory incentive to be applied during the continuation of R&D. Manufacturers, EPRI, or the relevant customers of OTEC cannot be expected to perform the necessary R&D in the absence of federal grants and contracts.

2) The classification of OTEC as a vessel provides major institutional and economic impacts during all phases of commercialization. In the R&D phase, it directly affects the design and economics of OTEC. In construction and operation, vessel status will give access to Maritime Administration subsidy support, leverage lease financing, and guarantee the application of tax incentives such as Investment Tax Credit and Foreign Trade Credit. No other institutional action has a more far-reaching impact: thus, our strongest recommendation is that OTEC's status as a vessel, under the terms of the appropriate legislation, be established as soon as possible.

### Prototype Phase

Current ERDA plans call for construction of a 25 MWe power cycle test as part of the prototype phase. As noted in the ERDA program plan, it would be desirable that this event, in 1983, be supported by private industry, with some incentives provided. Although we are skeptical about private industry being sufficiently motivated at that point for such a huge undertaking, the following incentives could be applied which would aid the industry's financial situation:

1) Continue the direct grant and expenditure program established under the R&D phase, begin to emphasize the role of cost sharing, and develop a convertible grant to loan program.

2) Provide push incentives that would encourage contractors and subcontractors to participate in the prototype program. The key tax incentives include favorable treatment of expenses and losses, the use of tax avoiding corporate structures and removal of the disincentives of depreciation recapture and investment credit recapture for the necessarily short-lived prototype.

3) Institutionally, the necessary permits for the testing of the prototype would have to be obtained in a timely fashion.

### Demonstration Phase

The demonstration phase would entail the construction and the in situ operation of a 100 MWe OTEC for the purpose of demonstrating the technology and verifying the performance standards. This demonstration phase could conceivably cost a total of $300 million. It is during this phase when sufficient push incentives and some pull incentives should be provided in order to commit the manufacturers and consumers to put up their own venture capital. Therefore, the recommended scenarios:

1) Solicit construction bids for a 100 MWe demonstration project, with the successful bidder being the one who offers the best combination of low price and high percentage of cost share. The rationale for requiring cost sharing would be to attract and commit those companies that foresee a future market in OTEC.

2) The tax provisions established for the demonstration of OTEC technology will directly impact the likelihood that contractors and subcontractors will participate and it will affect corporate structures that will be established for the demonstration and construction phases. Foremost in these considerations will be allowing leverage lease financing, classification as a vessel and generally the eligibility of as many tax incentives programs as are available; favorable depreciation, tax deferrals and treatment of interest during construction. The financial community and corporations engaged in OTEC commercialization will be seeking an early return on their investment through tax credits; this requires establishment of these incentives at least one year prior to any serious plans for engaging in commercialization.

### Construction Phase, Early Production

The construction phase incentives are subdivided (somewhat arbitrarily) into an initial set of units (1-7) and the later production units (8+), since we postulate that the incentives needed for the initial seven units would no longer be required for the later production units. It is during the construction phase that the full breadth of options becomes available. The major recommended incentives for the initial units are:

#### Expenditures

1) Loan guarantees up to 80% of the capital costs, with a total authorization of $3.0 billion.

2) Interest subsidies for the difference between the applied and prime interest rates up to 4% above the prime rate.

3) Government-subsidized "vessel" insurance.

TABLE 3

APPLICATION OF CANDIDATE INCENTIVES TO DEVELOPMENT PHASES

| Incentives | Phases I. R&D | II. Advanced R&D Pilot | III. Demonstration | IV. Construction | V. Operation |
|---|---|---|---|---|---|
| **GRANTS** | | | | | |
| 1. Direct grant | x | x | x | | |
| 2. Convertible grant | | x | x | | |
| 3. Other | | x | x | | |
| **LOANS** | | | | | |
| 1. Direct loan | | x | x | x | |
| 2. Loan guarantee | | x | x | x | |
| 3. Interest subsidy | | | | x | x |
| 4. Increase bank loan reserves | x | x | x | x | x |
| 5. Combination w/price guarantees | | | x | x | x |
| 6. Other (e.g., maritime types) | | | | x | x |
| **PRICE GUARANTEES** | | | | | |
| 1. Guaranteed price | | | | | x |
| 2. Guaranteed price w/loan guarantee | | | x | x | x |
| 3. Guaranteed price (alternative) | | | | | x |
| 4. Guaranteed price/loan guarantee (alternative) | | | | x | x |
| 5. Limited price & loan guarantee | | | | x | x |
| 6. Limited price guarantee/ advance payments | | | | x | x |
| 7. Sale of options/guararteed price | | | | | x |
| 8. Tariff & import quotas (indirect) | | | | | x |
| 9. Other--combination w/guaranteed price support | | | | | x |
| **GOVERNMENT PROCUREMENT** | | | | | |
| 1. Guaranteed procurement (fixed price) | | | | | x |
| 2. Guaranteed procurement (cost + fixed price) | | | | | x |
| 3. Two-step commercial procurement | | | | x | x |
| **INSURANCE** | | | | | |
| 1. Insurance or indemnity fund | | | | x | x |
| 2. Market loss insurance | | | | | x |
| 3. Market catastrophe insurance | | | | | x |
| **GOVERNMENT PLANT OWNERSHIP** | | | | | |
| 1. Government operation | | x | x | x | x |
| 2. Corporate Operation under Contract | | x | x | x | x |

4) Convertible grant to loan (although we estimate that the initial units will not be economical enough for grantee ever to exercise his conversion option).

Tax Incentives

1) Only the largest of financial institutions will have the capital resources to extend the venture capital necessary for the initial seven OTECs, and only these institutions will be large enough to fully utilize the tax credits and deferrals mentioned previously. It is therefore recommended that serious consideration be given to allowing advantageous corporate structures to form to fully attract the private capital resources necessary that will in turn reduce the dependency upon direct expenditures by the federal government.

2) Allow corporate structures mentioned in the R&D phase recommendations.

3) Allow the leveraged lease financing and accelerated depreciation of an OTEC.

4) Raise investment tax credit on "unconventional" energy sources to 15% instead of 10%.

5) Allow favorable treatment of interest during construction.

Institutional

1) Prepare EIS addressing the extraterritorial aspects of OTEC.

2) Clarify the International Order that would govern the international permissibility of OTEC operations beyond the current 3-mile Territorial Seas.

3) Create an OTEC site distribution system to mitigate any potential conflicts.

4) Provide favorable investment recapture treatment by Public Utilities Commissions (or the equivalent) where the owner/operators are public utilities.

Construction Phase, Later Production

The incentives required for the later production units would be substantially reduced to minimize the outflow of public funds. The remaining incentives to maintain OTEC's economic competitiveness would be:

Expenditures

1) Grant 80% loan guarantees for that sum which remains authorized but unappropriated.

2) Provide interest subsidies for the difference between the applied and prime interest rate, up to 2% above the prime rate.

3) Provide government-subsidized "vessel" insurance.

4) Give convertible grants to loans.

5) Allow construction differential subsidies if foreign shipyards begin to compete.

Tax Incentives

1) Continue to allow accelerated depreciation.

2) Continue to allow leverage lease financing of OTECs.

3) Maintain favorable corporate structures.

4) Eliminate existing disincentives.

Institutional

1) Continue to provide for protection of existing OTECs.

Operational Phase

The operational phase incentives would be provided primarily to eliminate any remaining economic differential between OTEC and conventional baseload sources. The precise incentive mechanism that should be applied would depend upon the owner/operator of the OTEC and the market being served. The eligible mechanisms include vessel insurance, guaranteed price for the product, market loss insurance, market catastrophe insurance, tariffs and import quotas, limited price guarantees and/or guaranteed procurement.

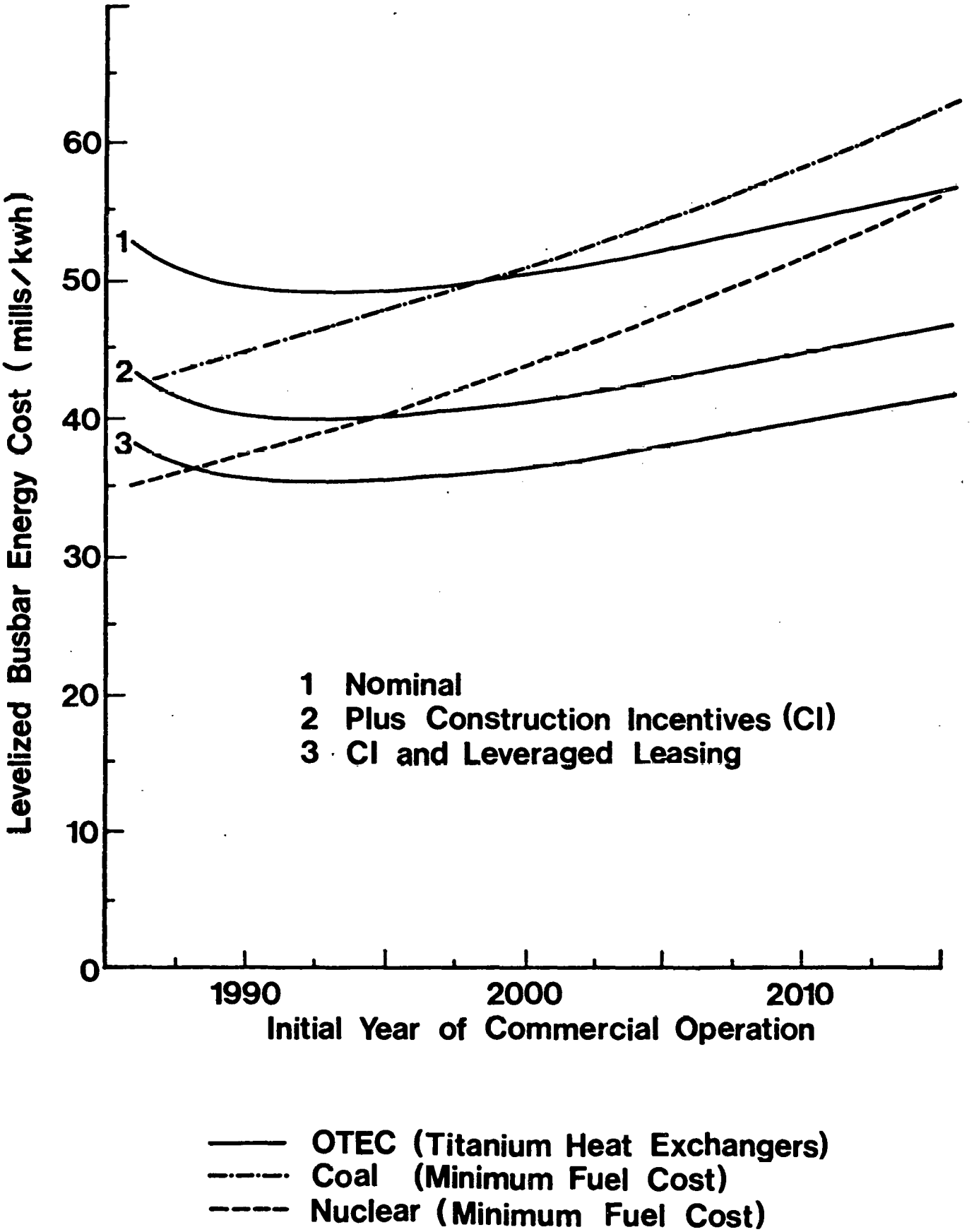
The incentives applied would be established on a unit-by-unit basis, for the amount and type of operating subsidy would be highly dependent upon the permissibility of leverage lease financing and the classification of the owner/operator of OTEC. Figure 4 illustrates that if leverage lease financing is available then only the first two OTEC units would require an operating subsidy, amounting to $300 million over the plants' 30-year life. If leverage lease financing were not possible then the operating subsidies would have to extend to the first 16 units, and the total authorization would amount to $2.66 billion over a period of 46 years. In essence, the eligibility of OTECs to be financed by leveraged leases reduces the dependency upon government expenditures by $2.36 billion over a period of 46 years.

Effectiveness of the Proposed Recommendations

The impact of the incentives proposed by this study should represent an effective and efficient means of accelerating the demonstration and commercialization of OTEC. Figure 4 depicts the effectiveness of the proposed incentives upon the levelized busbar energy costs of an annually-produced OTEC with titanium heat exchangers. The proposed R&D, Prototype, Demonstration, and Construction incentives were collectively able to shorten the time required to reach the indifference point on the cost curve. The previous indifference point year with minimum nuclear fuel costs schedule was 2015 (see Figure 1). This indifference point is moved to the year 1989 with the construction and leveraged lease financing incentives applied. For the succeeding years after the indifference point is reached, incentives can be rolled back substan-

FIGURE 4

BUSBAR ENERGY COSTS WITH RECOMMENDED INCENTIVES



tially without drastically altering the economic competitiveness. Thus, our original hypothesis proved correct: if sufficient expenditure and tax incentives could be provided for that period required to realize the effects of the learning curve, the high escalation rates of coal and nuclear fuel would soon make OTEC economically competitive.

It should be reiterated that the comparison in Figure 4 is between the most pessimistic OTEC costs and the most optimistic nuclear energy costs. When compared to coal energy, OTEC would have an 11% cost advantage on a busbar energy cost basis beginning in 1986, and expanding substantially in ensuing years. The need for extensive OTEC incentives would therefore not be as necessary if it is determined in the future that coal will represent a substantial source of baseload energy in the regions which OTEC would service. Furthermore, all of the cases computed used a capital cost escalation rate of 5% per annum, regardless of the type of power plant being considered. But, because of additional escalation factors related to the costs of equipment required to meet environmental standards, both coal and nuclear plants may have substantially higher capital escalations than shown here. The effect of these would make OTEC competitive earlier.

## Costs of the Proposed Recommendations

The recommendations put forth in this report can be divided into three basic time periods: 1977-1986, 1986-1993, 1993-2010. Each period represents a specific phase in which distinct economic and institutional incentives must be applied to make OTEC technically feasible and economically viable. We have estimated the effectiveness of the selected incentives in making OTEC economically competitive in the early 1990's on an individual plant basis. However, we must also examine the total costs for these incentives. By thus incrementalizing the phases and costs, definite decision nodes in the future can be identified for future public policymakers to weigh the emerging technical and economic information regarding OTEC.

### R&D to Initial Production

The period 1977 to 1986 would require approximately $500 million of direct government grants and contracts to successfully complete a 100 MWe demonstration program. The distribution of costs might be as follows:

$100 million in R&D expenditures
$100 million in Prototype expenditures
$300 million in Demonstration expenditures
$ 20 million in private capital investment
$ 80 million in private expenditures

### Initial Production

The period 1986 to 1993, represents the time required to produce the initial seven OTECs at a rate of one per year. The first seven units were determined as a differentiation point since the learning curve benefits are maximized during this period and level off thereafter; furthermore, the seventh unit reaches the indifference point when only the construction incentives are applied. Thus, the first seven units have been identified as those which would require substantial subsidies over the lifetime of the plant. *Therefore, the following expenditures represent the authorizations during this period (in 1976 dollars), but the appropriations would occur over the succeeding thirty years.* (They do not include the effects of inflation.)

$2900 million in interest subsidy authorization
$ 300 million in operating subsidy authorization
$3000 million in loan guarantees

The actual costs during the seven-year period would amount to a substantially smaller figure of $795 million. The breakdown would be:

$641 million in interest subsidies
$ 65 million in operating subsidies
$189 million in tax expenditures

$795 million in total expenditures

### Later Construction

The period of 1993 to 2010, represents the operation of the initial seven units and the construction and operation of the next eighteen units. During this period, expenditures would be incurred from previous authorizations and new authorizations would be required to cover the production units. The eighteen production units' authorization would be:

$2930 million in interest subsidy authorization
$ 100 million in loan guarantees

The corresponding expenditures during the seventeen-year period would be:

$1500 million in interest subsidies for initial units
$1642 million in interest subsidies for production units
$ 170 million in operating subsidies
$ 800 million in tax expenditures

$3112 million in total expenditures

The final period of 2010+ represents the residual expenditures for incentives authorized in the previous two periods. No authorizations would be necessary, but the appropriations could be:

$ 639 million in interest subsidies for initial units
$1297 million in interest subsidies for production units
$ 65 million in operating subsidies

$2001 million in total expenditures

## Conclusions

It seems clear that the level of economic investment associated with the development of a capital intensive new energy source such as OTEC, is so great that private industry alone cannot reasonably be expected to pursue this technological innovation. It appears that the federal government alone has the necessary resources and mechanisms at its disposal to orchestrate the sensitive application of push and pull incentives required to eventually develop the technology and market for OTEC. The rate at which the goal of eventual technological feasibility and economic viability will be achieved is a direct function of the level of support given by public policy.

The high level of economic support required for development of OTEC technology clearly constitutes a considerable barrier. However, there are three counterbalancing factors which also must be considered. First, the construction of the first few OTEC plants under conditions of substantial subsidy will result in an energy contribution exclusively within the United States. The learning experiences resulting from operation of the first few units will act to develop a competitive market, particularly if fuel costs continue to escalate and if capital costs of conventional plants increase at a higher rate than we have predicted. This long-term demonstration of the technology on a commercially feasible basis will greatly increase the potential for exportation and lease of OTEC plants abroad; we remain confident that this latter market is potentially the greatest. The loan guarantee authorization of $3 billion will, in effect, accelerate the rate at which U.S. corporations and public utilities will qualify early in the program, thereby developing the commercial infrastructure at a greater rate.

Secondly, the estimates given for a 4% differential interest subsidy on the initial units and a 2% differential interest subsidy on later units represent the upper limit of the potential need. It is not likely that financial institutions would demand up to 4% above the prime rate on qualified investors under an 80% loan guaranteed project. However, during the initial stages, the apprehension on the part of financial institutions for the long-term viability of new energy technologies, OTEC's dependence on public policy support, the lack of prior commercial demonstration, and the use of highly leveraged firms for ownership of OTEC plants, would clearly prompt these financial institutions to raise interest rates above the prime to reflect these uncertainties.

Finally, OTEC has a significant importance in that it is the only nonnuclear, nonfossil fuel baseload energy option available to the United States which does not use some form of energy storage. We feel that a national energy program which systematically develops and demonstrates OTEC technology is worth pursuing, based on the evidence available to date. The process of a staged technology development which has been recommended by ERDA is consistent with a sound process of continual review and evaluation of the merits of OTEC in terms of the public investment required for its development. This continuing process will afford public policymakers the opportunity to make conscientious and intelligent decisions as the results of OTEC's research and development phase progress.

# LEGAL, POLITICAL, AND ENVIRONMENTAL ASPECTS OF OCEAN THERMAL ENERGY CONVERSION: A REPORT ON AN ASIL/ERDA STUDY

H. GARY KNIGHT
*Louisiana State University Law Center*
*Louisiana State University*
*Baton Rouge, Louisiana*

ROBERT E. STEIN
*International Institute for Environment and Development*
*1525 New Hampshire, N.W.*
*Washington, D. C.*

J. DANIEL NYHART
*10-219 Massachusetts Institute of Technology*
*Cambridge, Massachusetts*

Abstract

The deployment of ocean thermal energy conversion (OTEC) devices in the world ocean raises a number of domestic and international legal, political, and environmental problems. International aspects include jurisdiction to deploy and operate OTEC devices, political implications of such deployment, regulation of operations, and protection of the marine environment. Domestic aspects include multiple use of ocean space, state and Federal regulation, responsibility and liability for damage to and by OTEC devices, protection of the marine environment, financing, and general economic issues. The American Society of International Law, pursuant to an NSF-ERDA grant, commissioned studies on these and related problems during 1975, the results having been disseminated at a workshop held in Washington, D. C., on January 15-16, 1976. The study provided an overview of legal/political problems contemporaneously with technical research work on OTEC devices. Since legal/political issues have usually been raised after the perfection of a new technology, this approach affords an opportunity for current feedback to forestall impediments to implementation of OTEC projects.

## Introduction: Methodology of Study

In 1974 the American Society of International Law ("ASIL") obtained a grant from the National Science Foundation ("NSF") to investigate the legal, political, and environmental implications of ocean thermal energy conversion ("OTEC") devices. The grant later came under the administration of the Energy Research and Development Administration ("ERDA"). The study requested was unique because it sought to identify and analyze legal and related nontechnical issues at the same time that fundamental work was being undertaken on the technical feasibility of OTEC devices.

In the past, legal and policy questions have often been deferred or not raised at all until a new technology reached the stage of practical application. The adverse effects of late blooming jurisdictional and environmental impediments to implementation of new technologies has a well known history, some examples being the SST, the Alaskan pipeline, and outer continental shelf oil and gas development.

The study commissioned by NSF/ERDA sought, in part, to avoid this error of the past by considering legal, political, environmental, and related issues from the outset, simultaneously with the development of OTEC technology. If the study results in appropriate action to ameliorate probable legal and political impediments, and if OTEC proves feasible and the deployment stage is reached, then hopefully no significant time loss would be incurred as a result of newly discovered non-technical problems. The study would presumably have alerted decision makers to the issues, and proper legislative, regulatory, or other action would have been taken to coincide with the target deployment date.

Another benefit of this approach was the interaction between the study group members and representatives of the companies (TRW and Lockheed) performing the basic feasibility studies. If legal or political problems discovered by the study group can be ameliorated at a pre-deployment stage by technological modifications, legal problems which might otherwise prove to be serious impediments to OTEC deployment could be eliminated entirely. Likewise, sufficient knowledge of the technology at hand on the part of study group members enabled them to identify problems which might otherwise have escaped their attention. Accordingly, the interaction of technology and law in this study may prove to have beneficial effects both for the developers of the technology and for the public interest.

The ASIL's approach to the study, which had

been utilized in prior ASIL projects, was to form a panel of experts in various fields such as law of the sea, environmental law, political science, and economics. Issues were then identified by the principal investigator and the two project co-managers, and research papers were commissioned to members of the Panel (a list of the OTEC Panel members is set forth at the conclusion of this paper). The Panel met five times during 1975 at ASIL headquarters in Washington, D. C. to critique the papers in first, second, and final draft form. This inter-disciplinary exchange process resulted in improvements in each draft of each paper, and also provided a wider range of inputs to the respective authors than could have been achieved by any author working alone.

Because the study's purpose was not to reach any definite conclusions but rather to identify and analyze legal, political and other issues which could have an effect on OTEC deployment, the papers were ultimately presented, without specific conclusions or recommendations, at a workshop held in Washington, D. C., on January 15-16, 1976.

## Some Major Issues Raised

Because the papers are for the most part quite long and detailed, this portion of the paper will simply identify each major issue area discovered, identify the paper commissioned and its author, and give a brief synopsis of the paper's contents. Those interested in pursuing particular issues further can obtain copies of the full texts through one of the methods indicated in the conclusion. The legal, political, environmental, economic, and other issues raised cover both international and domestic problems, the first four issues described below being concerned basically with international matters.

### 1. International Issues.

#### a. Jurisdictional Problems.

A nation's or an individual's right to make a particular use of the ocean depends on the jurisdictional legal regime applicable to the site in question. The right to deploy and operate OTEC devices depends on the particular zone of ocean space involved (e. g., territorial sea, economic resource zone, high seas). The legal content of such zones is in flux, with the final legal regime dependent on the outcome of the current law of the sea negotiations and the Third U.N. Law of the Sea Conference. It seems relatively certain, however, that coastal states will possess authority sufficient to warrant the deployment of OTEC devices off their coasts to a distance of 200 miles. Beyond 200 miles the outcome is less clear. A problem also exists with respect to "ownership" of ocean thermal energy. For the present it seems likely that it will be considered a "free" resource, with "ownership" vesting in the nation or person who first makes use of it. However, recent international economic developments, particularly involving underdeveloped nations (the so-called "new international economic order") indicate that international control over many ocean resources, perhaps including thermal energy, may not lie in the too distant future.

There are other, less compelling, problems raised by international law. For example, the protection of OTEC devices from accidental or deliberate interference may necessitate the promulgation of safety zones surrounding such installations. OTEC's may be subject to international terrorism. Issues will also arise concerning inspection, flags of convenience, and cables transmitting power to shore.

All of these questions are addressed in the paper by Prof. H. Gary Knight entitled "International Jurisdictional Issues Involving OTEC Installations," in which the author discusses the present state of the international law of the sea, the trends in development of that body of rules, and such concepts as the economic resource zone, the "common heritage of mankind," and the regulation of scientific research in the ocean. He also focuses on the "reasonable use" theory as a legal basis for deployment of OTEC installations.

#### b. Political Problems.

The international political ramifications of OTEC are discussed by Dr. Ann Hollick in "The International Political Implications of Ocean Thermal Energy Conversion Systems." Though such impacts are difficult to ascertain because of the time frame and the many variables involved, an examination of current international developments does indicate some possible future developments which could interact with OTEC. The paper discusses such issues as the political geography of OTEC operations, international political factors affecting OTEC, and operational issues affecting OTEC. Of particular interest is the possible effect on energy relations between developed and underdeveloped nations stemming from the fact that, with the exception of the United States, the nations situated within the equatorial band conducive to OTEC deployment are not major consumers of energy at the present time. Depending on the the quantity of OTEC energy produced, this could provide a new basis for "north-south" energy relations.

#### c. Regulatory Problems.

In "International Regulatory Authority Concerning Ocean Thermal Energy Conversion Devices," Capt. C. R. Hallberg observes that although there are no international organizations which can be said to be clearly seized with authority or competence to deal with OTEC devices at present, it is certain that some agencies will assert jurisdiction at or prior to the time of deployment. There are obviously national and international public interests of some importance to be protected -- environmental protection, labor standards, general economics of operation, safety of life and property at sea, to mention the more important -- and there is a multiplicity of international organizations apparently competent to deal with each such interest. The most likely body to become involved, however, is the International Maritime Organization (formerly IMCO) which is concerned with such matters as pollution of the sea by oil and safety of life at sea. Work already underway on the subject of ocean data acquisition systems (ODAS) by the International Oceanographic Commis-

sion (IOC) could also have an impact on OTEC deployment. These problems will not be ameliorated by the establishment of 200 mile economic resource zones under national (coastal state) control, for activities in such zones will still be subject to agreed international standards concerning pollution, safety, and so forth.

d. Environmental Protection.

One of the most important international issues analyzed is that of protection of the marine environment, addressed in Robert E. Stein's paper entitled "Ocean Thermal Energy Conversion: International Environmental Aspects." OTEC's may cause changes in ocean temperature and perhaps in the atmosphere which could have impacts far from the site; water intake and exhaust could affect biologic conditions and fish life in broad areas of the water column; and the use of fluids and chemicals of a potentially hazardous nature could produce adverse effects if spilled. Although some legal precedents exist to deal with international pollution, new initiatives stemming from the Stockholm Conference on the Human Environment and the United Nations Environment Program (UNEP) are more likely to have significant effects on OTEC deployment. There are also a number of international agreements which may impact OTEC, such as the 1972 Ocean Dumping Convention and the 1973 IMCO Convention for the Prevention of Pollution from Ships. The paper dealing with this subject concludes that there will inevitably be environmental effects from OTEC deployment and that there will as a result be a growth in multilateral regulation of OTEC devices.

2. Domestic Problems.

a. Multiple Use.

As the diversity and intensity of the use of ocean space has increased over the past three decades, several conflicts have arisen over proper allocation of resources or space in the marine environment. The list of old and new uses is long -- continental shelf oil and gas, merchant shipping, fishing, artifical islands, military operations, oceanographic research, dumping of wastes, deep seabed mineral mining -- and the introduction of still another use is certain to create at least minor conflicts with existing users of the area. In addressing this problem in his paper "Spatial and Emerging Use Conflicts of the Ocean Space," Dr. Byron Washom first identifies all of the significant present and emerging uses of the ocean, demonstrating that the intensity and diversity of ocean space use is already causing problems of accommodating conflicts for the same space or resources. The paper then identifies a range of probable conflicts of OTEC with a section on possible methods for the adjustment or resolution of such conflicts.

b. Regulatory Problems.

A common current complaint of the populace is overregulation by an increasingly large and pervasive state and Federal bureaucracy. Nowhere is this more evident than when one seeks to make a particular use of a portion of ocean space under the jurisdiction of the United States. Permits or approvals must be obtained from a plethora of departments, agencies, and bureaus. Often there is little or no effort toward consolidation or coordination of these requirements. James C. Higgins, Jr.'s paper, entitled "Ocean Thermal Energy Conversion Plants: Federal and State Regulatory Aspects," identifies a long list of state amd Federal agencies which will undoubtedly assert jurisdiction with respect to OTEC devices. Over a dozen such agencies are identified and the bases for their jurisdiction analyzed -- including the Army Corps of Engineers, the Coast Guard, ERDA, the Federal Energy Administration, the Federal Power Commission, and the Departments of Defense, Commerce, Interior, and Labor. The major problem foreseen is the multiplicity of permits and approvals which would have to be obtained before deployment.

c. Responsibility and Liability.

J. Daniel Nyhart's paper, "Problems of Legal Responsibility and Liability to be Anticipated in OTEC Operations," deals with the thorny questions of who bears the burden of responsibility for damage to or by OTEC devices, and who is ultimately liable for any such damage. Even though procedures for conflict avoidance may be developed, as pointed out in Dr. Washom's paper, it is inevitable that some other user of ocean space (perhaps a vessel) will cause damage to an OTEC, or that an OTEC will (perhaps through pollution or inadvertant collision) cause damage to some other object or area of land. This paper examines the applicability of traditional maritime law concepts to OTEC (including the issue whether OTEC devices will be considered as "vessels" for purposes of admiralty law), as well as complicated questions of liability resulting from various financing arrangements such as ship mortgaging and leveraged leasing. Because of the problems involved in applying "old" law to "new" technologies, it may be necessary to secure legislation specifically directed at OTEC devices.

d. Environmental Problems.

In his paper "Ocean Thermal Energy Conversion: Domestic Environmental Aspects," Thomas B. Steol addresses the effect of the National Environmental Protection Act (NEPA), subsequent litigation, and environmental impact statements. This paper differentiates between the research and development stage, the demonstration stage, and commercial development in discussing the likely applicable domestic environmental laws and regulations.

e. Financing.

"Legal Aspects of Financing Ocean Thermal Energy Conversion Plants," by John H. Riggs, Jr., analyzes a wide range of possible financing devices for OTEC. Included in the discussion are the financing of privately owned OTEC plants through such devices as unsecured debt or equity financing by the corporate owner, ship mortgage financing, and lease financing; financing of government owned OTEC plants; and mixed forms of financing. Riggs concludes that capital should be available for OTEC financing, despite the looming competition for capital funds over the next 10-15 years, but

that much will depend on the willingness of the Congress and the Executive branch to make available federal loan guarantees and tax advantages for such financing.

f. General Economic Analysis.

Finally, Prof. Carlos Stern, in "Economic Issues Related to Ocean Thermal Energy Conversion Plants" has addressed a wide range of general economic questions. Among the issues with which he is concerned are electric power in a utility system (power demand and market), the potential market for OTEC energy, cost comparisons between OTEC and other energy sources, cost estimates for OTEC, and direct on-site processing of OTEC electricity.

## Conclusion

Although the study was not designed to produce definite conclusions or make specific recommendations, it seems clear from the papers prepared that a variety of legal, political, and economic problems face OTEC, both at the domestic and at the international level. Consideration needs to be given, therefore, by appropriate legislative and executive personnel, to methods for coping with these impediments prior to the time that OTEC deployment -- even in the demonstration stage -- is upon us. One possible approach is to continue the work of the OTEC Panel, this time focusing on specific jurisdictional, legislative, and regulatory methods for coping with the problems already identified.

All of the papers described in this summary will be available shortly in a hard-cover book published under the auspices of the ASIL. Prior to that time a limited number of copies of the typescript versions remaining from the January 15-16, 1976, workshop will be available from the ASIL. Resort to individual authors is also appropriate for single issues. A list of the authors and OTEC Panel members, and their affiliations, is contained in the annex.

## Annex

OTEC Panel members and paper authors: Robert E. Stein (International Institute for Environment and Development), Prof. H. Gary Knight (Louisiana State University Law Center), Prof. J. D. Nyhart (Massachusetts Institute of Technology), Bennett Boskey (Volpe, Boskey & Lyons; Washington, D. C.), Dr. Robert Cohen (ERDA), Capt. C. R. Hallberg (U.S. Coast Guard), James C. Higgins, Jr.(Offshore Power Systems, Jacksonville, Fla.), Dr. Ann Hollick (Woodrow Wilson International Center for Scholars, Washington, D. C.), Dr. Arthur Konopka (NSF), John H. Riggs, Jr. (White & Case; Brussels, Belgium), Prof. Warren M. Rohsenow (Massachusetts Institute of Technology), Dr. Herman E. Sheets (Univ. of Rhode Island), Prof. Carlos Stern (Univ. of Connecticut), Thomas B. Stoel, Jr. (National Resources Defense Council, Washington, D. C.), Dr. Byron J. Washom (Massachusetts Institute of Technology), Norman A. Wulf (NSF).

# POTENTIAL MARICULTURE YIELD OF SEA THERMAL POWER PLANTS. PART 2—FOOD CHAIN EFFICIENCY

S. LAURENCE AND O. A. ROELS
*Port Aransas Marine Laboratory*
*The University of Texas Marine Science Institute*
*Port Aransas, Texas*

ABSTRACT

In the tropical and subtropical oceans where OTEC plants could operate, the deep-sea water is considerably higher in plant nutrients (such as nitrate and phosphate) than the surface water. We have demonstrated at our St. Croix Artificial Upwelling laboratory that these nutrients in the deep-sea water, brought to the surface and exposed to sunlight, can be used for phytoplankton production in a continuous system. This phytoplankton is then fed to shellfish so that animal protein can be produced from deep-sea water and sunshine.

In the small-scale, shore-based St. Croix system, utilizing a continuous flow of 80% deep and 20% surface water, 79% of the available dissolved inorganic "nitrogen" in the mixed flow was converted to phytoplankton protein-N. This phytoplankton was fed to clams (Tapes japonica) and 33% of the phytoplankton protein-N was converted into clam meat protein-N. This corresponds to a clam meat (wet weight) production of 18 $g/m^3$ of deep water.

A 160 $MW_{(e)}$ net OTEC plant requires a deep-water flow of 1804 $m^3$ of deep-sea water per second from the condensers—according to an ERDA-commissioned design by Lockheed (1). This corresponds to a net yield of $\cong$ .026 kWh for each $m^3$ of deep water pumped. From the estimated sales prices of clam meat and electricity, and from the capital and operating costs of the OTEC plant and the mariculture system, the relative cost of and profit from the $\Delta T$ and the nutrient content of the deep-sea water could be calculated.

Major problems facing a mariculture system linked to a floating OTEC plant are (1) the necessity of containment of the deep-sea water to prevent too great dilution with surface water and sinking, (2) the very large areas required if the entire deep-water discharge from an OTEC plant were utilized, and (3) the impact on the market value of clam meat produced on a gigantic scale.

## INTRODUCTION

A combination of increases in world population, energy utilization, rising expectations, depletion of petroleum resources, pollution, and the emergence of new political realities, has brought about a general recognition of the pressing need to develop renewable and environmentally acceptable sources of energy. Similar forces, exacerbated by limitations on the availability of arable land, have brought about great pressures on world food resources. Pimentel and his colleagues (2) have demonstrated that limitations on fossil-fuel and arable land resources make it impossible to feed the present world population a United States-diet, in which 69% of the total protein intake is of animal origin. They further estimate that the world-wide use of U.S. agricultural techniques at the present population level would entirely deplete known petroleum reserves in 13 years.

There are also restrictions on the amount of protein which can be provided by the sea using present techniques. Currently, the ocean provides only 5-10% of the world's protein, and the world fish catch has apparently stabilized at 1970 levels (3). Most of the protein from the sea comes from highly productive coastal and upwelling areas: the open ocean, constituting 90% of the world's surface area, produces 0.7% of its fish; coastal zones, which occupy 9.9% of the area, provide 54%; and upwelling areas, which constitute only 0.1% of the surface area, provide 44% of the total catch (4).

A partial solution to these problems may lie in a combined OTEC/Mariculture system, in which the discharged deep water—unchanged except for its temperature and rich in inorganic nutrients (Table 1)—could be used in combination with sunlight to initiate a variety of marine food chains. Since the deep water can be brought to the surface with a net gain in energy, this mariculture system would not depend on expensive and unpredictable outside energy sources, and since it may be used in coastal areas or in the open ocean, it places no further pressure on arable land and increases the overall productivity of the sea.

This paper summarizes the results of a series of experiments designed to determine the potential organic productivity of an OTEC/Mariculture system. The animal protein production potential of the deep water appears to be more important than its energy-producing potential. In small-scale experiments, the conversion efficiency of available nutrients, and the protein production per unit area of this mariculture system was superior to conventional agricultural systems. A combined energy- and food-producing OTEC system appears much more desirable than an energy-producing plant alone. Problems of combining the two systems are briefly discussed, and the need for more theoretical and experimental research is stressed.

Table 1. Typical nutrient concentration levels in the deep (870 m) and surface waters north of St. Croix, U.S. Virgin Islands

| | NUTRIENTS | | | | |
|---|---|---|---|---|---|
| | $NO_3+NO_2$-N | $NO_2$-N | $NH_3$-N | $PO_4$-P | $SiO_4$-Si |
| Offshore surface water (= 3 km) | .2 | .2 | .9 | .2 | 4.9 |
| Nearshore reef surface water | .2 | .2 | .8 | .3 | 2.1 |
| Deep-sea water at 870 m | 31.3 | .2 | .7 | 2.1 | 20.6 |

THE ARTIFICIAL UPWELLING INSTALLATION

The technical feasibility of Artificial Upwelling mariculture has been investigated since 1969 in a small plant on the North Shore of St. Croix, U.S. Virgin Islands (17°47'N; 64°48'W) in the Caribbean Sea. St. Croix was chosen because the ocean reaches a depth there of 1000 m approximately 1.6 km offshore. Three polyethylene pipelines, each 1830 m long and 7.5 cm in diameter, were installed in 1972 from shore to a depth of about 870 m. Present deep-water flow is 250 liters/min. The deep water is warmed by conduction and is at a temperature of 22±1°C when it reaches the surface. The deep water is pumped into two 45,000-liter pools. Diatoms grown in these pools are started from axenic laboratory cultures, then cultured in 757-liter tanks which are, in turn, used to inoculate the pools. One diatom, Chaetoceros curvisetus Cleve (STX-167) can be grown in continuous culture in unsupplemented deep water for up to 40 days, at a turnover rate of one pool volume per day. The pool cultures are pumped continuously into shellfish tanks at metered rates, depending on the feeding activity of the shellfish; an algal-stripping rate of up to 90% has been achieved. The system also contains a hatchery where the clam Tapes japonica (Deshayes) is regularly produced, a larvae-setting area for juveniles, an experimental shellfish area used to determine optimum feeding ratios, animal density, etc., and a pilot shellfish-rearing area. In the latter, an ongoing record of labor and energy costs and various growth parameters in the pools and in the shellfish tanks are incorporated into a computerized economic sensitivity analysis, which provides a cost-output ($/kg clam wet weight) as a function of changes in selected inputs. Cost-sensitive components can therefore be identified and used as guidelines for changes in the system and for designing research.

Table 1 gives the concentration of the major nutrients necessary for algal growth in deep and surface waters at St. Croix. Growth in the algal pools is nitrate-limited, and we have therefore concentrated on determining the efficiency with which this nutrient can be converted into usable plant and animal protein-N.

CONVERSION OF DEEP-WATER NUTRIENTS TO PHYTOPLANKTON PROTEIN

The inorganic nutrients in the deep water may be used to initiate a wide variety of marine food chains. We have concentrated on the use of phytoplankton (especially diatoms) as a primary producer since they can efficiently utilize the available nutrients with only sunlight as an outside energy source, and because they represent a high-quality, protein-rich food for secondary producers such as clams and oysters.

We have successfully initiated and sustained phytoplankton cultures using two different techniques: artificial inoculation of 100% deep water using unialgal cultures, and by using surface water as an inoculum, thus initiating 'natural' blooms. The former method is most applicable to a highly controlled, land-based operation, and is the one used regularly to maintain our pool cultures. Results utilizing this method have been described in detail elsewhere (5,6). The inoculation of deep water with surface water is more directly applicable to an open-bay or open-ocean OTEC/Mariculture system. It would also have advantages in a land-based system assuming that the results were reasonably predictable on a seasonal and yearly basis.

As illustrated in Table 1, the surface water off St. Croix, which has the same nutrient content as 'open-ocean' waters (7), contains a negligible quantity of the dissolved inorganic nutrients necessary for phytoplankton growth. Since the deep water contains a much higher concentration of nitrate, optimal blooms (high cell concentration under steady-state conditions) will require a high proportion of deep water. To generate a bloom fast, a sufficient number of cells is required. Some cells will be provided by the deep water, but the great majority will be supplied by surface water. Thus, an optimal combination of deep and surface water requires a trade-off between final cell concentration and lag time.

In a series of batch studies using various ratios of deep to surface water, it was found that if the proportion of deep water exceeded 80%, most cultures either failed to grow or had lag times of greater than 5 days. If the proportion of surface water exceeded 40%, the final yield measured in terms of nitrate uptake, cell growth and chlorophyll-a concentration was low. Mixtures containing 60 to 80% deep water and 40 to 20% surface water resulted in optimal blooms.

In an actual system, where the relative proportions of deep and surface waters would change over time, it is clear that the ideal situation is one in which an initially high proportion (40-50%) of surface water could be maintained until exponential growth began (3-4 days). Thereafter, it is desirable to maintain the highest possible level of nutrient input, which requires 100% deep water. Thus, the optimum ratio of deep to surface water is almost opposite to that which would obtain in an uncontained, open-sea OTEC system, where the highest concentration of deep water is at the discharge point, and where it is continuously diluted by surface waters thereafter. Containment is discussed in more detail below. To determine the potential efficiency with which inorganic nitrogen could be converted to phytoplankton protein in a deep water:surface water system, some control over the mixing rates would have to be maintained.

Cultures were initiated by mixing 500 liters of deep and 400 liters of surface water in 2000-liter concrete epoxy-coated culturing vessels ('reactors') under continuous aeration. The surface water was obtained through a polyethylene pipeline whose intake was 30 m offshore; the deep water was Antarctic Intermediate Water from 870 m pumped through the pipelines described earlier. Once peak yield was obtained (usually within 3-4 day

deep water was added until its total proportion was 80%. The cultures were monitored until peak density was again ieved; thereafter the culture was placed on continuous r with a mixture of 80% deep and 20% surface water at a turnover rate of 1.0/day. This proportion was used because, under open-sea or open-bay conditions, it is unlikely that a higher proportion could be maintained. This particular turnover rate was employed because microscopic examination of the successful cultures revealed that the dominant species was Chaetoceros curvisetus, which was known to culture well at this rate. The temperature in the reactors was 26±1°C.

Under these conditions, about 50% of the cultures failed to bloom. Failures were usually associated with the presence of high concentrations of bacteria (Pseudomonas sp.), or were dominated by small flagellates (<2μ in diameter) which are known to culture poorly; such cultures were discontinued. The successful cultures were dominated by Chaetoceros curvisetus (STX-167) which is the only species known to grow well in unsupplemented deep water. Over the course of a year, 50 separate cultures were studied. Five representative cultures (determined on the basis of periodic comparisons of turbidity, nitrate uptake, and cell composition and concentration) were subject to intensive analysis over the major proportion of their lifetimes, which averaged about 40 days from the time of initial inoculation. Samples for phytoplankton protein-N were analyzed using a modification of the Lowry-Folin method of Dorsey et al. (8), and samples for dissolved nitrate plus nitrite ($NO_3^-$ + $NO_2^-$) and for ammonium ion ($NH_4^+$) were analyzed employing an AutoAnalyzer and standard Technicon manifolds. Samples were taken once daily at 1400 hr; a number of 24-hr samplings at 4-hr intervals were also done. These data were used to determine the degree of 'nitrogen' uptake and the efficiency with which total available and total removed 'nitrogen' was converted into phytoplankton protein-N. The results are summarized in Table 2.

Table 2. Phytoplankton protein-nitrogen production and "nitrogen" conversion efficiency in 80% deep:20% surface water mixtures

| TOTAL DISSOLVED $NO_3$-N+$NO_2$-N+$NH_3$-N *AVAILABLE* (μg-at/l) | TOTAL DISSOLVED $NO_3$-N+$NO_2$-N+$NH_3$-N *REMOVED* (μg-at/l) | PHYTOPLANKTON PROTEIN-NITROGEN PRODUCED (μg-at/l) |
|---|---|---|
| 25.8 | 24.54 | 20.3 |
| UPTAKE OF TOTAL AVAILABLE INORGANIC NITROGEN | CONVERSION EFFICIENCY, TOTAL *AVAILABLE* 'NITROGEN' →PHYTOPLANKTON PROTEIN-N | CONVERSION EFFICIENCY, TOTAL *REMOVED* 'NITROGEN' →PHYTOPLANKTON PROTEIN-N |
| 95.1% | 78.7% | 82.7% |

A mixture of 80% deep and 20% surface water contains 25.8 μg-at/l of dissolved inorganic 'nitrogen'. On the average, the continuous-flow cultures produced phytoplankton protein-N at a concentration of 20.3 μg-at/l, for a conversion efficiency of 78.7%. Of the total available inorganic 'nitrogen', 24.54 μg-at/l was ed from solution by the phytoplankton, representing an uptake efficiency of 95.1%. Thus, 82.7% of the removed 'nitrogen' was converted to phytoplankton protein-N.

In Table 3 is illustrated—assuming full utilization of all of the deep water (6.48 x $10^7$ $m^3$/day) from the Lockheed-designed OTEC plant (160 $MW_{(e)}$ net)—the amount (2.34 g) of algal protein (= protein-N x 6.58) produced per $m^3$ deep water, the amount (5.0 x $10^4$ metric tons) of protein per year (330 days), and the estimated area (2,049 hectares) required, given a culture depth of 4.88 m and a turnover rate of 0.81/day (an optimized relation between depth and turnover rate based on experiments in St. Croix (6) by M.W. Farmer et al.), and a constant ratio of 80% deep:20% surface water: the amount of algal protein produced/hectare/year would be 24.4 metric tons. This compares to a production of 0.71 metric tons/hectare/year for alfalfa, currently the greatest terrestrial producer of plant protein (2). If the deep water discharged from an OTEC plant were fully utilized for mariculture, large areas are required. Undoubtedly, actual production in terms of total biomass and protein/ha/yr would be less in an actual system, but since such factors as the total amount of deep water discharged and its temperature remain as yet undefined for an actual plant, only estimates can be provided at this time. At present, the most relevant data remain the efficiency of conversion and the amount of plant and animal protein which can be produced per $m^3$ of deep water.

Table 3. Estimated phytoplankton protein production from a 160 MW (gross) OTEC plant

| | |
|---|---|
| Phytoplankton protein ($g/m^3$) | 2.34 |
| Phytoplankton protein production 160 MW plant (metric tons/330-day yr)* | 5.0 x $10^4$ |
| Estimated areal requirements for full utilization (hectares)** | 2,049 |
| Estimated phytoplankton protein production (tons/hectare/yr) | 24.4 |
| Plant protein production in highest terrestrial producer (alfalfa) (tons/hectare/yr)*** | 0.71 |

*Lockheed design (1), = 6.48 x $10^7$ $m^3$/day.
**Assumes 80% deep:20% surface water, with a culture depth of 4.88 m and a turnover rate of 0.81/day.
***From Pimentel et al. (2).

## CONVERSION OF PHYTOPLANKTON PROTEIN TO SHELLFISH MEAT PROTEIN

Once algal blooms are initiated and sustained through the use of proper management techniques, the phytoplankton may be used in a variety of ways. It has been suggested that a primary producer grown in a deep:surface water mixture could be directly harvested and used as human or animal food, or converted into fuel. Harvesting of phytoplankton is difficult and expensive and is

less efficient than 'biological' harvesting, i.e., filtration by a secondary producer. Conversion to fuels involves considerable loss of gross plant energy and, more important, represents a very poor use of phytoplankton since the latter is rich in protein (approximately 58% on an ash-free, dry-weight basis for Chaetoceros curvisetus) and can be converted very efficiently into high-quality animal protein.

The most promising use of phytoplankton grown in deep-sea water is as a food for a marine secondary producer. The latter 'harvest' and 'feed' in a single, continuous operation, and the conversion of plant to animal protein is generally quite efficient. The choice of a particular secondary producer depends on a large number of biological and economic considerations, including the cost of producing larvae, maintaining and harvesting the animals, dollar value of final product, etc.

At present, the most promising secondary producers are shrimp and shellfish. We have concentrated on the latter because they are known to be efficient filter-feeders, can be densely packed (thus leading to economical use of space and excellent control over feeding regimes), possess a high biological (protein) and economic value, and can be grown with relative ease from larvae to adults using established culturing techniques.

The conversion of algal protein to shellfish meat protein has been studied employing both 100% deep water and 80% deep:20% surface water mixtures. Shellfish feeding studies employing 100% deep water have been reported in detail elsewhere (5,6). In such a system, phytoplankton protein has been converted to shellfish meat protein with efficiencies as high as 35%. In deep and surface water mixture studies, cultures were initiated as described above, in 2000-liter reactors and placed on continuous flow of 80% deep:20% surface water at a turnover rate of 1.0/day. Cultures were dominated by Chaetoceros curvisetus; various Nitzschia sp. and microflagellates were also present. The cultures were gravity-fed continuously to several batches of juvenile Tapes japonica for 36 days. For determination of 'nitrogen' conversion through the second trophic level, replicate 4-liter trays containing 140 g whole wet weight of clams on Day 0 were fed either at 1 or 2 ml per sec. Previous work (5) had indicated that maximum conversion efficiency would be obtained by these two weight/flow-rate groups.

Samples for phytoplankton protein-N and for dissolved $NH_4^+$ and ($NO_3^-$+$NO_2^-$) entering and leaving the trays were measured daily. Every nine days, all the clams were weighed and a subsample measured for shell length. Enough clams were harvested every nine days to bring the total population weight back to its starting level of 140 g. The harvested clams were frozen, and later whole wet weight, dry meat weight and protein content of the meat, as well as wet and dry shell weights, were determined.

In this study, the 25.8 µg-at/l of total dissolved inorganic 'nitrogen' present in the 80% deep:20% surface water mixture was converted to 20.0 µg-at/l of phytoplankton protein-N, for a conversion efficiency of 77.5%. For the 140-g 1 ml/sec group, a mean total of 0.855 g phytoplankton protein-N was presented over the 36-day experiment, and 0.29 g protein-N was recovered in the clam meat. For the 140-g 2 ml/sec group, 1.733 g phytoplankton protein-N was presented and 0.59 g was recovered as Tapes japonica meat protein-N. This represents conversion efficiencies of 33 and 34%, respectively. This conversion efficiency is superior to that obtained with the most efficient known terrestrial plant-protein to animal-protein conversion (Table 4).

Table 4. A comparison of plant-to-animal protein conversion efficiency obtained in a mixture of deep and surface water to that obtained with other efficient secondary producers

| ANIMAL PRODUCT | ANIMAL PROTEIN OUTPUT / VEGETABLE PROTEIN INPUT X 100 |
|---|---|
| Milk* | 31.4 |
| Eggs* | 27.1 |
| Beef (feed lot)* | 6.5 |
| Catfish* | 10.5 |
| Shellfish (Tapes japonica)** | 33.0 |

*Comparative data from Pimentel et al. (2).
**Shellfish data from studies at the St. Croix "Artificial Upwelling" site.

For the 140 g 1 ml/sec group, this conversion efficiency translates to an animal protein production of 0.755 g/$m^3$ of deep water. Wet meat weight production for this group was 18 g/$m^3$ of deep water. A plant pumping 6.48 x $10^7$ $m^3$ deep water/day would produce 1.6 x $10^4$ metric tons protein/yr (=330 days), and 3.8 x $10^5$ tons meat/yr. These results, presented in more detail elsewhere (9), are summarized in Table 5.

Table 5. Estimated animal protein production from a 160 MW OTEC plant

| | |
|---|---|
| Shellfish (Tapes japonica meat protein (grams/$m^3$ deep water)* | 0.755 |
| Wet meat production (grams/$m^3$ deep water) | 18 |
| Protein production assuming full utilization of deep-water discharge (metric tons/330-day yr)** | 1.6 x $10^4$ |
| Wet meat production assuming full utilization (metric tons/330-day yr) | 3.8 x $10^5$ |

*Based on a 36-day "constant weight" feeding study in which 140 g whole wet weight of Tapes japonica was fed a mean concentration of algal protein-N of 20.0 µg-at per liter at a rate of 1.0 ml/sec.
**Lockheed design (1), discharging 6.48 x $10^7$ $m^3$/day.

## DISCUSSION

At the present stage of OTEC development, several variables relevant to the utilization of the deep-sea water nutrients (such as the temperature of the deep water discharge) remain undefined. Thus, truly useful comparisons of the potential energy and food-producing aspects of OTEC are very difficult to make at this time. The issue is important, for while the energy- and food-production capabilities of OTEC are compatible, conditions for optimization of one aspect are not necessarily identical for optimization of the other. A present

ocean OTEC design (1) calls for the discharge of the deep water at temperatures which are about 15°C lower than that required to maintain the deep water in equilibrium with the surface water, thus requiring containment if mariculture is to be accomplished.

Ongoing research into the energy- and food-producing aspects of OTEC is pursuing a divergent course: the decision to employ pilot-level testing in the open sea, for example, may be advantageous for development of the energy resource, but it makes mariculture very difficult. There is little doubt that the possible economic returns from a combined energy/mariculture OTEC plant are greater than that from an energy-producing unit alone. The Lockheed OTEC design (1) would produce $\cong$ .026 kWh for each $m^3$ of deep water pumped, worth about 1 mil. Assuming that 18 g of clam meat could be produced for each $m^3$, its value is $\cong$ 3.5¢ at going market prices. Of course, considerable depression of shellfish market values would undoubtedly occur if production were undertaken on the scale discussed above; the economically optimum scale for OTEC/Mariculture is not known. The economics of an integrated OTEC power and mariculture system making full use of the energy potential and nutrient characteristics of the deep-sea water should be determined and compared to that of an OTEC power plant alone. A systematic study taking into account the large-scale and long-term social benefits from each is required.

The use of OTEC-derived energy should be analyzed. If OTEC-supplied electrical energy were to be used for agriculture, for example, its benefit to society would most likely be less than if the direct production of food using deep-sea water were undertaken, even if the latter placed limitations on energy production per se. In short, food and energy production are equivalent at some level of analysis. Models, based on empirical research, are needed to guide decisions allocating economical and technical resources. Such decisions must reflect an awareness of the needs of society and the potential of the deep-sea water resource.

REFERENCES


Lockheed Corporation, 1975. Ocean Thermal Energy Conversion (OTEC) power plant, technical and economic feasibility. Vol. 1, Natl. Science Fdn. (RANN), SE/G1-C937/FR/75/1.

Pimentel, D., W. Dritshilo, J. Kummel and J. Kutzman, 1975. Energy and land constraints in food protein production. Science 190:754-761.

Mayer, J., 1976. The dimensions of human hunger. Scientific American 235(3):40-49.

Crisp, D.J., 1975. Secondary productivity in the sea. In: Productivity of World Ecosystems, National Academy of Sciences, Washington, D.C.

Roels, O.A., T.E. Dorsey, S. Laurence, P.W. McDonald and K.M. Rodde. Nitrogen balance and clam growth in an artificial upwelling mariculture system at different food flow rates and shellfish densities. Submitted to Marine Biology, 1977.

Roels, O.A., S. Laurence, M.W. Farmer and L. Van Hemelryck, 1976. Organic production potential of artificial upwelling marine culture. In: Microbial Energy Conversion, H.G. Schlegel and J. Barnea (eds.) Erich Goltze KG, Göttingen, pp. 69-81.

Amos, A.F., O.A. Roels, C. Garside, T.C. Malone and A.Z. Paul, 1977. Environmental aspects of nodule mining. Chap. 13, In: Marine Mining, G.P. Glasby (ed.), Elsevier Publ. Co., Amsterdam (in press).

Dorsey, T.E., P.W. McDonald and O.A. Roels, 1977. A heated Biuret-Folin protein assay which gives equal absorbance with different proteins. Analyt. Biochem. (in press).

Laurence, S. and O.A. Roels, 1976. Marine pastures: a by-product of large (100 megawatt or larger) floating ocean-thermal power plants. Final Rept. Contract E(11-1)2581, Energy Research & Development Admin., COO/2581-3, 170 pp.



University of Texas Marine Science Institute Contribution #167. Supported by National Oceanic & Atmospheric Administration, U.S. Department of Commerce, Sea Grant Number 04-6-158-44117 and by private foundations.

# ELECTRICAL ENERGY TRANSMISSION FOR OTEC POWER PLANTS

B. M. WINER AND J. NICOL
*Arthur D. Little, Inc.*
*Acorn Park*
*Cambridge, Massachusetts*

## Abstract

The OTEC Power Plant, will convert the energy stored in the waters of the oceans into electrical energy. Arthur D. Little, Inc. (ADL) has investigated the technical problems associated with transmitting this energy to shore via electric power cables and estimated the associated costs.

Electric power cables of the necessary size have never operated under the conditions that will pertain for the OTEC cables. However, there appear to be no insuperable technical problems associated with transmitting electrical energy from an OTEC plant located in reasonably shallow water (< 6000 ft.). Since most of the normally available cable design information has not yet been fixed, much of our work was a parametric analysis of the cost effect of various plant and cable design options. The normal method of ascertaining the number of redundant cables required to provide reliable energy transmission was not strictly applicable. The criterion used to develop this important design parameter was that the total cost of the energy delivered to shore should be minimized. This paper will present a detailed description of the methodology used to develop the cost estimates, the various cost elements that must be considered, and some of the study results.

## Introduction

The concept of building an Ocean Thermal Energy Conversion (OTEC) power plant to exploit the temperature difference between the warm surface water and cold deep water of the tropical seas has intrigued investigators since the late nineteenth century. This persistent temperature difference can run a heat engine to generate electric power. This power, delivered to shore, would reduce the need to burn more conventional fossil and nuclear fuels to generate electricity. It appears to be technically feasible to deliver electric power to shore from OTEC plants located in reasonably shallow water (< 6000 ft.) via submarine electric power cables using reasonable extrapolations of today's technology.

## Results

The power cable systems that would be required for the OTEC power plants would be the most advanced electric power transmission cable systems ever built. The length of the cables, the maximum depths, the power capacity and total cost of the system is likely to be greater than any other underwater system now in service or expected to be in service within the next ten years. No high voltage cable has ever been operated while being moved in the manner required of the cable section running from the ocean bottom to the floating platform. While it appears that the problems can be solved, much work remains to be done.

The general conclusions reached during the study of the OTEC power transmission system at Arthur D. Little, Inc. are:

1. All of the major technical problems associated with transmitting electrical power to shore from an OTEC plant in less than a mile of water which have been foreseen appear to be solvable or avoidable.

2. The incremental transmission costs for optimized cable systems are less than 5 mills/kW-hr delivered when the OTEC plant is within 25 miles of shore (ac and dc).

3. The incremental transmission costs for optimized cable systems (dc) are between 13 and 15 mills/kW-hr delivered when the OTEC plant is within 200 miles from shore.

4. While some connector between the riser and bottom cables will be required, a submerged swivel connector appears to be unnecessary.

5. If the final product is to be electrical energy and if it is technically feasible to transmit the energy as electric power, then electrical energy transmission is more economical than chemical transmission. The converse is true if the desired product is chemical energy.

## Cable Sections

The three distinctly different sections of the OTEC power cables are 1) the stationary cable along the ocean bottom, 2) the movable cable (riser) between the ocean bottom and the OTEC plant and 3) the connector between the stationary and movable cable sections. The stationary

cable is most similar to systems already in use and there is less uncertainty about the forms of the solutions ıe problems of these cables than for the other two.

The riser cable presents problems that have never before been encountered with high voltage, high capacity electric power cables. These problems arise primarily because of relative motion between the OTEC plant and the stationary cable due to waves, currents and winds. Almost certainly the upper end of the riser must share some of the motion of the OTEC plant, so the riser will be subjected to considerable flexure and changes in stress. The mechanical requirements of the riser will be quite high. It is not at all clear if these requirements can be met when the riser is completely supported by the OTEC plant; a separate buoyancy support system may be needed. Motion will reduce the life span of the riser, which should probably be designed to be replaceable, for repair of the riser cable in place, is probably not feasible.

The development of a submarine connector between the movable riser cable and the cable along the sea bottom is expected to be an important design problem. The final design of this element will depend critically on the OTEC plant design, the plant size, the life span of the riser cables and the connectors' own maintenance requirements.

In order to reduce the initial cost of the OTEC power plant, it may be desirable to hold the plant in place with a single tether. It would thus be possible for the plant to rotate about the anchor point. A swivel connector will then be needed to keep the riser cable from twisting. Lockheed has investigated a swivel connector at the anchor cable pivot. Its chief disadvantage is the potential unreliability of the resulting total system. The swivel connector itself would be large and probably expensive or else it would require frequent maintenance. Furthermore, the reliability of a single tether may not be high enough to prevent the unscheduled departure of the plant from the site; the probable cost of retrieving the plant should be significant. Finally, a single swivel connector would have to be de-energized and, as a result, the OTEC plant would have to be completely shut down each time a riser cable is replaced. If the life span of the riser cables is very short, this could be very costly.

Alternatives to the single point swivel are:

- Multiple, relatively inexpensive, tethers and anchors to prevent rotation; or
- Siting of the OTEC plants in relatively strong, dependable currents which would prevent rotation; or
- Running the riser cables to a swivel connector located in a buoy near the surface but outside the OTEC plant's radius of rotation; or
- Dynamic positioning using the plant effluent to prevent rotation around the single anchor point (standby conventional dynamic positioning systems for when the plant is not operating).

The solution to this problem must consider the total OTEC system, not just the energy delivery subsystem.

## Cable Types

The three cable systems which appear to be suitable for transmitting electrical power from an OTEC power plant to shore are 1) solid dielectric cables, 2) mass impregnated paper insulated (solid) cables, and 3) high pressure, oil-filled (HPOF) paper cables.

The solid dielectric cable using cross-linked polyethylene insulation appear to be the least expensive cable that might be used to meet the OTEC requirements. Its light weight and simple construction make it particularly suitable for use at great water depths (> 6000 ft.). However, several conventional installations of the solid dielectric cables operating at the higher voltages that will be required for OTEC (> 138 kV) have not proven to be as reliable as the paper-insulated cables. The development and demonstration of reliable extruded dielectric cables for use in land installations is presently being supported by ERDA and EPRI. It is hoped that these improved cables will be available for use with the OTEC power plant.

The mass or oil-impregnated paper cable system is the same type as the $\pm$ 250 kV cables installed between Denmark and Norway in 1976. The maximum water depth for those two cables was about 1500 ft. and their lengths were about 76 miles. This is the longest and deepest submarine power cable system ever installed and it is presently operating successfully.

The insulation in the paper cable system is oil-impregnated paper tapes wrapped tightly around the conductor; the required thickness of the wrapped paper depends on the operating voltage. A lead sheath, fit tightly around the insulation, provides the ground return and protection from water. The weight of the lead sheath is typically about equal to the weight of the copper conductor. The low fatigue resistance of the lead sheath requires that some other metal be used as the sheath for the riser cables.

The HPOF paper cable is roughly the same as the paper cable system with a pressurized oil-filled core; the core is installed primarily for the purpose of suppressing corona and ionization. However, it is also possible to use the oil core to protect the cable from water damage after the cable is cut by maintaining a small positive pressure difference between the cable core and the sea water. (Because the oil has roughly the same density as sea water, the pressure difference at the surface need not be excessive even if the pressure at the cable break is over 90 atmospheres.) This protection can be provided in cables less than roughly seventy miles long; the viscosity of the cool oil is too great to allow oil pumping through the small oil duct in the conductor over greater distances.

Although several other cable systems have been investigated, they all had characteristics which made them unsuitable for use with the OTEC power plant. HPOF Pipe Type Cables require the joining of many pipe lengths while holding both ends at the surface, then pulling three relatively short (< 1 mile) lengths of cable into the pipe, splicing the cables, welding the pipe and then

lowering the unit to the sea bottom. The large number of cable splices necessarily reduces the cable reliability. $SF_6$ cables with outer walls thick enough to withstand the sea bottom pressure differential (90 to 180 atmosphere) are extremely expensive. More seriously, when the cable is not energized, the $SF_6$ temperature would be below the critical temperature and at 90 atmospheres, the $SF_6$ would liquefy. While it may be possible to devise a method of solving this problem, the costs are likely to be very high. Cryogenic or superconducting cables require refrigeration units at frequent intervals; placing and maintaining these refrigeration units along the sea bottom raises serious reliability questions. In addition, these cables are being developed with a much larger capacity than that expected for the OTEC plants; the cost of using these cables at lower power levels is likely to be prohibitive.

## Optimized Cable Selection

A huge variety of cable voltages, core sizes and costs are available to transmit electrical energy from an OTEC power plant to shore. The choice of the optimum cable depends critically on the plant and site characteristics and these have not yet been defined. Any otudy of the cost of delivering electrical energy from an OTEC power plant to shore must consider many, usually fixed characteristics as variable parameters.

Among the factors to be considered in designing a transmission system for an isolated plant are plant characteristics and economic and site parameters not specific to the type of cable, and mechanical, electrical, reliability and termination characteristics specific to the type of cable system contemplated. A partial list of significant factors is given in the following tables.

[Not specific to any particular cable system]

Plant Characteristics

- Maximum Generating Capacity
- Capital Cost/Kilowatt of Capacity
- Average Plant Availability
- Operating Costs
- Required Reliability of the Transmission System
- Distance from Shore

Economic Parameters Which Determine the Fixed Cost Factor

- Effective Interest Rate (Debt/Equity Ratio)
- Taxes, Insurance, etc.
- Plant Construction Time
- Depreciation Schedule

Site Dependent Characteristics

- Maximum Water Depth Along Cable Route
- Maximum Slope of Sea Bottom Along Cable Ro...
- Water Currents Along Cable Route
- Weather
- Probability of Cable Fault due to Mechanical Interference
- Sea Bottom Material (Sand, Rock, etc.)
- Distance Between Site and Repair Base

[For Each Candidate Cable System]

Physical Characteristics

- Cable Diameter
- Cable Weight per Unit Length
- Maximum Stress and Stain
- Minimum Bending Radius
- Maximum Torsion
- Maximum Length Between Joints

DC Characteristics

- Conductor to Ground Voltage Rating
- Conductor Size
- Resistance per Unit Length at the Operating Temperature
- Shunt Resistance per Unit Length (Dielectric Losses)
- Cable Ampacity at Expected Load Factor and Ambient Temperature

AC Characteristics

- Phase to Phase Voltage Rating
- Conductor Size
- Resistance per Unit Length at the Operating Temperature
- Conductor Reactance per Unit Length
- Shunt Reactance per Unit Length
- Shunt Resistance per Unit Length (Dielectric Losses)
- Ampacity at Expected Load Factor and Ambient Temperature

Cable Reliability (Availability)

Failure Rate per Unit Cable Length for Shallow Water Cables, Deep Water Cables and Riser Cables

Mean Time to Repair Shallow Water Cables, Deep Water Cables and Riser Cables

AC Terminals

Reactive Compensation at Both Cable Ends

Voltage Support Requirements

Terminal Efficiency

Cable Switching Requirements

Terminal Maintenance Requirements

Terminal Capital and Operating Costs Per MVA Transmitted

DC Terminals

Harmonic Filtering Requirements

Conversion Efficiency

Voltage Support Requirements

Corrosion Characteristics of Sea Return

Switching Requirements

Terminal Maintenance Requirements

Terminal Capital and Operating Costs per MW Transmitted

Cost Characteristics

Cost per Unit Length of Cable (Stationary and Riser Cables)

Installation Cost per Unit Cable Length for Shallow or Deep Water and the Riser Cable

Cost per Cable Repair for Shallow or Deep Water and for the Riser Cable

Clearly, if each of these system characteristics is to be considered a variable parameter, it would not be possible to reach any conclusion about the cost of a transmission system for an OTEC power plant. In the study performed by Arthur D. Little, Inc. for the National Science Foundation, the following factors were considered to be variable:

Maximum OTEC Power Plant Generating Capacity

Capital Cost per Kilowatt of Capacity

Distance of OTEC Plant From Shore

Maximum Water Depth

Specific Cable Design Operated Either in the ac or dc Mode

All other factors were fixed either at reasonable values by reference to the literature or by the variable parameter (e.g. the specific candidate cable design). Where there was insufficient data to determine some of these factors for electric power cables (e.g. the mean time to repair cables), extrapolations were made from the history of submarine telephone cables.

When assessing the economic competiveness of OTEC power plants with land based systems, it is necessary to consider the generation and transmission units as subsystems of the total system. Thus, the figure of merit would be the total cost per kilowatthour delivered.

$$\text{Figure of Merit} = \frac{f(\text{total capital cost}) + \text{operating cost/yr.}}{\text{expected energy delivered/yr.}}$$

where the total capital and operating costs are the sums of the costs of the power plant and delivery subsystems and f is the fixed cost factor; the fraction of the total capital cost required each year for principal, interest, taxes, insurance, etc.

The expected energy delivered per year is $A \cdot pf \cdot h \cdot P_d$ where A is the availability of the transmission system; pf is the plant factor or the availability of the OTEC plant; h = 8760 hours per year and $P_d$ is the power delivered to shore from an OTEC plant.

The reliability of availability of the transmission system is seldom considered to be a variable parameter. Usually, the number of cables installed is n plus one, where n is the number of cables of a specific design required to transmit the total capacity of the power plant. However, because of the high cost of the cables and the power plant, and the relative inaccessability of the cables, a reexamination of the issue would be prudent.

If the number of redundant cables increases, the total capital and operating costs increase and the figure of merit could increase. However, at the same time, the availability of the transmission system increases, increasing the amount of expected energy delivered to shore and the figure of merit may decrease. The required number of redundant cables can be defined as that number which minimizes the figure of merit (Figure 1). For conventional systems, the optimum number of redundant cables is usually one. For OTEC power plants, this number will depend on the cost of each extra cable, the cost of the OTEC plant and the speed with which each cable can be required.

While the appropriate measure of the cost effectiveness of particular OTEC plant/transmission cable combinations is the total cost per kilowatthour delivered to shore, it is often desirable to compare the cost effectiveness of particular cables with a variety of assumed power plant characteristics. The appropriate measure of a

transmission subsystem's cost effectiveness would be the incremental transmission cost (ITC); this is defined as follows:

$$ITC = \frac{\text{total cost}}{\text{kW-hr delivered}} - \frac{\text{cost}}{\text{kW-hr generated}}$$

The dependence of the ITC for particular cables on the OTEC power plant size and cost can be clearly demonstrated by plotting (see Figure 2.) ITC for a circuit having a power transmission capacity of P against the maximum transmission capacity of the OTEC power plant. If the OTEC plant has a maximum generating capacity of less than P, only one circuit is required; OTEC plants with maximum generating capacities between P and 2P require two circuits, etc. The higher the unit cost of the OTEC power plant (dollars per kW), the higher the value of the transmission losses and thus the higher the incremental transmission cost for a particular power plant.

DETERMINATION OF THE NUMBER OF REDUNDANT CABLES

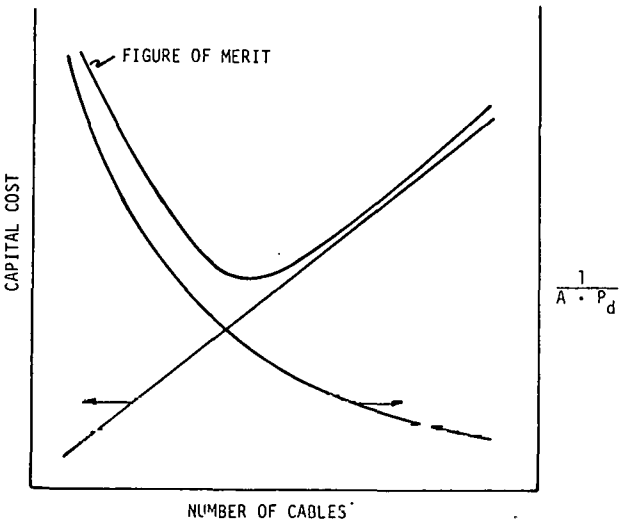



Figure 1.

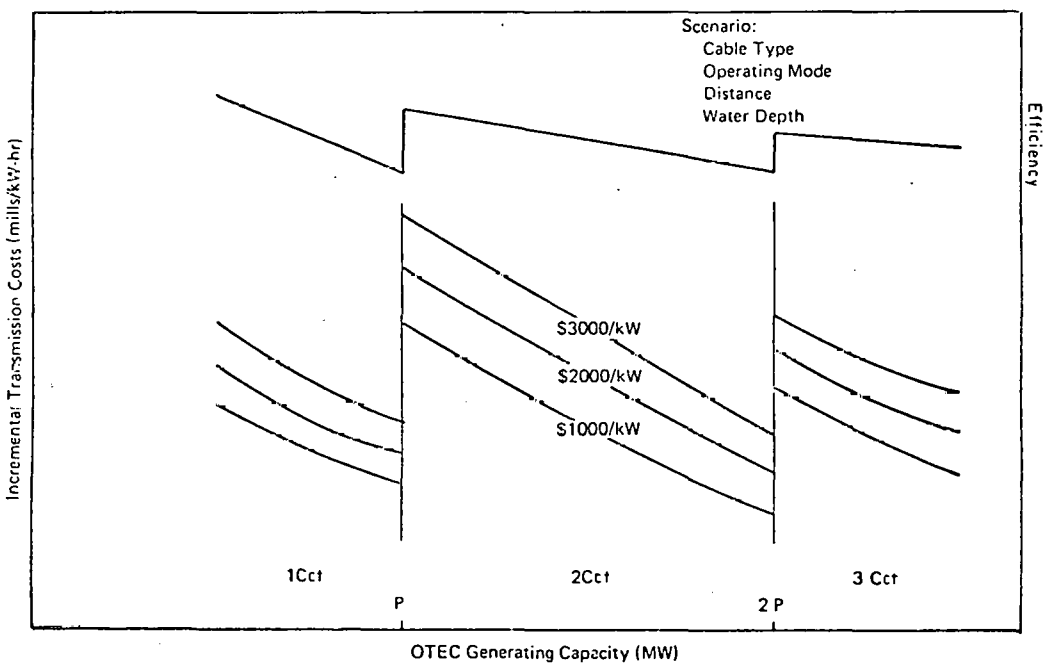



Figure 2.

The current in the cable and therefore the power transmission capacity, P, of a particular cable depends on the ability of the environment to dissipate the heat generated by ohmic and dielectric transmission losses. If the cable is operated in the ac mode, some of the current must be used to feed the shunt capacitance distributed along the cable. The magnitude of the required charging current varies along the cable; the longer the cable, the larger the maximum charging current. When the maximum charging current equals the thermally limited cable ampacity, the cable can transmit no useful power; the length of the cable when this occurs is the critical cable distance. The variation of an ac cable's power transmission capacity with transmission distance is shown in Figure 3. The larger the cable conductor, the higher the cable ampacity and the longer the critical distance. If the cable is operated in the dc mode, all of the current in the core can be used to transmit power to shore. The cable capacity diminishes only slightly with the transmission distance, because of resistive voltage drop.

THE AC POWER TRANSMISSION CAPACITY OF A CABLE DEPENDS ON THE TRANSMISSION DISTANCE

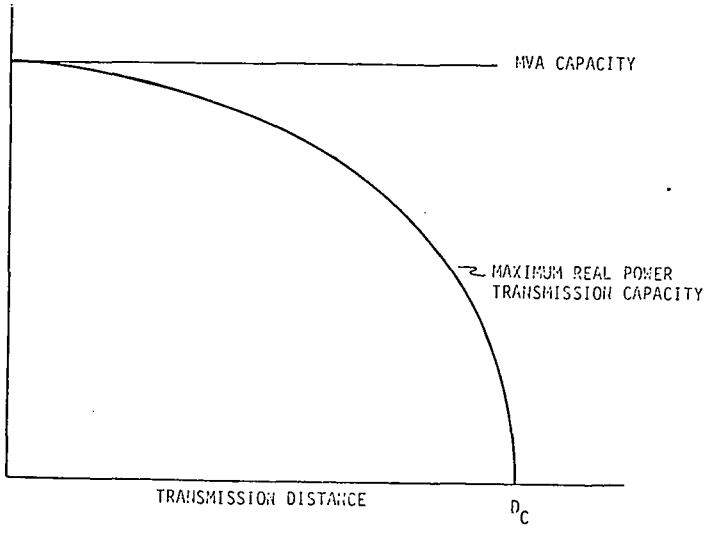



Figure 3.

Dc transmission systems have several significant advantages over comparable ac systems even over relatively short distances. Dc cables of the same capacity as ac cables are smaller, lighter and more efficient. While normally dc cables are operated in pairs, it is possible to operate a single dc cable using a sea return to complete the circuit; three ac cables must be available at the same time if usable power is to be transmitted. The major disadvantages of dc systems are related to the cost, efficiency and reliability of the ac/dc conversion equipment located at both ends of the transmission route. Since dc electric power is not generated at transmission voltages, the power must be generated as ac, stepped up to the transmission voltage and then converted to dc and transmitted.

Results for One Candidate Cable

In order to demonstrate how the suitability of a particular cable varies with OTEC plant characteristics and location, the ITC for one cable design has been calculated as a function of the plant parameters assuming that a) the cable is operated in the ac mode (Figure 4), and b) the cable is operated in the dc mode (Figure 5).

This cable can be operated in the ac mode at a phase to phase voltage of 230 kV and a transmission capacity of 230 MVA per three phase circuit. The power transmission capacity of a three phase circuit 25 miles long is 215 MW; the power transmission capacity of a circuit 50 miles long is only 150 MW. It would require only one circuit to transmit the power from a 200 MW OTEC plant located 25 miles out at sea; two circuits would be required if the plant were fifty miles from shore. Five circuits (15 cables) would be required to transmit the power generated by a 1000 MW OTEC plant located twenty five miles from shore. Laying and maintaining fifteen cables in this environment would be quite difficult; this figure indicates that if ac transmission is deemed to be desirable, a cable with a higher capacity than this candidate cable would be needed for the 1000 MW OTEC power plant.

The ITC of this same cable, operating in the dc mode at a conductor to ground voltage of roughly 300 kV, can be used to demonstrate how the optimal number of redundant cables varies with the cost of the OTEC power plant (Figure 5). Only one cable is required to transmit the power from a 200 MW OTEC power plant located two hundred miles from shore. If the power plant costs only $1000 per kilowatt of capacity, the high cost of the redundant cable is not justified by the expected increase in the amount of OTEC energy delivered to shore. If the power plant costs $2000 per kilowatt of capacity, the increased total cost per kilowatthour caused by the additional capital cost of the redundant cable would be slightly greater than the reduction in the per unit energy cost caused by the increase in the amount of energy delivered. If the OTEC plant costs $3000 per kilowatt, the increased availability of OTEC energy would justify the cost of the redundant cables.

A comparison of the ac and dc incremental transmission costs for this cable as a function of the transmission and distance is shown in Figure 6. Dc transmission and ac transmission, using this cable, have the same cost for this plant located roughly twenty miles from shore.

Figure 4.

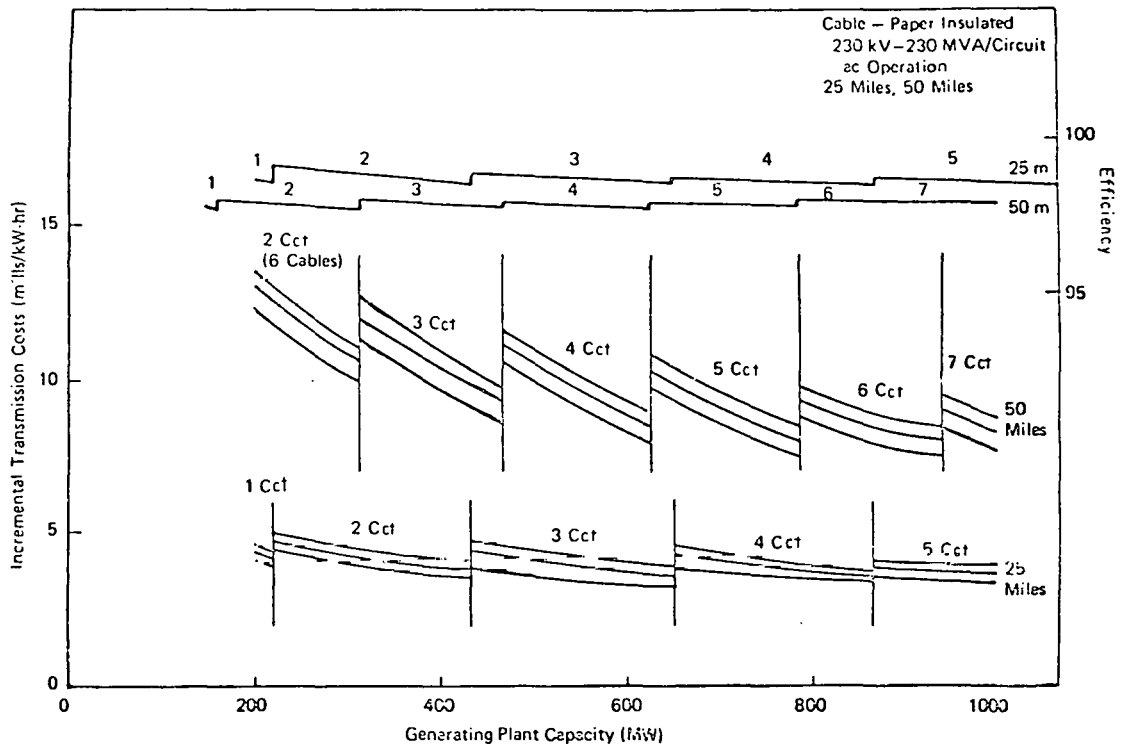
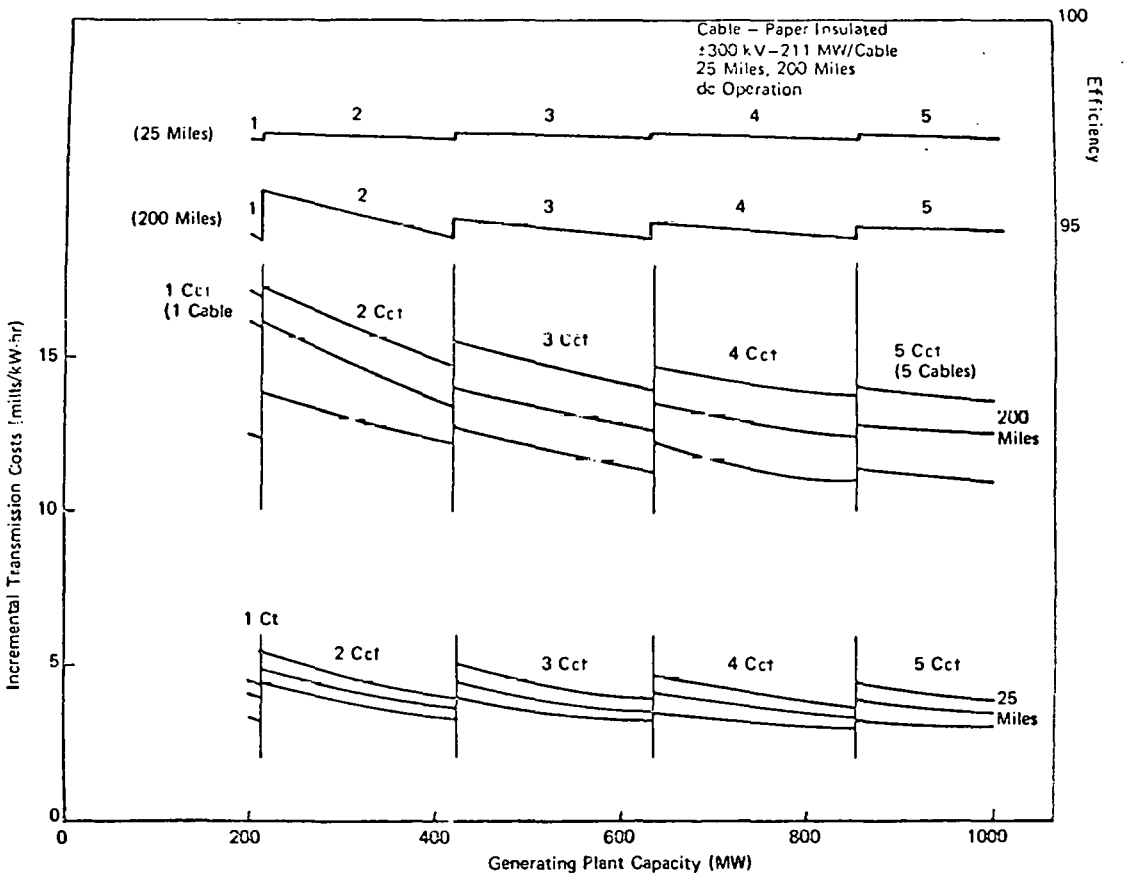



Figure 5.



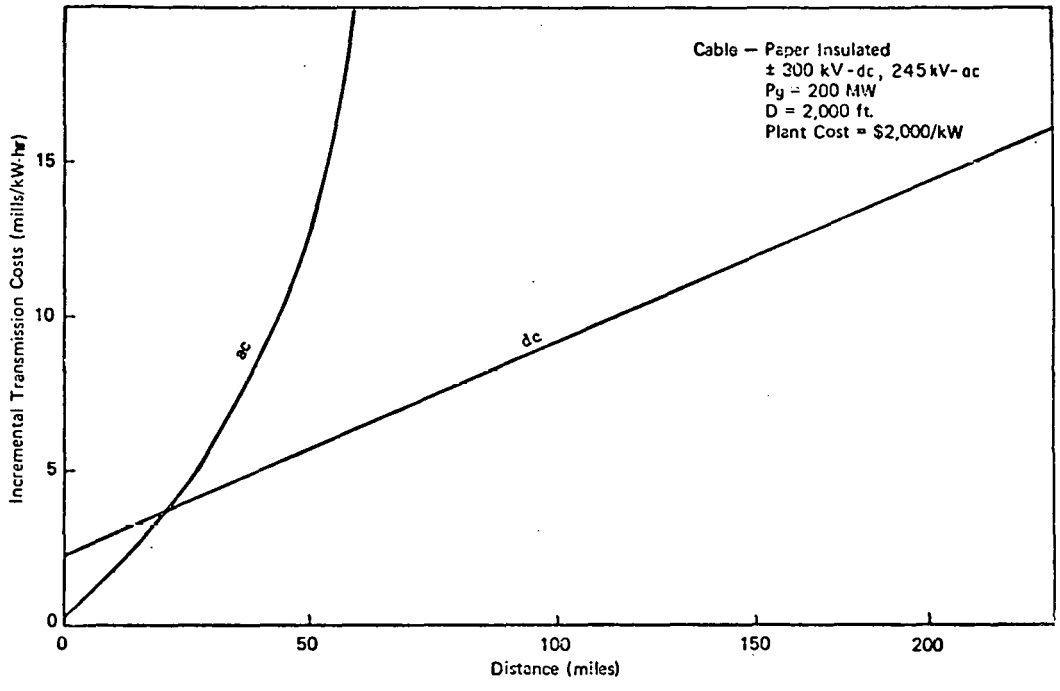

Cable — Paper Insulated
± 300 kV-dc, 245 kV-ac
Pg = 200 MW
D = 2,000 ft.
Plant Cost = $2,000/kW
δc
δc
Incremental Transmission Costs (mills/kW-hr)
0
5
10
15
0
50
100
150
200
Distance (miles)

Figure 6.

# OCEAN ENERGY INDUSTRIAL COMPLEXES

B. LINDAL, C. D. HORNBURG, AND N. EL-RAMLY
*DSS Engineers, Inc.*
*7483 Northwest 4th Street*
*Ft. Lauderdale, Florida*

Abstract

Results of a one year study on the feasibility of producing energy intensive products at ocean sites using electricity generated from Ocean Thermal Energy Conversion (OTEC) plants are presented.

Analysis of production methods and other data on 62 major products lead to selecting 23 of these for further study. Production was grouped into five separate, possible complexes. Further market and transportation studies showed that production of products in a sea chemicals complex and an organic chemicals and plastics complex had the highest economic potential. Detailed designs of these two complexes are presented. The three potential sites were selected for these OEICs.

An environmental assessment revealed that these complexes would have negligible adverse environmental impact. The selected products can be produced at ocean sites competitively with production at similar land-based complexes. Return on investment will be between 13% and 18% depending on actual power costs and details of the final designs.

## Introduction

One of the major problems to be solved, if floating energy conversion plants are to be economically feasible, is that of energy delivery. Systems for production and shipment of intermediate fuels such as hydrogen, and/or systems involving underwater electrical cables must be developed. These systems may substantially increase the cost of energy delivered to the mainland.

The alternate to this is to utilize the ocean energy at the source for production of energy intensive products. This would result in the maximum utilization of the extracted energy, not only due to eliminating delivery losses, but also by more direct use of the energy.

Seawater is the source of many raw materials used in the chemical industry. These raw materials can be extracted by thermal, chemical and mechanical methods. They can then be processed using large amounts of electric power in order to produce more valuable products like magnesium, sodium, and other electrolytic dissociation products of salts. These products can then be shipped to the mainland for further processing and use, or further cascade industries can be developed at the ocean site.

There are many other products that require large amounts of electrical energy to manufacture. It is possible that some of these could be produced at ocean sites in integrated complexes, using ocean thermal energy.

Thus, the U.S. Energy Research and Development Administration (ERDA) awarded a contract to DSS Engineers, Inc. to investigate the feasibility of developing Ocean Energy Industrial Complexes (OEICs). This investigation was recently completed and this paper presents the results.

## Objectives

The fundamental purpose of the study was to investigate the economic, technological, and environmental aspects of recovering marketable chemicals from sea water and producing other energy intensive products in conjunction with floating ocean thermal energy conversion plants.

The basic overall objectives were as follows:

1) Identify primary products that have a high potential for economical production at ocean sited thermal gradient power plants.

2) Provide technical and economic information on systems to extract the major marketable chemicals and magnesium from seawater, and produce other energy intensive products from raw materials imported by ships.

3) Determine limitations of integrated Ocean Energy Industrial Complexes with regard to minimum economic size and maximum plant capacity considering market conditions.

4) Assess the environmental factors related to Ocean Energy Industrial Complexes as compared to similar land industries and ocean energy conversion plants alone.

5) Determine the relative economics and competitive position of OEICs as compared to similar land-based complexes.

6) Identify research needs and opportunities related to energy utilization and processes used in OEICs.

## Research Tasks

The research was broken down into 7 main technical tasks with a total of 43 sub-tasks. The main technical tasks were:

1. Preliminary Identification of potential products & processes
2. Selection of product mix, complex sizes and sites
3. Analyze alternate processes
4. Design two typical (base case) complexes
5. Assess environmental factors
6. Prepare cost estimates and assess economics
7. Assess overall possibilities and determine research needs

Initial Selection of Products and Processes

Detailed technical and economic data was collected on producing 62 major chemicals and/or materials. An analysis of the production methods, process energy use and the technical status of these lead to selecting 23 products to study further for production at OEICs. The currently feasible methods to produce these products were then identified and the main technical requirements described.

Production of the selected products was grouped into five separate complexes: (1) Sea Chemicals; (2) Organic Chemicals and Plastics; (3) Fertilizers; (4) Aluminum and (5) Steel.

Market, Transportation and Raw Materials

A preliminary market analysis covering 30 possible products revealed that at least nine of these should not be studied further due to low demand, low growth rate or both. Among these are bromine, ethyl chloride, phosphorus (electric-furnace), manganese, sodium and titanium. The high demand, high growth rate products are as follows:

| Product | U.S.Demand, 1975 (1000s short tons/yr) | Predicted Growth Rate %/yr. |
|---|---|---|
| Potash | 4,999 | 5.0 |
| Chlorine | 11,753 | 6.0 |
| Caustic | 11,821 | 6.5 |
| Magnesium | 144 | 8.0 |
| Ethylene | 12,678 | 7.0 |
| Vinyl Chloride | 2,000 | 4.0 |
| Polyethylene (LD) | 3,324 | 9.0 |
| Polyethylene (HD) | 1,471 | 9.0 |
| Ethylene Oxide | 1,900 | 6.0 |
| Ammonia | 16,218 | 5.0 |
| Ammonium Nitrate | 8,750 | 7.0 |
| Aluminum | 6,400 | 6.0 |
| Steel | 113,000 | 2.4 |

A review of raw material requirements and sources of supply showed that raw materials required for producing the products listed could be obtained within reasonable shipping distance to probable locations for OEICs. The one possible exception to this is the use of Naphtha as raw material or feedstock for producing plastics via the electric arc process. A long term reliable supply of naphtha may be uncertain. However, there are many feedstocks that can be substituted for naphtha in this process. These include LNG, coal and, possibly onsite produced synthetic feed.

Shipping of the final products to main industrial ports presents no great problems and shipping costs relative to market prices are in the order of 1% to 5%. Exceptions to this are shipping potash and flammable gases such as hydrogen, acetylene, ethylene and oxygen. Thus, producing these gases for shipment to land for consumption was eliminated from further consideration.

From an examination of the various methods of ocean shipment it was concluded that special, long-term chartered vessels should be utilized for shipping products to markets or else vessels should be owned and operated by the OEIC. This would insure stable, long-term shipping costs and make it possible to balance storage requirements against shipping vessel size when designing the specific complexes.

Storage of raw materials, particularly bulk materials such as iron ore, coke, phosphate rock and alumina, at an ocean site will be a problem. This will contribute to increased production costs. Storage of finished products will require less volume and, with a properly designed platform, should present few problems.

An anlysis of various factors effecting locations for OEICs was made. This considered environmental, logistics and legal factors. It was concluded the following three areas would be most suited.

1. Caribbean Sea - approximately 200 miles north of Caracas
2. Pacific Ocean - approximately 200 miles south of Mexico
3. Pacific Ocean - between 5°N and 10°N, south of Hawaiian Islands

The region in the Caribbean is the most preferable for marketing and logistics requirements of an OEIC. This has been chosen as the location for a typical complex on which the economic analysis was made.

Process Descriptions

A total of 26 individual plants or processes were analyzed to determine if they would be appropriate to use in OEICs. These are listed in Table 1. The 100 series of numbers are for processes that might be used in the sea chemicals complex. Process numbers in the 200 series plus 302 and 303 are applicable to the organic chemicals and plastics complex.

Figure 1 shows the production of sea chemicals via the final processes selected.

For the initial concentration of the sea water prior to extracting minerals, four processes were compared: Freezing; vapor compression evaporation combined with multi-effect evaporation and multi-stage flash evaporation; electrodialysis and; reverse osmosis. The freezing process was selected as being the most suitable for this application.

Then, as can be seen from Figure 1, there are three separate crystallization steps required to extract sodium sulfate, sodium chloride, potash and magnesium chloride. By examining various processes available for achieving

TABLE 1

ALTERNATE PROCESSES ANALYZED

| PROCESS OR PLANT NUMBER | FUNCTION | METHOD | INPUT | PRODUCT |
|---|---|---|---|---|
| 101A | S.W. concentration | Freezing | Sea Water | 3 x conc. S.W. |
| 101B | S.W. concentration | V/C Evaporation | Sea Water | 3 x conc. S.W. |
| 101C | S.W. concentration | Electrodialysis(ED) | Sea Water | 3 x conc. S.W. |
| 101D | S.W. concentration | Reverse Osmosos(RO) Electrodialysis(ED) | Sea Water | 3 x conc. S.W. |
| 102 | Crystallization | Freezing | 3 x conc.S.W. | $Na_2SO_4$ |
| 103 | Crystallization | Freezing | Brine | NaCl Brine |
| 104 | Crystallization | Freezing | Brine | KCl&$MgCl_2$solution |
| 105 | Concentration | Evaporation | $MgCl_2$ solution | Conc. $MgCl_2$ |
| 106 | Mg production | Electrolysis | Conc. $MgCl_2$ | Magnesium |
| 107A | Caustic/chlorine production | Electrolysis (Mercury cells) | NaCl | Chlorine/Caustic, Hydrogen |
| 107B | Caustic/chlorine production | Electrolysis (Diaphragm cells) | NaCl brine | Chlorine/caustic, Hydrogen |
| 201A | Hydrocarbon conversion | Electric Arc | Naphtha | Acetylene |
| 201B | Hydrocarbon conversion | Electric Arc | Naphtha | Ethylene |
| 211A | Vinyl Chloride production | Acetylene & HCl | Acetylene | Vinyl Chloride |
| 211B | Vinyl Chloride production | Pyrolysis of Ethyl-dichloride | Ethylene | Vinyl Chloride |
| 211C | Vinyl Chloride | Balanced ethylene/ Acetylene | Ethylene | Vinyl Chloride |
| 212 | Neoprene Prod. | Balanced Process | Acetylene | Neoprene |
| 213 | Polyethylene production | High pressure polymerization | Ethylene | Polyethylene |
| 214 | Ethylene Oxide production | Catalystic oxidation | Ethylene & Air | Ethylene Oxide |
| 301A | Hydrogen Prod. | DeNora Cell electrolysis | Water | Hydrogen |
| 301B | Hydrogen Prod. | Allis-Chalmers Cell electrolysis | Water | Hydrogen |
| 302 | Ammonia Production | Synthesis | Hydrogen, Nitrogen | Ammonia |
| 303 | Nitrogen Prod. | Air Liquefication | Air | Nitrogen |
| 304 | Fert.Production | Ammonia & Nitric Acid | Ammonia Nitrogen | Ammonium Nitrate |
| 401A | Aluminum Prod. | Hall-Heroult | Alumina | Aluminum |
| 401B | Aluminum Prod. | Chloride | Alumina | Aluminum |

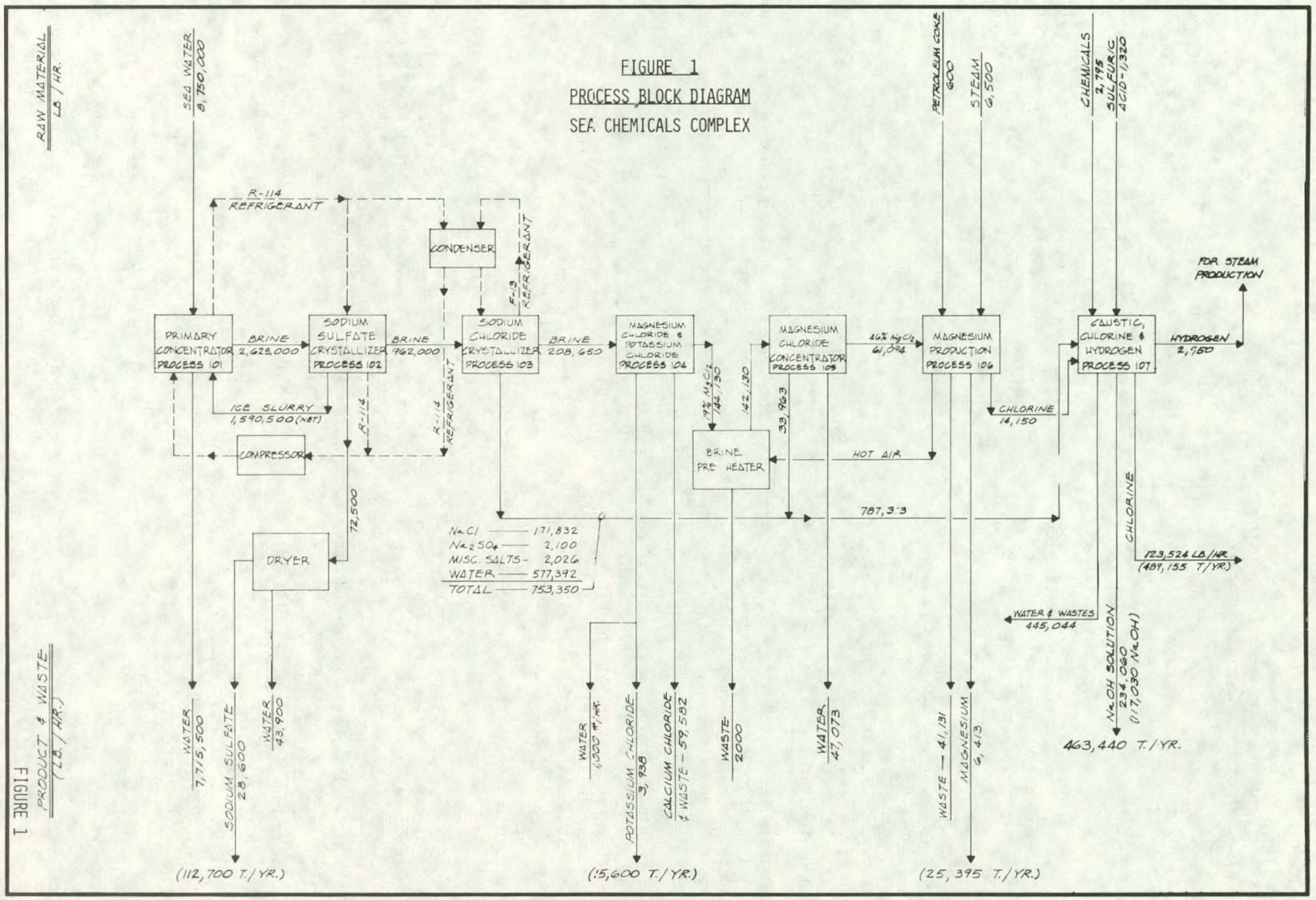

FIGURE 1
PROCESS BLOCK DIAGRAM
SEA CHEMICALS COMPLEX
RAW MATERIAL LB / HR.
SEA WATER 8,750,000
R-114 REFRIGERANT
CONDENSER
F-13 REFRIGERANT
PRIMARY CONCENTRATOR PROCESS 101
BRINE 2,625,000
SODIUM SULFATE CRYSTALLIZER PROCESS 102
BRINE 962,000
SODIUM CHLORIDE CRYSTALLIZER PROCESS 103
BRINE 208,650
MAGNESIUM CHLORIDE & POTASSIUM CHLORIDE PROCESS 104
MAGNESIUM CHLORIDE CONCENTRATOR PROCESS 105
46% MgCl2 61,394
MAGNESIUM PRODUCTION PROCESS 106
CAUSTIC, CHLORINE & HYDROGEN PROCESS 107
PETROLEUM COKE 600
STEAM 6,500
CHEMICALS 2,795
SULFURIC ACID-1,320
FOR STEAM PRODUCTION
HYDROGEN 2,750
ICE SLURRY 1,590,500 (NET)
R-114
R-114 REFRIGERANT
COMPRESSOR
72,500
DRYER
7% MgCl2 142,130
142,130
33,963
BRINE PRE HEATER
HOT AIR
CHLORINE 14,150
787,313
NaCl — 171,832
Na2SO4 — 2,100
MISC. SALTS - 2,026
WATER — 577,392
TOTAL — 753,350
123,524 LB/HR (489,155 T/YR.)
CHLORINE
WATER & WASTES 445,044
NaOH SOLUTION 234,060 (17,030 NaOH)
463,440 T./YR.
PRODUCT & WASTE (LB. / HR.)
WATER 7,715,500
SODIUM SULFATE 28,600
WATER 43,900
WATER 1,355 #/HR.
POTASSIUM CHLORIDE 3,938
CALCIUM CHLORIDE & WASTE - 59,582
WASTE- 2000
WATER 47,073
WASTE — 41,131
MAGNESIUM 6,413
(112,700 T./YR.)
(15,600 T./YR.)
(25,395 T./YR.)

FIGURE 1

these crystallization steps, a continuation of the freezing process down to a temperature of -45°F was selected. This results in the lowest energy requirements and is the simplest of the alternate processes studied.

The magnesium chloride from the last crystallization step (process 104) would then be concentrated and purified in conventional multiple effect evaporators (process 105) to give a 46% magnesium chloride solution.

For producing magnesium, the I.G. Farben type electrolytic cells were chosen over the Dow cells. Since these cells require dehydrated feed, spray drying of the 46% magnesium chloride solution is contemplated, followed by rechlorination.

The salt recovered via processes 103 and 105 flows to process 107 for production of caustic and chlorine.

The diaphragm cell was selected over the mercury cell for producing caustic/chlorine due to possible environmental problems as well as technical problems in maintaining a level base for mercury cells.

Figure 2 is the process flow block diagram for the organic chemicals and plastics complex. Process 201 which produces acetylene and ethylene, is the most important process in this complex and its performance is critical to the overall economics.

Various methods for this operation were compared and it was concluded that the electric arc process using naphtha as a feedstock was the best at the present time in OEICs. This process is adaptable to using many other feedstocks such as LNG, coal and synthesized hydrocarbons. The basic principle of this process involves the use of electricity for the supply of energy to the process, rather than burning fossil fuels in excess of that which is required for reactants.

Next, vinyl chloride will be produced in processes 211A and B by a balanced process from pyrolysis of ethylene dichloride and by combining acetylene and hydrogen chloride.

The production of low density polyethylene and ethylene oxide would be accomplished by conventional means. Some of the oxygen for ethylene oxide production will be obtained from the air-liquefaction and rectification process 303. Most of the nitrogen produced by this process is used in process 302 for the production of ammonia. The hydrogen is obtained from the arc process where it is produced as a by-product. The hydrogen and nitrogen are combined in a reactor at 300 atm using an iron oxide catalyst.

Base Case Complexes

The production rates selected for the Sea Chemicals Complex are as follows:

| Products | Tons/yr |
|---|---|
| Sodium Sulfate | 112,700 |
| Potash | 15,600 |
| Magnesium | 25,395 |
| Sodium Hydroxide | 463,440 |
| Chlorine | 485,155 |
| Total | 1,106,290 |

These products had a total sales value of $172,614.000 U.S. Gulf Coast, mid-1975. In addition to sea water required to produce these products, 2,376 tons/yr of petroleum coke, 19,641 tons/yr of miscellaneous chemicals and 273,584 KWe plus thermal energy are required. The energy requirements by process are as follows.

| Process Description | KWe | Thermal |
|---|---|---|
| Sea Water Concentration | 42,729 | -o- |
| Crystallization Step I | 9,218 | 506,880 |
| Crystallization Step II | 5,758 | -o- |
| Crystallization Step III | 2,169 | -o- |
| MgCl Concentration | 530 | 524,324 |
| Magnesium Products | 56,200 | 772,992 |
| Caustic/Chlorine Products | 156,980 | 2,785,068 |
| | 273,584 | 4,589,244 |

The thermal requirements given above are millions BTUs per year. About 1,168,200 MM BTUs of this are supplied by hydrogen produced. Thus, the net thermal requirements are 3,421,044 MM BTUs per year.

The production rates selected for the Organic Chemicals and Plastics Complex are as follows:

| Product | Tons/yr |
|---|---|
| Vinyl Chloride | 150,000 |
| Ethylene Oxide | 200,000 |
| Polyethylene | 200,000 |
| Ammonia | 211,250 |
| Total | 761,250 |

These products have a total sales value of $288,250,000 U.S. Gulf Coast, mid-1975. Production of these products will require 635,168 tons/yr Naphtha, 101,700 tons/yr Chlorine and 487.3 MWe. However, 115 Mw of this electricity can be generated from steam produced in waste heat boilers. Thus, the net electricity required from an OTEC would be about 372 MW.

The above information for feedstock requirements, electrical requirements and production in the organic chemicals complex was based on process data given in open literature. If current design data is utilized, then only 550,310 tons/yr Naphtha, 91,200 tons/yr chlorine and 331 MWe net from the OTEC would be required.

Environmental Considerations

The various discharges from the base case complexes were identified, their potential environmental impact assessed, and possible pollution control technology established.

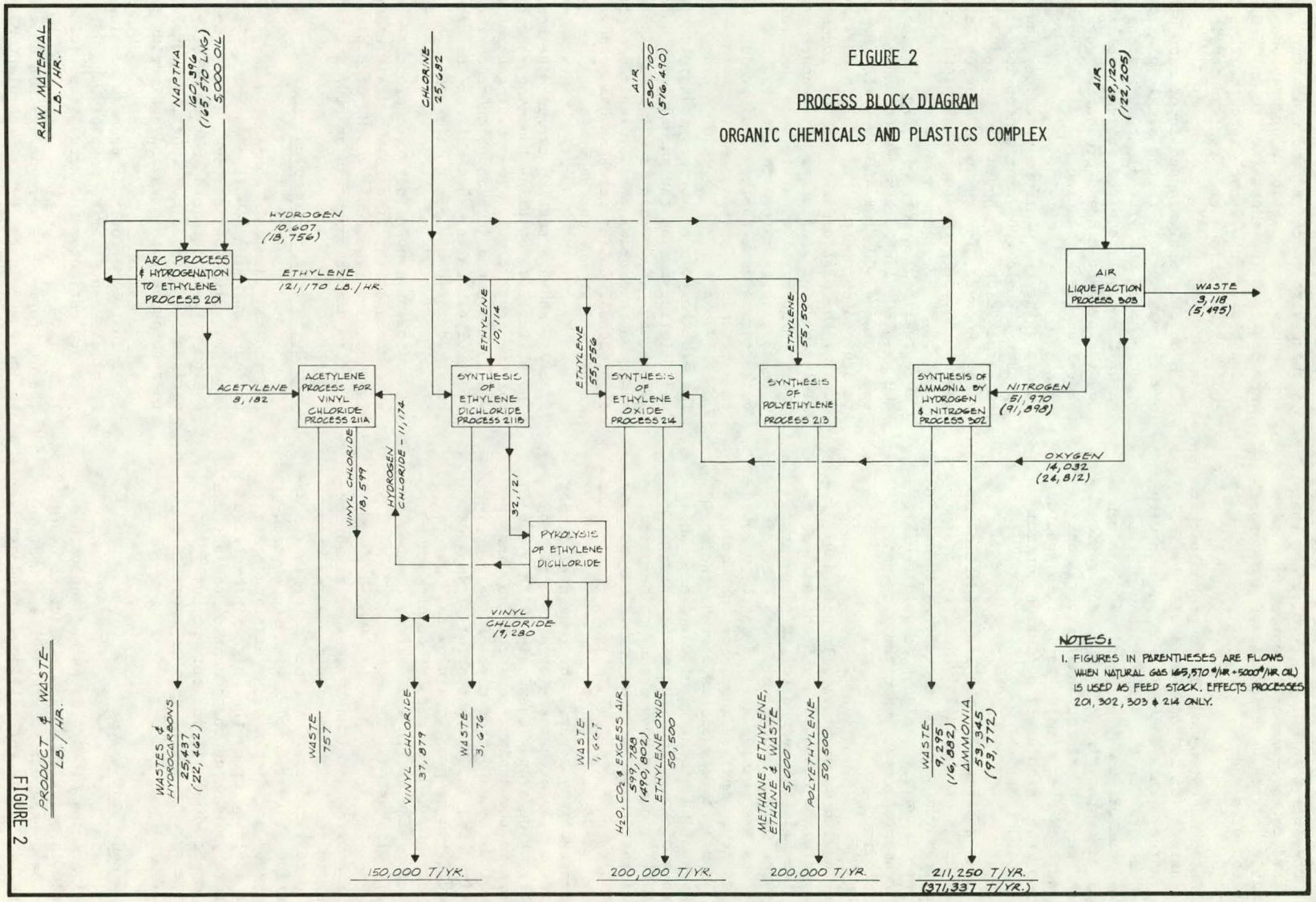

FIGURE 2
PROCESS BLOCK DIAGRAM
ORGANIC CHEMICALS AND PLASTICS COMPLEX
RAW MATERIAL LB./HR.
NAPTHA 160,396 (165,570 LNG) 5000 OIL
CHLORINE 25,692
AIR 580,700 (576,490)
AIR 69,120 (122,205)
HYDROGEN 10,607 (18,756)
ARC PROCESS & HYDROGENATION TO ETHYLENE PROCESS 201
ETHYLENE 121,170 LB./HR.
AIR LIQUEFACTION PROCESS 303
WASTE 3,118 (5,495)
ETHYLENE 10,114
ETHYLENE 55,556
ETHYLENE 55,500
ACETYLENE 8,182
ACETYLENE PROCESS FOR VINYL CHLORIDE PROCESS 211A
SYNTHESIS OF ETHYLENE DICHLORIDE PROCESS 211B
SYNTHESIS OF ETHYLENE OXIDE PROCESS 214
SYNTHESIS OF POLYETHYLENE PROCESS 213
SYNTHESIS OF AMMONIA BY HYDROGEN & NITROGEN PROCESS 302
NITROGEN 51,970 (91,898)
OXYGEN 14,032 (24,812)
VINYL CHLORIDE 18,599
HYDROGEN CHLORIDE - 11,174
32,121
PYROLYSIS OF ETHYLENE DICHLORIDE
VINYL CHLORIDE 19,280
PRODUCT & WASTE LB./HR.
WASTES & HYDROCARBONS 25,437 (22,462)
WASTE 757
VINYL CHLORIDE 37,879
WASTE 3,676
WASTE 1,617
H2O, CO2 & EXCESS AIR 599,788 (490,802)
ETHYLENE OXIDE 50,500
METHANE, ETHYLENE, ETHANE & WASTE 5,000
POLYETHYLENE 50,500
WASTE 9,295 (16,882)
AMMONIA 53,345 (93,772)
150,000 T/YR.
200,000 T/YR.
200,000 T/YR.
211,250 T/YR. (371,337 T/YR.)
NOTES:
1. FIGURES IN PARENTHESES ARE FLOWS WHEN NATURAL GAS 165,570 #/HR + 5000 #/HR OIL) IS USED AS FEED STOCK. EFFECTS PROCESSES 201, 302, 303 & 214 ONLY.

FIGURE 2

The present and possible future legal regulations that may apply in regard to environmental control were also explored. Possible hazards were identified and comparisons to land sites were made.

By the time OEICs are constructed, it is probable that their siting, construction and operation will be regulated to some degree. This fact, in conjunction with a conscientious concern for the preservation of the oceans, dictates that OEICs may be developed in a manmaner which will be compatible with their environment. OEICs located on the high seas may have several environmental advantages over similar facilities located on land but by no means should all pollution control technologies be abandoned.

Those waste streams generated in the Sea Chemicals Complex are all comprised of chemicals which were initially extracted from the sea and, therefore, through the use of proper disposal techniques, should exhibit no adverse environmental impact upon their re-entry into the eco-system.

In the base case design we combined all individual discharge streams and mixed these with ambient sea water. This combined stream is then close to the temperature and salinity of the water into which it would be discharged. Those waste streams generated in the Organic Chemicals Complex are comprised mostly of combustionable fluids and can be safely disposed of by incineration with the resulting discharge of $CO_2$, water and some small amounts of NOx. In light of the present findings of the EPA's research on ocean incineration, it can be stated that these emissions would be environmentally acceptable.

The greatest threat of any adverse environmental impact from an OEIC lies in the occurrence of accidents, resulting in spills of hazardous chemicals. With a conscientious effort in the design, construction, and operation of an OEIC, the causes of some of these accidents may be eliminated and the potential of damages which could result can be greatly minimized. Due to the remoteness of the OEIC the net effect of such a spill or accident on the health and welfare of the public is largely eliminated.

In comparing the environmental advantages or disadvantages of locating industrial complexes at sea or on land, it must be realized that a prime factor is the degree of interaction of that complex with its environment. The OEIC does not displace any existing habitats and is somewhat isolated from other highly productive eco-systems, thereby reducing the potential for adverse environmental impact while placing this potential in an area of reduced critical concern when compared with land sites.

Structure Design and Plant Layouts

Considerable comparisons of alternates and analysis of designs were made in order to select a platform design concept for the base case OEICs. Three basic units were first compared. These were: 1) power production plant; 2) chemical processing facility; 3) product storage facility. Various alternate configurations of these were conceived and compared. Alternate platform concepts as developed by previous investigators were analyzed for adaptation to an OEIC. These included the surface vessel concept, the spar buoy concept and variations on a semi-submersible concept.

Based on this analysis and input from other investigators, it was decided that a single platform could be used to house the OTEC plant, the process equipment for an OEIC and all required storage facilities. This is for the product mix and production quantities of the base-line cases selected.

In analyzing the platform concepts, the semi-submersible appears to hold good promise for long-term application in large OEICs and should be studied further in this regard. However, for the base case OEICs, the surface vessel concept proposed by TRW-Global Marine was adopted

Conceptualized layouts of a sea chemicals complex with a 300 MW OTEC plant are presented and described. This vessel would be 900' L x 450' W x 150' H, constructed of reinforced concrete. Figure 3 is the layout of the top deck of the platform showing the process arrangement, living quarters, offices, maintenance shops and storage areas. The arrangement is such that the main process streams flow from fore to aft (right to left) with main bulk storage next to the final production processes at the aft end.

The electrolytic cells for producing magnesium, caustic and chlorine are on the second level under processes 102 through 107. This is shown in figure 4. Also shown on this drawing is a plan and section of one block of process 101. This process has been divided into four sections like the one shown.

Figure 5 shows a section through the complete platform. The third level contains the evaporators and condensers for the power plant. The power generation equipment would be mounted just above those on the level below the electrolytic cells. One-half of the second level is reserved for power plant maintenance and parts storage.

In a similar manner, detailed process equipment layouts were made for the organic chemicals and plastics complex. This complex requires a 400 MW OTEC plant. The overall platform dimensions would be 900' L x 600' W x 150' H.

Cost Estimate and Economics

For the sea chemicals complex, a detailed capital cost estimate was made covering each item of equipment based on previously developed design data. Costs of major equipment were obtained from manufacturer's quotations. various elements of construction costs were estimated in accordance with standard estimating practice.

Total installed costs of process modules for the Organic Chemicals and Plastics Complex were determined from previous estimates and actual costs of similar plants.

The platform costs were determined as those attributed to increases in the basic OTEC plant platform structure needed to install all the process equipment with supporting facilities. Other costs, including start up

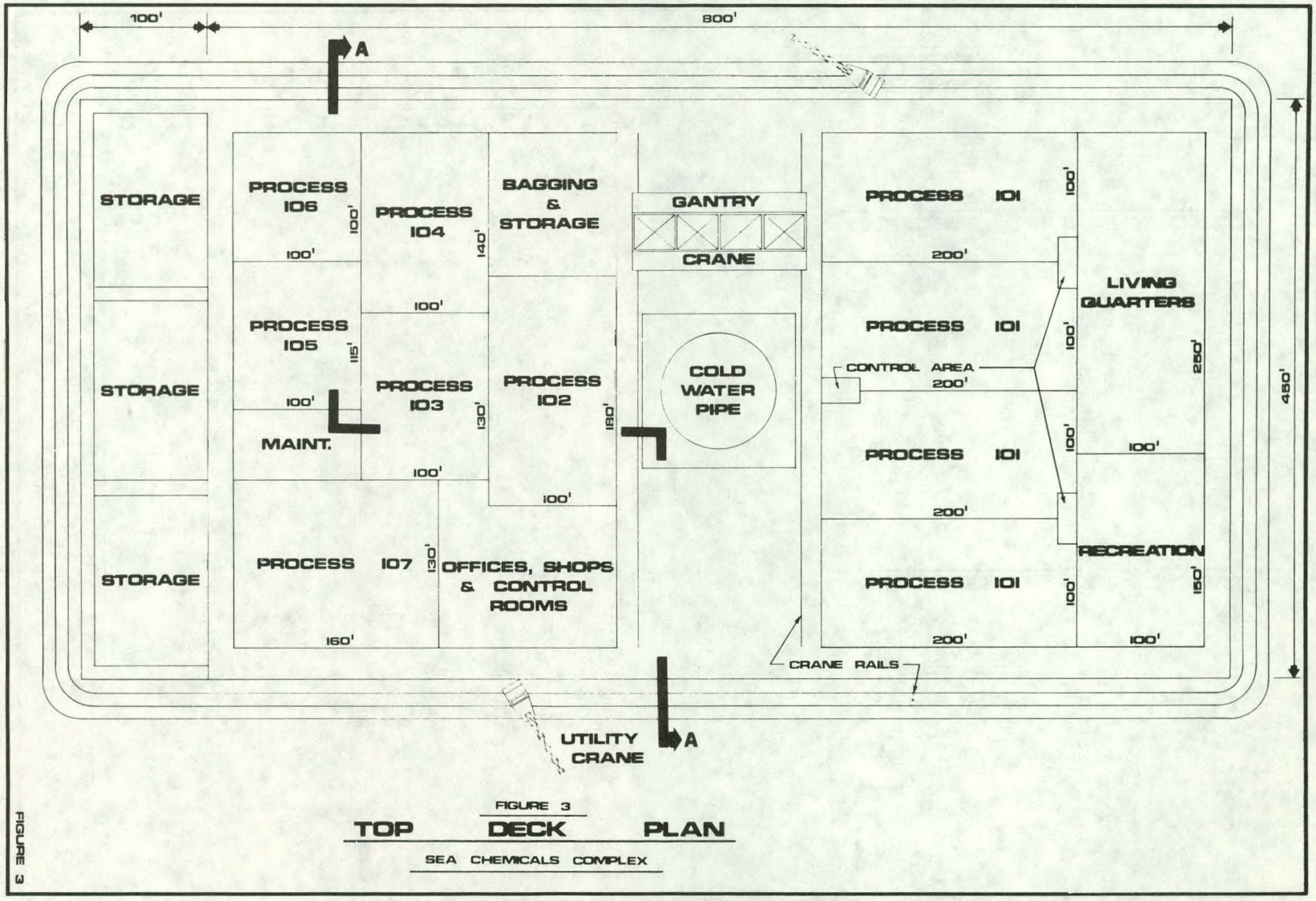



FIGURE 3

## TOP DECK PLAN

SEA CHEMICALS COMPLEX

FIGURE 3

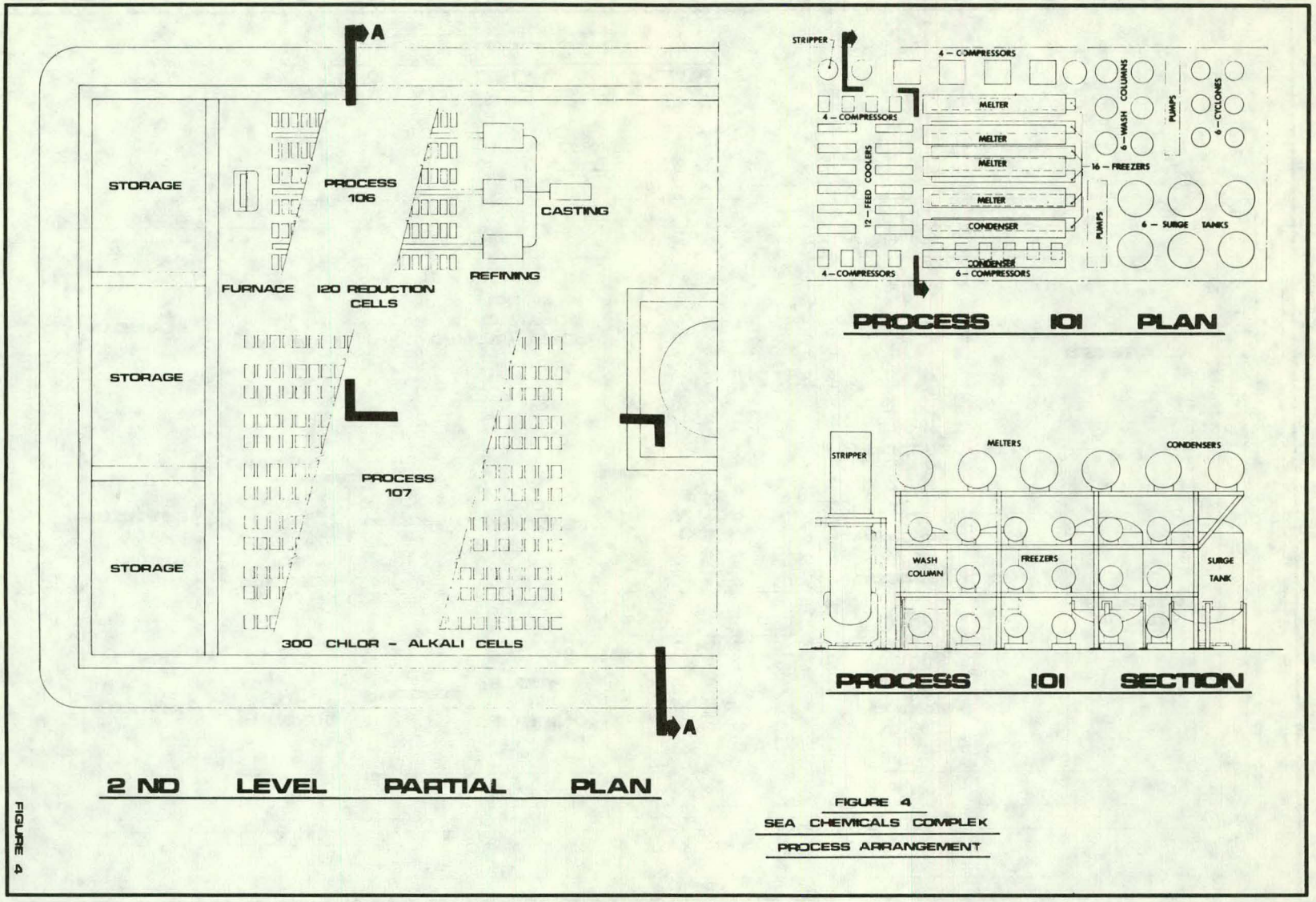



FIGURE 4

SEA CHEMICALS COMPLEX

PROCESS ARRANGEMENT

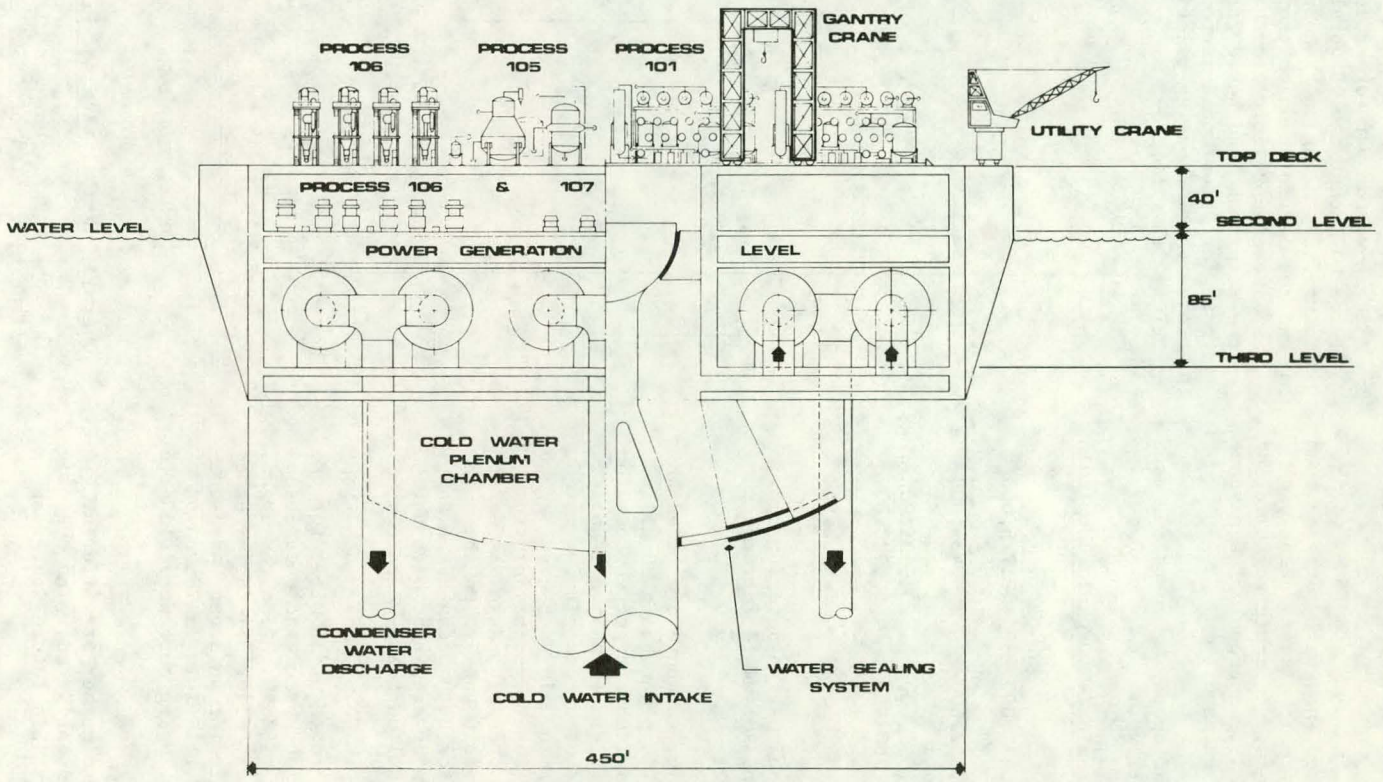



FIGURE 5

SEA CHEMICALS COMPLEX

**SECTION A-A**

PLATFORM ARRANGEMENT

FIGURE 15

costs, interest during construction, owner's costs and working capital were added to arrive at the total estimated investment.

Production costs were estimated in detail for each item of: feedstocks; electricity; fuel; miscellaneous process materials; and other items. An administrative and sales cost of 10% was deducted from gross sales revenue to arrive at a net operating revenue.

Based on this, the capital and operating costs for each complex were estimated as follows:

| Item | Sea Chemicals | Organic Chemicals |
|---|---|---|
| Total Capital Investment | $ 265,991,000 | $ 408,715,000 |
| Net Annual Operating Revenue | 155,352,600 | 259,425,000 |
| Annual Production Costs | 88,092,000 | 206,505,000 |
| Net Operating Profit | 67,260,000 | 52,920,000 |
| Return on Investment | 25.28% | 12.94% |

Utilizing current operating and design data for the organic chemicals complex, the ROI would increase to 17.45%.

The operating costs and ROIs given above are based on the cost of power from the OTEC plant being 20 mills/KWH. This was considered a suitable expected cost for comparison purposes. However, since the profitability depends primarily on the cost of electricity, a more exact expected cost was determined in each case. Then, the effects on profitability due to variations from this expected cost through a probable range was determined. This is shown in figures 6 and 7. On these the ROI vs. power cost is given for both ocean-based and land-based complexes. It can be seen that with the same electricity costs, the ROI on ocean-based complexes would be greater.

At the normal expected power costs of 29 mills for the sea chemicals complex, both land-based and ocean-based complexes yield approximately 18% ROI. For the organic chemicals and plastics complex (Figure 7) the expected power cost would be 19.1 mills for an ocean based complex and the ROI would be 13.7%. This was based on low yields for the processes. Using current yield data, the ROI would be 17.6%.

The effects of variations in a number of different other parameters were also investigated. The most significant of these was the possible future increases in fossil fuel costs.

After the start of operation large differences could become apparent if land-based power continues to increase while the ocean based power remains relatively constant. If we assume that product prices are set to maintain constant ROIs for land-based facilities, then the ROI of ocean facilities will increase with time. Figure 8 shows this graphically for two rates of increases in fuel costs, 6% and 12%, corresponding to 5% and 10% increases in electrical cost from fossil fuel-fired power plants.

This shows the very dramatic increases and potentiall large ROIs that may be obtained from these OEICs. Of course, depending on the market penetration of OEICs and the degree at which the cost of land-based power may increase relative to the cost of ocean-based power, the return on land-based facilities may decrease while those for OEICs would increase less. Still, this illustrates the increasing relative economical operation of OEICs with time.

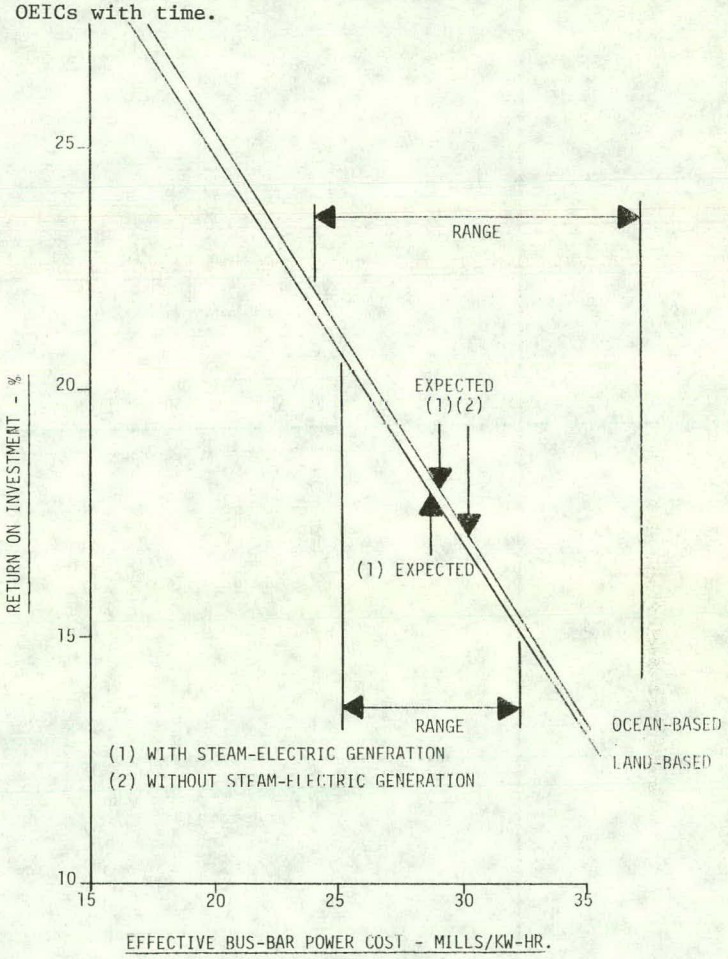



FIGURE 6
ROI VS. POWER COSTS - SEA CHEMICALS COMPLEX

-Overall Possibilities and Problems

The last task of our work involved determining the overall possibilities of OEICs and problems associated with their development. The total possibilities for production from, and electrical utilization by, OEICs were assessed. Supplying only a modest share of the world's increased demands between 1990 and 2000 would require production of 20,075,000 tons/yr at Sea Chemicals OEICs and 14,380,000 tons/yr at Organic Chemicals and Plastics OEICs. This production would require 40 OEICs similar to the base case complexes studied. These would consume 11,855 MWe net and require OTECs with a total capacity of 13,000 MWe. A deeper market penetration may be

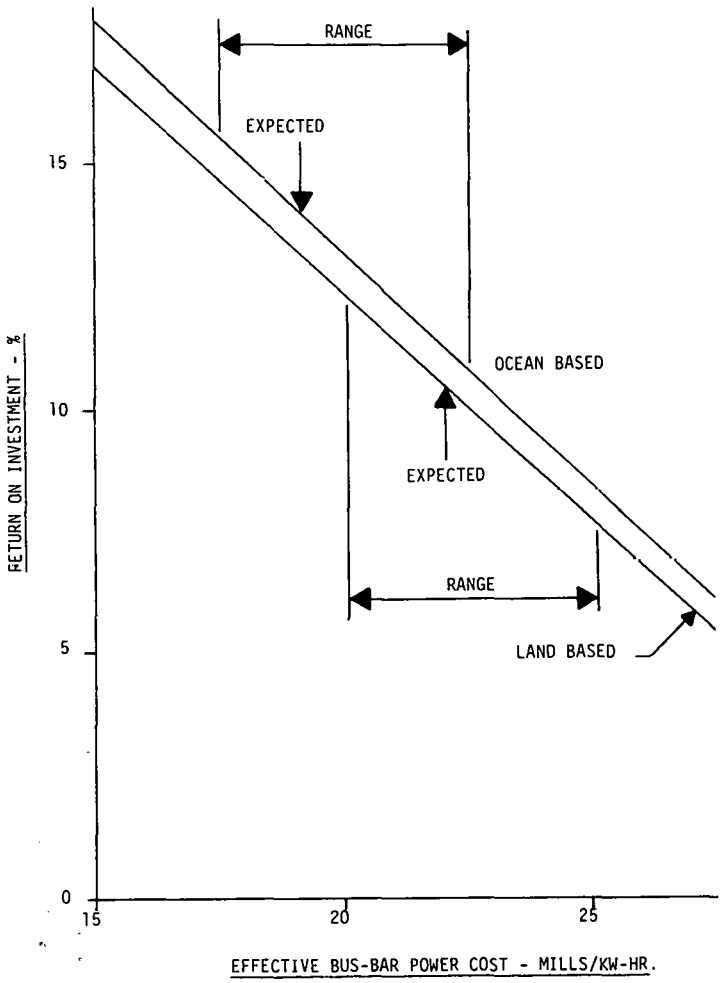



FIGURE 7

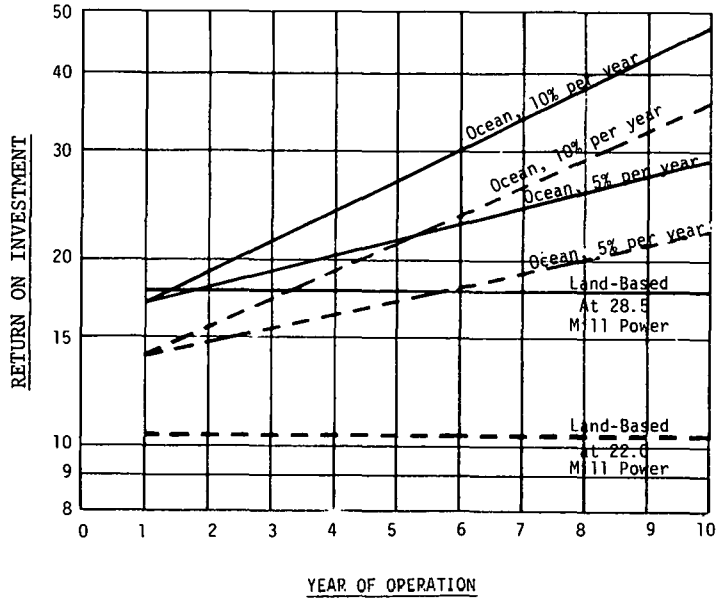
ROI VS. POWER COSTS - ORGANIC CHEMICALS COMPLEX

possible, up to about twice these production rates.

We did an investigation into the fuels and feedstocks for the electric arc process. This showed that a number of alternatives are available which could make it possible for the organic chemicals and plastics OEICs to be independent of hydrocarbons. The most promising of these may be synthesizing methane and methanol from coal.

A schedule for staged development and construction of OEICs was developed. This indicates that 14 years will be required to have a full size Sea Chemicals Complex operating. An Organic Chemicals and Plastics Complex could be fully operational in about 11 years. Allowing additional time to initially demonstrate the OTEC concept would mean that it would be 1990 to 1993 before the first fully operational OEIC could exist.

There will be many problems in implementing a project to construct many larger OEICs. They include legal, geopolitical, taxation, financing, ownership, planning and management. No amount of technical feasibility will




1. Solid lines are for Sea Chemicals Complex (300MW)
2. Dashed lines are for Organic Chemicals Complex (400 MW)
3. Increases for ocean sited complexes are based on 5% and 10% increases in land-based electrical costs with product prices increased accordingly.

FIGURE 8

RETURN ON INVESTMENT VS. YEAR OF OPERATION

ensure the success of OEICs unless, and until, the problems of implementation have been met and solved. This was true in the past concerning development projects, it is even more true today, and can be expected to be increasingly true in the future. Further studies should be organized and pursued with emphasis toward workable solutions of the problems identified.

Process 101 through 104 in the Sea Chemicals Complex are based on limited pilot plant and bench scale testing combined with theoretical considerations. There are areas for improvements and refinements as well as technical problems to solve. Further technical study of these processes are needed as well as pilot plant testing. It is believed that a more extensive and precise analysis of the overall arc process, as presented herein, is warranted. In this connection, there should also be a special and detailed study concerning the economical production of synthetic feedstock for this process.

## Conclusions

The overall conclusion of the study was that producing energy intensive products at integrated Ocean Energy Industrial Complexes is technically sound and economically viable.

Some of our specific conclusions are as follows:

a. The three sites most suited to locating OEICs are: 1) Caribbean Sea, approximately 200 miles north of Caracas; 2) Pacific Ocean, approximately 200 miles south of Mexico and; 3) Pacific Ocean,

south of Hawaiian Islands.

b. The freezing process is most suited for primary concentration of sea water as well as for the crystallization steps required.

c. The electric arc process using Naphtha as the feedstock is most suited in the near-term for production of acetylene and ethylene for subsequent production of organic chemicals and plastics.

d. A single platform concept housing the OTEC, process equipment and all required storage should be used in the size range selected for the base case OEICs. This should be a surface type vessel or a semi-submersible.

e. The two main complexes studied can be constructed and operated at the selected sites with no adverse environmental impact. Furthermore, the effort and cost to do this for an OEIC is considered less than for comparable land-based complex from which there will always be some adverse impact.

f. Products can be produced at a sea chemicals OEIC competitively with production at a similar land-based complex. The estimated Return on Investment is 25% based at power cost of 20 mills/KWH from an OTEC. At an expected power cost of 30 mills/KWH, the ROI would be about 18%.

g. Products can be produced at an organic chemicals and plastics OEIC competitively with production at a similar land-based complex. The estimated Return on Investment is 13% to 17% depending on operating yields obtained. This is with 20 mills/KWH power cost. At an expected effective power cost of 19.1 mills/KWH, the ROI would be about 13.7% to 17.6% depending on the operating yields obtained.

h. Problems that must be faced to implement construction and operation of OEICs will be many and large. Studies are needed to identify these problems and formulate solutions.

i. To supply only a portion of the world's increased demand for the nine products selected between 1990 and 2000 would require 40 base case OEICs. These would require OTEC power plants with a total design capacity of 13,000 MWe.

j. Further process studies are needed on both OEICs presented. Pilot plant testing will be required for the freezing processes involved in the sea chemicals complexes. Studies concerning synthesizing feedstock for the electric arc processes should be undertaken.

References:

1. Hornburg, C.D., Lindal, B., El-Ramly, N., "Preliminary Research on Ocean Energy Industrial Complexes", Report ORO-4915-3 prepared for the United States Energy Research and Development Administratic under Contract No. E-(40-1)-4915.

Eighty-four references were utilized in the preparation of this report and are listed therein.

CONF-770331--5

# ALTERNATIVE FORMS OF ENERGY TRANSMISSION FROM OTEC PLANTS

A. KONOPKA, N. BIEDERMAN, A. TALIB, AND B. YUDOW
*Energy Systems Analysis*
*Institute of Gas Technology*
*3424 S. State Street*
*Chicago, Illinois*

## ABSTRACT

This paper compares the transmission of OTEC-derived chemical and electrical energy. The chemical energy-carriers considered are the following:

- Gaseous and liquid hydrogen
- Liquid ammonia
- Methanol
- Gasoline
- Hydrazine hydrate
- Anhydrous hydrazine
- Unsymmetrical dimethylhydrazine (UDMH)
- 1,7-Octadiyne
- Tetrahydrodicyclopentadiene.

The assessment assumes that each of the above energy carriers were transported by barge and/or pipeline. The delivered costs were then compared with transmission of electricity by submarine cables. Because chemical and electrical energy are not equivalent, however, their comparison can only be done after the outputs are converted to a common form. Thus, in addition to presenting the delivered cost and overall energy efficiency of the chemical energy-carriers, we have provided a discussion of the equipment, costs, and efficiencies of converting the hydrogen and ammonia delivered into electricity, and the electricity delivered into hydrogen and ammonia.

As such, this paper provides a concise technical assessment and economic analysis of components associated with the conversion, storage, transportation, and shore-based receiving facilities for the conversion of OTEC mechanical energy to chemical energy, and compares this in a like manner to the conversion and transmission of electrical power.

Results concerning the hydrogen and ammonia analysis were determined as part of the OTEC program at IGT from May 1975 through May 1976 under Contract No. NSF-C1008 (AER-75-00033) with the National Science Foundation and ERDA. Information concerning carbonaceous fuels and high-energy fuels production was developed as part of the current IGT OTEC program under Contract No. E(49-18)-2426 with ERDA.

## INTRODUCTION

Considerable analysis has been carried out assessing the ways and means by which ocean thermal energy conversion (OTEC) plants could be used to provide energy for the U.S. economy. This energy, derived from the difference between the deep and surface ocean temperatures, must be delivered to shore, and the overall credibility of OTEC could significantly depend on this transmission system.

Electric cables generally offer the lowest delivered energy costs because of their simplicity and their small amount of conversion losses. This alternative, however, is dependent upon relatively close proximity between the OTEC plant and the energy market. It also requires the platform to be moved, restricting somewhat plant siting and keeping the platform from taking advantage of seasonal changes in the ocean temperature differentials. The cable alternative precludes the plant from serving more than a single energy market or delivering energy onshore at more than one point. Finally, it does not lend itself to other than base-load supply of power.

On the other hand, chemical energy transport of OTEC power is more expensive than electric cable transmission. Because electric power is generated first and the chemical energy-carriers are derived in a number of ways from electricity, the production of chemicals is more complex, and the delivery system is, consequently, less efficient. While the transmission of chemical energy-carriers by pipeline suffers some of the same drawbacks as electric cables, the use of barges or ships to

transport chemical energy to shore provides the opportunity for much more flexibility in plant siting and the points to which energy can be delivered. (The cost of barge transport is relatively inflexible to the distance between the OTEC plant and the delivery point.) Another, less assessed, advantage is that chemical energy-carriers are in a storable form; thus, they could be used to provide peaking energy for onshore use, and not be confined to base-load supply.

The Institute of Gas Technology (IGT) has studied chemical energy carriers as possible alternatives to electric transmission. We have analyzed gaseous and liquid hydrogen and liquid ammonia; high-energy fuels, such as hydrazine hydrate, anhydrous hydrazine, unsymmetrical dimethylhydrazine, 1-7-octadiyne, and tetrahydrodicyclopentadiene; and carbonaceous fuels, such as methanol, gasoline, and methane. Cost estimates for their production and transmission to shore are presented in this paper.

## Chemical Energy Production

We have chosen two OTEC plant sizes, 100 MW and 500 MW, to represent the size range currently under investigation and based our delivered unit energy cost calculations on these two plant sizes. We have also considered the technical aspects of producing chemical energy-carriers onboard an OTEC platform, basing the synthesis on electrically-derived hydrogen, and either ocean-derived or imported raw materials.

The basic building block for all the chemicals analyzed is hydrogen. Hydrogen production by electrolysis is an established industrial process, used most often where relatively inexpensive power is available. [12] Technical advances will make electrolyzers cheaper and more efficient.

Three stages of development of electrolyzer technology have been assumed in our analyses to indicate the benefits of technological improvements in electrolyzers:

a. Current Technology (CT), representing off-the-shelf technology. [13]

b. Short-Range Improved Technology (SRIT), representing a 1- to 3-year research goal realization. [17]

c. Long-Range Improved Technology (LRIT), representing possible technology of 1985. [5,6]

A vapor-compression-type water-desalination unit was chosen as the source of pure water for all the electrolysis systems. Rectified conventional a-c electricity generation was considered to provide d-c power for the electrolysis systems. Close coupling of a d-c acyclic generator with an advanced-technology electrolyzer is an alternative to rectification and appears cheaper and more efficient.

We evaluated this as a fourth stage technical improvement called the advanced long-range improved technology (ALRIT) production system. We selected high-efficiency individual components to get an overall high thermal efficiency for the chemical energy production. (Efficiency in our analysis is defined as the higher heating value of the product divided by the shaftpower input multiplied by 100.)

Production Capacity and Efficiency. The estimated production capacities and overall thermal efficiencies of the two OTEC plant sizes for the production of gaseous and liquid hydrogen and liquid ammonia are given in Table 1. The increase in production capacity of the different electrolyzer technologies becomes apparent as more advanced (higher efficiency) electrolyzers are used.

Table 1. CHEMICAL-PLANT PRODUCTION CAPACITIES AND OVERALL EFFICIENCIES

| Chemical Energy Carrier | Shaft Power Capacity, MW | CT Electrolyzer Capacity, tons/day | CT Electrolyzer Efficiency kWhr/lb | CT Electrolyzer Efficiency % | SRIT Electrolyzer Capacity, tons/day | SRIT Electrolyzer Efficiency kWhr/lb | SRIT Electrolyzer Efficiency % |
|---|---|---|---|---|---|---|---|
| Gaseous Hydrogen | 100 | 50 | 23.9 | 74.9 | 53 | 22.7 | 78.9 |
| | 500 | 250 | 23.9 | 74.9 | 264 | 22.7 | 78.9 |
| Liquid Hydrogen | 100 | 39 | 30.8 | 58.1 | 41 | 29.5 | 60.7 |
| | 500 | 194 | 30.8 | 58.1 | 203 | 29.5 | 60.7 |
| Liquid Ammonia | 100 | 250 | 4.8 | 59.0 | 262 | 4.6 | 61.9 |
| | 500 | 1236 | 4.9 | 58.4 | 1297 | 4.6 | 61.2 |

| Chemical Energy Carrier | Shaft Power Capacity, MW | LRIT Electrolyzer Capacity, tons/day | LRIT Electrolyzer Efficiency kWhr/lb | LRIT Electrolyzer Efficiency % | ALRIT System Capacity, tons/day | ALRIT System Efficiency kWhr/lb | ALRIT System Efficiency % |
|---|---|---|---|---|---|---|---|
| Gaseous Hydrogen | 100 | 56 | 21.6 | 83 | 57 | 21.31 | 84 |
| | 500 | 278 | 21.6 | 83 | 282 | 21.31 | 84 |
| Liquid Hydrogen | 100 | 92 | 28.5 | 62.9 | 93 | 26.86 | 66.6 |
| | 500 | 211 | 28.5 | 62.9 | 274 | 26.86 | 66.6 |
| Liquid Ammonia | 100 | 273 | 4.4 | 64.4 | 282 | 4.25 | 66.6 |
| | 500 | 1350 | 4.5 | 63.7 | 1396 | 4.29 | 65.9 |

A77040959

Mechanical energy available at the shaft of the turbines of the OTEC plant.

The overall thermal efficiency of gaseous-hydrogen production ranges from 75% to 84% for CT and ALRIT systems, respectively. The efficiency is identical for both 100-MW and 500-MW plant sizes, since electrolyzers are modularized in largest cell sizes. The general distribution of total electricity among the components for a gaseous hydrogen system is approximately 95% for electrolysis, 3% losses for a-c to d-c rectification and shaftpower conversion, 1% power input for water desalination, and 1% for the pipeline compressor.

The overall thermal efficiency of liquid-hydrogen production ranges from 58% to 67% for CT and ALRIT systems, respectively. The distribution of total electricity among the components of the liquid-hydrogen production plant is approximately 79% for electrolysis, 3% losses for a-c to d-c rectification and shaftpower conversion, 0.6% power input for water desalination, and 17.4% for the liquefaction unit.

The overall thermal efficiency of liquid-ammonia production ranges from 59% to 67% for CT and ALRIT systems, respectively, at an OTEC plant capacity output of 100 MW.

The general distribution of total electricity among the components of the liquid-ammonia production plant is approximately 88% for electrolysis, 3% losses in a-c to d-c rectification and shaftpower conversion, with a 0.6% power input for water desalination, 2.4% for air separation, and 6% for the ammonia-synthesis loop.

Hydrogen and Ammonia Production Economics. Costs of the hydrogen prdduction plant equipment were supplied by manufacturers. [6,13,18] As hydrogen production

requirements increase, more instead of larger electrolyzer cells would be used, making electrolyzer plant equipment costs linear with respect to plant capacity.

costs of a vapor-compression water desalination unit [4] and an a-c generator and rectification unit [5] were also used to obtain the hydrogen production facility's total cost. For an ALRIT system, the cost of the a-c generator and rectification unit was replaced by an acyclic generator's cost. [6]

A factor of 1.5 was used to approximate the total installed plant investment.

For liquid hydrogen liquefication equipment, Linde Division, Union Carbide Corp., provided costs. [19] The liquefier cost was added to the hydrogen production plant cost to obtain the total plant investment for the liquid hydrogen production facility.

For ammonia production, the costs of an air-separation plant and an ammonia synthesis loop were estimated from data provided by Union Carbide and J. F. Pritchard and Co. [13,20] The low energy consumption and high reliability of an air-separation technique make it a more suitable unit for obtaining nitrogen than the alternative hydrogen-air combustion technique.

Burning excess hydrogen in air to obtain synthesis gas of a 3:1 hydrogen/nitrogen mixture results in a decrease in ammonia production efficiency of almost 8% over the air-separation method to obtain nitrogen for ammonia synthesis.

Table 2 gives the total plant investment for producing gaseous hydrogen, liquid hydrogen, and ammonia, including the installed cost of all processing units with the necessary auxiliary systems but not including any incremental cost that might be required to expand the existing OTEC platform. It also does not include working capital, interest during construction, or any start-up costs.

Table 2. OTEC CHEMICAL PLANT CAPACITY AND CAPITAL INVESTMENT

| | 500-MW | | | | 100-MW | | | |
|---|---|---|---|---|---|---|---|---|
| | Plant Capacity | | Plant Investment | | Plant Capacity | | Plant Investment | |
| Chemical Energy Carrier | tons/day | kg/day | $10^6$ $ | $/kW (out) | tons/day | kg/day | $10^6$ $ | $/kW (out) |
| Hydrogen Gas | | | | | | | | |
| CT | 250 | 226,800 | 170 | 456 | 50 | 45,400 | 34 | 456 |
| SRIT | 264 | 239,500 | 127.6 | 324 | 53 | 18,100 | 25.61 | 324 |
| LRIT | 278 | 252,000 | 56 | 135 | 56 | 50,800 | 11.28 | 135 |
| ALRIT | 282 | 255,800 | 33.24 | 79 | 57 | 51,700 | 6.72 | 79 |
| Liquid Hydrogen | | | | | | | | |
| CT | 194 | 176,000 | 190.4 | 658 | 39 | 35,400 | 49.74 | 855 |
| SRIT | 203 | 184,200 | 154.45 | 510 | 41 | 37,200 | 43.12 | 705 |
| LRIT | 211 | 191,400 | 95.42 | 303 | 42 | 38,100 | 31.08 | 496 |
| ALRIT | 223 | 202,300 | 77.18 | 232 | 45 | 40,800 | 25.90 | 386 |
| Liquid Ammonia | | | | | | | | |
| CT | 1236 | 1,121,300 | 188.48 | 646 | 250 | 226,800 | 43.36 | 735 |
| SRIT | 1297 | 1,176,600 | 150.00 | 490 | 262 | 237,700 | 35.55 | 575 |
| LRIT | 1350 | 1,224,700 | 84.44 | 265 | 273 | 247,700 | 22.94 | 356 |
| ALRIT | 1396 | 1,266,400 | 65.90 | 200 | 282 | 255,800 | 19.11 | 287 |

A7704096

We calculated the unit cost of producing the various chemicals for both plant sizes, assuming -

- The fixed charge rate* is broken down as -

| | |
|---|---|
| Capital Recovery Factor | 12.8% |
| Income Tax Annuity | 3.8% |
| Other Taxes and Insurance | 2.0% |
| Fixed Charge Rate | 18.6% |

- An annual maintenance expense of 2% of the initial investment of which 1% is maintenance labor, and 1% maintenance supplies.
- A cost of labor, supervision, and administration and general overhead based on manpower requirements of both plant sizes. (The average pay for the operating labor was taken to be $11.42/hr. The cost of maintenance labor was taken as 1% of the initial plant investment. The cost of supervision was taken as 15% of the cost of operating and maintenance labor. General administration and overhead was taken as 60% of the cost of operating, maintenance labor, and supervision.)
- The shaftpower was purchased from the OTEC plant. (Because the shaftpower cost is uncertain, we presented the chemical energy production cost with a range of shaft-power costs.)

The total unit chemical energy production cost is obtained by dividing the total annual cost (annual fixed charges, annual operating and maintenance cost, and annual fuel cost) by the annual throughput of chemical energy. (Annual throughput of chemical energy is based on a 90% OTEC plant availability factor.) A representative unit production cost ($/GJ gaseous hydrogen, liquid hydrogen, and ammonia) is given in Figure 1. This figure shows the sensitivity of unit chemical energy production costs to OTEC shaftpower costs.

Hydrogen and Ammonia Energy Transport - Pipeline. We investigated gaseous hydrogen and liquid ammonia pipelines and liquid hydrogen and liquid ammonia ocean-going barges to transport energy.

For pipeline transportation of gaseous hydrogen, we assumed the following:

- Unit costs based on an annual throughput corresponding to a 0.9-plant availability factor for both 100-MW and 500-MW OTEC plants.
- Hydrogen gas from the electrolyzer at 400 psia (2760 kPa), and required onshore delivery pressure at 500 psia (3450 kPa)
- Use of a reciprocating compressor and intercooler with electric motor drive located on the OTEC platform. (The discharge pressure of the pipeline compressor was approximately 1500 psia (10,340 kPa) consistent with maximum pipeline pressures considered for safe operation.)

* Based on a debt/equity ratio of 60:40, an interest rate on debt of 9%, return on equity of 15%, 20-years straight line depreciation for taxes and cost accounting.

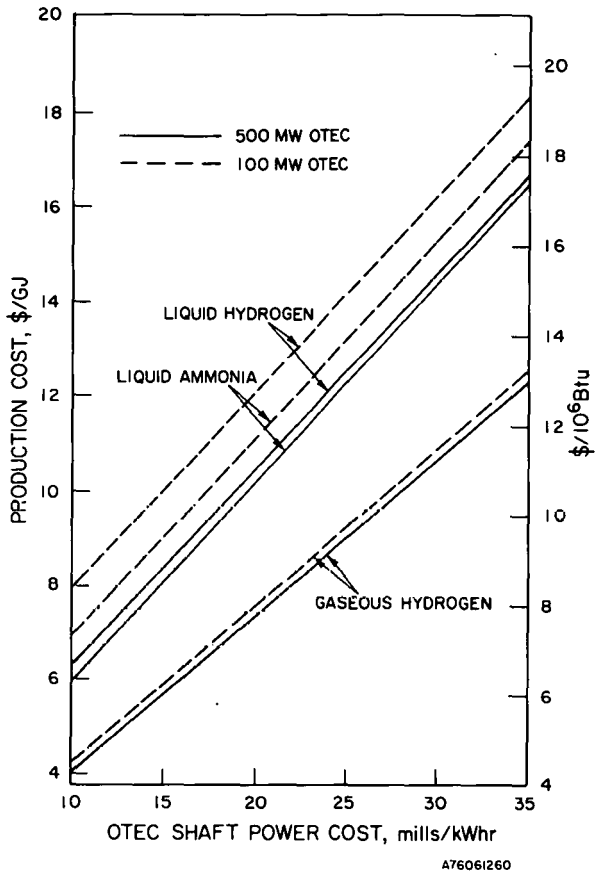



Figure 1. COST OF ONSHORE PRODUCED ELECTRICAL ENERGY AS A FUNCTION OF PLANT PRODUCED CHEMICAL ENERGY

- Reciprocating compressor installed costs ranged from $480/hp to $305/hp, decreasing with increased throughput, with installation costs of $150/hp included[9]

- An installed cost of the riser for gaseous hydrogen, consisting of the installed riser casing cost and the installed cost of auxiliary equipment including tensioning and control equipment[7]

- Total cost per mile of pipelines for either gaseous hydrogen and liquid ammonia installed in water depths of 1000 to 1500 ft (304.8 to 457.2 meter) ranging from $150,000/mile to $840,000/mile ($240,000/km to $1,104,000/km) for outside pipe diameters of 3.7-in. OD to 20.0-in. OD (9.4 cm to 50.8 cm), respectively. [3]

For pipeline transportation of liquid ammonia we assumed the following -

- Unit costs based on an annual throughput corresponding to a 0.9-plant availability factor for both plant sizes

- Liquid ammonia produced on the OTEC platform pumped up to near 1500 psia with a small temperature rise from liquid ammonia production conditions of -28° F (240° K) and 1 atm, and then sent to the pipeline

- An estimated total installed cost of the liquid ammonia pump and electric driver of $384/hp with $100/hp included for installation [8]

- That installed riser cost for liquid ammonia consisted of the installed riser casing cost and the installed cost of auxiliary equipment.[7]

We determined unit transport costs for pipeline gaseous hydrogen and liquid ammonia by adding the compressor or liquid pump installed costs, the operating costs of the compressor or liquid pump station, the energy costs for the electric drive, the cost of the riser, and the cost of the pipeline. Annual fixed costs were determined using a capital charge of 18.6%/year. We combined the unit transportation costs and terminal costs to obtain the delivered chemical energy costs.

Hydrogen and Ammonia Energy Transport - Barge. We investigated using ocean-going barges as an alternative to pipeline transport of liquid ammonia or gaseous hydrogen. The barge transport system would consist of OTEC on-site storage to accumulate enough energy carrier product to fill the barges, a system to load the barges with the energy carrier product, and the barges carrying the product to shore.

We used the notched-barge concept, which includes a notch in the stern into which an ocean-going tug's bow is semipermanently locked.

At each distance for which transport costs were developed, the on-site storage was sized to the barge capacity.

The energy carrier loading system consisted of loading arms, liquid transfer and vapor return lines, valves, fittings, and safety equipment.[11]

The design, construction, and operation of ocean-going liquid ammonia barges is well established, but the cost of cryogenic barges for liquid hydrogen transport is very uncertain. Although NASA has established liquid hydrogen transport by river barge, there is no design or operating experience in hauling large quantities of liquid hydrogen in ocean-going vessels.

We assumed barges of 15,000, 30,000, and 60,000 bbl (2385, 4770, and 9540 cu m) capacities. At each transport distance for which unit costs were evaluated, we selected the best barge size for delivering the annually produced energy carrier within the constraints of the length of the barge operating year, the speed of the barge-tug combination, the turnaround time at each end of the run, and of the 100% annual production of the energy carrier.[2]

Capital costs for liquid ammonia barges[2,16] ranged from $147/bbl ($925/cu m) for a 15,000 bbl (2385 cu m) barge to $103/bbl ($648/cu m) for a 60,000 bbl (9539 cu m) barge. Tug horsepower requirements ranged from 1000 shp to 2400 shp, with tug costs from $0.9 to $2.0 million.

Air Products Company's preliminary efforts to design a 15,000 bbl (2385 cu m) liquid hydrogen barge for the Space Shuttle program were used to establish a range of liquid hydrogen barge costs. In the proposed Air Products design, the cylindrical, vacuum insulated tanks, each of 7500 bbl (2385 cu m) capacity, are arrayed in-line on the barge deck to achieve the desired capacity of 15,000 bbl (2385 cu m). [18] An upper estimate of the liquid hydrogen barge cost was $600/bbl ($3774/cu m). Tug horsepower and costs corresponded to requirements for liquid ammonia barges.

The unit costs of energy carrier transport that we present are based on the annual OTEC energy carrier throughput (based on 90% OTEC plant availability) for plants using LRIT electrolyzers. Annual throughputs for liquid hydrogen transport were reduced by hydrogen losses due to barge boil-off and liquid hydrogen transfer to land. Boil-off losses during OTEC storage, transfer, and handling were assumed to be reliquefied.

We assumed the following -

- An annual charge rate of 20% of the capital costs of the tug and barge
- Annual Maintenance costs of 5% of the capital cost of the tug and barge
- Marine diesel oil costing $16.00/bbl ($10.11 cu/m) to fuel the tug. [15]

We combined barge transport unit costs with chemical energy production costs and terminaling costs to obtain the total delivered cost of chemical energy.

Hydrogen and Ammonia Land-Based Terminal Facility

Barge Terminal Facility. There must be a storage facility onshore to receive the energy carrier and to distribute it to the pipeline or powerplant.

We sized the receiving terminal's storage capacity to twice the capacity of the largest barge delivering the energy carrier to cushion against such contingencies as OTEC plant breakdown, barge transport delays, or variations in demand.

Table 3 presents liquid hydrogen and liquid ammonia terminal costs for energy quantities of both 100-MW and 500-MW OTEC plants and transmission distances of 100, 600, and 1000 miles (161, 965, and 1609 km).

Onshore-Pipeline Terminal Facility. Gaseous hydrogen or pipeline liquid ammonia require no onshore terminal facilities except possibly a compressor or pump station.

Table 3. UNIT TERMINALING COSTS AS A FUNCTION OF DISTANCE

| | 100 MW | | 500 MW | |
|---|---|---|---|---|
| | $/million Btu | $/GJ | $/million Btu | $/GJ |
| Liquid Hydrogen | | | | |
| 100 miles (161 km) | 0.76 | 0.72 | 0.57 | 0.54 |
| 600 miles (956 km) | 1.41 | 1.34 | 0.58 | 0.59 |
| 1000 miles (1609 km) | 2.73 | 2.59 | 0.58 | 0.59 |
| Liquid Ammonia | | | | |
| 100 miles (161 km) | 0.12 | 0.11 | 0.03 | 0.03 |
| miles (956 km) | 0.12 | 0.11 | 0.04 | 0.04 |
| miles (1609 km) | 0.14 | 0.13 | 0.04 | 0.04 |

High-Energy Fuels Production

We examined chemical processes for producing hydrazine; UDMH; 1,7-octadiyne; and tetrahydrodicyclopentadiene onboard an OTEC platform. The examination included determining feedstock requirements, production processes, and initial cost estimates for these products synthesized on an OTEC platform.

Our overall conclusions and recommendations indicate:

- Synthesis of hydrazine hydrate or anhydrous hydrate -
  1. OTEC production feasible without raw material backhaul
  2. Production costs competitive with current market prices
  3. Bayer Process is most economic, because of high process efficiency compared with competing processes.
- UDMH synthesis -
  1. OTEC production feasible with backhaul of dimethylamine
  2. Production cost competitive with current market price
  3. Raschig Process is preferred, because of high efficiency.
- 1,7-octadiyne synthesis -
  1. OTEC production possible, but almost entirely dependent on shore-based feedstocks
  2. Production costs are competitive with hydrazine fuels, but competitiveness with market price is unclear because it is not currently manufactured.
- Tetrahydrodicyclopentadiene synthesis -
  1. OTEC production possible, but unattractive since it would involve solely the hydrogenation of backhauled dicyclopentadiene.
- Hydrazine fuels have competitive costs as commodities, but not as OTEC energy carriers.
- High-energy fuels appear to be 3 to 5 times more expensive than hydrogen or ammonia produced under identical conditions.
- Size of the market for high-energy fuels is uncertain.

Carbonaceous Fuels Production

Costs of energy from an OTEC plant considering the energy being transported as methanol or gasoline has also been determined. Several chemical process contractors, such as Vulcan-Cincinnati [22] and Mobil Oil Company, [14] have been contacted to obtain process information

concerning the production of methanol and gasoline. Methanol and gasoline are synthesized from electrolytic hydrogen (produced onboard the OTEC platform) and carbon dioxide (available from onshore sources).

The cost of gasoline and methanol delivered by pipeline is compared with hydrogen delivered by pipeline and shown in Figure 2. For this example, we considered the utility financing method described previously assuming a 100-MW OTEC plant using advanced electrolyzer technology and OTEC shaftpower costing 20 mills/kWhr.

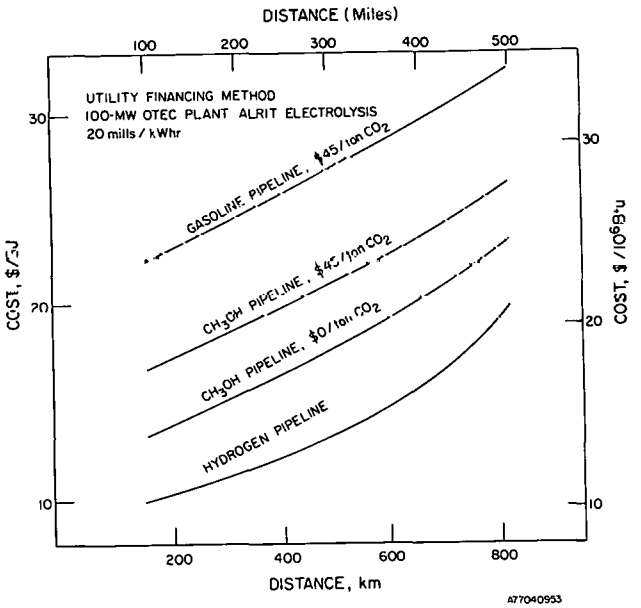



Figure 2. COSTS OF HYDROGEN, METHANOL, METHANE, AND GASOLINE AS A FUNCTION OF DISTANCE

As shown in Figure 2, the cost of energy delivered as hydrogen is always less expensive than methanol or gasoline over reasonable transportation distances. Costs of delivered hydrogen range from $10.50 to $20.00/million Btu ($9.95 to $18.95/GJ) for 100 to 500-mile (161 to 805 km) transmission distances. Methanol and gasoline delivered costs, assuming carbon dioxide costing $45/ton and a 100-mile (101 km) transportation distance, are $17.50 to $23.00/million Btu ($16.58 to $21.80/GJ), respectively. At 500-mile (805 km) distances the costs are $28.00 and $34.00/million Btu ($26.54 and $32.22/GJ), for methanol and gasoline respectively.

Compared with current energy prices, the figures for OTEC energy appear high. Natural gas city-gate (wholesale) prices in 1975 were $0.76/million Btu ($0.72/GJ) for interstate gas and $1.26 to $2.11/million Btu ($1.19 to $2.00/GJ) for intrastate gas. Studies at IGT indicate that by 1985, the costs for new natural gas supplies will be on the order of $3.00 to $4.00/million Btu ($2.84 to $3.80/GJ) in 1976 dollars. Supplemental sources of pipeline quality gas and methanol from coal are also expected to be in the same price range:

| | $/million Btu | $/GJ |
|---|---|---|
| SNG From Coal | 2.50-4.00 | 2.37-3.80 |
| SNG From Naphtha | 3.96-5.38 | 3.75-5.10 |
| Methanol From Coal | 6.00-7.50 | 5.69-7.11 |
| LNG | 3.27 | 3.10 |

Ammonia produced from gas supplies at this price is estimated to have a manufactured cost of $280 to $315/ton.

Other energy forms - electricity and oil - are expected to be substantially higher by 1985. Electric costs are estimated to average 3.75¢ to 4.0¢/kWhr in 1985. Fuel oil prices are anticipated to be approximately $3.50/million Btu ($3.32/GJ) or higher in 1985.

As such, it would appear that while OTEC power as electricity or chemical energy will be expensive, its cost relative to the traditional energy sources at the point in time when OTEC plants would become commercial will not be exorbitant. In fact, ammonia produced on OTEC platforms could be very competitive with domestically produced ammonia derived from natural gas.

## CHEMICAL ENERGY CONVERSION TO ELECTRICITY

When electricity is the desired product, onshore energy conversion devices will be needed to convert offshore-produced, high-cost chemical energy into electricity. For the sake of this analysis, we have chosen to convert only hydrogen and ammonia to electricity. Because the delivered costs of the high-energy fuels and the carbonaceous fuels are higher than hydrogen and ammonia, it is safe to assume that the cost of electricity derived from them will also be higher.

Energy Conversion Devices. We considered gas turbines and fuel cells for energy conversion because conventional Rankine cycle power plants appear to have lower overall thermal efficiency.

Unit Cost Summary. We calculated the cost of a-c electricity produced from fuel cells and gas turbines using delivered OTEC plant-produced gaseous and liquid hydrogen and liquid ammonia.

Figure 3 shows that the ammonia-air burning fuel cell [47] gives the highest electricity cost output followed by the hydrogen-air fuel cell. Although the combined efficiency of the hydrogen fuel and d-c to a-c inverter system at 40.5% is slightly greater than the gas turbine and a-c generator system (40.0%), the fuel cell system's higher fixed cost provides a higher electrical output cost.

## ELECTRICAL ENERGY TRANSMISSION SYSTEM

Design of an optimum electrical delivery system for OTEC is more complex than that for chemical energy delivery. The usual submarine cable should minimize the transmission costs for the specific 1) power to be transmitted, 2) transmission distance, 3) maximum water depth, 4) cost of transmission losses, and 5) required reliability. A cable which is over- or under-designed can cost much more than an optimum cable. The large choice of cable types and ratings and the decrease with distance of a cable

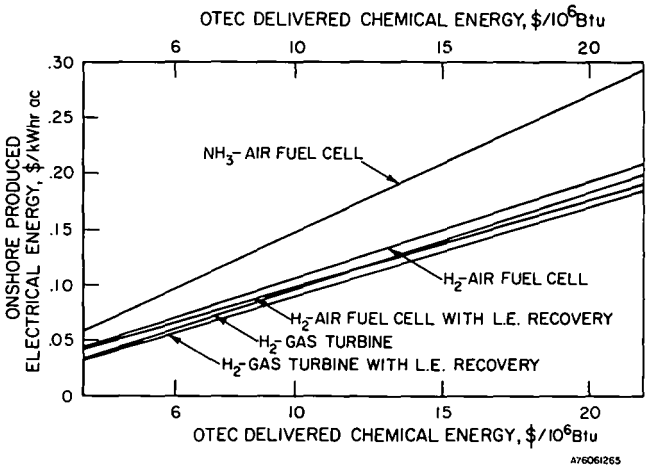



Figure 3. COST OF ONSHORE PRODUCED ELECTRICAL ENERGY AS A FUNCTION OF PLANT-PRODUCED CHEMICAL ENERGY

capacity and efficiency at full load further complicate this.

The a-c system components are 1) a switching system and step-up transformer, 2) cables to the sea bottom, 3) cables along the sea bottom, and 4) a land terminal including a step-down transformer. The number of cables will depend upon the plant size and cost, cable costs and the expected failure rate and repair time. The d-c system components are 1) a step-up transformer, 2) an a-c to d-c converter and switching system, 3) cables to the sea bottom, 4) cables along the bottom, and 5) the a-c to d-c converter station. The number and type of cables will depend upon the same factors as the a-c cables. The plant costs must include the cost of the converter stations.

The effect of the losses and costs of these systems on the delivered cost of energy is the incremental transmission costs, ITC, which Table 4 summarizes.

$$ITC = \frac{0.186 \times \text{costs} + (\text{losses} \times 0.9 \times 24 \times 365 \times 0.02}{\text{delivered power} \times 0.9 \times 24 \times 365}$$

Table 4. INCREMENTAL TRANSMISSION COSTS (mills/kWhr)[21]

| Distance/Plant Size | | 100 MW | 500 MW |
|---|---|---|---|
| 0 miles | a-c | 0 | 0 |
| (0 km) | d-c | 2.0 | 2.0 |
| 25 miles | a-c | 5.36 | 3.73 |
| (40.2 km) | d-c | 5.03 | 3.58 |
| 50 miles | a-c | 8.64 | 6.99 |
| (80.5 km) | d-c | 6.70 | 4.95 |
| 100 miles | a-c | | |
| (161 km) | d-c | 9.85 | 7.09 |
| 200 miles | a-c | | |
| (322 km) | d-c | 16.77 | 11.55 |

Fixed charge rate = 0.186. Plant availability = 0.9.
Cost of losses = $0.02/kWhr.

## COMPARISON OF ENERGY DELIVERY SYSTEMS AND CONCLUSIONS

The unit energy cost and overall energy efficiency of gaseous and liquid hydrogen and liquid ammonia used as energy carriers from an offshore OTEC plant have been compared. No attempt has been made to date to all inclusively compare high-energy fuels or carbonaceous fuels with hydrogen and ammonia. However, comparison of the results presented in Figure 2 with the following figures indicates that hydrogen and ammonia will always be delivered less expensively than the carbonaceous fuels.

The unit energy cost is the total of production, transmission, and terminaling costs. Tables 5 and 6 show delivered unit energy costs and overall efficiencies of hydrogen and ammonia as both chemical and reconverted electrical energy for 100-MW and 500-MW OTEC plants located 100 miles (161 km) and 1000 miles (1609 km) offshore. We assumed advanced hydrogen production technology and OTEC shaftpower costs of 20 mills/kWhr.

The cheapest chemical energy at 100 miles (161 km), for both plant sizes, is gaseous hydrogen by pipeline, at $10.08 and $8.44/million Btu ($9.55 and $7.99/GJ). At 1000 miles, liquid ammonia transported by barge is cheapest, at $13.15 and $11.56/million Btu ($12.45 and $10.95/GJ). The most expensive step is producing the chemical energy, except when long distance pipelines or liquid hydrogen barges are used or when the chemical energy is converted to electricity. The low efficiencies of chemical to electrical conversion (29% to 45%), plus the high cost of delivered chemical energy make the resulting electricity quite expensive. The cheapest reconverted electricity costs $0.09 and $0.077/kWhr ac and comes from hydrogen chemical energy delivered by 100-mile (161 km) long pipeline and reconverted to electricity by gas combustion turbine at 33% efficiency.

Energy transmission efficiency for chemical energy is of secondary importance because the most efficient parts of each transmission system are not always the cheapest ones. Overall, the most efficient energy conversion system at 100 miles (161 km) is the gaseous hydrogen pipeline, at 83.6% efficiency. Chemical energy reconversion to electricity has a 33.4% total efficiency.

We compared the delivered energy costs of hydrogen gas by pipeline, liquid hydrogen by ocean-going barge, liquid ammonia by pipeline and ocean-going barge, and d-c and a-c electricity transmission for various transmission distances. Electricity transmission costs were available only for distances up to 200 miles (322 km). We assumed OTEC shaftpower generating costs were 20 mills/kWhr and that 1 kWhr equals 3413 Btu.

This comparison assumes energy to be equally useful as hydrogen or electricity. In practice the breakeven transmission distances will be much different, because in nearly all applications hydrogen and ammonia are less useful than electricity because they are used at a lower efficiency. However, if hydrogen or ammonia is the desired onshore product, electricity transmission could be an expensive intermediate form of chemical energy transmission. Reconverted chemical energy to electricity costs can be compared with a-c or d-c electrical energy transmission.

Figure 4 compares the unit cost of energy for different energy carriers from a 100-MW OTEC plant as a function of transmission distance. Electrical energy transmission is cheapest at less than 200 miles (322 km) with d-c transmission cheaper than a-c at distances greater than 25 miles (40.2 km). If the unit cost line for d-c electricity is extrapolated beyond 200 miles (322 km), electricity remains cheapest up to about 300 miles (483 km). However, this extrapolation may be incorrect since d-c transmission costs after

Table 5. CHEMICAL ENERGY DELIVERED COST COMPARISON (100 MW)

| Chemical Energy Carriers | Distance, miles | Production Cost Efficiency[2] $/10⁶ Btu | % | Transmission Cost Efficiency $/10⁶ Btu | % | Terminal Cost Efficiency $/10⁶ Btu | % | Chemical Energy Onshore Total Cost Efficiency $/10⁶ Btu | % | Reconversion To Electricity[3] Cost Efficiency $/10⁶ Btu | % | a-c Electricity Cost From Chemical Energy Cost Efficiency $/kWhr a-c | % |
|---|---|---|---|---|---|---|---|---|---|---|---|---|---|
| Hydrogen Gas By Pipeline[1] | 100 | 7.98 | 84 | 2.10 | 99.5 | | | 10.08 | 83.6 | 16.29 | 40.0 | 0.090 | 33.4 |
| | 1000 | 7.98 | 84 | 25.00 | 98.8 | | | 32.93 | 83.0 | | | | |
| Liquid Ammonia By Pipeline[1] | 100 | 11.74 | 66.7 | 1.90 | 99.4 | | | 13.64 | 66.3 | 39.93 | 29.0 | 0.183 | 19.2 |
| | 1000 | 11.74 | 66.7 | 26.00 | 98.6 | | | 37.74 | 65.8 | | | | |
| Liquid Hydrogen By Barge | 100 | 12.75 | 66.6 | 2.07[4] | 98.2 | 0.66 | 99.9 | 15.48 | 65.3 | 21.73 | 44.5 | 0.127 | 29.1 |
| | 1000 | 12.75 | 66.6 | 7.09 | 92.8 | 2.37 | 99.9 | 22.21 | 61.7 | 29.94 | 44.5 | 0.178 | 27.5 |
| Liquid Ammonia By Barge | 100 | 11.74 | 66.7 | 0.82 | 99.5 | 0.11 | 99.9 | 12.67 | 66.3 | 37.14 | 29.0 | 0.170 | 19.2 |
| | 1000 | 11.74 | 66.7 | 1.29 | 96.0 | 0.12 | 99.9 | 13.15 | 64.0 | 38.71 | 29.0 | 0.177 | 18.6 |

[1] Assumes pipeline was constructed in 1000-ft-deep water.

[2] Based on an OTEC shaft-power cost of 20 mills/kWhr.

[3] Reconversion to electricity considers the most efficient process.

[4] Barge transport costs are based on the high estimate of $600/bbl for barges.

B76112494

Table 6. CHEMICAL ENERGY DELIVERED COST COMPARISON (500 MW)

| Energy Carriers | Distance, miles | Production Cost Efficiency[2] $/10⁶ Btu | % | Transmission Cost Efficiency $/10⁶ Btu | % | Terminal Cost Efficiency $/10⁶ Btu | % | Chemical Energy Onshore Total Cost Efficiency $/10⁶ Btu | % | Reconversion To Electricity[3] Cost Efficiency $/10⁶ Btu | % | a-c Electricity Cost From Chemical Energy Cost Efficiency mills/kWhr a-c | % |
|---|---|---|---|---|---|---|---|---|---|---|---|---|---|
| Hydrogen Gas By Pipeline[2] | 100 | 7.79 | 84.0 | 0.65 | 98.5 | | | 8.44 | 82.7 | 22.56 | 40.0 | 0.077 | 33.1 |
| | 1000 | 7.79 | 84.0 | 8.50 | 97.4 | | | 16.29 | 81.8 | 25.61 | 40.0 | 0.143 | 32.7 |
| Liquid Ammonia By Pipeline[1] | 100 | 10.79 | 66.0 | 0.60 | 99.4 | | | 11.39 | 65.6 | 34.02 | 29.0 | 0.155 | 19.0 |
| | 1000 | 10.79 | 66.0 | 8.85 | 98.6 | | | 19.64 | 65.1 | 54.20 | 29.0 | 0.252 | 18.9 |
| Liquid Hydrogen By Barge | 100 | 11.03 | 66.6 | 1.39[4] | 98.1 | 0.50 | 99.9 | 12.92 | 65.3 | 18.43 | 44.5 | 0.107 | 29.1 |
| | 1000 | 11.03 | 66.6 | 4.24 | 90.5 | 0.51 | 99.9 | 15.78 | 60.2 | 21.72 | 44.5 | 0.128 | 26.8 |
| Liquid Ammonia By Barge | 100 | 10.79 | 66.7 | 0.23 | 99.6 | 0.03 | 99.9 | 11.05 | 66.4 | 33.19 | 29.0 | 0.151 | 19.3 |
| | 1000 | 10.79 | 66.7 | 0.74 | 96.8 | 0.03 | 99.9 | 11.56 | 64.5 | 35.90 | 29.0 | 0.162 | 18.7 |

[1] Assumes pipeline constructed in 1000-ft-deep water.

[2] Based on an OTEC shaft-power cost of 20 mills/kWhr.

[3] Reconversion to electricity considers the most efficient process.

[4] Barge transport costs are based on the high estimate of $600/bbl for barges.

B76112497

200 miles (322 km) may not increase linearly because of reliability and capital costs.

Liquid hydrogen transported by ocean-going barge becomes cheaper than ammonia by pipeline at 185 miles (298 km) with a crossover cost of $16.50/million Btu ($15.63/GJ). Liquid hydrogen transported by ocean-going barge becomes cheaper than a gaseous hydrogen pipeline at 450 miles (724 km), costing $18.85/million Btu (17.85/GJ). Hydrogen gas pipelines appear to be the cheapest form of chemical energy transmission for distances less than 225 miles (362 km). Beyond this, liquid ammonia transported by barge appears to be cheapest.

Figure 5 compares different energy carriers from a 500-MW OTEC plant as a function of distance. A-c electricity becomes more expensive than d-c eleetrical energy at a distance of 25 miles (40.2 km), costing $7.00/million Btu ($6.63/GJ) at the crossover. Hydrogen gas transmission by pipeline becomes cheaper than d-c electrical energy transmission at 170 miles (274 km) with a cost of $9.00/million Btu ($8.52/GJ).

Liquid ammonia transported by ocean-going barge becomes cheaper than hydrogen gas by underwater pipeline at 480 miles, costing $11.30/million Btu ($10.70/GJ).

The effect of varied OTEC shaftpower costs on the delivered unit cost of chemical energy for 100-MW plants is shown in Figures 6, 4, and 7, which give the delivered unit costs versus transmission distance for 10, 20, and 30 mills/kWhr, respectively. Delivered chemical energy cost is fairly sensitive to OTEC shaftpower costs. For example, using ALRIT electrolysis, hydrogen gas delivered 100 miles by pipeline costs $6.50/million Btu ($6.16/GJ) if OTEC shaftpower is available at 10 mills/kWhr. If shaftpower is available

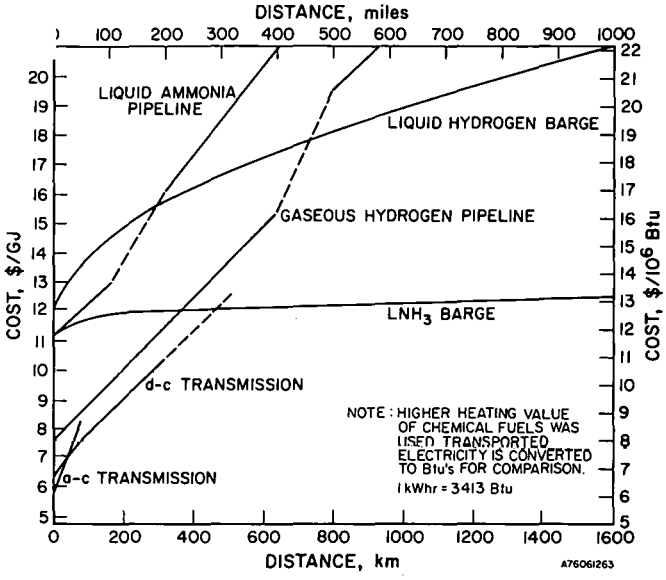



Figure 4. DELIVERED ENERGY TRANSPORTATION COST COMPARISON (100 MW, 20 mills/kWhr)

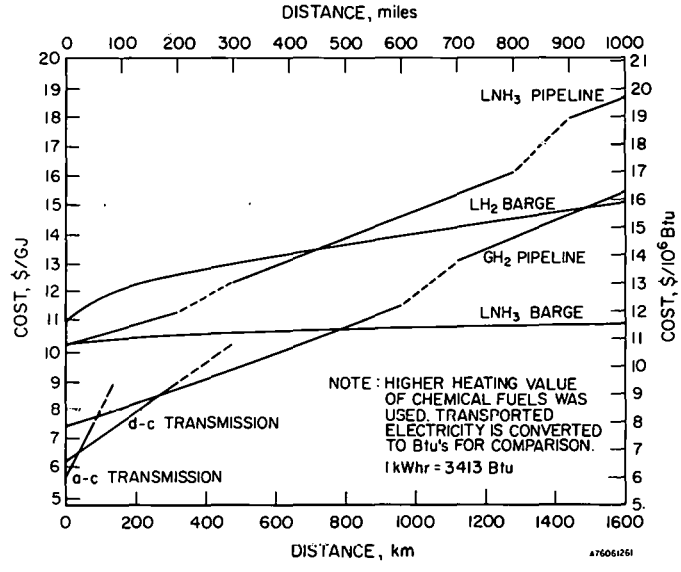



Figure 5. DELIVERED ENERGY TRANSPORTATION COST COMPARISON (500 MW, 20 mills/kWhr)

at 20 or 30 mills/kWhr, gaseous hydrogen would cost $10.00 and $13.70/million Btu ($9.47 and $12.97/GJ), respectively.

OTEC shaftpower costs also influence the point where one energy carrier becomes cheaper than another. For example, liquid ammonia transported by barge becomes cheaper than gaseous hydrogen transported by pipeline at 180 miles (290 km), 230 miles (370 km), and 270 miles (434 km) if OTEC shaftpower costs are 10, 20, and 30 mills/kWhr, respectively. This is due to the higher cost of OTEC shaftpower and the decreased production efficiency for ammonia.

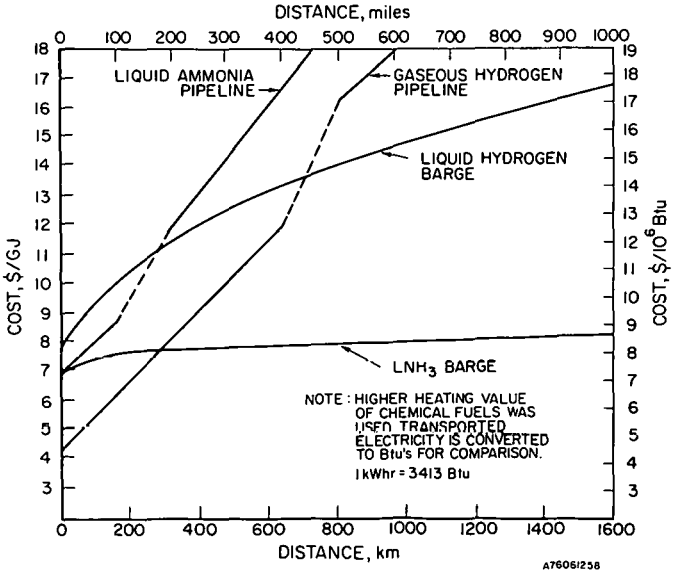



Figure 6. DELIVERED ENERGY TRANSPORTATION COST COMPARISON (100 MW, 10 mills/kWhr)

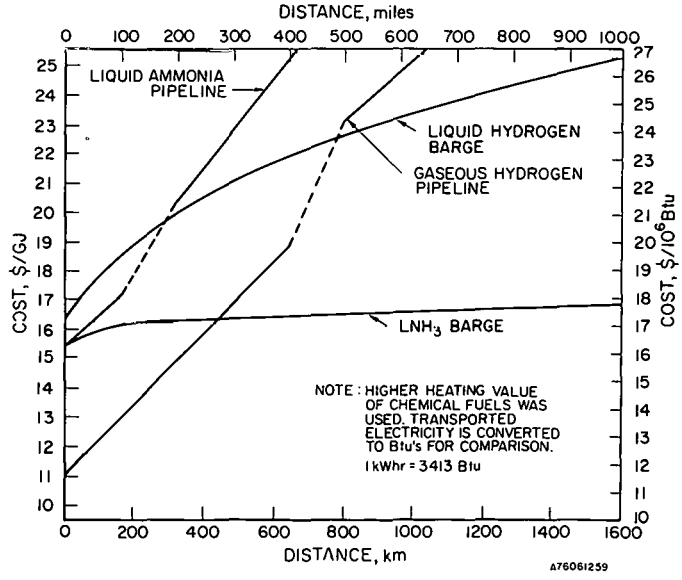



Figure 7. DELIVERED ENERGY TRANSPORTATION COST COMPARISON (100 MW, 30 mills/kWhr)

The effect of varied OTEC shaftpower costs on the delivered unit cost of chemical energy for 500-MW plant capacity is shown in Figures 8, 5, and 9, which give the delivered unit cost versus transmission distance for 10, 20, and 30 mills/kWhr, respectively. For example, using ALRIT electrolysis, hydrogen gas delivered 100 miles (161 km) by pipeline costs $5.00/million Btu

($4.74/GJ) if OTEC shaftpower is available at 10 mills/kWhr. If shaftpower is available at 20 or 30 mills/kWhr, gaseous hydrogen would cost $8.50 and $12.20/million Btu ($8.05 and $11.55/GJ), respectively.

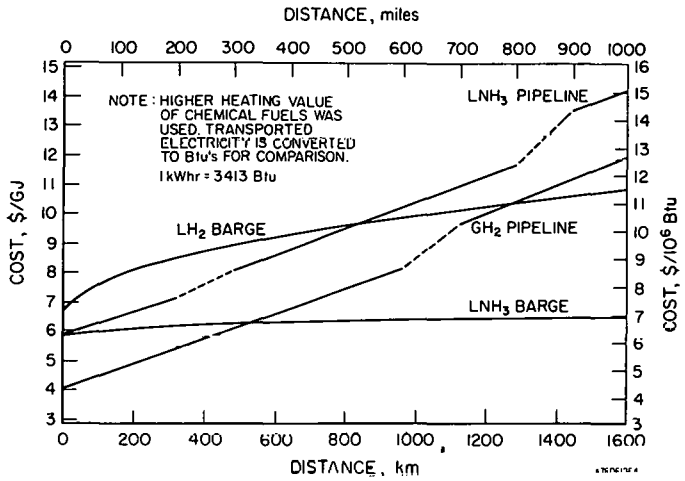



Figure 8. DELIVERED ENERGY TRANSPORTATION COST COMPARISON (500 MW, 10 mills/kWhr)

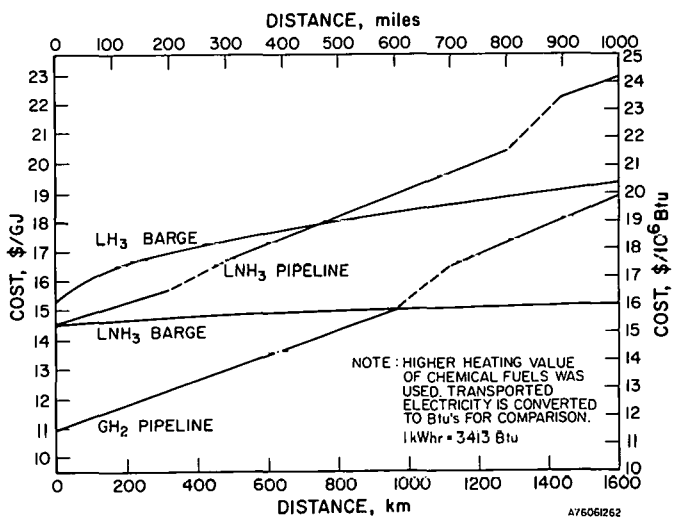



Figure 9. DELIVERED ENERGY TRANSPORTATION COST COMPARISON (500 MW, 30 mills/kWhr)

We determined the effect on unit energy cost of increasing OTEC-plant size from 100 MW to 500 MW. For example, the unit cost of hydrogen gas delivered by a 500-mile (806-km) pipeline, assuming an OTEC shaftpower cost of 30 mills/kWhr, decreases from $24.30/million Btu ($23.01/GJ) to $15.05/million Btu ($14.25/GJ), when the size is increased from 100 MW to 500 MW.

For the 500-MW plant, the points where barge-transported liquid ammonia becomes cheaper than piped gaseous hydrogen is at 375, 485, and 600 miles (603, 780, and 965 km), for shaftpower costs of 10, 20, and 30 mills/kWhr, respectively.

Hydrogen costs less at increased plant capacity (500 versus 100 MW) because hydrogen pipeline transmission costs decrease with throughput increase.

OTEC energy delivered 300 miles (480 km) or less should probably be moved as electricity, if that is what is required. But because costs of submarine pipelines and electric cables depend on the site, no clear choice of transport mode can be made until sites are selected. This choice also depends on the ultimate market - chemical commodity, chemical energy, or electricity.

## ACKNOWLEDGEMENT

This work is being carried out under contract to the Energy Research and Development Administration, and the National Science Foundation. Results concerning the hydrogen and ammonia analysis were determined as part of the OTEC program at IGT from May 1975 through May 1976 under Contract No. NSF-C1008 (AER-75-00033) with NSF and ERDA. Information concerning carbonaceous fuels and high-energy fuels production was developed as part of the current IGT OTEC program under Contract No. E(49-18)-2426 with ERDA.

## REFERENCES

1. Aqua-Chem, Inc., private communication of October 1975.

2. Biederman, N. P. and Dodd, C. A., "Economics of LNG Barge Transportation," LNG Surveillance Program, Chicago, 1971.

3. Brown and Root, Inc., private communication of January 1976.

4. Engelhard Minerals and Chemicals Corp., Ammonia-Air Fuel Cell System, East Newark, N.J., 1972.

5. General Electric Co., private communication of September 1975.

6. General Electric Co., private communication of November 1975.

7. Global Marine Development Co., Cost Study of Marine Risers for Deep Ocean Fluid Transport.

8. Gulf Central Pipeline Co., private communication of October 1975.

9. Ingersoll-Rand Co., private communication of November 1975.

10. J. F. Pritchard and Co., private communication of August 1975.

11. Kisiel, J., FMC Corp., private communication of October 28 1975.

12. Konopka, A. J. and Gregory, D. P., "Hydrogen Production by Electrolysis: Present and Future." Paper presented at the 10th IECEC, Newark, Del. August 17-22, 1975.

13. Lurgi Apparate-Technik GmbH, private communication of August 1975.

14. Mobil Oil Company, private communication of October 1976.

15. Platt's Oilgram Price Service, 53:201, 4A (1975) October 17.

16. Sallean, A., Breit and Garcia Engineering Co., private communication of November 1975.

17. Teledyne Isotopes, private communication of October 1975.

18. Tempke, W., Air Products and Chemicals, Inc., private communication of March 1976.

19. Union Carbide, Linde Division, private communication of August 1975.

20. Union Carbide, Linde Division, private communication of September 1975.

21. Winer, B., Arthur D. Little, private communication of May 1976.

22. Vulcan-Cincinnati, private communication of September 1976.

# MARKET DEFINITION, COMMERCIAL DEVELOPMENT PLAN, AND OTEC FINANCING: A SUMMARY OF 1976 APL WORK FOR THE U.S. MARITIME ADMINISTRATION

EVANS J. FRANCIS
*Aeronautics Division*
*Applied Physics Laboratory, The Johns Hopkins University*
*Johns Hopkins Road*
*Laurel, Maryland*

JOSEPH SEELINGER
*Office of Maritime Technology*
*U.S. Maritime Administration, Department of Commerce*
*Washington, D.C.*

Abstract

A concept for Ocean Thermal Energy Conversion (OTEC) plant-ships for the onboard production of ammonia or other products at tropical sites has been developed. Ammonia is of particular interest because it is presently produced from natural gas, our scarcest fossil fuel. Liquid ammonia could be shipped to the U.S. to supply fertilizer and chemical markets or as a carrier of hydrogen for use in fuel cells to produce electricity. A cost estimate for a 100-$MW_e$, 313-short-ton/day, demonstration-size OTEC/ammonia plant-ship provided the basis for cost estimates for commercial-size ships producing 1000 tons per day or more of ammonia. Economic and marketing analyses have been conducted to provide forecasts bearing on the commercialization potential for the 1983-2000 period, including ammonia production costs and prices, U.S. and world market penetration, and benefits to the U.S. and the world from a successful program. Less extensive analyses have been conducted for OTEC aluminum production and for the case of direct transmission of OTEC electric power to U.S. and foreign shores.

## Introduction

In April, 1976, an Executive Summary and Detailed Report (Ref. 1) published a conceptual design of a 100-$MW_e$, 313 short-ton/day OTEC/ammonia demonstration-size plant-ship. Extrapolations were then made from this design to the sixth and subsequent 500-$MW_e$, 1697 short-ton/day OTEC/ammonia commercial-size plant-ships which could produce and deliver anhydrous ammonia ($NH_3$) F.O.B. U.S. gulf coast ports at $96/short ton. This led to a projected gross profit of 47% at an estimated sales price of $180/short ton and a payback of total plant investment by cash flow of approximately 5.5 years. Aluminum production on board tropical OTECs was adjudged marginally profitable and the prospects for hydrogen generation and delivery to the U.S. for use as fuel or in the generation of electric power from fuel cells were adjudged potentially attractive for the long term.

Review of the work completed through early 1976 led the U.S. Maritime Administration to support further work on OTEC Commercial Development of ammonia, aluminum and other products and on a development plan for commercial implementation. That work provides the basis for this report.

## The OTEC/Ammonia Plant-Ship Concept

The baseline, 100-$MW_e$ (net), 313-short-ton/day, OTEC/ammonia pilot/demonstration plant-ship is shown in Fig. 1. The basic OTEC plant is 145 meters (475 feet) by 60 meters (196 feet) and of modular design with forty evaporator modules, forty condenser modules, twenty turbines, and four generators. Each heat exchanger module comprises an array of large diameter, horizontal, multiple-pass, aluminum tubes with ammonia working fluid inside the tubes. Sea water flows downward over the tubes by gravity. Each module is housed in a rectangular, open compartment within the concrete hull structure, so that no separate heat exchanger shell is required. The open arrangement permits *in situ* cleaning by water jets, as well as ready access for removal of a module for repair. Warm surface seawater is pumped by 20 outboard pumps into head ponds above the evaporator modules, from whence it flows downward and exhausts, slightly cooled, from the bottom of the vessel at about 21-m (70-ft) depth. Cold water is pumped from 760-m (2500-ft) depth by 19 pumps located near the top of the central, 18-m (60-ft) diameter, cold-water pipe (CWP) into ponds above the condensers. There are two condenser head ponds, one each fore and aft. Each has a sloped feed channel on each outboard side, deepest near the CWP, from which the water overflows transversely inward toward the pond centerline, thus providing a distributed flow over the ponds. The cold water also exits from the bottom of the vessel.

Demisters, turbines and generators are located on machinery decks between the rows of heat exchangers. These decks also house the electrolysis plant, which uses the OTEC power to produce hydrogen from fresh water (obtained from warm sea water by a reverse osmosis purification system) and the ammonia plant, which uses the hydrogen and nitrogen obtained by air liquefaction to produce liquid ammonia. The product ammonia is stored in tanks which, together with ballast tanks, are located in the hull between rows of heat-exchanger compartments. The product ammonia is off-loaded monthly by tanker. Station-keeping for the plant-ship is provided by propulsors at the corners of the vessel, which propel the

ship at a speed of about 0.5 knot relative to the local current to maintain its position or permit it to "graze" s[illegible]y in the area. The full-size platform and cold w[illegible] pipe with one 5-$MW_e$ heat exchanger module comprise the recommended tropical ocean pilot/demonstration plant configuration.

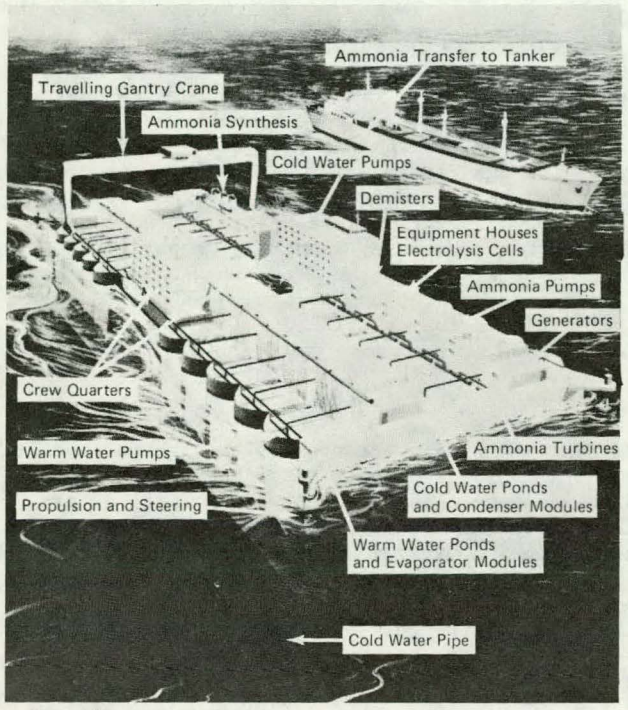



Fig. 1 Baseline OTEC/Ammonia Pilot/Demonstration Plant-Ship

Conceptual designs have not been completed for the commercial-size OTEC/ammonia ships or for OTEC/aluminum. Further investigations in 1976-1977 led to the conclusion that there would be no requirement for OTEC/liquid-hydrogen ships. The OTEC/ammonia product can be more easily and less expensively manufactured on the tropical ocean platform and transported to the U.S. user site. At or near that point, the ammonia can be dissociated into its component hydrogen and nitrogen gases and the hydrogen used as fuel or in fuel cells for the generation of electricity. For an optimized production and use cycle, which could be available in the late 1980's or early 1990's on the 25th OTEC/ammonia plant-ship, the total plant investment would be \$1400 per $kw_e$ delivered power and 23 mills per kwh for a coastal U.S. user (e.g., electric utility substation, hotel, industrial plant).

The general principles which led to the APL concept for the OTEC plant-ship are:

. The $\Delta T$ available is a powerful factor in overall costs. Within the range of interest, plant costs vary inversely with $\Delta T$ to a power of 2-2.5.

. The forces acting on the 60' diameter, 3000' long cold water pipe vary as the square of current velocity and control station-keeping. For grazing and station-keeping, power to maneuver at .9 knot is adequate. For the average conditions only 750 HP is needed for propulsion.

. To get accurate costs, we settled on barge construction that can be built in existing shipyards with known technology.

. The overall minimum systems cost is essential since the power source is large and diverse. The lowest overall cost does not necessarily result from optimized heat transfer characteristics.

. The quantity of OTEC power available in the tropical oceans, if used to produce ammonia, makes use of the vast solar energy stored near the equator and produces a product which conserves natural gas and is vitally necessary for food production.

## Site Selection and Grazing

Because of the powerful affect of $\Delta T$, with each degree F resulting in an approximately 5% increase or decrease in overall costs, recent work at APL has included the identification of grazing patterns in the tropical Atlantic and tropical Pacific oceans and an analysis of the structural forces which would be encountered in following these patterns. Figure 2 shows such a grazing pattern in the tropical Atlantic Ocean doldrums following the mean monthly "Hot Spots" of warm surface water and a near-maximum mean $\Delta T$ each month. This pattern lies between 4° and 11° South latitude. Our plant design is adequate to accommodate the loads from wind, waves, and currents which would be encountered on this pattern. Further, with the satellite navigation equipment on board the OTEC plant-ship and ammonia tankers and the gathering of oceanographic data by satellite, additional limited improvements using this approach can be expected.

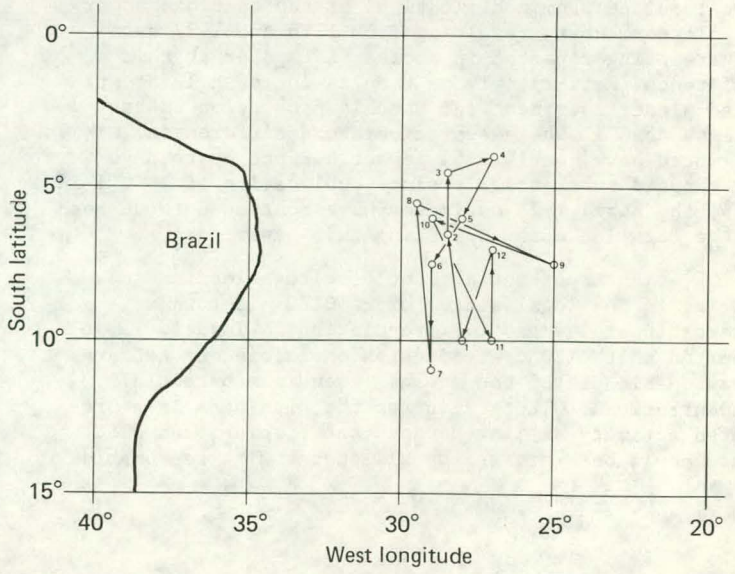



Fig. 2 OTEC Grazing Pattern, Tropical Atlantic Ocean

Figure 3 shows the comparative mean monthly ΔT's obtained with grazing in this South Atlantic pattern with an OTEC plant-ship and a 3000 foot (900 meter) cold water pipe (early results are quite similar with tropical Pacific Ocean grazing), and off Puerto Rico - a fixed site - with a 3000 foot (900 meter) cold water pipe. One of the more significant facts is that the tropical grazing approach allows the OTEC power cycle to be operated at or near optimum efficiency on a year-round basis, thus markedly reducing costs. It is our understanding that ERDA has more recent Puerto Rico data with a 4000 foot (1200 meter) cold water pipe with somewhat higher temperatures than those reported by the University of Puerto Rico and used in our presentation. These new data are to be reported in another paper at this conference. However, the more recent fixed site data continue to show wide variance in ΔT over an annual cycle.

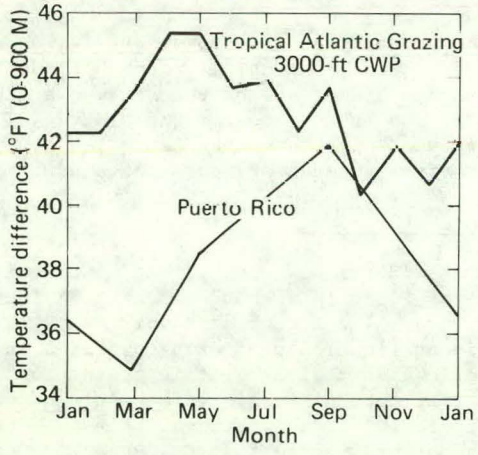



**Fig. 3 Temperature Differentials, Tropical Atlantic Ocean Grazing Pattern and Fixed Site Off Puerto Rico**

The recent work at APL on grazing patterns has been restricted to the use of existing data in oceanographic files. Since the ΔT is so important to OTEC efficiency and total system costs, proposals for specific related data gathering in the open ocean have been made, but have not been funded. Updated costs have resulted from modifications of the heat exchanger and platform costs resulting from 1976 and 1977 data and are being reported in another APL paper at this conference (Ref. 2). These results increase 1975 estimated plant investment and ammonia production costs by less than 1% whereas a temperature differential of 1°F would have nearly a 5% impact. Since costs have not changed substantially since publication of Ref. 1 in 1976, the April 1976 estimates have continued to be used in the detailed work supporting this paper.

An important element of site selection and grazing is the legal status of an OTEC plant under international law and U.S. regulations. In Ref. 1, we reported that OTEC operations as envisioned by APL are a reasonable use of the oceans, even in substantial concentrations; OTEC grazing on the high seas is a protected activity similar to deep sea fishing; and OTEC, thus, could be exercised by all states with reasonable regard to the interests of other states in their exercise of freedom of the high seas. Subsequent legal research has led to the following significant conclusions relative to U.S. regulations: An OTEC of the grazing variety could be documented as a vessel of th United States; the language of the existing maritime programs is sufficiently broad that OTEC could qualify under these programs if such qualification is the desire of Congress; the activity of non-U.S. entrants to the OTEC field could be deemed to represent foreign-flag competition; the impact of an OTEC on conservation of scarce national resources such as natural gas or ammonia fertilizer would support a finding of "otherwise useful to the United States in time of emergency," and operation of an OTEC in a foreign economic zone could be deemed to be foreign commerce if the resultant product were shipped to the United States or, alternatively, if OTEC products from operation in a United States economic zone were exported to another country. Of particular interest in connection with the OTEC program is the fact that a floating power station has been held not to be a vessel where the station was linked to the shore by a transmission cable.

## Plant Investment and Production Costs

Starting with the conceptual design for the 100 $MW_e$ OTEC/ammonia plant-ship described in Ref. 1, we analyzed the commercial-sized plant-ships first determining the construction and components technical restrictions in maximum and minimum size, and evaluated the sensitivity of plant investment, Government support and operating cost of various commercial-size options. Having thus defined the goal of the development process, it was possible to work backward to a judgment as to what must be demonstrated and to the specific objectives of a pilot plant program. This sizing analysis led to the following results:

- The early OTEC/ammonia commercial plant-ships are expected to be 325-$MW_e$ producing 1000-metric tons of anhydrous ammonia per day, 345 days of the year.
- A separate demonstration plant-ship is <u>not</u> needed.
- The pilot/demonstration hull can be constructed and deployed during 1978-1980, potentially in any of the 22 U.S. private shipyards listed in Table 1 at a cost of $37.5 million in constant 1975 dollars. This will require about $45 million in FY'78-'80 funds.

Table 2 shows the estimated capital and production costs for the 1st, 4th and 8th commercial-size OTEC/ammonia plant-ships if constructed in private U.S. shipyards. The 8th or 9th and subsequent plant-ships are expected to be commercially viable without Government support at $230-$240 million cost and anhydrous ammonia delivered F.O.B. New Orleans at $96-$99/short ton. With the rapidly increasing cost of natural gas in the U.S., earlier plant-ships may be fully competitive commercially. What we have addressed is essentially a state-of-the-art program. With a well supported R&D

Table 1
Potential OTEC Construction Yards

| Area | Construction Facility | Shipway* | Unemployment July 1976** |
|---|---|---|---|
| Bath, ME | Bath Iron Works Corporation | 700' x 130' x 40' | |
| Baltimore, MD | Bethlehem Steel Corporation - Sparrows Point | 1200' x 192' x 40' | 7.0% |
| | Maryland Shipbuilding & Dry Dock Company | 850' x 110' x 40' | |
| Boston, MA | General Dynamics Corp. - Quincy Shipbuilding Division | 860' x 144' x 40' | 8.2% |
| Newport News, VA | Newport News Shipbuilding & Dry Dock Co. | 1600' x 230' x 44' | 5.7% |
| Brooklyn, NY | Seatrain Shipbuilding Corporation | 1094' x 143' x 40' | 10.1%*** |
| Philadelphia, PA | Sun Shipbuilding & Dry Dock Company | 1600' x 200' x 40' | 8.6% |
| Mobile, AL | Alabama Dry Dock & Shipbuilding Company | 750' x 105' x 35' | 6.7% |
| New Orleans, LA | Avondale Shipyards, Inc. | 900' x 225' x 40' | 8.6% |
| | Marine Concrete Structures, Inc. | 500' x 150' x 12' | |
| Beaumont, TX | Bethlehem Steel Corp. - Beaumont Yard | 650' x 84' x 40' | 7.2% |
| Pascagoula, MS | Ingalls Shipbuilding Division/ Litton Industries, Inc. | 800' x 150' x 40' | 4.6%**** |
| Galveston, TX | Kelso Marine, Inc. | 700' x 100' x 12' | 7.3% |
| Orange, TX | Levingston Shipbuilding Co. | 1100' x 90' x 35' | 7.2% |
| Brownsville, TX | Marathon Manufacturing Company - Gulf Marine Division | 1400' x 200' x 35' | 11.6%**** |
| San Francisco, CA | Bethlehem Steel Corporation - San Francisco Yard | 950' x 148' x 40' | 11.5% |
| Portland, OR | FMC Corporation - Marine & Rail Equipment Division | 650' x 105' x 35' | 8.5% |
| Seattle, WA | Lockheed Shipbuilding & Construction Co. | 690' x 90' x 35' | 8.7% |
| | Todd Shipyards Corp. - Seattle | 550' x 96' x 40' | |
| Tacoma, WA | Concrete Technology Corp. | 500' x 150' x 11'10" | 11.3% |
| San Diego, CA | National Steel & Shipbuilding Company | 965' x 170' x 40' | 11.5% |
| Hawaii | Hawaiian Dredging & Supply Company | 390' x 53' x 30' | 8.7% |
| Puerto Rico | Guanica Bay | feasibility study only | 16.8% |

*Source: 1974 Report on Survey of U.S. Shipbuilding and Repair Industry, U.S. Department of Commerce Maritime Administration plus APL information. Depth figures will require verification.
**Source: Department of Labor, Bureau of Labor Statistics, Local Area Unemployment Statistics Division, September 1976.
***May 1976 data are the latest available.
****June 1976 data are the latest available.

program, further cost reductions in both plant investment and ammonia production costs would be possible.

The production costs in Table 2 for OTEC ammonia were based on 20 year straight-line depreciation. In actual commercial operation, more favorable balance sheet projections would be obtained by using the available investment tax credit, advanced depreciation methods and the available Internal Revenue Class 00.28 for vessels under U.S. flag to compute depreciation over a period of 14.5 years.

We also reviewed our earlier estimated ammonia price of $180 per year in constant 1975 dollars. This review led to the conclusion that the best projections of mid 1980 ammonia prices could be obtained by using percentage markups of price over production costs. The range used was between 40% and 100% over new U.S. shore plants' production costs giving a range in the mid 1980s of prices between $138 and $262 per short ton in constant

1975 dollars. The estimates for the first and sixth and subsequent OTEC/ammonia plant-ships, with the length of time to recover plant investment by cash flow and the compounded net profit over equity are shown in Table 3.

Table 2

Estimated Capital and Production Cost for 325-$MW_e$, 1000-MT/D OTEC/Ammonia Plant-Ships (1975 Dollars)

| CAPITAL COSTS ($M)[a] SHIP | 1st | 4th | 8th |
|---|---|---|---|
| HEAT EXCHANGERS | 99 | 89 | $85M |
| PLATFORM & CWP | 102 | 72 | 60 |
| OTEC MACHINERY & MISC. | 64 | 49 | 43 |
| DEPLOYMENT TO SITE | 2 | 2 | 2 |
| TOTAL BASIC SHIP | 267 | 212 | $190M |
| AMMONIA PRODUCTION AND TRANSFER PROCESS | 59 | 53 | 50 |
| NET PLANT-SHIP COST | $326 | $265 | $240M |
| WORKING CAPITAL (W.C., 120 DAYS) | 4 | 3 | 3 |
| **PRODUCTION COSTS ($/ST)** | | | |
| CHEMICALS, LABOR, OVERHEAD | 7 | 7 | 7 |
| FIXED CHARGES (12.8% OF P.I.) | 110 | 89 | 81 |
| INTEREST ON W.C. @ 8% | 2 | 2 | 2 |
| SHIPMENT TO U.S. | 9 | 9 | 9 |
| COST AT U.S. PORT | 128 | 107 | 99 |
| GROSS PROFIT ($180 PRICE) | 29% | 41% | 45% |

[a]COSTS INCLUDE CONSTRUCTION INTEREST AND ESCALATION @ 12%. PLANT OPERATES 345 DAYS/YEAR.

Table 3

Range of Forecast 1983 Ammonia Prices

| OTEC/$NH_3$ SHIP | $NH_3$ SALES PRICE (CONSTANT 1975 DOLLARS) | PI RECOVERED | FIRST 6 YEARS NET PROFIT/ EQUITY (COMPOUNDED) |
|---|---|---|---|
| FIRST (50% GOVT, 50% PVT) | $200/S.T. | 3.7 YRS. | 28%/YR. |
| SIXTH & SUBS. (100% PVT) | 200 | 4.6 | 29% |
| SIXTH & SUBS. (100% PVT) | 138 | 6.6 | 12% |
| SIXTH & SUBS. (100% PVT) | 158 | 5.7 | 14% |
| SIXTH & SUBS. (100% PVT) | 183 | 4.9 | 24% |
| SIXTH & SUBS. (100% PVT) | 197 | 4.6 | 28% |
| SIXTH & SUBS. (100% PVT) | 226 | 4.1 | 35% |
| SIXTH & SUBS. (100% PVT) | 262 | 3.6 | 41% |

The method used to compute cash flow and return on investment is shown in detail on Table 4. A general inflation rate of 7% per year for all variable costs was used. On the left, the per ton production costs less depreciation are added to shipping costs to New Orleans and to interest on working capital to get total cash costs. On the right side of the chart, these total cash costs are converted to annual costs in millions of dollars. Gross profit is then computed by subtracting total cash costs and double declining balance depreciation (converted to sum-of-the-years digits in the 3rd year) from annual sales at $200 per short ton. The full investment tax credit for solar energy equipment of 12% is then taken on the assumption that the owner-operator company has adequate other income against which this credit could be applied. The cash flow is then stated, its cumulative percent of total private plant investment calculated and the year's cash flow is then used as a sinking fund at the end of the year to retire a portion of the outstanding debt. Debt financing was assumed for this example at the 87-1/2% of total plant investment maximum allowed under Title XI Mortgage Guarantees. We assumed the approximate interest rate for an AAA-rated industrial corporate bond of 8%.

Table 4

Cash Flow Data[1], Sixth and Subsequent OTEC/Ammonia 500-$MW_e$ (NET) 585, 567 ST/Y Commerical

PI ANT-SHIPS (P.I. = $367.1 M)
1983 DEPLOYMENT (CONSTANT 1975 DOLLARS)

| | $/TON CASH COSTS | | | ANNUAL DATA (MILLIONS, 1975 DOLLARS) | | | | | | | | |
|---|---|---|---|---|---|---|---|---|---|---|---|---|
| YEAR | PROD. COSTS LESS DEPR. | SHIPPING & INTEREST ON WORKING CAPITAL | TOTAL CASH COSTS | SALES | TOTAL CASH COSTS | DDB & SYD DEPR. (14.5 YR) | GROSS PROFIT | INVESTMENT TAX CREDIT (12%) | FED. INC. TAX (48%) | CASH FLOW | CUMULATIVE % OF PVT P.I. RECOVERED | CUM. RETAINED NET CASH FLOW BY EQUITY R.O.I.) |
| 1 | 73 | 11 | 84 | $117 | 49 | 51 | 17 | 44[2] | – | 105 | 29% | (216)[3] |
| 2 | 59 | 11 | 70 | 125 | 41 | 44 | 40 | | 19 | 86 | 47% | (150)[3] |
| 3 | 51 | 12 | 63 | 134 | 37 | 40 | 57 | | 27 | 71 | 66% | (79)[3] |
| 4 | 42 | 12 | 54 | 143 | 32 | 37 | 74 | | 36 | 75 | 86% | (4)[3] |
| 5 | 33 | 13 | 46 | 153 | 27 | 34 | 93 | | 44 | 83 | PI Recovered in 4.6 years | 161% |
| 6 | 34 | 14 | 48 | 164 | 28 | 31 | 106 | | 51 | 90 | | 368% |
| 7 | | | | | | | | | | | | |
| 8 | | | | | | | | | | | | |
| 9 | | | | | | | | | | | | |
| 10 | | | | | | | | | | | | |
| 11 | | | | | | | | | | | | |
| 12 | | | | | | | | | | | | |
| 13 | | | | | | | | | | | | |
| 14 | | | | | | | | | | | | |
| 15 | | | | | | | | | | | | |
| 16 | | | | | | | | | | | | |

[1]1975 ESTIMATES ASSUMES 7 % ANNUAL RISE IN SALES PRICE, 7% TO SALE LABOR EACH YEAR AFTER 1983. ASSUMES 100% PRIVATE FINANCING (87.5% DEBT - $321.2 M WITH SINKING FUND FOR ANNUAL RETIREMENT AND 12.5% EQUITY - $45.9 M FINANCING). INCLUDES 8% INTEREST INCOME ON AVERAGE CASH FLOW BALANCE DURING THE YEAR AND ON CARRYOVER BALANCE DURING THE YEAR. SALES PRICE = $200/TON.

[2]IT IS ASSUMED THAT TOTAL COMPANY INCOME EXCEEDS TWICE THE 12% INVESTMENT TAX CREDIT FOR THE FIRST YEAR SO THAT THE 50% LIMITATION DOES NOT REDUCE IT. THUS THE INVESTMENT CREDIT PROVIDES SHELTER FOR THE $17.3 M GROSS PROFIT ON OTEC/AMMONIA PLUS AN ADDITIONAL $26.8 M OF TAX ON $55.8 M OF INCOME FROM OTHER SOURCES.

[3]BALANCE OF DEBT OUTSTANDING AT END OF YEAR IF 100% OF CASH FLOW FOR COMPANY WITH OTHER INCOME APPLIED TO DEBT REDUCTION ANNUALLY.

NOTE: RETURN ON INVESTMENT: NET PROFIT/EQUITY FOR EACH YEAR IS: YR 1 = 38%, YR 2 = 46%, YR 3 = 64%, YR 4 = 84%, YR 5 = 105%, YR 6 = 120%, AV. YR 1-6 = 76% (29%/YEAR COMPOUNDED).

For the state-of-the-art program, Fig. 4 shows the current estimates of ammonia production costs for new natural gas feedstock ammonia plants in the U.S. and for OTEC/ammonia plant-ships. The calculated 1976 production cost for an $80 million shore plant using 50% interstate natural gas at $1.41 per thousand cubic feet (MCF) and 50% intrastate natural gas at $1.80 per MCF is $93 per short ton. A "general" inflation rate of 7% per year has been assumed. Curves have been drawn from this point for three projected natural gas costs. Since it is probable that natural gas prices will rise faster than the inflation rate, the three curves represent natural-gas-feedstock ammonia production costs for the inflation rate plus 2.8% (the total rate of increase being 9.8%), inflation plus 8% (+15%), and inflation plus 13% (+20%). The first commercial OTEC/ammonia plant-ship is projected to begin operations in 1982 or 1983. The following year three more commercial OTEC/ammonia plants are projected. The fifth and subsequent plant-ships come in the third and subsequent years. The first OTEC/ammonia plant is shown in the figure to be marginally competitive from its first year of operation if natural gas prices rise at the inflation rate of 7% plus 13% per year. The sixth to ninth OTEC/ammonia plants are expected to be commercially competitive without government support even if natural gas prices rise relatively slowly.

Shown at the bottom of Fig. 4 are the projected prices we have used for natural gas and oil. The natural gas price is assumed to increase from the 1975 price of $1.01 per MCF (net) at the inflation rate of 7%

plus 2.8% and plus 8%. The oil price is expected to rise at the inflation rate plus 2.8% from the present ice of $11 to $14 per barrel. With the inflation us 13% rate of increase, the cost of natural gas per llion Btu does not reach the line for $14 per barrel oil until 1985. The inflation plus 8% line of natural gas does not reach the $14 per barrel level until 1996, and the inflation plus 2.8% line of natural gas (not shown) does not cross the oil price levels at all. If natural gas prices climb more rapidly than our projections, the OTEC/ammonia option becomes even more attractive.

Shown at the top of Fig. 4 are the projected costs of ammonia production for the first six OTEC plants after start-up. Since 77% of their ammonia production costs are fixed, the lines are nearly flat over time. Thus, OTEC/ammonia costs after start-up become increasingly competitive with existing natural gas feedstock ammonia plant costs which include large raw materials expenses that do inflate with each passing year.

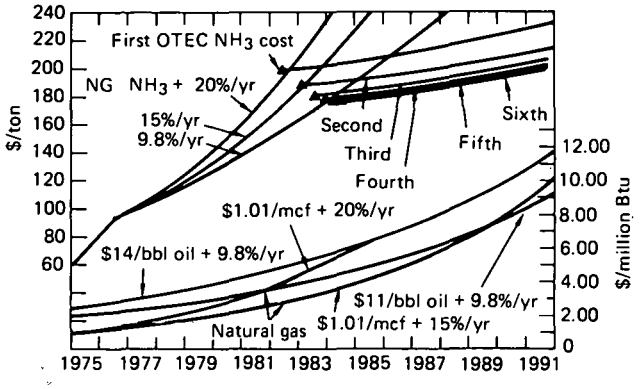



**Fig. 4 Projected Ammonia Production Costs for OTEC and New Domestic Plants**

## Domestic Market for OTEC/Ammonia, 1983-1995

In order to determine the forecast OTEC/ammonia capacity required, we have used the following assumptions: OTEC/ammonia plant-ships could capture 50% of the increase in capacity after 1982 plus 3% of the existing ammonia market per year (market served by in-place and replacement capacity) commencing in 1983; the ratio of domestic production to domestic capacity will be 90%; OTEC/ammonia plants, because of their higher fixed costs, will produce at or near maximum capacity.

Under these assumptions, we have forecast ammonia production from 1980 through 1990 as shown in Table 5.

Table 5
U.S. Ammonia Production Capacity Forecast
1980-1990
(Millions of short tons/year)

| | Est. | 1980 | 1982 | 1983 | 1985 | 1987 | 1990 |
|---|---|---|---|---|---|---|---|
| Total Capacity | High | 23.7 | 26.1 | 26.8 | 29.7 | 32.4 | 37.2 |
| | Low | 22.2 | 23.8 | 24.5 | 26.2 | 27.9 | 30.8 |
| Domestic Capacity | High | 23.7 | 25.7 | 25.3 | 25.1 | 25.2 | 25.4 |
| | Low | 22.2 | 23.4 | 23.0 | 22.8 | 22.2 | 21.7 |
| OTEC/$NH_3$ Capacity | High | - | .4 | 1.5 | 4.6 | 7.2 | 11.8 |
| | Low | - | .4 | 1.5 | 3.4 | 5.7 | 9.1 |
| No. of 325 $MW_e$ OTEC/ $NH_3$ Ships (Cum.) | High | - | 1 | 4 | 12 | 19 | 31 |
| | Low | - | 1 | 4 | 9 | 15 | 24 |

If a U.S. Government policy were announced that no new domestic natural gas supplies would be available for domestic ammonia plants after the OTEC/ammonia plant-ships are proved technically and economically feasible (a Government decision similar, though later in time than that postulated by APL a year ago), the number of OTEC/ammonia plant ships required would be increased to 34-47 OTEC/ammonia plant-ships by 1990. An additional 15 to 19 325-$MW_e$, 1000 metric ton per day OTEC/ammonia plant-ships would be needed for the period 1991-1995 under the 50% new market capture plus 3% of old market assumptions.

## Overseas Market for OTEC/Ammonia, 1983-1995

For the readily-accessible overseas OTEC/ammonia market for plant-ships grazing in the tropical Atlantic Ocean, we have included only the following countries: Brazil, Argentina, Guiana, Surinam, Uruguay, Ecuador, Angola, Cameron, Congo, Gabon, Ghana, Guinea, Ivory Coast, Liberia, Mauritania, Morocco, Nigeria, Senegal, Sierra Leone, and South Africa. Brazil is the largest consumer of nitrogen fertilizer of these countries. Consumption is projected to reach 1,054,000 metric tons (mt) in 1980 and 1,752,000 in 1985 or nearly 60% of the total. Brazil, like the U.S. is dependent upon imported oil and natural gas for a substantial part of its needs.

Consumption of nitrogen fertilizer in the tropical Atlantic Ocean nearby overseas market was 866,000 metric tons in 1975.* Projecting market growth at the rate for developing countries in general (10.7% per year), this growth will reach 1,440,000 mt in 1980; 2,393,000 mt in 1985 and 3,979,000 mt in 1990. We will ignore industrial uses of ammonia in these countries for purposes of our projection. Converting the above into anhydrous ammonia demand and applying the same assumptions that we used for domestic market share, we have an OTEC/ammonia requirement for 7 additional 325-$MW_e$ (net) 1000 mt/year plant-ships, Table 6. Brazil alone would require 4 of the 7 plant-ships.

*Monthly Bulletin of Agricultural Economics and Statistics, Food and Agriculture of the United Nations, Rome, Vol. 25, No. 3, March 1976.

Table 6
Overseas Ammonia Production Capacity Forecast
1980-1990
(Millions of Short tons/year)

| Est. | 1980 | 1982 | 1983 | 1985 | 1987 | 1990 |
|---|---|---|---|---|---|---|
| Total Capacity | 2.26 | 2.77 | 3.07 | 3.76 | 4.61 | 6.26 |
| Domestic Capacity | 2.26 | 2.77 | 2.67 | 2.96 | 3.11 | 3.56 |
| OTEC/$NH_3$ Capacity | - | - | .40 | .80 | 1.50 | 2.70 |
| No. of 325 $MW_e$ | - | - | 1 | 2 | 4 | 7 |

An additional 5 325-$MW_e$, 1000 metric ton per day OTEC/ammonia plant-ships would be needed for the tropical Atlantic Ocean nearby overseas market for the period 1991-1995.

Another country selected for special comment is India which produces much of its fertilizer needs from more costly processes than natural gas, using naptha and coal and in 1975 became the world's largest nitrogen fertilizer importer. In 1975, India reported nitrogen fertilizer imports of 880 thousand mt and production of nearly 1,200 thousand mt. With the vast areas of tropical ocean off India, serious consideration should be given to the promise of OTEC/ammonia in this area.

Other examples could be cited, including special considerations for the middle East countries. The point is that these countries and other tropical area nations could take the initiative independently, or in cooperation with the U.S. to establish a beneficial program using the new OTEC technology. APL has recently discussed its OTEC approach and the need for initiatives with an official of the United Nations.

A question has been raised relative to excess capacity within the domestic ammonia industry which could meet the needed demand. In 1975 and 1976, the industry produced at an actual and estimated 91% of plant capacity. With the published domestic ammonia plant building program (construction started, contracts let, and planned new construction), if all plants announced were to be built, the industry would be operating at 78% of capacity in 1978 under our low demand case and 81% of capacity under our high demand case. These percentages then move upward to 84% and 89% in 1980. By then, the domestic ammonia industry would be consuming approximately 5% of the lower-48 states natural gas supply. This figure would increase to 7% by 1985 and, as stated in President Carter's energy message of April 20, 1977, the industry would get priority allocation of natural gas and relief from the taxes on natural gas paid by other industries, because there is no economic alternative to the use of natural gas for feedstock. With the first successful commercial OTEC/ammonia plant-ship, however, there is an alternative and the whole situation is changed. If a definite program for the first OTEC plant-ship is announced, the excess domestic natural-gas-ammonia capacity beyond 1980 would not be built.

Additional questions have been raised as to the potential for meeting ammonia fertilizer needs by coal and from Middle-East "free" gas. Coal feedstock ammonia is significantly more expensive than natural gas or OTEC projections and environmentally is the least desirable. Cost reductions from 30%-70% would be necessary. While perhaps deserving of research, it does not present a present threat to the OTEC/ammonia market share. "Free" Middle-East natural gas based ammonia plants are not economically competitive with OTEC/ammonia plants at current operating factors if the gas used is valued at $0.80/MCF or more. With the other options available for Middle-East gas, U.S. ammonia sales do not offer an attractive profit potential. Since ammonia is vital to U.S. food production, substantial Middle-East production of ammonia for sale in the U.S. would almost certainly be met by tariffs or import restrictions. Such tariffs apply now at $25/ton for Middle-East production and $50/ton for Communist-sphere production of non-fertilizer ammonia.

## OTEC/Electricity Via Fuel Cells

The process for generating electricity using dissociated ammonia from a 500-$MW_e$ OTEC/ammonia plant-ship to fuel a hydrogen-oxygen fuel cell is shown in Figure 5. This process is for a plant with an optimized design which would be available in the late 1980's or early 1990's, on the 25th OTEC/ammonia plant-ship built in the U.S. It is expected that this electricity, which can be provided at any location in the U.S. or in the world, will become the major product from tropical OTEC plant-ships.

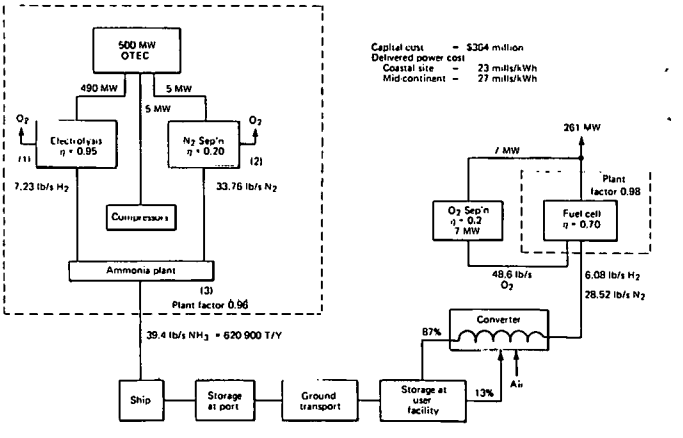



**Fig. 5 OTEC Produced Ammonia Dissociated to Power a Hydrogen-Oxygen Fuel Cell, Cycle and Costs for Optimized Design, 25th Plant-Ship**

The capital cost in constant 1975 dollars is $363 million or $1390/$KW_e$, consisting of $315 million plant investment for the OTEC/ammonia plant-ship, $11 million for the ammonia to hydrogen and nitrogen converter and auxiliaries, $7 million for the air liquefaction plant, and $30 million for the General Electric model fuel cell. For a coastal U.S. user, the produc-

tion cost of the electricity would be 23 mills/kwh. For a mid-continent user, the ammonia is shipped via rge and tank truck at a cost of 4 mills/kwh for the st remote locations, bring the cost at user site 27 mills/kwh. (For a baseline, 6th OTEC/ammonia plant-ship, the cost would be 38 mills/kwh and 43 mills/kwh respectively.) The above optimized cycle kwh costs are very competitive with baseline estimates for electricity from coal or nuclear power and are below optimized estimates we have seen from OTEC/direct transmission plants.

As shown in Figure 5, the 500-$MW_e$ optimized OTEC/ammonia plant-ship would produce 620,900 short tons per year of ammonia which would be shipped to the U.S., possibly have in-transit terminal storage at the port (e.g., New Orleans, Charleston), then move by barge, rail or tank-truck overland to the user site for operating tank storage at -28°F and atmospheric pressure at the user facility (e.g., an electric utility substation, an industrial plant, a hotel). The liquid ammonia would then be dissociated to hydrogen and nitrogen gas at point of use in a catalytic converter. In our estimate, we have used 13% of the ammonia product dissociated for its hydrogen as fuel to obtain the needed process heat. If it were more economical, this process heat could be provided by coal or other fuel. Then, the remaining 87% of the hydrogen gas is burned with oxygen gas obtained by air liquefaction in the hydrogen-oxygen fuel cell to produce electricity. The resultant electric power is 261-$MW_e$ of the original 500-$MW_e$ (net) power produced on the OTEC/ammonia plant-ship or an overall system efficiency of 52%.

OTEC/Aluminum

APL has received expression of interest by two major metal companies in the possibility for using the 10 mill/kwh busbar power on tropical ocean OTEC plant-ships for aluminum reduction and for smelting of ferro-alloys. The problem of stability for aluminum cells on an ocean platform exists for the conventional aluminum process and analysis has not been available for the new Alcoa aluminum reduction process. We anticipate that it will be possible to conduct at-sea tests with aluminum cells (possibly donated) on the OTEC/ammonia pilot plant to see if cell stability problems can be satisfactorily and cheaply resolved.

OTEC Pilot Plant

The APL concept for commercial-size plant-ships employs independent identical heat exchanger modules which are repeated to form a total power plant of the desired size. They are integrated with the platform to form the OTEC plant-ship. The platform structure itself forms the walls of the heat exchangers. This OTEC/ammonia plant-ship design lends itself to early verification with a 5 MW pilot plant, which will test a full scale portion (including manifolds, cold and warm water ponds, etc.) of a commercial plant.

The specific purpose of the pilot plant phase of the development program is to provide additional detailed information as soon as possible on the mechanical performance of the system and the component costs. This information is required to show prospective commercial interests the low risk construction and to project with adequate supporting data the cost-effective operation of full scale plants. The construction of the pilot/demonstration plant in a U.S. shipyard will require 24-27 months and about $45 million in FY'78-'80 U.S. dollars.

The subsystems of the baseline OTEC/ammonia plant-ship (see Fig. 1), at least one module of which must be tested in the pilot plant, are:

1. The heat engine: 20 identical units including piping and controls.
2. The platform: one central structure 475' x 196' + 20 identical heat exchanger cells with cold and warm water ponds and flow channels.
3. The cold water pipe: one 60' diameter 2500' long.
4. The water pumps: 19 identical cold water pumps + 20 identical warm water pumps.
5. The control system: 20 identical local control systems + one supervisory system.
6. The electric generators: 4 identical units available as commercial items in a range of sizes.
7. The heat exchanger cleaning system.
8. The electrolysis system: 20 identical units.
9. Air liquefaction and $N_2$ separation: one plant (optional, available as a commercial item).
10. Ammonia plant: one plant (optional, available commercially).

In addition, the pilot plant should be tested under tropical ocean conditions that accurately simulate the operational ocean environment that will be encountered in commercial use. The APL approach, which uses the 475' x 196' x 70' prestressed and reinforced concrete platform with one 5 $MW_e$ heat exchanger module and removable bottom covers in the unused areas is very flexible and would allow testing of alternative heat exchanger module sizes or types, aluminum cells and other items in a demonstration phase. This demonstration phase is expected to provide the basic information on technical operations and costs needed for commercial investment decisions. Therefore, no separate demonstration plant-ship should be required.

## Summary and Conclusions

Developments in 1976 and 1977 have reinforced conceptual OTEC/ammonia plant-ship design and the economic attractiveness of early commercialization for fertilizer and industrial uses. Refinements of site selection for a grazing tropical Atlantic Ocean plant have resulted in a nearly constant year-round $\Delta T$ of 43°F, providing economics in optimized power cycle design. Plant investment and production cost estimates for OTEC/ammonia have not changed significantly with hardware testing and further analysis since the publication of Ref. 1 in April 1976. An OTEC of the grazing variety can be documented as a vessel of the United States and would not legally be precluded from participating in established maritime programs.

The early commercial OTEC/ammonia plant-ships are expected to be 325-MWe producing 1000 metric tons of anhydrous ammonia per day, 345 days per year. 31-38 such plants would be supported by the domestic and nearby tropical Atlantic Ocean overseas markets between 1983 and 1990, an additional 20-24 between 1991 and 1995. Government support should not be required beyond the 8th or 9th plant-ship and may be terminated earlier in view of rapidly increasing natural gas prices. The fully private-financed OTEC/ammonia plant-ships will return the plant-investment in about 4.6 years with a compounded net profit over private equity of 28% per year. OTEC/ammonia dissociated to its component gases and used in hydrogen-oxygen fuel cells may become the largest market for the OTEC product in the late 1980's or early 1990's. At 23-27 mills/kwh for electricity delivered at the user site, this option would be very competitive with power from coal or nuclear fuel.

A government financed pilot plant costing approximately $45 million in FY'78-'80 dollars is needed to demonstrate technical operations and provide an acceptable basis of cost for commercial investment decisions. This pilot plant would be sufficiently flexible to allow testing of alternate heat exchanger designs and other products such as aluminum reduction or ferro-alloy smelting.

In summary, the OTEC/ammonia option looks sufficiently promising for the U.S. and the tropical nations of the world that we believe it would be imprudent not to investigate it thoroughly, at least through a pilot/demonstration plant designed to provide verified technical and financial data on a barge-type new construction hull in tropical ocean waters.

## References


1. Francis, E. J. (Principal Investigator), Executive Summary and Detailed Report, "Maritime and Construction Aspects of Ocean Thermal Energy Conversion (OTEC) Plant Ships," APL/JHU Reports SR 76-1A, 1B, April 1976 for the U.S. Maritime Administration, Department of Commerce, Contract No. 5-38054.

2. Dugger, G. L., Olsen, H. L., Pandolfini, P. P. and Avery, W. H., "Experiments on and Design of Low-Cost Aluminum Heat Exchangers for OTEC Plant-Ships," presented at the Fourth Ocean Thermal Energy Conversion Conference, University of New Orleans, March 22-24, 1977.

# A METHODOLOGY FOR OTEC MISSION ANALYSIS

ROBERT W. REID, JR.
*The Aerospace Corporation*
*2350 E. El Segundo Blvd.*
*El Segundo, California*

Abstract

An approach is described herein to evaluating alternate Ocean Thermal Energy Conversion (OTEC) concepts via a standard analysis simulation tool. The OTECOST computer program, which is currently being developed, is intended to simulate closed cycle OTEC power plant/transmission system performance and cost for a wide variety of design concepts and siting conditions. The intention is to provide a uniform economic basis for comparing candidate generation/delivery configurations on an overall system level.

Given power plant and transmission system designs, the OTECOST simulation scales the performance and capital cost of the candidate designs to suit prescribed siting and power generation conditions. Performance calculations for the closed cycle power plant initiate with the working fluid flow loop followed by calculations for the cool and warm seawater loops. A capital cost for each major equipment item is then computed as a function of the key performance parameters. The performance and capital cost of the transmission system is next calculated as a function of the OTEC power flow.

Capital expenditures, operating and maintenance costs, and the product flow to shore are distributed over the life of the plant in yearly segments. This capital/product flow schedule consists of three distinct phases which occur consecutively: the construction, checkout, and operational phases. A cost benefits analysis then uses the capital/product flow stream with a selected capital interest rate, inflation rate, and product selling price to determine the economic benefit of the particular power plant/product configuration being simulated.

A flexible optimization capability is built into OTECOST to minimize the capital cost per net power delivered by varying the inlet and outlet turbine and heat exchanger temperatures. This capability allows a consistent operational design comparison for varying sites, temperature differences, plant sizes, and configuration. A second mode of optimization allows the maximization of net power delivered for a fixed plant design operating in the presence of off-nominal ocean temperature variation and heat transfer performance (e.g., caused by biofouling).

## Introduction

The Ocean Thermal Energy Conversion (OTEC) concept is in a formative stage of development. Many design approaches have been investigated by the vast OTEC community of university researchers, industrial designers, and governmental representatives. For each major subsystem, several concepts have been studied and profferred to the community. These concepts range in detail from conceptual drawings to the level of preliminary hardware designs. The task of analyzing the mission potential of the OTEC concept in light of the varied designs, site locations, and potential products is, on a primary level, one of sorting and evaluating the large number of subsystem combinations which result. Mission analysis, as viewed at present, is: The study and evaluation of candidate power plants, site locations, and products in order to identify those candidates which, according to the evaluation criteria, best satisfy the mission objectives. This is our assumed understanding of the mission analysis task and serves to justify the approach taken here.

One further qualification is in order before proceeding. The work described below mainly addresses that portion of the mission analysis task which is amenable to quantitative evaluation. This does not mean that potential qualitative objectives (e.g., environmental protection, safety, legal and institutional constraints) are to be ignored or viewed as less important. The blending of qualitative and quantitative data for the candidate concepts must be performed at a higher level than the one assumed here. This paper attempts to address those measures of system success which can be quantified in order to prepare the way for the more subjective trade-offs which must follow.

The central topic of this paper is a computer simulation, designated OTECOST, which models power plant and transmission system performance and cost for the evaluation of candidate concepts. A view of where this simulation tool fits in the overall mission analysis task will be provided in the next section. An overview of OTECOST will then lead to a step-by-step discussion of its principle features and planned development. No attempt is made to describe the algorithms in detail, because the program is currently an analysis tool undergoing developmental changes. The model details will be deferred until the simulation checkout is complete.

## The Mission Analysis Flow

A simplified view of the mission analysis task is shown in Figure 4A-3-1. The objectives of the analysis form the basis for the task, because they define system success and failure. For the present study, the objective defined is quantitative and is to identify

- o The most economically profitable power plant/site/product combination among all candidates

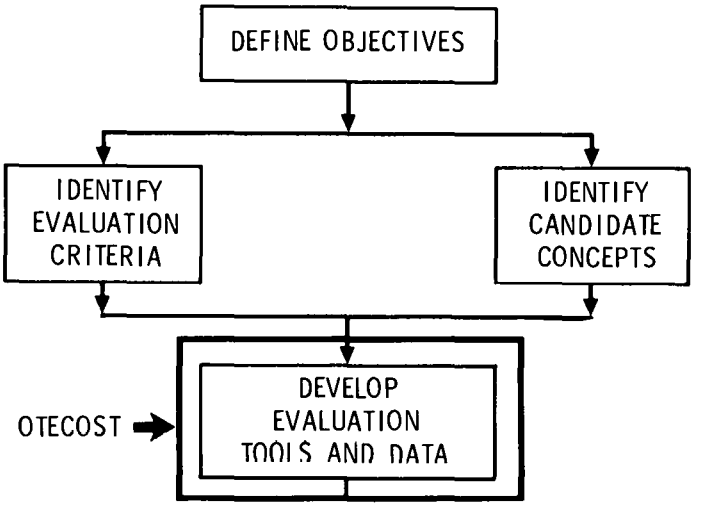



Figure 4A-3-1. Mission Analysis Flow

This objective currently leads to the identification of two possible evaluation criteria:

- o Maximize the net profit over the lifetime of the power plant/transmission system
- o Minimize the plant/transmission system capital cost to net delivered power ratio

It is conceivable that either criterion or some other might be selected depending on the interest of the investigator. The long term investor would choose the first criterion, whereas an investor who is limited by capital and power delivery constraints might well favor the second. This study will concern itself with the second criterion for reasons which will be explained in the benefits/cost analysis section.

Candidate concepts include various system levels (e.g., power plant structures, transmission concepts, heat exchanger, turbine, and pump candidates). The intention is to build a performance and cost scaling simulation which is capable of treating the component candidate concepts in a modular fashion so that many subsystem design combinations can be evaluated. This simulation tool, called OTECOST, will be used to evaluate alternate concepts using standardized evaluation criteria so as to identify those which show most promise.

## The OTECOST Simulation

The computer simulation referred to as OTECOST is being developed as a flexible system analysis tool capable of estimating both power plant and transmission system (be it electricity or product transmission) performance and cost. Such a tool allows sensitivity, trade-off, and off-nominal performance studies

for selected candidate concepts. It also promotes the standardization of evaluation criteria which aids an objective comparison process. Hopefully, OTECOST can also serve to focus OTEC community consensus regarding candidate performance and cost models and data. By structuring the simulation to accommodate various concepts and subjecting it to the critical view of the community, one might hope to realize an accelerated convergence of opinion concerning realistic performance and cost estimation.

Figure 4A-3-2 shows the computational flow of OTECOST at present. At the start of a given computer run three levels of parameter initialization are

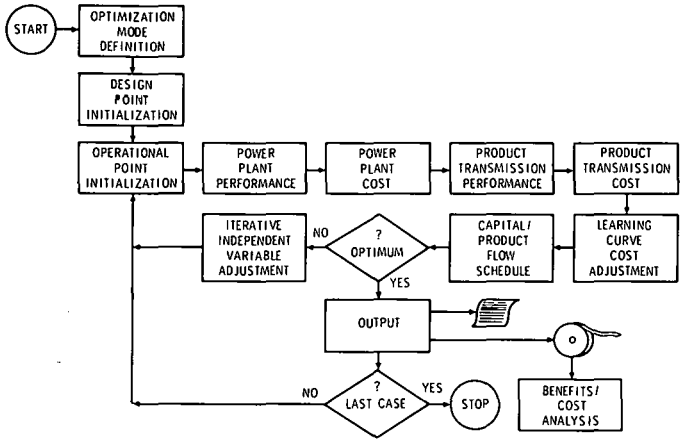



Figure 4A-3-2. OTECOST Flow

executed. First an optimization mode is selected from two candidates, these being the design point and off-nominal optimization modes. The design point mode selects plant performance to minimize the ratio of total power plant and transmission capital cost to net power delivered. The off-nominal mode defines the performance index to be maximized, under fixed hardware design constraints, as the net power delivered. Currently, OTECOST requires input data for over two hundred separate parameters. The majority of these parameters, which describe working fluid thermodynamic properties and detailed hardware design dimensions, are fixed for a given computer run at the design point initialization level and remain fixed thereafter. The remaining parameters, which number anywhere from a dozen to two dozen depending on the optimization mode chosen, are initialized at the start of a run. They are free to be changed by the optimization procedure or at the start of a new case when multiple cases per run are stacked. These independent variables, represented by the operational point initialization box of Figure 4A-3-2, will be described in more detail when the optimization procedure is discussed.

Each optimization pass through the performance and cost models begins with the OTEC power plant performance model. This model sizes major components needed to produce the user-specified gross plant power under user-specified operating conditions. Key performance values for each major component or capital item are then fed to the power plant cost model which determines the total capital cost and yearly operating and maintenance (O& M) cost corresponding to this item. The performance output of the power plant serves to scale the performance output of the product transmission model which in turn provides the key parameters needed to scale capital and O&M costs for each capital item within the product transmission cost model.

The learning curve model adjusts the average capital cost of each major power plant and transmission system capital item downward monotonically as a function of the number of units produced. These adjusted capital costs are then laid out on a time line over the lifetime of the plant as are the O&M costs and the yearly product delivered to shore. This capital/product flow schedule provides input data for the benefits/cost analysis when optimization is complete. At the end of a given performance and cost estimation pass, as described above, the optimization procedure determines whether or not the performance index is optimum and all constraints are satisfied. Iterative adjustment of the independent variables continues until convergence takes place or until it is determined that no solution can be found. At the completion of a given case, another case with different operational point initial conditions (i.e., independent variable initial conditions) can be executed in the same computer run. The data output for each case is used to perform benefits cost analyses.

## Power Plant Performance

A schematic view of the closed cycle OTEC power plant is shown in Figure 4A-3-3. Major pieces

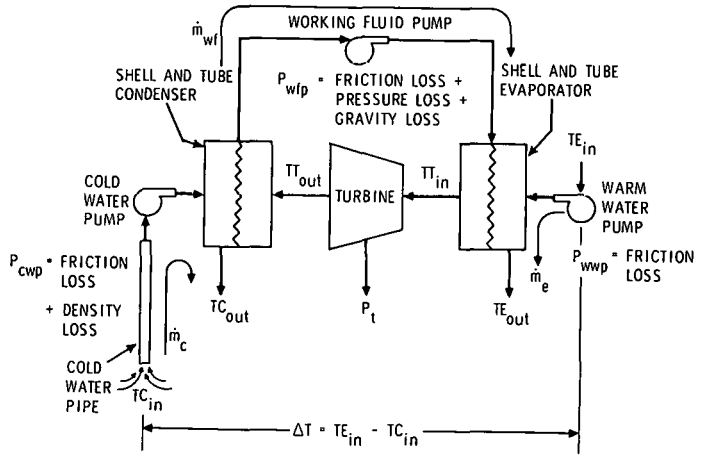



Figure 4A-3-3. Power Plant Performance (Closed Cycle)

of equipment include the condenser and evaporator heat exchangers, turbine(s), warm and cold water pumps, working fluid pump(s), and a cold water pipe. The mass of working fluid, $\dot{m}_{wf}$, required to generate the user-specified gross power, $P_t$, is determined as a function of this power level; the working fluid enthalpy properties; the temperatures in and out of the turbine, $TT_{in}$ and $TT_{out}$, respectively; and the turbine efficiency. Working fluid pump power, $P_{wfp}$, is calculated as a function of the fluid mass flow rate and the head due to friction, pressure differentials, and gravity. Many of the relationships used in the performance model are taken from Boot and McGowan (1) as well as standard fluid dynamic and thermodynamic texts (e.g., Pao (2); Jones and Hawkins (3)).

The mass flow rate of cold water, $\dot{m}_c$, needed to condense the working fluid may be determined from the required heat flux, the specific heat of water, and the condenser inlet and outlet temperatures, $TC_{in}$ and $TC_{out}$, respectively. The wetted surface area of the condenser is set by the total heat transfer coefficient and the velocity flow rate of cold water which influences this coefficient. Since the total surface area, the water velocity, and the heat transfer coefficient influence one another, three simultaneous nonlinear algebraic equations must be solved simultaneously to determine the values of these three parameters. Currently these equations are posed to the optimization problem as equality constraints which must be satisfied at the optimal solution. The cold water pump power requirement, $P_{cwp}$, is derived as a function of the water flow rate and the friction and density head. The warm water equations for the water flow rate, $\dot{m}_e$, pump power, $P_{wwp}$, evaporator surface area, flow velocity, and heat transfer coefficient are analogous to those for the condenser with the exception of cold water pipe friction losses and density losses which exist for the condenser only.

## Power Plant Cost

The cost scaling algorithms used in OTECOST are, for the most part, those assumed by the TRW final report (4). An exception is the hull structure algorithm which currently approximates a spar buoy hull cost as a function of the individual power module volume and the central core volume per the Lockheed final report (5). Figure 4A-3-4 shows qualitatively the parametric relationship between capital cost and performance for eight capital items of the power plant. Integration and contingency costs and engineering and management fees are added as a user-specified percentage of the direct capital cost. Operating and maintenance costs are also scaled from baseline values in proportion to scaled capital costs. The scaling philosophy used throughout OTECOST is one which requires baseline design cost and performance values which are used as initialization points for extrapolation via the cost algorithms.

It is realized that some or all of the current cost-performance relationships may prove inadequate

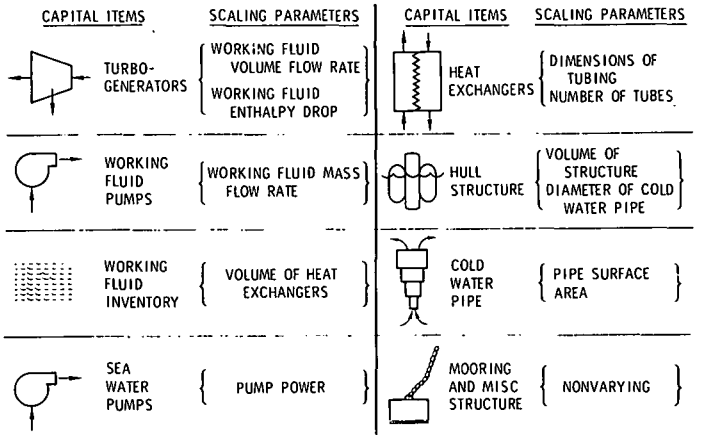



Figure 4A-3-4. Power Plant Cost (Closed Cycle)

to the task at hand. Mooring costs, for example, may very well be dependent on siting depth, platform size, and nominal current speed. Working fluid and water pump costs might also be scaled as functions of their respective fluid flow rates and heads. The OTECOST simulation is a growing program which will evolve toward the satisfaction of those goals set for it.

## Product Transmission Performance: Electricity

One example of a product transmission model presently available in OTECOST is that of electricity transmission to shore via submarine cable. Two modes of simulation are available to the user corresponding to the alternating and direct current methods of transmission. Figure 4A-3-5 depicts the power attenuation trends for a.c. and d.c. transmission.

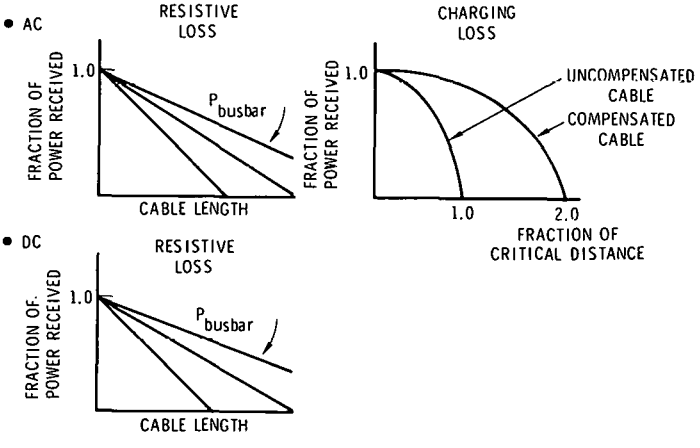



Figure 4A-3-5. Electricity Transmission Performance

For an a.c. design, the cable losses are the sum of resistive heating and cable capacitance charging. The former is linearly increasing with cable length and approximately quadratic in its increase with the busbar power level. Charging losses increase in a cubic manner with distance, where the critical distance is defined as that cable length which absorbs all input current in charging the cable's shunt capacitance. The critical distance of an a.c. submarine cable can be doubled by adding compensating inductors at both ends. This compensation, however, increases transmission system costs. The resistive and charging losses are root sum squared to approximate the magnitude of the complex power loss which exists. Direct current transmission losses are functionally analogous to the a.c. resistive losses. Only the power loss versus distance slope is different, as specified by the user.

The electricity transmission performance model is a simplification of more detailed models suggested by A. D. Little (6) and Kammer (7). The general transmission system design problem is a complex one, yet a reasonable scaling approximation is needed to strike a balance between realistic performance estimates and the programming simplicity needed to serve the needs of a much larger system simulation. Small power terminal losses, which are neglected, might be included as a first step toward updating the programs transmission performance accuracy.

Product Transmission Cost: Electricity

Electricity transmission costs are lumped under three capital item headings; power terminal costs, power cable costs, and cable installation costs. These items and their related performance scaling parameters are displayed in Figure 4A-3-6.

The terminal cost is linearly related to busbar power by separate user-specified coefficients for the

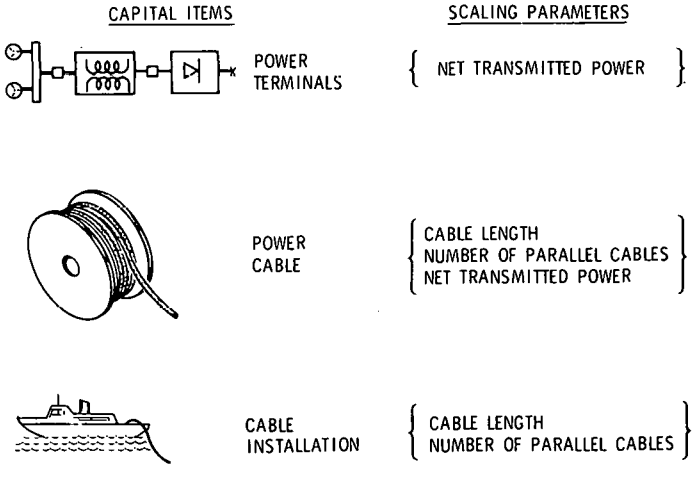



Figure 4A-3-6. Electricity Transmission Cost

a.c. and d.c. models. The power cable construction costs are dependent on the cable length and number of parallel cables as well as the plant busbar power level. The dependence on busbar power follows an empirically derived approximation to the cable cost vs. power data provided in reference (6) for paper insulated cabling. For a.c. transmission an additional percentage is added for cable compensation if the cable critical length is exceeded. If twice the critical length is exceeded by siting demands, an error message is printed.

Cable installation costs vary linearly with distance per reference (6) and the number of cable spans. The linear cost vs. distance slope which is a function of the laying ship's capacity is determined as a user-specified input.

Product Transmission Performance: Ammonia

An example of a chemical product application is that of anhydrous ammonia production. The production method selected for modeling is that described by APL (8) in which ammonia is produced from sea water and air. A schematic diagram of this procedure is presented in Figure 4A-3-7. Ammonia is synthesized from

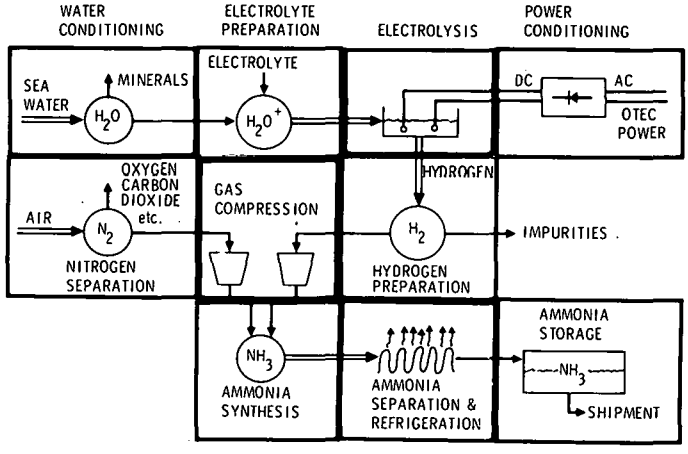



Figure 4A-3-7. Ammonia Production

a compressed mixture of hydrogen and nitrogen gases. The hydrogen is obtained by the electrolysis of fresh water to which an electrolyte is added. Fresh water is obtained from sea water by divesting the ocean water of its minerals. Power for the electrolysis process is provided by the a.c. to d.c. conversion of OTEC-generated power. The resultant hydrogen, which is purified and compressed, joins with nitrogen which is obtained via air liquefaction. After synthesis the ammonia product is purified, refrigerated, and stored for shipment to shore.

The flow rates of the various process substances are scaled by the power input to the ammonia plant given a baseline ammonia to power design ratio. Given the input power and thus the output ammonia flow rate, the hydrogen, nitrogen, water, and air flow rates are determined by the chemical weights needed for each substance and the user-specified process efficiencies. These flow rates then serve to scale the process equipment costs.

## Product Transmission Cost: Ammonia

Figure 4A-3-8 qualitatively shows the cost-performance functional relationships for the ten process flow items outlined in the previous figure. In

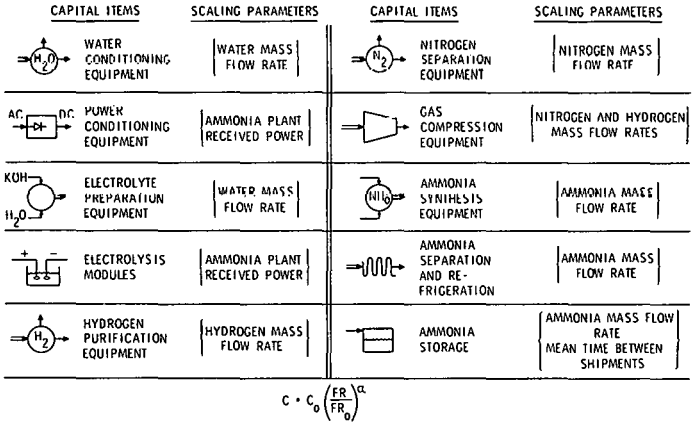


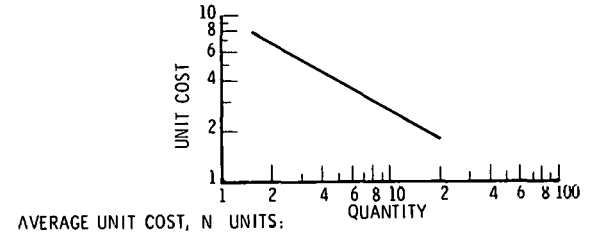

Figure 4A-3-8. Ammonia Production Cost

almost all cases the capital cost of the process equipment is related to the mass flow rate of substance through that particular element. The functional form of the cost-flow relationship is shown at the bottom of the figure. This relationship is commonly used in chemical engineering as a first cut approximation of equipment costs (see Mills (9) and Hoerner (10)). In some cases the same mass flow rate serves as a scaling factor for more than one piece of equipment. The water mass flow rate, for example, is used to scale water conditioning and electrolyte preparation equipment costs.

Ammonia storage costs depend not only on the ammonia flow rate, but also on the time between shipments to shore. The shipping cost which is a function of shipping distance and ship capacity is considered as an operating and maintenance cost associated with ammonia storage. It does not figure directly into the capital cost of storage under the current assumption (i.e., dedicated shipping is not assumed).

## Learning Curve Cost Adjustment

All capital costs for the power plant and transmission system are adjusted downward as a function of the number of units produced by a learning curve algorithm. It is assumed that the average per unit cost, $\bar{C}_N$, of producing N units of a given item is log linearly realted to the number of items produced. This assumption is displayed by the first equation in Figure 4A-3-9.




AVERAGE UNIT COST, N UNITS:

$$\bar{C}_N = C_1 N^b$$

TOTAL COST, N UNITS:

$$C_N = C_1 N^{1+b} = N\bar{C}_N$$

$n^{th}$ UNIT COST:

$$C_n = C_1 \left[ n^{1+b} - (n+1)^{1+b} \right]$$

$C_1$ = FIRST UNIT COST

b = LOG m/log 2

m = COST-QUANTITY CURVE SLOPE

Figure 4A-3-9. Learning Curve Algorithm

Also shown is a graphical representation of the log linear assumption, the total cost of N units (which is by definition $N\bar{C}_N$), and the nth unit cost (which is the difference between total costs for (N + 1) and N units). The first unit cost $C_1$ is calculated by the power plant or transmission cost routines depending on the capital item being adjusted. The number of units, N, is the total number for all plants (or transmission systems) produced. Empirical user-specified values of the cost-quantity curve slope, m, are used in the learning curve adjustment. In general labor costs display slope values in the range (0.75, 0.80) whereas material costs fall in the range (0.96, 0.99). Thus each capital item has a cost-quantity slope varying between these extremes depending on the relative mix of material and labor costs required for its production.

## Capital/Product Flow Schedule

Once the average capital cost is determined for each major capital item an expense and product flow schedule is developed for use in the benefits/cost analysis. At this point in the simulation all of the information is available for determining the capital cost per unit of power (or tons of product per day) delivered to shore. In order to calculate the cost of delivered energy rather than power, a time schedule of costs and energy produced must be planned. The features of such a plan are displayed in Figure 4A-3-10.

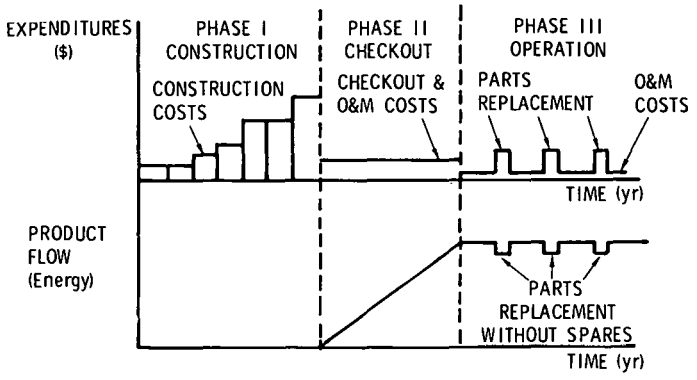



Figure 4A-3-10. Capital/Product Schedule

The power plant/transmission system lifetime is considered in three distinct phases, these being the construction, checkout, and operating periods. Each capital item has an associated construction lead time which is user specified at a design point and is scaled with the plant size for some items. The longest lead time determines the length of the construction phase. It is assumed that the total capital cost of each capital item is uniformly distributed over the lead time. As each lead time prior to deployment (i.e., the end of the construction phase) is reached, the capital expenditure for the corresponding item is summed with other outlays on a yearly basis to produce the total capital flow as shown by the construction costs in the figure. All expenditure and product flow units are expressed in yearly segments of the plant lifetime.

At the end of construction all capital costs drop to zero. The checkout period, which is user-specified, shows constant expenditures for operation and maintenance (O & M) of each major item at a higher level than the operational O&M costs. During the operational period the O&M costs remain constant and capital costs rise for each major item when a replacement is necessary. The simulated time between replacements, equal to the mean time between failures, is in part specified by the user and is dependant on the number of on-line items working in parallel.

The product flow is expressed as energy (kilowatt hours or tons of product) produced in a given yearly segment. During construction the product flow is zero. It rises linearly to its nominal operational level during checkout and remains fixed except for periods of parts replacement during the operational phase. If a major equipment item must be replaced without a spare on hand and this item is one of n acting parallel across the power stream, the energy level decreases by the fraction 1/n during the procurement period (i.e., lead time) needed for that particular item. The decision concerning spares maintenance is made in a separate subroutine which weighs the economic advantages of maintaining a spare against those of not doing so.

Iterative Independent Variable Adjustment

Figure 4A-3-11 summarizes the main features of

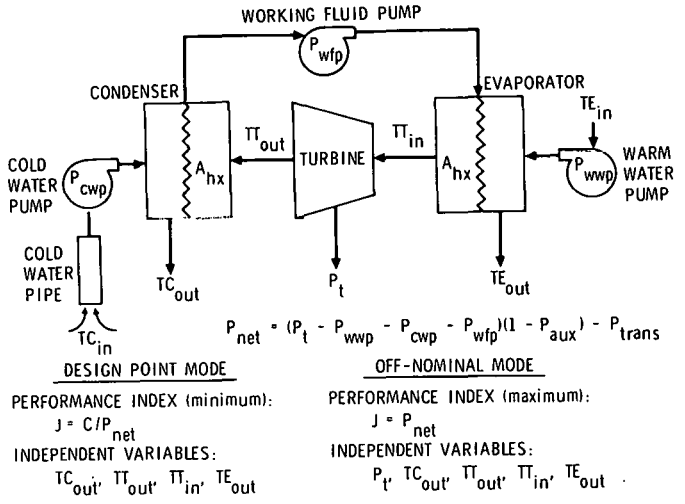



Figure 4A-3-11. Modes of Optimization

two optimization modes which are currently available to the user of OTECOST. The schematic power cycle diagram is reproduced at the top of this figure as a visualization aid in describing the optimization modes. The condenser sea water outlet temperature, $TC_{out}$; the turbine working fluid outlet temperature, $TT_{out}$; the turbine working fluid inlet temperature, $TT_{in}$; and the evaporator sea water outlet temperature, $TE_{out}$; serve as independent variables in both modes. The condenser and evaporator sea water inlet temperatures, $TC_{in}$ and $TE_{in}$, respectively, are fixed by site dependent conditions. Sizes of major equipment items are described by their power in the case of the fluid pumps ($P_{cwp}$, $P_{wfp}$, and $P_{wwp}$) and the turbine ($P_t$) or by the wetted area of the heat exchangers ($A_{hx}$). Net power, $P_{net}$, is defined as the gross power minus parasitic pump and auxilliary losses and the transmission power loss to shore, $P_{trans}$.

Design point optimization is used to define a nominal design size for the various equipment items by using the OTECOST power plant and transmission system scaling ability under user-specified temperature difference ($\Delta T = TE_{in} - TC_{in}$) and plant size ($P_t$) conditions. Thus, given a plant design for particular values of $P_t$ and $\Delta T$, one can scale this design to different operating environments (via $\Delta T$) and plant sizes (via $P_t$) using a consistent design methodology. The performance index to be minimized is the ratio of

total power plant and transmission system capital cost to net power delivered on shore. Independent variables include the four intermediate plant temperatures $TC_{out}$, $TT_{out}$, $TT_{in}$, and $TE_{out}$. Optimization constraints require that these temperatures be monotonically increasing, as written, on the range ($TC_{in}$, $TE_{in}$). In addition to independent variables listed in the figure, however, the evaporator and condenser surface areas, water flow velocities, and heat transfer coefficients are formally used as independent variables in the solution of six simulataneous algebraic equations or optimization equality constraints. These additional variables and constraints are not shown in Figure 4A-3-11 in order to help simplify the figure.

Given a nominal plant and delivery system design, it is reasonable to ask about its performance in the presence of off-nominal temperature differences, $\Delta T$, or off-nominal heat transfer characteristics (e.g., caused by biofouling). The off-nominal optimization mode can be used to investigate these problems. Since the design, and hence cost, is considered fixed, the natural desire is to maximize the benefit realized under off-nominal conditions. Thus, the performance index chosen for maximization is the net power delivered on shore, $P_{net}$. It is assumed that the pump and turbine power levels can be varied at or below their design values by some electromechanical control system. It is envisioned that such control will be necessary to operate the plant in the presence of seasonal, daily, or perhaps even hourly environmental fluctuations. Thus, the turbine power, $P_t$, is added to the list of independent variables already described for the design point mode. The power constraints mentioned above are added to the constraint list as is the requirement that the heat exchanger wetted surface area remain fixed at its design value (this constraint is imposed on the condenser and evaporator separately rather than the total heat transfer area).

The optimization procedure used employs an accelerated multiplier method developed by Betts (11). First derivative information is numerically generated by perturbation of the OTECOST simulation and second derivative, or Hessian matrix, data is iteratively developed by a rank one recursive process. Equality constraints are satisfied by an exterior point sequential unconstrained minimization technique, and inequality constraints are treated as equality constraints when an equality exists at a local optimum. This procedure is encoded in the Generalized Trajectory Simulation (GTS) at The Aerospace Corporation. The GTS input format, as described by reference (12), allows the user to define an optimization problem by specifying the performance index, independent variables, and constraints using program-specific symbols. This flexibility allows the structuring of many optimization problems with the ease of changing input data statements.

Some of the results obtained by exercising these optimization modes can be discussed qualtitatively. The total plant and transmission capital cost, the ne power delivered, and the ratio of cost to power can conveniently be plotted versus the temperature difference given a series of different cases. If data pairs of temperature difference (at a prescribed depth) versus distance off shore are available, the net delivered power can also be plotted from multiple case output. In general, there will be an optimum distance from shore for maximizing delivered power. This distance balances transmission losses against the performance advantage of a larger temperature difference as the distance increases.

If a power plant is operated in the presence of a known fixed yearly temperature variation, the question of choosing a nominal design temperature difference naturally arises. In general, a unimodal curve shows the result of plotting the operational cost to power ratio for various values of the design temperature difference. If a large design difference is chosen the plant is less costly than for lower values but the power is also less, because the plant operates all year long below its design difference. For lower design differences the power realized is greater than design, but the capital costs are very large. An optimum design temperature difference generally exists between these two extremes. The off-nominal mode, when used repeatedly for off-nominal temperature variations over a year's period, can produce yearly average power levels whose ratio to the design level produces a temperature variation use factor. A similar use factor can be plotted for off-nominal biofouling performance as a function of the fouling growth time, layer thickness, and cleaning interval.

## Benefits/Cost Analysis

Upon the completion of optimization convergence, the capital/product flow data is available to the benefits/cost analysis which utilizes the capital/product flow schedule described above to calculate an economic benefit/cost ratio. Figure 4A-3-12 shows a simplified

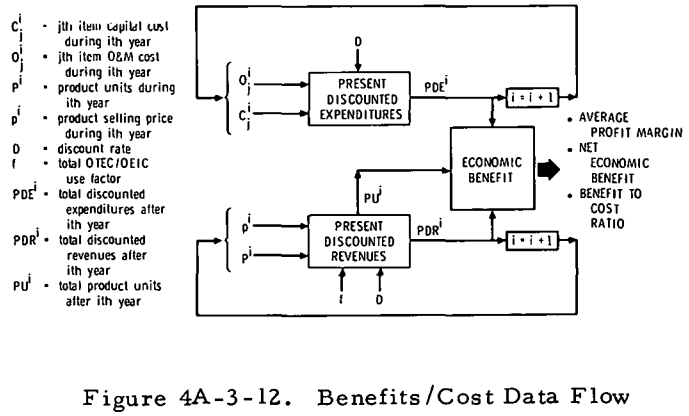



Figure 4A-3-12. Benefits/Cost Data Flow

flow of data through this analysis. The capital ($C^i_j$) operating and maintenance ($O^i_j$) cost streams for a year of the plants' lifetime, i, and each major pment item, j, are summed and discounted by D to produce the current present discounted expenditures. A similar procedure is used to calculate the present discounted revenues using the product flow stream ($P^i$) user-specified product prices ($p^i$) and a user-specified plant use factor (f) and discount rate (D). The total number of product units ($PU^i$) expenditures ($PDE^i$) and revenues ($PDR^i$) after the ith year are combined to produce the profit margin which is the revenues minus expenditures over units; the net benefit, which is revenues minus expenditures; and the benefit/cost ratio, which is revenues over expenditures.

The selection of the optimization performance index (capital cost over net power) allows the benefits/cost analysis and its assumptions to also be used separately from the OTECOST simulation. Thus the capital/product data from a given OTECOST case may be used in the benefits/cost analysis under varying economic assumptions without having to run the full simulation repeatedly. If the total cost of energy delivered to shore (i.e., mills/kwh) is desired as a performance criterion for optimization, it will be necessary to include the benefits/cost analysis within the optimization loop. This may be done in the future as an option if user demand reveals the need.

## OTECOST Status and Development

The OTECOST performance and cost simulation is, at the present time, an analysis tool which has been developed by The Aerospace Corporation in support of an ongoing mission analysis study. It is an engineering tool which is being modified and developed on a daily basis. Its input structure is suited to the useage of a limited group of users who are intimately familiar with the program structure and idiosyncracies.

Currently the program is batch processed on a CDC 7600 facility at The Aerospace Corporation via card decks or terminal access. The program, exclusive of optimization, consists of roughly 2000 Fortran-coded cards (i.e., 1 box). There are over two hundred input parameters which include hardware dimensions, working fluid and sea water properties, baseline cost and performance data, equipment failure and procurement times, equipment efficiencies, fluid flow coefficients, the gross power level, the number of power modules, and inlet and outlet flow temperatures. Of these, about one to two dozen are available as independent optimization variables, depending on the mode of optimization chosen. There are no excessive storage or run time requirements for OTECOST. The OTEC cost-performance simulation requires about 0.1 sec per pass, whereas the entire OTECOST package (including optimization) runs about 10 sec per case on the CDC 7600 computer.

In the months ahead, OTECOST will be documented and validated in more detail. Structuring will begin toward the goal of transforming the simulation into a production tool accessible to a wider community of . The performance and cost algorithms will be modified and increased to reflect OTEC community concensus where possible. This is an extremely useful but difficult result to achieve. The use of OTECOST as a sounding board for concept critique and concensus requires the active support and participation of the many technical and economic specialists within the OTEC community. Your interest and support are invited and encouraged in this ongoing effort.

## References


1.) Boot, J. L., and McGowan, J. G., "Feasibility Study of a 100 Megawatt Open Cycle Ocean Thermal Difference Power Plant," University of Massachusetts Mechanical Engineering Department, Report No. NSF/RANN/SE/GI-34979/TR/74/3, August, 1974.

2.) Pao, R. H. T., Fluid Dynamics, Charles E. Merrill, Columbus, Ohio, 1967.

3.) Jones, J. B., and Hawkins, G. A., Engineering Thermodynamics, John Wiley, New York, 1960.

4.) "Ocean Thermal Energy Conversion Research on an Engineering Evaluation and Test Program," TRW Report under Contract No. NSF-C958, June, 1975, Vol. II and III.

5.) "Ocean Thermal Energy Conversion (OTEC) Power Plant Technical and Economic Feasibility," Lockheed Report No. LMSC-D056566, NSF Report No. NSF/RANN/SE/GI-C937/FR/75/1, 12 April 1975.

6.) "Draft Interim Report on Energy Delivery, Ocean Thermal Energy Conversion," A. D. Little Report No. 78356 under NSF Contract No. NSF-C1019, May 8, 1976.

7.) Kammer, W. A., "OTEC Siting Report No. 3," Aerospace IOC. Dated August 4, 1976.

8.) Avery, W. H., Blevins, R. W., Dugger, G. L., and Francis, E. J., "Executive Summary: Maritime and Construction Aspects of Ocean Thermal Energy Conversion (OTEC) Plant Ships," Applied Physics Laboratory/Johns Hopkins University Report No. SR 76-1A, April 1976.

9.) Mills, H. E., "Cost of Process Equipment," Chemical Engineering, March 16, 1964, p. 133.

10.) Hoerner, G. M., "Nomograph Updates Process Equipment Costs," Chemical Engineering, May 24, 1976, pgs. 141-143.

11.) Betts, J. T., "An Accelerated Multiplier Method for Nonlinear Programming," Journal of Optimization Theory and Applications, Vol. 21, No. 2, February, 1977.

12.) "The Generalized Trajectory Simulation System, Volume IV: Numerical Operators," SAMSO-TR-75-255, Vol. IV, Aerospace TR-0076(6666)-1, Vol. IV, 15 April 1976.

# OTEC IMPLEMENTATION PROBLEMS FOR SPECIFIC MISSIONS*

E. TSCHUPP, B. BERKOWITZ, AND W. HAUSZ
*TEMPO-Center for Advanced Studies*
*General Electric Company*
*Washington, D.C.*

Abstract

The Ocean Thermal Energy Conversion (OTEC) concepts for the production of electricity or energy intensive products are generally conceded to be technically feasible within the foreseeable future. However, technical feasibility is only one requirement for enabling the OTEC program to make a significant contribution to the nation's energy requirement. Another major requirement on such systems is that they are commercially competitive with more conventional energy technologies and that no significant barriers to implementation will exist.

This study examines several specific applications or missions for OTEC systems that appear to have high probability for commercial viability; and addresses, locations, and conditions making marketplace conditions favorable for OTEC. In addition, it addresses institutional, industrial, and political factors to enable the identification of possible barriers to implementation and deployment and means of minimizing such barrier problems. The study describes the potential OTEC energy contribution and steps that should be taken to maximize that contribution.

## OTEC Implementation Problems for Specific Missions

The Ocean Thermal Energy Conversion System concept offers the potential of converting the large-scale renewable resource of solar energy into reliable base load electric power which is suitable for use in both commercial and industrial applications. Also, it can displace the use of fossil energy consumption that is approximately three times the energy content of the delivered electricity. As a result of the great potential offered by this concept, a mission analysis is required as part of the definition planning studies to support the development of system requirements and plans.

The basic Ocean Thermal Energy Conversion (OTEC) System Concept will use the difference in temperature that exists between the surface of the ocean and ocean waters at great depths (300 m. or more) as the energy source to drive turbine generator units for the production of electricity. This power can then either be delivered to shore via a transmission cable or be used in the production of electrical energy intensive products at sea (i.e., hydrogen, aluminum, chlorine, etc.) which will be used onshore. In either case, the OTEC production will contibute to the national energy requirements and displace fossil fuel that can be better utilized in other applications.

This report examines feasibility of four specific missions as commercial ventures. To do this, the competitiveness of OTEC products in the marketplace are considered as well as the impacts of the technology and the political, institutional, and environmental factors associated with OTEC operations. In addition, ancillary and/or non-commercial missions such as national security are considered for the purpose of identifying additional benefits that can accrue as the result of OTEC systems implementation.

The missions that are considered are:

- Near shore production of electric power delivered to shore via submarine cable.
- Offshore production of sea chemicals (such as chlorine, etc.) which are electrically intensive and in large-scale industrial use.
- Offshore production of aluminum, the most electrically intensive product in large industrial use and a product which is projected to increase in demand by a factor of four by the year 2000.
- Offshore production of fertilizers based on fixed nitrogen in the form of ammonia. Ammonia is currently produced by reforming methane and the demand for ammonia by the year 2000 is projected to exceed the methane resources available for its production.

To give some indication of the relative national significance of these energy intensive industries, the bar chart of Figure I shows the additional electrical capacity that will be required, using current technology to meet the additional demand in the post-1990 period when OTEC units for commercial operation can be readily available.

To be conservative, the additional capacity requirements for base load electricity were projected only for the Southeastern United States, where near-shore sea temperature and depth conditions are suitable.

The projections for the three product options were made based on national requirements because the at-sea production combined with existing national distribution systems indicated that the national market could be served.

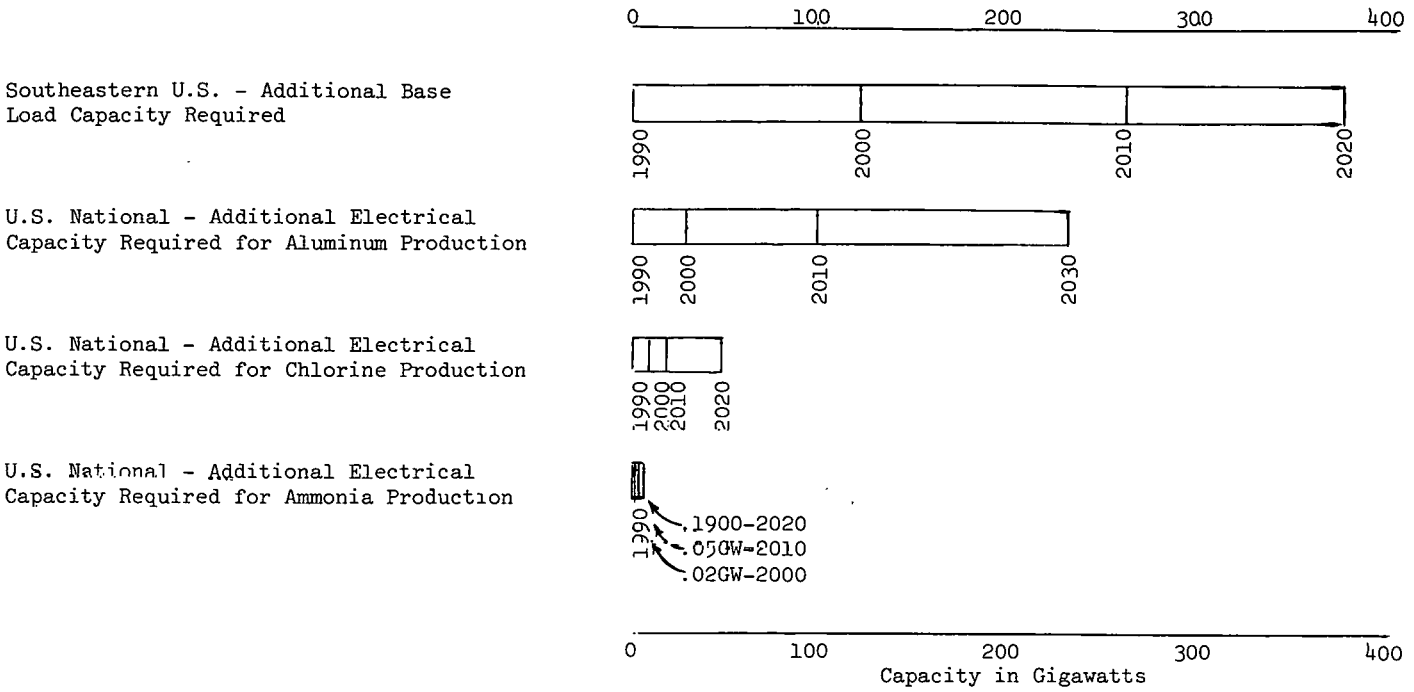



Fig. 1 Projected Additional Electrical Power Capacity Requirements (Post 1990)

The capacity requirements were based on estimates of the electrical energy content of the product and reasonable capacity factors for base load generating systems.

Because a number of configurations have been proposed and several options with respect to specific components have been discussed in the literature, the systems used were normalized as much as possible. However, there were some basic assumptions made.

- First, it was assumed that a generic OTEC power generation module would be used and that its design would be flexible enough so that the same evaluation could be used for moored or station-keeping units.
- Second, it was assumed that the product facility on the factory ship OTEC would be of the "package" type of unit currently under development in the chemical and minerals process industries.
- Third, the size was normalized presuming that the unit size would range between 100 MW and 500 MW.
- Fourth, defense and ancillary missions were examined for potential benefits that might supplement the basic benefits of providing high quality energy at negligible fossil fuel costs.
- Fifth, no ancillary cycles such as wind or wave power were assumed.

The basic missions examined were production of electricity for direct input to a shore-based grid, production of aluminum from alumina at sea, production of sea chemicals at sea and production of fertilizer at sea. Each of these were examined from the point of view of ease of implementation, competitiveness with shore-based alternatives and timing. The results of the examination are as follows.

Electrical power generation was considered as an alternative to base load coal fueled electricity. In this capacity, the Southeastern United States and some United States possessions were examined for maximum impact. It was found that, on a pure consumption basis, the greatest benefit would be in the United States. Examination of the utility industry structure indicates that OTEC will be most nearly competitive there. The major uncertainty with this mission is the flexible link which will connect the OTEC to the undersea transmission cable.

Aluminum smelting and production would appear to be feasible. Sea chemicals would not appear to be competitive at an early stage primarily because of the low cost of brines available on shore. Fertilizer production depends primarily on the cost of hydrogen. Onshore processes that do not use methane may or may not be competitive.

As the result of examining these missions, it appeared that the earliest competitive mission would be by direct generation of electricity followed by the at-sea deployment of aluminum, sea chemicals or fertilizer production.

Ends, goals, and schedules were examined for OTEC development and based primarily on ERDA 76-1, it was assumed that full-scale commercial deployment would begin in 1990,* three years after the full-scale prototype deployment. As a baseline, commercial uses would have approximately 12 gagawatts of OTEC capacity in place by the year 2000, and between 150 and 200 gigawatts in place by 2020.

Figure 2 indicates the projected penetration of OTEC into the base load power generation mission from the year 2020 for the Southeastern United States in the Southeastern Electric Reliability Council (SERC), South west Power Pool (SWPP), and the Electric Reliability Council of Texas (ERCOT) on the assumption that all OTEC power generated would be used within its reliability council and no export of power to other councils. A baseline estimate and reasonable high and low estimates are presented. The baseline OTEC penetration estimate was based on the penetration of nuclear power in the base load power generation market.

Figure 3 presents the impact of experience on technology improvement and cost reduction as well as the value of the OTEC power to the utilities in the reliability councils. It also shows the cumulative cost for the three penetration scenarios and the net investment or subsidy required to encourage the technological cost reduction needed to make OTEC competitive with projected coal generation costs. In the base line scenario, the break even point is achieved by the year 2000 at a total subsidy cost of four billion dollars incurred between the years 1990 and 2000. Following 2000, OTEC costs will be competitive with coal-fired base load plants in this region.

A similar analysis of the penetration of OTEC units into the three product missions was made. In this case, because the total factory unit was to be at sea, it was assumed that an additional ten years of OTEC operating experience and development of at-sea production plants would be required before the commercial operation of OTEC factory ships would be achieved. This analysis initiated commercial penetration into the aluminum, sea chemical, and ammonia fertilizer industry in the year 2000, and the projections through the year 2020 are shown in Table 1. These projections were based on the assumption that the at-sea aluminum production could service the Pacific, Atlantic, or Gulf Coast markets while the sea chemical and fertilizer production were assumed to be delivered to the Gulf Coast where the major concentration of these industries are currently centered.

*ERDA 76-1, A National Plan for Energy Research Development and Demonstration: Creating Energy Choices for the Future 1976, Volume 2, Program Implementation, pp 110, 111.

The analysis indicates that there are two major economic factors that will effect the commercial acceptability and viability. These factors are: the product unit cost and its competitiveness in the market, and the capital investment requirements of OTEC systems as compared to alternative approaches.

Comparison of OTEC costs for power delivered to shore indicates that it will be close to competitive with coal-fired base load systems in the Southeastern U.S., but that the power costs are high for the product industries examined primarily because manufacturers of areas where electric power is considerably cheaper than construction of OTEC-powered new plants will require both the increase in cost of alternative power sources and the reduction of cost of OTEC power to industrial levels.

The other factor, capital requirements, imposes another constraint. The utility and industrial willingness to incur capital debts are a function of the tradeoff between risk and capital requirements of alternative approaches and the return on investment. Thus, for a more capital intensive option to be selected over a less capital intensive option, it must offer a better return on investment and lower risk. As an example, utilities normally require a "fixed charge rate" (which is a measure of annual return on investment) of 15 to 18 percent of the capital cost. Utilities are a lower risk industry because they are regulated and amortize their installations over longer periods than other industries. Product manufacturing industries, because they have higher risk to contend with, normally require a much higher annual return on investment. The equivalent of "fixed charge rate" for manufacturing industries is normally 30 percent. As a result of the cost and capital factors, it appears that OTEC will be more acceptable for power delivery to shore earlier than for at-sea deployment in other industries. Then as learning curve cost reductions accrue as OTEC production and operation progresses, the OTEC costs will reduce to the point where the return on investment will become acceptable to higher risk industries.

Two areas required examination in the general area of political and institutional factors. They were the international area and the industrial area.

Because of the recent move to a 200-mile economic resource zone as a new institution and the changes in regulating the exploitation of the ocean's resources that will eventually occur (as indicated by the Law of the Sea Conference), it can be expected that OTEC operation will be regulated either by a national government or by an international agency. However, OTEC operation with proper pollution abatement safeguards for the purpose of harvesting a renewable resource will be much less controversial than deep-ocean mining or oil development. The major problem areas appear to be associated with possible conflicts with fishing industry interests and the need to reassure environmental concerns that the large volumes of cold and warm water modified and relocated to different depths in the ocean will not cause undesirable environmental modifications such as climatic effects or large plankton blooms. These concerns can only be allayed by performing environmental impact

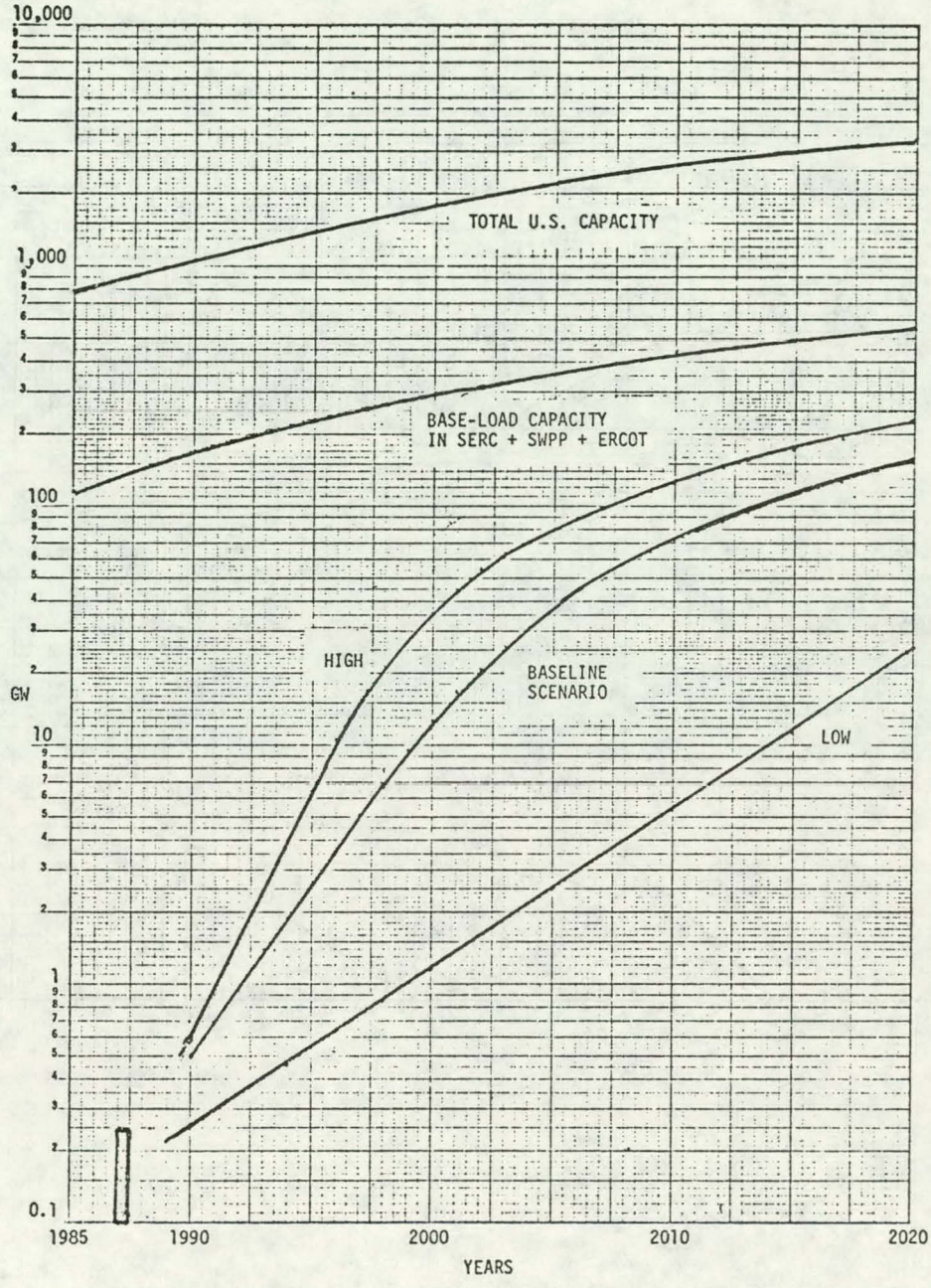



Fig. 2 OTEC Scenarios of Installed Capacity

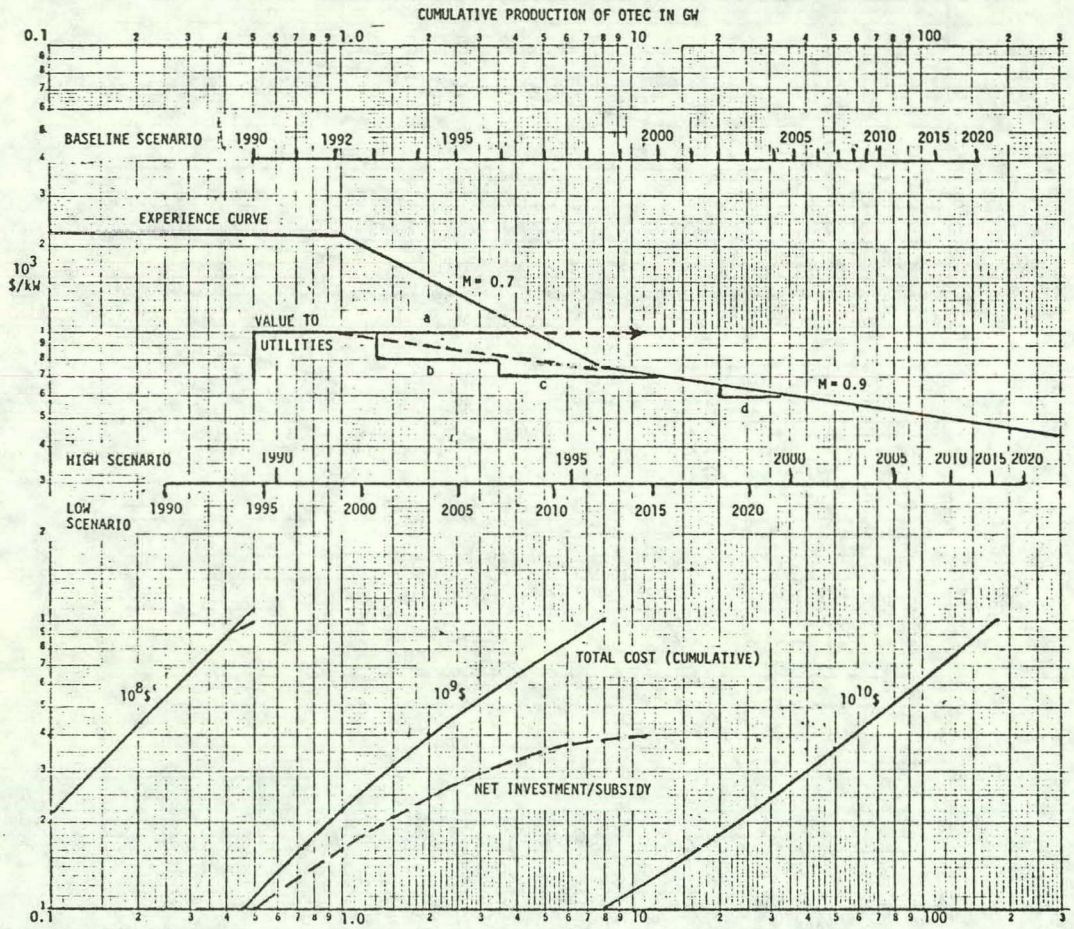



Fig. 3 Projection of OTEC Costs and Value

| | 2005 | 2010 | 2015 | 2020 |
|---|---|---|---|---|
| Aluminum | | | | |
| Baseline | | | | |
| Cumulative | .71 | 3.07 | 7.9 | 16.37 |
| Additions in Yr. | .25 | .64 | 1.22 | 2.05 |
| High | | | | |
| Cumulative | 1.00 | 4.29 | 11.06 | 22.92 |
| Additions in Yr. | .35 | .89 | 1.7 | 2.88 |
| Low | | | | |
| Cumulative | .43 | 1.84 | 4.74 | 9.82 |
| Additions in Yr. | .15 | .38 | .73 | 1.23 |
| Chlorine | | | | |
| Baseline | | | | |
| Cumulative | .11 | .46 | 1.19 | 2.49 |
| Additions in Yr. | .04 | .10 | .18 | .32 |
| High | | | | |
| Cumulative | .16 | .64 | 1.67 | 3.48 |
| Additions in Yr. | .05 | .13 | .26 | .44 |
| Low | | | | |
| Cumulative | .06 | .27 | .71 | 1.49 |
| Additions in Yr. | .02 | .06 | .11 | .19 |
| Ammonia | | | | |
| Baseline | | | | |
| Cumulative | .08 | .33 | .80 | 1.55 |
| Additions in Yr. | .03 | .07 | .11 | .18 |
| High | | | | |
| Cumulative | .16 | .66 | 1.6 | 3.1 |
| Additions in Yr. | .06 | .13 | .23 | .35 |
| Low | | | | |
| Cumulative | .03 | .13 | .32 | .62 |
| Additions in Yr. | .01 | .03 | .05 | .07 |

Table 1 OTEC Penetration Scenarios
(Gigawatts of Capacity)

assessments for specific installations. It is possible that some sites may have problems but initial indications are that most locations will have no serious problems.

## CONCLUSIONS

By a series of steps identifying missions and markets, projecting the market for capacity in these missions, estimating the performance characteristics of OTEC and the consequent cost per kilowatt and per kilowatt hour, estimating the penetration rate into the market and the consequent reduction in OTEC costs with the competing shore-based plants, it was concluded that:

- Initial OTEC plants would be non-competitive, but reaching break even costs or full economic competitiveness could be achieved by the year 2000.

- The shortfall, or difference between OTEC costs and the competitive value of units installed would total $4 billion. The maximum subsidy investment per year required is $400 million for four years. The total investment by industry in OTECs by 2020 will be of the order of $90 billion.

- The subsidization required to reach the break even point is very sensitive to the many parameters estimated. High and low values were considered that could greatly reduce, or increase, the amount needed. Strategies to reduce the shortfall were briefly considered.

The dollar values developed in this implementation scenario are large, but perspective may be gained by considering that $4 billion in 1976 dollars is far less than has been invested by the government in aiding the development of nuclear power to the same level of penetration, far less than the cost to put a man on the moon, and far less than the cost to develop any but the most trivial weapons systems: missiles, tanks, nuclear submarines, aircraft, and the Manhattan Project.

In estimating the OTEC capacity committed to these applications, care must be taken to avoid double counting, since the industries assumed to begin at-sea operation would do so at the expense of onshore expansion which the estimates of electrical power demand include. As a result, the projection for electrical power demand onshore should be reduced by the amount of onshore expansion replaced by at-sea expansion. To accomplish this would require a more detailed analysis of the markets than has been possible, so no attempt has been made to aggregate these quantities.

***Research supported by the Energy Research and Development Administration, Division of Solar Energy - Contract No. E949-18-2421, ERDA Program Manager - Dr. Robert Cohen.**

# IV. ENVIRONMENTAL & SITING CONSIDERATIONS

LLOYD LEWIS, CHAIRMAN
*Environment & Resource Assessments Branch*
*Division of Solar Energy, ERDA*

THIS PAGE

WAS INTENTIONALLY

LEFT BLANK

# AIR-SEA INTERACTION PERTURBATIONS BY PLANT OPERATIONS

S. A. PIACSEK AND A. C. WARN-VARNAS
*Naval Ocean Research and Development Activity*
*Department of the Navy*
*Bay St. Louis, Mississippi*

P. J. MARTIN
*Science Applications, Inc.*
*8400 Westpark Drive*
*McLean, Virginia*

## Abstract

The readjustment in the air-sea heat flow and the air-sea temperature contrast following a possible sea surface temperature lowering by OTEC operations has been calculated in the areas of Puerto Rico, Gulf of Mexico, and Hawaii. The net heat flow in these areas has been found to be +76, -27 and +50 cal/cm$^2$-day, respectively, and the perturbations due to OTPP operations are found to be 96, 81 and 67 cal/cm$^2$-day-°C.

## Introduction

This paper is concerned with a computation of the seasonal variation and annual average of the net heat flow crossing the ocean's surface in the vicinities of Puerto Rico, Gulf of Mexico and Hawaii, as well as their perturbation by OTPP operations. The formulas used for the calculations were assembled by Laevastu (1) and Wyrtki (2), and are a combination of empirical data fitting and physical laws. A preliminary study for the Puerto Rico area has been performed by Piacsek, et al. (3); a similar work for Hawaii has been carried out by Bathen, et al. (4).

## Heat Flux Calculations

The meteorological data for Puerto Rico has been abstracted from Atwood (5) and for the Gulf of Mexico from Reference 6. Heat fluxes were estimated using the bulk formulas detailed in Appendix I. The heat budgets, calculated for each month and averaged to obtain a yearly mean, are listed in Table I.

The uncertainty of the value for the net solar radiation is not known. Bathen, et al. (4) have reported that a solar radiation formula obtained from Wyrtki (2) allowed for a much greater correction for cloud cover than Laevastu's formula used here and predicted solar radiation levels about 20% lower. Bathen notes that the type of cloud cover, as well as the extent of the cover may govern the intensity of solar radiation of the sea surface.

Recently published estimates of the drag coefficient for latent heat loss vary within a range of $\pm$ 20%. Thus, allowing for an uncertainty of 15% in wind speed and humidity values, the uncertainty of the latent heat loss is about 30%.

A Bowen ratio of .1 was used to estimate the sensible heat flux. Based on the uncertainty regarding the latent heat flux and the Bowen ratio, the uncertainty of the sensible heat loss may be 40% or more.

Due to the fairly large uncertainties regarding the components of the net heat flux, not much can be said about the accuracy of the net heat flux itself. However, we are more interested in the components of the net heat flux that are strongly affected by changes in the sea surface temperature. Table II shows the heat budget estimations repeated with the sea surface temperature lowered in increments of .5°C from 0 to 1 from its observed value. It was assumed that the air temperature well above the sea surface was not affected by the local change in the sea surface temperature.

Table II shows a fairly linear change of sea surface heat flux with sea surface temperature of 96 cal/cm$^2$-day-°C for Puerto Rico, and 81 cal/cm$^2$-day-°C for the Gulf of Mexico. For small temperature changes of less than a few degrees centigrade, the back radiation and latent and sensible heat flux vary almost linearly with sea surface temperature.

TABLE I

ANNUAL MEAN SEA SURFACE HEAT FLUX

| Decrease of $T_S$ from ambient value | Puerto Rico | Gulf of Mexico |
|---|---|---|
| Net solar radiation ($cal/cm^2$-day) | 558* | 427 |
| Back radiation ($cal/cm^2$-day) | -119 | -137 |
| Latent heat loss ($cal/cm^2$-day) | -330 | -289 |
| Sensible heat loss ($cal/cm^2$-day) | - 33 | - 29 |
| Net surface heat flux ($cal/cm^2$-day) | 76 | - 27 |

* NOTE: Positive heat flux means flow from air into water

TABLE II

SEA SURFACE HEAT FLUX CHANGE WITH SURFACE TEMPERATURE DECREASE

($cal/cm^2$-day)

Decrease from ambient value

| | o°C | .50°C | 1.0°C |
|---|---|---|---|
| Puerto Rico | 76 | 125 | 172 |
| Gulf of Mexico | -27 | 13 | 54 |
| Hawaii | 55 | 88 | 122 |

Most of the change in the surface heat flux, almost 80%, is due to a decrease in the evaporative heat loss. And if the Bowen ratio R is used to estimate the sensible heat loss, the bulk formula for latent heat loss effectively models about 85% of the change in surface heat flux with sea surface temperature.

Differentiating the bulk formula for latent and sensible heat loss (Appendix A) with respect to sea surface temperature $T_S$, we obtain

$$\frac{d}{dT_s}(Q_E + Q_S) = -(1+R).\rho_a C_E . L . U_a . \frac{dq_s}{dT_s} \qquad (1)$$

The variables in equation (1) are defined in Appendix A. The mean wind speed $U_a$ is the only variable in (1) that might be expected to vary significantly from one region to another. Hence, regions with high wind speeds should show correspondibgly high changes of sea surface heat flux with sea surface temperature.

APPENDIX A

FORMULAE USED TO CALCULATE SURFACE HEAT FLUXES

The formulae used to calculate incident and reflected solar radiation, $Q_i$ and $Q_r$, respectively, are from Laevastu (1960).

$A_n \leq 75°$ $\quad Q_i = .014 \times A_n \; t_d \times (1 - .6C^3)$ $\quad cal/cm^2$-day

$A_n > 75°$ $\quad Q_i = 1.06 \times t_d \times (1 - .6C)$ $\quad cal/cm^2$-day

$\quad Q_r = .15 \times Q_i - (.01 \; Q_i)^2$ $\quad cal/cm^2$-day

FORMULAE USED TO CALCULATE SURFACE HEAT FLUXES - CONTINUED

ere

$A_n$ = altitude of sun at noon (day)

$t_d$ = length of the day (min)

C = cloud cover in tenths

FORMULAE USED TO CALCULATE BACK RADIATION (WYRTKI 1966)

$$Q_b = R.S.T_s^4 \times (.39 - .05e_a) \cdot (1 - .38\ C^2) \times 86400 +$$
$$+ 4\ R.S.T_s^3 \times (T_W - T_a) \times 86400 \qquad \text{cal/cm}^2\text{-day}$$

where

R = ratio of sea surface to black body radiation, ~.97

S = Stefan - Boltzmann constant, $(1.3553 \pm .001) \times 10^{-12}$ cal/cm$^2$-sec

$T_s$ = sea surface temperature in °K

$e_a$ = vapor pressure of the air well above the surface, in mb

C = cloud cover in tenths, ( 0 - 1.0)

$T_W$ = sea surface temperature in °C

$T_a$ = air temperature well above the surface

Another formula for $Q_b$ used by Laevastu was found to give values in close agreement with those given above.

FORMULAE USED TO CALCULATE LATENT HEAT

$$Q_E = \rho_a \cdot C_E \cdot L \cdot (q_w - q_a) \cdot U_a \times 86400 \qquad \text{cal/cm}^2\text{-day}$$

where

$\rho_a$ = air density (g/cm$^3$)

$C_E$ = drag coefficient for latent heat exchange

L = latent heat of evaporation for sea water, $597.8 - .573\ T_s$ (cal/g)

$q_a$ = specific humidity of the air well above the surface

$q_w$ = specific humidity at the sea surface

$U_a$ = wind speed (cm/sec)

A number of values of the drag coefficient $C_E$ have been obtained by various authors by fitting ($Q_E$) to experimental data. Table II provides a listing of some of these values from Pond et al. (1971). On the basis of their own work with data from the BOMEX experiments, Pond, et al. suggest that the best value for $C_E$ is $1.2 \times 10^{-3}$, with an experimental uncertainty of about 20%. Considering the range of values of $C_E$ listed in Table II a value of $1.25 \times 10^{-3}$ was chosen for working up the Puerto Rico heat budget with an uncertainty of about 20%.

FORMULAE FOR SENSIBLE HEAT LOSS FROM THE OCEAN'S SURFACE

$$Q_S = \rho_a \cdot C_S \cdot c_p \cdot (T_W - T_a) \cdot U_a \times 86400 \qquad \text{cal/cm}^2\text{-day} \qquad (2)$$

where

$\rho_a$ = air density

$C_S$ = drag coefficient for sensible heat exchange

$c_p$ = specific heat of air, .24 cal/g-°C

$T_W$ = temperature of water at surface in °C

$T_a$ = air temperature well above the sea surface

Hasse (1970) and Pond (1971) in working up data taken off San Diego obtained good correlation between the measured sensible heat flux $\overline{w'T'}$ and the quantity $(T_W - T_a).U_a$ using a value of $C_S = 1 \times 10^{-3}$. In evaluating the BOMEX data, however, Pond found very little correlation between $\overline{w'T'}$ and $\Delta T.U_a$ and concluded that the aerodynamic approach for calculating $Q_S$ was not very helpful. A more accurate estimate of $Q_S$ from the BOMEX data could be obtained using the Bowen ratio $R + Q_S/Q_E$, which varied between .08 and .14, with an average value of ~.10. Holland (1972), in reviewing the BOMEX data noted that $\overline{w'T'}$ correlated much better with $\Delta q.U_a$, which is another way of saying that the Bowen ratio should be used to calculate $Q_S$. Since Pond suggested that (2) may be unsuitable for calculating sensible heat fluxes in tropical regions, a Bowen ratio of .10 was used to calculate $Q_S$ for the Puerto Rico site.

REFERENCES


1. Laevastu, T., "Factors Affecting the Temperature of the Surface Layers of the Sea," Soc. Sci. Fennica, Commentationes Phys. - Math., 25, p. 1-136, 1960.

2. Wyrtki, K., "The Average Annual Heat Balance of the North Pacific Ocean and its Relation to Ocean Currents," J. Geophys. Res. 70, p. 4567, 1965.

3. Piacsek, S. A., Martin, P. J., and Roberts, G. O., "Recirculation and Thermocline Perturbations from Ocean Thermal Power Plants, " Proc. of Conference on "Energy From the Oceans: Fact or Fantasy," North Carolina State University, January 1976, p. 74; also NRL Technical Report NRL-GFD/OTEC 2-76.

4. Bathen, K. H., Kamins, R., Kornreich, D. and Moncur, J. E. T.," An Evaluation of Oceanographic and Socio-Economic Aspects of a Nearshore Ocean Thermal Energy Conversion Pilot Plant in Subtropical Hawaiian Waters," University of Hawaii Technical Report, April 1975.

5. Atwood, K. ," Ocean Thermal Energy Conversion: Resource Assessment and Environmental Impact for Proposed Puerto Rico Site," University of Puerto Rico, Report of Marine Sciences Report, 1976.

6. "Summary of Synoptic Meteorological Observations for North American Coastal Marine Areas," Volume 4, 1975; NTIS, Springfield, VA 22150.

# STRATIFIED TURBULENCE MODELING FOR THE NEAR FIELD EXTERNAL FLOW

GLYN O. ROBERTS
*Science Applications, Incorporated*
*8400 Westpark Drive*
*McLean, Virginia*

ABSTRACT

A simplified two-dimensional model is used to calculate the turbulent flow near the two outflows and the warm inflow associated with one power module of the Lockheed baseline OTPP design. A rectangular domain of depth 500 ft has three horizontal slots of height 72 ft on its left boundary, centered respectively at depths of 75, 150 and 315 ft, to represent the inflow and outflows. Four separate computations assume statistical uniformity across widths of 50 ft, 100 ft, 200 ft and 400 ft; we believe that the results for widths of 100 ft and 200 ft essentially bracket the results for the three-dimensional prototype flow. The assumed ambient temperature profile has a surface temperature of 80°F, and a thermocline at depth 300 ft where the temperature is 61.5°F. The temperature at 500 ft is 44.5°F. The assumed temperature at the cold inflow, at depth 1550 ft, is 42.6°F, this water is warmed by 2.4°F in the condenser and leaves the cold outflow at 45°F.

The numerical results for the average warm inflow temperature are 75.7°F, 77.2°F, 77.9°F and 78.6°F in the four cases. This inflow water is cooled by 3°F in the condenser before leaving the warm outflow. In all four cases, the far-field flow leaves or enters the computational domain horizontally, with temperature equal to the ambient profile. In the 50 ft and 100 ft computations, there is significant recirculation (4000 cu ft/sec and 1300 cu ft/sec, respectively) from the warm outflow back into the warm inflow, contributing to the reduced inflow temperatures. In all cases, the OTPP-generated turbulence is negligible at distances greater than 350 ft from the inflow and outflows.

## 1. INTRODUCTION

Near-field flow computations are of fundamental importance to the OTEC program, for three reasons. First, they determine the inflow temperatures, as a function of design and operation parameters and of the ambient conditions. Secondly, they determine the hydrodynamic forces on the plant, due to ambient currents and waves and to the current system driven by the inflows and outflows. And thirdly, they are a basic input to far-field environmental impact computations, since they determine the redistribution of heat, salt, horizontal momentum, biological species, and nutrient between different ocean layers and the possible addition of biocides and pollutants to certain layers. Thus, these computations provide the capability of optimizing design and operation parameters for a given environment, and avoiding huge wastage in construction costs.

There are no off-the-shelf engineering formulae capable of giving even approximations to these complicated stratified turbulent flows. Some previous related efforts have been made in the laboratory and numerical simulation of the intakes and outfalls associated with conventional ocean-cooled power plants, as discussed, for example, in Roberts (1). These are essential tools for the simulation of OTEC flows as well.

Laboratory simulations depend on the principle of dynamic similarity. The experiment should have the same geometry as the prototype flow, and the same Froude number,

$$F = U/LN \quad .$$

Here U and L are the velocity and length scales, and N is the scale of the Vaisala frequency,

$$N^2 = (g/\rho)\, d\rho/dz \quad ,$$

where $\rho(z)$ is the density profile. It is impossible to scale the experiment so that the Reynolds number

$$R = UL/\nu$$

is the same as in the prototype flow (here $\nu$ is the kinetic viscosity). Thus, molecular diffusion of momentum and heat are more important in the experiment than in the prototype flow. It is believed that if the experimental Reynolds number is greater than about $10^3$ throughout the experimental flow, then molecular diffusion is negligible and the macroscopic properties of the turbulence are the same as for the prototype. However, even this criterion is hard to achieve in the

laboratory. Laboratory simulations for OTEC are described in the papers by Jirka (2) and Sundaram (3) in this session of this volume.

Numerical simulations of these stratified turbulent flows may be classified according to the turbulence closure model adopted. Sub-grid closure, in which the large-scale fluctuations are computed explicitly while the large-scale effects of the small-scale fluctuations are modeled, is impracticable for these complicated flows because of cost. It is essential to use statistical closure, in which the mean flow $\bar{u}_i$ is computed using a model for the mean flow effects of the turbulent fluctuations $u_i'$. The mean flow variables are affected by the Reynolds stress

$$\tau_{ij} = - \overline{u_i' u_j'} \quad , \tag{1}$$

the turbulent heat flux

$$H_i = - \overline{u_i' T'} \quad , \tag{2}$$

and the corresponding fluxes of salt and of any passive scalars. Here $T$ is the temperature, and the horizontal bar denotes an average over the turbulent fluctuations.

In zero-order statistical closure models, the Reynolds stress is modeled as

$$\tau_{ij} = K \, (\bar{u}_{i,j} + \bar{u}_{j,i}) \quad , \tag{3}$$

where the turbulent diffusivity K is an imposed constant or function of position, and may be a tensor. The turbulent heat flux is

$$H_i = K \, \bar{T}_{,i} \quad . \tag{4}$$

Here $\bar{u}_{i,j}$ denotes $\partial \bar{u}_i / \partial x_j$ , with the usual suffix notation. In first-order closure, K is determined from an equation of the form.

$$K = L \, \bar{E}^{\frac{1}{2}} \quad , \tag{5}$$

where L is a length scale and $\bar{E}$ is the mean turbulent kinetic energy,

$$\bar{E} = \tfrac{1}{2} \, \overline{u_i}^2 \quad . \tag{6}$$

$\bar{E}$ is determined from a separate equation, with empirical diffusion and decay terms added to certain physical generation and loss terms. In one-equation first-order models, L is an imposed constant or function of position, while in two-equation models, L (or some equivalent variable) is computed from a second empirical equation. Finally, in second-order closure models, all the components of $\tau_{ij}$ and $H_i$ are computer from empirical equations, with operation and decay terms analogous to those in the $\bar{E}$ equation. The nomenclature for the different closure models is not yet standardized. Discussions of closure models and descriptions of particular models have been given by Mellor and Yam (4), Munk and Anderson (5), Vager and Zilitinkevich (6), Stuhmiller (7), Lewellen et al. (8), Launder (9), Piacsek et al. (10), and Yamada (11), among others.

As the above discussion shows, turbulence models are empirical and approximate, and are still in a development stage. The models have varying numbers of parameters, to which numerical values must be assigned on the basis of experiments. Clearly, we would like to have a model and a set of parameter values which yield numerical results in reasonable agreement with a wide range of experimental measurements. For OTEC purposes, this range should include experiments with inflows and outflows, as described in references (2) and (3). Progress is being made towards this goal, but no such model currently exists.

## 2. THE CODE NRFLO2

In this report we describe results obtained with our computer code NRFLO2. Details of this code have been presented in previous reports, in references (12), (13) and (14). The geometry, OTPP model, turbulence model, boundary conditions, and numerical methods used by the code are summarized in the following paragraphs.

The code is two-dimensional. A rectangular domain is assumed, with the flow variables independent of the third coordinate. Thus, the flow variables can be regarded as averages with respect to this third coordinate, in a three-dimensional rectangular domain with some constant assumed width.

The OTPP is modeled by boundary conditions at the left boundary. The horizontal velocity component $\bar{u}$ is imposed, and is into the domain for OTPP outflows and out of the domain for inflows; up to two of each are allowed. The k-th inflow or outflow is

$$\bar{u} = \frac{a_k}{r_k} \, f\left( \frac{z - z_k}{r_k} \right) , \tag{7}$$

where $z_k$ is the depth of the center of the inflow or outflow region, $r_k$ is a radius, and $a_k$ is proportional to the vertically integrated flux. The function $f(x)$ is $(1-x^2)^2$ for $|x| < 1$. The temperature $\bar{T}$, the vertical velocity $\bar{w}$, and the turbulent kinetic energy density $\bar{E}$ are also imposed for OTPP outflows ($a_k$ positive), with the formulae

$$\begin{aligned} \bar{T} &= T_k \quad , \\ \bar{w} &= \bar{u} \tan \alpha_k \quad , \\ \bar{E} &= E_k \, a_k^2 \, r_k^{-2} \quad . \end{aligned} \tag{8}$$

Here $\alpha_k$ is the angle of the outflow jet from the vertical, and $E_k$ is a dimensionless constant. The temperature is either an imposed constant or is determined by ing an imposed increment to a corresponding average OTPP inflow temperature $\overline{T}_{in}$ determined from the equation

$$\overline{T}_{in} = \int \overline{Tu}\, dz \Big/ \int \overline{u}\, dz. \qquad (9)$$

The code NRFLO2 uses a first-order one-equation statistical-closure turbulence model, with an imposed constant turbulence length scale L. The formula above is replaced by the turbulent diffusivity (15) to represent the suppression of vertical turbulent mixing by strong stratification, cf. references (9) and (11). The full set of equations is thus

$$\partial_t \overline{T} = \left\{ K\overline{T}_{,j} - \overline{u}_j \overline{T} \right\}_{,j} , \qquad (10)$$

$$\partial_t \overline{u}_i = (g\alpha\overline{T} - c_w K N^2 \overline{u}_3/\overline{E})\delta_{i3} + \left\{ -\overline{P}_E \delta_{ij} + K(\overline{u}_{i,j} + \overline{u}_{j,i}) - \overline{u}_j \overline{u}_i \right\}_{,j} , \qquad (11)$$

$$\overline{u}_{i,i} = 0 , \qquad (12)$$

$$\partial_t \overline{E} = K\left\{ -N^2 + \tfrac{1}{2}(\overline{u}_{i,j} + \overline{u}_{j,i})^2 - c_f \overline{E}/L^2 + c_w N^2 \overline{u}_3{}^2/\overline{E} \right\} + \left\{ K\overline{E}_{,j} - \overline{u}_j \overline{E} \right\}_{,j} , \qquad (13)$$

$$N^2 = g\alpha\overline{T}_{,3} , \qquad (14)$$

$$K = L\overline{E}^{1/2}/(1 + c_s N^2 L^2/\overline{E}) , \qquad (15)$$

where $\overline{P}_E$ is a total pressure, and $\alpha$ is the coefficient of thermal expansion, taken as the constant $1.3 \times 10^{-4}/^{\circ}F$. The turbulence model involves four parameters, the length scale L and the three dimensionless parameters $c_f$, $c_s$ and $c_w$. The $c_w$ term in equation (11) has the effect of suppressing mean vertical motions, and generates turbulent kinetic energy in equation (13) instead.

The code NRFLO2 assumes the ambient conditions

$$\overline{T} = T_t + T_r \tan^{-1}\left\{ (z + d_t) \Big/ z_t \right\} \qquad (16)$$

$$\overline{E} = E_o \exp\,(z/z_E) , \qquad (17)$$

$$\overline{w} = 0 . \qquad (18)$$

These are used as the initial conditions for the computation, and as the boundary conditions on the right whenever the flow is into the domain. In equation (16), $T_t$ is the thermocline temperature, $d_t$ is the thermocline depth, $z_t$ is the thermocline thickness, $T_r$ is the temperature range, and z is measured upward. In equation (17), $E_o$ is the amplitude, and $z_E$ is the depth scale. At the top and bottom of the domain, $\overline{w}$ and the z-derivatives of $\overline{u}$, $\overline{T}$ and $\overline{E}$ are zero. At the top and the sides, the x-derivatives of $\overline{T}$, $\overline{E}$ and $\overline{w}$ are set to zero when $\overline{u}$ is not into the domain, $\overline{u}$ is imposed on the left, and a hydromatic pressure balance with the ambient temperature distribution is imposed on the right so that the outflow fluid finds its own temperature level.

Efficient numerical methods are used by the code NRFLO2, in order to obtain convergence of the equations (10) through (15) in the smallest possible number of time-steps. The time-dependence in these equations is used merely as a device to obtain the steady mean-flow solutions. Second-order accurate representations are used for the spatial derivatives, except that upwind differencing is used for the advective terms in the $\overline{E}_e$ quation. Full details of the numerical methods are given in reference (12).

## 3. NRFLO2 MODEL OF THE LOCKHEED BASELINE OTPP DESIGN

Lockheed Missile and Space Company, and TRW, Inc., have suggested baseline OTPP designs, in references (15) and (16). We have selected the Lockheed design for our initial study because it is more suited to a two-dimensional approximation. The Lockheed spar design is illustrated in Figures 1 and 3, in which all dimensions are in feet. Four power modules are symmetrically placed around the plant body, which is a vertical cylinder of diameter 200 ft and height 445 ft. The warm inflow of 48000 cu ft/sec (or 12000 cu ft/sec per module) enters through the 45° conical filter attached to the superstructure, is cooled (by $2.4^{\circ}F$ in the four evaporators, and exits horizontally at depth 150 ft. The cold inflow of 60000 cu ft/sec enters the cold water pipe at depth 1545 ft, is warmed by $2.4^{\circ}F$ in the four evaporators, and exits at a depth of 315 ft, directed 10° below the vertical. The evaporators and condensers and their out low ports all have diameter 72 ft. The cold water pipe is 1000 ft long, and tapers to a diameter of 100 ft.

In modeling the external flow associated with the Lockheed design, we have chosen to confine our attention to the upper 500 ft, and to the flow associated with a single power module. We thus assume warm and cold outflow slots centered at depths of 150 ft and 315 ft. Each slot has a total height of 72 ft. For our two-dimensional computations, we have taken four different widths of the slots and of the flow region, respectively 50 ft, 100 ft, 200 ft and 400 ft as illustrated in Figures 2 and 4 (which show the

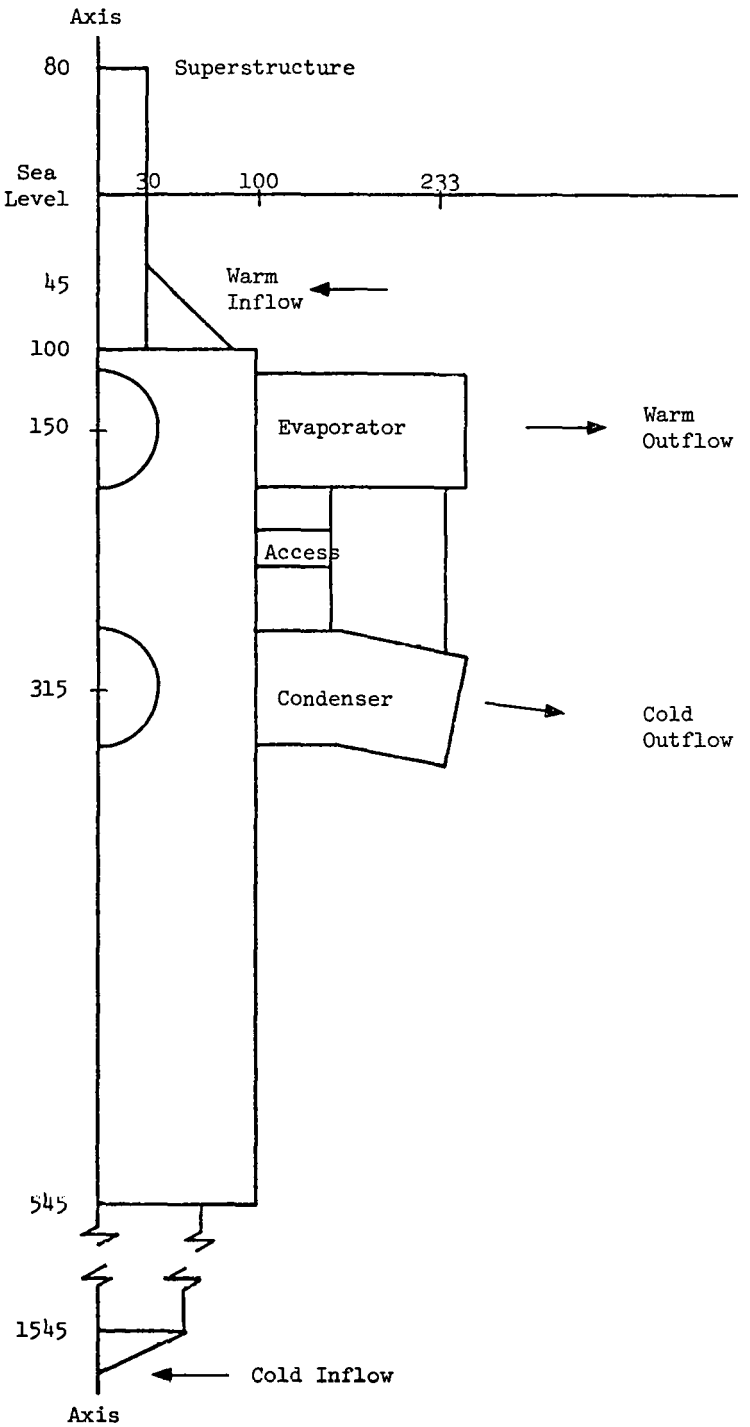



Fig. 1. Side View of the Lockheed Baseline OTPP Design.

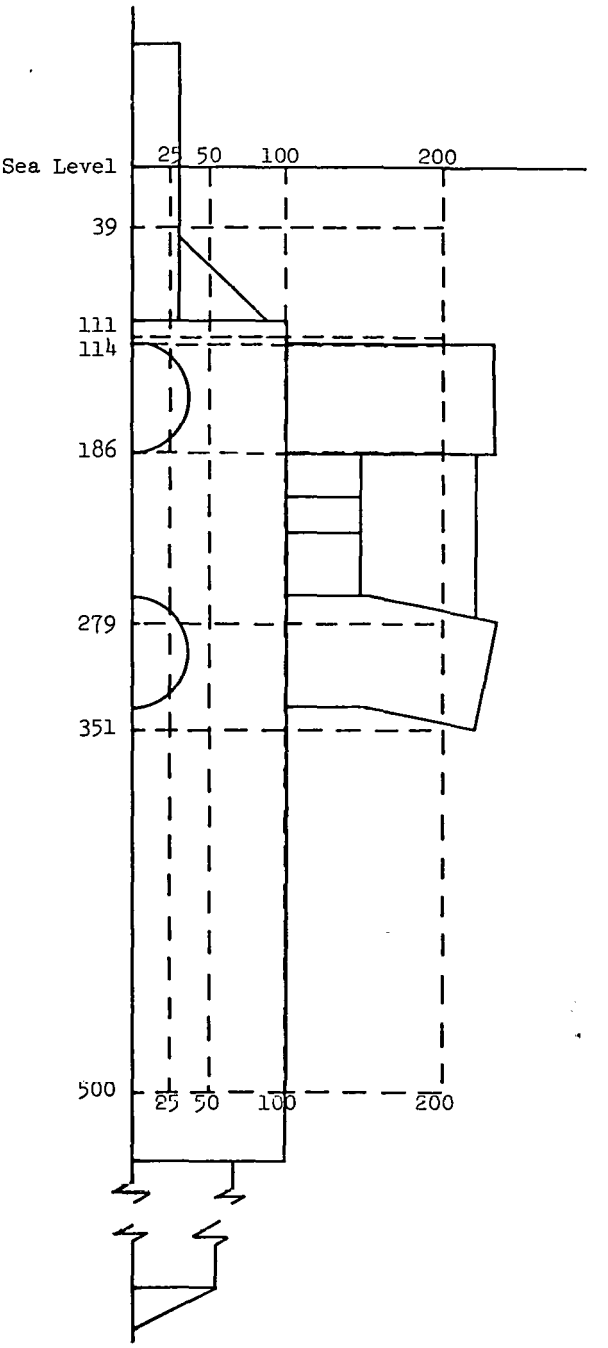



Fig. 2. Four Alternative Domain Widths and Three Horizontal Slot Locations for the NRFL02 Model of the External Flow associated with One Power Module.

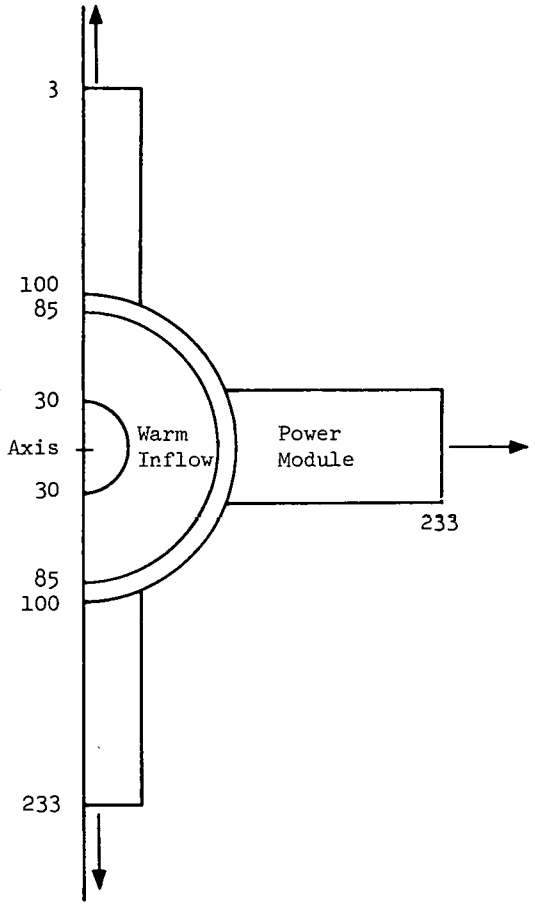



Fig. 3. Top View of the Lockheed Baseline OTPP Design

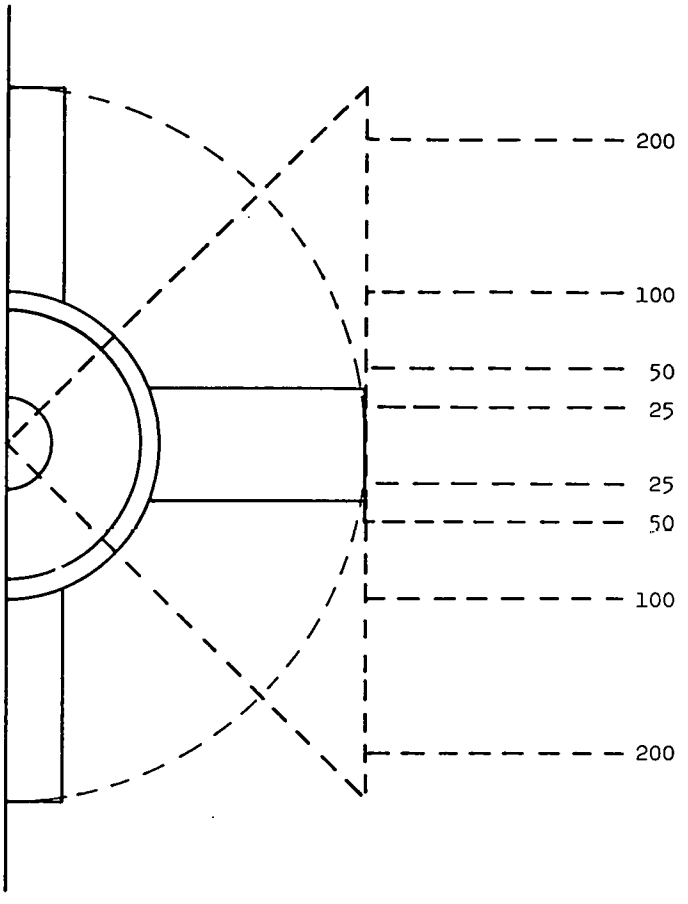



Fig. 4. The Four Alternative Widths for the NRFL02 Model of the Outflows and Warm Inflow for One Module.

half-widths). These widths should be contrasted with the outflow diameters of 72 ft, with the radius (85 ft) of the inflow cone, and with the distance of the outflows from the axis (233 ft).

The assumption of a two-dimensional flow is clearly a poor one. Physically, the warm inflow is roughly axisymmetric except to the extent that it is modified by the outflows. The turbulent outflow jets entrain the ambient fluid from the sides and from above and below. In a stratified environment, the turbulence decays rapidly with distance from the plant. Combining these factors, we feel that the two dimensional flow results for the width assumptions of 100 ft and 200 ft probably bracket the prototype flow. The 50 ft width assumption gives a rectangular outflow area of 3600 sq. ft, as compared with 4071.5 sq ft for the prototype circle. Similarly, the 400 ft width is extremely high, since the quarter-circumference of a circle of radius 233 ft is only 366 ft. Thus, if the four warm outflows were combined into a circular slot of height 72 ft, the flow would still be stronger than in the 400 ft model.

The three radii $r_k$ in equation (7) are set to 36 ft, to give a height of 72 ft. The depths $d_k$ are 75 ft, 150 ft, and 315 ft, respectively. The quantities $a_k$ are chosen to give warm fluxes of 12000 cu ft/sec and a cold flux of 15000 cu ft/sec. In equations (8), the warm outflow temperature is $3^{\circ}F$ cooler than the warm inflow temperature determined according to equation (9), and the cold outflow temperature is $45^{\circ}F$, or $2.4^{\circ}F$ warmer than an assumed inflow temperature of $42.6^{\circ}F$ at depth 1545 ft. For the cold outflow, $\alpha_k$ is $-10^{\circ}$, as designed by Lockheed. The quantities $E_k$ are set to 0.3, so that the turbulent kinetic energy flux is somewhat smaller than the kinetic energy of the mean flow.

For our turbulence model, we chose the four parameters on the basis of values used by previous workers and in our studies of turbulent wakes. These values have not yet been tuned to experiments on flows driven by inflows and outflow jets in a stratified environment. The adopted values were

$$L = 20 \text{ ft} \quad ,$$

$$c_f = 0.5 \quad ,$$

$$c_s = 0.1 \quad ,$$

$$c_w = 1.0 \quad .$$

The results are remarkably insensitive to these values.

For the ambient temperature profile (16), we adopted the values

$$T_t = 61.5^{\circ}F \quad ,$$

$$T_r = 14.0^{\circ}F \quad ,$$

$$d_t = 300 \text{ ft} \quad ,$$

$$z_t = 75 \text{ ft} \quad .$$

These values give a surface temperature of $80^{\circ}F$. The temperature at 500 ft is $44.5^{\circ}F$, while the temperature at very great depths is $39.5^{\circ}F$. The ambient turbulent kinetic energy density profile is given by equation (18), with

$$z_E = 125 \text{ ft} \quad ,$$

$$E_o = 7.4 \times 10^{-8} \text{ ft}^2/\text{sec}^2$$

The results are essentially independent of the ambient turbulence, provided it is not unreasonably large.

Efficient numerical methods are required so that the solution to equations (10) through (15) converges from the initial conditions to a steady-state in a reasonable number of time-steps. A non-uniform computational mesh is used, to give sufficient resolution where it is needed, without wasting mesh points in regions where small scales are not present. The spatial derivatives in the equations are represented with second-order accurate central differences throughout, except that upwind differencing is used for the advection terms in the $\overline{E}$ equation. (This exception avoids negative $\overline{E}$ values at locations where very sudden $\overline{E}$ gradients develop.) The scheme is basically leap-frog, with an alternating-direction implicit representation for the diffusion terms and with an implicit representation for certain terms in the $\overline{E}$ equation. In addition, there is an added term in the $\overline{w}$ equation, to damp vertical motion near the right-hand boundary and speed up the convergence. Details are given in reference (12).

For these Lockheed simulations, we chose a horizontal dimension of 750 ft and a vertical dimension of 500 ft. The cold outflow is warmed by turbulent mixing with the ambient fluid, and flows out horizontally at its own temperature level somewhat above 500 ft, as the results indicate. Similarly, the turbulence decays to negligible levels and the flow is practically horizontal at distances of only 500 ft, so we feel that our 750 ft domain is sufficient. Tests with larger domains have confirmed this.

## 4. NUMERICAL RESULTS FOR THE LOCKHEED NEAR-FIELD FLOW

Our numerical results for the four different width assumptions are summarized in Table 1 and displayed in the figures on the following pages, with their accompanying captions. In Table 1 the inflow and outflow speeds are determined by dividing the warm flux of 12000 cu ft/sec and the cold flux of 15000 cu ft/sec by the slot area, with allowance made for the assumed flow profile (7). The cold outflow temperature of $45^{\circ}F$ is imposed, as described above. The warm inflow temperature is calculated from equation (9). The warm outflow from the plant has been cooled by $3^{\circ}F$.

It may be seen from the table that for each case, the warm inflow flux of 12000 cu ft/sec comes partly from recirculated warm outflow. For the 50 ft width assumption, the recirculation flux is 4000 cu ft/sec. As a result of the recirculation and of the large values of the turbulent diffusivity K, the mean temperature of the warm inflow is lowered to $75.7^{\circ}F$. With a surface temperature of $80^{\circ}F$, this figure is unacceptably low. It is important to design an OTPP and its inflow and outflow speeds so that the inflow temperature is only a degree or so smaller than the surface temperature. Table 1 indicates that this is a practicable objective.

The warm inflow is cooled by two processes. The first is the recirculation of part of the warm outflow, after it has been cooled in the OTPP. The second is the turbulent mixing in the region near the plant. Turbulence is generated by the jet outflows and by the shear in the velocity field. The turbulent heat flux results in the cooling of the warm inflow and the warming of the cold outflow; the warm outflow is cooled by the cold outflow and warmed by the warm surface inflow. The table indicates that the maximum turbulent diffusivity is proportional to the imposed flow speeds. This maximum is achieved at the cold outflow. A more significant measure of the turbulent diffusivity magnitude is the minimum value on the left boundary between the outflows. If this is very small, as in the 400 ft width calculation shown in the table, there is effectively no cooling of the waters nearer the surface by the cold outflow.

The detailed numerical results are displayed in Figures 5 through 14, which are reductions of computer graphics. Figures 5 through 8 show the stream lines for the mean flow in the left half of the computational domain, for the four different assumed widths. The contour increments in cu ft/sec are 2000 for Figures 5 through 7 and 3000 for Figure 8. In each figure, the dimensionless data used for the computation, and the inflow temperature result, are also shown.

Table 1. Summary of Numerical Results

| QUANTITY | UNIT | VALUES | | | |
|---|---|---|---|---|---|
| Assumed Width | Ft. | 50 | 100 | 200 | 400 |
| Warm Inflow Speed | ft/sec | 6.38 | 3.19 | 1.60 | 0.80 |
| Warm Outflow Speed | ft/sec | 6.38 | 3.19 | 1.60 | 0.80 |
| Cold Outflow Speed | ft/sec | 8.50 | 4.25 | 2.12 | 1.06 |
| Warm Inflow Temperature | $^{o}F$ | 75.7 | 77.2 | 77.9 | 78.6 |
| Warm Outflow Temperature | $^{o}F$ | 72.7 | 74.2 | 74.9 | 75.6 |
| Cold Outflow Temperature | $^{o}F$ | 45.0 | 45.0 | 45.0 | 45.0 |
| Recirculation Flux | cu ft/sec | 4000 | 1300 | 300 | 100 |
| Warm Surface Flux | cu ft/sec | 8000 | 10700 | 11700 | 11900 |
| Maximum Turbulent Diffusivity | $ft^2/sec$ | 85.5 | 42.9 | 21.7 | 13.5 |
| Minimum Turbulent Diffusivity Between Outflows | $ft^2/sec$ | 40.1 | 18.7 | 7.1 | 0.4 |

In Figure 5 the cold inflow flux of 15000 cu ft/sec (lines 1 through 7) falls till it finds its own level, and entrains 8000 cu ft/sec from the warm outflow (lines 8 through 1). The remaining 400 cu ft/sec of warm outflow recirculates into the warm inflow (lines 2 and 3), and combines with 8000 cu ft/sec from the warm ocean surface (lines 8, 9, 0 and 1).

In Figure 6 the cold outflow flux of 15000 cu ft/sec and 10700 cu ft/sec of the warm outflow flux are entrained and merged and flow out horizontally (lines 1 through 9 and 0 through 2). The recirculation flux is only 1300 cu ft/sec, the remainder of the warm inflow comes from the ocean surface.

In Figure 7, the cold outflow (lines 1 through 7) falls past its own level and bounces back. In doing so, it entrains 2000 cu ft/sec from the warm outflow (line 8) and 4000 cu ft/sec from the ambient ocean (lines 9 and 0, entering the domain at depth 275 ft and leaving at 300 ft on the right). The remainder of the warm outflow (lines 9 and 0 through 3) flows horizontally out at the right, except that 300 cu ft/sec recirculates into the warm inflow, combining with 11700 cu ft/sec of surface water which flows in horizontally (lines 8, 9 and 0 through 3).

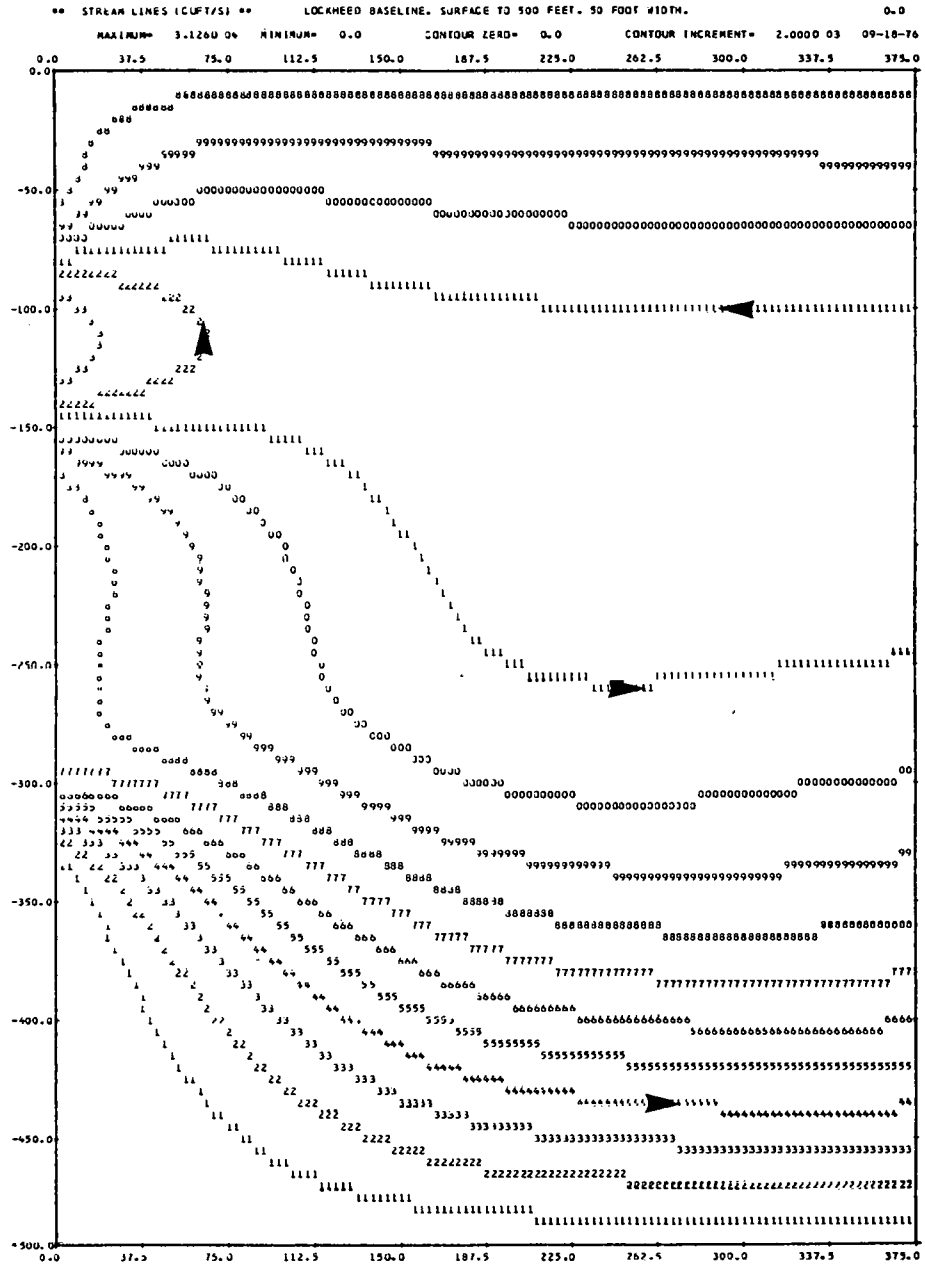
In Figure 8, the cold outflow jet (lines 1 through 5) entrains ambient ocean fluid from above (lines 6, 7 and 8) and below (lines 0 and A). The warm outflow jet (lines 6, 7 and 8) similarly entrains ambient ocean water from above (line 9) and below (line 5). The recirculation flux (line 9) is only about 100 cu ft/sec; the remainder of the warm inflow comes from the ocean surface (lines 6, 7 and 8).

Figures 9 and 10 display the temperature distribution and the stream lines in the whole computational domain, for the computations with assumed widths of 100 ft and 200 ft only. The corresponding figures for widths of 50 ft and 400 ft are in reference (13). In the upper panels, the contour increment is $3^{o}F$, so that the lines labeled 5 through 9 and 0 to 6 correspond to multiples from 15 through 26 of $3^{o}F$. Thus, the line 8, for example, is the $54^{o}F$ isotherm. In the lower panels, the contour increment is 3000 cu ft/sec. The left half of these lower panels is displayed in Figures 6 and 7.

In the upper panels of Figures 9 and 10, the isotherms are concentrated between 250 ft and 300 ft, showing the strong thermocline separating the warm surface layers from the cold deep water. The isotherms are roughly horizontal, like the streamlines in the lower panels. Comparison of the upper and lower panels indicates that the temperature is not constant on streamlines; this is because of turbulent heat transport between the streamlines of the mean flow.

Figures 11 through 14 have the same format, for each of the four assumed region widths. In the upper panel, the turbulent diffusivity distribution K is displayed, with contour increments in $ft^2/sec$ of 15, 7.5, 3 and 2. The figures are qualitatively similar, with maxima at the outflows and inflow. For large assumed width the stratification becomes dominant, and both K and $\bar{E}$ become negligible between the outflows. The minimum of K on the left boundary is displayed in Table 1.

The lower panels of Figures 11 through 14 show the horizontal velocity $\bar{u}$, the temperature $\bar{T}$, and the ambient temperature, at the left and right boundaries,




LOCKHEED BASELINE. SURFACE TO 500 FEET. 50 FOOT WIDTH.

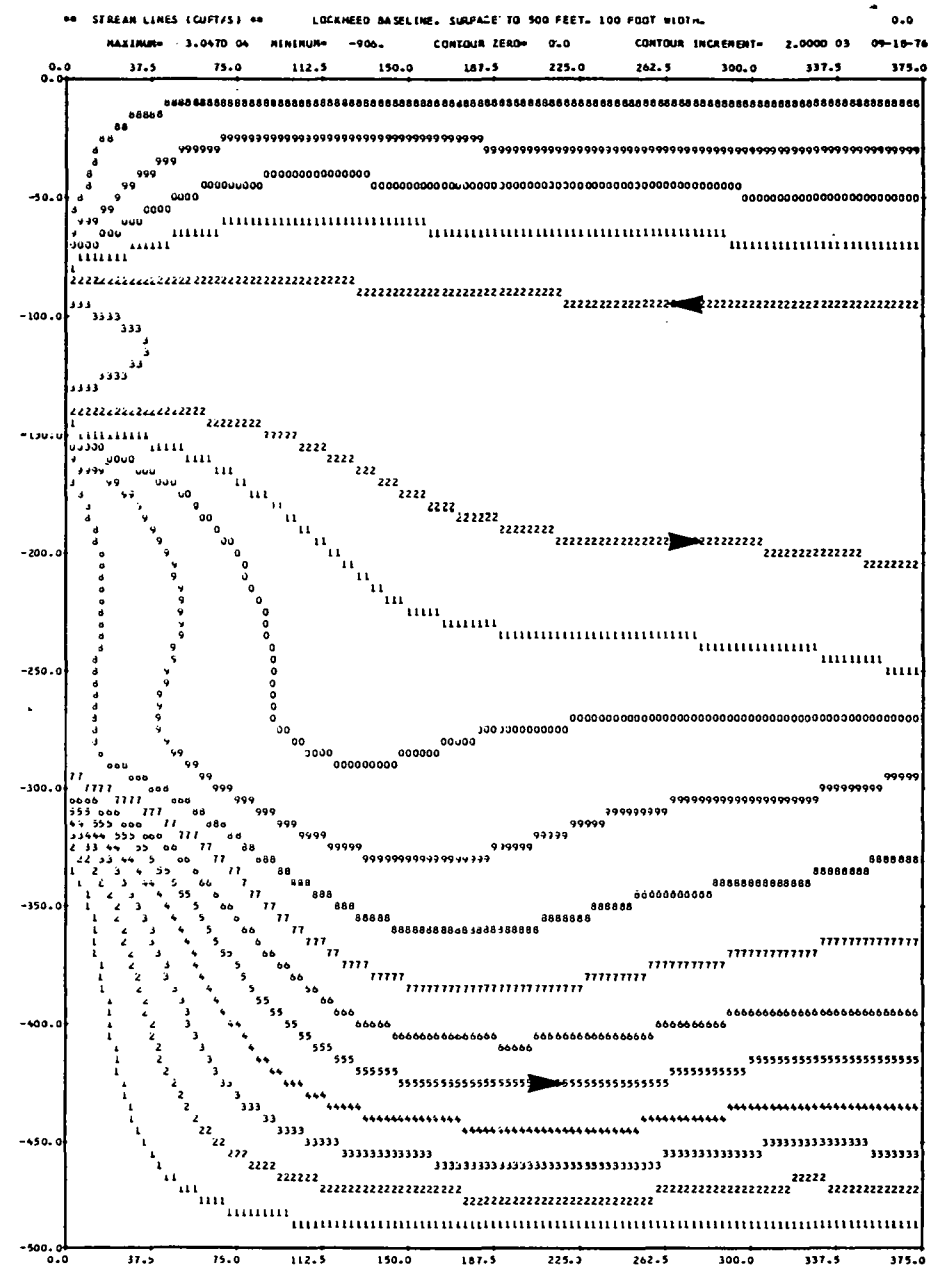
WARM PLANT INFLOW AT 75 FEET, WITH SAME RADIUS AS OUTFLOW.
OUTFLOW TEMPERATURE IS 3 DEGREES FAHRENHEIT COLDER THAN
MEAN INFLOW TEMPERATURE.
COLD PLANT OUTFLOW AT 315 FEET, TEMPERATURE 45 FAHRENHEIT.

MEAN PLANT INFLOW TEMPERATURE IS 75.7

| | | | | |
|---|---|---|---|---|
| AMPU | -0.0523 | 0.0523 | 0.0654 | 0.0 |
| AMPQ | 2.0 | 0.300 | 0.300 | 0.0 |
| TANALF | 0.0 | 0.0 | -0.160 | 0.0 |
| TFAMR | -3.0 | 70.0 | 45.0 | 45.0 |
| APL | 0.072 | 0.072 | 0.072 | 0.072 |
| ZCENT | 0.850 | 0.700 | 0.370 | 3.000 |
| TT,TB,ZTC,WID | 83.0 | 44.5 | 0.400 | 0.150 |
| JAMB,QDEP | | 1.00-09 | 0.25 | |
| FLEN,CF,CS,CW,PORC | 0.040 | 0.500 | 0.100 | 1.000 0.500 |
| GAP,XSTRC4,ZSTRCH,II,JJ | | 1.500 | 1.500 | 0.0 12 34 |
| TIME,CFL,NOUTPT,DSCALE,WIDFT | | 20.0 | 1.00 | 2 500.0 50.0 |

09-18-76

Figure 5. Stream Lines near the Plant for Width 50 Feet.




LOCKHEED BASELINE. SURFACE TO 500 FEET. 100 FOOT WIDTH.

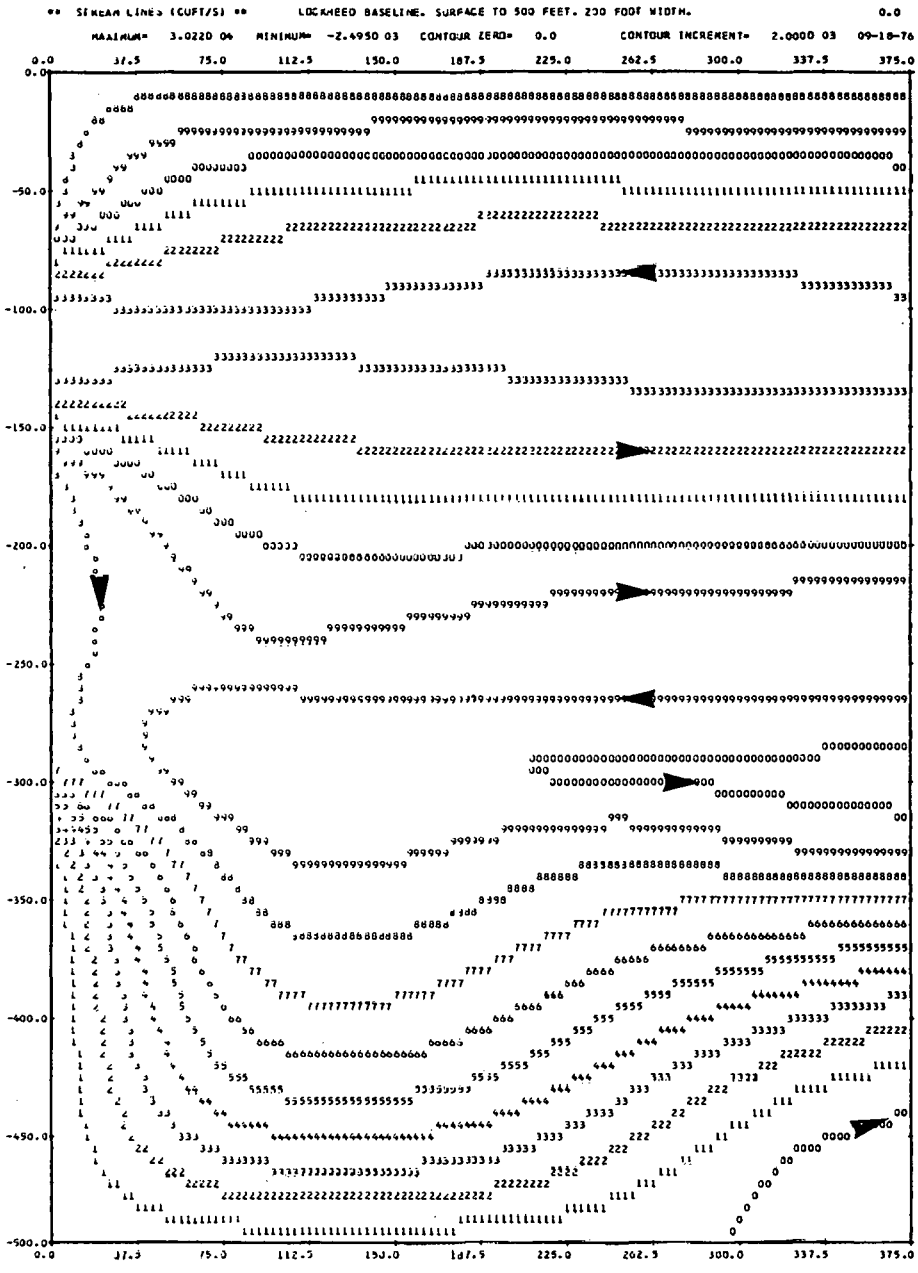
WARM PLANT INFLOW AT 75 FEET, WITH SAME RADIUS AS OUTFLOW.
OUTFLOW TEMPERATURE IS 3 DEGREES FAHRENHEIT COLDER THAN
MEAN INFLOW TEMPERATURE.
COLD PLANT OUTFLOW AT 315 FEET, TEMPERATURE 45 FAHRENHEIT.

MEAN PLANT INFLOW TEMPERATURE IS 77.2

| | | | | |
|---|---|---|---|---|
| AMPU | -0.0261 | 0.0261 | 0.0327 | 0.0 |
| AMPQ | 0.0 | 0.300 | 0.300 | 0.0 |
| TANALF | 0.0 | 0.0 | -0.160 | 0.0 |
| TFAMR | -1.0 | 70.0 | 45.0 | 45.0 |
| RPL | 0.072 | 0.072 | 0.072 | 0.072 |
| ZCENT | 0.850 | 0.700 | 0.370 | 3.000 |
| FT,FB,ZTC,WID | 80.0 | 44.5 | 0.400 | 0.150 |
| AMB,QDEP | | 1.00-09 | 0.25 | |

TLEN,CF,CS,CW,PORC 0.040 0.500 0.100 1.000 0.500
GAP,XSTRCH,ZSTRCH,II,JJ 1.900 1.500 0.0 12 34
TIME,CFL,MOUTPT,DSCALE,WIDPT 20.0 0.80 2 500.0 100.0
09-18-76

Figure 6. Stream Lines near the Plant for Width 100 Feet.




LOCKHEED BASELINE. SURFACE TO 500 FEET. 200 FOOT WIDTH.

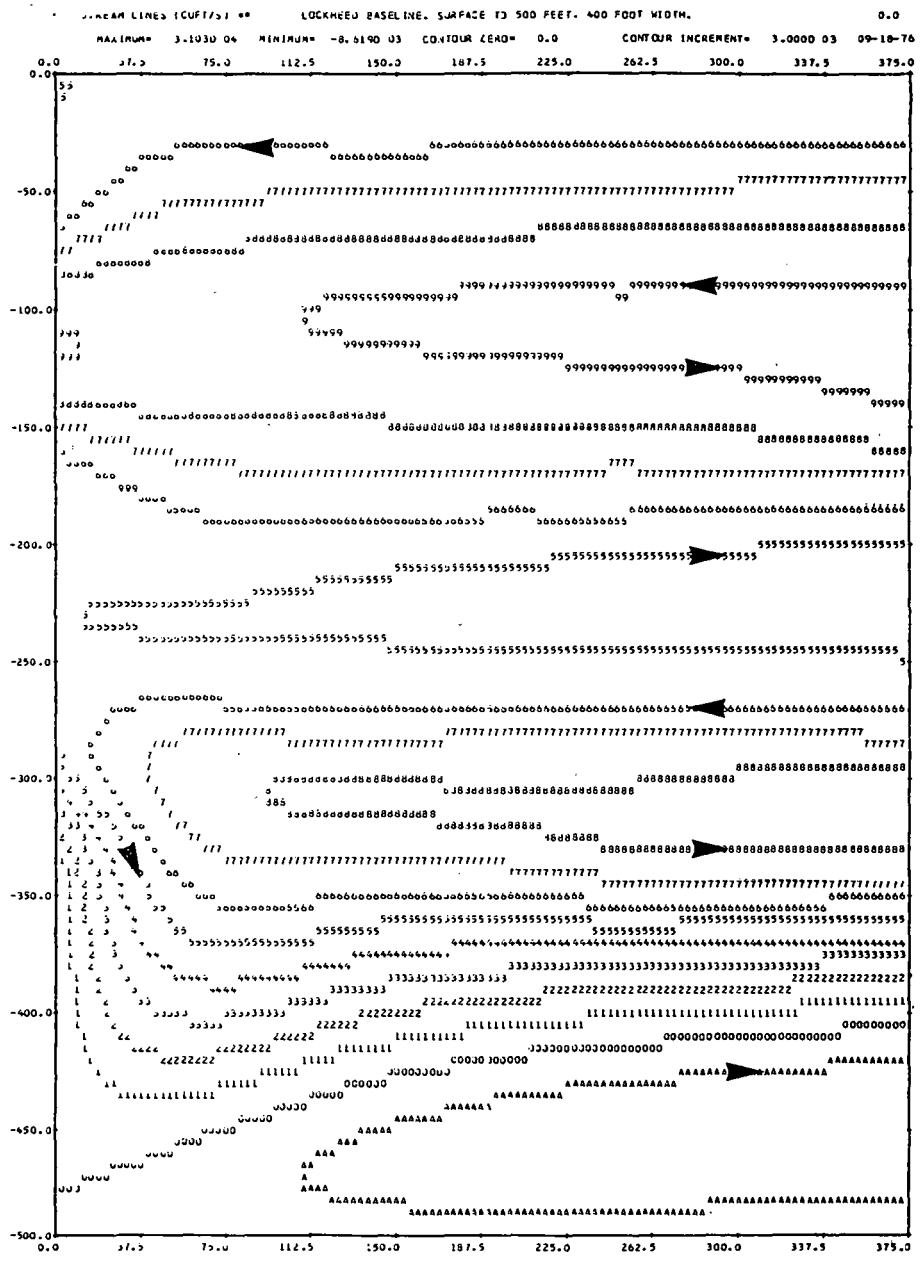
WARM PLANT INFLOW AT 75 FEET, WITH SAME RADIUS AS OUTFLOW.
OUTFLOW TEMPERATURE IS 3 DEGREES FAHRENHEIT COLDER THAN
WARM INFLOW TEMPERATURE.
COLD PLANT OUTFLOW AT 315 FEET, TEMPERATURE 45 FAHRENHEIT.

MEAN PLANT INFLOW TEMPERATURE IS 77.9

| | | | | |
|---|---|---|---|---|
| XMPU | -0.0131 | 0.0131 | 0.0163 | 0.0 |
| XMPQ | 0.0 | 0.300 | 0.300 | 0.0 |
| FANALF | 3.0 | 0.0 | -0.160 | 0.0 |
| TFANR | -3.0 | 70.0 | 45.0 | 45.0 |
| XPL | 0.072 | 0.072 | 0.072 | 0.072 |
| ZCENT | 0.850 | 0.700 | 0.370 | 3.000 |
| TT,TB,ZTC,WID | 80.0 | 44.5 | 0.400 | 0.150 |
| JAMB,QDEP | | 1.0D-09 | 0.25 | |
| FLEN,CF,CS,CW,PORC | 0.040 | 0.500 | 0.100 | 1.000 2.000 |
| GAP,XSTRCH,ZSINCH,II,JJ | | 1.500 | 1.500 | 0.0 12 34 |
| TIME,CFL,NOUTPT,DSCALE,WIDFT | | 10.0 | 0.80 | 2 500.0 200.0 |

09-18-76

Figure 7. Stream Lines near the Plant for Width 200 Feet.




LOCKHEED BASELINE. SURFACE TO 500 FEET. 400 FOOT WIDTH.

MEAN PLANT INFLOW AT 75 FEET, WITH SAME RADIUS AS OUTFLOW.
OUTFLOW TEMPERATURE IS 3 DEGREES FAHRENHEIT COLDER THAN MEAN INFLOW TEMPERATURE.
COLD PLANT OUTFLOW AT 315 FEET, TEMPERATURE 45 FAHRENHEIT.

MEAN PLANT INFLOW TEMPERATURE IS 78.6

| | | | | |
|---|---|---|---|---|
| XMPU | -0.0065 | 0.0065 | 0.0082 | 0.0 |
| XMP2 | 0.0 | 0.300 | 0.300 | 0.0 |
| FAHRLF | 3.0 | 0.0 | -0.160 | 0.0 |
| TFAHR | -3.0 | 70.0 | 45.0 | 45.0 |
| FPL | 0.072 | 0.072 | 0.072 | 0.072 |
| ZCENT | 3.853 | 0.700 | 0.370 | 1.000 |
| FT,FB,ZTC,WID | 80.0 | 44.5 | .0.400 | 0.150 |
| JAMB,QJEP | | 1.00-09 | 0.25 | |

FLEN,CF,CS,CW,PORC 0.040 0.300 0.100 1.000 0.500
SAP,ASFICH,ZSTACH,II,JJ 1.500 1.500 0.0 12 34
FINE,CFL,NOUTPT,DSCALE,WIDFT 10.0 0.80 2 500.0 400.0
09-18-76

Figure 8. Stream Lines near the Plant for Width 400 Feet.

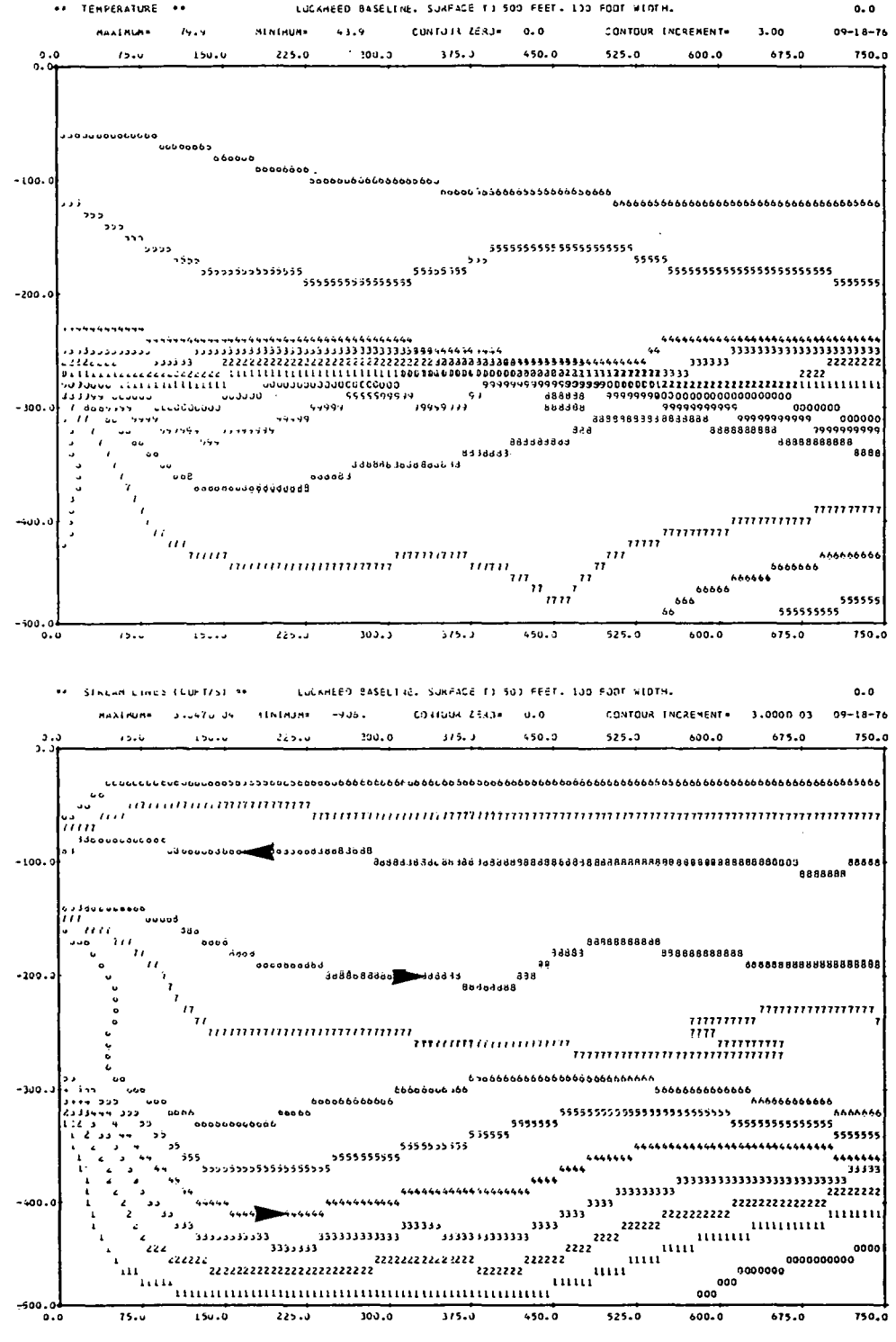



Figure 9. Temperature Distribution and Stream Lines for Width 100 Feet.

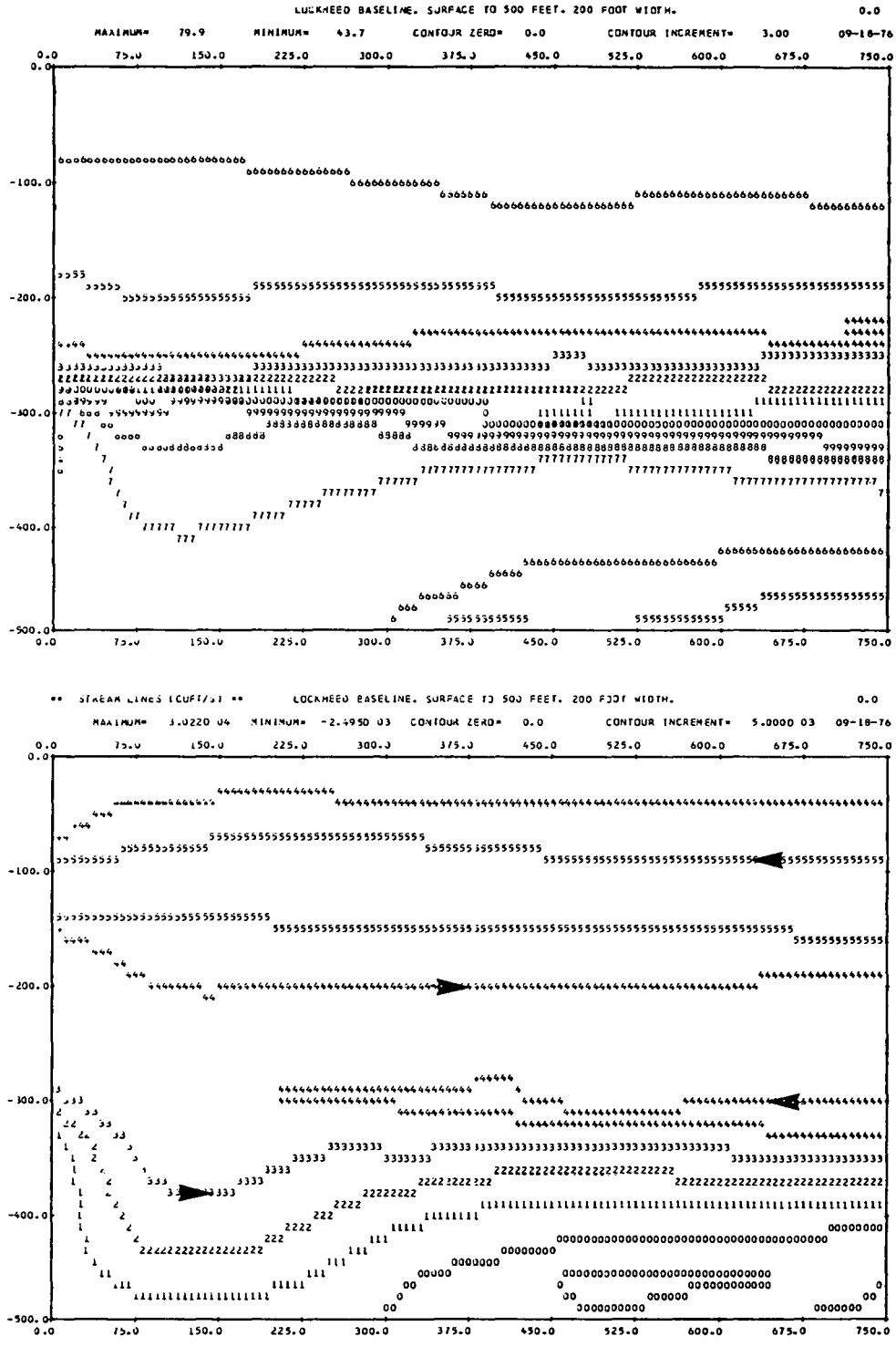



Figure 10. Temperature Distribution and Stream Lines for Width 200 Feet.

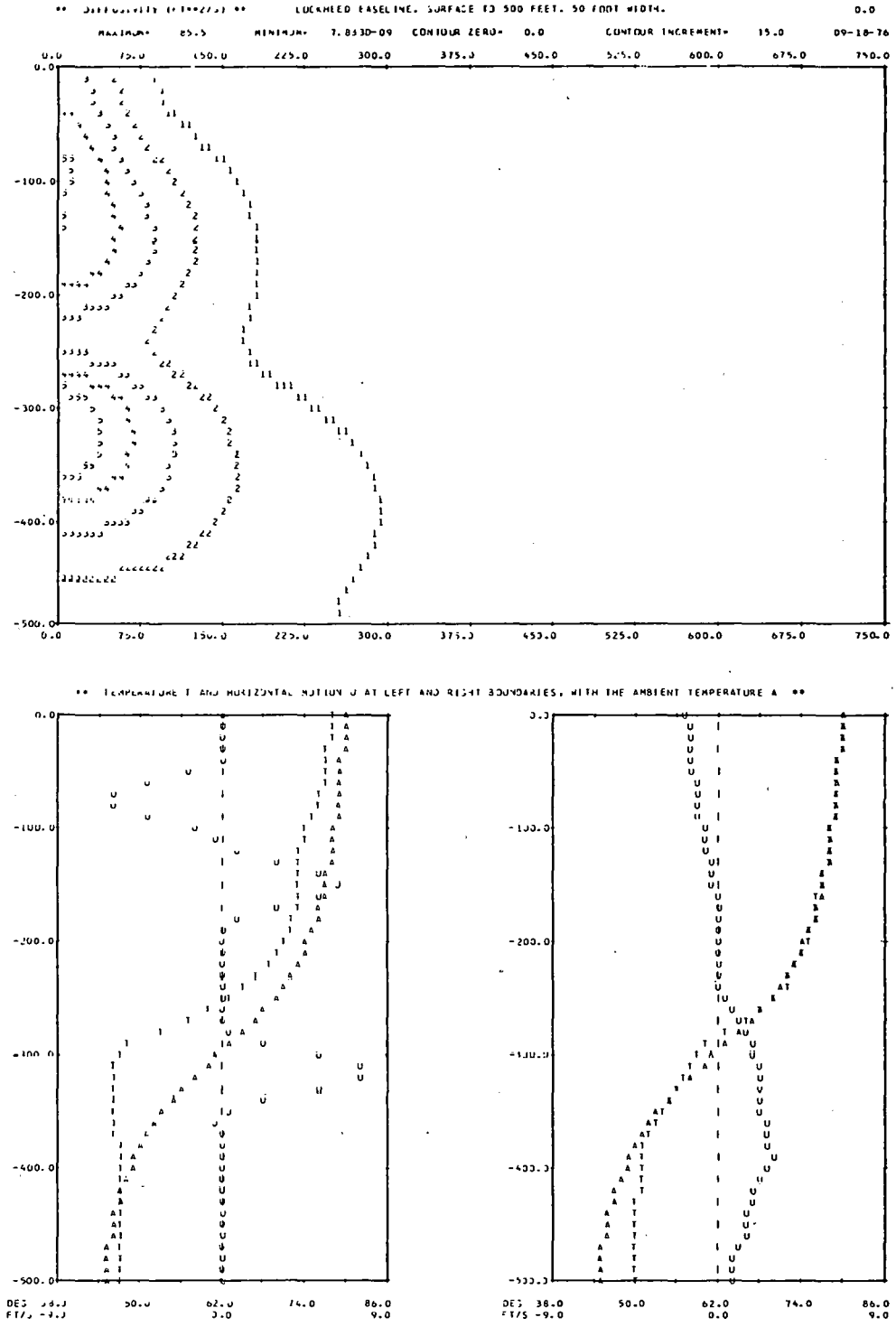



Figure 11. Diffusivity Distribution, and Boundary Profiles of Horizontal Flow and Temperature, for Width 50 Feet

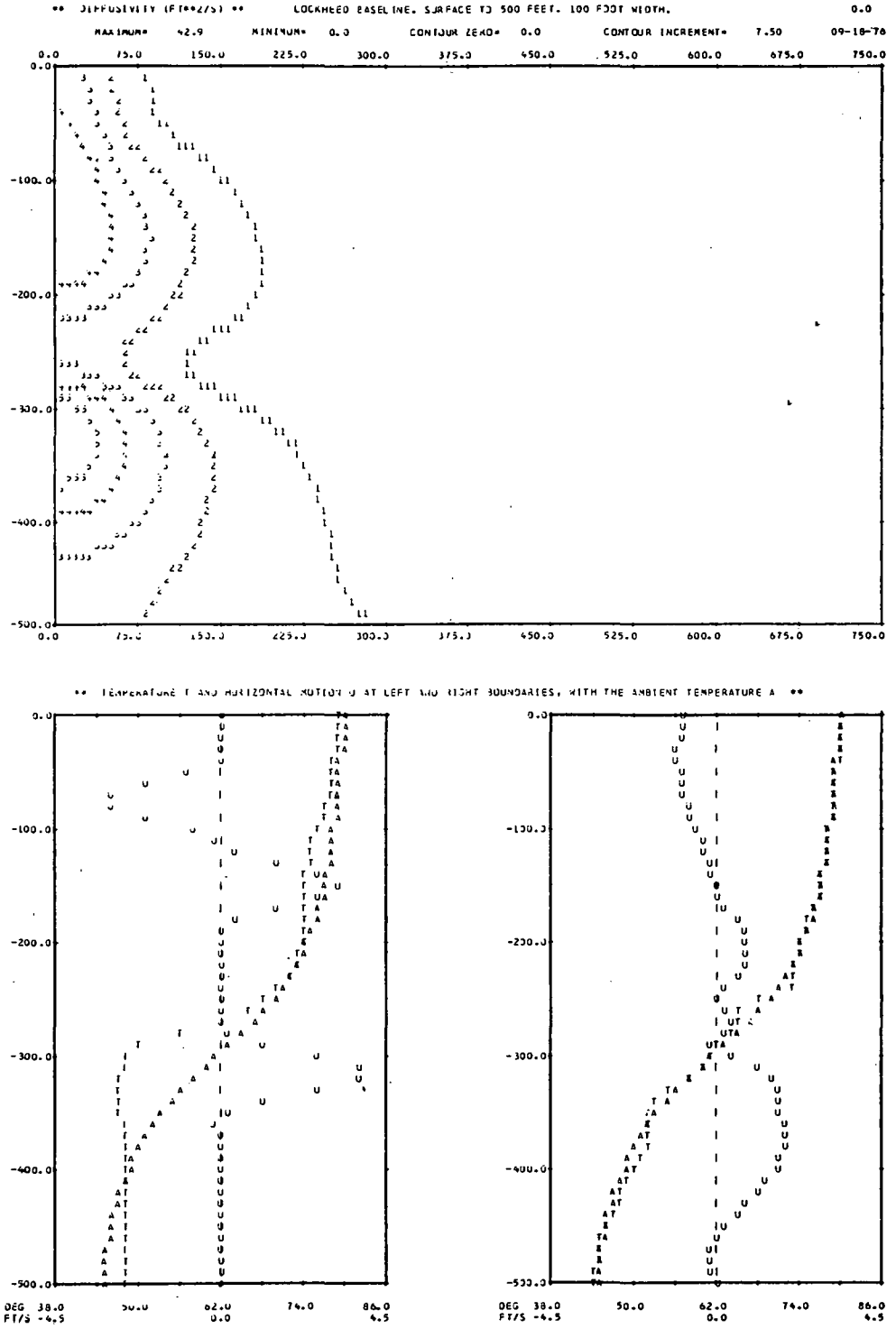



Figure 12. Diffusivity Distribution, and Boundary Profiles of Horizontal Flow and Temperature, for Width 100 Feet.

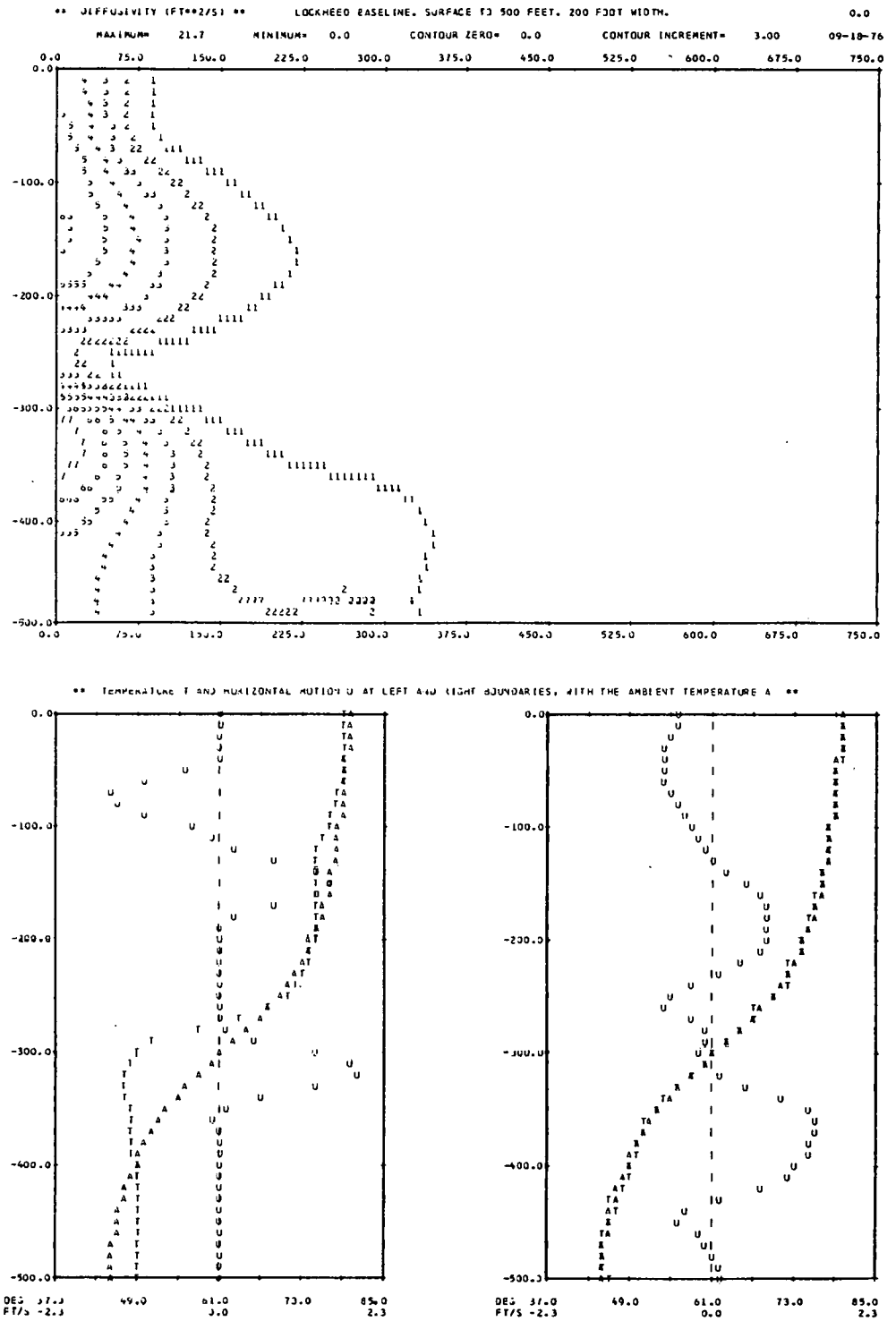



Figure 13. Diffusivity Distribution, and Boundary Profiles of Horizontal Flow and Temperature, for Width 200 Feet.

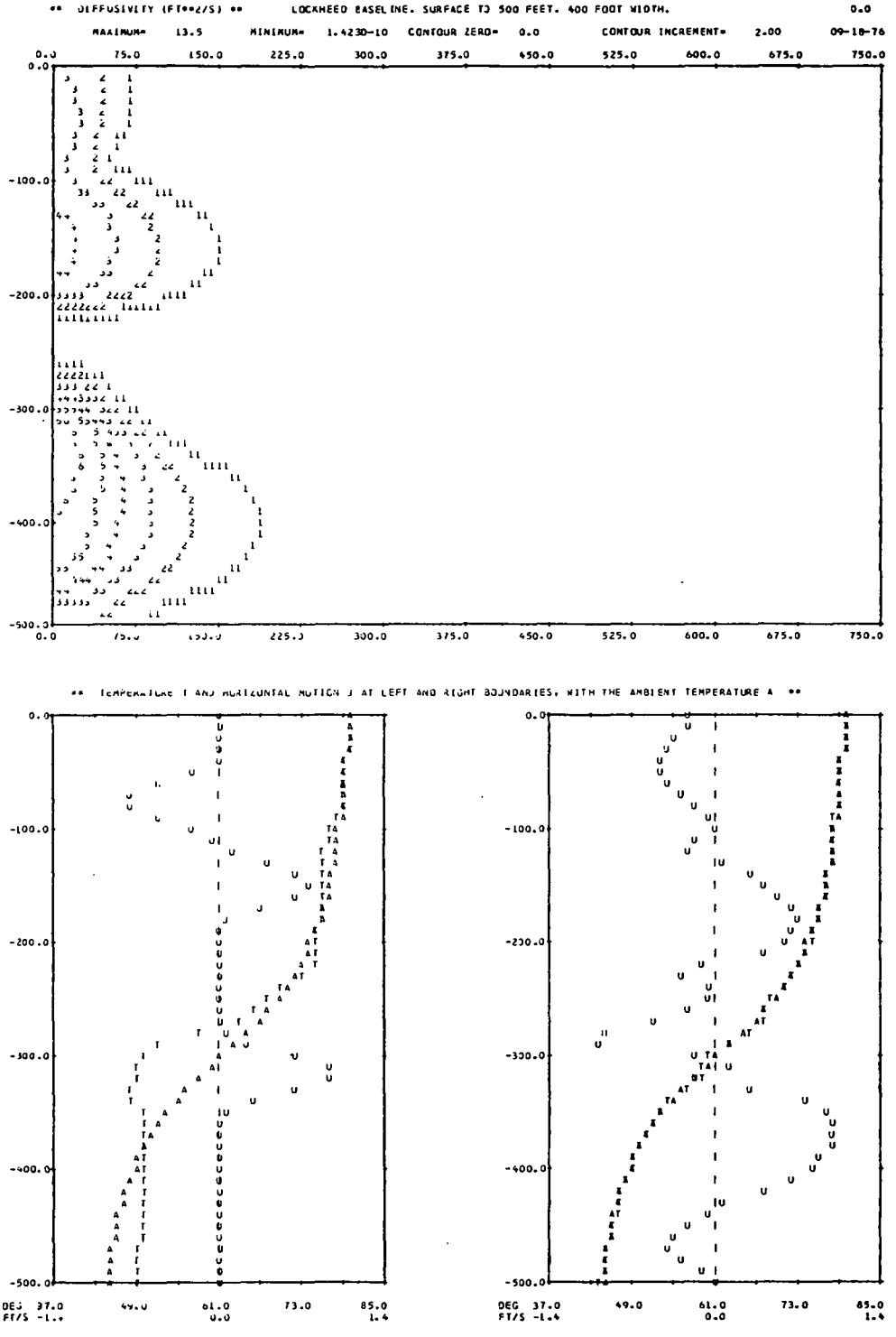



Figure 14. Diffusivity Distribution, and Boundary Profiles of Horizontal Flow and Temperature, for Width 400 Feet.

as functions of z. The ambient temperature is, of course, the same in each case, decreasing from 80°F at the surface to 44.5°F at 500 ft. The horizontal flow at the left boundary is halved for each doubling at the assumed width, the maximum speeds at the warm inflow, the warm outflow, and the cold outflow are given in Table 1. The temperature distributions on the left boundary are constant at the warm outflow (3°F cooler than the inflow) and at the cold outflow (45°F). The temperature on the right boundary is in close agreement with the ambient temperature, except in Figure 11 at the bottom, for the assumed width of 50 ft.

The horizontal flow at the right boundary, in the lower right panels of Figures 11 through 14, merits extra paragraphs. In Figure 11, for width 50 feet, the warm surface inflow occupies the top 150 ft, and the two outflows merge and occupy the lower 250 ft. In Figure 12, the outflows are distinct at the right boundary, and there is some entrainment above and below the cold outflow. In Figure 13, both outflows entrain fluid from above and below (as is confirmed by the stream lines in the lower panel of Figure 10). In Figure 14, this effect is more pronounced, and the warm surface inflow comes from the top 90 ft of the ocean.

It is noteworthy that in Figure 11, although the flow speeds are up to 8.5 ft/sec on the left boundary, the peak on the right boundary is only 2.6 ft/sec. The value is limited by the Richardson number distribution,

$$N^2 \Big/ (\partial \bar{u}/\partial z)^2 \quad ,$$

since values smaller than about unity result in a growth of turbulent kinetic energy.

Finally, it is the flow $\bar{u}(z)$ on the right boundary which determines the far-field environmental impact. In effect, the near-field flow withdraws water from the ocean in certain ranges of depth, temperature and density, and adds it in other ranges. With a large number of OTPP's operating in a limited ocean region, this will result in some modification of the temperature distribution and of the dynamics.

## 5. CONCLUSIONS

The code NRFLO2 should be regarded as a baseline near-field flow code. It is deficient in its geometry (two-dimensional) and in its turbulence model (constant length-scale, only one scalar diffusivity, and somewhat doubtful parameter values). Thus, our numerical results must be regarded as qualitative rather than quantitative. Within these limitations, we can draw the following conclusions.

First, it is possible to design an OTPP so that recirculation problems are negligible and the warm inflow temperature is very close to the surface temperature, even in the absence of an ambient current. To achieve this, the warm inflow and outflow speeds should be smaller than about 3 ft/sec, and the depth separation should be at least 30 ft. In addition, the warm inflow should be as close to the surface as possit

Secondly, the Lockheed designers were wise in seeking to place the warm outflow at its own temperature level. The downward slope of the cold outflow was suggested by the condenser design; it is a useful aid to the cold water in finding its own level, but not a major contribution.

Thirdly, the far-field environmental impact is determined by the details of the near-field flow. Depending on the width assumptions made in our computations, we obtained very different vertical distributions of flux addition to and withdrawal from the ambient ocean. Presumably, a good design will minimize the thermal impact on the ambient ocean.

## ACKNOWLEDGEMENTS

This report was prepared as part of the research program, "Theoretical Fluid Dynamical Studies of Resource Availability and Environmental Impact of Ocean Thermal Power Plants", in the Naval Research Laboratory, supported by the Ocean Thermal Energy Conversion Program, Division of Solar Energy, Energy Research and Development Administration, under ERDA contract E (49-26) 1005. The majority of the work was performed under the subcontract N00014-77-C-0033 with Science Applications, Inc.

## REFERENCES

1. Roberts, G.O., 1976: Evaluation of Thermal Plume Modeling for the San Onofre Nuclear Generating Station; Report SAI-76-627-WA. Science Applications, Inc., McLean, VA.

2. Jirka, G.H., 1977: Mixing and Recirculation Potential in the Vicinity of an OTPP; in this volume.

3. Sundaram, T.R., 1977: Experimental Studies on the External Flow Field, in this volume.

4. Mellor, G.L., and T. Yamada, 1974; A Hierarchy of Turbulence Closure Models for Planetary Boundary Layers. J. Atmos. Sci., 31, 1791-1806.

5. Munk, W.H., and E.R. Anderson, 1948: Notes on a Theory of the Thermocline. J. Marine Res., VII, 3 276-295.

6. Vager, B.G., and S.S. Zilitinkevich, 1968: A Theoretical Model of the Diurnal Variations of the Meteorological Fields. Meteorol, i. Gidrol, 7.

7. Stuhmiller, J.H., 1975: On the Phenomenological Modeling of Turbulent Flow; Report SAI-75-587-LJ, Science Applications, Inc., La Jolla, CA.

8. Lewellen, W.S., Teske, M., Contiliano, R., Hilst, G.R., and Donaldson, C. duP., 1974: Invariant Modeling of Turbulence and Diffusion in the Planetary Boundary Layer, Aeronautical Research Associates of Princeton, Inc., Report No. ARAP 225, Issued through Environmental Protection Agency, Report No. EPA-650/4-74-035 (PB No. 239 323/9ST).

9. Launder, B.E., 1975: On the Effects of a Gravitational Field on the Turbulent Transport of Heat and Momentum; Journal of Fluid Mechanics, 67, 569.

10. Piacsek, S.A., J. Toomre, and G.O. Roberts, 1975: Geophysical Fluid Dynamics Background for Ocean Thermal Power Plants; Report NRL-GFD/OTEC 11-75, Geophysical Simulation Section, Code 7750, Naval Research Laboratory, Washington, D.C.

11. Yamada, T., 1975: The Critical Richardson Number and the Ratio of the Eddy Transport Coefficients Obtained from a Turbulence Closure Model; Journal of Atmospheric Science, 32, 926.

12. Roberts, G.O., Piacsek, S.A., and Toomre, J., 1976: Two-Dimensional Numerical Model of the Near-Field Flow for an Ocean Thermal Power Plant. Part I. The Theoretical Approach and a Laboratory Simulation; Report SAI-76-624-WA, Science Applications, Inc., McLean, VA.

13. Roberts, G.O., Piacsek, S.A., and Toomre, J., 1976: Two Dimensional Numerical Model of the Near-Field Flow for an Ocean Thermal Power Plant. Part II. Simulation of the Lockheed Baseline Design; Report SAI-76-625-WA, Science Applications, Inc., McLean, VA.

14. Roberts, G.O., Piacsek, S.A., and Toomre, J., 1976: Two Dimensional Numerical Model of the Near-Field Flow for an Ocean Thermal Power Plant. Part III. Manual for the Computer Code NRFL02; Report SAI-76-626-WA, Science Applications, Inc., McLean, VA.

15. Trimble, L.C., 1975: Ocean Thermal Energy Conversion Power Plant Technical and Economic Feasibility; Lockheed Missile and Space Co., Inc., Report NSF/RANN/SE/GI-0937/FR/75/1, Sunnyvale, CA.

16. Douglass, R., 1975: Ocean Thermal Energy Conversion Research on an Engineering Evaluation and Test Program; Vols. 1-5, TRW, Redondo Beach, CA.

# AN ESTIMATE OF THE IMPACT OF OTEC OPERATION ON THE VERTICAL DISTRIBUTION OF HEAT IN THE GULF OF MEXICO

P. J. MARTIN AND G. O. ROBERTS
*Fluid Mechanics Division*
*Science Applications, Inc.*
*8400 Westpark Drive*
*McLean, Virginia*

ABSTRACT

The effect of OTEC operation on the thermal structure of the Gulf of Mexico is estimated by using a one-dimensional z-t heat conservation equation to predict the horizontal mean temperature. The surface heat fluxes are parameterized in terms of the observed air-sea temperature difference and the predicted sea surface temperature (SST). Advection of heat into the Gulf by the Yucatan Current is treated as a heat source for the surface layer of the Gulf. A constant mean upwelling is calculated to balance the overall heat budget. Within the mixed layer, the vertical diffusivity is calculated using the Mellor-Yamada Level 2 turbulent diffusion model. Below the mixed layer, a constant diffusivity is determined from a balance between vertical advection and diffusion to yield a realistic mean temperature profile.

The operation of 1000 OTEC plants in the Gulf is parameterized by the addition to the model of a mean vertical velocity profile required to complete the circulation between the near-plant intake and discharge flows. The result is a surface cooling and a warming at depth. The SST drops about 0.3°C during the first two years and then remains fairly constant. However, the deep water in the region above the cold water intake warms continuously at the rate of about 0.3°C per year. This rate of deep warming is about the worst that could be expected since the model does not allow the removal of this heat from the Gulf by the currents. For the operation of only 100 OTEC plants, the impact is correspondingly reduced. After 30 years, the model predicts a drop in SST of 0.05°C and a warming in the region above the cold water intake of 0.8°C.

## 1. INTRODUCTION

Recirculation between the intake and discharge flows of an OTEC plant is a potential problem for OTEC operations in that recirculation can bring about a decrease in the available thermal resource. Laboratory experiments and near-plant turbulent flow calculations have been performed by others to address the problem of recirculation in the immediate vicinity of an OTEC plant. This paper considers the effects caused by far field recirculation due to the operation of large numbers of OTEC plants in a semi-confined basin such as the Gulf of Mexico.

The operation of large numbers of OTEC plants in the Gulf of Mexico would undoubtedly have some effect on the balance of heat in that region. For example, a 200 megawatt OTEC plant will pump on the order of 1700 $m^3$ of sea water per second. For 100 such plants operating in the Gulf, this pumping rate is equivalent to a vertical velocity of $1.1 \times 10^{-5}$ cm/s if averaged over the entire area of the Gulf of Mexico. This velocity is equal in order of magnitude to estimates of the ambient upwelling in the ocean that helps maintain the permanent thermocline. Hence, the impact of large scale OTEC operation on the oceanic heat budget may not be insignificant and needs to be investigated.

We are using a one-dimensional z-t heat conservation equation to obtain a crude estimate of the effect of OTEC far field recirculation on the mean vertical temperature structure of the Gulf of Mexico. Our procedure is to set up a model that will maintain the observed mean temperature profile in the Gulf; then to perturb the model by simulating large scale OTEC operation. We assume that the OTEC plants drive a mean vertical velocity over the horizontal area of the Gulf in order to complete the circulation between the intake and discharge flows of the plants. Since the Gulf of Mexico is not a closed basin, this recirculation does not necessarily have to occur within the Gulf. The assumption that it does should provide a conservative estimate of the impact of OTEC operation on the mean vertical temperature profile of the Gulf.

## 2. FORMULATION AND DESCRIPTION OF THE MODEL

### 2.1 GENERAL DESCRIPTION OF THE MODEL

The model consists principally of using the one-dimensional z-t heat conservation equation to predict the mean temperature profile of the Gulf. The formulation of the model involves parameterizing the surface heat fluxes and the horizontal advection of heat into the Gulf through the straits, and determining the balance of advection and diffusion required to maintain the main thermocline.

### 2.2 SURFACE HEAT BUDGET FOR THE GULF OF MEXICO

The schematic in Figure 1 shows the principal elements involved in modeling the heat budget of the Gulf of Mexico. The largest heat source for the Gulf is solar radiation which is absorbed near the surface. There is a large net loss of heat at the surface due to back radiation and latent and sensible heat exchange with the atmosphere. Most of the difference between the heat lost from the surface and the heat gained from solar radiation is made up by the advection of heat into the Gulf through the Yucatan and Florida Straits.

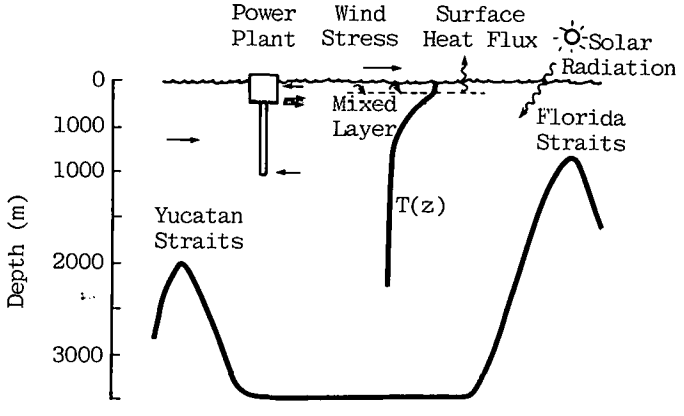



Fig. 1. Schematic Showing Elements of 1-D Gulf Basin Model.

The table in Figure 2 shows estimates of the mean annual heat budget for the Gulf given by Hastenrath (3) and Bunker (2). Also shown is an estimate of the heat budget calculated using bulk formulae and monthly meteorological data.

Hastenrath estimated the net heat budget of the Gulf of Mexico by three different methods: the oceanic heat budget, the atmospheric energy budget, and the calculation of surface fluxes using bulk formulae.

| | Hastenrath (1968) | Bunker (1976) | Used For Present Study |
|---|---|---|---|
| Solar Radiation | 344 | 320 | 427 |
| Back Radiation | -109 | | -137 |
| Latent Heat Flux | -270 | -300 | -289 |
| Sensible Heat Flux | | -50 | -29 |
| NET Heat Flux | -35 | -30 | -27 |

Fig. 2. Surface Heat Budget for Gulf of Mexico. Heat Fluxes are in Units of cal/cm$^2$/day.

He concluded that the Gulf suffers a net loss of heat from the surface over a typical yearly cycle and estimated this loss to be about 35 cal/cm$^2$/day.

Bunker calculated heat fluxes over the entire North Atlantic using bulk formulae and the large body of ship observations collected by the National Climate Center. His computations differed from the previous methods of Jacobs (5), Budyko (1), and others in that he used bulk coefficients that varied with wind speed and stability. From Bunker's maps of heat exchange, we estimated a mean heat loss by the Gulf of about 30 cal/cm$^2$/day which agrees very well with the value determined by Hastenrath.

Our own heat exchange calculations were made using the solar radiation formula of Laevastu (7), the bulk formulae of Wyrtki (17), and monthly meteorological data from Summary of Synoptic Meteorological Observations of North Atlantic Coastal Marine Areas, 1975 (15). We used a bulk coefficient for latent heat exchange of $1.5 \times 10^{-3}$ which is about the mean of the range of the values suggested by Bunker for the wind speeds and stabilities typical of the Gulf. Sensible heat exchange was estimated using a Bowen ratio of 0.1. The values for solar radiation calculated using the Laevastu formula appeared overly large and were reduced by 25 percent to yield a net heat flux in better agreement with the values determined by Hastenrath and Bunker.

he calculation of surface heat fluxes using bulk formulae is at present a fairly crude procedure. For example, even though Hastenrath and Bunker obtain similar values for the net surface heat flux of the Gulf, their determinations of the individual fluxes vary considerably. Hence, there seems to be room for considerable variability in the value for the net surface heat flux.

### 2.3 MEAN TEMPERATURE PROFILE OF THE GULF

The eastern and western Gulf constitute two fairly distinct regions. The eastern Gulf is dominated by the Loop Current which enters through the Yucatan Straits and exits through the Florida Straits. The

transport of the Loop Current averages about 30 x $10^6$ $m^3/s$ with surface currents as high as 200 cm/s (Nowlin and McLellan, 13). Because of the adjustment of the density field to the Loop Current, there are very large horizontal density gradients in the eastern Gulf (Leipper, 9). The currents in the western Gulf are not as strong as the currents in the eastern Gulf, and the corresponding horizontal density gradients are not as large. Typically, the water of the western Gulf is colder at a given depth than water in the eastern Gulf.

Figure 3 shows a spatial and temporal mean temperature profile for the Gulf of Mexico. The mean surface temperature, based on observations, is about 25.4°C. The mixed layer depth varies between 0 and 125 meters (Harding and Nowlin, 4), being shallower in the summer due to strong solar heating and deeper in the winter due to net surface cooling and resulting convection. From the base of the mixed layer down to about 500 m, the thermal gradient is very large. Below the depth of the sill in the Yucatan Straits (about 2000 m), the temperature and salinity are almost constant (McLellan and Nowlin, 10). The minimum temperature is about 4.2°C. The sill prevents Caribbean water colder than 4.2°C from entering the Gulf.

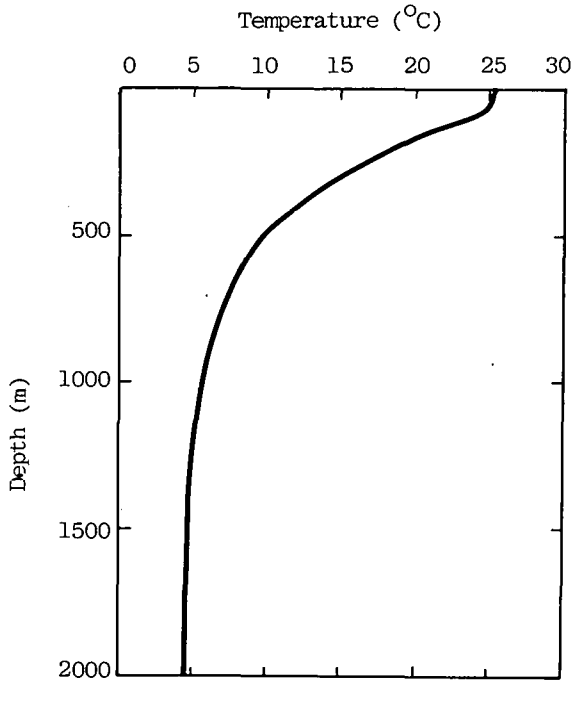



Fig. 3. Mean Temperature for the Gulf of Mexico.

## 2.4 HEAT CONSERVATION EQUATION

If the equation for the conservation of heat is averaged over the area of the Gulf, we obtain

$$\frac{\partial T}{\partial t} = \frac{1}{A}\left\{T\frac{\partial}{\partial z}(Aw) - \frac{\partial}{\partial z}(AwT) + \frac{\partial}{\partial z}\left(K_H A \frac{\partial T}{\partial z}\right)\right\} + Q_R, \tag{2.1}$$

where $T(z,t)$ is the horizontally averaged temperature, $A(z)$ is the horizontal area of the Gulf, w is the mean vertical velocity, $K_H$ is the vertical diffusivity for heat, t is the time, z is the depth, and $Q_R$ is a heat source term due to the penetration of solar radiation. The horizontal area of the Gulf as a function of depth used in equation (2.1) is shown in Figure 4. An extinction curve determined by Jerlov (6) for Type I, clear ocean water was used to describe the penetration of solar radiation.

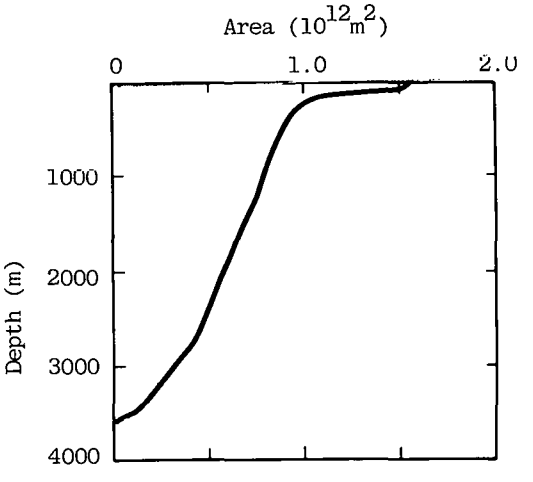



Fig. 4. Area of Gulf of Mexico vs. Depth.

Equation (2.1) is basically a balance between vertical advection and diffusion. In deriving the equation, it was assumed that these processes could be adequately parameterized in terms of horizontal mean values of temperature, vertical velocity, and diffusivity.

It was also assumed that inflow into the Gulf adjusts its depth to that of Gulf water of the same density. Hence, water entering or leaving a given layer of the model by horizontal advection has the same temperature as the layer. This assumption follows

from the tendency of horizontal flow to follow the isotherms. The vertical flowrate w can then be considered the flowrate in a direction perpendicular to the isotherms which balances the diffusion of heat along the thermal gradient.

The exception to this is water entering the Gulf through the Yucatan Straits which is warmer than the surface water in the Gulf. This water is assumed to mix with the surface water in the Gulf and is treated in the model as a component of the surface heat flux.

## 2.5 TRANSPORT THROUGH THE YUCATAN STRAITS

The transport through the Yucatan Straits was estimated by calculating the dynamic velocity field perpendicular to a density section just north of the Straits. The dynamic velocity field was determined using the equation

$$v = \frac{1}{\rho f} \frac{\partial}{\partial x} \int_{-D}^{z} - \rho g dz \quad , \qquad (2.2)$$

where $\rho$ is the density, g is the acceleration of gravity, and -D is a level of no motion where the horizontal density gradient is zero. The level of no motion was taken to be the deepest common density measurement between neighboring hydrographic stations along the section. This assumption no doubt contributes some error to the transport calculation. Some error may also be due to the fact that the density section data did not extend completely across the mouth of the Strait to Cuba, but ended at 85.02°W. The density data for the section were from the cruise of the R. V. Alaminos in May, 1972 (Morrison, Merrell, and Nowlin, 12).

Figure 5 shows the transport through the Yucatan Straits as a function of temperature. The total transport was calculated to be 26 x $10^6$ $m^3/s$ which is a little less than recent estimates of about 30 x $10^6$ $m^3/s$. Based on the Yucatan transport and the mean surface temperature of the Gulf, we estimated a net near-surface heat transport into the Gulf by the Yucatan Current of about 55 cal/$cm^2$/day, if averaged over the area of the Gulf. Given the assumptions involved, this is a very rough figure and could be in error by 50 percent or more.

## 2.6 ESTIMATE OF THE AMBIENT VERTICAL VELOCITY

A constant mean vertical velocity was determined to balance the overall heat budget of the Gulf. A loss of heat due to the surface heat flux of 27 cal/$cm^2$/day combined with a near-surface heat transport into the Gulf of 55 cal/$cm^2$/day yields a net supply of heat in the surface region of about 28 cal/$cm^2$day. We assume that this heat diffuses down the thermal gradient to warm colder water as it

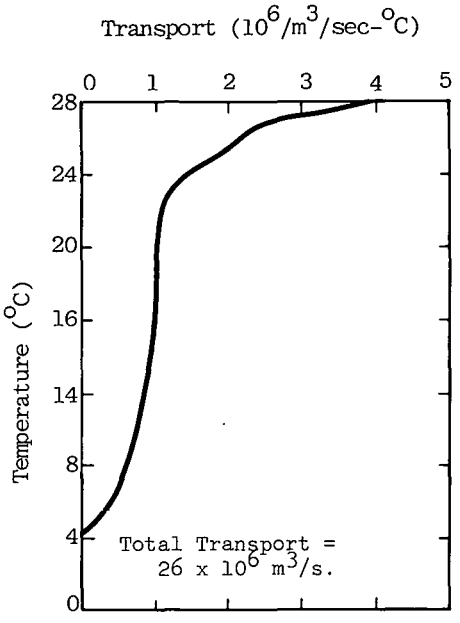



Fig. 5. Transport Through Yucatan Straits As A Function of Temperature

is advected upwards. A constant mean vertical velocity of 2.4 x $10^{-5}$ cm/s provides an upward flow of sea water sufficient to balance the downward diffusion of heat.

## 2.7 DETERMINATION OF MEAN VERTICAL DIFFUSIVITY

Within the mixed layer, the vertical diffusivity is estimated using the Mellor-Yamada Level 2 turbulence model (Mellor and Yamada, 11). This model calculates the vertical turbulent diffusivity from the local density gradient and the vertical shear of u and v, the components of the mean horizontal velocity. The mean temperature gradient is readily determined from the mean temperature profile predicted by Equation (2.1). Calculating the velocity gradients requires solving the u and v momentum equations, given by

$$\frac{\partial u}{\partial t} = fv + \left(K_M \frac{\partial u}{\partial z}\right) \quad , \qquad (2.3)$$

and

$$\frac{\partial v}{\partial t} = -fu + \left(K_M \frac{\partial v}{\partial z}\right) \quad , \qquad (2.4)$$

where f is the Coriolis parameter. The vertical diffusivity for momentum in the mixed layer $K_M$ is predicted by the Mellor-Yamada model along with the vertical diffusivity for heat. The surface boundary conditions for equations (2.3) and (2.4) are the two

components of the surface wind stress. As a second boundary condition, u and v are assumed to vanish at some depth well below the deepest penetration of the mixed layer.

Below the mixed layer, the vertical diffusivity is determined by the balance between vertical advection and diffusion. A constant mean vertical diffusivity was selected which yields a realistic temperature profile when equation (2.1) is integrated to steady state. The optimum value was found to be about 0.65 $cm^2/s$.

Therefore, main thermocline for the model is maintained by a constant mean upwelling of $2.4 \times 10^{-5}$ cm/s and a constant vertical diffusivity of 0.65 $cm^2/s$. These values were obtained rather crudely, but are within the range of other estimates of upwelling and vertical diffusivity for the open ocean (Veronis, 16).

## 2.8 MODEL SUMMARY

The model consists basically of using the conservation of heat to predict the mean temperature profile for the Gulf. All the variables are represented as horizontal mean values. The mean surface heat fluxes are calculated to be in fair agreement with the estimates of Hastenrath and Bunker. The warm surface flow into the Gulf through the Yucatan Straits is treated as a surface heat flux. A constant mean upwelling is determined to balance the overall heat budget, and a mean vertical diffusivity below the mixed layer is selected to yield a realistic temperature profile.

The formulation of the model included a number of assumptions. Hence, a high degree of accuracy cannot be claimed for all the parameterizations. The attempt was to set up a vertical balance of heat in the Gulf that agrees reasonably well with known conditions in the Gulf within the limitations of a one-dimensional model.

## 3. SEASONAL CYCLE OF GULF OF MEXICO

The seasonal variation of the mean sea surface temperature and mixed layer depth in the Gulf of Mexico was simulated with the model by seasonally varying the surface wind stress, solar radiation, and surface heat fluxes. Figure 6 shows a graph of the seasonal variation of the surface heat fluxes. The solar radiation exerts a dominating influence on the seasonal variation of the net surface heat flux throughout the year, with the Gulf gaining heat in the spring and summer and losing heat in the fall and winter.

The model, consisting of equations (2.1), (2.3), and (2.4) and their associated boundary conditions, was integrated numerically over several annual cycles using a time step of 1 day. A vertical grid with a spacing of 10 m in the upper 50 m and increasing logarithmically below 50 m was used. The surface heat

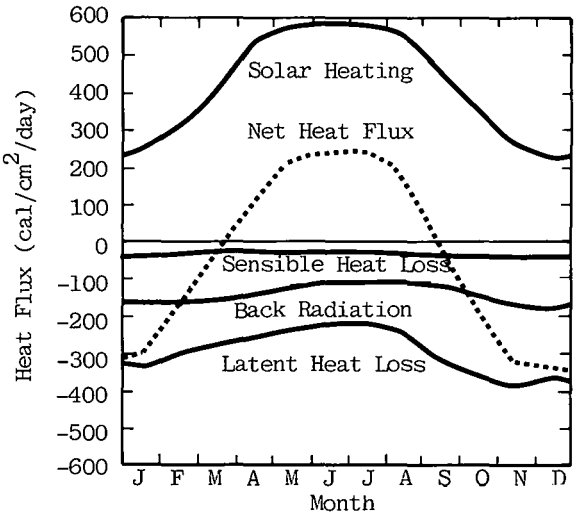



Fig. 6. Annual Cycle of Surface Heat Flux To The Gulf of Mexico

fluxes were calculated using the observed air-sea temperature difference and the sea surface temperature predicted by the model. Daily values of the observed forcing were interpolated from the monthly mean values. The diurnal variation of solar radiation was ignored. In previous simulations it was not found to affect significantly the seasonal variation of sea surface temperature and mixed layer depth. The initial temperature profile was fixed as depicted in Figure 3.

The annual cycle of the predicted sea surface temperature became fairly repetitive after about three cycles. Figure 7 shows a comparison of the predicted and observed sea surface temperature. The predicted and observed temperatures agree within about 0.5°C throughout the year. The predicted sea surface temperature depends principally upon the advective and surface heat fluxes, the mixed layer depth, and the rate of vertical diffusion below the mixed layer which helps determine the rate of descent of the isotherms due to heating in the spring and summer.

Figure 8 shows the seasonal variation of the mixed layer and isotherm depths predicted by the model. The mixed layer is fairly shallow in the summer due to strong solar heating, but deepens rapidly in the fall due to surface cooling and convection. The mixed layer rises rapidly again in the spring when the surface layers begin to warm. Harding and Nowlin (13) note that the mixed layer depth in the central Gulf in January and February, the coolest months, is about 90 m. The winter mixed layer depth predicted by the model agrees fairly well with this observation. The isotherms deepen slowly in the spring and summer due to downward diffusion, and rise rapidly in the fall due to convection. There is very little seasonal disturbance of the isotherms below 150 m.

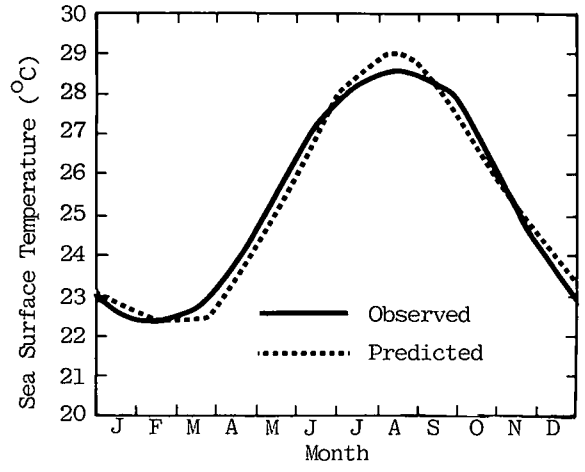



Fig. 7. Annual Cycle of Observed and Predicted Sea Surface Temperature for the Gulf of Mexico.

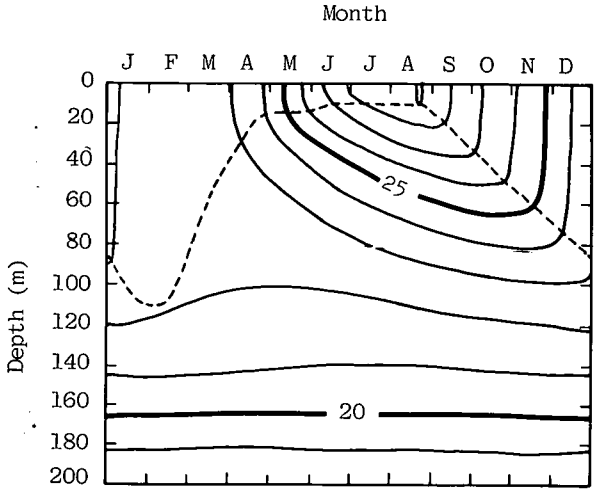



Fig. 8. Predicted Annual Cycle of Mixed Layer and Isotherm Depths for Gulf of Mexico. Mixed Layer Depth Shown with Dotted Line. Isotherm Depths (°C) Shown with Solid Lines.

## 4. IMPACT OF OTEC OPERATION ON THE GULF OF MEXICO

### 4.1 PARAMETERIZATION OF OTEC OPERATION

The operation of OTEC plants in the Gulf is parameterized by the addition to the model of a mean vertical velocity required to complete the circulation between the near-plant intake and discharge flows. It is assumed that this return circulation takes place within the Gulf and takes the form of a mean vertical velocity over the total area of the Gulf between levels where discharged sea water settles out and intake water is sucked in. These levels have been determined previously in near-plant flow calculations (Roberts, 14). Figure 9 shows the mean vertical velocity produced by the operation of a single OTEC plant. The figure shows upwelling near the surface between the warm water intake and discharge levels, and downwelling between the cold water discharge and intake levels between 500 and 1000 m. The bottom of the cold water pipe was assumed to be at a depth of 1000 m. For a single plant pumping 1700 $m^3/s$, the maximum expected mean vertical velocity is about $2 \times 10^{-7}$ cm/s when averaged over the area of the Gulf. To simulate the operation of a number of plants, the vertical velocity profile of Figure 9 is multiplied by the number of plants.

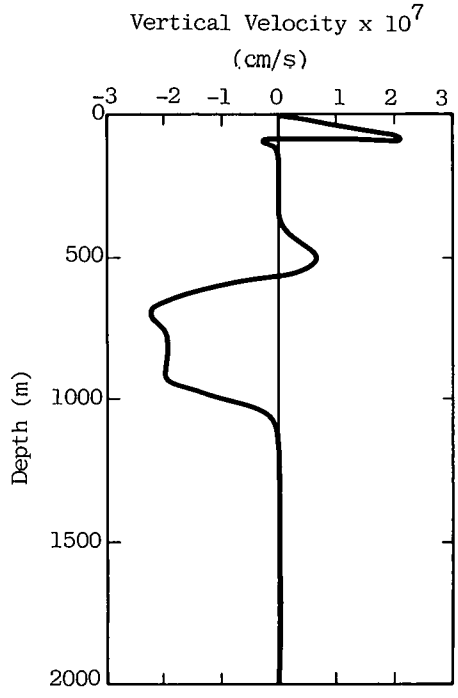



Fig. 9. Mean Vertical Velocity Due to Operation of a Single OTEC Plant in the Gulf of Mexico.

The averaging of the return circulation over the total area of the Gulf tends to minimize any local impact of OTEC operation that might occur around a plant or group of plants. The one-dimensional model assumes that once the discharge flow from a plant has settled out, it tends to move horizontally because of the stratification and forces a mean vertical motion only because of the physical boundaries of the Gulf basin. On the other hand, the assumption that the return circulation takes place completely within the Gulf is the worst that can be expected in the sense that the heat added to the Gulf in the region between

the cold water discharge and intake flows is not removed from the Gulf by the currents. Hence, the heat gained from the power plant condensers will build up in the model as time goes by. This behavior is probably unrealistic; however, we have not determined how to parameterize the removal of this heat by the currents.

## 4.2 BOUNDARY CONDITIONS FOR THE MODEL

The surface heat fluxes for the model were calculated using the predicted sea surface temperature and the observed air-sea temperature difference. For a body of water as large as the Gulf, it seems reasonable to assume that the air temperature depends upon the sea surface temperature. Laevastu and Harding (8) find that the air temperature over the sea adjusts to the sea surface temperature in about 4 hours. For a typical wind speed of 7 m/s, an air parcel will have traveled a distance of about 100 km. So, if the surface temperature of the Gulf changes, the mean air temperature over most of the Gulf is likely to change by a similar amount.

Calculating the surface fluxes using the observed air-sea temperature difference rather than, for example, the observed air temperature, results in a considerably weaker feedback between the latent and sensible heat fluxes and the sea surface temperature. For this reason, the main restoring force for the sea surface temperature is the warm water advected into the Gulf from the Caribbean. If the air-sea temperature difference is kept fixed, a drop in the sea surface temperature of 0.5°C results in an increase in the surface heat flux of only about 7 cal/cm$^2$/day, whereas, if the air temperature is kept fixed, the same sea surface temperature drop results in an increase in the surface heat flux of 40 cal/cm$^2$/day. For a drop in the sea surface temperature of 0.5°C, the net horizontal advection of heat into the Gulf increases by about 20 cal/cm$^2$/day.

As a bottom boundary condition for the conservation of heat (equation 2.1), the temperature was fixed at a depth of 1650 m. The temperature in the region below 1250 m was not affected by OTEC operation during the model runs.

Both annual mean data and seasonal data were used to force the model via the surface boundary conditions. Mean annual forcing was used in order that the effects of OTEC operation in the surface region would not be obscured by seasonal fluctuations. It might be expected that both types of forcing should give similar results below 150 m, which is about the maximum depth of seasonal influences.

## 4.3 RESULTS PREDICTED FOR OTEC OPERATION

Figure 10 shows the change in the mean temperature profile of the Gulf predicted by the model due to the operation of 1000 OTEC plants for a 10 year period. Mean annual values of the observed surface boundary conditions were used to force the model. The temperature above 200 m adjusts to OTEC operation afte about 2 years. Most of this adjustment occurs the first year. The sea surface temperature drops from 25.4°C to 25.1°C and then remains fairly steady.

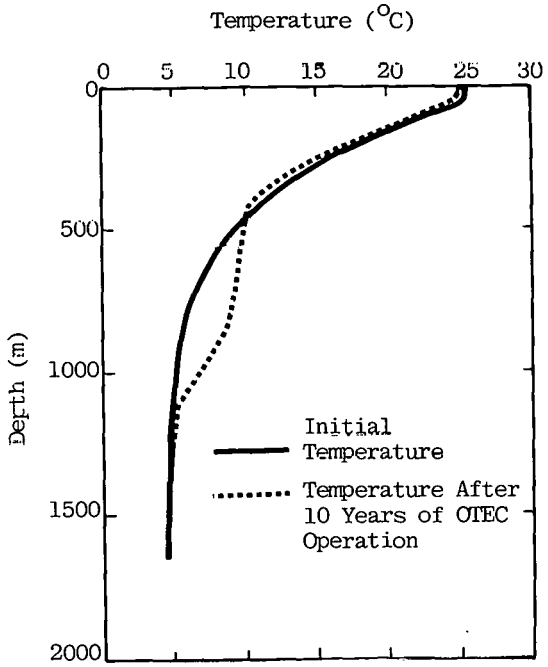



Fig. 10. Mean Temperature Profile in Gulf of Mexico After 10 Years of Operation With 1000 Plants.

The deeper region, however, never comes into adjustment. The downwelling between the settled out cold water discharge and the cold water intake continually warms the region from 500 to 1200 m at the rate of about 0.3°C per year. The increase of the heat storage in this region is fairly linear with time.

Near the surface, the warm Yucatan inflow and the latent and sensible heat fluxes help to maintain the temperature. The increase of these heat fluxes due to the decrease in the sea surface temperature balances the cooling due to the increased rate of upwelling. However, the deeper water is effectively insulated due to the small ambient vertical diffusivity. Assuming that the water flowing through the condensers of the OTEC plants is warmed about 3°C, 1000 OTEC plants will add about 27 cal/cm$^2$/day to the Gulf. This rate of heating is sufficient to raise the temperature of a column of water 500 m deep by 0.36°C per year. This is approximately the result predicted by the model.

Figure 11 shows the predicted change in the mean temperature profile in the Gulf due to the operation of only 100 OTEC plants. The impact is

considerably less than with 1000 plants, as might be pected. The sea surface temperature decreases only out .05°C and the region above the cold water intake warms at the rate of about .03°C per year.

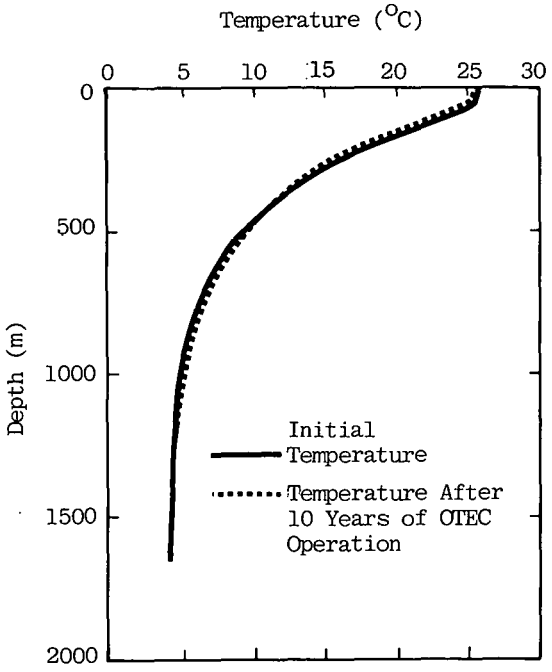



Fig. 11. Mean Temperature Profile in Gulf of Mexico After 10 Years of OTEC Operation With 100 Plants.

The use of seasonal forcing rather than mean annual forcing did not greatly affect the results predicted for OTEC operation in the Gulf. As expected, below 150 m the solutions are about the same. Figure 12 shows the effect on the January temperature profile of the operation of 1000 OTEC plants for a 10 year period for the case with seasonal forcing. The deop in sea surface temperature due to OTEC operation is greater in the winter than in the summer, being about .5°C in the winter but near zero in the summer. The mean drop in the sea surface temperature during the tenth year of OTEC operation is about 0.37°C.

## 5. SUMMARY

The results of this one-dimensional model indicate that the effect of the operation of one hundred 200 megawatt OTEC plants on the mean vertical thermal structure of the Gulf of Mexico would be fairly slight. With complete recirculation of the OTEC plant intake and discharge flows within the Gulf, the predicted drop of the mean sea surface temperature is about 0.05°C and the rate of warming of the deep water between the cold water intake and discharge

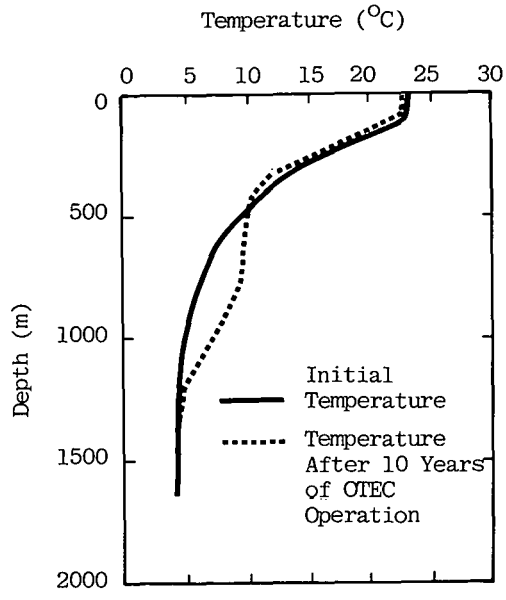



Fig. 12. Effect of Operation of 1000 OTEC Plants in Gulf of Mexico on January Temperature Profile.

levels is about 0.03°C/yr. Even with 1000 plants, the drop in the mean sea surface temperature is less than 0.5°C. However, recirculation between the cold water intake and discharge flows with such a large number of plants has the potential to decrease significantly the available thermal resource due to warming of the deep water. This model assumes the worst in the sense that it does not allow for the removal of this accumulating heat from the Gulf by the currents. It might be expected that cold water from the Caribbean would seek to displace warm water at an equivalent depth in the Gulf. Hence, the thermal resource available for very large scale OTEC operation in the Gulf may depend upon the rate of replacement of warmed deep water by colder water from the Caribbean.

## ACKNOWLEDGEMENTS

This report was prepared as part of the research program, "Theoretical Fluid Dynamical Studies of Resource Availability and Environmental Impact of Ocean Thermal Power Plants", in the Naval Research Laboratory, supported by the Ocean Thermal Energy Conversion Program, Division of Solar Energy, Energy Research and Development Administration, under ERDA contract E (49-26) 1005. The majority of the work was performed under the subcontract N00014-77-C-0033 with Science Applications, Inc.

REFERENCES


1. Budyko, M. I, 1963: Atlas of Heat Balance of the World. Glabnaia Geofiz. Observ. Also, Guide to the Atlas of the Heat Balance of the Earth, Transl. by I. A. Donehoo, U.S. Wea. Bur., WB/T-106, Washington, D.C.

2. Bunker, A. F., 1976: Computations of Surface Energy Flux and Annual Air-Sea Interaction Cycles of the North Atlantic Ocean. Mon. Wea. Rev., 104(9): p. 1122-1140.

3. Hastenrath, S. L., 1968: Estimates of the Latent and Sensible Heat Flux for the Caribbean Sea and the Gulf of Mexico. Limnol and Ocean., 13(3): p. 322-331.

4. Harding, J. L., and Nowlin, W. D., 1966: Gulf of Mexico. The Encyclopedia of Oceanography, R. W. Fairbridge Ed. Reinhold Publishing Corp., New York: p. 324-331.

5. Jacobs, W. C., 1942: On the Energy Exchange Between Sea and Atmosphere. J. Marine Res., 5: p. 37-66.

6. Jerlov, N. G.: Optical Studies of Ocean Water. Rept. of Swedish Deep-Sea Exped., 3, 1951.

7. Laevastu, T., 1960: Factors Affecting the Temperature of the Surface Layer of the Sea, Soc. Scient. Fennica, Comm. Phys. Mat., 25: p. 1.

8. Laevastu, T., and Harding, J. M., 1974: Numerical Analysis and Forecasting of Surface-Air Temperature and Water Vapor Pressure. J. Geo. Res., 79(30): p. 4478-4480.

9. Leipper, Dale F., 1970: A Sequence of Current Patterns in the Gulf of Mexico. J. Geo. Res., 75(3): p. 637-657.

10. McLellan, H. J. and Nowlin, W. D., 1963: Some Features of the Deep Water in the Gulf of Mexico, J. Marine Res., 21(3): p. 233-245.

11. Mellor, G. L., and Yamada, T., 1974: A Hierarchy of Turbulence Closure Models for Planetary Boundary Layers. J. Atmos. Sci., 31: p. 1791-1806.

12. Morrison, J. M., Merrell, W., and Nowlin, W. D., Jr., 1973: The Waters of the Eastern Gulf of Mexico as Observed during May 1972; I. Data collected aboard the R. V. Alaminos. Unpubl. Tech. Rept. of Dept. of Oceanogr., Texas A&M Univ., Ref. 73-10T: p. 330.

13. Nowlin, W. D., Jr., and McLellan, H. J., 1967: A Characterization of the Gulf of Mexico Waters in Winter. J. Marine Res., 25: p. 29-59.

14. Roberts, G. O., Stratified Turbulence Modeling for the Near-Field External Flow of an Ocean Thermal Power Plant; previous report in this volume.

15. Summary of Synoptic Meteorological Observations of North Atlantic Coastal Marine Areas, 1975. U. S. Naval Weather Service Command, Springfield, Va.: National Technical Information Service.

16. Veronis, G., 1969: On Theoretical Models of the Thermocline Circulation. Deep-Sea Res., 16 (Supp.): p. 301-323.

17. Wyrtki, K., 1965: The Average Annual Heat Balance of the North Pacific Ocean and its Relation to Oceanic Circulation. J. Geo. Rev., 70: p. 4547-4560.

# INVESTIGATIONS OF MIXING AND RECIRCULATION IN THE VICINITY OF AN OCEAN THERMAL ENERGY CONVERSION PLANT*

GERHARD H. JIRKA, DAVID J. FRY,
R. PETER JOHNSON, AND DONALD R. F. HARLEMAN
*R. M. Parsons Laboratory for Hydrodynamics and Water Resources*
*Department of Civil Engineering*
*Massachusetts Institute of Technology*
*Cambridge, Massachusetts*

Abstract

Experimental and analytical studies on the external fluid mechanics in the vicinity of an Ocean Thermal Energy Conversion (OTEC) plant are conducted. Schematic OTEC conditions defined by a mixed discharge mode and a discretely stratified ocean are assumed. The interaction of several fluid mechanical regions, a jet entrainment zone, an intermediate buoyant layer and an intake flow zone, is simulated in a shallow laboratory basin representing the upper layer of the stratified ocean. A concurrent analytical model development gives satisfactory agreement with the experiments and allows to define an approximate criterion for the existence of recirculation of discharge water back into the plant intake.

## INTRODUCTION

Studies of the disturbances of the ambient temperature and flow fields which are caused by the operation of Ocean Thermal Energy Conversion (OTEC) Plants and needed for purposes of resource assessment and environmental impact assessment. The OTEC energy resource is the temperature difference ($\Delta T$) which exists between the surface and lower layers of the tropical ocean. A decrease in $\Delta T$ may be caused by mixing and recirculation which are generated by the interaction of intake and discharge flows of the OTEC plant. Small decreases in $\Delta T$ have a significant effect on the power delivery of an OTEC plant. Using the data of economic analyses (1) it can be estimated that, for a base value of $\Delta T = 20^{\circ}C$, a $\Delta T$ drop of $1^{\circ}C$ will cause a 13% loss in power output. The environmental effect of OTEC relates to the multiplicity of changes of the physical, chemical and biological characteristics of the ocean waters surrounding the OTEC installation. These disturbances have to be considered relative to the baseline conditions prior to plant operation and a clear understanding of the external fluid transport processes is a prerequisite to their prediction.

The exact determination of the OTEC external fluid motion is a difficult task due to the complicated interaction of different fluid mechanical processes, the nature of the ocean ambient conditions and the numerous design details of the plant itself. The ongoing studies at the MIT Energy Laboratory, consisting of experimental and analytical investigations, are aimed at a schematic representation of OTEC external fluid mechanics, rather than at specific designs at a specific ocean site. In particular, our studies have the following objectives: 1) Identify the mixing and transport processes in the vicinity of an OTEC plant. 2) Demonstrate the feasibility of OTEC to operate without near-field recirculation. 3) Develop predictive analytical models and criteria for engineering design. 4) Provide experimental data on the entire OTEC flow field for concurrent numerical modeling efforts by other ERDA contractors.

## OTEC SCHEMATIZATION

Several schematizations of actual OTEC ocean and plant design conditions are introduced. These schematizations allow a considerable simplification in the experimental and analytical studies, but preserve the salient interaction of the different fluid transport processes and give a useful and accurate first indication of actual OTEC operating conditions.

a) Mixed discharge mode: The various industrial and and university teams which have developed conceptual OTEC designs during the past five years differ in the

*Work in progress under support from the Division of Solar Energy, ERDA, Contract No. E(11-1)2909 to M.I.T.

consideration of the discharge mode. In the separate discharge mode, the warm upper layer water, after passing through the evaporator, is discharged back into the upper layer and the cool lower layer water, after passing through the condenser, back to the lower layer. The two discharges are generally separated by a considerable vertical distance. In the mixed discharge mode, the evaporator and condenser flow are either directly mixed before discharging or are discharged close to each other so that mixing occurs outside but close to the plant. As a consequence, in the separate discharge mode separate jet paths exist in the upper layer and lower layer and some recirculation within the upper layer is likely to occur due to its limited depth and because of the low negative buoyancy of the evaporator jet with respect to the upper layer. The effect of the recirculation, however, is small due to the small temperature drop within the condenser (in the order of 2°C). In the mixed discharge mode, on the other hand, only one jet path will be established and located within the thermocline of the ocean. It appears that recirculation for this case may be altogether eliminated because of the stronger negative buoyancy of the mixed discharge jet with respect to the upper layer. A mixed discharge mode with a discharge depth at the thermocline has been assumed as the basis for our studies.

b) Discretely stratified ocean: The actual tropical ocean exhibits continuously varying profiles for density, temperature and velocity. It is possible, however, to distinguish a thermocline region of rapidly changing temperature and density. Thus, as shown in Fig. 1, it is assumed that the ocean is discretely

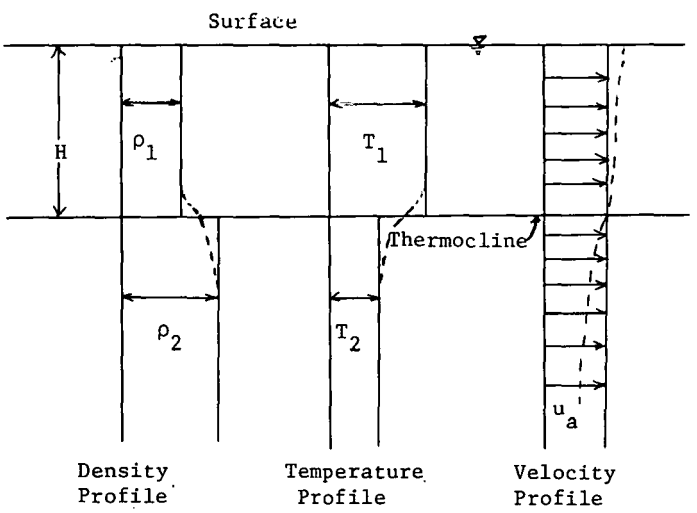



Fig. 1 Discretely Stratified Ocean Schematization (Dashed Lines Indicate Actual Ocean Profiles).

stratified with upper layer properties $\rho_1$ and $T_2$ and lower layer properties $\rho_2$ and $T_2$ and a thermocline depth H. The ambient velocity distribution is taken as uniform, $u_a$. In combination with the mixed discharge mode schematization, the discharge density is $\rho_o = 1/2(\rho_1 = \rho_2)$. A view of the OTEC flow field under this condition is shown in Fig. 2 for the case

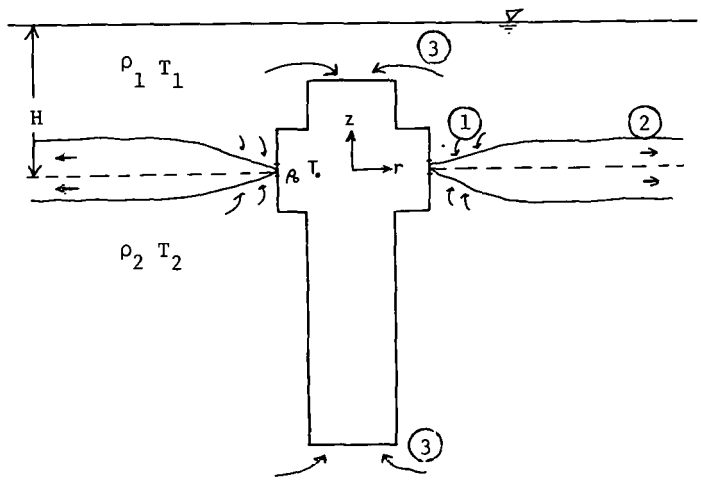
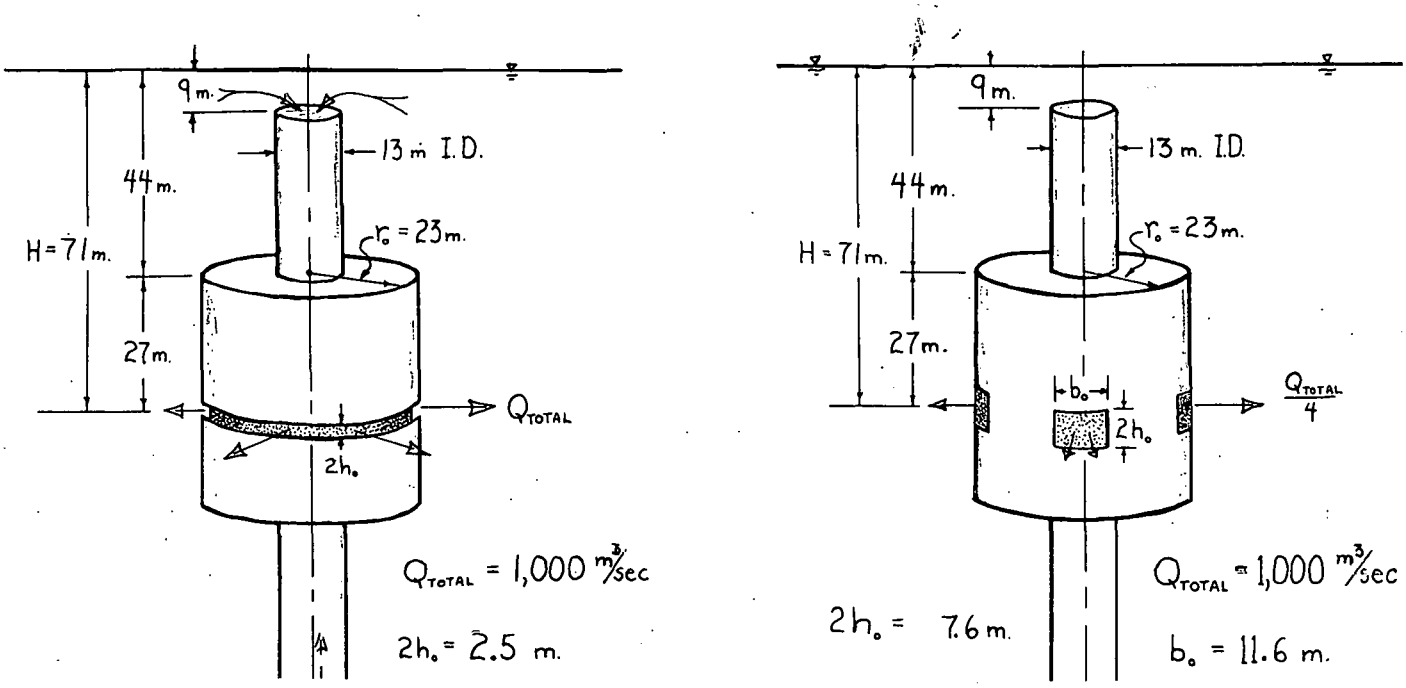



Fig. 2 Distinct Fluid Mechanical Zones for OTEC Operation in Stagnant Ocean. 1: Jet Zone, 2: Intermediate Buoyant Layer, 3: Intake Flow Zone.

of stagnant ambient conditions ($u_a = 0$) and in the absence of recirculation. Three distinct fluid mechanical zones can be hypothesized: 1) A jet zone in which entrainment of ambient fluid in the discharge flow occurs. 2) An intermediate buoyant layer (density current) which undergoes a transient spreading motion. 3) A intake zone in which flow toward the plant intakes occurs.

c) Plant design: A survey of previous design studies was made to determine values for flow rates, $Q_o$, discharge velocities, $U_o$, and size of intake and discharge ports, corresponding to a typical 100 MWe OTEC plant. This average design formed a baseline for the further studies in which the design parameters are varied, including an increase in plant size of up to 300 MWe. The basic plant shape was cylindrical (radius $r_o$) as shown in Fig. 3. A fixed intake design is assumed in the form of a vertically oriented pipe with an opening below the surface. Two types of discharge designs are simulated: (i) A radial jet discharge in form of a slot (height $2h_o$) extending around the periphery of the cylindrical plant (ii) Four separate jet discharges (height $2h_o$, width $b_o$) at angle of 90° to each other. Studies with and without ambient current were conducted.

Several non-dimensional parameters describe the external flow field. The most important ones are (neglecting the intake design which is of secondary order):




a) Radial Jet Discharge

b) Separate Jet Discharge

Fig. 3 Baseline Geometry and Flow Parameters for Mixed Discharge Conditions Assumed in Experimental Program ($\Delta T = 22^{\circ}C$) at an Assumed Scale Ratio of 1/200.

Densimetric Froude number $F_o^* = \dfrac{U_o}{\sqrt{\dfrac{\rho_o - \rho_1}{\rho_1} g L}}$

Discharge geometry $\dfrac{L}{r_o}$

Layer depth $\dfrac{H}{L}$

Volume flux parameter $\dfrac{u_a H^2}{Q_o}$

where $Q_o$ is the plant flow ($Q_o = 4U_oA$) and L is the governing scaling length given by

$$L = A^{1/2}$$

and A is chosen as the area of a quarter section of the radial discharge ($A = 1/2\pi\, r_o h_o$) or as the area of one of the four separate ports ($A = h_o b_o$). This choice of scaling length allows comparison of the different discharge designs with each other.

## EXPERIMENTS

Despite the above schematizations the experimental simulation of OTEC external fluid mechanics would be a formidable task. A further simplification is introduced by concentrating on the fluid motions in the upper layer only, where the recirculation potential is much higher due to the limited extent. Assuming that the discharge jet motion is symmetric with respect to the thermocline (see Fig. 2), the upper layer motion can be simulated in an inverted fashion using a shallow laboratory basin as shown in Fig. 4.

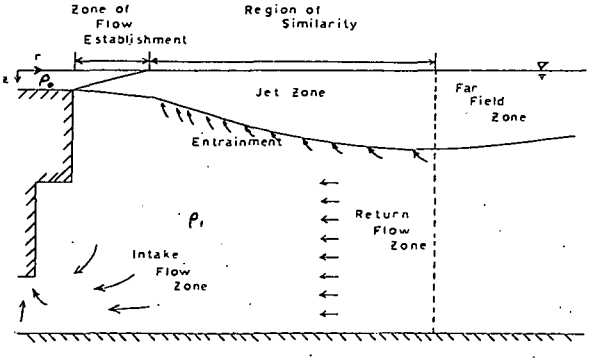



Fig. 4 Experimental Simulation of OTEC Operation in Ocean Upper Layer.

The inversion is necessary to avoid any jet wall friction at the bottom of the laboratory basin. Thus, the discharge jet which occurs at the interface of a discretely stratified prototype ocean is represented by a buoyant surface jet in the model. In the model the same initial jet density difference is maintained as in the prototype ($\rho_o - \rho_1$), only the direction of buoyancy is reversed. The shear which exists at the bottom of the model basin (corresponding to the ocean surface) is considered as negligible for the small motion. Note, however, that in the prototype (Fig. 2)

the density of the interface (z = 0) will be constant and equal to the discharge density ($\rho_o$) while in the model (Fig. 4) the density of the surface (z = 0) is variable and approaches the ambient density ($\rho_1$) at at large distances. This difference will make the model results conservative, i.e., in the model recirculation is more likely to occur as the effect of buoyant damping on jet mixing is smaller. The conservativeness can be estimated by applying the analytical model to both experimental and prototypical conditions.

The experiments were conducted in a 12 m x 18 m x 0.4 m laboratory basin. At an undistorted model scale of 1/200 this allows replication of an ocean surface area of about 2.5 km x 5 km and a thermocline depth of 70 m. The model parameters are scaled according to the densimetric Froude law and the discharge Reynolds number is large enough to model the jet turbulence. The data acquisition is primarily directed at measuring the mean temperature field in the OTEC vicinity ($\sim$ 1 km prototype). For this purpose a traversing probe frame with 100 thermistor probes (0.1°C accuracy) is utilized. Additional measurements include selected mean velocity profiles, turbulent temperature fluctuations and fluorescent dye concentrations in the intake as indicators of near-field recirculation.

Several series of experiments for various combinations of radial and separate jet geometries in stagnant and ambient current conditions have been conducted. The results are displayed in temperature maps, with examples given in Figs. 5, 6 and 7.

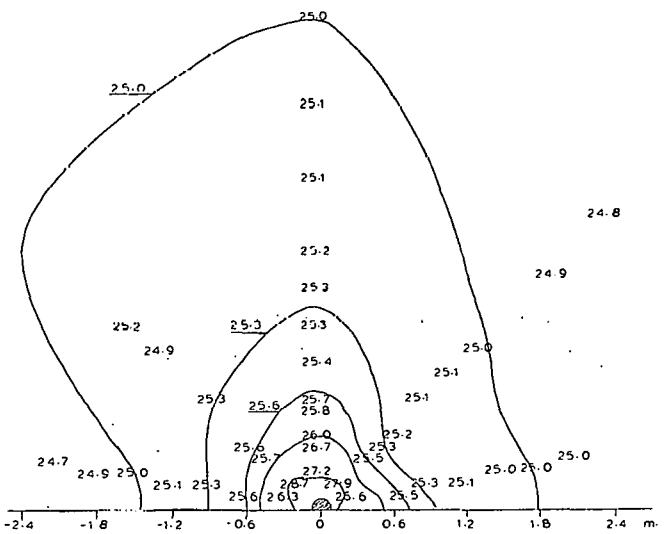



Fig. 5 Surface Isotherms (°C) for Radial Jet Discharge, Stagnant Ocean Conditions, $T_o$=34.6°C, $T_{ambient}$=23.5°C. Lower Boundary is Symmetry Line.

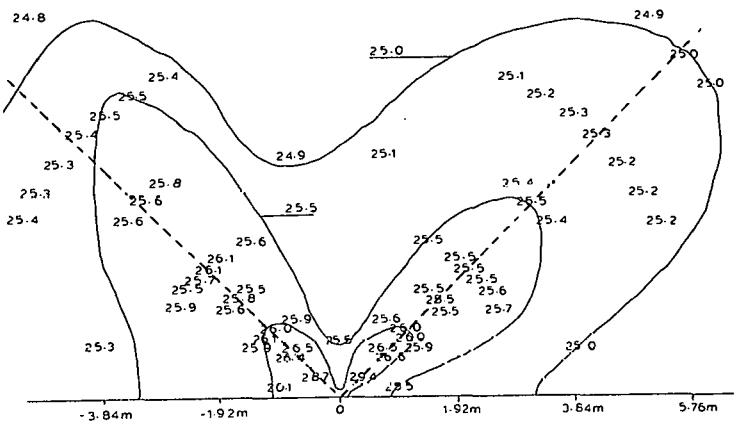



Fig. 6 Surface Isotherms (°C) for Separate Jet Discharge, Stagnant Ocean Conditions, $T_o$=35.0°C, $T_{ambient}$=23.9°C. Lower Boundary is Symmetry Line.

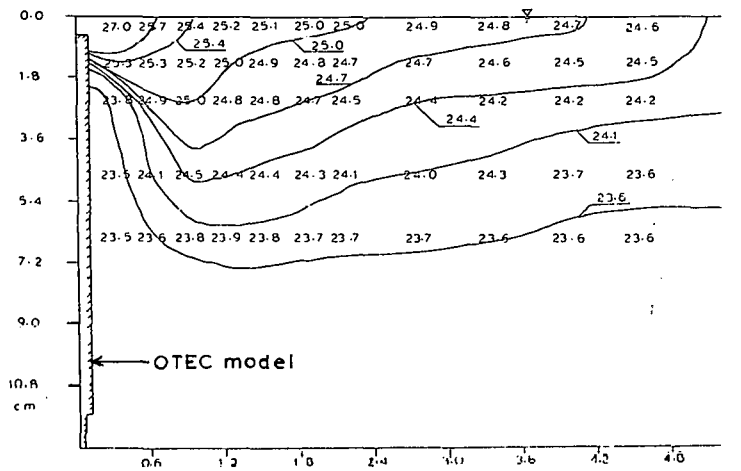



Fig. 7 Radial Transect of Radial Jet Structure for Conditions of Fig. 5. Vertically Distorted Plot.

Typically, the jet temperature difference drops off rapidly and approaches a relatively stable value $\Delta T_s$ at a larger distance, while the jet thickness increases initially and levels out at a certain maximum value. Thus, interesting jet properties are the stable dilution $S_s = \Delta T_s/\Delta T_o$, where $\Delta T_o = T_o - T_1$ is the initial temperature difference, and $h_{max}/L$. Comparison of the parameters for the different experimental series is given in Figs. 8 and 9. These comparisons demonstrate that the jet mixing capability (as indicated by $S_s$ and $h_{max}/L$) is relatively insensitive to the details of discharge design (whether radial or separate jet) and to the effect of an ambient current. The latter con-

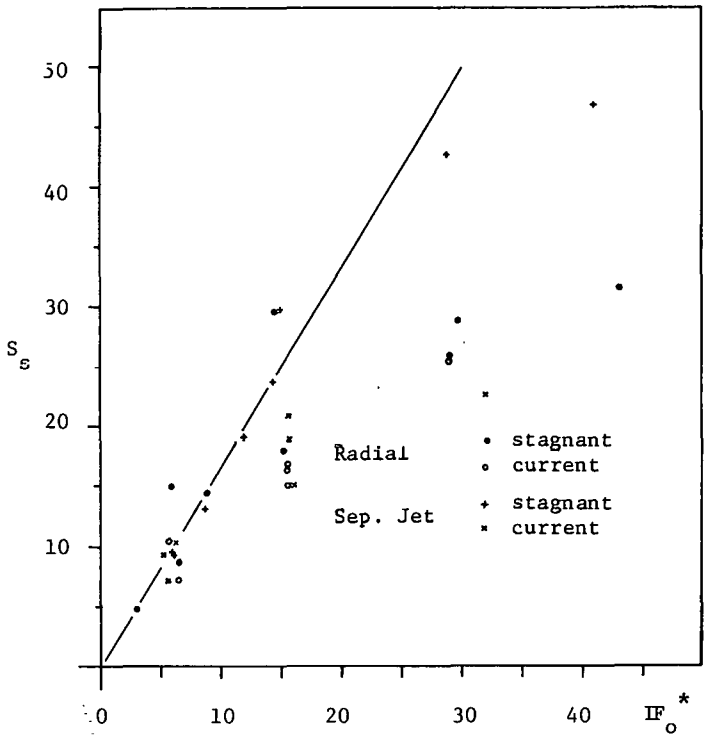



Fig. 8 Stable Dilutions, $S_s$, as a Function of Discharge Densimetric Froude Number, $F_o^*$, for Different Experimental Conditions.

clusion is limited by the experimental range which allowed similation of only small velocities (up to 0.1 m/s prototype). The near-field mixing is strongly dependent on the magnitude of the initial discharge velocity as expressed by the value of $F_o^*$. Some degree of near-field recirculation was evident in only two experiments with high values of $F_o^*$, representing a large OTEC site with extreme discharge conditions, as marked on Fig. 8.

## ANALYTICAL MODEL

The analytical model development is aimed at describing the buoyant jet mixing characteristics under stagnant ocean conditions which can be viewed as the most limiting case for OTEC performance. Models are developed for both the radial jet and separate jet geometries. The model formulation is given by the simultaneous differential equations for the conservation of mass, momentum and heat along the jet path. In particular, the radial jet model has an added term which accounts for the loss of jet momentum due to entrainment of fluid moving inward toward the plant intake and the jet initial region. The separate jet model represents an adaptation of an earlier surface jet model by Stolzenbach and Harleman (2). In both cases, the role of buoyancy is included as a damping

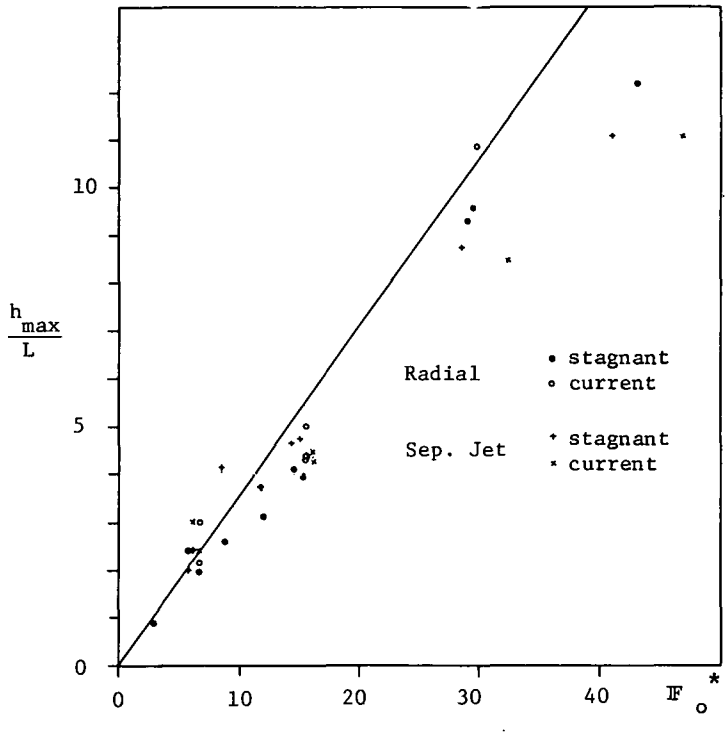
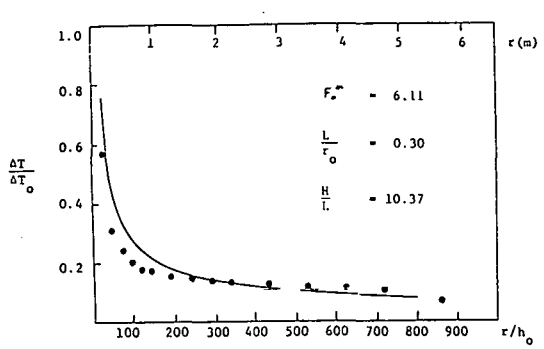


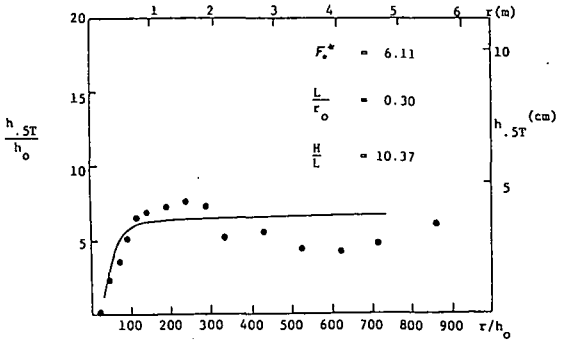

Fig. 9 Maximum Jet Depth $h_{max}/L$ as a Function of Discharge Densimetric Froude Number $F_o^*$ for Different Experimental Conditions.

factor for the vertical turbulent jet entrainment and as a pressure force acting to spread the less dense jet water in the horizontal direction. The jet equations are solved by a fourth-order Runge-Kutta numerical routine with appropriate initial conditions at the plant efflux.

a) Comparison with experiments (Surface jet): Using the appropriate boundary condition for temperature at the water surface ($dT/dz = 0$) and established jet entrainment coefficient, comparisons of the analytical model predictions with the experimental data give excellent agreement, as shown in Fig. 10 for the case of a radial jet discharge. Fig. 10a is a plot of predicted and observed normalized centerline temperature rises as a function of radial distance from the plant, while Fig. 10b compares the half-temperature depth, i.e., the depth where the temperature rise is half the centerline temperature rise. For those experiments, however, in which some near-field recirculation had been observed the analytical model failed to give satisfactory predictions, both with respect to centerline temperatures and to jet depths. This failure is attributed to the existence of significant dynamic pressure effects in the jet motion whenever the jet depth occupies a large portion of the available layer depth. In principle, the analytical model is applicable only to non-recirculating conditions. Using the available experimental information an approximate




a) Temperature Rise vs. Distance.




b) Half-temperature Depth vs. Distance.

Fig. 10 Comparison of Predicted and Observed Jet Parameters for Radial Jet, Stagnant Ocean Conditions.

limit of applicability is

$$\frac{h_{max}}{H} \lesssim 0.5 \qquad (1)$$

where $h_{max}$ is the predicted total jet depth. If equation (1) is not satisfied, it can be assumed that near-field recirculation will occur with the degree of recirculation increasing as $h_{max}/H$ increases. Large values of $h_{max}/H$ are generally associated with large discharge densimetric Froude number $F_o^*$ (as evident from Fig. 9), but also depend on $L/r_o$ and $H/L$.

b) Application to the prototype (Interface jet): The satisfactory agreement of the near-field mixing model with experimental data can be seen as a general validation of the model. In applying the model to prototypical conditions, the differences in the temperature (density) boundary condition has to be considered, as noted earlier. In fact, the analytical model can be used to demonstrate the degree of conservativeness with regard to the onset of recirculation in the experiments. Using the prototype boundary condition of the interface ($T=T_o$=const.), the predictions for the jet depth are shown in Fig. 11 and compared to the experimental case (surface jet). It can be seen that for a given value of $F_o^*$ the jet depth is almost twice as large for the experimental (surface jet) case as for the prototype (interface jet). Furthermore, for certain values of $F_o^*$, Equation (1) may not hold for experimental conditions indicating recirculation, while it holds for the prototype indicating absence of recirculation.

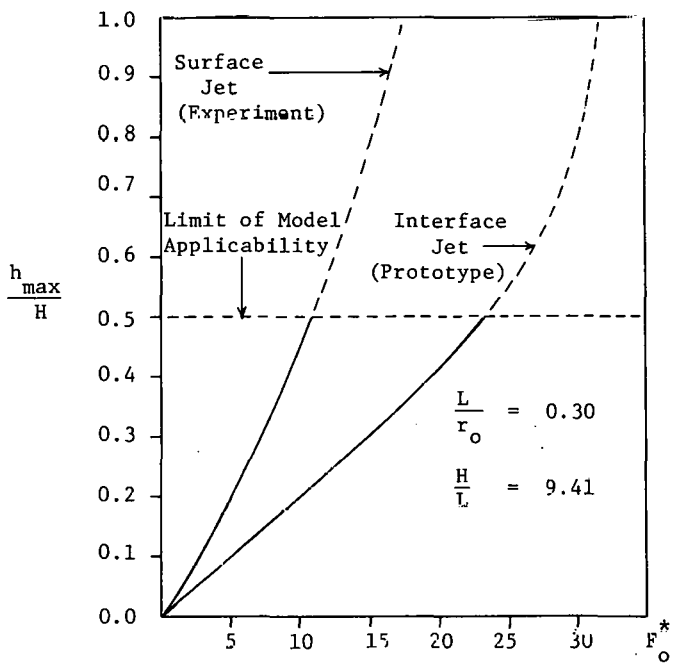



Fig. 11 Prediction of Jet Penetration Depth $h_{max}/L$ vs. $F_o^*$ for both Experimental and Prototype Conditions. Model Applicability is Constrained by $h_{max}/L \lesssim 0.5$.

## CONCLUSIONS

Our studies are continuing. However, the following preliminary conclusions can be offered on the potential for recirculation for OTEC plants and appropriate design strategies:

(i) The recirculation potential seems highest for stagnant ocean conditions with small ocean currents ($\sim$ 0.10 m/s) approaching this condition.

(ii) A separate discharge mode with the evaporator flow exhausting into the upper layer and the condenser flow into the lower layer carries a high likelihood for recirculation in the upper layer. The attendant $\Delta T$ depression may be small, however, due to the small temperature drop of the evaporator flow.

(iii) The mixed discharge mode (combined evaporator and condenser discharge) offers the possibility to completely prevent near-

field recirculation.

(iv) The likelihood for the near-field recirculation (as measured by the mixing capability of the discharge jets) is independent of the geometric details of the discharge ports but strongly dependent on the discharge velocity. Increasing discharge velocities carries a higher potential for recirculation.

(v) It appears that OTEC plants in the size range of 100 MWe to 200 MWe and under usual baseline stratification conditions can be designed to operate without near-field recirculation by using a low velocity (low densimetric Froude number) mixed discharge mode at the ocean thermocline.

REFERENCES

1. A. Lavi, Progress Report: Solar Sea Power Project, Carnegie Mellon University, Pittsburgh, Pa., August 1975.

2. K.D. Stolzenbach and D.R.F. Harleman, "An Analytical and Experimental Investigation of Surface Discharges of Heated Water," R.M. Parsons Laboratory Technical Report No. 135, M.I.T., Cambridge, Mass., February 1971.

# THE EXTERNAL FLOW INDUCED BY AN OCEAN THERMAL ENERGY CONVERSION (OTEC) POWER PLANT*

T. R. SUNDARAM, E. SAMBUCO, A. M. SINNARWALLA, AND S. K. KAPUR
*Applied Science Department*
*HYDRONAUTICS, Incorporated*
*7210 Pindell School Road*
*Laurel, Maryland*

Abstract

As an essential part of its operation, the OTEC plant withdraws large amounts of water (typically 6 x $10^4$ gpm per MW of capacity) from both the surface layers and the deeper layers of the ocean and discharges them at intermediate levels. The circulations induced in the ambient ocean of these large withdrawals and discharges are of paramount importance, since any adverse changes in the ambient stratification will directly influence the operational efficiency of the plant itself. Specifically, any "short circuit" between the outflows and the inflows will directly lead to a decrease in power production. Because of this direct "feed back" effect, the external flow induced by an OTEC plant has to be considered as an essential part of its operation. The present paper describes the interim results from an on-going experimental study to assess the recirculation potential under various design and environmental conditions. The method used is a "building block" approach in which "dissected" parts of the overall problem are isolated and studied experimentally. Specifically, experiments are described on two classes of problems, the first in which an ambient current is present but not ambient stratification, and the second in which the opposite is true. Recirculation is measured directly by introducing dye into the discharges and by measuring the dye concentration in the intake flow. Maps of the distributions in the jet flow of the mean and turbulent quantities are also given; such detailed measurements being of relevance to the "tuning" mathematical (turbulence) models of the flow field.

The similitude parameters governing the problem are identified and the manner in which the results of the "dissected" studies can be used to construct results for the overall problem is discussed.

## I. Introduction

Many of the factors that influence the environmental impact of an Ocean Thermal Energy Conversion (OTEC) power plant are essentially the same as those that influence the environmental impact of conventional power plants. Thus, at first sight it may appear paradoxical that the extensive body of literature which exists on the behavior of the thermal discharges from conventional plants cannot be used directly to predict the environmental impact of OTEC plants, or that any additional research into this problem is required at all. The reason for this apparent paradox is that there are two crucial differences, as far as environmental impact is concerned, between conventional power plants and an OTEC plant. Firstly, by its very nature of operation, an OTEC plant interacts with itself; that is, the plant alters the very resource (namely, the ambient thermal stratification) from which it derives its power. Moreover, any direct "short circuit" between the outflows and inflows will directly lead to a decrease in power production. Because of this direct "feed back" effect, the external flow induced by an OTEC plant has to be considered as an essential part of its operation.

The second essential difference between an OTEC plant and a conventional power plant is that the circulating flow in the former is approximately one hundred times larger than that in the latter. That is, an OTEC plant typically withdraws about 6 x $10^4$ gpm of water per MW of capacity from both the surface and deeper layers of the ocean and discharges it at intermediate levels. As will be seen below, the degree of interaction between the inflows and the outflows is directly dependent on the rate of circulating water flow.

*The research described in the present paper is being supported by The Energy Research and Development Administration under Contract No. E(49-18)-2348.

The present paper presents the interim results from an ongoing experimental study being conducted by HYDRONAUTICS, Incorporated on the internal flow field induced by the operation of an ocean thermal power plant. The principal objectives of the study are to assess the possibility of recirculation of the outflows into the inflows through controlled laboratory experiments on "dissected" parts of the overall problem and to make detailed measurements of the temperature, velocity and turbulence characteristics of the flow field.

In Section II of the present paper the characteristics of the external flow field of an OTEC plant are first described so as to set the objectives stated above in their proper perspective. In addition to a discussion of the rationale behind the objectives, Section II also contains a description of the selected method of approach to the solution of this complex problem. Some interim results are given in Section III and, finally, some preliminary conclusions are set forth in Section IV.

## II. Characteristics of the OTECPP Flow Field

The external flow field generated by the operation of an OTEC power plant is extremely difficult to predict because of the large number of factors influencing it. For example, the flow field is influenced by the plant geometrical characteristics (such as: intake and outflow dimensions, configurations and orientations, as well as their distances of separations; the geometry of the platform and the power plant "shell"; and so on), plant operating characteristics (such as the temperature differentials across the evaporators and condensers, and the volume rates of the withdrawn and discharged flows), and the ambient environmental conditions (such as density stratification, currents including current shear, turbulence and internal-wave motions). Theoretical understanding of such complex turbulent flow fields is not sufficiently advanced to permit detailed parametric calculations to be carried out on the combination of conditions under which recirculation may be expected to occur. Indeed our ability to predict the behavior of jet flows (discharges) in the presence of sinks (intakes) is woefully inadequate even under otherwise simplified external conditions, and to illustrate this dilemma several simplified elements of the OTECPP flow field are shown in Fig. 1.

The simplified problem shown in Fig. 1(a) is that of the head-on discharge of a jet into an oncoming current in the presence of a sink located above the discharge. In some of the proposed OTECPP designs, the (warm and cold water) discharges consist of four mutually perpendicular circular jets. Under these conditions it is highly likely that one of the discharge jets will be nearly head-on into an oncumming current, with the jet penetrating a finite distance into the current; beyond this point the jet flow will be turned around and flow past the OTECPP structure. Clearly a potential for recirculation exists in this case, but it cannot be predicted theoretically in quantitative terms. The problem shown in planview in Fig. 1(b) is that of the interaction of the OTECPP flow field (intake and discharge) with the wake of the OTECPP itself. Here again no satisfactory theoretical solution is possible.

The case in Fig. 1(c) is that of the withdrawal from, and discharge into, a stratified surrounding in the absence of an ambient current. In this type of flow, an increasingly deeper layer of water will be withdrawn into the intake at increasingly larger distances from it, as shown in the figure. The discharge will eventually mix with the intake flow as depicted in the figure, but our ability to describe theoretically when and how the mixing will occur is limited (1). The case described in Fig. 1(d) is that of a negatively buoyant discharge into a homogeneous surrounding in the absence of a current. Here again the influence of the intake on the behavior of the buoyant plume cannot be described theoretically.

Even from the brief description given above, the complexity of the possible interactions between an OTECPP and the surrounding ocean should be clear. As mentioned earlier,

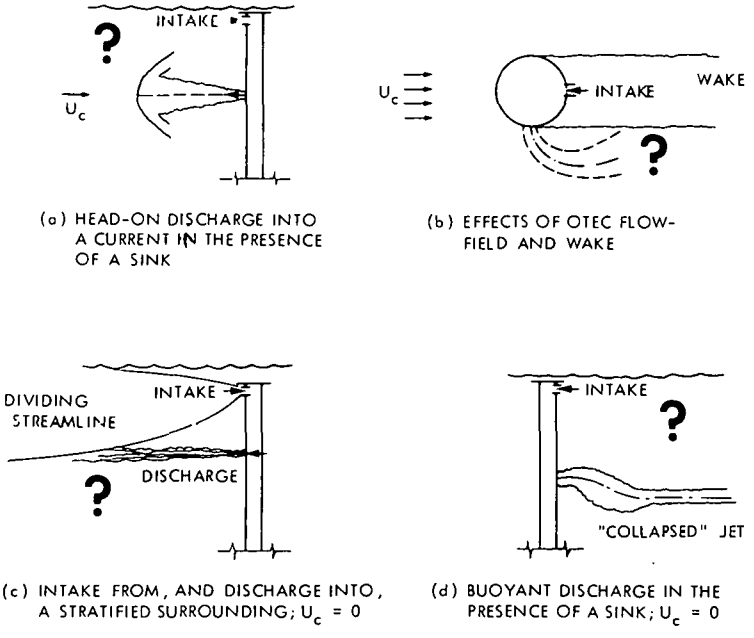



FIGURE 1 - SOME "DISSECTED" PROBLEMS RELEVANT TO AN OTECPP

present theoretically understanding of many of the operative turbulent-flow phenomena is inadequate, and a theoretical analysis of the complete flow field is impossible. While existing computational methods (2-4) for calculating turbulent flows, called "closure" models, offer some hope of being eventually able to treat such flows, their present state of development is not sufficiently advanced to provide satisfactory answers. The basic difficulty in the analysis of all turbulent flows is that the number of unknowns (including the fluctuating quantities and their correlations) is always larger than the number of equations available to solve for them. In the simplest cases, this difficulty is overcome by assuming that the effective "eddy diffusivity" is either constant, or that it is related to the gradients of the mean-flow quantities, through assumed relationships such as the mixing length hypothesis. In the "closure models", the above procedure is carried one step further, and relationships are postulated between some correlations of turbulent, fluctuating quantities and other correlations (often of higher order). However, such a procedure introduces a large number of empirical "constants" into the calculational framework, and, while it is hoped that these "constants" are universal ones, independent of the specific flow situations, this is far from certain. Thus, before these closure models can be utilized to analyze a specific problem of interest, controlled laboratory experiments are needed on that specific problem, so as to enable these models to be "tuned" to that specific situation. In this regard, it needs to be emphasized that measurement of the mean-flow variables (such as temperature and velocity) alone is inadequate for such "tuning", since the assumptions in the closure models are on the relationships between the turbulent fluctuations. Thus the assumptions can be directly verified only if the appropriate turbulence parameters are measured.

On the other hand, laboratory simulations of the entire flow field are difficult to achieve, and scale-model experiments on specific OTECPP designs are unlikely to lead to parametric information necessary for minimizing recirculation. It is our view that the optimum approach to advancing our level of understanding of this problem, and our ability to carry out parametric calculations, is to use a "building block" approach in which the individual phenomena of interest are isolated and studied separately. Complex interactions can be added gradually as success is achieved in delineating the relevant features of the simpler "building blocks".

The "building block" approach is also a logical one from a different point of view. Because of the direct impact of recirculation on power plant efficiency, it is appropriate to consider "worst case" examples; that is, extreme conditions (not ordinarily encountered) under which recirculation may occur. For example, it is relevant to consider the type of warm-water recirculation that can occur in th absence of any stratification in the upper oc layers between the levels of the intake and discharge, since such conditions can be expected to occur occasionally even with the best plant designs. Similarly, the recirculation potential in the absence of ambient currents has also to be considered, since there will always be periods, at any site, during which the ambient currents are either zero or are negligibly small.

Thus the approach that is used in the present study is to conduct controlled laboratory experiments on two classes of "dissected" parts of the overall problem. In the first class of problems, effects of an ambient current are included, but not those of ambient stratification; in the second class of problems the converse is the case. Specific examples of "dissected" experiments in the two classes of problems are described in the next section.

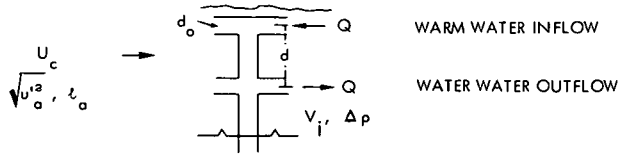
## III. Experimental Results and Discussion

### Similitude Requirements

When conducting laboratory tests simulating OTECPP flow fields, whether it be simulations of the entire flow field or some dissected parts of it, care must be taken to ensure that certain similarity parameters have the same values in the laboratory tests as they have in the full-scale flow field. These characteristic non-dimensional parameters are listed in Table 1.

TABLE 1 - IMPORTANT NON-DIMENSIONAL PARAMETERS

| | |
|---|---|
| $\frac{Q}{d^2 U_c}$ | - CHARACTERIZES EFFECTS OF FLOW RATE |
| $\frac{Q}{d^3 N}$ | - CHARACTERIZES EFFECTS OF STRATIFICATION |
| $\frac{d_o}{d}$ or $\frac{V_j}{U_c}$ | - CHARACTERIZES EFFECTS OF JET MOMENTUM |
| $\frac{V_j^2}{g\frac{\Delta\rho}{\rho} d_o}$ OR $\frac{Q^2}{g\frac{\Delta\rho}{\rho} d_o^5}$ | - CHARACTERIZES EFFECTS OF DISCHARGE BUOYANCY ( Relative to ambient ) |
| $\sqrt{\frac{u'^2_o}{V_j}}$, $\frac{\ell_o}{d}$ | - CHARACTERIZE AMBIENT TURBULENCE |



The first nondimensional combination shown (in which Q is the flow rate through the intake or discharge, d is the separation between the intake and discharge, and $U_c$ is the ambient current) characterizes the effect of the ambient current on recirculation, and is proportional to the ratio of the current induced at the discharge by the intake to that of the ambient current. It arises naturally, when considering the effect of an ambient current on recirculation in the absence of stratification. Indeed, when the effect of jet momentum is negligible, Sundaram et al. (5) have shown that a criterion for recirculation can be derived in terms of this parameter.

The second parameter, in which N is Brunt-Vaisala frequency of the ambient ocean, characterizes the inhibiting influence of the stable stratification on recirculation. It is essentially a Froude number based on the circulating water flow rate. The two parameters shown under the third category are equivalent, and characterize the effect of jet momentum including the penetration of the discharge into a cross current. In these parameters $d_o$ is the diameter of the discharge pipe and $V_j$ is the jet velocity. Both forms listed under the fourth parameter represent Froude numbers based on the outflow buoyancy, which characterize both the trajectory of the jet and its spread. The last two parameters shown in the table characterize the effects of embient turbulence. In general, the ambient turbulence can be characterized in terms of a characteristic velocity (namely, the root-mean-square intensity of turbulence, $(\overline{u'^2})^{\frac{1}{2}}$) and a characteristic length scale (namely, the integral scale of the turbulence, $\ell_a$).*

The physical significance of these similitude parameters is that the dependent variables (in their nondimensional form) can be written as functions of these parameters. Thus, for example, the degree of recirculation can be expressed in the form,

$$\text{Percent Recirculation} = f\left(\frac{Q}{d^2 U_c}, \frac{Q}{d^3 N}, \frac{d_o}{d}, \frac{V_j^2}{g\frac{\Delta\rho}{\rho} d_o}, \frac{\sqrt{\overline{u'^2}}}{V_j}, \frac{\ell_c}{d}\right) \quad [1]$$

The problem then becomes one of finding the specific functional form of f. One approach to solving the problem is to conduct controlled experiments on cases when one or more of the similitude parameters become "degenerate" (that is, no longer influences the flow phenomena), and to determine the functional form under these conditions. The general functional form is then inferred from the degenerate functional forms using semi-empirical theoretical arguments. The rationale behind this method of approach has its basis in similarity theory, and has been discussed in detail by Gukhman (6) and Sedov (7).

If Equation [1] is considered to represent a surface in a multidimensional, similitude space, then the degenerate cases represent "cuts" of this surface along various coordinate planes.

Since, in our view, the first two parameters in the right-hand side of Equation [1] are the most important, we have considered the cases where these separately become degenerate. In the absence of an ambient current, the first similitude parameter in the right-hand side of Equation [1] becomes infinite (and the last two become zero), while in the absence of an ambient stratification, the second parameter becomes infinite. If the functional dependences under these degenerate conditions can be determined experimentally, then they provide valuable information on the form of the generalized function.

Results from the two classes of experiments, one involving the absence of ambient currents and the other the absence of ambient stratification, are described separately later on in this section.

Experimental Facilities and Techniques

The experiments on the degenerate case in which an ambient stratification is absent were conducted in a 75-foot long flume with a 5-foot square cross section, while the experiments for the degenerate case in which an ambient current is absent were conducted in a transparent walled 6'x6'x6' cubical tank. A density stratification can be created in the latter facility either by thermal means or by the use of saline solutions.

Actual OTECPP discharge and inflows were simulated by the use of various simple source-sink rigs, two typical arrangements being shown in Fig. 2. The first arrangement shown simulates an axisymmetric withdrawal port and a single horizontal, circular discharge. The experimental rigs have provision for varying the inflow and outflow rates as well as the distance of separation between the two ports. Outflow buoyancy and horizontal orientation (to a current) can also be controlled. The second arrangement shown in Fig. 2 simulates an annular intake port and a circular discharge. As a part of the experimental setup, provision is also made for a number of different types of flow

*In the above discussion, Reynolds number has not been considered explicitly as a similitude parameter, since, in general, it cannot be duplicated in the laboratory tests without violating other requirements. It is implicit in the discussion that the Reynolds numbers in the laboratory flows are sufficiently high to assure Reynolds similarity (that is, Reynolds number independence).

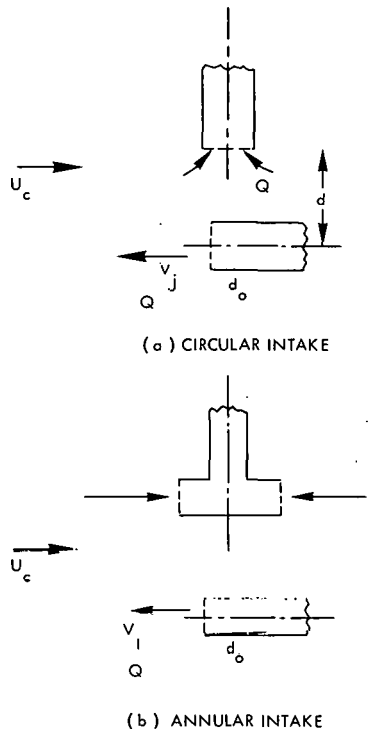



FIGURE 2 - SOURCE-SINK CONFIGURATIONS TESTED

measurements. For example, coloring dyes can be added to the discharges to enable visualization of jet trajectories. Any recirculation of the discharged effluents into the intake can also be assessed quantitatively by introducing a known concentration of dye into the outflow and by measuring the dye concentration in the inflow with the air of a spectrophotometer.

The mean and turbulent compounds of the temperature field are measured using Fast Response Thermistors (FRTs) made by Fenwall Electronics, Model K2206A, while the mean and turbulent velocities in the outflows are measured using hot-film anemometers made by Thermo Systems, Inc.

## Preliminary Results

While as a part of the ongoing program, a number of experiments have been conducted, only a few examples will be given here (for a more detailed discussion see Reference 8). Of specific interest herein are the experiments on the potential for recirculation or "short circuiting" between the warm water inflows and outflows. Data from some tests for the degenerate case without ambient stratification are shown in Figure 3.

The data shown in Fig. 3 corresponds to the case shown in Figure 1(a), that is, the discharge of a jet into a head-on current. In the specific tests under consideration, the discharge was nonbuoyant and the discharge diameter was fixed; however, the separation distance d, the discharge rate Q, and the current speed $U_c$ were all variable test parameters. Data for both of the intake configurations shown in Fig. 2 are presented. Note that for either intake configuration the effect of four simultaneous circular discharges at right angles to one another can be studied by using a sink inflow rate which is four times the discharge rate, by conducting separate experiments for the cases of counterflow, crossflow and coflow and by superposing the results appropriately. In Fig. 3 the data for the circular intake (such as that shown in Fig. 2(a)) are for the case when the intake and outflow rates are equal, while the data for the annular intake are for the case when the intake flow is four times the discharge rate.

From the data shown in Fig. 3, and the additional ones presently being acquired, it is possible to deduce semi-empirical expressions of the form,

$$\text{Percent Recirculation} = f_1\left(\frac{Q}{d^2 U_c}, \frac{d_o}{d}\right) \qquad [2]$$

where the simplified expression $f_1$ and the general expression f are related by the expression,

$$f_1\left(\frac{Q}{d^2U_c}, \frac{d_o}{d}\right) = f\left(\frac{Q}{d^2U_c}, \infty, \frac{d_o}{d}, \infty, \text{const.}, \text{const.}, \right) . \qquad [3]$$

Thus knowledge of the specific form of the function $f_1$ is of considerable value in deducing the functional form of the general function f.

Experiments have also been conducted to assess the potential for recirculation between the warm water outflows and inflow for the degenerate case in which an ambient stratification is present, but an ambient current is not.

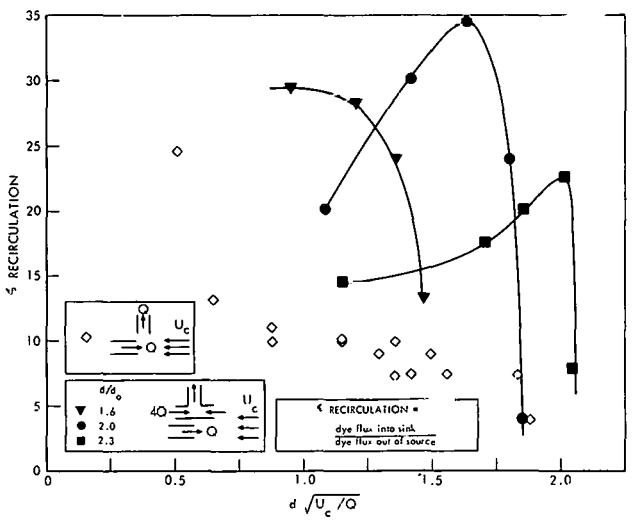



FIGURE 3 - NET-RECIRCULATION EXPERIMENTS

In many oceanic problems where it becomes necessary to include the effects of ambient stratification, the simplest manner in which this can done is to use the so-called "two-layer" approximation. In this approximation, the density stratification of the ocean is assumed to be comprised of an upper mixed layer, overlying another mixed layer of slightly higher density; the depth of the upper layer and the density difference between the two layers is so chosen as to give the "best fit" for the actual density profile. In the early estimates that were made on the potential for "short circuiting" between the intakes and discharges of an OTECPP, the two-layer approximation was used. For example, in an early estimate carried out by Zener (9), he assumed that the discharge is made just at the top of the bottom layer and that it mixes completely into this layer. The potential for recirculation was then assessed by computing the conditions under which fluid from the lower layer is likely to be withdrawn into the intake.

In the spirit of these early studies, the initial experiments on the effects of stratification that was conducted in the present program used a two-layer approximation. The lower layer consisted of a 5 percent salt solution, while fresh water formed the upper layer. The lower layer was dyed with the red dye. The suction pipe was held vertically with the opening 1.5 cm above the dyed lower layer. The conical waterspout formed by the radially upward flow of the dyed lower layer into the suction pipe was filmed for different suction velocities.

The critical velocity at which a waterspout forms, and the lower layer begins to be withdrawn into the inflow has been measured by Davidian, Glover and Appel (10) for the intake configuration shown in Figure 2(a). The semi-empirical relation given by these authors is,

$$\frac{V_c}{\left(g \frac{\Delta\rho}{\rho} d\right)^{\frac{1}{2}}} = 5.7 \left(\frac{d}{d_o}\right)^{\frac{3}{2}} \qquad [4]$$

where d is the vertical distance between the suction pipe and the interface, and $\Delta\rho$ is the difference in density between the upper and lower layers. Note that within the limitations of the two-layer approximation mentioned above, the quantity "d" also corresponds to the separation distance between the OTECPP intake and discharge.

The critical velocities measured in our tests are in excellent agreement with Equation [4]. In addition, in our tests the degree of recirculation that occurs, when the suction velocity exceeds the critical velocity, has also been measured utilizing the spectrophotometer method described. The results are shown in Fig. 4.

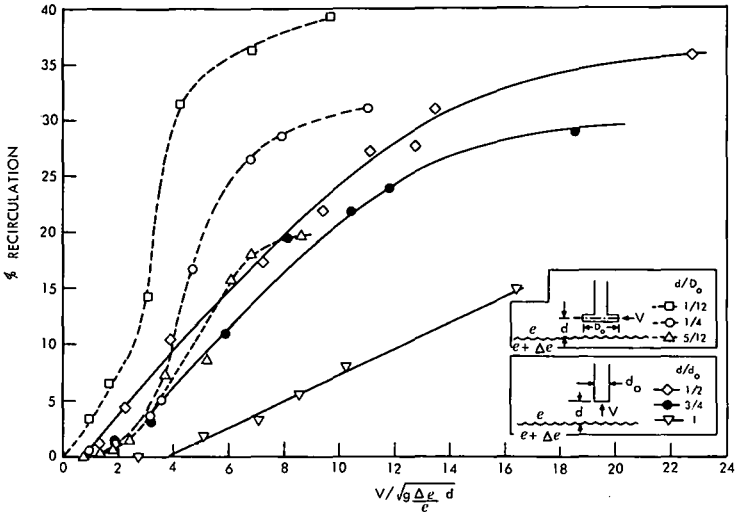



FIGURE 4 - RECIRCULATION POTENTIAL WITH STRATIFICATION ONLY

Figure 4 contains results for both of the intake configurations shown in Fig. 2. From the data given in this figure, expressions of the form

$$\% \text{ Recirculation} = f_2\left(\frac{V_j^2}{g \frac{\Delta\rho}{\rho} d}, \frac{d}{d_o}\right) \qquad [5]$$

can be deduced. Note that the first parameter on the right-hand side of Equation [5] is a specific form, applicable for the two-layer approximation, of the second parameter in the right-hand side of Equation [1].

Preliminary tests have also been carried out with source-sink pairs in a linearly stratified environment. The results from these tests are presently being analyzed and more tests are planned.

As mentioned earlier, one of the principal objectives of our study was to make detailed turbulence measurements in "dissected" parts of the OTECPP flow field so as to provide inputs to numerical codes currently under development. Note that these detailed measurements provide valuable insight into the complex turbulent transport phenomenon governing the flow fields, so that deduction of the generalized form of the function f in Equation [1], from the forms of the functions for the degenerate cases, is greatly facilitated.

Note also that by making detailed, comparison measurements in the absence and presence of currents, or the absence and presence of ambient stratification, much insight into the relevant characteristic features of the flow field (such as the suppression of entrainment by buoyancy gradients) can be obtained; such insight is seldom possible with dye visualization measurements alone or with limited mean-flow measurements.

Detailed measurements of the temperature distributions within a buoyant jet which is discharged into a nonflowing, unstratified ambient environment are shown in Figures 5 and 6. The discharge Froude number of the jet, $V_j^2/g \frac{\Delta\rho}{\rho} d_o$, was about 125. Note also that in this case, all the similarity parameters shown in Table 1 (and on the right-hand side of Equation [1]), except for the discharge Froude number, are degenerate.

The mean temperature contours at three lateral cross sections 6, 8 and 14 diameters downstream are shown in Figure 5. Note that the contours are nearly circular and concentric, apparently indicating nearly axisymmetric entrainment. On the other hand, the contours of the root-mean-square intensity of the temperature fluctuations, shown in Figure 6, display a kidney shape, symmetric about a vertical plane.

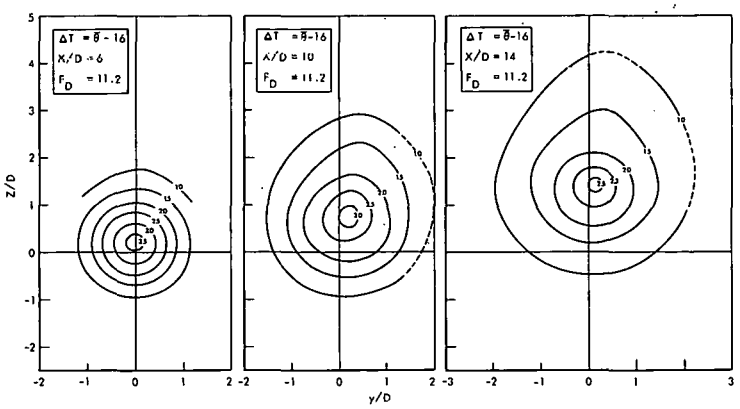



FIGURE 5 - ISOVALUE CONTOURS OF MEAN TEMPERATURE DEFECT ( ΔT )

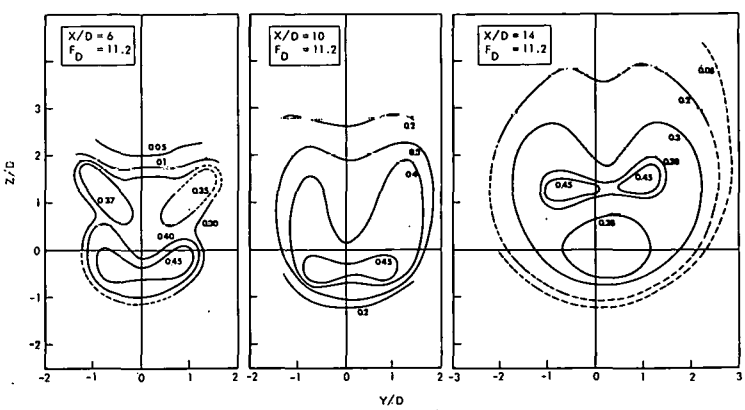



FIGURE 6 - ISOVALUE CONTOURS OF RMS INTENSITY OF TEMPERATURE FLUCTUATIONS

This is a significant result, though it may seem obvious after a little thought. Turbulent mixing of temperature occurs in different zones (vortex pairs) established by a balance of momentum and buoyant forces. Stated simply, th entrained fluid outside the core region shows greater influence of buoyancy in comparison to higher momentum fluid in the core and directly above the core.

## IV. CONCLUDING REMARKS

The external flow of an OTECPP is influenced by a large number of complex factors. Nevertheless, much insight into the conditions under which recirculation of the discharge flow into the intake flow can occur can be gained by performing controlled experiments on certain "dissected" parts of the overall problem. In the present paper, interim results have been presented from an ongoing study in which the two important factors which influence recirculation, namely, ambient stratification and ambient currents have been isolated and studied separately. Both of these factors tend to impede recirculation up to a point; experiments conducted in the present study have shown that recirculation will occur in spite of these impeding factors when certain critical values of the governing similitude parameters are exceeded. The appropriate similitude parameters, as well as their critical values, are being delineated in the present study. The degree of recirculation that occurs when the values of the similitude parameters exceed the critical value is also being delineated through controlled experiments.

Semi-empirical theoretical arguments will be used to generalize the results of the two "dissected" classes of experiments to the case involving both ambient stratification and currents.

## REFERENCES


1. Wechsler, L., Brown, C. E., and Sundaram, T. R., "Engineering Analysis of Systems for Extracting Useful Energy from the Sea," Proceedings of the Tenth Annual Conference of the Marine Technology Society, pp. 483-499, Washington, D. C., 1974.
2. Piacsek, S. A., Toomre, J., Roberts, G. O., "Geophysical Fluid Dynamics Background for Ocean Thermal Power Plants," Report NRL-GFD/OTEC 11-75, Geophysical Simulation Section, Code 7750, Naval Research Laboratory, Washington, D. C. 1975.
3. Piacsek, S. A., Martin, P. J., Toomre, J., Roberts, G. E., "Recirculation and Thermocline Perturbations from Ocean Thermal Power Plants," Report NRL-GFD/OTEC 2-76, Geophysical Simulation Section, Code 7750, Naval Research Laboratory, Washington, D. C., 1976.
4. Roberts, Glyn O., Piacsek, Steve A., and Toomre, Juri, "Two-Dimensional Numerical Model of the Near-Field Flow for an Ocean

Thermal Power Plant, Part I, The Theoretical Approach and a Laboratory Simulation," Geophysical Simulation Section, Code 7750, Naval Research Laboratory, Washington, D.C., 1976.

5. Sundaram, T. R., Scotti, R. S., and Mehta, G. D., "Some Environmental Effects of Ocean Thermal Plant Operation," Paper presented at the 1975 Fall Annual Meeting Geophysical Union, San Francisco, California, December 8012, 1975. Also HYDRONAUTICS, Incorporated Report ETG-3, 1975.

6. Gukhman, A. A., Introduction to the Theory of Similarity, Academic Press, New York, 1965.

7. Sedov, L. I., Similarity and Dimensional Methods in Mechanics, Academic Press, New York 1959.

8. Sundaram, T. R., Sambuco, E., Cinnarwalla, A., and Kapur, S. K., "The External Flow Field Associated with the Operation of An Ocean Thermal Power Plant," HYDRONAUTICS, Incorporated Technical Report 7621-1, Feb. 1977.

9. Zener, Clarence, et al., "Solar Sea Power," Progress Report NSF/RANN/SE/GI-39114/PR/73/1, Carnegie-Mellon University (1973 October 11). (Available from National Technical Information Service, Catalog PB-228 069).

10. Davidian, J., Glover, J. E., and Appel, D. W., "Development of the Noncirculatory Waterspout," Seven Exploratory Studies by Rouse—ASCE Proceedings Paper 1038, Journal of Hydraulic Division, Vol. 82, No. HY 4, August 1956.

# DEVELOPMENT OF A NUMERICAL OCEAN MODEL OF THE GULF OF MEXICO FOR OTEC ENVIRONMENTAL IMPACT AND RESOURCE AVAILABILITY STUDIES

J. DANA THOMPSON, H. E. HURLBURT, AND L. B. LIN
*JAYCOR*
*205 S. Whiting Street, Suite 500*
*Alexandria, Virginia*

Abstract

Short of actual operations the complex interactions of OTPP's and the environment can only be assessed using numerical ocean models and laboratory experiments. The best strategy for OTPP far-field modelling of the ocean is the selection of a single, well-observed ocean basin with well-defined boundary and surface input data with conditions in the basin representative of those to be encountered in the tropical and subtropical oceans. The basin should be large enough to represent open ocean conditions but small enough for economical computer modelling. The Gulf of Mexico is therefore appropriate for initial model studies.

We are developing a hierarchy of numerical models of the Gulf of Mexico for use in studies of OTPP operations. The first model is nonlinear, time-dependent, and retains both barotropic and first baroclinic modes. The model uses primitive equations on a β-plane and the external and internal gravity waves are treated implicitly. The model uses a uniform rectangular grid with $\Delta x = \Delta y = 16\ 2/3$ km and $\Delta t$ up to 1/7 day. The numerical model was driven for five years by an idealized wind field consistent with observational data presented by Franceschini and by Hellerman. The statistically steady-state model results show periods of upwelling along all the boundaries and downwelling in the interior. Baroclinic boundary currents of varying strength are found along all the boundaries, but are strongest along the western and northern boundaries. Eddies associated with nonlinear recirculation are found in the northwest and southwest corners with additional eddies representing baroclinic Rossby waves found throughout the model basin. A significant result of the model is the existence of strong baroclinic eddies in the Gulf even in the absence of the Loop Current.

## Introduction

We have been charged with investigating certain aspects of the interaction of ocean thermal power plants (OTPP's) and the mesoscale and large-scale ocean - the so-called "far-field." In this context, mesoscale refers to horizontal length scales from 10 to 100 km and large-scale encompasses scales larger than 100 km. Months to years are the relevant time scales.

One may view the need to study far-field oceanic interactions with OTPP's from two perspectives - resource availability and environmental impact. The latter view requires answers to such questions as: How will temperature disturbances be removed from the vicinity of an OTPP? How will changes in stratification modify the large-scale ocean circulation? How far down stream will the ecosystem be influenced by plant operations? How will the disturbed ocean interact with the atmosphere? From the resource availability viewpoint we must ascertain the natural variability of the thermal resource and ocean currents for a given site and also assess the long-term impact of an ensemble of OTPP's operating on the resource in a given region.

Short of actual OTPP operations, the low-order interactions of the plant with the far-field must be predicted either on theoretical grounds or from the results of small-scale analog studies. Essentially there are just three tools available for these predictive purposes - simple physical or budget models, more complex physical models usually solved by computer, and laboratory experiments. While no one tool is entirely satisfactory, all are necessary to the task.

In this presentation we explain why and outline how we are developing a complex numerical ocean model to study the interaction of OTPP's and the far-field.

## Requirements for OTPP Far-Field Modelling

The traditional picture of a rather static, sluggish ocean has rapidly faded during the past few years. We now know that in some ocean regions deviations from the annual mean for currents, mixed-layer depths, and stratifications are surprisingly large. This is particularly true in western boundary regions, near continental margins and in equatorial zones. Unfortunately, understanding and modelling this oceanic "weather" is a difficult task. Unlike meteorologists

oceanographers do not have a comprehensive observational data base from which to draw, particularly in the deep ocean, and are faced with measuring a medium quite unfriend to instrumentation. Not only is it difficult to develop theoretical models of ocean processes from observational clues, it is also difficult and expensive to verify them with independent data.

In designing a far-field ocean model for OTPP studies there are several formidable requirements. The model should be time-dependent, include advective processes, be baroclinic, and adequately parameterize small-scale turbulent processes. It must have some minimum capability of predicting stratification, sea surface temperature, and large-scale motion fields. Horizontal resolution must be comparable to the fundamental ocean length scale, the baroclinic radius of deformation, (of order 30 km). Model inputs, initial, and boundary conditions must be well known and at least the gross predictions of the model must be verified in observations. Otherwise the model is not credible and, hence, not useful.

Unfortunately, there does not exist an ocean model which completely satisfies all these requirements. Even with the largest computers it is not feasible to retain high vertical and horizontal resolution in a global ocean model which includes all the necessary, if incompletely known, physics. Consequently, it seems that the best strategy for OTPP far-field studies is to model a single, relatively well-observed ocean basin with well-defined boundary conditions and surface input data - first simulating the naturally observed features of the basin to establish model credibility, then perturbing that circulation with simulated OTPP operations. Given that the oceanic, meteorological, and biological conditions within the basin should be as representative as those to be encountered by OTPP's in the tropical and subtropical oceans, and given that the actual basin should be large enough to represent open ocean conditions but small enough for economical computer modelling, we suggest that the Gulf of Mexico is that oceanic region most appropriate for initial OTPP far-field studies.

Before discussing the Gulf of Mexico model development and results to date, some characteristics of the relatively well-observed Gulf that make it useful for OTEC far-field studies should be outlined. The Gulf is a semi-enclosed basin comprising a surface area of 1½ million $km^2$ (see Fig. 1). Its approximate dimensions are 1500 km east-west, 900 km north-south, and 3.5 km in the vertical in the deepest areas. About one-fifth of the area is covered by water less than 180 meters deep. The natural thermal resource in the Gulf seems adequate for OTEC operations over most of its area for every season except the winter season in the northern Gulf.

Less than ten percent of the Gulf bounds other oceans, with virtually all inflow coming through the Yucatan Channel and all outflow leaving through the Florida Straits. The inflow rate is roughly 30 million $m^3$ per second (Schmitz and Richardson (2)). With considerable seasonal variation the flow through the Yucatan Channel extends into the eastern Gulf, forms an anticyclonic loop, then exits through the Florida Straits, ultimately forming a segment of the Gulf Stream. This Loop Current may reach speeds up to 150 cm/sec, the width of the entire Loop being approximately 300 km. It does not penetrate much below 1000 m depth (see Fig. 2). The Loop undergoes systematic annual expansion and contraction, reaching as far north as the continental shelf off the Mississippi Delta by late summer and fall. The western Gulf is generally characterized as having weaker currents and less time variability - although direct current measurements off the continental shelf are virtually non-existent. Surface currents have been grossly estimated from ship observations.

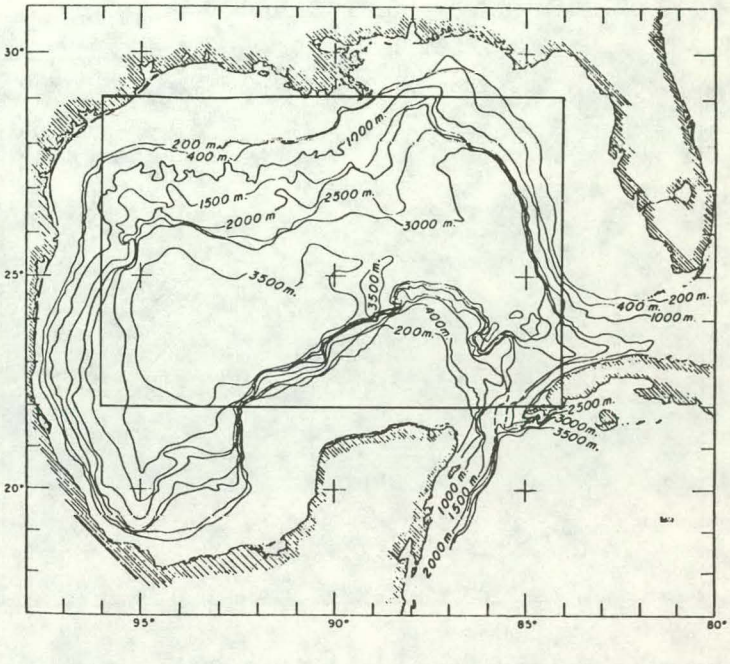



Fig. 1 Bathymetry of Gulf of Mexico based on U.S. Coast and Geodetic Survey Chart 1007 and soundings on file at the Department of Oceanography, Texas A&M University, from Nowlin (1). The rectangular box represents the approximate boundaries of the numerical model described in the text.

The thermal structure in the Gulf is closely tied to the circulation. For example, upwelling, the Loop Current, and mesoscale eddies can dramatically distort our simple mean picture of the basic stratification in the Gulf. Consider, for example, Fig. 3 (from Leipper, et al. (5)) which shows a NW to SE hydrographic section from near the Mississippi Delta to the western tip of Cuba. The section penetrated a detached eddy from the Loop Current and the Loop Current itself. Although eddies have been observed in the eastern and western Gulf, they have usually been assumed to be produced from the Loop Current. This may not always be the case as our research has clearly demonstrated.

In light of the present state-of-the-art in ocean modelling, our approach to the far-field problem in OTEC has been research oriented. It requires the development of a hierarchy of ocean models, ranging from

a low-vertical resolution (two-layer), high-horizontal resolution (15 km) hydrodynamical model with idealized geometry and forcing up to a high vertical and horizontal resolution model that includes mixed-layer physics, actual geometry, and observed forcing. At each stage of development the model must be carefully examined for scientific credibility. It must reproduce obvious features of the actual ocean or predict features yet to be verified in observations. The ultimate goal of course is to provide a credible, cost-effective far-field ocean model useful for OTPP far-field impact studies. However, if the far-field model cannot be proven valid in reproducing observed features in the Gulf of Mexico it is doubtful it could be credibly used in impact studies, either in the Gulf, or in modified form, at other prospective OTEC sites.

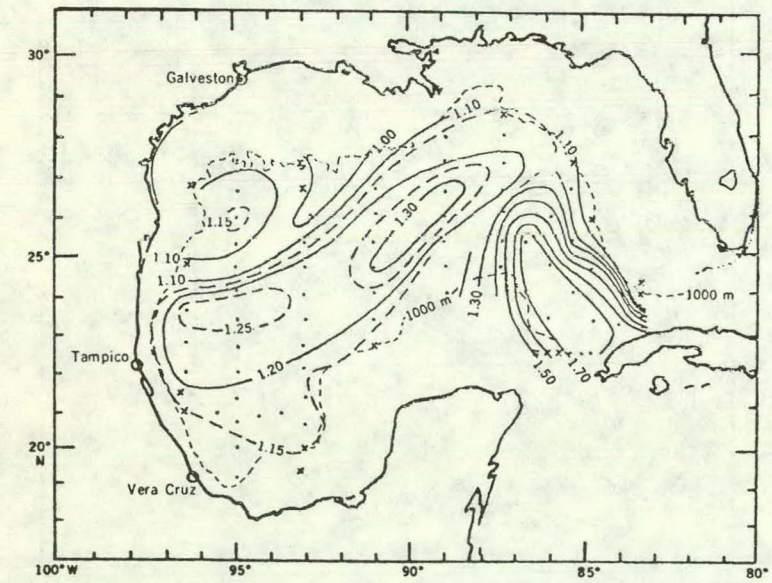



Fig. 2 Sea surface topography relative to the 1000-dbar surface (R. V. Hidalgo, February and March 1962). Adapted by Sturges and Blaha (3) from Nowlin and McLennan (4). The Loop Current and three eddy-like features are evident in the diagram.

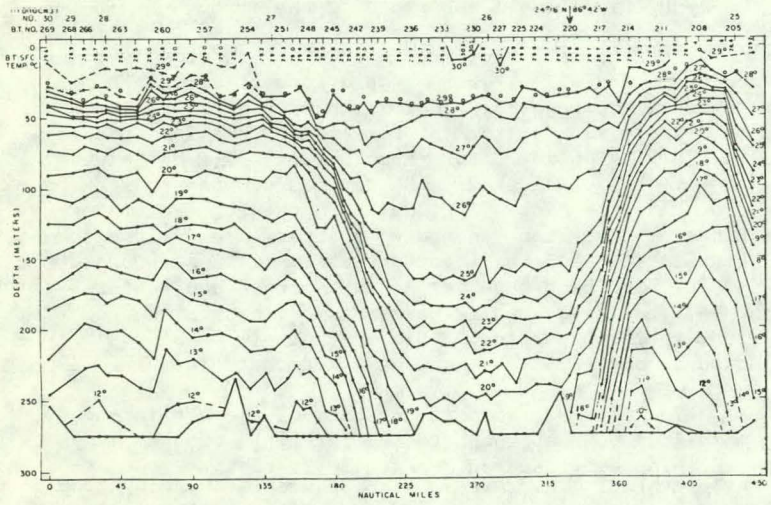



Fig. 3 North to south (left to right) temperature section (°C) in the eastern Gulf across a detached eddy (center) and the Loop Current itself (right), 20-22 August 1965. Line extends from about 87° W, 30° N to 85° W, 23° N (from Leipper, et al.,(5)).

## Model Development and Results

The first phase of our model development is complete. We have designed and run a 3 km deep, two-lay high resolution model of the Gulf of Mexico with a flat bottom in an idealized geometry. The model is schematically shown in Fig. 4. Fig. 1 shows its approximate spatial dimensions as superimposed on the depth contours in the Gulf.

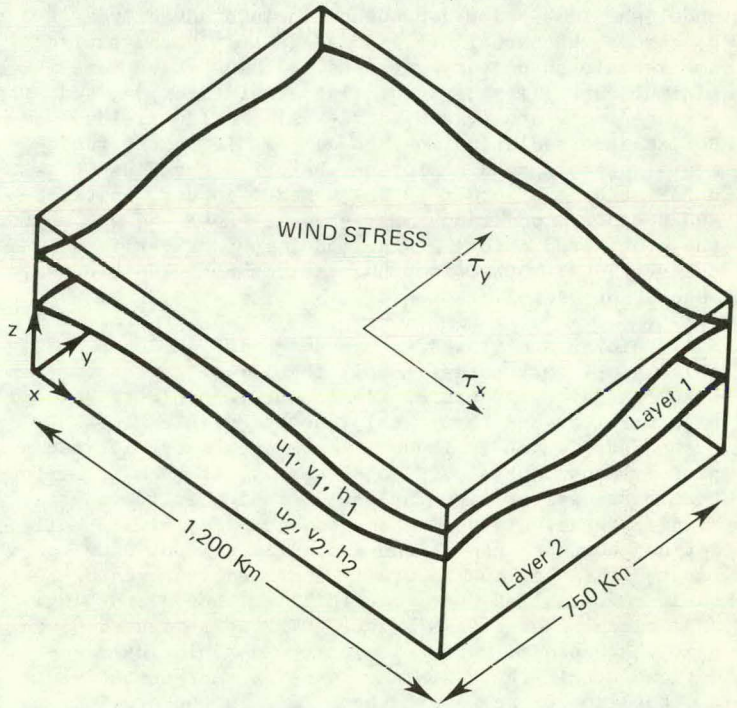



Fig. 4 Schematic diagram of the two-layer model used in the first numerical experiment. Note the walls are rigid and the bottom is flat.

Consider the model equations for a stably stratified, rotating ocean in a right-handed coordinate system. Thermodynamic effects are neglected except in determining the bulk stratification. Assume the fluid is hydrostatic and Boussinesq. Retaining only the first term in the perturbation expansion for the advective terms, the vertically integrated equations appropriate for a two-layer model are:

$$\frac{\partial \vec{v}_1}{\partial t} + \vec{v}_1 \cdot \nabla \vec{v}_1 + \hat{k} \times f \vec{v}_1 = -g\nabla(h_1 + h_2 + D) + \frac{\vec{\tau}_s - \vec{\tau}_I}{\rho h_1} + A\nabla^2 \vec{v}_1 \qquad (1)$$

$$\frac{\partial h_1}{\partial t} + \nabla\cdot(h_1\vec{v}_1) = 0 \tag{2}$$

$$\frac{\partial v_2}{\partial t} + \vec{v}_2\cdot\nabla\vec{v}_2 + \hat{k}\times f\vec{v}_2 = -g\nabla(h_1 + h_2 + D) + g'\nabla h_1 + \frac{\vec{\tau}_I - \vec{\tau}_B}{\rho h_2} + A\nabla^2\vec{v}_2 \tag{3}$$

$$\frac{\partial h_2}{\partial t} + \nabla\cdot(h_2\vec{v}_2) = 0 \tag{4}$$

where

$$\left.\begin{aligned}
\nabla &= \frac{\partial}{\partial x}\hat{i} + \frac{\partial}{\partial y}\hat{j} \\
\vec{v}_i &= u_i\hat{i} + v_i\hat{j} \\
g' &= g(\rho_2 - \rho_1)/\rho_2 \\
\vec{\tau}_I &= \rho C_I\bar{q}(\vec{v}_1 - \vec{v}_2) \\
\vec{\tau}_B &= \rho C_B\bar{q}\vec{v}_2 \\
\vec{\tau}_s &= \tau_{sx}\hat{i} + \tau_{sy}\hat{j} \\
q_i &= (u_i^2 + v_i^2)^{1/2} \\
\bar{q} &= (q_1 + q_2)/2
\end{aligned}\right\} \tag{5}$$

and i = 1, 2. Symbols are defined in the Appendix, although the notation used is common in oceanography. The height of the bottom topography above a reference level is given by D. Note that both barotropic and baroclinic modes are retained in the model.

Note that the model is time-dependent and non-linear and includes the physics of the earth's rotation, the β-effect, and a parameterization of sub-grid scale turbulence in terms of a numerically small eddy diffusion in the horizontal and a quadratic interfacial and bottom stress in the vertical. Interfacial stress is set to zero in the experiment we will describe. Wind stress is treated as a body force acting on the upper layer. The walls are rigid and a no-slip condition is prescribed on the tangential flow. The model was started from a state of rest. Parameter values and initial conditions for the height field are shown in Table 1.

Table 1: Model Parameter Values

| Parameter | Value | Parameter | Value |
|---|---|---|---|
| f | $5 \times 10^{-5}$ sec$^{-1}$ | $H_1$ | 150 m |
| g | $10^3$ cm sec$^{-2}$ | $H_2$ | 2850 m |
| g' | 2 cm sec$^{-2}$ | β | $2 \times 10^{-13}$ cm$^{-1}$ sec$^{-1}$ |
| A | $10^6$ cm$^2$ sec$^{-1}$ | Δx, Δy | 16 2/3 km |
| ρ | 1 gm cm$^{-3}$ | Δt | 2.4 hr |
| $C_I$ | 0 | D(x, y) | 0 |
| $C_B$ | $10^{-3}$ | | |

Both the external and internal gravity waves were treated implicitly, allowing exceptionally large time steps (2.4 hours) on a 16 2/3 km uniform grid without computational instability. A new technique termed Block Implicit Relaxation (Dietrich, et al., (6)) was used to solve the coupled implicit primitive equations in an economical manner. The model, in a 1200 km x 750 km domain, ran in less than 9 sec per model day on the NRL Texas Instruments ASC computer. The finite-difference scheme (leap-frog in time, scheme C from Grammeltvedt (7) for advection, and the scheme of Holland and Lin (8) for the Coriolis terms) conserves both total energy and mass, except for the explicit sources and sinks of wind stress, horizontal friction, and bottom friction. No additional smoothing or artifical numerical damping was used. A forward time-difference was used for the first time step and for restarting the model from a history tape roughly every six months. Saving one time level every ten days on the history tape was found to minimize tape storage requirements. At the end of five years of integrations total mass was conserved to one part in $10^{14}$.

To date we have been looking at the wind-driven circulation of the Gulf, closing off the inflow and outflow ports to isolate this component of the circulation. As in most forced ocean problems the wind stress and the wind stress curl distribution in space and time are extremely important in determining the circulation. We have taken great care to construct a forcing function for the model which faithfully represents the main features of the observed wind climatology over the Gulf. Hellerman (9), Franceschini (10) and others have published data concerning wind stress and wind stress curl over the Gulf. Based on this data we have constructed an analytical representation for the wind stress which can be written as:

$$\tau_x = A_x(\cos\omega t + 1) + B_x(.5\cos\omega t + \cos 2\omega t + 1)\left(\frac{y}{L_y} - .5\right) \tag{6}$$

$$\tau_y = A_y(\cos\omega t + 1) + B_y(.5\cos\omega t + \cos 2\omega t + 1)\left(\frac{x}{L_x} - .5\right)$$

where

$A_x = A_y = .2$ dynes $cm^{-2}$

$B_x = .18$ dynes $cm^{-2}$

$B_y = -.1125$ dynes $cm^{-2}$

$L_y = 750$ km

$L_x = 1200$ km

$\omega = 2\pi T^{-1}$ where T is one year.

The values for x and y are in km measured from the southwest corner of the model.

Sturges and Blaha (3) present evidence indicating that the extreme value in wind stress curl ($-7.5 \times 10^{-9}$ dynes $cm^{-3}$) occurs during December through February with another relative minimum in summer. The curl vanishes for the other two seasons. Fig. 5 shows the analytical representation of the wind curl versus time for the Gulf. The curl is uniform over the Gulf at any given time. The observed mean annual stress from Franceschini's compiled ship data is shown in Fig. 6 and the analytical representation is shown in Fig. 7.

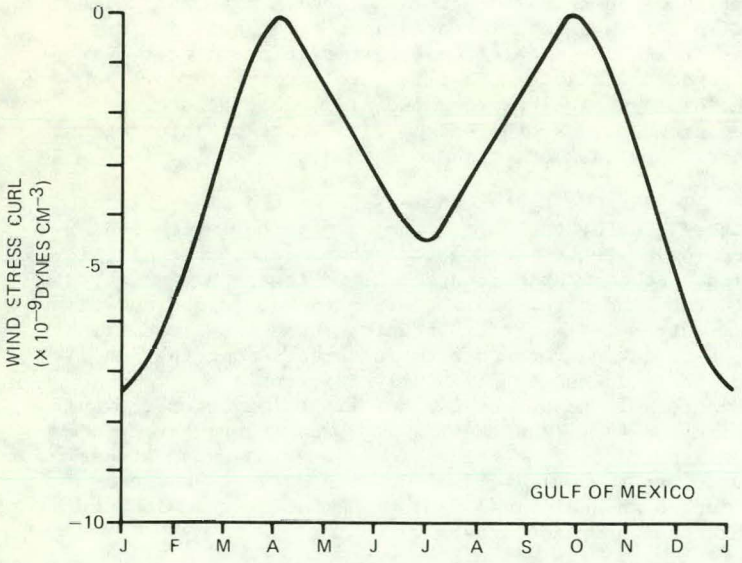



Fig. 5 The wind stress curl over the Gulf of Mexico versus time as given by the analytical representation used to drive the model.

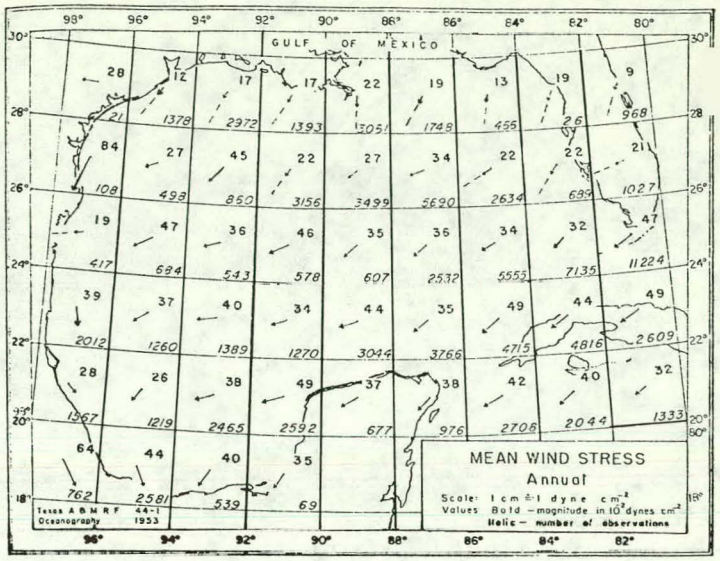



Fig. 6 The mean annual wind stress over the Gulf of Mexico as obtained from ship data by Franceshini (9) for the period 1850-1950.

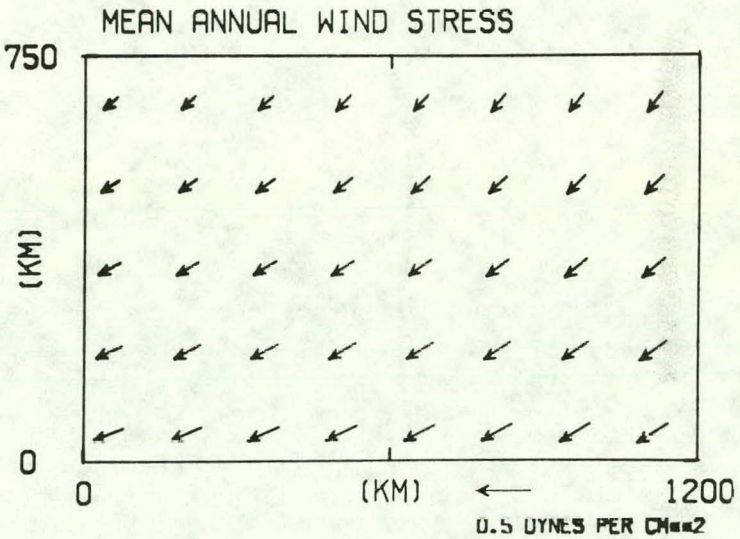



Fig. 7 The mean annual wind stress from the yearly average of the analytical representation.

Using these winds we drove the Gulf model for a period of five years to a statistically steady state from the initial rest state. Since the resulting enormous amount of model data was difficult to depict in a concise way, movies were constructed to show the evolution of the various fields of velocity and pynocline height anomaly (PHA). The pycnocline height anomaly is the deviation of the fluid interface from its initial value and may be thought of as a measure of the time-integrated effect of upwelling or downwelling on displacement of the thermocline. (Author's note: At this point the movie of pynocline height anomaly was shown before the New Orleans OTEC audience.) Snapshots from the movie at the end of each year from year one to year five are shown in Fig. 8. In examining

Fig. 8 it should be noted that the upper layer flow is roughly parallel to the contours of PHA and inversely proportional to the contour spacing. The model evolution has apparently reached a statistical steady state by the beginning of year four of the integrations.

Although we have yet to undertake a thorough dynamical analysis of the results for this experiment, a few major features are clearly evident. First, a north-west boundary current (and also a weaker eastern boundary current) develops rapidly during the first year and remains a significant feature during the integrations, with maximum speeds of about 60 cm $sec^{-1}$. Second, there occurs substantial positive values of PHA around most of the perimeter of the basin, indicating a net upward movement of the pynocline. This suggests that, at least during spin-up, coastal upwelling is important around most of the coastal margins. Third, mesoscale baroclinic eddies having horizontal scales of roughly 300 km dominate the interior circulation. One subset of the eddy group represents baroclinic Rossby waves moving from east to west at about 1.7 km per day. Another eddy group appears to owe its existence to shearing instabilities and nonlinear recirculations in the north-west boundary current. Both sets of eddies drift westward into the western boundary region and are "absorbed" into the current. As yet no evidence for baroclinic instability has been documented. Finally, a minimum in sea level at the coast is found during summer and winter, with the winter value being the stronger, in accord with observations.

## Conclusions

This simple wind-driven model of the Gulf of Mexico has reproduced a western boundary current consistent with the observational data described by Sturges and Blaha (3). It has also produced a sea level minimum during summer which appears in the observations and has not been satisfactorily explained before. It has produced ocean eddies which owe their existence to wind-forcing rather than the Loop Current.

Regarding applications to OTEC siting, we can, even at this early stage of model development, make some preliminary recommendations - keeping in mind that our present model is highly idealized and does not include the important Loop Current forcing. First, there may occur significant coastal upwelling within 30 km of the coast, around most of the Gulf, for most of the year. Since this upwelling is likely to reduce the thermal resource near shore an OTEC plant should be placed out of this upwelling area. Second, the central northern and northwest regions of the Gulf can be expected to have strong baroclinic 0(50 cm/sec)

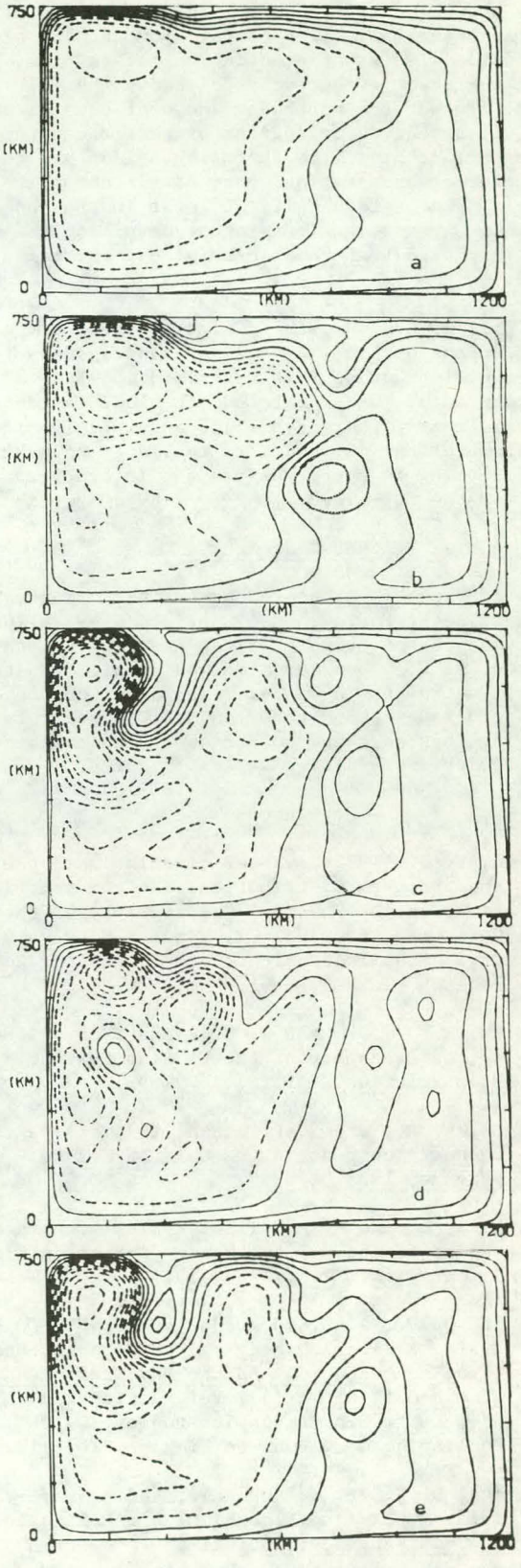



Fig. 8 The pycnocline height anomaly predicted by the numerical model at the end of year one (a), two (b), three (c), four (d), and five (e). The contour interval is 7.5 m with dashed lines indicating negative values. Note the mesoscale eddies and the strong north-west boundary current. The upper layer flow is roughly parallel to the contours and inversely proportional to contour spacing. Only the last two years may be considered in a statistically steady state.

currents above the main thermocline which would effectively flush thermal effluent away from an OTEC plant. Strong eddies also exist even in the central and eastern Gulf and would act effectively to remove thermal effluent. Third, the northwest and west central areas of the Gulf appear to be regions of persistent thermocline deepening, hence the thermal gradient may be expected to be strongest and most persistent there. Conversely, the eastern Gulf, at least in the absence of the Loop Current, has persistent upwelling and would be expected to have a less intense thermal resource.

Our preliminary success in simulating observed features in the Gulf of Mexico has encouraged us to continue development of this far-field model for OTEC. In the near future we plan to add the Loop Current, additional layers, thermodynamics, an explicit mixed-layer parameterization, and more realistic boundaries and wind forcing to better assess the interactions of OTEC and the far-field.

## Acknowledgements

This research is sponsored by the OTEC Program, Division of Solar Energy, ERDA Contract E(49-26)1005 under a subcontract from the Naval Research Laboratory, Washington, D. C. Computer time was supplied on the NRL Texas Instruments Advanced Scientific Computer. Appreciation is extended to Dr. Steve Piacsek for encouraging this work and to Margaret Mikota for typing the manuscript and drafting several figures.

## References

(1) Nowlin, W. D., 1972: Winter circulation patterns and property distributions. (From contributions on the Physical Oceanography of the Gulf of Mexico, Vol. 2, Texas A&M University Oceanographic Studies, Gulf Publishing Co., Houston, Texas), 3-51.

(2) Schmitz, W. J., Jr. and W. S. Richardson, 1968: On the transport of the Florida Current. Deep Sea. Res., 15 (6), 679-693.

(3) Sturges, W. A., and J. P. Blaha, 1976: A western boundary current in the Gulf of Mexico. Science, 192, 367-369.

(4) Nowlin, W. D. and H. McLellan, 1967: A characterization of the Gulf of Mexico waters in winter. J. Mar. Res., 25 (1), 29-59.

(5) Leipper, D. F., J. D. Cochrane, and J. F. Hewitt, 1972: A detached eddy and subsequent changes. (From contributions to the Physical Oceanography of the Gulf of Mexico, Vol. 2, Texas A&M University Oceanographic Studies, Gulf Publishing Co., Houston, Texas), 107-118.

(6) Dietrich, D. E., B. E. McDonald, and A. Warn-Varnas, 1975: Optimized Block-Implicit Relaxation. J. Comp. Physics, 18, 421-439.

(7) Grammeltvedt, A., 1969: A survey of finite-difference schemes for the primitive equations for a barotropic fluid. Mon. Wea. Rev., 97, 384-404.

(8) Holland, W. R., and L. B. Lin, 1975: On the generation of mesoscale eddies and their contribution to the oceanic general circulation. I. A Preliminary Numerical Experiment. J. Phys. Oceanogr., 5, 642-657.

(9) Hellerman, S., 1967: An updated estimate of the wind stress on the world ocean. Mon. Wea. Rev., 95 (9), 607-626.

(10) Franceschini, G. A., 1955: The distribution of mean monthly wind stress over the Gulf of Mexico, Technical Report. Texas A&M University, Department of Oceanography, College Station, 17 pages.

## APPENDIX
### List of Symbols

| | |
|---|---|
| $A$ | Horizontal eddy viscosity |
| $C_I$, $C_B$ | drag coefficients for interfacial and bottom stress |
| $D$ | height of the bottom topography above a reference level |
| $f$ | Coriolis parameter |
| $g$ | acceleration due to gravity |
| $g'$ | reduced gravity, $g(\rho_2 - \rho_1)/\rho_2$ |
| $h_1$, $h_2$ | instantaneous local thickness of the layers |
| $H_1$, $H_2$ | initial thickness of the layers |
| $t$ | time |
| $u_1$, $u_2$ | x-directed components of current velocity |
| $v_1$, $v_2$ | y-directed components of current velocity |
| $x$, $y$, $z$ | tangent plant Cartesian coordinates: x positive eastward, y positive northward, z positive upward |
| $\beta$ | df/dy |
| $\Delta t$ | time increment in the numerical integration |
| $\Delta x$, $\Delta y$ | horizontal grid increment |
| $\rho$, $\rho_1$, $\rho_2$ | densities of sea water |
| $\tau_{sx}$, $\tau_{sy}$ | x and y directed tangential wind stress at the surface |
| $\vec{\tau}_I$, $\vec{\tau}_B$ | interfacial and bottom stress vectors |

# MONTHLY ASSESSMENT OF TEMPERATURE RESOURCE FOR THREE POTENTIAL OTEC SITES

PAUL M. WOLFF
*Ocean Data Systems, Inc.*
*2400 Garden Road*
*Monterey, California*

LLOYD LEWIS
*Environment & Resource Assessments Branch*
*Division of Solar Energy*
*Energy Research & Development Administration*
*20 Massachusetts Avenue, North West*
*Washington, D.C.*

## Abstract

During 1975 Ocean Data Systems, Inc. assembled an ocean temperature data set for OTEC purposes from available soundings in Navy and NOAA files. In this study the OTEC data file was summarized monthly for three possible sites. The depth necessary to achieve a ΔT of 18°C, 20°C and 22°C was determined for each area for the most probable monthly temperature structure.

The data are presented in plan view and in tabular form. For each site the existence of a ΔT of 20°C at a depth less than 1500 meters was demonstrated for each month of the year.

Some information was provided on plans for expanded investigation of this type.

## Introduction

During 1975 ODSI assembled a data base of ocean temperature data for OTEC purposes, Wolff and Hubert (1). This data base contains all unclassified soundings available in Navy and NOAA files. From this data summaries were prepared identifying existing seasonal OTEC thermal gradients in the entire Northern Hemisphere. These summaries were for the four seasons and for 1° Lat Long areas.

As the ERDA OTEC program has progressed, the need for ΔT data on finer space and time scales for possible sites has become apparent. This report is a first step toward identifying the ΔT resource for specific sites on a continuous basis throughout the year. The full report and all tables and charts are contained in Wolff (2).

## Method

Deep soundings were sorted in 1° Latitude Longitude Squares and monthly in time. Sea surface temperature, shallow soundings and XBT casts were analyzed for areas about 15 miles on a side where data availability permitted.

Each location was marked on a siting chart (Fig. 1). Larger scale maps were then prepared showing the bathymetry of each area. This was done in order to show where sufficient water depth is present and to indicate rough estimate of depths for mooring cable lengths.

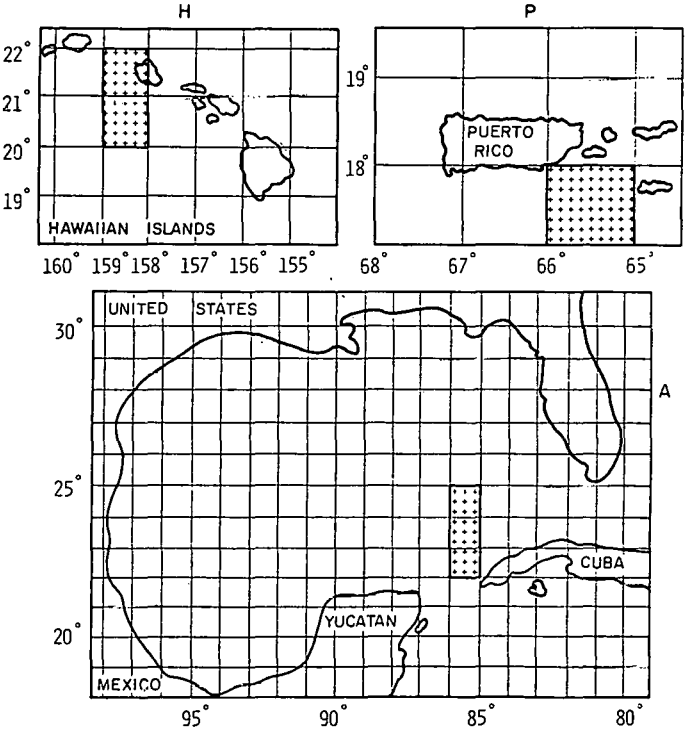



Fig. 1 Locations Studied.

Monthly mean sea surface temperature was extracted from charts for each of the three areas. Composite monthly mean temperature soundings were computed from shallow casts (less than 100 meters), XBT soundings (down to 450 meters) and deep casts from CSTD and Nansen instruments. The number of each type of cast involved in the composite was recorded.

ΔT's considered were 18°, 20°, and 22° C. Mean monthly surface temperatures were used for higher values and temperatures at depth subtracted from them.

ΔT = Sea Surface Temperature - Temperature at depth

The method is shown in Fig. 2 for a typical sounding.

Then interpolation was used in the temperature sounding to determine the depth required to obtain each of the prescribed ΔT's. The soundings were compared with data for the Puerto Rico area contained in Atwood, et al. (3) and with Hawaiian data contained in Bathen (4).

If the ΔT was not high enough by the time 1500 meter depth was reached, M was entered in the depth table. When there were only a few soundings available for an area or if a larger number of soundings were all taken in one or two years the depths were estimated by interpolation. These values were indicated by parentheses surrounding the depth. This was necessary mainly in the Gulf of Mexico where data availability did not permit resolution finer than the 1° square. Tables 1, 2 and 3 list the number of soundings available in this data base.

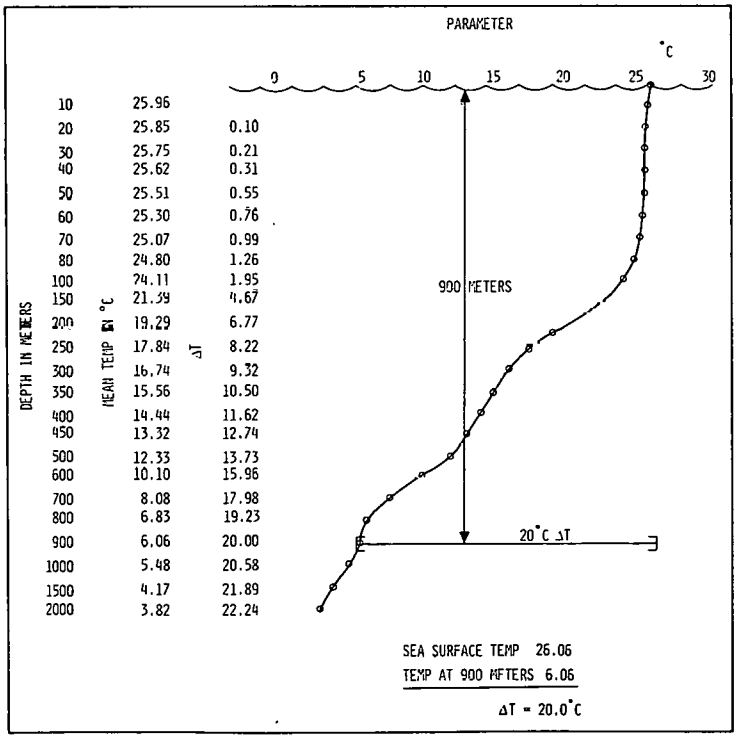



Fig. 2 Depth Determination

Table 1 Data Coverage (XBT's).

| LOCATION | SITE | J | F | M | A | M | J | J | A | S | O | N | D | YEAR TOTAL |
|---|---|---|---|---|---|---|---|---|---|---|---|---|---|---|
| HAWAII OAHU NORTH | 21°- 22°N 157°-158°W | 17 | 13 | 32 | 24 | 22 | 16 | 28 | 24 | 22 | 30 | 43 | 14 | 285 |
| HAWAII OAHU SOUTH | 20°- 21°N 157°-158°W | 6 | 6 | 13 | 21 | 26 | 29 | 17 | 13 | 29 | 22 | 9 | 4 | 195 |
| PUERTO RICO | 17°- 18°N 65°- 66°W | 26 | 34 | 26 | 19 | 38 | 112 | 88 | 73 | 93 | 37 | 13 | 30 | 589 |
| GULF OF MEXICO | 24°- 25°N 85°- 86°W | 10 | 7 | 1 | 1 | 11 | 18 | 3 | 21 | 18 | 20 | 5 | 14 | 127 |
| GULF OF MEXICO | 23°- 24°N 85°- 86°W | 6 | 5 | 0 | 6 | 13 | 7 | 2 | 32 | 20 | 22 | 18 | 9 | 140 |
| GULF OF MEXICO | 22°- 23°N 85°- 86°W | 0 | 7 | 2 | 5 | 11 | 4 | 9 | 21 | 22 | 15 | 16 | 5 | 117 |

Table 2 Data Coverage (Shallow Casts).

| LOCATION | SITE | J | F | M | A | M | J | J | A | S | O | N | D | YEAR TOTAL |
|---|---|---|---|---|---|---|---|---|---|---|---|---|---|---|
| HAWAII OAHU NORTH | 21°- 22°N 157°-158°W | 19 | 32 | 39 | 60 | 34 | 35 | 28 | 30 | 36 | 27 | 51 | 21 | 392 |
| HAWAII OAHU SOUTH | 20°- 21°N 157°-158°W | 30 | 27 | 45 | 24 | 27 | 36 | 26 | 33 | 31 | 34 | 27 | 28 | 368 |
| PUERTO RICO | 17°- 18°N 65°- 66°W | 28 | 30 | 14 | 29 | 40 | 90 | 69 | 95 | 115 | 45 | 10 | 35 | 600 |
| GULF OF MEXICO | 24°- 25°N 85°- 86°W | 8 | 5 | 2 | 2 | 14 | 16 | 4 | 19 | 21 | 17 | 2 | 16 | 126 |
| GULF OF MEXICO | 23°- 24°N 85°- 86°W | 4 | 3 | 0 | 5 | 15 | 6 | 3 | 28 | 19 | 19 | 17 | 8 | 127 |
| GULF OF MEXICO | 22°- 23°N 85°- 86°W | 0 | 4 | 1 | 4 | 13 | 3 | 8 | 20 | 23 | 14 | 13 | 6 | 109 |

Table 3 Data Coverage (Deep Casts).

| LOCATION | SITE | J | F | M | A | M | J | J | A | S | O | N | D | YEAR TOTAL |
|---|---|---|---|---|---|---|---|---|---|---|---|---|---|---|
| HAWAII OAHU NORTH | 21°- 22°N 157°-158°W | 1 | 4 | 8 | 6 | 11 | 5 | 6 | 5 | 5 | 9 | 8 | 1 | 69 |
| HAWAII OAHU SOUTH | 20°- 21°N 157°-158°W | 3 | 3 | 3 | 12 | 6 | 3 | 7 | 3 | 3 | 3 | 3 | 1 | 50 |
| PUERTO RICO | 17°- 18°N 65°- 66°W | 0 | 7 | 6 | 12 | 2 | 1 | 3 | 14 | 7 | 3 | 2 | 4 | 61 |
| GULF OF MEXICO | 24°- 25°N 85°- 86°W | 0 | 6 | 0 | 1 | 0 | 11 | 0 | 2 | 12 | 0 | 1 | 0 | 33 |
| GULF OF MEXICO | 23°- 24°N 85°- 86°W | 0 | 2 | 0 | 4 | 5 | 2 | 1 | 18 | 8 | 1 | 2 | 6 | 57 |
| GULF OF MEXICO | 22°- 23°N 85°- 86°W | 0 | 3 | 0 | 2 | 2 | 3 | 5 | 8 | 9 | 0 | 0 | 0 | 32 |

In the tables the areas involved are 1° in dimension for Oahu South and the Gulf of Mexico and for areas 15 minutes on a side for Oahu North and Puerto Rico. Data for only one smaller square is shown for these two sites and the location is hatched on the site location charts. Tables 4 and 5 show the resulting depths for ΔT = 22° and ΔT = 20°.

The plan view charts are intended to show horizontal variability within the areas. The deep temperature structure within each area was relatively constant throughout the year and over the area. The variation in the plan views is mainly a result of near surface temperature variability. Fig. 3 is a typical plan view chart.

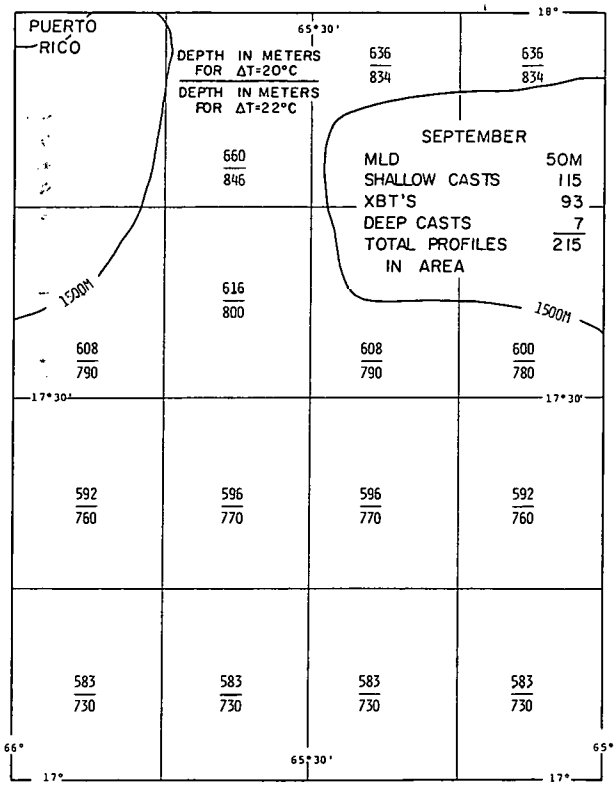



Fig. 3 Plan View Chart.

Table 4 Summary Table ΔT (20°C).

| LOCATION | SITE | J | F | M | A | M | J | J | A | S | O | N | D |
|---|---|---|---|---|---|---|---|---|---|---|---|---|---|
| HAWAII OAHU NORTH | 21°30'-21°45'N 157°15'-157°30'W | 1225 | 1268 | 1268 | 1311 | 903 | 627 | 636 | 566 | 556 | 566 | 700 | 781 |
| HAWAII OAHU SOUTH | 20°-21°N 157°-158°W | 906 | 850 | 970 | 837 | 690 | 588 | 571 | 590 | 490 | 500 | 573 | 635 |
| PUERTO RICO | 17°30'-17°45'N 65°45'-66°W | 822 | 906 | 922 | 858 | 730 | 687 | 673 | 667 | 608 | 600 | 680 | 730 |
| GULF OF MEXICO | 24°-25°N 85°-86°W | (1060) | 1121 | (1150) | (1150) | 880 | 682 | (600) | 475 | 502 | (600) | 885 | (1000) |
| GULF OF MEXICO | 23°-24°N 85°-86°W | (1040) | 1063 | (1100) | (1080) | 817 | 784 | 666 | 570 | 650 | 780 | 765 | (980) |
| GULF OF MEXICO | 22°-23°N 85°-86°W | (880) | 900 | (1050) | 845 | 785 | 753 | 611 | 590 | 675 | (760) | (770) | (825) |

( ) = INTERPOLATED, EXTRAPOLATED DATA.

ALL FIGURES REPRESENT DEPTH IN METERS.

Table 5 Summary Table ΔT (22°C).

| LOCATION | SITE | J | F | M | A | M | J | J | A | S | O | N | D |
|---|---|---|---|---|---|---|---|---|---|---|---|---|---|
| HAWAII OAHU NORTH | 21°30'-21°45'N 157°15'-157°30'W | M | M | M | M | M | 1182 | 1091 | 975 | 944 | 975 | 1354 | 1500 |
| HAWAII OAHU SOUTH | 20°-21°N 157°-158°W | M | M | M | M | 1234 | 1250 | 1000 | 1000 | 830 | 830 | 975 | 1250 |
| PUERTO RICO | 17°30'-17°45'N 65°45'-66°W | 1320 | M | M | 1500 | 970 | 894 | 870 | 858 | 790 | 780 | 882 | 970 |
| GULF OF MEXICO | 24°-25°N 85°-86°W | (M) | M | (M) | (M) | 1500 | 855 | (690) | 525 | 800 | (900) | (1000) | (1150) |
| GULF OF MEXICO | 23°-24°N 85°-86°W | (M) | M | (M) | (1450) | 1164 | 970 | 828 | 725 | (800) | 911 | 998 | (1100) |
| GULF OF MEXICO | 22°-23°N 85°-86°W | (1350) | M | (M) | 1162 | 1047 | 900 | 733 | 730 | (780) | (880) | (980) | (1090) |

( ) = INTERPOLATED, EXTRAPOLATED DATA.

M = REQUIRED ΔT NOT REACHED AT 1500 METERS.

ALL FIGURES REPRESENT DEPTH IN METERS.

## Work Now In Progress

The analysis reported here is being extended to cover the areas shown in Fig. 4. First the data base is being updated by the addition of all available additional data. Then an error checking procedure will be used to eliminate questionable data. A mean monthly sounding will be constructed for each of the squares in Fig. 4. From these soundings depth for specified ΔT values will be determined.

Statistics of variability and depth of mixed layer will be computed where the data quantity and distribution permits. The additional analysis will be complete in Fall 1977 and the OTEC thermal data base will be transferred to NODC at that time. This work is being done under ERDA contract, ODSI (5).

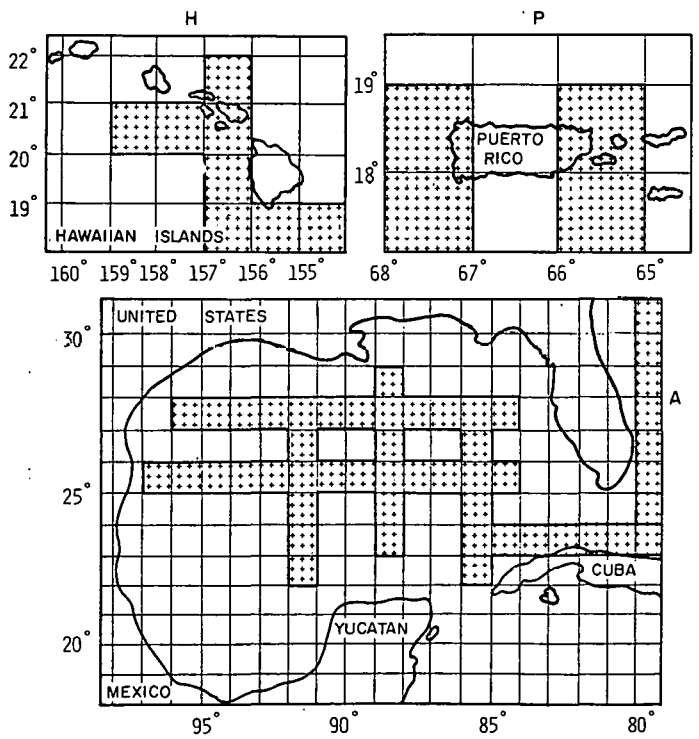



Fig. 4 New Work Areas.

## References


1. Wolff, Paul M. and William E. Hubert, "Ocean Thermal Energy Conversion: Resource, Ecological and Environmental Studies". Contract No. NSF-C1020, Ocean Data Systems, Inc., Monterey, CA, March 1976.

2. Wolff, Paul M. "Monthly OTEC Resource Availability for Three Sites". Purchase Order No. 29041 prepared for General Electric - Tempo, Santa Barbara, CA; Ocean Data Systems, Inc., Monterey, CA, January 1977.

3. Atwood, Donald K., et al. "Ocean Thermal Energy Conversion: Resource Assessment and Environmental Impact for Proposed Puerto Rico Site". NSF Grant No. AER 75-00145, 1 December 1975.

4. Bathen, Karl H. "An Evaluation of Oceanographic and Socio-Economic Aspects of a Nearshore Ocean Thermal Energy Conversion Pilot Plant in Subtropical Hawaiian Waters". NSF-Rand Grant No. AER 74-17421 A01, University of Hawaii, Honolulu, Hawaii, April 1975.

5. ODSI (Ocean Data Systems, Inc.) "Ocean Thermal Structure Analyses". Current ERDA Contract (No. EG-77-C-01-4028), 23 February 1977.

# OPERATIONAL SEA STATE AND DESIGN WAVE CRITERIA: STATE-OF-THE-ART OF AVAILABLE DATA FOR U.S.A. COASTS AND THE EQUATORIAL LATITUDES

CHARLES L. BRETSCHNEIDER
*Department of Ocean Engineering*
*University of Hawaii*
*Honolulu, Hawaii*

Abstract

Project OPSES-DEWAC stands for Operational Sea State and Design Wave Criteria. The work performed on this project was supported on a contract between the Energy Research and Development Administration and the University of Hawaii Department of Ocean Engineering. This was a "state-of-the-art" investigation on the availability of published material on the subjects of winds, waves, and surface currents for possible use in the determination of operational and design criteria for potential O.T.E.C. sites. It included the offshore areas of the U.S. East Coast, the Gulf Coast and the West Coast, the Hawaiian Islands, and all the equatorial oceanic areas between 20°S and 20°N latitude. No additional measurements and no generation of new data were made for increasing the "state-of-the-art". Actual data analysis by any statistical method was not part of the project. However, statistical techniques are briefly referenced that have been or are now being used for this purpose. Technical techniques for generating new data are given. Some presently used methods of application of OPSES-DEWAC data for preliminary design purposes are included in the graduate student educational parts of the project report.

The source of data are referenced and classified into one of four classes according to a pre-determined set of rules and opinions. There are various zones for which little or no adequate data are available, for example, the mid-Atlantic and Pacific Oceans of the northern hemisphere and the mid-Atlantic, Pacific and Indian Oceans of the southern hemisphere. Any plans for potential O.T.E.C. sites in such zones would have to include serious consideration for generating additional OPSES-DEWAC data by use of wave hindcasting techniques. On the other hand, the Gulf of Mexico (Zone 3) has the very best and most abundant data for use in operations and design of OTEC plants, followed by the U.S.A. East Coast, West Coast, and Hawaii zones, and also the Southeast Asia and India zones. There are some exceptions, however, where the deep water currents and sub-sea conditions are required, but these determinations were not part of the OPSES-DEWAC project.

The final report has about 450 pages of text, figures, and tables, 32 circulars/pages--one for each of the 32 OPSES-DEWAC zones, and the technical and student educational contributions mentioned above. Opinions given in the report are subject to change should any previous or future information become available.

It seems appropriate to present here only a generalized overview of the 32 OPSES-DEWAC zones as given in Vol. I of the Final Report and then give specific emphasis to the available data for Zone 3, the Gulf of Mexico.

## 2. Introduction

OPSES-DEWAC stands for Operational Sea State and Design Wave Criteria. The study was a current State of the Art literature search and was limited to winds, waves and surface currents. It included the offshore areas of the U.S.A. East Coast, Gulf Coast and the Pacific Coast, the Hawaiian waters and all of the equatorial oceanic areas between 20°S and 20°N latitude. The study areas included 32 OPSES-DEWAC zones, as shown in Fig. 1 and geographically demarcated in Table 1. A (final) report was prepared for these 32 zones, and a one table page for each zone summarizes pertinent primary and secondary references for OPSES winds, waves and currents and DEWAC winds, waves and currents.

There are many good references pertaining to winds and waves. There are theoretical works, laboratory studies and field studies. In fact, there are thousands of references on the subject that can be found in many well-recognized technical journals. However, many of these references are of fundamental and for basic concerns only. They are references that precede and make-up the various parts of something that has practical significance to papers and reports that can be used by engineers. One of the purposes of project OPSES-DEWAC is to make aware to the engineers of operation and construction disciplines the presently available pertinent data and sources of data for use in OTEC projects. It is hoped that little has been overlooked, but this is always a possibility. Certainly there must be available data of a proprietary nature that certain organizations are not permitted to make public for one reason or another.

The distinction between "primary", "secondary", and "other" references is made as follows. A primary reference is one which contains actual data which may be used

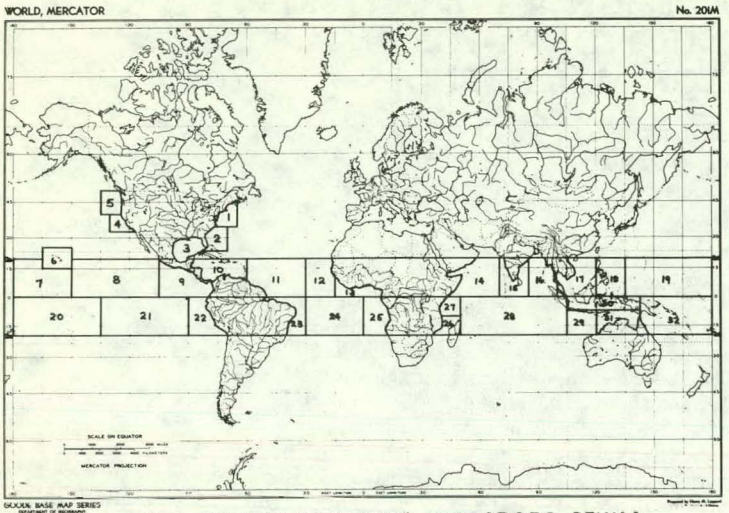



FIG.1 ZONE DESIGNATIONS FOR OPSES-DEWAC
(NOTE: COMPARE WITH FIGS. 2 AND 3; ZONE NUMBERS NOT THE SAME)

for operational as well as design criteria by employing statistical methods. A secondary reference is one which uses primary data sources in order to generate and/or analyze additional data. For example, Hogben and Lumb (9) together with (9A) is a primary source, whereas Flatseth and Pedersen (30), who have used the data of (9) for statistical analysis, is a secondary reference. Similarly, the SSMO data (19) is a primary source, whereas, Harris (31), who used the data also for statistical purposes, is a secondary source. Sometimes it is difficult to determine whether certain references should be classified primary or secondary since the distinction is not necessarily based on quality of work but rather on the importance of a particular source for its engineering use in either operational or design criteria. A reference which is designated primary for operational (OPSES) is not necessarily primary for design (DEWAC) criteria, and vice versa. For example, C.L. Bretschneider and R. Gaul (3) is a primary reference for OPSES, but not even a secondary reference for DEWAC, because all hurricane conditions were eliminated in the study. However, the hurricanes were included in Wilson (23) making this reference primary to DEWAC but is not even a secondary reference for OPSES because it does not include the data of (3). [Refs. (3) and (23) apply only to OPSES-DEWAC Zone 3 and not to Zones 1 and 2.]

Abstracts were prepared from about 150 of the references and these abstracts were used: (1) to prepare a code for the references and to distinguish between Primary (P), Secondary (S), OPSES (O), DEWAC (D), and Zones 1 thru 32; and (2) to prepare a circular sheet, one each for the 32 zones. The circular sheets also includes a code for a rating of the references:

> Two or more primary sources of data, complete (AA), two primary sources of data, almost complete (A), one primary source of data, partially completed (B), inadequate, no primary source of data (I), exceptions (E), strength (+) or weakness (-), and numbers designate the reference as cited (1, 2, 3, etc.).

At the bottom of each circular sheet evaluations are given for OPSES and DEWAC, together with recommendations. See Table II for Zone 3 as an example.

TABLE I

THE OPSES-DEWAC ZONES

| LOCATION DESIGNATIONS | | | |
|---|---|---|---|
| Zone No. | Geographic Area | Degrees Latitude | Degrees Longitude |
| | *U.S. MAINLAND AND HAWAII* | | |
| 1 | East Coast (Cape Hatteras to Maine) | 35.5°-45°N | 65°- 75°W |
| 2 | East Coast (Cape Hatteras to Key West) | 23° -35.5°N | 76°- 80°W |
| 3 | Gulf Coast | 18° -30°N | 80°- 95°W |
| 4 | Pacific Coast, California | 32.5°-40°N | 115°-130°W |
| 5 | Pacific Coast, Northwest | 40° -50°N | 125°-135°W |
| 6 | Hawaii | 15° -25°N | 150°-165°W |
| | *FROM HAWAII TO 20°N LATITUDE* | | |
| 7 | Central Pacific Ocean | 0°-20°N | 150°-180°W |
| 8 | Mid Eastern Pacific Ocean | 0°-20°N | 105°-150°W |
| 9 | Cocos Ridge Vicinity | 0°-20°N | 80°-105°W |
| 10 | Caribbean Sea | 0°-20°N | 60°- 85°W |
| 11 | Central Atlantic Ocean | 0°-20°N | 30°- 60°W |
| 12 | Eastern Atlantic Ocean | 0°-20°N | 15°- 30°W |
| 13 | Gulf of Guinea | 0°-20°N | 10°E- 15°W |
| 14 | Arabian Sea | 0°-20°N | 45°- 70°E |
| 15 | Mid-Indian Ocean | 0°-20°N | 70°- 85°E |
| 16 | Bay of Bengal and Andaman Sea | 0°-20°N | 85°- 95°E |
| 17 | South China Sea | 0°-20°N | 100°-120°E |
| 18 | Philippine Sea | 0°-20°N | 120°-135°E |
| 19 | Western Pacific Ocean | 0°-20°N | 135°-180°E |
| | *FROM EQUATOR TO 20°S LATITUDE* | | |
| 20 | Central Pacific Ocean | 0°-20°S | 135°-180°W |
| 21 | Eastern Pacific Ocean | 0°-20°S | 90°-135°W |
| 22 | Western South America | 0°-20°S | 70°- 90°W |
| 23 | Western Atlantic Ocean | 0°-20°S | 30°- 50°W |
| 24 | Central Atlantic Ocean | 0°-20°S | 0°- 30°W |
| 25 | Eastern Atlantic Ocean | 0°-20°S | 0°- 10°E |
| 26 | Mozambique Channel | 10°-20°S | 35°- 50°E |
| 27 | East Coast Africa | 0°-10°S | 40°- 50°E |
| 28 | Central Indian Ocean | 0°-20°S | 50°-105°E |
| 29 | Eastern Indian Ocean | 7°-20°S | 105°-120°E |
| 30 | Java and Banda Seas | 0°- 7°S | 105°-135°E |
| 31 | Timor and Arafura Seas | 7°-20°S | 120°-142.5°E |
| 32 | Coral Sea and Fiji Basin | 0°-20°S | 142.5°-180°E |

Out of very many references, only about 160 were selected as pertinent primary or secondary references for the entire 32 OPSES-DEWAC zones. The literature of the references include many more references that the reader may seek. Brief abstracts of about 150 of the pertinent

TABLE II

EXAMPLE ONE PAGE SUMMARY FOR ZONE 3
ZONE 3 REFERENCES

Zone 3: 23°-18°N by 80°-95°W, Gulf of Mexico

A. References for Operational Criteria

| | Winds | Waves | Currents |
|---|---|---|---|
| Code | AA | AA | A |
| Primary References | 14, 15, 18, 19r, 19bb, 20a, 20d, 24a, 24c | 3, 9, 9A, 14, 18, 19r, 19bb, 15, 21d, 24, 24a, 24c | 6, 8, 11, 14, 15, 18, 24c |
| Secondary References | 27, F | 26, 27, 31, F | 32, 33, 35, 37, F |

B. References for Design Criteria

| | Winds | Waves | Currents |
|---|---|---|---|
| Code | AA | AA | A |
| Primary References | 1, 4, 5, 7, 10, 14, 15, 17, 19r, 19bb, 24a, 24c, 151 | 1, 2, 3, 4, 9, 9A, 14, 15, 19r, 19bb, 23, 24, 24a, 24c, 151 | 8, 14, 15, 24c |
| Secondary References | 25, 28, 29, 34, F | 26, 30, 31, 36, F | 37, F |

EVALUATION FOR OPERATIONAL SEA STATE

All pertinent deepwater operational wave information is readily available in the references. The completeness of coverage exists also for the winds and currents, although current data for specific sites may require local measurements.

EVALUATION FOR DESIGN WAVE CRITERIA

Coverage of design information for winds and waves is adequate. Additional data may be obtained by a statistical analysis of the operational criteria. Current data is quite inadequate. It may be necessary to apply design wind information to existing theoretical current relationships to compute design current conditions.

RECOMMENDATIONS

Consider the effects of the Gulf Stream on waves according to refs. (12) and (24). Calculate and/or measure average current conditions.

[NOTE: Not all the references listed in Table II are included in the present paper, but are included in the Final Report, reference (F.).]

references are given in the Final Report. These references were used to make a subjective evaluation of the available data for each of the 32 OPSES-DEWAC zones, as well as statements of recommendations. Thus one page for each zone gives the reader an idea of the availability and quality of the data for each zone. Table II gives a sample of the one page summary for Zone 3, Gulf of Mexico. The evaluations and recommendations based on the subjective review of the referenced material was sometimes a trying task, and finally it appeared that additional guidances for the user might be necessary.

3. Classification of OPSES-DEWAC Zones

The references were further screened in order to make another presentation. The object was to classify the available data into one of four classes. This was an opinionated classification, but others may be entitled to other opinions. Table III gives 10 general rules for the classification. This resulted in a total of only 30 surviving references given in Table IV for the entire 32 OPSES-DEWAC zones. Each OPSES-DEWAC zones still had one or more than one reference, as some references applied to many zones. Working with only 30 references instead of 160 made it rather easy to set up 10 rules (see Table III) by which each classification was made.

TABLE III

GENERAL RULES FOR CLASSIFICATION

1. Deep water wind wave and swell hindcasts are Class I OPSES wave data and Class II DEWAC wave data [ref. (3), (13), (16), (41), (43), (62), (65), (74), (104) & (119)].

Hindcasts include simultaneous sea and swell, each having its one wave period, but are limited to onshore and along shore directions. Statistical methods are required to obtain DEWAC wave data from OPSES wave data, hence Class II DEWAC wave data.

2. Hurricane wind and wave measurements (1), hurricane winds (7), extreme winds (139), hurricane wind and wave calculations (2), (4), (23), and (152) and wave hindcasts from strong extra tropical storms (64) are Class I DEWAC wind and wave data.

3. Hogben and Lumb (9), (9A) are Class II OPSES and DEWAC wave data.

4. SSMO [all (19)] are Class I OPSES wind data, Class II OPSES wave data and Class II DEWAC wind and wave data.

5. Atlases [all (20), (21), (22) and (100)] are Class III and Class IV OPSES and DEWAC wind, wave and current data as the case may be. Class IV data are for areas where least data were used to prepare the charts.

6. Class I, II and Class III and IV OPSES current data become Class II, III and IV DEWAC current data, respectively, provided proper statistical techniques can be used. It is assumed that this is possible.

7. Ref. (8) was used to make Class II OPSES current data out of what otherwise would have been Class III DEWAC current data.

TABLE III (cont'd)

GENERAL RULES FOR CLASSIFICATION

8. Ref. (95) was used to make Class II OPSES wind data out of what otherwise would have been Class III or Class IV OPSES wind data, and then this becomes Class III DEWAC wind data.

9. The other references were used as an aid for doubtful cases of classification.

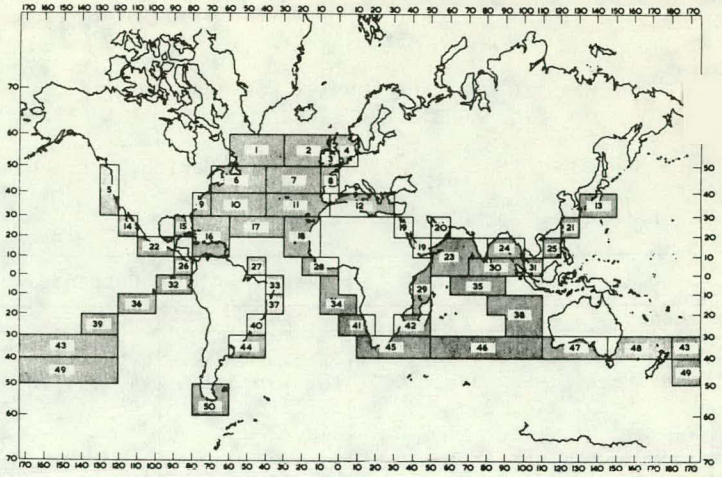
10. Ref. (24a), when such becomes available, will make all OPSES wind and wave data Class I and DEWAC data Class I or Class II, as the case may be.

[Table IV OPSES-DEWAC Classification was prepared by applying the above rules with due regard to the references as shown in Table II, although the other references given previously were not totally ignored.]

Class I wave data and only Class I must have wave hindcast statistics. All other wave data, such as short term wave recordings, ship observations, climatic wave charts, etc. are supplemental to Class I data. Wave hindcast statistics are the only available data having simultaneous occurrence of wind waves and swell not otherwise lost in other presentations. Class II wave data would have data of ship observations, such as Hogben and Lumb data (Fig. 2) and SSMO data (Fig. 3). Also see pertinent detailed SSMO areas given by Figures 4, 5 and 6. Class III and Class IV data do not have either Hogben and Lumb data or SSMO data. The data are of other sources having lesser observations. Sea and swell charts fall into Class III data and in some cases even Class IV data where observations are a minimum. Class I does not necessarily mean first class data; it merely means that there is plenty of good data from a number of sources. Class IV data does not mean that the data is bad; it merely means that there is not much good data and the number of sources are minimal. In fact there might well be a short period of several months of first class data in a zone classified as Class IV data because there is not a long enough period of time. Generally any short term recorded data does not affect but merely supports the classification, except perhaps a few locations in the Gulf of Mexico. Zone 3 is already Class I without the wave recordings from (1). The data of (1) also supports the value of (2) for use in Zones 1, 2 and 3.

Similarly the 10 rules were applied to all OPSES winds and currents as well as the waves and also to all DEWAC winds, waves and currents. Thus one of four classifications is applied to 6 conditions for each of the OPSES-DEWAC.

Finally Table V gives the classification for each of the OPSES-DEWAC zones. This is an opinionated classifaction which can change when more data become available, for example by use of wave hindcasting or wave forecasting techniques. This can be accomplished, for example, by use of the wave forecasting computer program at the U.S. Naval Fleet Numerical Weather Central, Monterey (24a). Also various other commercial computer programs are available for wave forecasting and wave hindcasting.



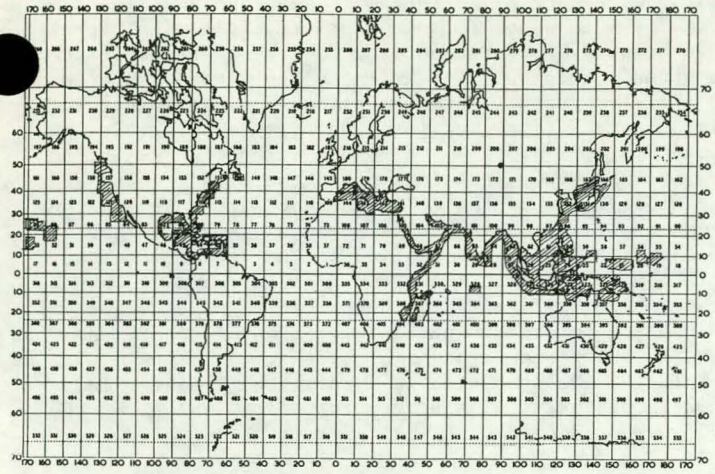
GROUPING OF MARSDEN SQUARES INTO AREAS
FIG. 2 ZONE DESIGNATIONS AFTER HOGBEN AND LUMB (1966)
(Only for USA coasts, Hawaii, and for 20°N Equator to 20°S Equator)
NOTE: Compare with Figs. 1 and 3: Zone numbers not the same

**TABLE IV**

**SUMMARY OF OPSES-DEWAC ZONES FOR THE LISTED REFERENCES**

| Listed References | ZONES | | | | | |
|---|---|---|---|---|---|---|
| | OPSES | | | DEWAC | | |
| | Wind | Wave | Current | Wind | Wave | Current |
| 1 | | | | 3 | 3 | |
| 2 | | | | 1,2,3 | 1,2,3 | |
| 3 | | | | 3 | | |
| 4 | | 3 | | | | |
| 7 | | | | 1,2,3 | 1,2,3 | |
| 8 | | | All | | | All |
| 9 | | 1,2,4,5,9, 10,12,13, 14,15,16, 17,18,22, 23,25,26, 27,28,29 | | | 1,2,4,5,9, 10,12,13, 14,15,16, 17,18,22, 23,25,26, 27,28,29 | |
| 13 & 16 | | 1 | | | 1 | |
| 19 | 1,2,3,4,5, 6,10,14, 15,16,17, 18,26,27, 30,31 | 1,2,3,4,5, 6,10,14,15, 16,17,18, 26,27,30, 31 | | 1,2,3,4,5, 6,10,14, 15,16,17, 18,26,27, 30,31 | 1,2,3,4,5, 6,10,14,15, 16,17,18, 26,27,30, 31 | |
| 21 | | 11,12,13 14,15,16, 17.18,19, 23,24,25, 26,27,28, 29 | | | | |
| 22 | | | 7,8,9,11, 12,13,14, 15,16,18, 19,26,27, 28,29,32 | | | 7,8,9,11, 12,13,14, 15,16,18, 19,26,27, 28,29,32 |
| 23 | | | | 3 | 3 | |
| 41 & 43 | | 4 | | | 4 | |
| 52 | | | 4 | | | |
| 62,65,&74 | | 6 | | | 6 | |
| 64 | | | | | 6 | |
| 93 | | | 7,8,9,18, 19,20,21, 22,32 | | | |
| 95 | 7,8,9,18,19, 20,21,22,32 | | | | | |
| 97 | 16 | 16 | | | | |
| 98 | | 16 | | | 16 | |
| 99 | | 14 | | | 14 | |
| 100 | 28,29,32 | | 28,29,32 | | | 28,29,32 |
| 104 | | 15 | | | 15 | |
| 119 | | 17 | | | 17 | |
| 139 | | | | 29,31 | | |
| 152 | | | | 6 | 6 | |

(see list of references)



MARSDEN SQUARE CHART

FIG. 3 AREAS OF THE WORLD WHERE SSMO DATA ARE OBSERVED AND REPORTED

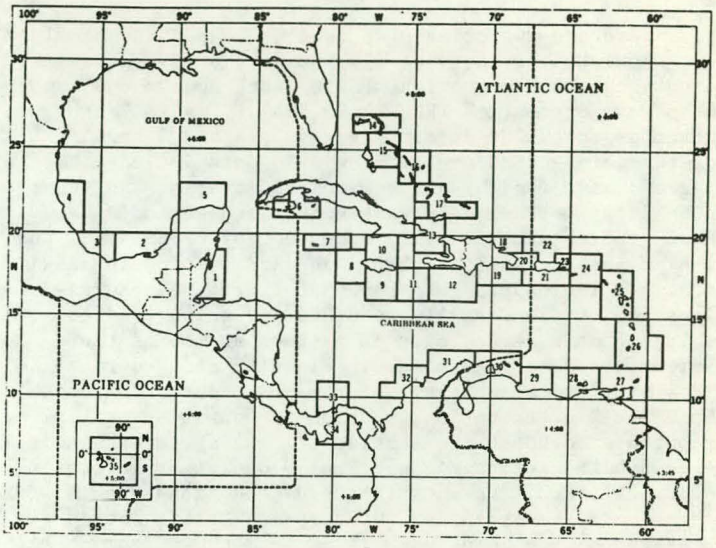



FIG. 5 CARIBBEAN AND NEARBY ISLAND COASTAL MARINE SSMO AREAS AND STANDARD TIME ZONES

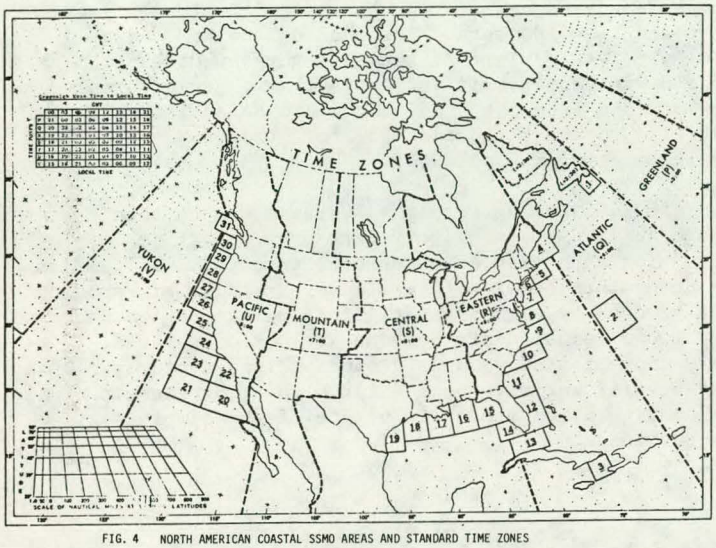



FIG. 4 NORTH AMERICAN COASTAL SSMO AREAS AND STANDARD TIME ZONES

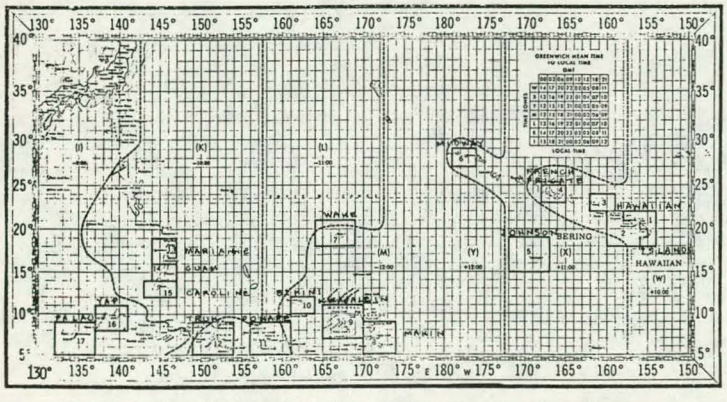



FIG. 6 HAWAIIAN AND SELECTED NORTH PACIFIC ISLAND COASTAL SSMO AREAS AND STANDARD TIME ZONES

TABLE V

OPSES DEWAC CLASSIFICATION

| Zone | OPSES | | | DEWAC | | |
|---|---|---|---|---|---|---|
| | Wind | Wave | Current | Wind | Wave | Current |
| 1 | I | I | I | I | I | II |
| 2 | I | II | I | I | I | II |
| 3 | I | I | I | I | I | II |
| 4 | I | I | I | I | II | II |
| 5 | I | II | I | I | II | II |
| 6 | I | I | I | I | I | II |
| 7 | II | III | II | III | III | III |
| 8 | II | III | II | III | III | III |
| 9 | II | II | II | III | II | III |
| 10 | I | II | II | I | II | III |
| 11 | IV | IV | IV | IV | IV | IV |
| 12 | III | II | III | III | II | IV |
| 13 | III | II | III | III | II | IV |
| 14 | I | II | II | I | II | III |
| 15 | I | I | II | II | II | III |
| 16 | I | I | II | I | II | III |
| 17 | I | II | II | I | II | III |
| 18 | I | II | II | I | II | III |
| 19 | II | III | II | III | III | III |
| 20 | II | III | II | III | III | III |
| 21 | II | III | II | III | III | III |
| 22 | II | II | I | III | II | II |
| 23 | III | II | I | IV | II | II |
| 24 | IV | IV | IV | IV | IV | IV |
| 25 | III | II | II | IV | II | III |
| 26 | I | II | I | I | II | II |
| 27 | I | II | I | I | II | II |
| 28 | IV | IV | IV | IV | IV | IV |
| 29 | I | II | II | I | II | III |
| 30 | I | II | II | I | II | III |
| 31 | I | II | II | I | II | III |
| 32 | II | III | II | III | IV | III |

| Class | NUMBER OF ZONES | | | | | |
|---|---|---|---|---|---|---|
| | OPSES | | | DEWAC | | |
| | Wind | Wave | Current | Wind | Wave | Current |
| I | 17 | 6 | 10 | 17 | 4 | 0 |
| II | 8 | 17 | 17 | 0 | 19 | 10 |
| III | 4 | 6 | 2 | 10 | 5 | 17 |
| IV | 3 | 3 | 3 | 5 | 4 | 5 |

## 4. Discussion of OPSES-DEWAC

There are two primary sources of wave data, namely U.S. Naval Weather Service (19) Summary of Synoptic Meteorological Observations (SSMO), and Hogben and Lumb Ocean Wave Statistics (HLOWS) (9, 9A). Figure 2 shows the areas for HLOWS data. Figures 3, 4 and 5 show coastal marine SSMO areas. The SSMO data includes both wind and wave (height and period) observations and the HLOWS data includes only wave height and period data. These reports are generally accepted for OPSES data, and with proper statistical techniques and caution for DEWAC data. It is important to remember that wave observations are not necessarily accurate and ships tend to avoid the most severe part of a storm and hence the maximum are sometimes missed. Flatseth and Pederson (30) did a statistical analysis of the HLOWS data. Although the Weibull distribution function is one of several acceptable methods, the statistical extrapolations must be used with caution. For example, one might interpret incorrectly from the data that sea conditions are greater off the Argentina, Uruguay and Brazil coasts than around Cape Horn, when it is well known from history books that this is not the case. The fact is that Cape Horn area (area 50) has some of the most severe storms and highest seas in the world. The reason very large waves were not observed, and hence cannot be predicted accurately from the statistical analysis, is that there were no ships going around the Horn or else they were heavily occupied with other hazard controls and not reporting data. Supertankers now make the trip.

Also, during the winter season, in particular, ships captains prefer to avoid the Horn and either go through the straits or route through the Panama Canal. This case at hand should be a reminder in using any SSMO or HLOWS data. In many cases, however, the SSMO and HLOWS data can be quite reliable, for example, HLOWS area 4 in the North Sea, where the wave observations have been calibrated by use of ship-borne wave recorder. Now that the supertankers are going around the Horn, perhaps better wave data will become available for HLOWS area 50.

Both the SSMO and the HLOWS wave height and period must be corrected to significant waves. The lower waves are generally observed too low and the higher waves too high. It can be determined from Hogben and Lumb (9) that the best fit relationship is

$$H_s = 2.04 + 0.82\, H_{v.o.s.} \quad \text{(meters)} \qquad (1\text{-a})$$

$$H_s = 6.7 + 0.82\, H_{v.o.s.} \quad \text{(feet)} \qquad (1\text{-b})$$

where $H_s$ = significant wave height in meters or feet and $H_{v.o.s.}$ is the visually observed wave height in meters or feet. Evidentally from equation (1) the observed and significant wave height are equal at 11.33 meters or at 37 feet, and observed wave heights below 37 feet are too low and above 37 feet are too high. This will have some effect on the statistical interpretation of the data. For example it can be shown that the statistical prediction equation for recurrence interval has the following form

$$H_I = A + m \ln I \qquad (2)$$

where I is the recurrence interval (I = 10, 25, 50, 100 years, etc.) and $H_I$ is the corresponding significant wave height. A is equal to some characteristic significant wave height, $H_R$, corresponding to some characteristic recurrence interval, $I_R$, and m is the slope of the line on semi-log graph. Thus, equation (2) is somewhat sensitive to predictions for large recurrence intervals because of the slope m. Also the value of A can be too low if the ship's captain avoided the higher seas, and the slope m can be too large because of the redistribution of the data. In addition m will always be too large if equation (1) is not applied to the raw data. What this combined effect means for 8 to 10 years of wave observation is first (a) the predicted wave height will be too low for recurrence intervals equal to or less than 8 to 10 years and second (b) because the slope m will be too large, the predicted wave height will be too large at some larger value of the recurrence interval, i.e. the 100 year predicted wave will perhaps be too high.

It seems that a simple prediction equation is given in normal form as follows

$$H/H_R = 1 + m \ln \frac{I}{I_R} \qquad (3)$$

where $H_R$ corresponds to $I_R$, e.g. the $H_R$ = the 10 year wave and $I_R$ = 10 years. For much of the SSMO data m = 0.16 ± 10%. In fact the data for New Orleans, Miami, Puerto Rico and Hawaii indicates that m deviates only a few percent from m = 0.16. It would be an interesting exercise to check equation (3) for other SSMO areas having plenty of good data.

The 10 year $H_R$ for $I_R$ = 10 years can be obtained graphically once the significant wave height is determined for a particular recurrence interval. It remains to determine the significant wave period. This should not be done by similar statistical relationships because the two marginal distributions are not correlated. A very convenient way to determine a close approximation to the significant wave period for high recurrence intervals (also high wind speeds) is by use of the simple expression

$$f_o^{-1} = 2.13 \sqrt{H_s} \qquad (4)$$

$$T_s = \sqrt{4/5}\, f_o^{-1} = 2.01 \sqrt{H_s} \qquad (5)$$

In equation (4) $f_o$ is the wave frequency corresponding to $S(f_o)$, the peak of the energy frequency spectrum.

## 5. Surface Currents and Other Currents

OPSES surface currents can either be obtained from U.S. Navy Hydrographic Office (currently the U.S. Naval Oceanographic Office) (22) or they may be calculated from wind stress data, for example, Hidaka (8), and appropriate formulae found in oceanography textbooks. Similarly, the currents can be calculated for depths below the sea surface. However, we must also remember that there are other currents to consider, such as those caused by river flow, density variation, and the large streams of the oceans of which the Gulf stream and the Peru current are examples. The work of Wyrtki (1975) is most appropriate for the Pacific Ocean from 30°S to 30°N latitude (93).

It is not intended to go into further details on

surface currents, since this paper is directed primarily toward waves.

### 6. Hurricane Winds and Waves

In the tropical areas north of the equator there will be places where hurricanes must be considered for DEWAC. This problem seems to have been solved for the U.S.A. Gulf Coast and East Coast states [see Graham and Nunn (7), Bretschneider (4), and Bretschneider and Tamaye (15)].

Figure 7 shows the areas in the Gulf of Mexico and the U.S.A. East Coasts where both the standard project and probable maximum hurricanes apply, and the hurricane wind fields can be determined by Graham and Nunn (7). Both the hurricane wind and wave fields can be determined from Bretschneider (4). Perhaps the lower zones can be extended southward with only a slight modification of the wind and wave fields.

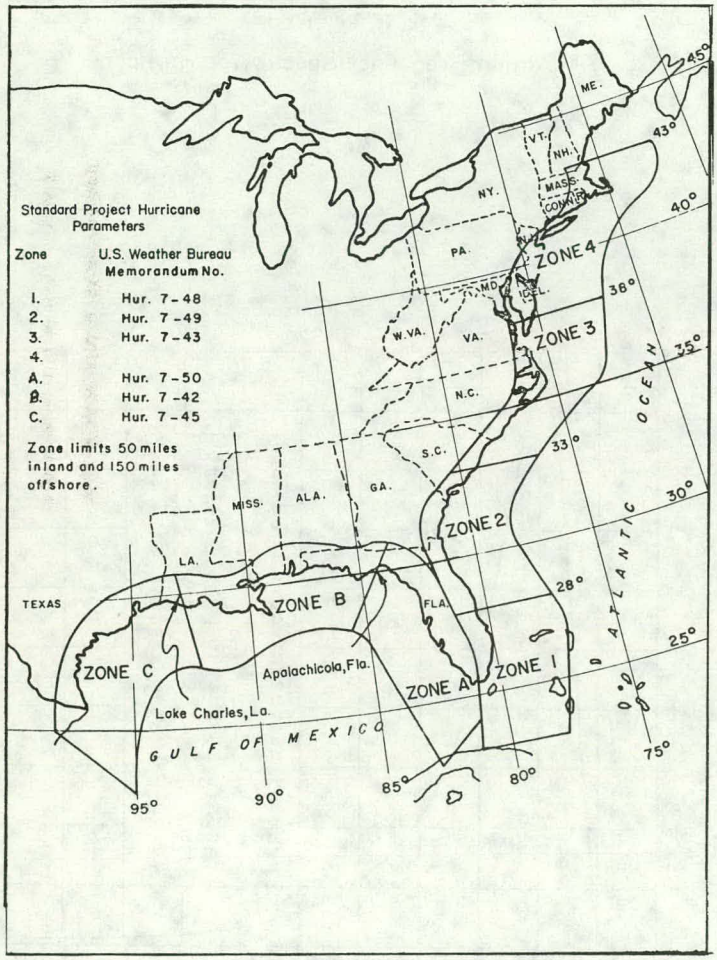



FIG. 7 HURRICANE ZONES, ATLANTIC AND GULF COAST, U.S.A., FOR U.S. WEATHER SERVICE

(NOTE: THE ZONES ARE NOT THE SAME ZONES AS OPSES-DEWAC, SEE FIG. 1.)

The project Mohole sea state survival hurricane spectrum for the Atlantic Ocean was given by Bretschneider and Collins (2). Fig. 8 shows that area in the Atlantic where the design spectrum (Figs. 10 and 11) will not be exceeded for a 100 year recurrence interval. Figs. 10 and 11 are most applicable for latitude 30°N off the U.S. East Coast. Further South and East in the shaded zone shown in Fig. 8 the conditions will be less severe.

FIG. 8 ATLANTIC OCEAN HURRICANE ZONE (FROM REFERENCE 2)

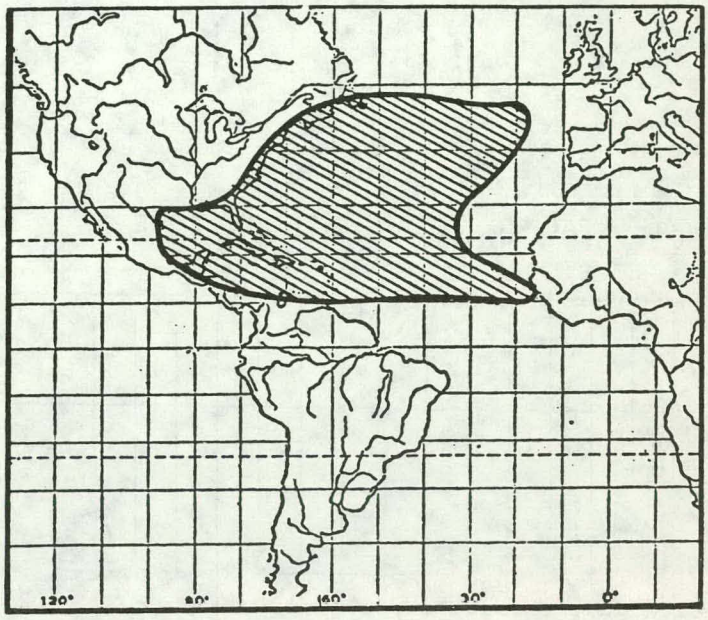



Fig. 9 shows the area in the Pacific Ocean where it is expected that the conditions might be exceeded. Figs. 10 and 11 should not be used in the Pacific Area until further studies on typhoons are made. The 100 year design hurricane waves decrease with decrease in latitude as can be found from Bretschneider (4).

Figures 12, 13 and 14 show the results of the analysis of Hurricane Camille (1969). Fig. 13 is the path; Fig. 12 shows the calculated wind field from the measured hurricane parameters and the calculated wave field using the model hurricane techniques of Bretschneider (4). Figure 14 shows a comparison between recorded and calculated or hindcast waves. The agreement is remarkably good, and could have been shown to be even better by rotating the hurricane ±45° from the path shown. This is allowable according to the U.S. Weather Service practices. The above verification of the model hurricane wave field is very encouraging. The technique has been applied to the conditions in Hawaii. Fig. 15 shows the paths of recent hurricanes for Hawaii and Fig. 16 the calculated hurricane wind and wave field by Tamaye and Rocheleau (152).

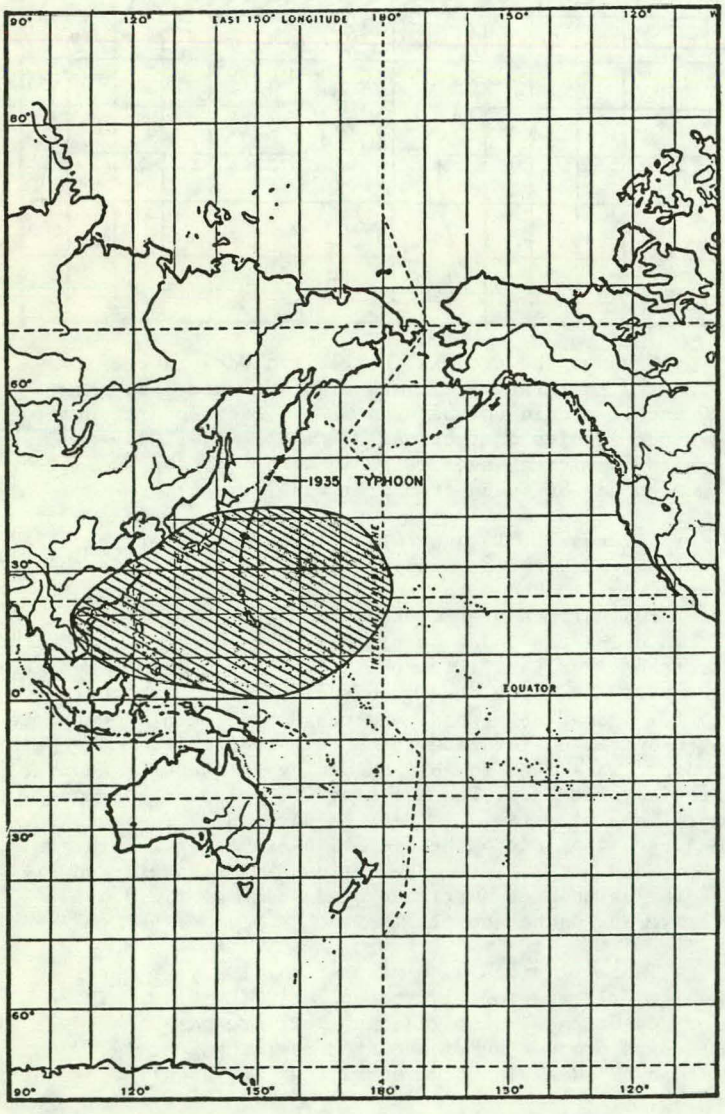
Table VI gives a summary of the 100 year Hurricane Design Criteria for five potential OTEC sites. Those for New Orleans, Miami and Key West are based on the standard project hurricane from Bretschneider (4), Puerto Rico by Hindcasting from Hurricanes and Hawaii from the

model hurricane given by Tamaye and Rocheleau (152). In Table VI: $U_S$ is the 10 meter level 10 minute average sustained wind speed; $G_S = 1.45\ U_S$ the gust speed; $H_S$ is the significant wave height. The significant wave period $T_S = \sqrt[4]{4/5}\ f_o^{-1}$, where $f_o$ is the wave frequency associated with $S(f_o)$ the maximum energy density and is obtained from the following equation

$$\frac{f_o^{-1}}{U} = 0.4 \tanh \left\{ \ln \left[ \frac{1 + \frac{40H_s}{U^2}}{1 - \frac{40H_s}{U^2}} \right]^{1/2} \right\}^{0.6} \qquad (6)$$

$f_o^{-1}$ = sec., $H_S$ = feet, $U = U_S$ = knots
$\overline{H} = 0.625\ H_S$, $\overline{T} = 0.906\ T_S$ and $H_{MAX} = 1.8\ H_S$.

FIG. 9 **PACIFIC OCEAN TYPHOON ZONE**
(FROM REFERENCE 2)



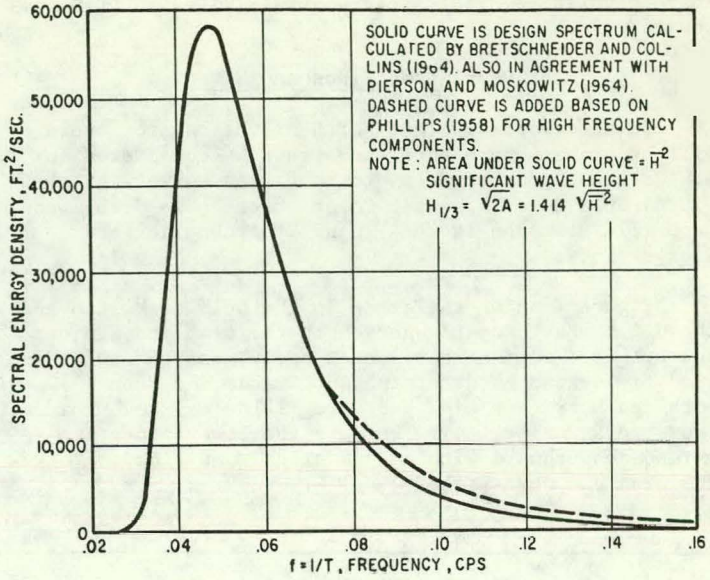




**Fig. 10** Maximum frequency spectra for Hurricane "B". (FROM REFERENCE 2)

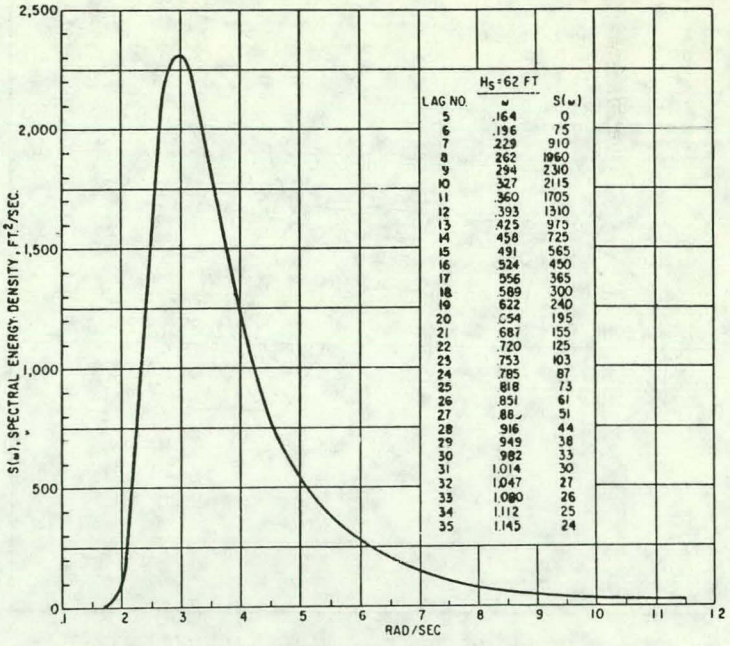



**Fig. 11** Floating drilling platform design sea state spectrum for survival condition. Note: This figure and the Energy Density were calculated by the Brown & Root Project Mohole staff. (FROM REFERENCE 2)

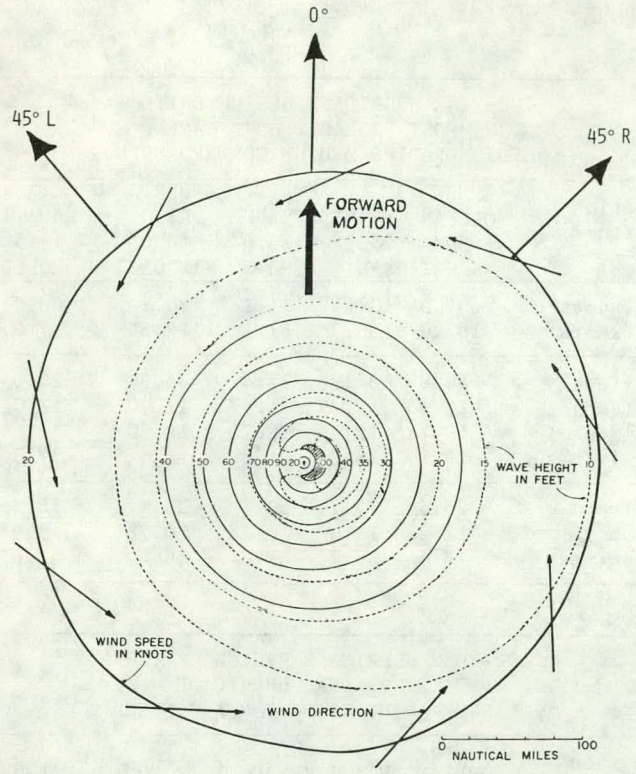



Fig. 12 Wind and Wave Field predicted for Hurricane Camille (1969). (from reference 151)

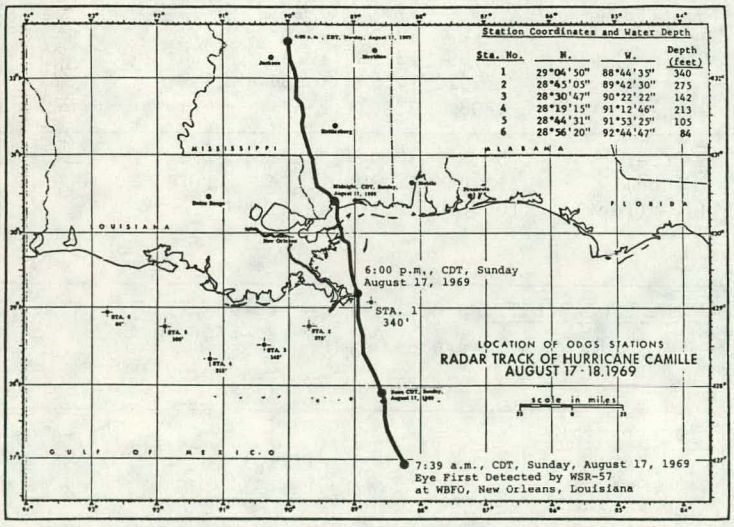



Fig. 13 Path of Hurricane Camille (1969) thru six measuring stations--of Shell's Ocean Data Gathering Program--in the Gulf of Mexico

The joint probability distribution of H and T and the wave spectrum S(f) are given by the equations at the bottom of Table VI. $T_s$ given by equation (6) is about 10% less than $T_R$ given by Bretschneider (4) and almost the same as given by the approximation given by equation (5).

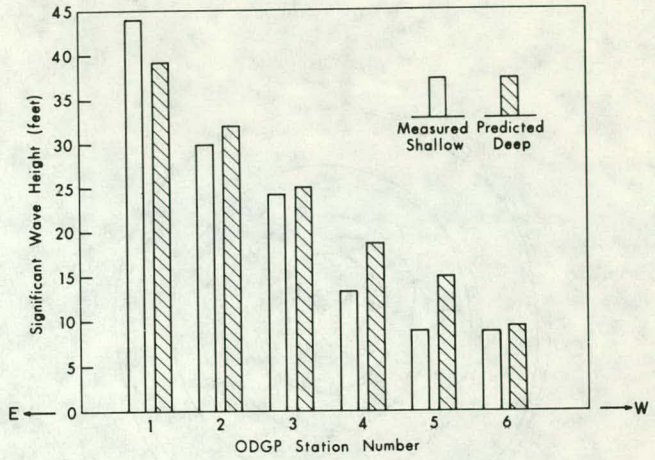



Fig. 14 Predicted and Measured Height of the Significant Wave Generated in the Gulf of Mexico at six different measuring stations--of Shell's Ocean Data Gathering Program--by Hurricane Camille, 1969. Values estimated from Fig. 11. (from reference 151)

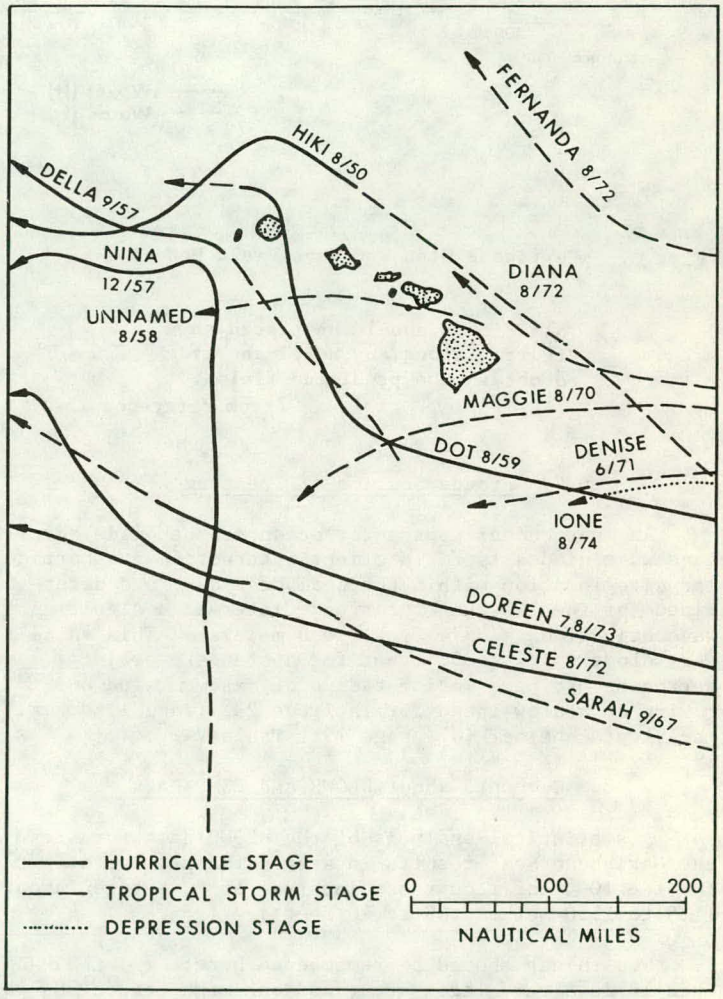



Fig. 15 Tracks of Hurricanes and Tropical Storms in the Vicinity of the Hawaiian Islands for the period 1950-1974. This Figure was provided through the courtesy of the National Weather Service of the National Oceanic and Atmospheric Administration of the government of the U.S.A. (from reference 152)

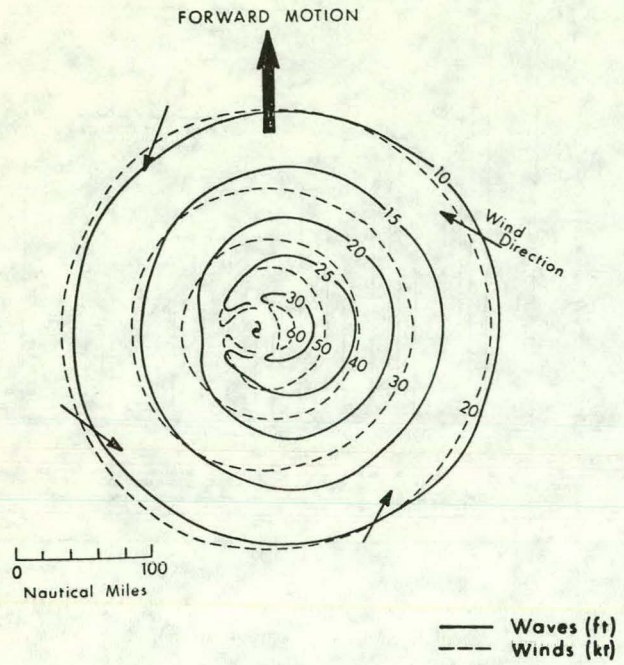



**Fig. 16** **Hurricane Wind and Wave Field Model.**

**This Figure should be placed on Figure 15 along any hurricane track to obtain the predicted fields.**

**(from reference 152)**

7. Froude Scaling of Spectrum

An independent contractor oceanographer made hurricane wave hindcasts for a client interested in a particular site location within the Caribbean Sea, and determined for the 100 year recurrence interval a significant wave height, $H_S$ = 35.4 feet (10.8 meters). This value is very close to $H_S$ = 35.1 feet for a standard project hurricane having a medium radius of maximum wind and moving at a slow speed for latitude 23° (zone 1, U.S.A.) [see Bretschneider (4), page 191, Table V-1].

8. Comments about HLOWS and SSMO Data

A statistical analysis of the HLOWS data for area 16, the Caribbean Sea, results in a significant wave height for the 100 year recurrence interval of $H_S$ between about 11.5 to 12.0 meters (39 to 40 feet).

Two things should be remembered here: (1) the HLOWS area 16 is a very large area, and one might expect $H_S$ to be larger and (2) captains of ships tend to avoid the storm areas of highest seas and thereby introduce what is termed a "Fair-Weather Bias" into observations from their ships. Thus, one might expect $H_S$ to be smaller and also the total number of observations are minimal.

TABLE VI

100-YEAR HURRICANE DESIGN CRITERIA
MOST PROBABLE HURRICANE
MEDIUM RADIUS MEDIUM FORWARD SPEED

| Location<br>Latitude<br>Type | NEW ORLEANS<br>30°<br>SPH I | MIAMI<br>25.5°<br>SPH I | KEY WEST<br>23.0°<br>SPH I | PUERTO RICO<br>18.0°<br>HINDCAST | HAWAII<br>19.5°<br>MODEL |
|---|---|---|---|---|---|
| $U_S$ (knots) | 94.5 | 107.1 | 111.1 | 84.8 | 60.0 |
| $G_S$ (knots | 137.0 | 155.3 | 161.1 | 122.5 | 87.0 |
| $H_S$ (feet) | 40.8 | 37.9 | 37.4 | 36.9 | 30.0 |
| $T_S$ (sec) | 12.46 | 11.72 | 11.57 | 11.90 | 11.01 |
| $f_o^{-1}$ (sec) | 13.16 | 12.39 | 12.23 | 12.60 | 11.64 |
| $S(f_o)$ ($ft^2$sec) | 1961 | 1593 | 1532 | 1536 | 938 |
| $\overline{H}$ (feet) | 25.5 | 23.7 | 23.4 | 23.1 | 18.75 |
| $\overline{T}$ (sec) | 11.28 | 10.62 | 10.48 | 10.78 | 9.97 |
| $H_{MAX}$ (feet) | 73.4 | 68.2 | 67.3 | 66.4 | 54.0 |

100-YEAR HURRICANE DESIGN CRITERIA
EXCEPTIONAL HURRICANE
LARGE RADIUS FAST FORWARD SPEED

| Location<br>Latitude<br>Type | NEW ORLEANS<br>30°<br>SPH II | MIAMI<br>25.5°<br>SPH II | KEY WEST<br>23.0°<br>SPH II | PUERTO RICO<br>18.0°<br>HINDCAST | HAWAII<br>19.5°<br>ESTIMATED |
|---|---|---|---|---|---|
| $U_S$ (knots) | 100.3 | 110.1 | 113.8 | 92.8 | 65.7 |
| $G_S$ (knots) | 145.4 | 159.6 | 165.0 | 134.6 | 95.2 |
| $H_S$ (feet) | 58.1 | 49.5 | 45.8 | 44.2 | 35.9 |
| $T_S$ (sec) | 15.05 | 13.58 | 12.98 | 13.0 | 12.03 |
| $f_o^{-1}$ (sec) | 15.91 | 14.36 | 13.67 | 13.8 | 12.72 |
| $S(f_o)$ ($ft^2$sec) | 4808 | 3150 | 2567 | 2414 | 1468 |
| $\overline{H}$ (feet) | 36.3 | 30.9 | 28.6 | 27.6 | 22.4 |
| $\overline{T}$ (sec) | 13.64 | 12.30 | 11.76 | 11.78 | 10.9 |
| $H_{MAX}$ (feet) | 104.6 | 89.1 | 82.4 | 79.6 | 64.6 |

JOINT PROBABILITY: $p(H,T)\,dH\,dT = p(H)\,dH \cdot p(T)\,dT$

$$p(H)\,dH = \frac{\pi}{2}(H/\overline{H})^2 e^{-\pi/4(H/\overline{H})^2}\,\frac{dH}{\overline{H}}$$

$$p(T)\,dT = 2.7(T/\overline{T})^4 e^{-0.675(T/\overline{T})^4}\,\frac{dT}{\overline{T}}$$

WAVE SPECTRA:

$$\frac{S(f)}{S(f_o)} = e^{5/4(f/f_o)^{-5}} e^{-5/4(f/f_o)^{-4}}$$

The hindcast value of $H_S$ = 35.4 feet therefore is selected as the most correct value for the 100 year recurrence interval for the particular location for which the wave hindcasts were made. Other locations within area 16 may have a larger value than $H_S$ = 35.4 feet and even larger than predicted by the HLOWS data, and other locations may have lower values than either HLOWS statistics and the 35.4 feet hindcast for the 100 year recurrence interval.

Perhaps the SSMO data will result even in different statistical results for the 100 year recurrence interval because (1) the SSMO data were observed from different ships over a different period of years than the HLOWS data, and (2) there are 28 SSMO areas within the HLOWS area 16, and yet area 16 is considerably larger than the sum total of the 28 SSMO areas. It would be interesting to do a comparative statistical study of all 28 SSMO areas within the single HLOWS area 16. Of course, wave hindcasting still would give better results than the observations; and, if one can establish the design hurricane parameters, then one might even find the design wave already in the published tables by Bretschneider (4).

## 9. Wave Hindcasting and Wave Forecasting

When no other reliable wave data is available, the best method of obtaining OPSES-DEWAC data is by using surface weather charts and wave forecasting techniques. The present state of the art of wave forecasting is quite accurate, but no more accurate than the winds from the meteorological charts. Today, for many areas of the world, the wind data from weather charts are fairly reliable, and, in particular, for those charts drawn more carefully and in greater detail at a later date for historical purposes. Sometimes the wave forecaster may wish to improve on the weather analysis. Wave data obtained by wave forecasting can be more accurate than ship observations. All modern methods of wave forecasting have been calibrated using very reliable wind and wave measurements. Computer programs are available to assist in the task.

For OPSES data one normally selects 6-hourly daily weather maps for a 3 to 5 year period spread over a longer period of time, say 10 to 15 years. In this case wind waves and swell hindcasts are tabulated by direction by the month or by season. Tables, histograms, cumulative graphs, or wave roses may be the method of presentation of such data.

For DEWAC data many more years of charts are required and the work becomes tedious and even expensive on a computer. What is usually done, is that the forecaster will scan all weather maps for the past 50 years or so and select at random what he thinks are the most severe storms, and selects the 100 worst storms and narrows it down to size, say about 30 storms. There may be as many as 10 to 15 consecutive maps that require an analysis for each storm. Hindcasts are made for the entire storm and statistical techniques are used to determine return intervals and risk factors. Statistical methods include the logarithmic distribution, Gumbel's distribution and the Weibull distribution, each of which is available readily in the literature.

When the forecaster limits the number of storms to 25 or 30, there is really no need for a computer unless one is available readily. The wave forecasting charts can be used with good reliability, but the forecaster must be experienced in determining the proper wind speed, fetches and wind duration.

## 10. Acknowledgements

This paper is based in part on the Final Report on Operational Sea State and Design Wave Criteria (OPSES-DEWAC) for Ocean Thermal Energy Conversion Projects (F.) which is the result of work supported by the U.S. Energy Research and Development Administration by Contract No. AT (04-3)-235 Project Agreement No. 13 with the Department of Ocean Engineering of the University of Hawaii.

Acknowledgements are made to Mr. J. T. O'Brien, Co-Principal Investigator, and to the four participating graduate students: Elaine Tamaye, John Cherry, Troy Pyles and Bruce Scott.

| | Author and Publication | Zones and Criteria≠ |
|---|---|---|
| *1. | U.S. National Oceanic and Atmospheric Administration. "Wind, Wave, Water Level and Air Pressure Measurements in Gulf of Mexico", (1969-70); Ocean Data Gathering Program (ODGP) in Gulf of Mexico as sponsored by Shell Development Co.; Raw data and analysis filed at Environmental Data Service (EDS) of U.S.A. National Oceanic and Atmospheric Administration, Ashville, N. Carolina 28801 (also Washington, DC 20235). | 3 P, D |
| *2. | Bretschneider, C.L. and J.I. Collins. (1964) "Design Sea State Study-Project Mohole", Final Report SN-187, National Engineering Co., Pasadena, CA (also published in Ocean Industry, Sept. 1967). | 1-3 P, D 10-12 18, 19 S, D |
| *3. | Bretschneider, C.L. and Roy Gaul. (1956) "Wave Statistics for the Gulf of Mexico", U.S. Army Corps of Engineers, Beach Erosion Board, Technical Memos No. 85, 86, 87, 88 and 89. | 3 P, O&D |
| *4. | Bretschneider, C.L. (1972) "Revisions to Hurricane Design Wave Practices", Proc. 13th Coastal Engineering Conference, Vancouver, B.C., Canada, July 1972. | 1-3 P, D |
| *7. | Graham, H.E. and D.E. Nunn. (1959) "Meteorological Conditions Pertinent to Standard Project Hurricane, Atlantic and Gulf Coasts of the United States", National Hurricane Research Project, Report No. 33, U.S. Weather Service. | 1-3 P, D |
| *8. | Hidaka, Koji. (1958) "Computation of the Wind Stresses Over the Oceans", Records of Oceanographic Works in Japan, Vol. 4, No. 2, March 1958. | All P, O&D |
| *9. | Hogben, N. and F.E. Lumb. (1966) Ocean Wave Statistics, Ministry of Technology, National Physical Laboratory. [see Ref. 9A below before using Ref. 9] | 1-5, 9-17, 21-28 P, O&D |
| (9A) | Hogben, N. (1974) "Ocean Wave Statistics--'Five Minutes Slow' After Six Years", Ministry of Technology, National Physical Laboratory. | 1-5, 9-17, 21-28 P, O&D |
| 12. | James, R.W. (1974) "Dangerous Waves Along North Wall of the Gulf Stream", Mariners Weather Log, NOAA Environmental Data Service, Washington, D.C., Vol. 18, #6. | 1-2 P, D |
| *13. | Neumann, G. and R.W. James. (1955) "North Atlantic Coast Wave Statistics Hindcasts by the Wave Spectrum Method", U.S. Army Corps of Engineers, Beach Erosion Board, BEBTM No. 57. | 1 P, O&D |
| *16. | Saville, Thorndike Jr. (1954) "North Atlantic Coast Wave Statistics Hindcast by C.L. Bretschneider-Revised Sverdrup-Munk Method", U.S. Army Corps of Engineers, Beach Erosion Board, BEBTM No. 55. | 1 P, O&D |
| 17. | Thom, Herbert C.S. (1973) "Distribution of Extreme Winds Over Oceans", ASCE Journal of the Waterways, Harbors, and Coastal Engineering Divison, Vol. 99, No. WW1, February 1973, pp. 1-17. | 1, 3, 6-11 14, 19 26-32 P, D |
| *19. | U.S. Naval Weather Service, 19-- Summary of Synoptic Meteorological Observations (SSMO), Vols. (about 150 volumes) as on index, U.S. Govt. Printing Office. | P, O&D |
| 20. | U.S. Naval Oceanographic Office (1955-74) [formerly U.S. Navy Hydrographic Office] U.S. Navy, Marine Climatic Atlas of the World, U.S. Govt. Printing Office. | P, O |
| 20a. | Vol. I, North Atlantic Ocean, Nov. 1955 (revised 1974) | 1-3, 9-12 |
| 20b. | Vol. II, North Pacific Ocean, July 1958 | 17-19, 4-8 |
| 20c. | Vol. IV, South Atlantic Ocean, Sept. 1958 | 11-13, 21-25 |
| 20d. | Vol V, South Pacific Ocean, Nov. 1959 | 2-3, 6-10 32, 20-22 |
| *21. | U.S. Naval Oceanographic Office (1974) [formerly U.S. Navy Hydrographic Office] Atlas of Sea and Swell Charts, Washington, D.C., U.S. Govt. Printing Office. | P, O |
| *22. | U.S. Naval Oceanographic Office (1974) [formerly U.S. Navy Hydrographic Office] Atlas of Surface Currents, Washington, D.C., Govt. Printing Office. | P, O |
| *23. | Wilson, Basil W. (1957) "Hurricane Wave Statistics for the Gulf of Mexico", U.S. Army Corps of Engineers, Beach Erosion Board, Technical Memo No. 98. | 3 P, D |
| 24. | "Wave Hindcast Statistics for the South Atlantic States", Research Proposal to the Army Corps of Engineers, CERC; by the Center for Engineering Research, Dept. of Ocean Engineering, University of Hawaii (for the period July 1968-Aug. 1969). | 1-3 P, O&D |
| 24a. | U.S. Naval Fleet Numerical Weather Central, Monterey, CA (1973) "Hemispherical Operational Wave Spectral Model (Numerical)". [also: Lazanoff, S.M. "same title as above" Proc. 15th Coastal Engineering Conf. publ. by Am.Soc.Civil Engineers, NY, NY, 1977]. | |
| 24c. | U.S. National Oceanic and Atmospheric Administration, National Climatic Center, Ashville, NC. (1870-date) "Wind, Wave and Current Observations from Shipboard". [Also, National Oceanographic Data Center in Washington, D.C., which is part of NCC.] | |
| 30. | Flatseth, J. and B. Pederson. "Distributions of Wave Height in Different Ocean Areas Around the World", Report No. 70-7-S for Research Department of Det Norske Veritas. | 1-5, 9-17 21-28 S, D |

*Denotes selected references (total of 30) used in classification of references and data. Reference numbers are same as in Final Report, given as Ref. (F.) at end of list.

≠P - Primary Reference
S - Secondary Reference
O - OPSES
D - DEWAC
1-3 - include Zones 1, 2, 3
1-5 - include Zones 1, 2, 3, 4, 5, etc.

| Author and Publication | Zones and Criteria≠ |
|---|---|
| . Harris, D.L. (1972) "Wave Estimates for Coastal Regions", Shelf Sediment Transport, Swift, Duane and Pilkey (eds.), Dowden, Hutchinson and Ross, Inc., Stroudsburg, PA. | 1-5<br>S, O&D |
| 36. Thom, H.C.S. (1973) "Extreme Wave Height Distributions Over Oceans", Journal of the Waterways, Harbors, and Coastal Engineering Division, ASCE, Vol. 99, WW3, August 1973. | All<br>S, D |
| *41. Marine Advisers (1961) "A Statistical Survey of Ocean Wave Characteristics in Southern California Waters", prepared for U.S. Army Corps of Engineers, Los Angeles District, by Marine Advisers, La Jolla, CA, January, 1961. | 4<br>P, O |
| *43. National Marine Consultants (1960) "Wave Statistics for Seven Deep Water Stations Along the California Coast", prepared for the Department of the Army, U.S. Army Corps of Engineers District, Los Angeles, CA, by National Marine Consultants, Inc., Santa Barbara, CA, December 1960. | 4<br>P, O |
| *52. Sverdrup, H.U. and R.H. Fleming "The Waters off the Coast of Southern California, March to July, 1937", University of California, Scripps Institute of Oceanography Bulletin, Technical Series, Vol. 4, 1936-1941, pp. 261-278. | 4<br>S, O |
| *62. Joy, Joseph W. (1964) "Characteristics of Deep-Water Waves in the Oahu Area for a typical year", prepared for Board of Harbor Commissioners, State of Hawaii, by Marine Advisers, La Jolla, CA, revised March, 1964. | 6<br>P, O&D |
| *64. Marine Advisers (1963) "Severe Storm Wave Characteristics in the Hawaiian Islands (1947-1961)", Marine Advsiers, Inc., 1963, prepared for the Board of Harbor Commissioners, Transportation Dept., State of Hawaii. | 6<br>P, D |
| *65. Moberly, Ralph Jr. and Theodore Chamberlain (1964) Hawaii Beach Systems, Hawaii Institute of Geophysics, Report No. HIG 64-2. | 6<br>P, O |
| *74. Marine Advisers (1963) "Wave Characteristics of Kona and Trade Wind Conditions for the Hawaiian Islands and their Channels", prepared for Board of Harbor Commissioners, State of Hawaii, by Marine Advisers, La Jolla, CA, June 19, 1963. | 6<br>P, O&D |
| *93. Wyrtki, Klaus (1974) "Equatorial Currents in the Pacific 1950 to 1970, and their Relations to the Trade Winds", Journal of Physical Oceanography, Vol. 4, No. 3, July, pp. 372-380. | 6-7, 19-20<br>32<br>S, O |

| Author and Publication | Zones and Criteria≠ |
|---|---|
| *95. Wyrtki, Klaus and Gary Meyers (1975) "The Trade Wind Field over the Pacific Ocean; Part I, The Mean Field and the Mean Annual Variation; Part II, Bimonthly Fields of Wind Stress, 1950 to 1972", HIG Publication HIG-75-1 and HIG-75-2, January, and April. | 6-9, 18-22<br>30-32<br>S, O |
| *97. Koninklijk Nederlands Meteorologisch Institut (1952) Indian Ocean Oceanographic and Meteorological Data, Charts and Text. | 14-16,26-29<br>P, O |
| *98. Srivastava, P.S., P.K. Vijayarajan and M.X. Joseph (1970) "Monthly Wave Characteristics of the Bay of Bengal", Indian J. of Meteorology and Geophysics, Vol. 21, No. 1, January. | 15-16<br>P, O |
| *99. Srivastava, P.S., D.K. Nair and K.R. Raman Karma (1968) "Monthly Wave Characteristics of the Arabian Sea", Indian Journal of Meteorology and Geophysics, Vol. 19, No. 3, July. | 14-15<br>P, O |
| *100. U.S. Oceanographic Office [formerly U.S. Navy Hydrographic Office] Atlas of Pilot Charts, U.S. Govt. Printing Office. South Pacific and Indian Oceans, H.O. Pub. No. 107 | 14-19<br>26-32<br>P, O |
| *104. Dattatri, J. and P.S. Renukaradhya (1971) "Wave Forecasting for West Coast of India", Journal of the Waterways, Harbors, and Coastal Engineering Division, ASCE, Vol. 97, WW3, August. | 15<br>S, O&D |
| *119. Vongvisessomjai, Suphat, Norbert L. Ackermann and Surasuk Muangman. "Wind Wave Computations in the Gulf of Thailand", informal paper, Asian Institute of Technology, undated. | 17<br>S, O&D |
| *139. Whittingham, H.E. (1964) "Extreme Wind Gusts in Australia", Bulletin No. 46, 1964, issued by the Director of Meteorology, Bureau of Meteorology, Melbourne, Australia, February. | 29, 31-32<br>S, D |
| 151. Bretschneider, C.L. and Elaine E. Tamaye (1976) "Hurricane Wind and Wave Forecasting Techniques", Look Lab/Hawaii, Vol. 6, No. 1, January, pp. 1-29. | 1-3, 6<br>D |
| *152. Tamaye, Elaine E. and Richard E. Rocheleau (1976) "What Hawaii Can Expect from the Next Hurricane", Look Lab/Hawaii, Vol. 6, No. 1, January, pp. 30-32. | 6<br>D |
| (F.) Bretschneider, C.L. et al. (1977) "OPSES-DEWAC Operational Sea State and Design Wave Criteria for Ocean Thermal Energy Conversion Projects", Final Report, OPSES-DEWAC. | |

# RESOURCE ASSESSMENT OF A HIGH POTENTIAL OTEC SITE NEAR PUERTO RICO

DONALD K. ATWOOD
*NOAA/AOML/OCL*
*15 Rickenbacker Causeway*
*Miami, Florida*

C. PETER DUNCAN
*Marine Sciences Department*
*University of Puerto Rico*
*Mayaguez, Puerto Rico*

MARVEL C. STALCUP
*Woods Hole Oceanographic Institution*
*Woods Hole, Massachusetts*

MICHAEL J. BARCELONA
*California Institute of Technology*
*Pasadena, California*

ABSTRACT

Environmental assessment of potential OTEC sites near Puerto Rico indicates that a high-potential site exists off the southeast coast. The $\Delta T$ to 1000 meters can be as high as 24°C (43°F) and is never less than 20°C (36°F). The insular slope at the site is steep, and water depths of 1000 meters exist within 1-1/2 miles off shore. Geostrophic conditions guarantee a warm, thick mixed layer with surface currents in the order of 1/3 of a knot. The supply of cold water can be considered limitless. The site is protected from north and northeast swell, and a mild sea state exists all year round (except during hurricanes). The salinity, temperature and nutrient distributions at the site are typical of open tropical seas making the site ideal for a prototype OTEC plant.

The northern Caribbean Sea is ideally suited oceanographically for exploitation of the Ocean Thermal Energy resource stored in tropical oceans. One reason for this is illustrated in Figures 1 and 2.

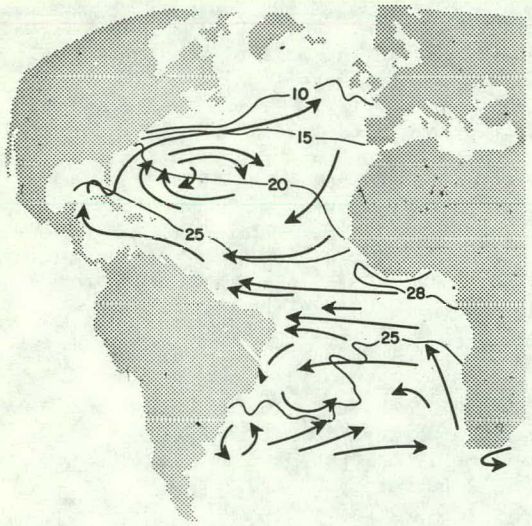



Fig. 1 Mean sea surface currents and. temperature for February. Arrows represent current directions and contours are for mean temperature in °C.

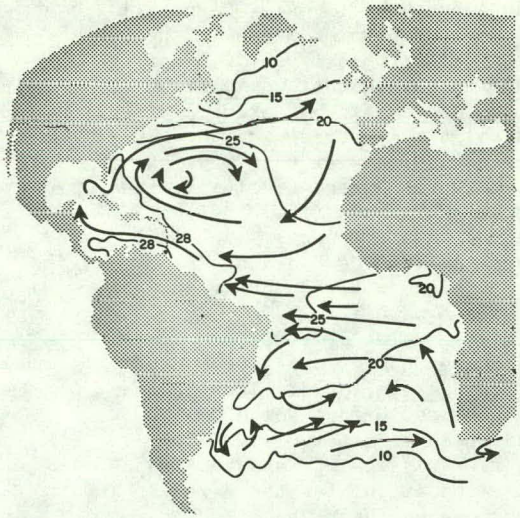



Fig. 2 Mean sea surface currents and temperature for August. Arrows represent current directions and contours are for mean temperature in °C.

Equatorial surface waters of the Atlantic store vast amounts of insolated heat. Westward flowing equatorial surface currents, and their extensions, move this warm water into the Caribbean where it continues flowing

westward as the Caribbean Current. The mean result is shown in Figure 1 for the month of February and in Figure 2 for August. In February the entire Caribbean has surface temperatures greater than 25°C. Note that at this time northern cooling of surface waters results in temperature throughout the northern Gulf of Mexico and Straits of Florida of less than 25°C. In August (Figure 2) both Caribbean and Gulf of Mexico surface waters have temperatures greater than 28°C. As these warm equatorial waters move along as the westward flowing Caribbean Current, the Ekman flow associated with the current moves them northward against the Greater Antilles where they form a thick warm surface layer. This is evident in Figure 2 where the southern part of the Caribbean has surface temperatures of less than 28°C due to this northward movement. The resulting warm thick mixed layer against the Greater Antilles is shown in Figure 3 which is a mean

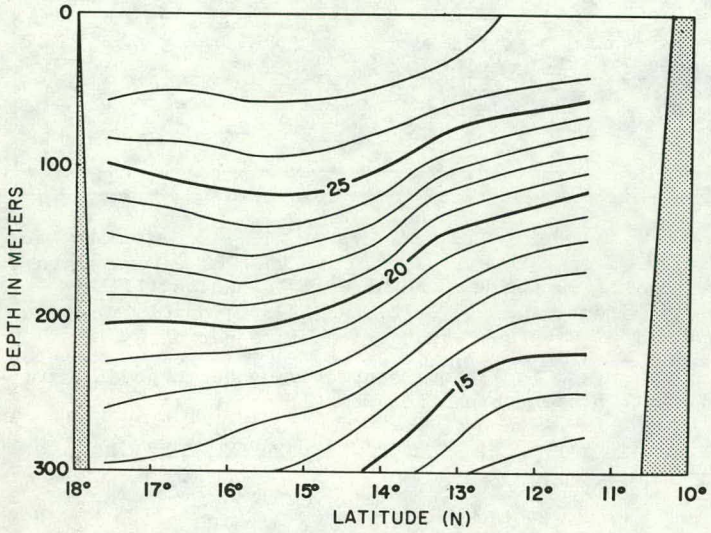



Fig. 3 Mean temperature section between Puerto Rico and Venezuela along 67°W. Contours are for mean temperature in °C.

temperature section down to 300 meters along 67°W between Puerto Rico (18°N) and Venezuela. Note that the mean situation yields water with temperature greater than 25°C down to 100 meters at the north end of the section.

Two other factors combine with the above to enhance the ability to use the area for OTEC exploitation. These are the presence of cold water (5°C) at 1000 meters and narrow insular shelves and steep insular slopes allowing accessibility to this cold water within a few miles of shore. Within this area, a high-potential OTEC site is located off the southeast coast of Puerto Rico as shown by the cross hatched portion in Figure 4. An initial resource assessment of this site was completed in May 1976 by the University of Puerto Rico Marine Sciences Department with funding from NSF/RANN (NSF Grant No. AER-75-00145). The assessment was made using historical data - much of which was taken at the University of Puerto Rico PESCA (Programa Estudios Caribe) Serial Hydrographic Station at 17°36'N, 67°00'W (Figure 4) -

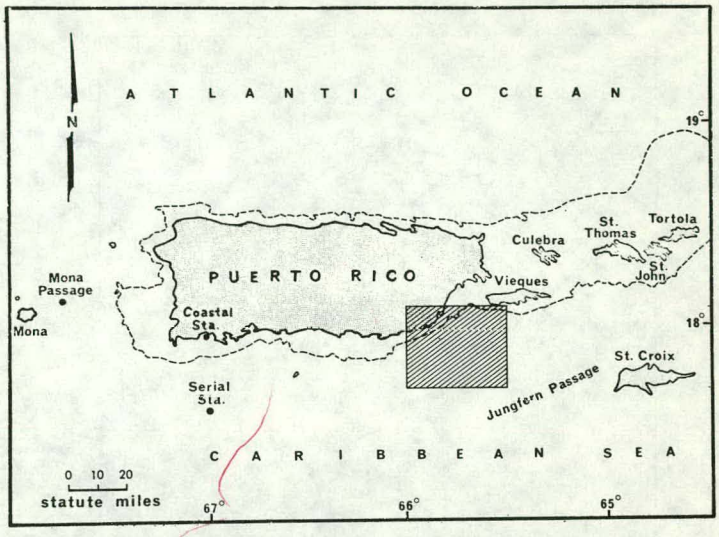



Fig. 4 Location of high-potential OTEC site near Puerto Rico (cross hatched area). Note position of University of Puerto Rico serial hydrographic station.

and data collected at the specific site during the study period. The site is particularly attractive because a ready market and distribution grid exist for any power generated. The south coast of Puerto Rico has extensive petroleum refining and petrochemical complexes including one adjacent to the site. These and other industrial complexes throughout the island plus a population of over 3 million people, result in power needs which are difficult to meet with Puerto Rico's present generating capacity (about 20,000 MWts). An excellent 115 KV power grid exists throughout the island and can be accessed from the site with minimal construction once lines are brought ashore. Since present power is generated by expensive oil fired generators, OTEC power could readily become a competitive source.

The following is a brief description of the results of the resource assessment done at the site. Complete details of the study are given in a report to NSF/RANN (1) which may be obtained from NSF or from the authors.

The position of the site on the south side of Puerto Rico and the Virgin Islands Platform protects it from North Atlantic swells. This insures a mild sea state all year long (except during hurricanes) and continuous access to the site.

Bathymetry at the site is shown in Figures 5 and 6. Figure 5 shows the regional bathymetry and Figure 6 depth profiles along the two lines labelled A and B in Figure 5. The site is located at the edge of the deep Virgin Islands Basin which receives virtually inexhaustible volumes of cold North Atlantic deep water

through the Anegada Passage to the northeast. Water a thousand meters deep can be reached within 2.5 to 3 kilometers from shore.

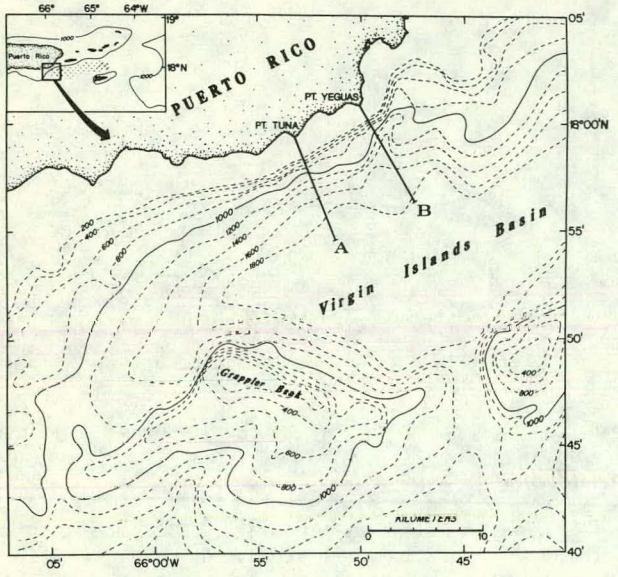



Fig. 5 Bathymetry at the Puerto Rico OTEC site. Data collected by Robert B. Starr aboard NOAA Survey Vessel WHITING and during this survey. Depth profiles along lines A and B are shown in Figure 6.

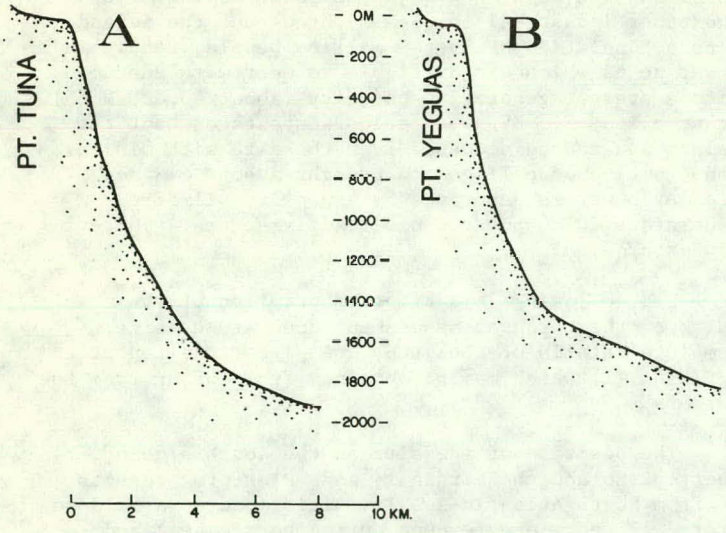



Fig. 6 Depth profiles along lines A and B in Figure 5. Note that depths of 1000 meters exist within 2.5 kms. of shore.

Figure 7 shows the temperature at the U.P.R. PESCA Serial Station contoured in a grid of depth versus time for the years 1971, 1972, and 1973. R/V CRAWFORD station numbers are shown above the contours to indicate sampling frequency. The upper third of the figure is a plot of $\Delta T$ in $^{o}C$ between 0 and 1000 meters for the same time period. Note that the $\Delta T$ is always greater than $20^{o}C$ and approaches $25^{o}C$ in September of each year.

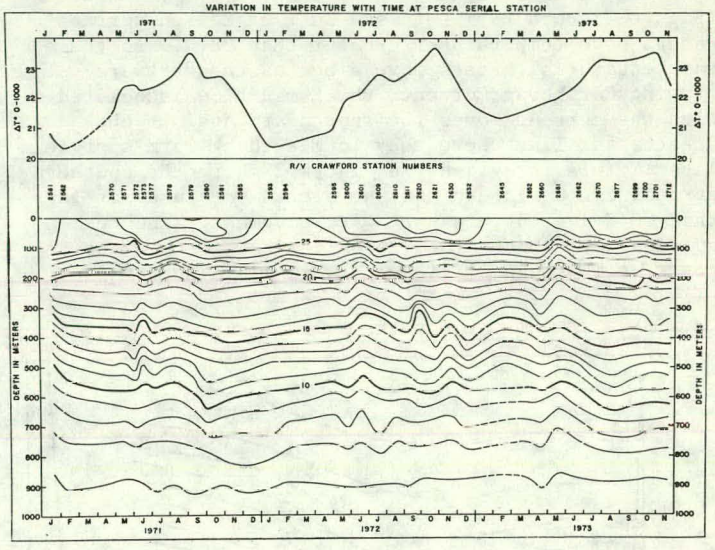



Fig. 7 Temperature ($^{o}C$) contours to 1000 meters at University of Puerto Rico PESCA Serial Station ($17^{o}36'N$, $67^{o}00'W$) during 1971, 1972, and 1973. Top of figure is plot of $\Delta T^{o}C$ versus time for the same period.

Figure 8 is a temperature versus depth profile for the site proper which includes all observations

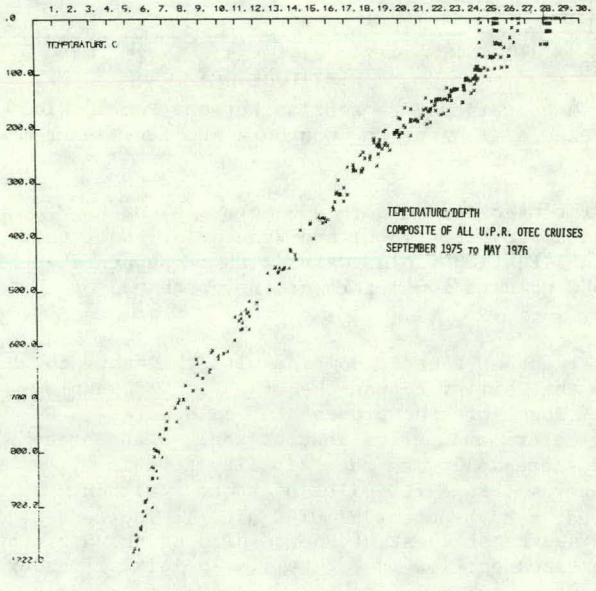



Fig. 8 Temperature ($^{o}C$) versus depth profile for a Puerto Rico OTEC site using all reversing thermometer observations taken during period of September 1975 to May 1976.

collected during four cruises to the site between September 1975 and May 1976. The data presented illustrate that the same ΔT's exist at the site as at the CA Serial Station. Figure 9 shows a series of XBT profiles taken hourly over a 24-hour period on 10 and 11 May 1976. These indicate that, except for some fluctuations in the thickness of the surface mixed layer (40 to 66 meters), the temperature regime is quite stable over one diurnal cycle. Surface layer variations occurred on approximately a 12-hour cycle indicating that they are probably tidal in origin. It is interesting to note the discontinuity in temperature at the base of the mixed layer which is probably due to warm equatorial water moving over the site with minimal vertical mixing.

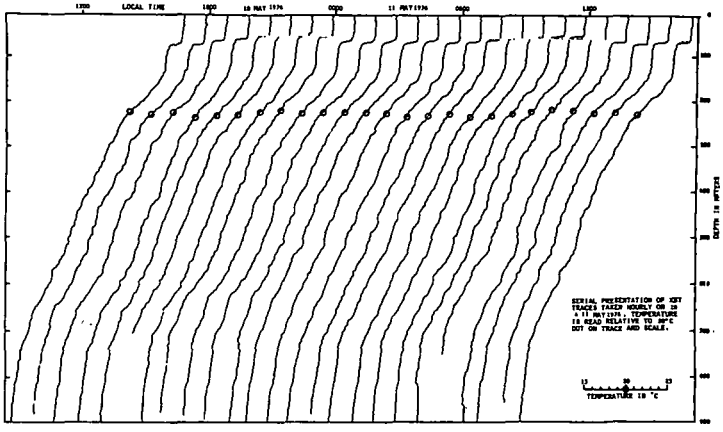


Fig. 9 Serial presentation of XBT data collected at the Puerto Rico OTEC site during period 1400 hours of 10 May 1976 to 1700 hours of 11 May 1976. Open circle represents depth of 20°C. Scale in lower right can be used to pick-up other temperatures on each XBT trace.

Figure 10 shows the salinity-depth profile at the site and includes all observations made during the assessment study. The profile is typical of the open Caribbean. Variations in surface salinity are quite large. These variations have been shown to result from a combination of rainfall to the equatorial waters of the Atlantic and outflow from the Amazon River (Froelich and Atwood, 2). The salinity maximum between 150 and 200 meters has origins at approximately 22° or 23°N and 50°W and results from high net surface evaporation during strong trade winds in that region (Worthington, 3). The salinity minimum at about 800 meters has origins at about 60°S (Subantarctic Intermediate Water), and the deepest water found at the site is formed in the Arctic (North Atlantic Deep Water, Wüst, 4).

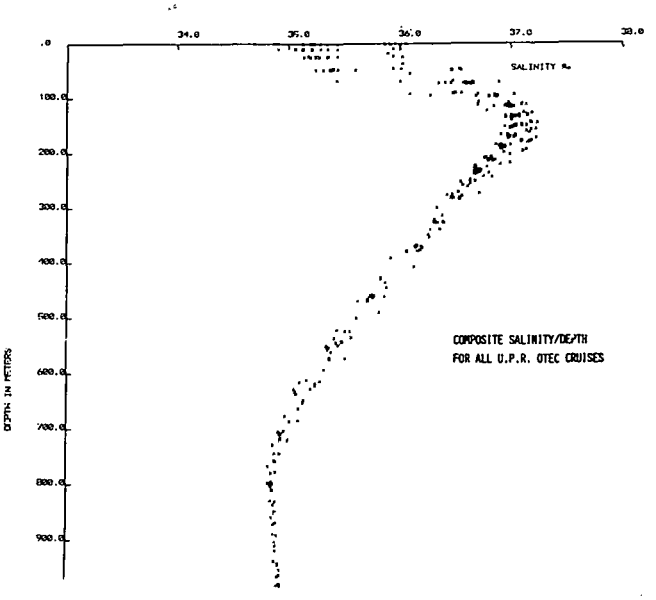



Fig. 10 Salinity (parts per thousand) versus depth profile for the Puerto Rico OTEC site using all observations collected during period of September 1975 to May 1976.

Figures 11 and 12 show depth profiles for the two nutrients which have the most control over primary productivity, i.e., phosphate and nitrate. In each case the profile is typical of open tropical seas. Concentrations are depleted at the surface due to assimilation by plankton in the photic zone. These

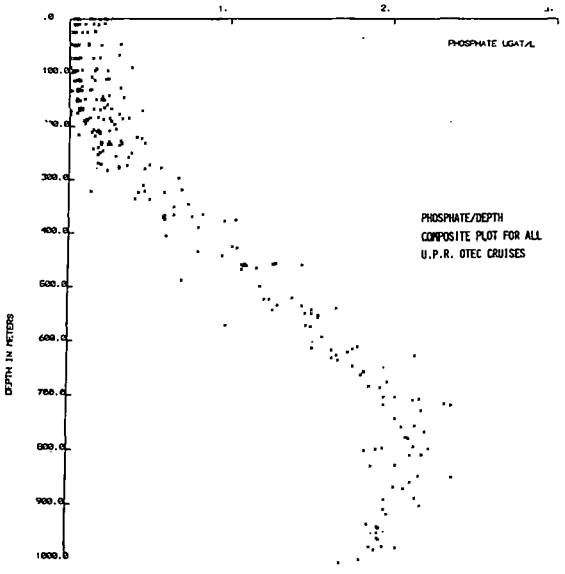



Fig. 11 Dissolved phosphate (micromolar) versus depth profile for Puerto Rico OTEC site using all observations collected during period of September 1975 to May 1976.

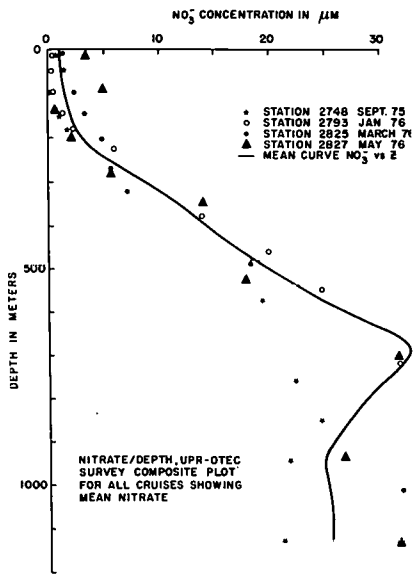



Fig. 12 Dissolved nitrate (micromolar) versus depth profile for Puerto Rico OTEC site using all observations collected during this survey. Symbols are keyed to cruise dates given. Solid curve is for mean observed nitrate concentration.

plankton then die, sink, and decay giving a maximum in nutrient concentrations at about 700 meters which is where maximum oxidation (decay) of dead planktonic material occurs. This depth also corresponds to an oxygen minimum of about 2.86 ml/l dissolved oxygen.

From this study it was concluded that the site is oceanographically excellent for OTEC exploitation. Its proximity to shore and a market for any OTEC power generated plus an existing 115 KV power distribution grid make it ideal for siting near shore OTEC plants. Since the site is typical of open tropical seas, the site is also ideal for siting early ocean test platforms or prototype OTEC plants.

## REFERENCES

(1) Atwood, Donald K., C. Peter Duncan, Marvel C. Stalcup and Michael J. Barcelona, Final Report. Ocean Thermal Energy Conversion: Resource Assessment and Environmental Impact for Proposed Puerto Rico Site, NSF Grant No. AER 75-00145, August 1976.

(2) Froelich, P. N. and D. K. Atwood, Dissolved Silicate and Salinity Structure of the Upper Waters of the Venezuela Basin, Caribbean Sea, Proceedings of Progress of Marine Research in the Caribbean and Adjacent Regions, CICAR-II Symposium, Caracas, Venezuela, July 1976.

(3) Worthington, L. V., On the North Atlantic Circulation, The Johns Hopkins Oceanographic Series Number 6, John Hopkins University Press, 11 pp., 1976.

(4) Wüst, G., Stratification and Circulation in the Antillean-Caribbean Basins, Part One, Spreading and Mixing of the Water Types, Columbia University Press, 201 pp., 1964.

# A FURTHER EVALUATION OF THE OCEANOGRAPHIC CONDITIONS FOUND OFF KEAHOLE POINT, HAWAII, AND THE ENVIRONMENTAL IMPACT OF NEARSHORE OCEAN THERMAL ENERGY CONVERSION PLANTS ON SUBTROPICAL HAWAIIAN WATERS

KARL H. BATHEN
*Department of Ocean Engineering*
*University of Hawaii*
*Honolulu, Hawaii*

Abstract

This work was performed as a five-month state funded extension to a previous 15-month NSF/RANN sponsored research project concerning the application of ocean thermal energy conversion in subtropical Hawaiian waters. Specifically, further definition of existing oceanographic conditions off Keahole Point (19°45'N, 156°04'W) and the environmental impact potentially resulting from conducting nearshore tests for both a 100 and 240 megawatt OTEC floating power plant off the Point are discussed.

Environmental analyses, as detailed in the previous 15-month NSF/RANN report, repeated for the case of a 100 MW and a 240 MW nearshore floating power plant located 2 km off Keahole Point. Both summer and winter conditions were considered. The intent was to evaluate just the approximate scale of impact for each case. Based on the temperature and discharge rate of cold water from the OTEC plant, and the local meteorological and oceanographic data, estimates were made of changes in surface heat exchange, alteration in heat content of the mixed layer, and rates of spreading of the discharged work. Work was completed using the surface heat exchange equations, and the two-dimensional heat conservation equation. Given then an estimate of the plume outfall characteristics and local biological data, the degree of nutrient addition and the extent of possible biostimulation were estimated.

The environmental analyses results showed that the cold water discharge plumes reached initial stability at approximately 275 m (100 MW case) and 305 m (240 MW case) from the point of discharge and centerline dilutions are 11 and 8, respectively at initial stability.

The maximum heat lost at the point of discharge for 100 MW, summer, slack water conditions was 1280 cal/cm$^2$ ($\Delta$T=0.33°C); with advection 920 cal/cm$^2$ ($\Delta$T=0.24°C). The areas of $\Delta$T greater than the background diurnal fluctuations were estimated at 11 and 33.5 km$^2$ for the slack water and advection conditions, respectively. During winter conditions with slack water/advection the areas impacted were 21/28 km$^2$, respectively.

The maximum heat lost for the 240 MW case, summer, with a northward advection was 2120 cal/cm$^2$ ($\Delta$T=0.54°C). The areas of $\Delta$T greater than the background diurnal fluctuations, at equilibrium, was estimated to be 42 km$^2$. The maximum decrease in the temperature of the mixed layer for the 240 MW case was estimated at 0.74°C, occurring during summer and slack water.

Potential biostimulation could occur out to 450 m from the point of discharge (100 MW case) and the areas impacted would be 1.6 km$^2$ (100 MW) and 4.4 km$^2$ (240 MW). Nutrient concentration increases over ambient surface water values would range from 120/160 times near the discharge to 1.7/2.4 times, respectively, some 450/600 m further downstream for the 100/240 MW plants.

This state-funded work is being expanded further through 1978. Included will be in situ, long-series observations of the deep ocean temperature, salinity, and currents at the 2,000-ft depth off Keahole Point. Acquisition of similar data are also planned in conjunction with pending OTEC bio-fouling experiments at Keahole Point. A critical evaluation of potential open ocean OTEC test sites in the North Pacific is also being developed. Included in that work will be a determination using available historical data at the University of Hawaii, of an optimum site considering maximum $\Delta$T, minimum depth to the cold water source, minimal current shear with depth, the most moderate sea state without occurrence of significant tropical storms, typhoons or hurricanes, and proximity to supporting logistics for initial OTEC testing at sea.

## Introduction

The work discussed in this report is a continuation of a project initiated in May 1974 and subsequently published in a report submitted to the National Science Foundation/ERDA in April 1975 (Bathen [1]). That report dealt with the possible effects of a 20 MW ocean thermal energy conversion (OTEC) pilot power plant, situated onshore at Keahole Point on the Kona coast of the island of Hawaii. The emphasis in previous work was twofold: first, to characterize the oceanographic conditions found seasonally off Keahole Point through an extensive historical literature survey and summer/winter field programs; and second, to develop the methodology and apply several environmental analyses aimed at estimating the approximate scale of physical and biological oceanographic impact of conducting 20 MW proof-of-concept OTEC tests at the Point.

The reader is referred to the initial report for a detailed introduction to the oceanographic environment of the Kona coast. The methodology described therein is repeated here, with additional clarification where this was thought necessary. Utilization of the historic data and field results cited in that report, as well as all assumptions underlying the methodology of environmental analyses, have not been changed. It was initially recognized, however, that additional summer 1975 field observations would be useful in providing a year to year comparison with the past summer 1974 results. A limited field effort was, therefore, planned and completed to obtain additional circulation and water column stratification data. These results are excluded here.

An OTEC plant utilizes cold seawater (in this case from a depth of 600 m), and warm seawater (from the surface), for the cooling and heating of a working fluid. The 20 MW pilot plant previously examined was assumed to discharge the degraded cooling and heating waters in a thoroughly mixed condition at a depth of 21.3 m (70 ft), into ambient waters characteristic of the locality and season. There were six ports, each of 7 ft diameter, at a spacing of 20 ft, discharging parallel plumes simulating one large single plume. Results of the past environmental analyses indicated that changes in the surface heat budget, changes in local stratification and the biological impacts should be almost insignificant, except in a small zone of approximately 1.1-2.6 $km^2$ within the immediate vicinity of the cold water outfall.

In the discussion following, the original conditions were changed. The OTEC plant was assumed to be floating offshore, discharging cold water through four horizontal ports 90° to each other. Plant capacity was increased, first to 100 MW, then to 240 MW. The discharge plume characteristics were recalculated for these large floating plants and the results are tabulated in the appendix. All original environmental analyses were then repeated based upon the behavior of the new plumes. It should be noted that in spite of the greater discharge rates, the size of the initial plumes were similar to the 20 MW case due to the new discharge geometry. In particular the dilution at initial stability (estimated to occur approximately 300 m from the discharge point), of the 100 MW plant plume was only slightly greater than that of the 20 MW plant, (11.35 vs 10.40). Initial stability was considered to occur when the plume had stabilized in vertical movement. Beyond this point the plume centerline remains essentially at a constant depth.

This paper deals with the results of the environmental analyses for the 100 MW and 240 MW nearshore floating OTEC plant. The emphasis here is on examining changes in the surface heat exchange and the possible effects thereon of an OTEC plant, the heat storage and temperature changes in the mixed layer resulting from the cold water discharge, and the extent of biostimulation in the mixing zone from the nutrient laden discharged cold water.

This work was funded by the Department of Planning and Economic Development, State of Hawaii. The schedule was restricted to June through October 1975. The field work was completed in July 1975 and all environmental analyses in the subsequent two months.

## Environmental Analyses

The major objective of this work was to evaluate the approximate scale of environmental impact that might result from conducting extensive OTEC tests off Keahole Point, Hawaii. Specifically, two OTEC power plants of 100 MW and 240 MW capacity were considered as these sized plants are approximately compatible with float plant concepts being investigated nationally. The analyses were limited to select environmental questions as dictated by the available data and the methodology developed in the previous NSF/RANN work for the 20 MW case (Bathen [1]). The questions posed of interest for the analyses were:

1. Given the characteristics of the Keahole Point receiving waters and considering the discharge from a 100 MW and 240 MW OTEC power plant what will be the discharge plume behavior, depth, dimensions, and dilution in the discharge area?

2. What is the normal local surface heat exchange budget and how might it be altered by cold water discharged from pilot plants of this size?

3. Given an estimate of the cold water plume(s) from the floating plant(s) how would this diluted mix of discharged and ambient water advect and mix horizontally as it moves away from the plant stationed just off Keahole Point?

4. What amounts and at what dilutions would nutrients be added to the surface mixed layer in the discharged water?

5. What are estimates of the potential changes in local biostimulation that might occur as a result of nutrients added to the surface photic zone?

6. Considering all results, what significant changes (area impacted and to what degree) could occur in the waters off Keahole Point from a 100 MW and 240 MW OTEC power plant as they relate to the State of Hawaii water quality standards?

The analyses previously developed were used in an attempt to answer each of these questions for each power plant size, summer, and winter conditions. Based on the temperature and discharge rate from the OTEC plant and

local meteorological and oceanographic data, estimates e made of changes in surface heat exchange, alteran in heat content of the mixed layer, and rates of eading of the discharged water. Work was completed using the surface heat exchange equations, and the two-dimensional heat conservation equation. Given then an estimate of the plume outfall characteristics and local biological data, the degree of nutrient addition and the extent of possible biostimulation were estimated by developing a numerical model relating nutrients and characteristic elements of the biological community.

## Surface Heat Exchange and Alteration

### Methodology

The net heat exchange between the surface of large bodies of water and the atmosphere is the result of five main processes:

1. incoming short wave solar radiation (insolation)
2. short-wave radiation reflected from the surface (reflection)
3. the net long wave radiation (back radiation) from the water to the atmosphere
4. heat exchange due to evaporation or condensation
5. sensible heat exchange

The usual approach to an analysis of surface heat exchange is to consider only these five processes, and to ignore minor processes such as heat transferred due to precipitation, surface runoff, chemical processes, and energy dissipation by surf and currents. The three processes of insolation, back radiation and evaporation/condensation are considered independent, while the reflected radiation is related directly to insolation, and the sensible heat exchange to evaporation losses. The relationships that have been developed attempting to predict these surface heat exchange components are of an empirical nature, principally because their application requires them to be in terms of readily measurable (and available) physical parameters.

The meteorological-oceanographic variables most commonly measured are wind, cloud cover, sea temperature, air temperature, and wet bulb temperature. It is to these five variables that nearly all relationships describing surface heat exchange are adapted. In spite of this limitation, a large number of equation sets for evaluating the five principal heat exchange processes exist. These have been reviewed by Laevastu (2), who also discussed the applicability of each equation. As a result he was able to select a set of relationships which he considered would give the best results under most conditions. No geographical limitations were set on the equations, which are as follows:

$$Q_i = 0.014 A_n t_d (1-0.0006C^3) \text{ cal/cm}^2\text{/day} \quad (1)$$

with the condition that when $A_n$ is greater than 75°

$$Q_i = 1.06 t_d (1-0.0006C^3) \text{ cal/cm}^2\text{/day} \quad (2)$$

where $Q_i$ = incident radiation on sea surface
$A_n$ = noon altitude of sun (deg)
$t_d$ = length of day (min)
$C$ = cloud cover (tenths of sky covered)

$$Q_r = 0.15Q_i - (0.01Q_i)^2 \text{ cal/cm}^2\text{/day} \quad (3)$$

where $Q_r$ = radiation reflected from sea surface

$$Q_b = 1440 \left[\frac{14.38-0.09T_w-0.046U_o}{69.72}\right][1-0.0765C] \text{ cal/cm}^2\text{/day} \quad (4)$$

where $Q_b$ = effective back radiation
$T_w$ = temperature of sea surface, °C
$U_o$ = relative humidity, %
$= \frac{100e_a}{e_{sata}}$, where $e_a$ = vapor pressure of the air, mb
$e_{sata}$ = saturated vapor pressure over water at the dry bulb temperature, mb

(Vapor pressures may be found in the Smithsonian Meteorological Tables.)

$$Q_e = \frac{L}{10}[(0.26+0.077W)(0.98e_{satw}-e_a)] \text{ cal/cm}^2\text{/day} \quad (5)$$

where $Q_e$ = heat exchange due to evaporation
$W$ = wind speed, m/sec
$e_{satw}$ = saturated vapor pressure over water at the temperature of water, mb
$L$ = latent heat of evaporation of sea water $= 594.5-0.51T_w$ cal/cm$^3$

The quantity in square brackets is the evaporation in mm/cm$^2$/day.

Equation (5) predicts some evaporation even under zero wind conditions. The term 0.26 is necessary, as convection will give rise to local air movement even though W=0. It is neglected when the sea temperature is less than the air temperature.

The surface film has been found to be about 0.6°C cooler than the water immediately beneath it (Boyum [3]; Laevastu and Inouye [4]). Thus if $T_w-T_a$ is less than 0.6°C,

$$Q_e = \frac{L}{10}(0.077W)(0.98e_{satw}-e_a) \text{ cal/cm}^2\text{/day} \quad (6)$$

$$Q_s = 38.9(0.26+0.077W)(T_w-T_a) \text{ cal/cm}^2\text{/day} \quad (7)$$

where $Q_s$ = sensible heat exchange
$T_a$ = air (dry bulb) temperature, °C

Equation (7) is derived directly from Bowen's ratio which, at sea level, is as follows:

$$R = 0.66 \left[\frac{T_w-T_a}{e_{satw}-e_a}\right]$$

If $T_w$ is less than $T_a$, Eq. (7) becomes:

$$Q_s = 3W(T_w-T_a) \text{ cal/cm}^3\text{/day} \quad (8)$$

The convention is to consider heat gained by the sea as positive, heat lost as negative. Thus, when

calculating the net heat exchange, the right hand sides of Eqs. (2) through (8) would each be preceded by a minus sign. Equations (1) through (8) (henceforth referred to as "method A") are valid on a daily basis, giving average values over a 24-hour period, if the five input variables are representative of their daytime averages.

A second set of surface heat exchange equations are those used by Wyrtki (5) in his study of the net surface heat exchange of the North Pacific Ocean. The equations (henceforth referred to as "method B") given in his report, without discussion, are:

$$Q_i - Q_r = Q_{io}(1-r)(1-0.38C-0.38C^2) \text{ cal/cm}^2\text{/day} \quad (9)$$

where $Q_{io}$ = some fraction of the solar constant (1.94 cal/cm$^2$/min) and is a function of latitude and month
$r$ = reflection, also a function of latitude and month

$$Q_b = RS\theta_w^4(0.39-0.05\sqrt{e_a})(1-0.38C^2) + 4RS\theta_w^3(T_w-T_a) \quad (10)$$

where $R$ = ratio of radiation of sea surface to that of a black body and = 0.97
$S$ = Stefan-Boltzman constant = $1.371\text{x}10^{-12}$ cal/sec/cm$^2$/°K$^4$
$\theta_w$ = temperature of sea surface in °K

$$Q_e = \rho_a C_D L(q_w-q_a)W \text{ cal/cm}^2\text{/day} \quad (11)$$

where $\rho_a$ = air density = $1.2\text{x}10^{-3}$ gm/cm$^3$
$C_D$ = drag coefficient, held constant at $1.55\text{x}10^{-3}$
$q_w$ = specific humidity at sea surface (i.e., the ratio of the mass of water vapor to the mass of moist air in which the water vapor is contained)
$q_a$ = specific humidity of air well above the sea surface

$$Q_s = \rho_a C_D C_p (T_w-T_a)W \quad (12)$$

where $C_p$ = specific heat at constant pressure of air = 0.24 cal/gm/°C

This method is somewhat less empirical than method A, in that the equations afford a better insight into how the constant parameters affect the surface heat exchange.

In applying methods A and B to computing the net surface heat exchange off Keahole Point, and its potential alteration due to local OTEC operations, four of five input variables ($W, C, T_a, T_w, T_{wb}$) were obtained from the 1966 weather reports taken at the old Kailua-Kona airport (Keahuolu Point). A characteristic mean value of wind speed, cloud cover, air temperature, and wet bulb temperature was computed for each day from 10 to 15 readings of each, taken generally from sunrise to sunset. Any apparently anomalous daily values were discarded and monthly averages were then computed. Monthly averages of sea surface temperatures were obtained from the report by Bathen (1). This report noted that Kona coast waters are generally a degree or two warmer than the average temperature of Hawaiian waters despite some local percolation cooling effects.

The 12 monthly values of the five variables were used in two independent computer programs involving Eqs. (1) through (8), and (9) through (12), respectively. In the program for method A, noon altitude of the sun, and length of day were taken for the 15th of each month from the Smithsonian Meteorological Tables. In the program for method B, insolation from a cloudless sky ($Q_{io}$) and reflection ($Q_r$) were found using Wyrtki's (5) method. Vapor pressures and relative humidity in both programs were found using the air and web bulb temperatures and the Smithsonian Tables.

Two different weather conditions were tested:

1. Characteristic monthly values of W, C, $T_a$, $T_{wb}$
2. Conditions of intense evaporation, i.e., strong winds and low cloud cover

The second condition was chosen because it was felt that if such conditions persisted for longer than a day or two, a significant heat loss from the sea might result --an important consideration when attempting to define the magnitude of the effects of the cool OTEC plant discharge waters. Table I summarizes the input data.

Results of the Computations

These have been plotted in Figures 1 and 2. The first figure shows the seasonal heat exchange components for characteristic local weather conditions. The solid lines are the results calculated using method A, the dotted lines using method B.

The upper pair of lines represent insolation less short wave reflection less long wave back radiation ($Q_i-Q_r-Q_b$) and gives an indication of the amount of incoming heat potentially available to warm the sea water. The large discrepancy between the two methods is largely due to the different cloud cover corrections applied. Method A always gives a smaller correction than method B. Under conditions of low cloudiness method A gives a very small correction, which seems reasonable, as during such conditions insolation may actually be increased by reflection from the clouds.

Results of Reed and Halpern (6) obtained off the Oregon coast indicated that Laevastu's cloud correction factor (method A) gave the best agreement with measured insolation values. However, the predominant cloud cover off Oregon during the time of measurement was stratocumulus,which might have somewhat different effects on insolation than the predominant low cumulus clouds off the Kona coast.

A secondary cause of the discrepancy was the choice of solar constant for each month. Under clear skies, method A resulted in smaller values of insolation during winter months (by about 55 cal/cm$^2$/day), and larger values during summer months (by about 55 cal/cm$^2$/day). The overall effect was to cause relatively small differences between the months during winter months, and larger differences during summer months. Back radiation

calculations were in good agreement with each other ›ughout the year.

The lowest pair of lines represent the sum of losses (or gains) due to sensible heat transfer and evaporation, ($Q_e$+$Q_s$). The sea surface temperature, with the exception of February (characteristic conditions), was less than the air temperature, resulting in a transfer of sensible heat from the atmosphere to the sea. Such heat gain was typically less than 15 percent of the evaporation loss. Methods A and B gave results in fairly good agreement. The anomaly appearing during September (characteristic conditions) resulted from the relatively high sea temperature (27.9°C). The anomaly during April (evaporative conditions) was caused by the very low wet bulb temperature selected for that month (19°C).

The net surface heat exchange, calculated as $Q_{net}=Q_i-Q_r-Q_b-Q_e-Q_s$, is the quantity of heat available for heating the ocean waters. Again, the different cloud correction factors caused the discrepancy in the results. If methods A and B are considered to give reasonable estimates of $Q_{net}$ near the upper and lower limits of the monthly ranges, then it is apparent that the waters off the Kona coast, under characteristic weather conditions gain heat throughout the year. The area between the pair of $Q_{net}$ curves has been shaded to indicate that, in general, the undisturbed net surface heat exchange may be expected to lie within this envelope throughout the year.

Intense evaporation conditions, likely to increase evaporation losses, may cause a small net heat loss from the sea during the winter months. Under these conditions, the reduction in cloud cover greatly increases insolation, which largely compensated for the increased evaporation losses.

Estimating the impact of the cold water discharge from an OTEC plant on the local heat budget was of interest. Utilizing results from the section following, maximum seawater temperature decreases within the immediate area of discharge were estimated to be 0.33°C (0.6°F), and 0.67°C(1.2°F), for 100 MW and 240 MW OTEC plants respectively. Figure 2 shows the results of computations using the same four weather variables, but postulating a seawater temperature decrease of 0.67°C to simulate the cold thermal discharge. The result is that overall losses are reduced and $Q_{net}$ increases by about 40 cal/cm$^2$/day, 50 cal/cm$^2$/day under conditions of intense evaporation. Under conditions of intense evaporation the increase in $Q_{net}$ is sufficient to cancel the net heat losses during the winter months.

Examining the separate components of the net heat increase, it is apparent that the changes due to a 0.33°C seawater temperature decreases are generally about half those due to the 0.67°C increase. Despite the temperature decrease, method A predicts a very small increase in back radiation. This is due to the empirical nature of Eq. (4). It takes no account of the Stefan-Boltzman law, which predicts a decrease in back radiation with a decrease in temperature of the radiating body. Method B does predict such a decrease. Both methods show a ase in evaporation, in good agreement. For a temperature drop of 0.67°C the yearly average decrease in evaporation losses is about 20 percent (char. cond.) and 10 percent (evap. cond.). There is a gain in sensible heat transfer from the atmosphere to the water, and again the two methods agree well. The percentage increase fluctuates monthly, at all times exceeding 50 percent (char. cond.) and lying between about 40 and 55 percent (evap. cond.).

The difference in $\Delta Q_{net}$ resulting from a local cold water intrusion as calculated by methods A and B, is principally caused by the difference in the $\Delta Q_{back}$ results. Both methods show an increase of heat flow into the sea, remaining fairly constant throughout the year at about 25 to 60 cal/cm$^2$/day for a 0.67°C temperature decrease. However, the percentage increase of $Q_{net}$ over the undisturbed local $Q_{net}$ varies considerably during the summer (June, July, Aug., Sept.), winter (Dec., Jan., Feb., March), and transition months (Oct., Nov., April, May). These variations are shown in Table II.

The additional heat flowing into the sea as a result of a local cold water intrusion would be expected to balance slightly the anomalous temperatures caused by such an intrusion. But it would also cause the local air temperature over the affected area to decrease somewhat. Whether a surface temperature decrease of about a degree would produce a significant decrease in the local air temperature, thereby increasing the possibility of changes in the micro-climate, is a question beyond the scope of this analysis.

## Heat Storage Changes in the Mixed Layer

### Methodology

The objective of these analyses was to estimate the area around Keahole Point over which temperature changes brought about by cool discharge waters might be significant. Significant was defined in this case as a temperature anomalies recognizable within normal diurnal temperature fluctuations. The examination of thermal changes was confined to those likely to occur in the surface mixed layer. Immediately below the mixed layer the stability of the pycnocline was assumed to prevent significant downward mixing and advection.

The problem was thus reduced to two dimensions by considering a vertically homogeneous mixed layer of constant depth. A relatively simple form of the heat conservation equation could therefore be used to predict changes in the heat content of the mixed layer. The differential form of the heat conservation equation in two dimensions is as follows (Bathen [7]).

$$\frac{\partial H}{\partial t} = A_h\left[\frac{\partial^2 H}{\partial x^2} + \frac{\partial^2 H}{\partial y^2}\right] - \left[u\,\frac{\partial H}{\partial x} + v\,\frac{\partial H}{\partial y}\right] + Q(x,y) \quad (13)$$

where $H$ = total heat content in the mixed layer
$t$ = time, sec
$A_h$ = horizontal mixing coefficient; this varies with latitude and at 20°N was assigned a value of $3\times10^6$ cm$^2$/sec (Bathen [7])
$x,y$ = distances along a horizontal coordinate grid system, cm x positive northward, y positive eastward

u,v = velocities in the x- and y-directions, cm/sec
Q(x,y) = net surface heat exchange, cal/cm$^2$/sec

The left hand side of Eq. (13) represents the local time rate of change of heat content, the right hand side the processes causing the change, i.e., horizontal mixing, horizontal advection, and the net surface heat exchange with the atmosphere. In order to account for changes in the depth of the mixed layer in shoaling water, where the bottom depth was less than the mixed layer depth, each term in Eq. (13) was divided by the mixed layer depth. If this had not been done, there would have resulted some heat transfer between two adjacent grid volumes at the same temperature, but of different depths.

The finite difference form (or recurrence equation) of Eq. (13) may be written as:

$$H_{i,j,k+1} = H_{i,j,k}\left[1.0 - \frac{4A_h\Delta t}{\Delta x^2} - \frac{u_{i,j,k}+v_{i,j,k}}{\Delta x}\Delta t\right]$$

$$- A_h \frac{\Delta t}{\Delta x^2}\left[H_{i+1,j,k}+H_{i,j+1,k}\right]$$

$$+ H_{i-1,j,k}\left[\frac{A_h\Delta t}{\Delta x^2} + \frac{u_{i,j,k}\Delta t}{\Delta x}\right] + H_{i,j-1,k}\left[\frac{A_h\Delta t}{\Delta x^2} + \frac{v_{i,j,k}\Delta t}{\Delta x}\right]$$

$$+ Q_{net}(x,y)[\Delta t] \qquad (14)$$

A computer program was written to solve this equation numerically. A square grid system ($\Delta x=\Delta y$; note that in Eq. (14) $\Delta y$ has been eliminated) was selected covering the area from 156°14'W to 156°00'W (or the coastline), and from 19°37'N to 20°00'N. The dimension of an element in the grid system was $61\times10^3$ cm (2000 ft). The location of the grid system was such that Keahole Point (19°44'00"N, 156°03'09"W) was positioned closer to the southern boundary than the northern. Recent data has shown the predominance of strong northerly currents during both flooding and ebbing tides (Bathen [1]).

Grid size and time step were selected so as to satisfy the requirements of convergence and stability, i.e., the numerical solution must be convergent to the exact solution, and the numerical solution must be stable with time. The rounding error caused by the difference between the exact numerical solution $H^*_{i,j,k}$, and the actual numerical solution $H_{i,j,k}$ must be bounded (finite) and decrease as $\Delta x$ and $\Delta t$ go to zero. By expanding the recurrence equation term by term into a Taylor series, and rewriting to include the error term, the finite difference round off error was found to be proportional to the derivatives of H as follows:

$$\text{error } \alpha \frac{\Delta t^2}{2} \cdot H_{tt}$$

$$\text{error } \alpha - A_h \frac{\Delta t \Delta x^2}{12} \cdot H_{xxxx} - A_h \frac{\Delta t \Delta y^2}{12} \cdot H_{yyyy}$$

$$\text{error } \alpha - u \frac{\Delta t \Delta x}{2} \cdot H_{xx} - v \frac{\Delta t \Delta y}{2} \cdot H_{yy}$$

where the subscripts denote differentiation. The derivatives are finite over the grid area. Thus as $\Delta x$ and $\Delta t$ diminish to zero, the error term disappears, a the actual solution converges to the exact numerical solution.

Stability was tested by the Fourier series method. A disturbance was introduced into the actual solution $H_{i,j,k}$. This disturbance was of the form $e^{L(\alpha i+\beta j)+\gamma k}$

where $L = \sqrt{-1}$
$\alpha,\beta,\gamma$ = constants
i,j,k = indices referring to x- and y-directions, and to time, respectively.

In this method it is usual to introduce the disturbance in terms of a finite Fourier series, but as Eq. (14) is linear, and therefore separate solutions are additive, the propagation of only a single term of the series needed to be considered. After substitution, and simplification of the result, the following conditions was obtained:

for the disturbance to decrease with time,

$$\frac{4A_h\Delta t}{\Delta x^2} + \frac{\Delta t}{\Delta x}\left(|u_{i,j,k}| + |v_{i,j,k}|\right) \leq 1.0$$

and with $A_h = 3\times10^6$ cm$^2$/sec, and a maximum value of $|u_{i,j,k}|+|v_{i,j,k}|=120$ cm/sec,

$$\frac{\Delta t}{\Delta x}\left(\frac{12\times10^6}{\Delta x} + 120\right) \leq 1.0 \qquad (15)$$

A requirement of secondary importance was that the grid size should not be so large as to render the volume of the plumes insignificant nor so small as to make the number of calculations excessive. Setting $\Delta x=61\times10^3$ cm, the stability requirement became:

$$t(197+120) \leq 61{,}000$$
$$t \leq 192 \text{ sec}$$

Therefore, a 3-min time step was selected.

Initial heat storage, before addition of the discharge plume, was calculated by vertically integrating the temperature profile from the surface to the mixed layer depth (MLD) and dividing by MLD to convert to cal/cm$^3$. A vertically decreasing temperature profile, decreasing 1°C per 100 m, was used. By selecting an appropriate sea surface temperature and MLD from the data given by Bathen (1), the mean heat storage in the water column for any month could be calculated.

$$H = \frac{\rho C_p \int_0^{MLD} T\, dz}{MLD} \text{ cal/cm}^3 \qquad (16)$$

where $\rho$ = density of sea water = 1.023 gm/cm$^3$
$C_p$ = specific heat at constant pressure = 0.954 cal/gm/°C
T = temperature of seawater (°C)

There was some evidence indicating that the bottom of the mixed layer tended to slope slightly downward towards the coast, suggesting the presence of the slow onshore drift believed to occur off Keahole Point

(Bathen [1]). Such a downward sloping mixed layer depth also indicates a geostrophic flow to the north. Calculations of geostrophic current velocities using typical ity profiles from two stations 13.1 km apart resulted orthward current velocities at the 0, 50, and 100 m depths, of 46.4, 47.8, and 48.5 cm/sec, respectively. The field data taken by Bathen (1) showed a northward moving net transport predominating off Keahole Point, with current speeds reaching 85 cm/sec (1.6 kt).

It was necessary to select from these results characteristic velocities for the Keahole area to use in the computer model. Velocities were assigned to each grid square by setting u=0, v=25 cm/sec along the southern boundary of the grid system. In addition u and v were set equal to zero along the eastern boundary of the grid system (not along the ocean-land boundary). Both velocity components in all other grid squares could then be calculated from the continuity equation, taking bottom bathymetry into account. A point to note here is that the velocity subroutine was written in such a way that changes in the v-component were weighted in inverse proportion to distance from shore, in order to provide a current velocity increase near Keahole Point, as suggested by both the recent field data and the historic data. Velocities were assumed constant with depth down to the mixed layer depth. This procedure resulted in u and v components of -33.0 cm/sec and 46.5 cm/sec (northwest flow) just southwest of Keahole Point during winter; and -40.6 and 42.7 cm/sec in the same grid square during summer. The maximum value of $|u_{i,j,k}|+|v_{i,j,k}|$ was 139.8+37.3=177.1 cm/sec. This occurred in the shallow bay off Honokahau. In all other grid squares $|u_{i,j,k}|+|v_{i,j,k}|$ was less than 120 cm/sec for both summer and winter velocity fields.

Five computer runs were made examining several meteorological and oceanographic conditions:

1. 100 MW plant
   a) summer conditions, velocity field = 0
   b) summer conditions, velocity field as described above
   c) winter conditions, velocity field = 0
   d) winter conditions, velocity field as described above
2. 240 MW plant
   d) summer conditions, velocity field as described above

Summer conditions consisted of a 40 m mixed layer depth, and a net surface heat exchange of 400 cal/cm$^2$/day, with a sea surface temperature of 26.7°C. Winter conditions were MLD=100 m, $Q_{net}$=-40 cal/cm$^2$/day, and surface temperature=24.9°C.

A shallow warm, summer mixed layer, with zero current velocities, would create a maximum impact, which would be somewhat offset by a positive net surface heat exchange. Winter conditions with a velocity field would result in a minimum impact. Changes in heat content due to the cold discharge were kept separate from changes due to surface heat exchange, and were compared at the end of each calculation cycle.

Following initialization, calculations were started by simulating for one time step the discharge of a small amount of cold water into the grid volume adjacent to Keahole Point, and assuming complete mixing with the grid ambient waters. The discharged water was at a temperature of 16.9°C, and contained 16.5 cal/cm$^3$. In comparison, the heat content of the ambient water was 23.8 cal/cm$^3$ during winter, and 25.9 cal/cm$^3$ during summer.

The net heat loss from the grid volume into which the simulated discharge took place, during the first time step, was calculated as follows. For the 100 MW OTEC plant the discharge rate was 22,208 ft$^3$/sec, or $11.34\times10^{10}$ cm$^3$/3 min. This is equivalent to 30.48 cm$^3$/3 min. This is equivalent to 30.48 cm$^3$/cm$^2$ surface area per time step.

$$\begin{aligned}\text{Heat discharged} &= \rho \times C_p \times T \times \text{volume}\\ &= 1.023 \times 0.954 \times 16.9 \times 30.48\\ &= 502.7 \text{ cal/cm}^2\text{/time step}\\ &\quad \text{or } 502.7/\text{MLD cal/cm}^3\text{/time step}\end{aligned}$$

$$\begin{aligned}\text{Heat lost from grid volume by displacement} &= 25.9 \times 30.48/\text{MLD cal/cm}^3/\Delta t\\ &= 789.4/\text{MLD}\end{aligned}$$

$$\text{Net heat loss} = \frac{1.0}{\text{MLD}}(789.4 - 502.9)$$

which during summer becomes $7.17\times10^{-2}$ cal/cm$^3$.

This loss was subtracted from the initial heat content. Then Eq. (14) was used to calculate the effect in adjacent grid volumes

During subsequent time steps an equal volume of cold water would enter into the grid volume adjacent to Keahole Point, resulting in a heat loss of:

$$H_{k+1} = \frac{11.34\times10^{10}(16.5-H_k)}{61{,}000^2 \times \text{MLD}} \text{ cal/cm}^3\text{/time step}$$

where $H_k$ is the heat content of the grid volume at time step k. After each "injection" of cold water, Eq. (14) was used to calculate the effect throughout the remainder of the grid system. Concurrently, a successive total of heat gained or lost due to surface heat exchange was calculated.

The change in heat content of selected grid volumes was printed at several time intervals following the start of cold water discharge. Computations were continued until a tendency toward equilibrium was approached in the grid volumes as a function of time, and as isopleths of heat losses (in cal/cm$^2$ surface area) at 1/2, 1, 3, and 6 hours after discharge commenced.

The range of existed diurnal temperature fluctuations off Keahole Point is large enough to mask the calculated small decrease in heat content over the large area of the entire grid system. However, a recognizable thermal impact will be confined to a mixing zone within the immediate vicinity of the point of discharge.

Data on diurnal temperature changes in the surface layer of Hawaiian waters were sparse. Laevastu and Inouye (4) noted that daily surface seawater temperature changes in lower latitudes average about 0.2°C, but they

did not state the depth at which daily temperature fluctuations become insignificant. Bathen (7, 8, 9) has measured the diurnal temperature range at several locations in Hawaiian waters, but restricted to shallow or sheltered areas. In the northwest channel of Kaneohe Bay (depth 12 m), during tidal inflow and outflow, the range at depths of 0, 5, and 10 m was 0.4°, 0.3°, and 0.2°C, respectively. At calm offshore locations he reports surface diurnal changes of 0.2° to 0.3°C, becoming negligible at 70 m. Assuming a diurnal range of 0.2°C, decreasing to zero at the 50 m depth, results in a diurnal heat content fluctuation of 488 cal/cm$^2$.

An alternate method to estimate the diurnal temperature range is provided by the surface heat exchange components previously calculated. The sea gains heat during the day, loses heat at night. Heat gained during the day is the total incoming radiation, less reflection, less approximately half (12 hr/24 hr) the sum of the back radiation ($Q_b$), evaporation losses ($Q_e$), and sensible heat transfer ($Q_s$). The heat loss at night is half the sum of $Q_b$, $Q_e$, and $Q_s$, calculated for characteristic night conditions, i.e., negligible cloud cover, no wind, lower air and wet bulb temperatures, and a seawater temperature equal to the daytime value. This data was also obtained from the old Kailua airport records. The surface heat exchange equations derived by Laevastu (2) accommodate this computation, because $Q_b$ was derived in terms of cal/cm$^2$/min, $Q_e$ was found to change little from day to night (except insofar as the temperature and wind speed changed), and $Q_s$ is directly related to $Q_e$ through Bowen's ratio.

The results of these calculations for the day to night changes in heat storage in cal/cm$^2$ are as follows:

| | ave. for 4 summer months | ave. for 4 winter months | ave. for transition months |
|---|---|---|---|
| daytime heat gain | +521 | +304 | +431 |
| nightime heat loss | -180 | -205 | -197 |
| net daily gain | +341 | + 99 | +234 |

If these daily changes are assumed uniformly distributed throughout the mixed layer, they would be equivalent to temperature changes of 0.13° and 0.03°C, summer and winter, respectively, calculated as follows:

$$T = \frac{\Delta H}{\rho x C_p x MLD} \ ^\circ C \qquad (17)$$

If, however, the changes are confined to the surface 10mm/15 m, as suggested by the field data (Bathen [1]), the diurnal temperature changes would be 0.52°C and 0.20°C, summer and winter, respectively. Because of the uncertainty in the depths to which diurnal temperature fluctuations extend, it was felt more useful to compare changes in heat content, rather than temperature.

Results of the Computations

In Fig 3 are plotted the computed changes in total heat content (cal/cm$^2$) as a function of time, for the grid volume adjacent to Keahole Point, and directly west of it (grid volume K.P.), under summer conditions with and without advection. The effect of advection on the equilibrium state, and the time taken to reach it, is considerable. By estimating an asymptote in the slack water case, the final changes in heat content are found to be 920 and 1280 cal/cm$^2$, representing temperature changes of 0.24° and 0.33°C, with and without advection respectively. These values exceed the estimated diurnal fluctuation in the surface 40 m (0.13°C) but are less than those estimated for the surface 10 m (0.52°C). If the latter estimate is approximately correct, the cooling of the mixed layer will have no significant effect on the surface heat exchange. Neglecting daily fluctuations, a surface temperature decrease of 0.33°C would result in an increase of $Q_{net}$ of less than 10 percent (20 cal/cm$^2$/day)(see Table II).

Figure 4 shows the heat losses under the same conditions in grid volumes 3.7 km north and west of grid volume K.P., and the heat gained due to surface heat exchange. Advection results in a considerable loss of symmetry of heat losses about the discharge point. Under slack conditions the net surface heat exchange approximately balances heat losses at 3.7 km from Keahole Point, but under conditions of advection, the heat loss 3.7 km west of Keahole Point is only a small fraction of the heat loss 3.7 km north of this point. As time progresses the zone in which the rate of change is a maximum moves steadily northward. Note also that the maximum rate of change of heat content at any given time decreases with time. From the shape of the curves it is apparent that the equilibrium heat loss in grid volume K.P. is the maximum under the imposed conditions.

The results show that heat losses under summer conditions with advection, to 9.7 km north of grid volume K.P. as a function of time, six hours after discharge commenced, equilibrium has been closely approached within 2.4 km of the outfall. Beyond 2.4 km the heat content is still changing appreciably at six hours. However, it is apparent that any further heat losses beyond 2.4 km will not exceed 520 cal/cm$^2$. As a first approximation, heat losses at complete equilibrium (i.e., at an effective equilibrium of the entire modelled area) are estimated to lie between 350 and 450 cal/cm$^2$ between 2-1/2 and 7 km north of Keahole Point, and to be less than 350 cal/cm$^2$ beyond 7 km. Heat losses at complete equilibrium exceeding 520 cal/cm$^2$ are estimated to occur within 2 km of grid volume K.P.

In this manner it is possible to establish positions in the grid system where the heat losses may be usefully compared to surface heat exchange gains. Then, by extending these points parallel to the isopleths in Fig. 5, areas can be defined over which the heat loss exceeds the estimated diurnal fluctuation in heat content.

The results without the imposition of a north-setting current show that at all distances from Keahole Point the tendency toward equilibrium has not become pronounced enough to allow fair estimates of heat losses at complete equilibrium. A crude guess would be that beyond 2 km from grid volume K.P. the equilibrium heat losses are less than 520 cal/cm$^2$. Beyond about 4 km, the average net surface heat exchange (+400 cal/cm$^2$/day) fully compensates heat losses caused by the cold water discharge at all times.

Figure 5 illustrates the spreading effect of the discharged waters under summer conditions with and without an imposed velocity field, as predicted by the model. The stated times are from commencement of discharge. The units of the isolines are cal/cm$^2$, and represent the change from ambient conditions at the specified time. After six hours, with exception of the 100 and 300 cal/cm$^2$ isolines, the areas bounded by the isolines are smaller under conditions of advection than under slack water conditions. Warm water flowing in from the south helps to diminish the impact of the cold water discharge.

The chain dotted curves enclose areas estimated to experience heat losses exceeding the diurnal range after 6 hours (curve P) and at complete equilibrium occurring at an underdetermined time (curve Q). Curve Q encloses areas of 3.5 km$^2$ (summer conditions with advection), and 11 km$^2$ (summer conditions without advection). Curve R is an estimate of the limit beyond which heat losses are always smaller than the heat gained by surface heat exchange.

Figure 6, 8, and 9 have been drawn in a similar manner for the winter conditions. The estimated asymptotes for equilibrium in grid volume K.P. (Fig. 6) are 750 and 1000 cal/cm$^2$ for advection and the slack water case respectively, equivalent to temperature decreases of 0.80°C and 0.10°C evenly distributed throughout the 100 m mixed layer depth. Both temperatures exceed the estimated winter diurnal fluctuations calculated for the total mixed layer depth (0.03°C), but are less than those calculated for the surface 15 m (0.20°C); similar to the summer results.

Comparison of results for summer and winter with advection reveals that the approach to equilibrium of grid volumes 2.4 km and further from grid volume K.P. is very similar under summer and winter conditions with advection. The winter diurnal fluctuation is less however (300 cal/cm$^2$), so that the area over which a significant effect would be noticed is larger; 12 km$^2$ after 6 hours, and 28 km$^2$ at complete equilibrium. The main effect of an increased mixed layer depth is to decrease the heat losses within 2.4 km of Keahole Point, by a maximum of((920-750)/920)x100=18%.

Under winter slack water conditions equilibrium is approached at about the same rate as during summer, but the final heat losses within 6 km of Keahole Point are estimated to be less by a maximum of ((1280-1000)/1280)x 100=22%. The area within which heat losses are estimated to exceed the diurnal fluctuation is 10 km$^2$ after 6 hours, and 21 km$^2$ at complete equilibrium. These areas are defined in Figs. 8 and 9.

It should be noted that significant impact during winter extended over a larger area than during summer, a result mainly of the diurnal fluctuation criterion. Also, during winter, advection has the effect of increasing the impacted area, whereas during summer advection has the opposite effect.

As it was assumed that the sea lost heat to the atmosphere under the imposed winter conditions (-40 cal/cm$^2$/day), there can be no compensation by net surface heat exchange. Curve R* in Figs. 8 and 9 indicates the boundary of the region beyond which heat losses due to the cold water discharge are always less than the heat lost through surface heat exchange.

It is apparent that in all cases discussed so far, the net surface heat exchange is insignificant in comparison with heat losses due to the cold water outfall. During summer, in order for $Q_{net}$ to fully compensate the loss of 502.7 cal/cm$^2$ every three minutes in grid volume K.P. (24.11x10$^4$ cal/cm$^2$/day), an area of ((24.13x10$^4$)/400)=603 grid volumes, would be required. This is equivalent to 225 km$^2$.

Two features stand out when comparing spreading of heat losses during summer and winter conditions (Figs. 5, 8, and 9). In both the slack water and advection case, heat losses exceeding 100 cal/cm$^2$ at any given time are confined to a smaller area during winter, whereas the isolines defining heat losses 25 cal/cm$^2$ or less encompass larger areas during winter. At values of the isolines near maximum, the ratio of the area encompassed by an isoline during summer to the area encompassed by the same isoline during winter exceeds 2.5 (100/40). As the isoline value decreases, the ratio decreases becoming unity at about 25 cal/cm$^2$. Thereafter the ratio further decreases at an accelerating rate. The size of the mixing zone is determined both by the surface area of the waters already affected, and the mixed layer depth. Mixing accelerates as the extent of the mixing zone increases, so that during winter the effects of the cold water discharge are spread more rapidly.

Second, during winter, the effect of the bottom topography less than 100 m deep is clearly noticeable, particularly in the slack water case. The shoaling waters along the coast act as a barrier to spreading, especially off Makalawena. The north-easterly advection north of Keahole Point somewhat offsets this effect.

Last, Figs. 10 and 11 illustrate the results for a 240 MW OTEC plant under summer conditions with advection. The heat loss at equilibrium in grid volume K.P. is 2120 cal/cm$^2$, equivalent to a 0.54°C temperature decrease. As in the advection cases previously discussed, equilibrium in grid volume K.P. is reached after about two hours. The temperature gradients existing from the outfall in three directions at equilibrium conditions were: (1) 0.012°C/100 m to the north; (2) 0.046°C/100 m to the west; and (3) 0.079°C/100 m to the south.

The distance from the outfall at which heat losses are equal to the diurnal fluctuation can be estimated from Fig. 10. This gives values of 7 km north of grid volume K.P. after six hours, and 8.5 km at complete equilibrium. The bounding curves are plotted in Fig. 11 (curves P and Q). At 11.5 km north of grid volume K.P. the heat loss is estimated to be fully compensated by $Q_{net}$ (curve R).

An estimate of the largest temperature decrease likely to result from the cold discharge of a 240 MW OTEC plant was made. This would occur during the summer slack water condition. From Table III, the temperature decrease would be approximately 0.33/0.24x0.54=0.74°C (1.33°F). In the prior section this was reduced to 0.67°C to permit an accurate comparison of changes in

surface heat exchange components resulting from a doubling of the seawater temperature decrease.

## Biostimulation

### Methodology

The objective of the work discussed in this section was to gain some insight into the possible effects of additional nutrients on the plankton community in the waters off Keahole Point. Nutrient concentrations greater than those presently existing might cause considerable local biostimulation. Water from depths of about 600 m contains inorganic nutrient (i.e., phosphates and nitrates) levels about 10 times those in the mixed layer. These additional nutrients would be expected to increase primary productivity in the euphotic zone. The degree of increase would diminish rapidly with distance from the discharge point because nutrient levels in the water column would decrease due to mixing, advection, and assimilation by phytoplankton.

The discharged cold water would contain about the same concentrations of nitrates and phosphates as fresh water percolating out from the island (Bathen [1]). The effects of percolation are apparent in coastal embayments, but have not been noted in the vicinity of points and headlands. The strong and persistent currents off Keahole and Keahuolu Points (Bathen [1]) would be effective in rapidly dispersing any additional nutrients, within the zone of influence of these currents. At this stage it is not known to what depths these strong currents extend. The biggest danger of biostimulation therefore appears to exist in the subsurface waters. (Note that the euphotic zone extends to well below 100 m off the Kona coast.)

The subtropical waters surrounding the Hawaiian Islands are known to be oligotrophic, but no definite indication has been given as to which is the limiting nutrient. Thomas (10) has shown that nitrogen might be the limiting nutrient in the eastern equatorial Pacific Ocean. Redfield, et al. (11) has shown that the inorganic nitrogen/phosphorus ratio in deep water (i.e., well below the euphotic zone) is approximately the same as the ratio in which these elements occur in phytoplankton. The cold water being discharged will be assumed to supply these nutrients in this same ratio (in addition to all required micro-nutrients and trace elements). Field data for total nitrogen and total phosphorus (i.e., including organic compounds of these elements) has shown that the surface waters off Kona tend to be richer in these major nutrients, than waters elsewhere in the Hawaiian Archipelago. This is partly a result of percolation, and partly a result of water upwelled offshore, moving slowly onshore.

The fraction of organic nitrogen and phosphorus, which is not directly utilizable by the primary producers, is unknown. The fraction of organic nitrogen in the mixed layer has been estimated to range from 0.3 to near unity (Riley and Chester [12]), while the fraction of organic phosphorus might constitute from 0.5 to near unity of the total phorphorus concentration (Riley and Skirrow [13]). It is known that the fraction of organic material decreases with depth. Below 1000 m, organic phosphorus is almost nonexistent, while the organic nitrogen constitutes less than 5 percent of the total.

A summary is given below comparing surface nutrient concentrations off Keahole and Keahuolu Points, and average values for Hawaiian waters (Bathen [1]). This shows the natural enrichment of Kona coast waters, perhaps one reason why the area enjoys successful sport fishing.

| | Total micro-gm at/l nutrient Kona coast | Inorganic micro-gm at/l (assuming an organic fraction of 0.8) | Average inorganic micro-gm at/l Hawaiian waters |
|---|---|---|---|
| Nitrogen | 8 - 15 | 1.6 - 3.0 | 0.4 |
| Phosphorus | 0.1 - 2.0 | 0.02 - 0.4 | 0.15 |

If the assumed organic fraction of 0.8 is representative, nitrogen enrichment appears to be more prevalent than phosphorus enrichment. Hence in the analysis following, phosphorus will be assumed the limiting nutrient.

The Machaelis-Menten nutrient uptake equation is frequently used in studying the overall effect of nutrient enrichment in oligotrophic waters. The rate at which nutrients are taken up by organisms is assumed to be equal to their growth rates. The equation is:

$$R_N = N \frac{V_{max}}{K_S+N} \qquad (18)$$

where $R_N$ = rate of nutrient uptake (micro-gm nutrient/hr per micro-gm of nutrient assimilated in the organism, or $hr^{-1}$)

$N$ = nutrient concentration per unit volume (micro-gm at/l)

$V_{max}$ = maximum nutrient uptake rate under ideal conditions ($hr^{-1}$)

$K_S$ = half saturation constant, or the nutrient concentration at which the uptake rate is 1/2 $V_{max}$

The growth characteristics of several diatom species have been published (Eppley, et al. [14]; Fuhs, et al. [15]) following limited studies of their growth in chemostats. These parameters were found to vary considerably from species to species, and variations in the results of experiments on the same species indicates that not all the relevant variables have been recognized.

The schematic model of plankton population dynamics use here (Caperon, et al. [16]), illustrates an increase in nutrient supply resulting in eutrophication. The total nutrient supply rate S (micro-gm at nutrient/hr) is the only independent variable. If S increases, the nutrient concentration N increases, and at the same time $P \cdot R_N$, and hence $H \cdot R_P$ and $C \cdot R_H$ also increase. In an oligotrophic system $R_N$, $R_P$, and $R_H$ are all in the maximum response region, so that the increase in S is

balanced by increases in these three uptake rates, without significantly affecting the respective population densities. In the minimum response region increases in N can only be balanced by an increase in the phytoplankton population P, and subsequently in the herbivore and carnivore populations H and C, respectively. These population increases are offset to some extent by a greater recycling rate (increases in p, h, and c), but this effect is usually too small to prevent eutrophication.

A change in nutrient concentration will not only serve to stimulate growth, but might also result in replacement of one dominant species by another, i.e., species succession. At low nutrient levels, species A will be at a competitive advantage. At nutrient concentrations greater than $N_1$, the faster growth rate of species B might cause it to become dominant.

The question which must remain unanswered at this stage is: how close are the waters off the Kona coast to the point where eutrophication becomes a possibility? (i.e., $R_N$ in the minimum response region). The complete lack of useful growth characteristics data pertaining to the indigenous plankton population necessitates a different, and cruder, approach to the problem.

Riley (17) has developed a simple mathematical model which will be utilized in an attempt to predict the magnitude of the change in plankton population density for a given potential increase in nutrient concentrations. Riley has proposed a set of three equations describing changes in nutrients, phytoplankton, and herbivorous zooplankton resulting from the overall effects of productivity and losses. The euphotic zone is assumed thoroughly mixed, a condition which is generally applicable off Keahole Point. Field measurements (Bathen [1]) have shown the mixed layer to be from 130 to 150 m deep during both summer and winter. With a characteristic extinction coefficient of 0.03 $m^{-1}$, the one percent light level is 154 m. The limiting nutrient off Keahole Point, assumed to be phosphorus, is assumed to be constantly replenished to the euphotic zone primarily via mixing with waters from just below this zone, but also by horizontal advection. In the equations which follow a single mixing coefficient is used to represent both sources of replenishment. The effect of the cold water discharge will be to augment this replenishment. The three equations are as follows:

$$\frac{dP}{dt} = P\left(P_r - gH - \frac{v}{L} - m - A\right) \qquad (19)$$

where P = phytoplankton population (gm carbon/$m^3$)
t = time (days)
$P_r$ = coefficient of phytoplankton production related to, but less than $R_N$($day^{-1}$)
= 0.663N for N less than 0.4 micro-gm at P/l, where N is the nutrient concentration
The factor 0.663 accounts for respiration losses, and the fact that productivity decreases in proportion as the nutrient concentration decreases
g = grazing coefficient
= 3.4 l swept clear per day per unit quantity of herbivore
H = herbivore population (gm carbon/$m^3$)
v = sinking rate
= 6 m per day (a value postulated for subtropical waters)
L = depth of euphotic zone (m)
m = mixing coefficient, or that fraction of the euphotic layer transported to the lower layer per day ($day^{-1}$)
A = an apparent mixing coefficient representing the OTEC plant discharge ($day^{-1}$). A is analogous to m in that the discharged water originating at the intake depth (600 m) will result in an additional mixing effect with the surface waters

Equation (14) describes the net rate of phytoplankton productivity in a given water column as the difference between net production and combined losses due to predation, mixing, and sinking. Note that the daily OTEC plant discharge has the continuity effect of moving an equal volume of water horizontally, out of the water column in question, carrying the plankton with it.

$$\frac{dH}{dt} = H(gP - r_H - fC) \qquad (20)$$

where gP = rate of food consumption by the herbivorous zooplankton ($day^{-1}$)
$r_H$ = respiratory rate
= 0.05 $day^{-1}$
f = feeding coefficient of the carnivorous zooplankton
= 0.005 $day^{-1}$ per unit carnivore population
C = carnivore population (gm carbon/$m^3$)

Equation (20) describes the net rate of herbivorous zooplankton increase with time.

$$\frac{dN}{dt} = kP(egH - P_r) + m(N_o - N) + A(N_D - N) \qquad (21)$$

where k = a conversion factor
= 0.774 micro-gm at P/l per gm carbon/$m^3$
$kPP_r$ = change in nutrient concentration caused by grazing
PgH = total carbon consumed by herbivores
kPgH = phosphate content of this food
e = regeneration coefficient
= 0.85, if the assimilation efficiency is assumed to be 15%
kPegH = total regeneration of nutrients (phosphate) from herbivore excretion
= 0.774P(0.85)3.4H
= 2.24PH
N = initial nutrient concentration (micro-gm at P/l)
$N_o$ = nutrient concentration just below the euphotic zone (micro-gm at P/l)
$N_D$ = nutrient concentration at depth of proposed cold water intake (micro-gm at P/l)

Equation (21) describes the time rate of change of nutrients resulting from regeneration, mixing, and grazing.

At equilibrium conditions dP/dt=0, dH/dt=0, and dN/dt=0. Since P ≠ 0, Eq. (19) reduces to:

$$H + \frac{v}{gL} = \frac{P_r - m - A}{g}$$

Substituting values for $P_r$ and g,

$$H = 0.195N - 0.294(m + A + \frac{v}{L}) \quad (22)$$

Similarly, since $H \neq 0$, Eq. (20) reduces to:

$$P = (\frac{r_H + fC}{g}) = 0.0147 + 0.00147L^2H^2 \quad (23)$$

Note that the carnivore population, C, was eliminated by using an empirical formula provided by Steele (16), which is based on the assumption that the carnivore population is proportional to the square of the herbivore population.

Next, since $P \neq 0$, Eq. (21) reduces to:

$$P = \frac{m(N_o - N) + A(N_D - N)}{0.513N - 2.24H} \quad (24)$$

Finally, by substituting Eq. (22) into Eqs. (23) and (24), two simultaneous equations were obtained, with unknowns P (phytoplankton concentration) and N (nutrient concentration):

$$P = 0.0147 + 0.00147L^2[0.195N - 0.294(m+A+\frac{v}{L})]^2 \quad (25)$$

$$P = \frac{m(N_o - N) + A(N_D - N)}{0.513N - 2.24[0.195N - 0.294(m+A+\frac{v}{L})]} \quad (26)$$

Typical solutions of Eqs. (25) and (26) can be sketched showing for each value of A there is a single unique solution.

In order to match this model to background conditions typical off Keahole Point, several values of m, L, and $N_o$ were substituted into Eqs. (25) and (26) with A held constant at 0. $N_D$ was also held constant at 3.0 micro-gm at P/l. L and $N_o$ were not independent, since the nutrient concentration increases with depth below the euphotic zone. Values were selected from the historic data supplied by Bathen (1). In this way 10 different values of N were obtained. That value of N was selected most closely corresponded to the inorganic phosphorus concentration assumed to exist off Keahole Point. This determined the values of m, L, and $N_o$ used in the subsequent calculations:

$m = 0.0025\ day^{-1}$
$L = 150\ m$
$N_o = 0.5$ micro-gm at P/l

giving

$N = 0.145$ micro-gm at P/l
$P = 0.023$ gm carbon/$m^3$
$H = 0.006$ gm carbon/$m^3$

Assuming a commonly used carbon:chlorophyll ratio of 100, the phytoplankton population would be equivalent to 0.25 mg Chl a/$m^3$. In oligotrophic waters, and particularly in areas of strong insolation, this ratio increases (Steele [18]). Values as high as 250 have been reported. Using a ratio of 200, the phytoplankton population would be equivalent to 0.12 mg Chl a/$m^3$, in reasonable agreement with the range of values reported by Bathen (1). [0.14 to 0.16 mg Chl a/$m^3$]

With values assigned to all parameters, Eqs. (25) and (26) were solved using values of A ranging from 0.0005 to 0.01 $day^{-1}$. The resulting solutions of N, P, and H are plotted in Figs. 13 and 14. Rapid increases in phytoplankton and zooplankton populations are apparent, particularly at small values of A.

Figure 12 shows the concentrations of inorganic phosphate to be expected in the euphotic zone in the vicinity of the discharge site, as a function of dilution. Dilution is here defined as the volume of water entrained by a unit volume of discharge water, plus this unit volume of discharge water. Thus for a dilution of 10, and an ambient phosphate concentration of 0.4 micro-gm at P/l, the phosphate concentration after dilution would be,

$$\frac{1(3) + 9(0.4)}{10} = 0.66 \text{ micro-gm at P/l,}$$

remembering that the phosphate concentration at the cold water intake is assumed to be 3.0 micro-gm at P/l. The two values of ambient phosphate concentrations used in deriving Fig. 12 were 0.15 and 0.40 micro-gm at P/l.

Results of the Computations

Given an ambient phosphate concentration of 0.15 micro-gm at P/l as a value typical off the Kona coast, and close to the median of the range reported by Bathen [1], any value of dilution given in Fig. 12 can be used to determine the corresponding phosphate concentrations. Then, using Fig. 13, the corresponding value of A can be found, and hence the phytoplankton and herbivorous zooplankton populations. Using the discharge plume from the 100 MW OTEC plant as an example, at initial stability the centerline dilution is 11.35. This results in a phosphate concentration of 0.401 micro-gm at P/l, and P and H are 0.155 and 0.064 gm carbon per $m^3$, respectively. Similarly, at 100 m from the discharge point, the centerline dilution is 3.61. At that point the phosphate concentration is estimated as 0.939 micro-gm at P/l, phytoplankton population as 0.805, and herbivore population as 0.208 gm carbon/$m^3$.

To extend this method beyond the region in which the plume is defined, dilutions were calculated as follows. Using the volumes of the four plumes as a starting point, dilutions as a function of distance from the discharge point would be estimated. The radius R, of the area around the discharge point required to contain the plumes, and the weighted, average vertical thickness D, of a single plume, defined an initial volume. At the seaward boundary of this volume the dilution was set equal to the weighted average dilution of the plumes. The dilution in successive circular volumes around the discharge point could then be calculated. R was increased in steps of 50 m, while D increased (per plume results) in steps of 14.7 m, until a thickness of 150 m (depth of euphotic zone) was reached. Beyond this point D remained constant.

Dilution at R =

$$[\text{Dilution at } (R-50)][\frac{\text{volume contained by radius R}}{\text{volume contained by radius (R-50)}}]$$

With the dilution thus estimated, nutrient and plankton concentrations were found as indicated above. Results are tabulated in Tables IV and V. Two regimes are recognized:

1. Since the plumes would stabilize at a depth of 60 to 70 m, appreciable biostimulation is predicted at depth, with the percentage increase of the phytoplankton population exceeding 500 for a 100 MW plant, and 1000 for a 240 MW plant. However, the velocity at the plume centerline in this zone is of the order of 1m/s, so that it would require only about 5 minutes for the discharged waters to reach this region. The steady state postulated by the model cannot have been attained, and it is unlikely that biostimulation of this magnitude will occur within the plume.

2. Outside the defined limits of the plumes, significant biostimulation is predicted only within 500 m of the outfall. On the assumption of a rapid and complete mixing within the 150 m euphotic zone, nutrient concentration and plankton populations decrease rapidly with distance from the discharge point. Diurnal and seasonal fluctuations have not been documented for waters within a few kilometers off the Kona coast. Total phosphorus concentrations measured during summer off Keahole and Keahuolu Points showed differences of up to 0.5 micro-gm at P/l between the two stations, and similar differences between different depths within the euphotic zone (Bathen [1]). Using the inorganic fraction assumed previously (0.2), inorganic phosphorus fluctuations are estimated to be about 0.1 micro-gm at P/l. With this figure as a standard of comparison, significant phosphate increases would occur within 225/275 m of the 100/240 MW plant outfall. Note that these are minimum estimates because mixing is unlikely to be complete. Nutrient concentrations will be higher than predicted by the model at the plume stabilization depth, decreasing upward and downward, as well as laterally. The overall result would be significantly affected areas larger than those predicted at the 60 to 70 m depth, and smaller affected areas above and below this depth.

Seasonal zooplankton population fluctuations are of the order of 100 percent in the oceanic waters off the island of Hawaii (Bathen [1]). Data on phytoplankton variations were not available, but would likely be similar in relative magnitude. Closer inshore, however, the steady supply of nutrients due to percolation and upwelling might dampen the fluctuations. Assuming background plankton population fluctuations of 25 percent, increases in both phytoplankton and herbivorous zooplankton populations would be significant within 450/600 m from a 100/240 MW plant outfall. The total affected area for the total discharge would be approximately 1.6 and 4.4 $km^2$, respectively. The net drift previously noted would spread the affected waters in a north to north-easterly direction, parallel to the inshore zone where the consequences of biostimulation would be most disruptive.

## Summary and Conclusions

The environmental analyses were concerned with estimating potential changes in the net exchange of heat at the surface, the changes in heat storage in the mixed layer, and potential biostimulation in the cold water discharge area from 100 MW and 240 MW floating nearshore OTEC power plants.

Two independent sets of equations were used to describe potential changes in the surface heat exchange processes. Under characteristic/high evaporation conditions net surface heat exchange ranged from 70/-30 cal/$cm^2$/day during January to 380/420 cal/$cm^2$/day during August/July. Under a large range of weather conditions the waters off Keahole Point gain heat throughout the year. This may be attributed to high insolation, and low evaporation losses. The effect of a 0.67°C (1.2°F) seawater temperature decrease was to decrease back radiation and evaporation losses, and to increase gains in sensible heat exchange, resulting in an overall increase in heat flow into the sea of 25 to 60 cal/$cm^2$/day, or an increase of about 15 percent during summer, and 40 percent during winter. The possible effects of the resulting heat loss from the atmosphere on the local micro-climate remain unknown.

Estimates made of the diurnal heat content fluctuations in the mixed layer for summer, winter, and transition months resulting from the cold water discharge were largest in the zone immediately surrounding the outfall. On the assumption that diurnal temperatures were confined to the surface 10 to 15 m thick layer, a 100 MW plant discharge (at the 21 m/70 ft depth) would cause no significant temperature decrease in this upper layer. Below the 15 m depth, temperature decreases would be significant. If diurnal temperature changes were assumed evenly distributed throughout the mixed layer (as was assumed for the heat loss computations), areas from 3.5 $km^2$ (summer with advection), to 28 $km^2$ (winter with advection), could be significantly affected. During summer, advection tended to decrease the significantly impacted area, whereas during winter this area was increased by advection. This condition resulted largely from the arbitrary choice of diurnal heat content fluctuations as measures of comparison, although there was also a tendency for more rapid advective mixing beyond the 25 cal/$cm^2$ isoline.

It was concluded from the single 240 MW plant case tested that the cold water discharge would result in maximum heat losses approximately double those due to the 100 MW plant, and the area of significant impact would be up to 10 times larger under similar conditions. The maximum temperature decrease was estimated to be 0.74°C, and would occur during summer slack water conditions. It was not possible to accurately define, on a monthly or seasonal basis, areas over which heat losses at complete equilibrium would exceed background diurnal fluctuations principally because of the uncertainty in existing diurnal heat content fluctuations, particularly the depth to which these extended. In addition, the depth of the mixed layer is an important factor changing with the seasons, and is subject to date of incomplete description.

The possibility of biostimulation was examined using three relationships describing rates of change of nutrients, phytoplankton, and herbivorous zooplankton, assuming steady state conditions. Within the plumes, the possibility of significant biostimulation is precluded because any particular parcel of discharged water would not remain within the plume sufficiently long for the plankton population to react appreciably to the high nutrient concentrations. Outside the defined plume limits, significant nutrient increases are predicted

within 300 m of the outfall. Beyond this region increases are similar in magnitude to background fluctuations caused by seasonal changes, percolation, or other factors. The areas likely to experience significant plankton population increases are approximately 1.6 and 4.4 $km^2$ for 100 and 240 MW plants, respectively. Under the prevailing current conditions, an OTEC plant positioned more than 1 km offshore, would likely have very little effect on the nearshore biota.

Attempts to relate the estimate of potential temperature and nutrient changes from the 100 MW and 240 MW cases to the Hawaii water quality standards proves inconclusive. With the exception of neighboring Honokahau and Kailua Bays, the nearshore waters within the Keahole area of interest are classified as AA, the highest state classification for preservation. Both bays are beyond the region of any significant impact. Waters classed as AA are required to remain in their pristine state, but uses of such water are not precluded if these are compatible with class AA standards.

The restriction regulating temperature is that this should not vary more than 2°C over ambient conditions during any 4-hr period. Bathen (1) has pointed out that diurnal fluctuation exceeding 2°C have been reported in many pristine locations presently classified as AA. The conclusion is that the state water quality standards require updating before they can be meaningfully applied to the environmental impact of the proposed OTEC plant. Discounting temperature changes within the limits of the plumes, which would require special concession and legal definition of mixing zones allowed in class AA waters, the maximum temperature change predicted by the heat conservation model was 0.75°C within 610 m of the outfall.

Limitations set on phosphates are that total phosphate should not exceed 0.64 micro-gm at P/l. According to this restriction, the existing undisturbed waters off Keahole Point are in violation of state regulations. Assuming an organic fraction of 80%, inorganic phosphate contribution from OTEC operations should not excced 0.13 micro-gm at P/l. The assumption made in the biostimulation model was that ambient inorganic phosphate was held constant at 0.15 micro-gm at P/l.

## References


1. Bathen, K.H. (1975): An evaluation of oceanographic and socio-economic aspects of a nearshore ocean thermal energy conversion pilot plant in subtropical Hawaiian waters. Report submitted to the National Science Foundation, University of Hawaii.

2. Laevastu, L. (1960): Factors affecting the temperature of the surface layer of the sea. Societas Scientiarum Fennica, Commentationes Physico-Mathematicae, 25(1), 1-136.

3. Bøyum, G. (1962): A study of evaporation and heat exchange between the sea surface and the atmosphere. Geofys. Publ., Geophys. Norv., 22(7).

4. Laevastu, T. and K. Inouye (1964): Sea-air temperature relations. Report No. 64-3, Hawaii Institute of Geophysics, University of Hawaii.

5. Wyrtki, K. (1966): Seasonal variation of heat exchange and surface temperature in the North Pacific Ocean. Report No. 66-3, Hawaii Institute of Geophys. University of Hawaii.

6. Reed, R.K. and D. Halpern (1965): Insolation and net long-wave radiation off the Oregon coast. Jour. Geophys. Res. 80, 839-844.

7. Bathen, K.H. (1970): Heat storage and advection in the North Pacific Ocean. Report No. 70-6, Hawaii Institute of Geophysics, University of Hawaii.

8. Bathen, K.H. (1968): A descriptive study of the physical oceanography of Kaneohe Bay, Oahu, Hawaii. Tech. Rep. No. 14, Hawaii Institute of Marine Biology, University of Hawaii.

9. Bathen, K.H. (1972): A descriptive study of the circulation and water quality in Kailua Bay, Oahu, during 1971 and 1972. Tech. Rep. No. 72-29, J.K.K. Look Laboratory of Oceanographic Engineering, University of Hawaii (in 3 vols.).

10. Thomas, W.H. (1969): Phytoplankton nutrient enrichment experiments off Baja, California and in the eastern equatorial Pacific Ocean. Jour. Fish. Res. Bd. Canada, 26, 1133-1145.

11. Redfield, A.C. and B.H. Ketchum, F.A. Richards (1963): The influence of organisms on the composition of seawater. In "The Sea" (M.N. Hill, ed.) vol. 2, 26-77, John Wiley and Sons, New York.

12. Riley, J.P. and R. Chester (1971): "An introduction to Marine Chemistry". Academic Press, New York, 197.

13. Riley, J.P. and G. Skirrow (1965): "Chemical Oceanography". Vol. I, Academic Press, New York, 326+.

14. Eppley, R.W. and W.H. Thomas (1969): Comparison of half-saturation constants for growth and nitrate uptake by marine phytoplankton. Jour. Phycol. 5, 375-379.

15. Fuhs, G.W. and S.D. Demerle, E. Cannelli, Min Chen (1972): Characterization of phosphorus-limited plankton algae. Am. Soc. Limnol. and Oceanogr., Nutrient and Eutrophication Symposium, vol. 1, 113-131.

16. Caperon, J. and S.A. Cattell, G. Krasnick (1971): Phytoplankton kinetics in a subtropical estuary: eutrophication. Limnol. and Oceanogr. 16, 599-607.

17. Riley, G.A. (1965): A mathematical model of regional variations in plankton. Limnol. and Oceanogr., suppl. to vol. 10, R202-R215.

18. Steele, J.H. (1958): Plant production in the northern North Sea. Marine Res., Scot Home Dept. 1958 (7), 1-36.

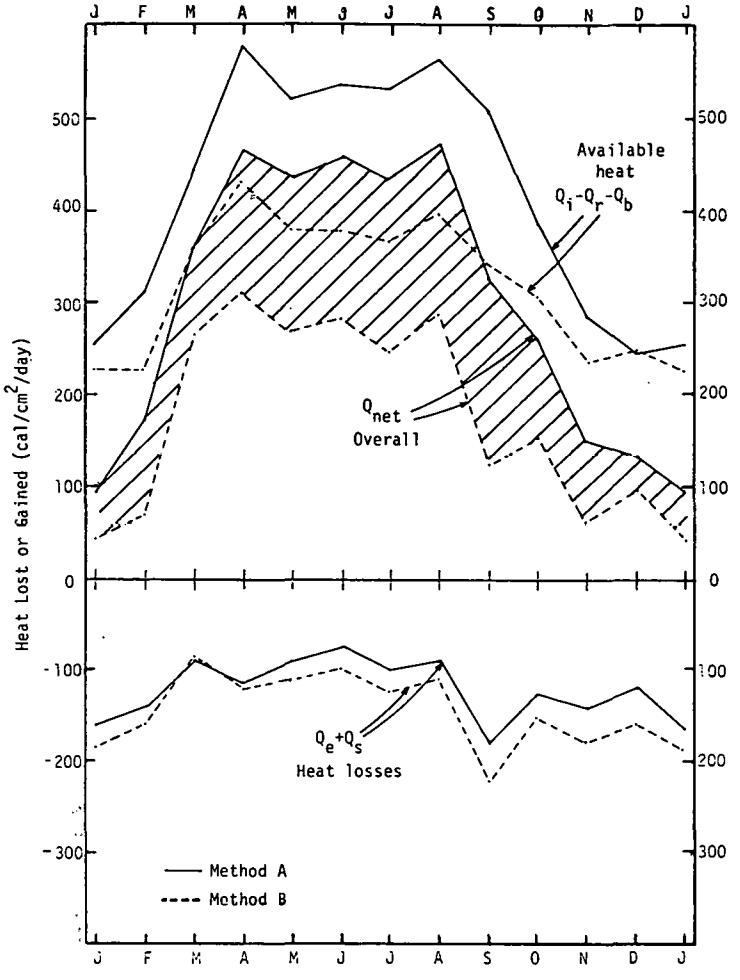



Fig. 1 Results of Surface Heat Exchange Computations Characteristic Conditions

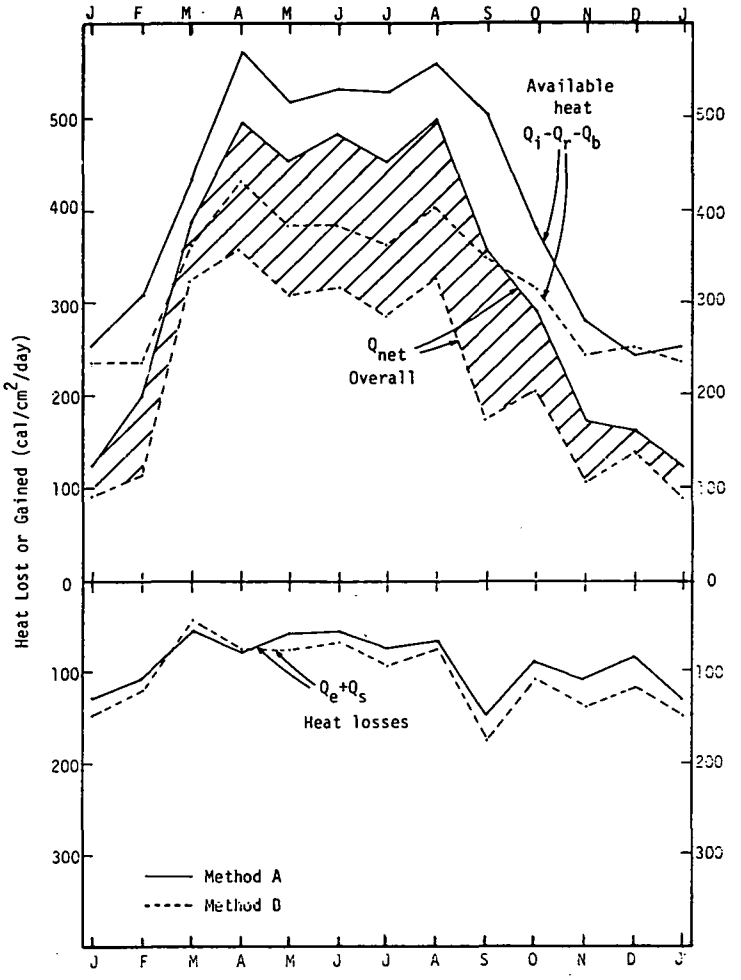



Fig. 2 Results of Surface Heat Exchange Computations Characteristic Conditions with Seawater Temperature Reduced by 0.67°C (1.2°F)

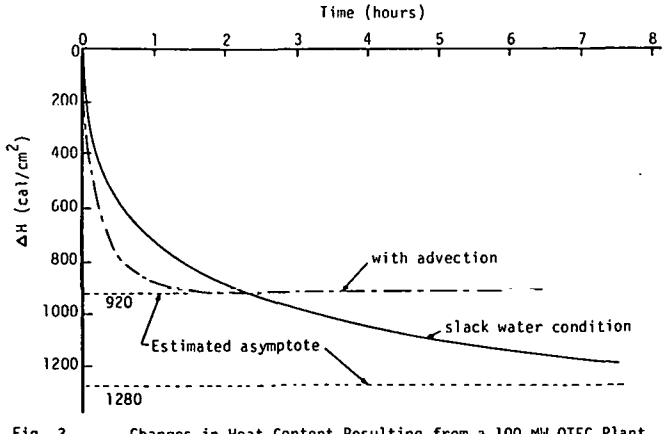



Fig. 3 Changes in Heat Content Resulting from a 100 MW OTEC Plant Discharge in Grid Volume K.P. under Summer Conditions

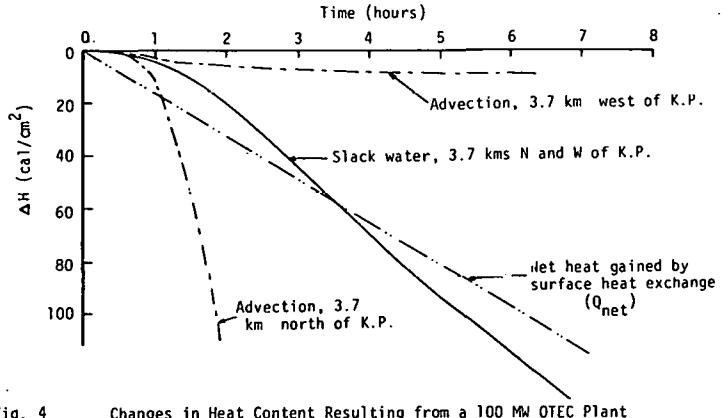



Fig. 4 Changes in Heat Content Resulting from a 100 MW OTEC Plant Discharge in Grid Volumes 3.7 km North and West of Grid Volume K.P. under Summer Conditions

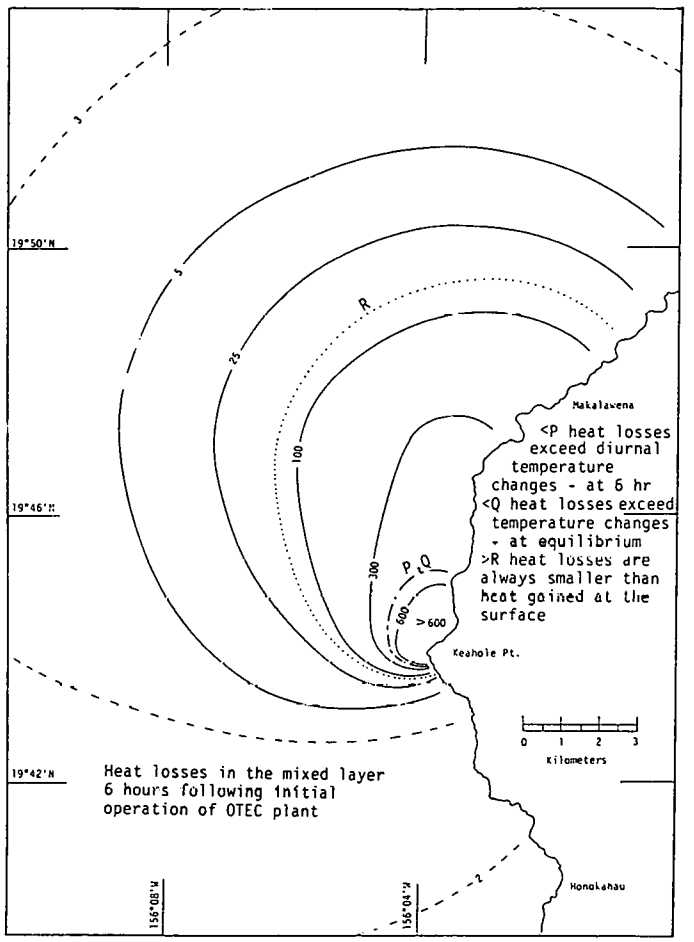



Fig. 5 Spreading of Heat Losses Calculated from the Heat Conservation Model (100 MW, Summer Conditions, Advection) (cal/cm$^2$)

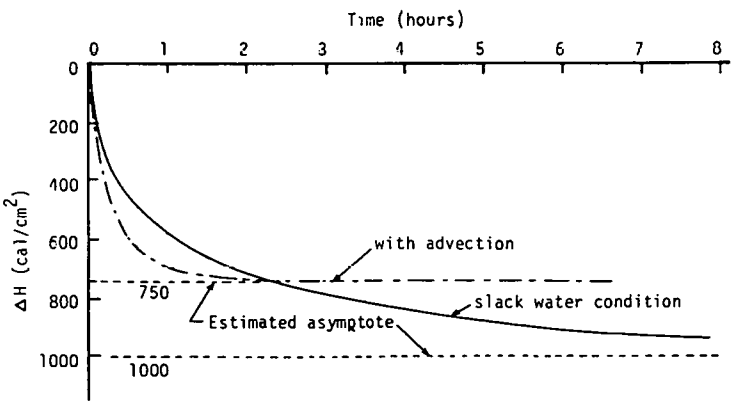



Fig. 6 Changes in Heat Content Resulting from a 100 MW OTEC Plant Discharge in Grid Volume K.P. Under Winter Conditions

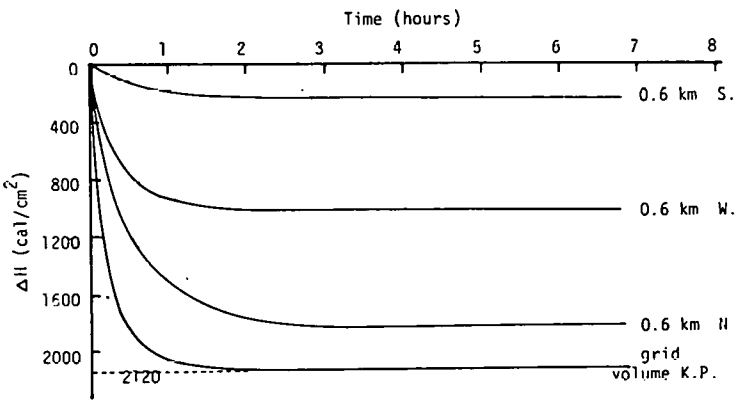



Fig. 7 Changes in Heat Content Resulting from a 240 MW OTEC Plant Discharge in Grid Volume K.P. and Adjacent Grid Volumes Under Summer Conditions with Advection

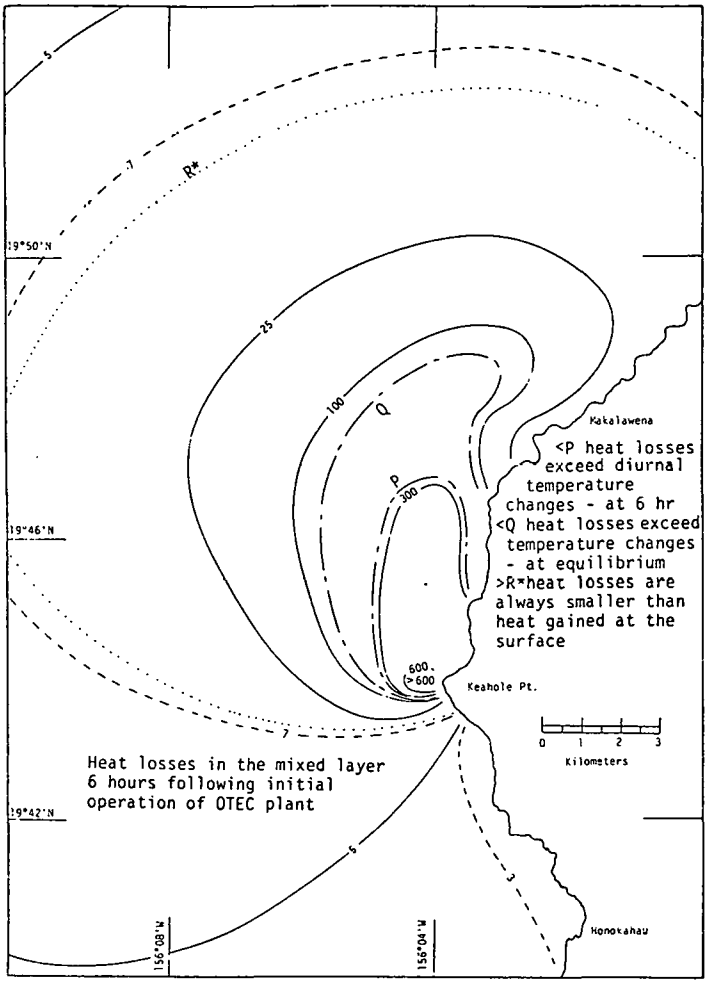



Fig. 8 Spreading of Heat Losses Calculated from the Heat Conservation Model (100 MW, Winter Conditions, Advection) (cal/cm$^2$)

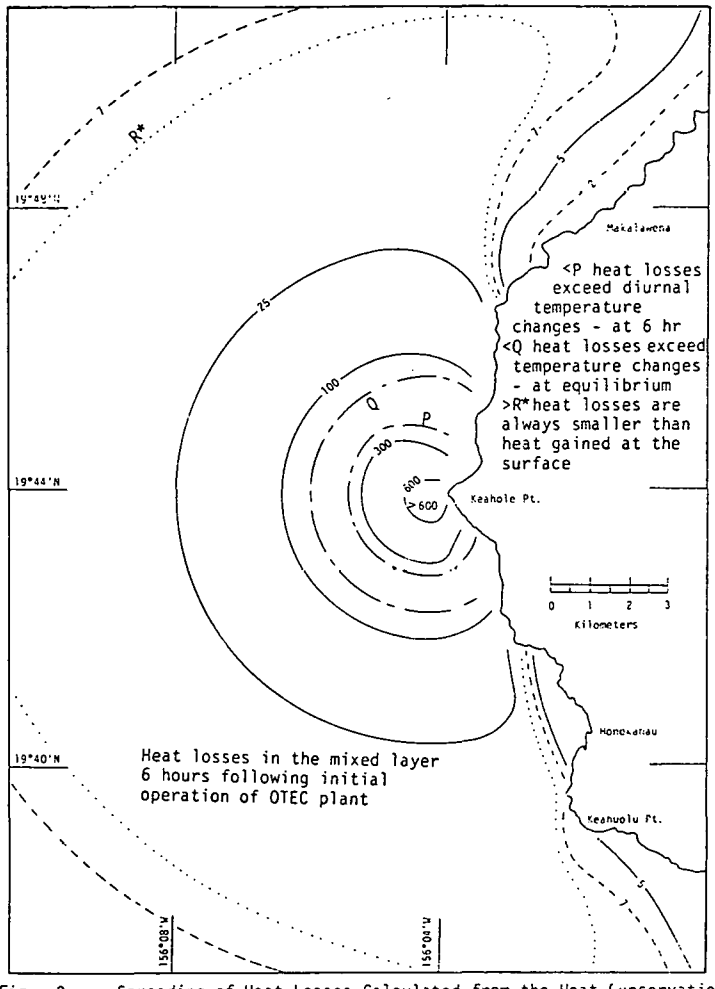



Fig. 9 Spreading of Heat Losses Calculated from the Heat Conservation Model (100 MW, Winter Conditions, No Advection) (cal/cm$^2$)

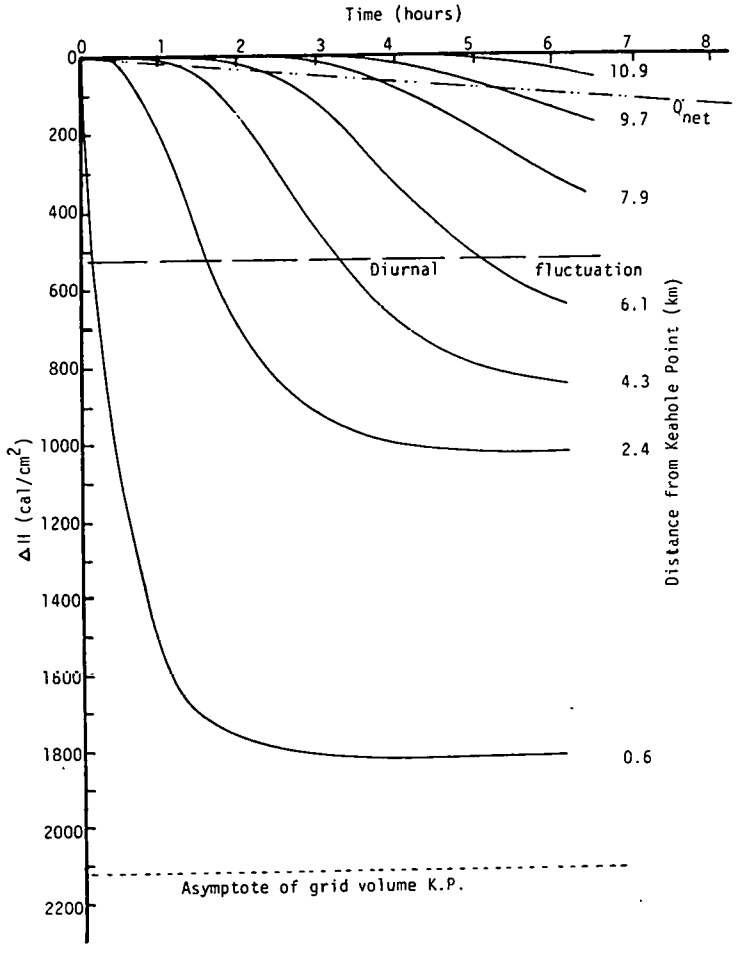



Fig. 10 Changes in Heat Content Resulting from a 240 MW OTEC Plant Discharge in 7 Grid Volumes Directly North of Grid Volume K.P. Under Summer Conditions with Advection

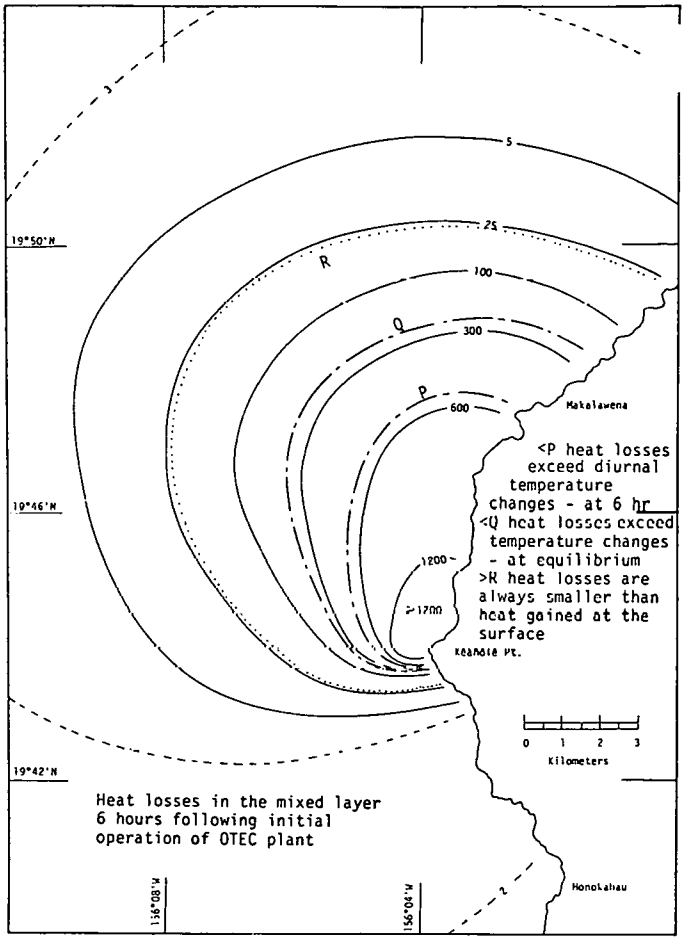



Fig. 11 Spreading of Heat Losses Calculated from the Heat Conservation Model (240 MW, Summer Conditions, Advection) (cal/cm$^2$)

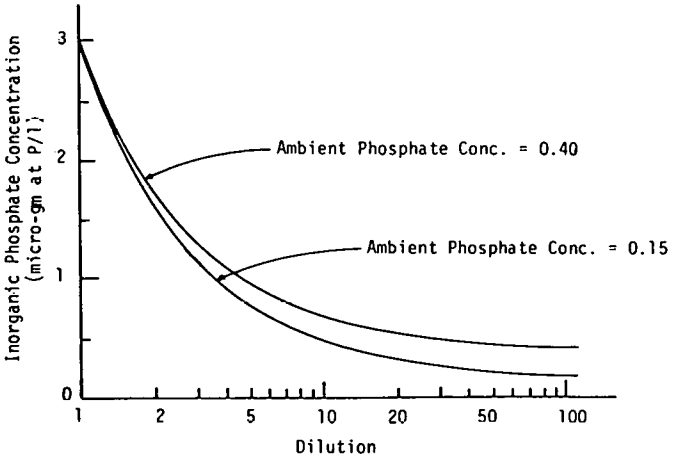



Fig. 12 Inorganic Phosphate Concentration after Dilution for Ambient Phosphate Concentrations of 0.15 and 0.40 micro-gm at/l

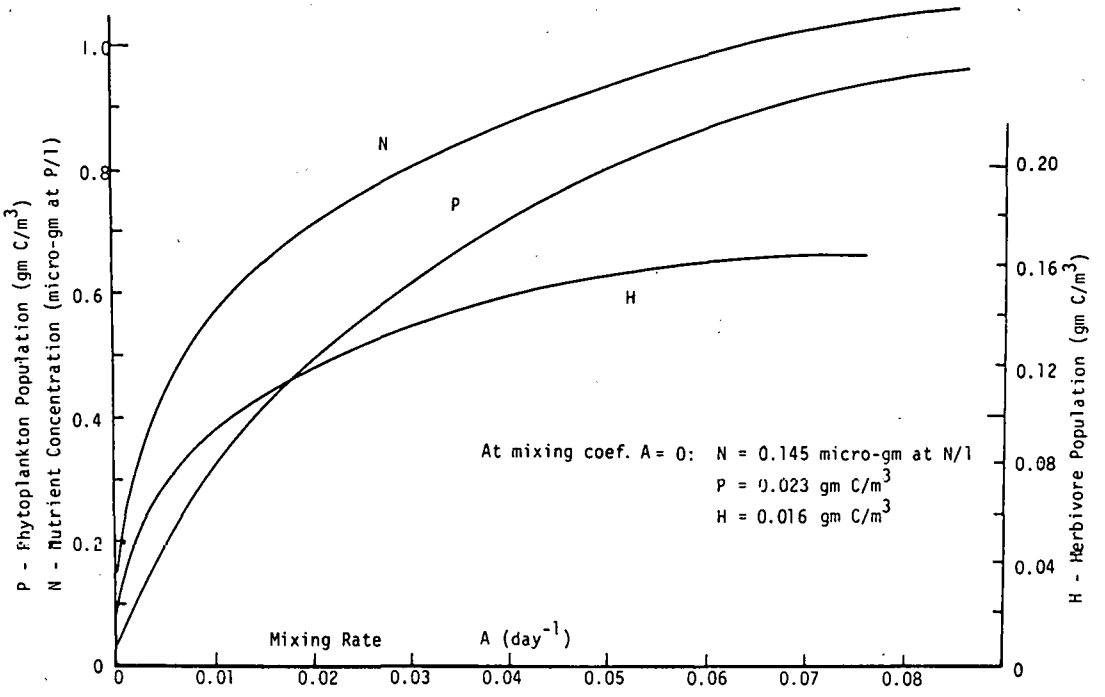



Fig. 13 Nutrient and Plankton Concentrations as a Function of the Apparent Mixing Coefficient A

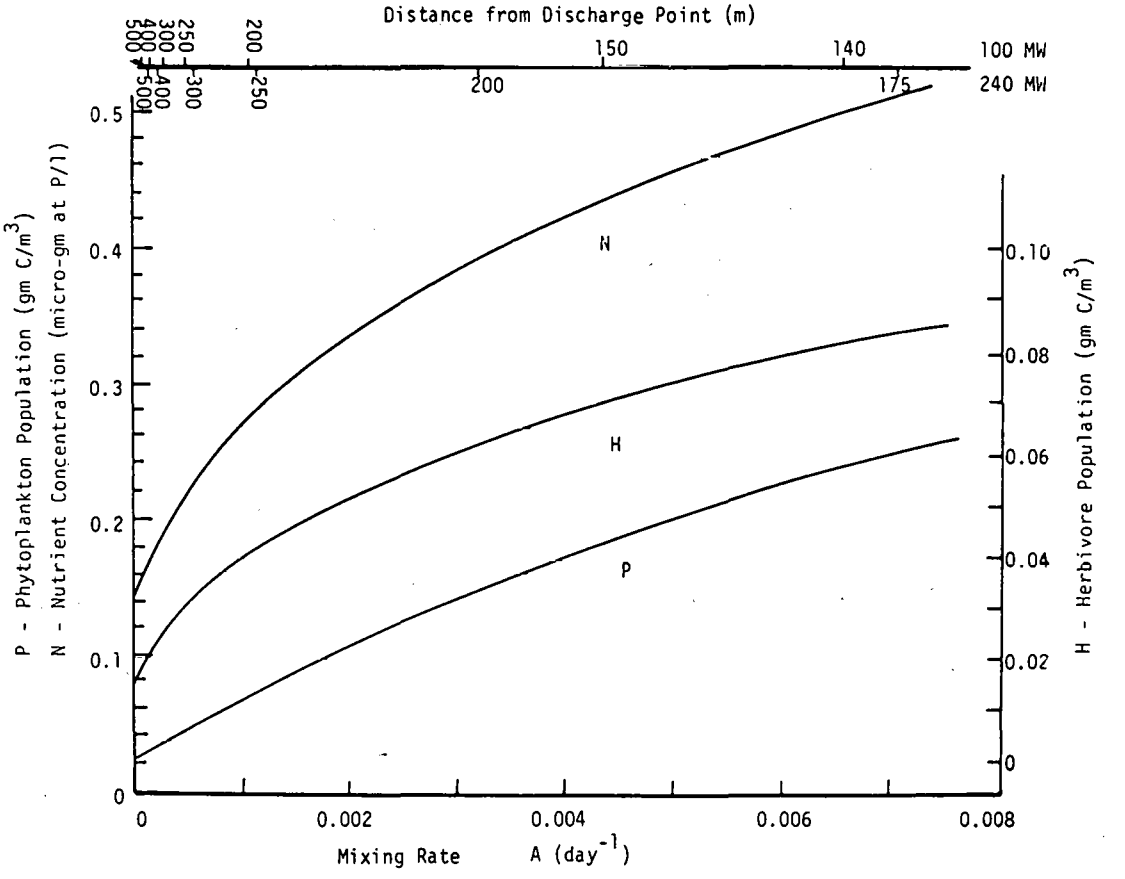



Fig. 14 Nutrient and Plankton Concentrations as a Function of A, and Distance from Outfall Discharge Point

Table I
Monthly Weather Data - Characteristic Conditions

| Month | Cloud Cover (tenths) | Temperature (°C) | | | Wind Speed (m/sec) |
|---|---|---|---|---|---|
| | | Sea Water | Air | Wet Bulb | |
| Jan | 5 | 24.9 | 25 | 21 | 4.1 |
| Feb | 7 | 24.4 | 24 | 21 | 4.1 |
| Mar | 6 | 24.0 | 26 | 22 | 4.6 |
| Apr | 5 | 24.7 | 26 | 22 | 4.1 |
| May | 7 | 25.4 | 28 | 23 | 3.6 |
| Jun | 7 | 25.8 | 28 | 23 | 2.6 |
| Jul | 7 | 26.0 | 27 | 23 | 3.1 |
| Aug | 6 | 26.7 | 28 | 24 | 3.1 |
| Sep | 6 | 27.9 | 28 | 24 | 4.1 |
| Oct | 6 | 26.8 | 28 | 24 | 4.1 |
| Nov | 6 | 26.2 | 27 | 23 | 4.1 |
| Dec | 4 | 25.7 | 27 | 23 | 4.1 |

Table II
Average Percentage Increases in Net Surface Heat Exchange Due to a Seawater Temperature Decrease

| | Seawater Temp Decrease | Summer | Winter | Transition |
|---|---|---|---|---|
| Characteristic Conditions | Method A | 3.1 | 10.0 | 5.8 |
| | 0.33°C | | | |
| | Method B | 10.7 | 32.2 | 18.7 |
| | Method A | 6.1 | 20.2 | 11.7 |
| | 0.67°C | | | |
| | Method B | 20.9 | 62.8 | 35.6 |
| Conditions of Intense Evaporation | Method A | 4.3 | -- * | 14.3 |
| | 0.33°C | | | |
| | Method B | 10.2 | -- * | 34.6 |
| | Method A | 8.9 | -- * | 29.0 |
| | 0.67°C | | | |
| | Method B | 20.1 | -- * | 66.0 |

*Surface heat exchange changes from a net loss to a net gain to the ocean.

Table III
Summary of Results of Heat Conservation Model Computations

| | | | Maximum heat loss (cal/cm$^2$) | Maximum temperature change (°C) | P: Area within which heat losses exceed diurnal (km$^2$) fluctuation after 6 hr | Q: Area within which heat losses exceed diurnal fluctuation at complete equilibrium (km$^2$) | R: Area beyond which $Q_{net}$ always exceeds heat losses (km$^2$) |
|---|---|---|---|---|---|---|---|
| 100 MW | Summer | Advection | 920 | 0.24 | 3.5 | 3.5 | 54 |
| | | Slack water | 1280 | 0.33 | 6.3 | 11 | 30 |
| | Winter | Advection | 750 | 0.08 | 12 | 28 | 200* |
| | | Slack water | 1000 | 0.10 | 10 | 21 | 285* |
| 240 MW | Summer | Advection | 2120 | 0.54 | 20 | 42 | 100 |

*During winter, beyond this area, heat losses due to the cold water discharge are always less than the heat losses due to the negative surface heat exchange.

Table IV
Nutrient (Phosphates) and Plankton Concentration in the Vicinity of a 100 MW OTEC Plant Outfall as Predicted by the Biostimulation Model

| Distance from dis. point (m) | Estimated thickness of bio-stimulated layer (m) | Dilution | Nutrient concentration | | Estimated phytoplankton population | | Estimated herbivorous zooplankton population | |
|---|---|---|---|---|---|---|---|---|
| | | | micro-gm at/l phosphates | % increase over ambient | gm C/m$^3$ | % increase | gm C/m$^3$ | % increase |
| a) Within the plume | | | | | | | | |
| 50 | 9.4 | 1.59 | 1.942 | 1195 | - | - | - | - |
| 100 | 21.9 | 3.61 | 0.939 | 526 | 0.805 | 3400 | 0.208 | 1200 |
| 150 | 35.5 | 5.83 | 0.639 | 326 | 0,405 | 1661 | 0.117 | 631 |
| 200 | 52.5 | 8.15 | 0.500 | 233 | 0.235 | 922 | 0.082 | 412 |
| 250 | 69.5 | 10.28 | 0.427 | 185 | 0.180 | 683 | 0.070 | 338 |
| 275 | 75.7 | 11.35 | 0.401 | 167 | 0.155 | 574 | 0.064 | 300 |
| b) Circular area spreading radially (see Fig. 5) | | | | | | | | |
| 141.8 | 48.4 | 8.69 | 0.478 | 219 | 0.220 | 856 | 0.080 | 400 |
| 150 | 50.8 | 10.19 | 0.430 | 187 | 0.182 | 691 | 0.070 | 338 |
| 200 | 65.5 | 23.36 | 0.272 | 81 | 0.068 | 195 | 0.044 | 175 |
| 250 | 80.2 | 44.48 | 0.214 | 43 | 0.044 | 91 | 0.031 | 94 |
| 300 | 94.9 | 75.82 | 0.188 | 25 | 0.035 | 52 | 0.027 | 69 |
| 350 | 109.6 | 119.20 | 0.174 | 16 | 0.032 | 39 | 0.023 | 44 |
| 400 | 124.3 | 176.56 | 0.166 | 11 | 0.030 | 30 | 0.021 | 31 |
| 450 | 139.0 | 249.90 | 0.161 | 7 | 0.028 | 22 | 0.020 | 25 |
| 500 | 150.0 | 332.92 | 0.159 | 6 | 0.027 | 17 | 0.019 | 19 |
| 550 | 150.0 | 402.83 | 0.157 | 5 | 0.026 | 13 | 0.018 | 13 |
| 600 | 150.0 | 479.38 | 0.156 | 4 | 0.025 | 9 | 0.018 | 13 |

Table V
Nutrient (Phosphates) and Plankton Concentrations in the Vicinity of a 240 MW OTEC Plant Outfall as Predicted by the Biostimulation Model

| Distance from dis. point (m) | Estimated thickness of bio-stimulated layer (m) | Dilution | Nutrient concentration | | Estimated phytoplankton population | | Estimated herbivorous zooplankton population | |
|---|---|---|---|---|---|---|---|---|
| | | | micro-gm at/l phosphates | % increase over ambient | gm C/m$^3$ | % increase | gm C/m$^3$ | % increase |
| a) Within the plume | | | | | | | | |
| 50 | 10.4 | 1.13 | 2.672 | 1681 | - | - | - | - |
| 100 | 20.6 | 2.17 | 1.463 | 876 | - | - | - | - |
| 150 | 33.8 | 3.50 | 0.964 | 543 | 0.850 | 3596 | 0.163 | 919 |
| 200 | 48.3 | 4.98 | 0.722 | 382 | 0.514 | 2134 | 0.125 | 681 |
| 250 | 65.9 | 6.46 | 0.591 | 294 | 0.350 | 1422 | 0.098 | 512 |
| 300 | 84.5 | 7.85 | 0.513 | 242 | 0.272 | 1083 | 0.087 | 444 |
| 305 | 85.5 | 7.99 | 0.507 | 238 | 0.267 | 1061 | 0.085 | 431 |
| b) Circular area spreading radially (see Fig. 11) | | | | | | | | |
| 164.9 | 49.9 | 6.60 | 0.582 | 288 | 0.340 | 1378 | 0.096 | 500 |
| 200 | 60.2 | 11.71 | 0.393 | 162 | 0.152 | 561 | 0.061 | 281 |
| 250 | 74.9 | 22.78 | 0.275 | 83 | 0.070 | 204 | 0.042 | 163 |
| 300 | 89.6 | 39.23 | 0.223 | 48 | 0.047 | 104 | 0.036 | 125 |
| 350 | 104.3 | 62.17 | 0.196 | 31 | 0.036 | 56 | 0.028 | 75 |
| 400 | 119.0 | 91.10 | 0.181 | 21 | 0.033 | 43 | 0.025 | 56 |
| 450 | 133.7 | 131.74 | 0.172 | 14 | 0.031 | 35 | 0.022 | 38 |
| 500 | 148.4 | 180.51 | 0.166 | 11 | 0.030 | 30 | 0.021 | 31 |
| 550 | 150.0 | 220.78 | 0.163 | 9 | 0.029 | 26 | 0.020 | 25 |
| 600 | 150.0 | 262.74 | 0.161 | 7 | 0.028 | 22 | 0.020 | 25 |

# V. OCEAN ENGINEERING

E. A. SILVA, CHAIRMAN
*Ocean Facilities Program*
*Naval Facilities Engineering Command*

THIS PAGE

WAS INTENTIONALLY

LEFT BLANK

# DYNAMIC RESPONSE OF MOORED BODIES TO WAVE MOTION

C. J. GARRISON
*Naval Postgraduate School*
*Monterey, California*

ABSTRACT

This paper reviews the analytic procedures for calculation of the hydrodynamic coefficients and the dynamic response of large displacement floating bodies in waves. The hydrodynamic analysis is based on the source distribution, or Green's function, technique. The excitation forces and moments as well as added mass and damping coefficients are used together with the equations of motion to compute the dynamic response of the body to regular waves.

## INTRODUCTION

Ocean Thermal Energy Conversion(OTEC) plants will be either moored or dynamically positioned in the ocean and, therefore, will be subject to wind, wave and current loading. This paper deals with the motion of a large displacement body of arbitrary shape floating in waves and represents the first phase of a project to develop a computer program for calculation of the dynamic response of an OTEC plant. In this phase of the work the immersed surface is represented by a surface distribution of sources and this surface is assumed to have no appendages which are not represented by the surface source distribution. The large diameter cold water pipe which will bring up the cold water from the ocean floor on all OTEC plants is also disregarded in this initial phase.

Spar buoy, barge and semi-submersible configurations have been proposed as possible OTEC plant configurations. In all cases the immersed portion of the structures includes or is solely composed of a large displacement hull. Such surfaces tend not to be "two dimensional" and it is necessary to resort to a truly three-dimensional hydrodynamic analysis as developed herein.

In the present analysis attention is restricted to regular waves although actual ocean vessels are subject to wave spectra. This, however, is not an actual limitation of the analysis because linear theory is applied. That is, the result of the present analysis is a linear transfer function for the dynamic response per unit of wave height. The transfer function is then used in conjunction with a wave spectrum to determine the response spectrum from which certain statistical characteristics of the response can be determined.

## ANALYSIS

The analysis of the motion of floating bodies relies on the principle of superposition of linear solutions. The formal development begins with the assumption that the amplitude of the wave which excites the motion of the floating body is small, say of order $\epsilon$, and the resulting induced motion of the body is also of order $\epsilon$. The boundary-value problem is formulated with terms of $O(\epsilon^2)$ and above disregarded in comparison to terms of order $\epsilon$.

*Supported by Energy Research and Development Administration, Ocean Thermal Energy Conversion program.

The result of this linearization procedure shows that it is possible to deal with rather complex motion associated with wave interaction with a floating body which is at the same time responding in six degrees of freedom in a fairly simple way. Through linearization the complex problem under consideration can be decomposed and treated as the sum of seven separate problems: the fluid motion produced by (1) surge, (2) heave, (3) sway, (4) roll, (5) yaw and (6) pitch motion of the floating body, one degree of freedom at a time in otherwise still water and (7) the interaction of a regular wave with the restrained body. The analysis outlined follows that presented by Garrison (1-3).

The small amplitude periodic motion of the floating body may be described by,

$$X_j = R_e\left[X_j^o e^{-i\sigma t}\right], \quad j=1,2,\ldots 6 \tag{1}$$

where $X_j$ (j=1,2,3) denots the complex amplitude of the displacemnts in surge, heave and sway, and

$$X_j^o = a\theta_j^o \qquad j=4,5,6 \tag{2}$$

where a represents the characteristic dimension of the hull (generally the radius) and $\theta^o$ denotes the complex angular amplitudes of the motion in roll,yaw and pitch. The linear and angular displacement about the body axes $O(x',y',z')$ are noted in the definition sketch, Fig.1.

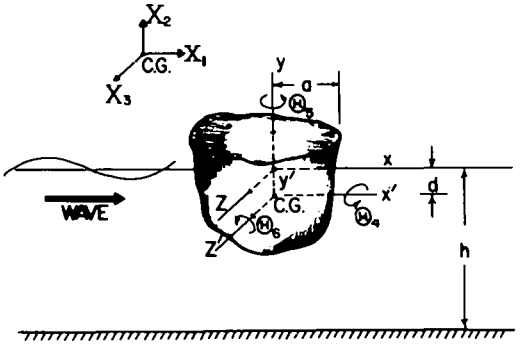



FIG.1 DEFINITIONS

The complex potential for wave interaction with the floating body is given by

$$\phi = \sum_{j=0}^{7} \phi_j \tag{3}$$

where $\phi_o$ = the complex potential associated with the incident wave and is given by,

$$\phi_o = -i \frac{gn^o}{\sigma} \frac{\cosh\left[k\ (h+y)\right]}{\cosh\ (kh)} e^{i(kx\cos\gamma + kz\ \sin\ \gamma)} \tag{4}$$

and $\phi_i$ (i=1,2,...6) denote the complex potentials associated with the six degrees of freedom of the body and $\phi_7$ denotes the complex potential associated with scattering of the incident waves by the restrained body. In Eq.(4) $k=2\pi/L$ where L denotes the wave length, $\sigma = 2\pi/T$ where T denotes the period and these two parameters are related through $\nu=\sigma^2/g=k\tanh(kh)$, in which h denotes the water depth. The space dependent part of the potentials are related to the velocity potentials according to

$$\Phi_j(x,y,z,t) = Re\left[\phi_j(x,y,z)e^{-i\sigma t}\right] \tag{5}$$

since the motion is assumed to be harmonic.

Each of the potentials must satisfy the Laplacian,

$$\nabla^2\phi_i = 0,\ i=0,1,2,....7 \tag{6}$$

the kinematic boundary condition on the bottom,

$$\frac{\partial\phi_i}{\partial y}(x,-h,0) = 0,\quad i=0,1,2,....7 \tag{7}$$

and the linearized free surface boundary condition,

$$\frac{\partial\phi_i}{\partial y}(x,0,z) - \frac{\sigma^2}{g}\phi_i(x,0,z) = ,\ i=0,1,2,....7 \tag{8}$$

On the surface of the body $\phi_i$ (i=1,2,....7) must satisfy kinematic boundary conditions. Linearization for small amplitude motion shows that it is sufficient to satisfy this boundary condition on the mean position of the hull when (i=1,2,...6) rather than on the exact instantaneous position. The kinematic boundary conditions to be satisfied on the immersed surface of the hull which is represented by S(x,y,z)=0 are:

$$\frac{\partial\phi_1}{\partial n} = g_1 = -i\sigma X_1^o n_x \tag{9a}$$

$$\frac{\partial\phi_2}{\partial n} = g_2 = -i\sigma X_2^o n_y \tag{9b}$$

$$\frac{\partial\phi_3}{\partial n} = g_3 = -i\sigma X_3^o n_z \tag{9c}$$

$$\frac{\partial\phi_4}{\partial n} = g_4 = -i\sigma\Theta_4^o\left[(d+y)n_z + zn_y\right] \tag{9d}$$

$$\frac{\partial\phi_5}{\partial n} = g_5 = -i\sigma\Theta_5^o\left[zn_x - xn_z\right] \tag{9e}$$

$$\frac{\partial\phi_6}{\partial n} = g_6 = i\sigma\Theta_6^o\left[xn_y - (d+y)n_x\right] \tag{9f}$$

$$\frac{\partial\phi_7}{\partial n} = g_7 = -\frac{\partial\phi_o}{\partial n} \frac{ign^o k}{\sigma\cosh(kh)}\left[n_y\sinh k(h+y)\right] + i(n_x\cos\gamma + n_z\sin\gamma)\cosh\left[k(h+y)\right]\Big] \tag{9g}$$

$$e^{i(kx\cos\gamma + kz\sin\gamma)}$$

in which $\vec{n} = i\vec{n}_x + j\vec{n}_y + k\vec{n}_z$ denotes the outward unit normal vector on $S(x,y,z)=0$ and d denotes the depth of submergence of the origin of the body axes which is located at the center of gravity of the body.

As a final condition on the solutions, the potentials $\phi_i$ (i=1,2,....7) must all represent radiated or outgoing waves and, therefore, must satisfy an appropriate radiation condition.

The solution to the boundary-value problems posed can be represented by the distribution of sources over the immersed surface,

$$\phi_k(x,y,z) = \frac{1}{4\pi}\iint_S f_k(\xi,\eta,\zeta)G(x,y,z;\xi,\eta,\zeta)dS \tag{10}$$

where G denotes the source potential (Green's function) and $f_k$ denotes the distribution strength function defined on the immersed surface.

The Green's function appropriate to the boundary value problem posed is given in two different forms by Wehausen and Laitone (4). One of these may be written

$$G = \frac{1}{R} + G^* \tag{11a}$$

where R represents the distance between the point $(\xi,\eta,\zeta)$ and the point (x,y,z), and G* denotes the regular function:

$$G^* = \frac{1}{R'} + 2P.V.\int_0^\infty \frac{(\mu+\nu)e^{-\mu h}\cosh\left[\mu(\eta+h)\right]\cosh\left[\mu(y+h)\right]Jo(\mu r)d\mu}{\mu\ \sinh(\mu h) - \nu\cosh(\mu h)} + i\,\frac{2\pi(k^2-\nu^2)\cosh\left[k(\eta+h)\right]\cosh\left[k(y+h)\right]}{k^2h-\nu^2h+\nu}\,Jo(kr) \tag{11b}$$

where

$$R' = \left[(x-\xi)^2 + (y+2h+\eta)^2 + (z-\zeta)^2\right]^{\frac{1}{2}} \tag{11c}$$

$$r = \left[(x-\xi)^2 + (z-\zeta)^2\right]^{\frac{1}{2}} \tag{11d}$$

P.V. denotes principal value of the integral. Faltinsen and Michelsen (5) have rearranged Eq. (11b) for purposes of improving the procedure of numerical evaluation. For details of the numerical evaluation of Eq. (11) and the alternate form proposed by Faltinsen and Michelsen as well as a third, series form of the Green's function the reader is referred to Ref.(6).

The expression for $\phi_k$ given by Eq. (10) has the property that it satisfies the boundary-value problem except for the kinematic boundary condition, Eq. (9). When this condition is applied the integral equation,

$$-f_k(x,y,z) + \frac{1}{2\pi}\iint_S f(\xi,\eta,\zeta)\frac{\partial G}{\partial n}(x,y,z;\xi,\eta,\zeta)dS = 2g_k(x,y,z), k=1,2,....7 \tag{12}$$

is otained

:e (x,y,z) denotes points on S(x,y,z) = 0 and n
:tes distance measured normal to the hull in the
:ard normal direction.

At this juncture it is necessary to discretize the problem in order to solve the integral equation. The surface S(x,y,z) = 0 is subdivided into, say N, quadralateral panels and over each panel the source strength function $f(\xi,\eta,\zeta)$ is taken to be constant. This results in the indicial equation,

$$-f_{k_i} + \alpha_{ij} f_{k_i} = 2g_{k_i}, \quad \begin{matrix} k=1,2,....7 \\ i,j=1.2,..N \end{matrix} \tag{14}$$

where the subscripts i and j denote the centroids of the i-th and j-th panels, respectively. After Eq.(14) has been solved for the vector $f_k$ the potential at the point i is given by converting the integral in Eq. (10) to the sum,

$$\phi_{k_i} = \beta_{ij} f_{k_j}, \quad \begin{matrix} k=1,2,....7 \\ i,j=1,2,..N \end{matrix} \tag{15}$$

In Eqs.(14) and (15) $\alpha$ and $\beta$ are defined as

$$\alpha_{ij} = \frac{1}{2\pi}\iint_{\Delta S_j} \frac{\partial G}{\partial n}(x_i,y_i,z_i;\xi,\eta,\zeta)dS \tag{16}$$

$$\beta_{ij} = \frac{1}{4\pi}\int_{\Delta S_j} G(x_i,y_i,z_i;\xi,\eta,\zeta)dS \tag{17}$$

The numerical evaluation of $\alpha_{ij}$ and $\beta_{ij}$ have been discussed in some detail in Ref. (6) and will not be discussed further here.

The linearized form of Bernoulli's equation gives the dynamic pressure on the immersed surface in terms of $\phi_k$ according to

$$P_k = \rho\sigma Re\left[i\,\phi\, e^{-i\sigma t}\right], \quad k=1,2,...6 \tag{18}$$

$$P_{o7} = \rho\sigma Re\left[i\,(\phi_o + \phi_7)\, e^{-i\sigma t}\right] \tag{19}$$

where $P_{o7}$ denotes the pressure associated with the wave interaction with the body held fixed.

The forces and moments casued by the dynamic fluid pressure acting on the immersed surface are determined from the surface integrals,

$$F_{ij}(t) = -\iint_S P_j h_i\, dS, \quad i,j=1,2,...6 \tag{20}$$

$$F_i(t) = -\iint_S P_{o7} h_i\, dS, \quad i=1,2,...6 \tag{21}$$

where $F_i$ denotes the i-th component of wave excitation force or moment arising from the j-th component of body motion. The functions $h_i$ are

$$\begin{aligned} &h_1 = n_x, \; h_2 = n_y, \; h_3 = n_z \\ &h_4 = (d+y)n_z - zn_y, \; h_5 = zn_x - xn_z, \; h_6 = xn_y - (d+y)n_x \end{aligned} \tag{22}$$

The excitation force and moment coefficients, respectively, may be represented by the complex coefficients,

$$\begin{aligned} C_j &= \frac{F_{j(max)}\, e^{i\delta_j}}{\rho g a^3 \eta_o}, \quad j=1,2,3 \\ C_j &= \frac{F_{j(max)}\, e^{i\delta_j}}{\rho g a^4 \eta_o}, \quad j=4,5,6 \end{aligned} \tag{23}$$

where $\delta_j$ denotes the phase shift of the force or moment with respect to the crest of the incident wave. A positive value of $\delta_j$ denotes lag.

In the case of the forces and moments due to the motion of the hull it is more common to describe the hydrodynamic loads in terms of added mass and damping coefficients:

$$-M_{ij} - iN_{ij} = \frac{F_{ij(max)}\, e^{i\delta_{ij}}}{\rho\sigma^2 a^3 X_j^o} \quad \begin{cases} i=1,2,3 \\ j=1,2,...6 \end{cases} \tag{24}$$

$$-M_{ij} - iN_{ij} = \frac{F_{ij(max)} e^{i\delta_{ij}}}{\rho\sigma a^4 X_j^o}, \quad \begin{cases} i=4,5,6 \\ j=1,2,...6 \end{cases}$$

where $M_{ij}$ and $N_{ij}$ denote the added mass and damping tensors, respectively.

The linearized equations of motion for the floating body for small amplitude motion written with respect to the centrodal axes are given by

$$\sum_{j=1}^{6}\left[-\nu(m_{ij}+M_{ij}) - i\nu N_{ij} + (K'_{ij}+K_{ij})\right]\frac{X_j^o}{\eta_o} = |C_i|e^{i\delta_i} \tag{25}$$

where

$$\nu = \sigma^2 a/g \tag{26}$$

$$\left.\begin{aligned} m_{ij} &= \begin{cases} 0, & i\neq j, \quad i,j=1,2,3 \\ \text{body mass}/\rho a^3, & i=j, \quad i,j=1,2,3 \end{cases} \\ m_{ij} &= -\int_m \frac{x'_{i-3}\, x'_{j-3}\, dm}{\rho a^5} \qquad i,j=4,5,6 \\ m_{ii} &= \int_m \frac{(x'_{i-3})^2\, dm}{\rho a^5} \qquad i=4,5,6 \end{aligned}\right] \tag{27}$$

and $x'_1 = x'$, $x'_2 = y'$, $x'_3 = z'$. The coefficients, $K_{ij}$ represent dimensionless force and moment coefficients associated with displacement of the body from its equilibrium position. These displacement coefficients result from the sum of the effect of the mooring lines and hydrostatic (or buoyant) loads. These coefficients are defined as

$$\left.\begin{aligned} K_{ij} &= \frac{\Delta i\text{-th force component}/\rho g a^3}{\Delta X_j}, \quad \begin{matrix} i=1,2,3 \\ j=1,2,...6 \end{matrix} \\ K_{ij} &= \frac{\Delta i\text{-th moment component}/\rho g a_4}{\Delta X_j}, \quad \begin{matrix} i=4,5,6 \\ j=1,2,...6 \end{matrix} \end{aligned}\right] \tag{28}$$

where the "delta" force or moments are those due to the mooring lines plus hydrostatic effect. In Eq. (25) $\eta^o$ is taken to be real, i.e., the surface elevation at x=z=0 is

$$\eta = \eta^o \cos(\sigma t)$$

and, therefore, all phase shift angles are measured with respect to the wave crest, positive values indicating lag. The phase shift angle, $\Psi_j$, is defined by $X_j^o = |X^o| e^{i\Psi_j}$.

## NUMERICAL RESULTS

The hydrodynamic coefficients as well as the resulting dynamic response has been computed for several example configurations. A fairly extensive set of results have been carried out for a rectangular 90m by 90m barge with a draft of 40m. This configuration was also studied by Faltinsen and Michelsen (5) and represents one of the few sources of experimental data for barge configurations. Results have been computed for two different subdivisions, 48 and 108 total source panels on the immersed surface.

The surge and heave excitation forces are shown in Figure 2 and 3, respectively. The fact that there is very little difference between the two sets of results corresponding to the 48 and 108 panel models indicates that the solution tends to converge very rapidly with increasing the number of panels. However, slower convergence should be expected at small periods.

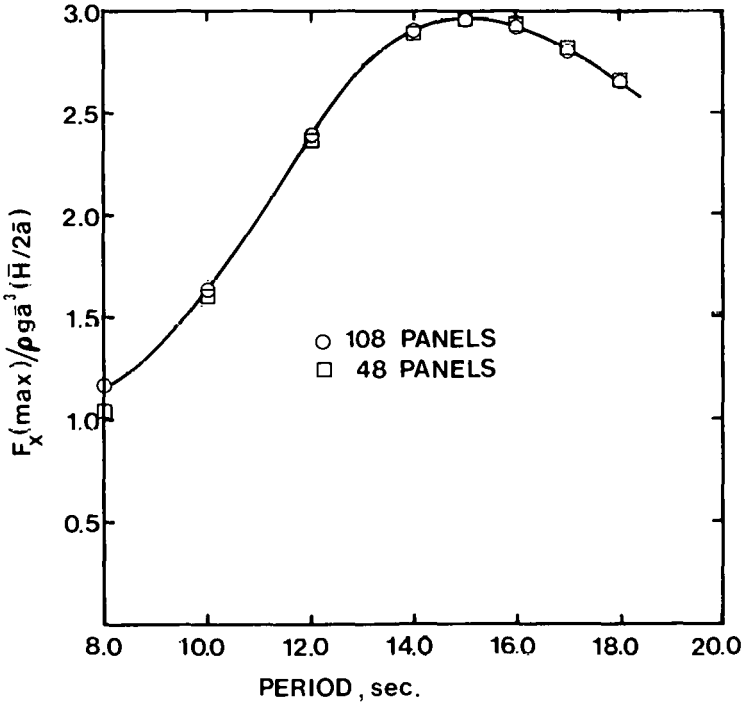



FIG.2 HORIZONTAL FORCE COEFFICIENT
(90m x 90m x 40m, Infinite Depth)

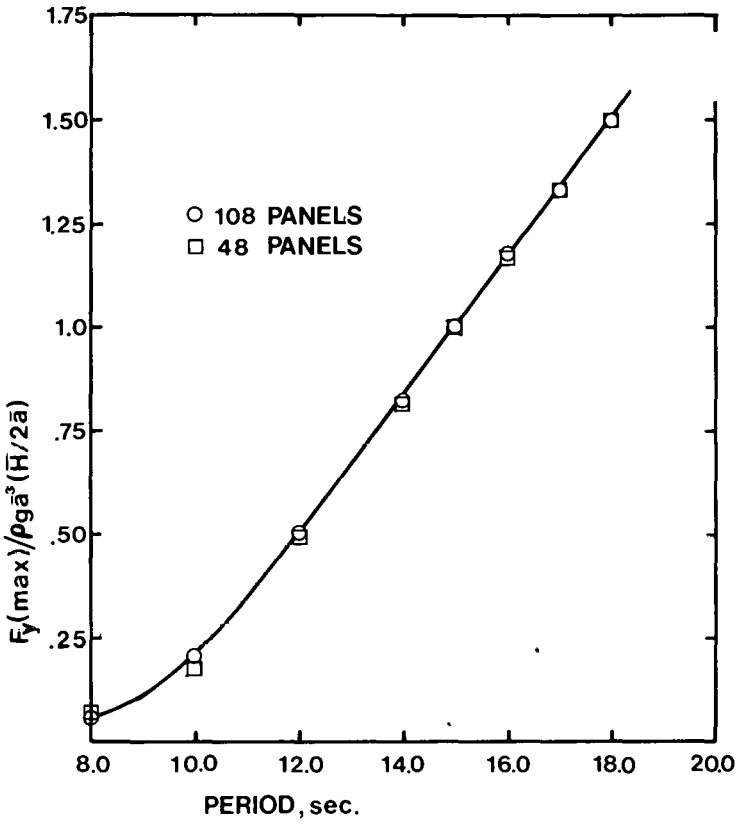



FIG.3 VERTICAL FORCE COEFFICIENT
(90m x 90m x 40m, Infinite Depth)

The pitch excitation moment about an axis through the c.g. was also computed. However, as it turned out in this particular case, the moment was extremely small and was masked by the "noise" caused by numerical error. For all practical purposes the pitch excitation moment was zero.

The surge added mass coefficient is shown in Fig. 4 and, here again, the results corresponding to 48 and 108 panels indicate that the solution has converged. The experimental results presented for comparison appear to agree well with the theory.

The corresponding damping coefficient in surge is shown in Fig. 5. These results are typical of most damping results. At high-frequency and low-frequency oscillation the wave-making damping tends to vanish since no waves are generated at the two extremes. In the intermediate frequency range, however, the wave-making ability reaches a maximum and the damping coefficient likewise shows a maximum. Although the scatter of the experimental results is fairly large the general agreement with the theory is quite good.

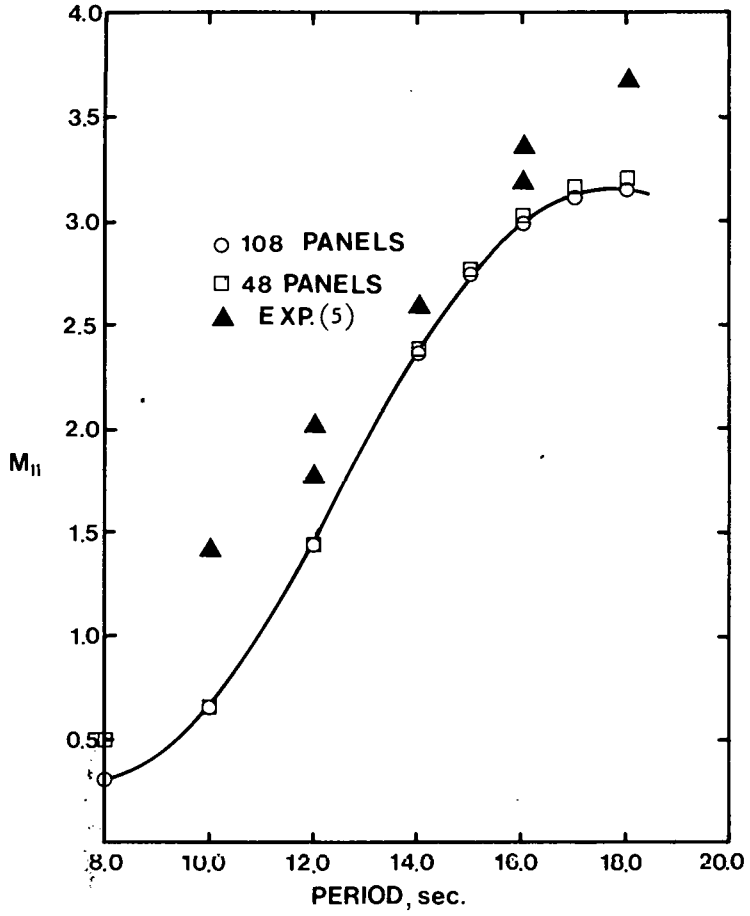



FIG.4 SURGE ADDED MASS COEFFICIENTS
(90m x 90m x 40m, Infinite Depth)

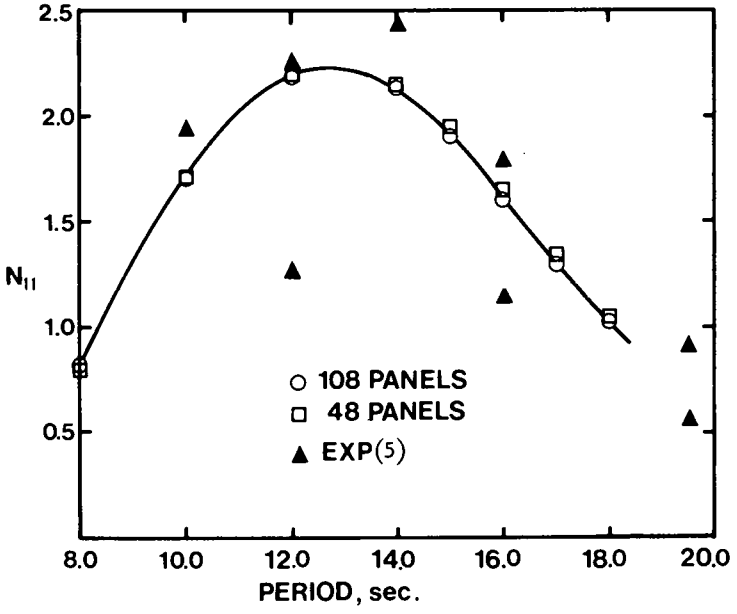



FIG.5 SURGE DAMPING COEFFICIENT
(90m x 90m x 40m, Infinite Depth)

The heave added mass coefficient, $M_{22}$, is shown in Fig.6 along with experimental values. These results show very little frequency dependence, particularly when compared to the surge damping coefficient, $N_{11}$. This results from the fact that the surface primarily involved in heave force is the bottom and this surface is fairly distant from the free surface. Thus, free surface effects which are frequency dependent are not pronounced in the case of heave motion whereas they are much more pronounced in the case of surge where surfaces near the free surface are involved.

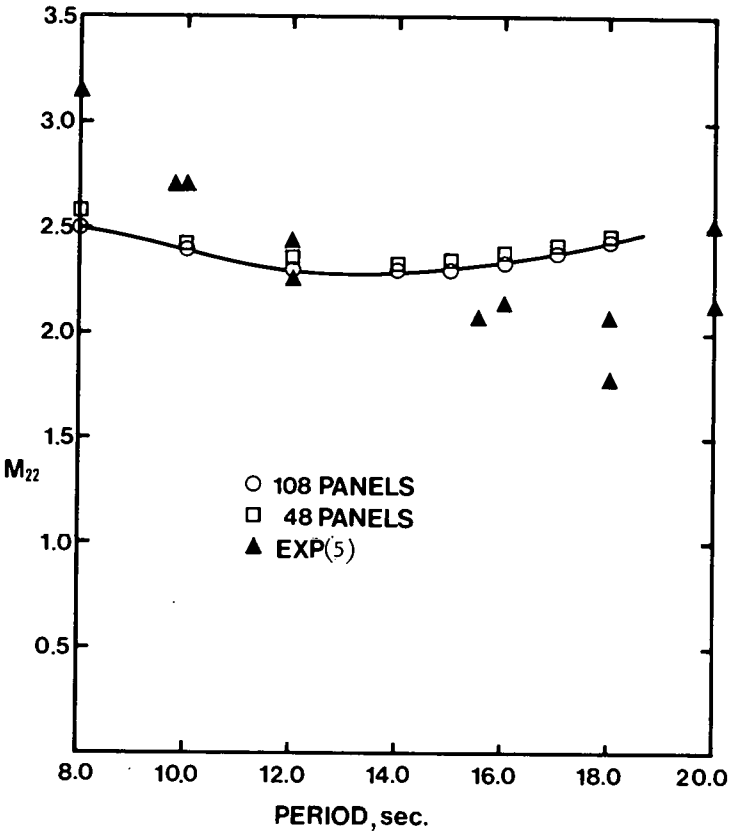



FIG.6 HEAVE ADDED MASS COEFFICIENT
(90m x 90m x 40m, Infinite Depth)

The computed heave damping coefficient is shown in Fig. 7 along with experimental values. It is interesting to note that compared to the surge damping coefficient the heave damping coefficient is rather small. This results from the fact that the bottom surface which acts as the primary wave-maker in heave is rather well-removed from the free surface and is, therefore, not too effective in generating waves and resulting damping.

It is also of interest to note that the experimental values of $N_{22}$ fall well above the theoretical results. This difference is attributed to viscous damping and appears to be pronounced in a relative sense because the computed wave-making damping is small.

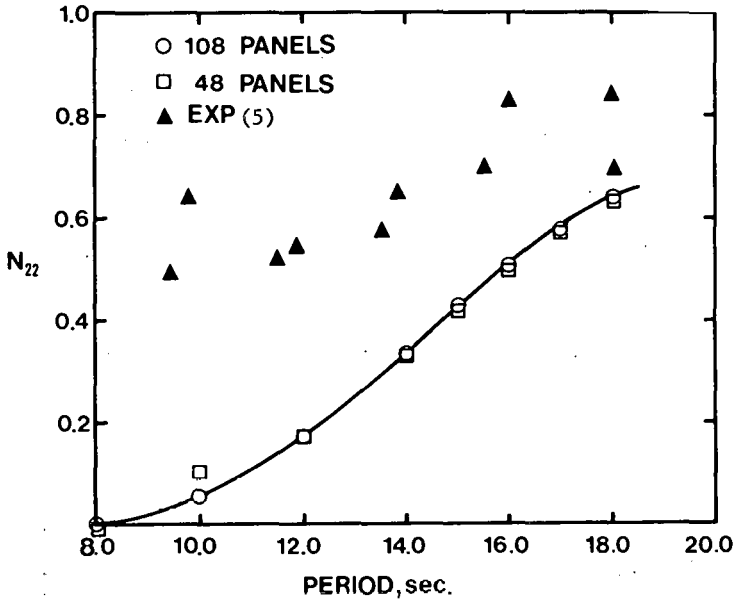



FIG. 7 HEAVE DAMPING COEFFICIENT
(90m x 90m x 40m, Infinite Depth)

The added moment of inertia coefficient shown in Fig. 8 is essentially independent of frequency (period). This appears to be typical of all results associated with floating caissons of the type in question. Moreover, the damping coefficient in pitch, $N_{66}$, which is not plotted, tends to be extremely small. These two features result from the fact that frequency dependence and damping is a result of wave production and very little wave generation occurs as a result of pitching motion. This is due to the fact that the bottom surface is far removed from the free surface and the vertical sides do not move in the normal direction appreciably as a result of pitching motion.

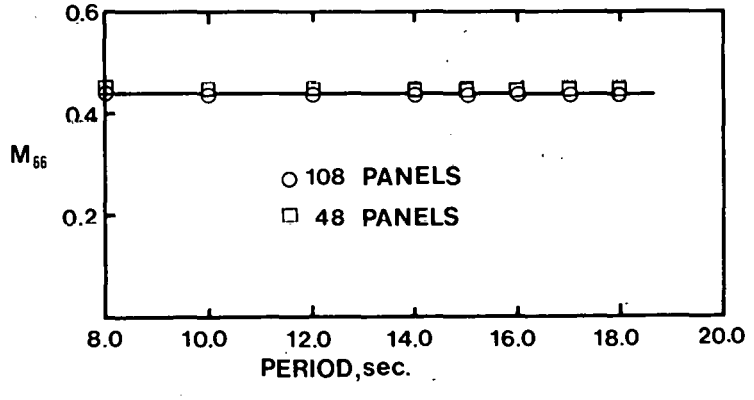



FIG. 8 PITCH ADDED MOMENT OF INERTIA COEFFICIENT
(90m x 90m x 40m, Infinite Depth)

The added mass coefficient in yaw, $M_{55}$, is shown in Fig. 9 along with experimental results. The agreement here appears to be generally good although the experimental data appears to possess considerable scatter.

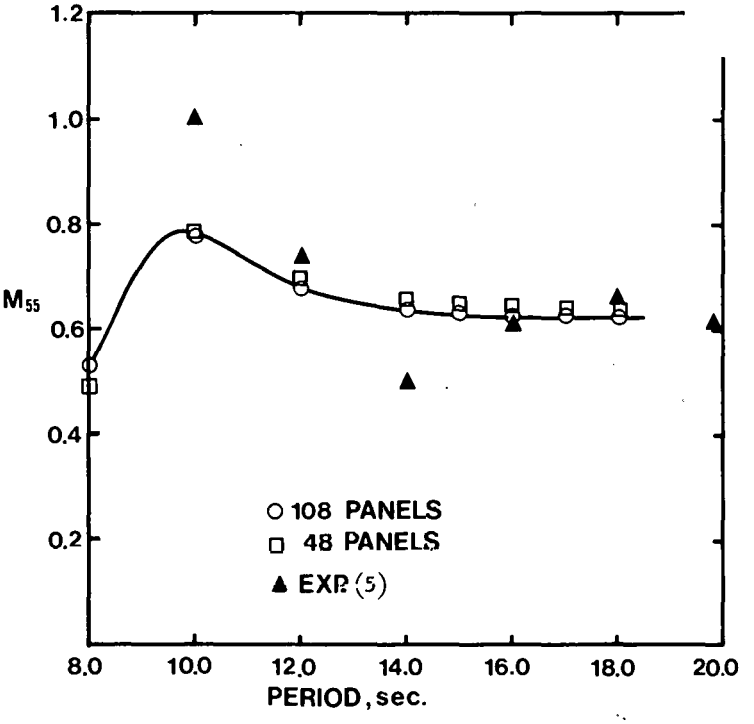



FIG. 9 YAW ADDED MASS COEFFICIENT
(90m x 90m x 40m, Infinite Depth)

Finally, the dynamic response of the box free-floating in waves is shown in Fig. 10. The pitch response, $\theta_6^o/(H/2a)$, is extremely small as was expected in view of small excitation moment. The resonance frequency in heave occurs at about 16.5 seconds period and, therefore, considerable dynamic amplification occurs. In the case of the heave response several experimental values are shown which tend to agree well with the theory.

Calculations have been made to compare with the wave channel test results of Kim, Henry and Chou (7) for a shallow-draft barge of 1.704 feet beam, by 2.558 feet length, by 0.16 feet draft. The location of the center of gravity and pitch gyradius is shown in Fig. 11.

The theoretical heave and pitch response is compared with the experimental values in Fig. 12. The results show excellent agreement between theory and experiment for the case of heave motion. This apparently results from the fact that the wave-making damping in heave for a shallow-draft barge is substantial and, therefore, the heave results are not too sensitive to the unaccounted for viscous damping.

The pitch results also show fairly good agreement. While there appears to be some scatter in the pitch results it appears that near resonance the experimental

values of the response fall below the theory. Here again, this is attributed to viscous effects which end to be significant compared to the rather small mount of wave-making damping in pitch.

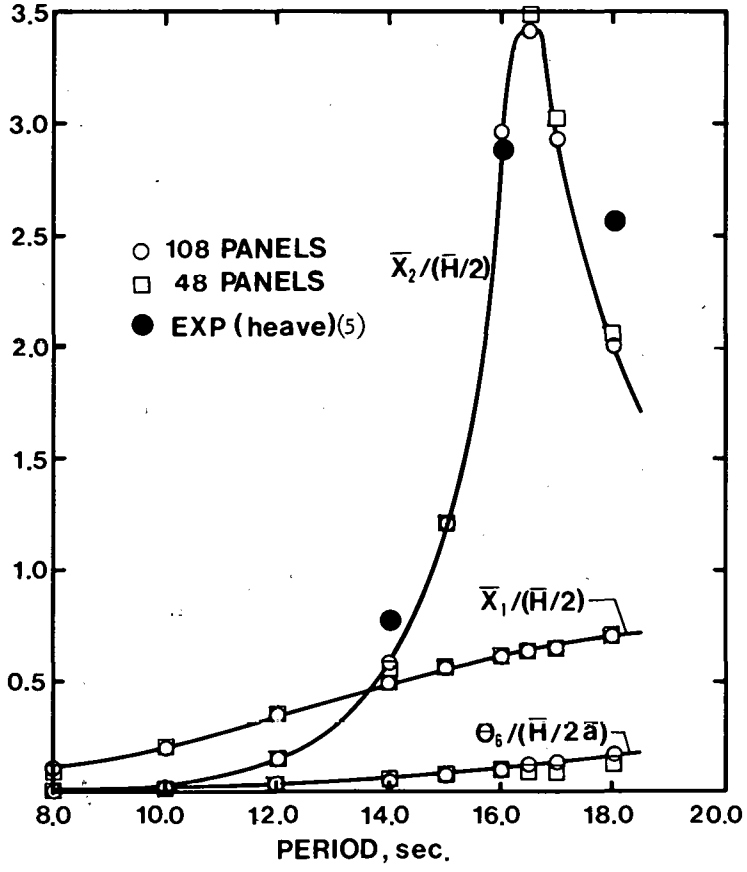



FIG. 10 SURGE, HEAVE AND PITCH RESPONSE
(90m x 90m x 40m, Infinite Depth)

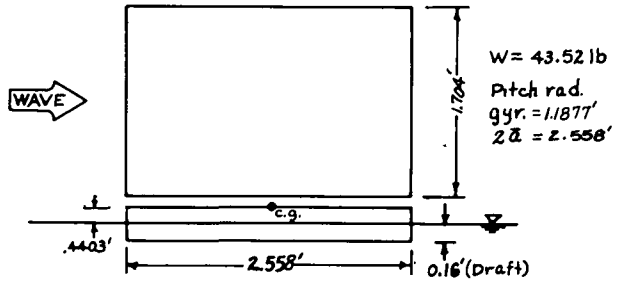



FIG. 11 SHALLOW DRAFT BARGE

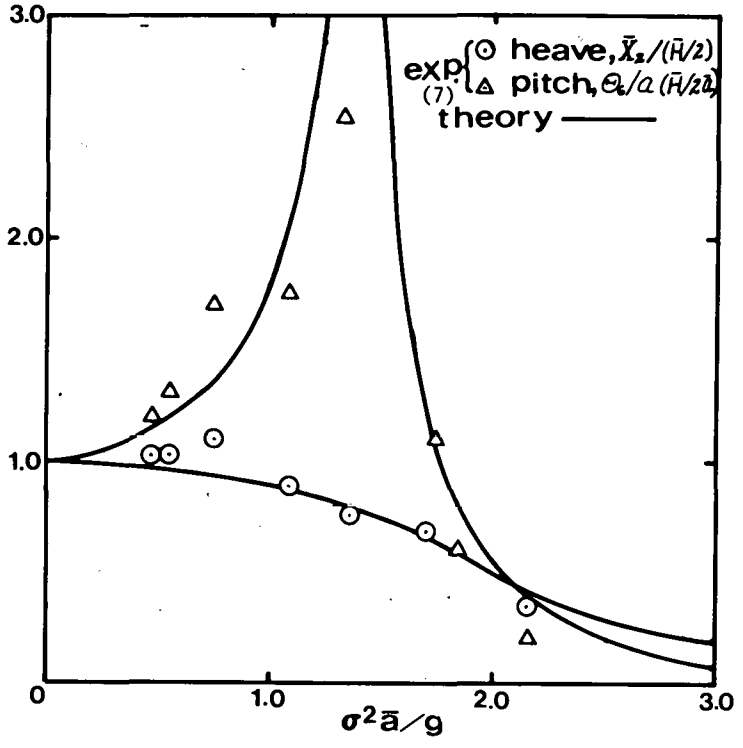



FIG. 12 HEAVE & PITCH RESPONSE OF A SHALLOW-DRAFT BARGE, DEEP WATER

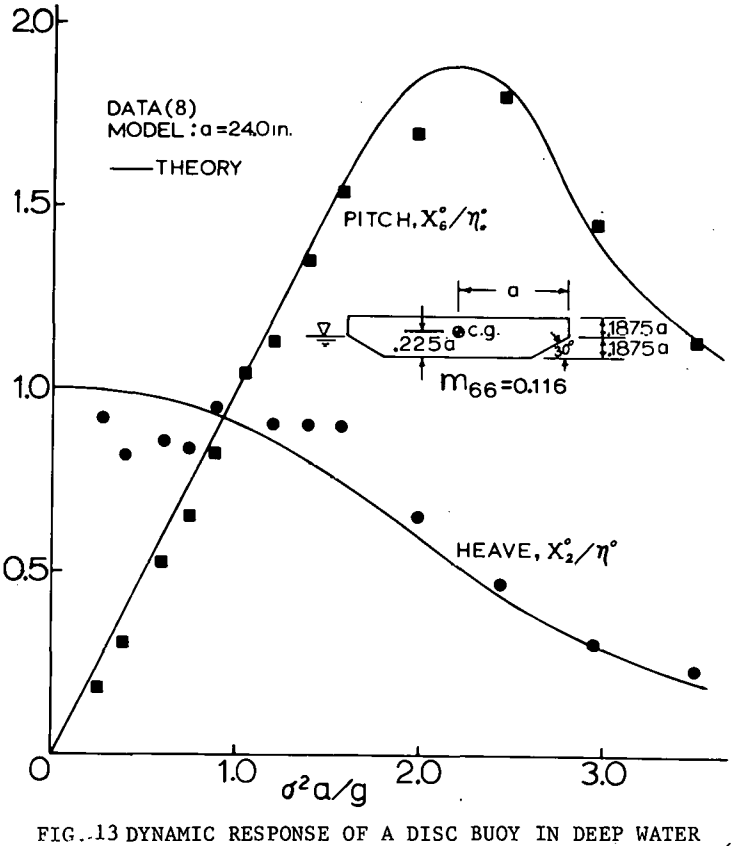



FIG. 13 DYNAMIC RESPONSE OF A DISC BUOY IN DEEP WATER

As a further example, the dynamic heave and pitch response for a rather shallow-draft disc buoy is shown in Figure 13. Unlike some of the previous results the pitch response as well as the heave response shows excellent agreement between the theory and experiment. This is likely due to the fact that the corners on the buoy configuration are beveled rather than sharp. This probably reduces the separation and resulting viscous damping. Consequently, the experimental results are in good agreement with calculations.

## CONCLUSIONS

An analysis based on linear theory and the use of Green's function has been outlined for determination of the hydrodynamic coefficients of large three-dimensional floating bodies. These hydrodynamic coefficients are used in conjunction with the linear equations of motion for a floating body to determine the dynamic response. Comparisons of the theory with experimental results for barge configurations indicates generally good agreement although in some instances, particularly near resonance, it appears that consideration of viscous may be necessary.

## REFERENCES


1. Garrison, C.J.,"Dynamic Response of Floating Bodies", Proc. Offshore Technology Conference, Paper No. OTC 2067, May 1974.

2. Garrison, C.J.,"Hydrodynamics of Large Objects i the Sea," Part I-Hydrodynamic Analysis," J. of Hydronautics, Vol.8, Jan. 1974.

3. Garrison,C.J.;"Hydrodynamics of Large Objects in the Sea,Part II-Motion of Free-Floating Bodies," J. of Hydronautics, Vol.9, April, 1975.

4. Wehausen,J.V. and Laitone,E.V.,"Surface Waves," Encyclopedia of Physics, Vol.9, Springer-Verlag, Berlin, 1960.

5. Faltinsen,O.M. and Michelsen,F.C.,"Motion of Large Structures in Waves at Zero Froude Number," The Dynamics of Marine Vehicles and Structures in Waves, Paper No.11, The Institution of Mechanical Engineers. July, 1974.

6. Garrison,C.J.,"Hydrodynamic Loading of Large Offshore Structures", Proc. International Symposium in Numerical Methods in Offshore Engineering, U. of Swansea, Wales, U.K., Jan. 1977.

7. Kim,C.H., Henry,C.J. and Chow,F.,"Hydrodynamic Characteristics of Prismatic Barges," Offshore Technology Conference, Paper No. 1417, 1971.

8. Hoffman, D.,Geller,E.S. and Niederman,C.S., "Mathematical Simulation and Model Tests in the Design of Data Buoys," SNAME,presented at the Annual Meeting, New York, N.Y., Nov. 15-17, 1973.

# SOME FACTORS AFFECTING THE SELECTION OF OTEC PLANT PLATFORM/COLD WATER PIPE DESIGNS

RODERICK A. BARR AND PIN YU CHANG
*HYDRONAUTICS, Incorporated*
*7210 Pindell School Road*
*Laurel, Maryland*

ABSTRACT

This paper discusses factors having an important influence on the selection of platform and cold water pipe designs for OTEC plants. A number of platform types have and are being considered for OTEC use, ranging from a ship or barge form to a semi-submersible to a submarine. In selecting the best type of platform for a given OTEC plant design and operating site, attention must be paid to these factors and to the interactions between the platform and cold water pipe.

## INTRODUCTION

This paper discusses many of the factors influencing the selection of the best platform and cold water pipe or CWP designs for a ocean thermal energy conversion or OTEC plant design. The paper has two purposes. The first is to provide a more comprehensive discussion than is currently available on the factors influencing selection of platform type. The second is to more widely disseminate results of two studies carried out for the U.S. Energy Research and Development Administration (ERDA) by HYDRONAUTICS. Results of these studies, which are described in detail in References 1 and 2, are highlighted in Appendices A, B and C.

Reference 1 describes five generic types of platforms proposed for OTEC plant use. These five can be described as ship or barge, submarine, semi-submersible, disc and spar. In addition to these five, the tuned sphere platform, which is described in Reference 3, will soon be considered for OTEC use. While work over the past few years has indicated that some platforms appear most attractive, and some least attractive, each platform type has unique advantages and disadvantages.

In general the best combined platform/CWP design will be the one which can meet all minimum design requirements and which will result in the lowest cost for OTEC plant product (electricity, ammonia, aluminum, etc.). The actual selection is therefore made largely on economic consideration. Such considerations are beyond the scope of this paper, which emphasizes the factors which affect plant performance and cost, and hence cost is discussed briefly only in a few areas.

## FACTORS AFFECTING SELECTION OF PLATFORM/CWP DESIGN

A large number of factors will influence the selection of the best platform/CWP design for an OTEC plant. These factors will, depending on OTEC plant size and operating environment, assume different relative importance. In addition to operating site and environment (waves, wind and current) the following factors are expected to be most important

- CWP loads and stresses due to motions and current
- Platform and CWP seaway induced motions
- Mooring, stationkeeping or grazing forces and power requirements
- Transit to operating site and CWP deployment
- Platform static and damage stability
- Platform and CWP materials and weight
- OTEC plant arrangements and accessibility
- Ease of platform construction (constructability)

The impact of these various factors on selection and design of platform and CWP is highlighted in this section. Quantitative results in the first three areas, from References 1, and 2, are presented in Appendices A, B and C.

Influence of Site and Environmental Conditions - The OTEC plant operating site and environment will have a dominant effect on many of the factors affecting platform and CWP design. Table 1 indicates typical relative influences of ocean waves and current and wind on the factors sensitive to the environment (+, 0 and - indicate large, moderate and insignificant sensitivity respectively). The magnitudes of these influences will depend on the relative magnitude of wave heights, current velocity and distribution and wind velocity.

Table 1

Influence of Environment on Various Factors Affecting Platform and CWP Design

| Factor/Environment | Waves | Current | Wind |
|---|---|---|---|
| CWP Loads and Stresses | + | + | 0 |
| Motions and Acceleration | + | 0 | - |
| Mooring/Stationkeeping | + | + | + |
| Transit to Site | 0 | - | 0 |
| CWP Deployment | + | + | 0 |
| Stability and Safety | + | - | + |

For operating sites where extreme wave heights or sea states occur, even if rarely, CWP loads and structural design will probably be dominated by seaway (ocean wave) induced platform/CWP motions. This is particularly true for large CWP diameters. Mooring and stationkeeping requirements will usually be determined by current for sites such as the Florida Straits, where large currents occur. Beam wind and wave induced roll motions will have a significant influence on safety, particularly when platform stability is reduced by platform damage and flooding.

The expected average and extreme environmental con-

ditions for the given site should be considered carefully in assessing the influence of these factors and in selecting the best platform/CWP design.

Interrelationship Between Platform and CWP Designs - It will generally not be possible to select the best type of platform for a given OTEC plant design without considering CWP design. Platform and CWP motions and accelerations and resulting CWP loads and structure are very sensitive to relative platform and CWP geometries. In particular, the selection of platform type can be significantly affected by CWP length and platform/CWP attachment characteristics (stiffness, damping, etc.) and CWP structure (wall thickness, stiffeners, etc.) will be determined largely by the choice of platform type.

CWP Loads and Structural Design Requirements - The fabrication and installation of a structurally adequate CWP is certain to be one of the most difficult problems facing OTEC plant designers. The CWP must be designed not only to withstand the largest single load occuring during its lifetime but must have adequate fatigue strength to survive 30 to 40 years of cyclic loading due to ocean waves. Using an average wave period of 10 seconds, a CWP will be subject to about $10^8$ load cycles during its lifetime. The strength of most materials in seawater is highly dependent on the load history for such large number of cycles, as described in Reference 2.

Methods for the structural analysis and design of the CWP, which take into account various loadings and failure modes, are described in detail in Reference 2. Appendix B provides a summary of some results in Reference 2 and provides some more recent calculated results. To date the methods of Reference 2 have not been used to carry out the detailed design of a CWP for a given application, although much of this work is being used in current studies of CWP structural design for OTEC ONE (EOTP-1).

Seaway induced CWP loads, which will usually be the dominant factor in determining CWP structural design, can vary greatly with platform type, as discussed in Appendix A. The choice of platform type will be limited to those platforms which result in structurally acceptable CWP's. For operating sites with large surface currents, platforms where the platform/CWP attachment is deeply submerged, such as the spar or submarine, will offer an advantage due to reduced current induced CWP loads.

Platform/CWP Motions and Accelerations - Excessive motions and accelerations can result in cessation of plant operation, reduced crew effectiveness, inefficient operation of or damage to heat exchangers or other power plant components and excessive CWP loads. In general it will be accelerations rather than motions which will be important. This is perhaps fortunate, as accelerations generally increase much more slowly than motions with increasing wave height or sea state. This is shown by results presented in Reference 1.

It seems likely that inefficient operation of or damage to heat exchangers and excessive CWP loads will be most sensitive to acceleration and will determine allowable operating platform accelerations. Data do not appear to exist for allowable accelerations for proposed OTEC heat exchangers. The detailed design of the plant components will determine if these components are most sensitive to vertical or horizontal accelerations.

Table 2 presents calculated vertical (heave) and horizontal (surge) accelerations for the five platform types considered in Reference 1. These results are for the 500MW baseline platforms of Reference 1 and for sea state seven (40 foot significant wave height) and long-crested (unidirectional) waves.

Table 2

Calculated Platform Accelerations for 500MW (500,000 long ton) Platforms in Sea State Seven

| Platform Type | Acceleration-Ft/Sec[a] | |
|---|---|---|
| | Vertical | Horizontal |
| Ship | 3.4 | 1.0 |
| Submarine | 1.2 | 0.4 |
| Semi-Submersible | 0.6 | 0.4 |
| Disc | 2.9 | 1.2 |
| Spar | 0.8 | 0.7 |

A number of studies of the effect of accelerations on human effectiveness exist. Reference 4 presents a recent summary of human tolerance data. Available data indicate that human tolerance is significantly less for horizontal accelerations than for vertical accelerations, and that tolerance is affected by frequency of motion. Human tolerance should not be overlooked in selecting platform type.

Mooring and Stationkeeping Loads - Mooring or stationkeeping systems can represent a major component of plant cost for plants operating in regions of significant current, waves and/or wind. For platforms that are "hard wired" to shore, the mooring or stationkeeping system must maintain the platform within a limited area, whose radius may be, typically, five to 20 percent of water depth. For platforms generating a product such as ammonia, the platform is required only to stay within a general or known area. Plants operating in specific sites such as the Florida Straits, even if dynamically positioned, will probably have to remain within an area whose radius is a few miles, while plants operating in areas such as the Atlantic Equitorial region can drift for tens or more of miles in the low current velocities typical of such areas.

In areas of high current flow, the current will help to insure a continual supply of fresh warm water. For areas of low current flow, it may be necessary for the platform to graze or to be propelled at speeds of one-half to one knot to insure this supply of fresh warm water. In a current such as the Gulf Stream, with a four knot surface current velocity, a free floating platform will drift at a speed of about one knot (see Reference 1). Appendix C discusses mooring or stationkeeping forces due to typical currents and propulsion forces required for grazing. Reference 1 discusses resultant propulsion powers required for stationkeeping or grazing. Reference 5 discusses mooring requirements.

Transit to Station - It is assumed that the OTEC plant will be moved from the building site to the operating e, or perhaps from one to another operating site, with- the CWP deployed. In this case the towing resistance or the platform will be highly dependent on the platform type and geometry, as described in Reference 1. When the distance between sites is large (as between a U.S. building site and an equitorial region) the transit cost may not be insignificant.

The data of Reference 1 can be used to estimate the cost of towing various platforms without CWP deployed. Consider, as an example, towing of a ship type platform at four knots and a semi-submersible platform at three knots for a distance of 4000 nautical miles. One and three 7500 to 10,000 horsepower tugs will be required for the ship and semi platforms, respectively. The estimated towing costs are about $500,000 and $2,200,000 for the ship and semi, respectively.

Cold Water Pipe Deployment - The primary factors affecting the difficulty and cost of CWP deployment, besides CWP length and diameter, are CWP weight per unit length and motions of the platform alone or with partically deployed CWP in moderate seas when deployment must occur. For very heavy CWP sections, as required by large seaway induced CWP loads, it may be necessary to use a separate crane barge for deployment, at significant additional cost. Unfortunately the effect on CWP design and motions on deployment cannot be quantified at present.

Plant Intact and Damaged Stability - Precedent exists for establishing intact and damaged stability requirements for drilling platforms, as described in References 6, 7 and 8. Intact stability criteria for OTEC plants are likely to be developed from these sources and will no doubt be based on platform ability to withstand a given wind velocity with a residual margin of righting moment. This ability is usually defined quantitatively in terms of areas under the righting moment curve and the wind heeling moment curve. Survival conditions for all types of drilling platforms are usually defined by 100 knot winds and this wind velocity is likely to be established for OTEC use.

Prudent design and regulatory requirements are likely to require a minimum capability of surviving damage and flooding of at least one compartment. Based on criteria of Reference 6, the platforms should survive in this damaged condition with a steady 50 knot wind. An OTEC plant will offer unique problems in compartmentation due to the large cold and warm water piping systems.

Platforms with large waterplane areas, such as the ship and disc types, should have no undue problems in meeting intact and damaged stability criteria which will be imposed by cognizant agencies or insurance considerations. The submerged platforms, such as the submarine and spar, on the other hand, may have great difficulty in meeting damaged stability criteria. While actual criteria do not now exist, the designer should select a platform which will meet the type of criteria discussed here and in References 6-8.

A rigidly attached CWP will greatly increase stability in intact and damaged cases. It will be necessary, however, to insure adequate intact and damaged stability in the absence of CWP, as occurs during transit or following loss of the CWP.

Platform and CWP Materials and Weights - The cost of the platform and CWP will be primarily determined by the choice of material (steel, aluminum, concrete, glass reinforced plastic, etc.) and by the total weight of material required. Cost will be increased by complex shapes, particularly for steel or aluminum platform construction.

The weight of the platform will be determined, for a given material, primarily by surface area and to a lesser extent, by draft and shape. Platforms with the smallest surface area, such as the disc, are likely to be cheapest to build, while platforms with the largest surface area, such as the semi-submersible or submarine are likely to be the most expensive to build. Experience in the offshore industry indicates that a semi costs two to three times as much as shipsfor a given payload.

The choice of material may, to some extent, be determined by platform type. Platforms, such as the ship, which may experience large hull bending moments, are likely to be constructed of steel, while platforms such as the spar and disc are likely to be constructed of reinforced light weight concrete. Studies to date indicate that concrete construction should be cheaper, at least for certain platform shapes, but it is not clear that, for example, a concrete disc platform would be cheaper to build than a steel ship for a given OTEC plant.

The weight and cost of the CWP will be determined primarily by seaway and current induced loads (bending moments). Large loads can result not only in large CWP weight but also in the need for more expensive or exotic materials and/or construction techniques. Increased weight will also increase the problems associated with the design of and the cost of the platform/CWP attachment.

Plant Arrangements and Accessibility - The arrangement of the OTEC power plant is important because of its impact on many important factors. These include piping and ducting requirement, system head losses, proximity of intakes and exhausts and possible flow recirculation, accessibility of plant components for maintenance, repair and removal for major overhaul or replacement and required plant deck area or volume. It is essential, for an economically attractive OTEC plant, to provide a plant arrangement which minimizes flow losses, recirculation and space and volume requirements and maximizes accessibility.

Plant arrangements will be largely influenced by the fact that cold water will reach the platform at one location (the CWP/platform attachment) and must be distributed from that point to all condensers. Warm water can be taken onboard at many locations. It is therefore desirable to provide a central location for the CWP attachment and to locate condensers as close to this attachment point as possible. Warm water intakes, which should be near evaporators, should be located upstream of cold water exhaust unless a large vertical separation can be provided.

Accessibility to plant components is maximized by use of a surface platform. Deck mounted cranes can be used to remove components to repair or storage areas and perhaps to deploy the CWP (see Reference 9). With submerged platforms, access must be completely internal or ex-

ternally mounted modules, which can be removed by deck mounted cranes or separate barge mounted cranes (see Reference 10), must be provided. Deployment of the CWP may be more difficult or costly for submerged platforms, although the shorter required length of pipe will be helpful.

Ease of Platform Construction - The constructability (ease or feasibility of construction) of the platform will be determined by platform maximum dimensions, maximum draft at platform float-out or launch and materials and methods of construction.

Some platforms, such as ship or barge and submarine, will probably be built of steel. For plant sizes up to at least 100MW these platforms can probably be built in existing U.S. building or graving docks. Semi-submersible platforms may be built of either steel or concrete; for plant sizes up to about 25MW, semi's can be built using existing U.S. construction sites. For larger sizes, new facilities permitting greater float-out drafts will probably be required. Axi-symmetric platforms, such as the disc or spar, will probably be built of concrete using slip forming techniques. Such platforms can probably be built using existing sites or techniques for platform sizes up to 50 to 100MW.

It should be noted that there is a definate advantage, in ease and cost of construction, in completing as much work as possible before platform launching. The ship and submarine platforms should offer the greatest advantage in this area, while slip formed concrete platforms are probably least advantageous.

## CONCLUSIONS

The selection of the best platform/CWP design for an OTEC plant will be significantly influenced by seaway and current induced motions, accelerations and CWP loads, OTEC plant arrangements and accessibility, platform static and damaged stability and platform and CWP weight, constructability and cost. Other important design factors such as mooring or stationkeeping and transit to site probably will have a somewhat lesser effect on selection of platform/CWP design.

As in any design problem, the design which can satisfactorily meet all minimum design requirements, can be constructed and has the lowest life cycle cost or cost per unit product will be selected. The best type of platform may well be quite different for different plant sizes and operating sites. For example, the use of an existing ship or barge, such as the Hughes Mining Barge, appears very attractive for evaluation of small OTEC plant components, but such platform shapes may not be attractive for large OTEC plants due to large CWP loads and structure.

## ACKNOWLEDGEMENTS

Much of the work described in this paper has been carried out under ERDA Contracts E(11-1)-2681 and EX-76-C-01-2424. The encouragement and support of the ERDA Ocean Thermal Energy Conversion Program Office throughout this work is appreciated.

## REFERENCES

1. Barr, Roderick, A., John F. O'Dea and Vladimir Ankdinov, "Theoretical Evaluation of the Seakeeping Performance and Resistance/Propulsion Characterist of Five Candidate OTEC Platforms", HYDRONAUTICS, Incorporated Technical Report COO-2681-1, July 1976.
2. Chang, Pin Yu, "Structural Analysis of Cold Water Pipes for OTEC Power Plants", HYDRONAUTICS, Incorporated Technical Report COO-2424-1 (in Press).
3. Tuned Sphere International, "Tuned Sphere Stable Platform for Ocean Thermal Energy Conversion Power Plants", Proposal submitted to ERDA, April 1976.
4. Payne, Peter R., "On Quantizing Ride Comfort and Allowable Accelerations", Paper 76-873 presented at the AIAA/SNAME Advanced Marine Vehicles Conference, September 1976.
5. Little, T.E., "Cold Water Pipe, Pumps and Deep Water Mooring", Paper 2C-1 presented at the Fourth Ocean Thermal Energy Conversion Conference, March 1977.
6. American Bureau of Shipping, Rules for Building and Classing Offshore Mobile Drilling Units, 1968.
7. Seymour, D.J. and C.R. McCardell, "Floating Type Offshore Drilling Vessels", Paper presented at Pacific Northwest Section of the SNAME, October 1966.
8. McTaggert, R.G. and R.H. Gundorson, "On Damaged Stability of Drilling Vessels", Transactions of the SNAME, Volume 81, 1973.
9. Avery, W.H., et al., "Maritime and Construction Aspects of Ocean Thermal Energy Conversion (OTEC) Plant Ships", APL/JHU Report SR 76-1A, 1976.
10. "Ocean Thermal Energy Conversion (OTEC) Power Plant Technical and Economic Feasibility", Lockheed Missiles and Space Company, Inc. Report LMSC-D056566, 1975.

A1 Barr, Roderick A. and John F. O'Dea, "Preliminary Evaluation of HMB Motions and CWP Loads for OTEC One", HYDRONAUTICS, Incorporated Technical Report 7513.3-1.

B1 Reissner, E., "On Finite Bending of Pressurized Tubes" Transactions of the ASME, September 1959, pp. 386-392.

B2 Brazier, L.G., "On the Flexure of Thin Cylindrical Shells and Other Thin Sections", Proceedings of the Royal Scoiety, Series A., Vol. 116, 1927.

B3 Baker, E.H., L. Kovalevsky, F.L. Rish, Structural Analysis of Shells , McGraw Hill Book Company, Inc., New York, 1972.

B4 Timoshenko, Stephen P., Theory of Elastic Stability, McGraw Hill Book Company, Incorporated, New York.

## APPENDIX A
## Platform Motions and Accelerations and CWP Bending Moments in Irregular Waves

Reference 1 describes methods developed to analyze the coupled motions in waves of five generic types of OTEC platforms with rigid CWP and the resulting CWP shear forces and bending moments. Reference 1 presents extensive calculated results for various platform and CWP geometries and CWP attachment restraints. These methods have been recently extended to flexible CWP's, as described in Reference A-1.

The motions and CWP loads are calculated in the frequency domain using linearized equations of motion. Responses in irregular waves are calculated using normal seakeeping statistical methods. Reference A-1 describes the various assumptions employed in the analysis methods. Some typical results are discussed below.

Results with Rigid CWP

Tables A-1 and A-2 and Figures A1-A3 summarize some results from Reference 1 for platforms with rigid or inelastic CWP's. The Tables summarize platform motions and CWP bending moments for 500 and 100MW plants (500,000 and 150,000 long tons displacements) with rigidly attached CWP. Figures A1 and A2 show calculated pitch motions and CWP bending moments for 500MW plants in head seas. Figure A3 shows calculated heave accelerations for 100MW plants in head seas.

The largest platform motions and accelerations and the largest CWP bending moments generally occur for the disc and ship platforms, the smallest motions, accelerations and bending moments generally occur for the semi-submersible and the spar platforms. The most important motions and accelerations are those in heave, which are insensitive to CWP attachment stiffness. CWP bending moments are, on the other hand, very sensitive to CWP pitch/roll attachment stiffnesses, decreasing with decreasing attachment stiffness. For the semi-submersible CWP bending moments are smallest in head seas; for the ship and submarine bending moments are largest in head seas.

Pitch and roll motions are insignificant for rigidly attached CWP, and are moderate for zero and finite CWP attachment stiffnesses. Heave accelerations range from 0.02 to 0.2 times gravitational acceleration. While such accelerations would be considered moderate in normal ship practice, they may represent a design problem for some OTEC plant components such as heat exchangers. The large CWP bending moments, particularly with rigidly attached CWP, may make fabrication and installation of the CWP difficult or infeasible.

Results with Flexible CWP

The methods of Reference 1 have been extended to include CWP bending flexibility. Table A3 presents calculated CWP bending moments and bending stresses (determined from linear beam theory) for the baseline 500MW ship platform/CWP of Reference 1 with various CWP structures, attachment rigidities and significant wave heights. The results for the rigid CWP are from Reference 1. The CWP wall thicknesses considered were based on estimated loads and stresses.

The comparison of results for the various CWP flexabilities is most interesting. For the steel CWP's, bending moment decreases with increasing wall thickness and is a minimum for the rigid CWP. Bending stress therefore decreases very rapidly with increasing wall thickness or decreasing flexibility. For GRP CWP's, bending moment increases with increasing flexibility and hence bending stress decreases more slowly with increasing wall thickness. Bending moments and stresses are significantly larger for the larger attachment stiffnesses for both steel and CRP CWP's. The one prestressed concrete CWP case considered appears to be relatively flexible and to have significantly larger bending moments than the rigid CWP. Bending moment and stress are less sensitive to attachment stiffness than is the case for the other CWP materials.

CWP wall thicknesses and weights can be estimated using results in Table A3. Table A4 gives results obtained by equating maximum expected sea state seven bending stress (see Reference 1) to assumed allowable working stresses (40,000, 20,000 and 2,500 psi for steel, GRP and reinforced concrete, respectively).

The estimated CWP wall thickness and weight are large, but they do not indicate the impracticability of steel CWP's, particularly for zero attachment stiffness. GRP CWP's are clearly the lightest but may present unique fabrication problems. The concrete CWP weight is excessive. The working stress use for the concrete CWP (plus or minus 2,500 psi with 2,500 psi prestress) is considered realistic for the light weight (140 pound per cubic foot) concrete assumed in Table A4.

As noted in References 1 and A1, CWP bending moments and stresses will be significantly different for different CWP diameters and lengths, and hence Table A4 should be considered only as indicative of relative CWP wall thicknesses and weights with a ship platform. CWP weights and wall thicknesses may be quite different with other platform types.

TABLE A1 - Comparison of Calculated Significant Motions for Different Platforms for Sea State Seven - 500 MW Plant, 2000 Foot Deep Pipe, Quasi-Infinite Pipe Attachment Stiffness

| RESPONSE, feet or degrees | SHIP | SUBMARINE | SEMI-SUBMERSIBLE | DISC | SPAR |
|---|---|---|---|---|---|
| Surge, feet | 8.57 | 4.17* 3.87 | 4.02 | 8.81 | 6.27* 5.45 |
| Sway, feet | 9.56 | 7.44* 6.44 | 4.17 | 8.81 | 6.27* 5.45 |
| Heave, feet | 21.47 | 8.57 | 5.44 | 21.16 | 6.25 |
| Roll, degrees | 0.38 | 0.27 | 0.12 | 0.36 | 0.22 |
| Pitch, degrees | 0.38 | 0.11 | 0.12 | 0.36 | 0.22 |
| Yaw, degrees | 1.37 | 0.98 | 0.54 | 0 | 0 |
| Axial B. M., ft-lb | | | | | |
| • Attachment | $1.15\times10^{10}$ | $1.56\times10^{10}$ | $7.15\times10^{9}$ | $2.77\times10^{9}$ | $6.83\times10^{9}$ |
| • Maximum | $1.15\times10^{10}$ | $1.56\times10^{10}$ | $7.15\times10^{9}$ | $5.27\times10^{9}$ | $6.83\times10^{9}$ |
| Lateral B. M., ft-lb | | | | | |
| • Attachment | $7.51\times10^{8}$ | $5.15\times10^{9}$ | $1.02\times10^{9}$ | $2.77\times10^{9}$ | $6.83\times10^{9}$ |
| • Maximum | $6.00\times10^{9}$ | $5.15\times10^{9}$ | $8.58\times10^{9}$ | $5.27\times10^{9}$ | $6.83\times10^{9}$ |

*Upper values at waterline, lower values at center of hull.

TABLE A2 - Comparison of Calculated Significant Motions for Different Platforms for Sea State Seven - 100 MW Plant, 2000 Foot Deep Pipe, Quasi-Infinite Pipe Attachment Stiffness

| RESPONSE, feet or degrees | SHIP | SUBMARINE | SEMI-SUBMERSIBLE | DISC | SPAR |
|---|---|---|---|---|---|
| Surge, feet | 8.27 | 7.14 | 6.32 | 11.58 | 8.79 7.97 |
| Sway, feet | 12.02 | 9.90 | 6.80 | 11.58 | 8.79 7.97 |
| Heave, feet | 22.49 | 10.93 | 7.53 | 23.34 | 8.68 |
| Roll, degrees | 0.49 | 0.38 | 0.22 | 0.49 | 0.33 |
| Pitch, degrees | 0.39 | 0.23 | 0.21 | 0.49 | 0.33 |
| Yaw, degrees | 1.83 | 1.45 | 0.68 | 0 | 0 |
| Axial B. M., ft-lb | | | | | |
| • Attachment | $3.60\times10^{9}$ | $3.74\times10^{9}$ | $2.03\times10^{9}$ | $9.60\times10^{8}$ | $1.47\times10^{9}$ |
| • Maximum | $3.60\times10^{9}$ | $3.74\times10^{9}$ | $2.03\times10^{9}$ | $2.10\times10^{9}$ | $1.47\times10^{9}$ |
| Lateral B. M., ft-lb | | | | | |
| • Attachment | $1.70\times10^{8}$ | $1.02\times10^{9}$ | $2.89\times10^{8}$ | $9.60\times10^{8}$ | $1.47\times10^{9}$ |
| • Maximum | $1.58\times10^{9}$ | $1.02\times10^{9}$ | $2.89\times10^{9}$ | $2.10\times10^{9}$ | $1.47\times10^{9}$ |

Table A3

Comparison of Calculated Significant Bending Moments and Bending Stresses for Various CWP's For Baseline 500 MW Ship Platform-Head Seas

a. Attachment Stiffness in Pitch = 0

| CWP Material | CWP Wall Thick-Feet | $H_{1/3}$ = 20 ft | | $H_{1/3}$ = 40 ft | | $H_{1/3}$ = 80 ft | |
|---|---|---|---|---|---|---|---|
| | | B.M.* | Stress** | B.M. | Stress | B.M. | Stress |
| Rigid Pipe | ∞ | 12.8 | -- | 32.4 | -- | 56.8 | -- |
| Steel | 0.4 | 44.2 | 8.16 | 81.4 | 15.0 | 115 | 21.2 |
| | 0.8 | 27.4 | 2.56 | 58.2 | 5.4 | 89.7 | 8.4 |
| GRP | 0.2 | 5.1 | 1.87 | 19.1 | 7.01 | 30.9 | 11.4 |
| | 0.4 | 8.6 | 1.58 | 18.1 | 3.35 | 35.2 | 6.51 |
| Concrete | 4.5 | 82.1 | 1.28 | 117 | 1.82 | 151 | 2.35 |

*IN HUNDRED MILLION ($10^8$) POUND-FEET

**IN THOUSAND ($10^3$) PSI

b. Attachment Rigidity in Pitch = $10^{14}$ (Quasi-Infinite)

| CWP Material | CWP Wall Thick-Feet | $H_{1/3}$ = 20 ft | | $H_{1/3}$ = 40 ft | | $H_{1/3}$ = 80 ft | |
|---|---|---|---|---|---|---|---|
| | | B.M. | Stress | B.M. | Stress | B.M. | Stress |
| Rigid Pipe | ∞ | 27.0 | -- | 103 | -- | 241 | -- |
| Steel | 0.4 | 62.4 | 11.5 | 150 | 27.7 | 260 | 48.0 |
| | 0.8 | 48.2 | 4.50 | 126 | 11.8 | 239 | 22.3 |
| GRP | 0.2 | 19.5 | 7.15 | 59.9 | 22.0 | 97.0 | 35.6 |
| | 0.4 | 19.5 | 3.61 | 69.1 | 12.8 | 190 | 35.1 |
| Concrete | 4.5 | 66.7 | 1.04 | 156 | 243 | 275 | 4.27 |

Table A4

Estimated CWP Wall Thickness and Weights in Air

| Material | Attachment K = 0 | | Attachment K = $10^{14}$ | |
|---|---|---|---|---|
| | $t_{wall}$-feet | W-long tons | $t_{wall}$-feet | W-long tons |
| Steel | 0.4 | 60,000 | 0.7 | 106,000 |
| GRP | 0.2 | 11,000 | 0.6 | 33,000 |
| Concrete | ≃ 6 | 273,000 | -- | -- |

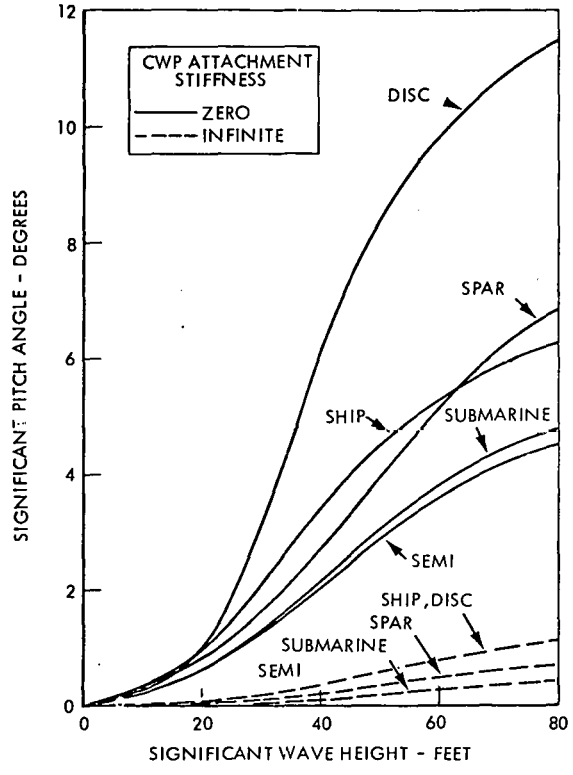



FIGURE A1 - SIGNIFICANT PITCH MOTION FOR 500 MW, 500,000 LT PLATFORM/CWP - HEAD SEAS

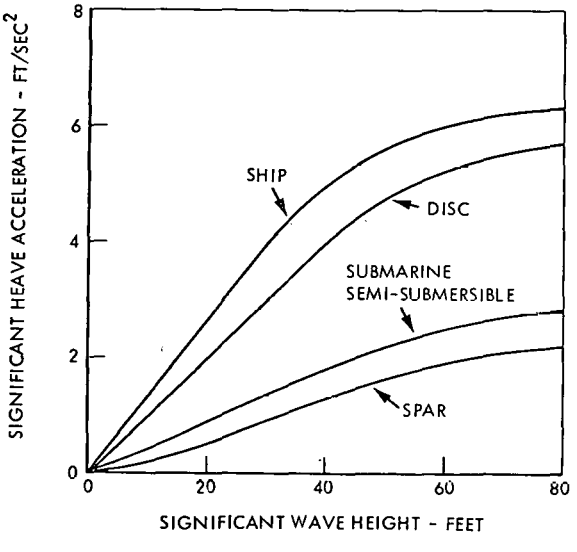



FIGURE A2 - SIGNIFICANT HEAVE ACCELERATION FOR 100 MW, 150,000 LT PLATFORM/CWP - HEAD SEAS

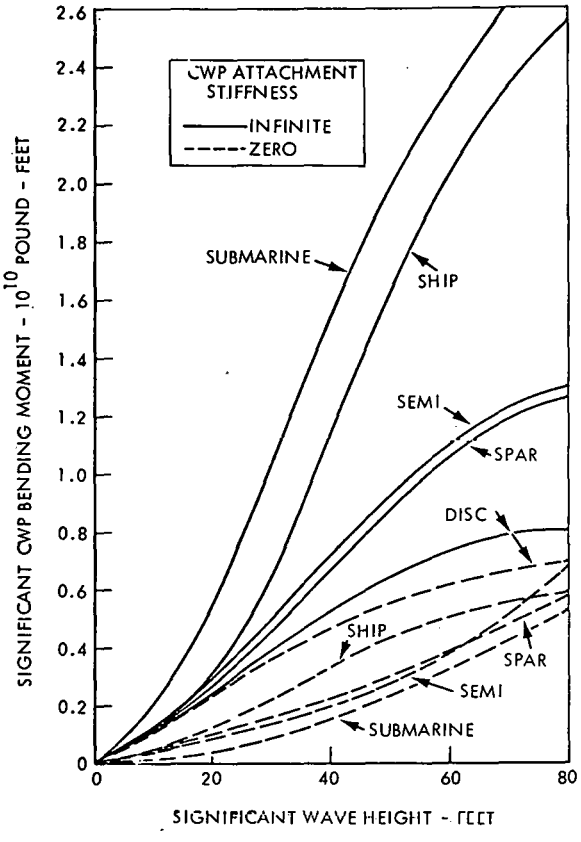



FIGURE A3 - SIGNIFICANT CWP MAXIMUM BENDING MOMENTS FOR 500 MW PLATFORM/CWP - HEAD SEAS

APPENDIX B
CWP Structural Design Requirements and Analysis

This appendix highlights results from Reference 2 and presents a brief discussion of CWP structural design requirements, methods and factors affecting CWP structural design. This appendix also includes some later results not included in Reference 2.

Reference 2 emphasizes nonlinear methods based on the work of Reissner and Brazier, References B1 and B2. Nonlinear effects can be very important, particularly when very thin wall CWP's are used. Most nonlinear effects are expressed in terms of a flexibility factor, the use of which requires an understanding of the theory.

Design Requirements of CWP Structure

In order to ensure safe and efficient operation of the OTEC power plant, the CWP structure must meet the following requirements:

a) Adequate transverse stiffness to maintain the cross-section shape and insure adequate and continuous cold water flow.

b) Adequate longitudinal bending strength to resist the forces due to the environment (current and waves) and due to platform/CWP motions.

c) Adequate overall and local strength for the duration of the design life of the OTEC platform, including the effect of fatigue.

Unique CWP Structural Design Problems

Several unique problems result from the large size of the CWP. Well developed methods for marine risers of one to two foot diameter may not be adequate. First, the linear theory for cylindrical shells which is used for risers, may lead to great error for the OTEC pipe. Second, since the OTEC pipe is subjected to long duration cyclic loads, fatigue failure is an important problem. Thirdly, since the deformation of the CWP cross-section can be significant, such deformationsmust be accounted for in predicting stresses. The errors due to linear approximations are illustrated in Figure B1 and Figure B2.

The Effects of CWP Nonlinear Deformations and the Flexibility Factor

The linear theory assumes that the shape of the CWP cross-section is unchanged by deformations. This assumption is valid for cases with small radius/thickness ratio or more accurately it is valid for small values of the flexibility factor which is defined by:

$$\xi = \frac{3(1-\nu^2)}{2(1-r_c)}^{\frac{1}{2}} \frac{B}{h}\frac{B}{R} \qquad [B1]$$

where

- $\nu$ is Poisson's ratio (0.3 for steel, etc.)
- B is CWP radius
- R is radius of curvature due to bending
- $r_c$ is the ratio of the external pressure to external pressure for pure compressive buckling at actual flow velocity
- h is thickness

Flexibility is hence determined by internal flow velocity, radius/thickness ratio, and the bending moment upon the CWP. This indicates that the radius/thickness ratio, used in the linear theory as a predominant parameter, does not cover the whole story of the CWP responses. If the internal cold water flow velocity approaches a critical velocity, $r_c$ approaches one and the flexibility factor becomes infinite. The effects of the flexibility factor, $\xi$, on the cold water pipe are quite complicated and are not yet fully understood. Nevertheless, it's effect on the most important design parameters have been determined. In general there are four significant effects of cross-section deformations which are briefly discussed below.

Figure B3 shows the various types of loadings and stresses which can occur in the CWP. Not all of these are equally important. Torsional stresses, in particular, are unlikely to be important for the CWP.

Additional Stresses Due to Cross-Section Deformations

If cross-section deformation is small, the most important stresses are bending stress, shear stress due to bending and loop stress due to pressure difference across the CWP wall. With significant deformation, the nonlinear solution of Reference 2 give the following formulas for these stresses

$$\sigma_b = \frac{M}{B^2 h\pi} \sin\theta \left\{\frac{f_2(\xi)}{f_1(\xi)}\right\} \qquad [B2]$$

$$f_2 = 1 - \frac{2}{3}\xi^2 - \frac{76}{135}\xi^4 + \frac{4}{15}\beta_2\alpha^4$$

$$f_1 = 1 - \xi^2 - \frac{2}{3}\xi^4$$

$$\tau = \frac{H}{\pi h B}\cos\theta \left\{\frac{f_2(\xi)}{f_1(\xi)}\right\} \qquad [B3]$$

$$\sigma_\theta = -\frac{B}{h}\frac{\rho}{2}V^2 + \left\{-\frac{B}{h}\rho V^2(\xi^2 + \frac{8}{9}\xi^4) + \frac{2}{3(1-\nu^2)}(\xi^2 + \frac{4}{9}\xi^4) \times \cos 2\theta\,[1 + 2(\xi^2 + \frac{8}{9}\xi^4)]\right\} \qquad [B4]$$

where

- $\sigma_b$ is bending stress
- $\tau$ is shear stress due to bending
- $\sigma_\theta$ is loop stress
- V is flow velocity inside CWP
- $\theta$ is angular position measured from the axis of bending

The factors or terms in braces, {}, represent the nonlinear effects. If $\xi$ is set equal to zero these equations reduce to the well known linear equations. In addition to these effects, cross-section deformations result in an additional bending stress given by:

$$\sigma_{\theta b} = \frac{E}{1-\nu^2}\left(\frac{h}{B}\right)\left[2(\xi^2 + \frac{4}{9}\xi^4)\cos 2\theta + \frac{12-8r_c}{5-r_c}\xi^4\cos 2\theta\right] \qquad [B5]$$

where E is modulus of elasticity.

Reduction of the Stability Strength

Using the nonlinear solution, the critical bending stress, that is the bending stress at which snap buckling, as illustrated in Figure B4, occurs is:

$$\frac{E}{\sqrt{3(1-\nu^2)}} \frac{h}{B} \left\{ 0.5708 \left[ 1 - \frac{V_c}{V_{cr}}^2 c \right]^{\frac{1}{2}} \right\} \qquad [B6]$$

where

$c = 1 + \tan^2 \frac{\pi a}{2}$

$a$ = the out-of-round ratio = $\frac{u}{B}$

$V_c$ = velocity of the internal cold water flow

$V_{cr}^2 = \frac{1}{\rho} \frac{E}{2(1-\nu^2)} \left(\frac{h}{B}\right)^3$ = the critical velocity of the internal cold water flow

The term in braces is the nonlinear correction. For $\frac{R}{h} > 200$ use Figure B6.

Figure B1 shows that reductions in stability strength are, typically, 43 to 50 percent. Available test data indicate reductions of about 30 to 45 percent for steel (B/h of 200 to 700) and 40 to 60 percent for brass, confirming the general validity of equation [B6].

Discrepancies between experimental and theoretical critical loads exist, however. One reason for these discrepancies is shell imperfections (out-of-roundness), the effect of which increases with increasing radius to thickness ratio (B/h). Figure B5 shows an empirical correction factor based on data from References B3 and B4. The factor is about 0.57 for B/h of 200 or less, confirming the validity of equation [B6]. For larger values of B/h, Figure B5 should be used, and transverse stiffners will probably be required. For OTEC CWP's, B/h should be less than 200 and equation [B6] can be used.

Reduction of CWP Strength

According to linear theory, CWP loop stresses are small compared to bending stresses and CWP failure is governed by uniaxial bending stress. According to the nonlinear theory, loop bending stress is important when flexibility factor is not small and CWP failure is governed by biaxial stress due to longitudinal and loop bending. For an allowable stress, $\sigma_a$, the biaxial stresses should be limited to

$$\sigma_a \geq \sigma_b^2 + \sigma_{\theta b}^2 - \sigma_b \sigma_{\theta b}$$

Figure B2 shows variations of this relationship, which can be expressed, approximately, by

$$\sigma_b \leq \sigma_a (1 - \xi) \qquad [B7]$$

The error of the linear theory is thus roughly proportional to the flexibility factor. This indicates that the bending stress should be lower than the allowable stress by a fraction about equal to the flexibility factor.

Reduction of CWP Stiffness

If CWP cross section deformation occurs, the linear relationship between bending moment and curvature must be replaced by

$$R = \frac{EI}{M} \left\{ 1 - \xi^2 - \frac{2}{3} \xi^4 + \ldots \right\} \qquad [B8]$$

Where the curly bracket represents the nonlinear effect. CWP design requirements will usually result in small values of flexibility factor and hence small nonlinearities. For typical CWP design cases the decrease in radius of curvature will be less than five percent. It is therefore realistic, for most realistic CWP designs, to predict CWP loads and stresses using linear theory.

Line Solution Method for CWP Bending and Extension

CWP bending and extension problems can be solved by many methods. As "optimum" CWP designs may be nonprismatic (variable cross section) or made of more than one material, methods other than simple beam theory are required. Finite element and finite difference methods are applicable, but may have computational problems. The line solution methods appears most attractive in terms of accuracy and computation costs.

The errors introduced by lumped masses in finite element and finite difference solutions can be large if a large number of masses are not used. As an illustration, consider a CWP which is simply supported at both ends and is modelled by five masses. The resulting errors in the first five modal natural frequencies are 0, 0.06, 0.55, 3.1 and 16.0 percent. As higher modes can be important for CWP's, a large number of lumped masses or elements can be required.

The Importance of Fatigue and Fatigue Strength

Operational OTEC plants and CWP's will have required lifetimes of 30 to 40 years. This will result, for a realistic ocean environment, in about $10^8$ stress cycles, and hence CWP fatigue failure will be a distinct possibility. The possibility of fatigue failure is increased by the significant reduction of material fatigue strength in a corrosive seawater environment. The fatigue strength of metals in seawater can be less than 50 percent of that in air after $10^8$ cycles and fatigue strength in seawater, unlike that in air, continues to decrease with increasing number of cycles. Methods and essential steps for designing a CWP with adequate fatigue strength are given in Reference 2.

Design Process for a Cold Water Pipe

Figure B6 shows a flow chart for a complete, nonlinear CWP structural design process. The process involves iterations and some calculations which require the use of a computer. The prediction of the loads on the CWP is discussed in Reference 1 and Appendix A. The Section numbers in Figure B6 refer to sections in Reference 2. As noted earlier, it may be possible with many CWP designs to neglect nonlinear effects and hence to considerably simplify the design process.

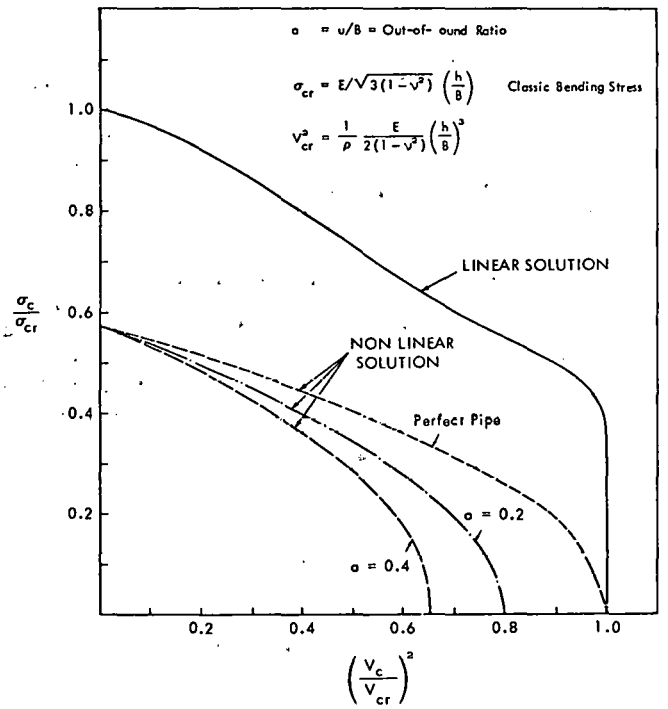



FIGURE B1 - CRITICAL BENDING STRESS AND CRITICAL FLOW VELOCITY

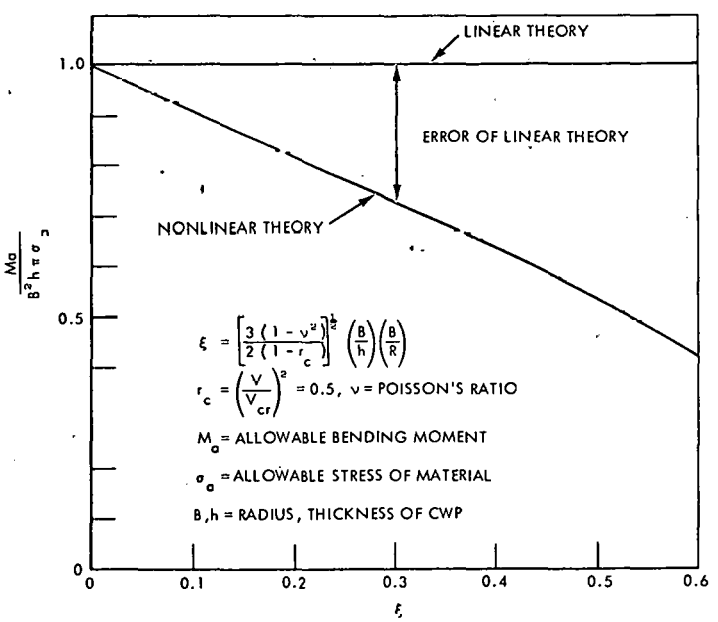



FIGURE B2 - ALLOWABLE BENDING MOMENT IN TERMS OF ALLOWABLE STRESS

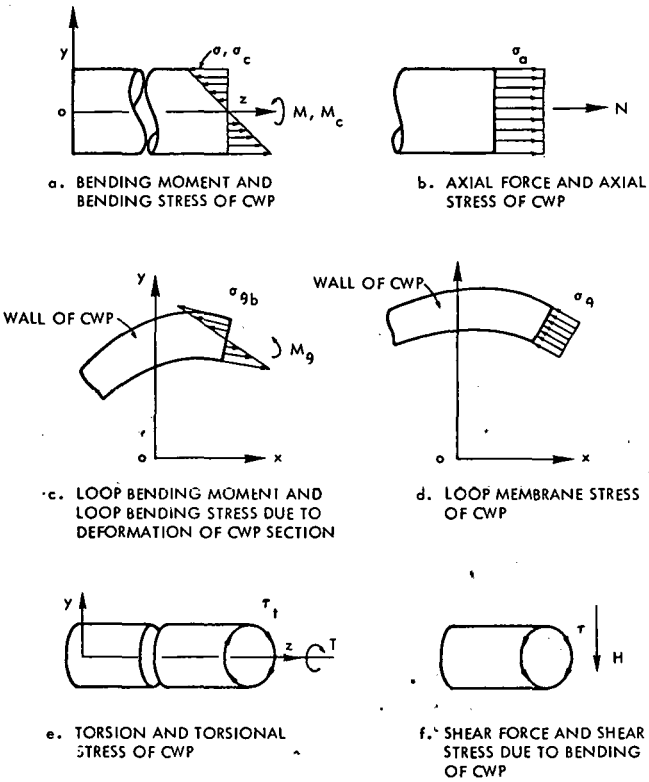
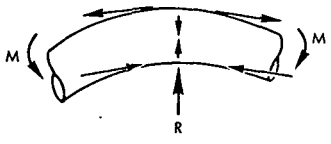


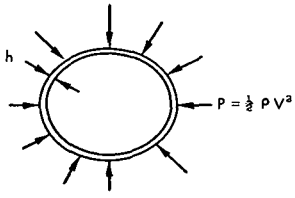

FIGURE B3 - STRESS COMPONENTS OF OTEC COLD WATER PIPE

SNAP BUCKLING

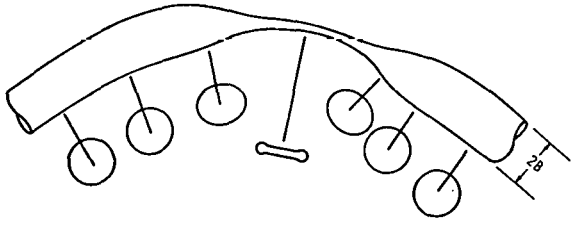
1. BENDING




2. EXTERNAL PRESSURE




3. AFTER CRITICAL STRESS OR YIELD STRESS




4. FLEXIBILITY FACTOR

$$\xi = \left[\frac{3(1-\nu^2)}{2(1-r_c)}\right]^{\frac{1}{2}} \left(\frac{B}{h}\right)\left(\frac{B}{R}\right)$$

$\xi_c = 0.5089$

FIGURE B4 - FACTORS INFLUENCING SNAP BUCKLING

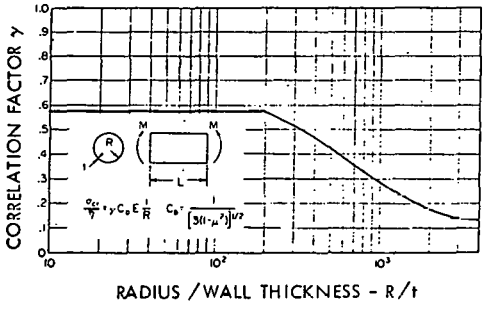



FIGURE B5 - CORRELATION FACTORS FOR UNSTIFFENED UNPRESSURIZED CYLINDERS SUBJECTED TO BENDING

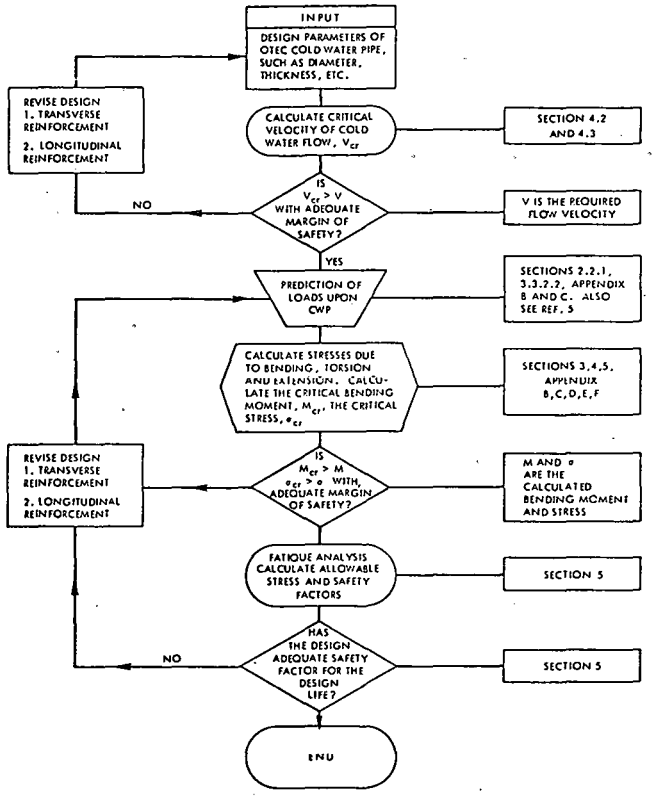



FIGURE B6 - DESIGN ANALYSIS PROCEDURE OF OTEC COLD WATER PIPE

## APPENDIX C
## Mooring, Stationkeeping and Grazing Forces

A potentially important factor in the selection and design of an OTEC plant may be the magnitude of current, wind and steady wave induced forces on the platform/CWP, particularly for operating sites having high velocity currents. For such sites, current forces will generally be much larger than steady wave and wind forces, and the cost of mooring or dynamic positioning systems can be a significant part of total plant cost. Table C1 compares current forces for surface current velocities of two and four knots for the five platform types considered in Reference 1. Forces are significantly smaller for the submarine and the ship than for the other platforms.

Table C1 also compares forces corresponding to grazing at one-half and one knot speeds in slack water (water without current). Here the force on the CWP is predominant and differences in forces between platforms are not significant.

Wind forces will generally be smallest for the submarine, spar and ship for head winds and smallest for the submarine and spar for beam winds.

Table C1

Forces in Pounds on 100MW Platforms with 2000 Foot Long, 50 Foot Diameter Cold Water Pipe in Head Current and Due to Grazing in Slack Water

| | Surface Current Velocity* $V_o$ | | Grazing Velocity | |
|---|---|---|---|---|
| Platform Type | 2 Knots | 4 Knots | 0.5 Knots | 1 Knot |
| Ship | 179,000 | 716,000 | 53,300 | 213,190 |
| Submarine | 100,000 | 640,000 | 51,900 | 207,600 |
| Semi-Submersible | 291,000 | 1,164,000 | 63,800 | 255,400 |
| Disc | 236,000 | 944,000 | 57,200 | 228,800 |
| Spar | 274,000 | 1,095,000 | 60,600 | 242,300 |

*Calculated for velocity distribution with depth (z) given by

$V = V_o (1-0.0005z)^2$ for $3 \leq 2000$ ft

$V = 0$ for $3 > 2000$ ft

# HYDRODYNAMIC LOADS ON THE COLD WATER PIPE

D. T. Hove and W. C. L. Shih
*Los Angeles Division*
*Science Applications, Inc.*
*101 Continental Boulevard, Suite 310*
*El Segundo, California*

Abstract

Ocean current and/or plant motion crossflows induce time dependent hydrodynamic loads on the cold water pipe. Initial estimates of lift, drag and Strouhal shedding frequency have been made based on a literature review for smooth and rough cylinders for the Reynolds number range of $10^6$ to $10^7$. An experimental program is underway to verify the design loads. Preliminary experiments were conducted at the CalTech Ten Foot Wind Tunnel, and a final experimental verification program will be conducted in the NASA Twelve Foot Pressure Tunnel during August 1977. An analytical technique is being developed to determine the validity of extending lower Reynolds number data to higher Reynolds numbers by modeling the influence of roughness on cylinder boundary layer flows.

## Introduction

Every proposed OTEC power plant design has included a long cylindrical pipe to bring cold water from the ocean depths to the surface where the cold water is used to condense the power system working fluid. The power plants will operate in either a station keeping mode held in place against the currents by an anchor or a dynamic positioning system or in a slow grazing motion to avoid thermal contamination in quiescent waters. Ocean current and/or plant motion crossflows will induce hydrodynamic loads on the cold water pipe, and design criteria are required for pipe structural and positioning system analyses.

Pressure variations exist on cylindrical bodies in crossflows because the fluid alternately decelerates, accelerates and then decelerates around the body. In an ideal inviscid potential flow, no net force would exist on the body, but in real fluids the viscous boundary layer causes the flow to separate from the cylinder leaving a low pressure base region which produces a net drag. Furthermore, the separation process is time dependent with alternate shedding vortices creating an oscillatory lift (normal) force. A key influence parameter (along with geometry, surface condition, turbulence, etc.) is the flow Reynolds number. Due to the large cold water pipe diameters, Reynolds numbers as high as $10^8$ may be encountered by OTEC plants, and $10^8$ is well beyond the range of experimental data.

The present program was undertaken to establish hydrodynamic design load criteria (pressure distributions, drag, lift and Strouhal shedding frequency) for the OTEC cold water pipe. Preliminary recommendations are made based on a review of the cylinder flow literature, and an experimental program is underway to verify the recommendations in the cylinder Reynolds number range of $10^6$ to $10^7$. Finally, analytical techniques are being studied to extend the test data to a Reynolds number of $10^8$ in a rational manner.

This work is sponsored by ERDA under contract E(49-18)-2331. Dr. E. Silva is the technical monitor. Professors Coles and Roshko have provided valuable suggestions.

## Cold Water Pipe Design Requirements

OTEC plants will operate in ocean currents which are a function of time, depth and location. Design curves must encompass peak currents expected to be observed (with high confidence) over the 40-year plant lifetime, and presumably the design criteria should not be site dependent. If the plants are to operate in the Gulf Stream, for example, peak currents $U_\infty$ could be 7 feet per second near the surface. With a cold water pipe diameter d of 150 feet and a kinematic viscosity $\nu$ of water of $10^{-5}$ ft$^2$/sec, a cylinder Reynolds number

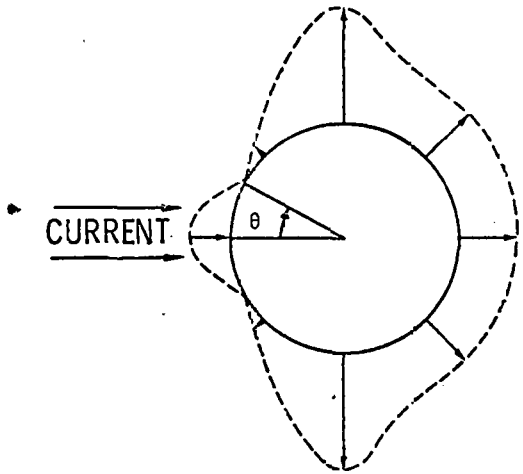
$$Re_d = \frac{U_\infty d}{\nu}$$

of $10^8$ results.

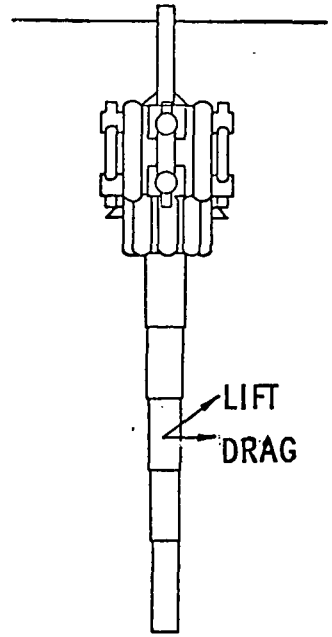
Preliminary OTEC plant design studies have been performed by TRW, Lockheed, University of Massachusetts and Johns Hopkins. In addition, structural analyses of the cold water pipe have been performed by Westinghouse and Hydronautics, Inc. Most cold water pipe design studies have emphasized bending of the pipe axis and buckling of the pipe wall. According to Albano, however, the dominant failure mode is deformation of the cylinder cross section into an oval shape such that the bending stress exceeds the allowable stress. Calculation of ovalling and buckling requires the specification of the sectional pressure distribution; axial bending calculations and positioning system design require the integrated lift and drag forces (Figure 1).

Unsteady hydrodynamic loads arising from vortex shedding can excite dynamic structural response phenomena including rigid body and flexible motion. A simplified analysis indicates the cold water pipe ovalling and

# OTEC
# COLD WATER PIPE HYDRODYNAMIC LOADS DESCRIPTION




PRESSURE DISTRIBUTION




INTEGRATED FORCES

FIGURE 1

bending natural frequencies are at or above the vortex shedding frequency for selected design alternatives. e natural frequencies near the shedding (exciting) quency raise the spector of load and response en- ...cement, and care must be taken to avoid such a design. With a pipe natural frequency greater than the shedding frequency, the pipe will respond to instantaneous loads and, therefore, peak values of the pressure distributions and lift and drag are required.

The spectral content of the forcing functions are important to dynamic structural response analysis and estimation of fatigue life. If the shedding process is periodic or quasi-periodic, a single characteristic Strouhal number

$$S = \frac{fd}{U_\infty}$$

is defined where f is the shedding frequency. The shedding process may be random (broadband) over a portion of the Reynolds number range; here statistical response analysis is required based on the spectral content. Also required is a measure of the correlation length along the cylinder axis. If the correlation lengths are long compared to the cylinder diameter, sectional analyses are valid, and the loads act in concert along the pipe. If short correlation lengths are present, the structural analysis must be three-dimensional, and the total loads on the pipe are diminished.

Cold water pipe construction materials may include concrete, steel, fiber reinforced plastic or aluminum with varying degrees of surface roughness. Cast concrete may have roughness heights on the order of $10^{-4}$ pipe diameters, and steel plates may have weld roughnesses on the order of $10^{-3}$ pipe diameters. Ocean biofouling is not well understood, but it is estimated that surface roughnesses of $10^{-3}$ to $10^{-2}$ pipe diameters could occur. External structural reinforcing rings are a cost effective method of strengthening the cylinder walls; the rings may be $10^{-1}$ cylinder diameters in height and spaced at one to three diameters. The effect of these various surface conditions on the hydrodynamic loads must be determined.

Drag forces may cause the cold water pipe to rotate from the vertical depending on positioning system design. The effect of this inclination angle on the hydrodynamic loads should be quantified.

## Preliminary Design Loads Recommendations

Hydrodynamic loads on the cold water pipe will be influenced by the ocean environment. Certain effects such as free stream turbulence can be dismissed because the scale of the turbulence is too large to have an effect. Other phenomena such as shear flow and stratification remain unquantified, but it is conjectured that their effect is to relieve the recommended loads developed from uniform flow experiments. Flow Reynolds number appears to be the key environment parameter.

Of equal importance is the design of the cold water pipe. Short (low aspect ratio) pipes will experience end effects due to pressure relieval and suction. Noncylindrical crossectional geometry will influence flow separation and, therefore, the pressure distributions. Exterior surface members may influence the pressure loading even if aligned with the flow, and surface roughness has a marked effect on the loads as will be demonstrated. Further complications are introduced by pipe motion and inclination angle.

In order to establish design loads in a systematic manner, only a fixed circular cylinder in a uniform cross flow is considered. The effects of flow Reynolds number and surface roughness on drag, lift, and Strouhal number are quantified, and flow inclination angle effects on mean drag coefficient are estimated.

### Mean Drag Coefficient:

The drag force on a body is usually expressed in terms of a nondimensional drag coefficient

$$C_D = \frac{\text{Drag}}{\frac{1}{2}\rho U_\infty^2}$$

where $\rho$ is the fluid density. Drag coefficients on circular cylinders have been the subject of investigation for many years. Early investigators experienced difficulty in reaching high Reynolds numbers due to a lack of adequate facilities, and there was (and still is) a tendency to force higher Reynolds numbers by exceeding prudent blockage ratios in wind tunnels. Only recently has the effect of surface roughness and freestream turbulence on drag coefficient been realized and quantified. Thus, the large scater in test data for smooth cylinders (Figure 2) can be accounted for in a rational manner.

In the most modern experiments, the critical regime (precipitous drop in drag coefficient) for smooth cylinders is delayed to a Reynolds number of about $2X10^5$, and a minimum drag coefficient of about 0.2 is reached followed by a gradual rise to a drag coefficient of 0.5 at a Reynolds number of $10^7$. A design curve is recommended which is representative of the results of a number of investigators in the critical regime and reflects the work of Szechenyi and of James and Malcolm from $10^6$ to $10^7$. The curve has been extended to a Reynolds number of $10^8$ based on a feeling that no new fluid mechanics phenomena will be encountered at the higher Reynolds numbers, and an analytical/experimental technique is being developed to verify this extrapolation.

At sufficiently high Reynolds numbers and surface roughness, the mean drag coefficient becomes independent of Reynolds number and is a function only of the relative roughness k/d where k is a measure of the roughness height (Roshko). This Reynolds number independence is observed in fully turbulent pipe flows, although the present phenomenon is related to effects of roughness on boundary layer transition and separation. For cylinder Reynolds numbers greater than $3X10^6$, and relative roughness heights between $10^{-5}$ and $10^{-2}$, the experimental data are a simple function of relative roughness (Figure 2). The recommended curve should not be used outside of the stated bounds as there is evidence that the curve flattens (at least for awhile) at higher roughness heights. At lower

# OTEC
# CYLINDER MEAN DRAG COEFFICIENTS

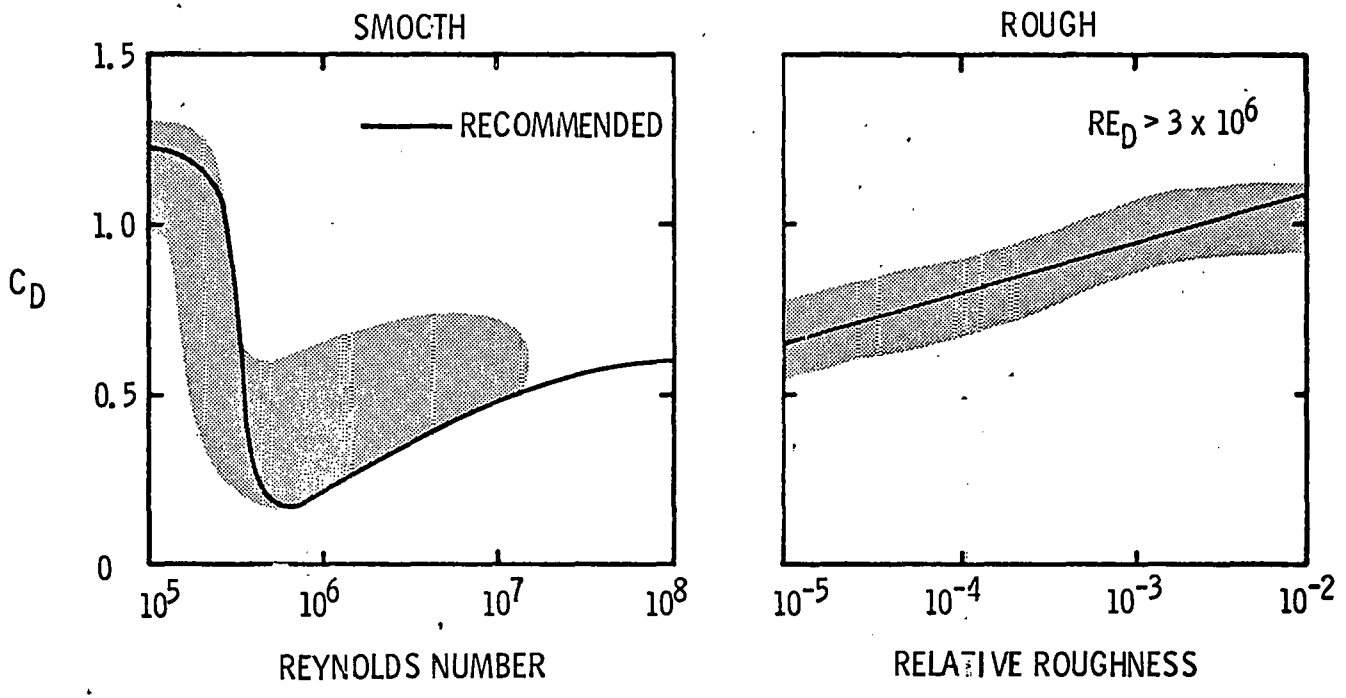



FIGURE 2

Reynolds number and roughness heights, individual experiments should be consulted.

Drag on inclined cylinders can be expected to be less an for normal flow. Based on measurements made in the subcritical region ($Re_d < 2X10^5$), the drag depends on the flow component normal to the cylinder for small inclination angles. Since the drag is normalized by the square of the velocity, and the drag component in the flow direction is D cos $\alpha$

$$C_D(\alpha) = C_D(0) \cos^3 \alpha$$

Hoerner cautions against this approach for supercritical flow but offers no alternative.

## Lift Coefficient

The unsteady pressure forces associated with the vortex shedding process lead to oscillatory lift (normal) forces on the cylinder, and a nondimensional rms lift coefficient

$$C_L = \frac{\text{Lift}}{1/2\rho U^2}$$

is defined analogous to the drag coefficient. There is a factor of two scatter in the smooth cylinder data (Figure 3); however, the upper bound of the data is due to Fung who noted the influence of model surface roughness. Therefore, a single rms lift coefficient of 0.1 is recommended for smooth cylinders.

The influence of surface roughness on lift coefficient is less certain than for the mean drag coefficient. Szechenyi has proposed a correlation (Figure 3) employing a roughness Reynolds number

$$Re_k = Re_d \left(\frac{k}{d}\right)$$

which collapses his lift coefficient data and that of Batham quite well. Preliminary design recommendations are 0.1 for $Re_k < 500$ and 0.27 for $Re_k \geq 500$.

## Strouhal Shedding Frequency

Power spectral density analyses of unsteady cylinder loads reveals that in certain Reynolds number regimes the shedding process is periodic and can be characterized by a single frequency. At subcritical Reynolds numbers the energy containing frequencies are confined to a narrow band, and the Strouhal number is about 0.2 for smooth cylinders (Figure 4). In the critical Reynolds number regime ($2X10^5 \leq Re_d \leq 3X10^6$) a broad band power spectral density is usually observed (e.g., Jones), but the center frequency Strouhal number is nearly 0.2. Some investigators have reported Strouhal numbers in excess of 0.4 in this region, but recent experiments have not verified this. At the higher Reynolds numbers, several investigators have observed that the Strouhal frequency rises to about 0.3. Jones has characterized the shedding process as quasi-periodic here.

For design purposes, a smooth cylinder Strouhal (center) frequency of 0.2 is recommended for $Re_d < 3X10^6$, and 0.3 is recommended for $Re_d \geq 3X10^6$. If broad band analyses are necessary, the work of Jones, Cincotta and Walker should be consulted.

Again, little is known about the effect of surface roughness on the unsteady separation process. Preliminary design recommendations are based on the roughness Reynolds number approach of Szechenyi. A Strouhal number of 0.2 is recommended for $Re_k < 30$ and 0.3 is recommended for $Re_k \geq 30$ (Figure 4).

## Wind Tunnel Test Program

A wind tunnel test program is being conducted to verify the design criteria established in the previous section. The test program will provide steady and unsteady pressure distributions as well as lift, drag and Strouhal shedding frequency for smooth and rough cylinders over the maximum available Reynolds number range. A secondary objective is to investigate the Reynolds number independence regime for rough cylinders to aid in developing a technique for extending the test results to higher Reynolds numbers.

Only a few investigators (e.g., Miller, Szechenyi, Achenbach, Guven, et.al.) have performed systematic measurements of the effects of uniform surface roughness on mean cylinder loads, and only Szechenyi has made detailed measurements of surface roughness effects on unsteady loads. Completely missing from the literature is a systematic description of the peak pressure distributions which are critical to the OTEC cold water pipe design.

## Facility Selection

During the test program design, numerous facilities were surveyed to determine the maximum achievable cylinder Reynolds number within nominal testing constraints (high cylinder aspect ratio, low blockage, negligible compressibility, availability, cost). Tow tanks are limited to a cylinder Reynolds number of $\sim 5X10^6$ and present severe aspect ratio, cavitation and surface effects limitations. Water tunnels were considered but are limited to a cylinder Reynolds number of $4X10^6$ and have cavitation problems. Wind tunnels provide the most attractive option since the majority of the cylinder flow investigations have been performed in wind tunnels and since a Reynolds number of the order of $10^7$ can be achieved.

The test facility selected for this work is the NASA Ames Research Center Twelve Foot Pressure Tunnel. This pressurized wind tunnel has an 11.3 foot square test section and can achieve a unit Reynolds number of $9X10^6$/foot at a Mach number of 0.25. With a 1 foot diameter cylinder spanning the test section, the blockage ratio is 11 percent, the length to diameter ratio is 11.3 and the cylinder Reynolds number is $9X10^6$. Compressibility effects on pressure coefficients are less than 1.5 percent.

An initial test program was conducted in the California Institute of Technology Ten Foot Wind Tunnel. This highly versatile, low speed wind tunnel presented a cost effective approach to developing the test proce- to be used in the upcoming Twelve Foot Pressure Tunnel

# OTEC
# CYLINDER RMS LIFT COEFFICIENTS

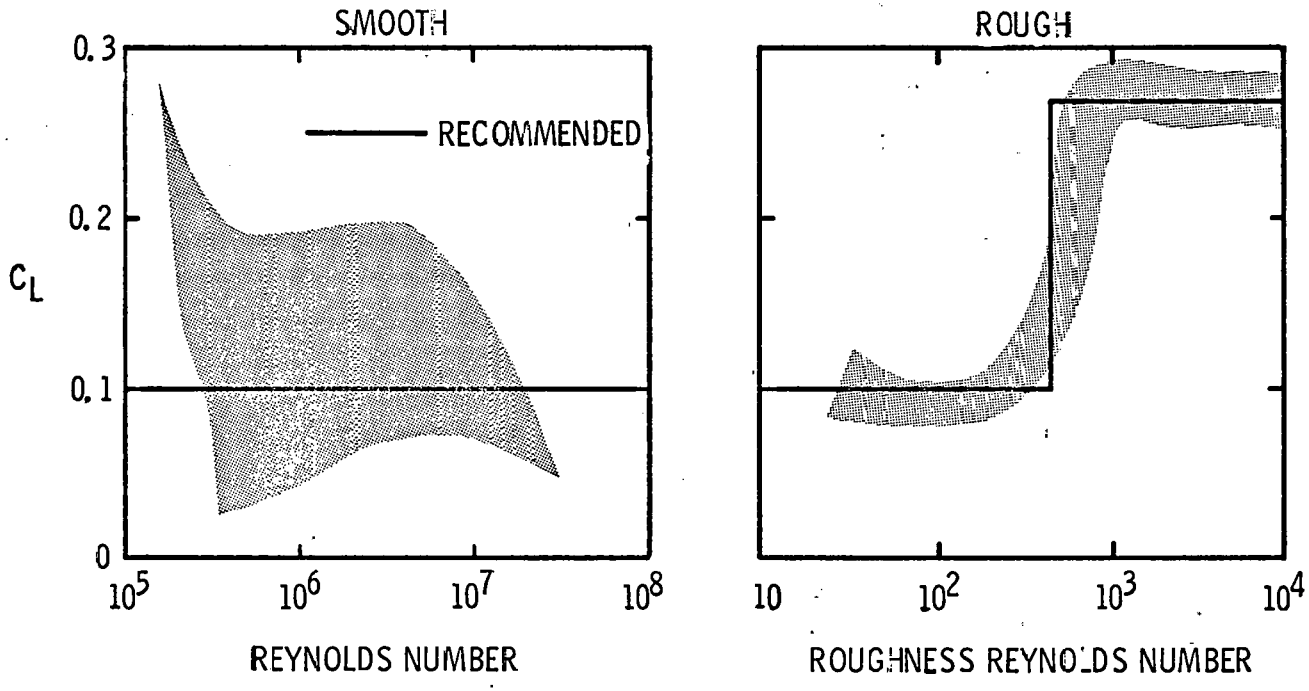



FIGURE 3

# OTEC
# CYLINDER STROUHAL SHEDDING FREQUENCY

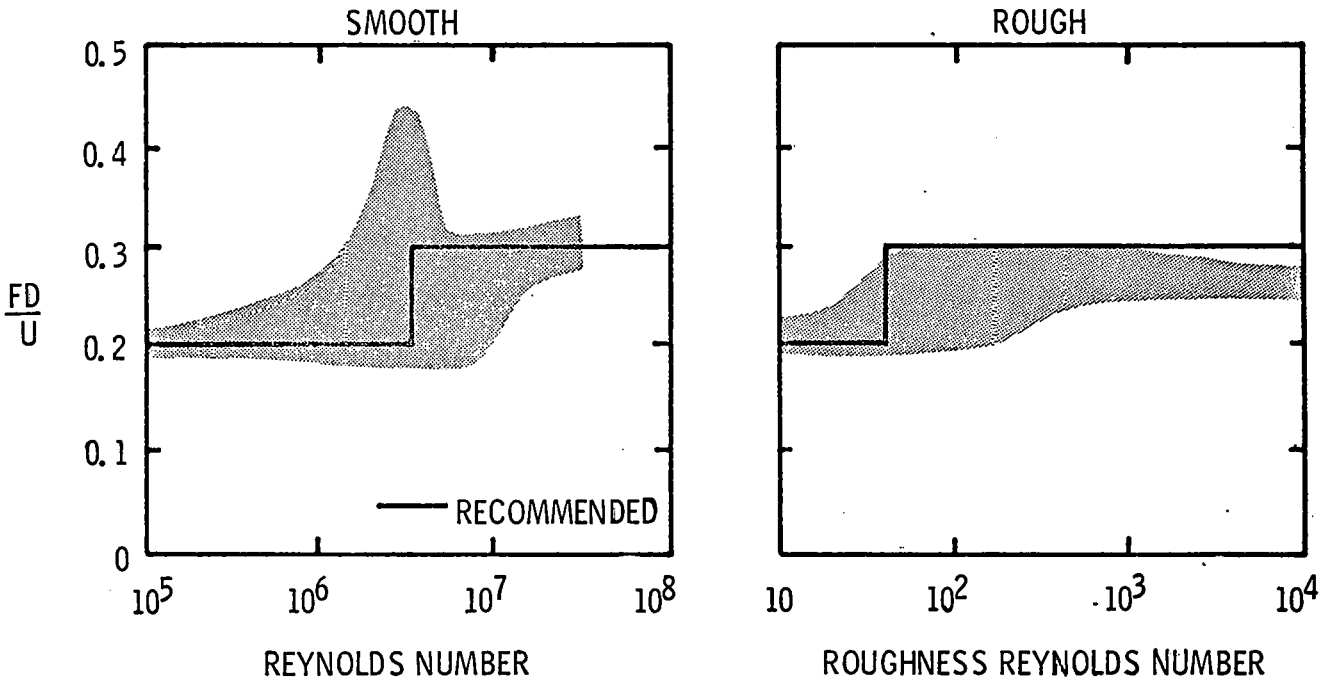



FIGURE 4

tests and to investigate the effects of flow inclination angle.

## Model Design

A series of smooth wall cylinder tests were conducted in September 1976 at the Twelve Foot Pressure Tunnel under the direction of Dr. W. James of Iowa State University and Dr. G. Malcolm of NASA Ames. Their twelve-inch diameter cylinder model is instrumented with 18 static pressure ports equally spaced around the model centerline, 5 rows of 8 static pressure ports along one half of the model length, 12 unsteady pressure transducers equally spaced around the model at a location 3 inches to the right (looking upstream) of the model centerline and 7 surface hot wire shear stress gages in 30-degree increments at a location 3 inches to the left of the centerline. Mean drag coefficients from the NASA tests were used in establishing the design load recommendations presented earlier.

The NASA/ISU test model has been made available for the present test program. In the CalTech tests, the 8.5 foot center section of the model spanned the wind tunnel test section (Figure 5). Large end plates eliminated end effects, and a special mounting mechanism allowed model rotation and inclination. The same instrumentation used at NASA Ames was employed at CalTech. Model surface roughness was varied by covering the cylinder with 40 percent open square mesh wire screens of wire diameters 0.065 and 0.0065 inches (Figure 6). Because the wires overlap, the equivalent roughness is taken to be two wire diameters, and the roughness to model diameter ratios are $10^{-3}$ and $10^{-2}$. Equivalence to a sand-grain type roughness requires experimental verification. Exterior structural reinforcing rings were simulated (Figure 7); the ring heights were $10^{-1}$ model diameters and were spaced at one model diameter. After the normal flow tests the model was yawed to 10 degrees to investigate inclination angle effects for a model with the simulated structural reinforcing rings (Figure 8) and one surface roughness ($k/d = 10^{-3}$).

## Preliminary Test Results

Wind tunnel tests were conducted for smooth and rough cylinders at a Reynolds number of $1.3X10^6$; one smooth wall test was conducted at a Reynolds number of $4X10^5$. The smooth cylinder centerline pressure distributions expressed in terms of a pressure coefficient

$$C_p = \frac{P - P_\infty}{1/2\rho U^2}$$

were asymmetric (Figure 9), and the model experienced a steady lift. It appears that the asymmetries are due to the effects of contamination of the model surface on boundary layer transition and separation. With the addition of the surface roughness, the pressure distribution became quite symmetric and the base pressure decreased (Figure 9). The effect of increasing roughness is to decrease the pressure minimum, a phenomena attributed to early boundary layer separation. The mean pressure distributions are accompanied by large unsteady pressure fluctuations; sample peak excursions are indicated by the bars in Figure 10.

Smooth wall mean drag coefficient data are generally in good agreement with the design curves despite the observed asymmetries in the pressure distribution (Figur 11). However, with the addition of the ring stiffener to the smooth model a low frequency pressure oscillati... was observed, and the mean drag coefficient nearly doubled (Figure 11). The measured mean values changed with model rotation angle (time) as indicated by the error bar. This phenomena is not understood, and will be investigated further in the final phase of the test program. The effect of the uniform surface roughness was to increase the mean drag coefficient as predicted (Figure 11).

When the model with ring stiffeners was yawed to 10 degrees, the low frequency pressure oscillation disappeared, and a well behaved pressure distribution was observed. However, the integrated drag coefficient was about 12 percent lower than expected from the $\cos^3 \propto$ law (Figure 12). Surface roughness ($k/d = 10^{-3}$) gave similar results; at 10 degrees yaw the measured drag coefficient was about 14 percent lower than expected. The effect of yaw angle can thus be conservatively estimated by the $\cos^3 \propto$ law.

## Future Plans

A final phase test program will be conducted at the NASA Ames Twelve Foot Pressure Tunnel in July 1977 using the techniques developed in the CalTech tests. The Reynolds number range will be $2X10^5$ to $8X10^6$. Ring stiffeners will be simulated at two spacings (1 and 1.5 cylinder diameters) on a smooth model. Surface roughness heights of $3X10^{-4}$, $10^{-3}$ and $10^{-2}$ cylinder diameters will be tested. The effect of roughness spacing (39 and 24 percent open screens) will be determined.

## High Reynolds Number Flows

No data is currently available for steady or unsteady pressure distributions on cylinders beyond Reynolds numbers of about $1.2X10^7$. Test facilities including wind tunnels, water tunnels and towing tanks are limited to Reynolds numbers below about $4X10^7$ even allowing for some relaxation of test constraints (e.g., permitting higher blockage ratios in the wind tunnels and lower aspect ratio cylinders). Towing tanks and water tunnels have further problems with surface effects and/or cavitation. Alternative means of simulating the higher Reynolds number flows have also been considered. They include ocean towing; gravity drop or pop up of cylinders in the ocean; and use of alternate fluids in existing facilities, but all appear to offer formidable cost and implementation problems.

Whether or not it is necessary to simulate the high Reynolds number regime beyond $10^7$ depends upon the uncertainty of extrapolating existing results. Current feeling is that no new fluid mechanical phenomena are anticipated with further increases in Reynolds number, however such conclusions require verification. In view of the experimental difficulties in achieving the high Reynolds number conditions, we are first using existing analytical numerical tools to study the parametric behavior and sensitivity of the cylinder boundary layer at high Reynolds number relative to separation and surface

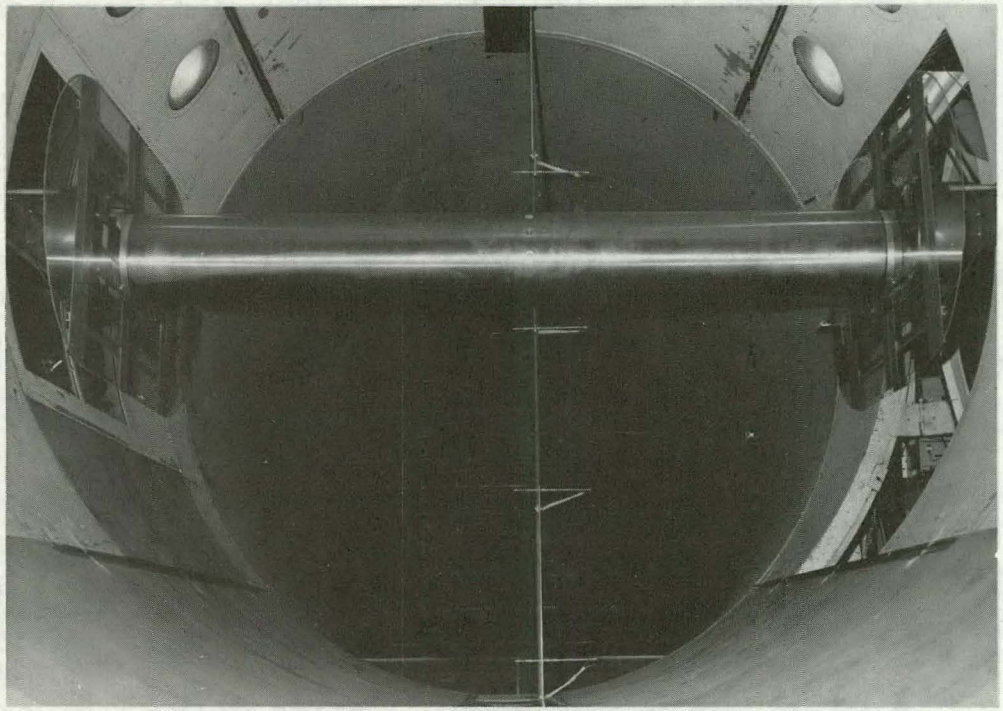


FIGURE 5

CYLINDER TEST ARRANGEMENT FOR CALTECH TEN FOOT TUNNEL TESTS

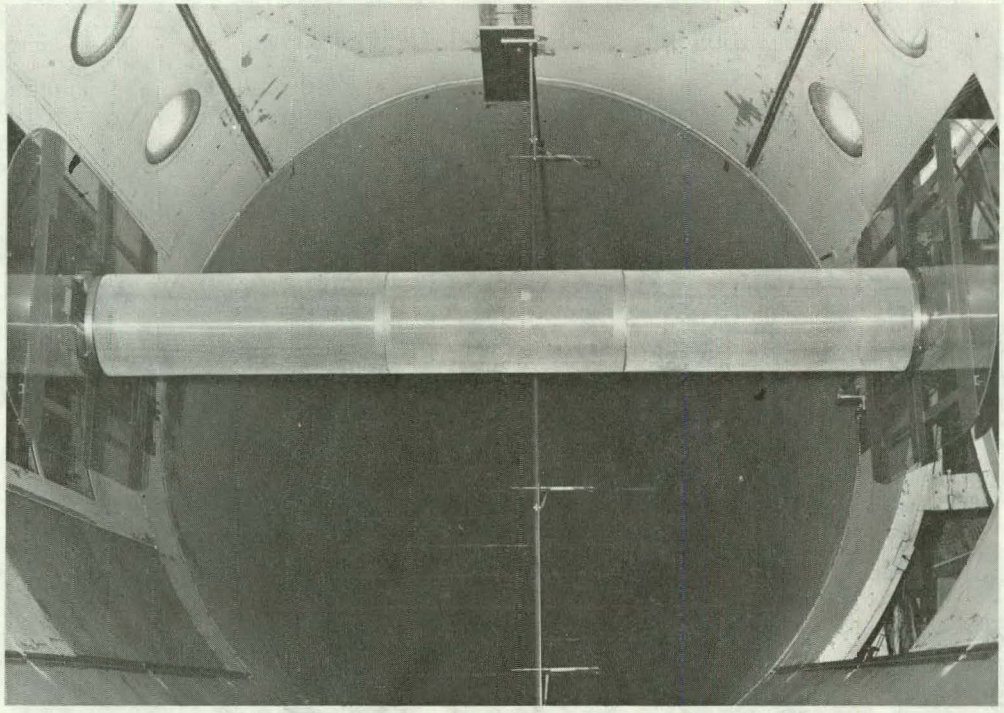


FIGURE 6

CYLINDER MODEL WITH SURFACE ROUGHNESS ATTACHMENT

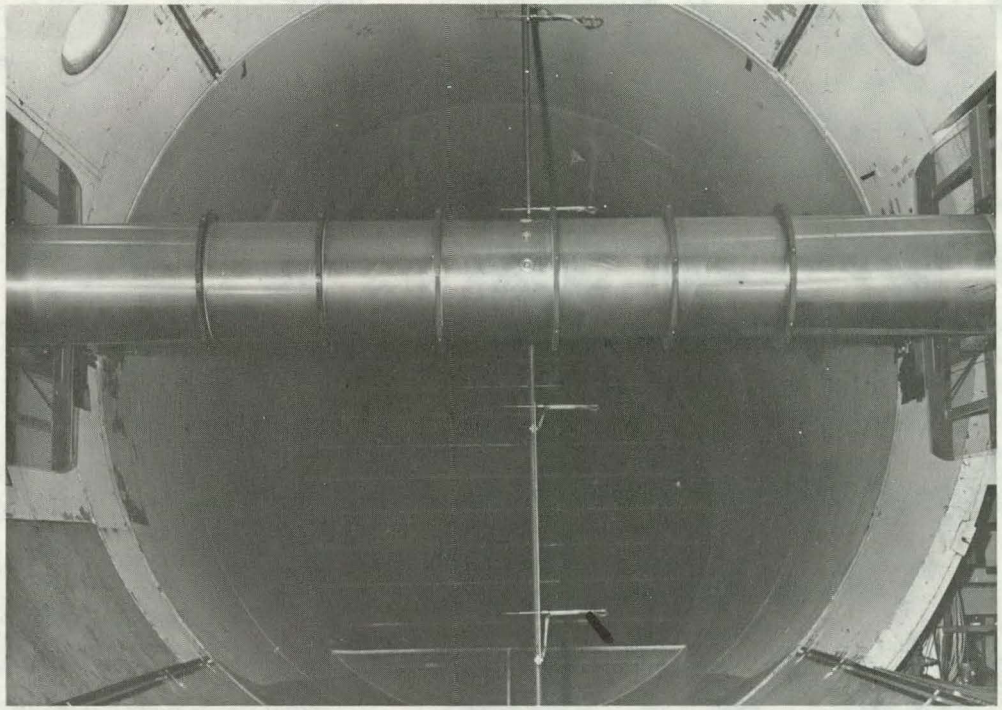


FIGURE 7

SIMULATED STRUCTURAL REINFORCING RINGS

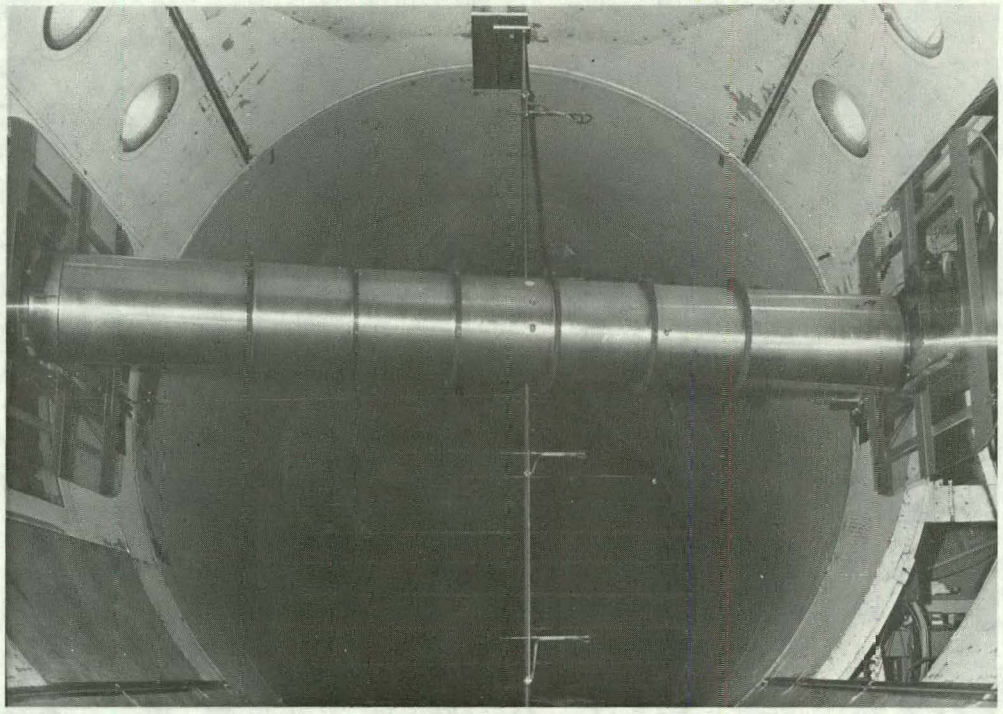


FIGURE 8

YAWED CYLINDER TEST GEOMETRY

# OTEC
# CYLINDER PRESSURE DISTRIBUTIONS

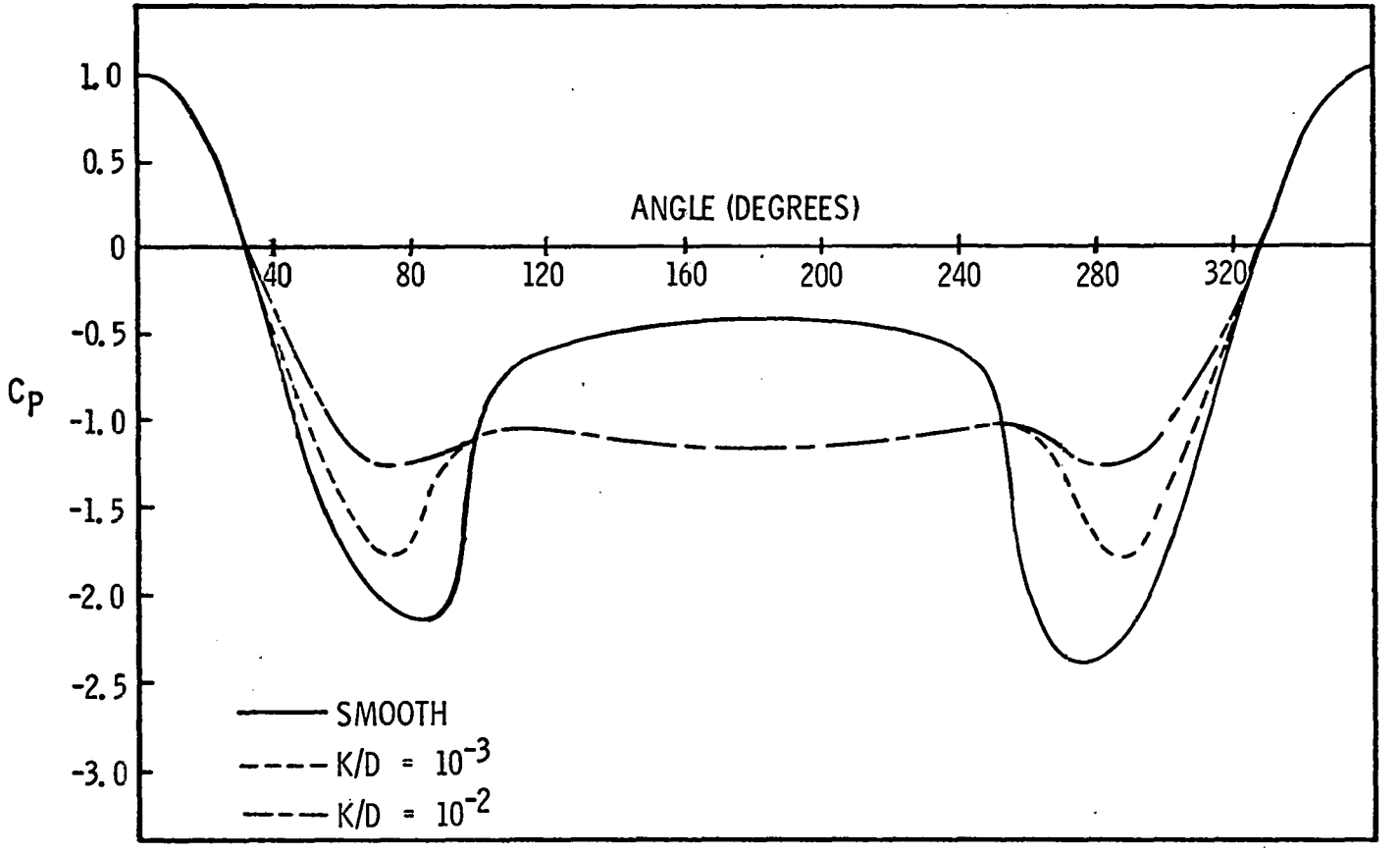



FIGURE 9

# OTEC
# UNSTEADY PRESSURE DISTRIBUTIONS

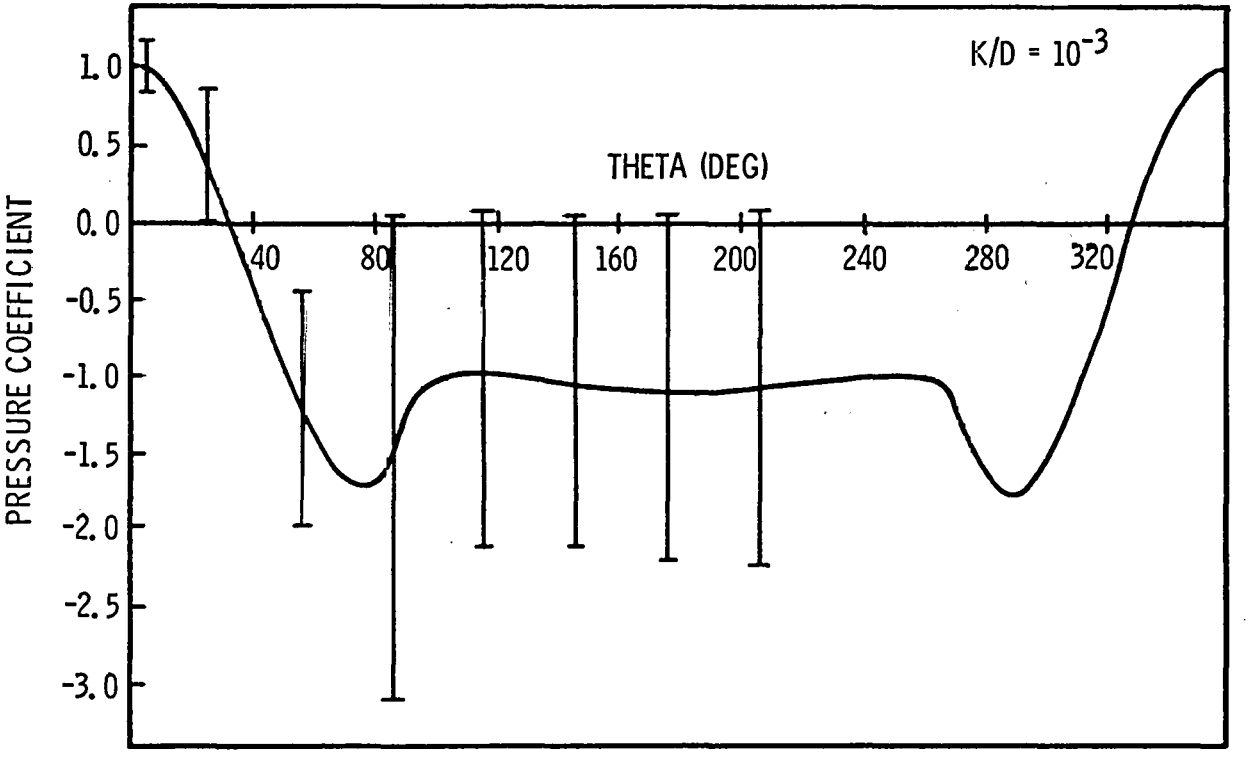



FIGURE 10

# OTEC
# CYLINDER MEAN DRAG COEFFICIENTS

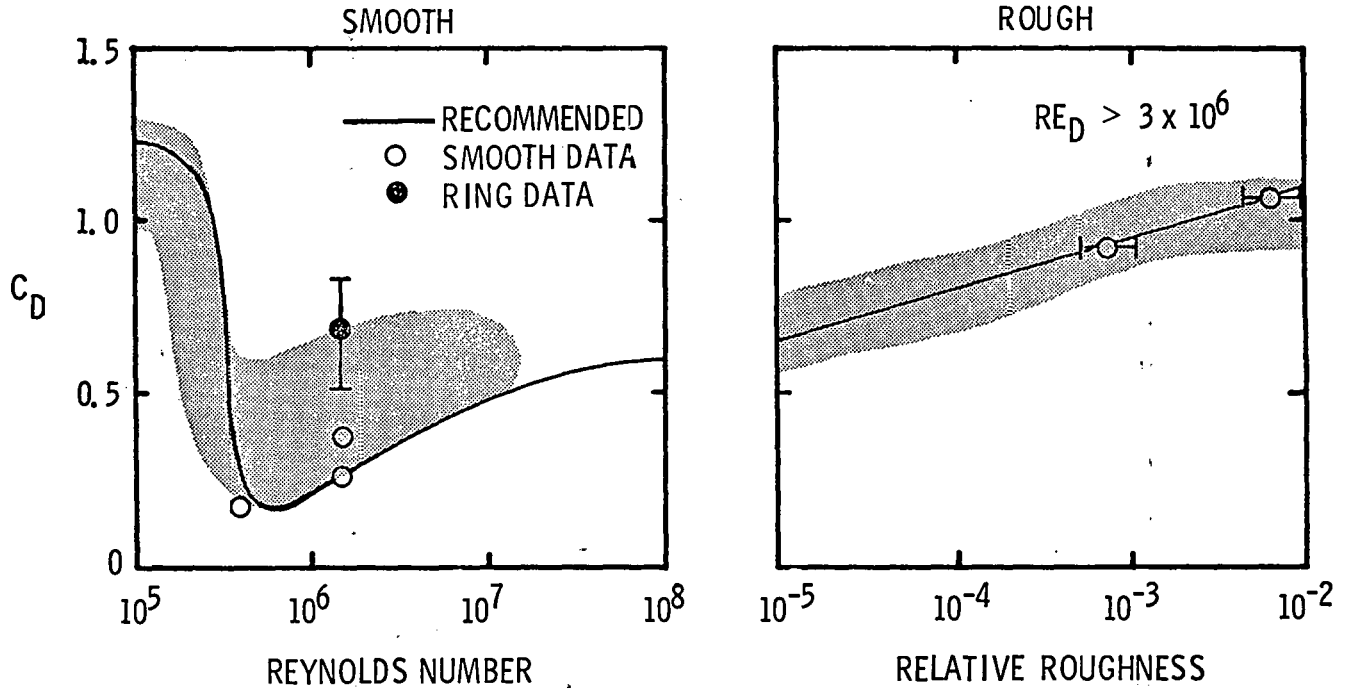



FIGURE 11

# OTEC
# EFFECT OF YAW ANGLE
# ON MEAN DRAG COEFFICIENT

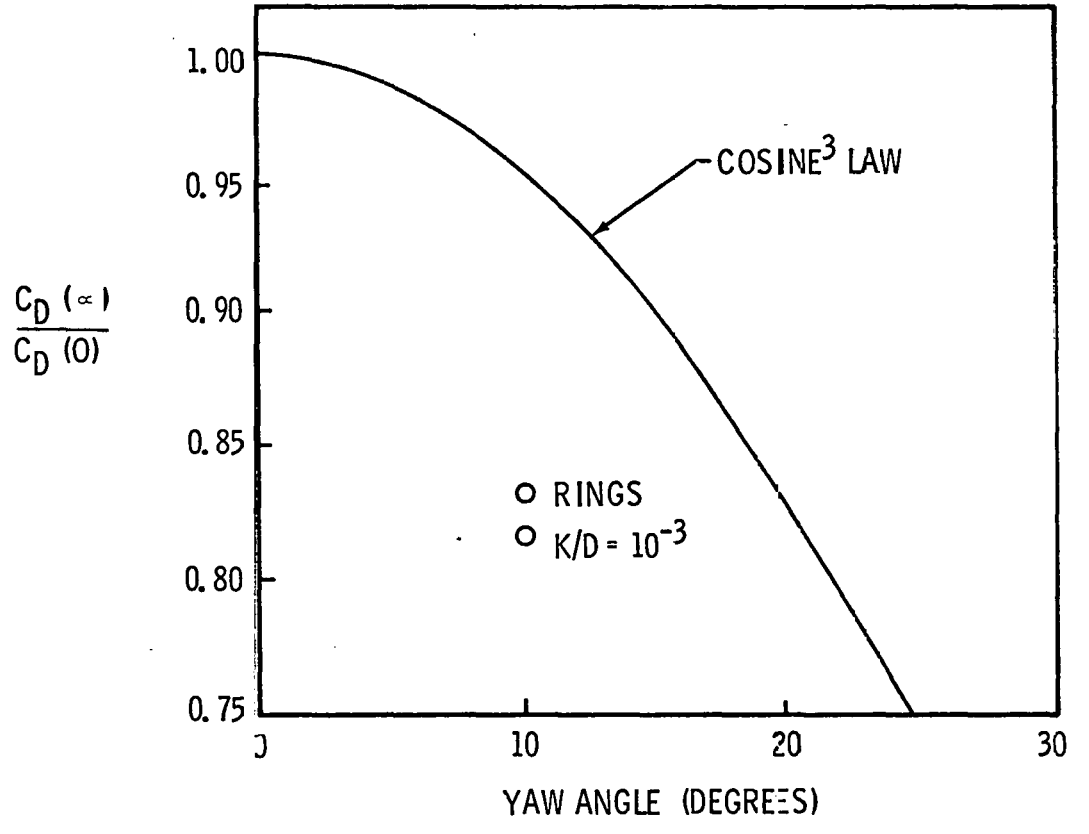



FIGURE 12

roughness. Results from this study will determine whether extrapolation of the current steady flow results reasonable and will identify possible high Reynolds ver simulation techniques using rough or partially gh cylinders at lower Reynolds numbers.

## Summary

Preliminary design criteria have been established for the hydrodynamic loads on the OTEC cold water pipe. Steady drag, rms lift and Strouhal shedding frequency have been specified for smooth and rough cylinders; the OTEC cold water pipe will most surely be rough due to construction or marine biofouling. The effect of inclination angle on steady drag has been demonstrated at one Reynolds number.

A test program is underway to verify the design loads and to provide time dependent pressure distributions which are not currently available in the literature. OTEC unique design geometries (exterior reinforcing rings) are included. Wind tunnel tests are expected to be conducted in July 1977, and the test data will be available by November 1977.

Analytical techniques are being developed to extend the data to higher Reynolds numbers based on the behavior of the cylinder wall boundary layer.

## References

Achenbach, E., 1968 "Distribution of Local Pressure and Skin Friction Around a Circular Cylinder in Cross-flow Up to Re = $5X10^6$," J. Fluid Mech. 34, pp. 625-639.

Achenbach, E., 1971, "Influence of Surface Roughness on the Cross-flow Around a Circular Cylinder," J. Fluid Mech. 46, pp. 321-335.

Albano, E., 1976, "Structural Design Considerations for the OTEC Cold Water Pipe," SAI-77-538-LA.

Fung, Y. C., 1960, "Fluctuating Lift and Drag Acting on a Cylinder in a Flow at Supercritical Reynolds Numbers," J. Aero Space Sci. 27, pp. 801-814 (also STL Rep. GM-TR-0165-00343).

Guven, O., Patel, V. C., and Farell, C., 1975, "Surface Roughness Effects on the Mean Flow Past Circular Cylinders," Iowa Inst. Hydr. Res., Univ. Iowa, IIHR Rep. 175.

Hoerner, S. F., 1965, "Fluid-Dynamic Drag."

Hydronautics, Inc., 1976, "Theoretical Evaluations of the Seakeeping Performance and Resistance/Propulsion Characteristics of Five Candidate OTEC Platforms," TR 7513-1.

James, W., and Malcolm, G., Personal Communication, November 1976.

Johns Hopkins University, 1976, Detailed Report, Maritime and Construction Aspects of Ocean Thermal Energy Conversion (OTEC) Plant Ships APL/JHU SR 76-1B.

Jones, G. W. Jr., Cincotta, J. J., and Walker, R. W., 1969, "Aerodynamic Forces on a Stationary and Oscillating Circular Cylinder at High Reynolds Numbers," NASA TR R-300.

Lockheed, 1975, "Ocean Thermal Energy Conversion Power Plant Technical and Economic Feasibility," Lockheed Missiles and Space Co., Inc. Report NSF/RANN/SE/GI-C937/FR/75/1, Sunnyvale, California.

Miller, B. L., 1976, "The Hydrodynamic Drag of Roughened Circular Cylinders," The Royal Institution of Naval Architects, Paper 9.

Roshko, A., 1970, "On the Aerodynamic Drag of Cylinders at High Reynolds Numbers," U.S.-Japan Research Seminar on Wind Loads on Structures, Honolulu.

Szechenyi, E., 1975, "Supercritical Reynolds Number Simulation for Two-Dimensional Flow Over Circular Cylinders," J. Fluid Mech. 70, pp. 429-542.

TRW, 1975, "Ocean Thermal Energy Conversion Research on an Engineering Evaluation and Test Program," TRW Systems Group, Volumes I through V.

University of Massachusetts, J. G. McGowan, W. E. Heronemus, 1976, "Gulf-Stream Based, Ocean-Thermal Power Plants" J. Hydronautics 10, 2.

# COLD WATER TRANSPORT, COLD WATER PIPE, AND DEEP WATER MOORING LINE ANALYSIS—A PARAMETRIC APPROACH

THOMAS E. LITTLE
*Westinghouse Electric Corporation*
*P. O. Box 1488*
*Annapolis, Maryland*

ABSTRACT

The successful implementation of the ocean thermal power plant is dependent upon the technical and economic feasibility of transporting large volumes of cold water from sea depths of 500 meters or more, through suitable ducting to the power plant condensers. In addition, plant/platform station keeping must be provided by a mooring arrangement and/or by use of dynamic positioning. Highlights of the analysis and evaluation of the cold water transport, cold water pipe, and deep water mooring lines are provided with a view toward judging the impact of these subsystems on the overall OTEC plant/platform concept and to provide an estimate of material and construction cost. Selected parameters, issues, and evaluation criteria are used to assess the merits of candidate subsystems over a range of plant size from 100 MWe to 1000 MWe net output power.

## I. Introduction

The ocean engineering issues affecting the design, construction, deployment, cost and operation of the OTEC power system deserve special consideration in any planned effort to alleviate deficiencies in available technology. In particular, the successful implementation of the OTEC plant is dependent upon the efficient transport of cold seawater from depths of 500 meters or more, upward through suitable ducting, to the power plant condensers. In addition, it is also necessary to maintain the plant/platform on station by a mooring arrangement and/or by use of dynamic positioning.

The study results provided by this paper were selected from OTEC studies (1) conducted by the Westinghouse Electric Corporation, Oceanic Division, for ERDA under contract E(11-1)-2642. In broad terms, the objectives of the Westinghouse study efforts have been directed toward expanding the OTEC ocean engineering technology base. The results provided here are the highlights of an analysis and evaluation of OTEC plant/platform cold water transport, the cold water pipe, and deep water mooring lines. A variety of c.w. pipe and mooring line configurations are identified and described over a range of OTEC plant size from 100 MWe to 1000 MWe net output power by using a parametric approach. It must be accepted that the depth of a parametric analysis does not equal the refined detail that could be carried out in establishing and evaluating one particular design configuration; however, this approach does provide a broad range and variety of plant parameters that can be used to describe OTEC subsystems and components in such a way that the usefulness of the results is not unduly jeopardized as overall plant concepts undergo evolutionary change.

The results presented in the subsequent sections of this report can be used to assess the merits of likely cold water pipe and passive mooring concepts and to provide a basis on which to match actual plant requirements as the thermal cycle issues are resolved. The technology data base provided can be used by OTEC system analysts and program planners as a basis for quantitatively evaluating actual plant/platform requirements and/or in making overall system tradeoff comparisons.

## II. Cold Water Transport

The mass flow rate of cold seawater required for an OTEC power plant is a function of the power cycle heat rejection, condenser design (heat exchanger effectiveness), and the available seawater temperatures. Cold water mass flow rate data available from various OTEC power system studies are summarized by Figure 1. The ratio of cold water mass flow rate to plant net power plotted here was found to be a very useful and pertinent parameter. A constant value of

$$\frac{\dot{m}_{cw}}{\dot{W}_{net}} = 4.17 \frac{kg}{s \cdot kW} \qquad (1)$$

was selected as the baseline for this study as a result of a review and evaluation of previous investigators' studies (see Figure 1). The selection of a constant value for the parameter $\dot{m}_{cw}/\dot{W}_{net}$ assumes that the overall condenser performance and plant efficiency remain constant with plant size. Ultimately the absolute level of $\dot{m}_{cw}/\dot{W}_{net}$ and the variation with plant size can only be determined by actual plant and heat exchanger performance.

The cold water flow path energy losses, pumping power required, and static pressure loads were determined using relevant hydraulic models such as the configuration shown schematically by Figure 2. The following assumptions apply to the models considered:

- The water velocity within the cold water pipe station ② to station ③ is 2 m/s.

- The cold water velocity at the pump inlet, station ⑤ , is approximately 7 m/s.
- The head loss resulting from flow through the condenser is 1.5 meters and is constant over the range of plant net power considered.
- The cold water effluent velocity at station ⑨ is 1 m/s.

The cold water pipe diameter, D, was determined using the assumption of a 2 m/s cold water velocity, an inlet seawater density of 1027.5 kg/m$^3$, and the cold water mass flow relationship provided by Eq. 1. Combining the above it is found from the continuity equation for incompressible flow that

$$D = 1.61 \left(\dot{W}_{net}\right)^{1/2} \qquad (2)$$

where D is in meters and the plant net power, $\dot{W}_{net}$, units are megawatts (MW).

Figure 2 presents the results of a hydraulic analysis using a typical flow-through model as indicated. The cold water is drawn through a screen at station ① , travels up a c.w. pipe of length L and diameter D, makes a right angle turn to enter a particular plant power module, flows through the plant condensers and exits at station ⑨ at approximately 1 m/s. Using the c.w. pipe diameter that is defined by Eq. 2 and a condenser head loss of 1.5 meters, the parametric relationship between ideal pumping power, $\dot{W}_p$, plant net power, $\dot{W}_{net}$, and c.w. pipe length is determined. For example, Figure 2 indicates that for a 1200-meter c.w. pipe the ideal pumping power required is 13% of the plant net output power. The "ideal" notation used here indicates the pumping power required of a 100% efficient pump. An appropriate pump efficiency must be used to obtain the actual pumping power required. Actual c.w. pump efficiency is anticipated to fall within the 85% to 90% range.

The pump head, H, expressed by Figure 2 is required to overcome a viscous dissipation loss, $\dot{E}_k$, that is a combination of the screen loss, contractions, expansions, turning, and the condenser head loss; also contributing to H are the c.w. pipe wall friction, $\dot{E}_f$, the density effect loss $\dot{E}_\rho$, and the effluent kinetic energy loss rate, $\dot{E}_v$. Figure 3 presents analogous results for a pond configuration hydraulic model. As indicated here the results of both hydraulic models are very nearly the same although the physical arrangement of components is somewhat different.

In general the ideal pumping power parameter, $\dot{W}_p/\dot{W}_{net}$, is directly proportional to pump head required and c.w. flow rate. Thus,

$$\frac{\dot{W}_p}{\dot{W}_{net}} \propto H\left(\frac{\dot{m}_{cw}}{\dot{W}_{net}}\right), \qquad (3)$$

and as shown by Figures 2 and 3, the pump head required, H, is directly proportional to the c.w. pipe length, L, indicating that for every 450-meter increase in c.w. pipe length the pump head required will increase roughly 1%. Regarding the relationship provided by Eq. 3, it is instructive to note that the pump head required is determined in large part by the condenser head loss and

**Cold Water Mass Flow Rate**

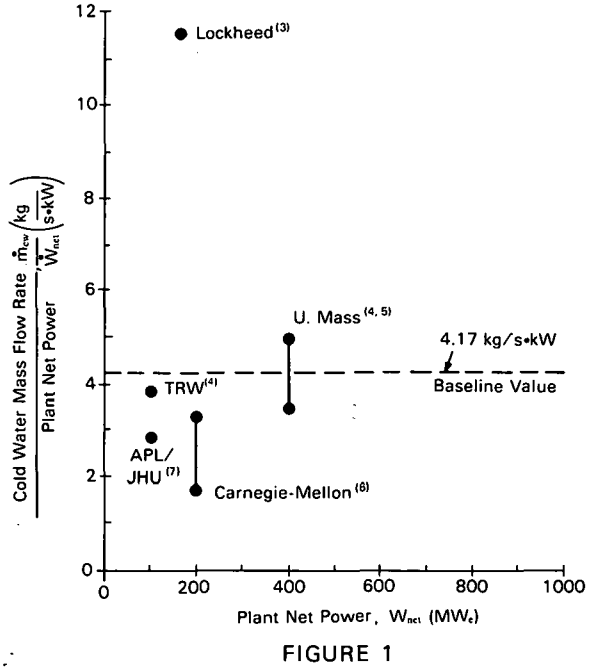



FIGURE 1

**Hydraulic Model - Flow Thru Configuration**

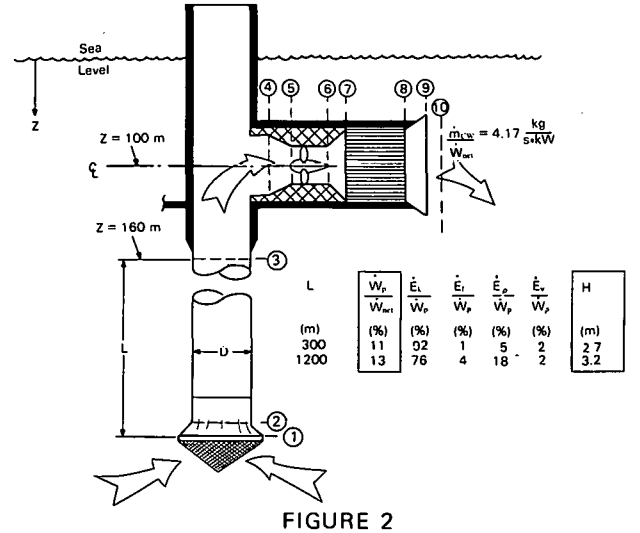



FIGURE 2

Hydraulic Model - Pond Configuration

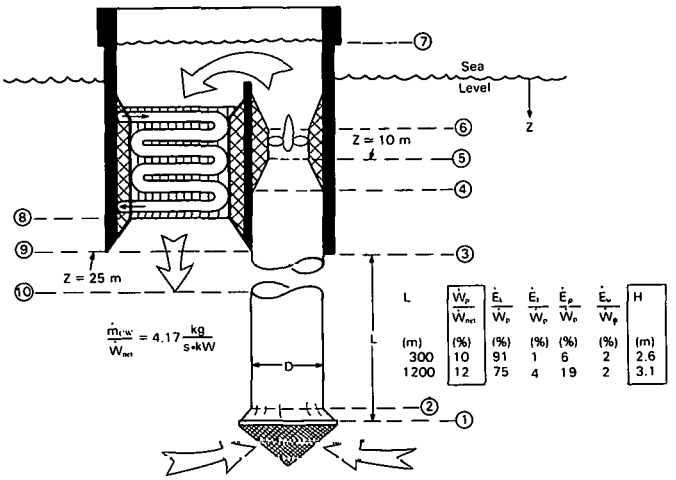



FIGURE 3

Pressure Difference Across C.W. Pipe Wall

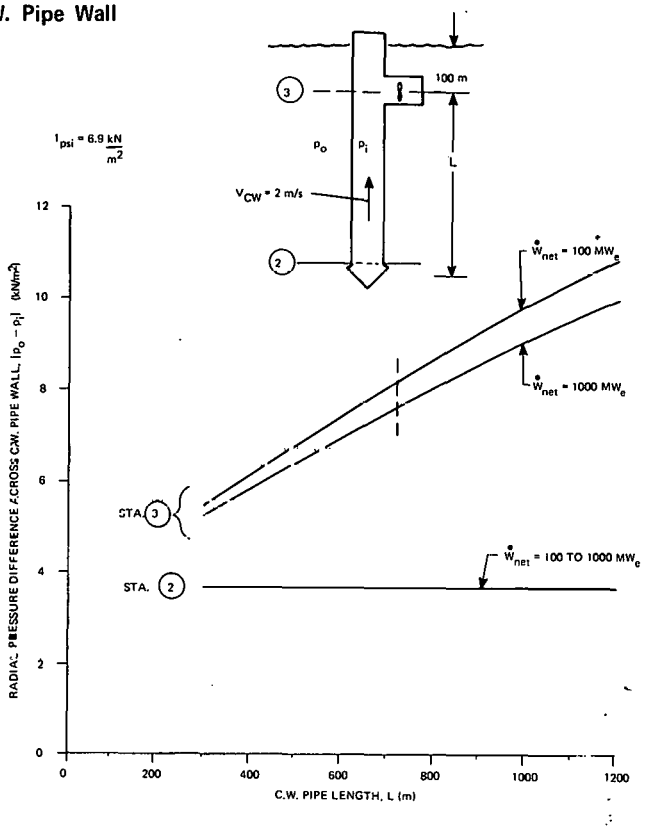



FIGURE 4

the density effect loss, $\dot{E}_\rho$. The density effect loss results from lifting the relatively higher density cold water at station (1) up to a greater potential level, Z, at the effluent exit station (9) . The designer can do little to influence $\dot{E}_\rho$; however, the condenser head loss is a potential tradeoff factor for consideration in future plant power system optimization studies. Eq. 3 can be used to scale from the 1.5-meter condenser head loss assumed in this study. For example, a condenser head loss increase from 1.5 m to 3 m, assuming a 1200-m long c.w. pipe, would increase the pump head required, H, from 3.2 m to 4.7 m. The ideal pumping power parameter, $\dot{W}_p/\dot{W}_{net}$, would in turn increase from 13% to 19.1%.

The static pressure difference across the c.w. pipe wall has a direct influence upon pipe wall structural configuration. In short, the loads due to the radial pressure difference across the wall will in most cases dictate the structural configuration needed to prevent buckling collapse by elastic instability. The static pressure load across the c.w. pipe wall at stations (2) and (3) are shown by Figure 4. The radial pressure difference at station (2) results from the internal flow viscous dissipation losses through the inlet screen, the pipe contraction losses, and the reduction of internal static pressure due to momentum increase of the accelerated internal fluid. Station (2) pressure difference is independent of plant net power and pipe length whereas station (3) pressure difference is a function of plant net power and pipe length. The latter variation occurs because of pipe friction losses and density effect losses.

III. Cold Water Pipe

The cold water pipe concepts outlined by Figure 5 were surveyed based on static loads imparted by the specific design current profile shown and the static pressure loads resulting from cold water flow internal to the pipe. The objective of the static analysis presented here is to quantify the forces applied by a severe ocean environment, including the effects of basic gravity and buoyance forces, upon a spectrum of c.w. pipe configurations. This information in turn is used to determine a first cut c.w. pipe size, weight, and cost as a function of plant net output power.

Ideally, a complete treatment of the dynamic behavior and response of an OTEC platform/pipe coupled system, as well as static behavior, should be a feature of platform and cold water pipe design efforts; however, quantification of the motions of representative OTEC platforms and the influence of such motions on the dynamics of the cold water pipe remain burdened with a host of unresolved questions. ERDA is now funding parallel studies concerned with alleviating deficiencies in this area of available technology. Some of the initial results of investigators concerned with platform dynamics will be presented at this conference.

A steady state load analysis is a necessary, although perhaps not a sufficient, criterion for verifying the structural integrity of candidate c.w. pipe design configurations. With this limitation in mind it is instructive, and not altogether premature, to establish and evaluate conceptual designs of the cold water pipe considering only the influence of severe steady state loads.

A design current profile was used to determine the current moment and shear loads on the c.w. pipe. The current profile used assumes a surface value of 2 m/s that is constant down to a 50-m depth. Below 50 meters the current decreases exponentially with depth in accordance with the relationship shown by Figure 5. In general, it was found that the static radial pressure load on the c.w. pipe was the controlling load that dictates pipe structural configuration necessary to prevent a pipe buckling failure. In other words, for a pipe wall structure that is designed to prevent buckling (due to elastic instability) it is found that the stresses resulting from the design current moment and shear loads, hoop loads, and self-weight loads fall below allowable limits. Specifically, a c.w. pipe wall thickness to pipe diameter ratio, t/D parameter was established for a ring-stiffened cylindrical shell such that the critical buckling pressure exceeded the calculated radial pressure by a factor of 2 (i.e., buckling safety margin = 2). The buckling equation for long, thin, ring-stiffened cylindrical shells subject to an external radial pressure (8) was used to calculate the critical collapse pressure. The stresses resulting from all other static loading conditions are then calculated to confirm that the established pipe configuration has sufficient strength under combined loading conditions.

Table 1 provides a summary of the configuration, maximum stress ratio, and weight evaluation of ring stiffened cold water pipe structures constructed of aluminum, steel, and glass-reinforced plastic. The pipe diameter versus plant net power was determined from Eq. 1. The shell parameter, t/D, at station ③ of the c.w. pipe is based on the radial pressure loads (shown by Figure 4) acting on a cylindrical structure with ring stiffeners spaced two pipe diameters apart and a critical buckling safety margin of 2.

The maximum stress due to the tensile, compressive, and shear loads was determined by combining the stresses from each load to obtain the maximum overall shear stress, $\tau_{max}$, that may occur within the pipe structure. The allowable stress, $\tau_{allow}$, comes from the Maximum Shear Theory (9) failure criteria and is defined as one-half the material yield stress. The ratio $\tau_{max}/\tau_{allow}$ shown is therefore a quantitative measure, a measure of the proximity of maximum stresses occurring in the c.w. pipe to an allowable limit based on the Maximum Shear failure criteria. It is of interest to note that the stress ratio $\tau_{max}/\tau_{allow}$ increases rapidly as the pipe diameter decreases (lower net plant power range). This trend, shown by Figure 6, indicates that for pipe diameters less than 16 meters the controlling structural criteria for a cantilevered pipe shift to a consideration of current loads instead of the previously described buckling criteria. This particular difficulty could possibly be eliminated by reducing the stress contribution due to bending by using additional longitudinal stiffening or by utilizing a cold water pipe that is free to pivot at the platform interface.

**Cold Water Pipe Concepts Selected For Analysis And Evaluation**

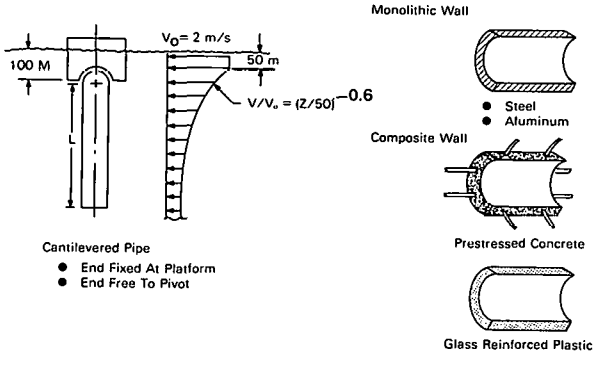



FIGURE 5

**Maximum Stress From Combined Tensile, Compressive, And Shear Loads (Current Forces Only) Top Of 600m C.W. Pipe**

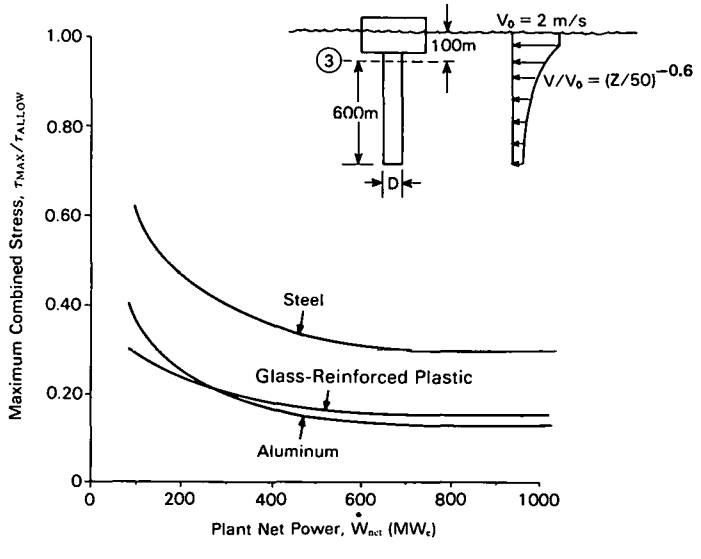



FIGURE 6

TABLE 1

**Aluminum Cold Water Pipe**
**Ring Stiffened Cylindrical Shell**

| PLANT NET POWER, $\dot{W}_{net}$ (MWe) | PIPE LENGTH, L (m) | PIPE DIAMETER, D (m) | SHELL[a] THICKNESS, $\frac{t}{D} \times 10^3$ | COMBINED[b] STRESS RATIO, $\frac{\tau_{max}}{\tau_{allow}}$ | PIPE WEIGHT IN AIR, $\frac{Wt}{\dot{W}_{net}}$ (metric ton / MWe) | PIPE WEIGHT IN SEA WATER, $\left[\frac{Wt - \Delta}{\dot{W}_{net}}\right]$ (metric ton / MWe) |
|---|---|---|---|---|---|---|
| 100 | 300 | 16.1 | 1.97 | 0.16 | 12.8 | 8.1 |
| 400 | ↓ | 32.2 | ↓ | 0.07 | ↓ | ↓ |
| 800 | ↓ | 45.5 | ↓ | 0.06 | ↓ | ↓ |
| 100 | 600 | 16.1 | 2.18 | 0.35 | 27.1 | 17.1 |
| 400 | ↓ | 32.2 | ↓ | 0.15 | ↓ | ↓ |
| 800 | ↓ | 45.5 | ↓ | 0.13 | ↓ | ↓ |
| 100 | 1200 | 16.1 | 2.48 | 0.64 | 58.5 | 36.8 |
| 400 | ↓ | 32.2 | ↓ | 0.27 | ↓ | ↓ |
| 800 | ↓ | 45.5 | ↓ | 0.23 | ↓ | ↓ |

**Steel Cold Water Pipe**
**Ring Stiffened Cylindrical Shell**

| PLANT NET POWER $\dot{W}_{net}$ (MWe) | PIPE LENGTH, L (m) | PIPE DIAMETER, D (m) | SHELL[a] THICKNESS, $\frac{t}{D} \times 10^3$ | COMBINED[b] STRESS RATIO, $\frac{\tau_{max}}{\tau_{allow}}$ | PIPE WEIGHT IN AIR, $\frac{Wt}{\dot{W}_{net}}$ (metric ton / MWe) | PIPE WEIGHT IN SEA WATER, $\left[\frac{Wt - \Delta}{\dot{W}_{net}}\right]$ (metric ton / MWe) |
|---|---|---|---|---|---|---|
| 100 | 300 | 16.1 | 1.37 | 0.28 | 25.5 | 22.2 |
| 400 | ↓ | 32.2 | ↓ | 0.18 | ↓ | ↓ |
| 800 | ↓ | 45.5 | ↓ | 0.16 | ↓ | ↓ |
| 100 | 600 | 16.1 | 1.52 | 0.55 | 53.9 | 46.8 |
| 400 | ↓ | 32.2 | ↓ | 0.32 | ↓ | ↓ |
| 800 | ↓ | 45.5 | ↓ | 0.30 | ↓ | ↓ |
| 100 | 1200 | 16.1 | 1.73 | 1.10 | 116.4 | 101.2 |
| 400 | ↓ | 32.2 | ↓ | 0.66 | ↓ | ↓ |
| 800 | ↓ | 45.5 | ↓ | 0.58 | ↓ | ↓ |

**Glass-Reinforced Plastic Cold Water Pipe**
**Ring Stiffened Cylindrical Shell**

| PLANT NET POWER, $\dot{W}_{net}$ (MWe) | PIPE LENGTH, L (m) | PIPE DIAMETER, D (m) | SHELL[a] THICKNESS, $\frac{t}{D} \times 10^3$ | COMBINED[b] STRESS RATIO, $\frac{\tau_{max}}{\tau_{allow}}$ | PIPE WEIGHT IN AIR, $\frac{Wt}{\dot{W}_{net}}$ (metric ton / MWe) | PIPE WEIGHT IN SEA WATER, $\left[\frac{Wt - \Delta}{\dot{W}_{net}}\right]$ (metric ton / MWe) |
|---|---|---|---|---|---|---|
| 100 | 300 | 16.1 | 3.16 | 0.13 | 12.7 | 5.0 |
| 400 | ↓ | 32.2 | ↓ | 0.08 | ↓ | ↓ |
| 800 | ↓ | 45.5 | ↓ | 0.07 | ↓ | ↓ |
| 100 | 600 | 16.1 | 3.51 | 0.27 | 26.9 | 10.6 |
| 400 | ↓ | 32.2 | ↓ | 0.16 | ↓ | ↓ |
| 800 | ↓ | 45.5 | ↓ | 0.15 | ↓ | ↓ |
| 100 | 1200 | 16.1 | 3.98 | 0.47 | 57.9 | 22.9 |
| 400 | ↓ | 32.2 | ↓ | 0.28 | ↓ | ↓ |
| 800 | ↓ | 45.5 | ↓ | 0.24 | ↓ | ↓ |

(a) Shell thickness at station ③ based on a ring stiffener spacing S/D = 2 and a critical buckling safety margin $\frac{\Delta P_{cr}}{\Delta P_{allow}} - 2$.

(b) Combined tensile, compressive, and shear stress ratio for a cantilevered pipe with end fixed at the platform.

The pipe weights shown by Table 1 were calculated based on the shell thickness at station ③ tapering linearly to station ② . The shell thickness at station ② is determined from the radial pressure loads at that point (see Figure 4) using a buckling safety margin of 2.

A prestressed concrete cold water pipe is somewhat unique relative to the metal and reinforced plastic pipe designs because of the pretension involved and the generally accepted requirement for coverage of the reinforcing and prestressing steel to prevent corrosion. A steel coverage of 4 cm to 6 cm suggested from Ref.(10) can, in some cases, increase shell thickness to a point where the total wall thickness exceeds that required to withstand all other loads. Experimental work by Haynes (11) with concrete hydrostatic pressure vessels indicates that Bresse's equation (12) is applicable to long, thin-wall ($t/D < 0.03$) concrete cylinders.

Table 2 provides a summary of the configuration, stress ratios, and weights of a concrete c.w. pipe with a shell thickness that provides a critical pressure buckling margin of 2 and/or 5 cm of structural steel coverage. As indicated, the prestress in the concrete is taken to be 80% of the allowable concrete yield strength. The allowable concrete yield strength used here is taken to be 45% of the uniaxial compressive yield strength. The pretension to achieve the above concrete prestress was assumed to come from steel tendons with a cross-sectional area of 10% of the total. These pretension conditions lead to a prestress in the tendons of 14.4% of the steel yield strength.

Cold water pipe costs for the individual conceptual designs analyzed are summarized in Table 3. The cost reflected here is a combination of materials cost plus in-place construction cost. The concrete pipe design is the only configuration where the pipe cost per unit plant net power is not a constant value. This is due to the requirement for 5-cm steel coverage which begins to control the shell thickness at plant power levels less than 200 MWe (D < 23 meters) whereas for plant net power above 200 MWe (D > 23 meters) the buckling criteria dictates shell thickness.

## IV. Deep Water Mooring Lines

A passive mooring system for an OTEC plant/platform will consist of mooring lines, line handling machinery (winches, etc.), attachment hardware, and an appropriate anchor. In the study effort reported here, only the performance potential and costs or mooring lines themselves were treated; the objective is to provide parametric information about line capacity and cost in a very general way without reference to a particular platform configuration or anchor type. As an example of the technique and results that can be obtained, two mooring line configurations will be described; the first is a line using currently available hardware and the second is an advanced concept that can be sized to develop considerably more holding power in a greater range of water depths than any of the conventional mooring line types. The physical properties of the mooring lines considered

TABLE 2

**Prestressed Concrete Cold Water Pipe**

| PIPE NET POWER, $\dot{W}_{net}$ (MWe) | PIPE LENGTH, L (m) | PIPE DIAMETER, D (m) | SHELL[a] THICKNESS, $\frac{t}{D} \times 10^3$ | COMBINED[b] STRESS RATIO IN TENDONS, $\frac{T_{max}}{T_{allow}}$ | COMBINED[b] STRESS RATIO IN CONCRETE, $\frac{T_{max}}{T_{allow}}$ | PIPE WEIGHT IN AIR, $\frac{Wt}{\dot{W}_{net}}$ (metric ton / MWe) | PIPE WEIGHT IN SEA WATER, $\left[\frac{Wt - \Delta}{\dot{W}_{net}}\right]$ (metric ton / MWe) |
|---|---|---|---|---|---|---|---|
| 100 | 300 | 16.1 | 9.32 | 0.19 | 0.62 | 63.1 | 41.0 |
| 400 | ↓ | 32.2 | 6.34 | 0.18 | ↓ | 42.9 | 27.9 |
| 800 | | 45.5 | 6.34 | 0.17 | | 42.9 | 27.9 |
| 100 | 900 | 16.1 | 9.32 | 0.24 | 0.47 | 120.3 | 78.4 |
| 400 | ↓ | 32.2 | 7.04 | 0.22 | ↓ | 90.0 | 59.2 |
| 800 | | 45.5 | 7.04 | 0.22 | | 90.9 | 59.2 |
| 100 | 1200 | 16.1 | 9.32 | 0.34 | 0.20 | 228.5 | 148.8 |
| 400 | ↓ | 32.2 | 7.99 | 0.27 | ↓ | 195.9 | 127.6 |
| 800 | | 45.5 | 7.99 | 0.26 | | 195.9 | 127.6 |

(a) Shell thickness at station ③ based on a critical buckling safety margin $\left(\Delta P_{cr} / \Delta P_{allow}\right) = 2$ and/or a 5 cm (2 in.) rebar coverage.

(b) Combined tensile, compressive, and shear stress ratio for a cantilevered pipe with end fixed at the platform, where
- Prestress in concrete = 0.8 $S_y$ (compression)
- Prestress in steel = 0.144 $S_y$ (tension)
- Steel Tendons cross-sectional area, x, assumed as 10 percent of total

TABLE 3

**Cold Water Pipe Cost Summary**

(Mid-1976 Dollars)

| Plant Net Power, $\dot{W}_{net}$ (MWe) | Pipe Length, L (m) | Pipe Cost/Plant Net Power, $\frac{\text{Dollars}}{\dot{W}_{net}}$ $\left(\frac{\$}{kWe}\right)$ Steel | Aluminum | Prestressed Concrete | Glass-reinforced Plastic |
|---|---|---|---|---|---|
| 100 | 300 | 23.6 | 47.4 | 15.8 | 67.1 |
| 400 | ↓ | ↓ | ↓ | 10.7 | ↓ |
| 800 | | | | 10.7 | |
| 100 | 600 | 49.9 | 100.3 | 30.1 | 142.0 |
| 400 | ↓ | ↓ | ↓ | 22.7 | ↓ |
| 800 | | | | 22.7 | |
| 100 | 1200 | 107.7 | 216.4 | 57.1 | 305.7 |
| 400 | ↓ | ↓ | ↓ | 49.0 | ↓ |
| 800 | | | | 49.0 | |

TABLE 4

**Mooring Line Physical Properties**

| MATERIAL | CONFIGURATION | SIZE | STATIC BREAKING STRENGTH, $T_{max}$ (MN) | WEIGHT IN AIR, Wt. (N/m) | WEIGHT IN WATER $\left[Wt. - \Delta\right]^*$ (N/m) | DATA SOURCE |
|---|---|---|---|---|---|---|
| Steel | Chain (ORQ) | 15.2 cm dia. | 16 | 5251 | 4570 | Ramnas Bruk[13] |
| Steel (alluy) | Chain (Super) | 12.7 cm dia. | 13 | 3682 | 3206 | Ramnas Bruk[13] |
| Steel | Wire Rope | 6.4 cm. dia. | 1.7 | 126 | 110 | U.S. Steel[14] |
| Synthetic Fiber | Nylon Braid | 76.2 cm. circ. | 10 | 389 | 48 | Sampson[15] |
| Steel (HY80) Hollow Cylindrical Links, L/D = 10 | Design Depth (m) 1500 | Diameter (m) 0.520 | Wall Thickness (cm) 1.72 | 15 | 2595 | 714 | Westinghouse |
| | 3000 | 0.466 | 1.93 | ↓ | | 908 | Conceptual |
| | 6000 | 0.337 | 2.80 | | | 1297 | Design |
| | 1500 | 1.62 | 5.35 | 146 | 25,261 | 6947 | |
| | 3000 | 1.46 | 6.06 | ↓ | | 8841 | |
| | 6000 | 1.05 | 8.71 | | | 12630 | |
| | 1500 | 2.84 | 9.37 | 445 | 76,996 | 21174 | |
| | 3000 | 2.54 | 10.54 | ↓ | | 26949 | |
| | 6000 | 1.84 | 15.27 | | | 38498 | |

* $\Delta$ = sea water displacement (buoyant force)

are summarized in Table 4. In developing the parameters indicative of mooring line performance the following assumptions were used.

- The current and wave forces acting along the mooring line are insignificant in comparison to the forces at the platform connection, $F_H$, due to platform drag.
- The mooring line is flexible and inelastic.
- All forces acting on the mooring line are of a steady-state nature (i.e., motion dynamics was not considered).

A two-component mooring line, shown by Figure 7, consisting of a 76.2-cm circumference nylon braid and a 12.7-cm diameter steel alloy chain represent the most promising state-of-the-art approach to deep water mooring using currently available hardware. A multi-component catenary analysis was used to obtain the line performance presented by Figure 8. The relationship between line tension ratio, $T/T_{max}$, as a function of horizontal force at the platform connection, $F_H$, and water depth, Z, is based on a $T_{max}$ equal to the static breaking strength of the weakest line section. All mooring lines have a design line length to seawater depth ratio (scope) such that the line angle $\theta_1 = 0^\circ$ up to the point where $T/T_{max} = 1$. This procedure of selecting a design scope ensures that the anchor will not be subjected to a vertical pulling force until the mooring line tension exceeds the line's static breaking strength. The static breaking strengths, $T_{max}$, used here are listed in Table 4.

The performance parameters of the braid-chain mooring lines and a pure chain mooring line are shown by Figure 8. In water depths less than 1500 m the pure chain line compares favorably with the braid-chain line; however, as depth increases the chain self-weight begins to limit its holding power. At 4600 meters water depth, the pure chain will reach its breaking strength due to self-weight alone, whereas the braid-chain line continues to provide a significant horizontal restraining force.

**Nylon Braid-Chain**
**Two Component Mooring Line**

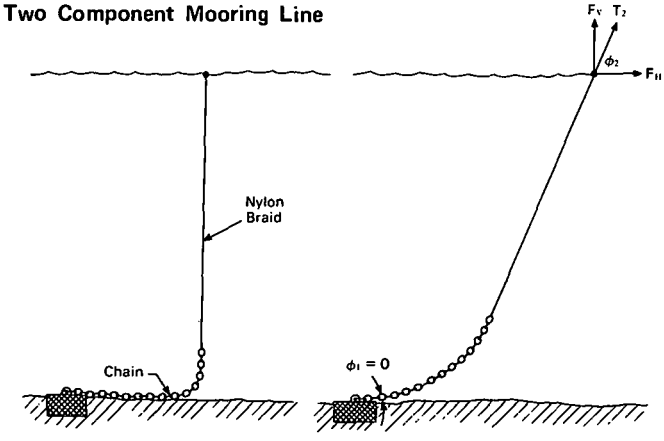



FIGURE 7

**Nylon Braid-Chain (Two Component Mooring Line)**
**Line Tension Vs. Horizontal Force**

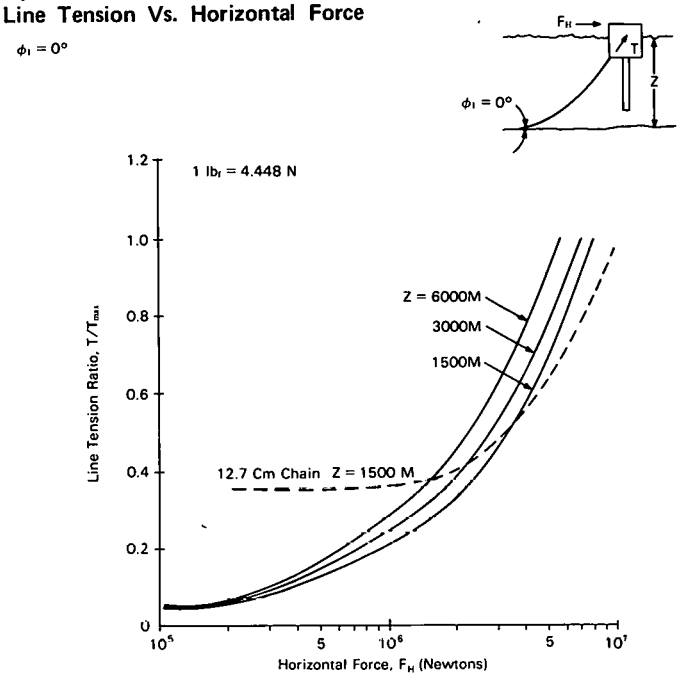



FIGURE 8

As a guide, it is accepted practice in the offshore drilling industry (16) to limit line tension to 33% of the static breaking strength (i.e., $T/T_{max}$ = 0.33) for operating conditions and to 50% of the breaking strength ($T/T_{max}$ = 0.50) for storm conditions. Using a maximum of $T/T_{max}$ = 0.33, Figure 8 indicates that the braid-chain line will provide 2 x $10^6$ newtons (2MN) of horizontal restraining force in 1500-m deep water while the all chain line at this sea depth exceeds the $T/T_{max}$ limit due to its self-weight along.

An advanced concept mooring line, consisting of interconnecting hollow cylindrical links (HCL) as shown by Figure 9, can be sized to develop considerably more holding power in a greater range of water depths than any of the conventional mooring line types. The HCL's are steel pressure vessels with internal buoyancy voids to reduce their in-water weight. They have many of the advantages of chain (ruggedness, corrosion allowance capacity, high strength) without the debilitating weight penalty of chain. The HCL's do have their shortcomings in that they are not a standard commercially available item like chain and braid and must be designed and built specifically for the OTEC application; hence their cost is estimated to be relatively high. The end fittings that interconnect the links must be sized to transmit loads from link to link and provide a moveable joint for ease of deployment and the ability to respond to platform motions.

Table 4 provides a physical description of the HCL conceptual design configurations used for mooring line performance presented by Figure 10. The performance potential of the HCL line concept is evident from the results provided by Figure 10. For example, at a sea depth Z = 1500 meters and a line tension ratio $T/T_{max}$ = 0.33 a HCL mooring line with a static breaking strength of 15 MN will provide 4 MN horizontal restraining force at the platform connection. This restraining force is a factor of 2 times better than the braid-chain line. A HCL line designed for a static breaking strength of 146 MN has the potential to provide 40 MN of horizontal restraining force. In theory HCL lines designed for breaking strengths up to 445 MN might be considered; however, the difficulty of fabricating such thick wall pressure vessels becomes a limiting factor.

**Hollow Cylindrical Link (HCL) Concept**

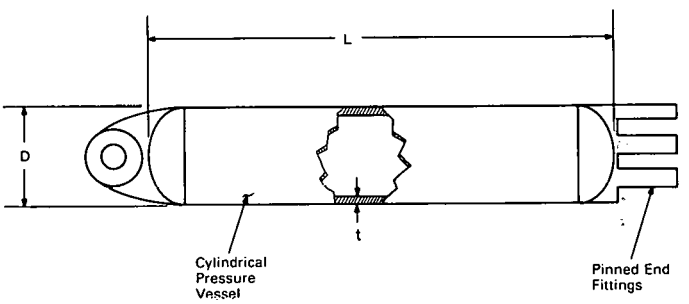



FIGURE 9

**Hollow Cylindrical Link Mooring Line**
**Tension Vs Horizontal Force**
**Z = 1500 Meters**

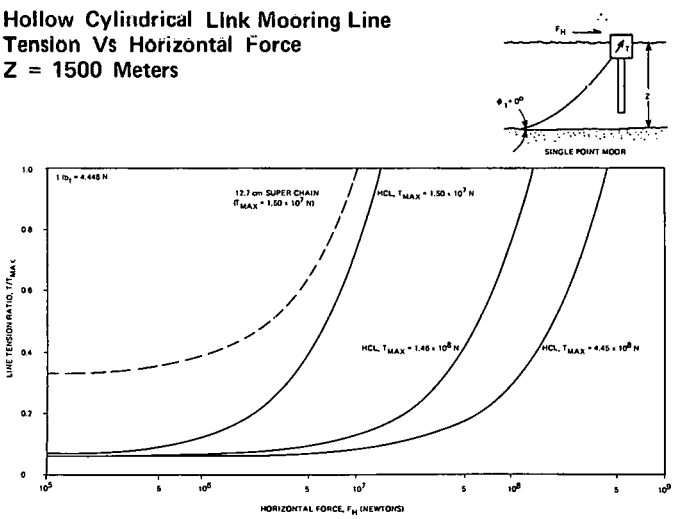



FIGURE 10

The cost comparison of a pure chain line, a two-component braid-chain line, and hollow cylindrical link es of various breaking strengths are provided by Figure 11. Cost at sea depths of 1500 m, 3000 m, and 6000 m are shown for the two-component and HCL lines. Cost for sea depths of 600 m and 1500 m for pure chain lines are shown for comparison.

**Single Point Mooring Line Cost Vs. Line Breaking Strength**

**(Mid-1976 Dollars)**

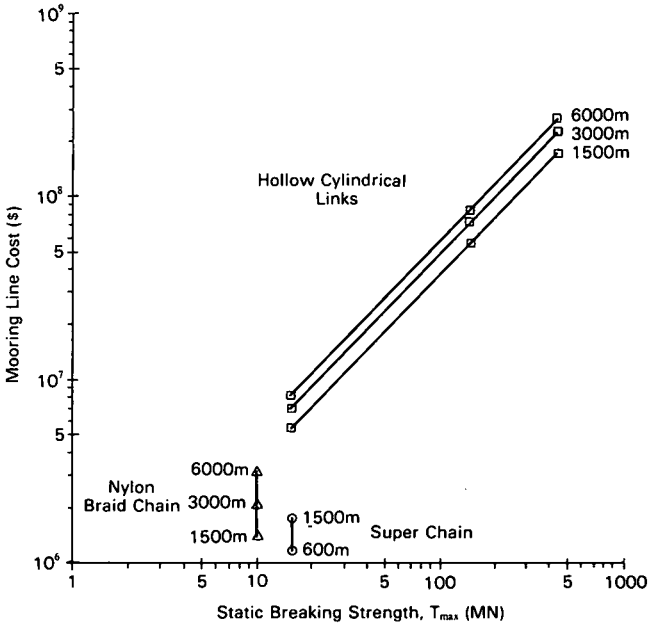



FIGURE 11

## V. Conclusions

A parametric approach was used to provide a description of OTEC plant/platform cold water transport, the cold water pipe, and deep water mooring lines and to assess the merits of candidate concepts over a range of plant size from 100 MWe to 1000 MWe net output power. In light of the analyses and evaluations performed, the following conclusions are offered:

1. A review and evaluation of previous investigators' studies indicates that an OTEC plant will require a cold water mass flow rate of approximately 4.2 kg per second for every kilowatt of net power generated. A high of 11.5 kg/s•kw for a very conservatively rated plant condenser and a low of 1.7 kg/s•kw for a high performance condenser covers the range of surveyed data.

2. Using a baseline cold water mass flow rate parameter, $\dot{m}_{cw}/\dot{W}_{net}$, of 4.17 kg/s·kw and a condenser head loss of 1.5 meters, the ideal pumping power (100% pump efficiency) required for the cold water flow path was found to be roughly 12% of plant net power,

$$\frac{\dot{W}_p}{\dot{W}_{net}} = 0.12.$$

An increase in condenser head loss from 1.5 m to 3 m increases the cold water pumping power (ideal) to 19% of plant new power.

3. Assuming steady state loads only (i.e., no dynamic loads), it was found that the radial pressure difference across the cold water pipe wall dictates the pipe wall structural configuration. For cylindrical c.w. pipes with diameters greater than 16 meters, the pipe shell thickness needed to prevent buckling collapse of the pipe by elastic instability is in excess of the thickness required to safely handle the loads resulting from self-weight and current forces.

4. The weight in seawater of a 600-meter long, ring-stiffened, cylindrical glass-reinforced plastic (GRP) cold water pipe was found to be 10.6 metric tons per megawatt of plant net power. As contrasted with the other materials evaluated, a GRP pipe offers the least weight penalty. In comparison an aluminum c.w. pipe weighs 17.1 metric tons/MWe, a steel pipe 46.8 metric tons/MWe, and a concrete pipe weighs roughly 59.2 metric tons/MWe in seawater.

5. The cost of a 600-m, prestressed concrete pipe was estimated to be roughly $23 to $30 per kilowatt of plant net power, depending on the design criteria used to establish the pipe wall thickness. In comparison the 600-m steel pipe cost estimate was $50/KWe, an aluminum pipe $100/KWe, and a glass-reinforced pipe was $142/KWe.

6. The largest commercially available mooring lines are capable of exerting horizontal restraining forces in the range of $1 \times 10^6$ to $5 \times 10^6$ newtons (1 MN - 5 MN), assuming the line tensions are not allowed to exceed 50% of the static breaking strength of the line. The cost of a single mooring line of this type ranges from $1.2 million to $3.3 million depending on mooring depth.

7. To achieve holding forces above $5 \times 10^6$ newtons (5 MN) requires advanced mooring concepts such as a specially designed and constructed Hollow Cylindrical Link (HCL) mooring line. Single line cost for this type line ranges from $5.7 million to $240 million depending on line strength and mooring depth.

References


1. Little, T.E., et al, "Deep Water Pipe, Pump, and Mooring Study: Ocean Thermal Energy Conversion Program", Final Report, Westinghouse Electric Corporation, ERDA/COO-2642-3, June 1976.

2. Douglas, R.H., et al, "Ocean Thermal Energy Conversion Research on an Engineering Evaluation and Test Program - Final Report Vol. 1-5", TRW Systems Group, NSF/RANN/SE/GI-C958, June 1975.

3. Trimble, L.C., et al, "Ocean Thermal Energy Conversion (OTEC) Power Plant Technical and Economic Feasibility - Final Report Vol. 1 and 2", Lockheed Missiles and Space Company, Inc., NSF/RANN/SE GI-C937 , April 1975.

4. Adams, C.R., "A Preliminary Analysis of Ocean Thermal Power Plant Architecture and Statics", U. of Mass. Report No. NSF/RANN/SE/GI-34979/TR/73/8; June 1973.

5. McGowan, J. and Connell, J., "Heat Exchanger Design for Ocean Thermal Difference Power Plants", ASME Paper No. 74-WA/Oct. -4, Dec. 1974.

6. Lavi, A., "Solar Sea Power Project - Final Report", Carnegie-Mellon University, NSF/RANN/SE/GI-39114/ PR/74/6, January 1975.

7. Dugger, G.L. and Francis, E.J., "Maritime Aspects of Producing Products at OTEC Plants at Sea and Delivering them to the United States", Energy From the Oceans Fact or Fantasy Conference Proceedings, Raleigh, North Carolina, Jan. 27-28, 1976.

8. Pulos, J.G., "Structural Analysis and Design Considerations For Cylindrical Pressure Hulls", Report 1639, David Taylor Model Basin, April 1963.

9. Popov, E.P., Mechanics of Materials, Prentice-Hall Inc., Englewood Cliffs, N.J., pg. 229, 1963.

10. Hansen, R.H., and Waagaard, K., "Some Recommendations For Design Loads and Design Criteria For Concrete Vessels", Concrete Ships and Vessels, Continuing Education In Engineering, University Extension, Univ. of Calif., Berkeley, September 15-19, 1975.

11. Haynes, H. and Ross, R., "Influence of Length to Diameter Ratio on Behavior of Concrete Cylindrical Hulls Under Hydrostatic Loading", Tech. Report R-696, Naval Civil Engineering Laboratory, Port Hueneme, California, 1970.

12. Timoshenko, S.P. and Gere, J.M., Theory of Elastic Stability, McGraw-Hill Book Company, Inc., New York, pp. 289-297, 1961.

13. "Ramnäs Anchor Chain", Ramnäs Bruk Division of Bulten-Kanthal AB, Ramnäs, Sweden, Catalog No. 51, Edition 4, April, 1973.

14. "Tiger Brand Wire Rope", United States Steel Catalog, ADUSS 55-2460-01, reprinted November, 1968.

15. "New High Strength Rope Systems to 30-Inch Circumference", Sampson Cordage Works, Boston, Mass., Tech. Data Sheet SBRC-A2, June, 1975, and Price List No. A-6, March, 1976.

16. Huff, J.R. and Sisk, J., "Modifications For Deepwater Mooring", Petroleum Engineer, Feb. 1976, pp. 11-12.

# ANCHOR SYSTEMS

PHILIP J. VALENT AND J. MICHAEL ATTURIO
*Ocean Engineering Department*
*Civil Engineering Laboratory*
*Naval Construction Battalion Center*
*Port Hueneme, California*

## Abstract

The Ocean Thermal Energy Conversion (OTEC) power plants will impose lateral loads from 5 to 100 MN (1 x $10^6$ to 23 x $10^6$ lb), on its anchor systems, depending on the particular site environment. This report compares anchor systems to identify those best suited to scaling up to the sizes required by OTEC. Deadweight anchors with base shear keys are identified as the best choice for the deep ocean environment. Pile anchors attached to a common frame (template) are identified as a possible better anchor choice on hard (rock) seafloors and in high energy, shallow water areas typified by the Gulf Stream. Concepts for transporting and lowering the required deadweight and pile anchor systems to the seafloor site are described and their limitations noted. The attractiveness - and technical feasibility - of using a free-fall-emplaced deadwight anchor installation is highlighted.

## Introduction

The Civil Engineering Laboratory began its OTEC anchor systems effort in May 1975. The Phase I effort was directed toward identifying those anchor types best suited for mooring OTEC. First, a state-of-the-art review was conducted, collecting all available information necessary to analytically scale the existing anchor types up to the sizes required to moor OTEC (1). Second, the existing anchor types were scaled up to provide the required holding capacities in five possible seafloor materials. Those anchor types proving not feasible or practical were omitted from further consideration. The configurations of the remaining anchor types were optimized to provide a high ratio of lateral holding capacity to weight (2). Recommendations of anchor types for OTEC are presented in Atturio et al. (3). In September 1976, the Phase II anchor effort was initiated to: (a) evaluate fabrication, transport, installation, and seafloor construction techniques and their impact on the proposed anchor designs; (b) select those anchor designs offering an optimal balance between technical feasibility and cost; and (c) prepare a technical development plan outlining the shortcomings in present analytical techniques and construction/installation equipment capability, and outlining the course of action necessary to overcome these problems. This effort is now complete and is reported herein.

## Site and Loading Conditions

The anchor loading conditions assumed for this effort are based on two quite different environments: (a) a benign, deep ocean environment and (b) a demanding, Gulf Stream environment.

In the deep ocean environment, water depths range from 2,000 to 6,000 m (6,000 to 20,000 ft). The seafloor material is calcareous ooze or pelagic clay. Wind and current load on the power plant was estimated to be about 9 MN (2 x $10^6$ lb) (4, 5). For the Phase I effort a safety factor of two was applied, yielding an ultimate horizontal component of mooring line load at the anchor of 18 MN (4 x $10^6$ lb). The mooring line angle with the horizontal was assumed ranging from zero to 1.4 radians (80 deg) depending on the mooring system design (Figure 1) Raising the mooring line angle from the horizontal introduces a vertical load component at the anchor. At a mooring line angle of 1.4 radians, this vertical load component amounts to 100 MN (23 x $10^6$ lb).

In the Gulf Stream environment, water depths expected are about 500 to 1,000 m (1,500 to 3,000 ft). The likely seafloor material is sand, gravel, or rock. Loads on the power plants in the Gulf Stream environment are approximately ten times those in the deep ocean environment (4, 5), resulting in an assumed ultimate horizontal component of mooring line load at the anchor of 180 MN (40 x $10^6$ lb). For this environment, the mooring line angle with the horizontal was assumed to range from zero to a maximum of 0.8 radian (45 deg), depending on the mooring system design (Figure 2). The vertical load component corresponding to a line angle of 0.8 radian is 180 MN (40 x $10^6$ lb).

## Anchor Types Considered

The anchor types were placed in four groups to facilitate evaluation (Figure 3): (a) drag embedment anchors, such as the STATO, Paravane, or Bruce; (b) plate anchors (steel plates which are driven edgewise, vertically deep into the seafloor and then rotated into a horizontal position); (c) pile anchors; and (d) deadweight anchors. The first two anchor types, drag embedment and plate anchors, were eliminated as contenders because: (a) a single anchor could not be made sufficiently large to provide the required holding capacity, and because (2) a sufficient multiple anchor configuration would require the bridling together of several drag embedment or plate anchors. This bridling system would be necessary to equalize the load between the anchors. Such a bridling system would be very difficult, if not infeasible, to install in deep water.

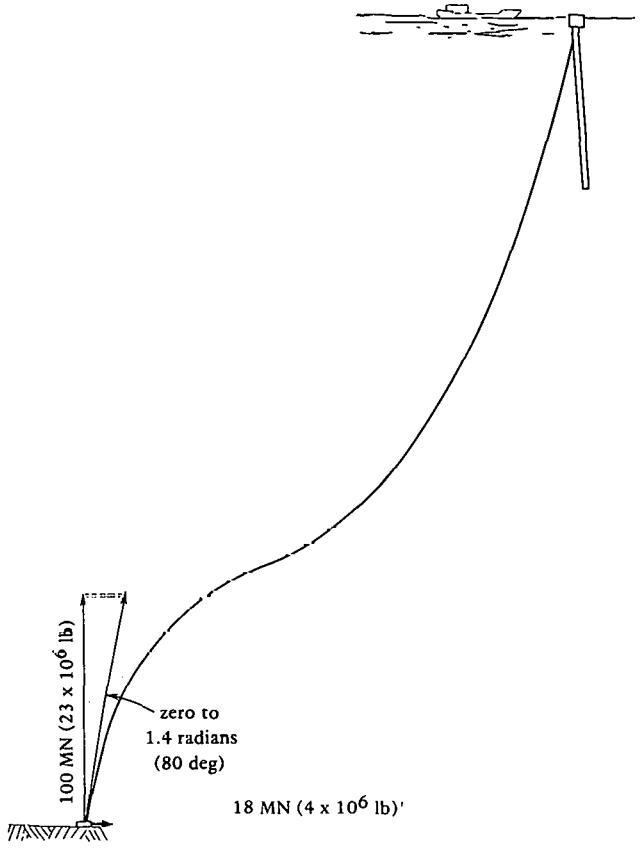



Figure 1. Anchor Loadings, Deep Ocean Environment, Phase I.

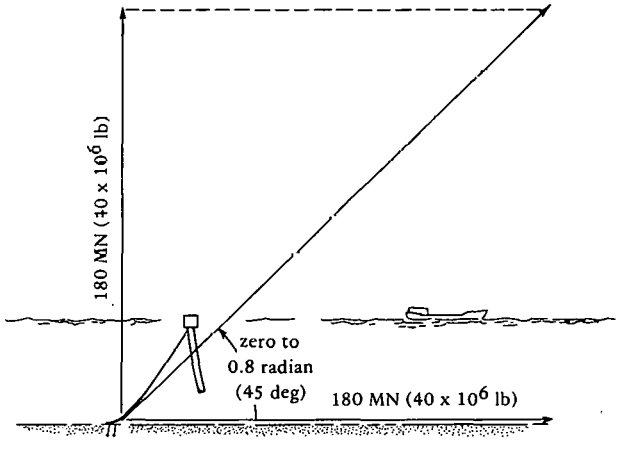



Figure 2. Anchor Loadings, Gulf Stream Environment, Phase I.

The configuration of pile anchors for the OTEC pow plant is influenced heavily by the large horizontal loa component applied. The relatively soft deep-ocean bottom sediment allows large lateral deflection of the pile head. The large deflections result in a large bending moment in the pile which dictates the pile cross section necessary. Steel pipe piles are capable of resisting these large bending moments; reinforced or prestressed concrete piles are not. To resist the 18 MN (4 x $10^6$ lb) horizontal load for the deep ocean environment, three steel pipe piles are required, each 5 m (16 ft) in diameter by 50 m (160 ft) long (Figure 4). Shafts for the piles would probably be predrilled through a template, and the pipe piles grouted into the shaft and into the template. The air weight of this pile group including the template is about 32 MN (7 x $10^6$ lb).

The configuration of deadweight anchors, as with pile systems, is influenced by the large horizontal load component applied. To resist this horizontal load component, the deadweight employs shear keys arranged in a grid pattern (Figure 5). The shear keys drive the soil shear plane (sliding) deep into the seafloor and into the stronger soils. Parametric analysis of deadweight anchors shows that the optimum ratio for skirt length to anchor width in deep ocean cohesive soils is 0.1 (2). To minimize the possibility of anchor overturning, the maximum ratio of anchor height to width was set at 0.1. On a deep ocean cohesive soil a deadweight equipped with shear keys may resist up to three times the lateral load of a similar deadweight without shear keys. To resist the 18 MN (4 x $10^6$ lb) horizontal load for the deep ocean environment, the deadweight anchor depicted in Figure 5, 40 m (130 ft) square and weighing 35 MN (7.9 x $10^6$ lb), would be necessary. If the design mooring line angle with the horizontal is raised above zero, causing some vertical load to be applied to the anchor, this vertical load must be balanced (opposed) by adding mass to the deadweight. Mass can be added by increasing the thickness of the concrete base plate or by adding other weighting materials, even dredged seafloor soil, on top of the anchor base plate.

Comparison of the deadweight and pile group anchors for mooring line angles of zero shows them to be almost equivalent from an efficiency standpoint (efficiency = anchor holding capacity/anchor air weight). This balance does shift as the mooring line angle at the anchor is raised and the pile anchor system is able to mobilize the soil friction in resisting the vertical component of mooring line load. However, installation of the pile group is more complicated than that of the deadweight, offsetting any efficiency advantages. For this reason the deadweight anchor was selected as the better anchor type for use in the deep ocean.

When the pile and deadweight anchor types are sized to resist the loadings of the Gulf Stream environment, the efficiency balance is noted to shift quite markedly toward pile type anchors. The seafloors beneath the Gulf Stream, where the Stream is close to land, are dense and strong and oftentimes are rock. These high strength, near surface materials can be utilized to resist the high horizontal load component. Thus, the pile section design can be changed considerably, significantly increasing the efficiency of the

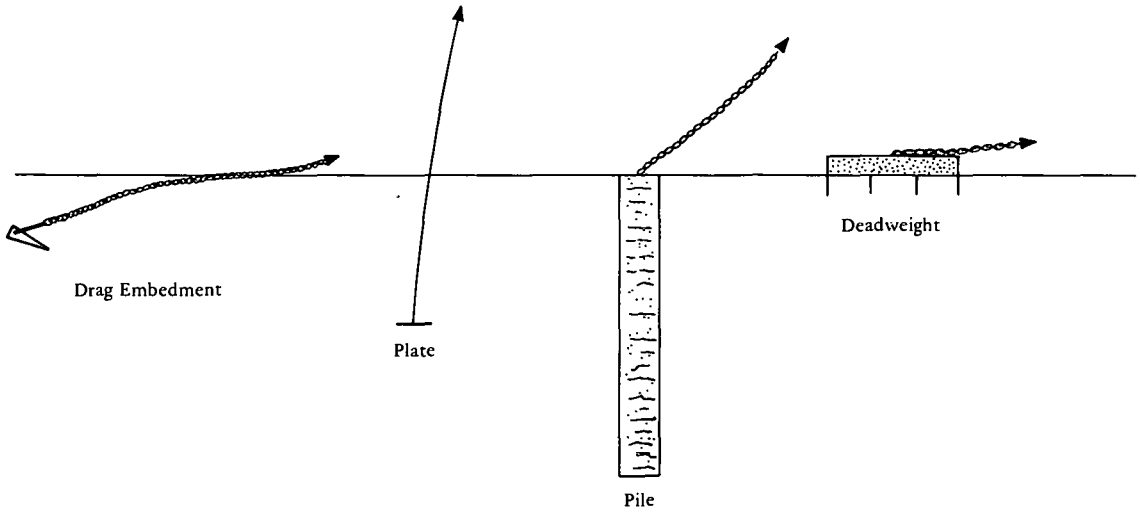



Figure 3. Anchor Groups Considered.

pile type anchor over the deadweight on hard seafloors. A modified pile anchor design for use in hard seafloors will be presented later in this paper.

## Anchor Lowering

The above discussion considers only in-place, service performance of the pile and deadweight anchor types. These anchors, or components of them, must be transported to an OTEC anchor site and then lowered through the water column and safely emplaced on/in the seafloor. The anchors for the deep ocean environment will weigh about 35 MN ($8 \times 10^6$ lb) in air and about 18 MN ($4 \times 10^6$ lb) in water. Two basic installation techniques were considered: (a) controlled lowering in one piece or in five elements, or (b) free-fall emplacement.

Figure 6 graphically presents the state of the art in the handling of heavy loads in the deep ocean. Two cases were considered for controlled lowering. First, the deep ocean deadweight anchor was assumed to be broken into five components, each weighing 3.6 MN ($0.8 \times 10^6$ lb) submerged. Alternately, the deadweight was assumed lowered as one unit weighing 18 MN ($4 \times 10^6$ lb) submerged. The drillship falls far short of the required lift capability. Even if the drillship were equipped with 100%-effective motion compensation, it would be able to lower the desired anchor components only to maximum depths of 2,000 m (6,000 ft). Of course such a motion compensation system is far from reality. The derrick barge, when coupled with a "pipe link" line, such as that proposed for mooring the Lockheed OTEC platform (4), at first glance appears to have significantly greater load handling capacity than the drillship. However, the time required to make and break the joints of the pipe link chain is considerably longer than that required to make and break drill pipe joints: using the pipe link chain, lowering of the anchor to 6,000 m (20,000 ft) will take in excess of six days. To make economical use of the derrick barge with its pipe link chain, the anchor would probably have to be lowered as a unit, limiting the maximum handling depth to about 2,000 m (6,000 ft). As with the drillship analysis, this derrick barge analysis assumed 100%-effective motion compensation — which is not realistic. The comparison of state-of-the-art heavy-load handling systems shows that the Glomar Explorer is the only vessel capable of lowering the 18 MN OTEC anchor to water depths of 2,000 to 6,000 m (6,000 to 20,000 ft). That vessel has demonstrated the capability to apply a lifting force estimated at 36 MN ($8 \times 10^6$ lb) in 5,100 m (17,000 ft) water depth. However, the Glomar Explorer is one of a kind, is quite costly to mobilize, maintain, and operate, and may not be available when needed for OTEC anchor emplacements.

The idea of dividing the anchor into components or building blocks as a means of reducing the payload weights was referred to above when discussing the possibility of anchor emplacement by drillship. The idea of adding buoyancy to the anchor during lowering was also investigated as a possible means of facilitating anchor emplacement by drillship. Light petroleum products (e.g., aviation gasoline), syntactic foams, and air-filled pressure hulls were all considered as possible sources of buoyancy. Buoyancy did serve to reduce the net static load on the lift system, although the added mass of the buoyancy also acted to increase the dynamic forces arising from vessel motion. This evaluation of buoyancy assist in anchor handling showed that the probability of developing a snap load condition when lowering the complete 18 MN anchor by drillship was quite high. It was also determined that buoyancy assist in handling 3.6 MN ($0.8 \times 10^6$ lb) anchor components by drillship would make

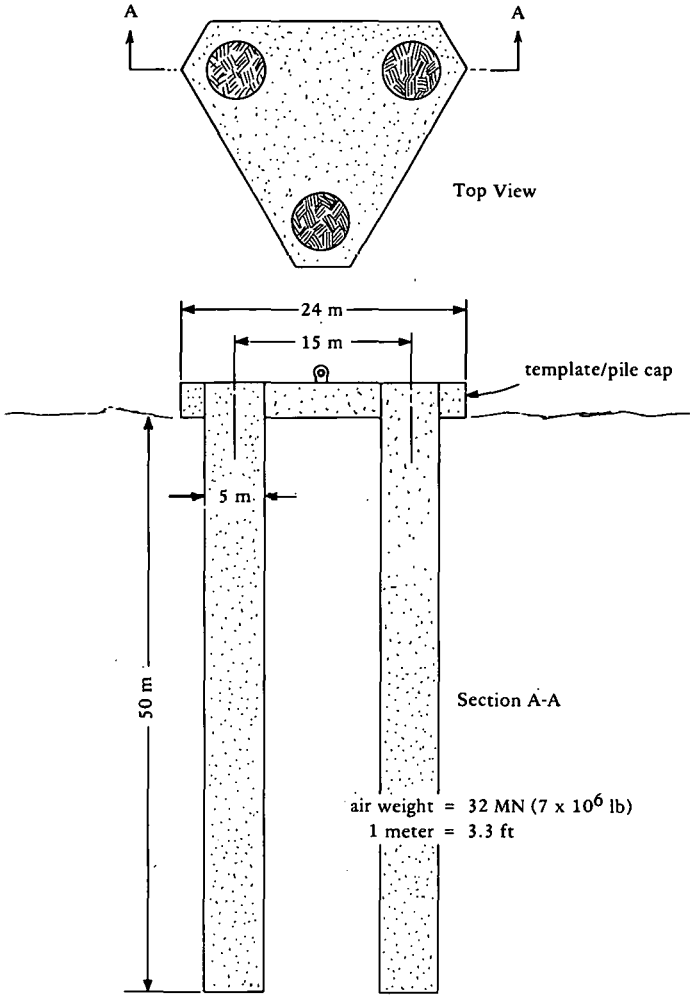



Figure 4. Deep Ocean Anchor Pile Group.

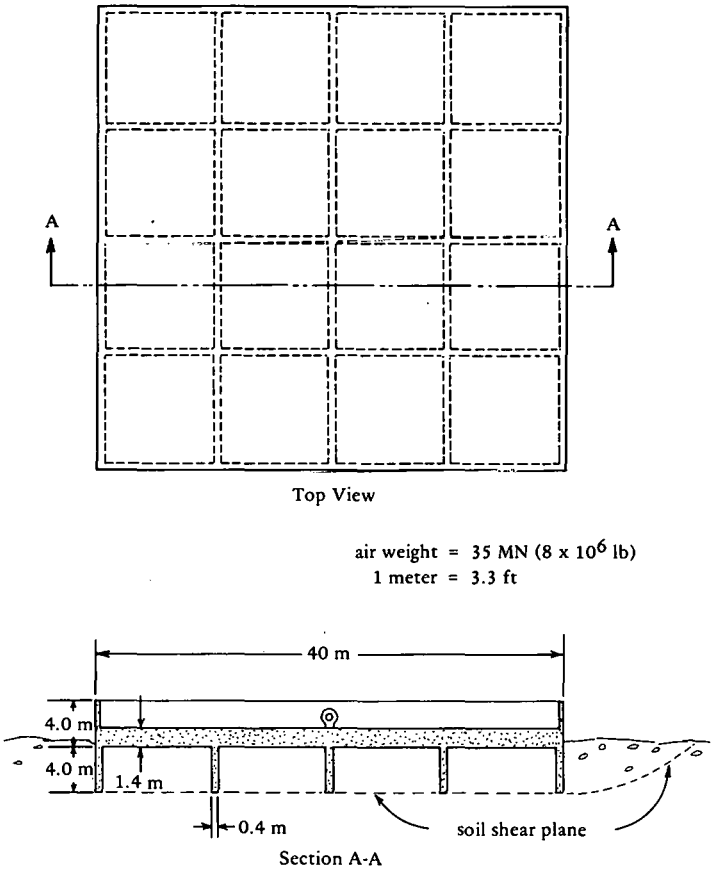



Figure 5. Deep Ocean Deadweight Anchor.

feasible the controlled lowering of those components to water depths of 6,000 m (20,000 ft). A buoyancy system using air-filled pressure hulls, reusable for lowering several OTEC anchors, is the best buoyancy assist approach. However, even this sophisticated system requires five trips to the seafloor to complete the anchor installation. In addition, a sophisticated seafloor positioning control system would be required in order to assemble the anchor components on the seafloor. Techniques and systems for controlled lowering and emplacement of the 18 MN OTEC anchor are complicated and expensive.

Initially, free-fall emplacement of 18 MN anchors was considered, but not highly regarded because of apprehensions regarding stability during free-fall and structural integrity on landing. The free-fall concept does have certain inherent advantages: it is simple, requires no special equipment, and requires very little ship time on station for installation. Conceptual development of the free-fall concept has reinforced confidence in the advantages of the free-fall concept and has largely dispelled apprehensions regarding stability and structural integrity.

## Free-Fall, Deadweight Anchor

The free-fall-emplaced deadweight anchor (Figure 7) is a direct descendant of the high lateral load capacity deadweight anchor designed for controlled lowering (Figure 5). The grid pattern shear keys of the controlled lowering design has been changed to a radial pattern to provide easy egress for the trapped water beneath the anchor during landing on the seafloor. Also, the periphery of the anchor has been fitted with a device to control vortex shedding to minimize pitching motion during free-fall. Otherwise the free-fall configuration is the same as the controlled lowering configuration (except for being circular versus square). The free-fall anchor

(Figure 7) has been designed for a mooring line load with components of 9 MN (2 x $10^6$ lb) horizontal and 9 MN (2 x $10^6$ lb) vertical (line angle of 0.8 radian (45 deg) to the horizontal). The free-fall anchor for the new loading conditions weighs 18 MN (4 x $10^6$ lb) in seawater and is 34 m (100 ft) in diameter. Air weight for the anchor would be about 31 MN (7 x $10^6$ lb).

The free-fall anchors will be constructed in the dry in a shipyard atmosphere. The construction material will likely be reinforced concrete with some prestressing in critical areas. The anchors will be transported to the OTEC sites either on barges, or by making the anchors themselves temporarily buoyant and towing them. Loading of a 31 MN (7 x $10^6$ lb) payload on a barge and transporting the payload are demonstrated offshore oil-platform installation capabilities.

Offloading of a nonbuoyant payload weighing 18 MN (4 x $10^6$ lb) in seawater has not been done before, but the feat does not appear overly difficult. Alternately, the anchor itself can be made to resemble a barge by adding temporary buoyancy topside to safely float the anchor during its long tow to the OTEC site. Once at the site, the buoyancy compartments would be flooded to initiate the free-fall descent.

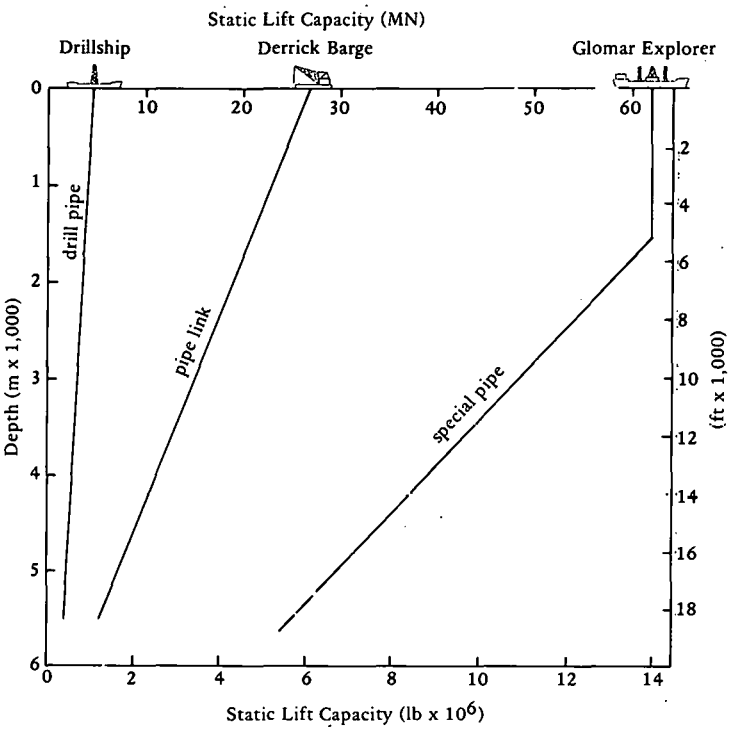



Figure 6. State of the Art in Heavy-Lift Vessels.

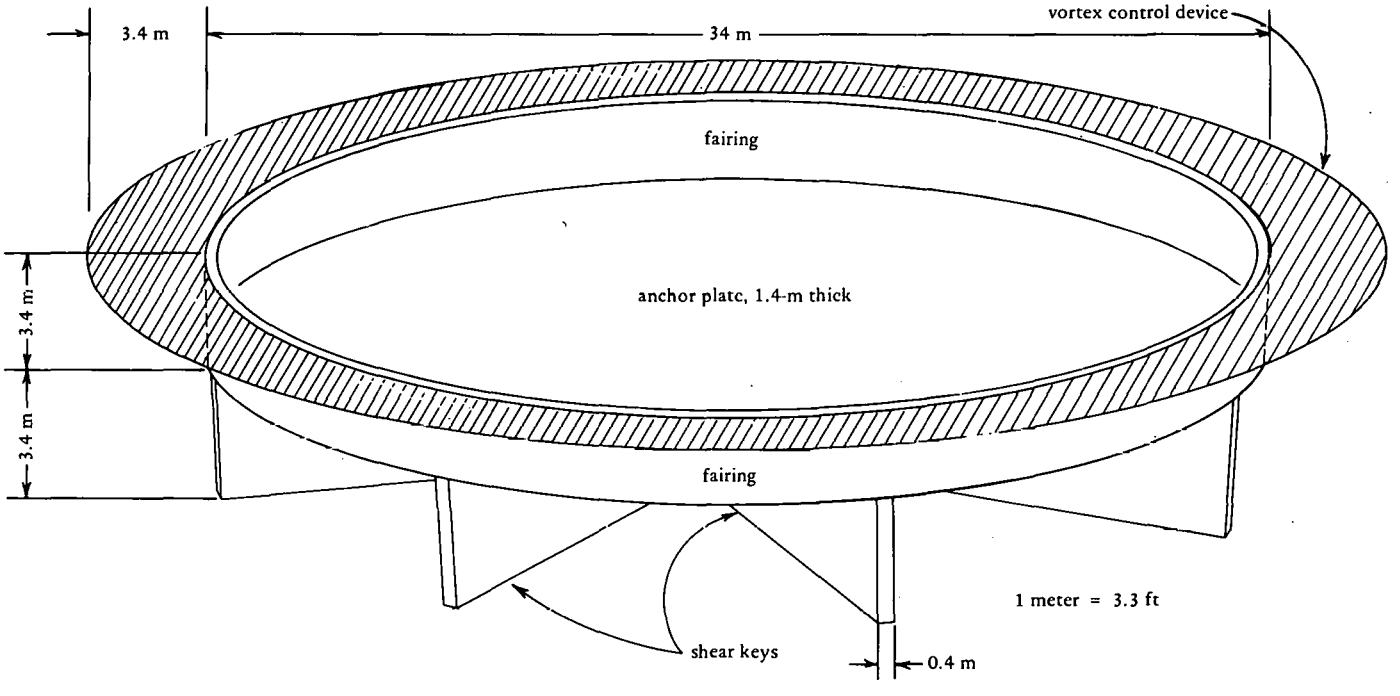



Figure 7. Oblique View of Free-Fall-Emplaced Deadweight Anchor.

The mooring line will be installed either by carrying it to the seafloor on the anchor topside during emplacement or by lowering and attaching the line to the anchor after emplacement. If the mooring line is carried to the seafloor on the anchor, then the upper end will be released from the anchor after seafloor contact and will be returned to the surface by a syntactic foam-filled float. If the seafloor end of the mooring line is attached after anchor emplant, the line lowering, positioning, and attachment operation will be carried out by an appropriately equipped drillship.

Tests with a 0.15-m (6-in.) diameter, scaled model of the free-fall anchor show that the anchor is stable during free-fall: the anchor will quickly right itself to a horizontal attitude; it does not translate nor rotate during free-fall, and pitching motions are not of serious magnitude (about ±0.1 radian). Terminal velocity of the prototype is predicted to be 6 m/s (20 fps) or less.

The structural integrity of the proposed free-fall anchor on landing has not been verified. Verification will require an analytical description of the interaction between the anchor, the water, and the soil on landing followed by model tests to confirm the analysis. Once the force history and pressure distribution on the anchor are understood, then structural analysis and design of the anchor can proceed. Time and funding limitations have precluded such an analysis. However, the approximate analyses did show that structural integrity of the free-fall deadweight when landing on typical deep ocean soil seafloors will not be critical. Even if this preliminary conclusion should prove faulty, structural integrity during landing can be maintained by slowing the free-fall velocity of the anchor system. The velocity can be slowed by decreasing the submerged weight of the anchor during free-fall by temporarily adding buoyancy, or by increasing the drag on the anchor system by adding drogue buoys.

The free-fall emplaced deadweight anchor system is also usable on soil seafloors in the Gulf Stream environment, provided that the seafloor is sufficiently compliant to allow complete embedment of the shear keys without structural distress occurring in the anchor. Rather than use one very large anchor to resist the 180 MN (40 x $10^6$ lb) ultimate lateral load, multiple free-fall deadweight anchors weighing about 20 MN (5 x $10^6$ lb) submerged each would probably be used. Individual mooring lines would connect the plant to each anchor with load equalization among lines being accomplished by an automatic system on the plant.

## Pile Anchor System

OTEC power plant sites are proposed in the Gulf Stream where a deadweight anchor is not expected to serve well. These sites are those with seafloors of near-surface or exposed hard material, often rock. In such areas an anchor incorporating piles will often provide the desired anchor holding capacity with far less material weight, and probably at lower total cost.

The vertical component of mooring line load and overturning forces on the pile cap/framework would be resisted by tension piles 0.4 to 0.8 m (15 to 30 in.) in diameter by 40 m (130 ft) in length (Figure 8).

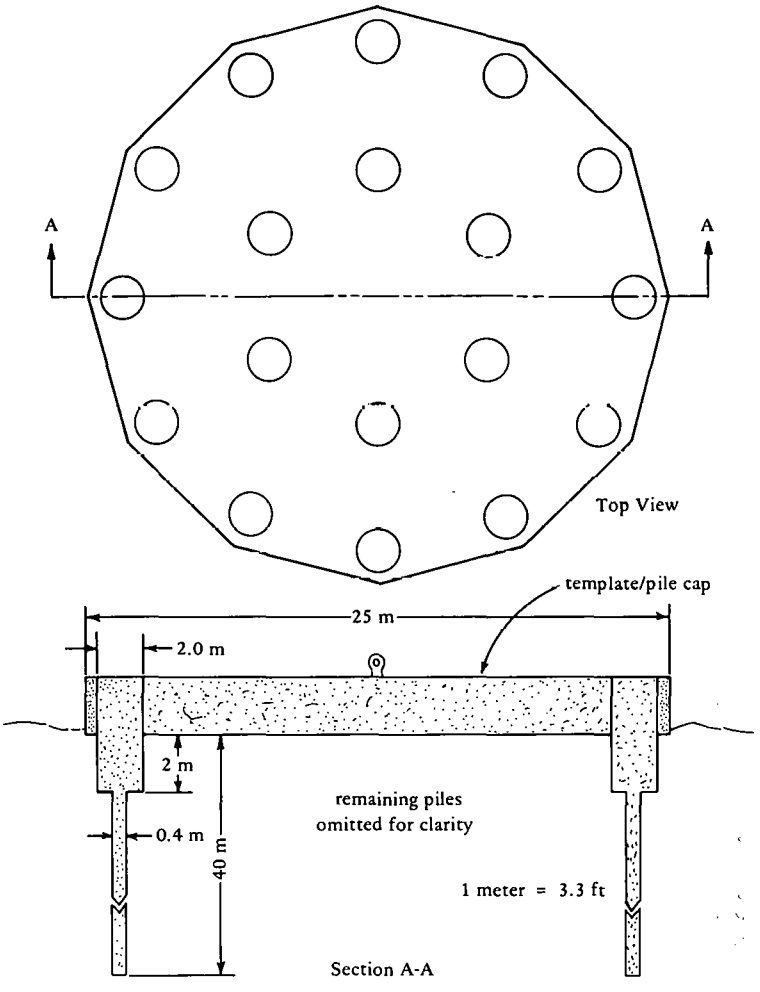



Figure 8. Anchor Pile Group for Gulf Stream Environment.

The horizontal load component would be resisted by short, large diameter stub piles acting much like shear pins between the pile cap and the rock mass. Quite likely the upper ends of the tension piles will be reamed out to serve as the "shear piles" as shown in Figure 8.

Installation of the pile group anchor would be carried out by first lowering a framework to the seafloor. Lowering of this framework weighing about 4 MN (1 x $10^6$ lb) in 500 to 1,000 m (1,500 to 3,000 ft) water depths would be handled by a crane barge or possibly by a drillship (Figure 6). The framework would initially serve as a guide during pile installation. After the pile shells had been grouted into the guides, the framework would serve to distribute the mooring force from the mooring line attachment point to the individual piles. Drilling of holes for the piles would be done from a drillship using conventional drillhole re-entry techniques for maneuvering the drillstring into the framework drill guides. "Walking" of the drill bit on the rock surface would be prevented by the drill guides. Required drill

bit feed thrust would be reduced to manageable magnitudes eveloping a hydraulic powered, rotary impact tool drilling of holes up to 800 mm (30 in.) in diameter. ...matic tools are now available for drilling such holes in shallow water depths (6). Hydraulically powered, rotary-impact tools, suitable for drilling holes up to 100 mm (4 in.) diameter in water depths of 1,000 m (3,000 ft), have been developed (7). Thus, when needed, the required 800-mm (30 in.) diameter rotary-impact drill can be developed. Sufficient thrust for conventional reaming of the upper drillhole to diameters of 2 m (6 ft) can be realized by hanging a drill collar-like assembly from the reamer bit and allowing the reamer bit to support this mass in the tension pile drillhole.

After each drillhole is completed, a steel tension member and integral shear collar would be grouted into the drillhole and template drill guide using conventional techniques. The drillship would later attach the mooring line to the anchor framework attachment point.

Procedures for analysis of the pile group anchor on rock seafloors are satisfactory. No development in this area is necessary at this stage, although some design and installation specifics do need to be worked out. The solutions to these problems will likely be highly site specific.

## Conclusions and Recommendations

Reliable, long-lasting anchor systems capable of maintaining the OTEC power plant on station in a single or multiple point moor are technically feasible. The free-fall emplaced, deadweight anchor for use on soil seafloors is very attractive because it does not require any specialized ship support except the ocean-going tugs required to tow it to the proposed anchor location. A deadweight anchor is not efficient in a rock seafloor. A specialized pile anchor installed by drillship appears to be workable for this situation.

Because most of the proposed OTEC plant locations are in areas having soil seafloors, the free-fall emplaced, deadweight anchor merits high development priority. Reliable procedures for predicting the forces on the free-fall anchor should be assembled and verified by model tests. A near prototype scale free-fall anchor should be fabricated, transported, installed, and test-loaded if possible, to verify all aspects of the free-fall anchor system.

Development work on a pile anchor system should be deferred until a necessary site floored with near surface or exposed rock has been identified. Deferral is prudent at this time because the design of the pile system will likely be highly site specific.

## Acknowledgments

The authors gratefully acknowledge the assistance of their many colleagues in various facets of this effort: Robert J. Taylor, Robert D. Rail, Homa J. Lee, Joseph F. Wadsworth, Richard M. Beard, Donald B. Jones, Robert J. Odello, Leonard J. Woloszynski, and Fred O. Lehnhardt.

## References

1. Civil Engineering Laboratory, Technical Memorandum M-42-76-1, "State-of-the-Art in High-Capacity, Deep-Water Anchor Systems," by P. J. Valent, R. J. Taylor, H. J. Lee and R. D. Rail. Port Hueneme, Calif., Jan 1976, 109 pp.

2. Civil Engineering Laboratory, Technical Note N-1463, "OTEC Single Anchor Holding Capacities in Typical Deep Sea Sediments," by P. J. Valent, R. J. Taylor, J. M. Atturio and R. M. Beard. Port Hueneme, Calif., Dec 1976, 131 pp.

3. Civil Engineering Laboratory, Technical Report R-853, "Preliminary Selection of Anchor Systems for OTEC," by J. M. Atturio, P. J. Valent and R. J. Taylor. Port Hueneme, Calif., Mar 1977, 45 pp.

4. "Ocean Thermal Energy Conversion (OTEC) Power Plant Technical and Economic Feasibility," vol I and II, Technical Report, LMSC-D056566, Lockheed Missiles and Space Co., Inc. Sunnyvale, Calif., 1975.

5. Ocean Thermal Energy Conversion Research on an Engineering Evaluation and Test Program, vol 1-5, for Contract No. NSF-C958, prepared for U.S. Energy Research and Development Administration, Washington, D.C., by TRW Systems Group, One Space Park. Redondo Beach, Calif., 1975.

6. Advertising literature. "Superdrills," brochure Form 4405A, by Ingersoll-Rand. Rock Drill Division. Phillipsburg, N.J., 1976, 4 pp.

7. Brackett, R. L., P. K. Rockwell, S. A. Black, L. W. Hallanger, W. R. Tausig, and S. Sergev (1976), "Recent Development in Diver Construction Equipment," The Working Diver 1976, Symposium Proceedings, Mar 2-3, 1976, Columbus, Ohio, 55-76 pp.

# SCREENS FOR THE OTEC PLANTS

JOHN H. NATH
*Department of Mechanical Engineering*

JULIE W. AMBLER
*School of Oceanography*

ROBERT M. HANSEN
*Department of Civil Engineering*

*Oregon State University*
*Corvallis, Oregon*

Abstract

This progress report describes the work to date for the contract time period of 15 September 1976 to 14 September 1977. An overview of screens for onshore plants is in progress while an overview of micronekton abundance has been completed. A tentative schematic design for a screening system for completely enclosed conduit flow is presented. In addition, a tentative proposed design for sampling micronekton in a manner similar to an OTEC plant is presented. It is concluded that possibly large volumes of micronekton will need to be filtered from the warm and cold water flows at times in order to protect the heat exchangers and other items. Most of the screened fish will die and will need to be disposed of in such a manner so as to not attract large numbers of predators.

## INTRODUCTION

Ocean thermal energy conversion plants will intake very large quantities of warm ocean water relatively near the surface and cold waters at relatively great depths. The biological material and other matter at these two depths may be greatly different. Various fishes and other organic matter will need to be excluded from the plant in order to protect the heat exchangers and other items. Therefore, because of possible large concentrations of certain species, the screening process will be of major concern.

The screens, or filter system, should also give adequate protection to the environment. Large species, such as whales, sharks and large tuna, etc., can be excluded from the plant by means of large gratings at the intake structures. Bell-shaped intakes can reduce head losses from entrance conditions and gratings, and entrainment or impingement problems from fish. Because of corrosion and biological growths, and clogging, a fine-meshed screen will require frequent cleaning and should probably not be placed at the intakes. It is proposed to place them downstream from the pumps for completely closed conduit systems. Most biological species that pass the intakes and pumps and are then stopped at the secondary screens and directed back into the environment, will die. It is unlikely that any practical means of screening these smaller species can be accomplished without killing the majority of them. Thus, the intakes should be arranged so as to discourage entrance by the smaller species.

### Purpose

The purpose of this research is to determine the kinds and quantities of biological materials that must be excluded from an OTEC plant and to develop candidate methods for so doing. Biological activity, particularly fish and other micronekton, is considerable in some parts of the oceans. These fish must be prevented from impinging upon the heat exchangers. They are numerous and in some areas very dense. The screens may be quite large and expensive to construct and operate. Thus, the main purpose of this research is to bring to light the considerations that must be made for effective construction.

The objectives of the work can be separated into three considerations as given below. The work is a "paper and pencil" study where many things need to be determined. They are:

Engineering Determinations

- A criteria review for onshore power plant heat exchangers which utilize ocean water.
- Shape and location of intakes and how they influence the ingestion of fish.
- Estimation of energy losses for various details within the screening system.

- Considerations for cleaning and operating screens (major items).
- Development of a candidate schematic design which may be expanded into actual designs.
- Broad cost estimates to illustrate the magnitude of financial problems with regard to capital construction vs. annual operating costs and parasitic losses of energy.

Biological Determinations

- Horizontal and vertical abundance of species of fish and plant organisms.
- Dimensions and motion capabilities of various fishes.
- Effectiveness of devices other than screens.
- Prediction of problems with candidate schematic designs from experiences gained with existing power plants.

Joint Engineering and Biological Determinations

- Coordination of efforts.
- Design of a fish sampling device which will simulate the flow around OTEC intakes.
- Summary of preliminary design criteria.
- Final report.

Scope

This paper is a progress report. Approximately seven months have elapsed since the beginning of the work. The biological work is well developed but the engineering will require considerably more effort prior to completion of the one-year contract. The biological data have been reviewed for $\pm$ 20° latitude and along the coastlines of the contiguous 48 states, plus Hawaii. However, a preliminary temperature difference survey illustrates that certain areas within this region are unfavorable for OTEC siting and they will not be covered with regard to biological surveys.

The screens and screen operations presented herein are schematic in nature. The development of screen structural details is a function of final design and is not within the scope of this work. Preliminary design criteria will be developed. The importance of the screening operation will require a considerable engineering effort for the final design.

We emphasize that the existing biological information is obtained from the results of sampling fish with mid-water trawls. These trawls are about 10' wide at the mouth and are pulled in a mostly horizontal path through the water at a speed of about 2 to 5 knots. They entrap the fish that cannot escape the advancing trawl. This sampling condition will be considerably different than that of an OTEC plant which will be sucking in large quantities of warm and cold water. The plant will act like a giant vacuum cleaner as it operates in the water. Thus, one task for this work is to develop a device that can be used from oceanographic and other types of vessels to sample fish volumes at various depths with a "vacuum cleaner" type of action.

## BIOLOGICAL OVERVIEW

Sites considered for OTEC development include an enormous area of the Earth's surface. This overview (primarily a literature review) includes biological information from an area within 600 miles of the coast of the contiguous United States, the equatorial regions, within $\pm$ 20° latitude, and the Hawaiian Islands. This area is a sizeable fraction of all of the world's oceans. Many parts of it have never been sampled with gear that would provide information relevant to OTEC performance. Only the sites with the highest OTEC potential were considered. They are areas where the temperature difference between surface and deep waters (1000m) is greater than 18°C. In general, the tropical oceans between 20°N and 20°S have the highest potential. This is illustrated for the Pacific Ocean in Fig. 1. The Pacific Coast of the United States, and most of the East Coast, has relatively low potential. However, the Florida current and the Gulf of Mexico have good potential. Therefore, we have concentrated on the biota of the subtropical and tropical oceans.

Studies on conventional power plants, which require ambient water for heat disposal, show that the animals most affected by screens are those too large to go through and those which cannot avoid the intake stream. Many become pressed against the screens and usually die. The very small ones are ingested by the plant. Large numbers of menhaden fish on the screens of conventional power plants in the Hudson River have caused shutdowns. The high mortalities of impinged animals can significantly affect population abundances. This study concentrates on animals larger than 5 mm. These animals are quite well known from the catches of midwater trawls and are called *micronekton* by biologists. Nekton are animals that can swim against a current--animals ranging in size from shrimps to porpoises and whales. Micronekton have been defined as the assemblage of actively swimming fishes, crustaceans, and cephalopods (squids, octopi) ranging from 1-10 cm in their greatest dimension (3). Biologists most frequently measure the lengths of animals to estimate age and growth. Length is a useful measurement for impingement studies, because fish usually are trapped lengthwise on the screens.

Even though the velocities at their inlets are comparable, an OTEC plant will most likely catch more animals of larger sizes than do midwater trawls. Midwater trawls are towed at 2-5 knots (1.0-2.6 m/sec). The flow speed in the cold and warm water pipes of an OTEC plant may be about 2 m/sec, but outside the speeds will be less. However, the size of the cold water pipe is much greater than the 3 m midwater trawls (mouth area = 7.9m$^2$) which are used to sample micronekton. The few larger midwater trawls usually catch larger

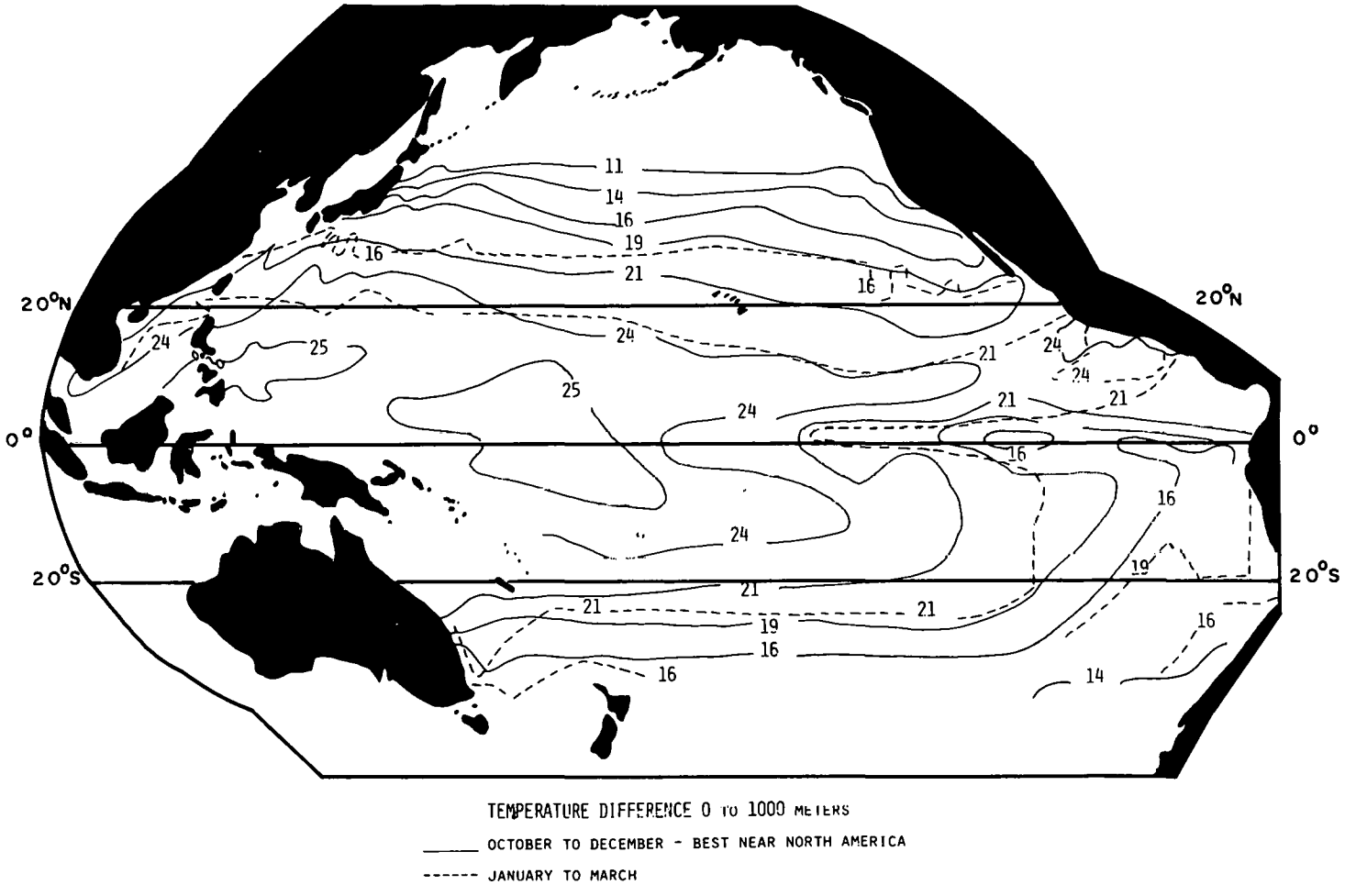



Fig. 1 Temperature Difference Chart, 0 to 1000 m, for the Pacific Ocean

animals, which suggests that an unscreened OTEC inlet will catch more and larger animals than the 3 m midwater trawls. For example, a small Cobb trawl, a commercial fisheries net, with a 10 m diameter mouth catches larger animals than does the 3 m midwater trawl (Dr. W. G. Pearcy, personal communication). A large commercial net like the Engels trawl with a 100 m diameter mouth can catch any size of fish, even fast swimming fish like salmon. The diameter of the cold water pipe for OTEC 1 will be about 2 m, which is comparable to the mouth area of a 3 m midwater trawl. The diameter of the cold water pipe for a 100 MW plant will be about 15-30 m. Warm water intakes may be of comparable size. Therefore, it is reasonable to assume that OTEC plants probably will catch animals never caught by typical midwater trawls. Nevertheless, the only existing data from potential OTEC sites has been collected with small 3 m midwater trawls, and these results are presented in this report.

An extensive literature search for references on micronekton abundances and distributions in potential OTEC sites was made. For cross referencing, the OTEC zones in (4) were used. Although these zones are smaller than the zoogeographic regions described below and do not follow zoogeographic boundaries, they do allow references to be sorted into small geographic areas.

Other subject headings were used to reference behavioral aspects of micronekton as given in Table 1 They will be utilized in the final report.

Table 1. Subjects used for biological cross referencing

Geography

Bretschneider OTEC zones
Indo-Pacific Ocean
Pacific Ocean
Indian Ocean
Atlantic Ocean
World Oceans
Kuroshio Current

Organisms Behavior

Floating objects
Artificial islands and reefs
Drifting seaweeds
Sound scattering
Light--effect on animals
Electrical fields
Sound--effect on animals
Submersible observations
Intake screens--impingement
Inner plant kills
Temperature differences between 0-1000m ($\Delta T$)
Gear used to collect micronekton
Misc. references

## Geographic Distribution

The general geographic distribution of micronekton can be described by zoogeographic regions, which are large oceanic areas with fairly homogeneous physical characteristics and fauna. Zoogeographic regions are shown in Fig. 2, which were developed by using descriptions from (5, 9, 13).

On a worldwide scale, the distributions follow latitudinal bands around the earth. Some species, adapted to live in a wide range of conditions, can be found in all three major oceans from the northern subtropical convergence near 45°N to the southern subtropical convergence near 45°S. The north and south equatorial currents which flow westward divide the subtropical central water gyre distributions from the equatorial distributions. Species that live in a north central gyre are often found in the south central gyre, but not in the intervening equatorial zone. Equatorial species are sometimes found from 23°N to 23°S, while others are very narrowly restricted.

Continents are barriers which break up the distributions so that the Atlantic and Pacific Oceans have distinct zoogeographic regions at the same latitudes. Many species are found throughout the tropics of the Indian and Pacific Oceans, but are not found in the Atlantic. On the other hand, there are species that are only found in the Atlantic. The transfer of species between the Indo-Pacific and the Atlantic Oceans is inhibited by the cold water barriers at Cape Horn and the Cape of Good Hope.

The wide expanse of the Pacific Ocean or the East Pacific Barrier divides the Indo-Pacific tropical region from the eastern tropical region. The physical environments of the eastern and western sides of the Pacific are different because the vertical distributions of hydrographic features tend to tilt upward from the west to the east. The eastern tropical Pacific is highly productive because the thermocline is close to the surface and physical processes generate upwelling. The eastern tropical Pacific is a distinct zoogeographic region with a large number of endemic species (i.e. species only found there).

Micronekton abundance is low in tropical, offshore oceanic areas. Abundance is defined as the volume of micronekton divided by a unit volume of water (usually $1000m^3$). Abundance figures are estimated from trawl results and are, therefore, very approximate. Displacement volumes less than 20 $ml/1000m^3$ are typical. Subarctic regions have much higher abundances than subtropical regions. This is illustrated from Fig. 3, which is reproduced from (1). Central water gyres, such as the Sargasso Sea, have the lowest abundances. As the distance offshore increases, abundances decrease due to less nutrient runoff from the land as shown in Fig. 4. Since early OTEC plants will be within 40 miles of land, these sites will have the greatest micronekton abundances of all potential OTEC sites.

It is possible that large volumes of micronekton will be ingested by the plant and impinged on the screens. In the eastern tropical Pacific, a highly productive area, the highest micronekton volume recorded was 80 $ml/1000m^3$ (10). The intake pipe of a 100 MW OTEC plant may take up about 25,000 $m^3$/minute, which would include micronekton at a rate of 2 liters/minute based on Love's data. Assuming a passive screen system of about 200 $m^2$ in area, a 1 cm thick layer could accumulate in about 17 hours. Of course, some will pass through, but these numbers give one a rough idea of the magnitude of the problem. Although micronekton abundances are relatively low in the open ocean, the flow rates of OTEC will concentrate significant volumes of animals on the screens, which must therefore be cleaned. A few OTEC plants will not destroy a a significant portion of the micronekton populations, but fleets of clustered 100 MW plants could be harmful regionally.

## Depth Distribution

The depth range that OTEC plants will occupy is from 0 - 1200 m (4000 ft). This includes the vertical zones termed by biologists as the epipelagic (0 - 200m), mesopelagic (200 - 1000m), and the bathypelagic (1000 - 4000m) regions as shown in Fig. 5. Epipelagic and mesopelagic animals have similar horizontal distributions as described above for the zoogeographic regions. The species distributions of bathypelagic animals are not very well known, but many species cover large geographic areas, for which one zoogeographic region may suffice (5). In this review the distributions of bathypelagic animals are not emphasized.

The warm water inlet for an OTEC plant will be in the epipelagic zone, where temperatures in the upper part of this zone are fairly constant with depth due to

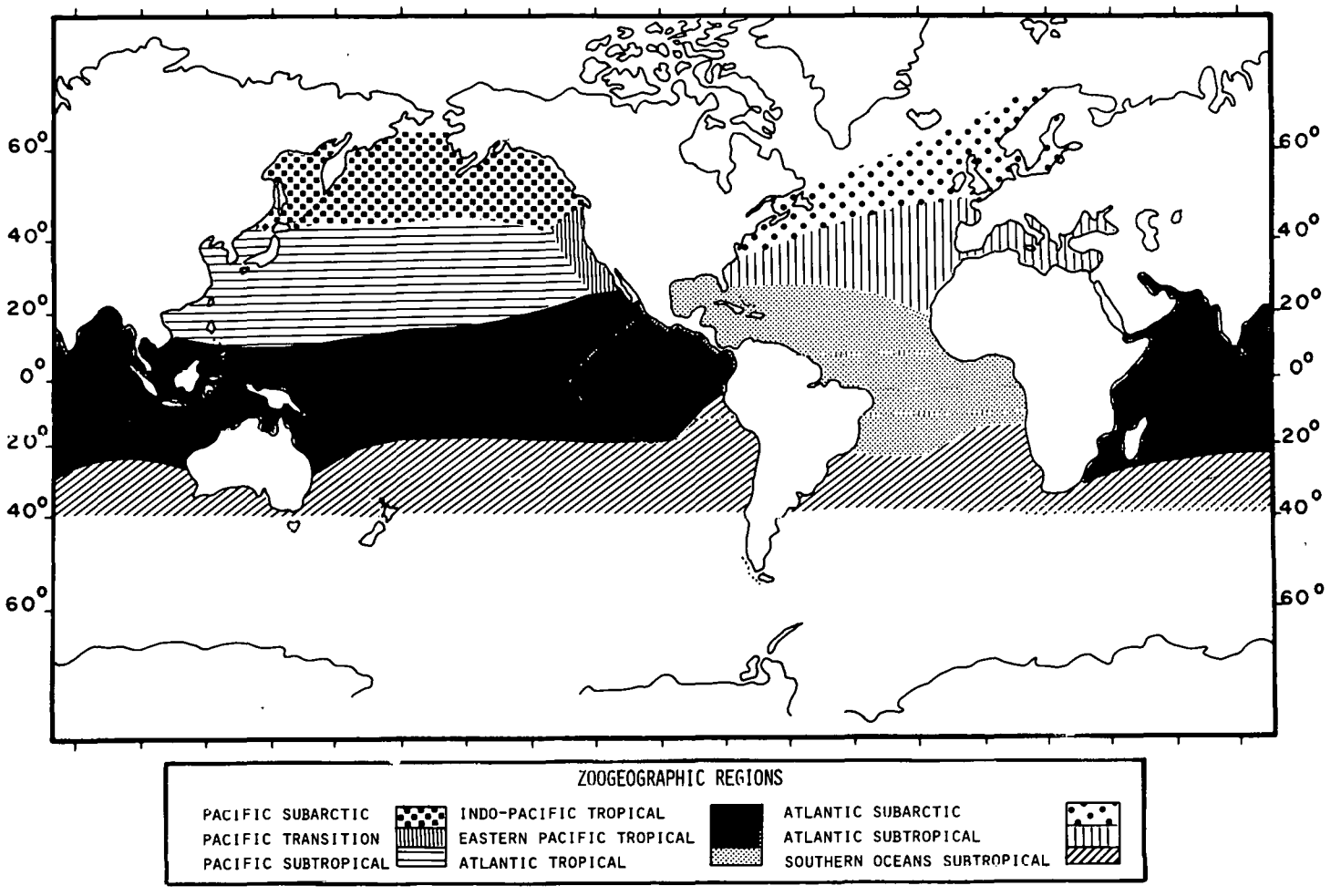



Fig. 2 Zoogeographic Regions for much of the Earth's Oceans

wind mixing. Light penetrates through this layer to support growth of phytoplankton (microscopic plants), which are grazed by zooplankton (microscopic animals). Larvae of almost all oceanic animals (fish, crustaceans, cephalopods) are found in the epipelagic zone, even though many of the adults live in deeper waters or on the bottom nearshore. The adult squids and fish (tunas, flying fish, sharks, and jacks) are fast swimmers and some are quite large. Sargassum, a floating seaweed, is found in subtropical oceans, especially in the Atlantic.

The twilit mesopelagic zone is located below the thermocline where the cold water pipe will be located. Many mesopelagic animals have photophores, or light organs, which may help camouflage them, help them recognize their own species or catch prey. There are no quantitative estimates of large animals such as sharks, whales, tunas, and larger squid, although these animals are known to be found here. A large percentage of the micronekton are vertical migrators, living at several hundred meters during the day and migrating to epipelagic waters at night. Mesopelagic squid caught by midwater trawls are small, active swimmers, usually 4-5 cm in length and rarely greater than 30 cm (16). The nektonic crustaceans include euphausiids, and bright red shrimps and mysids. The great majority of mesopelagic fish belong to the families Myctophidae (lantern fishes) and Gonostomidae (bristlemouths). Many mesopelagic fish mature at small sizes, i.e. 25-50 mm in length (1).

It is doubtful that mesopelagic fish can survive after being collected by the warm or cold water intakes. These fish are quite sensitive to mechanical disturbance and have only been kept alive for a few hours even when carefully dipnetted (2). Animals collected by the cold water pipe will undergo rapid pressure changes. From

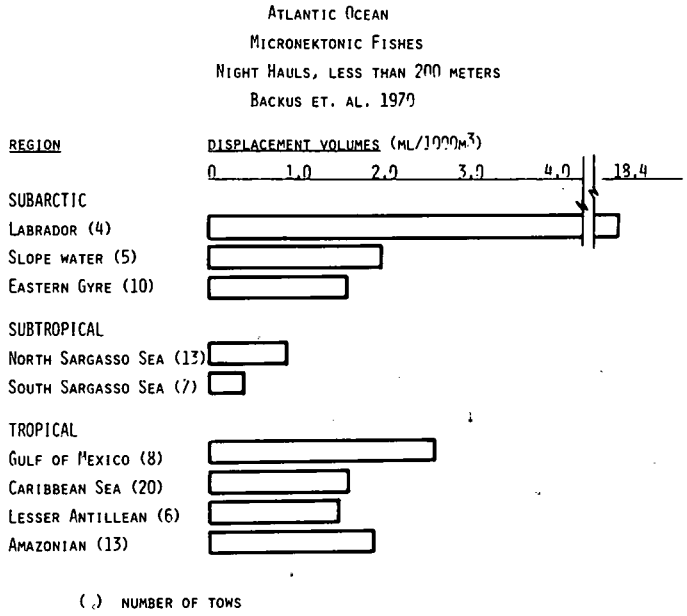



Fig. 3 Micronekton Abundance in the North Atlantic Ocean

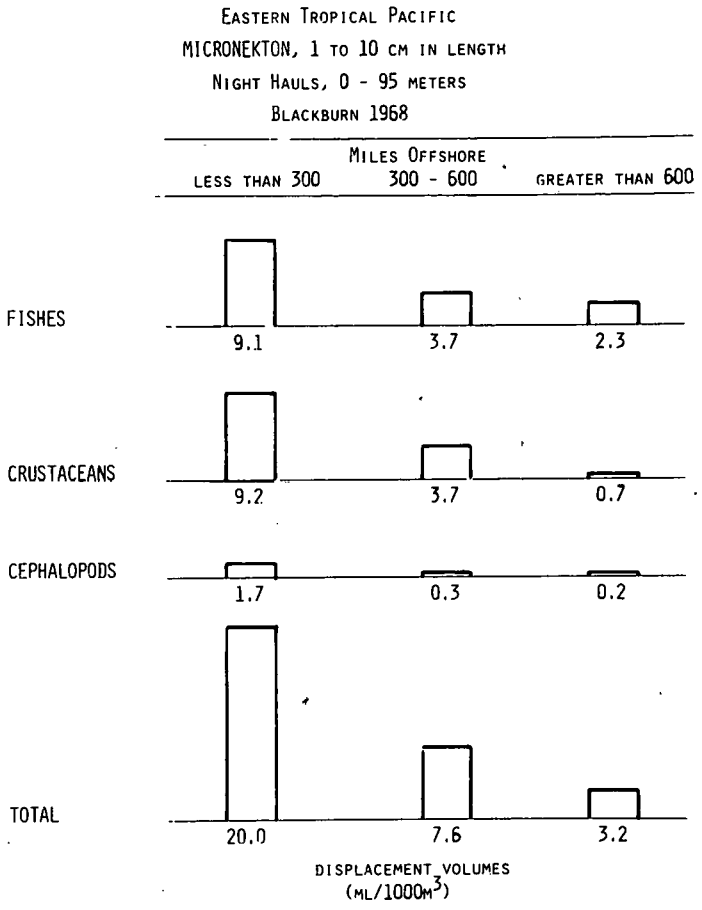



Fig. 4 Micronekton Abundance as a Function of Distance Offshore

experience with midwater trawls, all the mesopelagic fish collected are dead, probably due to suffocation since few of the fish with gas-filled swim bladders have everted stomachs. Therefore, to protect the fish that OTEC can collect, the fish must be repelled before they enter the intake pipes. The existing literature on "scarefish" devices used in conventional power plants has not been exhausted. This information probably is not applicable to OTEC plants anyway because the behavior of open ocean deep water fish is different from nearshore species. Furthermore, it is controversial whether these devices are effective (15).

The micronekton of bathypelagic waters are not vertical migrators. They are weak swimmers with poorly developed muscles. Unless the cold water pipe is very long (deeper than about 1000m), OTEC plants may not affect this zone.

Micronekton samples collected at night in the epipelagic layer are dominated by fish and crustaceans which inhabit mesopelagic layers in the daytime. This conclusion is based on studies in the eastern tropical Pacific and near Hawaii (12). In the tropical and subtropical Atlantic, in the sampled range of from 40-200 m, maximum fish catches per hour were made between 40-80 m in depth and at night (1). Midwater trawl samples collected during the day near the surface are usually small because the vertical migrators have descended. Off Hawaii, day samples from 0-400 m include jelly-like animals--mainly Cnidaria (jellyfish, siphonophores) and Tunicata (salps, pyrasomes), as well as other invertebrates. In this area, 47% of the micronekton biomass deeper than 400m during the day migrated

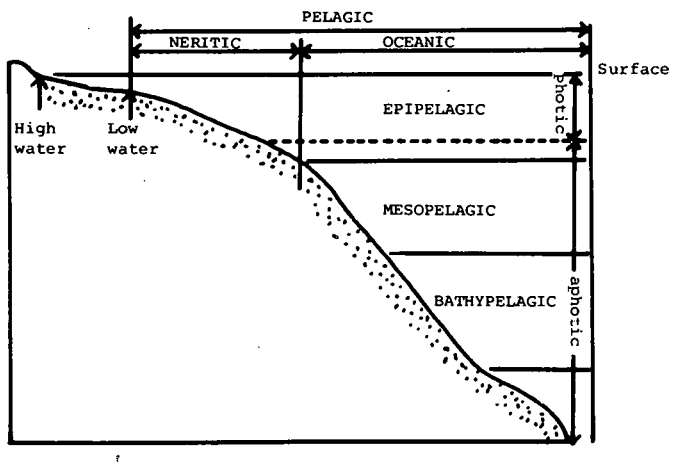



Fig. 5 Definition of Pelagic Depth Regions (After Hedgpeth, 1957)

into the upper 400 m at night (12). Cephalopods have been sampled from 0-1200 m in the eastern Atlantic. The highest number were found in the upper 100 m (11).

Few investigators have studied all micronekton categories, or have included detailed vertical distributions. However, such studies would be useful for the design and operation of OTEC plants. Echo sounders detect scattering layers where midwater fishes concentrate and have been used to determine the depth for midwater trawls (1). Thus, echo sounders are useful tools to study the depths of fish concentrations.

Observations from submersibles reveal important aspects of the behavior of mesopelagic fish (2). Mesopelagic fish orient themselves differently depending on their location in the water column. At night, many are at the surface (less than 100 m) and are oriented horizontally. During the day, they are found below 300 m, oriented vertically. The vertically oriented fish are stimulated to swim downwards by an approaching submersible's lights. Otherwise they hang motionless in the water. However, fish found near the surface at night are attracted by ships' lights, can be dipnetted at the surface and have been known to follow a submersible to deeper waters. The fish at the surface swim vigorously but are incapable of repeated swimming activity to escape predators such as squid. Thus, these fish may be caught by nets more easily than resting fish which are oriented vertically (2).

Two types of myctophids representing different specie groups are probably present: an active type that migrates to the surface and an inactive type that does not migrate all the way to the surface (2). The active type is characterized by large eyes, firm body, is attracted to lights, and lives at intermediate depths during the day and the surface at night. The inactive type has small or medium sized eyes, a soft body, is repelled by light, rests in a vertical position during the day, and migrates at night towards the surface.

Several observations relevant to OTEC plants can be made about fish behavior.

- The abundance of fish at all depths changes with the time of day, especially in the epipelagic layer.
- During the night, myctophids susceptible to capture will occur at the surface. However, during the day there will be virtually none.
- Lights at the surface will certainly attract myctophids; lights at depth will probably repel them.
- Myctophids orient vertically at depth (greater than 200 m), resting in a vertical position, and escape by swimming downward.

The orientation of these fish is important because experience with conventional power plant designs shows that coastal and estuarine fish are better able to resist horizontal currents than vertical currents. Perhaps the midwater fish will behave oppositely. Mesopelagic fish in deep layers do not encounter any strong horizontal currents and certainly no detectable gradients in velocity as do nearshore fish. Therefore, they probably will show different responses to currents introduced by OTEC plants.

### Floating Object Fish Attraction

An OTEC plant itself will create an environment attractive to animals. Fish whose permanent habitat is in the epipelagic zone, e. g. pilot fish and jacks, will be especially attracted. Any structure in open water, from flotsam (logs) to artificial reefs or observation rafts, attracts fish (6, 7). Small fish seek shelter from predators under the object, or in its crevices. Therefore, the concentrations of animals around an OTEC plant will be much higher than those typical of the surrounding ocean. This can be expected to amplify screening problems primarily for the warm water inlets during both day and night operations.

## SCREENS FOR ONSHORE PLANTS

Screens for onshore power plants (both nuclear and fossil fueled) require a continuous flow of "clean" water to remove excess heat. Typically, the water temperature rises by 10°C within about one minute and remains at an elevated temperature for some time after discharge into the receiving body of water. In contrast, a similar net power output OTEC will be circulating 100 times as much water through each intake with a probable temperature change of about 3°C. Condenser design flow speeds for both types of plants range between 5 and 8 ft/s.

### Shoreline Intakes

Screens are almost always located at the intake well upstream from the pumps, as shown in Fig. 6. The coarse bar rack and log boom serve to exclude large debris and protect the fine screens. The traveling

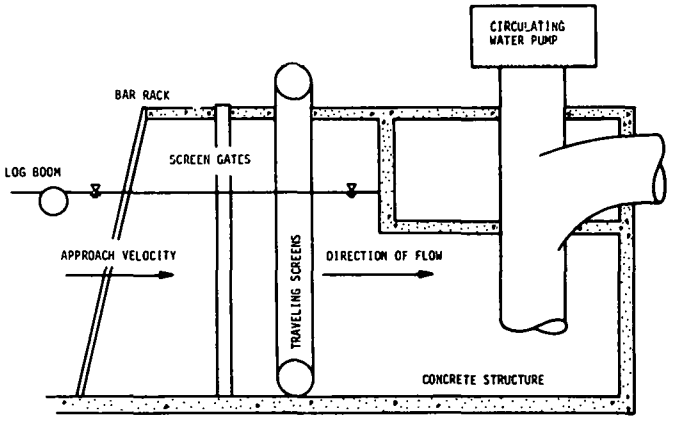



Fig. 6 Typical Shoreline Intake Structure ( 14 )

wire screen is of a small mesh size. The screen gates may be closed when maintenance of the traveling screen requires dewatering that portion of the intake structure. Most screening systems take advantage of a free surface for fish diversion, debris removal and cleaning. Present ideas for OTEC screening systems may not include a free surface. They may be completely encased in a closed conduit under pressure. Thus, it may be impossible to adapt existing schemes to an OTEC plant. However, it is useful to review existing plants for background information.

However, the possible use of a surge tank in the warm and cold water systems may provide a free water surface in which case the screen designs may be simplified. This interim report concentrates on the closed conduit system.

## Guidance

A large group of methods may be categorized as behavioral screens that depend on an organism's ability to learn to avoid an unpleasant environment or be guided through bypass routes. There is much information on fish protection (primarily trout, salmon and striped bass) at water diversions, intakes and dams but simple extrapolation of results to ocean species is not justified (8, 14, 15).

The use of sound to repel fish was unsuccesful at the Indian Point Power Plant. Fish will avoid chemicals such as copper, zinc, chlorine and some herbicides and pesticides when introduced at sublethal doses. This procedure is still experimental and unpopular due to cost and environmental concern. Air bubble curtains are expensive to operate and have had only marginal success. They have proved to be ineffective in estuaries. There has been some limited success with electrical barrier guidance systems in fresh water applications (70%-80% efficiency for velocity <.3m/s) but they have not been used in salt water. The use of light produces conflicting results, causing both attraction and repulsion.

Many fish have a natural tendency to avoid entering a zone of high flow velocity when they can remain in a region of lower velocity. A strong vertical velocity at the intake is usually avoided since shore fish react to vertical flow fields much more slowly than to horizontal flows. Combinations of several of the above may improve performance for onshore plants.

## Screen Examples

Screens are the most effective means of preventing fish from entering an area. The simplest, a bar screen (trash rack), consists of vertical parallel bars placed over the intake. The principal function is to prevent entrainment of large objects that might damage the pumps and secondary screening system. Shore based intakes normally use 3 1/2" by 1/2" flat steel bars with 3" to 4" clear openings. A traversing rake or brush assembly may be used for regular cleaning. An angle of $15^{o}$ to $20^{o}$ to the vertical is preferred. If entrainment of large surface debris becomes a problem, a log boom may be used to prevent blockage of the bar screen.

Fine meshed stationary screens with moving scrapers or brushes are a successful means of plant protection but impinged fish are subject to high rates of mortality and damage. Rotating disc screens are sometimes used for relatively small flows. The disc rotates about a horizontal axis and is cleaned with a high pressure spray above the free water surface.

Vertical traveling screens with 3/8" mesh size are the standard type used on power plants in the U.S.A (15). The usual criterion is a mesh size not greater than half the condenser tube diameter. In salt water applications, monel wire is the preferred mesh material. The screen is cleaned with a high pressure water spray (80-120 psi) and flushed debris is returned to the environment. The main advantages to this screen are proven performance and availability. These screens are usually run intermittently, but if head loss due to clogging becomes significant, continuous operation is in order. Continuous operation is sometimes preferred to reduce fish impingement time which should be less than 40 sec for increased survival rates. Fish normally become impinged broadside on the screens when exhausted, thus a 3/8" mesh may effectively screen elongate fish whose smallest dimension is less than 3/8". Refinements providing improved fish protection include fish buckets, nets or pumps. An example of the vertical traveling screen is shown in Fig. 7.

Variations of the vertical traveling screen are the horizontal traveling, Beloit-Passant, and revolving screens (15). Horizontal traveling screens are quite successful but have not been constructed in large sizes as yet. This screen is effective in diverting fish when placed at an angle to the flow. This guidance is based on the observations that some fish will orient themselves perpendicular to and facing away from the screen. An example of the horizontal traveling screen is shown in Fig. 8. The revolving drum screen is a large perforated drum that may be revolved either vertically or horizontally and operates similar to a vertical traveling screen.

## Fouling and Corrosion

The most common method for control of biofouling is cleaning with high pressure sprays. Mechanical brushes or scrubbers are also used. Other methods are heat treatment, chlorination, toxic coatings or low fouling materials such as copper alloys. To some extent, higher water velocities will reduce fouling but this must be balanced against higher impingement rates and greater head losses. Corrosion is best controlled by proper material selection. Coatings and cathodic protection may also be effective but require diligent inspection.

Head Loss

The energy loss through the screen is expressible in terms of head loss. The U.S. Department of the Interior uses the following equations to estimate head losses

$$h_L = k \frac{V^2}{2g}$$

$$k = 1.45 - 0.45\,\xi - \xi^2$$

$$\xi = \frac{\text{Area of opening}}{\text{Gross Area}}$$

where V is the flow speed through the openings and g is the gravity constant. The importance of keeping the screen clean is shown in Fig. 9.

Large installations with unique characteristics have head loss coefficients determined from detailed laboratory model studies.

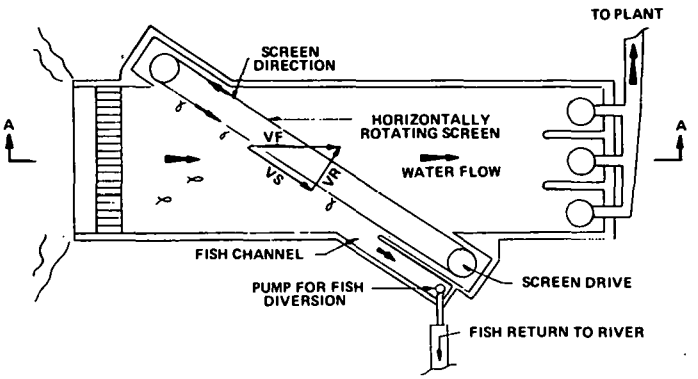



Fig. 8 Horizontal Traveling Screen (15)

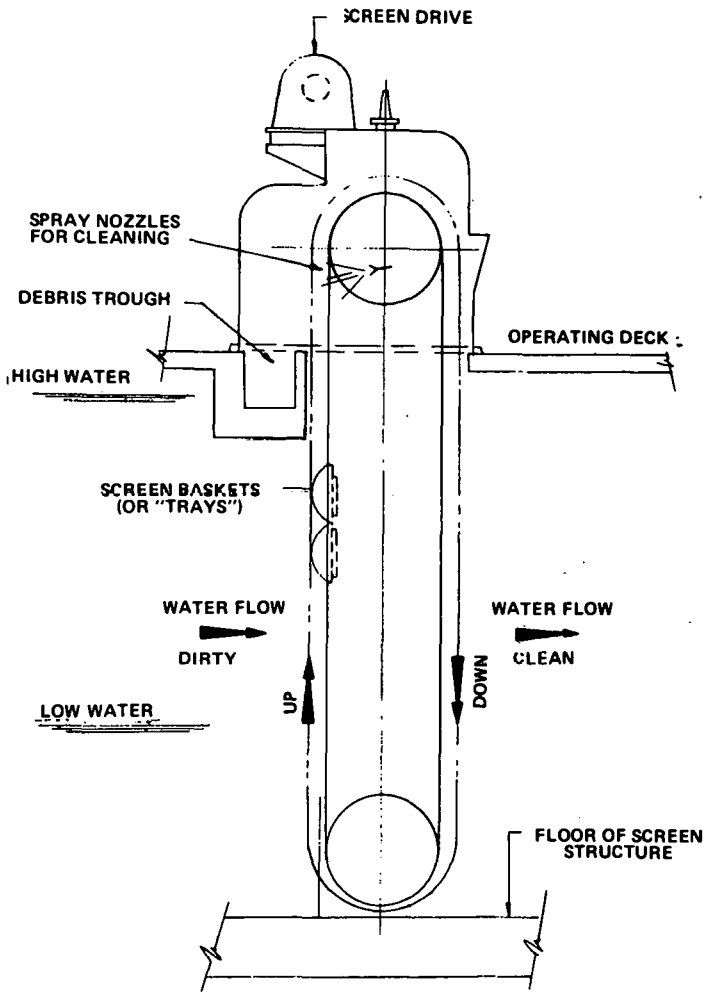



Fig. 7 Conventional Vertical Traveling Screen (15)

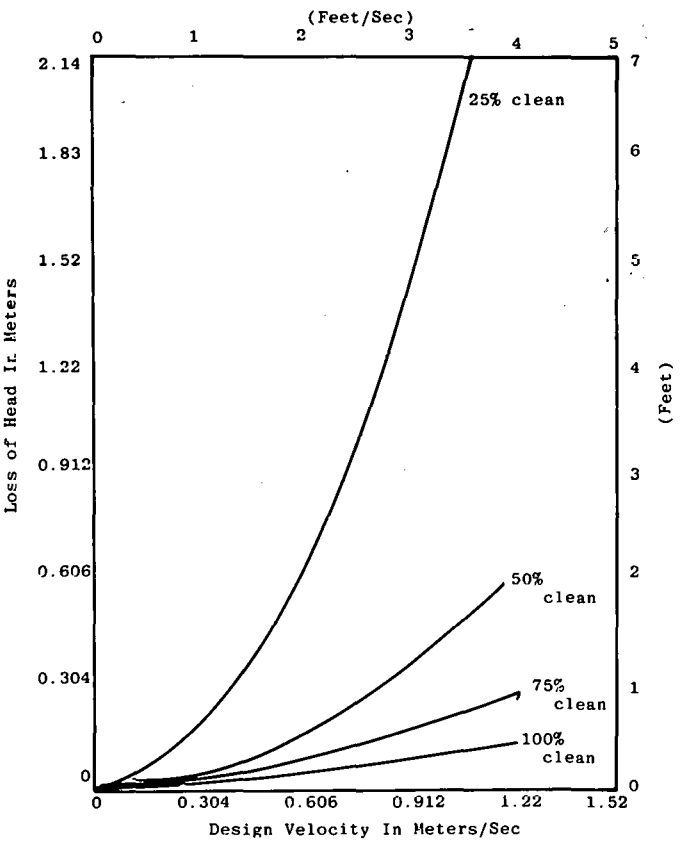



Fig. 9 Head Loss Through Traveling Water Screens of 3/8" Opening

SCREENS FOR OTEC PLANTS

The final design for screens will depend on the configuration around the plant and how biological material is pulled into the plant. In addition, the screens will become clogged at times and will need to be cleaned. This section reviews these needs.

Entrance Velocity

The flow speed at the entrances will influence the biological material that will be ingested into the plant. Present schemes indicate the possibilities of speeds on the order of 2-3 meters per second at the entrances. Of course, these speeds decay with distance from the entrance. The flow into a point sink from an infinite fluid medium is well known. However, it is still not known what the flow configuration around an OTEC plant will be. We now know only that the speeds may be as high as 3 m per second.

Only the larger very strong fish will be able to escape such flow speeds. Even the larger species may not be able to escape vertical speeds of such magnitudes. It may be required to design both the warm water and cold water intakes so that the flow velocities are primarily horizontal. These conditions are shown in Fig. 10. It is anticipated that only large fish will be able to escape the entrance flow speeds that will result in the final design. It may be necessary to design the warm water intakes for a lower intake speed because of the greater abundance of fish in the epipelagic region.

Cleaning

Cleaning of the screens is a major consideration for existing cold water intakes for heat dissipation at existing plants. Therefore, the screens are accessible. For an OTEC plant the warm and cold water intakes may be relatively inaccessible. Thus, cleaning at the intakes may be extremely difficult.

Cleaning may involve backflushing of screens to dislodge material that has clogged on the upstream side. In addition, biological growths may occur, such as barnacles, etc., which may need to be scrubbed at various times. If some operations can be dependent on the general flow, and thus made automatic, a savings in final costs will probably be made.

The present plan from this research is to provide large gratings at the intake openings as shown in Fig. 10 which will exclude only the large species of animals. A bank of secondary screens will then be placed downstream from the pumps so that automatic flushing of the screens can be made.

Intake Grating

The openings in the intake grating may range from about 0.3 to 1.0 m in size. Thus, most micronekton, plants, and non living materials will pass through the grating but large fish such as large sharks, whales, tuna, etc. will be excluded, particularly if they can escape the intake flow speed. The intake gratings will need to be cleaned from time to time, especially in the warm water intake. It may be that the cold water intakes will not require cleaning.

The head losses at the intakes for such large gratings will be relatively small. In addition, the intakes should be belled with approximately an ogee shape so as to reduce entrance head losses and the ingestion of some fish sizes.

A likely choice for the grating material is 90/10 copper nickel (1.5 iron). The alloy is relatively inexpensive and readily available and would provide essentially maintenance-free performance. It combines excellent corrosion resistance (uniform corrosion rate less than 1 mil per year) over a wide range of velocities and proven fouling resistance. These properties may be particularly useful at the warm water intakes where fouling rates are proposed to be higher. Above a 3 ft/sec continuous velocity, fouling organisms have increasing difficulty in attaching to a surface. If this condition can be assured, then carbon or low alloy steels (corrosion rate 5 to 10 mpy) may be a viable substitution. The risk of significant biofouling resulting in increased head loss through the screen and possible plant shutdown must be weighed against the increased cost of the copper alloy. Antifouling paints or coatings require regular inspection and maintenance making them a poor alternative.

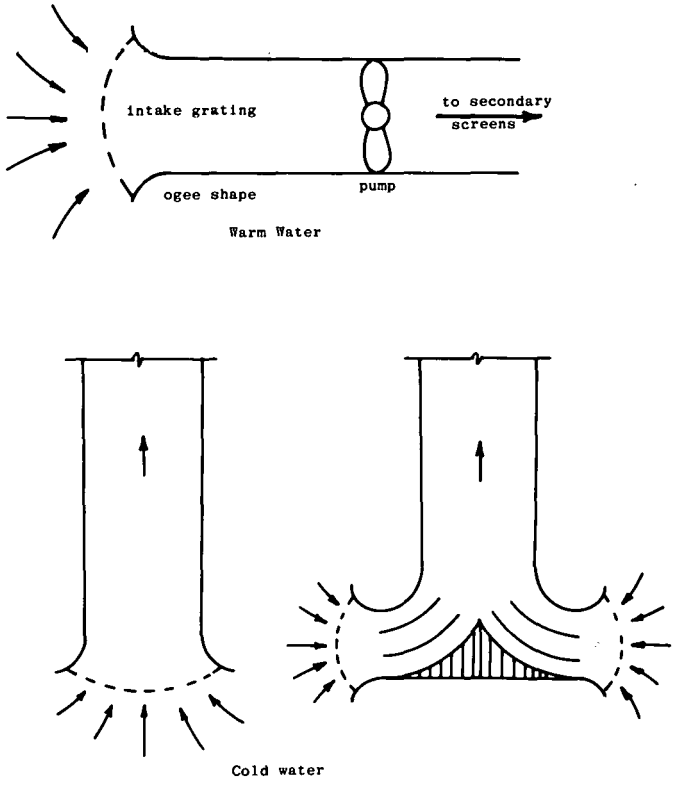



Fig. 10 Schematic of Intake Configurations

Secondary Screens

In order to exclude material larger than about 1/2" from the heat exchangers, it will be necessary to provide a screen with openings about 3/8" in size. This is presently being done for onshore plants. Such a small screen size will require frequent backflushing and cleaning for the warm water intakes. It is not known, even qualitatively, how often cleaning will be required for such small screens in the cold water pipes.

It would be desirable to be able to collect the material and divert it back to the outside environment. However, the pressure distribution in closed conduit flow must be taken into careful consideration. Figure 11 shows that if an opening is made in the side of the pipe upstream from a pump, that the water will flow from outside the pipe into the pipe. However, if an opening is made downstream from the pump, the flow will then be from inside the pipe to the outside environment. This mechanism makes it quite desirable to place the secondary screens downstream from the pump systems for closed conduit flow.

If the final design of the OTEC plant permits a free water surface to appear after the intake sections but prior to the pump system, then an effective cleaning system for the screens can be placed upstream from the pump. This is presently done, as presented in previous sections, for onshore plants.

Figure 12 indicates a possible bar screen arrangement in a circular pipe section which would provide relatively automatic cleaning and backflushing of the screens. As shown, the figure indicates the main flow divided into two sections, one taking the main flow while the other cleans the screens. The flow passes the pump and turns to the left through turning vanes (which can be rotated so as to divert the main flow to the right). The flow then passes through a diffuser and flow direction change into a section of much larger diameter than the main conduit. The increase in diameter is accomplished in order to reduce the flow velocities at the screens. Accordingly, this will reduce head losses considerably at the screens. The material in the water will impinge upon the screen and some of it will slide along the bar grating to the outside periphery of the pipe, which also concentrates the material into a naturally occurring nozzle section, as the plane screens intersect the circular pipes.

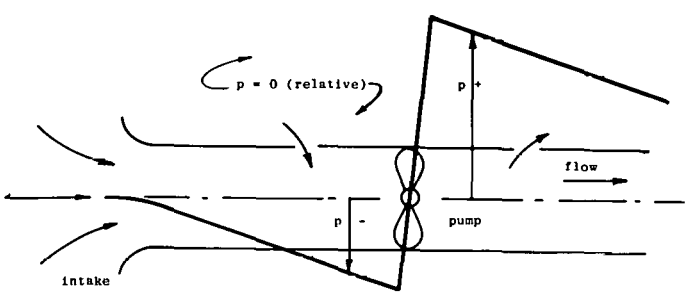



Fig. 11 Pressure Gradient for Closed Conduit Flow

Because the pressure inside the pipe is greater than that outside, a small amount of flow will be diverted to the outside which represents an energy los to the total system. However, this energy cost will b_, a certain amount of cleaning of the screens. As shown the figure also indicates that the right hand screens are being backflushed from a small amount of flow which returns from the Y section in the upper section of the figure and from the submerged jets that can be focused on the screen from the center support section as shown near the section A-A cut.

The fixed fine-meshed screening system outlined above may consist of monel bars (nickel alloy) which is commonly used for shorebased intakes in salt water environments. The corrosion resistance is usually quite good (1 mpy) except for susceptibility to pitting. However, at low velocities, monel does not resist biofouling and will require more frequent cleaning. The flushing and cleaning operations must be effective to prevent clogging of the screen causing increase in the head loss as shown in Fig. 9.

Thus, there will be a need for repair, maintenance and special cleaning of the screens. Biological growths, corrosion and other structural problems may occur which will require a more intensive treatment.

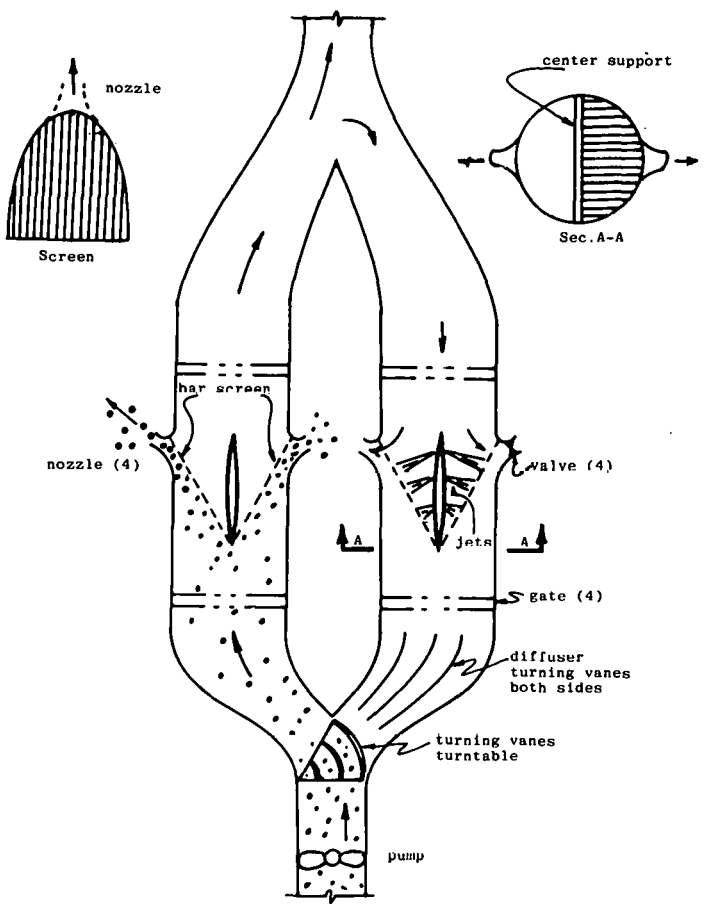



Fig. 12 Automatic Secondary Screen Cleaning Schematic for Closed Conduit Flow

Gates and Valves

Figure 12 indicates four gates, two on each twin system. The gates can close the tubes and the valves in the nozzles can be closed so that the volume around the screens can be dewatered. This region can then be entered by workmen to scrub and clean the screens as required. During this operation on one set of screens, the other set of screens can still be in operation. In addition, it may be possible to remove the screens and replace them with previously cleaned and maintained screens, in order to reduce to a minimum the shutdown time of one tube. It may be required to locate other gates and valves in other sections for maintenance and operations.

Energy Losses

The cold and warm water intake pipes are planned to be very large in size. The construction for the screening systems, including any bifurcated designs, as indicated in Fig. 12, will require major construction and fabrication problems. It will be a major design problem to reduce energy losses through the intakes, turns, vanes, valves, screens, etc. Similar energy loss considerations must be made in large conduits for existing hydroelectric projects.

Experience with large existing plants indicates that it is not possible to predict accurately the head losses or energy losses in new configurations such as those shown in Fig. 12. Therefore, laboratory model testing is utilized for estimating these losses for a given design. Frequently, designs are changed based upon the results of such studies. In addition, undesirable flutter and other pressure fluctuation problems can be investigated and corrected through laboratory model studies. Therefore, it is strongly recommended that laboratory model studies be conducted to test the energy losses and other hydraulic problems involved in the screening system as indicated herein.

BIOMASS SAMPLING EXPERIMENT

The resistance to horizontal or vertical flows by fish in the mesopelagic region is not known. Some information exists on resistance to horizontal and vertical flows for salmon-type of fish. However, no data exists on mesopelagic fish because they die when brought to the surface and cannot be retained for experimentation. Even their swimming speeds are not well documented.

The amount of mesopelagic fish taken into the cold water pipe will be a function of how the pipe sucks in the water among other things. However, present estimates of the abundance of mesopelagic fish are based on midwater trawls. The physical action of capturing the fish is grossly different between a midwater trawl and the suction action of the cold water pipe for an OTEC plant. Therefore, new information is required in order to be able to even approximately predict problems from fish impingement on the secondary screens for the cold water pipe. Therefore, it is proposed to conduct an experiment which will approximate the action of the cold water pipe intake in order to sample the fish in this manner.

In order to avoid construction of a test pipe extending a long distance into the ocean from an oceanographic research vessel or from some other relatively small craft, the sampling device shown in Fig. 13 is proposed. Two samplers will be required. One with a vertical intake and the other with a horizontal intake. The details of the experimentation will be proposed in the second half of this first year of this research. At this time, it is anticipated that the details of the experimentation may be as follows. The research vessel will be located at a desirable station. One sampler, say the vertical sampler, will be lowered over the side to the desired depth and the thrusters will be activated, which will suck in fish to the bar screens as shown. The fish will tend to accumulate at the top of the interior cylindrical screen. After a predetermined time of sampling, the first valve will be closed, entrapping the fish and materials in the upper most section. The thrusters at this time will be deactivated. The sampler will then be lowered to another desired location and the process repeated until the second valve is closed. The sampler can then be lowered again to a third level for additional sampling.

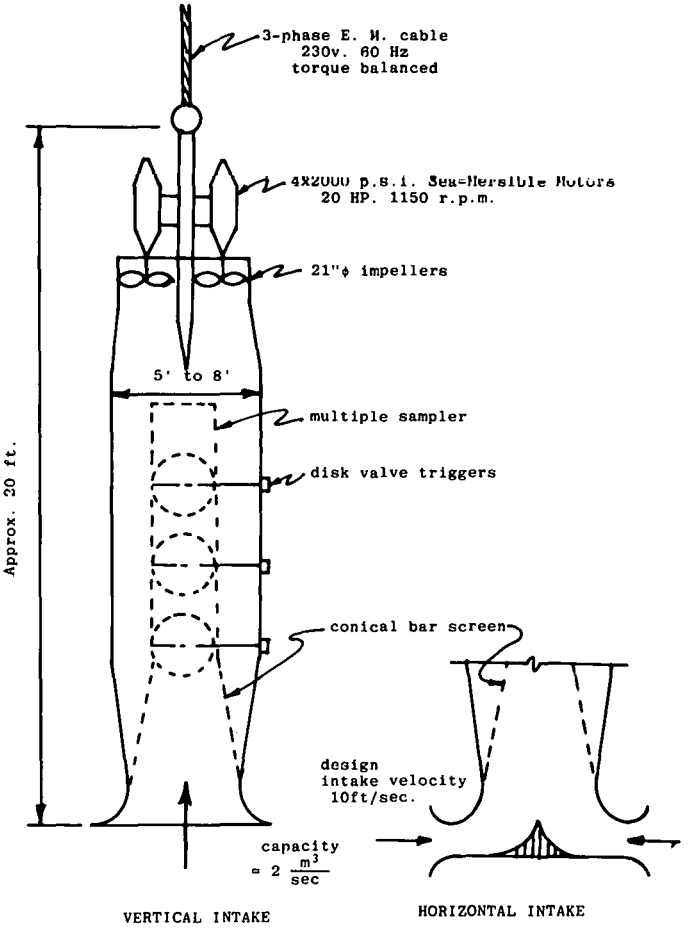



Fig. 13 Deep Sea Fish Sampler

After sampling with the vertical sampler, the horizontal intake sampler will be lowered over the side and the process repeated. At different stations, the vertical sampler will be lowered first whereas at other stations the horizontal sampler will be lowered first. By sampling in a statistically representative manner, the differences between the material collected from the horizontal and the vertical sampler can be determined. In addition to that difference, data will be obtained for the first time of the biomass in the mesopelagic region by methods other than midwater trawls.

## CONCLUSIONS

The eastern and southern coasts of the United States, as well as the tropical seas to $\pm 20^{o}$ latitude and the region around the Hawaiian Islands, were considered in determining the biomass that will need to be screened out of OTEC plants. The western coast of the United States does not have a desirable temperature differential to warrant the consideration of an OTEC plant. Therefore, this area is not included in this study.

The epipelagic fish are of most concern for the warm water intake. They are abundant and pose a major problem to the warm water intake systems. Hopefully, horizontal intake velocities can be avoided by many of these fish. However, it is unknown whether mesopelagic and bathypelagic fish can resist horizontal velocities any better than vertical velocities. The intake pipes of OTEC plants will sample micronekton differently than trawls used by biologists, even though the inlet velocities are similar to those of typical midwater trawls. The cold water pipe of 50-100 MW plants can be expected to ingest larger micronekton than are caught by standard trawls because its inlet area is much larger.

The response of mesopelagic fishes to intake pipes and screens is unknown. Behavioral studies of coastal and estuarine fish from conventional power plants are suggestive but not definitive because mesopelagic fish do not experience strong currents in the deep ocean.

An OTEC plant, like other floating structures, will be attractive to micronekton. Concentrations around the plant will be higher than in the surrounding ocean.

Micronekton populations should be assessed to evaluate impacts of clusters of OTEC plants on these populations.

An open ocean experiment for mesopelagic fish is proposed primarily to estimate the following - their ability to resist horizontal and vertical currents and whether a pump catches different animals than a midwater trawl. However, these preliminary evaluations must be viewed with caution because of scale effects. That is, for a 100 MW plant with 15-30 m diameter cold and warm water intakes, the action on micronekton is unpredictable because of the huge flow volumes, even if velocities are maintained at a minimum.

Large gratings are proposed to be installed at the intakes. These will exclude large fish only. For closed conduit systems secondary screens with small openings should be located downstream from the pumps in order to facilitate cleaning operations. The exact type of screens have not been determined.

Somewhat automatic cleaning can be designed for the secondary screens if they are placed downstream from the pump so that openings in the pipe will create a flow from inside the pipe to the outside. Energy losses from such flow, as well as losses from special pipe configurations, will need to be studied carefully with scaled physical model studies in the same manner as is done by the U. S. Bureau of Reclamation and the U. S. Corps of Engineers for large hydroelectric plants.

For systems that permit a free water surface, it may be possible to design a fairly standard traveling screen that permits continuous cleaning.

It is assumed that all fish entering the system will be killed from impingement on the screens or the pumps. Thus, a major concern exists for the material that may be returned to the environment which may attract large quantities of fish. (The material may be collected, but that will probably entail a further energy loss.) This attraction in turn may accentuate the problems of screening.

The costs in terms of dollars and energy loss for screening systems will be considerable. More details on losses will be available at the completion of this research.

## REFERENCES


1. Backus, R. H., Craddock, J. E., Haedrich, R. L. and Shores, D. L., "The Distribution of Mesopelagic Fishes in the Equatorial and Western North Atlantic Ocean," Journal Marine Research, 1970, 28(2):179-201.

2. Barham, E. G., "Deep-Sea Fishes: Lethargy and Vertical Orientation," Proceedings of an International Symposium on Biological Sound Scattering in the Ocean, U. S. Government Printing Office, Washington, DC 20402, 1970, pages 100-118.

3. Blackburn, M., "Micronekton of the Eastern Tropical Pacific Ocean: family composition, distribution, abundance, and relations to tuna." Fishery Bulletin 67: 71-115, 1968.

4. Bretschneider, C. L., "Operational Sea State and Design Wave Criteria, A Generalized Study for OTEC," Proceedings Third Workshop on Ocean Thermal Energy Conversion (OTEC), Houston, Texas, John Hopkins University, Applied Physics Laboratory, May 8-10, 1975.

5. Briggs, J. C., "Life in the Open Sea," Marine Zoogeography, McGraw-Hill Book Co., NY, 1974.

6. Gooding, R. M. and Magnuson, J. J., "Ecological Significance of a Drifting Object to Pelagic Fishes," Pacific Science, 1967, 21: 486-497.

Hunter, J. R. and Mitchell, C. T., "Association of Fishes with Flotsam in the Offshore Waters of Central America," Fishery Bulletin, 1967, 66: 13-29.

8. Jensen, L. D., editor, "Entrainment and Intake Screening Proceedings of the Second Entrainment and Intake Screening Workshop," John Hopkins University, Baltimore, MD, Edison Electric Institute, Electric Power Research Institute, 3412 Hillview Ave., Palo Alto, CA, EPRI Publication No. 74=049-005, December 1974.

9. Johnson, M. W. and Brinton, E., "Biological Species, Water Masses and Currents," The Sea, Vol. 2, pgs 381-414, 1963, Interscience, NY.

10. Love, C. M., editor, "Biological and Nutrient Chemistry Data," Eastropac Atlas, 1972-75, Vol. 2,4,6,8,10, NOAA, NMFS, Circular 330.

11. Lu, C. C. and Clarke, M. R., "Vertical Distribution of Cephalopods at 11°N, 20°W in the North Atlantic," Journal Marine Biological Association of the United Kingdom, 1975, 55(2):369-389.

12. Maynard, S. D., Riggs, F. V., and Walters, J. F., "Mesopelagic Micronekton in Hawaiian Waters: faunal composition, standing rocks and diel vertical migration." Fishery Bulletin, 1975, 73(4): 726-736.

13. McGowan, J. A., "Oceanic Biogeography of the Pacific," B. M. Funnell and W. R. Riedel, editors, The Micropaleontology of Oceans, 1971, Cambridge University Press.

14. Sonnichsen, J. C., Bentley, B. W., Bailey, G. F., and Nakatani, R. E., "A Review of Thermal Power Plant Intake Structure Designs and Related Environmental Considerations," Report from Hanford Engineering Development Laboratory, P. O. Box 1970, Richmond, WA, May 1973.

15. Train, R. E., et al, "Development Document for Best Technology Available for the Location, Design, Construction and Capacity of Cooling Water Intake Structures for Minimizing Adverse Environmental Impact," by the Affluent Guidelines Division Office of Water and Hazardous Materials, U. S. Environmental Protection Agency, Washington, DC, 20460, April 1976.

16. Voss, G. L., "The Biology and Bathymetric Distribution of Deep-Sea Cephalopods," Studies Tropical Oceanography, 1967, Miami 5:511-535.

# CONCRETE OTEC STRUCTURES—FABRICATION METHODS

H. H. HAYNES AND R. D. RAIL
*Ocean Structures Division*
*Civil Engineering Laboratory*
*Naval Construction Battalion Center*
*Port Hueneme, California*

## Abstract

Fabrication methods using cast-in-place and precast concrete techniques for large floating structures are discussed. OTEC structures of various configurations and sizes up to 500,000 tons or larger can be constructed in Puget Sound, Washington. At other potential U.S. construction sites, with water limitations of 35 to 45 feet, OTEC structures of about 150,000 tons (about 100 MWe power plant size) can be built of concrete using existing facilities. Techniques for reducing the draft of structures during construction and towout, such as temporary buoyancy and the use of lightweight concrete, are also discussed.

## Introduction

Concrete is a prime candidate material for the construction of Ocean Thermal Energy Conversion (OTEC) structures. These structures will be quite large. Methods, developed in Europe, for fabrication of large concrete ocean structures utilize fjords and similar deep water sites not commonly found in the U.S. The relatively shallow water available at most potential U.S. construction sites imposes draft constraints and raises the question of how to build the massive OTEC structures in U.S. waters.

The objective of this paper is to describe the methods available for the fabrication of large floating structures from reinforced and prestressed concrete. In this way, readers who are interested in the overall aspects of OTEC, but not necessarily knowledgeable about concrete construction, may learn of the wide diversity and flexibility for building with concrete.

## OTEC Size Requirements

Table 1 shows full-load displacements of various structures, both actual and conceptual, as an indication of relative sizes. Full-load displacement is the weight of water displaced by the hull when the structure is carrying its full pay load and associated ballast.

Concrete-hulled OTEC concepts proposed by Lockheed, TRW, University of Massachusetts, Carnegie-Mellon University, and Johns Hopkins University have displacements ranging from 140,000 to 355,000 tons.[1-5]*

Hydronautics evaluated five candidate OTEC platforms and used 500,000 long tons as a baseline for a 500 MWe power plant with 150,000 to 900,000 tons considered as the range of interest.[6] Hull configurations included two surface platforms--a ship shape and a disc--and three submerged platforms--submarine, spar, and semi-submersible. Based on sea keeping performance, the semi-submersible was the most attractive. Ithas twin horizontal cylindrical hulls 600 feet long by 120 feet in diameter with six 80-foot diameter vertical cylinders for stability.

The OCEAN RANGER at 50,000 tons (one-tenth the displacement of the OTEC baseline platform) is the largest steel semi-submersible offshore drilling platform built to date. The 91,000-ton aircraft carrier NIMITZ is the world's largest military ship and the 630,000-ton BATILLUS the largest crude oil carrier.

Concrete structures include the ARCO LPG barge (65,000 tons), the Genoa, Italy floating dry dock (about 220,000 tons), and various large bottom-resting offshore oil platforms, such as the Brent B CONDEEP (440,000 tons) built in Norway and currently in place in the North Sea, and the Ninian platform (600,000 tons) nearing completion in Scotland. The offshore platforms are pertinent since they are floating during most of their construction and the several hundred mile towout to operational sites.

Thus we see that large floating structures have been built in the size range of proposed OTEC power plants, though not specifically of the hull configuration, internal arrangement or weight distribution of the OTEC structure.

## Construction Sites

Construction of a ship or other large floating object is usually started in the dry and then, after a greater or lesser amount of construction, the hull is launched or floated. Construction and outfitting is completed with the ship afloat in a wet dock, often at an outfitting pier.

OTEC structures are in general too large to start on marine railways or barges. If possible, they will be started in dry docks, but if too large for dry docks, then special flooding basins can be constructed.

* Numbers in parenthesis indicate references listed following the text.

Availability of sites to build such basins is a major problem.

Puget Sound in Washington State is the only deep r harbor site in the continental U.S. It has protected waters to depths of 550 to 700 ft near industrial areas and a minimum towout depth of about 130 ft.

In Puget Sound the size of an OTEC structure to be built is not significantly restricted by water depth. The dry dock or flood basin approach is feasible and becomes a matter of choice to the designer. OTEC structures of 500,000-ton displacement or greater (500 MWe and larger power plants) can be built in any of the major configurations: semi-submersible, spar, submarine, barge and disc.

At other U.S. construction sites the designer's choice is more constrained. Harbors, dry docks and towout waterways have draft limitations of 35 to 45 ft. Outside of harbors, the sites are less protected from open ocean weather conditions. It would appear economically desirable to use existing dry docks with their established services. Another major advantage is that since they already exist, they would not need environmental approvals, as would be required for the construction of flooding basins. The main disadvantages of existing shipyards, in addition to depth limitations, may be width and overhead clearance limitations.

The Applied Physics Laboratory, Johns Hopkins University, has compiled information on commercial shipyards in the United States. Construction facilities are available on the Atlantic, Gulf and Pacific coasts with shipways of 40-ft (12-m) depth, and 150-ft (45-m) or more width (444-ft (135-m) width in one case).[7] Sizes of U.S. Navy dry docks are another indicator of U.S. industrial capabilities. The U.S. Navy has dry docks on the Atlantic and Pacific coasts and in Puerto Rico and Hawaii with widths greater than 140 ft (42 m), depths of 47 ft (14 m) or more, and lengths around 1100 ft (330 m).

At the present time, OTEC power plants of surface ship and of some semi-submersible configurations can be built at existing facilities in sizes up to about 100 MWe (assuming displacement of about 150,000 tons). In all cases the overall system design requires a careful integration of the internal arrangement of the power plant, the external hull configuration, the gross displacement, the fabrication methods and the construction site characteristics.

The use of modular construction, temporary additional buoyancy, lightweight concrete and other fabrication and deployment methods discussed below are particularly useful in overcoming water depth limitations.

## Fabrication

Two basic approaches to building massive floating concrete structures are to build the structure as a whole using cast-in-place concrete or to build the structure, for the most part, from components of precast concrete elements that are joined together in various ways. Most structures are built using a combination of cast-in-place and precast but the predominate use of one or the other method classifies the construction approach.

### Cast-In-Place Concrete

This method typifies the approach that has been used for the North Sea offshore concrete structures, that is, to cast concrete into forms and build the structure as a whole. The general procedure is to use a large flooding basin where the base section of the structure is built. The base consists of the bottom section, internal partitions, and side walls up to a height of about 40 ft (12 m). The forms for the partitions and side walls are built so that they can be slipped upward as the concrete is cast. The forms are suspended from steel reinforcing bars embedded in the concrete walls and climb the steel bars as casting proceeds. This technique for the vertical walls is called slip-formed concrete construction.

After the walls are slip-formed to a sufficient height, the basin is flooded and the base is floated out and moored in protected waters. Construction of walls, towers and deck, as well as outfitting , is then completed with the structure afloat in its "wet dock". In Figure 1, a CONDEEP structure is shown under construction while ballasted down by sand and water to a 30- to 40-ft freeboard. At the time shown, construction was just beginning on the three towers which eventually brought the overall height of the platform to 530 feet. For the construction phase shown, a draft of 120 feet was used. Water depth greater than 550 ft was used later for mounting of the steel superstructure. For this operation the concrete structure was ballasted down so that only the tips of the towers were above water. The superstructure, which had been fabricated in a ship yard, was mounted on two large hulls, towed to the deep water site, and brought over the top of the submerged concrete structure. CONDEEP was then deballasted so that it lifted the superstructure.

Such a procedure could be used for the construction of OTEC platforms in Puget Sound. However, OTEC structures would not require the same water depths as the offshore platforms since the configurations of the structures are much different.

Hoyer-Ellefsen, builders of the CONDEEP structures, have proposed floating concrete platforms for the oil industry. Their CONDRILL concept, displacing about 107,000 tons, is designed for construction in a dry dock and has a towout draft of 50 to 60 feet. A production version, CONPROD, has a towout draft of 43 feet (Figure 2). These structures will use cast-in-place concrete for the major part of the construction. Similar techniques are naturally available to OTEC.

### Precast Concrete

In this method precast elements are joined together to build the main structure of subassemblies, which in turn are joined to each other or to the structure.

Precast elements may be produced at several locations simultaneously, thus leading to shorter overall construction time and to less congestion at the major job site. Casting beds are used repetitively thus requiring a smaller working area. Re-use of forms for like elements leads to other cost savings, as do rapid curing methods, specialized jigs for preparing and handling reinforcing and prestressing steel, and various other assembly line methods.

Quality control is easier in this factory-like environment. Thus, higher strength concrete can be dependably produced; this can lead to thinner, lighter-weight sections in many cases. Handling of materials may be less critical since it is not necessary to maintain an uninterrupted flow of large quantities of material to one central point, as required for the continuous around-the-clock placing of concrete commonly used for the large cast-in-place structures.

Another very important advantage of the precast approach is that a much shallower wet dock will suffice during most of the construction period. Various assemblies and major modules, such as one of the hulls of a semi-submersible, would require a relatively shallow draft. Deeper water would then be needed only for the comparatively short time required to assemble the major modules together.

An example of combined cast-in-place and precast fabrication is the seawall for the Ekofisk oil storage structure shown in Figure 3 under construction while afloat. Cast-in-place storage tanks were surrounded by a perforated seawall built up of precast elements, Figure 4. These were stacked in place, forming a "hollow wall". Reinforcing and prestressing steel were placed in the voids which were then filled with concrete. Construction of the composite seawall was completed by post-tensioning.

Another example of combined precast and cast-in-place construction is the 65,000-ton ARCO LPG barge designed by ABAM Engineers, built at Tacoma, Washington by Concrete Technology, Inc., towed across the Pacific Ocean and moored in the Java Sea off Indonesia.[8] As seen in Figure 5, gas processing equipment, offices, quarters and six steel storage tanks are mounted on the deck of the 460-ft (140-m) long barge. Six additional storage tanks are placed within the concrete hull.

A combination of segmental precast shell members and cast-in-place walls and decks were post-tensioned in three directions to produce a watertight composite structure which resists bending and shear loads as well as hydrostatic pressure with relatively thin walls. Curved hull segments, each about 45 ft wide by 11 ft long, were match cast one against another in a dockside casting yard. After suitable curing the 40-ton segments were placed sequentially in the graving dock (Figure 6). The joints were sealed with epoxy. Longitudinal walls were cast in place and the transverse walls and bow section constructed by precast and cast-in-place methods. The partially completed hull was post-tensioned and floated to an outfitting dock (Figure 7). Six storage tanks were placed in the bottom of the hull and then the upper portion of the concrete walls and decks were cast and post-tensioned, and outfitting completed.

There are various sites in the United States where a barge such as the ARCO barge, with a launch draft of 13 ft and a fully loaded draft of 45 ft, could be built. Also, using similar fabrication method the barge could be scaled up in size either as a unit or by modular construction in which the final structure would consist of several modules each about the size of the ARCO barge.

A comparable floating LPG facility has been proposed by Transenergy International, Inc. for the North Sea (Figure 8). This concept has a twin-hulled semi-submersible configuration, more appropriate to severe sea conditions than a barge-shaped hull. For this concrete structure, segmentally constructed hulls could be built individually in dry docks and then floated and joined together after which the vertical cylinders would be built up of precast segments or slip-formed in place.

Another concept for a floating LPG facility, this one somewhat larger with a total displacement of about 200,000 tons, has been developed by Global Marine Development, Inc. (Figure 9). A preliminary design of the 860- by 192- by 96-ft deep hull uses a double wall which functions both as the exterior of the hull and the interior of the LPG tanks. Most of the construction would be in a dry dock using established precasting and post-tensioning methods.

Modular Construction

In addition to the large floating structures built and proposed by industry for industrial application, the Department of Defense has investigated concepts for large mid-sea "Mobile Ocean Basing Platforms". These stable platforms have been suggested in various configurations and sizes from a 300- by 300-ft communciations station up to a mid-ocean airfield 1000 ft wide by 4000 ft long. The various configurations have in common a construction approach in which modules are towed to deep water, open ocean sites and assembled into the final structure. This is shown in Figure 10 for a 300- by 1200-ft version displacing about 600,000 tons.[9]

An approximately one-tenth scale model of a 300- by 300-ft semi-submersible platform was built by the Civil Engineering Laboratory to evaluate construction methods and structure behavior (Figure 11). Segments for the 5½-ft diameter model hulls were cast at a concrete pipe manufacturing plant using conventional methods. The segments were joined by post-tensioning. The saddles between the horizontal and vertical cylinders were cast in place after which the vertical column were post-tensioned to the hulls.

A modular construction approach can be visualized for Hydronautic's 500,000-ton baseline semi-submersible platform (Figure 12). The cylindrical hulls and the cross members would be individually constructed in a dry dock. The ends of the cross members and the corresponding openings in the main hull members would be temporarily bulk-headed. As each cylinder is constructed, the dry dock is flooded, that cylinder floated out

and worked on until both hulls and the cross members are completed, at which time they are all assembled ether while afloat. Vertical members would then be p-formed, or constructed by other methods, with the ___ucture afloat. Due to its very stable configuration, draft could be kept at a minimum during the remaining construction and fitting out.

Individual cylindrical hulls 600 ft long by 120 ft diameter with 2-ft thick walls can be built with a draft of 27 ft. This wall thickness provides adequate strength for the cylinders while floating "light". At their proposed maximum operating depth of 220 ft a 4.6-ft wall thickness would be required (at least at the most highly loaded section of cylinder). The additional wall thickness can be constructed within the cylinder afloat in its wet dock. For the final semi-submersible configuration with twin hulls, one cross member and six vertical columns (all with final wall thicknesses) with the dimensions and layout as shown in Figure 12, a draft of about 53 feet is required. If lightweight concrete were used throughout, the required drafts could be reduced from 27 to 23 ft in the dry dock, and from 53 to 46 ft in the wet dock.

A variety of precast techniques have been mentioned from assembling small components into large structure sections or modules to assembling modules while afloat into the final structure. The flexibility in using this construction approach is quite wide.

## Joining Methods

Fast, practical methods for joining both small elements and major modules with watertight, structurally adequate joints is an important consideration for precast concrete construction.

The use of high quality concrete and careful workmanship are probably the most important factors in producing reliable cast-in-place joints between precast elements. Continuity of reinforcing steel may be developed by a variety of lap splices and in some cases by welding. Elastomeric waterstop prevents water flow through construction joints.

Cement mortar and expanding grout may be used as a bedding material when placing precast elements. However, epoxy, though a more expensive material, often permits easier and faster construction of better joints at a lower overall cost.

Bolts have been used for fastening elements together, however, post-tensioning is in most cases more desirable for assembling small elements into large members and joining major modules together. Bolts and post-tensioning techniques have the advantage of being reversible. Thus, major modules could be disassembled for maintenance or for replacement.

A number of major structures have been assembled from large modules while afloat. Three floating bridges, two on Lake Washington and one across Hood Canal, in the Seattle, Washington area, were constructed in this manner. Typically, individual pontoons each up to 360 ft long by 50 ft wide were constructed in dry docks and then towed to the bridge site. There they were connected by post-tensioning and other methods into highway bridges 0.9 to 1.6 miles long.

The 3.4-mile Bay Area Rapid Transit tunnel between Oakland and San Francisco was constructed of sections 350 ft long by 50 ft wide. The sections were floated to the site, lowered into a trench that had been dredged in the bay bottom, and connected together in place on the bottom.

The large Genoa dry dock was constructed of 15 sections each with a displacement of about 14,000 tons that were joined together while floating in the bay at Genoa.

The Kish lighthouse in Ireland is basically a vertical cylinder built of concentrically telescoping sections. It was towed in the "closed-telescope" position to its site in the Irish Sea. Once on the bottom, the telescoped sections were extended and permanently joined together and the structure was post-tensioned to the seafloor.

## Towout

Passages to the open ocean may be shallower than wet dock areas. Chesapeake Bay has a critical depth 45 ft at the underwater tunnel portion of the Chesapeake Bay Bridge-Tunnel. Much of San Francisco Bay is considerably deeper than the 5-mile stretch of 45-ft water depth outside the Golden Gate. In such situations, two basic approaches can be taken (assuming lightweight concrete is already being used): use temporary buoyancy and modular construction techniques.

Temporary buoyancy relies on methods to augment the inherent buoyancy of the structure itself. Naturally, auxillary buoyancy structures are an alternative, but this is one of the more costly techniques. However, if no other approach provides a solution, then auxilliary buoyancy structures become cost effective as a necessary expense. However, a less expensive approach is to work with the structure as much as possible.

Portions of the structure can be used for buoyancy that under operating conditions will be flooded or open-bottomed. For example, the cold water pipe well could be closed at the bottom with a temporary bottom and then de-watered. The entrances and exits for the heat exchanger and condenser compartments could be closed-off and de-watered.

Also, added ballast to the structure could be held back so that only a sufficient quantity was added for safety under towage. Any additional ballast could be added after deeper water was reached.

Probably the most flexible method is to use modular construction, dividing the structure into several independent floatable modular secitons. These sections can be built in relatively shallow water and then assembled together in deep water. The assembly method will be designed for a speedy execution (one or two days) because most deep water sites outside of U.S. harbors are exposed to the ocean ocean. Advanced weather pre-

diction techniques are accurate enough to forecast sea conditions for the duration of the connection process. An excellent example of the modular structure approach is the T. Y. Lin International concept.[11]

## Lightweight Concrete

Lightweight concrete is essentially the same as normal weight (hard rock) concrete except some or all of the aggregate is a natural or processed porous material rather than sand, gravel or crushed rock. For concrete compressive strengths of interest (5000 psi or greater) for OTEC applications the aggregates are generally made by expanding naturally occurring shales, clays and slates and industrial by-products such as slag and pelletized fly ash. In all cases the aggregates are light in weight due to the cellular structure of the individual aggregate particles. The cells may vary from microscopic to macroscopic and are both interconnected or non-interconnected. The aggregates are produced by various processes but in one widely used approach the cellular structure is formed by heating the raw materials to incipient fusion (about 1100° C) at which point entrapped gases or injected water or steam cause bloating. The cellular structure is retained when the material cools to a vitrified hard material.

Reinforced normal weight concrete, when fully saturated, has a unit weight in air of about 160 lbs/ft$^3$ (2560 kg/m$^3$). Reinforced saturated lightweight concrete weighs up to about 130 lbs/ft$^3$ (2080 kg/m$^3$). Thus, for the hull of the OTEC platform the weight savings is about 20%, assuming fully saturated concrete, which is the worst case. For interior concrete walls, decks and other platform elements that do not become saturated the weight savings is about 25%. For wholly submerged elements, such as the walls of the cold water pipe, the net in-water weight savings (taking into account the buoyancy due to displaced water) is about 30%.

The reduction in platform self-weight leads to a reduction in platform size for a given payload. The smaller sized platform has less drag and therefore requires less propulsion power during towout or during operations in the grazing mode; moored platforms may have smaller mooring lines and anchors. All of these lead to cost reduction. Of particular importance is the reduced draft during construction and towout. Thus, more construction sites may be available.

Many engineering properties of lightweight concrete are similar to those of normal weight concrete. One of the first applications for lightweight aggregate was in concrete ships built during World War I. The USS Selma, 7,500 ton displacement, was the first vessel built in 1919. Due to an accident the Selma was grounded on a beach in Galveston, Texas; its operational life was short, but its research life has been long. In 1953 after 34 years of exposure to wetting and drying for the upper part and continuous submergence for the lower part, samples of the hull from both parts showed no signs of corrosion for the steel reinforcement and an increase in compressive strength for the lightweight concrete.[12]

Thus, field experience shows good long-term behavior of lightweight concrete at shallow depths. However, additional knowledge is needed on the material properties of both normal weight and lightweight concrete while partly and fully saturated in a hydrostatic environment.

## Summary

This report discussed construction approaches that can be used to build concrete OTEC structures. One of the main considerations was methods to build massive structures in relatively shallow water. In general, it is recommended to utilize modular construction, temporary buoyancy and lightweight concrete in order to maximize the size of the structure that can be built in water depths of 40-45 ft.

## References


1. Lockheed Missiles and Space Company, Inc., Ocean Thermal Energy Conversion (OTEC), Power Plant Technical and Economic Feasibility, Vol I Technical Report, Vol II Supporting Data. Prepared for National Science Foundation Research Applied to National Needs Program, NSF/RANN/SE/G1-C937/FR/75/1 and LMSC-DO-56566, Sunnyvale, CA, April 1975.

2. TRW Systems Group, Ocean Thermal Energy Conversion, Research on an Engineering Evaluation and Test Program, Vol 1, 2, 3, 4 & 5, Final Report. Prepared for Energy Research and Development Administration for Contract No. NSF-C958, Redondo Beach, CA, June 1975.

3. University of Massachusetts. Progress report NSF/RANN/SE/GI-34979/PR/74/1: Research Applied to Ocean Sited Power Plants, by W. E. Heronemus, et al., Cambridge, MA, 30 April 1974.

4. Carnegie-Mellon University, Progress Report NSF/RANN/SE/GI-39114/PR/74/3, Solar Sea Power, by C. Zener, et. al., Pittsburgh, PA, April 1974.

5. The Johns Hopkins University, Applied Physics Laboratory, Maritime and Construction Aspects of Ocean Thermal Energy Conversion (OTEC) Plant Ships, by W. H. Avery, R. W. Blevins, G. L. Dugger, and E. J. Francis, Laurel, Maryland, April 1976.

6. Hydronautics, Incorporated, Theoretical Evaluations of the Seakeeping Performance and Resistance/Propulsion Characteristics of Five Candidate OTEC Platforms, by R. A. Barr, J. F. O'Dea, and V. Ankudinov, Laurel, Maryland, July 1976.

7. Private correspondence with E. J. Francis, of the Johns Hopkins University, Applied Physics Laboratory, Laurel, Maryland, April 1977.

8. Anderson, A. R., World's Largest Prestressed LPG Floating Vessel, Journal of the Prestressed Concrete Institute, Vol 22, No. 1, January - February 1977, 21 pages.

9. Civil Engineering Laboratory, Technical Note N-1144,

Mobile Ocean Basing System - A Concrete Concept, by J. J. Hromadik, et al., NCBC, Port Hueneme, CA, January 1971.

Andrew, C. E., Problems Presented by the Lake Washington Floating Bridge, Proceedings of the American Concrete Institute, Vol 37, January 1941, pg 253 - 268.

11. T. Y. Lin International, Engineering Analysis of Ocean Thermal Energy Conversion Structures of Concrete, San Francisco, CA, November 1976.

12. Expanded Shale, Clay, and Slate Institute, Story of the Selmia, National Press Building, Washington DC, November 1953, 11 pages.



Figure 1. CONDEEP Under Construction

Table 1. Comparative Sizes of Various Large Floating Structures

| | Approximate Full-load Displacement (long tons) |
|---|---|
| OTEC Concepts (Concrete Hulls) | |
| Johns Hopkins University (100 MWe) | 142,000 |
| TRW, Inc. (100 MWe) | 212,000 |
| Lockheed Missiles & Space Co., Inc. (160 MWe) | 355,000 |
| University of Massachusetts (400 MWe) | 400,000 |
| Hydronautics, Inc., "Baseline" (500 MWe) | 500,000 |
| Actual Structures (Steel) | |
| OCEAN RANGER, Semisubmersible Drilling Platform | 50,000 |
| NIMITZ, Aircraft Carrier | 91,000 |
| BATILLUS, Crude Oil Carrier | 630,000 |
| Actual Structures (Concrete) | |
| ARCC Barge, LPG Processing Plant | 65,000 |
| GENOA Floating Drydock | 220,000 |
| CONDEEP, Offshore Platform* | 440,000 |
| NINIAN, Offshore Platform* | 600,000 |

*Floating during construction and deployment

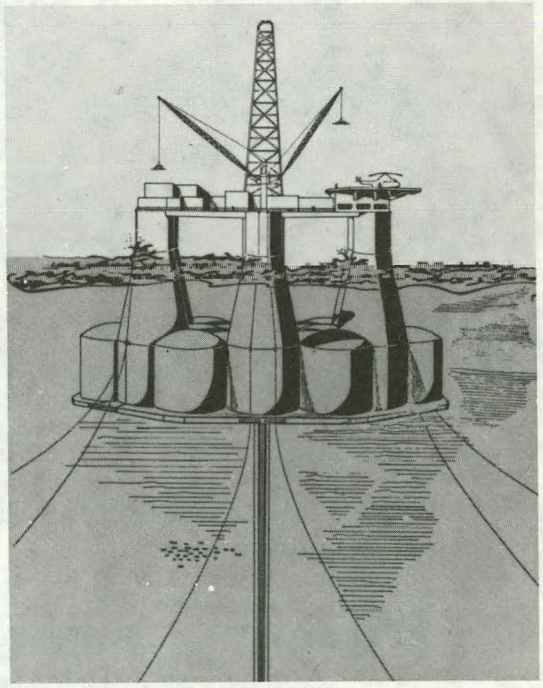


Figure 2. Floating Concrete Platform, CONPROD

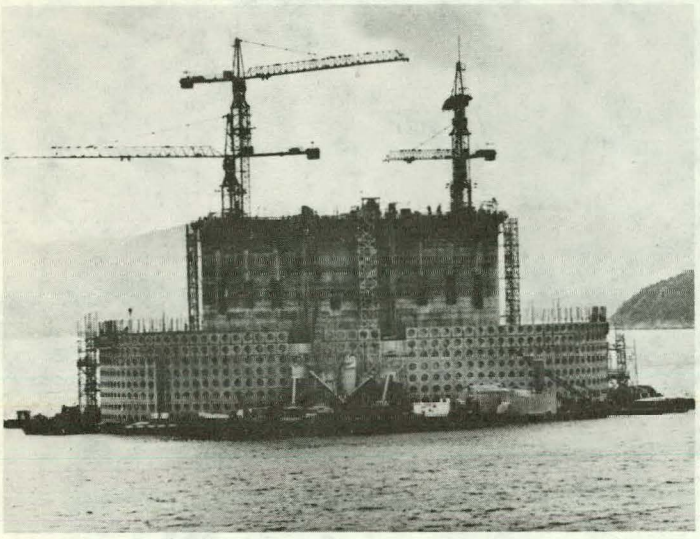


Figure 3. Ekofisk Oil Storage Tank Under Construction.

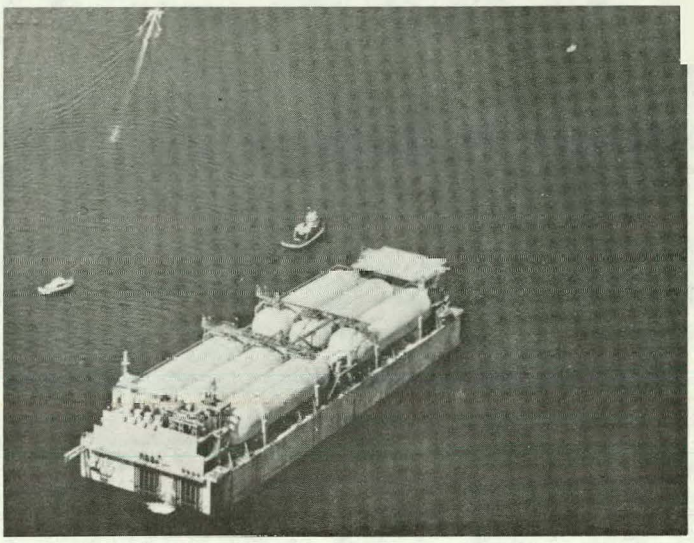


Figure 5. ARCO Barge LPG Processing Plant Under Tow.

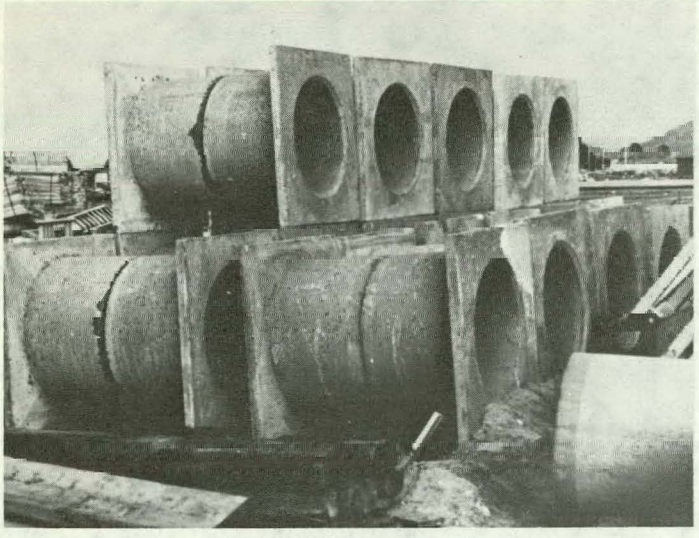


Figure 4. Precast Elements For Ekofisk Tank Seawall.

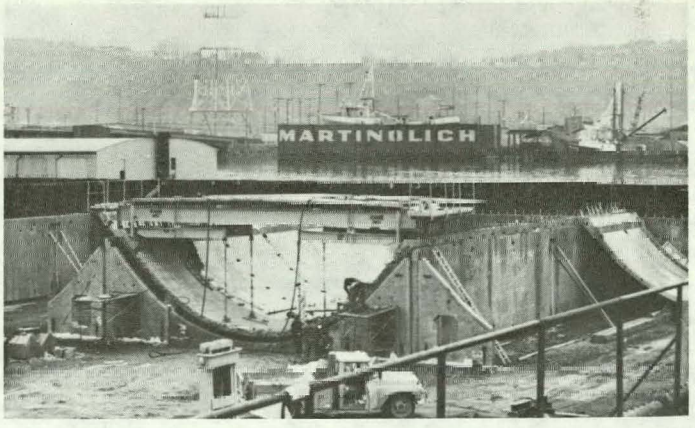



Figure 6. Precast Bottom-hull Sections for ARCO Barge Being Assembled in Dry Dock.

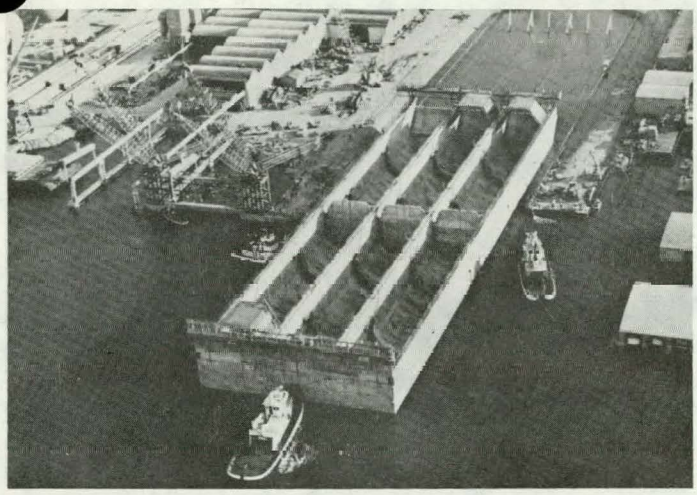


Figure 7. Partially Completed ARCO Barge Being Floated Out of Dry Dock.

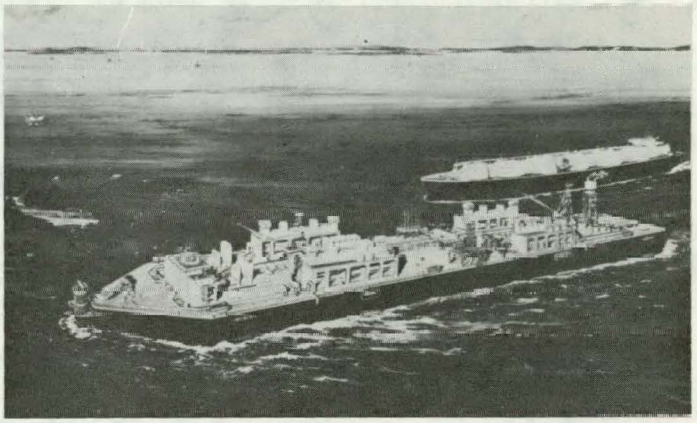


Figure 9. Surface-ship Concept for LPG Processing Facility (Global Marine Development, Inc.).

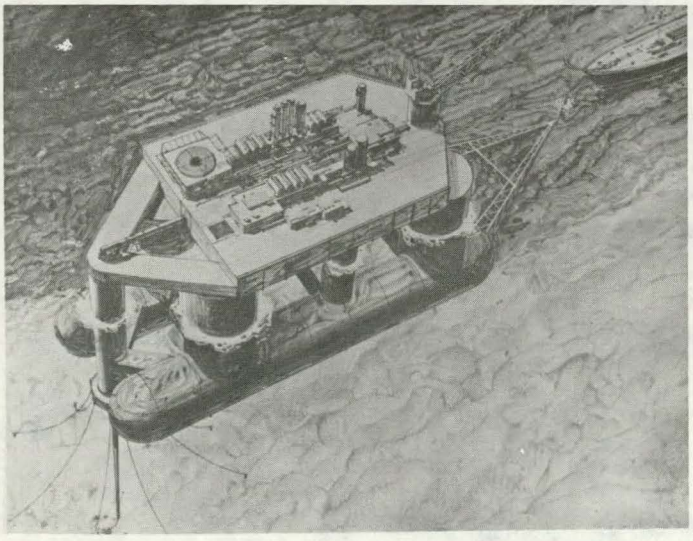


Figure 8. Semisubmersible Concept for LPG Processing Facility (Transenergy International, Inc.).

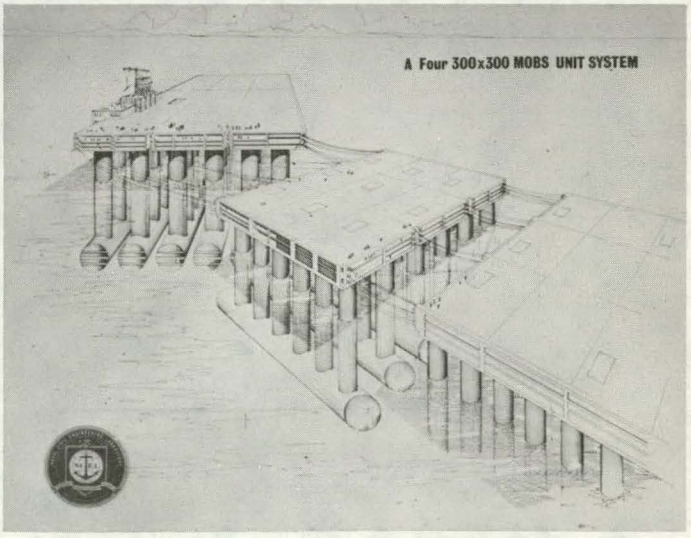



Figure 10. At-sea Assembly of Modules of Large Mobile Ocean Basing System.

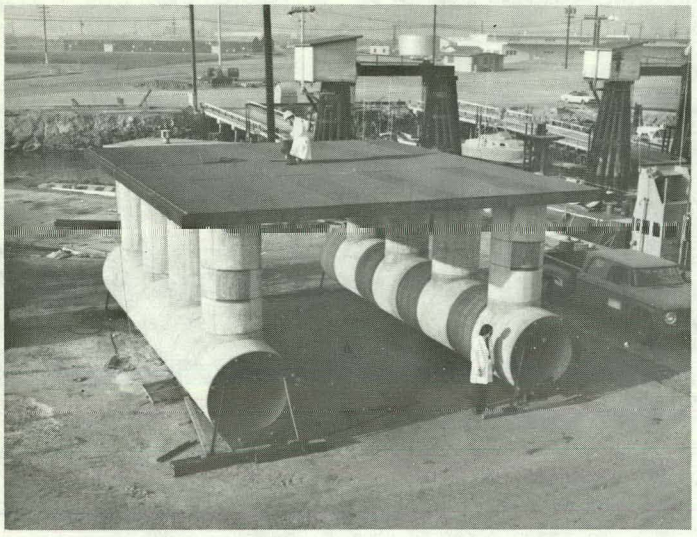


Figure 11. One-tenth Scale Model of Module of MOBS Platform.

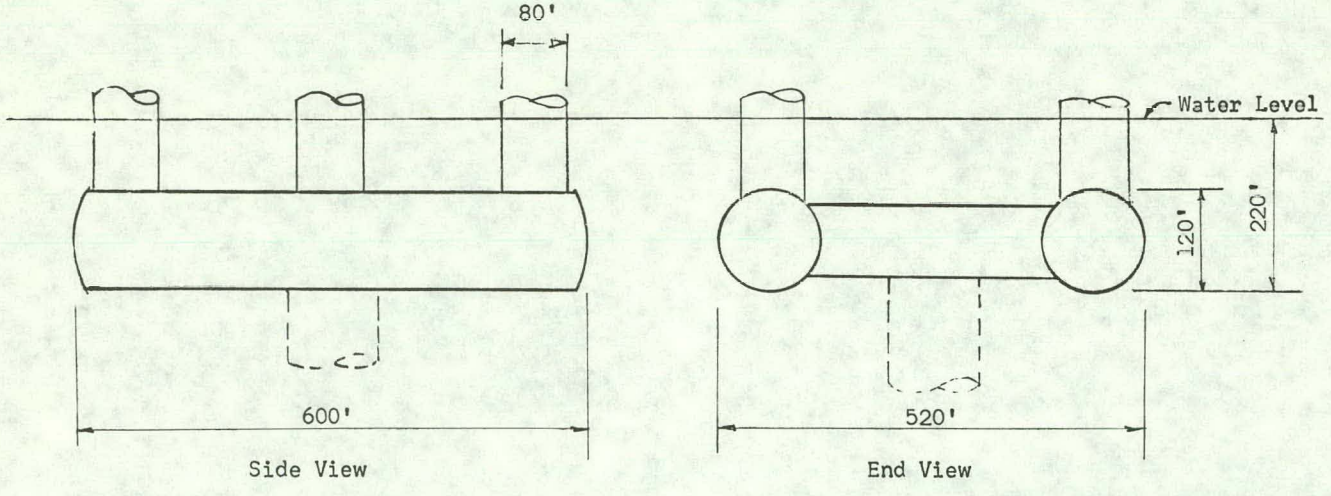



Figure 12. Baseline 500,000-ton Semisubmersible Platform (Hydronautics, Inc.).

# VI. HEAT EXCHANGERS

## SESSION 1

KENNETH J. BELL, CHAIRMAN
*Oklahoma State University*

THIS PAGE

WAS INTENTIONALLY

LEFT BLANK

# COMPACT HEAT EXCHANGERS FOR SEA THERMAL POWER PLANTS

J. HILBERT ANDERSON AND JAMES H. ANDERSON, JR.
*Sea Solar Power, Inc.*
*2422 S. Queen Street*
*York, Pennsylvania*

ABSTRACT

It has, for a long time, been recognized that the key element affecting the economic feasibility of ocean thermal power is the cost of the heat exchangers. Because of the huge potential of the sea as a viable source of energy, no avenue should be left unexplored in the search for heat exchangers that are optimally suited to this application. This search should include, in addition to conventionally used exchangers, innovative designs such as those of plate and fin construction.

This paper examines the applicability and possibilities for using compact plate-fin exchangers, with emphasis on practicality of manufacture, cost effectiveness, heat transfer capability, and adaptability for use in the ocean environment.

There seems to be universal agreement that the cost of converting ocean thermal energy to electric power is dependent, more than anything else, on the design and development of effective and low-cost heat exchangers for both boiling the working fluid into vapor and condensing the vapor back to liquid. Since sea thermal power has more potential for supplying our total energy needs and many other needed chemicals than does any other available solar energy source, it seems logical to concentrate every possible effort on the development of effective and low-cost heat exchangers for this purpose.

Both boilers and condensers are similar in the sense that very large amounts of heat must be transferred at very small temperature differences. Therefore it might be expected that similar heat exchanger constructions can be used for both boilers and condensers. While condensing vapors is a relatively straightforward process, and since the water from deep in the ocean is already known to be fairly clean and free of fouling mechanisms, it can generally be stated that the condenser design problem is somewhat easier than the boiler design problem. For this reason, I shall concentrate, in this paper, on discussion of the problem of designing boilers for sea thermal power plants.

Refrigerant liquid evaporators for transferring heat from water to boil a refrigerant are in common use and have been used for many, many years to evaporate ammonia, hydrocarbons and halocarbons which, as a group, encompass most of the usual refrigerants that are used to lower temperature by removing heat. These exchangers are used at very similar temperature differences and temperature levels to those required in a sea thermal power plant. Therefore the general technology for the design of refrigerant evaporators, or boilers, is not at all new. Therefore, also, we should be able to utilize the experience gained over many years of practice in the air conditioning and refrigeration industry to help us design effective boilers for sea thermal power plants.

The basic problem of evaporation of a liquid from a heat transfer surface is somewhat more difficult than that of condensing a vapor on a heat exchange surface. The reason is that, when the liquid turns into a vapor, it tends to produce a dry spot at the heat transfer interchange. One of the problems, then, is to keep the heat transfer surface effectively wetted throughout the exchanger.

The other associated problem is that, when a liquid is passed through the heat exchanger in the evaporating mode, the resistance to mass flow is much greater for the high specific volume vapor than it is for the liquid itself. For this reason, there is a strong tendency for the liquid to segregate and flow through one part of the boiler, and for the gas to flow through another passage, thereby greatly reducing the effective boiling heat transfer area. This is a common problem in refrigerant evaporators. In refrigeration terminology, this is normally called the "distribution problem" and results from this natural instability of distribution of flow through the evaporator. Many years of effort have been spent on trying to solve this problem, yet it always remains a serious and fundamental problem in the design of evaporators.

We experienced this phenomenon on a small scale when we built the world's first operating model of a sea thermal power plant, in which we submerged the boiler in a tank of hot water to evaporate R-11 refrigerant and run the turbine. This boiler, shown on Figure 1, is a simple multiple-tubed evaporator normally used for air conditioning purposes. The liquid flows from a header at the bottom up through the tubes and is supposed to boil as it flows up through the tubes. When we first assembled this, we did not consider the problem of distribution of liquid within the tubes and hoped that, because it was so small, it would operate successfully anyhow. Much to our

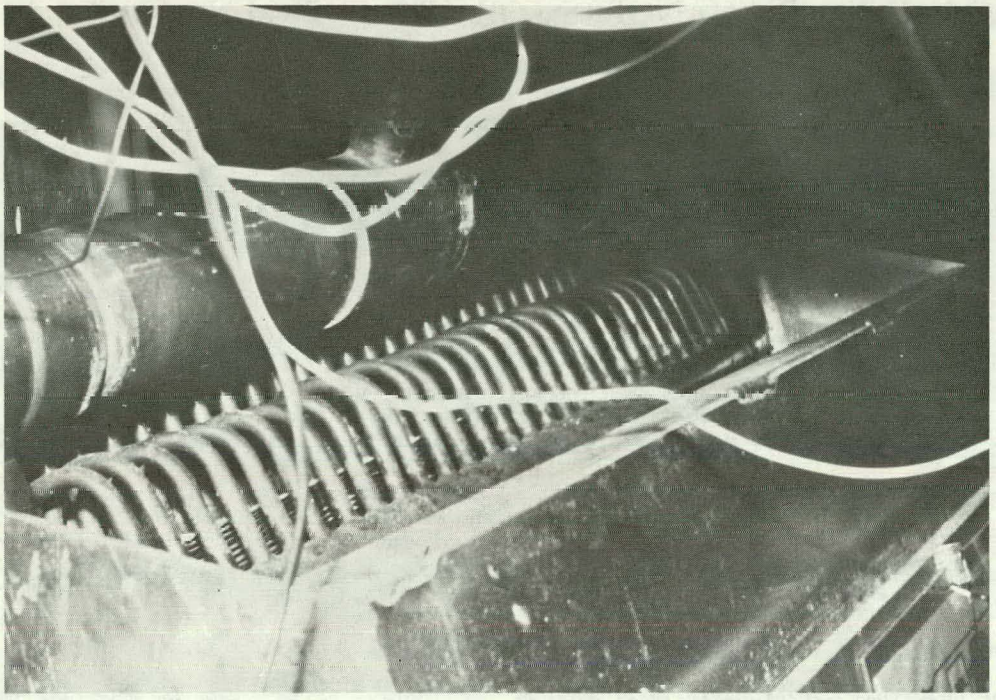
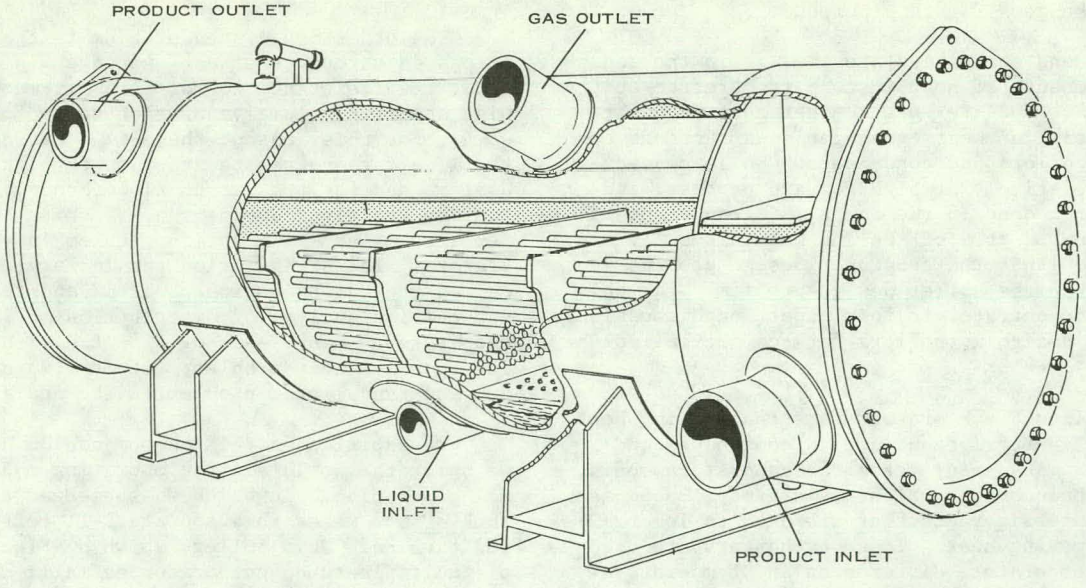


FIG. 1




FLOODED EVAPORATOR WITH SUCTION SLOT

FIG. 2

chagrin, the boiler would produce almost no vapor worth mentioning and was, essentially, a complete failure. In order to make the boiler work, we had to add a complete large, recirculating header going across the top and returning to the bottom so that it could be filled with liquid sufficiently to cause the liquid to flow up and recirculate, thereby assuring all the tubes to be wetted. This simple example serves to illustrate the trap that can so easily befall us in trying to design an evaporator for a sea thermal power plant. Many people have fallen into this trap and, to this day, continue to do so in the refrigeration industry.

In looking at the problem of evaporators for a sea thermal power plant, it should be noted that there is one distinct difference between them and a refrigerant evaporator. In a refrigerant evaporator, the fluid entering the evaporator passes through an expansion valve with high pressure drop. As it passes through the expansion valve entering the evaporator, part of the liquid is flashed into vapor at the inlet of the evaporator, due to the energy in the high-pressure liquid. This is a considerable advantage because it provides energy to produce high velocity over the heat exchanger surfaces, and also provides a means for assuring distribution of the liquid throughout the evaporator.

In the sea thermal plant, the liquid enters well below saturation temperature, and therefore there is no initial energy provided to insure distribution and good circulation over the heat exchange surfaces. This makes an evaporator for a sea thermal plant more difficult to design than that for a refrigerant evaporator in a refrigerant cycle.

The types of evaporators used in refrigeration work can be divided into four broad classes, as defined by their mode of operation.

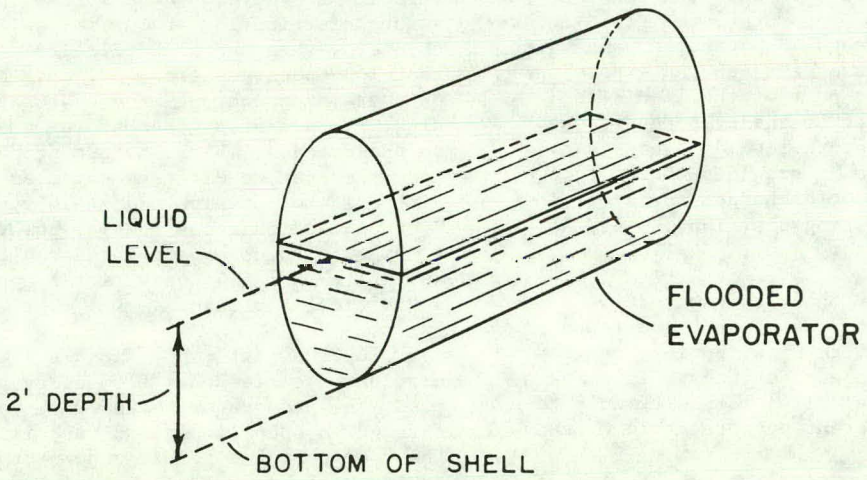
(A) We have the spray type or, more broadly speaking, the downflow evaporator. In this type, the liquid is sprayed over the heat exchanger surface and flows downward by gravity over the various surfaces, with the vapor then rising from the surfaces in reverse flow to the liquid flow. This type is theoretically attractive because, supposedly, you can put a minimum film of liquid directly on the surface, distributed over the surfaces, and leave a maximum area for the vapor to escape. It also has the advantage that the vapor pressure throughout the evaporator remains nearly constant, and therefore the evaporating side of the exchanger is at practically a constant temperature. This type of evaporator is no longer used to any great extent in refrigeration work. The reasons are that it is difficult and expensive to make sure that the liquid is indeed distributed well over all of the surfaces. There is the basic tendency for not all of the surfaces to be well wetted, and this becomes extremely difficult in larger sizes. While theoretically very attractive, it is doubtful whether this type of evaporator can ever be a very practical design for sea thermal plants. This does not mean that we should not attempt to solve the problems inherent in this type of evaporator, but it does mean that this type is not, by any means, the easiest and most logical approach to the problem.

(B) The second common type is referred to as the "DX", or direct expansion, evaporator. This is very common in small refrigeration systems and utilizes the expansion energy of the throttled refrigerant to produce a high velocity through tubes or over surfaces to keep them wet and thereby induce velocities that enhance the heat transfer coefficients. Unfortunately, this type is extremely difficult to insure good distribution of liquid over wetted surfaces. In a refrigeration system where ample energy is available at the inlet, and with the liquid flashing into vapor at the inlet, distribution nozzles can be used to assure reasonably good distribution. This situation is not present in a sea thermal plant evaporator unless a lot of additional liquid pumping power is made available, which in turn causes losses in the power circuit. If high pressure drop and high velocity are developed by more pumping power in order to assure distribution at the inlets to the vaporizing channels, then the high velocity liquid also dictates that long passages are used, and this in turn causes high pressure drops through the evaporating passages. These high pressure drops then affect the boiling temperature on the passage, which in turn produces a smaller effective temperature difference across the exchanger. It is difficult to conceive that this type of evaporator could ever be used on a sea thermal power plant. Despite this, a number of people have suggested this type of evaporator, but there is really very little hope of this ever being a practical approach.

(C) The next type which is commonly used in refrigeration is called the "flooded evaporator." In this case, the evaporator is an open type with tubes passing through an open liquid and vaporizing chamber. This is the most common type of evaporator used in large refrigeration systems. A cutaway picture of a typical shell and tube evaporator is shown on Figure 2. The liquid enters at the bottom, and the vapor is released to the space above the tube, which usually fills about one-half the shell height. By having the liquid essentially flood the tubes, this insures that the tubes are always wetted by splashing as the vapor comes off the tubes. By this means, relatively high heat transfer rates can be produced, and reasonably effective evaporation can be achieved. The disadvantage of this system is that the liquid level produces a pressure due to the static height of the liquid column. That is, the pressure at the bottom of the evaporator is higher than the pressure at the upper surface. This means, then, that the saturation, or boiling temperature at the bottom of the evaporator is higher than that at the top. This introduces a heat transfer temperature difference penalty, and in order to minimize this penalty, this type of evaporator should be used with very low levels of liquid. This, in turn, means that very large diameter tube bundles or shells are almost self-defeating in a sea thermal plant, simply because the depth of the liquid creates what is normally called a "static head penalty," and the static head penalty in a large-diameter shell can very appreciably reduce the effective temperature difference to produce boiling. When you are working with small temperature differences, as is required in a sea thermal plant, this static head penalty can easily become a major factor in the performance of the evaporator.

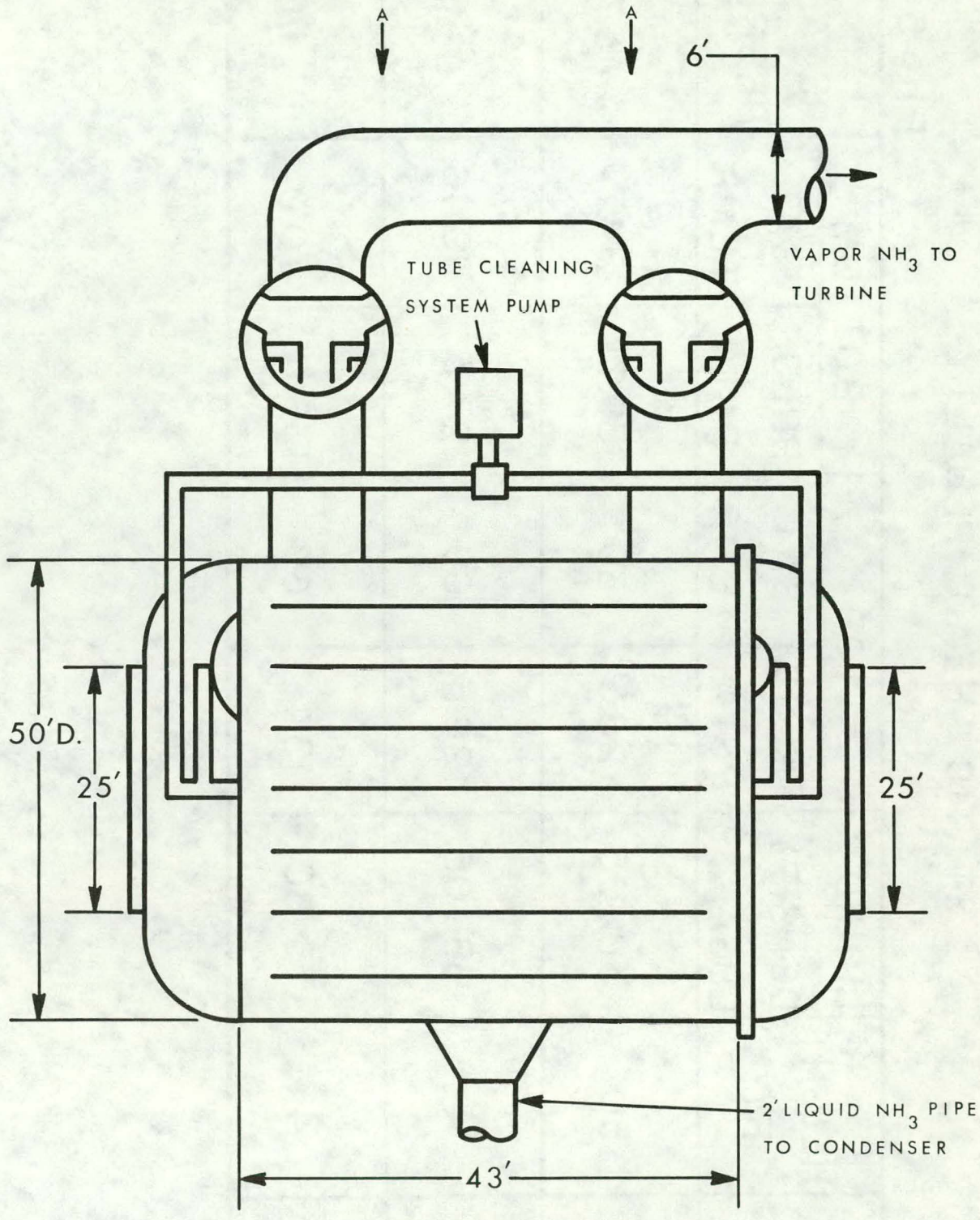
(D) The recirculating type of flooded evaporator. This evaporator is similar to the flooded evaporator,

# EFFECT OF REFRIGERANT LIQUID DEPTH ON THE EVAPORATING TEMPERATURE




| REFRIGERANT | 113 | 11 | 21 | 133a | 114 | 31/114 | 12 |
|---|---|---|---|---|---|---|---|
| TEMPERATURE AT SURFACE (°F) | 35° | 35° | 35° | 35° | 35° | 35° | 35° |
| PRESSURE AT SURFACE (PSIA) | 2.33 | 6.26 | 11.08 | 12.27 | 13.55 | 25.47 | 47.26 |
| PRESSURE EFFECT OF 2 FEET OF LIQUID (PSIA) | 1.40 | 1.33 | 1.23 | 1.20 | 1.32 | 1.16 | 1.21 |
| TOTAL PRESSURE AT BOTTOM OF SHELL (PSIA) | 3.73 | 7.59 | 12.31 | 13.47 | 14.87 | 26.63 | 48.47 |
| EVAPORATING TEMPERATURE @ BOTTOM PRESSURE (°F) | 53.3° | 43.5° | 39.7° | 39.0° | 39.3° | 37.2° | 36.4° |
| Δ T PENALTY AT BOTTOM (°F) | 18.3° | 8.5° | 4.7° | 4.0° | 4.3° | 2.2° | 1.4° |

FIG. 3




SIDE VIEW

FIG. 4

# STATIC HEAD PENALTY

FIG 5

| LIQUID | HEIGHT FT. | LIQUID DENSITY LBS/FT$^3$ | TOP | | BOTTOM | | PENALTY DEGREES |
|---|---|---|---|---|---|---|---|
| | | | PRESS. PSIA. | SAT. TEMP. | PRESS. PSIA. | SAT. TEMP. | |
| $NH_3$ | 50 | 38.05 | 126.5 | 69 | 139.71 | 74.7 | 5.7 |
| $NH_3$ | 4 | 38.05 | 126.5 | 69 | 127.5 | 69.46 | .46 |
| R-22 | 4 | 75.60 | 134 | 69 | 136.1 | 70.0 | 1.0 |

but in this case, excess liquid is circulated through the evaporator so as to produce somewhat higher liquid velocities and boiling coefficients at the bottom of the evaporator, where the liquid enters. This also tends to produce better distribution of liquid over the surface, and avoid the problem of having gas flow through part of the surfaces with poor distribution of flow and incomplete wetting of the surfaces. It is very probable that this type can be the most effective type for use in sea thermal plants, if we keep in mind that the vertical height of the flow path must be kept low enough so that the static head penalty does not become too large.

In order to illustrate the effect of static head penalty on boiling temperature of a refrigerant, Figure 3 shows a chart of static head penalties for a typical refrigerant evaporator, and also shows the construction of the evaporator. The evaporator in this case is shown as a shell and tube with tubes filling about one-half of the shell diameter. The liquid floods the tubes to about the middle of the evaporator, and the space above the tubes is used for separation of the vapor from the liquid as it splashes up through the tubes. Typical static head penalties in degrees are shown for several varieties of refrigerants at normal evaporation temperatures incurred in air conditioning systems. Note that the static head penalty on temperature is highest for low-pressure refrigerants and lower as the pressure of the refrigerant goes up. The static head penalties are shown for approximately two ft. liquid height, and even at this low level of liquid height, can be a quite appreciable percentage of the temperature difference available for producing evaporation.

In order to relate static head penalty to sea thermal power directly, we have shown the attached figure from the TRW report on a basic evaporator designed for a sea thermal plant. This evaporator is a shell and tube type with a 50 ft. diameter shell filled with titanium tubes. The evaporator is the flooded and liquid recirculation type. If, as shown on Figure 4, the evaporator is filled with liquid, then the static head penalty at 50 ft. depth amounts to 5.7°F. This means that the boiling temperature at the bottom of the tube bundle is actually 5.7° higher than the boiling temperature at the top of the bundle. If there is any flow pressure drop in addition to the static head drop, then the temperature difference can be even greater than this. Since, in this particular case, the supposed value of log mean temperature difference to produce evaporation is given as 7.83°F., then it is obvious that a static head penalty of 5.7°F. will make a tremendous difference in the heat transferred in this boiler, and it could not possibly meet the supposed design conditions. In other words, this means that the amount of heat transfer surface required for these design conditions would nearly double over that presented. This shows how serious the problem of static head penalty can be.

The lower two lines in Figure 5 show what the static head penalty would be for ammonia and for a halocarbon refrigerant such as R-22 at 4 ft. depth. If this type of boiler is used, then it is obviously important to keep the level of the liquid in the boiler to a low value in order to have effective heat transfer.

Let us now look at some sample heat exchanger types and present-day costs. First, Figure 6 shows a picture of a boiler for a geothermal plant on test in the Nevada desert. This is a shell and tube heat exchanger for using water to boil isobutane in a geothermal power plant. The water flows in the shell, and the isobutane flows through the tubes. The shell is 17" in diameter and 20 ft. long, and is unique in that it provides true counterflow exchange, which is extremely important in a geothermal plant. The true counterflow design not only permits maximum heat transfer coefficients and maximum effective temperature differences, but also minimizes pressure drop on both the water and the isobutane side, thereby greatly improving the effective efficiency of the plant. Figure 7 shows a model of the isobutane heaters, boilers, and superheaters for a 10,000 kw geothermal plant using the design shown on the previous slide. The heat exchangers for this plant are a very major part of the cost of the plant, and the design of the true counterflow shell and tube exchangers made a large difference in the overall cost and effectiveness of the plant. Shell and tube exchangers are a very common design for large refrigeration systems, and can be an effective choice for sea thermal plants, although the cost is likely to be higher than we would like.

Figure 8 shows a picture of what has recently become a common type of exchanger used in the low temperature refrigeration field. This is a compact plate-fin design of aluminum exchanger assembled and brazed into one integral unit. This design provides a large amount of heat transfer surface in a minimum of space, thereby reducing the cost of the surrounding enclosure and making it possible to contain relatively high pressures with a minimum external shell cost. We believe this type of design can be utilized in sea thermal plant boilers and condensers and believe the potential low cost of such a system is well worth the development effort to attempt a practical design for sea thermal plant operation.

An exploded view of typical brazed aluminum exchanger parts is shown on Figure 9. This type exchanger can be assembled in many more complex forms, with many connections, as shown on Figure 10. This feature can be used to attain a more effective design of sea thermal plant evaporators.

We have shown on Figure 11 a table of a few selected examples of heat exchanger types that give an idea what the potential costs might be. The first line shows a propane boiler for a geothermal plant, which was recently purchased. The diameter of the shell is 52", and the length is 52 ft. The tubes are carbon steel, and the pressure rating is 150 psi., which is very similar to that required in a sea thermal plant. The actual purchase price for an ordinary carbon steel tube exchanger in this rather large size is approximately $7.00 per square foot. This does not include the cost of installation, but is merely the price of the manufactured exchanger.

The second line shows the description of the exchanger described above for heating and boiling isobutane with water on the shell side of the exchanger. These exchangers are rated at approximately 650 pounds per square




FIG. 6

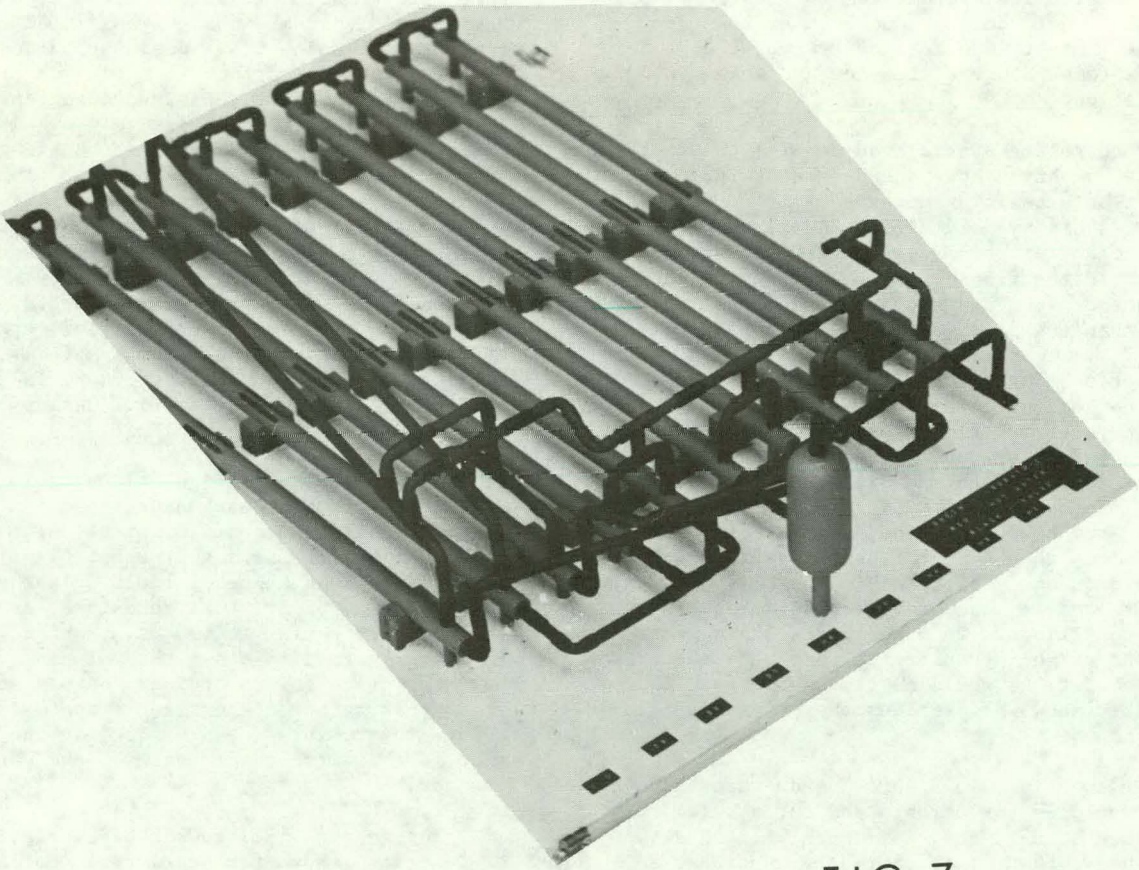


FIG. 7

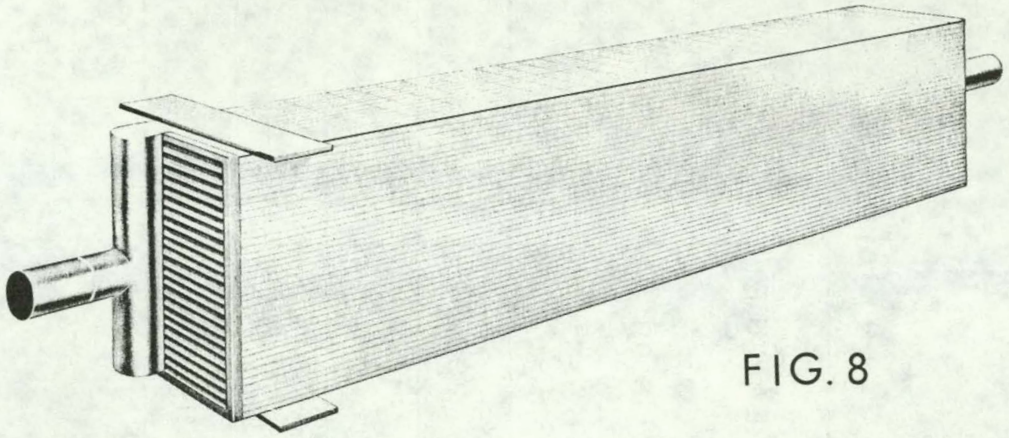


FIG. 8

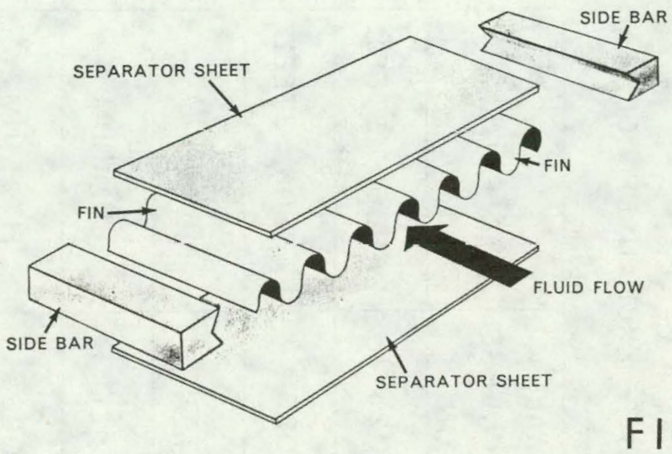



FIG. 9

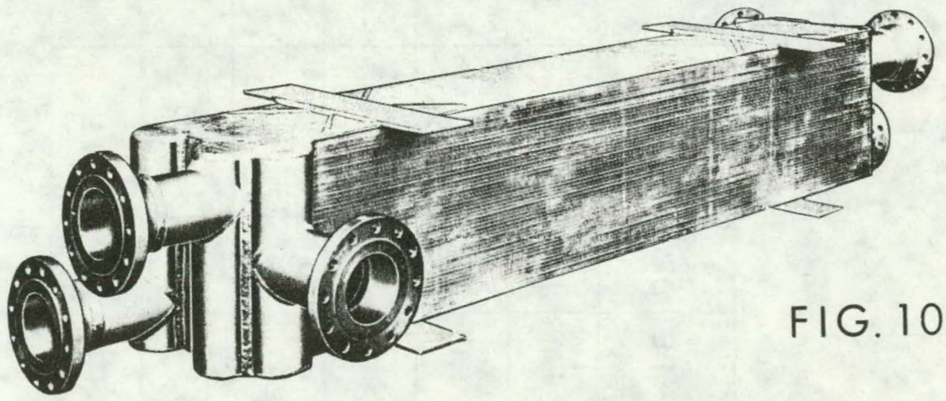


FIG. 10

HEAT EXCHANGER COMPARISON

FIG II

| TYPE | DIA. | LENGTH FT. | TUBE DIA. IN. | WALL THICKNESS IN. | MATERIAL | PRESS. PSI. | AREA/CU.FT. | COST/SQ.FT. |
|---|---|---|---|---|---|---|---|---|
| S+T | 52" | 52 | .75 | .028 | CARBON STEEL | 150 | 18.89 | 7.80 |
| S+T | 17" | 70 | 1.187 | .028 | CARBON STEEL | 670 | 21.5 | 17.00 |
| PLATE | 47" x 47" | 17.7 | — | — | ALUMINUM | 200 | 290 | .68 |
| PLATE | 35" x 43" | 22 | — | — | ALUMINUM | 200 | 289 | .74 |
| S+T | 72.7' | 52.5 | 2 | .028 | TITANIUM | 110 | 15.11 | 8.97 |
| S+T | 50' | 43 | 1.5 | .037 | TITANIUM | 136 | 14.45 | 8.22 |

inch and have carbon steel tubes. The actual purchase ... was approximately $17.00 per sq. ft. of surface, again this does not include cost of installation in field.

The next two lines show rather typical large brazed, compact surface aluminum plate-fin exchangers that were recently sold. Note that the physical size of these exchangers is somewhat near the magnitude of that of an exchanger that might be used in a sea thermal power plant in multiple modules. The purchase price of these exchangers was in the neighborhood of $0.67 per sq. ft. of exchange surface. This is not perhaps a well-described price, because these exchangers are very complex, and the definition of heat exchange surface is somewhat different from that which we normally use. It would be expected that the equivalent price of an exchanger for a sea thermal plant would be higher than these values. However, it seems reasonable to expect that the price would still be considerably lower than that for an ordinary carbon steel shell and tube exchanger. One of the reasons for the potential low cost of the compact aluminum exchanger is that the amount of square feet of surface contained in a cubic foot of volume is much larger than that of a typical shell and tube exchanger. This results in a more compact size and results in a smaller physical exchanger, which in turn, then, requires smaller containment vessels. All of this tends to reduce the cost of the exchanger and, obviously, also reduces the installation cost. An additional advantage of such an exchanger is that it is quite easy to put extended fin surface on the refrigerant side. This largely eliminates the differences between various refrigerants as far as heat transfer coefficients are concerned, and the water side becomes the controlling side for heat transfer.

The last two lines show the physical size and type of construction proposed by TRW and Lockheed for sea thermal power plant evaporators. In one case, the proposed evaporator is 50 ft. in diameter, and in the other, more than 70 ft. in diameter with titanium tubes. Note that the number of sq. ft. of surface per cubic foot of volume is lower than any of the examples shown above, yet the proposed cost is less for titanium tubes than that shown for the purchase price of carbon steel tubes in the samples shown above. These prices are supposed to be installed costs of field-erected exchangers. When you realize that any large field-erected exchanger is required to be completely annealed after welding the shell together in the field, then you begin to realize the stupendous problem involved in constructing such an exchanger in the field. It is indeed difficult to conceive that installed costs such as those proposed could ever be approached with this tremendous physical size of titanium tube exchanger. From our experience in actual design, manufacture and purchase of exchangers, we cannot believe that such estimated cost could ever be even close to being met.

Because of the cost problem, we believe that it is well worthwhile making the effort to develop plate and fin exchangers. While the brazed aluminum design is already established as a potential possibility for compact exchanger construction, and also lends itself to ease of manufacture in mass-production, it does have ...al disadvantages in that aluminum is, so far, the only material that has successfully been used in large exchangers. It also has the disadvantage that, in seawater, the use of brazing alloys, which have a slightly different composition than the exchanger material, is a potential source of trouble due to electrolytic action in seawater.

For these basic reasons, we have carefully considered the possibility of developing a mechanical plate and fin construction which does not require brazing of the surfaces together. This opens the door to utilization of other materials than aluminum and other combinations of materials. That is, it would not be necessary to use the same material on the refrigerant side of the exchanger as is used on the seawater side. Careful study of the problems in manufacturing such an exchanger has convinced us to believe that it is indeed possible to develop a suitable mechanical construction, which would have the advantage of potentially lower cost of manufacture than a brazed construction, and also permit the use of materials other than aluminum. While it is too early to say positively that this can be done, the potential gain and the potential requirement for sea thermal plants are so large that we believe it highly important to embark on a study of such potential designs.

No heat exchanger for sea thermal plants, particularly at the warm water end, would be feasible unless we plan for some suitable method of cleaning. In the conceptual design, we must obviously think of designing water passages that are free and clear and easy to clean. For this reason, the water side passage of a flat plate heat exchanger should be simple, straight, rectangular passages that are easily accessible for chemical cleaning, hydraulic nozzle cleaning, or even for mechanical scraping and brushing. The refrigerant side can have finned surfaces, which increase the effective transfer area. While we have reasonable expectations of reducing the need for too frequent cleaning by suitable water control methods, it is still important to have an exchanger design that is easily cleanable. With this type of compact design, which can be made up in multiple modules, it is easily conceivable that entire modules can be removed and brought to the surface of the plant for thorough cleaning. They also have the advantage that there is immediate access from the major water passage plenums, and there is no need to remove heads in order to have access to the water passages. Therefore we believe that this type of design has an excellent chance of being practical from the point of view of cleanability.

The problem of marine fouling, and particularly of crustacea forming on the warm water surfaces of sea thermal power plant boilers, must be recognized and certainly can be a very major problem. While this may not be directly related to heat exchange itself in the sense that, no matter what heat exchanger you use, this problem will be with you on the seawater side; nevertheless, we should recognize that some effort must be made to eliminate this problem. All of the indications are, from experience, that there will be no crustacea or no serious fouling problem on the cold water or condenser end of the plant, but there should be very serious potential problems on the warm water, or boiler, end of the plant. Various possible control means for prevention of fouling are already in use in thousands of heat exchangers at marine

installations and aboard ships. Therefore we should not despair and say that this is an insurmountable problem, because this problem is being dealt with in hundreds of thousands of actual operating installations at sea. However, this does not mean that we should blithly ignore the problem. The various possible control schemes that have been suggested and are, in some cases, already in use, are the following:

(1) Velocity Control - It is well known that barnacles will not adhere to a surface if there is sufficient velocity over the surface. Therefore the velocities through heat exchanger passages must be kept reasonably high in order to minimize attachment of barnacles to those surfaces.

(2) The second most used means of control of fouling in heat exchangers is to use a poisonous nickel-copper alloy in the exchangers. This is a very common solution aboard marine condensers in ships. By developing a mechanical construction of exchangers, it is quite possible to consider the use of these alloys as an exchanger material. However, it should be noted that these alloys cannot be used in an ammonia plant.

(3) The next popular method of control of fouling mechanisms is to use chlorination of the water. This is commercially used, and is potentially usable in a sea thermal power plant. However, it is rather undesirable because of cost. The tremendous quantity of water required to heat the boilers in a sea thermal plant will require a tremendous amount of chlorine, and this can become a rather large cost factor in the operation of the plant.

(4) The next potential method of fouling control is simply to remove part of the oxygen from the water prior to entering the boilers. This appears to be much lower in cost than chlorination, and probably has the additional advantage that it tends to reduce corrosion in general as well as to starve crustacea. Not much work has been done in this area, but what has been done indicates that this is a promising approach. The other advantage of this method is that the gases removed from the water can be separated and are saleable as by-products from the plant. Therefore this method of control should be virtually free of any cost penalty, and can actually add to the income produced by the plant.

(5) A fifth possibility is to develop ozone generation for killing organisms in the water. Probably not too much is known about this, but it does have the potential of being lower cost than chlorination.

While we cannot say at this stage, with any degree of authority, what is the final best solution to the fouling problem in heat exchangers, there seems to be enough encouragement to believe that this problem can be solved. As pointed out above, we are living with it in hundreds of thousands of installations and believe that it can be lived with in a sea thermal power plant.

In summary, let us again state that the potential for ocean thermal energy conversion is so vast that it justifies any and every effort for development of suitable low-cost heat exchangers. We are firmly convinced that this justifies the attempt to design plate-fin exchangers which do have the potential of reducing the c of exchangers, as well as improving their efficiency, reducing their physical size. They also have the potential of reducing physical size of a plant and improving maintenance and accessibility.

## DISCUSSION

Castelli (U.S.Navy): Mr. Anderson, you mentioned during your paper that some benefit could be gained through deoxygenation of the sea water: A) How do you propose to remove these quantities of gases from literally cubic miles of sea water? B) Do you expect this deoxygenation to eliminate bacterial (biological) sliming, which is the major impediment to efficient heat transfer? Slimes do form in anaerobic environments.

Anderson: Corrosion and much bio-fouling have been shown to be decreased with removal of dissolved oxygen in sea water. Since there is a considerable amount of oxygen in the air dissolved in the warm sea water, it is logical to pass the warm water through a deaerator prior to passing through the boiler.

By passing the warm water through a chamber where the pressure is reduced below the saturation pressure, the dissolved air bubbles out and can be collected. Enough gases - oxygen, nitrogen, $CO_2$ and others - can be collected, separated and sold commercially!

We have worked out a simple deaerator which requires a small amount of compressor power. The value of the commercial gases will pay for the chamber. The deaerator thus removes oxygen which helps prevent corrosion and bio-fouling in the boiler and at the same time provides extra income by sale of the valuable gases.

We expect to live with anaerobic slimes as is presently done in other sea water applications.

This work is reported in publications of the University of Massachusetts prepared for the National Science Foundation.

CONF-770831--1

# ANALYTICAL AND EXPERIMENTAL STUDIES OF OTEC HEAT TRANSFER PROBLEMS AT OAK RIDGE NATIONAL LABORATORY

JOHN W. MICHEL
*Energy Division*
*Oak Ridge National Laboratory*
*P. O. Box Y*
*Oak Ridge, Tennessee*

## Abstract

During the past year, Oak Ridge National Laboratory has been involved in assisting ERDA in the analysis, planning, and implementing a program to develop advanced heat exchangers for ocean thermal energy conversion (OTEC) application. An analysis of the $NH_3$ binary cycle and the current state of commercial heat exchanger technology indicated that the goals of this program should be to improve the seawater heat transfer coefficients by a factor of 2, the ammonia heat transfer coefficients by a factor of 2 to 4, and to be able to control fouling factors at a value of 0.0003 or below. These improvements coupled with qualifying aluminum for this seawater/ammonia service would go far toward assuring the economic viability of the OTEC concept.

A single tube ammonia heat transfer loop has been built and operated to evaluate the heat transfer characteristics of fluted tubes. Preliminary ammonia condensation results are presented.

## Introduction

Oak Ridge National Laboratory (ORNL) has been informally involved in the OTEC Program for several years, but direct ERDA support for program assistance in the area of heat transfer began in February of 1976. The intent of this paper is to summarize the significant activities of this work up to the present time. The work covers two broad categories: (1) Analytical Studies and Program Support and (2) Experimental Heat Transfer Studies. Table 1 summarizes the work completed and planned as part of these activities.

## Analytical Studies

### Heat Transfer Development Goals

Although much of the early work in this category of analytical studies was of a program support nature, proposal review, contract monitoring, and program planning, some work was done to define the OTEC heat exchanger development goals. From the "baseline" design studies (1, 2), it was obvious that decreasing the cost of the heat exchangers could materially improve the overall economic attractiveness of the OTEC concept. This could be done by reducing the size (heat transfer area) via enhanced heat transfer and/or reducing the

Table 1. ORNL-OTEC Activities

ANALYTICAL

General

- Review proposals and assist SEB's
- Monitor and assess results
- Assist program planning

Ad Hoc

- Optimization work
- Core test loop design and siting
- Bottoming cycle
- Open cycle
- Literature reviews and discussion papers (heat exchanger and materials)

EXPERIMENTAL

- Condensation tests (tube geometry, length, temperature)
- Two evaporator types
- Double enhancement
- Tilted operation
- Test cores

*Research sponsored by the Energy Research and Development Administration under contract with the Union Carbide Corporation.

fabrication cost through use of less costly materials and new improved design and fabrication concepts.

Figure 1 illustrates the potential for improving (over the baseline designs) the heat transfer performance of ammonia evaporators or condensers. This figure, a plot of the ammonia-side heat transfer coefficient vs the heat exchanger overall coefficient, emphasizes the importance of improving the seawater-side coefficient. Assuming that current state of the art is represented by the baseline design point indicated ($h_{NH_3}$ = 1500, $h_{H_2O}$ = 843, and a fouling factor of 0.0003) an increase in $h_{NH_3}$ by say a factor of 2 only improves the overall coefficient by 7%. Doubling the water-side coefficient, however, increases $U_o$ by a factor of about 1.8 and increasing both the seawater and ammonia sides by a factor of 2 improves the overall coefficient by a factor of 1.9. With these enhanced heat transfer values, the importance of reducing the fouling factor is of increased benefit; e.g., reducing the fouling factor at these heat transfer enhancements from 0.0003 to 0.00015 gives an additional 13% improvement in the overall coefficient. Thus, the combined effects of these improvements could reduce the heat transfer area required and hopefully the cost by over a factor of 2.

Questions now arise concerning the possibilities for doubling the seawater- and ammonia-side heat transfer coefficients and halving the fouling factor. Figure 2 shows one mechanism for improving the boiling and condensation coefficients for the working fluid. This type of fluted (Gregorig) surfaces takes advantage of the working fluid surface tension to maintain a thin film and thus high coefficients on the ridges while utilizing the grooves for drainage (in condensation) or a source of waves for rewetting the ridges (for thin film evaporation).

This type of surface was extensively evaluated at ORNL as part of the OSW ocean desalting program and more recently with fluorocarbons and hydrocarbons for the geothermal energy program. Sample tube geometries evaluated in these programs are illustrated in Fig. 3 with increasing condensation performance occurring from Tube A to Tube E, respectively. This improvement, ratio of h for Tube E to the h for Tube A (smooth), is shown in Fig. 4 for several fluorocarbons as a function of heat flux on 4-ft long 1-in.-diam tubes. It may be seen that improvements of a factor of 5 can be achieved at the low heat fluxes typical of OTEC operation. We would expect a similar improvement with ammonia. Another type of enhancement demonstrated to be effective for boiling is the "Linde" high flux nucleation promoting surface (3) where improvement factors of up to 10 have been reported.

Seawater-side enhancement is complicated by the importance of associated pressure loss and biofouling considerations. Ignoring biofouling for the moment, Fig. 5 illustrates several types of internal low fins which are capable of doubling the water-side heat transfer coefficient for the same pumping power expended. It may be noted that the top two tube configurations show heat transfer enhancements greater than the area increase — these two tubes have ribs or fins which spiral down the internal length of the tube.

It would appear that this type of surface may be difficult to keep free of biofouling, but it should be recognized that the ERDA biofouling and corrosion R&D program will be evaluating prevention and cleaning schemes which could prove to be suitable for such enhanced surfaces.

Based on the above brief surveys, a reasonable statement of OTEC heat transfer development goals may be defined as given in Table 2.

Table 2. Development Goals for Closed Cycle OTEC Heat Exchangers

1. Two-fold increase in seawater coefficient
   - pressure loss
   - tube cost
2. Three- to five-fold increase in ammonia
   - evaporator
   - condenser
3. Maintain biofouling/scaling factors below 0.0003 hr·ft$^2$·°F/Btu
   - costs
   - reliability
4. Qualify aluminum
   - fabrication costs
   - reliability/lifetime

Heat Exchanger Size

Another OTEC heat exchanger problem area briefly addressed was the unprecedented large size required for projected full-size commercial units. Simple approximate relationships can be used to define shell and tube heat exchanger size in terms of the number of tubes required and the tube bundle diameter. These relationships are shown below and shown graphically in Fig. 6:

$$N = 20 \frac{MWe}{\eta_{cy}} \left( \frac{1}{V \delta t d_i^2} \right)$$

$$D^* = 1.05 \, P d_o \sqrt{N} \quad \text{or} \quad = 4.7 \, P \frac{d_o}{d_i} \sqrt{\frac{MWe}{\eta_{cy} V \delta t}}$$

where

N = number of tubes,

MWe = net power output,

$\eta_{cy}$ = power cycle efficiency,

V = seawater tube velocity, ft/sec,

$\delta t$ = seawater temperature change, °F,

*Allowances for fabrication clearances, vapor lanes, etc., not included.

$d_i$ = inside tube diameter, ft,

$d_o$ = outside tube diameter, ft,

P = ratio of tube pitch to diameter (triangular pitch).

Since the baseline and other studies have shown the optimum values of V to be near 5 ft/sec, $\delta t$ in the range of 2 to 4°F and the tube diameters to be in the range of 1 to 2 in., Fig. 6 is based on these values. It may be seen that the tube bundle and, therefore, (approximately) the containment shell diameter is not sensitive to tube diameter and that a diameter of 45 to 65 ft is required for a 25 MWe module. The number of tubes required is sensitive to tube diameter and the temperature change of the seawater. It may be noted that developing new types of improved tubes from single tube laboratory tests will require some four order of magnitude scale up to reach the projected full-size modules.

The remaining heat exchanger size parameter to be defined is the tube length and this may be found from the following relationship:

$$L = 55{,}000 \frac{d_i}{d_o} \frac{V}{U} \ln\left(\frac{\Delta T_1}{\Delta T_1 - \delta t}\right),$$

where

L = tube length, ft,

U = overall heat transfer coefficient, Btu/hr·ft$^2$·°F,

$\Delta T_1$ = heat exchanger inlet approach temperature, °F.

Figure 7, a plot of L vs U, is based on the above relationship with V constant at 5 ft/sec and the tube diameter and temperature drops shown as parameters over a range of interest as indicated by previous plant optimization studies. As indicated on this figure, if the heat transfer development goals are achieved, i.e., overall coefficients of 800 to 1000 obtained, then the tube lengths would decrease from the baseline values of 20 to 50 ft to 5 to 15 ft.

## Experimental Studies

An experimental program on enhanced ammonia heat transfer has begun at ORNL. Figures 8 and 9 show a schematic diagram and a photograph of an ammonia condensation test loop that has been built and will later be converted to perform ammonia evaporation studies. This is a natural circulation loop with an elevated condenser test section that is designed to obtain ammonia condensation heat transfer coefficients as a function of heat flux by the Wilson-line method. Figure 10 shows a typical Wilson plot, $1/U_o$ vs (1/water flow rate)$^{0.8}$, which gives an ammonia condensation coefficient (1/intercept) of ~1300. Figure 11 shows the effect of heat flux on the ammonia condensation coefficient on a 4-ft vertical 1-in.-diam smooth tube and indicates that the coefficient varies from ~1400 Btu/hr·ft$^2$·°F at low heat flux to ~800 at high heat flux. The data so far obtained on a smooth vertical tube correlate well with the theoretical McAdams equations as indicated in Fig. 12. Preliminary results with Tube E (Fig. 3) indicate that these condensation coefficient values can be increased by about a factor of 4 to 5 by use of an enhanced Gregorig-type tube surface.

## Conclusions

Based on our analyses of the OTEC heat transfer situation, development goals were proposed which would improve the heat exchangers performance by more than a factor of 2. Brief surveys of past work indicate that the heat transfer improvements are achievable but need to be verified, especially in the expected ocean environment. Of particular importance and currently of considerable uncertainty is the problem of maintaining low fouling factors, especially with aluminum.

## References


1. Ocean Thermal Energy Conversion (OTEC) Power Plant Technical and Economic Feasibility, Lockheed Missile & Space Company, Report No. NSF/RANN/SE/GI-C937/FR/75/1, LMSC-D0565666 (Vol. 1), April 12, 1975.

2. Ocean Thermal Energy Conversion Research on an Engineering Evaluation and Test Program, TWR Systems Group, Redondo Beach, California, Final Report (Volume 1 — Executive Summary), June 1975.

3. C. F. Gottzmann, J. B. Wulf, and P.S. O'Neill, "Theory and Application of High Performance Boiling Surfaces to Components of Absorption Cycle Air Conditioners," in Proceedings of the Conference on Natural Gas Research and Technology, held in Chicago on February 28—March 3, 1971, Institute of Gas Technology, Chicago, Illinois, CONF 710234.

4. A. P. Watkinson et al., "Turbulent Heat Transfer and Pressure Drops in Internally Finned Tubes," *Heat Transfer, AIChE Symposium Series*, 69(131), 94—103 (1973).

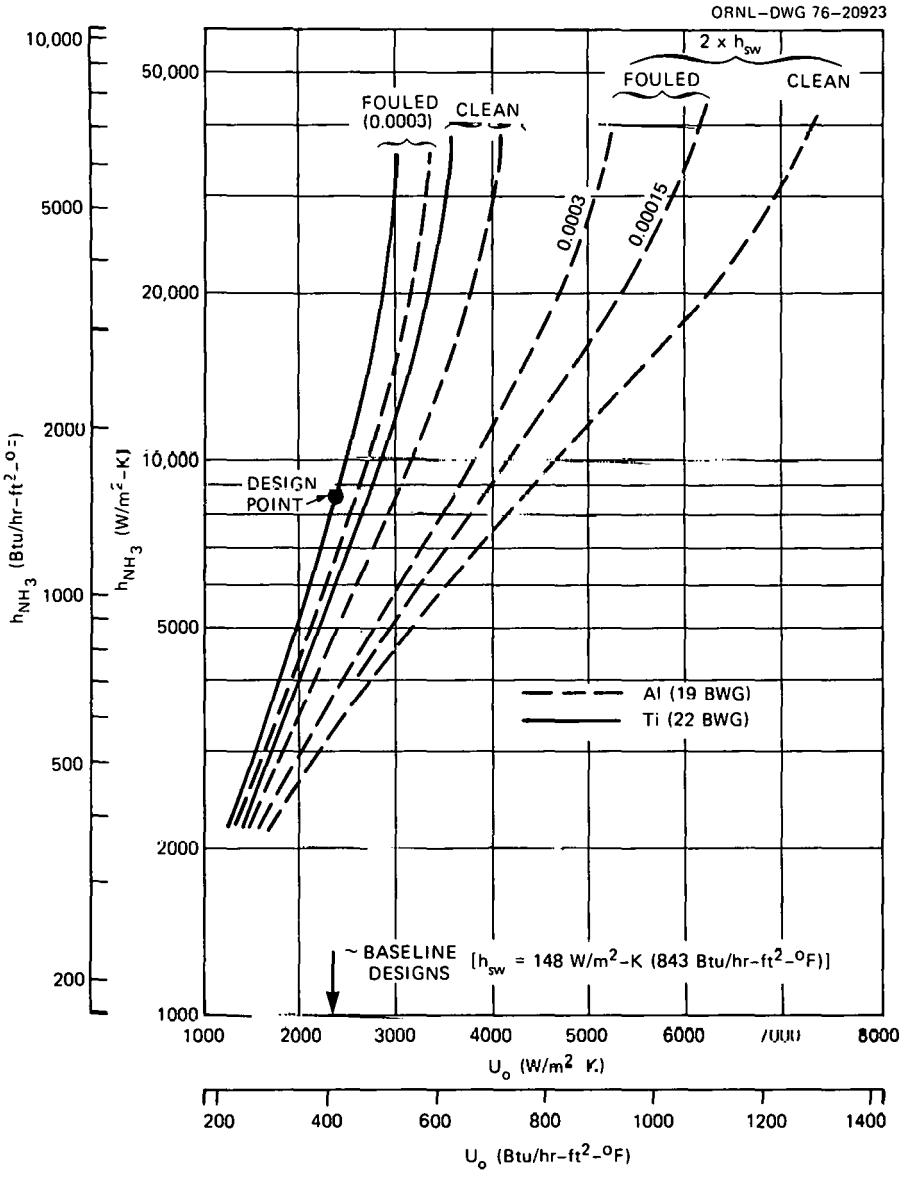



Fig. 1. The potentials and limitations for improving heat transfer in OTEC heat exchangers.

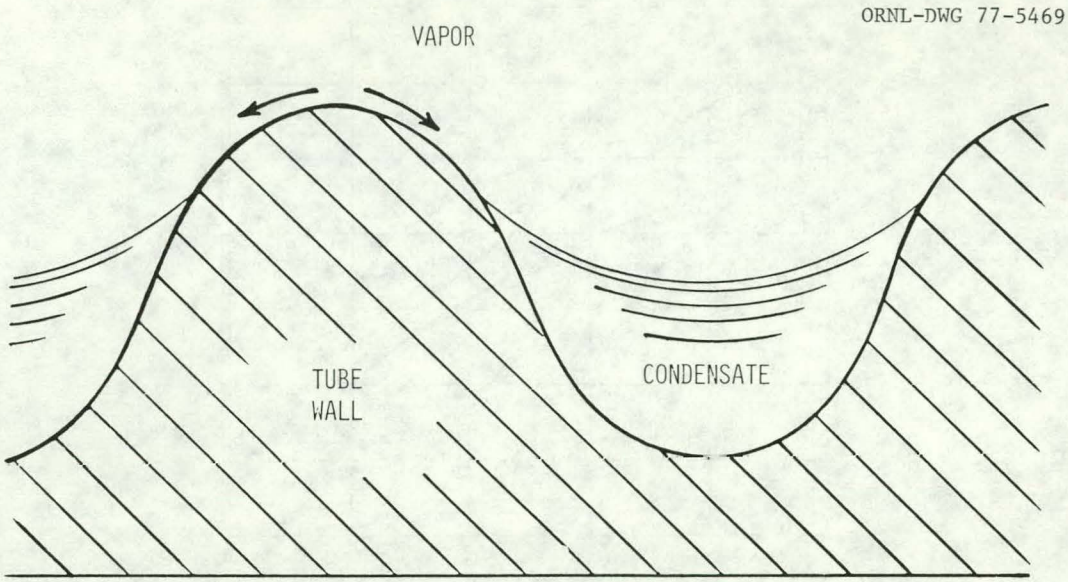



Fig. 2. Gregorig surface heat transfer mechanism.

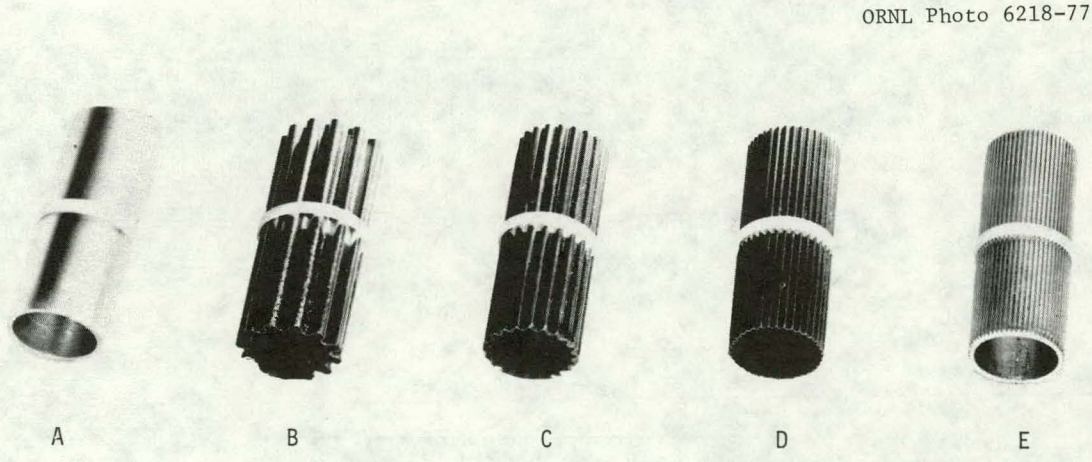



Fig. 3. Samples of enhanced tube types evaluated.

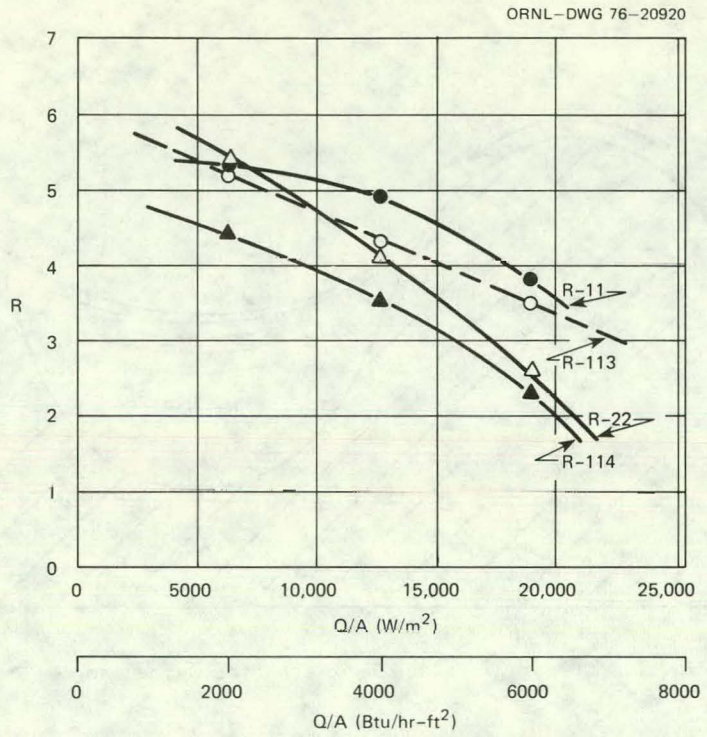



Fig. 4. Condensation enhancement using fluted tubes.

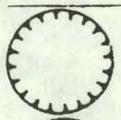
| Tube | $\frac{A_{fin}}{A_{sm}}$ | $\frac{h_{fin}}{h_{sm}}$ | $\frac{f_{fin}}{f_{sm}}$ | $\left[\frac{h_{fin}}{h_{sm}}\right]_{PP}$ |
|---|---|---|---|---|
|  | 1.66 | 2.6 | 2.6 | 2.3 |
|  | 1.63 | 2.3 | 2.0 | 1.9 |
|  | 1.54 | 2.3 | 3.1 | 1.6 |

Fig. 5. Seawater heat transfer improvement posibilities. [Derived from Watkinson et al. (4).]

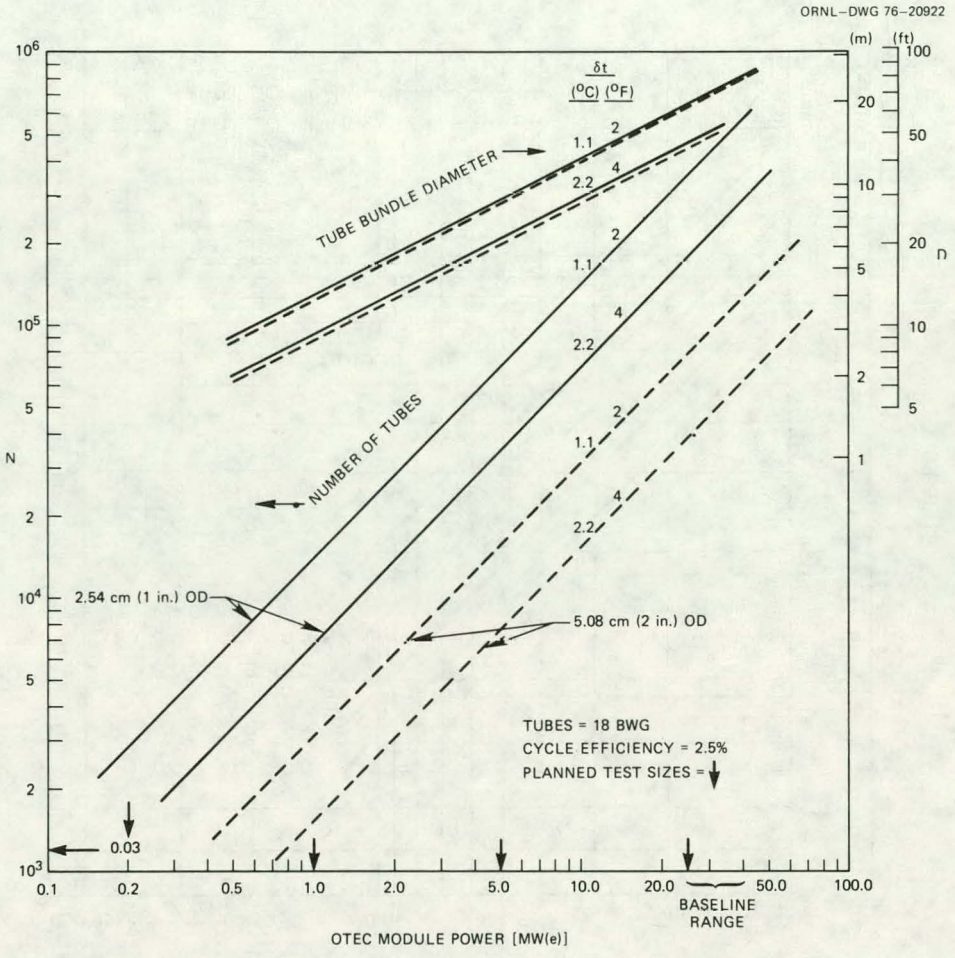



Fig. 6. Effect of design parameters on OTEC heat exchanger tube bundle size.

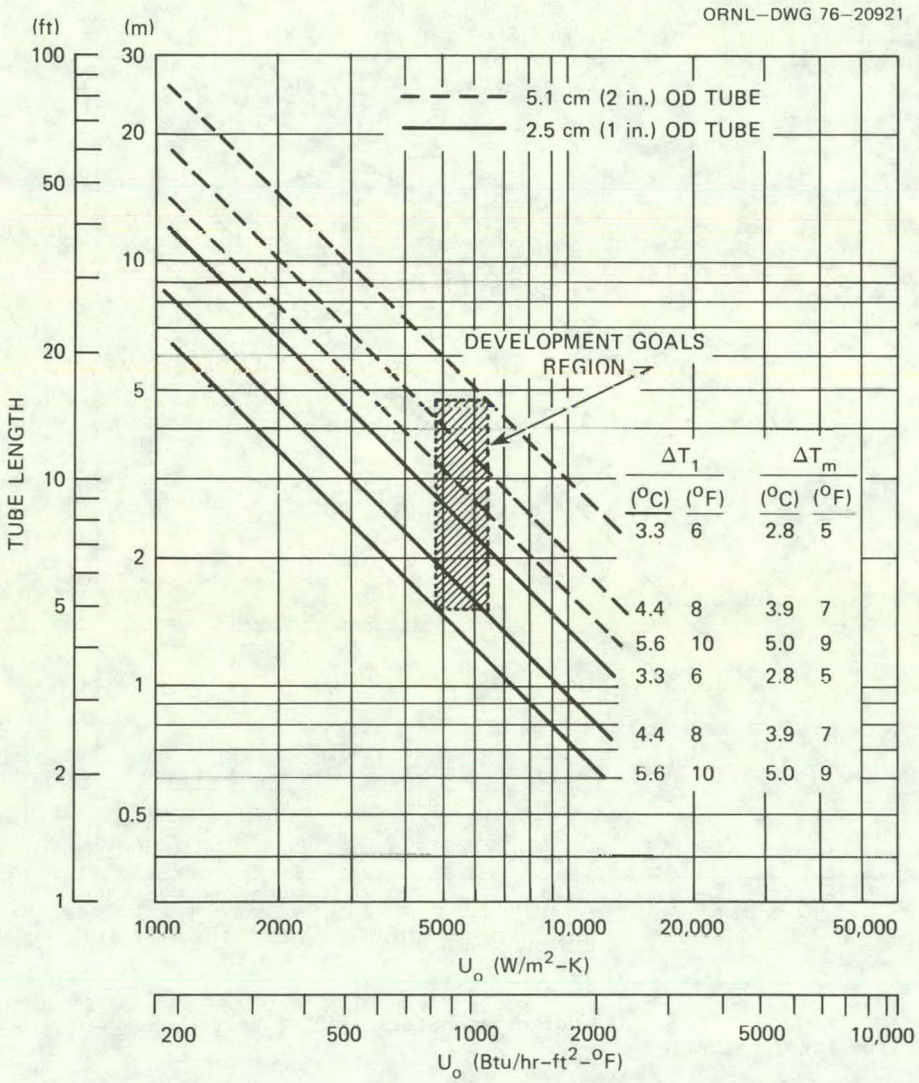



Fig. 7. Effect of design parameters on OTEC heat exchanger tube length

ORNL Photo 6174-77

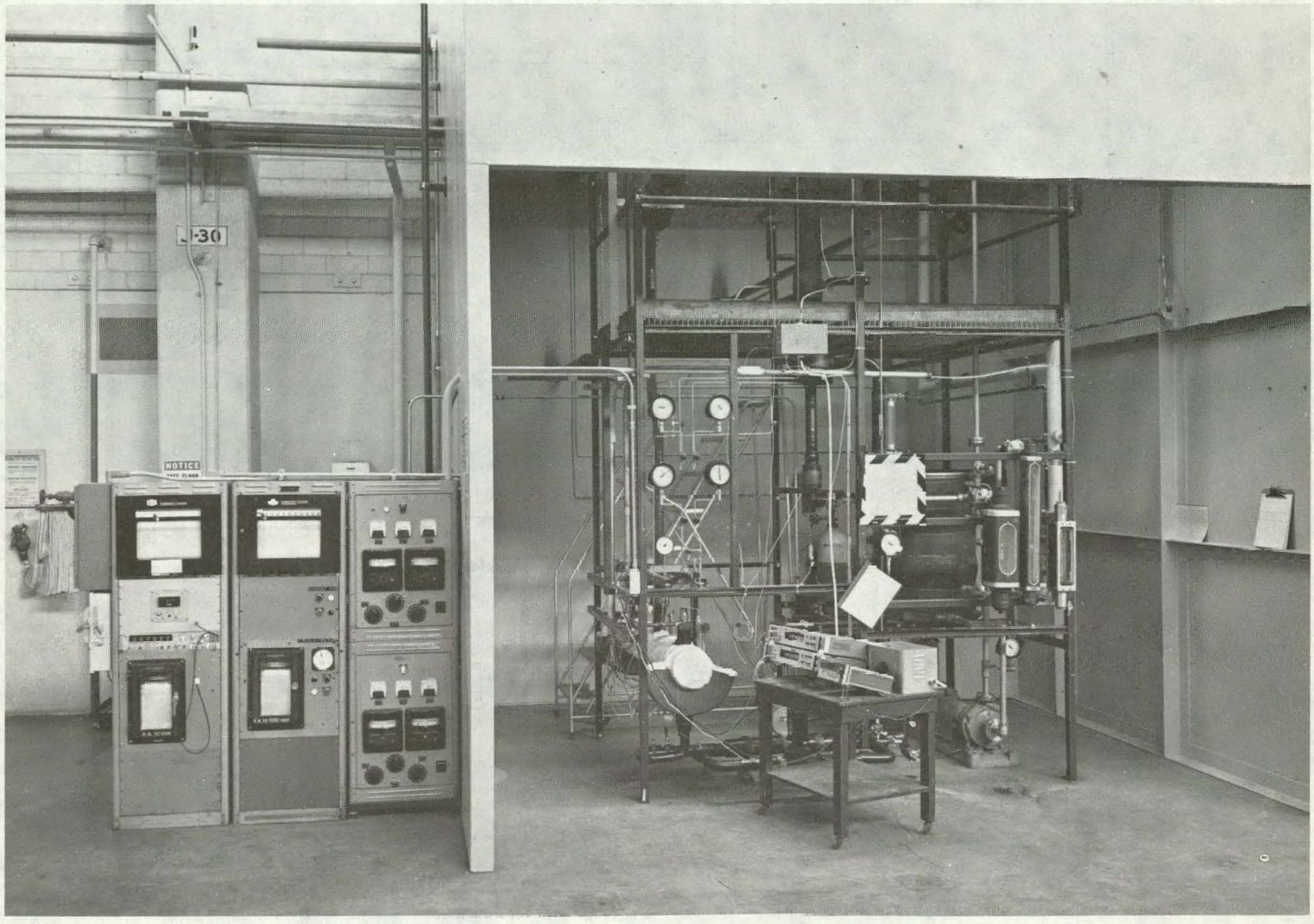



Fig. 9. Photograph of the ORNL $NH_3$ condensation test loop.

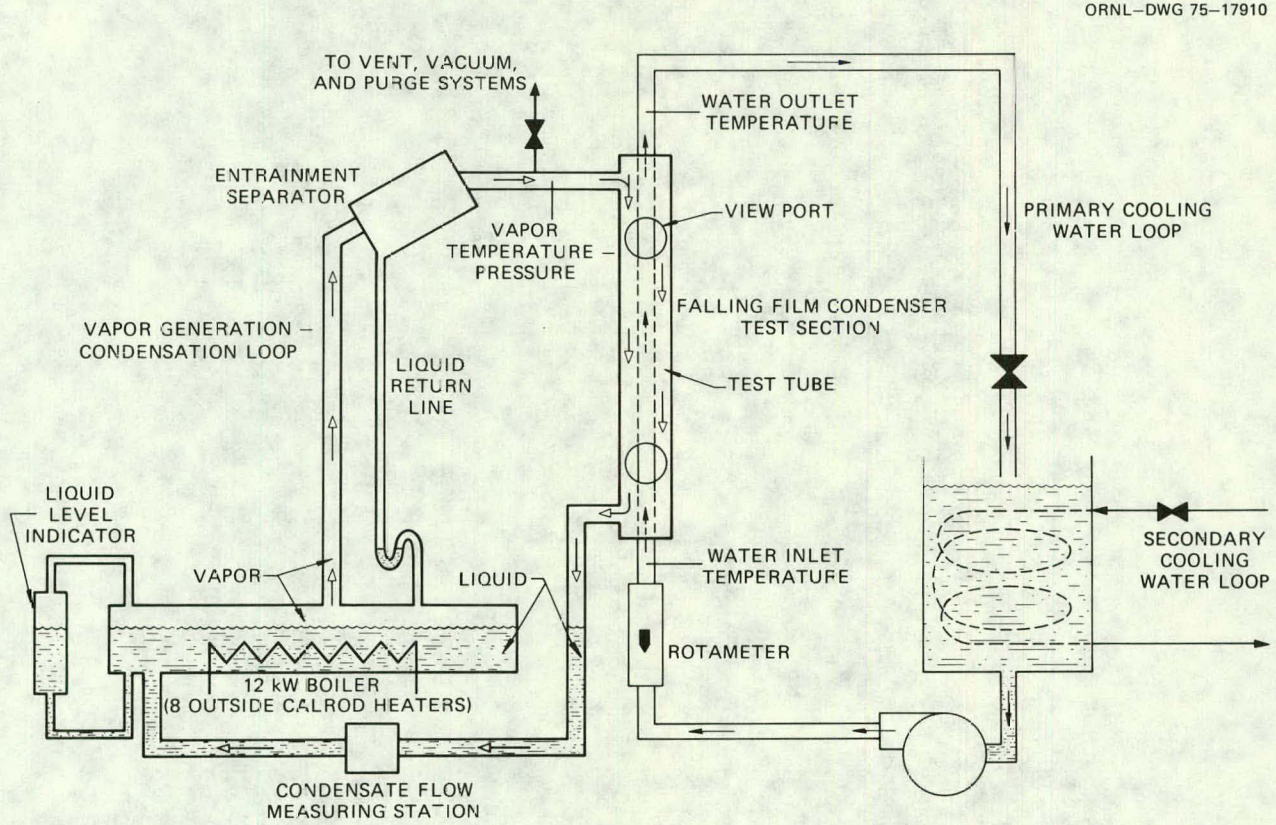



Fig. 8. Schematic diagram of the ORNL $NH_3$ condensation loop.

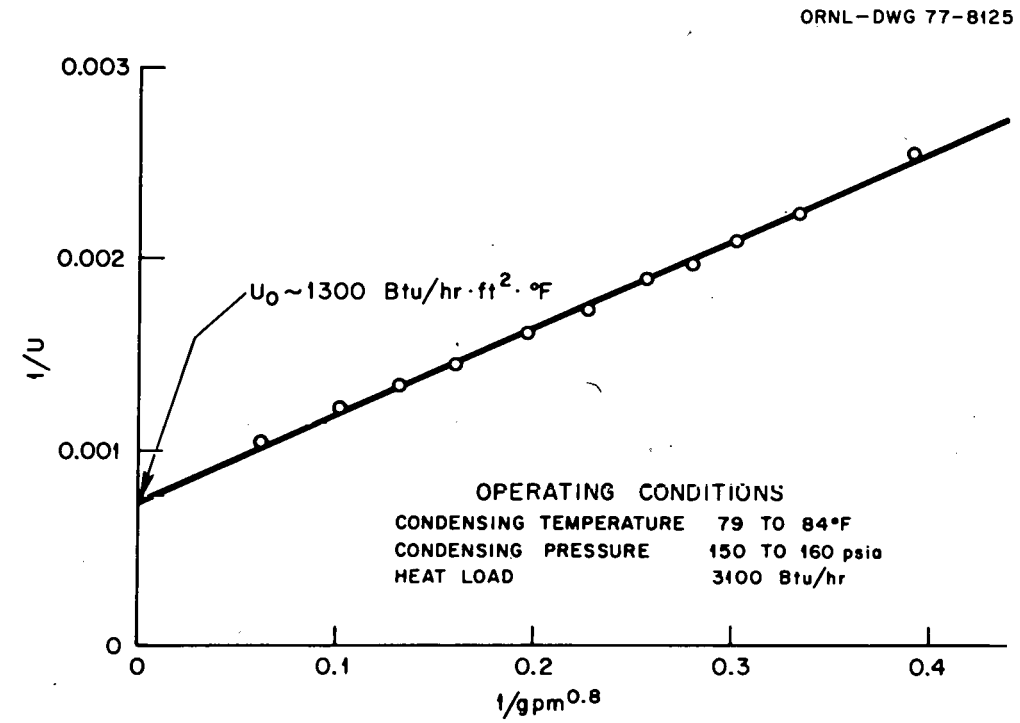



Fig. 10. Wilson plot for ammonia condensation data.

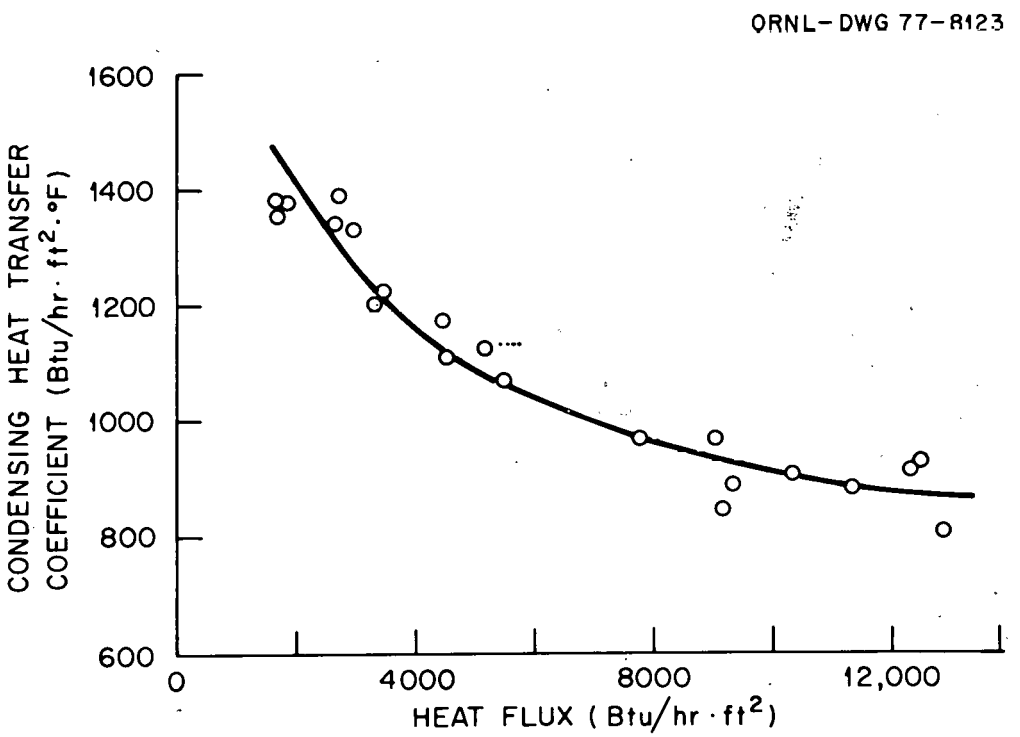



Fig. 11. Effect of heat flux on ammonia condensation coefficients — smooth vertical tube.

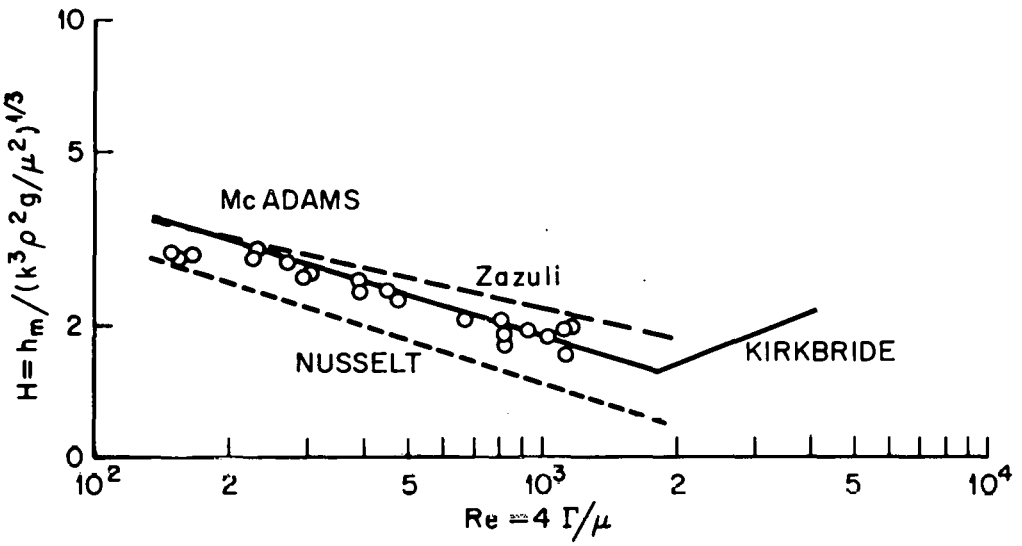



Fig. 12. Ammonia condensation correlation for smooth vertical tube.

## DISCUSSION

Joplin (Florida Power and Light): To what extent are Oak Ridge's performance findings a function of the heat transfer fluid being on the outside of a tube and the water being on the inside? What might be the effects of putting the water on the outside and the heat transfer fluid on the inside under pressure?

Michel: The heat exchanger size relationships in this paper are for shell and tube designs with the seawater flowing inside the tubes. The possible effects of inverting this arrangement would be that a different and probably less practical system of tube cleaning would be required, but it may be possible to eliminate a large pressure vessel shell to contain the ammonia vapor and, thus, perhaps realize a cost savings. A rather complex manifolding system would, however, be required.

Aronson (Gilbert's Associates): How will the evaporator and condenser design be influenced by enhanced performance of heat transfer tubes? (1) Will tube length be shortened? (2) Will tube diameters be increased? (3) Would the optimum temperature change of the seawater be changed?

Michel: The best answer to your question is that the best heat exchanger geometry will be determined from plant optimization studies. Hopefully, a complete system optimization model and program including appropriate cost functions will be available to help establish the optimum design. Qualitatively, as the overall heat transfer coefficient is increased, I would expect the tube length to decrease and possibly the tube diameter and seawater $\Delta T$ to increase somewhat.

# ACCELERATED HEAT EXCHANGER CORE TESTING

NORMAN F. SATHER
*Energy and Environmental Systems Division*
*Argonne National Laboratory*
*9700 South Cass Avenue*
*Argonne, Illinois*

Abstract

A program has been started at Argonne National Laboratory to test high performance evaporators and condensers being considered for the 1-MWe ocean test of OTEC heat exchangers. The experimental part of the program will be carried out in a test facility containing three loops -- warm water, cold water, and ammonia. The test units will be about 1/40th the size of those for the ocean test, and fresh water will be used instead of sea water. Otherwise, test conditions will be typical of the ocean test. The objectives of the program are to measure performance of the units and to compare performance with that expected from data obtained from single-tube tests and design calculations. Testing of the first group of heat exchangers -- three evaporators and two condensers -- is scheduled to start with overall performance tests, beginning in August 1977.

A program was recently started at Argonne National Laboratory to test high-performance evaporators and condensers being considered for the 1-MWe ocean test of OTEC heat-exchanger components planned for 1979. The experimental program has two primary objectives: to measure the performance of the test units for use in ammonia-cycle OTEC power plants; and to compare the measured performance of the test units with that expected from single-tube data and design calculations.

The Argonne program includes design and construction of a facility to measure the performance of at least three candidate evaporators and two condensers of 1-MWt capacity -- about 1/40th of the size of the units for the 1-MWe ocean tests. The program was begun last December with initiation of the design of the test facility. Testing of the heat exchanger units is planned to begin late in the summer of 1977 and preliminary evaluations of their performance will be completed by the fall. Further testing of these and other units will be carried out in 1978. The Argonne program also includes a supporting modeling effort (to be reported on later) to provide reliable design methods for sizing evaporators and condensers of the types being contemplated for OTEC use.

## Units to be Tested

Five units will be investigated in the first round of testing. A flooded-bundle evaporator being built by Union Carbide/Linde is the first (see Fig. 1). This unit, to be delivered July 1, 1977, is a horizontal

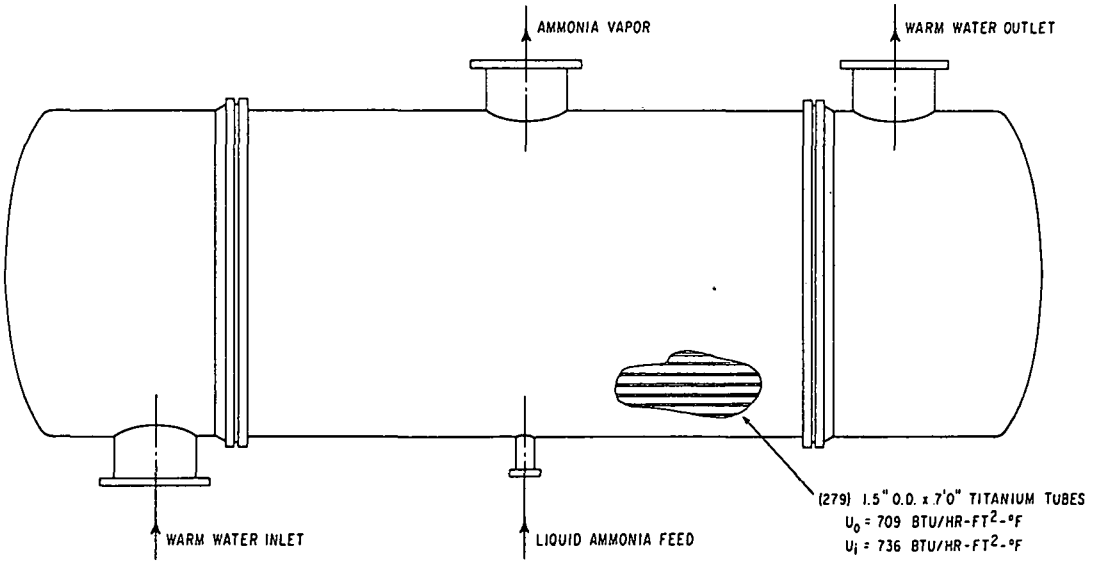



Fig. 1 Union Carbide/Linde Flooded Bundle Evaporator

shell-and-tube evaporator containing 279 titanium tubes 1.5-in OD by 7-ft long. Liquid ammonia is pumped into a pool of ammonia on the shell side, where it boils on the outside of the tubes. Tube surfaces are coated with a layer of porous titanium that enhances the rate of nucleate-boiling heat transfer. The ammonia is vaporized by heat from warm water flowing through the tubes in a three-pass configuration. The expected overall heat-transfer coefficient based on the outside area of the tubes is 709 Btu/hr-ft$^2$-°F, about twice that for smooth titanium tubes. Experimental data on heat-transfer coefficients for porous-surface titanium tubes measured in single-tube studies at Union Carbide are reported in paper No. 3B-2 of this volume.

The second evaporator to be tested is a vertical shell-and-tube unit of the falling-film type (see Fig. 2), developed at Carnegie-Mellon University. The unit contains 240 fluted aluminum tubes 1-in OD x 14-ft 3-in long. Liquid ammonia is pumped into a plenum chamber so constructed that the ammonia flows down the outside of each tube in a thin film. Ammonia evaporated from the tube surfaces is discharged through the ammonia-vapor nozzle; that reaching the bottom of the tubes without evaporating is collected and recirculated to the liquid-ammonia feed nozzle. Warm water flows upward through the condenser on the tube side.

The first condenser to be tested, (Fig. 3), is nearly identical to the Carnegie-Mellon falling-film evaporator. This unit also has 240 vertical fluted aluminum tubes of the same overall dimensions. Ammonia vapor is charged to the shell side of the condenser through a nozzle midway between the upper and lower tube sheets; the condensate collects on the tubes and flows downward in thin films to the bottom tube sheet, where it discharges through a condensate nozzle. The heat of condensation is removed from the condenser with a cold-water stream that flows upward on the tube side. The design for the fluted-tube condenser, also developed at Carnegie-Mellon University, is based on data described in paper 3B-1 of this volume. The Carnegie-Mellon evaporator and condenser are scheduled for delivery to Argonne on September 1, 1977.

Two other heat exchangers, to be supplied by Union Carbide/Linde, are scheduled for testing in the fall of 1977. One is a horizontal shell-and-tube evaporator in which liquid ammonia is sprayed onto the outside surfaces of titanium tubes coated with porous titanium and warm water is on the tube side. The other is a condenser, a horizontal shell-and-tube unit containing fluted tubes. Ammonia condenses on the shell side and water flows through the tubes.

## Test Program

The performance of the test exchangers will be characterized by the overall heat-transfer coefficient and the pressure drops on both the shell and tube sides. In addition, effort will be made to determine the separate water-side and ammonia-side heat-transfer coefficients and the variability of performance of individual tubes. The separate heat-transfer coefficients will be determined by varying the water-flow rate through the exchangers and extrapolating the

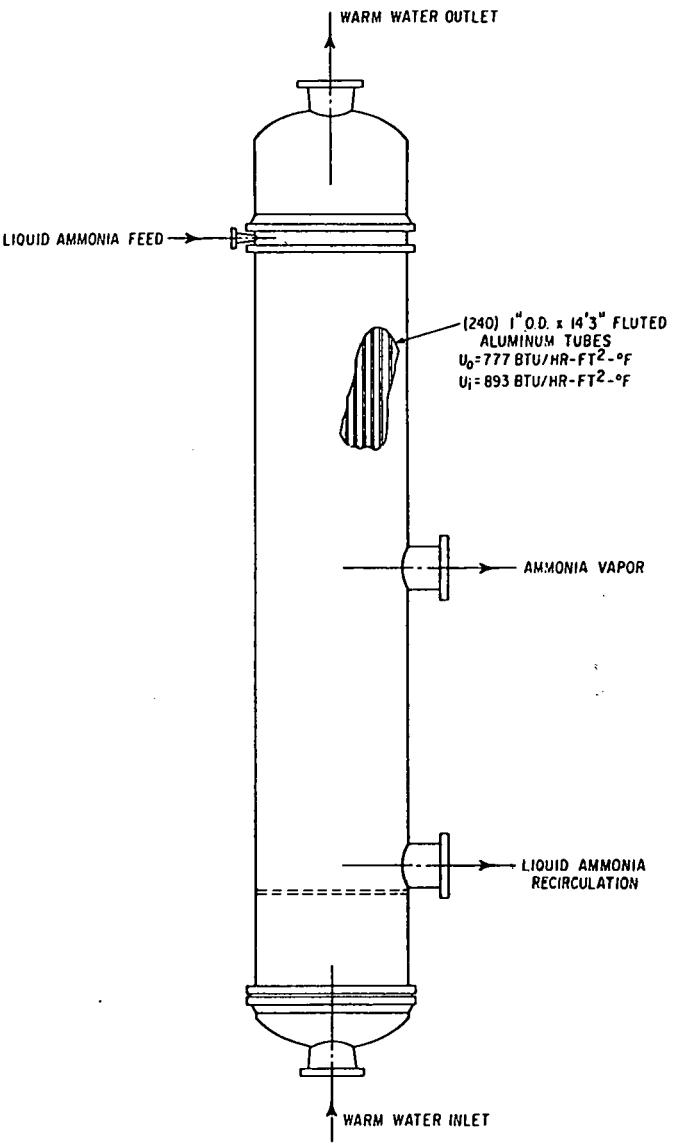



Fig. 2 Carnegie-Mellon Falling Film Evaporator

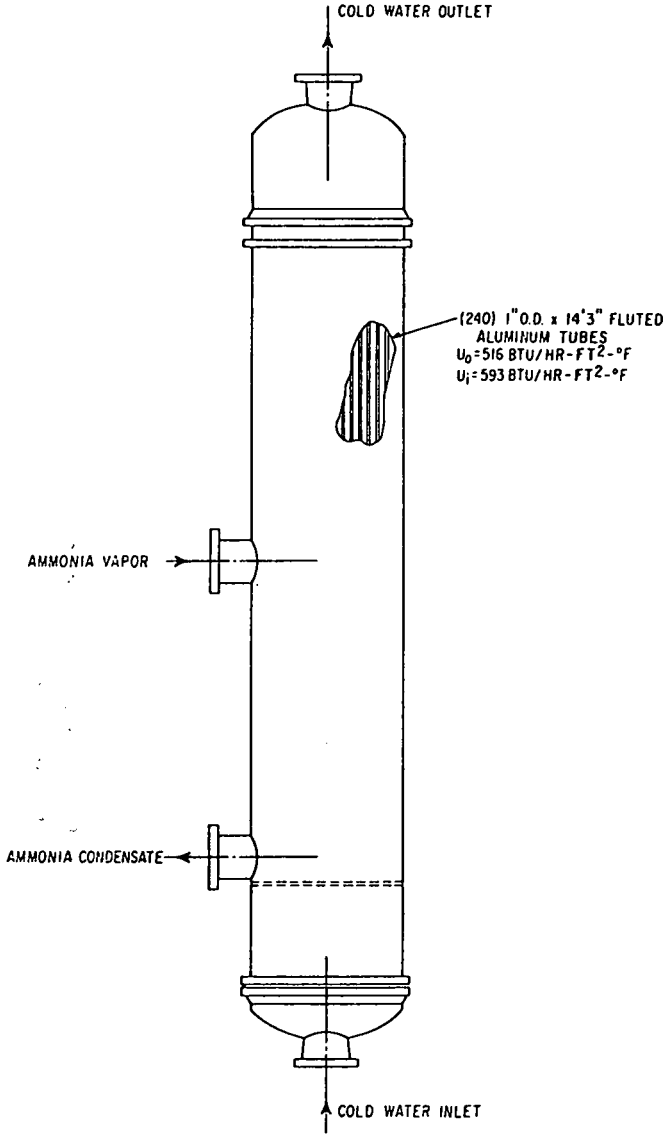



Fig. 3 Carnegie-Mellon Falling Film Condenser

overall heat-transfer coefficient to zero water-side resistance by the standard Wilson procedure. Use of this procedure requires data on the dependence of the water-side coefficient for single tubes. Performance of individual tubes will be measured by instrumenting selected tubes in the bundle to determine flow rates and temperatures, from which the local tube heat-transfer coefficients can be estimated.

## Test Facility

Measuring performance of the test units required a facility to provide simulated warm ocean water to the evaporator under test and simulated cold ocean water to the condenser. Such a facility is under construction at Argonne. The test units are designed to handle a heat duty of $3.2 \times 10^6$ Btu/hr and a change in water temperature of 2°F. Other operating conditions will be typical in all respects of expected operating conditions for OTEC plants except that chemically treated fresh water will be used instead of ocean water; and thus effects of fouling of heat-transfer surfaces will be kept as small as possible. These data on clean-tube systems will be supplemented with information from the OTEC programs on biofouling and corrosion to predict performance of the test evaporators and condensers in an ocean environment.

A piping diagram for the test facility at Argonne is given in Fig. 4. The facility will consist of three flow loops -- one for supplying warm water to the evaporator under test, a second to supply cold water to the condenser under test, and a third for circulating the working fluid (ammonia) through the evaporator and condenser. The facility is designed for operation at steady state over the range of heat duties and flow rates of warm and cold water and temperatures given in Table 1. Provision will be made for control of

Table 1. Operating Conditions of Test Facility

| | Nominal Value | Range |
|---|---|---|
| Heat Duty of Test Units, $10^6$ Btu/hr | 3.2 | 2.4-4.0 |
| Warm-Water Supply Temperature, °F | 80 | 75-85 |
| Cold-Water Supply Temperature, °F | 40 | 38-45 |
| Water-Temperature Change, °F | 2 | 2-4 |
| Log Mean Temperature Difference, °F | 9 | 6-12 |
| Water Flow Rate, gpm | 3200 | 1200-4000 |

temperatures and flow rates and for measurement of parameters necessary for determining the overall heat-transfer coefficient and pressure-drop characteristics on the test units over the specified ranges of operating conditions.

The warm-water supply loop, of 14-in piping, includes a circulating pump for supplying the 80°F water to the evaporator and a steam heater for reheating the

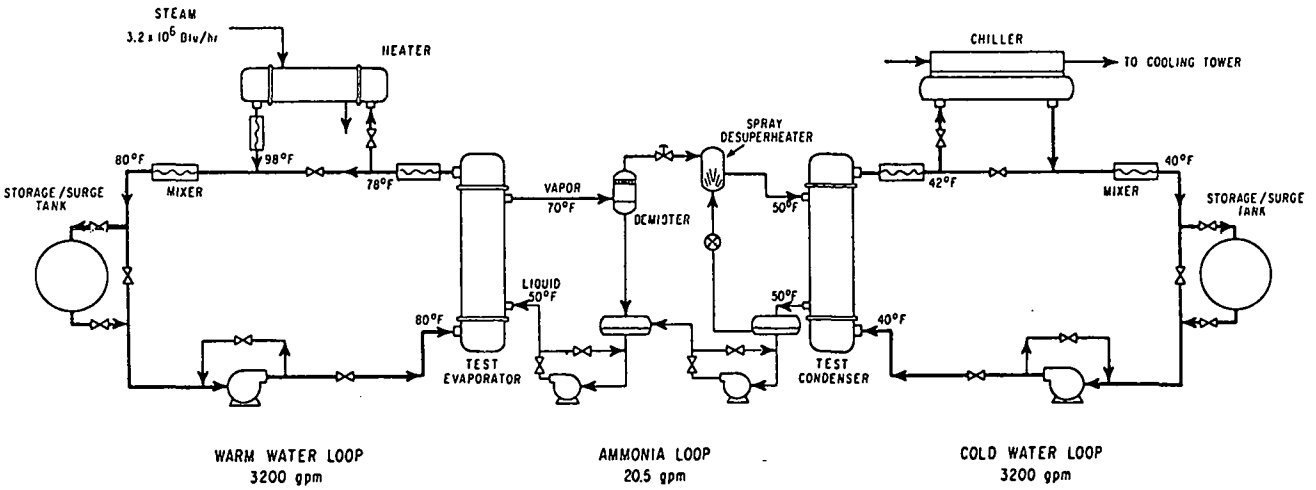



Fig. 4 OTEC Heat Exchanger Test Facility

water from 78°F to 80°F after passage through the evaporator. The warm-water loop also includes a storage/surge tank and mixers to eliminate radial variations in water temperature across the pipe where mixed mean temperatures are measured. There will also be valves as shown for control of flow rates; and instrumentation for measuring flow rates, temperatures, temperature differences, pressures, and pressure differences in the loop.

The cold-water supply loop, shown on the right side of Fig. 4, is a similar 14-in piping loop having a circulating pump; a 500-ton refrigeration unit; a similar 10,000-gal storage/surge tank; flow-control valves; and instrumentation for measuring flow rates, temperatures, and pressures.

The ammonia loop, shown in the center of Fig. 4, is identical to that in an OTEC power plant, except that the turbine has been replaced with an expansion valve and a spray desuperheater, which together provide a vapor feed to the condenser of the same thermodynamic state as that of a turbine exhaust. Ammonia vapor from the evaporator passes through an 8-in line to a demister, where entrained liquid is removed; through the expansion valve, where the pressure drop occurs, through the spray desuperheater, and into the condenser. Condensate from the condenser is collected in an accumulator, which also collects liquid from the demister and from test evaporators for which recirculation of unevaporated liquid is required. Liquid ammonia is pumped from the second accumulator to the test evaporator. Under nominal operating conditions, the pressure in the evaporator is 129 psia and that in the condenser 89 psia. The ammonia loop has instrumentation to measure flow rates, temperatures, temperature differences, pressures, and pressure drops across the test units.

Vapor quality will be measured as follows: the temperature and pressure of the vapor from the expansion valve are measured directly. The operating conditions are such that this vapor will always be superheated. The quality of the vapor leaving the evaporator is then calculated from its temperature and pressure and the measured flow rate of liquid from the demister. Similarly, the quality of the vapor being fed to the condenser is determined from the temperature and pressure of the vapor at the condenser inlet and the measured flow rate of liquid ammonia fed to the spray desuperheater.

The facility will have an auxiliary ammonia storage system and equipment for filtering the ammonia as it circulates in the loop, for degreasing the ammonia loop, and for removal of air with a nitrogen purge before charging with ammonia. Noncondensable gases will be purged from the ammonia loop during operation. Both the warm- and cold-water loops have equipment for filtering and chemically treating loop water to control corrosion and pH. All piping and equipment in the water and ammonia loops are of carbon steel, except for the chiller tubes, which are copper. The facility will have a data-handling system that accepts inputs from thermocouples, from digital transducers, and from a digital clock. Raw or reduced data from an associated minicomputer can be displayed on LED numeric displays and recorded for later analysis by an off-site digital computer.

The accuracy goals for the measurements characterizing the overall performance of the test units are ± 10% for the overall heat-transfer coefficients, ± 5% for the water-side pressure drops across the units, and ± 10% for the ammonia-side pressure drops. To determine the individual heat-transfer coefficients with meaningful

accuracy, the overall heat-transfer coefficients must be sured to within ± 5%. These requirements set the cision for quantities measured directly. The results shown in Table 2. Equipment to be used for these

Table 2. Required Experimental Precision of Directly Measured Quantities

| | |
|---|---|
| Water and Ammonia Temperatures, °F | ± 0.1 |
| Water Flow Rates, gpm | ± 5 at 3200 |
| Ammonia Flow Rate (Liquid), gpm | ± 0.1 at 20.5 |
| Ammonia Pressures (Vapor Line), psia | ± 0.02 |
| Ammonia Pressures (Test Units), psia | ± 0.02 |

measurements includes Type-E thermocouples for all temperatures, turbine flow meters for both the water and ammonia flow rates, and high-precision transducers for all pressures in the ammonia and water loops.

The procedure in the operation of the test facility is as follows: for evaporators tests, first the flow rate of the warm water to the evaporator is set at the desired value, as is the ammonia-side pressure by the controller that operates the expansion valve in the vapor line. This fixes the ammonia-side saturation temperature. The rate of steam feed to the warm-water heater is adjusted until the desired temperature of the warm water entering the evaporator is reached. The sequence of inlet-water temperatures will be (°F): 80, 82, 78, 84, and 75. The tests will be made at the following conditions:

| Water Flow Rate, gpm | Ammonia Side | |
|---|---|---|
| | Saturation Temp, °F | Saturation Pressure, psi |
| 3200 | 72 | 133 |
| 2400 | 72 | 133 |
| 4000 | 72 | 133 |

Additional runs will be made to assess the effects of varying the ammonia-side saturation temperature. A similar procedure will be used in testing the condenser units.

The sequence of inlet-water temperatures will be (°F): 40, 42, 38, and 45. The test will be run at the following conditions:

| Water Flow Rate, gpm | Ammonia Side | |
|---|---|---|
| | Saturation Temp, °F | Saturation Pressure, psi |
| 3200 | 48 | 86 |
| 2400 | 48 | 86 |
| 4000 | 48 | 86 |

Again, the water flow rate is set first, then the ammonia-side saturation temperature, and lastly the cold-water inlet temperature to the condenser by adjustment of the set point on the controller of the referigeration unit.

## Schedule

According to the schedule in Fig. 5, planning of the test program and the design and construction of the test facility, begun in December 1976, should be completed in July, 1977. After several weeks of calibration and shakedown runs, tests of overall performance of the Linde flooded-bundle evaporator will be started. The same tests will be run on the other four heat exchangers by December, 1977, after which further tests of these same units, particularly those on the variability of performance of individual tubes, will be made. Tests of other heat exchangers being designed are also planned for 1978.

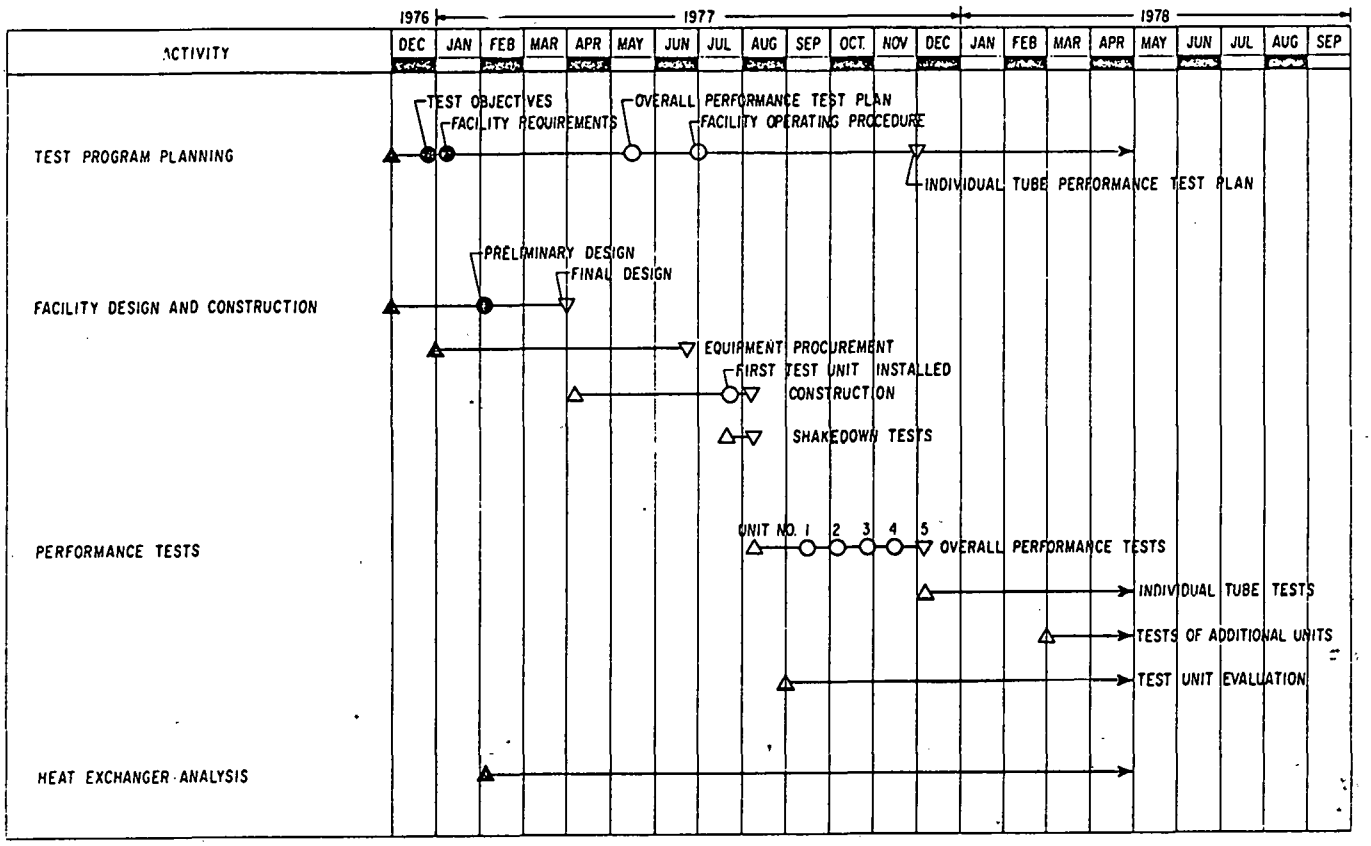



Fig. 5 Schedule for Heat-Exchanger Test Program

## DISCUSSION

singer(Lockheed): What means will be used for determining the quality of ammonia at the exit of the evaporator?

Sather: We are expecting, by the way, a quality range of 85% to 100%. The procedure we will use is to calculate the quality at that point by working backwards from a known vapor state after the expansion valve and measuring the liquid flow rate from the demister itself, which is returned back to the evaporator. So we'll calculate the quality on the basis of those measurements and the known vapor flow rate.

Messinger(Lockheed); What provision will the facility have for measuring heat exchangers that are slightly tilted either from the horizontal or vertical?

Sather: I assume that you are talking about intentionally tilted. The units themselves (based on the Carnegie-Mellon design) are to operate vertically, and we are expecting to test them vertically, as vertically as we can make them. There would be no difficulty at all to carry out tests with the units oriented at a prescribed angle from the vertical. We will be constructing support racks, or support structures for the test units and they can rather easily be modified to permit canting the units themselves.

Messinger(Lockheed): My interest is, first, in the deviation from the vertical position; I am concerned with operation under actual sea-state conditions on a platform which would be subject to some swaying motion, and particularly with the question of the distribution problem of the ammonia among the various tubes. The concern about the horizontal units is the already published Lockheed impression that there can be possibly significant enhancement in at least the condenser and possibly in the evaporator by going to small angles of declination from the horizontal.

Sather: I guess that I have no further comment. I would think it would be better to ask Al Czikk and Bob Rothfus tomorrow about that. Rather than speak to me, you might as well speak to the source.

Manikowski(Lockheed): How did they select the saturation pressures, in effect, for the ammonia side of the cycle?

Sather: Perhaps I shouldn't have emphasized that these are firmly fixed. It is relatively easy to change the set point on the controller to adjust the pressure so that the temperature will be whatever value within its range we would want. We have picked those as the values for our first test and they represent in both cases a 7°F log mean temperature driving force based on the nominal conditions of operation. We plan to cover in subsequent tests temperature drop differences between 6 and 12°F. There's nothing special about the numbers except as a starting point.

Reid(Aerospace Corp.): 1) How are you going to monitor the cleanness of the water? Are you going to measure fouling even under these conditions? (Which I would not discard as being absolutely non-existent.) And 2), How are the test data to be used in the furtherance of the project?

Sather: I think there are three questions there. First, monitoring of ammonia in the water: We will be monitoring concentrations of ammonia in the water continuously. We haven't yet settled on the method by which we will do this, but certainly we recognize it as quite important to do this and we are considering several alternative means now. Second, with respect to measuring effects of fouling: We don't plan to do that, at least in our first round of tests. We haven't really discussed or decided whether we will subsequently. The tests themselves will be carried out over a period of weeks, and we will be looking for changes in performance and going back and checking data against earlier baseline runs as one indication of potential fouling. But we have no specific plans at the moment. Third, how do we plan to use the test data? There is an embryonic test plan for verifying models. I guess I don't know the answer to that, except to say that we will be comparing the results of various models with the test data, attempting to check existing models and perhaps validating refinement of revised versions of models that are currently used, where necessary. I guess to answer that properly requires being able to anticipate where we expect analytical methods to be inadequate. We, I think at this point, don't have enough of a feel for how this will turn out. So I can't really give more of an answer than that.

CONF-770331--2

# AN OUTLINE FOR OPTIMIZING AND EVALUATING PROPOSED OTEC SYSTEMS

R. N. LYON
*Engineering Technology Division*
*Oak Ridge National Laboratory*
*Oak Ridge, Tennessee*

Abstract

It appears to be possible to begin now the development of a mathematically tractable, generalized model of OTEC plants that can be used in optimizing those plants, predicting their power cost and highlighting areas of needed information. This can be accomplished most quickly by cooperation between OTEC groups, and pooling their present optimization work.

The absence of such a development brings ever nearer the hazard of erroneous but irreversible program decisions.

By "modeling of OTEC systems," I mean a set of relationships that tie together the variables in an OTEC system. For example, in an open or closed Rankine type OTEC plant, the flow rate of cold seawater is obviously related to the pumping power required for the seawater flow. That pumping power is related to the diameter and length of the cold-water duct, to the geometry of the duct system for delivering the water to the active portion of the condenser, to the geometry of the cold-water disposal system, and to the geometry of the water flow system in the active portion of the condenser. The flow rate is inversely proportional to the temperature rise of the cold water at a given rate of heat removal from the heat exchanger, and the net power for a given heat removal rate is affected by the cold water pumping power, warm water pumping rate, evaporator and condenser characteristics, and the turbine and feed pump efficiencies.

The fundamental relationships between operating and design variables of this type do not constitute a complete model, however, they put both restraints and constraints on other variables, such as system layout and hull design, but they do not specify those designs. Both types of variables in turn affect the bus bar cost of the net power that is produced.

Finally, the form in which the power is delivered to the ultimate market — electricity, aluminum, ammonia, hydrogen, or something else — affects the effective power cost at the market, and may influence the most effective hull design, the system layout, and the fundamental design and operating variables.

A complete model relates all of these variables, including the cost of the product delivered to the market.

Optimization, in the case of OTEC, consists ideally of finding the set of values and decisions that will result in the minimum delivered cost and, of course, specifies that cost.

As we all know, we lack much of the information needed for the ideal optimization, but I submit that we won't know what we need until we begin to develop the model on a formal basis. Even at our present stage of ignorance, I believe we can begin to develop a generalized model to fit most if not all of the OTEC concepts and begin to project brackets for the minimum delivered cost.

In the process, we will get answers to other questions: Which concept should be pushed for early development? Which concepts should be carried for possible long-term cost reduction? How sensitive are power costs to deviations from optimum operation and design? Where are the soft areas in data and other technical knowledge?

Modeling and optimization are particularly helpful in forcing us to face the real obstacles. Obviously, it would be uneconomical to triple the evaporating conductance while doubling the cost per square foot of heat transfer surface, if even initially the combined water side and wall conductance is only one-third the evaporating conductance. We might reduce the required heat transfer surface by about 17%, but we would increase the cost of that surface by about 67% in the process.

The large number of variables, the complexity of their relationship in a model — including in some cases banks of discontinuous data — suggests the use of a

*Research sponsored by the Energy Research and Development Administration under contract with the Union Carbide Corporation.

digital computer. Computers are fast, precise, and tireless. On the other hand, computers are stupid — have no innate judgement. Errors of fact and s in vocabulary and syntax when instructing a computer produce erroneous results.

This first law of computers, "garbage in; garbage out" or GIGO, is so generally recognized that only after a computer program has been in use for some time and subjected to general scrutiny and testing are its results generally accepted without reservations. That fact argues strongly for early development of a generalized computer model and optimization program that can be subjected to that scrutiny and testing — and modified accordingly — before the OTEC program finds itself forced by a large number of more or less irrevocable decisions to move along less than optimum paths.

A truly general model will fit all possible OTEC concepts. To date those concepts include:

1. Vapor-Turbine (or "Rankine Cycle") Systems

These may include open systems, using steam evaporated from the warm seawater, or closed system that use some other working fluid, such as ammonia.

2. Hydraulic-Turbine Systems

These systems proposed by Earl Beck, by Zener and Fetkovich of CMU, and by Ridgeway of RDA, use the thermal difference for differing types of vapor lifts to raise the warm water and provide the differential hydraulic head to operate an hydraulic turbine.

Other concepts that have been suggested but are not now under active consideration include:

1. An hydraulic turbine driven by a thermal fountain — an upwelling produced by warming deep, lower-salinity water from depth with heat from this warm surface water.

2. A Nitinol engine that uses the remarkable deformation memory and change in elastic modulus with temperature of a roughly 50-50 alloy of nickel and titanium.

3. Thermocouples. Cost and low efficiency have kept thermocouples from serious consideration.

All these concepts are restricted by the first two laws of thermodynamics:

1. Power out = heat flow in − heat flow out.

2. Power out $\leq$
(heat flow in/temp. in)(temp. in − temp. out),

or

heat flow out/temp. out $\geq$ heat flow in/temp. in.

These laws are only concerned with the thermal conversion part of the process. They include the theoretical work needed for a feed pump in a closed Rankine cycle, but do not, for example, include the work required to raise the denser cold water up to the plant.

On the other hand, they can be applied to any closed part of the conversion process. Thus, when the second law is applied to a closed Rankine cycle, "heat in" can mean the total heat required to raise the temperature of the feed and to evaporate it, and "temperature in" can be taken as the absolute temperature of the saturated vapor at the outlet of the evaporator.

In general, "temperature out" can be taken as the saturation temperature of the vapor entering the condenser, unless the vapor is superheated and an important amount of heat must be removed to lower its temperature to saturation.

Application of these laws to an open system is slightly more complicated, since we do not have a feed pump as such. Instead, we have to pump the condensate from the lower, condenser pressure up, past the evaporator pressure to the disposal pressure. In theory, that is partly compensated by the reduced amount of warm water that must be pumped, or allowed to flow by gravity back to disposal pressure. In practice, we will find that these and other physical laws are usually taken care of automatically as we design a system.

Other input to our model includes:

Concepts and variations.
Variables (or more precisely values of variables).
Parametric relationships.

Concepts include not only the system itself, as described earlier, but the type of hull (spar, floating pan, barge, etc.) and the form of the product (electricity, aluminum, ammonia, etc.).

Variations are modifications of these concepts, such as a surface (closed) condenser with an open system.

Variables, in general, are characteristics of the systems that can be expressed by specific numerical values — the diameter of a shell and tube heat exchanger, and the diameter, length, and number of its tubes, etc.

We can rather arbitrarily divide the variables into parameters, independent variables, and dependent variables. Only values of parameters and independent variables represent input.

It is essential that all of the dependent variables of interest be unambiguously computable from a given set of input values for the parameters and independent variables. The set of input values, of course, must also be internally consistent with the natural laws and parmetric relationships. That requirement and the desirability for rapid convergence in optimization dictate care in separating input variables from dependent or output variables.

The distinction between parameters and independent variables comes when setting up the optimization method. During a given optimization, the values for the parameters are held constant. At one extreme, all input variables except one are given temporarily fixed values, and the system is optimized with respect to that one unfixed independent variable. A computer may be needed only for computing specific cases if that method is chosen, since a few values of the power cost can be plotted versus the independent variable to show graphically the optimum value of that variable. This does not, however, give the true optimum value when the values of other input variables are allowed to change. On the other hand, optimizing with a very large number independent variables may take a great deal of computer time, and may never converge using presently available techniques. In general, computer time is much less valuable than human time, and optimization development should strive toward the fewest parameters. An example of an exception might be the temperature of the warm surface water, since at a given site that is not a variable over which we have control.

Parametric relationships are relationships, between the variables, that may change from site to site or from variation to variation. Thus, the list of a plant as a function of wind velocity will depend on the hull concept, the method of anchoring or positioning, and in some cases on the concept of the conversion system and its layout. Similarly, the relationships between cost and geometry of a shell and tube heat exchanger will be different from that of a plate and fin heat exchanger, and the change in water temperature with depth will vary from site to site.

Since the evaporator and condenser, in most of the front-running concepts, account for up to half the cost of the plant, the parametric relationships affecting their design and cost are particularly important. The size, and thereby the cost, of a heat exchanger to transfer heat at a given rate can, in principle, always be reduced by increasing the temperature differences across the heat exchanger. In an OTEC plant where the inlet temperature of the warm water is not controllable, and where the minimum inlet temperature of the cold water is limited, increasing the temperature drop across the heat exchanger reduces the temperature drop across the actual conversion portion of the system; and, as we have seen, that tends correspondingly to reduce the power production from a given heat flow.

The evaporator and condenser cannot be optimized independently. The fractional reduction in net power caused by increasing temperature difference across the evaporator will depend on the corresponding diversion of temperature drop and power to the condenser, and vice versa. The power used to bring warm and cold water to the heat exchangers and to dispose of the water also enters that calculation, and thus the size and cost of the ducting must enter the calculation. If the cold water duct is lengthened, the power diverted for pumping the cold water is increased, but the temperature of the cold water may be reduced.

On the other hand, reducing the size of the heat exchanger may permit reduction of the hull size and cost.

All of these interactions can be represented by parametric relationships that will change with concept and variation.

Similarly, we can reduce the size of the heat exchanger by increasing the velocity of the seawater through the heat exchanger, but the ratio of pumping power per unit area to thermal conductance on the seawater side along a smooth surface increases with about the square of the velocity of the seawater. That pumping power must be drawn from the gross output of the conversion system which, of course, tends to reduce the net power output per unit area of heat exchanger. Further, increasing the seawater velocity reduces directly only the thermal resistance between the water and the wall. It does not change the thermal resistance of the wall. Increasing the heat flow per unit area tends to decrease the thermal resistance in a nucleate boiling system as well, but it does not materially affect the evaporating thermal resistance on a smooth tube spray evaporator, and it tends to increase the condensing thermal resistance, particularly on enhanced condensing surfaces.

The relationship between pumping power and conductance in single-phase forced convection is not always the same, particularly when the nature of the surface is changed. In general, the pressure drop in a flowing system results from two phenomena: friction at the wall and changes in fluid velocity (including merely changes in direction). Since surface conductance is a surface phenomenon, it is related directly only to the surface friction and turbulence near the surface. Changes in velocity direction affect surface conductance largely as that change in velocity affect surface friction and that local turbulence. Often this effect is small compared with a corresponding pressure drop directly related to surface friction.

The relationship between "effective" surface friction and surface conduction is affected by the fluid properties — notably, the Prandtl number (Pr), or ratio of thermal diffusivity to momentum diffusivity. Thus, that relationship for the warm water (Pr $\approx$ 6.5) may be somewhat different from that for cold water (Pr $\approx$ 11.5). I suggest for that reason that the results of studies of enhanced seawater surface be listed to include the Prandtl number, and that the studies cover an appropriate range of Prandtl numbers. Plots of f, friction factor $\equiv$ 1/4 X hydraulic diameter X pressure drop per unit length/velocity pressure, versus Reynolds number, and plots for several values of Pr of j $\equiv$ Stanton number X $(Pr)^{2/3}$ versus Reynolds number, would appear to be useful forms.

In any case, experimenters should eschew an understandable tendency to attempt "evaluation" of surface modifications by such misleading combinations as the ratio of modified conductance to unmodified conductance

at constant pumping power, or the ratio of $(j)^3/f$ at Reynolds number. While these may often allow a s comparison, they do not provide enough information nodeling and for a valid optimization and comparison where both evaporator and condenser must be considered.

As implied in the preceding paragraphs, students of heat transfer often find it useful to separate the thermal conductances that make up the overall conductance. In many systems, including some OTEC systems, that sepration allows separate study of the variables that affect each conductance. Synthesis of the individual results into overall conductances is not always easy, however. Local boiling and conduction conductances vary with heat flux or wall temperature. Initiation of boiling is a strong function of local temperature. Circumferentially, local conductances are not uniform in flow across either single tubes or tubes in a bank. In some OTEC systems, several of these phenomena must be combined by integrating around the tubes, along the tube length, or perhaps both in order to find the "mean" or "effective" overall conductance. Even the definition of the "mean" conductance will depend on what kind of "mean" temperature drop is to be used in designing the heat exchanger.

None of these problems is particularly difficult, but they need to be addressed and answered in a way that meets with general concurrence if the resulting parametric relationships put into OTEC models and, therefore, the results of optimization of these models are to be valid and generally acceptable.

Many of the trade-offs in open systems are analogous to trade offs in closed systems. For example, in a closed channel involving forced single-phase convection, four times the Stanton number [conductance/(mass velocity times heat capacity)] is equal to the rate of relaxation of bulk water temperature in units of temperature difference between the bulk temperature and the wall temperature toward the wall temperature per unit length of channel measured in hydraulic diameters of the channel. In turbulent flow with smooth walls, that relaxation rate decreases only slowly with velocity (about the one-fifth power). In a falling film along an adiabatic wall with only its vapor on the free side of the film, the rate of relaxation, per unit length of descent of the bulk temperature, in units of temperature difference between bulk temperature and the satuation temperature will be only a mildly changing function of flow rate per unit width of film.

In the channel case, the overall temperature change in the stream is altered either by changing the wall temperature or by changing the length of the channel; in the falling film case, the overall temperature change is altered by changing the saturation temperature (changing the pressure of the vapor), or by changing the distance of the fall. In both cases, one change alters the temperature at which heat is received or removed, and the other involves an alteration in the work expended by the stream or film.

Thus, although the actual relationship may differ, a generalized model appears to be possible for handling both concepts.

I have used examples here from the field of heat transfer but similar examples are available in the areas of ocean engineering, structural engineering, and cost analysis.

A logical order of computation for a given set of values for the parameters and independent variables might be as follows:

1. Calculate the resulting values for the dependent design and operating variables for the system.

2. Calculate values for those layout and hull variables that remain after specifying the concepts and variations.

3. Calculate the construction and deployment costs.

4. Calculate or introduce maintenance costs, other operating costs, and utilization factor.

5. Calculate the bus-bar cost of power.

I believe that at present the plant model should stop at this point, although I recognize that the ultimate goal is the cost of the ultimate product delivered to the market. The cost of the power plant will outweigh the effect on total cost of modifying the plant to produce a different voltage or frequency, or to produce direct current.

Later, if the plant modeling and optimization is successfully developed, it can be combined, if desirable, with one or more modeling and optimization programs for product production, where applicable, and for appropriate delivery systems.

The final part of an optimization program, which may in fact dominate the modeling, is the arrival at the optimum (minimum-power-cost) set of values for the independent variables. If all the relationships between the variables can be put in certain forms, then that set of values can be arrived at directly.

For example, the first partial derivatives of cost with respect to the independent variables can be set at zero while requiring the second partial derivatives to be greater than zero, and the corresponding values for the independent variables found by matrix algebra or some other algebraic methods.

Alternatively, if the relationships can be put in the form of an appropriate "posinomial," geometric programming, developed by Zener and Lavi, can be used. In attempting to use these methods, we must be careful not to distort the model seriously by forced linearization or other approximations.

These or other methods, such as Newton or Taylor series methods, may be applicable for semidirect approach by successive approximation to the optimum.

The most generally applicable methods are search methods in n-dimensional space, where n is the number of independent variables. A powerful, but time consuming, process of this type is the method of maximum descent (or ascent) developed by statisticians. The "simplex" method is another type of search approach. It has been successfully used on problems with up to 20 variables, and may be usable in some cases for even more variables.

To date, I have found the maximum ascent method most usable for an eight variable system to find the maximum power per dollar of total (evaporator plus condenser) heat exchanger cost.

The system discussed in the present paper will involve much more than eight variables, however. Its development will require cooperation of most of the groups that are developing concepts as well as considerable mathematical help. It will also require, as already indicated, the cooperation of research people in aiming their work at the real, obstructive problems in OTEC development, and in reporting their results in the most usable form. It seems likely that the development of this program will consume at least four or five man-years, if it is to be reliable and usable, and if its output is to be acceptable.

On the other hand, the current piecemeal parallel efforts at optimization not only duplicate each other, but lead to highly questionable and often conflicting results. A good generalized program can result from a pooling of the current individual efforts.

OTEC needs now to begin comprehensive and energetic development of a general modeling and optimization method for assistance in making a wide variety of administrative and design decisions. The absence of such a method casts doubt on those decisions and jeopardizes the entire OTEC program.

# VI. HEAT EXCHANGERS

## SESSION 2

ABRAHIM LAVI, CHAIRMAN
*Ocean Systems Branch*
*Division of Solar Energy, ERDA*

THIS PAGE

WAS INTENTIONALLY

LEFT BLANK

# ENHANCED SINGLE-PHASE HEAT TRANSFER FOR OTEC SYSTEMS

A. E. BERGLES AND M. K. JENSEN
*Department of Mechanical Engineering and*
*Engineering Research Institute*
*Iowa State University*
*Ames, Iowa*

## Abstract

This paper reports on an initial study directed toward assessing the potential for heat transfer enhancement of the sea water, or single-phase side, of Ocean Thermal Energy Conversion (OTEC) heat exchangers. Of primary interest in large-scale heat exchange equipment are a number of "passive" enhancement techniques which do not require external power to generate and sustain the improvement. These techniques are: rough surfaces, extended surfaces, displaced enhancement devices, and swirl flow devices. The world literature was surveyed to locate representative data for these techniques. Heat transfer and friction factor data are presented for various techniques and subgroups of techniques.

The enhancement data are screened using a performance evaluation criterion which represents a measure of the reduction in heat transfer surface area with enhancement, subject to the constraints of constant heat duty and fluid pumping power. Rough tubes (particularly those with repeated-ribs or spiral protuberances), internally finned tubes, and tubes with twisted-tape inserts are shown to be the most effective. Using the best configurations of these techniques, it is possible to reduce the required heat exchanger surface area by 30 percent.

## Introduction

Preliminary studies have shown that the heat exchanger costs for Ocean Thermal Energy Conversion (OTEC) systems represent approximately one-half of the total capital cost. Much of the OTEC research is now directed at development of lower cost heat exchangers which are not unduly affected by biofouling. It appears that reduced size (and cost) will require utilization of enhanced heat transfer surfaces for both the boiler and condenser. The present study was directed toward assessing the potential for heat transfer enhancement on the sea water, or single-phase side, of these heat exchangers.

As noted in References 1 and 2, single-phase, forced-convection heat transfer can be enhanced by a wide variety of techniques. Of primary interest in large-scale heat exchange equipment are a number of the "passive" techniques which do not require external power to generate and sustain the improvement. These techniques are:

- Rough surfaces
- Extended surfaces
- Displaced enhancement devices
- Swirl flow devices

Combinations of several passive techniques (compound techniques) are also a possibility.

The first task in this study was to survey and evaluate the world literature on these techniques as applied to forced-convection flow of single-phase fluids. The basis for the survey was the bibliography and library of world literature on heat transfer enhancement which have been developed at the Iowa State University Heat Transfer Laboratory. From the literature pertaining to the four enhancement techniques, for the second task, the heat transfer and flow friction characteristics of representative surface configurations and inserts were assembled. The third task of the data evaluation was to apply appropriate performance evaluation criteria to the data. This evaluation led to an estimate of the reduction of heat exchanger size which can be achieved through use of enhanced heat exchanger tubes.

*Sponsored by Oak Ridge National Laboratory

## Literature Survey

The literature on heat transfer enhancement has grown rapidly in recent years. In order to provide rapid access to this literature a computerized literature retreival system was developed in the Iowa State Heat Transfer Laboratory. The references are given a reference number according to enhancement technique, mode of heat transfer, and sequential number for a given technique-mode. The reference number, citation information, and several descriptive key words are stored in a computer. The data requested are retrieved using a basic program developed by the Iowa State University Computation Center and adapted to this application. Retrieval is accomplished by specifying author, publication, date, key words, or a combination thereof.

Of the 70 possible cases (14 techniques and 5 modes) of data on heat transfer enhancement, only four cases are of interest for the present study. These cases represent the four passive techniques noted above, each only for the case of single-phase forced convection. The total number of references selected by the retrieval

system was 367 (out of a total of over 1,200). Out of these references a number of sets of data for turbulent flow of water flowing inside circular tubes were selected to show representative improvements which can be expected if these techniques were to be applied to OTEC heat exchangers. The studies selected are summarized in Tables 1-4.

## Discussion of Data for Selected Enhancement Techniques

Appreciable roughness may result from normal manufacturing processes; examples include pierced steel galvanized steel pipe, and cast iron pipe. Several studies have examined the thermal-hydraulic performance of commercially rough pipes with air; however, no data appear to have been reported for water. In any event, it would seem that the small increases in heat transfer which are observed should be discounted in practice, as slight fouling or rusting could negate any effect of the roughness.

Table 1. Representative Studies of Rough Surfaces

| Investigators | Reference this Report | Bibliographic Code | Investigators' Reference | Comments |
|---|---|---|---|---|
| Nagaoka and Watanabe | 4 | 022002 | 17 | wire coil insert |
| Cope | 5 | 022003 | A | knurling |
| Savage and Myers | 6 | 022024 | e = 1 in., L = 1 in. | transverse fin |
| Kolar | 7 | 022037 | 3 | thread |
| Kajic | 8 | 022038 | 1.25 mm lead, 0.06 mm depth | thread |
| Gowan | 9 | 022051, 022058 | R-1 | roughness screen |
| Kalinin et al. | 10 | 022055, 022074, 022091, 022126 | 4 | rolled protuberance |
| Eissenberg | 11 | 022071 | 2 | spiral protuberance (rope) |
| Webb et al. | 12 | 022093, 022011 | 2/10 | repeated rib |
| Kramer and Gater | 13 | 022098 | 2 | convoluted (flexible hose) |
| Grass | 14 | 022100 | Nur Querrillen | spiral groove |
| Blumenkrantz and Taborek | 15 | 022105 | 21 | Turbotec (convoluted) |
| Dipprey and Sabersky | 16 | 022021 | A-4 | sand grain (-cast) |
| Blumenkrantz et al. | 17 | 022117 | 2 | Phelps Dodge (convoluted) |
| Brouilette et al. | 18 | 022142 | 4 | spiral groove |
| Smith et al. | 19 | 022151 | p/D = 1.80 | single spiral rib |
| Kumar and Judd | 20 | 022124 | H/D = 1.06 in., D = 0.063 in. | wire coil insert |

Table 2. Representative studies of extended surfaces.

| Investigators | Reference this Report | Bibliographic Code | Investigators' Reference | Comments |
|---|---|---|---|---|
| Bergles et al. | 22 | 032020, 032014 | 5 | Forge-Fin low spiral |
| Watkinson et al. | 23 | 032023 | 13 | Forge-Fin straight |
| Watkinson et al. | 23 | 032023 | 18 | Forge-Fin high spiral |
| Watkinson et al. | 23 | 032023 | 19 | Forge-Fin low spiral |

Table 3. Representative studies of displaced enhancement devices.

| Investigators | Reference this Report | Bibliographic Code | Investigators' Reference | Comments |
|---|---|---|---|---|
| Evans | 24 | 042001, 042002 | d = 0.875 in., s = 12 in. | disc insert |
| Megerlin et al. | 25 | 042005 | 15 | mesh insert |
| Megerlin et al. | 25 | 042005 | Fig. 6 | brush insert (average) |

Table 4. Representative studies of swirl flow devices.

| Investigators | Reference this Report | Bibliographic Code | Investigators' Reference | Comments |
|---|---|---|---|---|
| Gambill and Bundy (Greene) | 26 | 000020 | A | twisted ribbon on axial core |
| Gambill et al. | 27 | 052006 | y = 2.49 | twisted tape |
| Ibragimov et al. | 28 | 052038 | y = 2.12 | twisted tape |
| Smithberg and Landis | 29 | 052011 | H/D = 3.62 | twisted tape |
| Lopina and Bergles | 30 | 052023, 052017 | y = 3.15 | twisted tape |
| Nagaoka and Watanabe | 31 | 022002 | 7 | twisted tape |

Artificial surface roughness can be classified as random or regular, with the roughness elements being either attached or integral. The final result may be strongly influenced by the manufacturing process (casting, forming, machining, or welding). Accordingly, it is not surprising that the literature on rough surfaces surpasses that for any other technique. Studies for water representing most of the possible types are included in Table 1. For each study cited the geometry which yielded the largest heat transfer coefficients is selected. It is noted that "convoluted" tubes are included in this classification. This is on the assumption that the en-

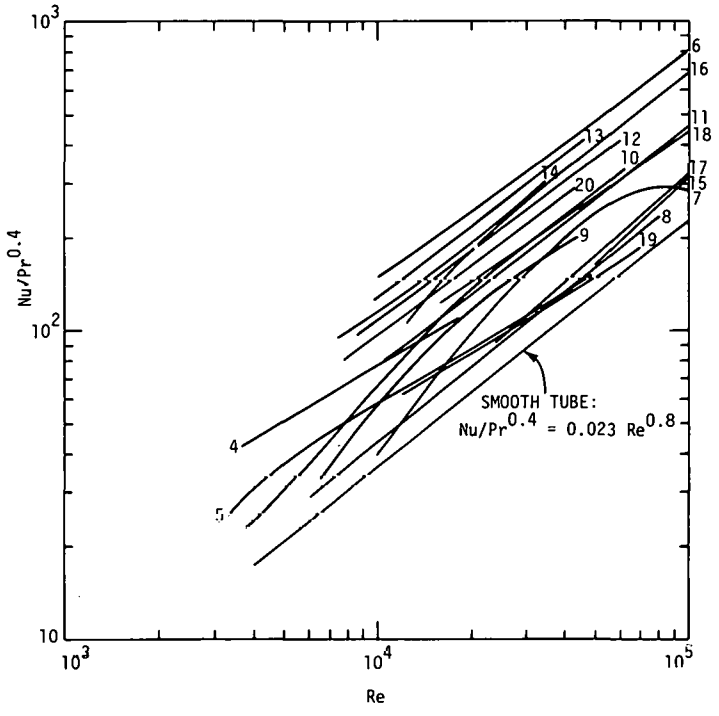



Fig. 1. Heat transfer data for tubes with various types of roughness.

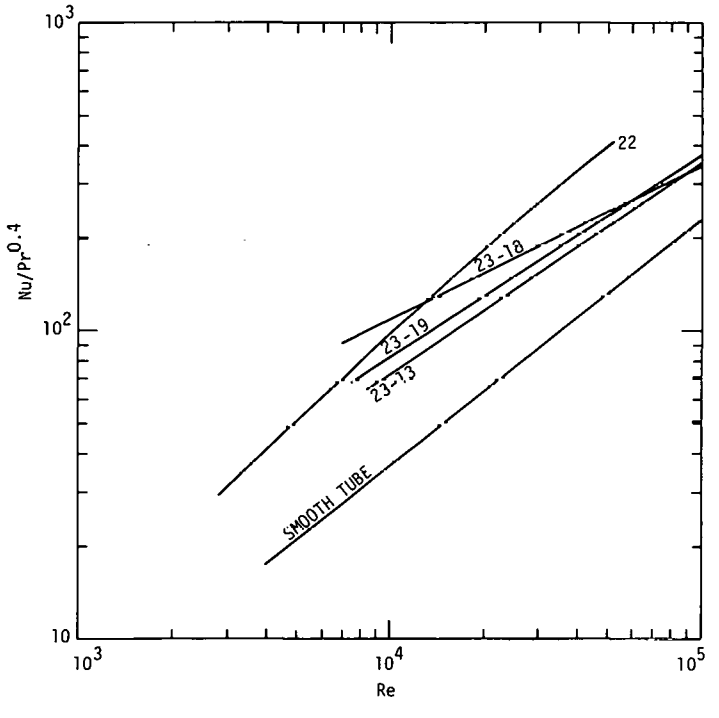



Fig. 3. Heat transfer data for internally finned tubes.

hancement is due primarily to flow over essentially transverse protuberances, rather than to the additional surface area or flow swirling.

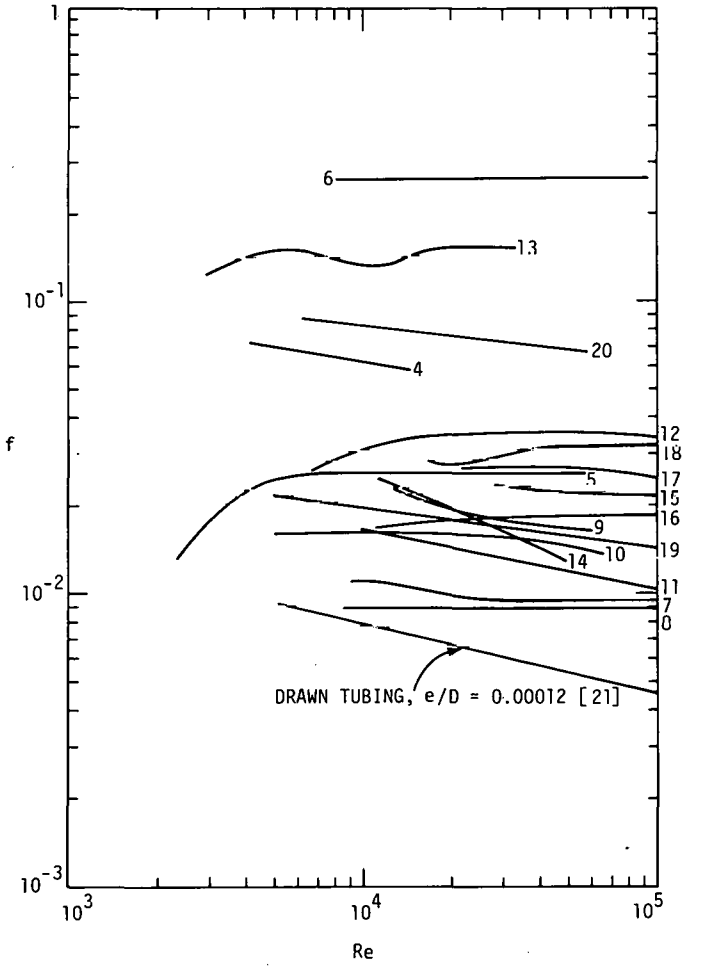



Fig. 2. Friction factor data for tubes with various types of roughness.

Rough surface behavior is indicated in Figs. 1 and 2. The data in these figures and subsequent figures are presented on a nominal basis, i.e., no allowance is made for increased surface area or cross-sectional area change due to roughness elements. The rather wide range of data is noteworthy, but it is of primary importance to note that improvements of several hundred percent in heat transfer coefficient can be obtained with different types of roughness. The accompanying increase in friction factor is generally much larger than the increase in heat transfer coefficient.

## Extended Surfaces

Tubes with internal surface extensions have been fabricated by machining of grooves, extrusion, brazing of strip inserts, and drawing-swaging operations. It is only recently that comprehensive studies have been conducted to determine the heat transfer and hydraulic characteristics of internally finned tubes with turbulent flow of water. The data selected for Table 2 include both straight and spiral fins.

The heat transfer results summarized in Fig. 3 in-

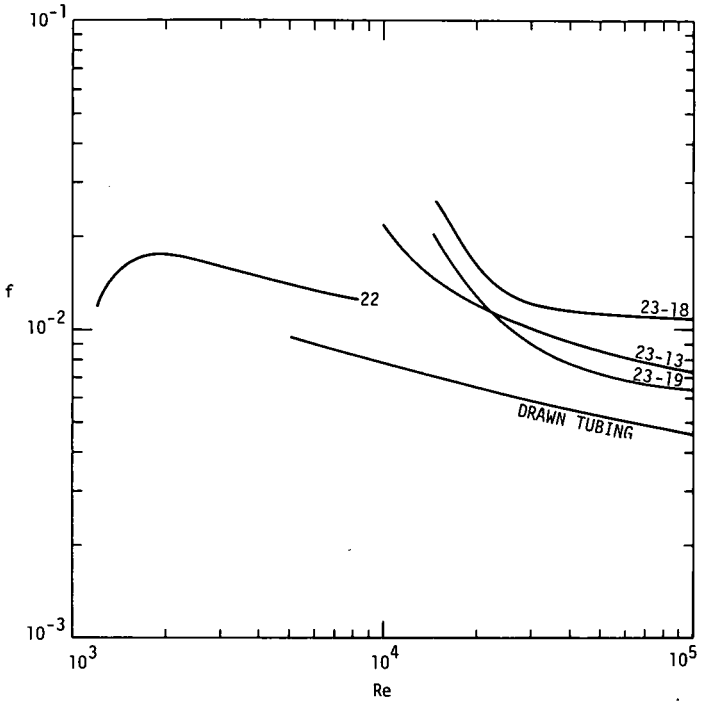



Fig. 4. Friction factor data for internally finned tubes.

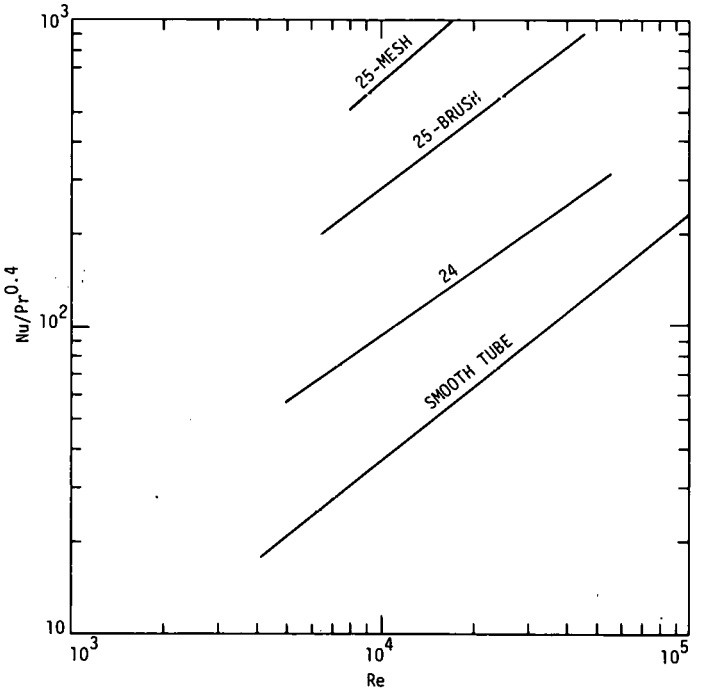



Fig. 5. Heat transfer data for tubes with several types of displaced enhancement devices.

dicate maximum improvements of about 200 percent. The friction data in Fig. 4 suggest increases of the same order. In general, the best performing tubes have spiralled fins and exhibit an enhancement well above that

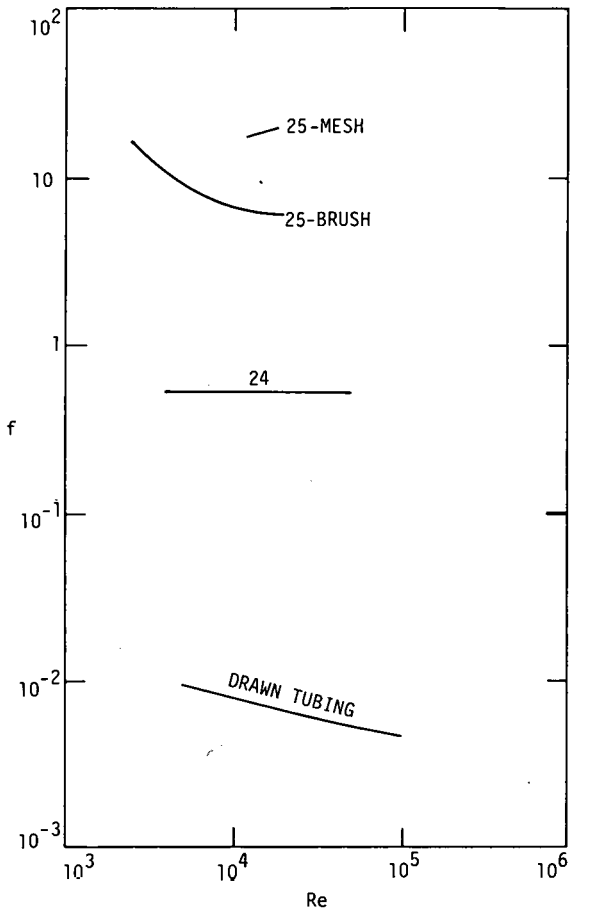



Fig. 6. Friction factor data for tubes with several types of displaced enhancement devices.

expected simply from the area increase. The spiralling apparently promotes flow separation in the manner of a transverse protuberance.

## Displaced Enhancement Devices

A rather wide variety of tube inserts fall into the category of displaced enhancement devices. The common characteristic is that flow in the vicinity of the heated surface is disturbed by a device not attached to the surface. These include the following types of inserts: core, mesh, brush, static mixer elements, rings, discs, and streamlined shapes. Data for water are somewhat limited as there has been little application of these inserts with liquids at high or even moderate velocities due to the large pressure drop. The data noted in Table 3 and in Figs. 5 and 6 represent three of the geometries noted above. The mesh tube data [25] are of at least academic interest as the heat transfer coefficients obtained are probably the highest ever observed for single-phase flow of water. Unfortunately, the friction factors for this insert are also extremely high. In general, the device which disturbs the flow also causes appreciable form drag in the main flow; hence, the pressure drop is quite large.

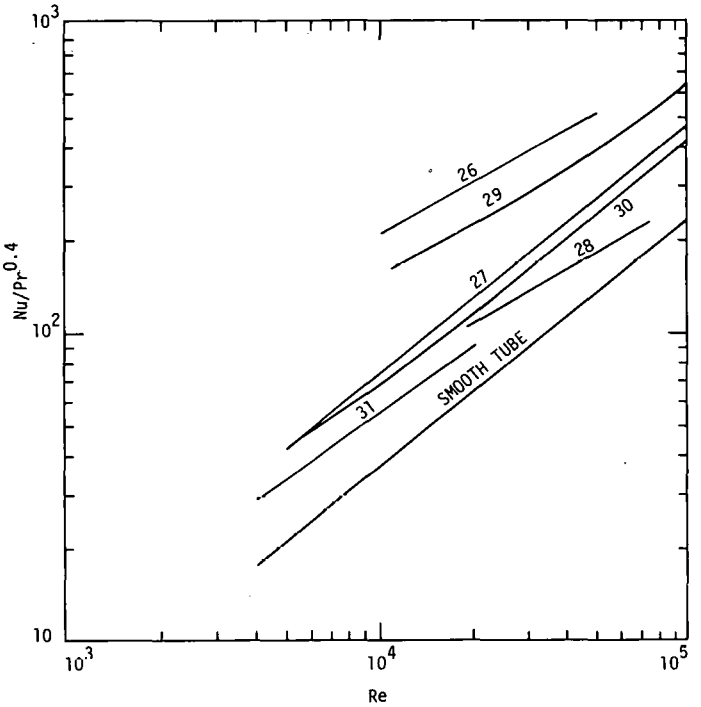



Fig. 7. Heat transfer data for tubes with twisted-tape inserts.

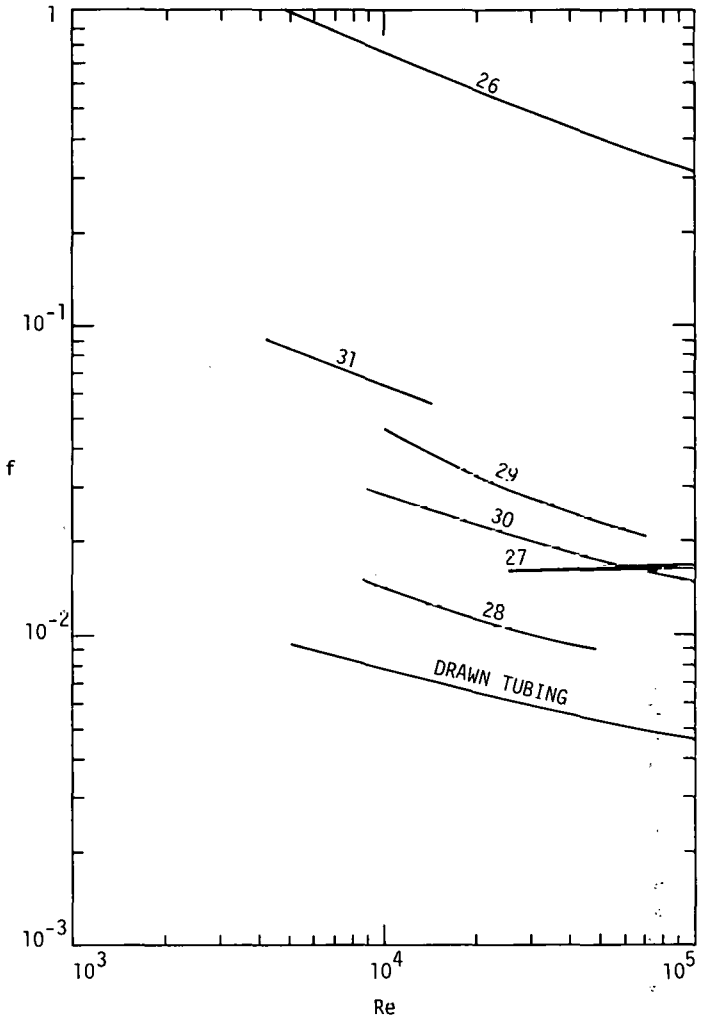



Fig. 8. Friction factor data for tubes with twisted-tape inserts.

## Swirl Flow Devices

Swirl flows may be produced by inlet vortex generators, periodically spaced propellers, and twisted-tape inserts. The simple twisted tape, which has been the subject of many investigations, dominates Table 4. The only exception is the axial core insert which permits twisting of a strip of metal to a smaller pitch than is possible with the usual tape insert. The enhanced heat transfer is due to several factors: increased path length of flow, secondary flow caused by flow over a curved surface, secondary flow induced by centrifugal force field, and fin effect of the tape. The coefficients presented in Fig. 7 indicate a maximum improvement of several hundred percent, and it is evident from Fig. 8 that the accompanying pressure drop increases are at least as large.

## Compound Techniques

The literature search yielded only several references to studies of two or more enhancement techniques operating simultaneously. The general expectation is that heat transfer will be improved beyond that observed with one of the individual techniques alone. An example of such a study is given in Reference 32 where swirl flow in a rough tube was studied. The heat transfer coefficient was increased as expected, and an additive correlation was developed. The increase in heat transfer coefficient is small, however, and further studies would be required to establish an optimum combination of roughness and tape twist ratio.

## Performance Evaluation of Enhanced Tubes

### Constant Flow Rate Comparison

A variety of measures of performance have been proposed in the literature [33-36]. If pumping power were of no concern, the heat transfer data alone (Figs. 1,3,5, 7) could be used to estimate the reduction in heat exchanger surface area made possible by enhancement. However, for the OTEC equipment, and indeed for most practical heat exchangers, it is necessary to consider both heat transfer and flow friction when selecting enhancement techniques.

### Constant Pumping Power Comparison

For the present problem it appears that the screening of tubes can be better accomplished by computing for each tube the performance criterion referred to in previous studies such as $R_S$ [33-35]. This factor denotes the area of the enhanced heat exchanger to that of the normal heat exchanger, subject to the constraints of constant heat duty and pumping power. Assumptions a

made similar to those noted for the previous criterion, the ratio is specified as

$$R_5 = \left(\frac{A_a}{A_o}\right)_{q,P,D,\bar{T},\Delta T_{\ell m},R_{ext} = 0} \quad (1)$$

By combining expressions for rate of heat transfer

$$q = hA\ \Delta T_{\ell m} \quad (2)$$

and pumping power

$$P = NV \frac{\pi D^2}{4} 4f \frac{L}{D} \frac{\rho V^2}{2g_o} \quad (3)$$

for both augmented and reference exchangers, the following relation is obtained:

$$\frac{A_a}{A_o} = \frac{h_o}{h_a} = \frac{V_o^3 f_o}{V_a^3 f_a} \quad (4)$$

In terms of dimensionless groups the desired area ratio is given by

$$\frac{A_a}{A_o} = \frac{Nu_o/Pr^{0.4}}{Nu_a/Pr^{0.4}} = \frac{Re_o^3 f_o}{Re_a^3 f_a} \quad (5)$$

Since Nusselt numbers and friction factors are available in terms of Reynolds numbers, $R_5$ can be readily obtained as a function of one of the Reynolds numbers. The usual method of solution is to use smooth tube heat transfer and friction factor correlations, e.g., $Nu_o/Pr^{0.4} = 0.023\ Re_o^{0.8}$ and $f_o = 0.046/Re_o^{0.2}$. By choosing $Re_a$, $f_a$ and $Nu_a/Pr^{0.4}$ can be picked off plots such as Figs. 1 and 2. Equation (3) is then solved for $Re_o$, and $A_a/A_o$ can be calculated.

An example of the application of this performance criterion is presented in Fig. 9. For the rough tubes it is apparent that the $R_5$ values extend over very wide ranges. In some cases the pressure drop is so high that the enhanced exchanger requires a larger area than the normal exchanger. The enhanced heat exchanger can have the area distributed in any convenient way as long as the NL product is maintained constant.

This potential reduction of 60 percent in heat exchanger area is very encouraging; however, the results must be interpreted with caution since the performance criterion still contains rather restrictive assumptions. In particular, the assumptions of constant log-mean temperature difference and zero external thermal resistance lead to an optimistic assessment of area reduction. Several alternate performance criteria are now examined.

## Other Comparisons

If the length scale of the heat exchanger is specified, the assumption of constant temperature difference can be relaxed. This condition has been referred to as $R_{5b}$ in previous studies [34,35]. The only conditions under which $R_5 \cong R_{5b}$ is at low NTU or effectiveness (NTU < 0.25). Since OTEC boilers and condensers are designed for low NTU to keep the required surface area from getting exorbitant, the present use of $R_5$ is a fair approximation, except for the fact that the external resistance is not taken into account.

By further specifying the external thermal resistance or the ratio of that resistance to the prime surface resistance, a still more realistic ratio can be obtained ($R_{5c}$). The fourth possibility, constant temperature difference but variable external resistance, has not been discussed in the literature.

One interesting criterion, referred to as $R_8$ previously, involves the area ratio at fixed heat duty, pumping power, and flow rate. $R_8$ is numerically equal to $R_5$; however, the additional constraint leads to a specified relation between length and number of tubes depending on the level of the flow rate. Case A suggested by Webb and Eckert [36] is equivalent to $R_8$, or more generally to $R_{8c}$.

In the absence of ammonia side enhancement, the external resistance is very important; therefore, it is best to turn to some typical OTEC heat exchanger calculations to get an accurate estimate of the potential for area reduction through use of enhancement. The calculations basically represent use of the extended performance evaluation criterion discussed in References 34 and 35.

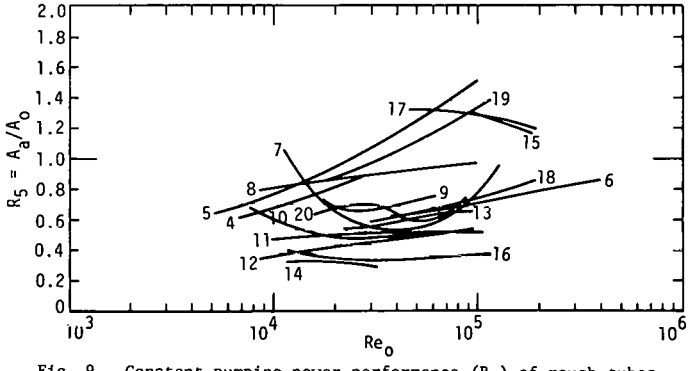



Fig. 9. Constant pumping power performance ($R_5$) of rough tubes.

## Effect of Enhancement on a Baseline OTEC Heat Exchanger

### Reference Exchanger

In order to refine the estimate of the maximum benefit of enhancement, it is necessary to consider as a reference exchanger an actual baseline heat exchanger. The unit chosen is similar to the shell-and-tube evap-

orator used in the Lockheed 160 $MW_e$, net, (4 units) power plants [37]. The design parameters are

$D_{out}$ = 2.0 in.

$t_w$ = 0.040 in.

material: aluminum, "as drawn" (e = 0.00006 in.), $k_w$ = 92 Btu/hr ft F.

$L_o$ = 55.23 ft

$N_o$ = 120,000

$V_o$ = 5.3 ft/sec

$T_{NH_3}$ = 72 F

$T_{H_2O,in}$ = 80 F

$(1/h)_f$ = 0.0003 hr $ft^2$F/Btu

$h_{NH_3}$ = 1500 Btu/hr $ft^2$F

Sea water properties (77 F): $\rho$ = 64.06 lbm/$ft^3$, $C_p$ = 0.94 Btu/lbm F, k = 0.340 Btu/hr ft F, $\mu$ = 2.32 lbm/hr ft

Using a standard correlation for single-phase heat transfer in tubes

$$Nu_o = 0.023\, Re_o^{0.8} Pr^{0.4} \qquad (6)$$

$h_o$ is calculated to be 897 Btu/hr $ft^2$F. The overall heat transfer coefficient is then calculated from

$$\frac{1}{U_{out,o}} = \frac{A_{out}}{h_o A} + \frac{A_{out}}{h_f A} + \frac{\ell n (D_{out}/D)\pi D_{out}}{2\pi k_w} + \frac{1}{h_{NH_3}} \qquad (7)$$

$$= .0011613 + 0.0003125 + 0.0000370 + 0.0006667$$

$$= 0.0021775 \text{ hr } ft^2\text{F/Btu}$$

$$U_{out,o} = 459 \text{ Btu/hr } ft^2\text{F}$$

The heat duty is then calculated from

$$q = C_{min}\Delta T_{in}(1 - e^{-NTU}) \qquad (8)$$

where

$$NTU = \frac{UA}{C_{min}} \qquad (9)$$

$$= 459 \times 3.47 \times 10^6/0.2772 \times 10^{10} = 0.575$$

$$q = 0.2772 \times 10^{10} \times 8 \times 0.437 = 9.69 \times 10^9 \text{ Bt}$$

This heat exchanger will now be used to test the effects of using various enhanced surfaces for which laboratory results are available.

Enhancement of Seawater Heat Transfer

Typical enhanced tubes were examined to demonstrate the effect of enhancement on the design of a heat exchanger which has the same heat duty and pumping power as the baseline exchanger described in the previous section.

Equation (7) is used in the following form:

$$\frac{1}{U_{out,a}} = \frac{A_{out}}{h_a A} + A_{out} R_{ext}$$

together with equations (8) and (9). Equation (3) completes the system of equations. As calculated in the previous section

$$q = 9.69 \times 10^9 \text{ Btu/hr}$$

and the pumping power is

$$P = 8.49 \times 10^9 \text{ ft lbf/hr}$$

The iterative solution procedure is conveniently carried out by fixing $N_a$, guessing $Re_a$, and calculating $L_a$ from both equations (3) and (8). When the two values of $L_a$ converge, that value of $L_a$ and $Re_a$ constitute the solution. The area ratio is then given by $N_a L_a / N_o L_o$.

The 2/10 repeated-rib roughness of Webb et al. [12] is used for example calculations as it stands high in the $R_5$ ranking derived from Fig. 9. This type of surface has been studied extensively, both experimentally and analytically. Computed values of $L_a/L_o$ and $A_a/A_o$ as functions of $N_a/N_o$ are given in Fig. 10. The curves clearly demonstrate that reduction of the surface area requires an increase in the number of tubes (frontal area). Assuming that shell diameter is proportional to the square root of N, doubling the diameter would permit a surface area reduction of 36 percent. The tubes would be only 16 percent as long.

The solutions are generally rather insensitive to velocity, i.e., $Re_a$ varies over a narrow range. This is a consequence of the significant effect of the external resistance. With a substantial enhancement, the water side contributes less to the overall resistance.

At large $N_a/N_o$, $A_a/A_o$ approaches a constant value as a result of the decrease in NTU to the point where $\epsilon \cong$ NTU. With the present constraints and large $h_a$, $\epsilon \cong$ NTU requires that $A_a/A_o$ be approximately constant.

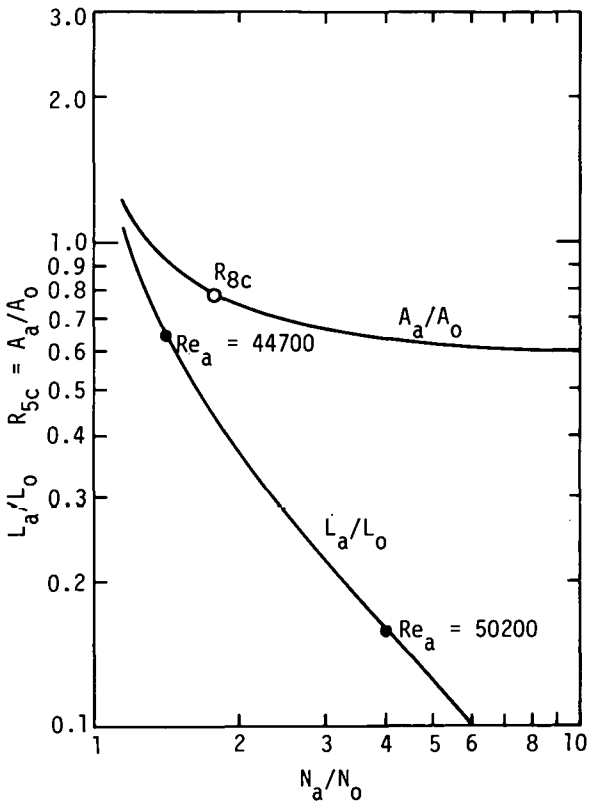



Fig. 10. Constant pumping power performance ($R_{5C}$ and $R_{8C}$) of a heat exchanger using tubes with repeated-rib roughness.

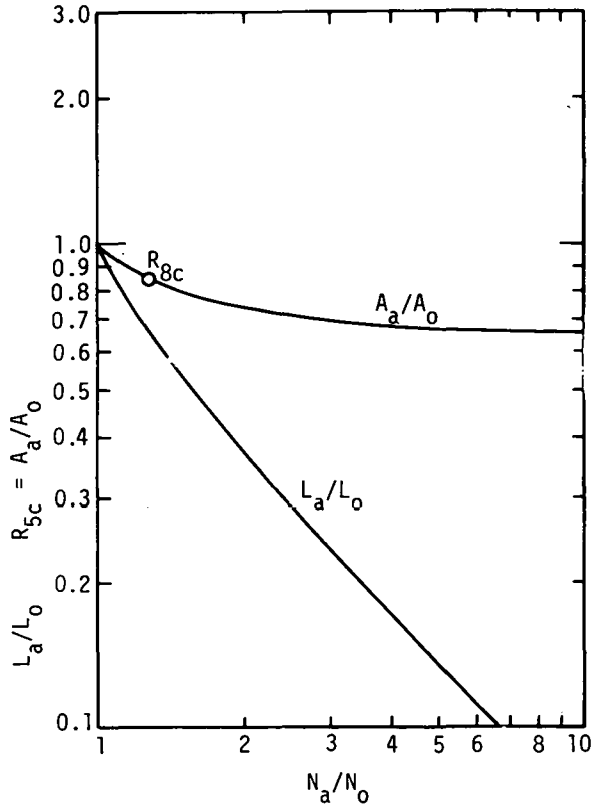



Fig. 11. Constant pumping power performance ($R_{5C}$ and $R_{8C}$) of a heat exchanger using internally finned tubes.

Figure 10 cannot be related directly to the $R_5$ values presented earlier since the reference heat exchanger has a moderately high NTU. In other words, the log-mean temperature difference varies considerably as the geometrical parameters are altered.

Included on Fig. 10 is the single point representing $R_{8c}$. For this criterion, flow rate is fixed ($2.949 \times 10^9$ lb/hr); hence, there is a unique solution to the set of equations.

Figure 11 presents the performance characteristics of an internally finned tube. $R_{8c}$ corresponds to a rather high value of $A_a/A_o$, suggesting that for this surface the constant flow rate assumption is overly restrictive.

The mesh tube is represented in Fig. 12. Obviously, this enhancement device should not be considered for an application of this type. It is important to note that the results shown in Fig. 3 were rather encouraging regarding this tube. The basic problem is that the extremely high friction factor requires that the augmented velocity be very low. The heat transfer coefficient, then, is little improved over the smooth tube value.

Figure 13 presents the data for a representative twisted-tape insert. The performance is generally similar to that for the rough tubes and the inner-fin tubes, as demonstrated in the composite plot of Fig. 14.

The general conclusion to be drawn from these calculations is that enhancement of the seawater side alone, by use of rough tubes, inner-fin tubes, or tubes with twisted-tape inserts, can reduce the heat exchanger surface area by about 30 percent at $N_a/N_o = 2$.

Enhanced Seawater and Ammonia Heat Transfer

As a final example of the benefits to be derived from use of enhancement techniques in OTEC heat exchangers, it is useful to consider enhancement of both seawater and ammonia heat transfer.

Without regard for the specific techniques which might be utilized, assume that the ammonia vaporization coefficient can be increased by 200 percent. The results of the performance calculation are shown in Fig. 15. The evaporator surface area can now be reduced by 50 percent at $N_a/N_o = 2$. With this potential for size (and cost) reduction, it is evident that serious consideration must be given to use of enhancement in OTEC heat exchangers.

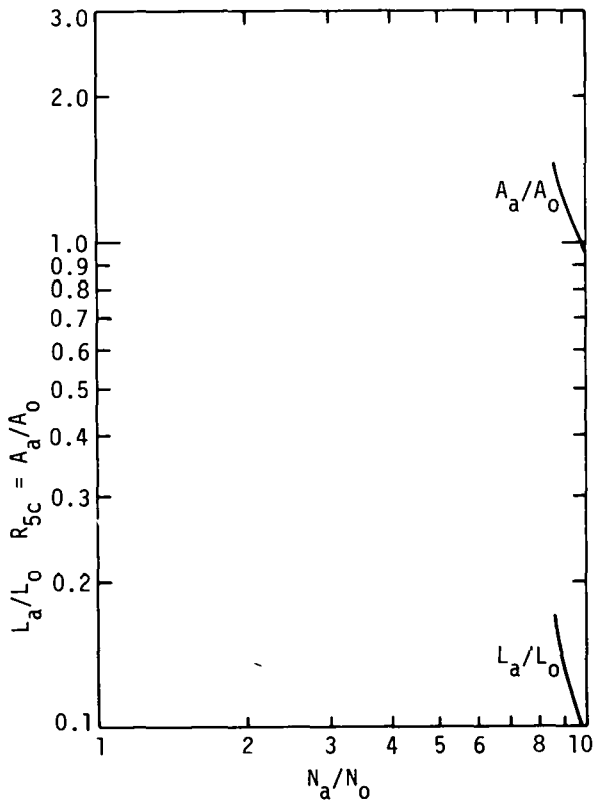



Fig. 12. Constant pumping power performance ($R_{5C}$ and $R_{8C}$) of a heat exchanger using tubes with a mesh insert.

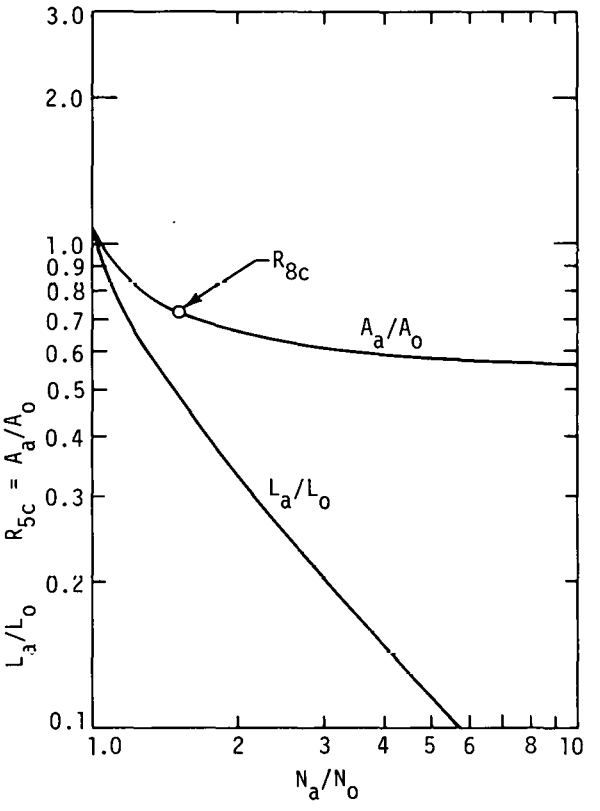



Fig. 13. Constant pumping power performance ($R_{5C}$ and $R_{8C}$) of a heat exchanger using tubes with a twisted-tape insert.

Selection of an Optimum Enhanced Surface

It is of interest to examine an enhanced surface for which considerable data are available, with the intent of specifying the optimum surface configuration. As noted previously, tubes with repeated-rib-roughness have been thoroughly investigated, both experimentally and analytically. Furthermore, it is probable that this type of tube can be manufactured commercially, at least with aluminum tubes. The ribs could be produced by rolling grooves on the exterior surface, as proposed by Soviet investigators [10] or by deforming the interior surface over a mandrel as done for a commercially available tube [38]. The procedure utilized by Webb et al. [12], painstakingly building up the tube from a stack of machined short cylinders, is not appropriate.

Webb and Eckert [36] have suggested a procedure for optimization of the roughness configuration to provide the minimum area augmented heat exchanger. Using general correlations developed in an earlier paper for the experimental results [12], a chart was prepared for $R_{8c}$ for p/e = 10, Pr = 10, $Re_o$ = 100,000, and $e^+$, the roughness Reynolds number, ranging from 15-25. The results were presented for other values of p/e; however, the expectation is that the results will not change appreciably with small changes in spacing. (Other studies have shown that the optimum spacing for transverse protuberance is about p/e = 10[1].) A minimum $R_{8c}$ occurs at $e^+ = 20$. An approximate solution for the desired roughness height is given for $e^+ = 20$ as $e/D = 37.4/Re^{0.83}$. Referring to Fig. 10, a probable value of the rough tube Reynolds number is 45,000. Hence, e/D = 0.005, and for D = 1.92 in., e = 0.01 in. It is expected that this surface would yield performance ratios more favorable than those of the 2/10 surface presented in Figs. 9 and 10 since that surface has e/D = 0.02.

The very small optimum protuberance is a consequence of the thin laminar sublayer. To avoid form drag or pressure loss in excess of that which represents heat transfer improvement, the protuberance must not extend too far beyond the laminar sublayer. While the small protuberance requires modest material deformation, it would appear that there could be severe problems from fouling. A slight fouling of the surface could obscure the protuberances and void the enhancement. No information is available on the biofouling of this type of roughened surface; however, it is anticipated that the experience would be similar to that for smooth tubes.

In the event that other types of enhanced tubes are desired, similar analyses can be performed to select the optimum geometry. In particular, sufficient results are

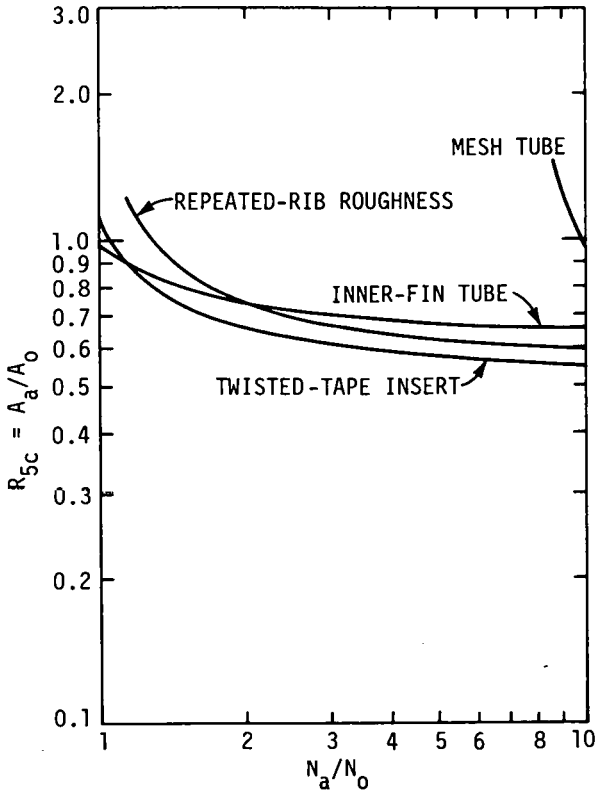



Fig. 14. Composite plots of constant pumping power performance ($R_{5C}$ and $R_{8C}$) of a heat exchanger using tubes with various enhancement techniques.

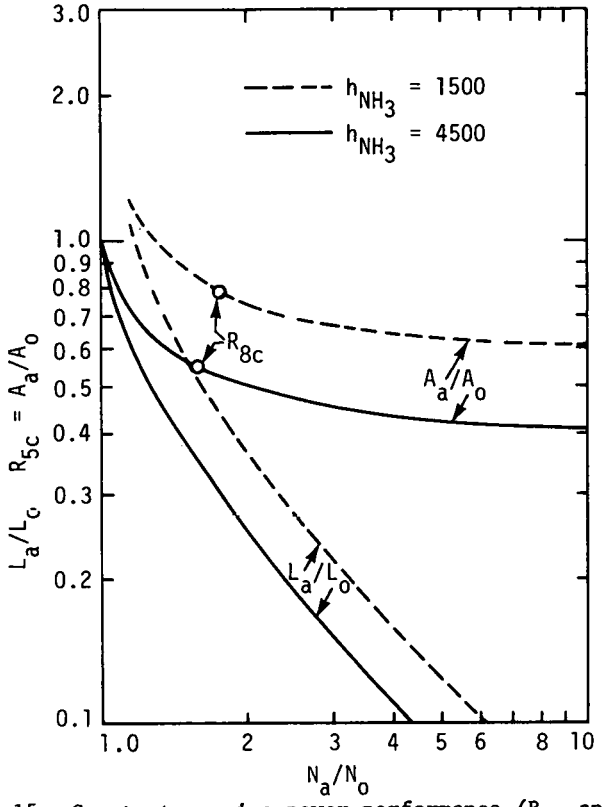



Fig. 15. Constant pumping power performance ($R_{5C}$ and $R_{8C}$) of a heat exchange using tubes with enhancement of both the sea water and ammonia heat transfer.

probably available to make the selection for internally finned tubes and tubes with twisted-tape inserts.

## Conclusions and Recommendations

This study has suggested a number of techniques which should be considered for enhancement of the seawater heat transfer coefficients in OTEC heat exchangers.

A computerized bibliography of heat transfer enhancement techniques has been utilized to provide data for a specific application. The search for single-phase, forced convection enhancement studies yielded 367 references for the four practical techniques specified. Most of the studies for turbulent flow of water flowing inside circular tubes were considered and the configuration was chosen which gave the highest heat transfer coefficients. The data for heat transfer coefficient and friction factor are presented on a nominal basis for convenient comparison with conventional smooth tube correlations.

For each of the techniques--rough surfaces, extended surfaces, displaced enhancement devices, and swirl flow devices--it is possible to find test data which indicate at least several hundred percent increase in the heat transfer coefficient over the smooth tube value at constant flow rate.

The constraint of constant pumping power is suggested as being most appropriate for OTEC heat exchangers. The representative data are given a screening using a performance evaluation criterion based on constant pumping power. Enhancement techniques which fare the best on this test were employed in heat exchanger design calculations. These calculations of "extended performance evaluation criteria" indicate that tubes with repeated-rib roughness, internal fins, or twisted-tape inserts can reduce required heat exchanger surface area by 30 percent. If the average heat transfer coefficient for evaporating ammonia can also be increased by 200 percent, the surface area can be reduced by 50 percent. It is recognized, however, that the enhanced tubes will cost more.

While the repeated-rib roughness can be optimized to yield outstanding performance, the optimum protuberance height for probable OTEC conditions is only 0.01 in. A small biofouling deposit could destroy the effect of such roughness elements.

Rough tubes (particularly those with repeated ribs or spiral protuberances), internally finned tubes, and tubes with twisted-tape inserts should be considered for enhancement of seawater heat transfer in OTEC heat exchangers. The data summarized in this report can be used directly in optimization studies of the complete system, e.g. [39]. It is recommended, however, that additional

tests be conducted which are more nearly similar to expected OTEC conditions. Specifically, the following tests should be considered: tests of large diameter tubes (assuming that system optimization studies continue to call for tubes of large diameter), tests under cooling conditions (for the condenser), and tests with biofouling.

While these tests are important, caution should be exercised in relying too heavily on "separate effects" tests. It will be difficult to assure uniform flow distribution in the very large heat exchangers. The most concern has been directed toward the two-phase streams; however, it should be noted that uniform flow of seawater inside a bundle of over 100,000 tubes may require special baffling or orificing arrangements since the frictional pressure drop in the tubes is quite small.

## Nomenclature

| | |
|---|---|
| $A$ | nominal heat exchanger surface area, $N\pi DL$ |
| $C_{min}$ | capacity rate, $wC_p$ |
| $C_p$ | specific heat at constant pressure |
| $D$ | nominal tube diameter; diameter of wire coil insert |
| $d$ | tube diameter |
| $e$ | protuberance height |
| $e^+$ | roughness Reynolds number, $(e/D)Re\sqrt{f/2}$ |
| $f$ | Fanning friction factor |
| $g_o$ | gravitational conversion factor |
| $H$ | spacing of wire coil insert; pitch of twisted tape |
| $h$ | heat transfer coefficient |
| $k$ | thermal conductivity of fluid |
| $k_w$ | thermal conductivity of tube wall |
| $L$ | protuberance spacing; tube length |
| $N$ | number of tubes |
| $P$ | pumping power |
| $p$ | rib spacing |
| $q$ | rate of heat transfer |
| $R$ | performance evaluation criterion |
| $R_{ext}$ | thermal resistance external to heat transfer surface being enhanced |
| $S$ | spacing of tube inserts |
| $\bar{T}$ | average fluid temperature |
| $t_w$ | tube wall thickness |
| $\Delta T_{in}$ | temperature difference between entering streams |
| $\Delta T_{lm}$ | logarithmic mean temperature difference |
| $U$ | overall coefficient of heat transfer |
| $V$ | average flow velocity |
| $w$ | mass flow rate |
| $y$ | tube diameters per $180^o$ tape twist |
| $\epsilon$ | heat exchanger effectiveness |
| $\mu$ | dynamic viscosity |
| $\rho$ | density of fluid |
| NTU | number of transfer units, $UA/C_{min}$ |
| Nu | Nusselt number, $hD/k$ |
| Pr | Prandtl number, $C_p\mu/k$ |
| Rc | Reynolds number, $\rho VD/\mu$ |

### Subscripts

| | |
|---|---|
| a | denotes enhanced heat exchanger |
| f | denotes fouling conditions |
| in | denotes entering fluid condition |
| o | denotes normal heat exchanger |
| out | denotes condition at outside tube wall |

## References


1. Bergles, A. E., "Survey and Evaluation of Techniques to Augment Convective Heat and Mass Transfer," in Progress in Heat and Mass Transfer, Vol. 1, Pergamon Press, 1969, pp. 331-424.

2. Bergles, A. E., "Recent Developments in Convective Heat Transfer Augmentation," Applied Mechanics Reviews, Vol. 26, 1973, pp. 675-682.

3. Jordan, J. R., Sun, R. P. and Maple, C. G., "Operation and Maintenance of the Rare-Earth Information Center's Information Retrieval System (RICIRS)," USAEC Report IS-3388, July 1974.

4. Nagaoka, Z. and Watanabe, A., "Maximum Rate of Heat Transfer with Minimum Loss of Energy," Proceedings 7th International Congress on Refrigeration, Vol. 3, 1936, pp. 221-245.

5. Cope, W. F., "The Friction and Heat Transmission Coefficients of Rough Pipes," Proceedings Institution of Mechanical Engineers, Vol. 145, 1941, pp. 99-105.

6. Savage, D. W. and Myers, J. E., "The Effect of Artificial Surface Roughness on Heat and Momentum Transfer," American Institute of Chemical Engineers Journal, Vol. 9, 1963, pp. 694-702.

7. Kolar, V., "Heat Transfer in Turbulent Flow of Fluids through Smooth and Rough Tubes," International Journal of Heat and Mass Transfer, Vol. 8, 1965, pp. 639-653.

8. Zajic, V., "Some Results on Research of Intensified Water Cooling by Roughened Surfaces and Surface Boiling at High Heat Flux Rates," ACTA Technica CSAV No. 5, 1965, pp. 602-612.

9. Gowen, R. A., "A Study of Forced Convection Heat Transfer from Smooth and Rough Surfaces," Ph.D. thesis in Chemical Engineering and Applied Chemistry, University of Toronto, 1967.

10. Kalinin, E. K., Dreitser, G. A. and Yarkho, S. A., "Experimental Study of Heat Transfer Intensification under Condition of Forced Flow in Channels," Japan Society of Mechanical Engineers 1967 Semi-International Symposium. September 1967, Paper 210.

11. Eissenberg, D., "Tests of an Enhanced Horizontal Tube Condenser under Conditions of Horizontal Steam Cross Flow," Heat Transfer 1970, Vol. I, Paper HE2.1, Elsevier Publishing Company, Amsterdam, 1970.

12. Webb, R. L., Eckert, E. R. G. and Goldstein, R. J., "Heat Transfer and Friction in Tubes with Repeated-Rib Roughness," International Journal of Heat and Mass Transfer, Vol. 14, 1971, pp. 601-618.

13. Kramer, J. M. and Gater, R. A., "Pressure Loss and Heat Transfer for Non-Boiling Fluid Flow in Convoluted Tubing," American Society of Mechanical Engineers Paper No. 73-HT-23, 1973.

14. Grass, G., "Verbesserung der Waermeuebertragung an Wasser Durch Kuenstliche Aufrauhung der Oberflaechen in Reaktoren Waermetauschern," Atomkernenergie, Vol. 3, 1958, pp. 328-331.

15. Blumenkrantz, A. and Taborek, J., "Heat Transfer and Pressure Drop Characteristics of Turbotec Spirally Grooved Tubes in the Turbulent Regime," Heat Transfer Research Inc., Report 2439-300-7, 1970.

16. Dipprey, D. G. and Sabersky, R. H., "Heat and Momentum Transfer in Smooth and Rough Tubes at Various Prandtl Numbers," Jet Propulsion Laboratory, Technical Report No. 32-269, June 1962. International Journal of Heat and Mass Transfer, Vol. 6, 1963, pp. 329-353.

17. Blumenkrantz, A., Yarden, A. and Taborek, J., "Performance Prediction and Evaluation of Phelps Dodge Spirally Grooved Tubes. Inside Tube Flow Pressure Drop and Heat Transfer in Turbulent Regime," Heat Transfer Research Inc., Report 2439-300-4, 1969.

18. Brouillette, E. C., Mifflin, T. R. and Myers, J. E., "Heat Transfer and Pressure Drop Characteristics of Internal Finned Tubes," American Society of Mechanical Engineers Paper No. 57-A-47, 1957.

19. Smith, J. W., Gowan, R. A. and Charles, M. E., "Turbulent Heat Transfer and Temperature Profiles in a Rifled Pipe," Chemical Engineering Science, Vol. 23, 1968, pp. 751-758.

20. Kumar, P. and Judd, R. L., "Heat Transfer with Coiled Wire Turbulence Promoters," Canadian Journal of Chemical Engineering, Vol. 8, 1970, pp. 378-383.

21. Anonymous, "Pipe Friction Manual," Hydraulic Institute, New York, New York, 1954, pp. 61-62.

22. Bergles, A. E., Brown, Jr., G. S. and Snider, W. D., "Heat Transfer Performance of Internally Finned Tubes," American Society of Mechanical Engineers Paper No. 71-HT-31, 1971.

23. Watkinson, A. P., Miletti, D. L. and Tarassof, P., "Turbulent Heat Transfer and Pressure Drop in Internally Finned Tubes," American Institute of Chemical Engineers Symposium Series, Vol. 69, No. 131, 1973, pp. 94-103.

24. Evans, L. B., "The Effects of Axial Turbulence Promoters on Heat Transfer and Pressure Drop Inside a Tube," Ph.D. Thesis in Chemical Engineering, University of Michigan, 1962.

25. Megerlin, F. E., Murphy, R. W. and Bergles, A. E., "Augmentation of Heat Transfer in Tubes by Means of Mesh and Brush Inserts," Journal of Heat Transfer, Vol. 96, 1974, pp. 145-151.

26. Gambill, W. R. and Bundy, R. D., "An Evaluation of the Present Status of Swirl Flow Heat Transfer," Oak Ridge National Laboratory Report ORNL 61-461, 1961. American Society of Mechanical Engineers, Paper No. 62-HT-42, 1962.

27. Gambill, W. R., Bundy, R. D. and Wansbrough, R. W., "Heat Transfer, Burnout, and Pressure Drop for Water in Swirl Flow Tubes with Twisted Tapes," Chemical Engineering Progress Symposium Series, Vol. 57, No. 32, 1961, pp. 127-137.

28. Ibragimov, M. H., Nomofelov, E. V. and Subbotin, V. I., "Heat Transfer and Hydraulic Resistance with the Swirl-Type Motion of Liquid in Pipes," Teploenergetika, Vol. 8, No. 7, 1961, pp. 57-60.

29. Smithberg, E. and Landis, F., "Friction and Forced Convection Heat Transfer Characteristics in Tubes with Twisted Tape Swirl Generators," Journal of Heat Transfer, Vol. 86, 1964, pp. 39-49.

30. Lopina, R. F. and Bergles, A. E., "Heat Transfer and Pressure Drop in Tape Generated Swirl Flow of Single-Phase Water," Journal of Heat Transfer, Vol. 91, 1969, pp. 434-442.

31. Nagaoka, Z. and Watanabe, A., "Maximum Rate of Heat Transfer with Minimum Loss of Energy," Proceedings 7th International Congress on Refrigeration, Vol. 3, 1936, pp. 221-245.

32. Bergles, A. E., Lee, R. A. and Mikic, B. B., "Heat Transfer in Rough Tubes with Tape-Generated Swirl Flow," Journal of Heat Transfer, Vol. 91, 1969, pp. 443-445.

33. Bergles, A. E., Blumenkrantz, A. R. and Taborek, J., "Performance Evaluation Criteria for Enhanced Heat Transfer Surfaces," Heat Transfer 1974, Vol. II, The Japan Society of Mechanical Engineers, 1974, pp. 234-238.

34. Bergles, A. E., Bunn, R. L. and Junkhan, G. H., "Extended Performance Evaluation Criteria for Enhanced Heat Transfer Surfaces," Letters in Heat and Mass Transfer, Vol. 1, 1974, pp. 113-119.

35. Bergles, A. E., Junkhan, G. H. and Bunn, R. L., "Performance Criteria for Cooling Systems on Agricultural and Industrial Machines," HTL-6, ISU-ERI-Ames 74267, December 1974, PB 246 418.

36. Webb, R. L. and Eckert, E. R. G., "Application of Rough Surfaces to Heat Exchanger Design," International Journal of Heat and Mass Transfer, Vol. 15, 1972, pp. 1647-1658.

37. Trimble, L. C., Messinger, B. L., Ulbrich, H. E., Smith, G. and Lin, T. Y., "Ocean Thermal Energy Conversion System Study Report," Proceedings, Third Workshop on Ocean Thermal Energy Conversion (OTEC), APL/JHU SR 75-2, August 1975, pp. 3-21.

38. Wolverine Division UOP, Inc., "Type S/T Turbo-Chil$^{R}$ Finned Tube," Product Bulletin HPE 5M 2/76.

39. Lyon, R., "An Outline for Optimizing and Evaluating OTEC Systems," paper presented at the 1977 Ocean Thermal Energy Conversion Conference, New Orleans, March 1977.

CONF-770331--3

# THE OTEC PROGRAM AT CARNEGIE-MELLON UNIVERSITY HEAT TRANSFER RESEARCH AND POWER CYCLE TRANSIENT MODELING

ROBERT R. ROTHFUS AND CHARLES P. NEUMAN
*Carnegie Institute of Technology*
*Carnegie-Mellon University*
*Pittsburgh, Pennsylvania*

Abstract

Results of experiments on falling film, fluted, vertical tube heat transfer surfaces are reported. It is found that flutes enhance the heat transfer coefficient far in excess of what might be expected from increased surface. Data for refrigerant 11 and ammonia are presented.

Fine axial flutes on the water side seem to increase the heat transfer coefficient and the pressure drop in proportion to the increase of surface brought about by the flutes. It is concluded therefore that enhancement on the water side can result in a substantial reduction in heat transfer surface requirements and so also a reduction in volume for OTEC heat exchangers.

Finally, analytical models for the transient behavior of OTEC power cycle components are exhibited. These models form the basis for control system design and operational strategies for OTEC.

## Introduction

The heat exchangers of an OTEC system are large and costly. One approach to reducing the cost is to diminish the size by enhancing heat transfer. The essential problem is to design a unit which will yield acceptably high heat transfer under low temperature potential with minimal parasitic power loss.

One interesting design alternative is the vertical shell-and-tube type of exchanger with seawater flowing inside the tubes and working-fluid flowing layer-wise under gravity down the outside surfaces. Both the inner and outer surfaces of the tubes contain fine axial flutes to enhance the heat transfer. Fig. 1 illustrates the essential elements of such an exchanger as they might appear in a conventional unit. When the exchanger is operated as an evaporator, liquid working fluid is supplied to the plenum out of which it flows through apertures onto the exterior surface of each tube. Unevaporated liquid is recycled from the bottom of the tubes back to the supply plenum where it is joined by make-up liquid.

An evaporator-condenser combination rated at 1 $MW_t$ such as is shown in Fig. 1† has been designed by CMU for testing at Argonne National Laboratory. In order to extend the general design concept to much larger OTEC exchangers, work in several pertinent areas of heat transfer and fluid flow is continuing on the laboratory scale. The current related projects at CMU are summarized in Table 1. Basically, they address the steady-state and time-dependent aspects of heat transfer and of the distributed movement of fluids in, out and through typical components of the very large exchangers projected for OTEC use.

The matter of enhanced heat transfer is central to the conceptual design. Substantial reduction in the size of the evaporator or condenser can be anticipated when r e enhancement is attained on both the water side and working-fluid side of the heat transfer area. Axial flutes afford means of enhancement through macroscopic alteration of the surface on each side. The experimental work reported here deals with enhancement by flutes under typical OTEC conditions involving typical OTEC fluids. The working-fluid data cover evaporation and condensation of R-11 and ammonia. The water-side data include both heat transfer and fluid friction in single-phase flow.

Table 1. Current CMU OTEC Projects

| | |
|---|---|
| 1. | Working-fluid side heat transfer experiments. |
| 2. | Water side heat transfer experiments. |
| 3. | Transient and steady-state modeling, simulation, and control system design of the complete OTEC power cycle. |
| 4. | Working-fluid liquid distribution experiments. |
| 5. | Pressure drop in $NH_3$ vapor experiments. |
| 6. | Water distribution system design. |
| 7. | Erosion of flutes and joints experiments. |

## Working-Fluid-Side Heat Transfer

The use of axial flutes to improve heat transfer in thin liquid layers is not new. Early work (Gregorig, 1959) applied the idea to laminar condensate films. It remained, however, for a study at ORNL (Alexander and Hoffman, 1971) to make possible a quantitative evaluation of the effect of the mode of liquid flow on the heat transfer coefficient. The coefficient was found to attain a local maximum in the range of laminar-turbulent transition (Zener, 1974). The same seemed to be true for both evaporators and condensers.

† Figures are presented at end of paper, beginning 3B-1-11.

Alexander and Hoffman suggested that enhancement is largely the result of naturally occurring waves which intermittently lave the crests of the flutes as shown in Fig. 2. When the trough between waves passes by, surface tension dries the crest of the flute by pulling the liquid into the rill, thus producing a higher heat transfer coefficient, on the average, than can be attained on a flat surface at the same mass rate of flow. That picture is consistent with observations (McLeod, 1951; Belkin, 1953) that transitional waves are large and frequent. The waves contain disturbance eddies but the troughs are in pseudo-laminar flow, a combination which appears to maximize the net heat transfer coefficient. The objectives of the CMU experimental program are to determine whether the ORNL results apply to OTEC working fluids and operating conditions (Rothfus and Neuman, 1977).

## Experimental Study

An experimental unit has been constructed as shown schematically in Fig. 3 with a single-tube evaporator and a single-tube condenser in parallel. A detailed description of the apparatus is given in Technical Report No. COO/2641-4. One of the vertical tubes is fluted, the other is smooth. Either can be the evaporator in a given experiment while the other can be the condenser. Thus, a single run produces data on the smooth evaporator and fluted condenser or on the fluted evaporator and smooth condenser, depending on which side of the unit is heated or cooled. To replicate OTEC conditions, a difference of about 20°F is maintained between the inlet temperatures of the hot and cold water when testing ammonia. Typical inlet temperatures for such runs are 38°F to the condenser and 58°F to the evaporator.

The smooth tube is an aluminum 1-inch, 16 BWG tube (OD = 1.000 inch, ID - 0.870 inch). The fluted tube is the companion piece, but with 26-mil, constant-radius flutes on its outer surface only. The external flutes are essentially as is shown in Fig. 4 with $d = D =$ 26 mils and $\lambda = 0$ . Such flutes have a fluted-to-smooth surface area of 1.57 in theory, but slight flattening of the crests causes an observed area ratio of ~1.50.

Experiments have been run on R-11 and ammonia. Attention has been centered on the upper-laminar and transitional regimes of flow. It is important to recognize the nature of the experimental heat transfer coefficients. Only a small fraction of the liquid fed to the top of the test section was normally evaporated or condensed. Consequently, the mass flow rate (and the Reynolds number) of the liquid layer did not change much over the length of the test section. The heat transfer coefficient was therefore identifiable with a particular Reynolds number. In this sense, it is a "local" quantity.

## Smooth-Tube

As shown in Fig. 5, the smooth-tube condenser behaves in the normal way. In the laminar range, the coefficients are predictable from Nusselt's classical theory (Nusselt, 1916) and the R-11 and ammonia data are drawn together by normalizing the heat transfer coefficients on the quantity $\phi = \left(k^3\rho^2 g/\mu^2\right)^{1/3}$ in the usual way. The smooth-tube evaporator exhibits the expected dependence on Reynolds number as shown in Fig. 5. However, the coefficients are about twice those of the smooth condenser. No reason for the difference has been uncovered in either the present experiments or the open literature. Whatever the reason, the behaviors of R-11 and ammonia are consistent, since both sets of data are drawn together by means of the $\phi$-factor normalization.

## Fluted-Tube

As shown in Fig. 6, the fluted-tube condenser exhibits an enhanced heat transfer coefficient. In the laminar region, the fluted-tube coefficients are about 2.8 times those of the smooth tube. Since the area ratio is only 1.5, this suggests a considerable fluid-mechanical contribution to the enhancement. (Heat transfer coefficients reported here are based on the area of the smooth tube having the same nominal diameter.) As expected, a local maximum is reached at a Reynolds number of about 1500, but it is a shallow one, increasing the coefficient by only about 20 per cent. The R-11 and ammonia data are again correlated through the $\phi$-factor.

As shown in Fig. 6, the fluted evaporator exhibits the greatest dependence on Reynolds number. Up to a Reynolds number of about 400, the fluted tube has lower coefficients than the comparable smooth tube. This is largely due to the fact that at low flow rates the liquid does not wash the crests of the flutes. (Unlike the condenser, the evaporator has no way of wetting the crests except by liquid motion.) The coefficient rises steeply with increased Reynolds number, reaching a peak at a Reynolds number of about 3200. The peak, best seen in the R-11 data, is confirmed by other points not included in the graph. The R-11 and ammonia data are correlated reasonably well by means of the $\phi$-factor.

## Conclusions

a. Heat Transfer in non-aqueous liquid layers can be sharply enhanced by fine axial flutes. Enhancement factors of 3 to 5 have been demonstrated.

b. As in aqueous systems, the heat transfer coefficient goes through a local maximum in the range of laminar-turbulent transition. Fluted-tube evaporators and condensers differ in their dependence on Reynolds number, but in both cases, the degree of enhancement is large enough to suggest a substantial fluid-mechanical contribution.

c. To the extent suitable for most design purposes, data on R-11 and ammonia can be drawn together by the ordinary $\phi$-factor normalization of the heat transfer coefficient.

These conclusions are based on results obtained from one style and one size of flute, namely a constant-radius flute of 26-mil height. It remains for current experiments with other styles and sizes to show whether the conclusions can be generalized.

## Water-Side Heat Transfer

Seawater velocities in OTEC heat exchangers are ... to be in the range of 4 to 8 ft per second. With ammonia as the working fluid, enhancement on the ammonia side (as by flutes) puts the major resistance to heat transfer on the water side at these velocities. Enhancement on the water side therefore becomes essential. Two features of water-side enhancement are recognizable. First, the degree of enhancement must be considerable in order to match that on the ammonia side. Second, enhancement must be accomplished with no more than about an equal percentage increase of friction in order to maintain favorable economics.

The present work addresses the following questions:

a. At what water velocity do the flutes become fully effective?

b. How is that velocity (or Reynolds number) related to the size and style of the flutes?

## Experimental Study

To answer these questions, a horizontal, single-tube heater has been constructed as shown schematically in Fig. 7. The test section, 8 ft long, is heated electrically by means of external tapes to the level of 0.8 to 1.5 kilowatts. Insulation makes losses negligible. Thermistors or thermocouples measure inlet and outlet water temperatures and 5 wall temperatures along the length of the test sections. Pressure drops are measured by means of manometers. The test liquid is recirculated tap water flowing at a steady, volumetrically-measured rate.

To establish the basis of comparison between smooth and fluted tubes, data were first obtained on a smooth, 1-inch, 16 BWG, aluminum tube. The fluted tube contained internal, constant-radius flutes of 26-mil height. It was rolled and welded. Allowing for the bead, the fluted-to-smooth area ratio was found to be 1.50 rather than 1.57 as theoretically required by constant-radius flutes. Two other aluminum fluted tubes were tested. They were extruded, seamless tubes of nominal 1-inch size containing internal, constant-radius flutes of 45-mil and 60-mil height. In both tubes, the fluted-to-smooth area ratio was 1.57. The description of the flute is shown in Fig. 4.

The flutes already tested or currently under test at CMU can be described in terms of three parameters:

a. The fluted-to-smooth area ratio (AR).

b. The flute height ($\Delta$) in mils.

c. The ratio of height to rill diameter ($\Delta/D$).

As shown in Fig. 4, the diameter of the crest is d, the diameter of the rill is D, and the tangent (straight portion) connecting the crest and rill is $\lambda$. It follows that

$$\frac{\Delta}{D} = \frac{\lambda}{D} + \frac{1}{2}\left(1 + \frac{d}{D}\right)$$

and

$$AR = \left(\frac{\pi}{2} - 1\right) + 2\left[\frac{\Delta/D}{1+(d/D)}\right]$$

The flute design can therefore be identified through the code (AR-$\Delta$-$\Delta$/D). AR and $\Delta/D$ establish the crest-to-rill diameter ratio d/D and in turn the ratio $\lambda/D$. The absolute flute height $\Delta$ then sets all the other dimensions. Table 2 identifies the flutes in the current scheme of research at CMU.

Table 2. Inside Fluted Tubes

| $\Delta$ (mils) \ AR | 1.57 | | 2. |
|---|---|---|---|
| 26 | 1 | | |
| 45 | 1 | 1.5 | 1.5 |
| 60 | 1 | 1.5 | 1.5 |

The Fanning friction factors for tubes (1.57-45-1.0) and (1.57-60-1.0) are compared in Figure 8. Any difference is confined to the low turbulent range. At Reynolds numbers greater than 13,000 (corresponding to a water velocity of about 2-1/2 ft/sec) the results are indistinguishable. As the Reynolds number increases, the friction factor moves from somewhat above to somewhat below the enhancement corresponding to the area ratio of 1.57. On the average, the flutes are fully effective with respect to friction over the whole Reynolds number range of interest.

Fig. 9 shows the comparison of Fanning friction factors for tubes (1.57-26-1.0) and (1.57-60-1.0). The friction factors for the lower flute height reach the degree of enhancement equal to the area ratio at a Reynolds number of about 32,000 (corresponding to a water velocity of about 6-1/2 ft/sec) while those for the higher flute height are up to the area-ratio level of enhancement over the whole Reynolds number range investigated.

Heat transfer data for the same tubes (1.57-26-1.0) and (1.57-60-1.0) are compared in Fig. 10. The j-factors for the lower flute height reach the area-ratio level at a Reynolds number of about 18,000 (corresponding to a water velocity of about 3-1/2 ft/sec) while those for the higher flute height are up to the area-ratio level of enhancement over the whole Reynolds number range investigated. The comparable smooth tube follows the Sieder and Tate equation (Sieder and Tate, 1936).

On the whole, these results are consistent with the simple-minded notion that the flute must "poke its head" above the equivalent momentum or thermal "film" before it is felt by the fluid. Likewise, it can be imagined that the flute becomes fully effective when its height exceeds the equivalent "film" thickness by a fixed percentage. This view of the flute behavior is described more fully in CMU Technical Report COO/2641-4.

## Conclusions

a. Both heat transfer coefficients and friction factors are increased by fine axial flutes on the water side of the heat transfer surface. At moderate water velocities well within the range of projected OTEC

operation, the degree of enhancement equals the fluted-to-smooth surface area ratio.

b. Constant-radius flutes reach full effectiveness at a water velocity which is lowest for flutes of greatest height. Flutes of 45-mil or greater height inside a nominal 1-inch, 16 BWG tube are fully effective over the whole lower turbulent range of flow. The behavior of flutes having other than the constant-radius configuration is currently being tested.

## Overall Heat Transfer Coefficients

On the water side of the heat transfer surface, the coefficients obtained in the present study are immediately applicable as length-mean values. This is due to the fact that water properties change very little from one end of the tube to the other.

Quite differently, the "local" coefficients for the working fluid side have to be averaged in order to be useful to the designer. In the condenser, the length-mean coefficient $\bar{h}$ is best correlated as a function of the condensate Reynolds number at the bottom of the tube. This is the common type of correlation found in textbooks. Fig. 11 presents the length-mean coefficient for ammonia condensing on a 1-inch aluminum tube with 26-mil constant radius external flutes.

The evaporator is more complicated. It is most convenient to correlate the mean heat transfer coefficient $\bar{h}$ with the Reynolds number at the top of the tube since this is the control variable. The average Reynolds number on the evaporator tube, however, is a function of the heat load. It is possible to express the effect of the heat load in terms of a recycle ratio $\sigma$ where

$$\sigma = \frac{\text{mass rate of liquid flow from bottom of tube}}{\text{mass rate of evaporation}} .$$

If attention is limited to the Reynolds number range of the present data and if it is assumed that the "local" values of the heat transfer coefficient apply to successive points along the length of the evaporator, the effect of recycle ratio on the mean heat transfer coefficient is as shown in Fig. 11. The recycle ratio has a significant influence. There is a trade-off to be made between the pumping cost of the recycle and the first cost of the evaporator.

The connection between the individual mean heat transfer coefficient and the overall coefficient cannot be generalized since the ammonia-side coefficient depends on the heat load. However, a particular situation can be used to illustrate the efficacy of enhancement by means of flutes.

### (a) Condenser

Assume that cooling water is supplied at 40°F to condense ammonia saturated at 50°F. The tube is aluminum, nominally 1-inch, 16 BWG, 20 ft long. A scale-resistance factor of 0.0005 exists on the water side. The overall coefficient $U_i$ based on the inside area of the nominal smooth tube is shown in Table 3. The table indicates that

- Enhancement on the ammonia side is strongly beneficial.

Table 3

Effect of Flutes on Overall Heat Transfer Coefficient of Condenser

$U_i$ = Btu/(hr)(sq ft of inside surface)(°F)

Example: Water inlet temperature 40°F
Ammonia saturation temperature 50°F
1-inch, 16 BWG, Al. tube 20 ft long
Scale-resistance factor = 0.0005

| Water Velocity (ft/sec) | $AR_{water}$ = 1.0 | | | $AR_{water}$ = 1.57 | | | $AR_{water}$ = 2.0 | | |
|---|---|---|---|---|---|---|---|---|---|
| | 4 | 6 | 8 | 4 | 6 | 8 | 4 | 6 | 8 |
| Case I. $U_i$ = | 310 | 340 | 350 | | | | | | |
| Case II. $U_i$ = | | | | 350 | 390 | 410 | 370 | 420 | 430 |
| Case III. $U_i$ = | 400 | 460 | 510 | 500 | 550 | 590 | 540 | 590 | 630 |

Case I. Base Case: Smooth Tube Inside & Outside
Case II. Water-side Enhancement Only
Case III. Enhancement on Both Sides:

$[AR_{NH_3} \sim 1.5]$

- The water side must also be enhanced by a factor of at least 1.57 if overall coefficients of 600 Btu/(hr)(sq ft)(°F) or more are to be realized.

### (b) Evaporator

The comparable case for the evaporator maintains the same tube and scale-resistance factor. However, warm water is supplied at 80°F to evaporate ammonia saturated at 70°F. Again, the overall coefficient $U_i$ is based on the inside area of the nominal smooth tube. Table 4

Table 4

Effect of Flutes on Overall Heat Transfer Coefficient of Evaporator

Example: Water inlet temperature 80°F
Ammonia saturation temperature 70°F
Inlet Reynolds No. of liquid $NH_3$ = 3200
1-inch, 16 BWG, Al. Tube 20 ft long
Scale-resistance factor = 0.0005

| Water Velocity (ft/sec) | $AR_{water}$ = 1.0 | | | $AR_{water}$ = 1.57 | | | $AR_{water}$ = 2.0 | | |
|---|---|---|---|---|---|---|---|---|---|
| | 4 | 6 | 8 | 4 | 6 | 8 | 4 | 6 | 8 |
| Case I. $U_i$ = | 450 | 520 | 570 | | | | | | |
| Case II. $U_i$ = | | | | 550 | 610 | 650 | 600 | 650 | 690 |
| Case III. $U_i$ = | 570 | 680 | 760 | 730 | 830 | 890 | 810 | 910 | 960 |

Case I. Base Case: Smooth Tube Inside and Outside
Case II. Water-side Enhancement Only: $U_i$
Case III. Enhancement on Both Sides: $U_i$

$[AR_{NH_3} \sim 1.5]$

indicates that in this case

Substantial enhancement on the water side is even more important since the ammonia-side coefficient is higher than in the case of the condenser.

- Overall coefficients in the range of 900 Btu/(hr)(sq ft)(°F) require water-side enhancements of 1.57 or more. Although fluted surfaces with area ratios of 1.2 or 1.3 may be easier to fabricate and clean, they result in significantly larger exchangers.

## Dynamic Modeling and Control of OTEC Power Cycles

An integral component of the CMU OTEC activity involves the analytical transient modeling, simulation, and control of OTEC power cycles (Hetyei and Neuman, 1975-1976 and Dykstra and Zener, 1976). This activity is being directed to

- Evolve control strategies and to estimate the time required to bring under control both small and large disturbances in system input;
- Establish proper procedures for protecting an OTEC plant during operating emergencies;
- Study the stability of an OTEC power system module and to identify its natural frequencies; and
- Identify how the control requirements affect the plant design.

- These issues are being addressed by proceeding systematically through the following steps:

- Analytical modeling of the transient behavior of the OTEC power cycle components.
- Interconnection of the component models to develop a complete transient model of an OTEC power cycle.
- Linearization of the transient model about realistic sets of consistent steady-state operating conditions.
- Simulation of the linearized model on a digital computer.
- Evaluation of each control option to achieve the desired response.
- Design of controllers using linearization and testing of controllers using more exact models.
- Development of start-up and shut-down procedures.

Because of the complexity of an OTEC plant, dynamic modeling is an essential step concurrent with the design and construction of a prototype plant. The essential components of an OTEC power plant, which employs a closed Rankine cycle, are: evaporator (and pre-heater), turbine-generator, condenser, working fluid pressurizing pump, and cold and warm water pumps and pipes. Each of these components is being examined in turn. Schemes for controlling these components, and the OTEC power cycle, constitute the next phase of activity. The transient models are developed by considering the flow processes (energy, mass, and momentum) associated with each of the components. Initially, each component is idealized. Later, the assumptions will be evaluated and relaxed, if necessary, to extract models which characterize the operational behavior of an OTEC plant.

## Transient Modeling of Falling Film Evaporators

To illustrate the approach, the development of a lumped parameter, transient model of a tube-and-shell evaporator incorporating falling films is sketched (10). Even though the model is designed to characterize the transient behavior of falling film smooth-tube evaporators, provision has been made to incorporate both the CMU and Argonne core-test data as they become available. Dynamic models will then be developed to characterize the transient behavior of falling film fluted-tube evaporators. In the sequel, all heat transfer coefficients and material properties are considered to be constant, independent of both time and position along the tube.

Dynamic models of the evaporator are developed by writing heat and mass balances on an incremental section of the evaporator $\Delta z$ long. The z-axis, which coincides with the centerline of the tube, starts at the top of the tube (at $z = 0$) and ends at the bottom (at $z = L_e$). Since the dynamics of the vapor flow are not considered, it is possible to conceptualize the vapor as being produced from the falling liquid film, flowing into the region between the tube and the shell, and then exiting radially out of the evaporator through a porous shell. The symbols employed are listed in Table 5 along with their units of measurement. An equilibrium operating point is assumed to illustrate the numerical values of the evaporator parameters. The working fluid is assumed to be ammonia and the temperature of the saturated vapor leaving the evaporator is 68°F. The tube and shell are assumed to be made of aluminum. The cylindrical shell is 1" thick with an inside diameter such that the cross-sectional area of the vapor $A_v$ equals the cross-sectional area of the water. The temperature of the incoming water is 77°F and has a velocity of 6 ft/sec based upon a 0.87" ID tube. The values of the evaporator parameters are summarized in Table 6.

The heat balance for the water states that

$$\left\{\begin{array}{c}\text{the rate of heat accumulation} \\ \text{in the water control volume}\end{array}\right\} = -\left\{\begin{array}{c}\text{the heat conducted from the} \\ \text{water to the tube wall}\end{array}\right\} + \left\{\begin{array}{c}\text{the enthalpy of the} \\ \text{entering water}\end{array}\right\} + \left\{\begin{array}{c}\text{the enthalpy of the} \\ \text{exiting water}\end{array}\right\} \quad (1)$$

In writing the heat balance for each evaporator tube, we consider the tube to be thin with a finite heat capacity. Since the tube is thin, negligible heat is conducted along the length of the tube. The heat balance on the tube states that

$$\left\{\begin{array}{c}\text{the rate of heat accumulation} \\ \text{in the tube control volume}\end{array}\right\} = \left\{\begin{array}{c}\text{the heat conducted from the} \\ \text{water to the tube}\end{array}\right\} - \left\{\begin{array}{c}\text{the heat conducted from the} \\ \text{tube to the working fluid}\end{array}\right\} . \quad (2)$$

In writing the heat balance for the vapor, the shell is assumed to be at the vapor temperature. The heat balance on the vapor states that

$$\left\{\begin{array}{c}\text{the heat conducted from}\\ \text{the tube to the vapor}\end{array}\right\} = \left\{\begin{array}{c}\text{the enthalpy of the vapor}\\ \text{exiting through the porous shell}\end{array}\right\} - \left\{\begin{array}{c}\text{the enthalpy of the liquid being}\\ \text{evaporated}\end{array}\right\} + \left\{\begin{array}{c}\text{the time-rate of change of the}\\ \text{energy of the vapor contained}\\ \text{between the tube and the shell}\end{array}\right\} + \left\{\text{the heat conducted to the shell}\right\}. \quad (3)$$

The mass balance on the working fluid side of the evaporator states that

$$\left\{\begin{array}{c}\text{the amount of}\\ \text{liquid being}\\ \text{vaporized}\end{array}\right\} = \left\{\begin{array}{c}\text{the amount of vapor}\\ \text{leaving through the}\\ \text{porous shell}\end{array}\right\} + \left\{\begin{array}{c}\text{the change in the amount}\\ \text{of vapor between the}\\ \text{tube and the shell}\end{array}\right\}. \quad (4)$$

Multiplication of (4) by the specific enthalpy of the condensate ($H_L$) yields {the enthalpy of the liquid being evaporated}. Substitution of this enthalpy into the vapor heat balance (3) to eliminate the evaporation terms leads to

$$\left\{\begin{array}{c}\text{the heat conducted from}\\ \text{the tube to the vapor}\end{array}\right\} = \left\{\begin{array}{c}\text{the enthalpy of the vapor}\\ \text{exiting through the porous shell}\end{array}\right\} - \left\{\begin{array}{c}\text{the enthalpy of the vapor}\\ \text{leaving through the porous shell}\end{array}\right\} - \left\{\begin{array}{c}\text{the change in the enthalpy of}\\ \text{the vapor between the tube and}\\ \text{the shell}\end{array}\right\} + \left\{\begin{array}{c}\text{the time-rate of change of the}\\ \text{energy of the vapor contained}\\ \text{between the tube and the shell}\end{array}\right\} + \left\{\text{the heat conducted to the shell}\right\}. \quad (5)$$

Equations (1), (2) and (5) constitute the partial-differential equations describing the transient behavior of the evaporator.

For OTEC plant control, lumped parameter (ordinary differential equation) models are sought to describe the input-output characteristics of the system components. The average value of a quantity $\square$ is denoted by the bracket symbol $\langle\square\rangle$. To average these heat balances, equations (1), (2) and (5) are integrated over the length of the tube, from z=0 to z=$L_e$, and the results are divided by the tube length $L_e$. Thereby:

Water heat balance

$$\rho_w A_w C_w \langle\dot{T}_w\rangle = -\pi D_t h_{wt}\left[\langle T_w\rangle - \langle T_t\rangle\right] + \frac{W_w C_w}{L_e}\left[T_w(0) - T_w(L_e)\right] \quad \langle 1\rangle$$

Tube heat balance

$$\rho_t A_t C_t \langle\dot{T}_t\rangle = \pi D_t h_{wt}\left[\langle T_w\rangle - \langle T_t\rangle\right] - \pi D_t h_{tv}\left[\langle T_t\rangle - T_v\right] \quad \langle 2\rangle$$

Table 5. Symbol Table

| Symbol | Definition | Dimensions |
|---|---|---|
| $A_s$ | Cross-Sectional Area of Shell Material | $ft^2$ |
| $A_t$ | Cross-Sectional Area of Tube Material | $ft^2$ |
| $A_v$ | Cross-Sectional Area Between Shell and Tube | $ft^2$ |
| $A_w$ | Cross-Sectional Area of Water | $ft^2$ |
| $C_s$ | Heat Capacity of Shell Material | Btu/lb/°F |
| $C_t$ | Heat Capacity of Tube Material | Btu/lb/°F |
| $C_w$ | Heat Capacity of Water | Btu/lb/°F |
| $D_s$ | Inside Diameter of Shell | ft |
| $D_t$ | Diameter of Tube | ft |
| $D_t'$ | Inside Diameter of Tube | ft |
| $H_L$ | Specific Enthalpy of Condensate | Btu/lb |
| $H_v$ | Specific Enthalpy of Vapor | Btu/lb |
| $h_{wt}$ | Heat Transfer Coefficient, Water to Tube | Btu/°F/$ft^2$/sec |
| $h_{tv}$ | Heat Transfer Coefficient, Tube to Vapor | Btu/°F/$ft^2$/sec |
| $L_e$ | Length of Evaporator Tube | ft |
| $Th_s$ | Thickness of Shell | ft |
| $U_v$ | Specific Internal Energy of Vapor | Btu/lb |
| $V_w$ | Velocity of Water | ft/sec |
| $W_v$ | Mass Flow Rate of Working Fluid Vapor | lb/sec |
| $W_w$ | Mass Flow Rate of Water | lb/sec |
| $\rho_s$ | Density of Shell Material | $lb/ft^3$ |
| $\rho_t$ | Density of Tube Material | $lb/ft^3$ |
| $\rho_v$ | Density of Working Fluid Vapor | $lb/ft^3$ |
| $\rho_w$ | Density of Water | $lb/ft^3$ |
| $\lambda$ | Latent Heat of Evaporation | Btu/lb |
| $T_t$ | Temperature of Tube | °F |
| $T_w$ | Temperature of Water | °F |
| $T_{w(0)}$ | Temperature of Inlet Water at z = 0 | °F |
| $T_{w(L_e)}$ | Temperature of Outlet Water at z = $L_e$ | °F |
| $T_v$ | Vapor Temperature | °F |
| $\gamma$ | Transit Time of Water through the Evaporator Tube | sec |
| $\gamma_{ave}$ | Transit Time of the Water from Point along the Tube where the Local Water and Tube Temperatures Attain their Average Values. | sec |
| t | Time | sec |
| $\sigma$ | Recycle Ratio | - |

Vapor heat balance

$$\rho_s A_s C_s \dot{T}_v + A_v \frac{d(\rho_v U_v)}{dt} - A_v H_v \dot{\rho}_v = \pi D_t h_{tv}\left[\langle T_t\rangle - T_v\right] - (H_v - H_L)\frac{W_v}{L_e} \quad \langle 5\rangle$$

Table 6. Illustrative Evaporator Parameter Values

/elocity $v_w$ = 6 ft/sec (on a 0.87" inside diameter tube)

| | | | | |
|---|---|---|---|---|
| Densities | | | | |
| Water | $\rho_w$ | = 62.24 | lb/ft$^3$ | |
| Tube and shell | $\rho_t = \rho_s$ | = 168.48 | lb/ft$^3$ | |
| Heat Capacities | | | | |
| Water | $C_w$ | = 1.0 | Btu/lb/°F | |
| Tube and shell | $C_t = C_s$ | = 0.2151 | Btu/lb/°F | |
| Heat Transfer Coefficients | | | | |
| Tube-water | $h_{tw}$ | = 0.3376 | Btu/ft$^2$/°F/sec | |
| Vapor-tube | $h_{vt}$ | = 0.5215 | Btu/ft$^2$/°F/sec | |
| Specific Enthalpy | | | | |
| Vapor | $H_v$ | = 628.8 | Btu/lb | |
| Heat of Vaporization of Ammonia | $\lambda$ | = 510.5 | Btu/lb | |
| Steady-State Values | | | | |
| Vapor density | $\rho_v^*$ | = 0.4179 | lb/ft$^3$ | |
| Vapor internal energy | $U_v^*$ | = 573.745 | Btu/lb | |
| Dimensions | | | | |
| Tube diameter (OD) | $D_t$ | = 1 inch | | = 0.0833 ft |
| Tube diameter (ID) | $D_t'$ | = 0.87 inch | | = 0.0725 ft |
| Shell diameter (ID) | $D_s$ | = $\sqrt{2}\, D_t$ | | = 0.118 ft |
| Tube length | $L_e$ | = 20 ft | | |
| Shell Thickness | $Th_s$ | = 1 inch | | |
| Water Flow Rate | $W_w$ | = $\rho_w \pi \frac{(D_t')^2}{4} v_w$ | | = 1.542 lb/sec |
| Areas | | | | |
| Water cross-sectional area | $A_w$ | = $\frac{\pi}{4} D_t^2$ | | = 0.005454 ft$^2$ |
| Tube cross-sectional area | $A_t$ | = $\frac{\pi}{4}[(D_t^2 - D_t'^2)]$ | | = 0.00133 ft$^2$ |
| Shell cross-sectional area | $A_s$ | = $\frac{\pi}{4}[D_s + Th_s)^2 - D_s^2]$ | | = 0.0209 ft$^2$ |
| Vapor cross-sectional area | $A_v$ | = $\frac{\pi}{4}[D_s^2 - D_t^2]$ | | = 0.005454 ft$^2$ |

In <5>, the difference between the specific enthalpies of the vapor ($H_V$) and the condensate ($H_L$) is the latent heat of evaporation (Btu/lb):

$$\lambda \triangleq H_V - H_L \quad .$$

The above equations constitute the basic lumped-parameter evaporator model. At first glance, there appear to be six dependent variables: namely, $\langle T_w(t) \rangle$ , $T_w(L_e)$ , $\langle T_t(t) \rangle$ , $T_v(t)$ , $U_v(t)$ , and $\rho_v(t)$ , and only three equations. $\dot{\rho}_v$ and $\dot{U}_v$ can be expressed in terms of $\dot{T}_v$ . The enthalpy (H) and the internal energy (U) of the vapor are related thermodynamically by

$$U_v = H_v - P_v V_v \quad .$$

$P_v$ is the pressure of the saturated vapor and $V_v$ is the volume of one pound of saturated vapor. The enthalpy, the pressure, and the specific volume are determined by the vapor temperature. Therefore, $U_v$ is specified by the temperature. A change in the vapor temperature produces a corresponding change in the enthalpy, pressure, and specific volume, and thus a change in the internal energy. The pressure in the volume of the evaporator is assumed constant. With this assumption, the vapor density is directly related to the vapor temperature through the (ideal gas law) equation of state. Increasing (decreasing) the vapor temperature increases(decreases) the vapor volume and decreases (increases) the vapor density.

What remains is to relate the outlet water temperature $T_w(L_e)$ to the inlet water temperature $T_w(0)$ and the vapor temperature $T_v(t)$. This is accomplished by writing the steady-state water and tube heat balances. Upon rearranging (1-2), we find that these steady-state heat balances are, respectively:

Water heat balance

$$\left(\frac{W_w C_w}{\pi D_t h_{wt}}\right)\frac{dT_w(z)}{dz} + T_w(z) = T_t(z) \qquad (6)$$

Tube heat balance

$$0 = h_{wt}\left[T_w(z) - T_t(z)\right] - h_{tv}\left[T_t(z) - T_v\right] \qquad (7)$$

Upon substituting (7) into (6) to eliminate the tube temperature $T_t(z)$, we obtain the first-order linear differential equation in $T_w(z)$:

$$\zeta \frac{dT_w(z)}{dz} + T_w(z) = T_v \quad , \qquad (8)$$

with the length constant (ft)

$$\zeta \triangleq \left[\frac{1}{h_{wt}} + \frac{1}{h_{tv}}\right]\left(\frac{W_w C_w}{\pi D_t}\right) \quad .$$

For

$$C_w = 1 \quad \text{Btu/lb/°F}$$

$$h_{tw} = 0.3376 \quad \text{Btu/ft}^2\text{/°F/sec}$$

$$h_{vt} = 0.5215 \quad \text{Btu/ft}^2\text{/°F/sec} \quad ,$$

and for the water velocity $V_w$ = 6 ft/sec in a $D_t'$ = 0.87" inside diameter tube,

$$D_t = 1 \text{ inch}$$

$$W_w = \rho_w \frac{\pi}{4} (D_t')^2 V_w = 1.54 \text{ lb/sec} \quad ,$$

the length constant

$$\zeta \cong 28.73 \text{ ft} \quad .$$

For a constant vapor temperature $T_v$, the solution of (8), evaluated at the bottom of the evaporator tube ($z = L_e$), is

$$T_w(L_e) = T_w(0) e^{-L_e/\zeta} + \left[1 - e^{-L_e/\zeta}\right] T_v \quad . \qquad (9)$$

Equation (9) relates the outlet water temperature $T_w(L_e)$ to the inlet water temperature $T_w(0)$ and the vapor temperature $T_v$ in the steady-state. To approximate the dynamic behavior of $T_w(L_e,t)$, the transit times of the water and vapor are introduced as time delays on the inlet water and vapor temperatures.

Let $\gamma$ = the transit time of the water through the evaporator tube, from z=0 to z=$L_e$.

The inlet water time delay

$$\gamma \triangleq \left(\frac{L_e}{V_w}\right)$$

is the transit time of the water through the evaporator. $V_w$ is the average velocity of the water through the tube (ft/sec), and

$\gamma_{ave}$ = the transit time of the water in the steady-state (11) from the point $z_{ave}$ along the tube, where the local temperatures $T_w(z)$ and $T_t(z)$ attain their average values $\langle T_w \rangle$ and $\langle T_t \rangle$, to $z = L_e$.

That is, $z_{ave}$ is defined implicitly by

$$T_w(z=z_{ave}) = \langle T_w \rangle \qquad \text{for } \gamma_{ave} .$$

For the outlet water temperature equation (9), the time delay

$$\gamma_{ave} = \left(1 - \frac{z_{ave}}{L_e}\right)\gamma .$$

$L_e = 20$ ft

$z_{ave} = 10$ ft

$\frac{z_{ave}}{L_e} = 0.5$

$\gamma = 3.33$ sec

$\gamma_{ave} = 0.5\,\gamma = 1.67$ sec .

To incorporate the dynamic behavior of the outlet water temperature $T_w(L_e,t)$, equation (9) is replaced by

$$T_w(L_e,t) = T_w(0,t-\gamma)\exp(-L_e/\zeta) + [1-\exp(-L_e/\zeta)]T_v(t-\gamma_{ave}) . \quad (10)$$

Equation (10) specifies $T_w(L_e,t)$ as a time-delayed function of the inlet water temperature and the vapor temperature, delayed by their respective transit times. In the simulation studies, the transient response of the evaporator will be examined in detail, along with the behavior of the model in the vicinity of operating points. The approximations leading to (10) will be evaluated and the need for introducing variable time-delays and length parameters assessed.

The lumped parameter single-tube evaporator model is illustrated in Fig. 12. This transient model is specified by the three coupled nonlinear differential equations <1>, <2>, and <5> and the algebraic equation (10). The system of differential equations is nonlinear because of the water flow-rate and outlet water temperature product $[W_w T_w(L_e,t)]$ appearing in <1> and the two equation of state terms $[\dot{U}_v$ and $\dot{\rho}_v]$ in <5>. Upon substituting (10) into <1>, we find that the dynamic behavior of the evaporator is characterized by three coupled nonlinear differential equations with the two time-delays $\gamma$ and $\gamma_{ave}$. The three inputs or control variables are the inlet water temperature $T_w(0,t)$, the water flow-rate $W_w(t)$, and the vapor flow rate $W_v(t)$. The dependent variables are the water temperature $\langle T_w(t) \rangle$, tube temperature $\langle T_t(t) \rangle$, and vapor temperature $T_v(t)$. The two outputs are the outlet water temperature $T_w(L_e,t)$ and the vapor temperature $T_v(t)$.

In OTEC power plant evaporators, only partial evaporation of the falling film is obtained on each tube. The inlet working fluid flow rate is several times higher than the evaporation rate in order to take advantage of the higher heat transfer coefficients available in the turbulent flow regime. This results in the recirculation of the liquid not evaporated after passing through the evaporator. Corresponding to each value of the recycle ratio, there is a heat transfer coefficient $h_{tv}$. The recirculation ratio enters the model through the specification of $h_{tv}$.

## Linearization of the Evaporator Model

The stability of the single-tube model is analyzed prior to designing feedback control schemes for the evaporator. To investigate the stability of the transient evaporator model in the vicinity of the stable operating point, each of the time-varying model variables is replaced by its equilibrium steady-state value (denoted by an asterisk) plus a time-varying deviation from that equilibrium value. That is,

Inputs

$$\begin{cases} T_w(0,t) = T_w^*(z=0) + \Delta T_w(0,t) \\ W_w(t) = W_w^* + \Delta W_w(t) \\ W_v(t) = W_v^* + \Delta W_v(t) \end{cases}$$

State Variables

$$\begin{cases} \langle T_w(t) \rangle = T_w^* + \Delta T_w(t) \\ \langle T_t(t) \rangle + T_t^* + \Delta T_t(t) \\ T_v(t) = T_v^* + \Delta T_v(t) \end{cases}$$

Parameters

$$\begin{cases} U_v(t) = U_v^* + \Delta U_v(t) \\ \rho_v(t) = \rho_v^* + \Delta \rho_v(t) \end{cases}$$

Outputs

$$\{ T_w(L_e,t) = T_w^*(z=L_e) + \Delta T_w(L_e,t)$$

Upon substituting the listed variables in equations <1>, <2>, <5>, and (10), subtracting the steady-state equations, and neglecting the higher-order terms, we find the linearized transient evaporator model is

Water heat balance

$$M_w C_w \frac{d(\Delta T_w)}{dt} = - \pi D_t h_{wt}[\Delta T_w - \Delta T_t] + \frac{C_w}{L_e} W_w^* [\Delta T_w(0) - \Delta T_w(L_e)] + \frac{C_w}{L_e} [T_w^*(0) - T_w^*(L_e)] \Delta W_w \quad (A22)$$

Tube heat balance

$$\frac{\rho_t A_t C_t}{\pi D_t} \frac{d(\Delta T_t)}{dt} = - h_{tv}[\Delta T_t - \Delta T_v] + h_{wt}[\Delta T_w - \Delta T_t] \quad (A23)$$

Vapor heat balance

$$\frac{-\lambda}{L_e} \Delta W_v + A_v H_v \frac{d(\Delta \rho_v)}{dt} = - \pi D_t h_{tv}[\Delta T_t - \Delta T_v] + A_v \frac{d[U_v^* \Delta \rho_v + \rho_v^* \Delta U_v]}{dt} + \rho_s A_s C_s \frac{d(\Delta T_v)}{dt} \quad (A24)$$

Outlet water temperature

$$\Delta T_w(L_e,t) = \Delta T_w(0,t-\gamma) e^{-L_e/\zeta^*} + \Delta T_v(t-\gamma_{ave})(1 - e^{-L_e/\zeta^*}) + \alpha_{T_w W_w} \Delta W_w(t-\gamma) - \alpha_{T_v W_w} \Delta W_w(t-\gamma_{ave}) \quad (A25)$$

In (14),

$$\alpha_{T_w W_w} \Delta W_w(t-\gamma) =$$

$$\{\exp[-L_e/\zeta(W_w^* + \Delta W_w)] - \exp[-L_e/\zeta^*]\} T_w^*(0)$$

and

$$\alpha_{T_v W_w} \Delta W_w(t-\gamma_{ave}) =$$

$$\{\exp[-L_e/\zeta(W_w^* + \Delta W_w)] - \exp[-L_e/\zeta^*]\} T_v^* \quad .$$

The linearized evaporator model is characterized by the three first-order linear differential equations (11-13) and the algebraic equation (14) with two time-delays.

Having linearized the evaporator model, we derive the relationships between $\dot{\rho}_v$ and $\dot{T}_v$, and between $\dot{U}_v$ and $\dot{T}_v$. The pressure, density, specific enthalpy, and specific volume of the working fluid (ammonia) are obtained at various temperatures from thermodynamic tables. The data are plotted, and the local slopes are calculated to approximate the derivatives.

In the vicinity of 68°F, for example,

$$R \triangleq \frac{\Delta \dot{\rho}_v}{\Delta \dot{T}_v} = 0.00719 \quad \text{lb/ft}^3/°\text{F}$$

and

$$S = \frac{\Delta \dot{U}_v}{\Delta \dot{T}_v} = 0.144 \quad \text{Btu/lb/°F} \ ,$$

where

$$U = H - \frac{144}{778} PV = H - 0.185\ PV \quad .$$

Thereby, (13) becomes, upon collecting terms,

$$\left\{A_v[U_v^* R + \rho_v^* S - H_v R] + \rho_s A_s C_s\right\} \frac{d(\Delta T_v)}{dt} =$$

$$- \pi D_t h_{vt}[\Delta T_v - \Delta T_t] - \frac{\lambda}{L_e} \Delta W_v$$

The three state-variables of the linearized model are:

$\Delta T_w(t)$ = Deviation of the water temperature from the equilibrium value $T_w^*$

$\Delta T_t(t)$ = Deviation of the tube temperature from the equilibrium value $T_t^*$

$\Delta T_v(t)$ = Deviation of the vapor temperature from the equilibrium value $T_v^*$ .

The two outputs are:

$\Delta T_w(z=L_e,t)$ = Deviation of the outlet water temperature from the nominal equilibrium $T_w^*(z=L_e)$

$\Delta T_v(t)$ = Deviation of the vapor temperature from the equilibrium value $T_v^*$ .

## Transfer Functions of the Evaporator

The open-loop transfer function matrix of the linearized evaporator model (11-13) is calculated. The transfer function matrix $\underline{G}(s)$ relates the Laplace transform of the inputs to the Laplace transform of the state variables. Symbolically,

$$\underbrace{\begin{bmatrix} \Delta T_w(s) \\ \Delta T_t(s) \\ \Delta T_v(s) \end{bmatrix}}_{\text{State Variables}} = \underline{G}(s) \underbrace{\begin{bmatrix} \Delta T_w(z=0,s) \\ \Delta W_w(s) \\ \Delta W_v(s) \end{bmatrix}}_{\text{Inputs}}$$

In turn, from (14), the output

$$\Delta T_w(L_e,s) =$$

$$\Delta T_w(0,s) e^{-\gamma s} e^{-L_e/\zeta^*} + \Delta T_v(s) e^{-\gamma_{ave} s} \left[1 - e^{-L_e/\zeta^*}\right]$$

$$+ \alpha_{T_w W_w} \Delta W_w(s) e^{-\gamma s} - \alpha_{T_v W_w} \Delta W_w(s) e^{-\gamma_{ave} s}$$

## Stability Analysis of the Evaporator Model

The stability of the linearized evaporator model is assessed by applying the Bode method of classical control engineering. The characteristic equation $\Delta(s) = 0$ is written in the form

$$1 + M(s) = 0 .$$

M(s) is the open-loop transfer function of a unity negative feedback system with characteristic equation $\Delta(s) = 0$. For sets of nominal evaporator parameters, it is demonstrated that the magnitude $|M(j\omega)|$ is always less than unity when the phase $\angle M(j\omega)$ is less than $-180°$ for all frequencies $\omega$, $0 \leq \omega < +\infty$. Consequently, the single-tube evaporator model is stable for perturbations about equilibrium operating points.

What remains is to evaluate the dynamic behavior of the evaporator model. A salient aspect of current research involves developing simulation models and control strategies for OTEC power plants. The evaporator model constitutes an integral component of the OTEC power cycle model.

## Transient Power Cycle Model

The OTEC power cycle model being assembled is depicted in Fig. 13; the pre-heater is not included in this exhibit. As illustrated, the model is specified by eleven coupled nonlinear differential equations, four time-delays, and the associated algebraic equations incorporating the operating characteristic curves of each component. It is noted that each pump contributes one differential equation to the model.

The transient model described lays the foundation for a digital computer simulation package of the OTEC power cycle. This simulation package, along with the linearized model, provides the tool for designing and evaluating control strategies for an OTEC plant. Representative problem areas to be addressed are highlighted in the sequel:

- The stability of an OTEC power system module will be examined and the natural frequencies will be identified for a realistic range of operating conditions. This step entails analyzing and simulating the linearized model on the digital computer.
- Control strategies, designed to dampen out both small and large disturbances in the plant inputs, will be evaluated. In so doing, the time required to bring the system under control will be estimated. Throughout the control system design and evaluation activity, controllers will be designed for the linearized model and then tested on the more exact (nonlinear) model.
- Start-up and shut-down procedures will be developed and evaluated.
- Procedures for protecting an OTEC plant during operating emergencies will be developed and evaluated.
- A control scheme will be developed for operating the plant at constant speed (constant frequency output) while maintaining the power output within 1% of its peak value for the ambient ocean surface temperature.
- On the basis of these control studies, the impact of the control requirements on OTEC plant design will be identified.

## References


1. R. Gregorig, "Hautkondensation an feingewellten Ob flächen bei Berücksichtigung der Oberflächenspannu Zeitsch. fur. ang. Math. und Physik, 5, 1954, pp. 36-49.
2. L.G. Alexander and H.W. Hoffman, "Performance Characteristics of Advanced Evaporator Tubes for Long-Tube Evaporators," ORNL-TM-2951 (OSW R&D Reports 644 and 699), 1971.
3. C. Zener et al., Solar Sea Power Third Quarterly Progress Report, April 30, 1974, NSF/RANN/SE/GI-39114/PR/74/3 (NTIS Accession No. PB235469).
4. A.A. McLeod, "Liquid Turbulence in a Gas -Liquid Absorption System," D.Sc. Thesis (Chemical Engineering), Carnegie-Mellon University, 1951, pp. 41-42.
5. H.M. Belkin, "Mass Transfer in Turbulent Liquid Films," Ph.D. Thesis (Chemical Engineering), Carnegie-Mellon University, 1953, pp. 45-49.
6. R.R. Rothfus and C.P. Neuman, "The OTEC Program at Carnegie-Mellon University, Heat Transfer Research and Power Cycle Transient Modeling," March 1977, COO/2641-4.
7. W. Nusselt, Ver. deut. Ing. Zeit., 60, 541, 569 (1916).
8. E.N. Sieder and G.E. Tate, Ind. Eng. Chem., 28, 1429 (1936).
9. S.A. Hetyei and C.P. Neuman, "Dynamic Modeling and Control of Solar Sea Power Plants," Carnegie-Mellon University, June 1975, NSF/RANN/SE/GI-39114/TR/75/7; NTIS Accession No. PB252983.
10. S.A. Hetyei and C.P. Neuman, "Steady State Evaporator Models of Solar Sea Power Plants - Part I," Carnegie-Mellon University, August 1976, ERDA TIC No. COO/2895-5.
11. S.A. Hetyei and C.P. Neuman, "Dynamic Models of Falling film Evaporators for Ocean Thermal Energy Conversion Plants," Carnegie-Mellon University, September 1976, ERDA TIC No. COO/2641-3.
12. L.J. Dykstra and C. Zener, "Transient Behavior of a Solar Sea Power Plant," Carnegie-Mellon University, July 1976, ERDA TIC No. COO/2895-4.

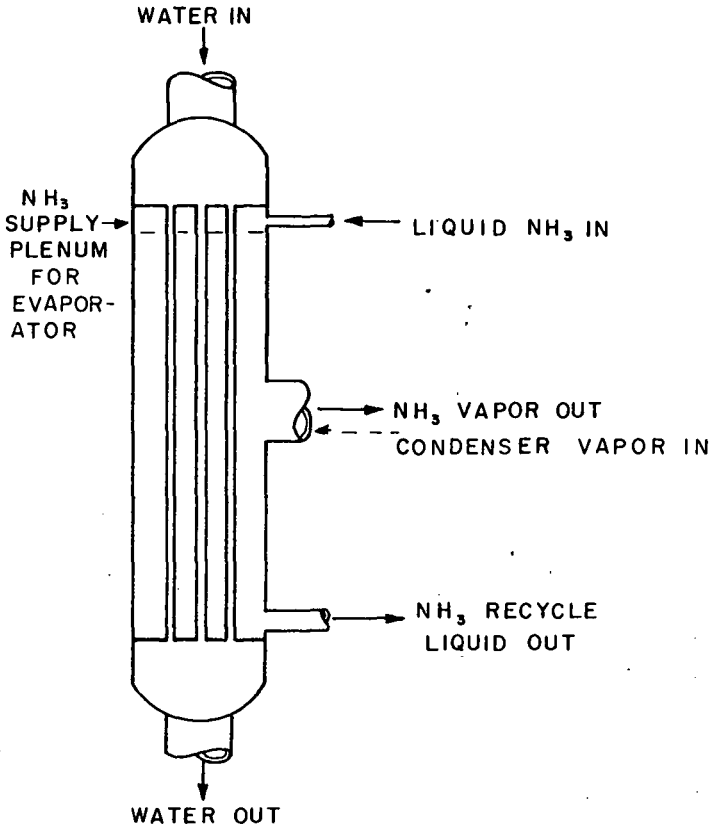



Figure 1.

VERTICAL TUBE EXCHANGER

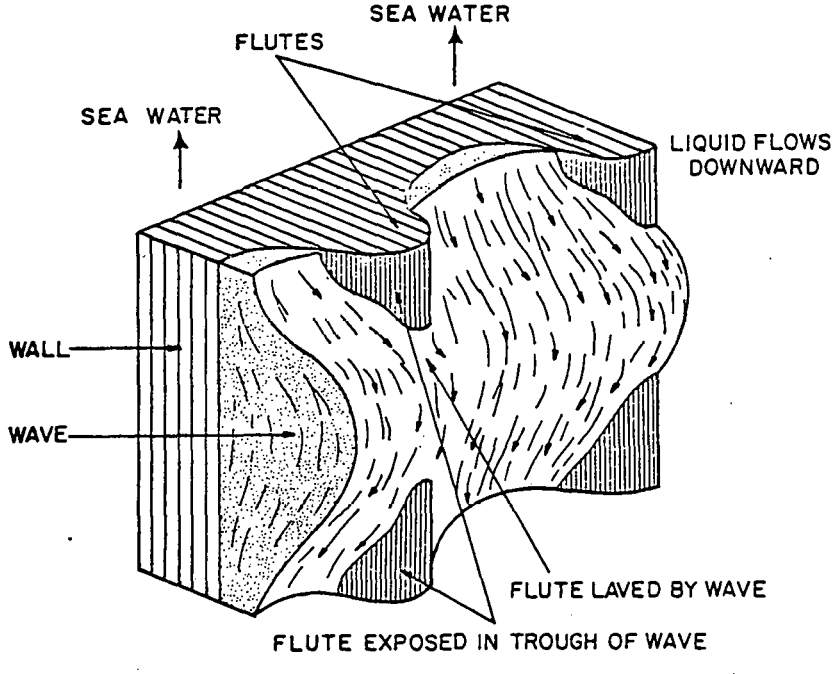



Figure 2.

WAVEY MOTION OF FALLING FILM ON FLUTED SURFACE

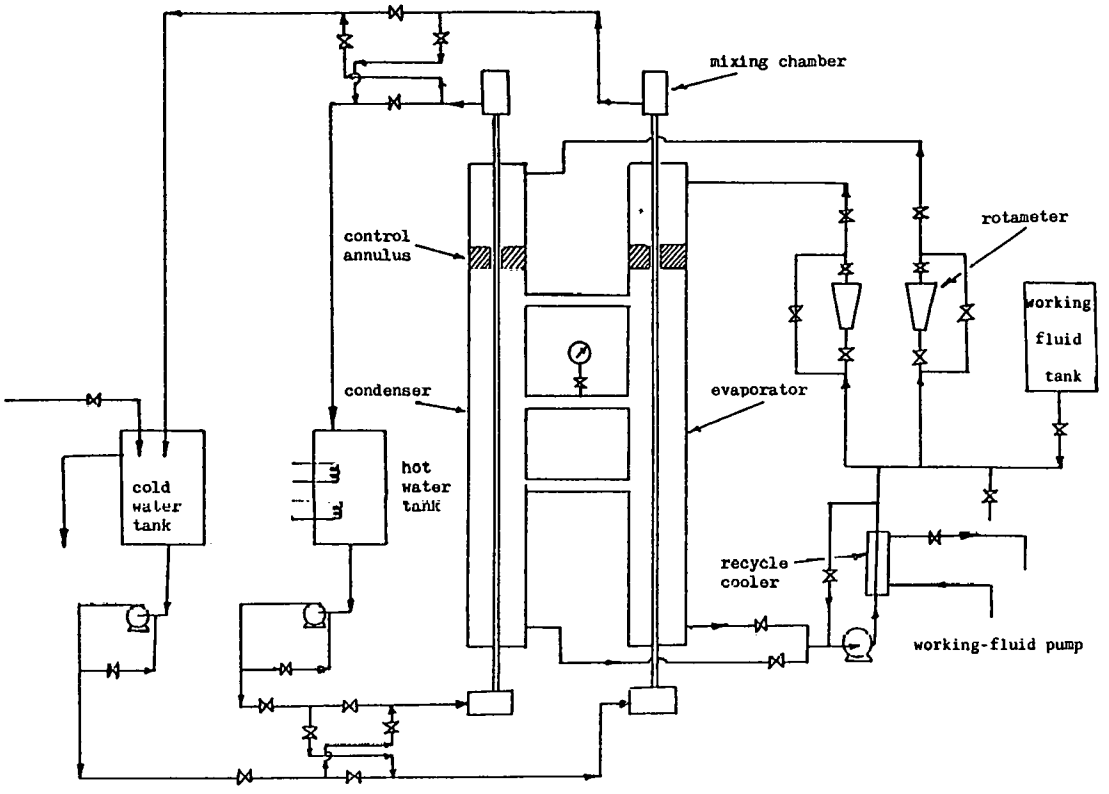



Figure 3

SCHEMATIC DIAGRAM OF TEST LOOP FOR WORKING-FLUID EXPERIMENTS

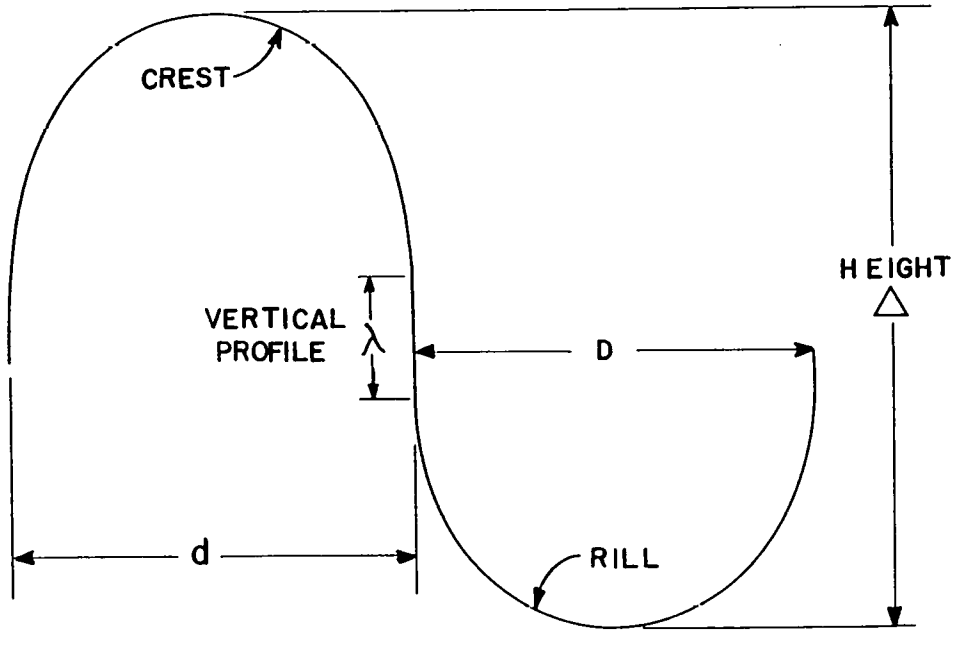



Figure 4.

FLUTE GEOMETRY

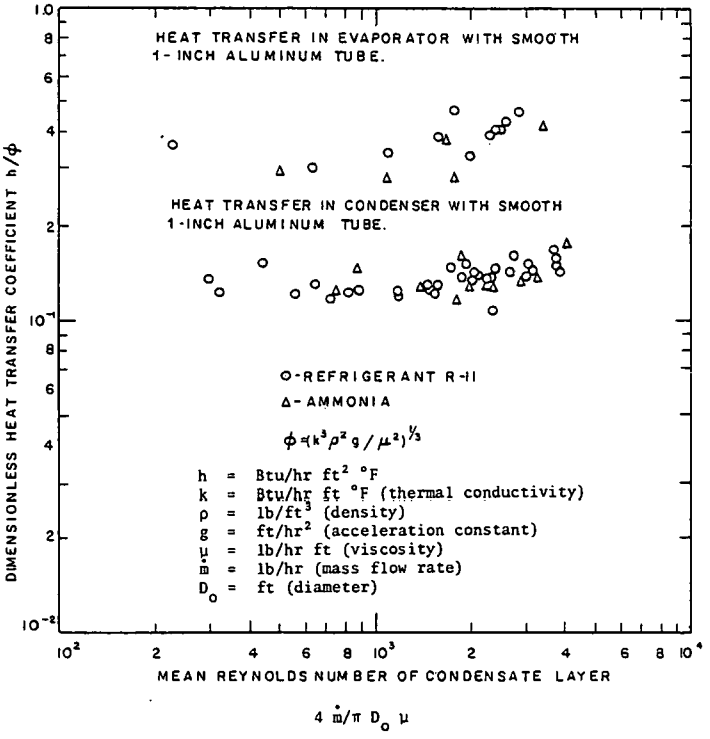



Figure 5.

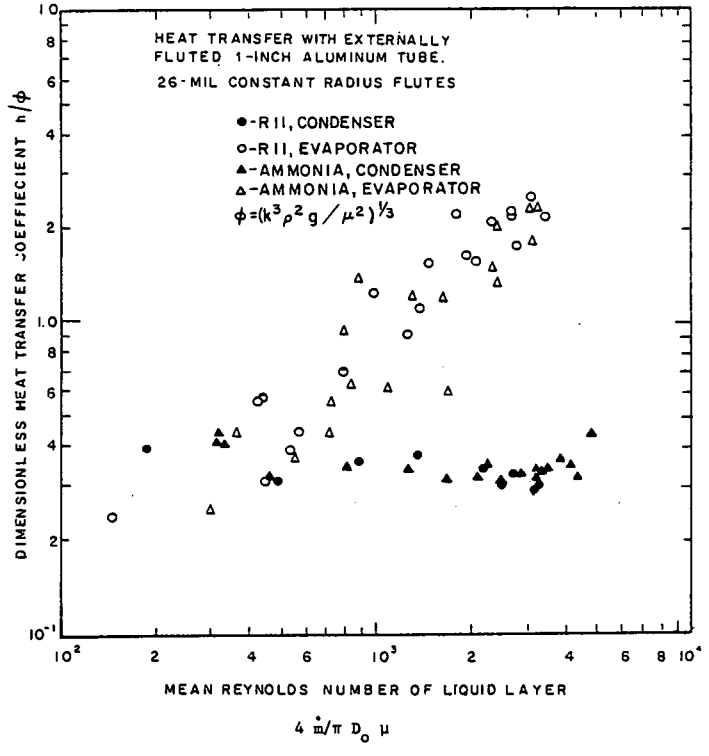



Figure 6.

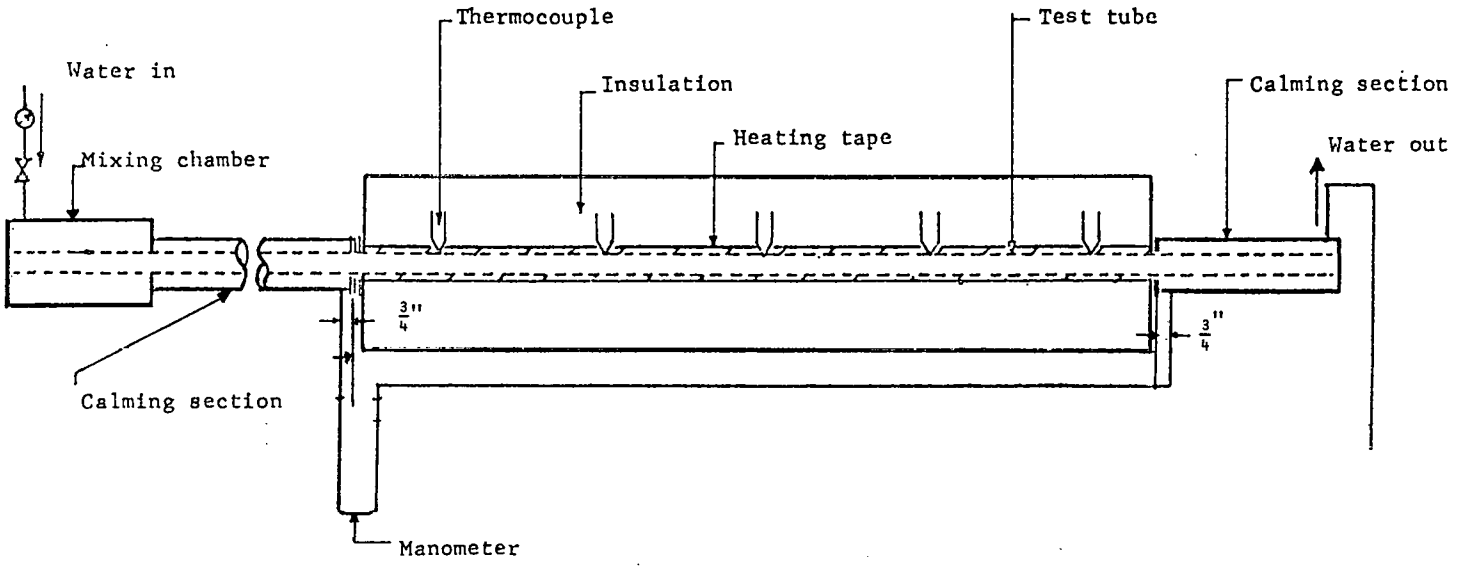



Figure 7. SCHEMATIC DRAWING OF APPARATUS FOR WATER-SIDE EXPERIMENTS

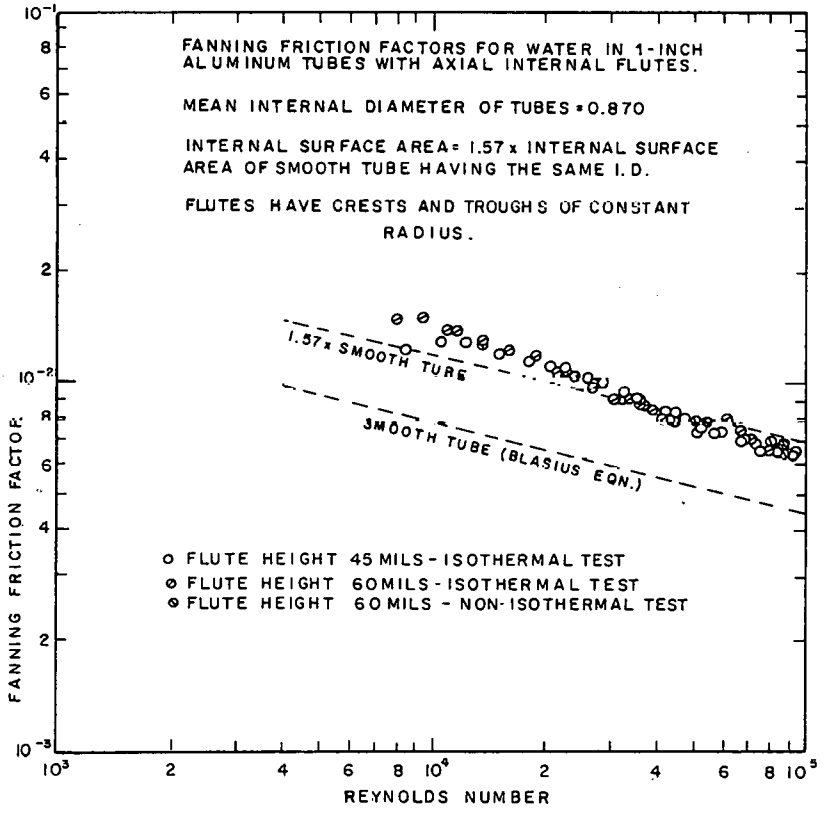
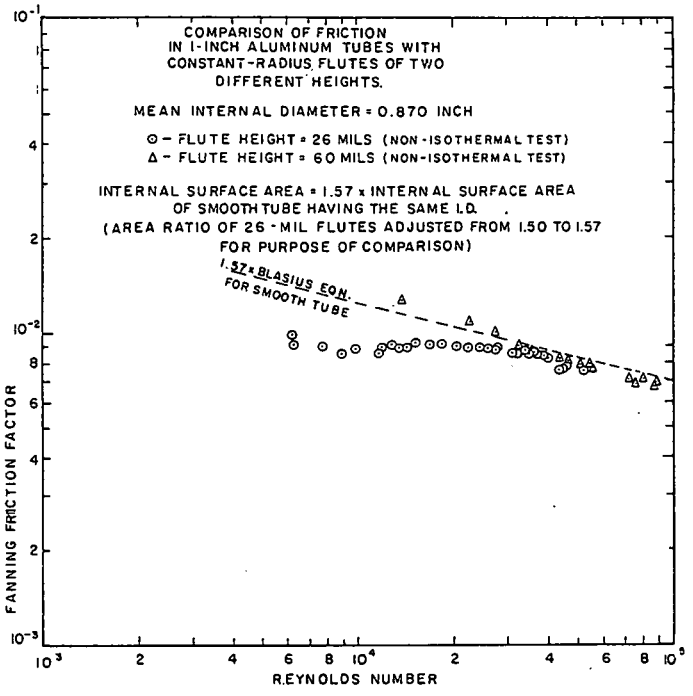
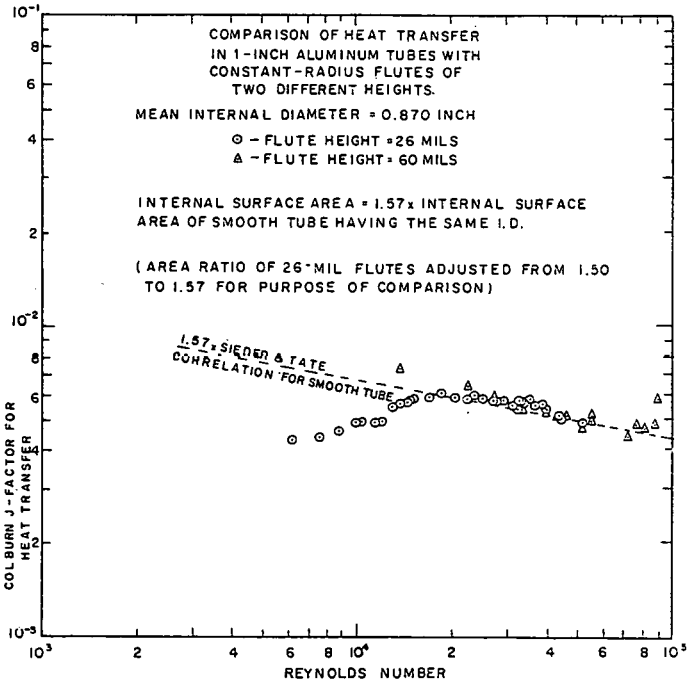



Figure 8.

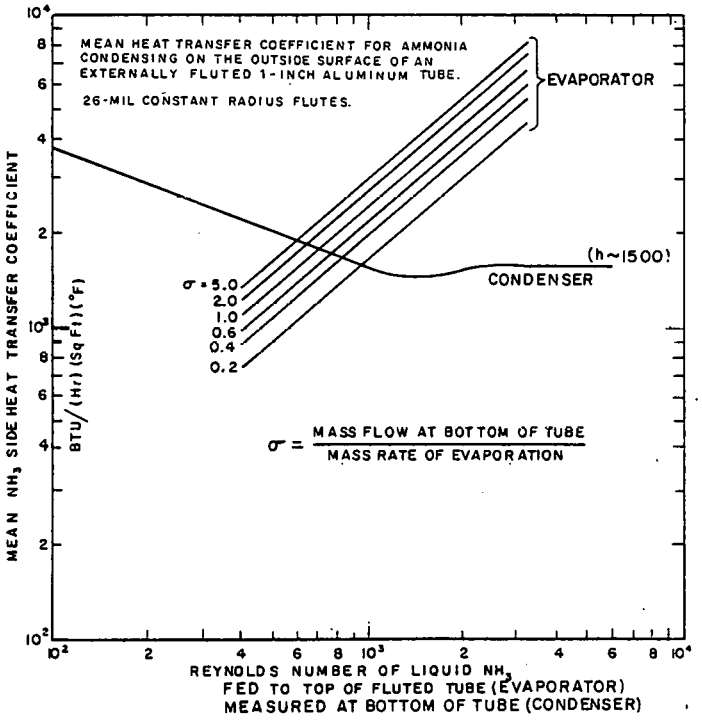



← Figure 9.

Figure 10. →




← Figure 11.



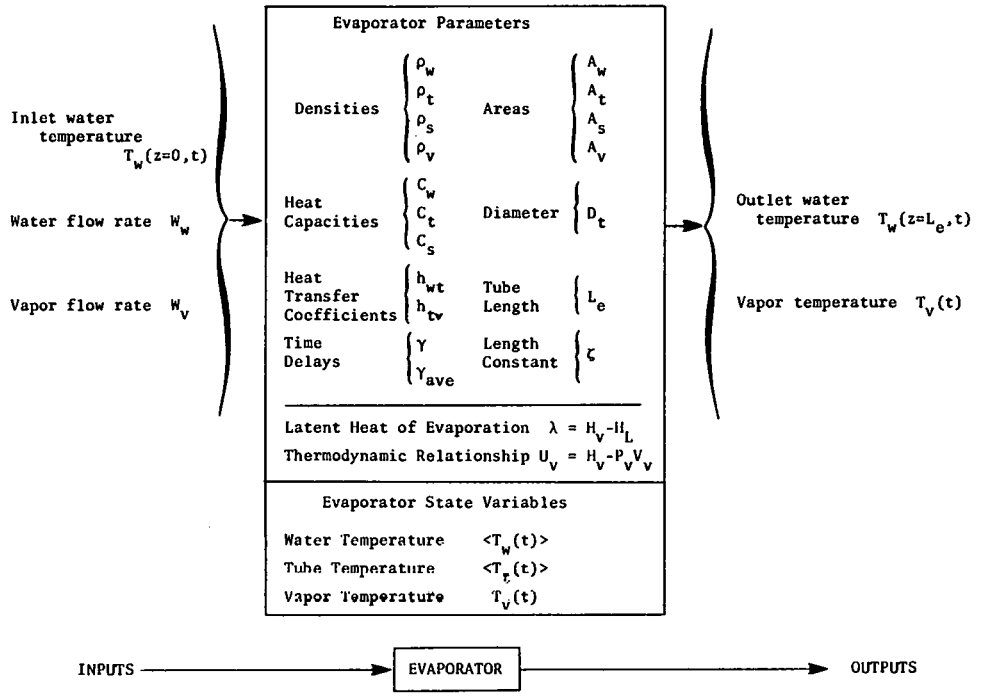



Figure 12. SCHEMATIC REPRESENTATION OF EVAPORATOR MODEL

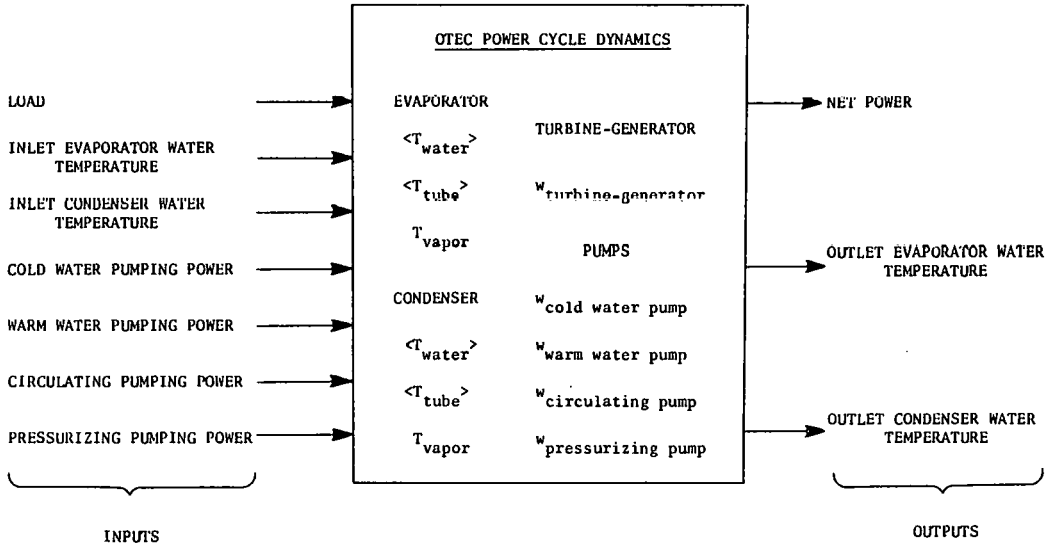



Figure 13. OTEC POWER CYCLE MODEL

# ENHANCED PERFORMANCE HEAT EXCHANGERS

A. M. Czikk, H. D. Fricke, and E. N. Ganic
*Linde Division*
*Union Carbide Corporation*
*Tonawanda, New York*

ABSTRACT

This program involves development of enhanced performance shell and tube evaporators and condensers for the OTEC application, using proprietary heat transfer enhancement devices. The work includes: analytical development of thermal and fluid flow models for sprayed bundle and flooded bundle evaporators; experimental determination of the heat transfer and fluid flow factors necessary for the evaporator models; designing, building and testing three pilot scale heat exchangers, comprising a sprayed bundle evaporator, a flooded bundle evaporator, and a horizontal tube condenser.

## 1. General

It has been estimated that the heat exchanger costs for Ocean Thermal Energy Conversion (OTEC) plants represent approximately one-half of the total capital cost. The low cycle efficiency, due to the low source-sink temperature difference, causes the heat duty of the exchangers to be very large. Therefore, the heat exchangers are the key item in the OTEC cycle. Much of the current OTEC research is directed at development of lower cost heat exchangers.

The cost-performance characteristics of OTEC heat exchangers were the subject of a previous UCC/Linde study (1). A number of heat exchanger concepts were analysed for the evaporator and condenser. Basically two heat exchanger types have been considered: (1) plate-fin and (2) shell-and-tube. We have preferred shell-and-tube exchangers because manufacturing techniques for fabricating very large plate-fin heat exchangers have not yet been developed. Although the plate-fin units represent a more compact heat exchanger, the required unit size would still be beyond the state-of-the-art.

Overall results or our preliminary study (1) suggest the use of shell-and-tube heat exchangers with the seawater in-tube. Because the seawater is tube-side, allowing close control of the seawater velocity, bio-fouling and corrosion can be minimized. In addition, mechanical tube cleaning is possible, and leaks which may occur can be isolated.

Heat transfer enhancements are necessary in order to decrease exchanger costs (1). For the evaporator, a nucleation promoter, (i.e., a porous boiling surface) is recommended. For the condenser, a surface tension motivated condensate film thinner is recommended as the most effective and practical enhancement.

Waterside enhancement was not analysed in our preliminary study (1). Choice of a waterside enhancement will depend on the method of fouling control and the choice of tube material. Of primary interest in the large scale OTEC heat exchangers, are the "passive" techniques (2): rough surfaces, extended surfaces, displaced enhancement devices and swirl flow devices. Combination of these techniques are possible. Waterside enhancement, like the shell-side enhancement, reduces the required heat exchanger area. However, the more expensive enhanced tubing must justify itself more economically.

More research is needed on the choice of material of construction, and in fouling control, before an "optimum" waterside enhancement can be chosen. Because of this, our preliminary study (1) considered only shell-side (i.e., ammonia side) enhancement.

## 2. Heat Exchanger Concepts - Preliminary Study

### 2.1 Evaporator

Two concepts were considered for the evaporator: (1) a large sprayed bundle, and (2) multiple flooded bundles. In the large sprayed bundle, (see Figure 1 where a 25 MWe evaporator is shown) the seawater would be in-tube, and the working fluid would be sprayed on the tubes. The scheme suggested for spraying the tubes is to pump the pressurized ammonia between double tubesheets, causing the ammonia to flow through perforated spray tubes. Since no liquid pool exists, the hydrostatic head problem is eliminated.

The tubes in this concept are coated with Linde's High Flux boiling surface. This seems to be most applicable to this type of service because of its ability to boil fluids with a low temperature difference. The High Flux surface consists of a porous metal layer bonded to heat transfer surface substances (Figure 2). This is capable of increasing the boiling heat transfer coefficient by one order of magnitude. The boiling heat transfer resistance is reduced by trapping large

vapor nuclei (activation) surrounded by very thin liquid layers attached to the walls of the porous matrix.

In the multiple flooded bundle concept, the seawater would be in-tube, and the bundle would be flooded by the working fluid (Figure 3). This concept is essentially an extrapolation of the current state-of-the-art flooded bundle heat exchangers. It is desirable to make the bundles as large as possible, for economy in construction and manifolding. A limit of the allowable bundle diameter for a flooded, horizontal tube evaporator exists because the hydrostatic head of the liquid pool decreases the temperature difference available for heat transfer. Also, head required to feed the bundle with liquid becomes too great, so that the tubes at the top of the bundle dry out and become incooperative.

Our preliminary analysis shows that a bundle diameter in the neighborhood of 15 feet will operate with a tolerable hydrostatic head loss, and without dry-out. In our conceptual design (Figure 3), three levels of flooded bundles are shown. For the OTEC application, manifolding of the seawater is eliminated by exposing the tubesheet to the ocean environment. The working fluid would have to be manifolded as shown in the Figure. Since this concept is simply an extension of current practice to an optimum bundle dimension, there is no question of its practicality.

A single large sprayed bundle is inherently more compact than several flooded bundles which are its equivalent, for geometric reason. The average temperature difference in the flooded bundles is smaller than in sprayed bundles, because of the hydrostatic head loss.

### 2.2 Condenser

The concept suggested in the preliminary study for the condenser was a vertical shell-and-tube unit with the seawater tube-side and the working fluid condensing shell-side (Figure 4). It was proposed to enhance the condensing performance through the use of fluted tubing (1). In the chemical process industry, this type of enhancement has been successfully used to obtain condensing coefficients higher than those from horizontal units. The major unsolved condenser problems are those of manufacturing common with the evaporator (1). The functional problems experienced in the condenser relate to major distribution and purging, and appear to be minimal when compared to the evaporator.

### 2.3 Materials

The tube materials considered (1) were 90/10 cupronickel, titanium, and aluminum. The higher resistance to biofouling, which would be especially important in the evaporator, tends to give the cuprous alloys an edge over titanium. 90/10 cupronickel exhibits an excellent combination of corrosion resistance and biofouling resistance, and is currently considered the standard in seawater-cooled condensers. However, the cuprous alloys can not be used if ammonia is the working fluid because of stress corrosion cracking problems.

Aluminum is an attractive material for OTEC application because of its low cost, high thermal conductivity, and ease of fabrication into fluted or finned tubes. The reported corrosion results in seawater have shown great variability. For best results, aluminum needs careful treatment, including passivation, protection from heavy metals, and perhaps some form of anodic protection. Development work and corrosion tests under actual OTEC conditions are necessary to fully qualify aluminum.

Titanium is unparalleled in seawater corrosion resistance, is highly resistant to erosion even at high velocities and has exhibited a long maintenance-free lifetime. Because of the excellent corrosion resistance of titanium and its high strength, thin wall tubing can be used, affording good heat transfer properties and material savings. For these reasons, titanium was used in the design of the evaporator for this study.

In the condenser, it is generally felt that the corrosion and biofouling potential of the cold seawater is considerably less than that of the warm seawater experienced in the evaporator. For the same reason as in the evaporator, titanium was chosen for the design of the smooth tube condensers. Aluminum was chosen in the design of the fluted tube condensers because: (1) the lower corrosion and biofouling potential of the cold seawater may allow aluminum to exhibit a reasonable life, (2) the substantial cost saving of substituting aluminum for titanium, and (3) the ease of manufacturing a fluted aluminum tube compared to titanium as mentioned above.

Table 1 summarizes the material selection and characteristics for seawater application.

### 2.4 Optimization Results (Cycle Cost Support)

The OTEC cycle was optimized, assuming the use of particular heat exchangers, and the results for a 100 MWe OTEC power plant are shown in Table 2. The optimized total heat exchanger cost for the plain tube evaporator and condenser is $1,408/KW (evaporator $721/KW and condenser $687/KW). The High Flux evaporator and fluted aluminum condenser gave a heat exchanger cost of $942/KW (evaporator $528/KW and condenser $414/KW). This repesents a savings of $466/KW or 33%, on the heat exchanger costs (savings on evaporator $193/KW and condenser $273/KW) when the High Flux evaporator and fluted aluminum condenser are substituted for the plain titanium units.

## 3. Current Results

The current UCC/Linde OTEC effort includes an ERDA funded analytical-experimental program directed at the thermal and fluid flow performance of the heat exchangers, and UCC/Linde funded development work on the application of proprietary heat transfer enhancement devices to the OTEC heat exchangers.

### 3.1 Heat Transfer Enhancement Devices

An extensive in-house program to develop an

aluminum porous boiling surface applied to titanium s has been undertaken. The pool boiling perfore of these tubes in ammonia at 75°F is shown in Figure 5. The heat transfer coefficient is 6,500 Btu/(hr-ft$^2$-°F) at the heat flux of interest.

A proprietary condensation enhancement has also been studied for OTEC application. Details of this device must be witheld until a patent application is filed, but it is a surface tension motivated condensate film thinner which can be easily applied to the outer surface of tubes. The main advantage of this device is that it can be applied to titanium tubes, since it is questionable whether fluted titanium tubes can be produced economically. The performance of this condensation enhancement is shown in Figure 6. It shows a 2.7 improvement relative to the experimental performance of a smooth tube in ammonia at 75°F.

### 3.2 Thermal Hydraulics of the Condenser

It is well-known that in a large horizontal condenser bundle, the average performance of a tube located deep inside the bundle will be less than that of a single isolated tube because of condensate loading. These problems were discussed in reference (3). The Nusselt analysis gives:

$$h_{c,N} = h_{c,1} N^{-\frac{1}{4}}$$

where $h_{c,N}$ is the heat transfer coefficient of the $N^{th}$ tube in a vertical column. Several experimental studies (4, 5, 6) indicated that the Nusselt relation is severely conservative as shown in Figure 6. As pointed out by Bell and Mueller (3), the inviscid condensate tested in (4) and (5) require little or no correction for the bundle effect. Ammonia (the OTEC working fluid) certainly qualifies as an inviscid liquid since its viscosity at 75°F is only half that of R-11 (4) and one-third that of R-12 (5).

The performance shown on Figure 6 for Linde's horizontal tube enhanced condensation device is for 9X loading, which is the maximum loading possible in the apparatus (9X = liquid loading which corresponds to the 9th tube located in vertical column). It seems reasonable to accept the Young and Wolenbery data (Figure 7) as the means to extrapolate this data to higher degrees of loading. These heat transfer results will be incorporated into a program which considers tube diameter, tube arrangement and vapor distribution system to give the performance of the condenser for a specified phasing arrangement.

### 3.3 Flooded Bundle Model

The effort has been focused on developing a model for the thermo-hydraulic analysis of flooded horizontal tube bundles. The model considers both heat transfer and two-phase fluid flow in the bundles.

The method applied is that of subchannel analysis widely used in water-cooled nuclear reactor studies. The tube bundle is subdivided in small flow channels as schematically shown in Reference (7). The basic conservation equations: continuity, momentum, and energy, are written for each channel. These equations are coupled with empirical equations for the heat transfer coefficient (on the shell-side) for each expected heat transfer mechanism, for two-phase frictional pressure drop and for void fraction. Due to the possibility that liquid ammonia at the bottom of a bundle may be subcooled, the following shell-side heat transfer mechanisms are considered:

convective heat transfer to liquid
subcooled boiling under flow conditions
saturated boiling under flow conditions

The selection of the local heat transfer coefficient is based on the local flow conditions and the wall (tube) temperature. The in-tube heat transfer coefficient is given by the Dittus-Boelter equation.

The model predicts the enthalpy and the structure of the two-phase flow of the working fluid on the shell-side. Preliminary results are presented in Reference (7) and for that reason, are omitted here. As shown in Reference (7) (Page II-19, Figure IIA-7), the model predicts the hydrostatic head effect on the local saturation temperature. The dry out phenomenon can be predicted by the model.

### 3.4 Sprayed Bundle Model

The sprayed bundle evaporator is a shell-and-tube heat exchanger where hot fluid flows inside, and cold fluid is sprayed on the outside surfaces of the horizontal tubes. Depending on the characteristics of the surface and fluid, boiling can occur on the shell-side. Otherwise, heat is conducted through the liquid film to the liquid vapor interface where vaporization takes place.

A sprayed bundle model involves various two-phase phenomena such as liquid entrainment, liquid film stripping and deflection, dry patch formation, liquid jet disintegration, drop motion and evaporation. The distribution and motion of the liquid phase inside the sprayed bundle is the most important problem. Good design requires that tubes are completely wetted. Even at modest velocities, the vapor tends to deflect the liquid sideways as it drops from one row of tubes to another. As a result, dry areas may develop in the interior of the bundle. Increasing the supply of liquid can overcome the dry out problem, but liquid in excess of that required for vaporization must be collected and recycled through the evaporator, decreasing the useful power. An effective spray system, which will maintain the heat transfer surface wetted at minimum recycling ratio is the optimum point of the evaporator.

For thermo-hydraulic modeling, experimental data for the local flow and heat transfer conditions in the bundle are necessary. Several bench scale experiments were designed for that purpose, and the following results are being generated:

- Deflection of falling liquid in the direction of vapor flow.

- Liquid jet disintegration when exposed to the local vapor cross-flow.
- Minimum liquid flow rate to keep an evaporator tube completely wet for all possible local vapor conditions in the bundle.

The analytical model predicts the liquid-vapor interaction by establishing mass flow balances in successive elements of the tube field, for any specified arrangement of spray and heat transfer tubes. The above mentioned experimental data are used as input data to couple the vapor cross-flow rate to the deflection of the falling liquid. The model tests for complete tube wetting in each element of the tube field.

Predictions of the program will be checked against the $3.2 \times 10^6$ Btu/hr demonstration sprayed evaporator which has been designed and will be tested at Argonne National Laboratory at the end of 1977.

Use of the program will enable rapid prediction of the shell-side flow performance of sprayed bundles for various choices of tube layout and bundle size, spray feed geometry and thermal duty.

### 3.5 Large Bench Scale Experiments

The first sprayed bundle-related experimental data for liquid deflection and wetting were obtained using an air-water apparatus. Some of the data and the experimental apparatus are described in Reference (7).

Currently, a sprayed bundle test loop is being constructed, using ammonia as the test fluid. A 12-tube bundle will be fed with liquid ammonia and exposed to transverse vapor ammonia flow of up to 10 ft/sec. The heat transfer performance of an instrumented tube, and the liquid deflection will be measured. The minimum liquid flow required to keep the instrumented tube fully wetted will be determined.

## 4. Core Test Heat Exchangers

The specific objective of this task is to design, fabricate, deliver and support the testing of the following (pilot scale) core test heat exchangers:

- Flooded Bundle Evaporator - Mark I
- Sprayed Bundle Evaporator - Mark I
- Horizontal Condenser - Mark I

All three units will feature enhanced heat transfer surfaces, which will be tested for their heat transfer and hydraulic performance by Argonne National Laboratories (Argonne, IL).

### 4.1 Flooded Bundle Evaporator

A Linde-developed computer program was employed for the thermal design of this unit. This effort basically involved a parametric study, searching for an optimum combination of a number of tubes, tube length and water velocity in the tubes (between 4 to 8 ft/sec) while constraining the search by imposing a required pumping power/kilowatt thermal. Tube diam and the required pumping power were previously esta lished by system optimization.(1).

The evaporator is conceptually shown in Figure 8. It is basically a shell-and-tube heat exchanger with fixed tube sheets and a three-pass tube side. The working fluid, ammonia, is on the shell-side, flooding the tubes which carry the "warm" water inside. Titanium tubes (1.5" O.D. x 1.430" I.D. x 84" long), incorporating Linde's High Flux boiling surface on the outside and plain surface on the inside, are utilized.

The shell, bonnets and tubesheets are carbon steel with titanium-cladding on that side of the tubesheets where the tubes are seal-welded. A protective coating is applied inside of the bonnets (water side) to minimize rust and galvanic corrosion. As noted in the figure, sufficient pipe nipples at selected locations are provided for temperature, pressure and liquid level sensor installations. The 2" nipples at the bonnets will be utilized for single-tube heat transfer measurements, in the future only; not for the initial demonstration tests.

Further pertinent nominal design and operating conditions are listed below:

| Design/Operating Parameter | |
|---|---|
| Number of Tubes | 279 |
| Effective Outside Heat Transfer Area | 685 $Ft^2$ |
| Shell Inside Diameter | 49 inches |
| Heat Duty | $3.2 \times 10^6$ Btu/Hr |
| Ammonia Boiling Temperature | $72^oF$ |
| Water Inlet Temperature | $80^oF$ |
| Water Outlet Temperature | $78^oF$ |
| Overall Heat Transfer Coefficient(1) (No Tube Side Fouling, but S.F.=1.?) | 709 Btu/Hr-$Ft^2$-$^oF$ |
| Mean Water Velocity in Tubes | 6.8 Ft/Sec |
| Overall Heat Exchanger $\Delta P$ | 1.75 psid |
| Shell-Side Design Pressure | 215 psig |
| Tube-Side Design Pressure | 100 psig |

(1) Referenced to outside tube surface area.

### 4.2 Sprayed Bundle Evaporator

The same computer program and experimental heat transfer data used for the flooded bundle heat exchanger was also employed for the thermal design of the sprayed bundle unit; except that design criteria from vapor/liquid displacement tests using air and water to simulate ammonia vapor/liquid interaction, were incorporated to ensure that the tubes would remain fully wetted.

The conceptual drawing of this unit is shown in Figure 9. It is a new type of shell and tube heat exchanger where "hot" fluid (water) flows inside the tubes onto which liquid ammonia is sprayed from perforated tubing strategically located throughout the tube bundle. Titanium tubes (1.5" O.D. x 1.43" I.D. x 50" long), incorporating Linde's High Flux boiling surface on the outside and plain surface on the inside, wil

be used. Plain tubing is utilized for the spray tubes. Arrangement of the spray tubes in relation to the functional tubes in the bundle is shown in Figure 10.

The shell, bonnets and tubesheets are carbon steel and Ti-cladding is provided on those sides of the tubesheet where the tubes are seal-welded. Nominal design and operating conditions are listed below:

Design/Operating Parameters

| | |
|---|---|
| Number of Heat Transfer Tubes | 388 |
| Number of Spray Tubes | 81 |
| Shell Inside Diameter | 71 inches |
| Heat Transfer Area, | 589 $Ft^2$ |
| Overall Heat Transfer Coefficient(1) | 782 $Btu/Ft^2\text{-}Hr^oF$ |
| Heat Duty | $3.2 \times 10^6$ Btu/Hr |
| Ammonia Boiling Temperature | $72^oF$ |
| Water Inlet Temperature | $80^oF$ |
| Water Outlet Temperature | $78^oF$ |
| Water Velocity in Tubes | 6.87 Ft/Sec |
| Water Side Pressure Drop | 2 psid |

(1) No tube-side fouling but S.F. = 1.2.

4.3 Horizontal Condenser

A parametric thermal design study for the Horizontal Condenser* was conducted, which included a preliminary cost analysis for the various designs. This effort basically involved comparing heat transfer performance and fabrication costs between heat exchangers utilizing aluminum tubes of differing outside diameters having either plain, straight-longitudinal fins, or spiral-longitudinal fins on the inside. Heat transfer and fluid friction correlations from Reference (8) were utilized for the tube-side; while for the shell-side, experimentally established condensing enhancement (3.5 times the classical Nusselt coefficient) was employed.

In all cases, Linde's proprietary outside (condensation) enhancement was assumed. Pumping power/$KW_{th}$, approach-$\Delta T$ and other nominal design operating conditions** remained constant. Even though tubes with spiral fins exhibited maximum performance (highest overall heat transfer coefficient - minimum surface area for the given pumping power/ $KW_{th}$), the excessive tubing cost precluded its use in the core test condenser. The reduction in surface area, due to the higher-performing spiral fins did not result in a significant decrease of overall heat exchanger cost. The higher cost is characteristic of this particular process: spiral-finned tubes are forged; while straight-finned tubes are generally extruded--a significantly less costly operation.

A conceptual drawing of the horizontal condenser is presented in Figure 11. It is basically a shell-and-tube type heat exchanger with fixed tubesheets, featuring a single-pass tube and shell-side. The ammonia vapor condenses on the outside of 3102 alloy aluminum tubes (1.50" O.D.*x 1.37" I.D.*x 163" Long). They are longitudinally straight-finned on the inside and incorporate Linde's external condensation enhancement. A cross-section of the condenser tube is shown in Figure 12. The external enhancement is not shown for proprietary reasons.

* Linde's standard Condenser Computer Program was utilized which accounts for inside-fin-tube geometries and Linde's external-tube (condensation) enhancement.

** Consistent with OTEC environment.

4.4 Heat Exchanger Test Flow Loop

The purpose of the flow loop is to test the core test heat exchangers at design (representative OTEC environment) and off-design conditions. The primary measurements will be the overall heat transfer coefficient and the pressure loss for the units. The experiments will be conducted by Argonne National Laboratories (ANL), which is presently constructing the facility. It was developed by ANL in collaboration with Lester B. Knight & Associates and features several ideas, previously established by Gilbert Associates.

This facility, schematically shown in Figure 13, basically encompasses a closed warm water loop, a closed ammonia cycle and a closed cold water circuit. The warm water loop consists essentially of the subject evaporator, a water heater (steam), a storage/surge tank, and a circulating pump. The heat input to the test unit will be determined indirectly by the heat exchanged in a by-pass loop containing the steam water heater, thereby guaranteeing a sufficiently large $\Delta T$ (approximately $20^oF$) for more accurate measurements. This heat input is verified on the ammonia side from the flowrate and enthalpy change (temperature and pressure measurements) determinations.

The ammonia cycle features a demister, an expansion valve, a spray desuperheater (for decreasing the ammonia from its boiling - to condensing temperature), liquid return pumps and , of course, the test evaporator and condenser, which are common to both loops.

The closed water loop encompasses the subject condenser, a chiller for conditioning the water inlet temperature, a storage/surge tank and a circulating pump.

The test loop is extensively instrumented for the heat transfer and fluid flow measurements. Controls are incorporated for regulating the heat input, water/ammonia flows, inlet water temperatures to the evaporator and condenser and ammonia temperatures.

The test matrix shown in Table 3 summarizes the initial experiments planned for nominal and near-nominal operating conditions. Reproducibility will be verified with repeat-tests. It should be noted that the evaporator and condenser must be tested independently at their respective conditions.

However, they will operate simultaneously. In other words, adjusting the evaporator's parameters (i.e., water flow, water inlet temperature and ammonia

* Nominal diameter.

boiling temperature )automatically fixes the condenser's operating conditions (which are not necessarily according to the test matrix). Similarly, subjecting the condenser to the desired running conditions, will cause the evaporator to seek its own operating level

Following Phase I testing, ANL has planned to characterize these units at off-nominal conditions by varying the warm water inlet temperature over an extended $76^{o}F$ to $85^{o}F$ range, changing the cold water inlet temperature between $35^{o}F$ and $44^{o}F$ and altering the water flowrate within possibly 2,000 and 8,000 GPM. The corresponding heat duty will then vary between $2.2 \times 10^{6}$ and $4.2 \times 10^{6}$ Btu/Hr. Single tube heat transfer measurements with individual water and ammonia film coefficient determinations are also considered as part of the latter test group.

List of References


1. A. M. Czikk et al, "Ocean Thermal Power Plants Heat Exchangers--Final Report, UCC-Linde Division, Tonawanda, NY, May 21, 1977, (Available from NTIS, U.S. Dept. of Commerce, Springfield, VA 22161).

2. A. E. Bergles, Private Communication, (Seminar on Augment Heat Transfer, UCC-Linde), Feb. 1977.

3. K. J. Bell and A. C. Mueller, "Condensation Heat Transfer and Condenser Design", AIChE Series, 1971.

4. B. E. Short and H. E. Brown, in "Proceedings of the General Discussion on Heat Transfer," Section I, pp. 27-31, Am. Soc. Mech. Engrs. and Inst. Mech. Engrs, (London), 1951.

5. F. L. Young and W. J. Wohlenberg, Trans. Am. Soc. Mech. Engrs, 64, No. 11, pp. 787-794, 1942.

6. D. O. Kern, "Mathematical Development of Tube Loading in Horizontal Condensers," AIChE Journal, Vol. 4, No. 2, pp. 157, 1958.

7. First, Second and Third Quarterly Report Submittal to ERDA from UCC-Linde Division, Tonawanda, NY (Sept. 30, Jan. 19, April 12, 1977), OTEC Contract E(49-18) 2448, (Sections written by E. N. Ganic.)

8. A. P. Watkinson and D. L. Miletti, "Heat Transfer and Pressure Drop of Forge-Fin Tubes in Turbulent Water Flow," Noranda Research Center, Point Claire, Quebec, Internal Report No. 255, January 1977.


Acknowledgements


Some of the current research program is sponsored by the Energy Research and Development Administration, Contract # E(49-18)2448. The preliminary study results presented here and in reference (1) were supported by the National Science Foundation, Grant # 43441-RANN.

The work on the UCC proprietary condensation enhancement was done by Dr. C. F. Liao.

TABLE 1

SUMMARY OF MATERIAL AND HEAT EXCHANGER PARAMETERS FOR SEAWATER SERVICE

| ITEM | TITANIUM | CUPRO-NICKEL | ALUMINUM |
|---|---|---|---|
| A. Corrosion Properties | | | |
| 1. General Corrosion Rate | Nil | 0.1 - 0.5 MPY | .055 - .333 MPY |
| 2. Pitting Rate | Nil | 1 - 5 MPY | .30 MPY - 13.9 MPY |
| 3. Crevice Corrosion Resistance | Excellent | Good | Poor |
| 4. Galvanic Corrosion Resistance | Excellent | Good | Poor |
| 5. Erosion Corrosion Resistance | Excellent | Good | Fair |
| B. Fouling Resistance | Poor | Excellent | Poor |
| C. Heat Exchanger Parameter | | | |
| 1. Configuration | Shell & Tube with Seawater on Tube Side | Shell & Tube with Seawater on Tube Side | Shell & Tube with Seawater on Tube Side |
| 2. Velocities (Recommended) | 4 fps - 20 fps | 4 fps - 8 fps | 4 fps - 12 fps |
| 3. Lifetime assuming corrosion is limiting | Unlimited | 5 - 30 Years | 1 - 10 Years |
| 4. Dimensions | .75" OD Min. x .028" Wall | .75" OD Min. x .070" Wall | .75" OD Min. x .070" Wall |
| 5. Evaporator Suitability | Fair Good | Excellent,(1) Fair(2) | Poor Fair |
| 6. Condenser Suitability | Excellent | Very Good,(1) Fair(2) | Fair |

Notes: 1) Propane as working fluid
2) Ammonia as working fluid

TABLE 2

100 MW OTEC POWER PLANT

Tube Diameter = 1½", $T_h$ = 79.75°F, $T_c$ = 46.5°F

| | Case 1 | Case 2 |
|---|---|---|
| **Work:** | | |
| Net MWe | 100 | 100 |
| Cold Water Work MWe | 8.20 | 9.20 |
| Warm Water Work Mwe | 5.46 | 7.02 |
| Working Fluid Work MWe | 2.88 | 2.89 |
| Gross Power MWe | 116.54 | 119.11 |
| Net Cycle Eff % | 2.357 | 2.362 |
| **Evaporator:** | | |
| Type of Tube | Plain Titanium | High Flux Titanium |
| Approach °F | 7.567 | 7.802 |
| Range °F | 2.285 | 2.111 |
| $PP/KW_{th}$ | .001284 | .001658 |
| No. of Tubes | 524700 | 401800 |
| Length Ft | 34.06 | 23.46 |
| Area x $10^6$ sqft | 7.018 | 3.702 |
| Heat Duty x $10^{10}$ Btu/Hr | 1.453 | 1.446 |
| LMTD °F | 6.546 | 6.884 |
| U Btu/Hr-Sqft-°F | 316 | 567 |
| Seawater Velocity Ft/Sec | 4.84 | 6.81 |
| Shell Diameter Ft | 65.1 | 57.0 |
| Cost $/KW | 721 | 528 |
| **Condenser** | | |
| Type of Tube | Plain Titanium | Fluted |
| Approach °F | 7.577 | 6.873 |
| Range °F | 2.359 | 2.688 |
| $PP/KW_{th}$ | .001218 | .001626 |
| No. of Tubes | 521800 | 442200 |
| Length Ft | 34.28 | 28.36 |
| Area x $10^6$ sqft | 7.024 | 4.925 |
| Heat Duty x $10^{10}$ Btu/Hr | 1.414 | 1.406 |
| LMTD °F | 6.631 | 5.653 |
| U Btu/Hr-Sqft-°F | 304 | 505 |
| Seawater Velocity ft/sec | 4.59 | 5.89 |
| Shell Diameter Ft | 62.2 | 57.25 |
| Cost $/KW | 687 | 414 |
| **Total:** | | |
| Heat Exchanger Cost $/KW | 1408 | 942 |
| $Sqft/KW_e$ | 140.42 | 86.27 |

---

$T_h$ - Source Temperature.

$T_c$ - Sink Temperature.

TABLE 3

PHASE I TEST MATRIX

| DEMONSTRATION UNIT | HEAT DUTY, Q (BTU/HR) | $H_2O$ INLET TEMP., $T_i$ ($^oF$) | $H_2O$ FLOWRATE, $W_{H_2O}$ (GPM) | $NH_3$ BOILING/CONDENSING TEMPERATURE, $T_{NH}$ ($^oF$) |
|---|---|---|---|---|
| EVAPORATOR | $3.2 \times 10^6$ | 80 | 3200 | 72 |
| | $4.0 \times 10^6$ | 82 | 3200 | 72 |
| | $3.2 \times 10^6$ | 80 | 3200 | 72 |
| | $2.4 \times 10^6$ | 78 | 3200 | 72 |
| | $3.2 \times 10^6$ | 80 | 3200 | 72 |
| CONDENSER | $3.2 \times 10^6$ | 40 | 3200 | 48 |
| | $4.0 \times 10^6$ | 42 | 3200 | 48 |
| | $3.2 \times 10^6$ | 40 | 3200 | 48 |
| | $2.4 \times 10^6$ | 38 | 3200 | 48 |
| | $3.2 \times 10^6$ | 40 | 3200 | 48 |

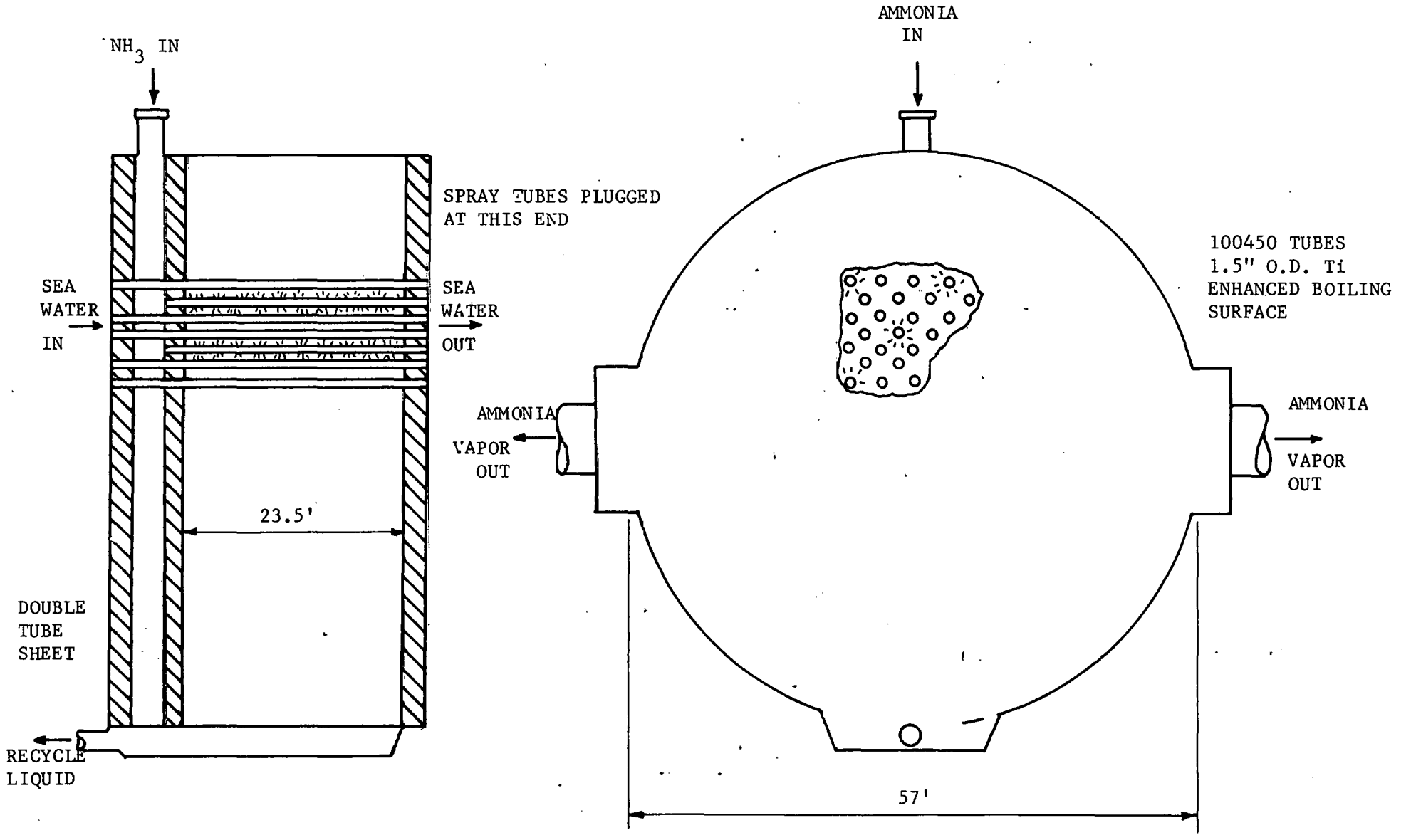
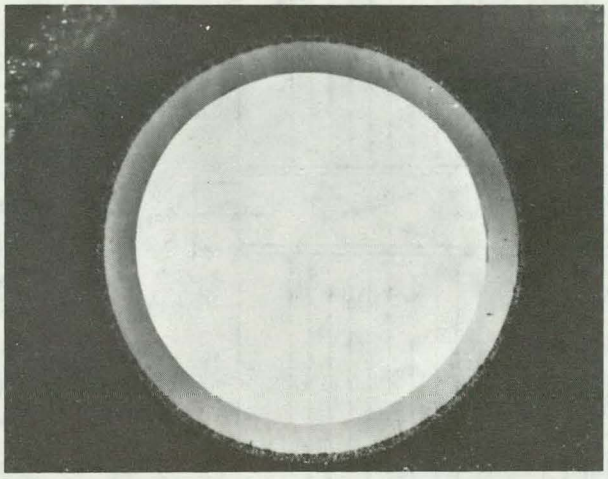


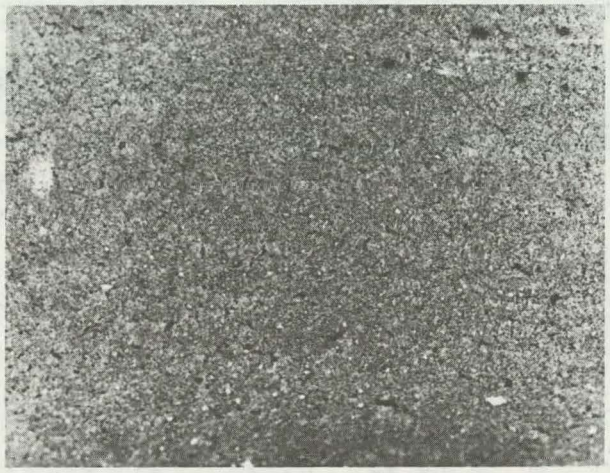

FIGURE 1 25 MWe EVAPORATOR MODULE

# PHOTO MICROGRAPHS OF POROUS COATED TUBING



1/2 DIA. TUBE

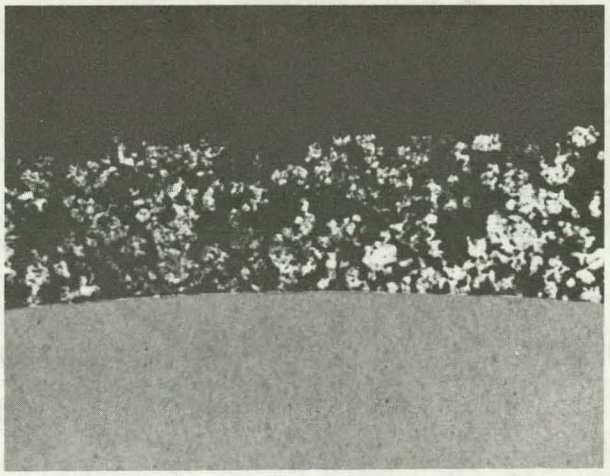
12X



EXTERNAL VIEW

OF COATING

20X



CROSS SECTION

OF TUBE & COATING

200X

FIGURE 2

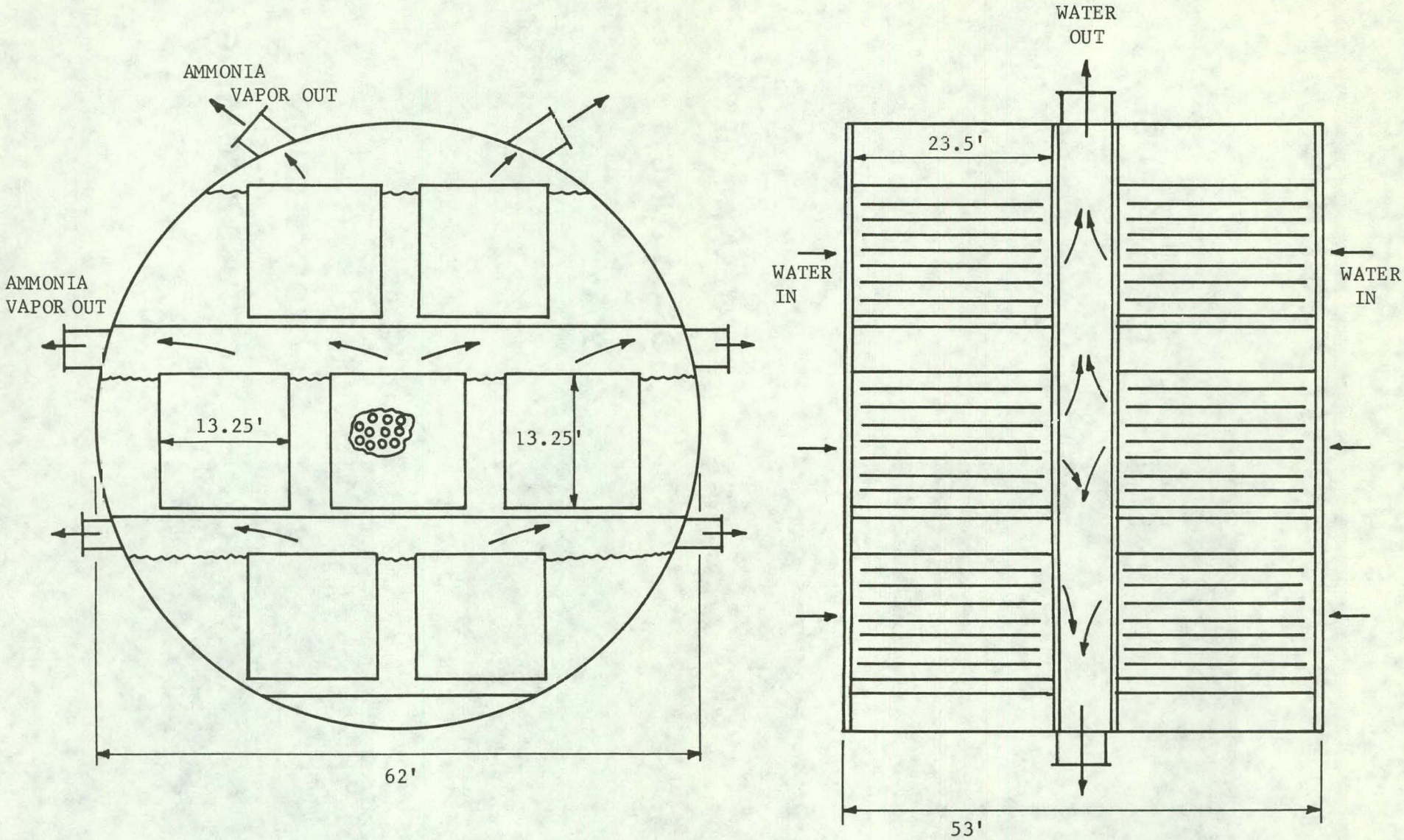





FIGURE 3

25 MWe EVAPORATOR MODULE
MULTIPLE FLOODED HIGH FLUX BUNDLES

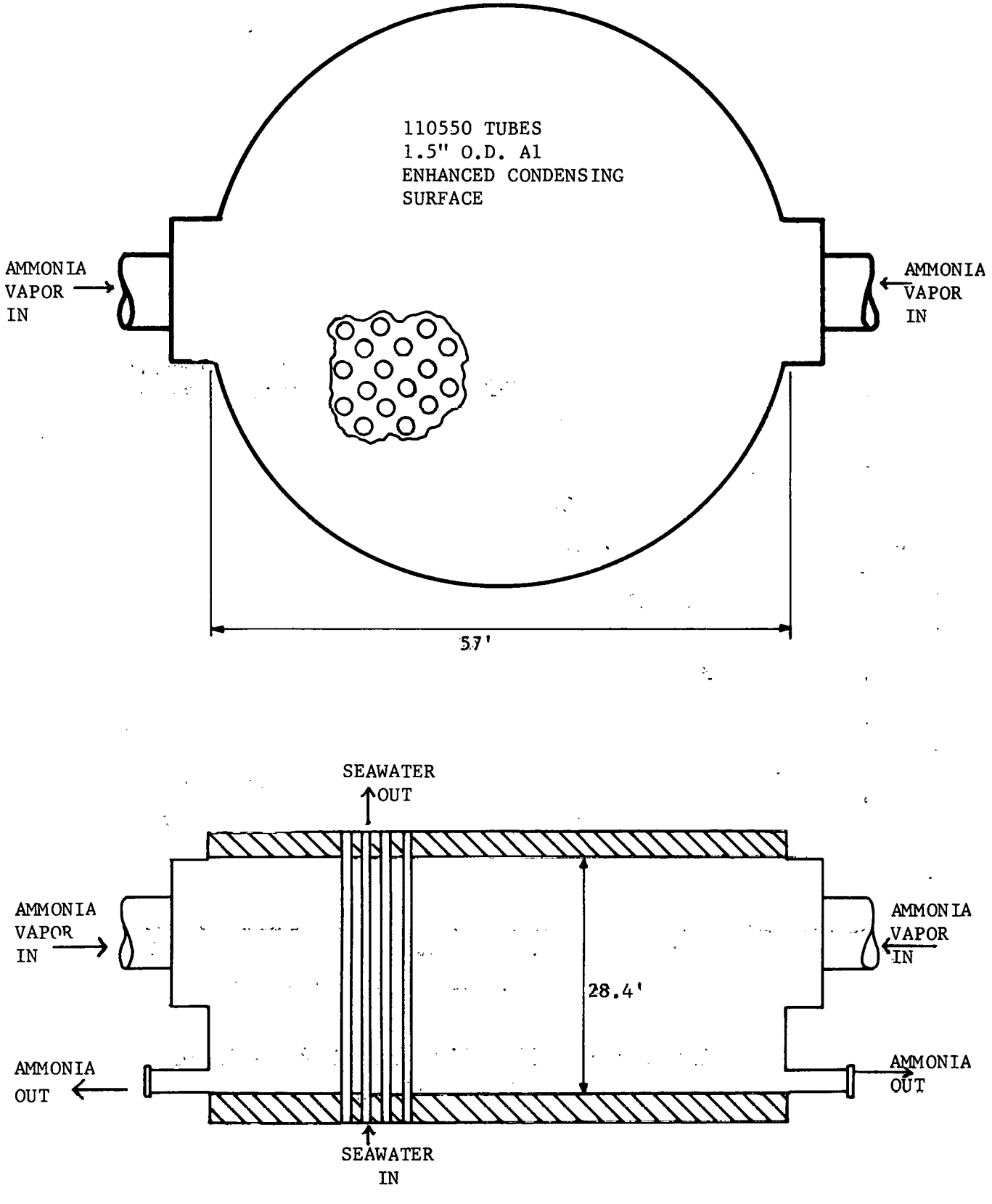



FIGURE 4 - 25 MWe CONDENSER MODULE

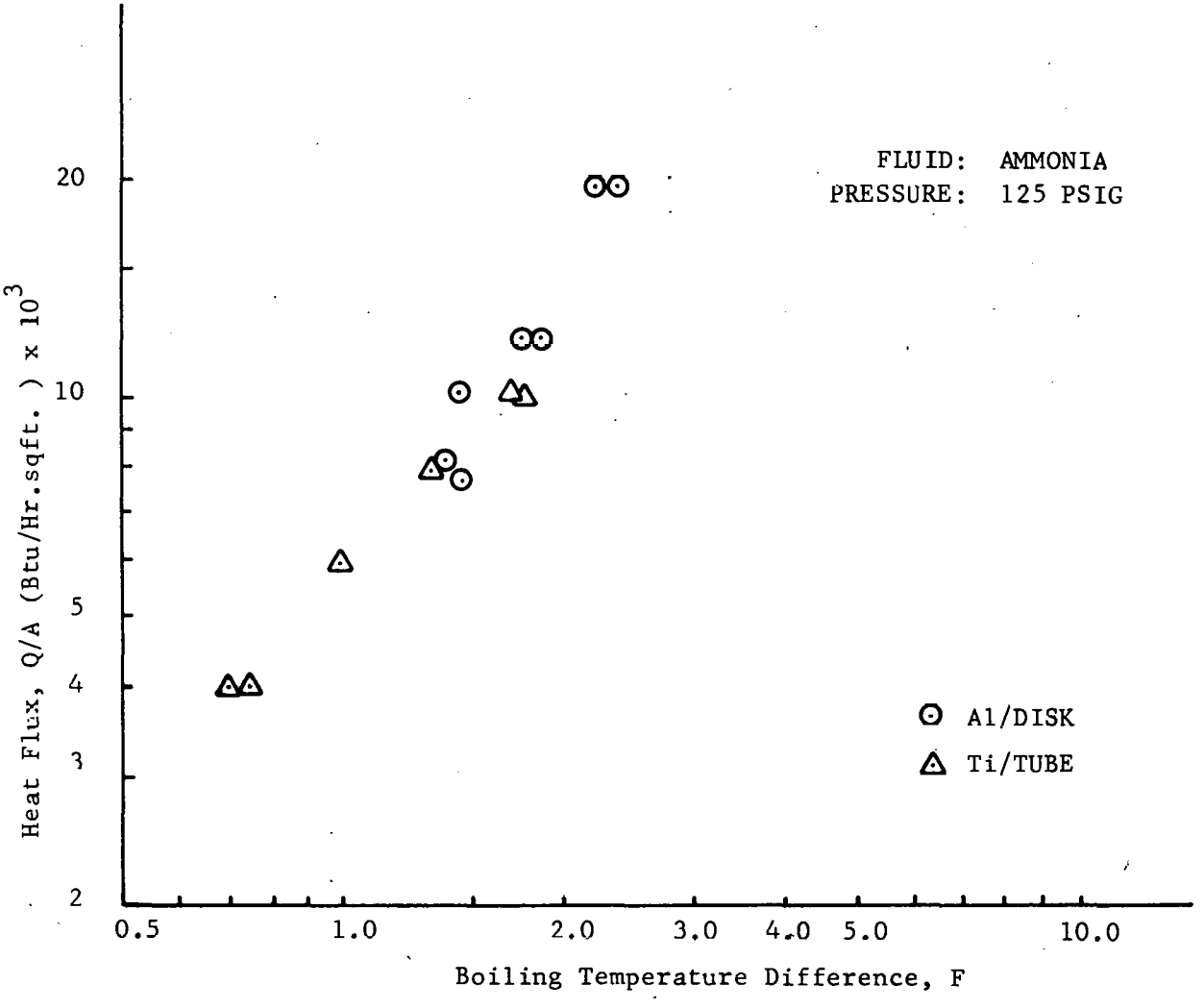



FIGURE 5 - ALUMINUM HIGH FLUX EVAPORATIVE SURFACE POOL-BOILING DATA

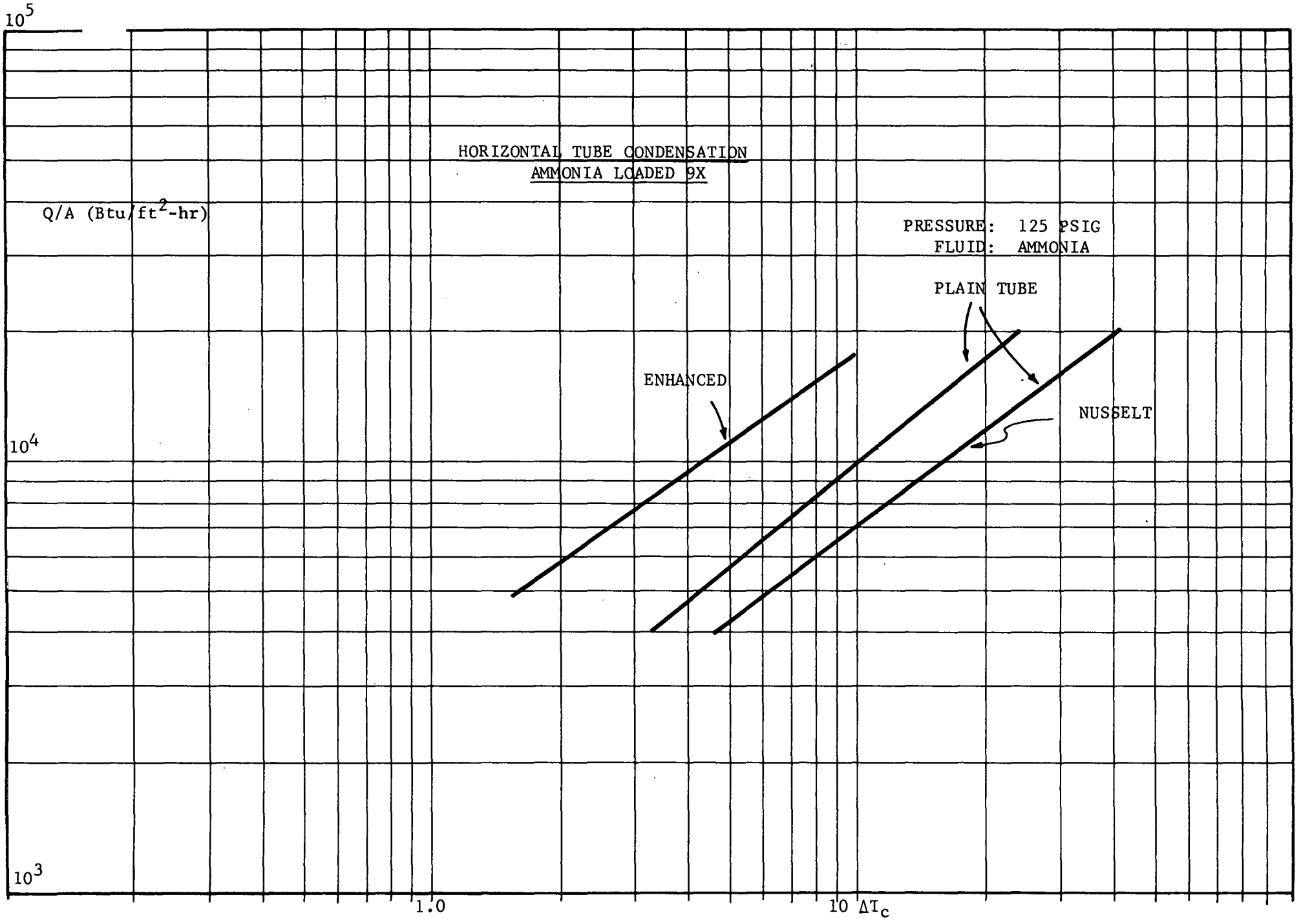



FIGURE 6 - HEAT FLUX VS. TEMPERATURE DIFFERENCE

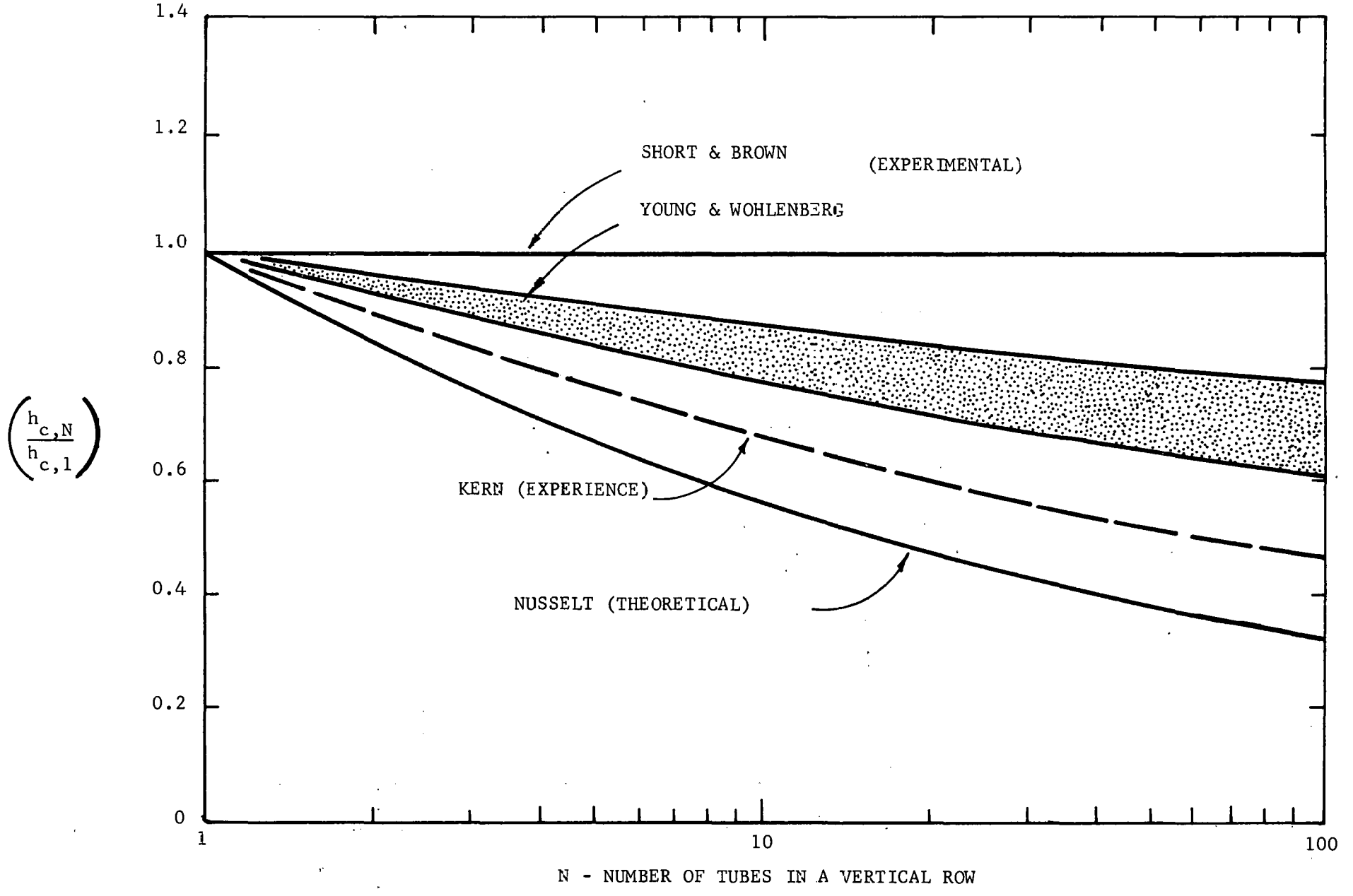
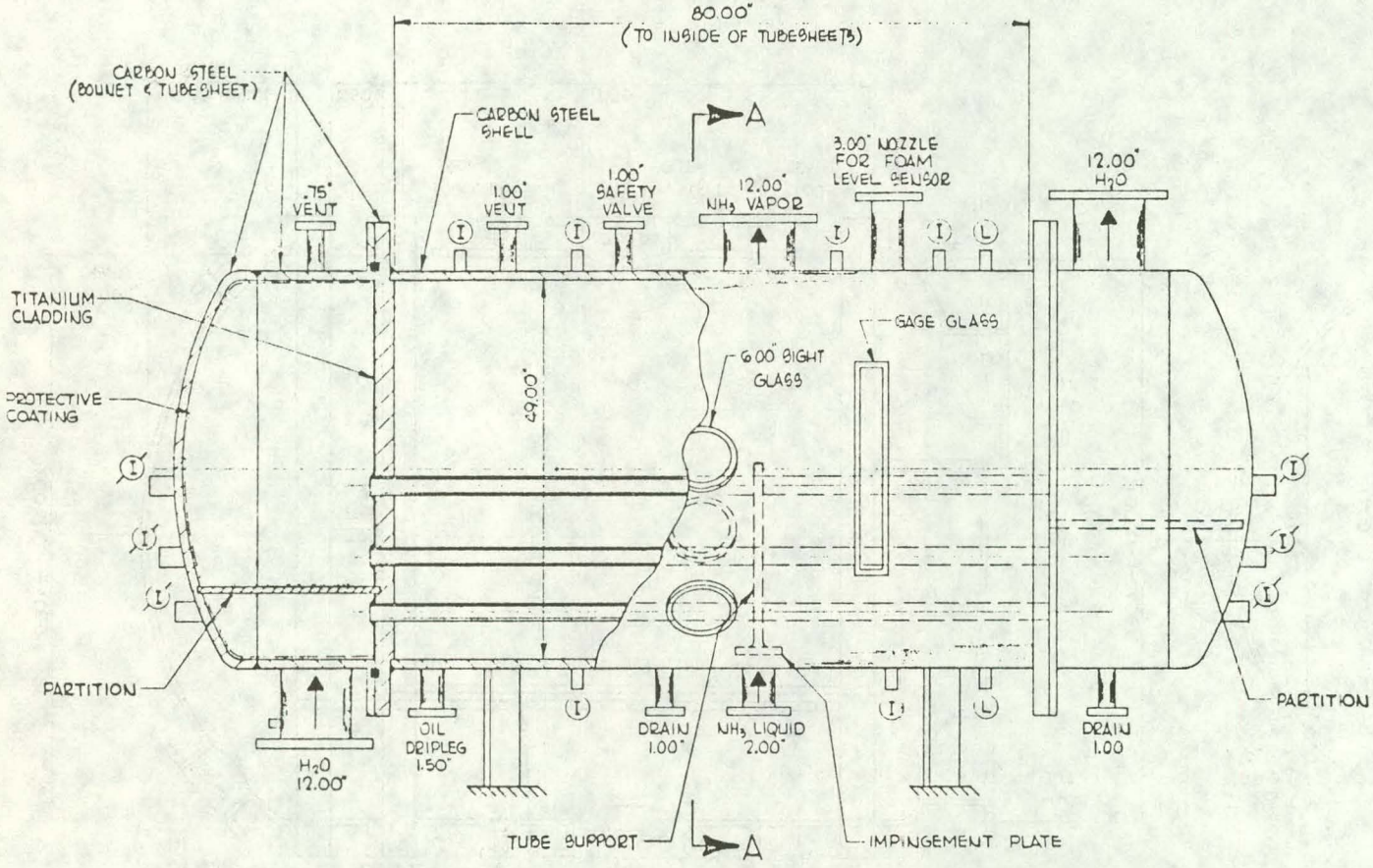
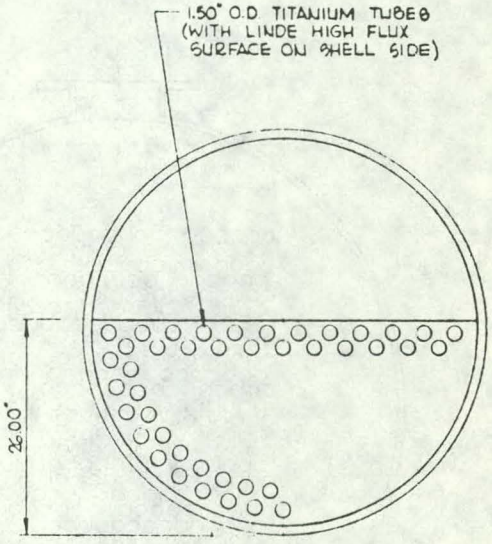



FIGURE 7 THE CORRECTION TO THE NUSSELT EQUATION FOR NUMBER OF TUBES IN A VERTICAL ROW (3)

ALL DIMENSIONS IN INCHES



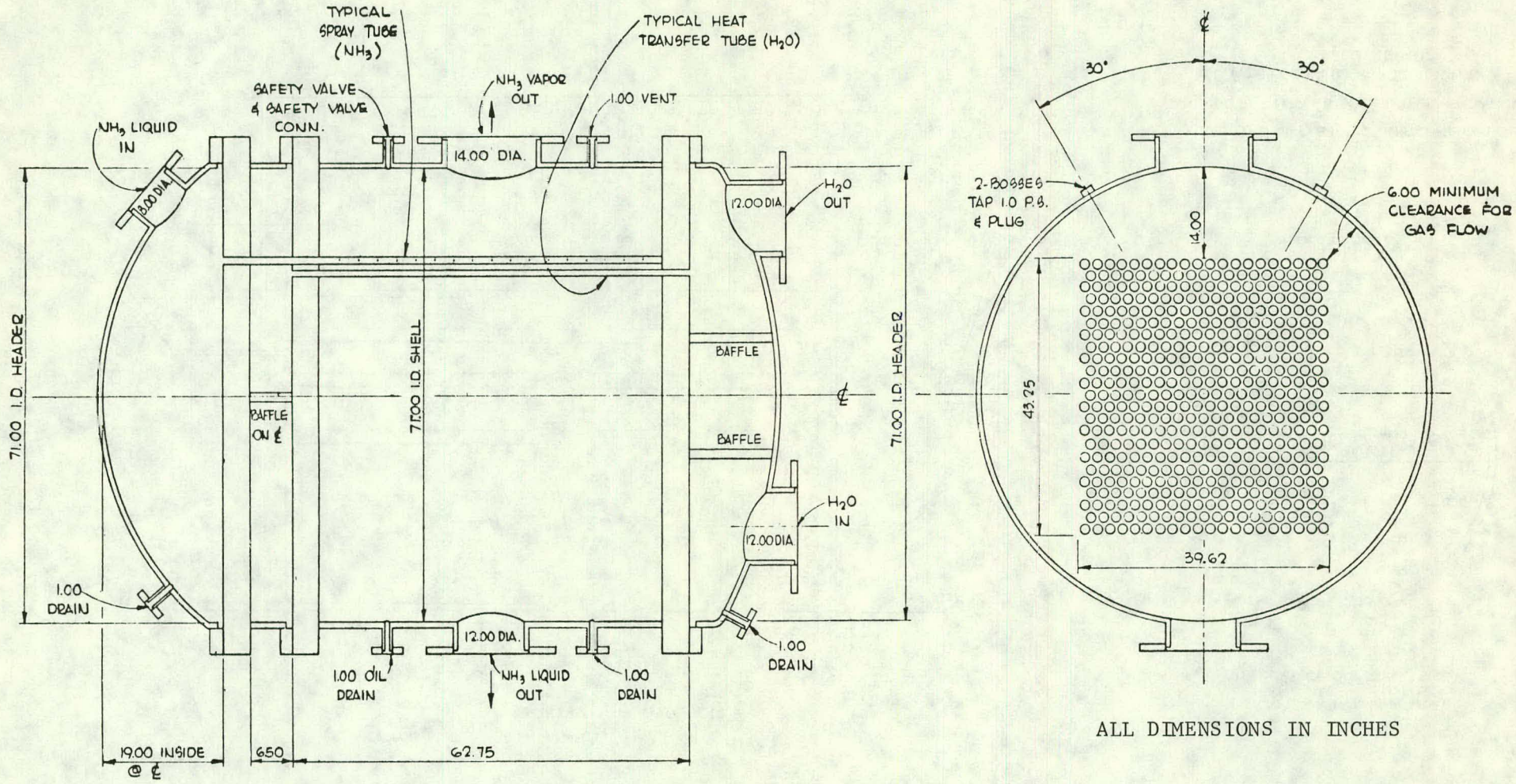

SECTION "A-A"

FIGURE 8 - FLOODED BUNDLE CORE TEST EVAPORATOR

(I) (6) 2" NIPPLES FOR INSTRUMENTATION

(I) (6) 1" NIPPLES FOR INSTRUMENTATION

(L) (2) .75" COUPLINGS FOR LIQUID LEVEL SENSOR




ALL DIMENSIONS IN INCHES

FIGURE 9 - SPRAYED BUNDLE EVAPORATOR

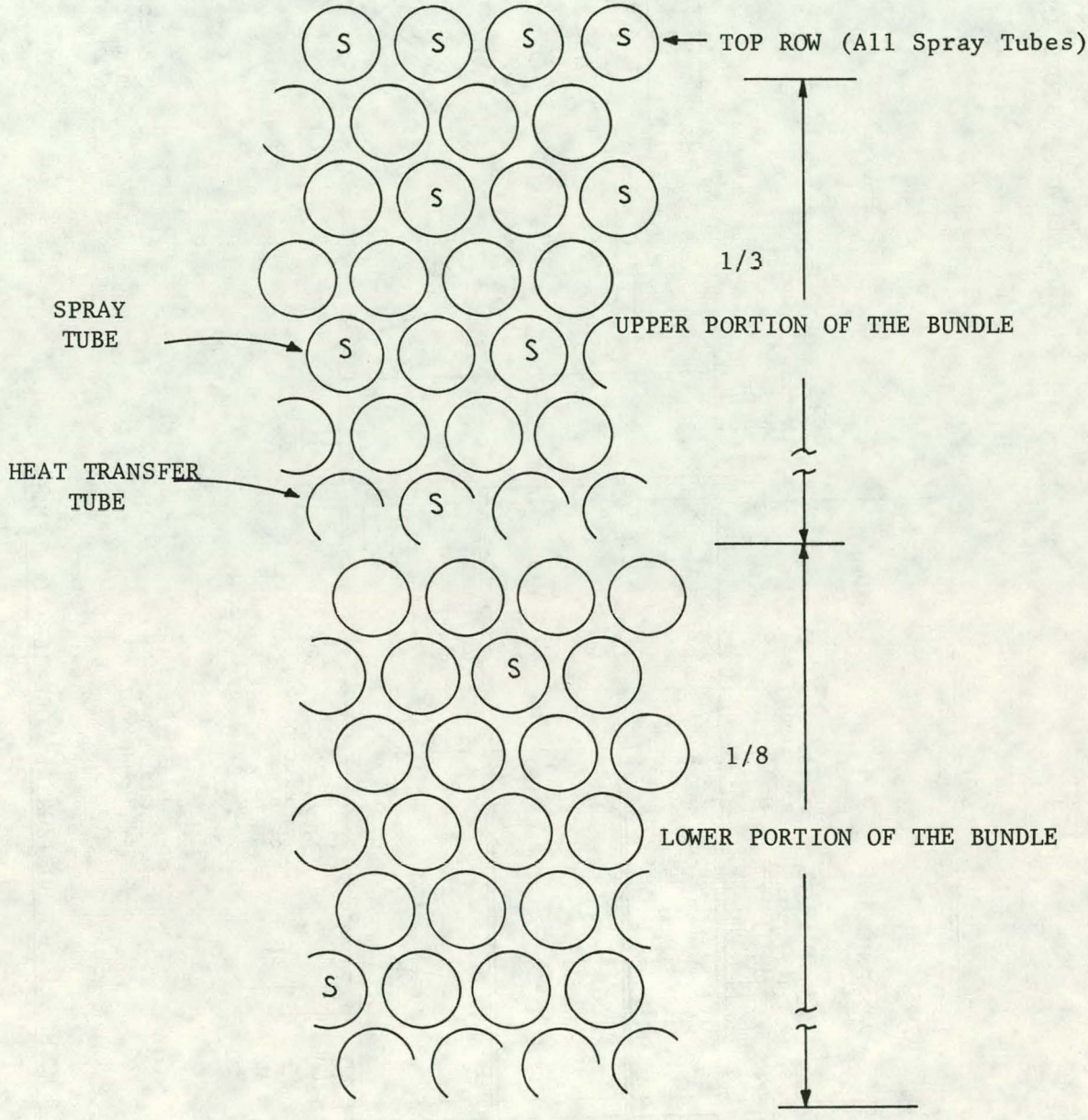



FIGURE 10 - SPRAYED BUNDLE TUBE ARRANGEMENT

ALL DIMENSIONS IN INCHES

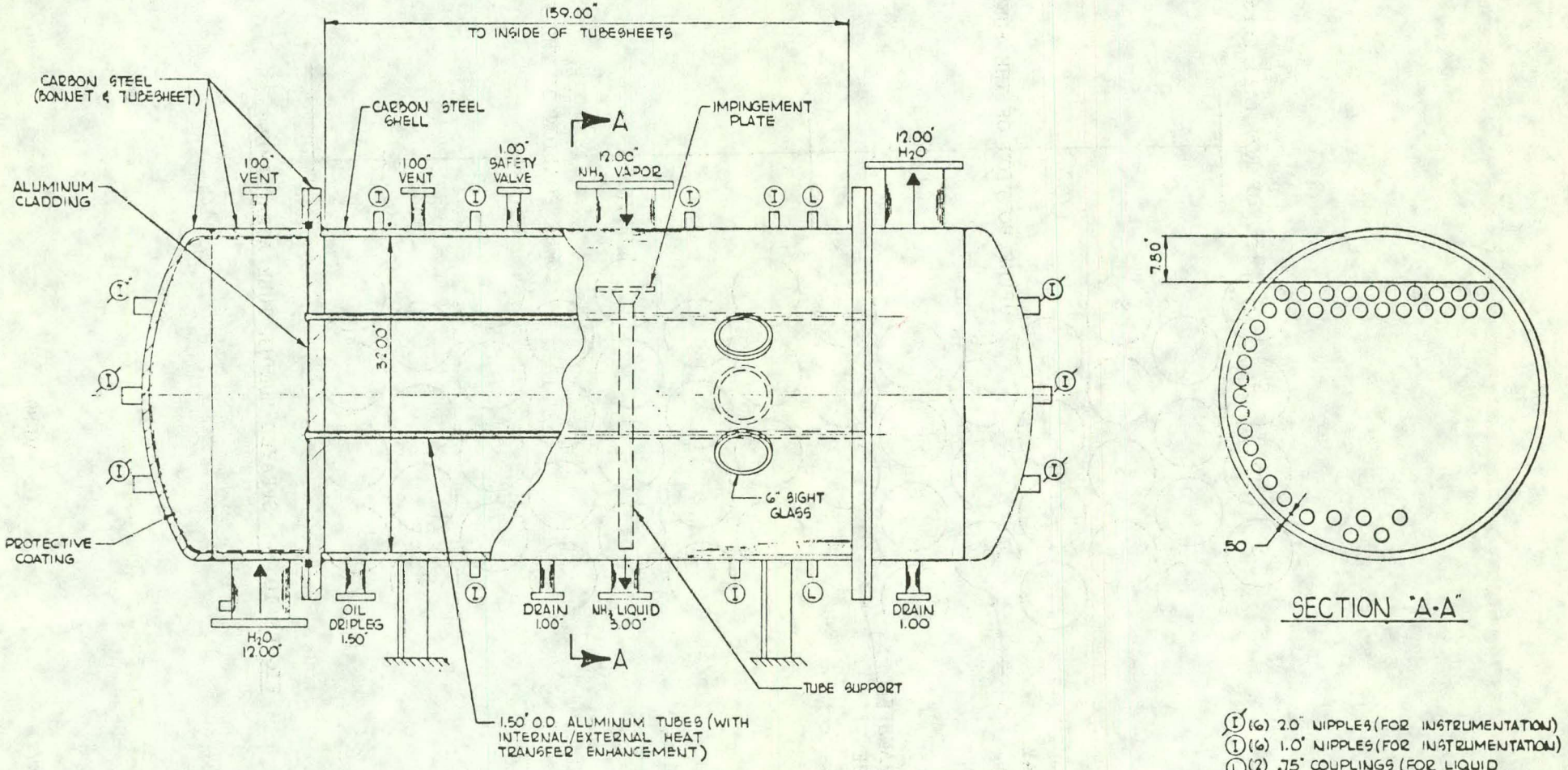



FIGURE 11 - HORIZONTAL CORE TEST CONDENSER

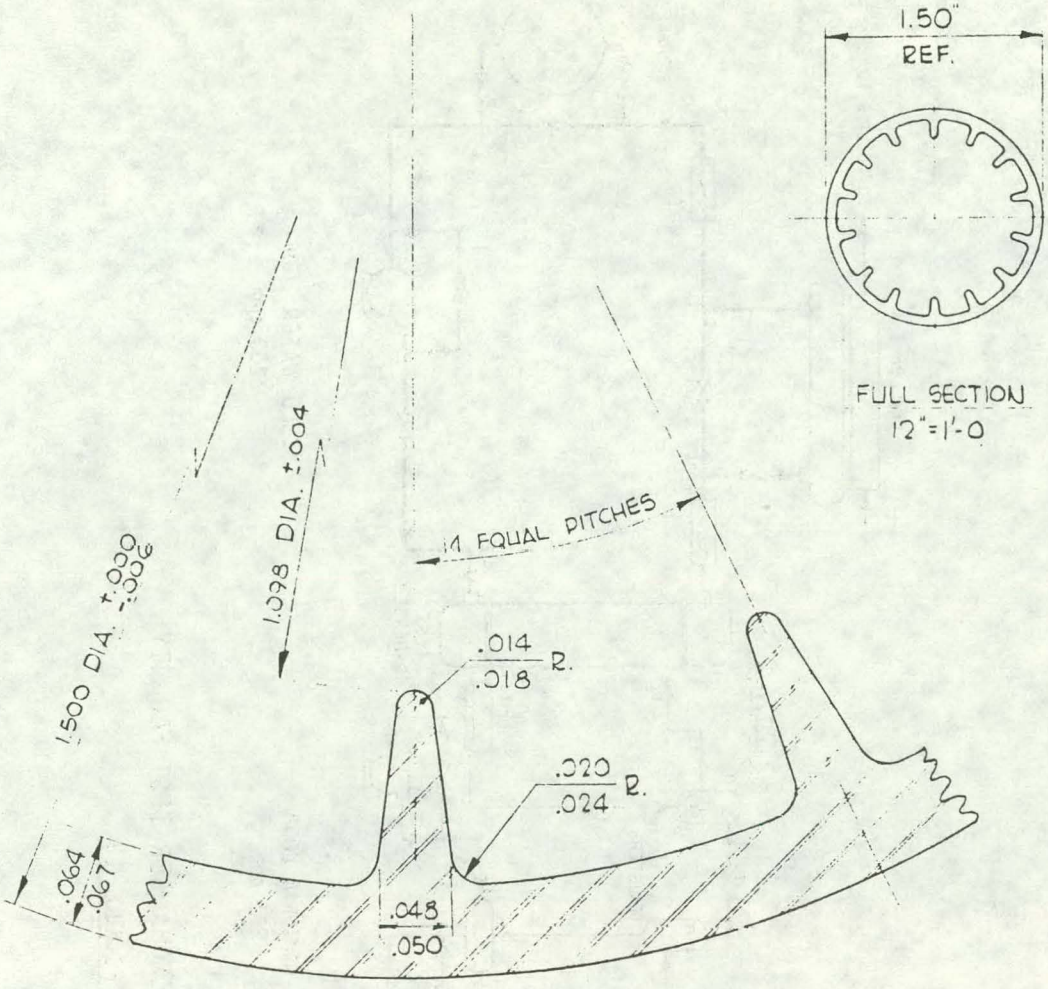
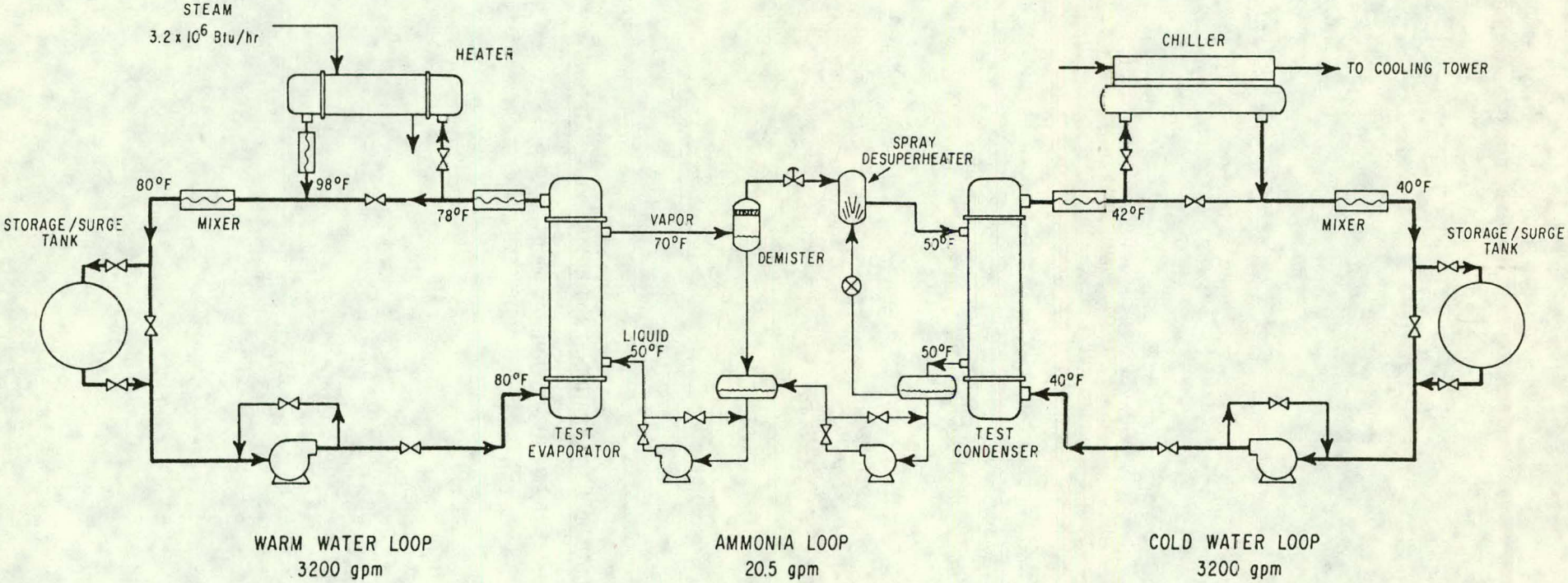



FIGURE 12 - CONDENSER TUBE CROSS-SECTION

(Condensation Enhancement Not Shown)




OTEC HEAT EXCHANGER TEST FACILITY

FIGURE 13

# HEAT TRANSFER ENHANCEMENT FOR EVAPORATORS

C. M. Sabin and H. F. Poppendiek
*Geoscience Ltd.*
*410 South Cedros Avenue*
*Solana Beach, California*

Abstract

Geoscience Ltd has been conducting an exploratory program for about two years on the enhancement of heat transfer conductances of water flowing through round tubes and ammonia boiling over horizontal submerged tubes. Recently a third task, a study of ammonia film evaporation, has been added to the program.

The ammonia boiling work has been directed toward the identification of tube surface modifications which, in addition to high heat transfer conductance, exhibit nucleation at very low temperature difference and uniform long term behavior. Several surfaces which satisfy these criteria have been found. The performance of one particular surface modification, consisting of two layers of woven screen, is described.

The water heat transfer conductance enhancement work has been undertaken on two different concepts. Both utilize only the tube wall itself for heat transfer surface, so that the effects of modifications are hydrodynamic. In one concept, inserts modify the flow adjacent to the tube wall to increase radial transport by relatively large scale motions. In the other concept, the laminar sublayer adjacent to the tube wall is disturbed by surface treatment. For higher Prandtl modulus fluids, such as water, in Reynolds modulus ranges of interest to OTEC, the reduction of the thermal resistance in the laminar sublayer can be significant if this layer is partially destroyed. One such surface modification, consisting of thin annular rings, is described together with its performance.

The potential impact of enhancement techniques is described. It is shown that under some circumstances, significant heat transfer area reductions result from application of these techniques.

## Introduction

Geoscience has a contract with ERDA to investigate enhancement of heat transfer conductances in the OTEC plant vapor generator.

The program consists of three parts. One part is related to the heat transfer from water flowing through round tubes; another part to the vaporization of ammonia over submerged horizontal tubes; and the third part is related to the vaporization of ammonia in thin films flowing over horizontal tubes. The thin film work is in its initial stages and is not described here.

The work undertaken so far is exploratory; that is, the investigation has been intended to assess the usefulness of concepts rather than to provide exhaustive studies of any one particular mechanism. Several concepts appear to warrant study in more depth. The planned follow-on program is intended to carry these concepts to the point that the results will be usable for design purposes.

## Water Heat Transfer Enhancement

The water heat transfer enhancement work is based on two different concepts. One of these utilizes large scale motions to enhance conductances, i.e., motions which involve a significant portion of the water flow in the tube. The other concept involves modification only of the flow adjacent to the wall, i.e., the laminar sublayer and buffer layer regions.

The water heat transfer investigation is being conducted in a circulation apparatus containing partially degassed water. The test section is a heavy walled copper tube approximately three inches inside diameter and fifteen feet long. A portion of the apparatus is shown in Figure 1. The entire length of the tube has spiral wrapped heaters in ten sections. The present experiments have been performed with a uniform heat flux boundary condition. The pressure drop is measured in the last four feet of the test section and the heat transfer data are being taken near the extreme downstream end adjacent to the transparent section which can be seen in the figure. The heat transfer conductances reported are based on averages of ten thermocouples, so that the axial conductance variations which occur with some of the flow modifying inserts are averaged. Details of the apparatus and procedures are given in references (1) and (2).

### A. Studies of Large Scale Motions

The heat transfer literature contains a number of studies of pipe flows with multiple orifices or bluff body protuberances installed. Such systems enhance heat transfer conductance by increased turbulence level. The increased turbulence is generated from the edges of stalls behind the insert. There is a large profile drag associated with such devices, and, in addition, motions are

generated which do not contribute to the radial transport of heat. The pressure losses associated with the generation of these extraneous motions is wasted.

It appeared that it would be possible to design low drag devices which modify the flow in the tube for increased radial heat transport and that such devices should require considerably lower pressure loss than the bluff body devices to provide an equivalent increase in heat transfer conductance. Conceptual insert designs were constructed and the resulting fluid motions observed in an open water channel, using a dye tracer. On the basis of these observations, six insert geometries were subjected to heat transfer testing.

Figures 2 and 3 contain sketches of the inserts tested. The inserts were fabricated by hand, formed into rings, and inserted into the tube at various intervals. They spring against the tube wall to hold them in position. Each set was tested at one, two, or three spacings, depending upon the effectiveness which it showed in enhancing heat transfer.

It may be observed that these inserts are not heat transfer surfaces but are, in fact, heat transfer barriers. There is an insulating layer of water between the support ring and the tube wall which locally adds to the thermal resistance.

The Style 1 configuration is a reference surface used to assess the heat transfer resistance and pressure drop associated with the insert vane supports.

Style 2 is a converging vane geometry which causes fast and slow striations in the flow. There is also an axial roller generated from the inner edge of the vane but it does not sweep the wall so probably does not contribute significantly to the transport of heat.

Style 3 is a twisted vane, or propeller type which forms an axial vortex close to the wall. Adjacent vanes are twisted in opposite directions so that vortices reinforce each other where they adjoin.

Style 4 is a bluff body, with a fairly large stalled region behind it. It does form a strong vortex on either side close to the wall and it was hoped that the heat transfer enhancement from this structure would compensate for the high profile drag.

A photograph of samples of the inserts is shown in Figure 4.

Typical of the results which were obtained in the experimental program are those for the converging vane configuration, which is shown in Figure 5. The data represent friction factor and heat transfer for three different spacings. Also shown on the graph are the solid line representing the Blasius correlation for friction factor in turbulent pipe flow, and the solid line representing the Dittus-Boelter correlation for heat transfer conductance in turbulent pipe flow. It may be seen that both the heat transfer and the friction factor are increased significantly. The friction factor for the 2-1/2 inch spacing, represented by the circles in the figure, exhibits typical rough wall behavior, with little dependence upon Reynolds modulus. The four inch data, on the other hand, exhibit strong dependence upon Reynolds modulus, and at about 10,000 the four inch spacing friction factor actually crosses that for the 2-1/2 inch spacing. The friction factor for the six inch spaced inserts exhibits high scatter in the Reynolds modulus region between 10, and 25,000. This appears to be caused by some interfer between flow patterns of successive insert assemblies at this spacing. The other inserts provided data which is similar to this set in general appearance although of course different in detail.

There are a number of dimensionless numbers and ratios which can be used to compare heat transfer surfaces. One comparison number, which is useful in comparing modifications to a basic geometry, is shown in Figure 6. The comparison number is the ratio of the heat transfer increase to the friction factor increase as a function of Reynolds number. This ratio has been referred to by some authors as the "efficiency index." It is a measure of the success of the modification in converting increased pressure drop into increased heat transfer conductance. It may be seen that none of the inserts which were tested in this program increase the heat transfer conductance as much as they increase the friction factor. The efficiency of the better inserts is in the order of seven-tenths. Some of the inserts which were tested were rather poor. The Style 4 inclined vane system, which has a stalled region downstream, had the worst performance. Typical multiple orifice systems fall in about the same range of efficiency as does the inclined vane Style 4.

The efficiency in conversion of the increased friction to heat transfer is not the only quantity of interest to the heat exchanger designer. He is also interested in how much the heat transfer is increased.

Figure 7 shows the ratio of the heat transfer conductance with and without inserts plotted against the friction factor ratio for the configurations at discrete Reynolds moduli. Lines of constant efficiency index are also shown on this graph. The configurations which fall highest on the graph are those which allow the largest decrease in heat transfer area while those which fall farthest to the left are those which cause the least pressure drop increase.

The inserts tested exhibit their optimum performance at rather low Reynolds moduli compared to those used in existing OTEC heat exchanger designs. This may be attributed to a compromise made in the design of the experiments. The inserts in order to be most effective, should be in the region of the flow where velocity gradients are steep. However, the inserts, to be made by hand and inserted into the tube without damage, have to be fairly large. It is believed that configurations similar to these, but smaller, would exhibit optimum behavior at Reynolds moduli of interest in the OTEC plant.

It is obvious that no consideration has been given to producibility of these configurations. However, it is the fluid motions which cause the heat transfer enhancement, and simple vanes, formed from the tube wall material, could be envisioned which are as effective and producible in a production facility.

An example of the application of a heat transfer surface modification which has performance similar to that of the better inserts described here, is given in a later portion of this paper.

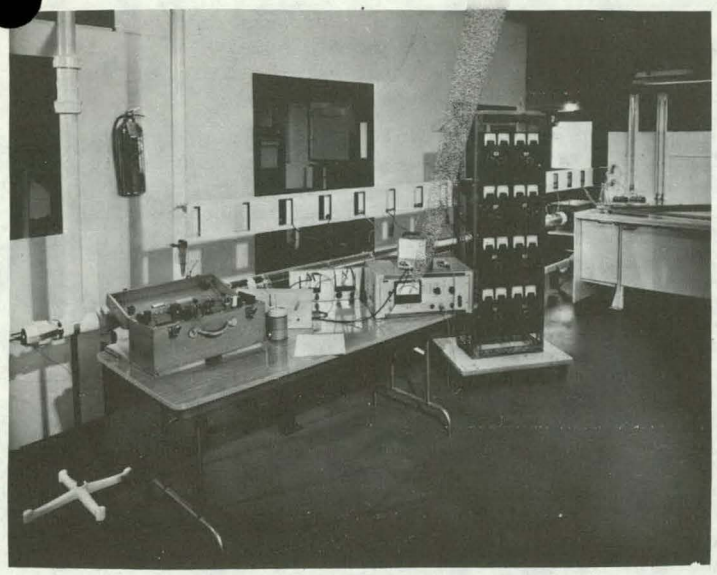


Figure 1. Overall view of water heat transfer apparatus.

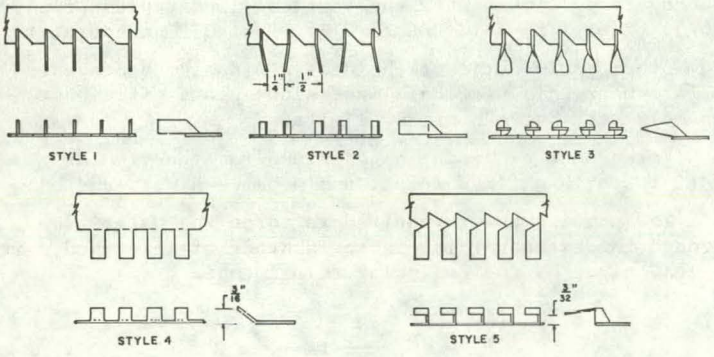



Figure 2. Insert geometries.

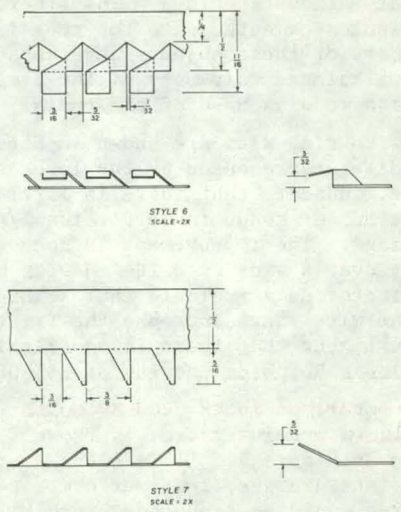



Figure 3. Insert geometries.

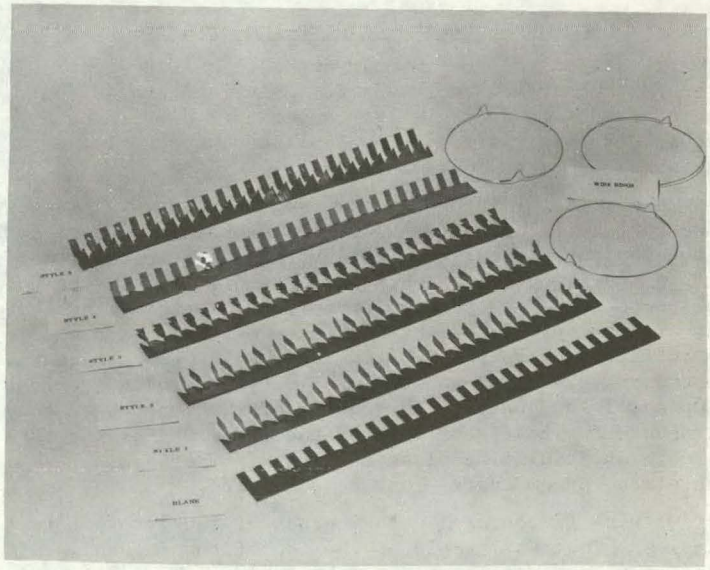


Figure 4. Photo of inserts laid out on a table.

B.- Studies of Wall Layer Modification

Two surface modifications have been tested which change the flow in the laminar sublayer and buffer layer. One of these consists of annular wire rings, inserted into the tube at various spacings. The other consists of copper granules cemented onto the tube interior. The sizes of both of these objects were chosen to coincide with the calculated thickness of the laminar sublayer in the Reynolds modulus band of the tests.

The wire ring data are shown in Figure 8. The heat transfer data, represented by the lower set of points on the figure, indicate that there is little difference in the heat transfer conductance for the 1/4-inch and 1/2-inch spacings. The improvement in conductance is 30 to 40 percent over a wide Reynolds modulus band. The friction factor data indicate that at high Reynolds modulus the wire rings increase the friction factor by a large amount, but that there is no friction factor increase below a Reynolds modulus of 25,000.

The comparison index used by Colburn, the friction factor-Colburn modulus ratio, is shown for this configuration in Figure 9. It is clear that the wire ring configurations are excellent performers. Smaller diameter wires would be expected to exhibit optima at higher Reynolds modulus.

Some preliminary copper granule data are shown in Figure 10, for a low grain density case. The friction factor behavior is similar to that reported by Nikuradse for sand grain surfaces. The heat transfer conductance is enhanced somewhat. These data have not been corrected for the heat transfer resistance of the varnish layer used to cement the granules to the tube.

Other aspects of the water heat transfer enhancement work will be described later.

Ammonia Nucleate Boiling Enhancement

The intent of the ammonia nucleate boiling heat transfer enhancement work was not only to increase conductance, but to decrease the temperature difference required for initiation of nucleation, and to relieve the sensitivity to contamination.

A portion of the apparatus used in this work is shown in Figure 11. The boiler vessel is a stainless steel tank with view ports, heating, filling, and lighting systems, and is installed in a double-walled steel room for personnel protection. Of particular interest in this figure is the arrangement of four boiler tubes extending from one end of the tank to the other. The outside two are guard tubes, and are continuous. The other two, which are test samples, extend only to the center of the tank where they attach to two test samples from the other end of the tank through an insulating plastic fairing. The tank, therefore, accommodates four test samples.

Figure 12 contains a photograph of four typical test samples. The test sample at the top of the figure is a section of unmodified, as-wrought tubing. The next has had a very fine screw thread turned on it. The thread has subsequently been rolled over by burnishing. The other two have a portion of the as-wrought tube surface covered by two layers of screen, coarse screen against the tube, and fine screen on the outside.

Data for unmodified surfaces are presented in Figure 13.

It may be seen that these surfaces require from 3 to 4.5°F temperature difference to bring about nucleate boiling. It may also be seen that the four test samples are not very uniform in behavior.

Data for some unmodified surfaces are presented in Figure 14. The temperature differences required to provide a given heat flux are much lower for the double screen tube, and the temperature difference required to initiate nucleate boiling was below that detectable with the instrumentation used.

Additional aspects of the nucleate boiling work will be discussed in another portion of the paper.

Application of Water-Side Heat Transfer Enhancement Techniques to An OTEC Evaporator

The basic heat exchanger design to be considered is one which has a heat transfer enhancement surface on the boiling ammonia side, but which has the water side unmodified. A reasonable approximation for such a heat exchanger is that the boiling ammonia heat transfer resistance and tube wall resistance are negligible compared to the resistance on the water side. Another reasonable idealization is that the ammonia saturation temperature is uniform throughout the exchanger. Subject to these idealizations, the behavior of the heat exchanger may be described by the equation shown in Figure 15. This equation is dependent only on the laws of thermodynamics and the definition of heat transfer conductance.* The same figure contains a graph of the equation, in a range of values suitable for an OTEC evaporator of a plant of 1 megawatt electrical output.

Shown on the graph are points locating three OTEC evaporator designs developed by an ERDA contractor utilizing an optimization program which minimizes heat exchanger cost (4). Despite the fact that virtually every characteristic of the power plant was carried as a parameter except the electrical power output, these three heat exchangers fall very near the vertical line representing a $q/\Delta t_{max}$ of $1.88 \times 10^9$ Btu/hr °F. Most OTEC evaporators from other optimization techniques would also be expected to fall near this vertical line, since plant efficiency can only vary between narrow limits.

For a heat exchanger constrained to a particular $q/\Delta t$, there is a fixed relationship between $w, \epsilon$, and $hA$.

The pumping power required to force the water flow through the exchanger is, in the absence of inlet and exit losses, given by the following relationship.

$$P = C_1 \frac{w^3}{A_c^3} fA \qquad (1)$$

*See for example Reference 3.

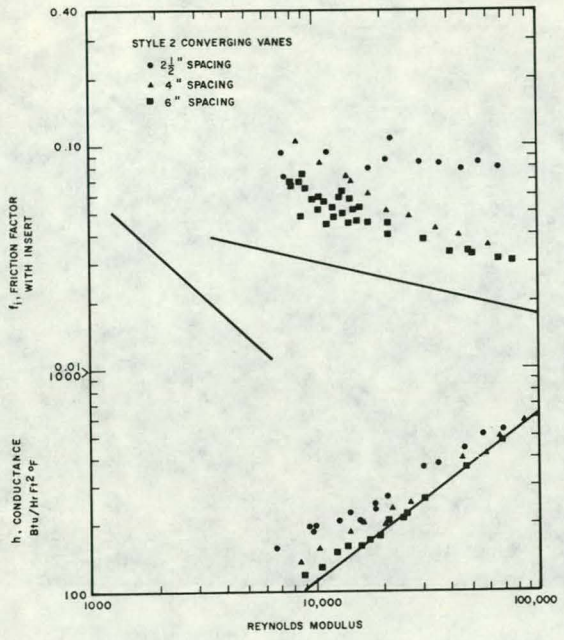



Figure 5. Friction factor and heat transfer conductance data for Style 2 vanes.

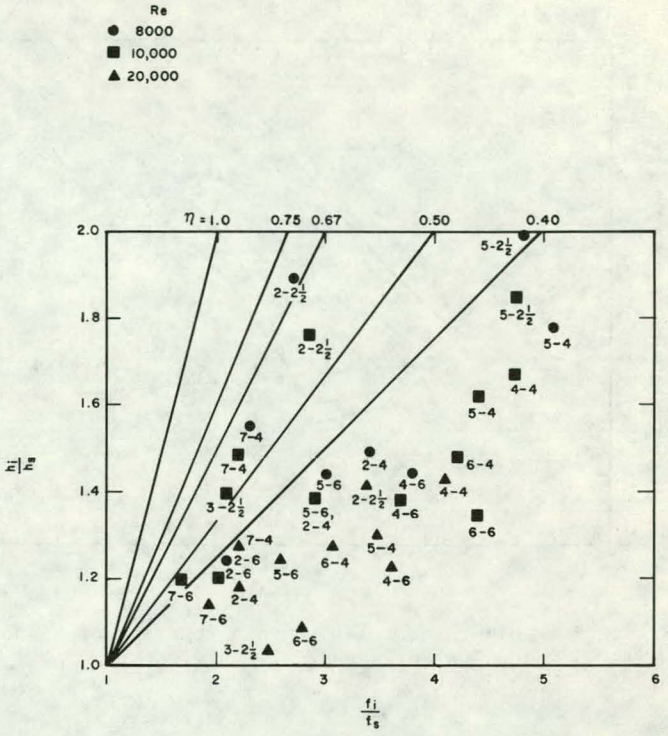



Figure 7. Heat transfer increase as a function of friction factor increase.

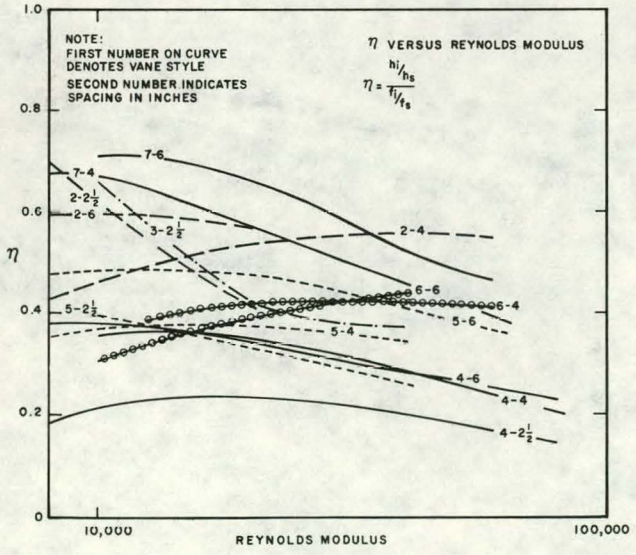



Figure 6. Efficiency index as a function of Reynolds modulus.

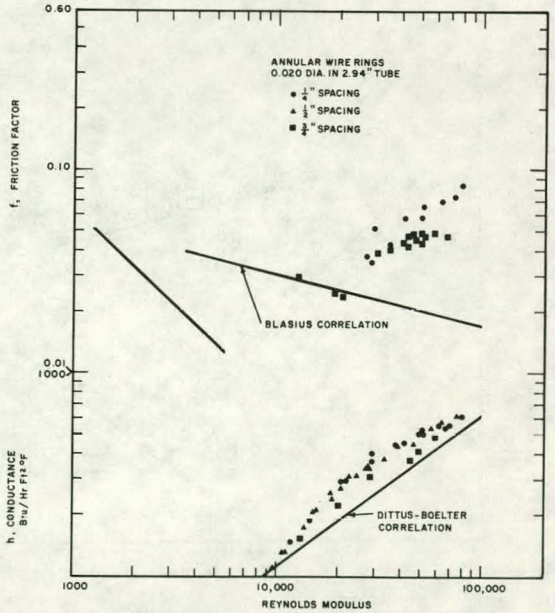



Figure 8. Heat transfer conductance and friction factor data for annular wire rings.

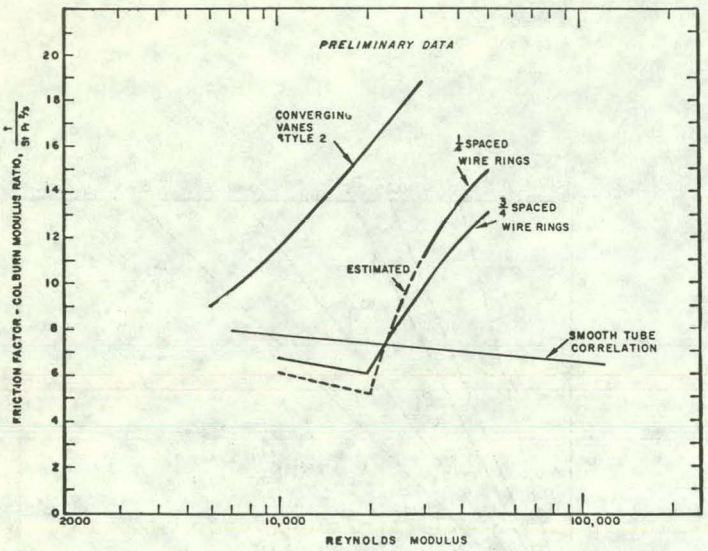



Figure 9. Colburn correlation as a function of Reynolds modulus for several geometries.

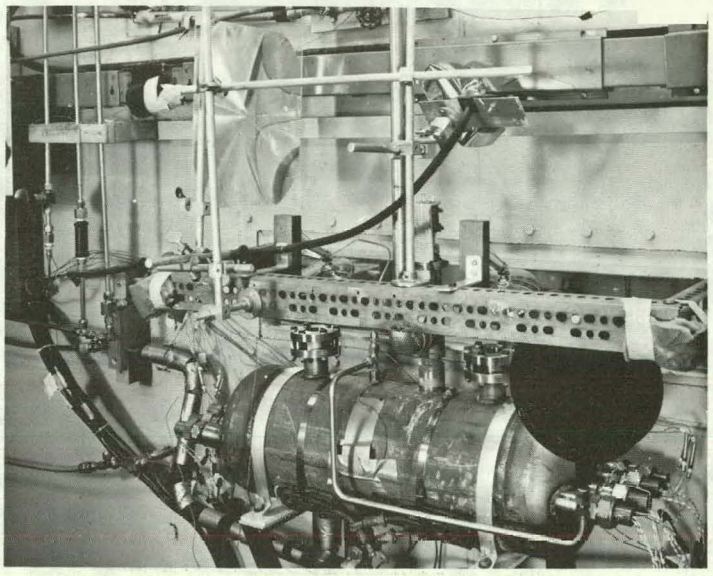


Figure 11. Ammonia boiling apparatus.

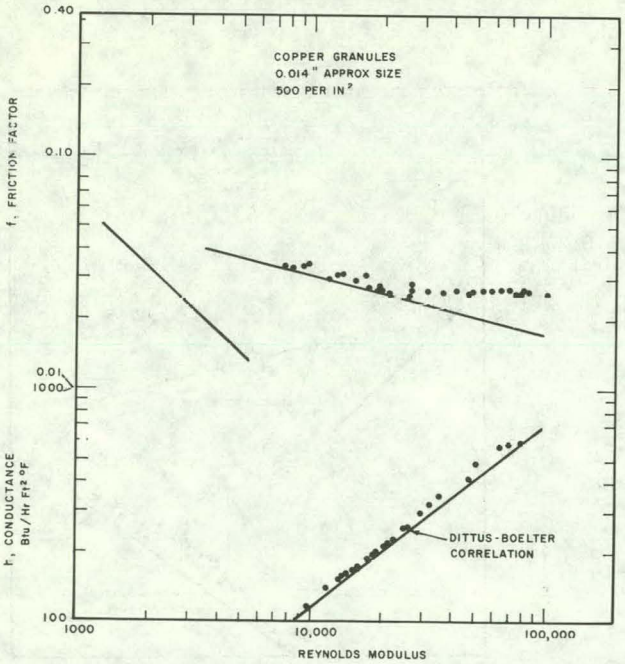



Figure 10. Heat transfer conductance and friction factor data for copper granule surface.

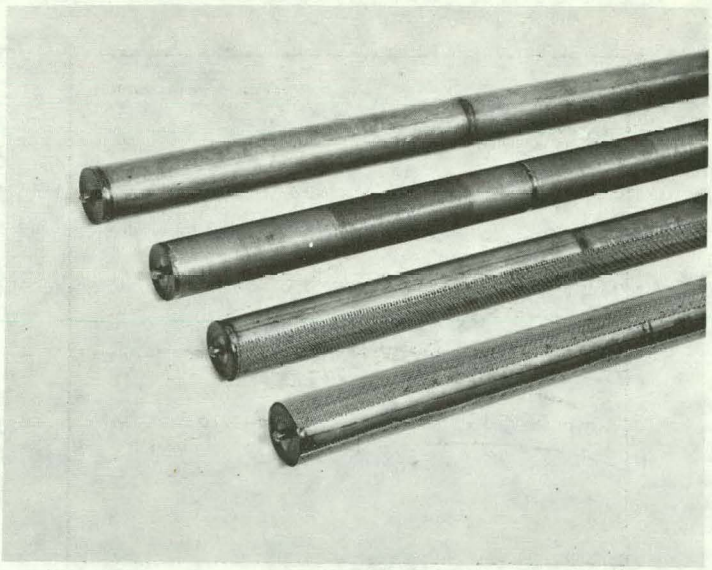


Figure 12. Four typical boiling surface test samples.

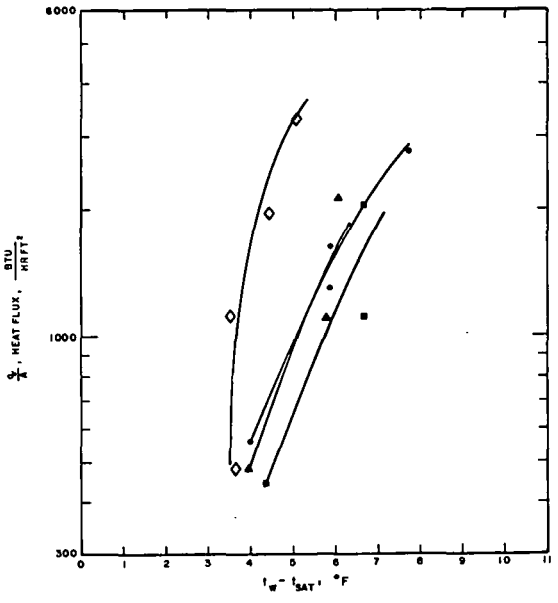



Figure 13. q/A versus ($t_w$ - $t_{sat}$) for smooth, untreated tubes.

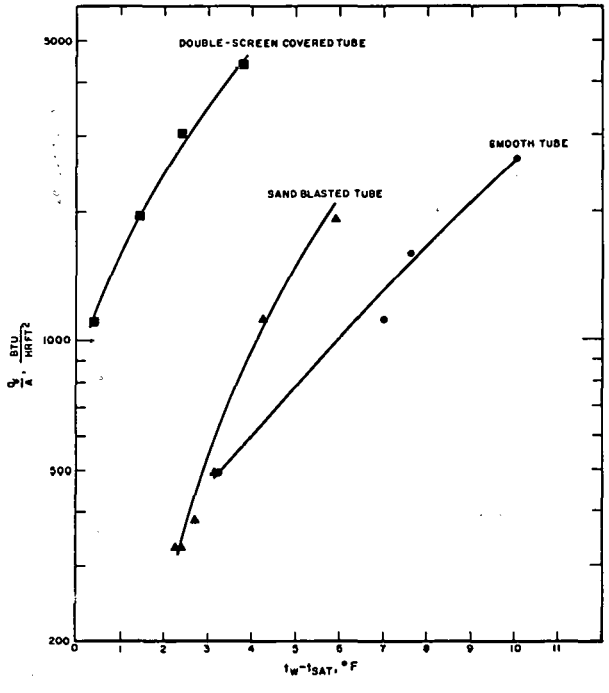



Figure 14. q/A versus ($t_w$ - $t_{sat}$) for tubes with sand-blasted and screen-wrapped surfaces.

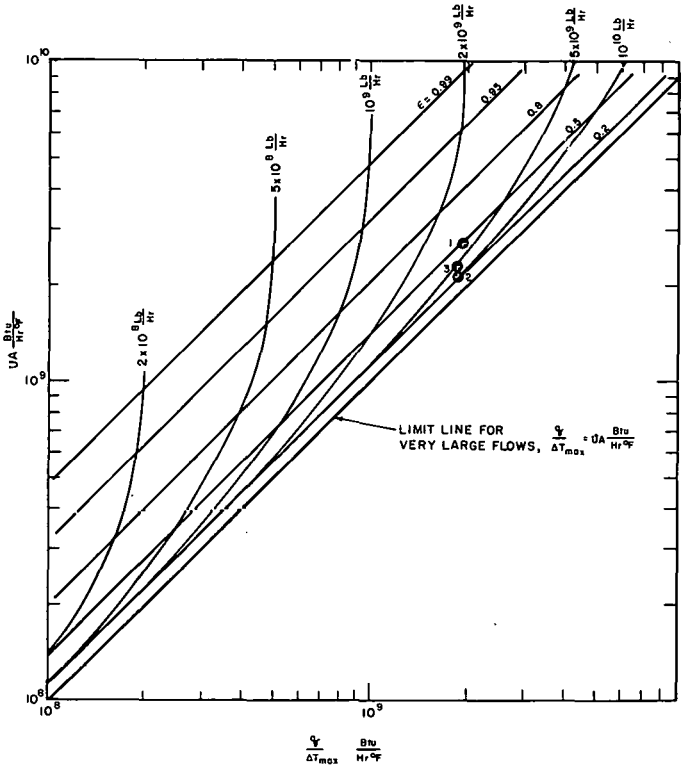



Figure 15. Thermal relationships for an OTEC evaporator.

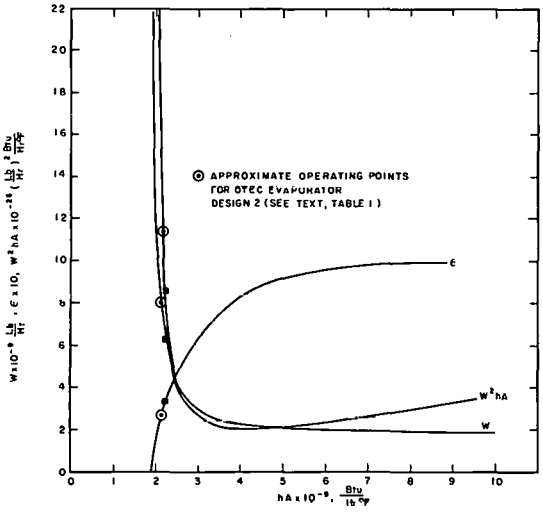



Figure 16. Pumping power multiplier and other quantities as functions of heat transfer conductance-area product.

For many heat transfer surfaces, the Colburn comparison index, the ratio of friction factor to Colburn modulus defined in Equation (2)

$$R_c = \frac{f}{St\ Pr^{2/3}} \qquad (2)$$

has an approximately constant value over a useful range of Reynolds moduli. For example, the value of this index for a smooth tube, using the Blasius friction factor correlation and the Dittus-Boelter heat transfer conductance correlation is

$$R_c = \frac{0.3164}{0.023} \frac{Pr^{0.07}}{Re^{0.05}}$$

the value of this expression ranges from 8.5 to 9.5 at Reynolds moduli from $10^4$ to $10^5$. The index given in Equation (2) can therefore be used as an approximate relationship between friction factor and heat transfer conductance. When this relationship is introduced into Equation (1), one obtains the following expression

$$P = \frac{C_2}{A_c^2} (w^2\ hA)\ R_c \qquad (3)$$

Equation (3) shows the relationship between pumping power, $R_c$ and a pumping power multiplier, $(w^2\ hA)$, dependent upon the thermodynamics of the heat exchanger. The pumping power multiplier is shown in Figure 16 for a case of fixed $q/\Delta t_{max}$. Shown on the curve is one of the three economically optimized designs shown in Figure 15.

Suppose that it is desired to assess the usefulness of a heat transfer enhancement modification which has the performance

$$\frac{h_2}{h_1} = 1.5, \quad \frac{f_2}{f_1} = 2$$

The efficiency index for this modification is therefore

$$\eta = 0.75$$

The modified design is to be subject to the following constraints

(1) The pumping power is unchanged
(2) The total heat flow is unchanged
(3) The overall temperature difference is unchanged
(4) The free flow area remains constant.

The first three constraints insure that the configuration change will not affect the performance of the plant. The fourth constraint clarifies the comparison between the original and modified heat exchangers. It could, however, be relaxed in order to optimize heat changer configuration.

By constraint (1)

$$(w^2\ hA)_2\ R_{c_2} = (w^2\ hA)_1\ R_{c_1}$$

It may be shown that

$$\frac{R_{c_2}}{R_{c_1}} = \eta$$

These relationships specify the new value of $(w^2\ hA)$ which must apply. This new value, together with Figure 16, specifies a new value of $(hA)$, which is somewhat greater than the original. The new values are indicated on the figure by the solid squares.

The ratio of the heat transfer area with the modification to that without the modification is simply

$$\frac{A_2}{A_1} = \frac{(h_2\ A_2)}{(h_1\ A_1)} \frac{h_1}{h_2}$$

$$= 0.7$$

This is a substantial decrease in area, and was obtained with a modification which increased friction factor significantly more than it increased heat transfer conductance.

Discussion of Ammonia Boiling Enhancement Mechanisms

A brief recapitulation of the results of two earlier boiling studies conducted by Geoscience (5) is believed to be useful in the interpretation of the ammonia boiling data presented here.

Figure 17 shows a system that was used to study boiling in a simplified cavity; it consisted of a glass syringe that had a small sealed capillary tube at one end which could be lowered into a hot water bath. The purpose of the experiments was to visually observe nucleate boiling in a glass cavity with the aid of a microscope. Sometimes the capillary was completely filled with Freon and at other times it was only partially filled (with some vapor and gases at its lower end). At low superheat wall temperatures, boiling would only start at a liquid-vapor interface. Under this condition, two kinds of boiling patterns were observed. At times bubbles were observed in the capillary center with liquid return at the wall. At other times cyclic flows of vapor slugs out of the capillary followed by the return of liquid slugs were observed. In all cases, once boiling started it continued as long as heat was added to the Freon. When the capillary was completely filled with liquid, boiling could not

be initiated at low superheats.

A second past study that is thought to be helpful in understanding nucleate boiling mechanisms relates to liquid superheating phenomena in forced flow through a boiler tube. Figure 18 shows an idealized representation of the wall temperature at the exit of a boiler as a function of time. Three simplified processes were postulated to exist at the end of the boiler tube for the case of continuous heat addition. In step 1 to 2, the wall and liquid are superheating above the saturation temperature. The process is analogous to the charge of two condensers in parallel, as shown in the figure. In step 2 to 3, the superheated liquid flashes into high velocity saturated vapor which then cools the wall. This process can be thought of as the discharge of one condenser through a low resistance. In step 3 to 4, the continuous heat addition increases the wall temperature rapidly until liquid reenters the tube. This process can be thought of as the charging of a single condenser. Then the cyclic pattern repeats itself. These idealized processes describe liquid superheating, vapor generation and expulsion and liquid flow return in a boiler tube. Figure 19 shows an experimental recorder trace of the wall temperature at the exit of a boiler under forced flow conditions as a function of time. Note the similarities between the idealized and experimental sawtooth cyclic, temperature patterns shown in Figures 18 and 19. It is pointed out that actual flow reversals in the boiler tube were also experimentally verified. It is suggested that the cyclic heat transfer and fluid flow patterns observed in the glass capillary system are analogous to those occurring in a boiler tube. Thus, to obtain low superheats for a nucleate boiling surface, one should use cavities that can retain vapor or gas volumes and that readily allow the cyclic expulsion of vapor and return flow of liquid. If the cavity density is high, high heat fluxes will also occur. It is Geoscience's position that rough surfaces with interlocking cavities will thus yield low superheats and high boiling fluxes.

One of the two temperatures that define the boiling conductance is the saturation temperature. Geoscience utilized three different simultaneous ways of measuring this quantity. One method consisted of measuring the wall temperatures of the non-heated boiler tubes positioned on both sides of the one heated tube. A second method consisted of measuring the vapor temperature in the space above the liquid in the boiler vessel. A third method consisted of measuring the vapor pressure in the space above the liquid and then determining the vapor temperature from the vapor pressure-temperature curve. The three methods of measuring the saturation temperature were then compared and found to be within one-half a degree Fahrenheit of each other. The differences were explainable on a physical basis. The second temperature that arises in the boiling conductance definition is the wall temperature. Figure 20 shows an enlargement of the thick-wall boiler tube which contained drilled holes for sheathed thermocouples. After measuring the wall temperature at the depth indicated, an extrapolation to the wall-liquid interface temperature was performed using the annulus conduction equation. The fin conduction equation was used to calculate the temperature error for the thermocouple for the system parameters that existed. It was found that the thermocouple error was about 0.03°F. On the basis of the errors in the wall-saturation temperature difference and the heat flux, the boiling conductance error was found to be less than 10 percent for temperature differences greater than 2°F.

Boiling conductances versus wall-saturation temperature differences for two treated surfaces and a smooth tube are shown in Figure 21. The conductances for the sandblasted and double-screened tubes fall significantly above those for a smooth tube; in addition, boiling inception occurred at significantly lower superheat conditions.

## Discussion of Water Forced Convection Heat Transfer Mechanisms

The following remarks describe some of the parameters and mechanisms that control forced convection heat transfer enhancement in tubes having small roughness parameters. Figure 22 shows the classical sand grain friction factor data of Nikuradse (6) in terms of the Reynolds modulus and the roughness parameter (asperity ratio $\epsilon/R$). Of particular interest are the rough tube data that lie along the smooth tube friction factor curve. In this discussion, the Reynolds modulus at which a given rough tube friction factor data set begins to depart from the smooth tube friction factor curve will be called $Re_{max}$. It will subsequently be shown that the heat transfer conductances in these low roughness parameter regions can be enhanced over smooth tube values without increases in friction factors.

By way of recapitulation, Figure 23 shows the classical generalized velocity profile for turbulent flow in tubes indicating the well known laminar sublayer, the buffer layer, and the turbulent core regions. From the generalized velocity profile, it can be shown that the ratio of the velocity at the laminar sublayer boundary to mean fluid velocity, $u_{LSL}/u_m$, is

$$\frac{u_{LSL}}{u_m} = \frac{0.75}{Re^{0.1}} \qquad (4)$$

The corresponding ratio of the temperature drop across the laminar sublayer to the wall-mixed mean fluid temperature drop (as determined from the heat-momentum transfer analogy for ordinary fluids (7)), $\Delta t_{LSL}/\Delta t_m$ is

$$\frac{\Delta t_{LSL}}{\Delta t_m} = \frac{Pr}{\frac{\Delta t_m}{\Delta t_{max}}\left[Pr + \ln(1 + 5\,Pr) + 0.5 \ln\left(\frac{Re}{60}\sqrt{\frac{\zeta_\epsilon}{8}}\right)\right]} \qquad (5)$$

where $\Delta t_{max}$ is the wall-centerline temperature difference. These laminar sublayer velocity and temperature difference ratios are shown in Table I as functions of Reynolds and Prandtl moduli. Note that the velocity ratios are relatively small, namely about 0.3. The corresponding

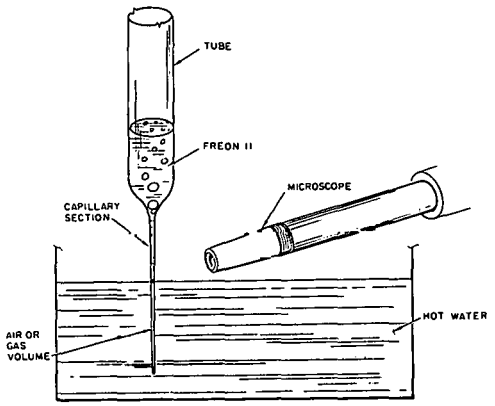



Figure 17. Boiling experiments with Freon-11 in capillary tubes.

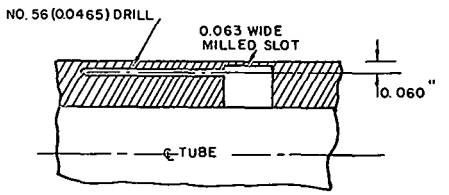



Figure 20. Thermocouple hole detail.

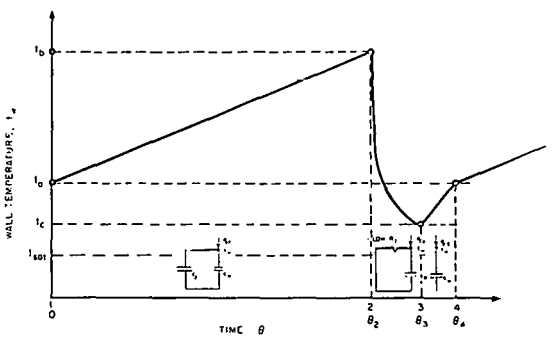



Figure 18. Idealized transient wall temperature variation in a forced flow boiler with periodic liquid superheating.

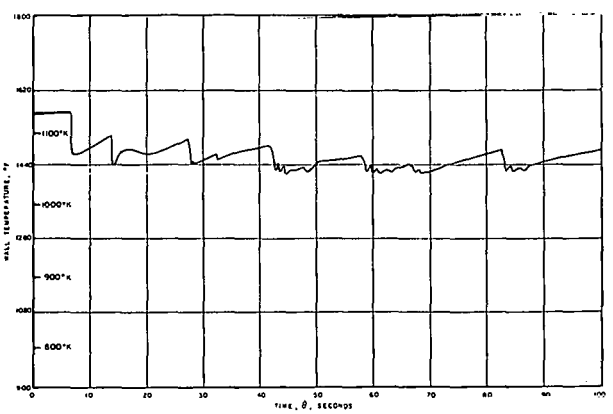



Figure 19. Experimental time-tube wall temperature trace obtained during liquid superheating studies.

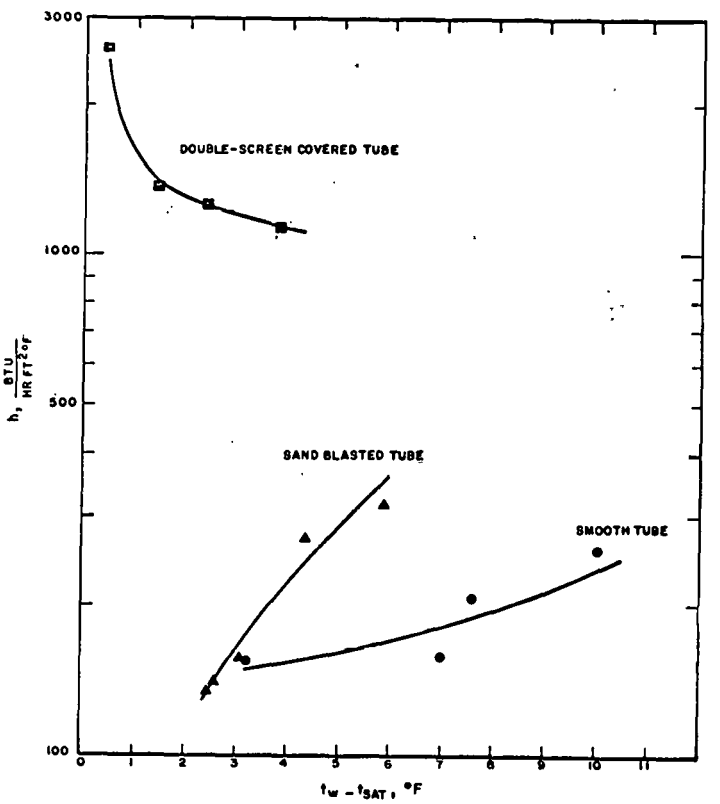



Figure 21. Boiling conductances for smooth, sandblasted and double-screen covered tubes.

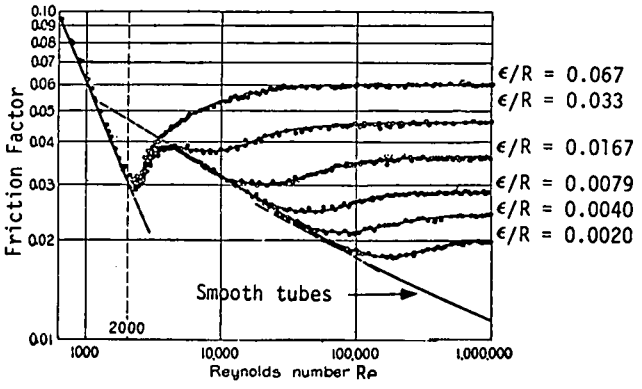



Figure 22. Variation of the friction factor for flow in a tube as a function of Reynolds modulus and the roughness parameter $\epsilon/R$.

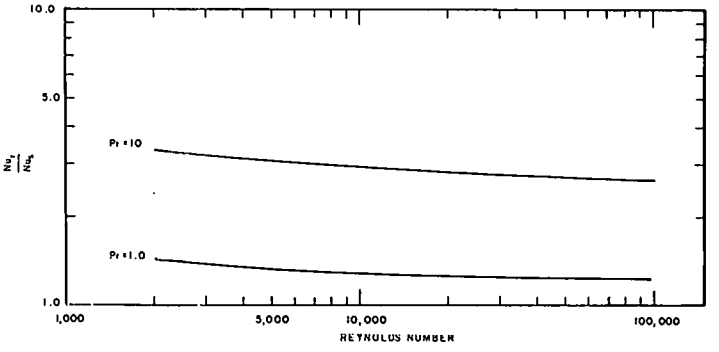



Figure 24. $Nu_r/Nu_s$ versus Re for Pr = 1 and 10.

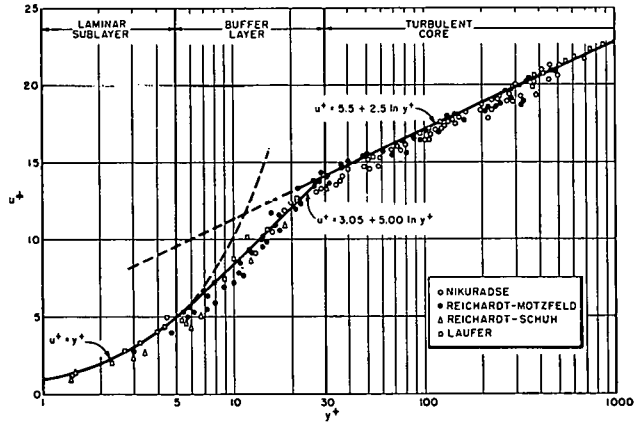



Figure 23. Generalized turbulent velocity profile in circular pipes and in channels.

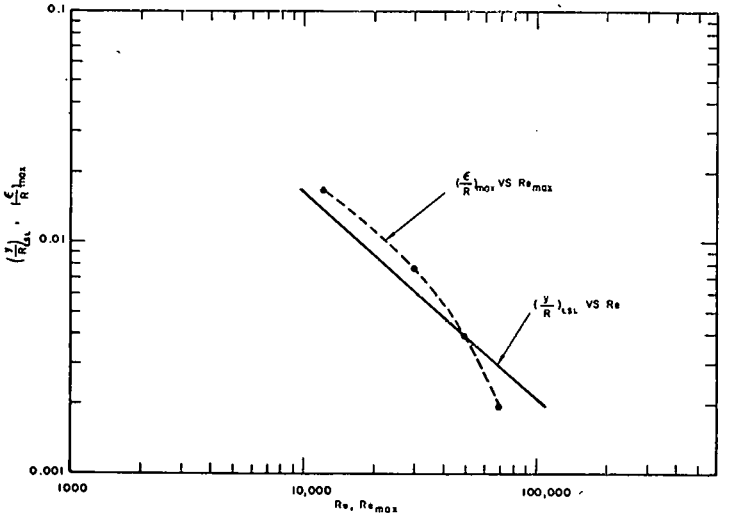



Figure 25. $(y/R)_{LSL}$ versus Re and $(\epsilon/R)_{max}$ versus $Re_{max}$.

$$\frac{u_{LSL}}{u_m} \;\&\; \frac{\Delta t_{LSL}}{\Delta t_m} \quad \text{versus} \quad Re \;\&\; Pr$$

| Re | $\frac{u_{LSL}}{u_m}$ | $\frac{\Delta t_{LSL}}{\Delta t_m}$ for Pr = 1 | $\frac{\Delta t_{LSL}}{\Delta t_m}$ for Pr = 10 |
|---|---|---|---|
| 2000 | 0.351 | 0.388 | 0.738 |
| 10000 | 0.298 | 0.296 | 0.691 |
| 50000 | 0.254 | 0.246 | 0.657 |

Table I. Comparison of the laminar sublayer ratios.

temperature difference ratios for Pr = 1 are also small, having a value of about 0.3. On the contrary, however, the temperature difference ratio for Pr = 10 is now significantly larger, namely, a value of about 0.7. In other words, the temperature difference ratios for higher Prandtl modulus fluids such as water are markedly larger than the corresponding velocity ratios. This means that if there are changes in the structure of the laminar sublayer as a result of the small surface roughnesses, one would not expect the total velocity field to be changed a great deal. On the other hand, for higher Prandtl modulus, one would expect changes in the laminar sublayer structure to influence significantly the total temperature field. This is the principle that can be used to enhance the convective heat transfer. Incidentally, the conclusion that the velocity field does not change very much when the laminar sublayer is degraded is supported by the Nikuradse rough tube friction factor data that fall on the smooth tube curve (i.e., in the region $2300 < Re < Re_{max}$).

The classical Nusselt modulus analogy relation for turbulent flow in a smooth tube is given by (7)

$$Nu_s = \frac{\sqrt{\frac{\zeta_s}{8}}\ Re\ Pr\ \frac{\Delta t_{max}}{\Delta t_{mean}}}{5\left[Pr + \ln(1 + 5\,Pr) + 0.5\ln\left(\frac{Re}{60}\sqrt{\frac{\zeta_s}{8}}\right)\right]} \qquad (6)$$

To establish an upper bound for heat transfer enhancement from tube roughness, it is presumed that the laminar sublayer is completely removed. For this condition, the first term in the denominator of Equation (6) would be removed leaving only the second two terms. The resulting expression defines the Nusselt number for rough tubes,

$$Nu_r = \frac{\sqrt{\frac{\zeta_s}{8}}\ Re\ Pr\ \frac{\Delta t_{max}}{\Delta t_{mean}}}{5\left[\ln(1 + 5\,Pr) + 0.5\ln\left(\frac{Re}{60}\sqrt{\frac{\zeta_s}{8}}\right)\right]} \qquad (7)$$

Removal of the Prandtl modulus in Equation (6) can be thought of as the replacement of the laminar sublayer by a low resistance turbulent layer or by replacing the thermal conductivity in the Prandtl modulus by a turbulent conductivity, thereby significantly reducing the value of the Prandtl modulus. Figure 24 shows a plot of $Nu_r/Nu_s$, as determined from Equations (6) and (7). Again, for Prandtl moduli in the range of unity, little heat transfer enhancement results by removal of the laminar sublayer resistance, but for a Prandtl modulus of 10 there is a threefold enhancement. The upper bound conductance enhancement for water (Prandtl moduli of 6 to 7) would be about twofold.

Figure 25 shows a plot of the roughness ratio $\nu$ $Re_{max}$ and the dimensionless laminar sublayer thickness versus Re; the two curves cross at about Re = 50,000. This graph can be used for establishing the grain size needed to remove the thermal resistance of the laminar sublayer. Specifically, the dimensionless roughness should at least be as high as $(y/R)_{LSL}$ but no higher than $(\epsilon/R)_{max}$.

Essentially all of the rough tube heat transfer and friction data in the literature deal with large roughness ratios. Only one set of data was found for a small roughness ratio, namely, the measurements of Dipprey and Sabersky for $\epsilon/R = 0.004$. Their friction factor enhancement was 26 percent and their conductance enhancement was 41 percent for a water flow system at a Reynolds modulus of about 100,000.

The experimental verifications of convective conductance enhancements for the Geoscience wire ring and copper granule tube treatments have already been presented in Figures 8 and 10. Neither roughness system has yet been optimized. Further, in the case of the copper granule work, it is estimated that correction for the presence of the varnish film will increase the conductances by another five to ten percent.

## Concluding Comments

In summary, it is believed that there are a number of methods by which ammonia boiling and water-side convection can be practically enhanced. The application of such results through optimization efforts should make it possible to reduce evaporator sizes.

## References


1. Sabin, C. M.; Poppendiek, H. F.; Connelly, D. J.; and Meckel, P. T.; "Annual Report, Nucleating Vaporization and Extended Surface Heat Transfer at Low Temperature Difference," ERDA Contract AT(04-3)-1094, Geoscience Ltd Report GLR-165, May 1976.

2. Sabin, C. M.; Poppendiek, H. F.; Connelly, D. J.; and Dunbar, J. G.; "Topical Report on Water Flow Heat Transfer Conductance Enhancement in Round Tubes by Means of Flow Modifying Inserts," ERDA Contract AT(04-3)-1094, Geoscience Ltd Report GLR-177, March 1977.

3. Kays, W.; and London, A. L.; COMPACT HEAT EXCHANGERS, 2nd Ed, McGraw-Hill, 1964.

4. Czikk, A. M.; Fenner, G. W.; Notaro, F; Zawierucha, R.; "Ocean Thermal Power Plant Heat Exchangers," Joint Conf American Section of International Solar Energy Society and the Solar Energy Society of Canada, Inc., pp 461-484, Vol 5.

5. Sabin, C. M.; Poppendiek, H. F.; Mouritzen, G.; Meckel, P. T.; and Cloakey, J. E.; "Liquid Metal Boiling Inception," NASA CR-2095, Geoscience Ltd report, Aug 1972.

6. Nikuradse, J., "Strömungsgesetze in rauhen Rohren," V.D.I. Forschungsheft, 361, 1933.

7. Boelter, L. M. K.; Martinelli, R. C.; and Jonassen, Finn; "Remarks on the Analogy Between Heat and Momentum Transfer," ASME Trans, Vol 63, pp 447-455, 1941.

# COMMENTS ON SEA WATER SIDE ENHANCEMENT FOR OTEC HEAT EXCHANGERS

W. L. OWENS
*Lockheed Missiles & Space Co.*
*Box 504*
*Sunnyvale, California*

## Introduction

It is well recognized that closed cycle Ocean Thermal Energy Conversion heat exchangers represent a significant fraction of the total OTEC plant costs. This has naturally led to the investigation of techniques such as shell side and tube side enhancement in an effort to reduce the physical size and cost of the evaporator and condenser as compared to a plain tube design. Most of the methods for tube side enhancement investigated to date have relied on either turbulence promotion or extended surfaces. The present comments are primarily directed to the effects of enhancement on evaporator design and cost with particular emphasis on tube side enhancement as it affects the overall thermal system design including the influence of pumping power on net power output. Most of the present observations are also applicable to the effects of enhancement on condenser design.

## Optimization

The manner in which the overall heat transfer coefficient, based on the outside tube area, varies with the evaporation and sea water heat transfer coefficient is shown in Fig. 1 for 2 in. by 0.034 in. titanium or stainless steel tubes. Experimental data obtained at LMSC's Palo Alto Research Laboratory indicates a value of approximately 1000 Btu/hr ft$^2$ °F for the ammonia evaporation heat transfer coefficient over most of the applicable flow rate range for plain horizontal tubes. The optimum sea water velocity corresponding to this value of evaporation heat transfer coefficient is generally on the order of 5.5 to 6 ft/sec. One must also determine the heat exchanger surface area requirement based on the maximum expected fouling factor, which is typically assumed to be on the order of 0.0003 to 0.0005 (Btu/hr ft$^2$ °F)$^{-1}$. The unenhanced performance of a plain tube has been indicated in Fig. 1 as a reference point against which shell and tube side enhancement can be compared. Shell side enhancement, in general, produces an improvement of the overall heat transfer coefficient at the expense of greater tube cost per unit length. Sea water side enhancement not only produces a greater tube cost per unit length but, in addition, it results in an increased friction factor and greater pumping power penalty, along with greater difficulty in incorporating most methods of biofouling control.

Two general cases will be considered in an attempt to estimate the efficacy of sea water enhancement. One case assumes enhancemcnt of the sea water side only; the other considers both shell and tube side enhancement. The general conditions are shown in Table 1. An enhanced shell side heat transfer coefficient of 4000 Btu/hr ft$^2$ °F was assumed based on data from Refs. 1 and 2 and LMSC data for evaporation of ammonia from circumferentially grooved horizontal tubes. A range of sea water enhancement of from one to two has been chosen based primarily on the data of Ref. 3 where the term

Table 1

ENHANCEMENT CONDITIONS

| Case | Tube | Fouling (Btu/hr ft$^2$ °F)$^{-1}$ | $h_{NH_3}$ Btu/hr ft$^2$ °F | h'/h | $\eta$ |
|---|---|---|---|---|---|
| 1 | 2-in. × 0.034-in., Ti | 0.0005 | 1000 | 1-2 | 0.5, 0.75, 1 |
| 2 | 2-in. × 0.034-in., Ti | 0.0005 | 4000 | 1-2 | 0.5, 0.75, 1 |

h'/h (enhancement factor) refers to the ratio of enhanced to unenhanced heat transfer coefficients for the same sea water velocity. Three values of the "efficiency index," $\eta = h'/h/f'/f$, have been selected to cover the range of data covered in Refs. 1 and 3.

Comparison of the various enhanced conditions to the unenhanced sea water condition will be accomplished using a computer optimization program for the general OTEC operating conditions shown in Table 2.

Table 2

OTEC OPERATING CONDITIONS

| | |
|---|---|
| Tube diam., in. | 2.0 |
| Tube wall, in. | 0.034 |
| Tube length, ft | 34 |
| Tube conductivity, Btu/hr ft$^2$ °F | 10.4 |
| Fouling factor, (Btu/hr ft$^2$ °F)$^{-1}$ | 0.0005 |
| Hot sea water temperature, °F | 80 |
| $NH_3$ evaporation temperature, °F | 70 |
| $NH_3$ condensation temperature, °F | 50 |
| Cold sea water temperature, °F | 40 |
| Tube entrance plus exit loss coefficient | 0.75 |
| Efficiencies | |
| Rankine | 0.0368 |
| Pumps | 0.86 |
| Motors | 0.90 |
| Generator | 0.985 |
| Turbine | 0.87 |

Making some general assumptions regarding the cold water pipe pumping power requirement allows estimation of the heat exchanger surface area per net power output for the conditions of Table 1. The influence of sea water velocity and the degree of enhancement, h'/h, on evaporator area per net power output, $A_o/P$, is shown in Fig. 2. The top curve shows the relationship between velocity and $A_o/P$ for a tube with shell side enhancement only, for which an optimum value of 27.8 ft$^2$/kW occurs

at a velocity of 6.9 ft/sec. Increasing degrees of enhancement produce reduced values of $A_o/P$ at lower optimum sea water velocities reflecting the increasing friction factor and pumping power penalty. Minima data such as those shown in Fig. 2 have been plotted in Figs. 3 and 4 for the two cases given in Table 1. Also shown is the relationship between optimum velocity and enhancement factor and efficiency index. The unenhanced tube side condition is given in Figs. 3 and 4 at $h'/h = \eta = 1$ yielding 27.8 and 39.2 $ft^2$/kW respectively. This results in a reduction in evaporator surface area of approximately 30 percent from shell side enhancement alone, which represents a significant decrease in heat exchanger size with an attendant cost reduction on the order of 10 percent.[4] Using the results of Figs. 3 and 4, it is possible to estimate the net reduction or gain in evaporator surface area resulting from sea water enhancement for the two cases of Table 1. Figure 5 shows the effect of sea water enhancement compared with a completely unenhanced tube ($h_{NH_3}$ = 1000 Btu/hr $ft^2$ ° F) and a tube with shell side enhancement only ($h_{NH_3}$ = 4000 Btu/hr $ft^2$ ° F).

The design value for fouling factor has a significant impact on the required heat exchanger surface area, which raises a question concerning the influence of fouling factor on the reduction or increase in surface area with sea water enhancement. It should be noted that reference to surface area change for the fluted tube refers to change in the total length of tubing. The internal area ratio due to fluting is accounted for by the enhancement factor, h'/h, as if the inside tube area were given by $\pi D_i L$. The influence of fouling factor design value on the increase or decrease in evaporator surface area is shown in Fig. 6 for two values of efficiency index and enhancement factor. These results indicate that the percent change in surface area due to sea water enhancement is only slightly affected by the value of fouling factor assumed.

## Discussion

The conditions shown in Tables 1 and 2 were chosen to make the assessment of sea water enhancement as general as possible while covering the expected range of shell side and tube side enhancement. Heat exchanger cost studies generally show a minimum occurring for a tube diameter of between 1.5 and 2.5 inches, depending on tube material and cost assumptions. Minimum cost also occurs at a tube L/D greater than that which will produce minimum surface area. Minimum surface area generally occurs at a tube L/D of approximately 100, while minimum heat exchanger cost occurs in the range of 200 to 450, depending on tube diameter and material.

An indication of current sea water enhancement capability is given in Fig. 7 for the two general techniques presently being pursued. It would appear that enhancement through turbulence promotion using the techniques investigated by Sabin and Poppendiek[3] and the corrugated tube[6] are generally limited to an efficiency index of 0.6 or less. The data for vanes shown in Fig. 7 were taken from Fig. 7 of Ref. 3 at the largest Reynolds number shown, which was 20,000. The sea water Reynolds number at 80 ° F is given by Re = 8500 VD where velocity is in ft/sec and diameter is in inches. Based on a minimum optimum sea water velocity of 5 ft/sec, the applicable Reynolds number range is 42,600 to 85,200 for tube inside diameters of between one and two inches, which is substantially larger than the value of 20,000 for the vane data. The trend of the data shown in Figs. 6 and 7 of Ref. 3 indicates that the efficiency index and enhancement factor will be even less than that shown in Fig. 7 when evaluated at representative OTEC Reynolds numbers should also be noted that the family of lines shown in Fig. Ref. 3 does not represent the efficiency index as indicated since the efficiency index has $h'/h = f'/f = 0$ as its point of origin.

Based on the curves of Fig. 5, it would appear that the use of vanes and rings for turbulence promotion as proposed in Ref. 3 would lead to an increase in evaporator heat transfer surface area rather than a reduction. This is in rather sharp contrast to the 30 percent reduction in surface area indicated in Ref. 3 for $\eta = 0.75$ and $h'/h = 1.5$. It is felt that this disparity results from the assumption made in Ref. 3 that all other thermal resistances are negligible compared to the water side. An indication of the relative proportion of the various thermal resistances is shown in Fig. 8 for the case of an enhanced shell side heat transfer coefficient. In this instance, the tube side resistance is less that half the total, which also reflects the importance of fouling considerations on the overall heat transfer coefficient. The net effect is to make the overall heat transfer coefficient much less sensitive to changes in the tube side heat transfer coefficient as indicated in Fig. 1 and probably led to the optimistic result of a 30 percent area reduction in Ref. 3.

The corrugated tubes of Ref. 6 appear to have a substantially better enhancement factor than the other enhancement devices of Fig. 7 and, for the enhanced shell side case, a reduction in surface area over the unenhanced sea water case of from five to ten percent appears possible. Unfortunately, the shell side enhancement does not appear to be too favorable based on condensation data for steam from Ref. 6, where roughly a 50 percent improvement over a plain tube was reported. This is substantially less than that attainable with fluted or grooved tubes as indicated by the data of Refs. 1 and 2 and by LMSC's experience with evaporation from horizontal tubes. If the relatively poor condensing enhancement with steam is also typical for evaporation and condensing of ammonia, then the use of corrugated tubes for OTEC heat exchangers would not appear to be justified.

Based on the results of Fig. 5, the extended surface tubes of Ref. 1 appear to offer the best hope for reduction in the size of the evaporator and condenser through tube side enhancement. This can be seen to result, primarily, through its larger efficiency index, which yields a 10 percent reduction at an enhancement factor of 1.5 for the shell side enhanced case. Unfortunately, the increased material costs for the fluting will most likely exceed any gains resulting from a reduction in the lineal footage of heat exchanger tubing required. For a 0.065-in. thick wall, the addition of 0.026-in. fluting would increase the material costs by approximately 20 percent, not considering fabrication costs. Greater flute heights such as 0.045 in. and 0.060 in. would make the material costs of tube side enhancement even more costly. The increased tube costs plus the associated problems with biofouling control on other than plain tubes would tend to make tube side enhancement with extended surfaces less than promising for OTEC application.

## Conclusions

An attempt has been made to evaluate the efficacy of tube side enhancement in a manner that incorporates the pumping power penalty for an optimized OTEC plant. Obviously, it is not possible to cover every conceivable operating condition in the limited time and space available for the present comm---

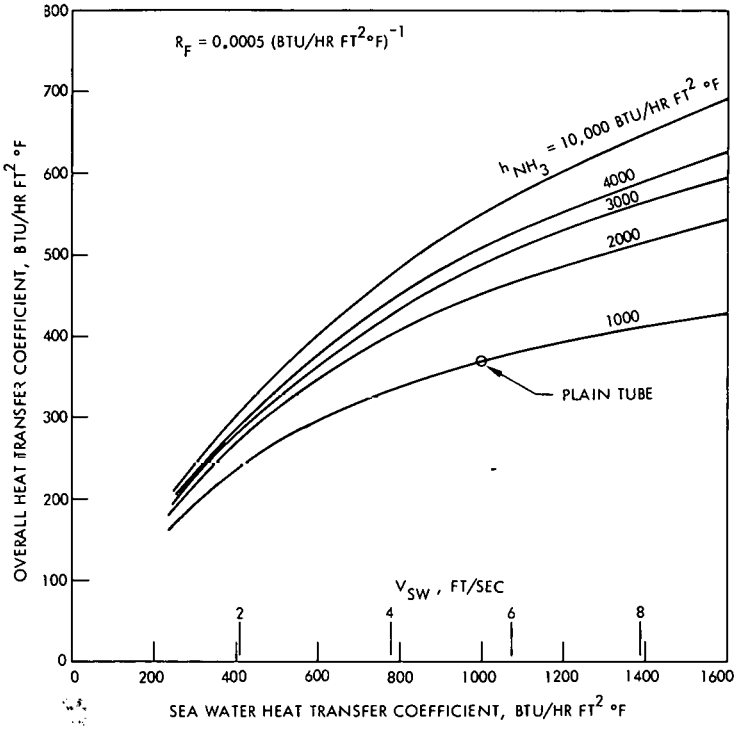



Fig. 1 Overall heat transfer coefficient dependence on sea water and ammonia evaporation heat transfer coefficient

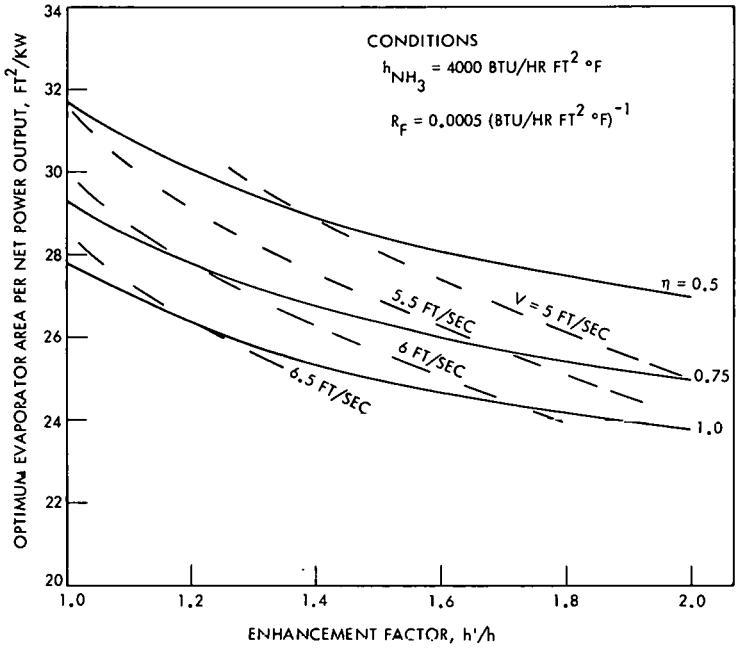



Fig. 3 Optimum evaporator area per net electrical power output with shell side enhancement

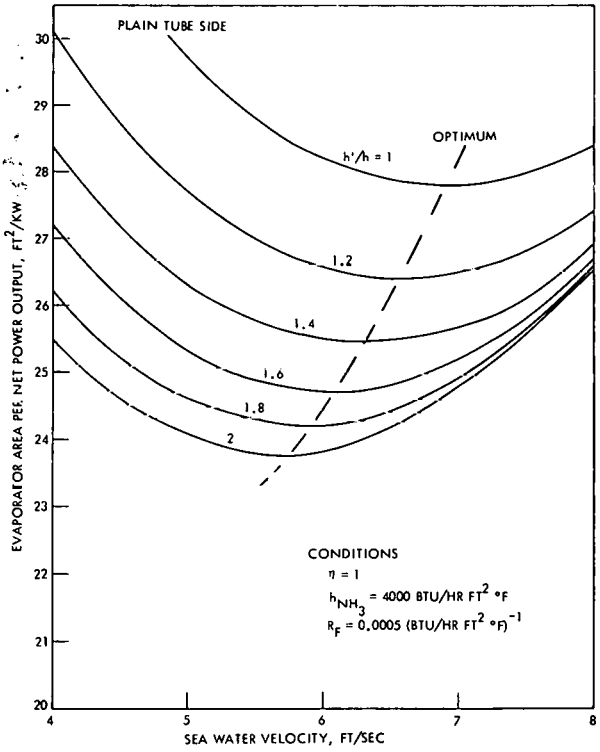



Fig. 2 Variation of evaporator area per net electrical power output with sea water velocity and enhancement factor

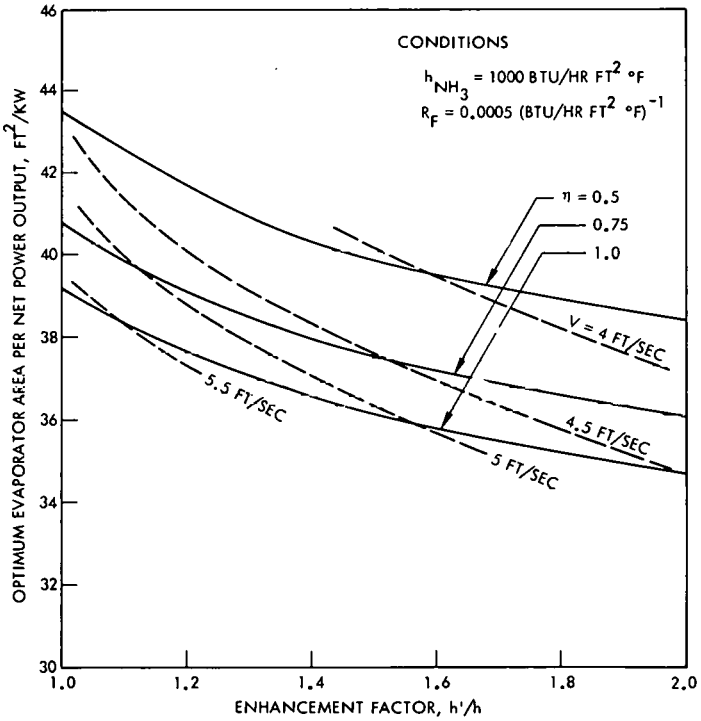



Fig. 4 Optimum evaporator area per net electrical power output without shell side enhancement

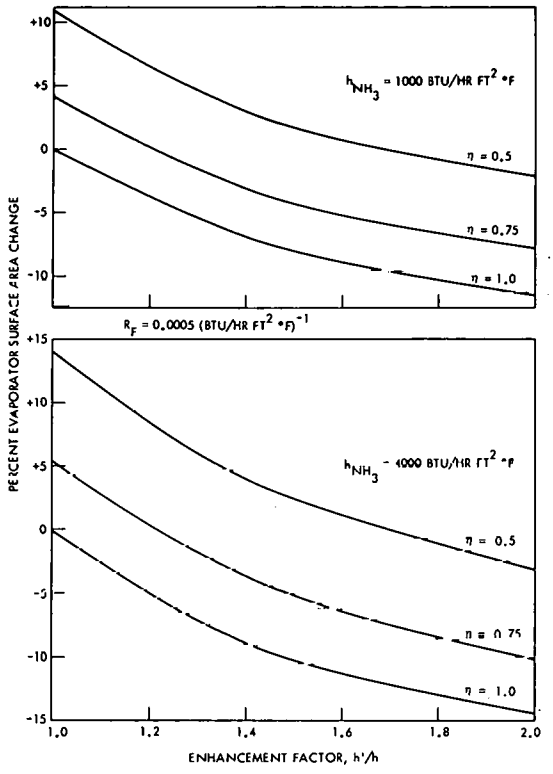



Fig. 5 Variation of percentage evaporator surface area change as a function of enhancement factor

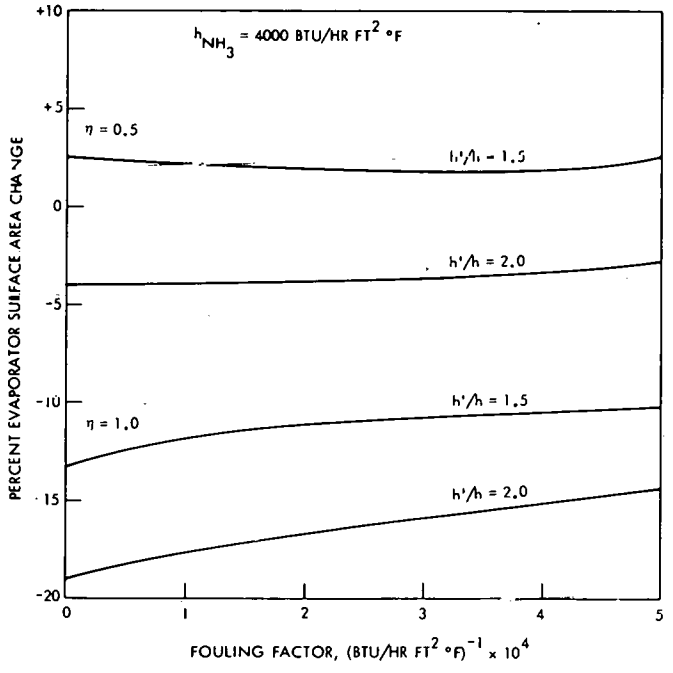



Fig. 6 Variation of percentage evaporator surface area change as a function of fouling factor

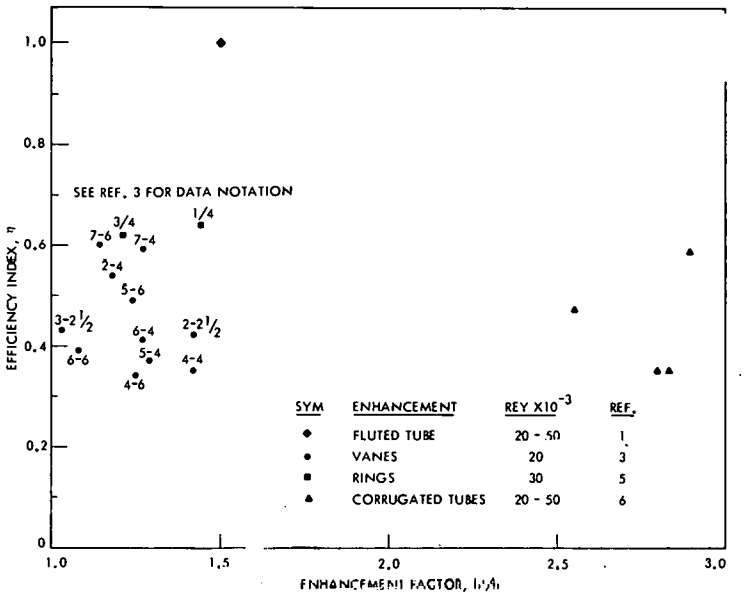



Fig. 7 Experimental values of efficiency index and enhancement factor

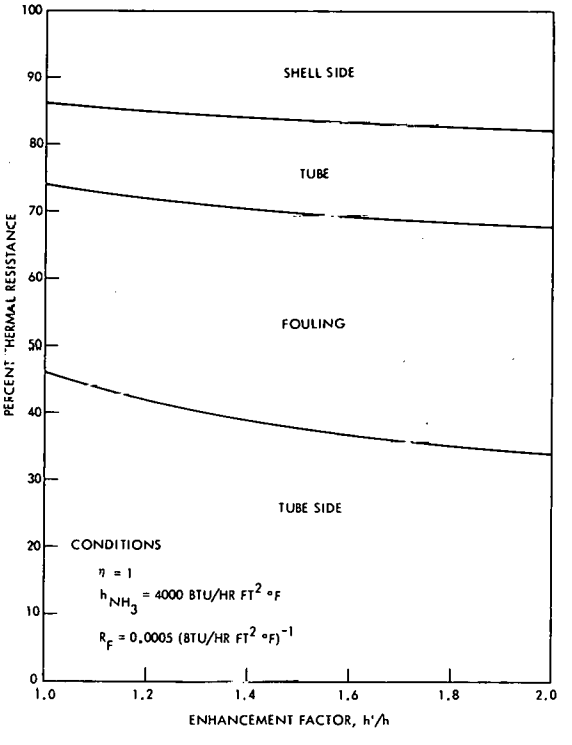



Fig. 8 Percent thermal resistance as a function of enhancement

Had more time been available, along with the necessary cost data, it would have been possible to treat the optimum cost rather than optimum heat exchanger surface area. In spite of these obvious shortcomings, it is felt that results of the present examination of sea water enhancement will allow several general observations.

1. The percent change in surface area as a function of enhancement factor and efficiency index is relatively insensitive to the fouling factor and shell side heat transfer coefficient.

2. Turbulence promotion devices such as vanes and rings, in most cases, will result in an increase in the total heat exchanger surface area required when compared to a tube without sea water enhancement. In addition, this type of enhancement will complicate most methods presently envisaged to control biofouling.

3. Corrugated or spiral tubes have the capability of reducing surface area by approximately 5 to 10 percent as a result of tube side enhancement, although this appears to be offset by its somewhat lower apparent shell side enhancement when compared with other techniques. Evaporation and condensation data for corrugated tubes with ammonia will probably show this technique to be less effective from an overall cost standpoint than tubes with fluted or grooved shell side enhancement. Biofouling control may also be difficult with the corrugated tube.

4. The extended surface form of sea water enhancement offers the potential of a 10 to 15 percent reduction in total tube length as a result of its generally higher efficiency index. Unfortunately, any potential reductions in total required tube length will be more than offset by increased tube costs. This technique will also offer some disadvantages from the standpoint of biofouling control.

5. Tube side enhancement for OTEC heat exchangers awaits the development of a surface with a suitable combination of efficiency index and enhancement factor that allows a net reduction in tube cost and does not complicate biofouling control. Until such a surface is developed, it is felt that the plain tube side with shell side enhancement offers the best current solution for application to OTEC heat exchangers.

## References


1. Rothfus, R. R. and Neuman, C. P., The OTEC Program at Carnegie-Mellon University – Heat Transfer Research and Power Cycle Transient Modeling, Fourth Ocean Thermal Energy Conference, New Orleans, La., Mar 1977.

2. Czikk, A.M., et al., Ocean Thermal Power Plant Heat Exchangers, Joint Conference American Section, International Solar Energy Soc. and Solar Energy Society of Canada, Inc., Aug 1976, Winnipeg, Canada.

3. Sabin, C.M. and Poppendiek, H.F., Heat Transfer Enhancement for Evaporators, Fourth Ocean Thermal Energy Conference, New Orleans, La., Mar 1977.

4. Owens, W.L., Cost Comparison for Three OTEC Heat Exchanger Designs, LMSC IDC 5702/175, 18 Jan 1977.

5. Sabin, C.M., et al., Nucleating Vaporization and Extended Surface Heat Transfer at Low Temperature Difference, ERDA Contract No. E(04-3)-1094, Geoscience Ltd., Report GLR-165, May 1976.

6. Young, E. H., et al., Heat Transfer Characteristics of Corrugated Tubes in Steam Condensing Applications, AICHE Paper No. 3, The 15th National Heat Transfer Conf., San Francisco, Calif., Aug 1975

# REPLY TO COMMENTS ON SEAWATER SIDE ENHANCEMENT FOR OTEC HEAT EXCHANGERS

C. M. SABIN AND H. F. POPPENDIEK
*Geoscience Ltd.*
*410 South Cedros Avenue*
*Solana Beach, California*

W. L. Owens is to be commended for taking the time and effort to comment on seawater side heat transfer enhancement. Unfortunately, he appears to have missed some key points in our paper; they are briefly discussed below.

1. "Efficiency factors" for enhancement techniques are by no means limited to a value of 0.6. Figures 8 and 9 of our paper clearly show that in certain Reynolds modulus bands, the wire ring geometries exceed an efficiency factor of unity. This fact was not given special attention in our paper; it was our feeling that the performance of this geometry was remarkable enough that individuals familiar with heat transfer surface development could not fail to recognize its significance.

2. All of the approaches to water heat transfer enhancement utilized in the Geoscience tests depend upon mechanisms which are strongly Reynolds modulus dependent. An enhancement technique which shows useful behavior at a specific Reynolds modulus must be modified geometrically to adapt it for use at another Reynolds modulus (in order that one would obtain optimum behavior). If a specific geometry were to be utilized at a Reynolds modulus different from its optimum point, poor performance could be expected.

3. None of the approaches to water heat transfer enhancement utilized in the Geoscience tests have recourse to turbulence generation for their effects. The poorer vane configurations, at off-optimum conditions, exhibit efficiencies almost as low as turbulence generators. The better vane configurations, near their optima, exhibit efficiencies three to four times better than turbulence generators. It appears that more efficient vane devices than those tested in the Geoscience program could be readily developed. In the case of Geoscience's wire rings, no additional fluid friction is involved in optimum regions.

4. In the area reduction example given in our paper of the application of a "low efficiency" enhancement technique, it was shown that regimes exist in which significant advantages can result. The example used was based on one specific cost-optimized design which exhibited a heat transfer effectiveness of about 0.25. We understand that the Lockheed cost-optimized designs (because of differences in basic input data) exhibit effectivenesses about twice this value. By consideration of the equations and Figures 15 and 16 of our paper, it is obvious that the application of a "low efficiency" surface modification is not appropriate at this specific effectiveness. Owens' suggestion that the differences are due to additional heat transfer resistances is not correct. The addition of other heat transfer resistances does not change the nature of the result shown in our paper; it does change the magnitude of the area reaction obtained, as one would expect.

The example mathematics presented were reduced to their most elementary form in order that the reader could readily recognize the simple, and somewhat inflexible, relationship between the principal parameters. Inclusion of additional effects would obscure the interrelationship between controlling parameters.

Inasmuch as Owens has addressed topics in his comments which are unrelated to the subject matter of our paper for the reasons cited above, we believe that it would be inappropriate for us to comment further.

# EXPERIMENTS ON AND DESIGN OF LOW-COST ALUMINUM HEAT EXCHANGERS FOR OTEC PLANT SHIPS

G. L. Dugger, H. L. Olsen, P. P. Pandolfini, and W. H. Avery
*Aeronautics Division*
*Applied Physics Laboratory, The John Hopkins University*
*Johns Hopkins Road*
*Laurel, Maryland*

## Abstract

Successful commercial implementation of ocean thermal energy conversion (OTEC) plant-ships will require achievement of a capital cost competitive with land-based plants. The most expensive components of an OTEC system are the evaporators (heated by warm surface water), the condensers (cooled by water from 700-1000 m depth), and the floating ocean platform. To minimize these costs, simple two-phase-flow heat exchangers made of large-diameter aluminum tubes (ammonia inside, sea water outside) have been designed for integration with a simple, barge-type, reinforced concrete hull. Each 2.5-$MW_e$(net) evaporator or condenser module has 259, 76-mm (3-in.)-O.D. tubes approximately 730 ft long, folded to 27 horizontal passes each; 7 of these tubes are "nested" in a vertical plane in each of 37 "elements." The method of analysis and a concept for assembling these modules are presented. The estimated costs for the sixth and subsequent 500-$MW_e$(net) commercial plant-ships are \$19/$m^2$ (\$1.77/$ft^2$) for the heat exchangers and \$573/$kW_e$ of net onboard power for the OTEC plant-ship. Experiments have been conducted with an ammonia flow loop containing a 77-mm (3.02-in.)-O.D. x 6-m (20-ft)-long aluminum tube simulating one pass in an evaporator. Inlet quality (mass percent vapor) was varied from 0 to 20% by means of a digitally modularized, steam-jacketed preheater. The test section was heated externally by electric tape. Some flow stratification occurred as expected at these low qualities, but the internal (ammonia-side), two-phase heat transfer coefficients were in agreement with the Chaddock-Brunemann correlation.

## Introduction

The development of low-cost heat exchangers for the OTEC power plant is vital to the achievement of economic viability for OTEC applications (Refs. 1-11). The small temperature differences available from the ocean require that the neat exchangers have areas of 5 to 13 $m^2$ (50-130 $ft^2$) per $kW_e$(net) of plant output. The need for a low-cost design (compared to current industrial heat exchanger costs) in order to make OTEC power plants competitive with alternative power sources has been a driving principal in the development of the APL approach. Two important subsidiary considerations have been:

1) The system design must utilize currently available technology, so that a 5-$MW_e$ pilot plant (one full-scale power module) installed on a platform large enough to permit expansion (by adding 19 more identical power modules) to a 100-$MW_e$ demonstration plant-ship could be constructed and deployed by 1980, and

2) The heat exchangers immersed in the ocean water must permit periodic removal of biofouling *in situ*, without interruption of operation, by an inexpensive and practical method.

Employing these basic criteria, and working in conjunction with the Energy Research and Development Administration (ERDA), the U.S. Maritime Administration (MarAd) and Office of Sea Grant, Department of Commerce, and with shipbuilders and the water-electrolysis, ammonia and aluminum industries, and many others (see Acknowledgment), APL has developed an overall "plant-ship" concept which promises a timely and economically viable means for implementation to relieve demands on U.S. fossil fuel resources (Refs. 1,6).

In the APL concept, OTEC plant-ships would operate in the tropical oceans in regions of maximum ocean temperature difference ($\Delta T$ = 24°C or 43°F) and minimum winds, waves, and currents (Ref. 6). The plant-ships comprise OTEC power plants plus onboard plants to manufacture energy-intensive products for shipment to U.S. or foreign ports. The preferred region for initial siting of OTEC/ammonia plant ships is in the mid-Atlantic Ocean, from 20° to 30° west longitude at 5° south to 5° north latitude. The liquid, anhydrous ammonia produced on board would be delivered to New Orleans for eventual use as fertilizer in the grain belt of midwestern USA.

This paper summarizes the method of heat exchanger analysis, estimated heat exchanger and plant-ship costs, and results of initial internal heat transfer experiments.

## The OTEC/Ammonia Plant-Ship Concept

The baseline, 100-$MW_e$(net), 300-short-ton/day, OTEC/ammonia demonstration plant-ship is shown in Fig. 1. The basic OTEC plant is of modular design with forty evaporator modules, forty condenser modules, twenty turbines, and four generators. Each heat exchanger module com-

prises an array of large-diameter, horizontal, multiple-pass, aluminum tubes with ammonia working fluid inside the tubes (Fig. 2). Sea water flows downward over the tubes by gravity. Each module is housed in a rectangular, open compartment within the concrete hull structure, so that no separate heat exchanger shell is required. The open arrangement permits in situ cleaning by water jets, as well as ready access for removal of a module for repair. Warm surface seawater is pumped by 20 outboard pumps into head ponds above the evaporator modules, from whence it flows downward and exhausts, slightly cooled, from the bottom of the vessel at about 21-m (70-ft) depth. The ponds probably will have removable covers (not shown) to mitigate free-surface dynamic effects and minimize growth of marine slimes (biofouling) on the tubes by excluding sunlight. Cold water is pumped from 760-m (2500-ft) depth by 19 pumps located near the top of the central, 18-m (60-ft) diameter, cold-water pipe (CWP) into ponds above the condensers. There are two condenser head ponds, one each fore and aft. Each has a sloped feed channel on each outboard side, deepest near the CWP, from which the water overflows transversely inward toward the pond centerline, thus providing a distributed flow over the ponds. The cold water also exits from the bottom of the vessel.

Demisters, turbines and generators are located on machinery decks between the rows of heat exchangers. These decks also house the electrolysis plant, which uses the OTEC power to produce hydrogen from fresh water (obtained from warm sea water by a reverse osmosis purification system) and the ammonia plant, which uses the hydrogen and nitrogen obtained by air liquefaction to produce liquid ammonia. The product ammonia is stored in tanks which, together with ballast tanks, are located in the hull between the rows of heat-exchanger compartments. The product ammonia is periodically off-loaded to tankers. Station-keeping for the plant-ship is provided by propulsors at the corners of the vessel, which propel the ship at a speed of about 0.5 knot relative to the local current to maintain its position or permit it to "graze" slowly in the area. They can produce 4800 HP for a maximum speed of 0.9 knot.

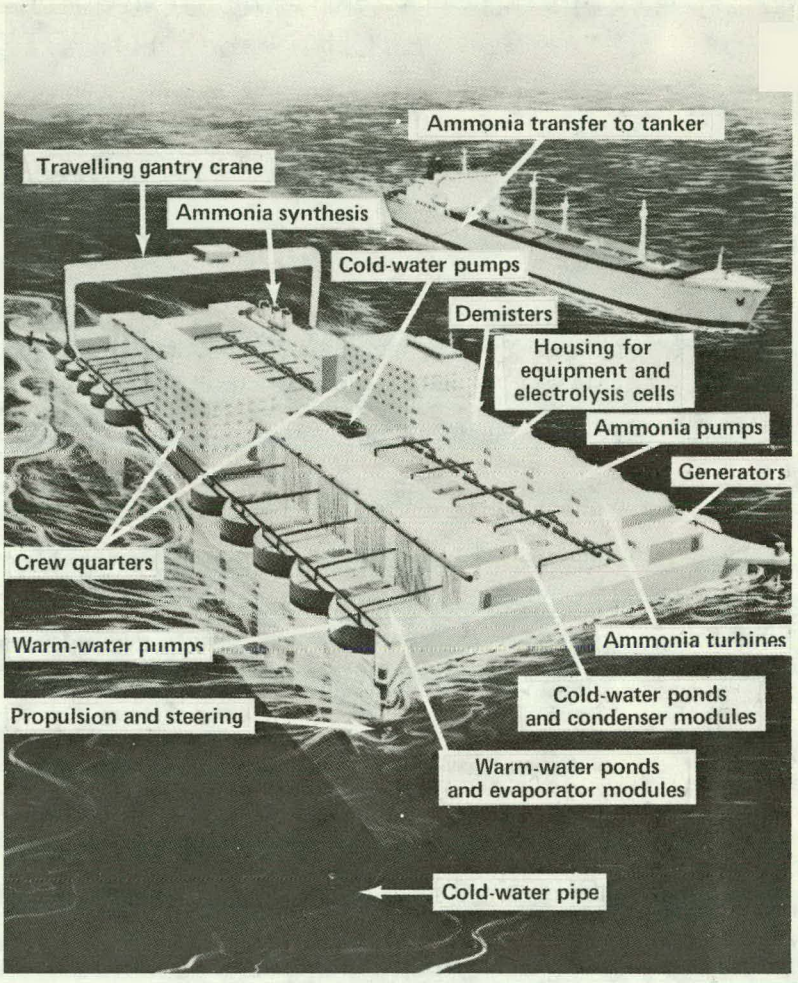



Fig. 1 Concept for 100-$MW_e$(net), 300-Short-Ton/Day, OTEC/Ammonia Demonstration Plant-Ship for Siting in Tropical Oceans

## APL Heat Exchanger Concept

The primary objective is to minimize the overall plant-ship cost. The heat exchanger design that meets this objective may not necessarily be the most efficient one from the standpoint of heat transfer. Low cost, modularity, cleanability, and maintainability are more important. After consideration of several heat exchanger types and configurations, a promising, novel type was investigated in detail to determine its potential for meeting these goals. It employs convective, two-phase-flow heat transfer from ammonia inside 77-mm (3-in.) O.D., multipass aluminum tubes to seawater flowing normal to the staggered tube arrays. This approach has been selected for the following reasons:

(a) Use of a relatively large tube diameter reduces the number of tube joints, thus reducing fabrication and assembly costs.

(b) No heat exchanger "shells" per se are required.

(c) A strong potential for economical, in situ cleaning of the heat exchangers using a water-jet system, such as the Hydronautics Cavijet™ (Ref. 12), without interruption of operations, results.

(d) The high degree of modularity will permit regularly scheduled inspection and maintenance, one module at a time, without a large reduction in the total power output.

These advantages of a simple heat exchanger design could outweigh the initial higher efficiency of a more complex design.

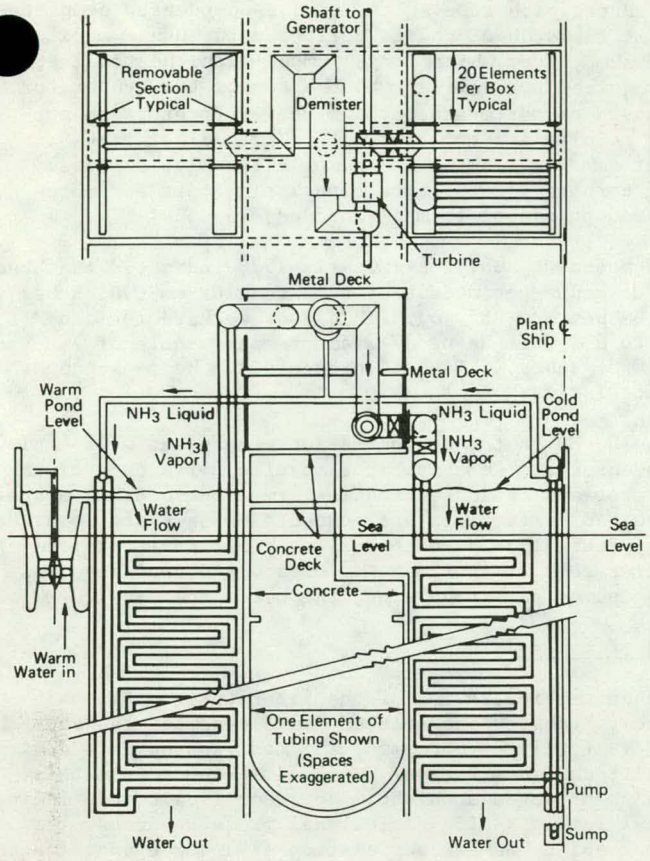



Fig. 2 Simplified Schematic of a 5-$MW_e$(net) Power Module

## Working fluid and tube material selection

Ammonia is by far the most attractive working fluid thermodynamically for OTEC plants (Refs. 8-10,13). (After ammonia, propane, which has been proposed by the Andersons (14), is the next best choice thermodynamically.) The selected heat exchanger tube material must be compatible with long-time contact with both ammonia and sea water. The leading candidates are titanium, stainless steel, and aluminum. Aluminum is by far the least expensive of the three for equivalent heat exchange performance. Aluminum alloys do suffer gradual corrosion and pitting in sea water, but suitable alloys can be found which will assure 20-year life at small penalty in corrosion allowance. Fink and Boyd (15) did an excellent review on the subject which shows that certain 5000 and 6000 series alloys would have an average corrosion of less than 1 mil (0.025 mm) per year. Verink (16) reported successful use of various alloys in the heat exchangers of an experimental desalting plant at far more severe conditions than will be faced by OTEC heat exchangers. The Kaiser Aluminum and Chemical Corporation has recommended to APL the use of Alclad 3004 (17). They judge that a sacrificial 0.08-0.13 mm (3- to 5-mil) cladding thickness of aluminum will provide the desired life for 76-mm-O.D. tubes with an overall wall thickness of 1.5 mm (0.06 in.). Our weight and cost estimates are based on the latter.

## Tube diameter and configuration tradeoffs

In selecting the tube diameter, pass length, number and arrangement of tubes in one multiple-tube "element" in a vertical plane, and spacing between elements, the best tradeoff among the following effects is sought:

1. For a given total power output requirement and a given enthalpy drop (or pressure ratio) across the turbine, the total ammonia flow rate is essentially fixed. (It will change slightly with the water pumping power requirements, which, in turn, depend on the heat exchanger design, as brought out later.) If ammonia velocities entering the heat exchanger tubes also remain the same, the total number of tubes $N_T$ required is inversely proportional to inside tube diameter squared, $D^2$. However, the required total length L of a multipass tube increases approximately as $D^{1.2}$. Two effects cause this exponent on D to exceed 1.0: heat transfer efficiency decreases slightly as D is increased, and, for a given heat exchanger compartment width (available tube pass length l), the number of return bends per tube $n_r$ increases with D, so that internal loss increases (see item 3). Letting $A_T$ = total heat exchanger surface area, $N_R$ = total number of return bends, $V_T$ = total internal volume of the tubes, and $V_m$ = volume of ammonia being circulated, the following approximate relations apply ($\propto$ = proportionality sign):

$$N_T \propto D^{-2}; \quad L \propto D^{1.2}; \quad n_r \propto L/l \propto D^{1.2} \tag{1}$$

$$N_R = N_T n_r \propto D^{-2} D^{1.2} = D^{-0.8} \tag{2}$$

$$V_T \propto V_m = N_T L\frac{\pi}{4} D^2 \propto D^{-2} D^{1.2} D^2 = D^{1.2} \tag{3}$$

$$A_T = N_T L\pi D \propto D^{-2} D^{1.2} D = D^{0.2} \tag{4}$$

2. Although volume $V_T$ decreases as D is decreased, $N_R$ and $N_T$ increase, making the plumbing more complex.

3. The internal pressure losses affect not only the ammonia pumping power requirement, but also the local water-to-ammonia temperature differences ($\Delta T$'s) for heat transfer, because the saturation temperature at which the ammonia boils increases with pressure. As D is increased, a higher initial pressure in the evaporator is required to overcome losses due to more bends (higher $n_r$) and to a larger gravity head (depth reached by the multipass tube), resulting in a lower $\Delta T$ and lower heat flux.

4. Tube spacings must be sufficient for practical tube-bundle fabrication, and a uniform lateral spacing between rows is important because it controls water flow distribution. Since variations in straightness of low-cost-production tubing may run near 1% per 8 m, engineering judgement indicates that design spacings should be at least 19 mm (3/4 in.), so a 19-mm spacing in the vertical plane is used in all cases. This desire for large spacings reduces the volumetric advantage achieved by reducing D.

5. Sea water velocity $v_w$ is inversely related to the minimum passage width between tubes of adjacent elements.

A $v_w$ of several feet per second is desired (a) to keep the water-wide heat transfer coefficient $h_w$ up and (b) to minimize the rate of biofouling, especially in the evaporators. However, a clear space of approximately 32 mm (1.25 in.) between elements is desired to permit the translation of a cleaning head in the vertical plane between the elements; this calls for a compromise toward the lower end of a $v_w$ range.

6. The water-side pressure drop is proportional to $v_w^2$ and to the number of tube passes in an element. Since the water pumps are among the major OTEC cost items, and the required water-pond height above the heat exchangers adds to ship buoyancy requirements, the system cost optimization leads to $v_w$'s near 1 m/sec.

7. To take advantage of a reasonable platform depth, striking a balance between required planform area and depth, it is desirable to "nest" several of the multipass tubes in the vertical plane (Fig. 2). Several multipass tubes run in adjacent, parallel passes, so that all experience essentially the same full seawater $\Delta T$ and essentially the same internal ammonia head conditions throughout. The resulting set of tubes in one vertical plane is called a heat exchanger element. This leads to a multiple of the minimum water passage width since approximately the same quantity of water per tube must flow, for a given tube diameter and a given water temperature change through the total depth, to accomplish the heat transfer. Increasing the number of tubes per element increases the space for cleaning, but it also directly increases the water head required.

Conceptual design of the heat exchangers

A computer program was used to explore the aforementioned tradeoff factors, including tube diameters from 3 in. to 9 in. (Ref. 11). The configuration initially selected in October 1975 for the development of the baseline concept for the demonstration-size plant ship of Fig. 1 was based on triply nested 152-mm-O.D. tubes. For simplicity, the schematic diagram for that configuration is shown in Fig. 2. The upper (planform) view illustrates the use of two each of the evaporator and condenser modules per turbine. The plant-ship centerline is at the right edge of the drawing; a mirror-imaged right half of the ship would complete a typical section through the beam. The lower (elevation) view illustrates typical evaporator and condenser elements, in which the tube banks will be made identical to simplify construction and inventory problems. Only the inlet and outlet plumbing and the ammonia flow direction differ.

In an evaporator element each of the nested tubes is fed liquid ammonia via a downcomer pipe in which part of the liquid heatup is accomplished. A short (about 1.5 m) riser, in which the liquid flows upward, is then provided to induce the onset of nucleate boiling within the riser while avoiding the possibility of gas bubbles forming too soon and flowing up the feed pipe. As the ensuing two-phase mixture flows upward through the multipass tube, 70% of the liquid is vaporized, i.e., a mixture of 70% quality goes from the top of the evaporator to a demister. The demister returns the liquid to the evaporator inlet. The vapor drives the turbine and then goes to the condenser. In a condenser element, ammonia vapor enters each tube at the top, is condensed completely as it flows down, and is delivered through a manifold to the sump, from which it is pumped with the total pressure required for delivery to the top of the evaporator. The closed compartments between the evaporator and condenser modules are employed either as ballast tanks or product ammonia tanks. For simplicity, Fig. 2 shows square corners for the tube bends. The cost estimates are based on use of formed (rounded) bends.

Subsequent analyses in early 1976 indicated that use of 22 elements per module of 6 nested 102-mm-O.D. tubes would be better (Ref. 6). This year we have revised again to a system using 37 elements per module of 7 nested 76-mm-O.D. tubes.* Table 1 presents the heat-exchanger characteristics.

A 100-$MW_e$(net), demonstration-size plant will employ 40 condenser and 40 evaporator modules. Two each of the evaporator and condenser modules drive one 6.6-$MW_e$ output turbine. Five turbines are connected on a shaft to drive each of four 31.7-$MW_e$-output, a.c.-generator/transformer/rectifier sets. With 26.6 $MW_e$ of power output required for the pumps and propulsion, the net output is 100 $MW_e$.

Method of analysis

An extensive review of the literature on two-phase-flow heat transfer and related fluid dynamics was conducted (Ref. 11) to determine the most appropriate analytical techniques for our proposed system. From this review we selected a Chisholm approach (18) to estimating internal (ammonia-side) frictional pressure drops, the Chaddock and Brunemann correlation (19) for evaporator heat transfer, an ASHRAE-recommended correlation (20) for condenser heat transfer, and estimates of the effects of gravity, acceleration, and tube bends on the pressure drop following Collier (21). Since none of the references provided experimental data or correlations covering all of our conditions simultaneously, the correlations have to be extrapolated from the conditions for which they were developed. The potential problem of operational instabilities in the heat exchangers was investigated (Ref. 11), and instability criteria were taken into account in the application of the developed program.

The analytical results for heat transfer and pressure drop are believed to be accurate within $\pm$ 30%, as is true for most initial designs of heat exchangers. Experimental work has begun at APL under ERDA support to provide the accuracy that will be needed for pilot plant design. Details of the analysis by Olsen and Pandolfini (11) and the initial experiments by Olsen et al. (22) are available. Only a brief description of the analysis can be given here.

Evaporator heat transfer and internal pressure drop.--The initial warmup (enthalpy change $\Delta h_0$) is accomplished in the downcomer, with turbulent convective heat transfer from the warm sea water, in concurrent

*This revision resulted after William Owens of Lockheed pointed out two errors in the APL code to the third author. We are grateful to Mr. Owens.

Table 1 Configuration of Heat Exchangers Using Seven-Nested 76-mm-O.D. Tubes

| | |
|---|---|
| :r of evaporator modules = number of condenser modules | 40 |
| Tubes per module | 259 |
| 7-tube elements per module | 37 |
| Required length per multipass tube (not counting evaporator downcomer or exit riser) | 222 m |
| Number of passes/tube | 27 |
| Required length/pass = 222 m/27 | 8.2 m |
| Length per pass comprises: | |
| Straight horizontal run | 7.6 m |
| Length in bend | 0.7 m |
| Downcomer length for evaporator (21.1 m down, 0.7-m bend, 1.5 m up) | 23.3 m |
| Riser from evaporator to demister | 7.6 m |
| Total length per evaporator tube (222 + 23.3 + 7.6) | 253 m |
| Horizontal spacing (center to center) of elements | 0.108 m |
| Vertical spacing (center to center) of passes | 0.095 m |
| Heat exchanger depth (189 passes) | 19.6 m |
| Module compartment width (ship beam direction) | 8.9 m |
| Module compartment length (ship length direction, 37 x 0.108 m) | 4.0 m |
| Sea water velocity | 0.84 m/s |
| Sea water temperature drop | 2.78 K |
| For 100 $MW_e$net: | |
| Evaporator water flow | $1.50 \times 10^9$ kg/hr |
| Condenser water flow | $1.46 \times 10^9$ kg/hr |
| Ammonia flow through turbine | $1.41 \times 10^7$ kg/hr |
| Evaporator HX area, incl. downcomer | $0.61 \times 10^6$ m² |
| Condenser HX area | $0.54 \times 10^6$ m² |

flow, to the liquid ammonia inside the tube. The onset of nucleate boiling in the subcooled region in the riser (or the beginning of the first horizontal pass; see Fig. 2) is predicted by the method of Bergles and Rohsenow (23) as modified by Frost and Dzakowic (24).

The two-phase-flow portion of the multipass tube is then divided into N computation sections of equal mass quality change, $\Delta x_i$ (per section) = $x_{me}/N$, where $x_{me}$ is evaporator exit quality. For the $i^{th}$ section the ammonia-side heat transfer coefficient is calculated from the Chaddock-Brunemann correlation (19):

$$h_i = 1.91\, h_{L_i}\, (Bo \times 10^4 + 1.5\, X_i^{-2/3})^{0.6} \qquad (5)$$

where Bo is the boiling number (heat flux divided by weight flow rate times latent heat), $X_i$ is the Martinelli parameter, and $h_L$ is the coefficient for all-liquid flow,

$$h_{L_i} = 0.023\, (k_f/D_{in})\, Re_i^{0.8}\, Pr_i^{0.4} \qquad (6)$$

where $k_f$ is thermal conductivity of liquid; $D_{in}$, inside diam; and Re and Pr are the Reynolds and Prandtl numbers.

For the water-side heat transfer coefficient $h_w$ for flow normal to a staggered tube bank, the correlation from Zukauskas (25) is used:

$$h_w = 0.022\, (k_w/D_{out})\, Re_w^{0.84}\, Pr_w^{0.36} \qquad (7)$$

The overall heat transfer coefficient for the $i^{th}$ section is

$$U_i = (h_w^{-1} + t/k_{Al} + h_{scale}^{-1} + h_i^{-1})^{-1} \qquad (8)$$

where t is aluminum wall thickness, and $h_{scale}$ (water side) is taken to be 2000. In determining $\Delta t_{mi}$ for the $i^{th}$ computation section, the effect of local pressure changes on the local ammonia saturation temperature is taken into account. The friction drop for the $i^{th}$ section is

$$\Delta p_{f_i} = \ell_i\, (1 + 10\, X_l^{-1} + X_l^{-2})(1 - x_i)^2 \cdot 2 f \rho v^2 / g D_{in} \qquad (9)$$

where f is the friction factor, v the all liquid flow velocity, g the gravitational constant, and the constant 10 is typical for large-bore pipe (Ref. 21). The acceleration pressure drop, $\Delta p_{a_i} = \Delta p_{a_i}\, (\rho_f, \rho_g, v_f, x_i, \alpha_i)$, is given by the second term of Eq. 2.35 of Ref. 21 with denominator taken to be unity. Subscripts f and g denote liquid and vapor, respectively. The void fraction $\alpha_i$ is found from the drift-flux model as

$$\alpha_i = Q_{g_i}/[1.2\, (Q_g + Q_f)_i + v_b\, A] \qquad (10)$$

where Q is volumetric flow rate, and $v_b$ is the bubble-rise velocity (in the horizontal run, $v_b = 0$). The gravity loss for a height change $\Delta z_i$ due to return bends in the $i^{th}$ computation section is:

$$\Delta p_{z_i} = -[\rho_g \alpha_i + \rho_f\, (1 - \alpha_i)]\, \Delta z_i \qquad (11)$$

The bend loss for $n_{b_i}$ bends within the $i^{th}$ section is:

$$\Delta p_{b_i} = n_{b_i}\, (\rho_f v_f^2/g)(1 + C_b\, X^{-1} + X^{-2})^{0.5} \cdot (1 - x_i)^{0.875} \qquad (12)$$

where $C_b$ is the Chisholm constant calculated from Collier's Eqs. 3.95 and 2.72 (21).

Since the evaporator outlet temperature is specified, a backward, iterative solution for the evaporator is done to obtain the evaporator tube length $L_e$ (and total two-phase heat exchange area, $A_e = N_e\, \pi\, D_{in}\, L_e$) and pressure drops that are converged for the evaporator. Finally, the total system analysis must be subjected to a global iteration which computes the cycle states and the heat exchanger analysis until satisfactory global convergence is obtained.

Condenser heat transfer and internal pressure drop.-- The total ammonia mass flow in the evaporator $\dot{w}_{me}$ is greater than the mass flow through the turbine $\dot{w}_m$ by the amount of liquid ammonia recirculated, i.e., $\dot{w}_{me} = \dot{w}_m/x_{me}$, where $x_{me}$ is the exit quality of the evaporator (nominally, 0.7). Complete condensation is required in the condenser (exit quality $x_{mc} = 0$).

The equation chosen for $h_i$ [Ref. 20, Chap. 2, p. 52, Eq. (14)] is

$$h_i = 0.057\ (c_p k\rho/\mu)_f^{0.5} (gD/4)^{0.5} (1 + CX_i^{-1} + X_i^2)(dp/d\ell)_{L_i}^{0.5} \qquad (13)$$

where $\mu$ is viscosity (and the g is deleted for S.I. units), and

$$(dp/d\ell_i)_{L_i} = [(1 - x_i)v_L]^2 f\rho_L/gD_{in};$$

$$v_L = 4\dot{w}_m/\pi D_{in}^2\, \rho_f N_c \qquad (14)$$

where $N_c$ is the total number of tubes in the condenser, and $v_L$ is the liquid (exit) velocity with the tube running full of liquid. This equation is strictly valid for only the vapor-shear controlled region, but it has been used in our analysis for the entire condenser because it yields conservative results (i.e., longer condenser tubes) and is easily used. [The $h_i$'s computed by the recommended (Ref. 21) equation for gravity-controlled regions are always higher than those given by Eq. (13).]

The $h_w$ is determined by Eq. (7) using the appropriate value of $Re_w$, and $U_i$ is given by Eq. (8). The method for obtaining $\Delta t_{mi}$ and the pressure drops for the condenser is essentially the same as outlined for the evaporator, except that a forward solution is employed, since the condenser inlet temperature $T_3$ is specified.

Water-side pressure drops in heat exchangers.-- For the water flow normal to the staggered tube bank with Reynolds numbers greater than $2 \times 10^5$, the Euler number, $Eu = g_c\, \Delta p/\rho v_w^2$, is essentially independent of Reynolds number (25) and is taken to be 0.08. The resulting pressure drop per tube pass (taking into account that there are two restrictions per pass) is

$$\Delta p_w = 2\, \rho v_w^2\, Eu/g_c = 0.16\, \rho v_w^2/g_c \qquad (15)$$

Parasitic power.--The baseline plant generates an equivalent of 132 $MW_e$ at the turbine shaft (126.6 $MW_e$ gross output from the four generators) in order to net 100 $MW_e$. The program includes calculations of the ammonia and water pumping requirements plus the 0.5-knot propulsive power. The global iteration must result in heat exchangers large enough to deliver 100 $MW_e$ net after subtracting these parasitic power requirements.

## Assembly of Heat Exchanger Modules

The concept for assembling the heat exchanger modules is as follows:

1) Obtain the materials: a) 76-mm-O.D., 1.5 mm-wall, aluminum tubes, cut by manufacturer to desired lengths, and b) the support structure items shown in Fig. 3. Extruded aluminum I-beams have recesses stamped out to cradle the tubes and provide the desired spacings. These "support strips" are pulled together by tie bolts that pass through predrilled holes in the support strips and in the tie-bolt collar-spacers. Three support strips per element [3 x (37 + 1) = 114 per module ] and (27 passes + 1) = 28 tie rods/support strip row (x 3 = 84 tie bolts/module) are required.

2) In shop, form the bends for each pass.

3) For each of the 7 complete tubes which are to be nested to form one heat exchanger element, make a welding rack with clamps to hold the 27 passes with the formed bends.

4) Place the tube sections in this rack, clamp them, and weld the passes together with an orbital welder to make a complete welded tube. Pressure check it and repair welds as needed (estimated at 15% of initial welding time).

5) Move this tube in its welding rack to the heat exchanger support rack, position it in the three support strips, unclamp the welding rack and return latter to the welding position. Repeat steps 2-5 for 6 more tubes to complete first element.

6) Insert tie bolts with the collar-spacers on the bolts. Put support strips for the next element in place. Repeat until all 37 elements are in place.

7) Tighten tie bolts. The combination of bolted support strips and welded tubes forms a rigid module.

8) Attach lifting cables and move to ship.

9) Install module. The details of the holddown structure are yet to be established, but the concept is as follows: Since the tubes are to be cleaned in place, it is only necessary to remove the module when repairs are required. The removal technique consists of flooding the tubes with liquid ammonia to counteract 60% of the buoyancy, placing weights on top of the module to achieve neutral buoyancy, removing holddown pins, removing the weights while the module rises in guide tracks installed in the compartment walls, and finally lifting the module with a crane. Thus, tracks and holddown pin supports are required in the compartments, and weight support racks and lifting eyes are required on the modules.

10) Install and connect ducts, valves, and manifolds.

The resulting estimated cost for a first-of-a-kind, 100-$MW_e$ demonstration plant ship is $35.2 M for the heat exchangers (Table 2). The technique is assumed to have been worked out when the first 5-$MW_e$ power module used on the pilot plant (requiring 2 modules each of evaporators and condensers) was constructed.

Since the heat exchanger module weight, 82 metric tons (Table 2), is relatively small for the 100-$MW_e$

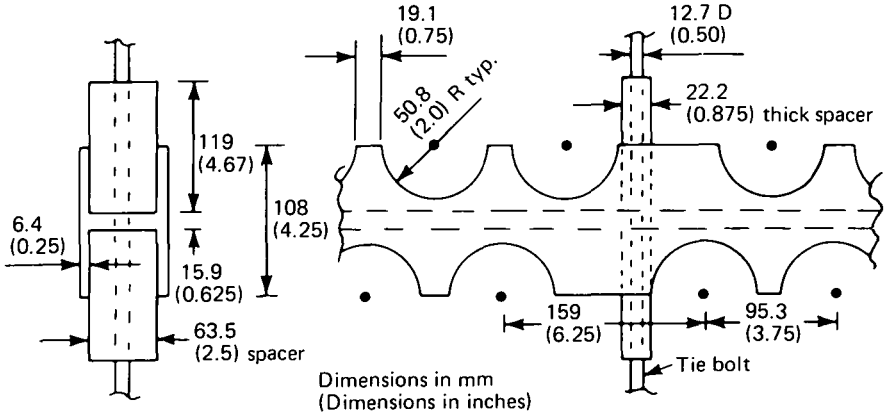



Fig. 3 Schematic Design of Support Strips, Spacers, and Tie Bolts. The 159-mm Spacing Applies for Tightest Bends (Every Seventh Space ).

Table 2 Estimated Costs of Heat Exchangers Using Seven Nested 3-in. Tubes (1975 Dollars)

| | | |
|---|---|---|
| Step 1, Material costs (averaged for condenser and evaporator): | | |
| Tubing, at $1.56/m plus 1 cut/pass at $1.50 | | |
| $1.56 (222 + 253)/2 + $1.50 x 27 | = $411/tube | |
| Elbows: $2.25 x 4 | = 10/tube | |
| Prorated cost of welding rack ($10K distributed over 37 x 80 tubes | = 3 | |
| Subtotal | $424/tube | |
| Per module (7 x 37 = 259 tubes) | = $109,800 | |
| Support strips 114 @ 121 kg @ $3.3/kg | = 45,500 | |
| Tie-bolts and spacers, 84 @ 15.5 kg @ $3.3/kg | = 4,300 | |
| Total tube-bank material/module | = $159,600 | |
| Steps 2-5, Labor per 7-tube element: | | |
| 30.7 man-hr per tube @ $15 | = $ 460 | |
| 0.8 hr for crane + operator @ $50/hr | = 40 | |
| Subtotal labor cost per tube | = $ 500 | |
| Subtotal per element (7 tubes) | = $ 3,500 | |
| Step 6, Advance tie-bolts and emplace spacers and next 3 strips, 3.3 man-hr @ $15 | = 50 | |
| Subtotal labor cost per element | = $ 3,550 | |
| For 37 elements, labor cost (for 6200 man-hr = 3.1 man-yr) | = $131,400 | |
| Step 7, Tighten tie-bolts, 3.3 man-hr @ $15 | = $ 50 | |
| Step 8, Attach cables and move to ship: | | |
| 2 hr, crane & operator @ $100/hr plus 8 man-hr @ $15 | = $ 320 | |
| Subtotal labor cost to ship (rounded) | = $131,800 | |
| Add material cost (rounded) | = 159,600 | |
| Subtotal per tube bank/module to ship | = $291,400 | |

(continued next column)

| | | |
|---|---|---|
| For 80 modules incl. 20% contingency: | | |
| Labor (321 man-yr + 20%) = $12.7 M | | |
| Material (+ 20%) = 15.3 M | | |
| Subtotal, 80 modules | | = $28.0 M |
| Step 9, Install holddown equipment and heat exchangers: | | |
| Labor (8 man-mo./module x 80 = 53 man-yr + 20% contingency) | = $ 1.9 M | |
| Material ($4000/module x 80 x 1.2) | = 0.4 M | |
| Subtotal, 80 modules + 20% contingency | | = $ 2.3 M |
| Step 10, Install valves and ducting to machinery (for 80 modules incl. 20% contingency) | | |
| Labor (0.5 man-yr x 80 = 40 man-yr + 20%) | = $1.6 M | |
| Material ($34,000 x 80 x 1.2) | = $3.3 M | |
| Subtotal, 80 modules | | = $ 4.9 M |
| Total installed cost of heat exchangers | | = $35.2 M |
| The overall split between labor and material is: | | |
| Labor (510 man-yr) = $16.2 M = 46% | | |
| Material = $19.0 M = 54% | | |
| Heat Exchanger Weight (Average for an Evaporator or a Condenser Module) | | |
| Tubing: 1.5 x $10^4$ $m^2$ (0.00152-m wall) x (2770 $kg/m^3$) | | = 63,000 kg |
| Support strips, tie bolts (144 x 121) + (84 x 15.5) | | = 18,700 kg |
| Hold-down material | | = 500 kg |
| Total | | = 82,200 kg |
| Buoyancy per module | | = 261,100 kg |
| Net buoyancy per module | | = 178,900 kg |
| The net buoyancy provided to the ship (80 modules) | | = 14,312 metric tons |

plant-ship (a 200-metric ton crane will be available, we assume that an optimal module configuration for a 500-$MW_e$, commercial-size plant ship will be twice as large, containing 518 tubes instead of 259. Then there will be 100 each of condenser and evaporator modules. If a "95% learning curve" is assumed (see Ref. 6), the second module will cost 0.95 times as much as the first; ourth, 0.95 times as much as the second; the eighth, 0.95 times the fourth, etc. The average cost of 100 evaporator or condenser modules will be 0.766 times the cost of the first module. Thus, the total heat exchanger cost for the first plant-ship is $35.2M x 5 x 0.766 = $134.8M. The next lots of 100 each of evaporator and condenser modules will cost 0.9 times the first lots, so the total heat exchanger cost for the second commercial plant-ship is $121.3M. The gain due to learning is

assumed to level out for the sixth and subsequent plant ships at a cost of \$110M, or \$19/$m^2$ (\$1.77/$ft^2$) of heat transfer area.

The reduction in cost from \$30.5/$m^2$ for the first-of-a-kind demonstration ship to \$19/$m^2$ for the sixth commercial ship is a 37.7% reduction. A 0.9 learning curve to the 550th unit of either evaporators or condensers would reduce the labor cost by 61.8%, saving 0.618 (\$16.2M x 5) = 50.1M of the total (35.2M x 5) - \$110.2M = \$65.8 M. A 14% reduction in heat exchanger cost due to better optimization (e.g. use of longer passes) would take care of the other \$15.7M with no credit for reduction in material cost. However, if we assume a 10% reduction in material cost due to learning for the fabrication of the framing items and to large quantity orders of tubing and bar stock (for framing), this would save 0.1 x \$19.0M x 5 = \$9.5M. The remaining \$6.2M to be saved would then require only a 3.5% improvement due to optimization of design. The learning curve rate required for the 10% saving on material would be near 98%.

The corresponding estimated total costs for OTEC plant-ships (to busbars) are \$1148/$kW_e$(net) for the 100-$MW_e$(net) demonstration plant-ship and \$574/$kW_e$(net) for the sixth and subsequent 500-$MW_e$(net) commercial plant-ships (first and third columns of Table 3). The economies due to scaling up the various OTEC machinery components and the first-lot (first commercial plant-ship) and sixth-lot (sixth ship) learning curve savings were computed by the method described in Ref. 6, using 90% learning curves. The basic hull costs are slightly smaller than shown in Ref. 6, because the required hull depth is reduced by 17% with the smaller-diameter heat exchanger tubes. The OTEC machinery costs are slightly higher because the parasitic power increased from the 16 $MW_e$ of Ref. 6 to 26.6 $MW_e$ per 100 $MW_e$(net).

The final column of Table 3 shows the estimated cost for the 25th 500-$MW_e$(net) plant-ship using 93% learning curves [Lockheed value (26)] from the first ship to the 25th ship for all components and assuming that:

a) The heat exchanger fouling coefficient can be reduced from 0.0005 to 0.0002 average (0.0003 before biweekly cleaning to 0.0001 after cleaning), and

b) A 15% reduction in the costs of the heat exchangers and the basic hull can be achieved through R&D and optimization of the integrated system on the commercial plant-ships.

With these assumptions, the costs of the 25th plant-ship could be as little as \$237 M for the basic OTEC plant-ship (\$474/$kW_e$) and \$316 M including the ammonia plant. The latter figure is well below the \$367 M used to estimate an ammonia production cost of \$96/ton for the sixth and subsequent plant-ships in Ref. 6.

Table 3 Cost Estimates for 100-$MW_e$(net) Demonstration-Size and 500-$MW_e$(net) Commercial-Size Plant-Ships (Millions of 1975 Dollars)

| | 100-$MW_e$ Demo. | 500-$MW_e$ Commercial 1st | 6th | Opt. 25th |
|---|---|---|---|---|
| Heat Exchangers | 39.4[a] | 151 | 123 | 92 |
| Basic Hull | 14.1 | 72 | 47 | 35 |
| Other Platform | 17.4 | 54 | 30 | 29 |
| OTEC Machinery | 35.8 | 101 | 68 | 63 |
| Cold Water Pipe | 7.1 | 22 | 17 | 16 |
| Subtotal OTEC | 113.8 | 400 | 285 | 235 |
| Deployment to Site | 1.0 | 2 | 2 | 2 |
| Total OTEC | 114.8 | 402 | 287 | 237 |
| (\$/$kW_e$) | (1148) | (804) | (574) | (474) |
| Ammonia Plant[b] | 28.1 | 96 | 83 | 79 |
| Total OTEC/$NH_3$ | 142.9 | 498 | 370 | 316 |

[a] All costs include 12% allowance for interest and escalation during construction; thus, the \$35.2M heat exchanger cost from Table 2 becomes \$39.4M.

[b] Includes desalinization, electrolysis, air liquefaction, ammonia synthesis, storage and transfer system; see Ref. 6.

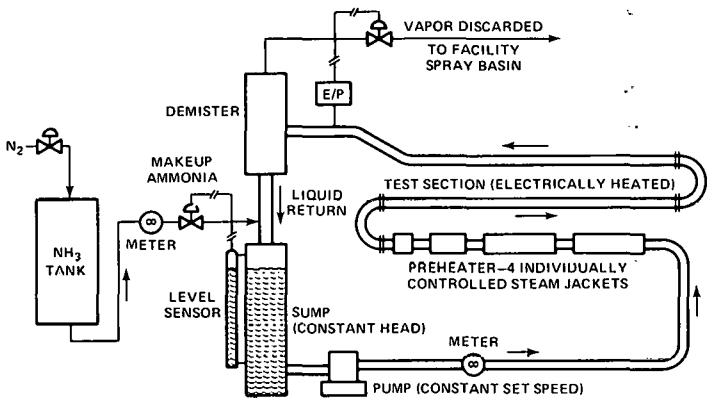



Fig. 4 Simplified Schematic Diagram of Internal Heat Transfer Test Setup.

## Two-Phase-Flow Experiments

### Experimental Setup and Test Procedures

Figure 4 is a simplified schematic of the Internal Flow Heat Transfer Experiment (IFHTE) simulating a single evaporator pass. Ammonia from a temperature-controlled storage tank is transferred (by nitrogen pressure) to fill the ammonia sump to an automatically-controlled head of 1.2 m to preclude cavitation in the double-sealed, positive-displacement ammonia pump, which provides a constant mass flow rate set by a Graham variable speed drive and measured by a rotating vane flowmeter. The ammonia quality entering the test section is changed by varying the heat input from a horizontal, steam-jacketed preheater which comprises four steam jackets of lengths 0.3, 0.6, 1.2, and 1.2 m. Any desired combination of the steam jackets can be supplied with saturated steam at a controlled pressure. Thus, a wide range of heating rates can be obtained, and ammonia quality can be controlled from a low level of 2% for an ammonia flow rate of 1100 kg/hr to maxima ranging from 40% for 1100 kg/hr to 10% for 4500 kg/hr. The preheater is connected to the test section inlet by a 0.23-m center-to-center return ben

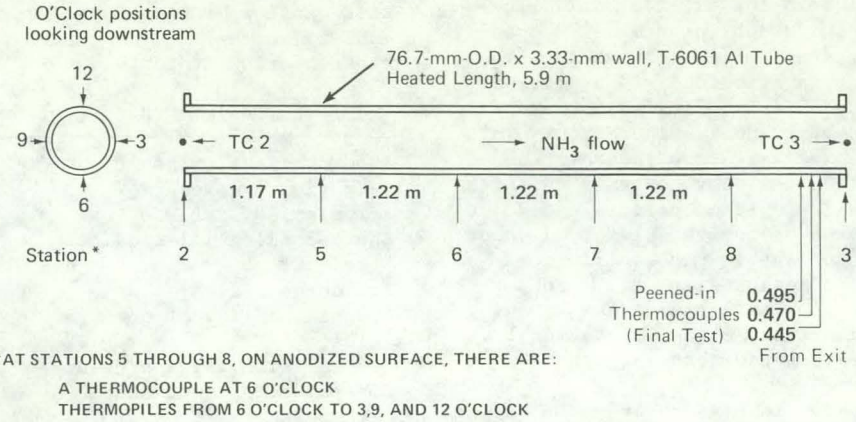
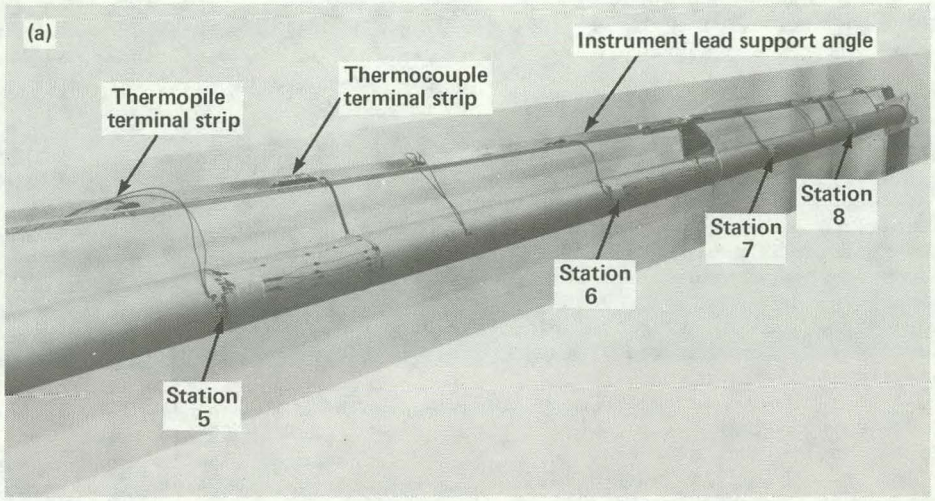



Fig. 5 Test Section Schematic Showing Instrumentation Locations.



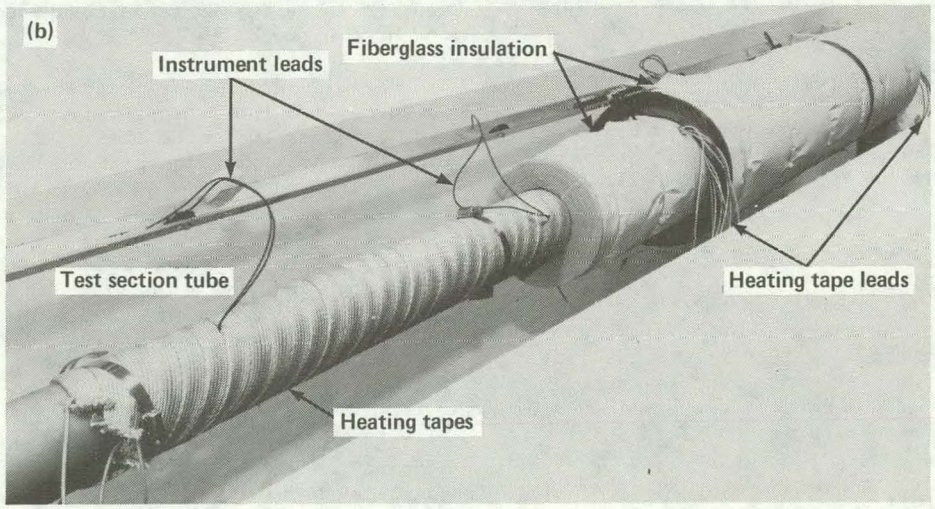




Fig. 6 Photographs of Test Section Showing a) Instrumentation at Stations 5 through 8 and b) the Heating Tape Wrapping and Insulation.

Electric heating tape on the test section provides a uniform external heat flux to the outside wall. The ammonia flows from the test section through a 180° bend and return line into a demister, which returns the liquid to the sump. The vapor is discarded via a pressure regulator into the facility water cooling system and escapes from a spray basin by gradual evaporation. This approach avoids the need for a large condenser in the loop. A remotely-controlled regulator controls the pressure at the demister inlet. Liquid ammonia is added continuously to the sump to make up for the discarded vapor and maintain a constant sump level. For equilibrium conditions, the ratio of the measured ammonia makeup rate to the (constant) total pumping rate yields the ammonia quality (x) entering the demister, which is assumed to be equal to the quality leaving the test section.

The test section is shown in Figs. 5 and 6. The inlet and exit flanges contain a static pressure tap at the 3 o'clock position (looking downstream) connected to a pressure transducer, and a copper-constantan thermocouple at the 9 o'clock position. The thermocouple is inserted into the flow (to a depth to divide flow area into equal areas) to measure the bulk temperature. Thermocouples and thermopiles are mounted on the outside wall of the tube at measuring stations 1.2, 2.4, 3.6, and 4.8 m from the inlet flange.

At each station the temperature reading at the 6 o'clock position is obtained from a copper-constantan thermocouple. A precision resistance thermometer is attached near each thermocouple; measurements from this thermometer are obtained when the test section assembly is at thermal equilibrium and are used to calibrate the thermocouple output. The tube wall temperatures at the 12-, 3-, and 9-o'clock positions are determined from differential temperatures (referenced to the value measured at 6 o'clock) by four-junction thermopiles, which have outputs double those of single-junction thermocouples. The thermopile junctions are flat, butt-welded, 0.005-mm-thick, copper-constantan elements that are pressed mechanically on the anodized surface and held in place by a thin coat of Glyptal (< 0.013 mm) over the top of the junction. The tube is uniformly anodized to isolate electrically the thermopiles from the aluminum tube surface. The thin (~ 0.005-mm) anodized layer has both a high electrical resistance (~ 100 ohm/m$^2$) and a relatively high thermal conductivity (~ 3600 J/hr-ft-K). The instrumented tube is uniformly wrapped with 24 heating tapes and covered with two layers of fiberglass insulation each 38 mm thick.

The test loop is initially filled with ammonia by bypassing the ammonia supply line control valve until the correct liquid level is obtained in the sump. (The aforementioned bypass and auxiliary plumbing for draining and purging by $N_2$ have been omitted from Fig. 4 for simplicity; see Ref. 22.) The ammonia pump is then started and the automatic level control system allowed to draw additional liquid from storage to re-establish the required level in the sump. The output signals of the various instruments are transmitted to a digital data acquisition and control system for signal conditioning and for recording on magnetic tape. The valves to the steam jacket of the preheater and the ammonia pump speed are set manually. The system pressure at the demister inlet, the steam pressure, and the power to the test section heating tapes are controlled remotely. Table 4 summarizes the ranges of conditions tested in runs covering 29 tests.

Table 4 Ranges of Conditions Tested

| | |
|---|---|
| Tube declination angle, $\alpha$ (positive downward)[a] | +0.26, -0.21, -2.0 deg |
| Ammonia flow rate, $\dot{w}_m$ | 0.45 - 1.3 kg/s |
| Corresponding all-liquid velocity, $v_L$ | 0.19 - 0.54 m/s |
| Inside heat flux, $\emptyset_1$ | 3500 - 7280 W/m$^2$ |
| Ammonia quality at demister inlet, x | 0-20 mass % vapor |
| Test section inlet pressure | (8.1 - 1.15) $10^5$ N/m$^2$ |
| Corresponding saturation temperature | 292 - 303 K |
| (Most of the tests were at (8.7- 9.1) $10^5$ N/m$^2$, $T_{sat}$ = 294-296 K.) | |

[a]The tube tilt angle $\alpha$ is taken as positive when the tube declines in the direction of flow in accord with some of the two-phase-flow literature [e.g., Tartel and Dukler (27)].

Experimental results

The six runs provided a progressive learning experience in the handling and expected behavior of ammonia flowing in two phases through a large diameter pipe. Results of runs 1-5 indicated that there were thermal contact resistances in the thermocouple and thermopile mountings which required a correction procedure (described in detail in Ref. 22). Therefore, an instrumentation mounting procedure which was not initially used (i.e., peening of thermocouples into the relatively thin tube wall) because of safety precautions was examined further and found to be feasible and was employed for the last series of tests: peened-in thermocouples were installed at three downstream stations (Fig. 5). As a result, the confidence in the data from the last run (run 6 representing 16 of the 29 tests conducted) is much higher than in those of runs 1-5.

Results from the all-liquid-inlet tests of run 6 are compared with the Dittus-Boelter equation in Fig. 7. Heat balances indicated that small amounts of boiling did occur in these all-liquid-inlet tests, as indicated by the quality numbers ($x_{out}$, %) beside the data points, but agreement with Eq. (6) is good. Therefore, Eq. (6) is used to compute $h_L$ for the Chaddock-Brunemann correlation, Eq. (5), for comparison with the two-phase flow results of run 6 (Fig. 8).

The ratios of the overall tubewise averages (all stations and all four circumferential positions) of the two-phase heat transfer coefficient ($h_{1(4)}$ to $h_L$ are plotted in Fig. 8. Equation (5) is represented by curves for two values of Bo x $10^4$ (0.090 and 0.285) which bracket the values for the tests. The experimental points agree well with these correlation curves.

Table 5 summarizes the predicted and measured heat transfer coefficients.

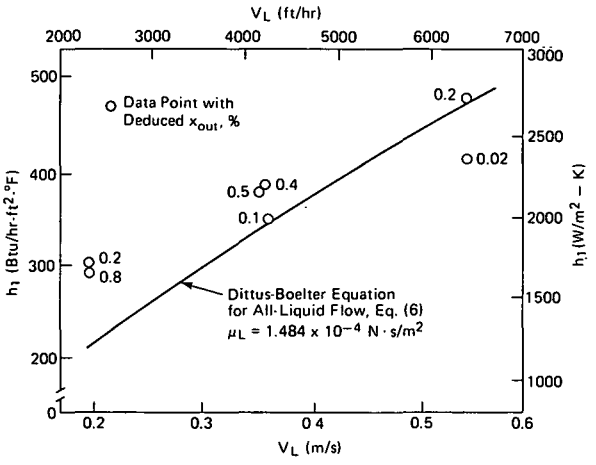



Fig. 7 Comparison of All-Liquid-Inlet Test Data with Dittus-Boelter Equation.

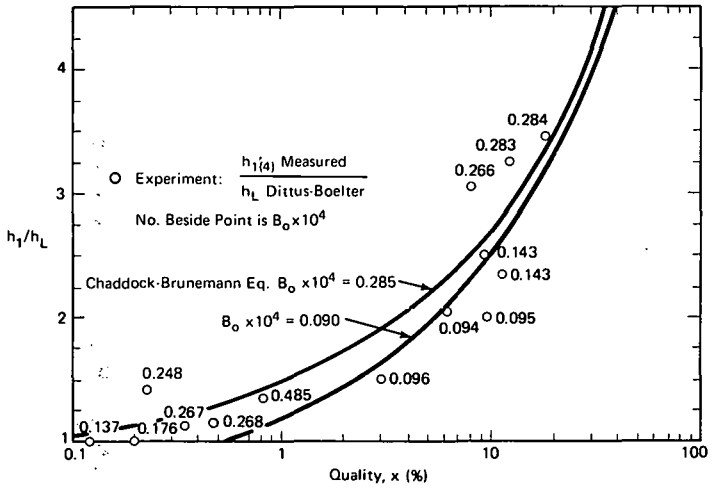



Fig. 8 Comparison of Measured Heat Transfer Coefficients to Chaddock-Brunemman Equation ($\alpha = -2^o$).

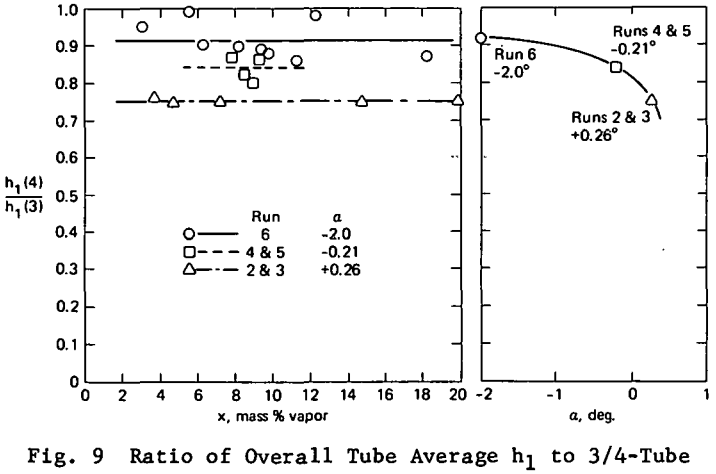



Fig. 9 Ratio of Overall Tube Average $h_1$ to 3/4-Tube Average $h_1$.

Table 5 Predicted and Measured Heat Transfer Coefficients

| $v_L$, m/s | x, % | $\Delta T_b$,[a] K | $\phi_{1_2}$ W/m² | Bo[c] x $10^4$ | Coefficients, W/m² - K: h Eq.(6) | $h_1$ Eq.(5) | $h_{1(4)}$ Meas. |
|---|---|---|---|---|---|---|---|
| a) Run 6, $\alpha = -2^o$, All-Liquid Inlet Tests[b] | | | | | | | |
| 0.196 | 0.2 | 1.49 | 3510 | 0.249 | 1230 | -- | 1730 |
| 0.196 | 0.8 | 2.14 | 6820 | 0.485 | 1220 | -- | 1650 |
| 0.357 | 0.1 | 0.86 | 3520 | 0.137 | 1970 | -- | 1990 |
| 0.356 | 0.4 | 1.41 | 6840 | 0.267 | 1970 | -- | 2230 |
| 0.355 | 0.5 | 1.04 | 6840 | 0.268 | 1960 | -- | 2160 |
| 0.540 | 0.02 | 0.71 | 3520 | 0.091 | 2750 | -- | 2390 |
| 0.538 | 0.2 | 0.96 | 6820 | 0.176 | 2740 | -- | 2740 |
| b) Run 6, $\alpha = -2^o$, Two-Phase-Flow Tests | | | | | | | |
| 0.181 | 12.2 | -.07 | 3690 | 0.283 | 1150 | 3310 | 3720 |
| 0.181 | 18.1 | 0.05 | 3690 | 0.284 | 1150 | 3830 | 3960 |
| 0.358 | 8.1 | -.01 | 6840 | 0.266 | 1970 | 4930 | 6010 |
| 0.359 | 9.3 | 0.09 | 3690 | 0.143 | 1980 | 4950 | 4940 |
| 0.360 | 11.2 | 0 | 3690 | 0.143 | 1990 | 5310 | 4650 |
| 0.535 | 3.0 | -.02 | 3690 | 0.096 | 2720 | 4510 | 4090 |
| 0.543 | 6.2 | -.13 | 3690 | 0.094 | 2760 | 5840 | 5640 |
| 0.542 | 9.7 | -.10 | 3690 | 0.095 | 2760 | 6870 | 5490 |
| c) Runs 4 and 5, $\alpha = -0.21^o$, Two-Phase-Flow | | | | | | | |
| 0.376 | 9.2 | 0.2 | 3790 | 0.140 | 2050 | 5110 | 6750 |
| 0.427 | 7.7 | 0.2 | 3750 | 0.122 | 2280 | 5270 | 7260 |
| 0.425 | 8.4 | 0.2 | 7290 | 0.239 | 2270 | 5670 | 6640 |
| 0.426 | 8.9 | 0.04 | 3760 | 0.123 | 2280 | 5550 | 5900 |
| d) Runs 2 and 3, $\alpha = +0.26^o$, Two-Phase-Flow Tests | | | | | | | |
| 0.189 | 2.7 | 0.6 | 3760 | 0.277 | 1190 | 2160 | 3260 |
| 0.186 | 4.7 | 0.9 | 3550 | 0.265 | 1170 | 2480 | 4480 |
| 0.188 | 7.2 | 0.9 | 3640 | 0.270 | 1180 | 2840 | 4570 |
| 0.188 | 19.9 | -- | 3640 | 0.270 | 1180 | 3990 | 5020 |
| 0.282 | 14.8 | 0.4 | 3630 | 0.179 | 1630 | 4910 | 5840 |

[a] $\Delta T_f$ = measured bulk temperature rise in test section - $T_3 - T_2$.

[b] For all-liquid-inlet tests, x is deduced from: $\phi_1 A_1 = \dot{w}_m\ (c_p\ \Delta T_b + x i_g/100)$, where $A_1 = 1.302$ m²; $c_p = 4810$ J/kg-K; $i_g$ = heat of vaporization = $1.18 \times 10^6$ J/kg

[c] Bo = boiling number = $\phi_1/i_g \rho_L v_L$; $\rho_L = 608$ kg/m³

Stratified wavy or intermittent flow occurs to various degrees for the low-quality ($x \leq 20\%$) two-phase-flow conditions tested. To observe the overall statistical effect of poor heat transfer at the top of the tube, the ratio of the overall tubewise average heat transfer coefficient covering all four circumferential positions, $h_{1(4)}$, to that of the tubewise average for the lower 3/4 of the tube (3, 6, and 9 o'clock positions), $h_{1(3)}$, is plotted in Fig. 9. The points from run 6 ($\alpha = -2.0^o$, meaning $2^o$ upward tilt in the flow direction) fall near a value of 0.91; those of runs 4 and 5 ($\alpha = -0.21^o$) fall near 0.84; and those from runs 2 and 3 fall near 0.75 reflecting the low coefficients at the top of the tube when the tube was declining at $\alpha = +0.26^o$. The right part of Fig. 9 shows the tube declination angle effect. The shape of the curve indicates that a tilt to $\alpha = -0.5^o$ (0.76 pipe diameter elevation) would be almost as good as a tilt to $\alpha = -2.0^o$. A better determination of this

effect including tests at zero inclination will be an objective of future testing.

## Concluding Remarks

This simple, two-phase-flow, plain-aluminum-tubed heat exchanger concept is believed to offer the required combination of low cost (approximately $\$19/m^2$ for the sixth and subsequent commercial plant-ships with a $24^\circ$ $\Delta T$), modularity to facilitate mass production and assure a high plant capacity factor, and cleanability that is needed to yield a competitive OTEC plant cost. We have estimated (Ref. 6) that such plant-ships can produce liquid ammonia at a cost, delivered to New Orleans, of approximately \$96/short ton in late 1975 dollars, compared to f.o.b. sales prices near \$180/ton [see also Ref. 28 for economic analyses].

An experimental setup has been developed for determining internal, two-phase-flow, heat transfer coefficients for ammonia in a single pass of nearly horizontal, 77-mm-O.D. aluminum tubing, and for evaluating stratification effects at mass qualities up to 20%. Results to date indicate that the heat transfer coefficients agree with the Chaddock-Brunemann correlation.

The stratification that occurred at these typical OTEC operating conditions (low mass velocity, low $\Delta T$, low heat flux) at low qualities decreased as the tube declination angle $\alpha$ was changed from $+0.26$ (downward in the flow direction) to $-0.21^\circ$ and was nearly eliminated at $\alpha = -2.0^\circ$ (3 diameters inclination over a 20-ft length). At this inclination the flow was in an intermittent flow regime which kept the top of the tube wetted over at least the last 80% of its length. A smaller inclination angle (say, $0.5^\circ$ or 0.76 diameter on the 20-ft length) apparently would provide most of this favorable effect. Even at $0^\circ$ the effect on overall heat transfer probably will not be great enough to warrant the complications in heat exchanger fabrication that would result from a requirement to tilt the tubes. (The exit mass quality from a complete multipass tube is expected to be at least 60%, and an annular two-phase-flow regime is expected to pertain at some quality above 20%.) The OTEC plant-ship itself will be very stable with a roll of only $0.02^\circ$ for normal conditions and $0.1^\circ$ for extreme conditions at the selected initial operating site in the Atlantic Ocean ($5^\circ$ S latitude to $5^\circ$ N latitude, $25^\circ$-$30^\circ$ W longitude).

Plans for further testing with the apparatus include a study of the occurrence of nucleation in the subcooled ammonia flow in both the plain tube and one with an enhanced (porous) surface to be obtained from Union Carbide, and further characterization of the stratified flow phenomena at design and off-design operating conditions. In these future tests all wall temperature measurements will be made with peened-in thermocouples, and more points along the test section will be instrumented.

## Acknowledgment

The authors gratefully acknowledge the efforts of many others in the development of the APL heat exchanger and plant-ship concepts. Among those at APL who have contributed to the work are W. B. Shippen, R. A. Makofski, E. J. Francis, M. B. Tate, V. J. Dietz, A. S. Polk, J. L. Keirsey, R. T. Cusick, J. L. Rice, M. E. Rose, J. E. Creeden, R. F. Wolff, and J. A. Funk. Peter Griffith MIT gave valuable advice on our heat exchanger design and analysis. The Sun Shipbuilding and Dry Dock Co., Chester, Pa., has made an extensive contribution to the overall ship design and the method for integrating the heat exchangers with the concrete hull, for which we thank Mr. Eugene Schorsch and his associates. Mr. Dale Doerr and others at the Kaiser Aluminum and Chemical Corporation's Center for Technology, Pleasanton, Calif., provided the heat exchanger design and aluminum material and welding costs. Dr. A. F. Conn and others of Hydronautics, Inc. helped us assess heat exchanger cleaning methods. We gratefully acknowledge support of the basic heat exchanger analysis and testing by Drs. Robert Cohen and Abrahim Lavi and Mr. Sigmund Gronich of the Division of Solar Energy of ERDA; helpful critiques by Prof. Kenneth Bell (Oklahoma State U.), Dr. Richard Lyon (ERDA/ONRL), and Prof. J. G. Knudsen (Oregon State U.); and support of the plant-ship investigation by the U.S. Maritime Administration, for whom Mr. James Gross is Head of the Office of Advanced Ship Development and Messrs. James Lisnyk and Joseph Seelinger have been Program Managers, Office of Maritime Technology.

## References

1. Dugger, G. L., Francis, E. J. and Avery, W. H., "Technical and Economic Feasibility of Ocean Thermal Energy Conversion," Applied Physics Laboratory, The Johns Hopkins University, Laurel, Md., AEO-76-060, presented at ISES Sharing the Sun Conference, Winnipeg, Canada, August 1976.

2. Dugger, G. L., Editor, "Proceedings, Third Workshop on Ocean Thermal Energy Conversion," Houston, Texas, May 8-10, 1975, APL/JHU Report SR 75-2, August 1975.

3. Hornburg, C. D., Lindal, B. and El-Ramy, N., "Preliminary Research on Ocean Thermal Energy Complexes," DSS Engineers, Inc., Fort Lauderdale, Fla., presented at ISES Sharing the Sun Conference, Winnipeg, Canada, August 1976.

4. Snyder, J. Edward, "Energy Utilization Aboard OTEC Platforms," Ocean & Energy Systems Project, TRW Systems, Redondo Beach, Calif., presented at ISES Sharing the Sun Conference, Winnipeg, Canada, August 1976.

5. Zener, Clarence, "A Comparison of the Economics of Nuclear and Solar Power," Carnegie-Mellon University, Pittsburgh, Pa., presented at ISES Sharing the Sun Conference, Winnipeg, Canada, August 1976.

6. Francis, E. J. (Principal Investigator), "An Analysis of the Maritime and Construction Aspects of Ocean Thermal Energy Conversion (OTEC) Plant-Ships," APL/JHU Report SR 76-1A, 1B, April 1976, for the U.S. Maritime Administration, Department of Commerce, Contract No. 5-38054.

7. Goss, W. P., Heronemus, W. E., Mangarella, P. A. and McGowan, J. G., "Summary of University of Massachusetts Research on Gulf Stream Based Ocean Thermal Power Plants," pp. 51-62 of Ref. 2.

8. "Ocean Thermal Energy Conversion (OTEC) Power Plant Technical and Economic Feasibility," Report NSF/RANN/SE/GI-C937/FR/75/1, LSMC-D056566, by Lockheed Missiles and Space Co., Inc. to the National Science Foundation, April 12, 1975 (2 volumes; Lloyd C. Trimble, Principal Investigator).

9. "Ocean Thermal Energy Conversion," Final Report by TRW Systems Group, Redondo Beach, Calif., to U.S. Energy Research and Development Administration; Contract NSF-C 958, June 1975 (5 volumes; Robert Douglass, Principal Investigator).

10. Olsen, H. L., et al., "Preliminary Considerations for the Selection of a Working Medium for the Solar Sea Power Plant," Solar Sea Power Plant Conference and Workshop, A. Lavi, ed., Carnegie-Mellon Univ., Pittsburgh, Pa., June 27-28, 1973, pp. 185-204.

11. Olsen, H. L. and Pandolfini, P. P., "Analytical Study of Two-Phase-Flow Heat Exchangers for OTEC Systems," APL/JHU Report AEO-75-37, November 1975, for Division of Solar Energy, U.S. Energy Research and Development Administration.

12. Conn, A. F. and Rudy, S. L., "Parameters for a Ship Hull Cleaning System Using the CAVIJET™ Cavitating Water Jet Method," Hydronautics, Inc., Technical Report 7510-1, July 1975.

13. Anderson, J. Hilbert and Anderson, James H., Jr., "Thermal Power from Sea Water," Mechanical Engineering, Vol. 88, April 1966, pp. 41-46.

14. Lavi, A., Final Report, Solar Sea Power Project, Report NSF/RANN/SE/GI-39114/PR/74/6; Carnegie-Mellon University, Pittsburgh, Pa., January 31, 1975.

15. Fink, F. W. and Boyd, W. K., "The Corrosion of Metals in Marine Environments," DMIC Report 245, May 1970, Defense Metals Information Center, Battelle Memorial Institute, Columbus, Ohio.

16. Verink, E. D., Jr., "Aluminum Alloys for Saline Waters," Chemical Engineering, Vol. 81, April 15, 1974, pp. 105-110.

17. Private communication from Dale D. Doerr, Kaiser Aluminum and Chemical Corporation, Pleasanton, Calif., to W. H. Avery, APL/JHU, May 7, 1976.

18. Chisholm, D., "Pressure Gradients Due to Friction During the Flow of Evaporating Two-Phase Mixtures in Smooth Tubes and Channels," Proceedings of the Institute of Mechanical Engineers, National Engineering Laboratory, Glasgow, Scotland, May 1972, pp. 347-357.

19. Chaddock, J. B. and Brunemann, H., "Forced Convection Boiling of Refrigerants in Horizontal Tubes--Phase 3," Report HL-113, School of Engineering, Duke University, Durham, N. C., July 1967.

20. Handbook of Fundamentals, American Society of Heating, Refrigeration, and Air Conditioning Engineers, New York, 1972.

21. Collier, J. G., Convective Boiling and Condensation, McGraw-Hill, London (1972).

22. Olsen, H. L., Pandolfini, P. P. and Rice, J. L., "Internal Heat Transfer in a Simulated OTEC Evaporator Tube," Applied Physics Laboratory, The Johns Hopkins University, Laurel, Md., AEO-76-066, November 1976.

23. Bergles, A. E. and Rohsenow, W. M., "The Determination of Forced Convective Surface Boiling Heat Transfer," Paper No. 63-HT-22, 6th National Heat Transfer Conference, Boston, August 1963.

24. Frost, W. and Dzakowic, G. S., "An Extension of the Method for Predicting Incipient Boiling on Commercially Finished Surfaces," Paper No. 67-HT-61, ASME-AIChE Transfer Conference, Seattle, August 1967.

25. Afgan, N. H. and Schlünder, E. U., Heat Exchanger: Design and Theory Source Book, Chap. 4, p. 75, Scripta Book Co., Washington, D.C., 1974.

26. "Ocean Thermal Energy Conversion (OTEC) Test Facilities Study Program," Vol. I, ERDA Report SAN/1156-77/1, LMSC-D506781, by Lockheed Missiles and Space Co., Inc., Sunnyvale, Calif., 17 January 1977.

27. Taitel, Y. and Dukler, A. E., "A Model for Predicting Flow Regime Transition in Horizontal and Near Horizontal Gas-Liquid Flow," A.I.Ch.E. Journal, Vol. 22, No. 1, Jan. 1976, pp. 45-55.

28. Francis, E. J. and Seelinger, J., "Market Definition, Commercial Development Plan and OTEC Financing," presented at this Conference.

# A DESIGN AND PRODUCIBILITY STUDY OF HEAT EXCHANGERS FOR OCEAN THERMAL ENERGY CONVERSION SYSTEMS

A. F. MANIKOWSKI AND A. R. PFLUGER
*Ocean Systems, Lockheed Missles & Space Company*
*Sunnyvale, California*

## Abstract

This paper addresses the design and producibility of shell and tube heat exchangers for use in ocean thermal gradient power plants. The results of an ERDA-sponsored 4-month preliminary design and manufacturing study of heat exchangers for this application are reviewed. Both titanium-tubed and aluminum-tubed designs were investigated. Pressure vessel concepts evaluated included monocoque cylinders and spheres, and ring-stiffened cylinders fabricated with aluminum, steel, and concrete. A manufacturing study was carried out in parallel with the design study to ensure that a producible design concept was evolved, and to provide a basis for making preliminary cost estimates of the heat exchangers.

The study indicates that OTEC is economically attractive when the marine alloys of aluminum are selected as the material of construction for the heat exchangers, and when mass production techniques are employed in the manufacture of the heat exchangers. Estimates of the costs of aluminum heat exchangers manufactured on a production line basis with appropriate investment in jigs tooling and automatic welding equipment were also made.

The critical development aspects of the OTEC shell and tube heat exchangers was found to be the tube-to-tubesheet joint. It is imperative that this joint be sound and reliable from a leakage standpoint. Neither leakage of ammonia working fluid from the system, nor leakage of sea water into the system, can be tolerated. The results of an exploratory development program carried out during the study indicate that explosive welding or magnetic forming in conjunction with conventional welding or elastomeric seals are feasible for joining aluminum tubing to the tubesheets. Further engineering and manufacturing development is required in this area.

## Introduction

The Ocean Thermal Energy Conversion (OTEC) power cycle is a means of extracting electric power from the thermal gradient of tropical oceans. The available temperature difference that exists between the warm surface waters and the cold water that lies below the mixed layer is typically 35° to 40° F. When applied to a Rankine cycle, this thermal potential is equivalent to a hydroelectric plant operating on a head of 100 ft of water. The cold water resource is drawn to the surface with pumps via a cold water pipe that is typically greater than 1,500 ft long. A Rankine cycle driven by the small temperature difference available between the warm and cold water powers the electrical generating plant.

The low temperature differentials available lead to low Rankine cycle efficiencies (2-1/2 to 3 percent thermal efficiencies). Hence, large heat transfer surface areas are required for the OTEC power plant. Typically, OTEC heat exchangers will required about 15 times the heat flow and 50 times the surface area required for the condensers of a conventional fossil fueled steam power plant. Thus the heat exchangers are the most significant component of the OTEC plant and as such have received considerable analytical and experimental attention.

This study considered potential shell and tube heat exchanger design concepts that are economical and within the reach of current technology. Since the largest heat exchanger constructed to date is about one fourth the size of a 25-MW(e) OTEC heat exchanger, it was recognized that some departure from current practices would be required to achieve this goal.

## Design Description

The design requirements established for this study were largely based upon the configuration of Lockheed's power module concept reported to the National Science Foundation in 1975 (see Fig. 1). The power module is a completely self-contained Rankine cycle power plant and consists of evaporator, turbine generator condenser and condensate pumps, sea water pumps, and a buoyancy control system. Although the Lockheed concept was used as a basis, the design and manufacturing approaches identified in this study are generally applicable to any large shell and tube heat exchanger. In fact, the Lockheed concept represents the most demanding requirement for the OTEC heat exchangers because the shells must be designed for external as well as internal pressurization.

The conceptual design study investigated the use of aluminum and titanium for heat transfer surfaces. Preliminary design layouts were made of pressure vessels constructed with aluminum, steel, and concrete. The pressure vessel configurations studied included both monocoque and ring-stiffened cylinder designs, and spherical unreinforced membrane designs. Table 1 summarizes the results of the design study and gives an indication of the relative material requirements for the 25-MW(e) heat exchanger pressure vessel designs investigated. Table 2 summarizes the weight and cost tradeoffs that are associated with the candidate pressure vessel configurations studied. The costs indicated in this table presume an automated production process for the manufacture of the pressure vessels. The table indicates that spherical or monocoque cylinders fabricated with SA516 steel will result in minimum

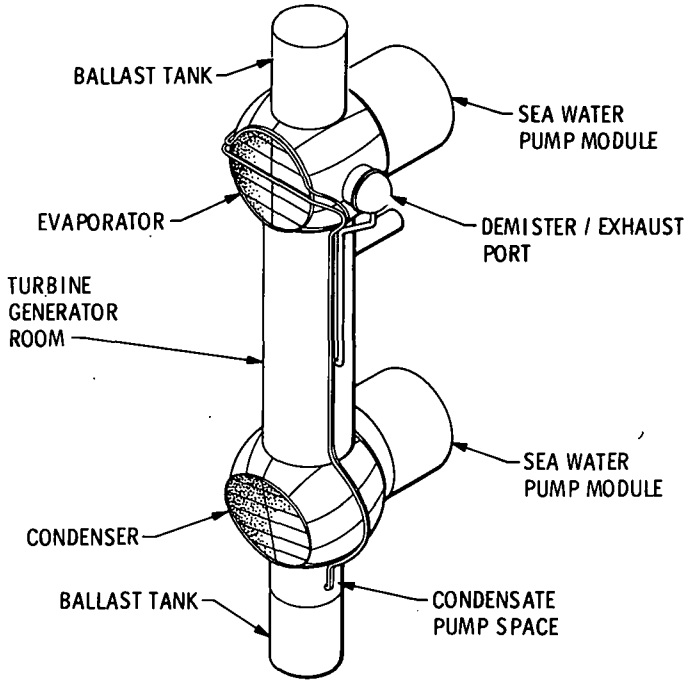



Fig. 1 Power Module

Table 1 PRESSURE VESSEL MEMBRANE THICKNESS REQUIREMENTS

| Material | Evaporator Membrane Thickness (in.) | Condenser Membrane Thickness (in.) |
|---|---|---|
| Aluminum 5083-0 | | |
| Sphere | 3 | 4-1/8 |
| Monocoque cylinder | 3-3/4 | 6-3/4 |
| Steel HY-80 | | |
| Ring stiffened cylinder | 1-1/2 | 1-1/2 |
| Monocoque cylinder | 1-1/2 | 4-1/2 |
| Sphere | 1-1/2 | 1-3/4 |
| Prestressed concrete cylinder | 43 | 43 |

cost pressure vessels. However, since titanium heat transfer tubes cost approximately three times those of aluminum, the overrall cost of the heat exchangers using steel pressure vessels and titanium tubes does not compare favorably with the aluminum designs. The all-aluminum heat exchanger designs were estimated to cost $350/kW(e) when constructed by a production manufacturing method. The titanium-tubed steel pressure vessel was $750 kW(e) using a similar manufacturing method. The use of aluminum heat transfer tubing with steel pressure vessel construction was not considered because of the design and manufacturing difficulties that result from use of this combination of materials in sea water.

The design configurations shown in Figs. 2 and 3 were selected as the baseline heat exchanger designs. The design incorporates 2-1/2 inch diameter 5052 aluminum tubing with a 0.058-inch wall thickness. The pressure vessel, tubesheets and tube support are constructed from 5083 aluminum alloy. The total weight of the assembled units are 850 long tons for the evaporator and 950 long tons for the condenser. The alternate design configuration using titanium tubes and steel pressure vessel construction is similar except that the pressure vessel size is somewhat smaller, 65 feet in diameter, weighing 1135 long tons and 1200 long tons for the evaporator and condenser, respectively. The aluminum baseline design was used as the basis for developing manufacturing plans and estimating costs of the heat exchangers. The costs developed for the titanium/steel heat exchangers were predicated on geometrical similarity to the baseline aluminum design.

## Cost Estimates and Manufacturing

Manufacturing and construction of the OTEC heat exchangers does not represent a major extension of current technology. Aluminum LNG tanks larger than the size of the 25-MW(e) heat exchangers have been constructed for the maritime industries. The design and construction of a heat exchanger of the size required for OTEC does, however, represent an advancement in the current state of the practice in terms of size. This study explored ways of exploiting manufacturing methods which are readily available for construction of a prototype or demonstration power plant. In addition, innovative manufacturing methods which promise significant reductions in manufacturing costs through the use of mass production methods were also investigated.

## PROTOTYPE HEAT EXCHANGER CONSTRUCTION

The construction of the prototype heat exchanger for the 25-MW(e) demonstration power plant should occur at or near the power plant construction site. The construction site would be located on a major river or within a harbor to facilitate water borne transport of the heat exchanger to the final construction or staging areas of the power plant. Field construction is the most appropriate construction method for the prototype heat exchanger because it minimizes capital investments in tooling and facilities. Figure 4 indicates the major elements of the proposed manufacturing plan. The preferred material of construction for the heat exchangers is aluminum-5083 alloy for the shell, and 5052 alloy for the heat transfer tubing.

Table 3 summarizes the projected construction costs for the prototype heat exchangers. These cost estimates are based upon cold forming of the spherical pressure vessel plates and welding up of the pressure vessel in a field construction environment. This implies a minimum of tooling and fixturing equipment. The cost estimates are based upon the use of drawn 5052 aluminum tubing and rolled and welded titanium tubing. The cost of heat transfer tubing was estimated to be $2.20/lb for drawn aluminum tubes, and $5.50/lb for the titanium tubes. The pressure vessel material costs are based upon $1.00/lb for 5083 plate and $0.36/lb for high strength steel plate. Labor was estimated at a $25/hr rate.

Table 2 PRESSURE VESSEL CONSTRUCTION COST AND WEIGHT COMPARISON

| Material | Material Cost ($/lb) | Spherical | | Ring-Stiffened Cylinder | | Monocoque Cylinder | |
|---|---|---|---|---|---|---|---|
| | | Weight[a] (lb × $10^3$) | Constr. Cost[b] [($/kW(e)] | Weight[a] (lb × $10^3$) | Constr. Cost[b] [($/kW(e)] | Weight[a] (lb × $10^3$) | Constr. Cost[b] [($/kW(e)] |
| Steel | | | | | | | |
| SA 516 | 0.21 | 2,627 | 58 | 3,642 | 63 | 3,050 | 49 |
| HY-80 or -100 | 0.36 | 2,260 | 64 | 3,081 | 80 | 2,476 | 52 |
| Aluminum | | | | | | | |
| 5083-H321 | 1.00 | 1,226 | 90 | – | – | 1,485 | 106 |
| 5083-0 | 1.00 | 1,334 | 94 | – | – | 1,615 | 111 |
| Prestressed Concrete | 0.17 | – | – | – | – | 6,300 | 102 |

(a) Weight for pressure vessel and tubesheet ring only. Does not include tubesheets, tube supports, or tubes.

(b) Cost data indicated for production manufacturing process includes 25 percent construction allowance.

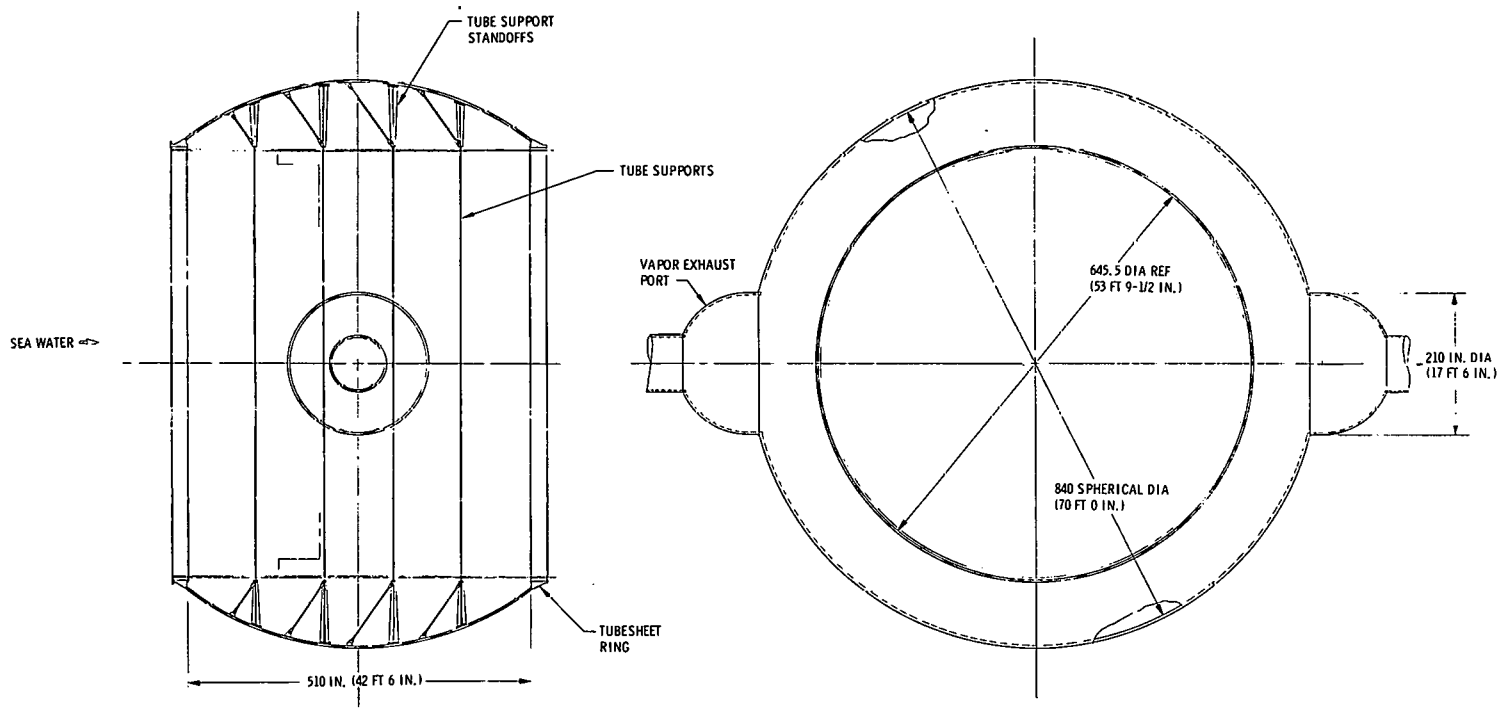



Fig. 2 25-MW(e) Evaporator Spherical Shell – Aluminum Tubes

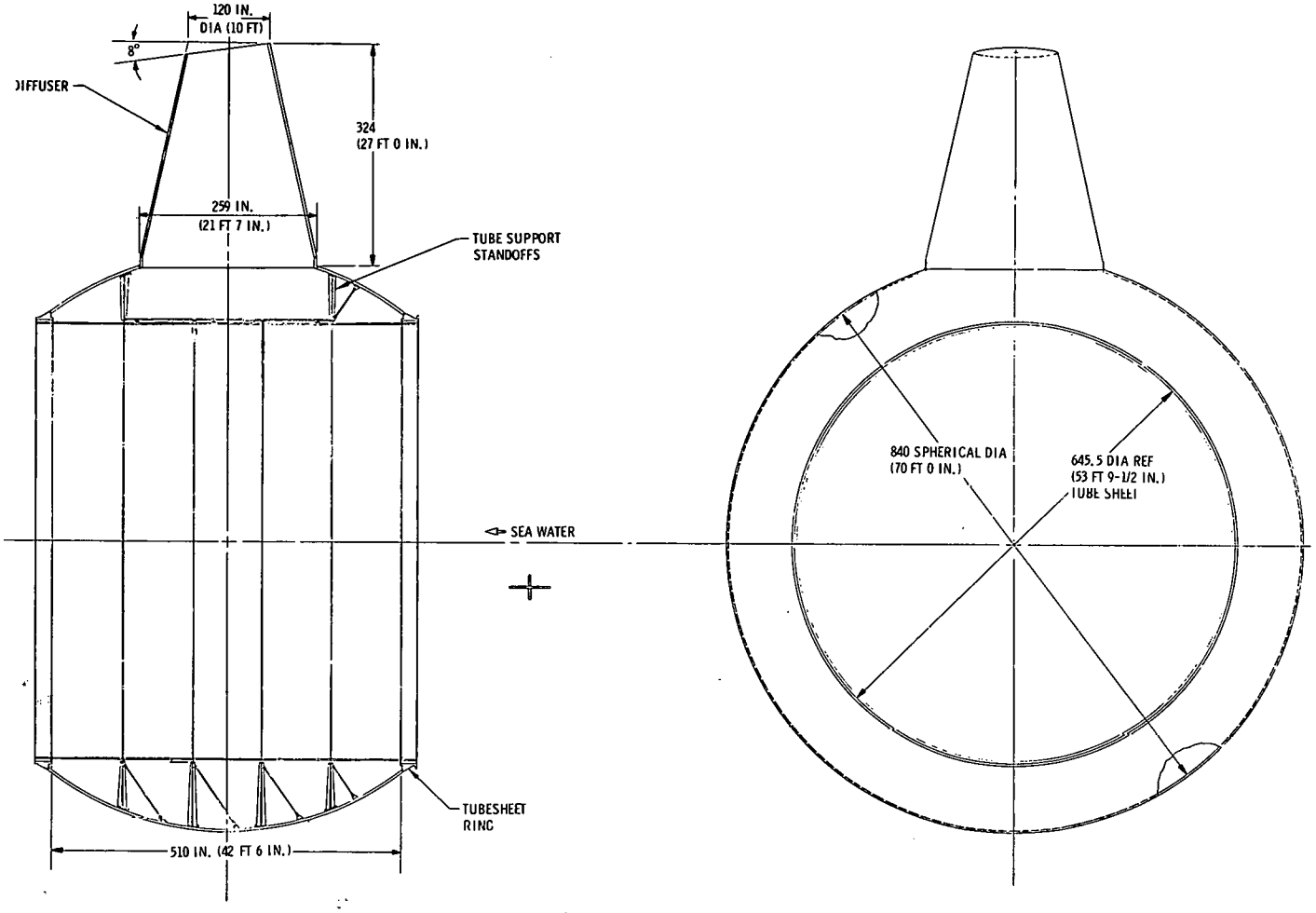



Fig. 3 25-MW(e) Condenser Spherical Shell – Aluminum Tubes

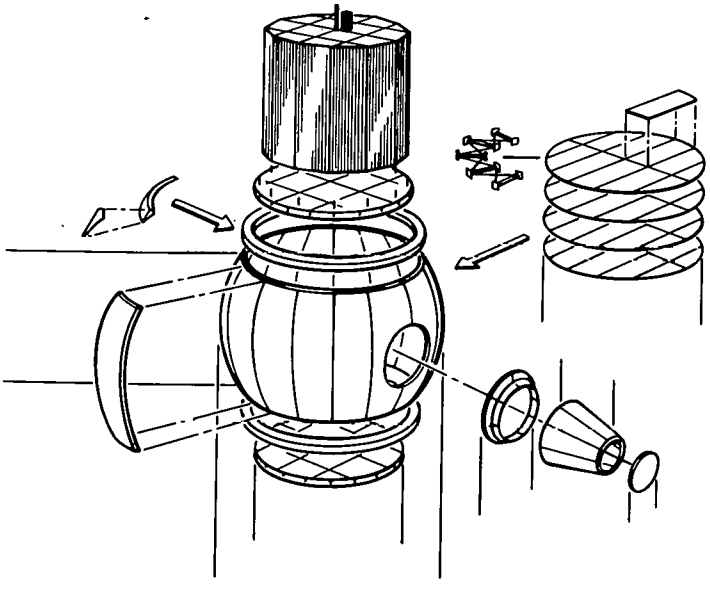


Fig. 4 Candidate OTEC Evaporator/Condenser

## MASS PRODUCTION OF OTEC HEAT EXCHANGERS

Upon completion of the technology development program for OTEC heat exchangers, economical exploitation of the ocean thermal resource can be anticipated. At that time, a mature manufacturing industry will have been developed to mass produce the aluminum heat exchangers at a rate of possibly eight to ten sets of heat exchangers per year. There are two major components of the heat exchangers that are amenable to cost reduction by use of methods of mass production. These components are the pressure vessel and the heat transfer tubing. Since the cost of the assembled pressure vessel represents approximately one half of the construction cost of the prototype aluminum heat exchangers, significant cost savings should result from the use of an automated construction method. The other significant area for cost savings is the aluminum heat transfer tube manufacturing process. Approximately 2 million pounds of aluminum tubing is required for each 25-MW(e) power plant. The purchase of a tube roll-and-weld line at the heat exchanger construction site can be economically justified for this quantity of tubing.

The cost of 5052 aluminum tubing manufactured in an onsite roll and weld line is estimated to be about $1.25/lb. Some further

Table 3 COST SUMMARY FOR 25-MW(e) PROTOTYPE HEAT EXCHANGERS

| Item | Estimated Cost ($ × $10^3$) | | | | | |
|---|---|---|---|---|---|---|
| | All Aluminum Construction | | | Steel/Titanium Construction | | |
| | Materials | Labor | Tools | Materials | Labor | Tooling |
| Pressure Vessel Shell (Constructed in Place) | 6,500[b] | | 200[b] | 6,050[b] | | 200[b] |
| Tubesheets | 250 | 530 | 450 | 144 | 503 | 450 |
| Baffles and Supports | 385 | 445 | | 290 | 423 | |
| Tubes | 4,750 | – | – | 11,400 | – | – |
| Installation – Tubesheets/Baffles | – | 110 | 250 | – | 104 | 250 |
| Installation – Tubing | – | 910 | 50 | – | 805 | 50 |
| Subtotal | 13,880 | | 950 | 13,769 | | 950 |
| Total Including 42% Allowance[a] | 18,245 | | | 26,810 | | |
| $/kW(e) | 729 | | | 1,072 | | |

(a) Allowance includes 20% contingency, 15% administration and engineering, and 3% fee.

(b) Turnkey cost; 42% allowance not applied to the quotation.

cost savings are indicated if the choice of tube material were 3003 Alclad, which was estimated to be $1.15/lb.

The proposed method of manufacturing the pressure vessel shell is shown in Fig. 5. The weld positioner is capable of supporting the entire 320-ton weight of the completed spherical pressure vessel shell. This approach allows the use of high deposition rate automatic welding processes that require weld material be applied in a locally horizontal position. The proposed process is based upon the Alcoa 649 process and is capable of joining 3-1/2-inch thick aluminum plates at a rate of 7 inches per minute. The cost savings in labor hours, elapsed time, weld quality, and contour control should justify the capital cost of the weld positioner in one production run of eight heat exchangers required for a 100-MW(e) power plant. Table 4 summarizes the estimated construction costs for the production heat exchangers.

THERMAL DESIGN

A computer optimization program was used to define the power cycle parameters for a 25-MW(e) power module. This computer program is capable of performing thermal and fluid dynamic design calculations as well as parametrically evaluating the effect of numerous design variables on heat exchanger size and cost. Table 5 indicates the power plant design parameters for a minimum cost heat exchanger design using aluminum tubing. In this particular optimization, the evaporator and condenser sizes were constrained to fit into geometrically identical spherical pressure vessels.

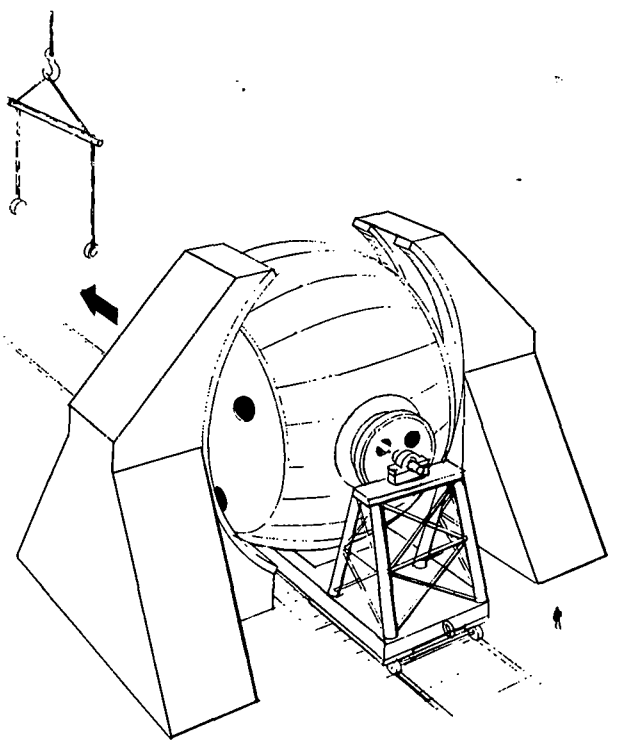


Fig. 5 Construction of Pressure Vessel on Gimballed Weld Positioner

Table 4 COST SUMMARY FOR ALUMINUM 25-MW(e) PRODUCTION UNIT HEAT EXCHANGERS

| | Estimated Costs ($ × $10^3$) | | | | | |
|---|---|---|---|---|---|---|
| | First Item | | | 25th Item[b] | | |
| | Materials | Labor | Tools | Materials | Labor | Amor. Tools |
| Pressure Vessel Shell | 1,380 | 170 | 6,500 | 1,380 | 120 | 570 |
| Tubesheets | 250 | 530 | 450 | 250 | 370 | 75 |
| Baffles | 385 | 445 | | 385 | 315 | |
| Tubes | 2,700 | – | – | 2,700 | – | 120 |
| Installation – Tubesheets and Baffles | – | 110 | 250 | | 80 | 40 |
| Installation – Tubing | – | 910 | 50 | | 640 | 10 |
| Subtotals | 4,715 | 2,165 | 7,200 | 4,715 | 1,525 | 815 |
| Total Including 25% Allowance[a] | 17,662 | | | 8,820 | | |
| $/kW(e) | $706/kW(e) | | | $352/kW(e) | | |

(a) Allowance includes 10% contingency, 10% administration and engineering, and 3% fee.
(b) Learning curve slope parameter = 0.93.

Table 5 25-MW(e) POWER PLANT DESIGN SUMMARY

| | |
|---|---|
| THERMAL RESOURCE | 79.75°F–43.38°F |
| POWER | |
| Rankine cycle efficiency | 2.83% |
| Net power output | 25 MW(e) |
| Gross turbine output | 32.2 MW(e) |
| Warm water pumping power | 2.46 MW(e) |
| Cold water pumping power | 3.28 MW(e) |
| Ammonia condensate pump power | 1.40 MW(e) |
| TURBINE (1 required) | |
| Ammonia flow rate | 2,007 lb/sec |
| Ammonia isentropic head | 17.57 Btu/lb |
| Efficiency | 87.7% |
| Turbine diameter | 8.64 ft |
| Turbine speed | 1800 rpm |
| Turbine inlet temperature/pressure | 70.9°F/130.8 psi |
| Turbine exhaust temperature/pressure | 52.9°F/94.2 psi |
| SEA WATER PUMPS (4 required/heat exchanger | |
| Warm water flow rate | 1,946 cfs |
| Warm water circuit pressure drop | 180.7 psf |
| Cold water flow rate | 1,888 cfs |
| Cold water circuit pressure drop | 284.3 psf |
| Cold water pump diameter | 17 ft |
| Pump shaft speed | 46.2 rpm |

Both the evaporator and condenser used sea water flowing inside the tubes and ammonia flowing over the tubes. This configuration is desirable for sea water shell and tube heat exchangers because of the need for cleaning the water-swept heat transfer surface. The smooth inside bore of the tubes provides the option of mechanically cleaning the sea water side of the tube.

The operation of the ammonia evaporator is based upon the principle of thin film evaporation. The thin film evaporation process has two potentially attractive advantages for OTEC. First, it offers high ammonia side heat transfer coefficients; second, it allows large tube bundle diameters to be used without the attendant problem of suppression of saturation temperature due to the large hydrostatic head of fluid that results when flooded evaporators are used.

The condenser is of a conventional design with the exception that the tubes are inclined 8 to 10 deg with respect to the horizontal in order to provide a drainage path for the condensate along the vertical tubes support walls. This drainage concept was found to be more attractive from the standpoint of simplicity than the conventional techniques using vapor lanes and drainage trays.

The thermal design specifications for the all aluminum evaporator and condenser are summarized in Table 6.

## CRITICAL DEVELOPMENT AREAS

Conventional shell-and-tube heat exchangers consist of an array of tubes joined to one or more thick tubesheets which are joined to the shell at their perimeter. For any shell-and-tube heat exchanger, the most critical manufacturing operations are the insertion of the tubes through the tubesheets and the formation of satisfactory tube-to-tubesheet joints. It has been determined that the most critical development area for the OTEC shell-and-tube heat exchangers is the tube-to-tubesheet joint, and that new departures from current practices should be developed to obtain a tube-to-tubesheet joint that is both economical to produce and will result in zero-leakage. Neither leakage of ammonia from the heat exchanger, nor leakage of sea water into the working fluid can be tolerated. In the 25 megawatt OTEC heat exchanger there are approximately 20 linear miles of tube-to-tubesheet joint. The potential leakage problem presented by this vast amount of joint area poses a significant challenge to the manufacturing of these joints.

A consideration in selecting the method for making the tube-to-tubesheet joints is the amount of axial load to be applied to the joint in service. Most conventional shell-and-tube heat exchangers utilize thick tubesheets capable of resisting the hydraulic load by themselves. As the diameter of the tubesheet increases, the thickness of the tubesheets must also increase, and for heat exchangers of the size of the 25 megawatt OTEC, the tubesheet thickness can become formidable. An alternative, permitted by the ASME Boiler Code, is to allow the tubes to act as stays which support or contribute to the strength of the tubesheets in which they are engaged. However, the degree to which the tubes may be permitted to support the tubesheets depends on the type of tube-to-tubesheet joint and on the method of joining.

Another consideration influencing the selection of the joining process for the tube-to-tubesheet joints is the use of a double-tubesheet design configuration. In addition to providing

Table 6 HEAT EXCHANGER THERMAL DESIGN SPECIFICATIONS

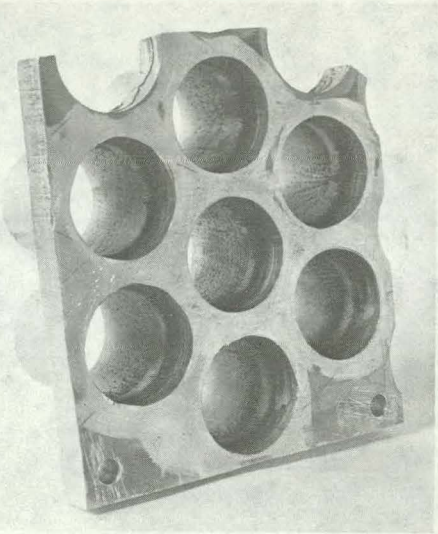
| Item | Condenser | Evaporator |
|---|---|---|
| Tubes | 2.5 in. × 0.058 5052 Aluminum | 2.5 in. × 0.058 5052 Aluminum |
| Number of tubes | 40,903 | 40,903 |
| Tube length (ft) | 42.5 | 42.5 |
| Tube pitch to diameter ratio | 1.2 | 1.2 |
| Tube bundle diameter (ft) | 52 | 52 |
| Heat load (Btu/sec) | 1,020,443 | 1,050,181 |
| MW(th) | 1,076 | 1,108 |
| Log mean temperature difference (° F) | 8.0 | 7.7 |
| Overall heat transfer coefficient (Btu/hr-ft$^2$-° F) | 423 | 452 |
| Sea water inlet temperature (° F) | 43.6 | 80 |
| Sea water exhaust temperature (° F) | 45.85 | 77.73 |
| Sea water flow rate (cfs) | 7,551 | 7.782 |
| Ammonia temperature (° F) | 52.5 | 70.85 |
| Ammonia pressure (psia) | 93.6 | 133.7 |
| Ammonia vapor flow rate (lb/sec) | 2,007 | 2,007 |

a greater insurance against leakage, this configuration most nearly meets structural requirements when combined with the [redacted] of the tubes as stays to permit reduction of the tubesheet [redacted]ness. In the proposed design configuration, the heat transfer tubes carry about 2/3 of the tubesheet hydraulic load, and the remaining load is reacted in a bending moment at the tubesheet perimeter. The double tubesheet configuration influences selection of the tube-to-tubesheet joining method in that it may restrict accessibility and it may also require greater tube/hole clearance to permit easy insertion of the tubes.

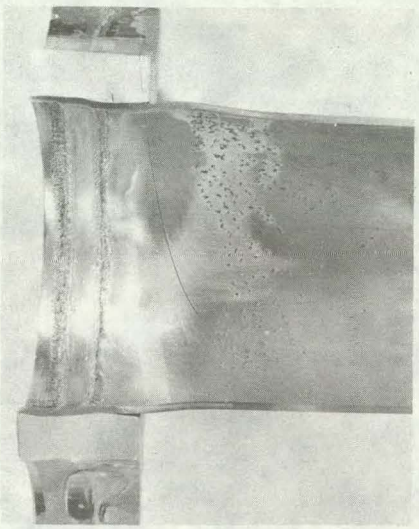
A further consideration in selecting the manufacturing method is that it must be compatible with the requirement for tube replacement in the event that a tube leak should occur, either during the manufacturing process or operation of the power plant.

The technology evaluation program carried out during this study was not intended to result in a qualified tube-to-tubesheet joint for the OTEC heat exchangers. Rather, it was to serve as an exploratory first step in obtaining data required to direct further research and development into this critical technical area. The scope of work included consideration of the more conventional methods of joining tubes to tubesheets, such as rolling and welding, as well as more innovative concepts such as explosive welding, electromagnetic forming (Magnaforming) and propellant expansion. In addition, the use of punched holes in the tubesheets in lieu of machined holes was also evaluated. Results of the technology evaluation of explosive welding carried out at The University of Denver is shown in Fig. 6.

The Magnaforming process for expanding tubes has proven to be attractive because the tube can be mechanically joined to both the inner and outer tubesheet simultaneously as indicated in Fig. 7. This technique of electromagnetic forming is based upon the principle that an electrically conducting tube will respond to a pressure wave generated by a transient magnetic field generated by a coil placed within the tube. The developmental evaluation program carried out at Maxwell Laboratories incorporated a specially designed coil that was capable of forming both the inner and outer tube/tubesheet joints simultaneously. It should be pointed out, however, that Magnaforming is applicable to aluminum tubes only. Because of its higher strength and higher electrical resistivity, titanium tubing cannot be successfully Magnaformed at this time.



Simultaneous Explosive Welding of Aluminum Tubes



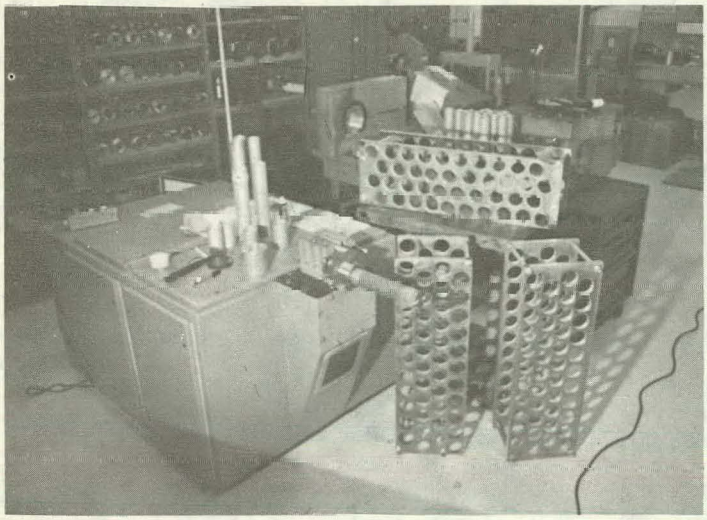
Cross-Section of Aluminum Explosive Joint

Fig. 6 Tube-to-Tubesheet Joint Evaluation Technology

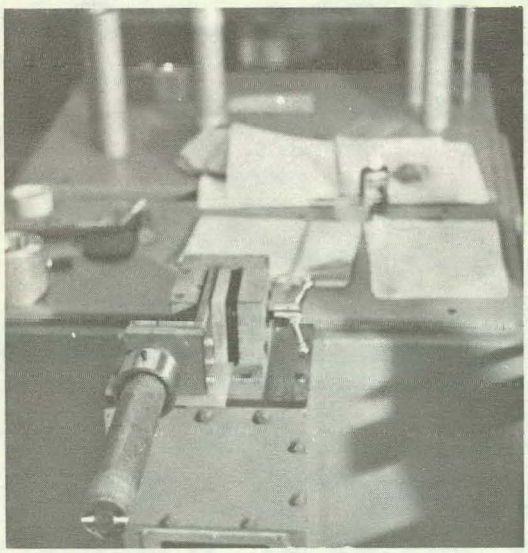
## Structural Design Requirements

Service conditions for OTEC heat exchangers require consideration of hydrostatic submergence in the development of structural design criteria. Ideal design conditions would result from pressure balancing the internal ammonia pressure with the external hydrostatic pressure. However, when the resulting sea water circulation problems are considered, it is difficult to justify this idealized design condition. For example, the cooled evaporator sea water discharge should be such as to minimize reingestion and the condenser cold sea water discharge should be deep enough to be under the mixed (isothermal) warm surface layer dilution of the resource. Table 6 summarizes the hydrostatic pressures used in the design of the evaporator and condenser. For purposes of this study, the 163-psid collapse pressure was established as the most stringent design requirement.

Although this study emphasized the design of heat exchangers for submerged application, the surface design condition was also considered. Heat exchangers designed for surface application have the advantage of being internally pressurized vessels which have less stringent manufacturing requirements and are not subjected to the possibility of sea water leakage into the ammonia working fluid. On the other hand, heat exchangers designed for surface conditions – such as within the hull of a ship or platform – will be subjected to higher internal design pressures associated with normal ambient air temperature excursions. A 105° F day is specified by the U.S. Coast Guard regulations for the design of pressurized ammonia tanks. This corresponds to an internal pressure of 250 psi. It should be noted that the design criteria will result in an aluminum pressure membrane that is 13 percent thicker than the 163-psid collapse pressure developed in Table 1.



A. Overall View Showing Capacitor Bank, Coil, and Three Tube-Sheet Assemblies Prior to Insertion of Tubes



B. Close-up of Special Coil and Die Assembly

Fig. 7 Magnaform Equipment at Maxwell

Table 6 HYDROSTATIC DESIGN PRESSURES FOR SUBMERGED HEAT EXCHANGERS

| Element | Depth at Centerline (ft) | External Pressure (psia) | Internal Pressure (psia) | Working Pressure (psid) |
|---|---|---|---|---|
| Evaporator | 150 ± 14 | 60 to 104 | 15 to 155 | -89 to +95 |
| Condenser | 315 ± 14 | 134 to 178 | 15 to 155 | -163 to 21 |

The design codes to be used in the design of large heat exchangers for operation in the ocean environment are not fu established at this time. It is expected that eventually a cl fication will be established by the Coast Guard or other regula tory body for the design of submersible power systems. In defining the structural criteria for these heat exchangers, Lockheed has used its best judgment to define a tentative set of structural design criteria. These design criteria are considered to be realistic, judging from past experience with regulatory agencies regarding the design of submersible power systems. The design criteria set forth by the American Bureau of Shipping Rules for Manned Submersibles have been used as a guideline for the design of the submerged heat exchangers. These design criteria permit the use of a factor of safety of 1.5 on collapse for man-rated submersibles.

The selection of a spherical pressure vessel for an externally pressurized design condition presents options relative to design and manufacturing. Figure 8 indicates one of the tradeoffs that can be made between manufacturing tolerance required of the pressure vessel and the amount of material required for the pressure vessel. A local out-of-roundness deviation of 8 percent can be considered representative of a tightly controlled manufacturing process. A 20 percent out-of-roundness deviation may be associated with normal industrial practice. For purposes of this study, the 8 percent out-of-roundness normal deviation was selected as the design criteria along with a 525-ft design collapse depth for the condenser which is located at a maximum depth of 350 ft.

The 8 percent out-of-roundness deviation may be related to a ± 1/4-inch radial tolerance over the critical arc length of 85 inches. This tolerance is representative of the specification to which LNG tanks are manufactured.

HYDRODYNAMIC LOADS

Since the OTEC heat exchangers are intended to be surface transportable, they must be designed to withstand the dynamic loads experienced while under tow. Here again the LMSC power module configuration was used to analyze and define these loads. The power module is designed to be towed in the horizontal position on the surface of the ocean. Both static and dynamic loads were derived for towing at 5 knots in sea states 3, 5, and 6. It was assumed that the heat exchangers would be vented to the atmosphere during surface operation, and that the ballast tanks would be partially flooded to obtain a 24-ft draft. Table 7 indicates the hydrodynamic loads that have been estimated for the power module during various operational modes. The most difficult design problem caused by the transport of the heat exchangers on the surface of the ocean relates to the structural support of the tubes and tube support plates. Under tow, the tubes are oriented in the vertical direction. The horizontally oriented tube support sheets are to be designed as self-supporting members that are compatible with heave and pitch response characteristics of the power module. Figure 9 summarizes the heave and pitch response spectra for a Sea State 6 and indicates the magnitude of the accelerations and wave encounter frequencies that may be expected while the power module is under tow.

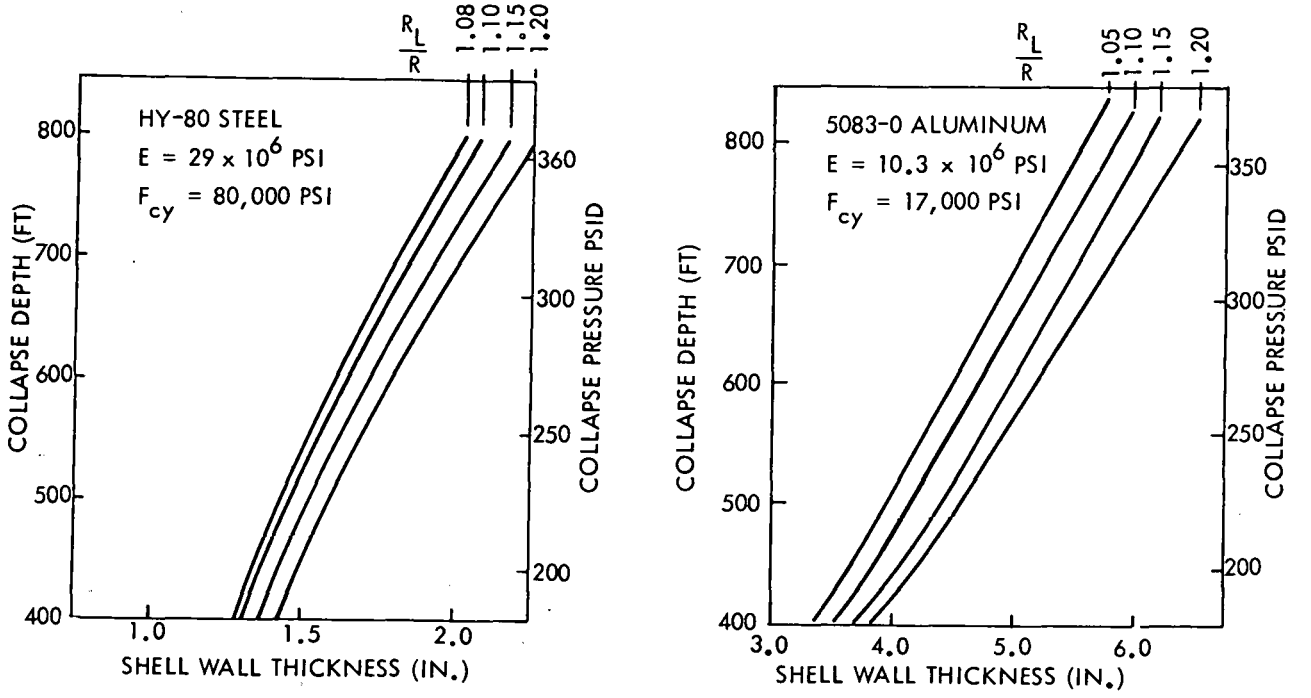
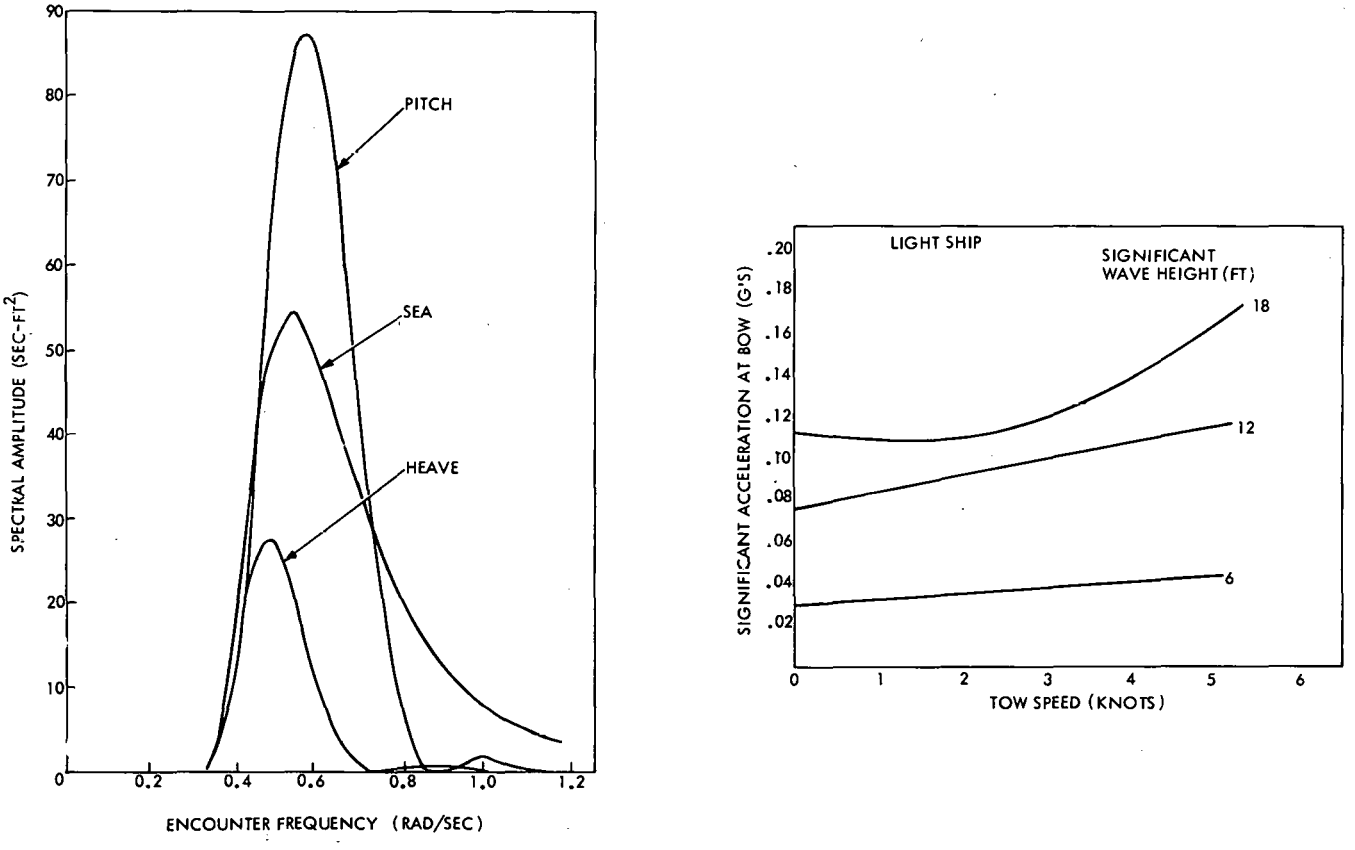



Fig. 8 Collapse Depth for Spherical Condenser Pressure Vessels




(a) Wave Encounter Frequency

(b) Significant Accelerations at Bow

Fig. 9 Summary of Heave and Pitch Response Spectra for Sea State 6

Table 7 SUMMARY OF MAXIMUM LOADS

| Operation | Condition | Shear (LT) | | Moment (ft-LT) | | Acceleration (g) | | Comments |
|---|---|---|---|---|---|---|---|---|
| | | Evap | Cond | Evap | Cond | Evap | Cond | |
| Towing | Hogging, Ballasted | 935 | 1,100 | 63,000 | 18,000 | 0.25 | 0.16 | Range of Period: 8 to 16 Seconds |
| Righting | Ballast | 150 | 560 | 10,000 | 16,000 | – | | Tow Resistance: 22,000 lb |
| Docking | Vertical | | 418 | | 33,000 | – | | |
| OTEC Plant | Heave | 40 | | 40 | | 0.02 | | SS-C Response: 1/2 ft Heave 100 sec Period |

## Conclusions

The design and construction of heat exchangers that are economically attractive for ocean thermal energy power plants is within the current state of the art. The use of aluminum marine alloys in the construction of these heat exchangers offers an economically attractive option whereby the materials cost and manufacturing cost can be minimized. The proposed materials of construction are 5052 aluminum for the heat transfer tubes and 5083 aluminum alloy for all components of the pressure vessel. The use of a spherical configuration for the pressure vessel results in minimum weight and cost pressure vessel. By incorporating the technology base developed for the construction of aluminum LNG tanks, it has been shown that it is possible to produce the 25-MW(e) OTEC heat exchangers on a production-line basis for $350 per kilowatt. The study also indicates that field construction of these heat exchangers is possible with a minimum investment in capital equipment and tooling for $730/kW.

In order to achieve the economies indicated with aluminum construction, an engineering and manufacturing development program is warranted to develop the tube-to-tubesheet joining techniques. It is imperative that this joint be sound and reliable from a mechanical and leakage standpoint. Both explosive welding and mechanical forming (in conjunction with the use of elastomeric seals or conventional welding) appear to be feasible approaches to this problem. Further development is required to select and optimize the manufacturing process and to evaluate long-term performance in the marine environment.

## Acknowledgements

The OTEC Heat Exchanger Design and Producibility Study(1) was performed by Lockheed Missiles & Space Company under contract to the Energy Research & Development Administration. An extensive amount of technical and manufacturing data was contributed by the various organizations that participated in the study. The efforts of the contributors listed below are gratefully acknowledged.

T.Y. Lin International, San Francisco, California
Yuba Heat Transfer, Tulsa, Oklahoma
Alcoa Laboratories, Alcoa Center, Pennsylvania
Bechtel Corporation, San Francisco, California
Pittsburgh Des Moines Steel, Des Moines, Iowa
Lockheed California Company, Burbank, California
University of Denver, Denver, Colorado
Maxwell Laboratories, San Diego, California
McKey Perforating, Milwaukee, Wisconsin

(1) Lockheed Missiles & Space Company,Inc., Heat Exchanger Design and Producibility Study, SAN/1291-7[illegible] Distribution Category UC-64, Oct 1976

## COMMENTS

Written Comments by J. Hilbert Anderson:

This paper is particularly unfortunate, because it is based on several impossible and/or impractical design premises. In essence this means that it represents an exercise in futility.

The first design assumption that is inconceivably bad is that you can spray liquid over a 52 ft. diameter tube bundle containing 41,000 tubes, and maintain a boiling liquid film over the entire surface of every tube. Spray type evaporators have been tried many times in the history of refrigeration. They have almost universally been discarded in favor of liquid flooded types, simply because the flooded evaporators work better. The flooded evaporator does at least solve the problem of wetting all the tubes. While the flooded evaporator does have the problem of static head penalty, this can be solved by using multiple low head evaporators. The use of multiple low head evaporators make the development of manufacturing capability for large shells completely unnecessary.

The assumption that the condenser should be designed for 350 ft. depth in the ocean is completely unwarranted. While diver maintenance is possible at this level it is below the level where diving costs are modest, and this depth would unnecessarily add to maintenance problems. We have pointed out many times that the value of food produced from the condenser discharge is almost certain to be greater than the value of the power produced by a sea thermal plant. This has been well established over a period of at least five years by the experimental station at St. Croix. To me it is unthinkable that we should deliberately throw this most valuable product away by discharging the condenser water below the upper warm layers. The condenser water should definitely be discharged above the boiler discharge so as to mix it and hold it in the upper levels. This has the additional benefit that it reduces boiler feed pump power and improves cycle efficiency.

The rigid requirement of no leaks is a consequence of selecting ammonia for the working fluid. Ammonia is highly soluble in water. Therefore, it is difficult to remove the water that leaks into the system, and it is difficult to detect ammonia leaks outward into the sea. To anyone who has actually built large heat exchangers it is obvious that a completely leak proof heat exchanger is terribly costly to build, and requires many more hours of shop time than to build and test an exchanger with modest leak tolerances.

The authors have apparently ignored the ASME Code requirement that pressure vessels that are field welded must also be annealed as a complete unit. This would indeed be difficult and costly, and I see no mention of

this in the table of estimated costs.

The requirement for double tube sheets adds an additional costly item. It is inconceivable to me that the estimated costs could ever be met for this size and type of exchanger. Very ordinary carbon steel exchangers, without double tube sheets, in easily manufacturable sizes today cost more than $7.75 per square ft. estimated here.

We recently purchased ten medium size shell and tube heat exchangers with carbon steel tubes at a price of $17.00 per sq. ft. Another carbon steel tube exchanger, 52" in diameter by 52 ft. cost $7.80 per sq. ft.

The statement that shell and fabrication costs are equal to or greater than the cost of tubes is an important point. We have concluded many years ago that a very major factor in heat exchanger cost is the pressure shell, and that this can be greatly reduced by minimizing pressure differences across the housing. This study only confirms our beliefs.

In summary we must conclude that the only real reason for continuing this development is to create another bottomless pit into which taxpayer funds can be poured forever without producing any useful results.

Reply by Authors:

The following additional background information developed during the course of the heat exchanger producibility study is offered in reply to the comments of Mr. Anderson. It is hoped that this information will clarify some of Mr. Anderson's misconceptions regarding this study.

## Thin Film Evaporators

The evaporator design proposed by Lockheed can best be described as a thin falling film evaporator. Boiling within the film is not intended to occur because of the low temperature differential (2-3 degrees F) available between the tube, and the evaporating ammonia film. This concept has been the subject of extensive research and development programs carried out with sea water by the Office of Saline Water, Department of Interior. References 1-5 are indicative of this development work. Further, the Israeli's have successfully applied the thin film evaporation concept to an aluminum tubed shell and tube heat exchanger used for desalting sea water. They have produced twenty-five of these units over the past eight years. These aluminum heat exchangers using the thin film evaporation technique have proven very successful from an economic standpoint.

The problem of adequately wetting all the tube heat transfer surfaces within the tube core is solved by irrigating each tube with an excess of liquid over and above that which is evaporated from each tube. Experience with the previously mentioned sea water desalination plants indicate that a reflux ratio of about 3 is adequate to insure complete wetting of all heat transfer surfaces and prevent local dry out of the heat transfer surfaces. The proposed evaporator design concept set forth by Lockheed in the subject report is considerably larger (54 ft. diameter tubesheet) than that upon which the desalination experienced is based (15 ft. diameter tubesheets). The tube non-wetting problem may be adversely affected by the scale up to these larger tube sheet geometries. Two design solutions have been identified to alleviate the ammonia maldistribution problem in the event that it should be more severe than anticipated. The first solution is to reduce the number of tubes in a vertical row supplied by each of the liquid ammonia distribution tubes. Designs that represent the two extremes for the configuration of the ammonia distribution system are depicted in figure 1. This design concept is sufficiently flexible so that heat transfer tubes can readily be converted to liquid distributor tubes during development testing. The second solution is to increase the ammonia reflux ratio. This can be readily accorplished by increasing the speed on the evaporator reflux pumps. One of the purposes of the OTEC heat exchanger development program is to identify the most effective distribution tube arrangement and reflux ratio.

## Condenser Location

Lockheed located the condenser at the depth of 350 ft. in an attempt to prevent mixing of the cold water effluent with the warm water of the mixed layer. It was recognized that any mixing of cold water within the mixed layer would result in a reduction of the OTEC thermal resource. For this reason, the condenser was located at a 350 ft. depth, which is below the mixed layer. It is reasonable to consider locating the condenser at a depth not greater than 170 ft. Location at this depth would also minimize leakage of sea water into the condenser by essentially "pressure balancing" ammonia and sea water pressures. Further studies are required to investigate the effects of discharging cold water into the mixed layer and to evaluate both the effects of recirculation and the thermal stability of the mixed layer under these conditions.

## Mariculture

We recognize the potential value of food products that can be obtained by cultivating the nutrients in the cold water drawn up by OTEC. However, we have not been able to reconcile the conflicting requirements of mariculture and electric power generation in a single system. Mariculture requires an environment that promotes the growth of Marine biota as a feedstock; electric power generation on the other hand, operates best in a sterile environment where marine biota are not available to foul the heat exchangers. In addition, mixing of cold water within the mixed layer is desirable for mariculture, whereas this practice would adversely affect the production of electric power.

## Ammonia Leakage

Both Lockheed and TRW have identified ammonia as the most promising working fluid for the OTEC system. Lockheed studies indicate that plain unenhanced heat transfer surfaces using propane as a working fluid will

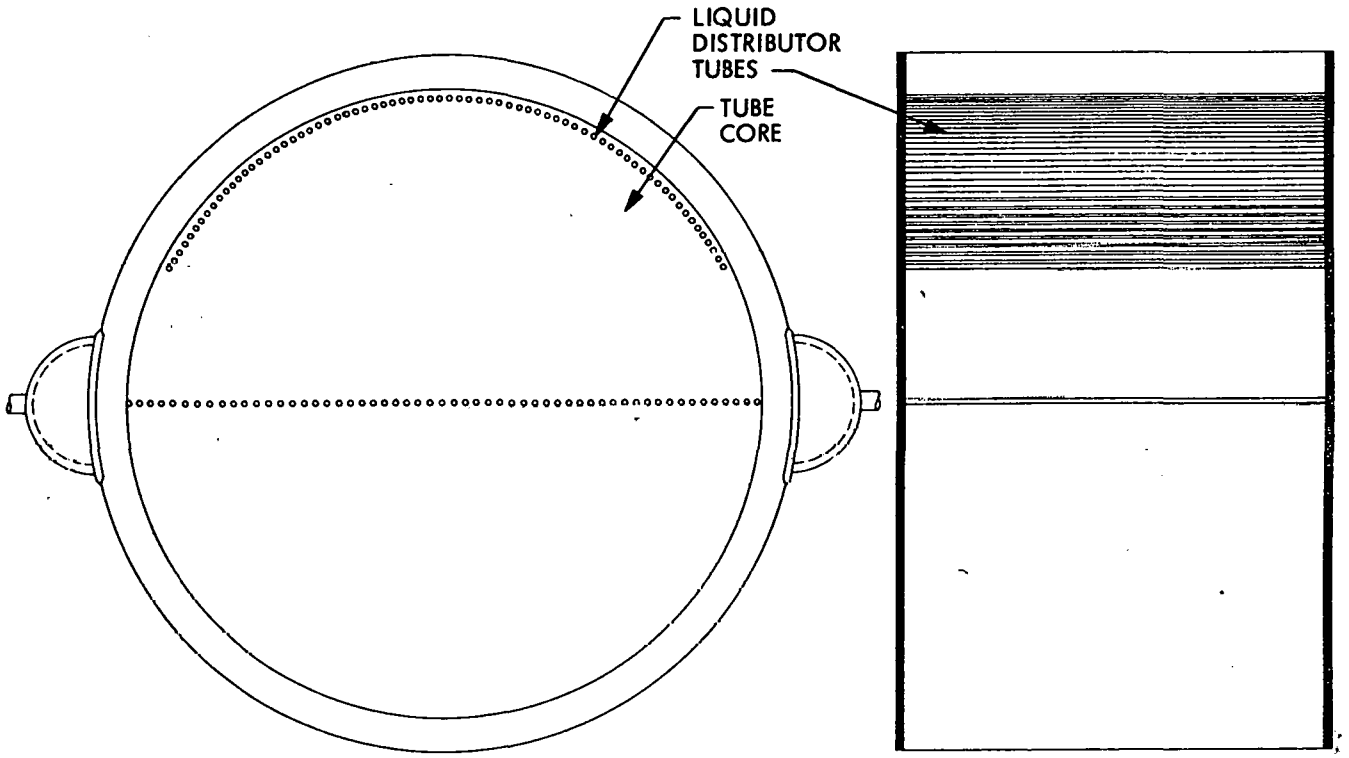



Fig. la Baseline Ammonia Liquid Distribution

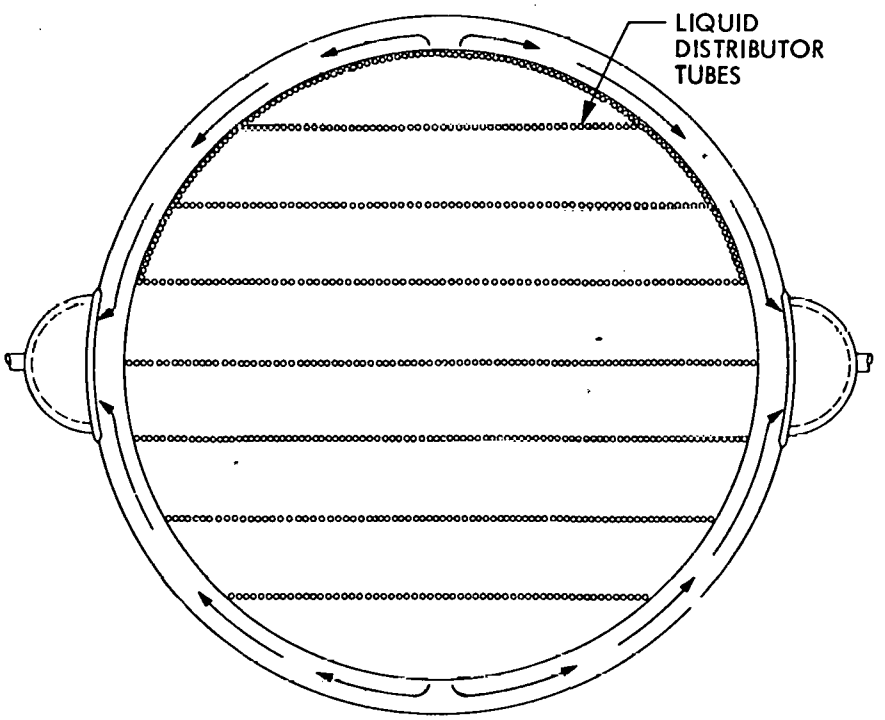



Fig. lb Alternate Ammonia Retrofit Configuration

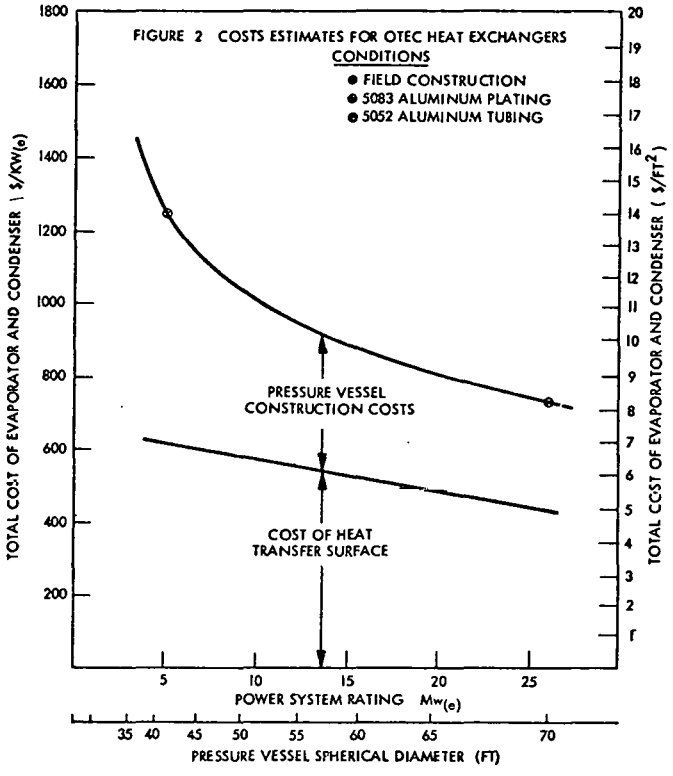
require approximately twice the heat transfer surface area as for ammonia. We believe that manufacturing techniques can be developed that are cost effective, will result in a leak free heat exchanger. Our study indicated that explosive welding of the tube/sheet interface is one of the most promising approaches to this problem.

## Annealing of Field Welded Structure

The requirements for annealing welded pressure vessels vary depending upon material and wall thickness. There are no requirements to anneal 5083 aluminum welded pressure vessels. The HY80 steel pressure vessels considered in the subject study for titanium tubed heat exchangers were designed and welded such that post weld heat treatment was not required. Adequate design margins, and proper control of the welding process eliminated the need for post weld heat treatment. In any case, several companies, including Lockheed, have developed economical methods for field heat treatment of heavy walled pressure vessels.

## Heat Exchanger Cost Estimates

The purpose of the study conducted for ERDA by Lockheed, was to investigate design concepts and manufacturing technologies for shell and tube heat exchangers as applied to OTEC power plants. The study was limited to an investigation of the manufacturing technology required to economically produce shell and tube exchangers. LMSC identified the monolithic heat exchanger as the most cost effective approach to the construction of OTEC heat exchangers because of the economics of scale that are inherent in the construction of large pressure vessels. During the course of this study, we investigated heat exchangers constructed for a 5 MW(e) power system, and for 25 MW(e) power output. The resulting cost estimates for these two heat exchangers which incorporated a spherical 5083 aluminum pressure vessel is shown in figure 2. It is apparent from this curve that there are economies of scale that do favor use of large monolithic heat exchangers for OTEC application. The technology required to economically construct vessels of this size exists in the LNG tank construction industry. If tooling intensive mass production methods are employed in the construction of the pressure vessels further cost improvements are indicated. We estimated that over a production run of twenty five megawatt power systems, (50 heat exchangers) a cost of $\$4/ft^2$ can be obtained for the OTEC heat exchangers using all aluminum construction.





Reference 1. Final Report Horizontal Spray Film (HTEX) and Vertical Tube (VTEX) Evaporator OSW San Diego Test Facility U.S. Department of Interior, Office of Saline Water, Thermal Process Division, May 1973, Burns and Roe Construction Corp., Paramus N.O. Office of Saline Water Contract 14-3014.

Reference 2. Horizontal Spray Film Evaporator Aqua Chemical Corporation, Office of Saline Water, R&D No. 209, NTIS Order Number PB 206284.

Reference 3. Experimental and Analytical Studies of Heat Transfer in a Falling Film System (Part I) Houston Research Institute, Office of Saline Water R&D No. 287, NTIS Order Number PB 207020.

Reference 4. Third Progress Report on Horizontal-Tube Multiple-Effect Process Plant Tests, Universal Desalting Corp., Office of Saline Water R&D No. 740, NTIS Order Number 208058.

Reference 5. Personnel Communications, A. F. Manikowski, Lockheed Missiles & Space Company, Inc., Robert Zeitlin, Israel Desalination Engineering, Tel Aviv, Israel 4 Feb. 1976.

THIS PAGE

WAS INTENTIONALLY

LEFT BLANK

# VII. BIOFOULING & CORROSION

LYLE D. PERRIGO, CHAIRMAN
*OTEC Biofouling & Corrosion Project*
*Battelle Pacific Northwest Laboratories*

THIS PAGE

WAS INTENTIONALLY

LEFT BLANK

CONF-770331--4

# THE OTEC BIOFOULING AND CORROSION PROGRAM[a]

LYLE D. PERRIGO AND GEORGE A. JENSEN
*OTEC Biofouling and Corrosion Project*
*Chemical Technology Department*
*Battelle Pacific Northwest Laboratories*
*Battelle Boulevard*
*Richland, Washington*

Abstract

The Energy Research and Development Administration (ERDA) is sponsoring a program to explore the possibilities for beneficially using the temperature difference between warm surface water of the tropical oceans and the deeper colder water to operate a heat engine. One of the major technical hurdles that must be crossed to make this source of energy available for commercial use is the solution to biofouling, corrosion and deposition reactions that are expected to reduce heat transfer efficiency. In January 1976, ERDA established a Project Activity Office at Battelle-Northwest. The mission of this Office is to develop, procure, monitor and evaluate projects to define, prevent and/or alleviate biofouling and corrosion problems expected in OTEC power plants. Since startup, this project activity office has: 1) developed a methodology to guide work, 2) assumed responsibility or contracted for 10 projects, and 3) expects to have several more contractors work on various aspects of biofouling and corrosion problems in the near future. The priorities for near and intermediate term work are identified and the operation of the Project Activity Office described in this paper.

## INTRODUCTION

The control of biofouling and corrosion in OTEC power plants is mandatory if this concept is to be commercially viable. Recognition of the importance of these factors led the Energy Research and Development Administration (ERDA) to establish a project activity office at the Pacific Northwest Laboratories, Battelle Memorial Institute. The mission of this project activity office is to assist ERDA in planning, identifying projects, securing contractors, controlling projects and evaluating the results of efforts to define, prevent and/or alleviate biofouling and corrosion problems that may by found in OTEC power plants.

The authors believe it is important to describe the program that has been developed to address the OTEC biofouling and corrosion problems. Such a description should provide a context for the following papers for the Ocean Thermal Energy Conversion Workshop. A discussion of the whole program, although brief, also should provide a background for those who are interested in the field and may wish to explore other methods to define, prevent and/or alleviate biofouling and corrosion problems.

Our information on the OTEC Biofouling and Corrosion Program will be covered in four sections that describe the Project Activity Office: 1) the program need, 2) approach and emphasis, 3) project organization, and 4) projects.

## PROGRAM NEED

There are a large number of reasons why the prevention and/or alleviation of biofouling and corrosion problems are important for the commercial operation of OTEC. There is, however, one overriding aspect of this problem. Because of the very low temperature differences

(a) This paper is based on work performed under Energy Research and Development Administration Contract E(45-1)-1830.

between the warm surface and cold deep ocean waters and the working fluid, heat transfer surfaces must be maintained with little or no fouling if electrical power is to be produced efficiently. If bacterial films, slimes and corrosion deposits cannot be kept at very low thicknesses heat transfer efficiencies would drop dramatically.

Laity's(1) analysis of the problem is instructive. Using common heat transfer calculational techniques and the assumption that the biofouling layer would have heat transfer characteristics similar to a stagnant film of water he developed the curves shown in Figure 1. As can be seen from these curves, a 2-mil thick deposit can lower heat transfer efficiency by about 15 to 30%. A 3-mil thick deposit is considerably worse. The usual methods for coping with heat transfer losses such as increasing the amount of surface area of fluid flow are not generally applicable. An OTEC power plant is expected to be a capital-intensive facility. Therefore an increase of the heat exchanger surface area by 25 to 50% would likely increase overall costs by 12 to 25%. Anticipated operation at flows of 6 ft/sec result in a parasitic power loss of about 30% of the plant's generation capacity. Increases in flow rates would cause a spectacular increase in pumping power requirements.

The results that were obtained by Fetkovich and his coworkers, although very preliminary, at Keahole Point, Island of Hawaii, tend to confirm the serious nature of bacterial films, slimes and corrosion deposits on heat transfer.(2) Fetkovich will provide additional details on his Keahole Point work later in this session.

## APPROACH AND EMPHASIS

The approach to the definition, prevention and/or alleviation of OTEC biofouling and corrosion problems and the emphasis being given to various parts of the program directed toward the control and/or solution of those problems is described in this section. The first subsection describes a methodology that has been adopted by PNL and was given in our first annual report,(2) the second subsection discusses a program master plan that will soon be published and the final subsection presents information on the emphasis being placed on the OTEC Biofouling and Corrosion Program.

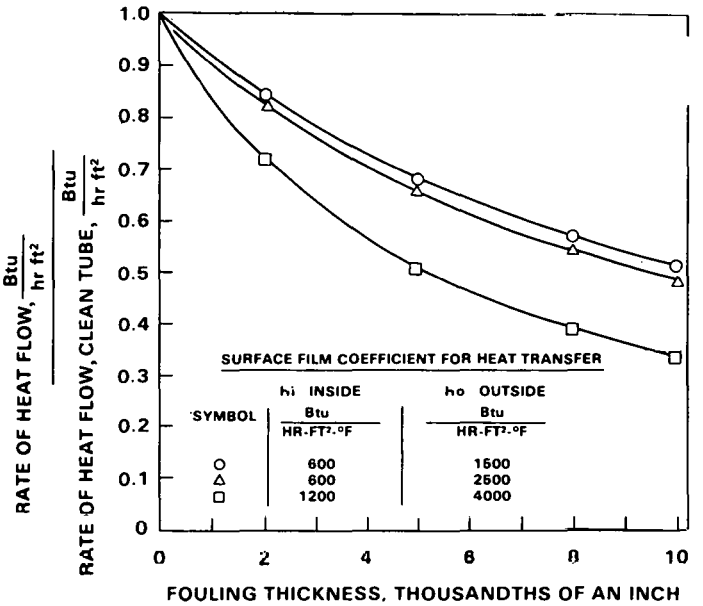



FIGURE 1. Effect of Fouling Film Thickness on Heat Transfer Across Tube Wall

## METHODOLOGY

The methodology to direct R&D efforts on OTEC biofouling and corrosion problems is shown in Figure 2. The overall effort is comprised of three major elements concerned with problem definition, preventative techniques, and methods for overcoming deleterious biofouling and corrosion in operating systems. Each of the major elements consists of several subelements dealing with specific approaches to, or methods for, solving the allied problems of biofouling and corrosion in OTEC systems. More detailed information on each of the major project elements and its constituent parts are described in the following subsections.

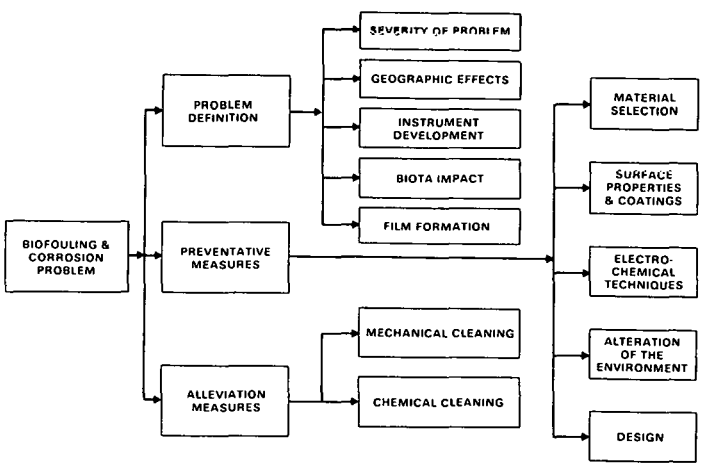



FIGURE 2. Methodology for OTEC Biofouling and Corrosion Program

Problem Definition

The proposed program provides for a substantial effort to define the nature and extent of biofouling and corrosion because little information is available on the nature and extent of biofouling or corrosion for many of the conditions under which an OTEC unit would operate. It is acknowledged that there is a wealth of data available on biofouling and corrosion of various materials and systems in coastal waters and harbors. However, since the systems may operate in mid-ocean, there may be considerably different and perhaps fewer problems for OTEC systems. Another important consideration is the cold, deeper ocean waters that will be employed as the heat sink for the OTEC system. Little is known about the biofouling or corrosion potential of such waters or about the perturbation effect of the OTEC system on mid-ocean biota, which will also be examined. Since biofouling and corrosion are critical path items for the OTEC system, the following definitional studies will be required to achieve mission objectives.

- Severity Studies. The unknown effects of biofouling and corrosion in mid-ocean and with surface and deep, cold ocean waters are to be defined by a number of key experiments.
- Geographic Effects. Appreciable uncertainty exists within the scientific and technical community about both the relative effects of biofouling and the allied corrosion problems in different geographic areas that might employ OTEC systems. Work in this sector will be focused on defining differences, if any, for the areas of interest to the United States.
- Instrument Development. At the present time, there is one design for a device to measure the biofouling and corrosion effects in ocean waters potentially applicable to OTEC. There are, however, only limited operating data in an ocean environment showing that this device will provide the information needed for the program. Effort will be applied to provide the necessary testing capability required to define the severity of the biofouling and corrosion problem. Additional test instruments will be developed, tested, and evaluated to obtain corroborating measurements of the biofouling and corrosion effects of ocean waters where OTEC systems may be located.
- Biota Impact. The water taken from the cold strata deeper in the ocean is likely to be richer in nutrients than the surface or near-surface waters where the OTEC system is expected to be located. Since pumping these nutrients closer to the surface is expected to have a significant effect on the abundance of flora and fauna in and adjacent to the OTEC system, the impact of this effect must be defined including aspects pertaining directly to OTEC heat transfer surfaces. The impact of OTEC system operations on the enviornment must also be assessed. For example, in chemical cleaning the release of chemicals or other cleaning products may be detrimental to the biota in the waters surrounding the OTEC system. The effects of low concentrations of heavy metals and even chlorine on biota in OTEC locations, for example, may be severe and must be defined.
- Film Formation. Organic chemicals, such as proteins, wastes from biological species, and decomposition residues exist in sea water. Many of these materials can precipitate on all surfaces exposed to sea water in the OTEC system. In particular, the formation of a film as little as 0.010-in. thick on the heat transfer surface can reduce heat transfer by a minimum of 50%. The rate, character, and composition of film formation in areas where OTEC systems are to be located must be identified, particularly the rate of formation, composition, and thickness of films forming on heat transfer surfaces. These films may also corrode the materials used in the construction of heat transfer surfaces. The corrosion effects of these films on the materials proposed for OTEC heat exchanger surfaces and biota impact of the film on these materials will also be investigated.

Preventative Measures

A number of measures have been used to a greater or lesser extent in the past several decades to prevent or reduce the unfavorable effects of biofouling and/or corrosion. In this program, these preventative procedures are to be examined to determine their merits in coping with OTEC biofouling and corrosion problems. The existing and substantial technology base in this area will be used as the starting point for work in this sector. Details on specific fields of study follow.

- Material Selection. Certain materials are known to suffer less biofouling and corrosion in coastal and harbor waters than others. The OTEC biofouling and corrosion tendency of these and other candidate materials will be examined in this portion of the study. An important consideration in selecting candidate materials for such examinations is their availability in the amounts needed for OTEC systems and their economics compared with competitive materials.

- Surface Properties and Coatings. One of the methods to avoid or minimize biofouling and corrosion problems is to provide for: 1) special surface conditions, or 2) coatings that will impede/inhibit undesirable effects. Work in this area will be focused on an examination of what, how and if these techniques may be applied beneficially to OTEC systems.

- Electrochemical Techniques. The application of electrochemical procedures is one of the classical approaches to the prevention of corrosion on a wide variety of systems in a number of environments. The examination of the feasibility of using this approach to avoid biofouling and corrosion in OTEC systems is expected to be one of the techniques studied in this program.

- Alteration of the Environment. Alteration of the environment is terminology used by corrosion engineers to describe procedures for changing the corrosive nature of the medium in which materials are exposed. Careful examination of this approach to minimize or avoid biofouling and corrosion problems in OTEC systems is warranted. Some discussion has already been directed toward the possible use of chlorine to impede-inhibit biofouling of OTEC systems. Effort in this sector of the project will be focused on examining the feasibility and desirability of using chlorine to solve the biofouling problem as well as other potentially useful techniques of this nature that would have a beneficial impact. The effects of these methods and their corrosion potential will also be evaluated.

- Design. One of the well-accepted methods for preventing or minimizing corrosion is to design the plant to avoid conditions that accelerate or initiate such undesirable effects. A similar set of conditions may be possible for biofouling and will be examined in this proposed study. It should be recognized that design and a preventative measure is markedly different from design in its usual sense. Antibiofouling and corrosion design is concerned with the effects of geometry, orientation, layout, relative location, configuration, fluid flow characteristics, etc., and not specific plans for particular pieces of hardware or facilities. It impacts the latter by indicating favorable or unfavorable conditions of design. Although well recognized as a corrosion prevention technique, it has not been widely used because few people know enough about anticorrosion design principles to effectively apply the method. However, these techniques are straightforward and are proposed for study as another means of avoiding biofouling and corrosion problems.

Alleviation Measures

A number of simple as well as more sophisticated measures are routinely used to remove biofouling buildup and corrosion films from marine heat transfer and other surfaces. Current technology involves both mechanical and chemical methods to accomplish this. Ideally, a combination of conditions, preventative measures, and operational techniques would avoid biofouling and deleterious corrosion effects in OTEC systems. Practically, however, the optional combination of variable

will merely minimize these undesirable effects. It then is a matter of providing cleaning procedures that might be online or shutdown techniques that might maintain heat transfer and other surfaces in an optimal state of cleanliness so that the OTEC mission may be achieved. This portion of the project is focused on measures that will provide this optimal level of system cleanliness.

- Mechanical Cleaning. One mechanical method for possibly maintaining desired cleanliness of heat transfer surfaces in OTEC systems has already been considered on a conceptual basis. A proprietary method reportedly uses soft rubber balls that are frequently fed into various tubes in a heat exchanger to wipe undesirable substances from these surfaces. A second method uses cavitation in a hydraulic system to remove undesirable materials from surfaces. These are two of many procedures that should be examined, some of which will be procedures for the heat source, as well as the heat sink side of the OTEC system. Key factors that should be evaluated in the development and selection of any candidate mechanical cleaning method as well as a chemical method are: 1) the long-term effectiveness in maintaining desired surface conditions, 2) erosion/corrosion/defilming effects that may result from cyclical use of cleaning methods, 3) the need/desirability of having multiple cleaning options to beneficially supplement each other to achieve desired conditions, and 4) operational versus shut-down methods to maintain desired conditions.
- Chemical Cleaning. As with mechanical cleaning procedures, there are many chemical cleaning methods that potentially could be used for maintaining the proper surface conditions in OTEC systems. Viable procedures should be identified, examined, and developed for this particular application. An important consideration in the development of a useful chemical process will be the handling and disposal of the cleaning medium after it is used. The key factors involved in the selection of viable cleaning processes mentioned in the previous subsection also apply to chemical cleaning and are considered integral and necessary parts of this study.

MASTER PLAN

A Master Plan for the effort to define, prevent and/or alleviate biofouling and corrosion problems in OTEC systems is now nearly complete and will be published in the near future. The primary objective of this plan is to define how the Project Activity Office will: 1) manage a technical program which will utilize or adapt existing technology whenever possible and 2) develop new technology where needed to cope with biofouling and corrosion problems in OTEC systems. The administrative aspects of this supportive effort, its organizational structure and prerogatives are also defined in the plan.

The plan recognizes that the pacing components of the OTEC power plant in achieving economic viability are the heat exchangers. The methodology identified earlier in this paper is expanded into definitive milestones which are required if the long-term performance capability of the OTEC system and its options are to be demonstrated. In the early phases the methodology is specifically directed toward identifying, evaluating, and utilizing available technology for defining, preventing, and/or alleviating the potential biofouling and/or corrosion problems in the OTEC heat exchangers.

In addition, the plan is flexible to ensure that the longer-ranged requirements of the OTEC system be met. For example, it addresses various programmatic issues which need resolution such as hull cleaning and corrosion, the unique materials problems of such a large ocean structure and the biofouling and corrosion effects on these materials, and the institutional considerations relative to biofouling which must be addressed.

EMPHASIS

The emphasis placed on defining, preventing and/or alleviating OTEC biofouling and corrosion problems is closely tied to and coordinated with efforts to solve other OTEC problems and to exploit the concept successfully. The OTEC thrust, as the authors of this paper understand the situation, is to use state-of-the-art

technology, insofar as possible, in demonstrating the viability of OTEC. Exploratory work and research is done to provide ideas, methods, and information to elucidate those areas where existing science and technology does not cover conditions adequately for design and demonstration. In a sense the current approach might be labeled as development and research. This approach is different from the more common research and development mode of operation that is often followed in similar endeavors.

Emphasis in the early work in the biofouling and corrosion area was focused on the acquisition of biofouling data from areas where OTEC power plants might be located. This emphasis was related to a need to define how serious the biofouling problem might be and what the attendant impact would be on heat transfer. Work was initiated to acquire the required data. Concurrently, a deeper analysis of the potential effects of fouling films was made by Laity showing that very thin deposits of 2 to 3 mils could reduce heat transfer efficiency by 25% or more.

The acquisition of the limited data by Fetkovich and his colleagues at Keahole Point, Island of Hawaii, Laity's information, and a thorough analysis of critical path activities controlling the development of OTEC resulted in a reordering of biofouling and corrosion program priorities in October 1976. The development of effective methods for cleaning OTEC heat transfer surfaces became equal in importance to the acquisition of long-term biofouling data from at least one geographic location. There is now a general recognition that cleaning of OTEC heat transfer surfaces will be an integral and necessary step in the normal operation of OTEC power plants.

The October 1976 examination of the OTEC Program had other effects. Analysis of existing information showed the importance of using aluminum for heat exchanger tubes, if at all possible. Aluminum has good thermal conductivity properties, it is easy to fabricate, there is a suitable production capacity to supply the potential demand and its costs are considerably less than other candidate tubing materials. The latter is an extremely important consideration in the commercialization of a capital intesive concept. Because there is an incentive for using aluminum, the Biofouling and Corrosion Project Activity Office is stressing projects for the near-term that will acquire information on the possibilities of using this material for OTEC heat exchanger tubes.

Other areas of great interest to the Biofouling and Corrosion Project Activity Office are: 1) the acquisition of biofouling data in the Atlantic and Caribbean areas, 2) cold water biofouling, corrosion and deposition data, 3) the development of another biofouling measurement device, 4) supporting data on titanium, and 5) the possibilities for using various methods for altering the bulk water or boundary layer water to impede or limit biofouling problems. The Project Activity Office is always interested in new, different, and potentially viable ideas for the solution of OTEC Biofouling and Corrosion problems.

## PROJECT ORGANIZATION

The Biofouling and Corrosion Project Activity Office was established at PNL in January 1976 in response to a request by ERDA. It was believed that such an operation, following ERDA procedures and procurement policies that were already in place at PNL because this laboratory is a prime contractor to ERDA, would help achieve OTEC Program objectives in a timely and cost-effective manner. The primary mission of the PNL Project Activity Office is project development and management, and the functional work is planning, procurement, monitoring, evaluation and liaison. Although the directive establishing the Project Activity Office at PNL allows up to 10% of the development and research funds to be spent within Battelle, none have been so allocated to date.

For most practical purposes the Biofouling and Corrosion Project Activity Office acts as an arm of ERDA. Figure 3 shows how it fits into the OTEC Program.

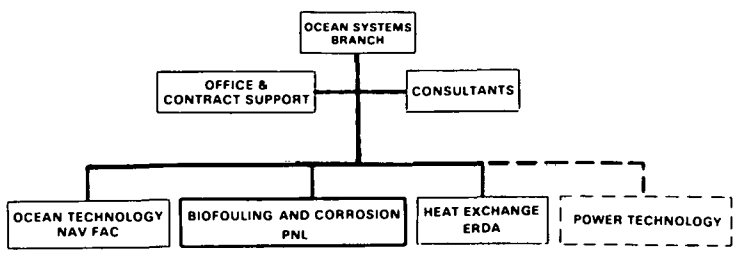



FIGURE 3. OTEC Organization

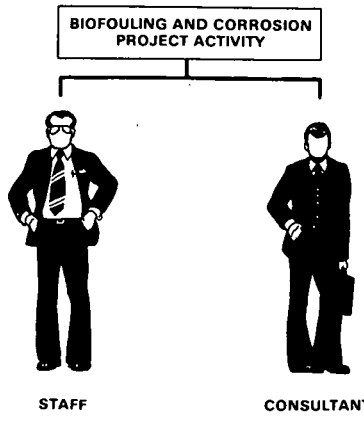



FIGURE 4. Biofouling and Corrosion Project Organization

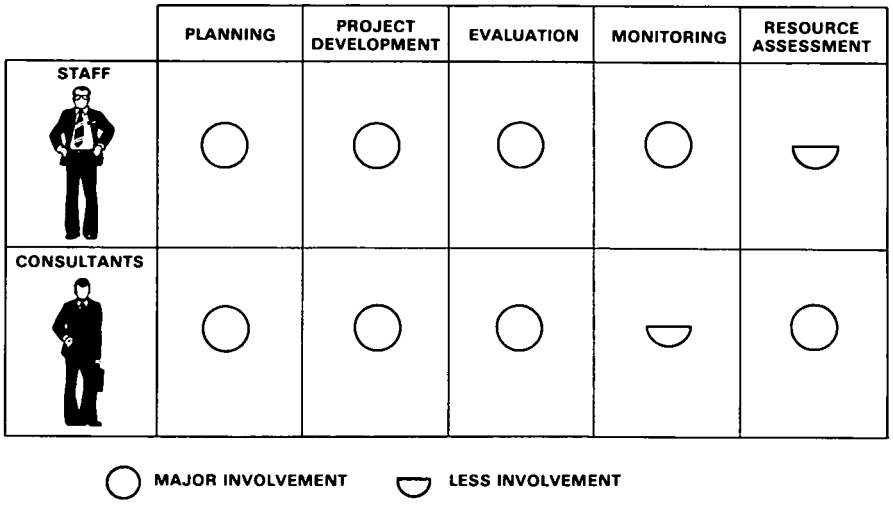



FIGURE 5. Joint Functions

The project activity office was organized to utilize two general categories of people: 1) staff members at PNL, and 2) consultants. It was believed that a multidisciplinary effort with major responsibilities for strong project management would best be served by such an arrangement. Figures 4 and 5 illustrate this two-category arrangement and some of the joint functions undertaken by the two groups. In addition, the PNL staff of the Biofouling and Corrosion Project Activity Office has other functions concerned with administration, budgeting, communications, coordination, procurement and technology transfer. Communications and liaison are very important aspects of the PNL operation. Figure 6 shows the Biofouling and Corrosion Project Activity Office is involved with these various other entities.

## PROJECTS

At the present time there are nine projects underway to define, prevent and/or alleviate OTEC biofouling corrosion problems that are being sponsored by the Project Activity Office. In addition there is one project that has been completed and the final report is in preparation. Papers are being delivered in this session on most of these projects so our discussion will be limited solely to their identification with a brief statement of their scope.

- Development and Use of a Biofouling Measuring Device--Carnegie Mellon University, Pittsburgh, Pennsylvania. This work effort is directed toward the development, proof testing and use of a device to acquire open biofouling and corrosion data similar to those expected to exist in OTEC power plants.
- A Study of Methods for the Prevention and Control of Fouling on Floating Platforms and Non-Heat Exchanger Surfaces Exposed to Sea Water for OTEC Power Plants--David W. Taylor Naval Ship Research and Development Center, Annapolis, Maryland. This effort is directed at developing information on cleaning and fouling control techniques that might be used for prevention and alleviation of fouling on OTEC platforms.
- Investigation of Heat Exchanger Cleaning Methods--Hydronautics, Inc., Laurel, Maryland. This project is directed toward establishing the state-of-the-art for cleaning OTEC heat exchangers and using the data obtained conceptualizing new or modified heat exchanger cleaning methods.
- A Study to Evaluate Existing Data on Primary Films--The Naval Post Graduate School, Monterey, California. This project is an effort to establish what is known about primary film formation so that the information can be used to guide other biofouling and corrosion projects.

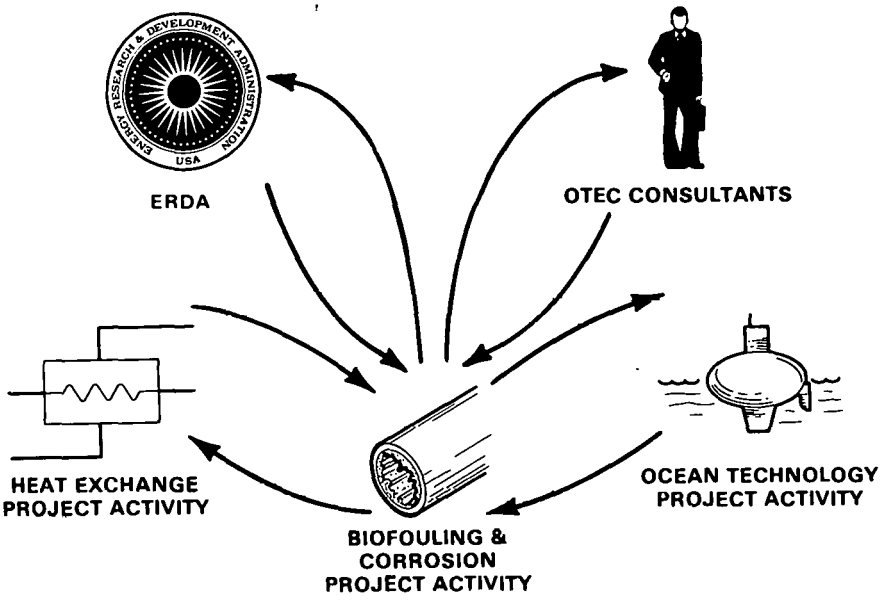



FIGURE 6. OTEC Communications and Liaison

- Catalog Information on the Performance of Aluminum in Sea Water--Alcoa, Technical Center, Alcoa Center, Pennsylvania. The objective of this effort is to establish and catalog what is known about aluminum corrosion in sea water for those alloys which may be used in the OTEC systems to help guide future project development activities.
- Compatibility Studies for the System Water-Ammonia-Titanium as Related to Ocean Thermal Energy Conversion--Sigma Research, Inc., Richland, Washington. This study is focused on determining the stress corrosion cracking behavior of titanium in sea water-ammonia mixtures.
- Preparation of a Catalog of Oceanographic Data Parameters for Potential OTEC Sites--The University of Miami, Miami, Florida. This effort is expected to provide oceanographic information on variables affecting biofouling and corrosion in the Gulf of Mexico, near Puerto Rico, and the Virgin Islands, around Hawaii, in the Gulf of Mexico and the area around Guam.
- A Critical Review of Design Factors Influencing Biofouling and Corrosion of OTEC System Surfaces--The Civil Engineering Laboratory, Port Hueneme, California. This project has as its objectives to examine the existing information to determine what the effect of orientation shape, geometry, and layout is on biofouling and corrosion to define potentially attractive design tools for reducing biofouling and corrosion.

We anticipate having signed contracts for several more projects within the next 4 to 6 weeks. The distribution of funds to support development and research work in Biofouling and Corrosion as of February 25, 1977 was as follows:

Universities - 65.0%

Government Laboratories - 12.3%

Industrial Organizations - 22.7%

In the longer term, we would continue to expect to have a substantial number of university and industrial contractors. Also the favored process for acquiring needed assistance will be by competitive procurement procedures.

REFERENCES

1. W. W. Laity, Unpublished Proceedings of Biofouling and Corrosion Workshop, Seattle, Washington, February 1976.
2. L. D. Perrigo and G. A. Jensen, An OTEC Annual Report to the Division of Solar Energy for FY-1976 and the Transition Quarter, BNWL-2154/UC-64, Battelle, Pacific Northwest Laboratories, Richland, Washington, 1976.

# ULTRA CLEAN HEAT EXCHANGERS—A CRITICAL OTEC REQUIREMENT

ANDREW F. CONN, MARK S. RICE, AND DAHLIA HAGEL
*HYDRONAUTICS, Incorporated*
*Applied Science Department*
*7210 Pindell School Road*
*Laurel, Maryland*

Abstract

Cleanliness of the heat exchanger tube, so as to maintain large heat transfer coefficients, has been identified as one of the critical requirements for successful operation of an OTEC power plant due to the already very low thermal efficiency which is projected for this concept. It has been estimated that it may be necessary to keep the microfouling layer (slime and other deposits) on the seawater side of the tubes down to a thickness of only 0.001 in. (25μ).

The objective of this study is to provide a catalog of methods now used to maintain the cleanliness of conventional heat exchangers, either by preventing or removing fouling, and to critically assess the applicability of each method for OTEC. Preliminary results and conclusions from this on-going study are presented.

## 1. Introduction

1.1 Objectives: The requirement for maintaining a high degree of cleanliness on the seawater side of the heat exchanger tubes in the OTECPP motivated this study of available cleaning methods, both mechanical and chemical, in order to identify which, if any, might be adapted for use in this new energy conversion system. Under the first task, our objective is to provide a critical compilation and evaluation of those methods now currently in use for cleaning heat exchanger surfaces. The objective of the second task is a conceptual study of those methods which have been identified as being potentially suitable for OTEC.

1.2 Definition of the Problem: Effective operation of an OTECPP requires heat exchanging areas and seawater flows which, in ratio to the amounts of power generated, are over two orders of magnitude larger than those in a conventional fossil-fueled power plant. In addition, the higher thermal efficiencies of the conventional plants permit them to successfully operate under less stringent cleanliness requirements. Estimates, which appear to be supported by ongoing experiments (1), have indicated that a microfouling growth of only 0.001 in. (25μ) will cause a loss of about ten percent in the heat transfer coefficient at the values of 400-500 BTU/ft$^2$-hr-$^o$F (2).

It is therefore seen that the experience and requirements of conventional power plant operators are vastly different from those of OTEC. Hence, at this time, only estimates can be provided as to the performance of any existing water treatment or cleaning method, based on various assumptions relating to the OTEC heat exchanger fouling conditions and cleanliness requirements. Final qualification of any of these methods must await a rigorous testing of its effectiveness under conditions which simulate those anticipated for OTEC.

## 2. Approaches Used to Develop Data Base

A questionnaire, accompanied by a form letter which described OTEC and the objectives of our study, was sent to every manufacturer we could identify as having even a remote possibility of contributing to this effort. The source list was developed from a variety of catalogues, trade, and technical magazines. From the responses, promising sources were identified, and one or more face-to-face, intensive interviews were conducted with representatives of those methods which seemed to

*Supported under Battelle Pacific Northwest Laboratories Contract No. B-31927-A-L.

have OTEC potential.

After initial analyses, it was often necessary to follow up with additional discussions. Data was also obtained from the technical literature and through valuable visits to a number of power plants on both the Atlantic and Pacific coasts. Discussions with individuals having expertise in certain specific areas such as microfouling and OTEC heat exchanger design were also held.

## 3. Discussion of the Methods

3.1 Types of Methods: The maintenance of a clean heat exchanger surface may be achieved in several ways. We have categorized the methods which may have potential for OTEC usage into three types: water treatment, surface treatment, and cleaning methods. Although the report (3) now in preparation for the first task of our study will provide detailed discussions (with cost factors) for all of the methods we have been able to identify, only those methods which seem to have potential OTEC applicability will be discussed in this paper.

3.2 Water Treatment: The following water treatment methods all share the advantages of applicability to any heat exchanger geometry and automated operation, and the disadvantage of being inherently incapable of removing attached nonorganic fouling. Although biocides, such as sodium hypochlorite and ozone may weaken and hence remove some attached micro-organisms, the effectiveness of this removal process in terms of OTEC heat transfer requirements remains to be studied experimentally.

3.2.1 Chlorination: On-site generation of sodium hypochlorite by electrical means is envisioned, at the rate (about 0.5 to 1.0 ppm) required for biofouling control. The main advantages of this on-site generation process are the lack of dependence on external supplies, no requirement for large storage containers, and the option of automation. The incompatibility with admiralty brass and many aluminum alloys, and the possible adverse effects to surrounding marine life are the chief disadvantages, as well as the inability to remove nonorganic fouling and perhaps attached organisms. The decision on chlorination for OTEC use requires definition of dosage requirements and the environmentally acceptable residual levels.

3.2.2 Ozonation: Involves on-site production of ozone from dried air, for use in much the same manner as chlorine. In existing large-scale ozone production facilities a corona discharge method is used to ionize oxygen molecules in the clean, dry air which has been provided by a previous step in the process. Ozone is a very potent biocide in concentrations as low as 0.5 to 1.0 ppm, and produces almost no permanent residual toxicity. However, in addition to its incompatibility with many plastics, copper-nickel, and Inconel, the power requirements to create the requisite dried air by existing production techniques are prohibitive. Thus, although the potency and environmental aspects of ozonation are quite attractive for OTEC, a breakthrough in the reduction of power costs is needed before it could be utilized.

3.2.3 Ultraviolet Treatment: Water in the conduits leading to the heat exchanger would be irradiated by an array of UV lamps. This method, although not used in power plants, is a standard water purification process for many applications. Irradiation at a wavelength of 2537A at a nominal dosage of 16,000 microwatts/$cm^2$-sec. causes resonance of DNA and protein molecules, resulting in microorganism destruction. This method is virtually nonpolluting, and will not enhance erosion or corrosion. However, the requirements for frequent maintenance and lamp replacement may make the use of UV too labor-intensive and expensive for the OTEC. Experimentation at intensities well below those levels now used to sterilize water, and a determination of the effectiveness with seawater operation, are required before a final evaluation can be made.

3.3 Surface Treatment: A method which would render the heat exchanger surfaces inhospitable to all types of fouling, both organic and inorganic, would be the ideal solution to our problem. A low surface energy, monomolecular coating now being developed by the Allied Chemical Corporation (4) would seem to provide this very solution, if the coating lifespan can be increased beyond the present limit of several weeks. This concept consists of depositing, on the seawater side of the tubes, a monomolecular layer (hence producing minimal heat transfer impediment) of a compound which has a surface energy very close to that of seawater. Thus, the driving mechanism which encourages adherence of proteinaceous films, micro-organisms and inorganic inert particles is minimized. If the lifetime of these coatings can be extended to practical durations, and the difficulties of seawater incompatibility and in-situ deposition are overcome, this method might be an eventual solution to the OTEC heat exchanger fouling problem.

3.4 Cleaning Methods:

3.4.1 Chemical Cleaning: As currently utilized, this method requires shutdown and isolation of a heat exchanger module and replacement of the seawater therein with either an acidic or basic cleaning solution. These methods are well-established, and an extensive background of commercial experience is available to correlate solution strengths with cleaning requirements. Additional advantages include applicability to any OTEC geometry, and low power and installation costs. These

are offset by disadvantages which include lost er generation associated with the shutdown irement, corrosive attack of tubing (espec- ly aluminum), storage and disposal problems, and chemical costs if cleaning frequencies are high. The applicability of this method to OTEC would require full integration into the base-line design, and will depend on the fouling rates, the nature of the substrate and corrosion products, and hence how frequently such chemical cleaning would be required.

3.4.2 Flow Driven Brushes: Are the devices used in a commercial heat exchanger cleaning system which is sold by the American M.A.N. Corporation (5). Flow reversal propels the brushes through the tubes, abrasively removing fouling and corrosion products. During the intervals between cleaning cycles, these brushes reside within "baskets" which are attached at both ends of every heat exchanger tube. The list of advantages for this method includes long brush life (five years or more); cleaning of each tube automatically; usage with some enhanced surfaces; and compatibility with chemical treatment methods.

The disadvantages are: the flow reversal requirement with its associated controls, valves, piping, and power losses; head losses due to flow restrictions by the brushes and baskets; usability only for internal tube surfaces; the possibilities of fouling of the brushes and baskets themselves; and possible enhancement of the corrosion and/or erosion of the tube walls.

This method is a definite contender for OTEC usage, however, questions related to effectiveness and required frequency of usage, and how to adapt the flow reversal requirement to OTEC, must be answered before a final assessment and comparison with other prime candidates can be made.

3.4.3 Recirculating Rubber Balls: Are the cleaning devices in the Amertap Corporation's system (6). These natural rubber sponge balls are injected at the upstream water box, randomly enter and wipe along the inside tube surfaces, are collected by screens at the downstream water box, and are then recirculated back to the upstream end of the tube bundle. Among the advantages are: almost continuous, automatic cleaning; considerable power plant experience in the U.S.A.; compatibility with chemical treatment methods; and variability of the abrasive forces through a selection of available ball designs.

The disadvantages are: dependence upon a random tube selection process which can be adversely biased by changes in the balls (due to contamination); head losses due to the collection screens; complex equipment to size, sort count the balls automatically; short ball life (about a month in conventional plants); usability only inside smooth-walled tubes; and possible enhancement of the corrosion and/or erosion of the tube walls.

This method is another definite contender for OTEC usage, however, questions related to cleaning effectiveness, ball wear rates, and handling, and how to redesign the collection method for OTEC so as to reduce head losses must be answered before a final assessment and comparison with other prime candidates can be made.

3.4.4 Ultrasonic Cleaning: Is now used, at high intensities, for a variety of cleaning applications, but not for power plant purposes. If this concept were to be adapted to OTEC, it would be practical only if a low level of ultrasonic energy could be propagated within either the tube walls and/or the tube sheets, at sufficient intensity to increase the fluid shear stresses at the seawater/heat exchanger interface, thereby discouraging the growth of microbial fouling and possibly removing both organic and inorganic foulants. The potential advantages of this concept include heat transfer enhancement from boundary layer turbulence; usability for either internal or external tube surfaces; no pollution; and a long (up to twenty years) operating life for the critical components.

The prime disadvantage is that no large scale systems of the type envisioned here exist, and hence the OTEC requirements for installation, power, and operating costs are undefined and could become prohibitive. Also, continuous, even low level, ultrasonics may lead to cavitation erosion and/or fatigue cracking, and the head losses due to ultrasonically induced turbulence may outweigh heat transfer enhancement. Thus, although this concept has many potential advantages, considerable experimentation is required before its practical applicability to OTEC can be assessed.

3.4.5 Water Jet Cleaning: Is a commonly used technique for cleaning heat exchanger tubing. However, the usual hand-held cleaning lances and nozzles would have to be adapted to a large, multi-nozzle automated cleaning system to be usable in an OTEC power plant. Possible reductions in pressure and power requirements might be gained by use of cavitating water jets (7). Since water jets are a noncontact cleaning method, they can be used to clean either the inside or outside of tubes, as well as irregular geometries and enhanced surfaces. Jets could be automatically deployed, and introduce no pollutants.

These advantages are offset by the lack of available experience in deployment of numerous jets in the complex, automated configuration

required by OTEC. Hence, the costs associated with installation and operation are undefined and may be very large. Erosion damage due to prolonged usage, and quantification of heat transfer enhancement under OTEC conditions are remaining questions. Thus, although existing methods have been developed specifically for internal tube cleaning, water jets should be given further consideration for cleaning OTEC heat exchangers which have other geometries.

## 4. Concluding Remarks

As mentioned, this paper has been written in the midst of our study of heat exchanger cleaning methods. We can, however, present the following preliminary conclusions:

4.1 There are vast differences between the cleaning problems of any existing power plant and an OTEC power plant.

4.2 Thus, no existing cleaning method can be qualified for OTEC use, as is, without further R&D, and/or new design adaptations.

4.3 Commercial power plant experience suggests that some combination of water treatment plus a cleaning method may provide the most practical and economical solution to meeting the ultra clean OTEC heat exchanger requirement.

## 5. References


1. Fetkovich, J. G., "Biofouling Experiments at Kiahole Point, Hawaii," Paper 3B-3, Proc. Fourth Ocean Thermal Energy Conversion Conference, New Orleans, March 22-24, 1977.

2. Stupian, G. W., "Potential Fouling of OTEC Heat Exchangers by Marine Organisms," The Aerospace Corporation Rept. No. ATR-77 (9401-02)-1, Nov. 1976.

3. HYDRONAUTICS, Incorporated Technical Report 7701-1 (In preparation).

4. Jones, P. E., and Ostrozynski, R. L., "The Prevention of Biofouling of Heat Transfer Surfaces of Ocean Thermal Energy Converters," Proceedings of the Third Workshop of OTEC, Houston, Texas, May 1976.

5. McAllister, R. A., "On-Steam Cleaning of Heat Exchanger Tubes: Fouling Prevented by Regular Brushing," ASME Publication #68-PET-12, Sept. 1968.

6. Kuester, C. K., and Lynch, G. E., "Amertap at English Station," ASME Paper No. 66-WA/CT-1, Presented at the Winter Annual Meeting and Energy Systems Exposition of the ASME, November 27 - December 1, 1966.

7. Conn, A. F., Mehta, G. D., and Sundaram, T. R., "Cavitating Water Jets -- I. Review and Applications," ASTM Cavitation and Polyphase Flow Forum -- 1976, pp.12-15, March 21-25, 1976.

# STUDIES OF BIOFOULING IN OCEAN THERMAL ENERGY CONVERSION PLANTS*

J. G. FETKOVICH, G. N. GRANNEMANN, L. M. MAHALINGAM, AND D. L. MEIER
*Carnegie-Mellon University*
*Department of Physics*
*Pittsburgh, Pennsylvania*

F. C. MUNCHMEYER
*University of Hawaii*
*Department of Mechanical Engineering*
*2540 Dole Street*
*Honolulu, Hawaii*

ABSTRACT

Ocean Thermal Energy Conversion (OTEC) plants will require large heat exchangers carrying immense quantities of seawater. The inevitable biofouling of the heat transfer surfaces will rapidly reduce the efficiency of such plants below acceptable levels unless suitable measures are taken. A group at Carnegie-Mellon University, in collaboration with one at the University of Hawaii, has begun a study, in the waters off Keahole Point, on the Big Island of Hawaii, of the problem of biofouling in simulated heat exchanger tubes under OTEC conditions.

One series of experiments was conducted with the apparatus mounted on a moored boat in the interval July-September 1976. In these experiments, water was pumped up to the apparatus from a depth of 20 feet. The tube was 1" ID aluminum, 8-1/2 feet long. Studies were conducted at nominal flow velocities of 3 and 6 feet per second.

At present a second series of experiments is underway. In these, the apparatus is mounted on a submarine buoy at a depth of about 50 feet. Three experiments are in progress. Two of these nominally duplicate the conditions described above. In the third, a similar titanium tube is being used at a velocity of about 6 feet per second.

In this paper we briefly describe the apparatus and methods being used, and discuss in detail the conditions of the experiments. The results of the analysis of the first series of experiments are also presented and discussed. All available preliminary results from the second series are also presented.

## I. Introduction

There exists little data which is relevant to the problem of the effects of biofouling on the heat-transfer characteristics in OTEC heat exchangers. We are concerned here with the regime of "Microfouling"; a slime layer only a few thousandths of an inch thick could reduce the heat transfer rates to unbearably low values. Fouling rates are expected to depend on a number of variables: surface material, surface condition, flow velocity, depth, temperature, time of year, location, as well as other details of the system configuration. The economically efficient design of a plant will depend critically on the ability to predict the effects of biofouling on its operation.

For all of these reasons, it is necessary to study biofouling as nearly as possible under OTEC operating conditions. These conditions are not yet well-defined (e.g., what is the optimum velocity?), and indeed will in part be determined by the results of these studies. It is necessary, therefore, to make measurements under a wide range of conditions.

A system has been developed (1) specifically to facilitate the necessary measurements. The system was designed to provide high flexibility in fixing operating conditions, and to have high precision in sensing changes in heat transfer rates due to fouling (better than 1% sensitivity limited by flow velocity determination; potential to go to 0.1% to 0.2% sensitivity under controlled conditions). That these design goals have been met has been confirmed now by extensive laboratory tests, by field tests, and now by over four months of field operation.

* supported by U.S. ERDA.

The details of the method and the theory of operation have been extensively covered in previous reports and publications (1,2), and we will therefore only briefly discuss these here.

The main parts of the system are shown semi-schematically in Fig. 1. The 1 in. PIPE carries the seawater at a selected velocity which is measured by the FLOWMETER. Not shown is a thermistor, attached to the 1 in. PIPE, to measure the seawater temperature. The heat transfer coefficient, h, from the metal pipe wall to the seawater is measured in the following way. A small amount of heat is applied to the outer surface of the Cu BLOCK raising its temperature an amount $\Delta T$ above that of the water. When the heat is turned off, $\Delta T$ is observed (after a brief transient) to decay exponentially to zero with a time constant which is approximately inversely proportional to h. The value of $\Delta T$ is measured directly by the output of a thermopile whose measuring junctions are embedded in the Cu BLOCK, and whose reference junctions are embedded in the Cu REFERENCE BLOCK which is at seawater temperature. In this way h is determined by measuring the time constant of the thermal decay.

This rather unorthodox method of measuring h has two significant advantages. First, it has inherently high precision for two reasons: the direct measureme of $\Delta T$ is done by means of a thermopile, and the other critical aspect of the measurement is time which can be determined to extraordinary precision using quartz clocks. Second, it is insensitive to variations in calibration of all but the flowmeter (which is what at present limits precision).

In the geometry of our system, a power input of 100 watts produces a $\Delta T$ of 1°F at a flow velocity of 6 ft/sec (clean tube). Without significant degradation in precision, $\Delta T$ may be lowered to 0.1°F with a power input of 10 watts. If desired, $\Delta T$ could also be increased.

The system (Fig. 1) is contained in a water-tight PVC housing which helps to prevent variations in ambient conditions (wind, sunlight) from affecting the critical $\Delta T$ measurements when the system is operated above surface. The housing is designed also to allow submerged operation at depths to at least 100 feet.

Figure 2 shows how the system of Fig. 1 would be connected to a pump in typical submerged operation. The Throttle Valve is adjusted to achieve the desired flow velocity. Figure 3 and 4 depict a system under test in the laboratory, without the PVC housing.

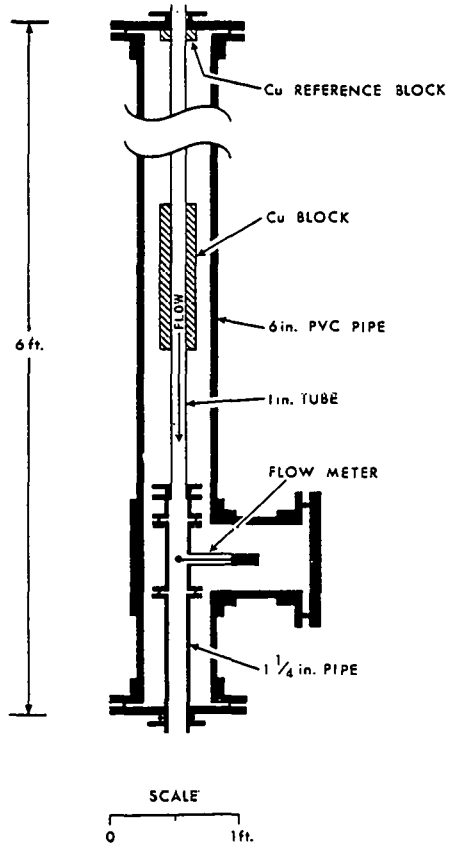



Fig. 1. Biofouling Measurement System

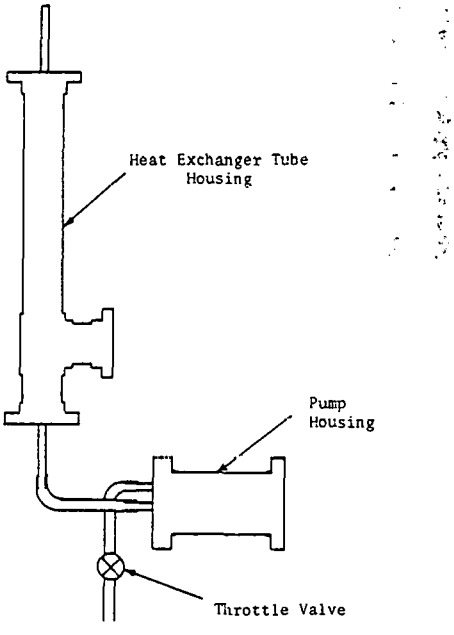
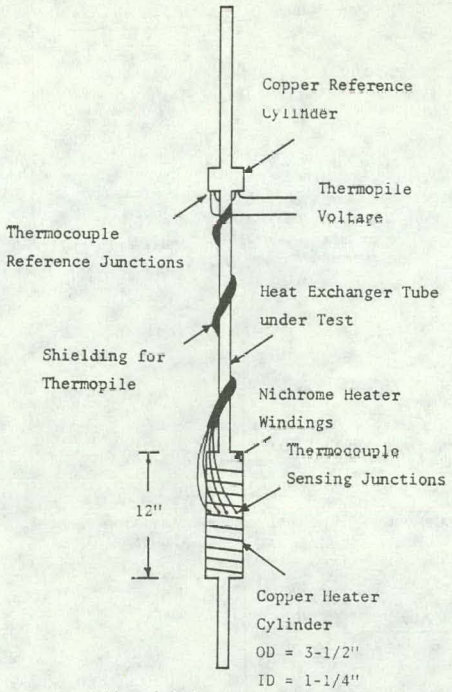



Fig. 2. System Plumbing



Tube with Instrumentation.

Fig. 3. Instrumented Tube

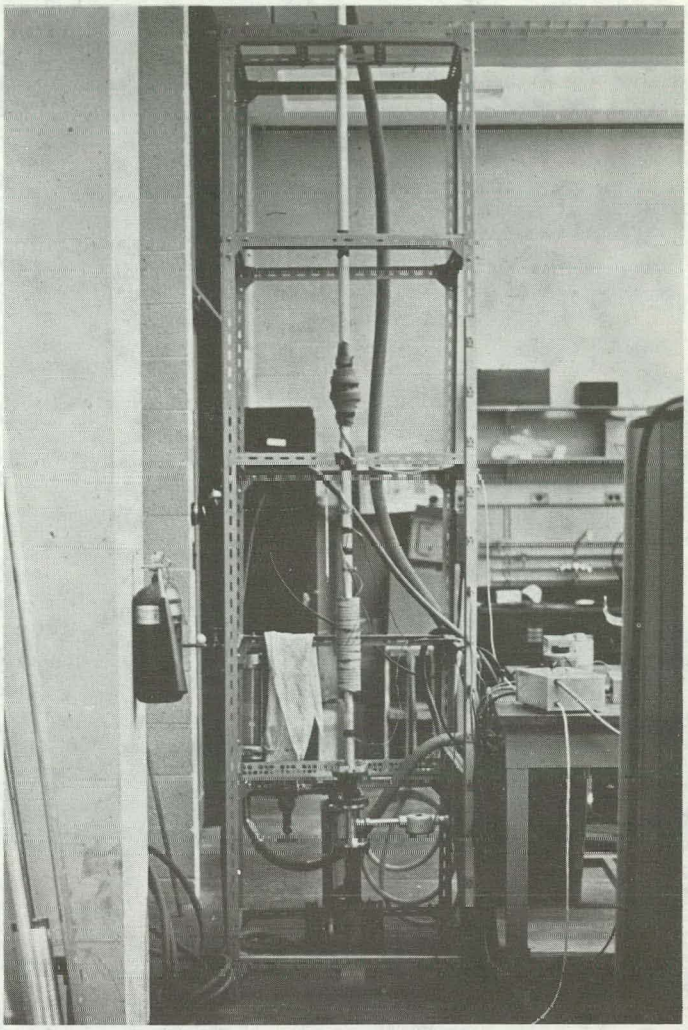


Fig. 4. Laboratory Setup



Fig. 5. 3ft/sec Experiment Mounted on NOI'I

## II. Field Setup

Two field setups have so far been in operation. In the first, two units (as shown in Fig. 1) were mounted on the deck of a boat (RV NOI'I, U. of Hawaii). Each unit was connected to a pump on the downstream side. The seawater was brought to the system, through approximately 40 feet of 2 in. reinforced plastic hose, from a depth of 20 feet.

Figure 5 shows the NOI'I with one of the two units mounted on the stern. The data acquisition electronics (not visible) is housed in the aft cabin. This system was used for taking data from mid July through September 1976.

In January 1977, a second submerged system was put in place, at about the same location as the first. In this system, up to six units may be mounted on a submarine buoy: Fig. 6 is an underwater photograph of the buoy with 3 units in operation. Figure 7 shows the mooring system in preliminary form. The main difference from reality is that now the electromechanical cable also serves as the mooring line. The cable (about 1500 feet long) connects the system to an electronics system located in a shelter on the beach.

After various tests and initialization procedures were completed, data taking started on February 12, 1977 and is still in progress.

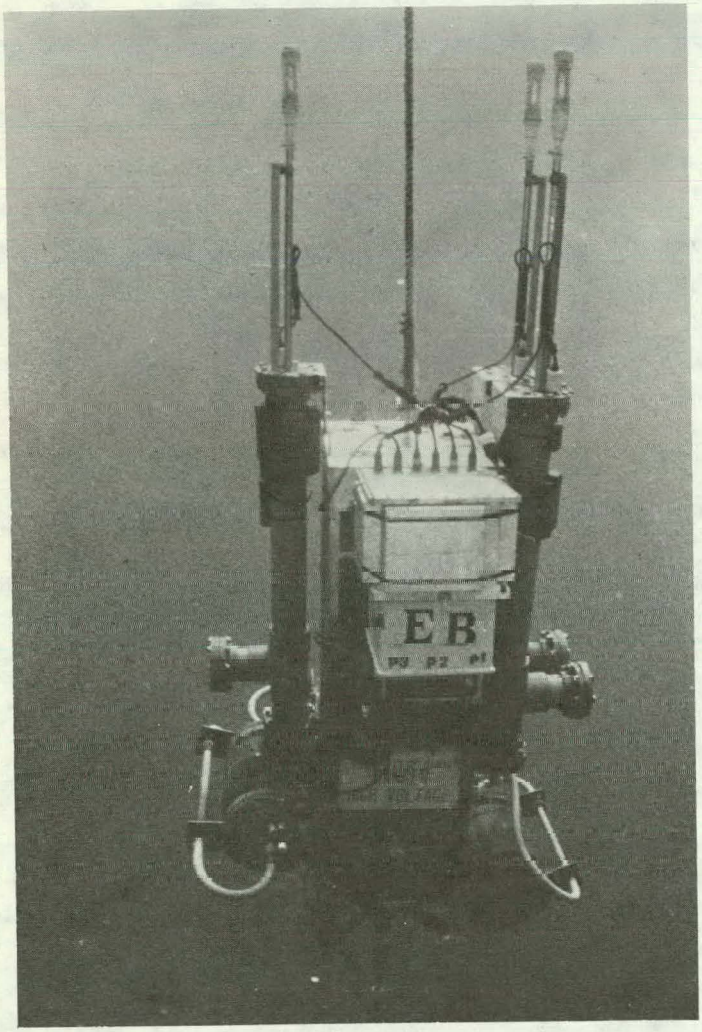



Fig. 6. Keahole Buoy in Operation Feb. 1977

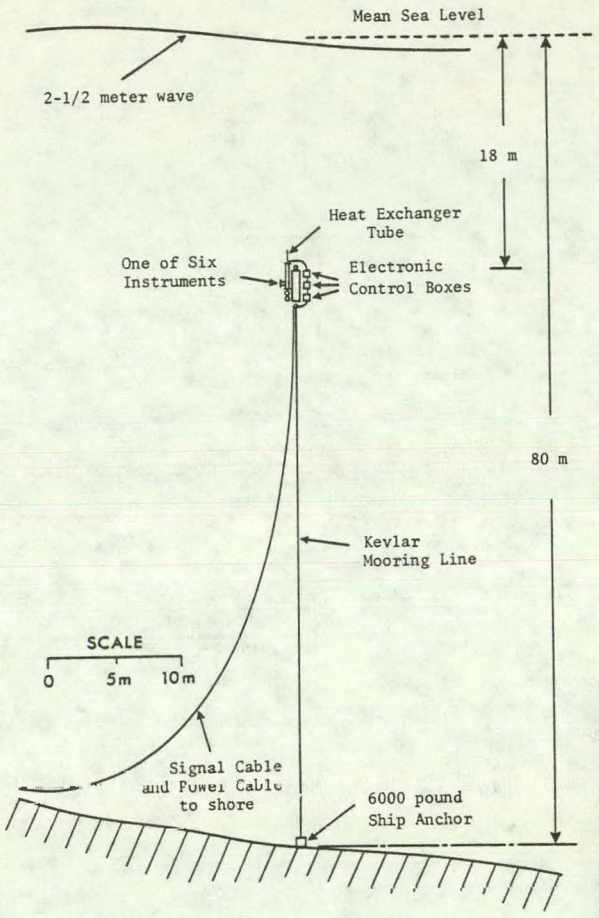



Fig. 7. Buoy Mooring System

## III. Data

To date, this system has been used to obtain data using freshwater in the laboratory, seawater from dockside, seawater from the deck of a boat (NOI'I), and sea water using a submerged system. Various checks have been made to ensure that the system operates as it should. Some of these have been described in detail elsewhere (2). Here we mention only the most important.

If, for a clean, smooth tube, h is measured over a range of v, then 1/h should be related to $v^{-0.8}$ as follows

$$1/h = (3.44 \times 10^{-3})/v^{0.8}$$

(with h in BTU/hr $ft^2$°F and v in ft/sec) for fresh water and

$$1/h = (3.64 \times 10^{-3})/v^{0.8}$$

for seawater. We have confirmed, by measurements, that the system yields a linear relationship to high precision. Furthermore, the slope of the line has been

shown quantitatively to agree with the semi-empirical theoretical expectation, as shown in Table 1.

TABLE 1

Comparison of slope of 1/h vs. $v^{-0.8}$ for different conditions

| Material | Conditions | Slope $\frac{hr\ ft^2°F(ft/sec)^{0.8}}{BTU} \times 10^3$ |
|---|---|---|
| Al | lab | 3.44±0.03 |
| 90 Cu 10 Ni | lab | 3.47±0.01 |
| Ti* | lab | 3.45±0.02 |
| Al** | on NOI'I | 3.50±0.2 |
| Handbook value (3) | | 3.44 |

* Thermal grease used between Cu cylinders and Ti tube.
** Data taken with ocean water. Value quoted is corrected to fresh water properties using h(ocean water) = 0.945±0.008 h(fresh water). See (1).

On board the NOI'I, two units were run. Both used Al 6061-T6 alloy pipes, one at nominal 3 ft/sec velocity (actual 2.9 ft/sec) and the other at nominal 6 ft/sec (actual 5.5 ft/sec). In taking data, the water temperature was found to vary slightly from time-to-time. For tabulation and plotting purposes, the data points are normalized to the same temperature (70°F) using the relation (3),

$$h_{T_o} = h_{T_w} \frac{1+.012\ T_o}{1+.012\ T_w}$$

where $T_o$ is the standard temperature in °F and $T_w$ is the water temperature. Similarly, the water velocity varies slightly. The 1/h vs. $v^{-0.8}$ relation (above) is used to normalize each datum to the nominal velocity.

The NOI'I results are tabulated in Tables 2 and 3. As shown, h is measured at various times. The difference between the value of 1/h measured at any given time and that measured initially (t=0; clean tube) is equated to $R_f$, the thermal resistance of the accumulated fouling layer. The average thickness of the fouling layer, $t_f$, is calculated from $R_f$ assuming that the thermal conductivity of the fouling layer is equal to that of seawater.

In Fig. 8, $R_f$ is plotted vs. time for the two units on the NOI'I.

In our more recent setup on the submerged buoy, we started three experiments on February 12, 1977, which are still in progress. Two of these duplicate the NOI'I experiments (Al 6061-T6 at 3 ft/sec and 6 ft/sec nominal velocities). The third involves a titanium pipe at 6 ft/sec nominal.

The data, treated as described above, are tabulated in Tables 4, 5 and 6, and $R_f$ for each case is plotted in Figs. 9 and 10.

TABLE 2

Nominal Flow Velocity: 3 ft/sec
Material: Al 6061-T6 (Tube No. 1)

| Date | $\langle h \rangle$ $\left(\frac{BTU}{Hr\ Ft^2\ °F}\right)$ | $\langle 1/h \rangle$ $\left(\frac{Hr\ Ft^2\ °F}{BTU}\right) \times 10^5$ | $\Delta\langle\frac{1}{h}\rangle = R_f$ $\left(\frac{Hr\ Ft^2\ °F}{BTU}\right) \times 10^5$ | $\frac{d}{dt}(R_f)$ $\left(\frac{Hr\ Ft^2\ °F}{BTU\ Week}\right) \times 10^5$ | $t_f$ (mils) |
|---|---|---|---|---|---|
| July 13...17, 1976 | 627.2±8.0 | 159.4±2.0 | 0.0 | --- | 0.0 |
| Aug. 10, 1976 | 608.8±7.5 | 164.3±2.0 | 4.9±2.8 | 1.23±0.7 | 0.21±0.12 |
| Aug. 31, 1976 | 551.6±4.3 | 181.3±1.4 | 21.9±2.4 | 5.67±1.2 | 0.92±0.10 |
| Sept. 15, 1976 | 478.8±3.3 | 208.9±1.4 | 49.5±2.4 | 13.14±1.62 | 2.08±0.10 |
| Sept. 22, 1976 | 435.4±3.7 | 229.6±2.0 | 70.2±2.8 | 20.70±3.69 | 2.95±0.12 |

TABLE 3

Nominal Flow Velocity: 6 ft./sec.

Material: Al 6061-T6 (Tube No. 2)

| Date | $\langle h \rangle$ $\left(\frac{BTU}{Hr\ Ft^2\ °F}\right)$ | $\langle 1/h \rangle$ $\left(\frac{Hr\ Ft^2\ °F}{BTU}\right) \times 10^5$ | $\Delta\langle(\frac{1}{h})\rangle = R_f$ $\left(\frac{Hr\ Ft^2\ °F}{BTU}\right) \times 10^5$ | $\frac{d}{dt}(R_f)$ $\left(\frac{Hr\ Ft^2\ °F}{BTU\ \ Week}\right) \times 10^5$ | $t_f$ (mils) |
|---|---|---|---|---|---|
| Aug. 19, 1976 | 1083.9±30.0 | 92.3±2.6 | 0.0 | --- | 0.0 |
| Aug. 30, 1976 | 1079.0±12.9 | 92.7±1.1 | 0.4±2.8 | 0.25±1.78 | 0.02±0.12 |
| Sept. 13, 1976 | 963.1±11.1 | 103.8±1.2 | 11.5±2.9 | 5.55±2.02 | 0.48±0.12 |
| Sept. 18, 1976 | 946.6±24.6 | 105.6±2.7 | 13.3±3.7 | 2.50±6.53 | 0.56±0.16 |
| Sept. 26, 1976 | 848.0±14.9 | 117.9±2.1 | 25.6±3.3 | 10.79±4.35 | 1.08±0.14 |

TABLE 4

SUMMARY OF DATA FROM SUBMERGED BUOY AT KEAHOLE POINT, HAWAII

Nominal Flow Velocity: 3.0 ft/sec
Material: Aluminum (6061-T6)

| Date | $\langle h \rangle$ $\left(\frac{BTU}{hr\ ft^2\ °F}\right)$ | $\langle 1/h \rangle$ $\left(\frac{hr\ ft^2\ °F}{BTU}\right) \times 10^5$ | $\Delta\langle 1/h \rangle \equiv R_f$ $\left(\frac{hr\ ft^2\ °F}{BTU}\right) \times 10^6$ | $t_f$ (mils) |
|---|---|---|---|---|
| Feb. 14, 1977 | 680 ± 7 (5) | 147 ± 1.5 | 0.0 | 0.0 |
| Feb. 21, 1977 | 671 ± 7 (1) | 149 ± 1.5 | 2.0 ± 2.1 | 0.08 ± 0.09 |
| Feb. 25, 1977 | 673 ± 7 (4) | 149 ± 1.5 | 1.6 ± 2.1 | 0.07 ± 0.09 |
| Mar. 7, 1977 | 661 ± 7 (1) | 151 ± 1.5 | 4.1 ± 2.1 | 0.17 ± 0.09 |
| Mar. 14, 1977 | 670 ± 7 (3) | 149 ± 1.5 | 2.3 ± 2.1 | 0.10 ± 0.09 |
| Mar. 21, 1977 | 662 ± 7 (1) | 151 ± 1.5 | 3.9 ± 2.1 | 0.16 ± 0.09 |
| Mar. 28, 1977 | 654 ± 7 (2) | 153 ± 1.5 | 5.8 ± 2.1 | 0.24 ± 0.09 |

TABLE 5

SUMMARY OF DATA FROM SUBMERGED BUOY AT KEAHOLE POINT, HAWAII

Nominal Flow Velocity: 6.0 ft/sec
Material: Aluminum (6061-T6)

| Date | $\langle h \rangle$ $\left(\frac{BTU}{hr\ ft^2\ °F}\right)$ | $\langle 1/h \rangle$ $\left(\frac{hr\ ft^2\ °F}{BTU}\right) \times 10^5$ | $\Delta\langle 1/h \rangle \equiv R_f$ $\left(\frac{hr\ ft^2\ °F}{BTU}\right) \times 10^5$ | $t_f$ (mils) |
|---|---|---|---|---|
| Feb. 15, 1977 | 1155 ± 12 (2) | 86.6 ± 0.9 | 0.0 | 0.0 |
| Feb. 22, 1977 | 1129 ± 11 (1) | 88.6 ± 0.9 | 2.0 ± 1.3 | 0.08 ± .05 |
| Mar. 6, 1977 | 1115 ± 11 (1) | 89.7 ± 0.9 | 3.1 ± 1.3 | 0.13 ± .05 |
| Mar. 6, 1977 | 1120 ± 11 (1) | 89.3 ± 0.9 | 2.7 ± 1.3 | 0.11 ± .05 |
| Mar. 16, 1977 | 1117 ± 11 (2) | 89.6 ± 0.9 | 3.0 ± 1.3 | 0.13 ± .05 |
| Mar. 22, 1977 | 1073 ± 11 (3) | 93.2 ± 0.9 | 6.6 ± 1.3 | 0.28 ± .05 |
| Mar. 29, 1977 | 1041 ± 10 (1) | 96.1 ± 1.0 | 9.5 ± 1.3 | 0.40 ± 0.05 |

TABLE 6

SUMMARY OF DATA FROM SUBMERGED BUOY AT KEAHOLE POINT, HAWAII

Nominal Flow Velocity: 6.0 ft/sec
Material: Titanium (B337-76)

| Date | $\langle h \rangle$ $\left(\frac{BTU}{hr\ ft^2\ ^\circ F}\right)$ | $\langle 1/h \rangle$ $\left(\frac{hr\ ft^2\ ^\circ F}{BTU}\right) \times 10^5$ | $\Delta\langle 1/h \rangle \equiv R_f$ $\left(\frac{hr\ ft^2\ ^\circ F}{BTU}\right) \times 10^5$ | $t_f$ (mils) |
|---|---|---|---|---|
| Feb. 16, 1977 | $1116 \pm 11^{(2)}$ | 89.6 ± 0.9 | 0.0 | 0.0 |
| Feb. 23, 1977 | $1102 \pm 11^{(4)}$ | 90.7 ± 0.9 | 1.1 ± 1.3 | 0.05 ± 0.05 |
| Mar. 7, 1977 | $1055 \pm 11^{(2)}$ | 94.8 ± 0.9 | 5.2 ± 1.3 | 0.22 ± 0.05 |
| Mar. 9, 1977 | $1061 \pm 11^{(3)}$ | 94.2 ± 0.9 | 4.6 ± 1.3 | 0.19 ± 0.05 |
| Mar. 17, 1977 | $1047 \pm 10^{(1)}$ | 95.5 ± 0.9 | 5.9 ± 1.3 | 0.25 ± 0.05 |
| Mar. 23, 1977 | $1012 \pm 10^{(2)}$ | 98.8 ± 1.0 | 9.2 ± 1.3 | 0.39 ± 0.05 |
| Mar. 30, 1977 | $966 \pm 10^{(1)}$ | 103.5 ± 1.0 | 13.9 ± 1.3 | 0.58 ± 0.05 |

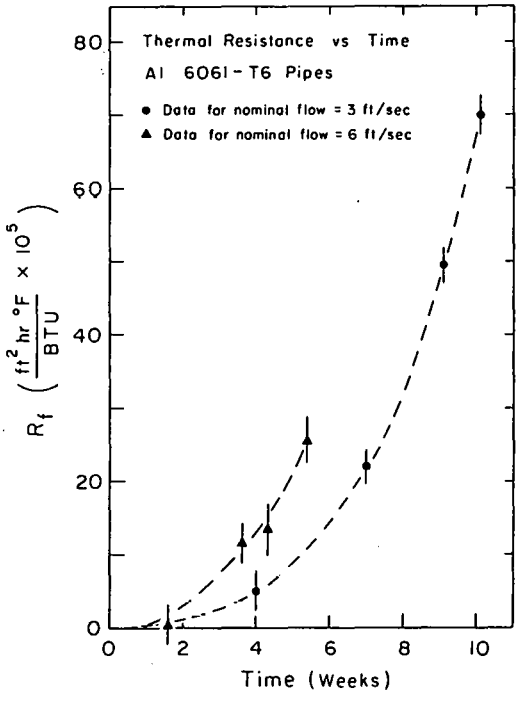



Fig. 8. NOI'I Data Al Pipes

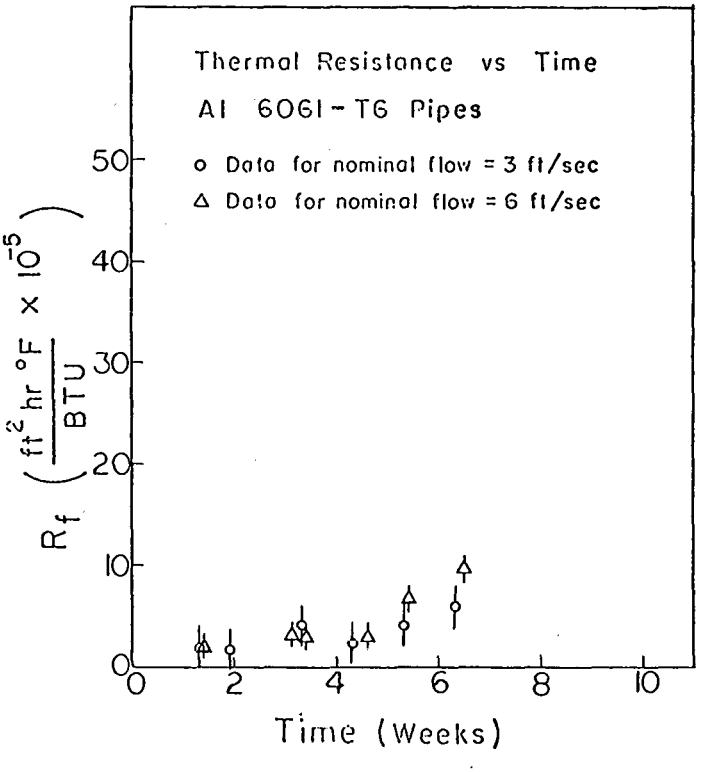



Fig. 9. Buoy Data Al Pipes

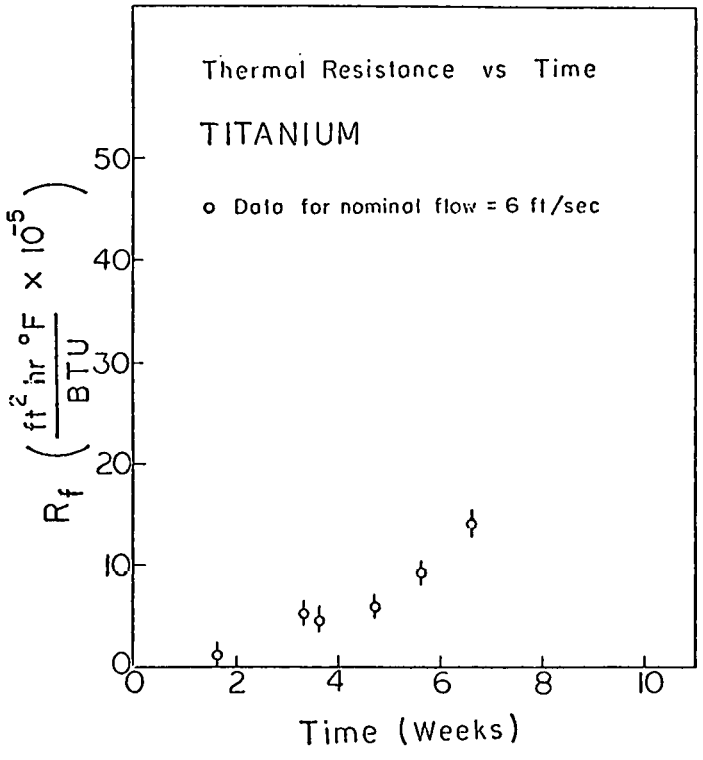



Fig. 10. Buoy Data Ti Pipe

## IV. Discussion

The system which was used to obtain the data described here was specifically designed for OTEC biofouling studies. It is quite a general system which is now being used to study warm-water biofouling in 1 inch smooth tubes. However it is easily modified for other purposes or conditions. For example, it could be used for studies of biofouling in cold, deep water (or non-biological fouling), it could be used with other tube diameters or geometries (i.e., enhanced surfaces), it could be used with any desired temperature difference (in the OTEC range) between the tube wall and the seawater ($\Delta T=0$ in current experiments).

This is the first time a system of this sort has been developed or used. In order to ensure successful operation, the system was overdesigned in some ways. There are various modifications and improvements which could be impelemented to make the system simpler to use or to produce (1). So far, the urgent press for data has left us little time to implement these obvious improvements. However, as discussed earlier in this paper, the system has worked well beyond initial expectations.

The trends in our preliminary results are seen most clearly in Figs. 8, 9 and 10. In Fig. 8, the thermal resistance of the fouling layer is plotted vs. time for the two units run above the surface on board the NOI'I. These runs are now complete. There are tv features of the data which are of obvious significance. First for each flow velocity, we find nearly zero slope at t=0, with the buildup accelerating with time (over the intervals covered). Secondly, we find that the biofouling rate is greater at the higher velocity.

The fact that the fouling rate is so slow at early times (it takes 2 to 4 weeks for the fouling resistance to reach 0.00005) is, in a sense heartening. It probably means (since the corresponding fouling layer averages less than 1/4 mil in thickness) that the fouling will be easier to remove at that stage than many had expected.

That the fouling rate is higher at the higher velocity will come as a surprise to some. In fact we must be careful about drawing premature conclusions about this, since there were some other differences between the two cases in addition to velocity. In particular there are two other possible sources of this difference which must be investigated.

One is that the two sets of data were not taken at the same time (the two experiments ended, rather than started, simultaneously). If the general biological activity in the area changed in the meantime, this could conceivably account for the difference. However, such a large change in so short a time seems unlikely in these waters.

A possible second difference between the two experiments is in the surface roughness. Although the two tubes were essentially identical as received from the supplier, they were cleaned differently. The one used at six feet per second merely had the surface film (oil, dirt, etc.) removed by swabbing with solvents. The one used at three feet per second, on the other hand, was in addition partially polished using an abrasive (cleaner) and a bristle brush. It is possible that the lower surface roughness of one tube led to a correspondingly lower fouling rate.

As a partial check on these questions, when the next set of experiments was started, this time using units operating in a submerged mode (mounted on a subsurface buoy at a depth of about 50 feet), all three experiments were started simultaneously, and all three tubes received the same treatment (including the partial polishing).

So far, we have analyzed data from six weeks of running (the experiments are being continued). The results for fouling resistance vs. time are shown in Fig. 9 for the two aluminum tubes at nominal flow velocities of 3 and 6 ft/sec, and in Fig. 10 for the Titanium tube at a nominal flow velocity of 6 ft/sec.

In the early stages of the experiments (t<5 weeks) the fouling buildup is so slow that the data points differ little from zero and from each other (relative to the experimental erros shown by the vertical bars), and few conclusions can be drawn. However, as we look at the last two sets of data points, we see again the beginning of a trend indicating that the 6 ft/sec Aluminum fouling rate is greater than the 3 ft/sec Aluminum rate. In this case, the difference cannot be ascribed to different treatment of the tubes or to different starting times of the experiments. It would seem to be an actual velocity effect. However, considering the experimental

errors, it is evident that after only 6.5 weeks of ---ing no firm conclusions can yet be drawn. More are required (and are being obtained) on this t.

Comparing Figs. 9 and 10 we see another interesting effect. The fouling rate at 6 ft/sec in the Titanium tube is greater than that at 6 ft/sec in the Aluminum tube. It is possible that this may be a surface roughness effect, and that rougher surfaces foul more rapidly than smoother ones. This possibility suggests itself for two reasons. First, Titanium, being harder than Aluminum will be less affected by the polishing which is done (100 strokes of the bristle brush through the tube). Second, although no quantitative measurements were made (this will be done in the future) the Titanium tube "appeared" rougher than the Aluminum tubes when received from the supplier.

Another interesting effect may be observed by comparing Fig. 8 (data taken with the units above surface) with Figs. 9 and 10 (data taken with the units submerged). The fouling rates are consistently lower in the latter case. This difference is possibly due to one or both of the following causes. There may be a larger-than-expected seasonal variation (July vs. February) in the general level of biological activity of those organisms responsible for microbiofouling. (Seasonal variations are expected to be much less in these waters than, for example, in the temperate zones.) Another possibility is that there is a significant vertical gradient in the density of microbiofouling organisms (for example, bacterial densities are expected to be greater at the surface than at greater depths in the mixed layer). Since the data of Fig. 8 correspond to water taken from 20 ft. depth, and the data of Figs. 9 and 10 correspond to water at about 50 ft. depth, this could explain the differences.

We do not have measurements of the level of biological activity in the waters corresponding to these data. Although such measurements were in the general plan, the press of time deadline militated against implementation in these experiments. (Of course, biological, chemical and physical measurements of water conditions are planned for future work, as soon as these plans can be realized.)

In summary, the data indicate the possible existence of certain phenomena which could be important to OTEC design and should be investigated further. Among these are:

a) Biofouling rates are very slow at early times, but accelerate rapidly after several weeks.
b) Biofouling rates probably increase with pumping velocity.
c) The surface roughness of a tube may significantly affect the biofouling rate. If so, the use of schemes such as Amertap or M.A.N. brushes, which would be expected to polish the surfaces, might be beneficial not only in removing existing fouling, but also in slowing further growth.
d) There may be a strong depth dependence of the biofouling rates.
e) There may be a significant seasonal variation in biofouling rates even in the relatively constant-condition waters of the tropical Pacific.

We re-emphasize that these conclusions are very tentative and will be so until considerably more data are available.

There are many other factors which could affect fouling rates. Some of those which are likely to be important, and which we therefore hope to study soon are the following.

We need to extend the velocity range studied. It may be that at higher velocities, the stresses experiences by the organisms make it difficult to attach and the fouling rate may level off or decrease. The range of materials and surfaces tested should be expanded. The effect of a change in temperature of the water passing through the system should be studied. Other tube geometries should be looked at (i.e., does the fouling rate go with diameter as expected; what will be the effects of attempts at enhancement, such as fluting, etc.). The effect of placing the pumps upstream of the test section should be looked at (the pumps so far have been downstream in all cases). If the added stresses experienced by the organisms significantly reduce the fouling rates this could be an important design factor in OTEC plants. There is obvious need to look at other kinds of water in other ocean locations.

We hope to study these and other important parameters as soon as conditions allow.

## Bibliography


1. Design Report, to be published.
2. Fetkovich, J. G., et al., Fouling and Corrosion Studies in OTEC-Related Heat Exchanger Tubes, Semiannual progress report. Fetkovich, J. G. et al., "A Study of Fouling and Corrosion Problems in a Solar Sea Power Plant", Proceedings, Third Workshop on Ocean Thermal Energy Conversion, Houston, 1975, pp. 155-156. Fetkovich, J. G., et al., "A Novel Method of Measuring Heat Transfer Coefficients with High Precision" and "Heat Transfer Problems in an Ocean Thermal Power Plant", Proceedings, Twelfth Southeastern Seminar on Thermal Science, Charlottesville, 1976, pp. 1-6, 81-86. Fetkovich, J. G., et al., "Studies of Biofouling in Ocean Thermal Energy Conversion Plants", Proceedings, International Solar Energy Society, Winnipeg, 1976, to be published.
3. Standard Handbook for Mechanical Engineers, Theodore Banmeister and Lionel S. Marks, McGraw-Hill, 1966 (pp. 4-100).


## Acknowledgments


C. William Fette and Frank Sharkey have made important contributions to this effort. The work of Robert Findley and the electronics shop personnel along with Paul Kuharic and the machine shop personnel deserves special mention. This effort was supported by the National Science Foundation and by the U.S. Energy Research and Development Administration.

# PRIMARY BIOFOULING FILMS AND OTEC HEAT EXCHANGERS

E. C. HADERLIE
*Department of Oceanography*
*Naval Postgraduate School*
*Monterey, California*

Abstract

It has been recognized for some time that the development of thin biological films produced through the activities of marine microorganisms could reduce the efficiency of heat exchangers proposed for closed-cycle OTEC power plants. Yet the published and unpublished literature dealing with marine microbial films has been so widely scattered that it has been difficult for design engineers to review what is known and what is not known at the present time regarding the nature of these films. A report has been prepared for ERDA which surveys all the pertinent literature, brings together an extensive bibliography, and points out areas where further research is needed to give possible answers to a number of critical questions.

## Introduction

From the very beginning of the development of the OTEC concept the specter of potential problems associated with biofouling on the heat exchangers has worried engineers. It is essential for planning and design purposes that one know how serious the biofouling problem is likely to be at potential OTEC sites and be able to predict performance degradation as a function of time. However, the diversity and scattered nature of biofouling literature, the general lack of data from open ocean sites, and the belief that data from coastal areas has little applicability, has forced engineers to include a "fouling factor" of questionable validity in their heat exchanger designs. To make possible a more rational determination of this fouling factor it would be desirable to have readily available a compilation of all pertinent literature and a brief up-to-date review of potential problems posed particularly by marine film-forming microorganisms. A report has been prepared for ERDA that covers these areas (1).

## Marine Molecular Fouling and Biological Films

Most marine fouling research has been concerned with the gross fouling of ship's hulls and salt water piping systems by large marine organisms such as barnacles, mussels and algae. However, whenever a new solid substrate, be it stone, wood, metal, glass or plastic, is placed in natural sea water, the first fouling events to occur involve dissolved organic molecules and living microorganisms and their products. The adsorption of these organic materials and living organisms occurs almost at once and over a period of hours or days the films created increase in thickness. It is these so-called primary organic films, rather than the later developing barnacles and other macro-foulers, which are of critical importance to the OTEC concept, for these films may degrade the efficiency of heat exchangers to an unacceptable level. The nature and behavior of thin organic films have been studied in coastal waters, and such films have been detected in all oceanic waters so far investigated. All present data indicate that the films develop in much the same manner in coastal and in open ocean water. What is not known in any detail at present is the rate of development and the ultimate thickness of the films which adsorb to surfaces in tropical ocean waters.

The fundamental nature of marine primary films has been investigated recently by many workers. Neihof and Loeb at the Naval Research Laboratory and Baier and his colleagues at Cornell University have studied the adsorption of organic molecules to solid substrates, a process which preceeds the attachment of living microorganisms (see references 2 and 3 which include bibliographies to earlier work). Corpe, Marshall, Mitchell, and Young, among others, have elucidated the kinds of microorganisms involved in primary film formation, the nature of their extracellular cementing material used in adhesion, and their behavior during attachment (see references 4, 5, and 6 which include bibliographies). We therefore have considerable knowledge of these primary films as they develop in coastal waters. Our information on film-formers from open water of the sub-tropics and tropics, however, is exceedingly limited. The scanty data we do have from potential OTEC sites indicate that films do form on solid surfaces submerged in surface waters, but detailed information on the nature of the organisms involved and the rate of film build-up is still lacking. Everything that is known leads us to believe that primary film formation on OTEC heat exchangers will be a problem, and common sense dictates that we attempt to prevent the films from forming or attempt to remove them as fast as they form. None of the classic methods employed to discourage fouling on ship's hulls appear to be feasible for OTEC heat exchangers, and the presently-used techniques for cleaning industrial heat exchanger tubes have not been tested in experimental OTEC heat exchangers.

## Areas Where Research is Needed

If the problems associated with the development of primary films on OTEC heat exchangers are to be satisfactorily solved we need additional research to more fully answer the following questions:

1. What is the fundamental nature of the molecular fouling film and how does it "condition" the surface so that film-forming bacteria settle, attach and reproduce?
2. At potential OTEC sites, how severe is the primary film problem likely to be?
3. What is the distribution, horizontally and vertically, or film-forming bacteria in the open sea? Is ocean water below depths of 500m free of potential film-forming microorganisms as has been reported?

4. What is the detailed chemical and physical nature of the acid polymers secreted by film-forming marine bacteria, and exactly what role do the polymers play in anchoring bacterial cells to surfaces?
5. Are there agents which could be added to the sea water or applied to the heat exchanger surfaces which would block synthesis of extracellular polymers and thus prevent the irreversible settlement of bacterial cells?
6. How does the velocity of sea water flowing over a heat exchanger surface influence the formation of bacterial films?
7. Do the first arriving and settling bacteria in the primary film prepare or condition the surface for later arriving bacteria and other microorganisms?
8. What are some of the environmental factors that influence the rate of growth of bacterial films?
9. Is the formation of a microbial film essential for the later settlement of macrofouling organisms?
10. How can the surface of metals and plastics be altered to make them unattractive to film-forming bacteria and other microorganisms? Is it possible to manipulate the initial wettability properties of heat exchanger surfaces so that bacterial films will not develop? Can the negative chemotactic behavior of film-forming bacteria to non-lethal concentrations of hydrocarbons be taken advantage of to repell bacteria from settlement on heat exchanger surfaces?
11. Is chlorination or ozonization of sea water a really effective method of controlling potential film-forming organisms?
12. What mechanical and chemical methods could be employed efficiently to periodically remove the bacterial films from OTEC heat exchanger surfaces and keep the surfaces clean?

References


(1) Haderlie, E.C. 1977. The nature of primary organic films in the marine environment and their significance for Ocean Thermal Energy Conversion (OTEC) heat exchange surfaces. Naval Postgraduate School Tech. Rept. NPS-68Hc77021.

(2) Neihof, R. and G. Loeb. 1977. The interaction of dissolved organic matter in seawater with metallic surface. p. 359-361, In Romanovsky, V. (ed.) Proc. 4th Int. Congress on Marine Corrosion & Fouling (In Press)

(3) Baier, R.E. 1973. Influence of the initial surface condition of materials on bioadhesion. p. 633-639, In Acker, R.F. et al. (eds.) Prof. 3rd Int. Congress on Marine Corrosion & Fouling, Northwestern Univ. Press, Evanston, Ill.

(4) Corpe, W.A. 1977. Primary bacterial films and marine microfouling. p. 97-100, In Romanovsky, V. (ed.) Proc. 4th Int. Congress on Marine Corrosion & Fouling (In Press).

(5) Marshall, K.C. 1973. Mechanism of adhesion of marine bacteria to surfaces. p. 625-632, In Acker, R.F. et al. (eds.) Proc. 3rd Int. Congress on Marine Corrosion & Fouling, Northwestern Univ. Press, Evanston, Ill.

(6) Young, L.Y. and R. Mitchell. 1973. The role of chemotactic responses in primary film formation. p. 617-624, In Acker, R.F. et al. (eds.) Proc. 3rd Int. Congress on Marine Corrosion & Fouling, Northwestern Univ. Press, Evanston, Ill.

# CATALOGUING OF OCEANOGRAPHIC PARAMETERS OF INTEREST TO BIOFOULING AND CORROSION

H. LEE CRAIG, JR. AND ROBERT S. C. MUNIER
*Rosenstiel School of Marine and Atmospheric Science*
*University of Miami*
*Miami, Florida*

Abstract

The Energy Research and Development Administration (ERDA) through its agent, Battelle Pacific Northwest Laboratories, is sponsoring programs to deal with biofouling and corrosion problems affecting Ocean Thermal Energy Conversion (OTEC) plants currently under development. One of the deciding factors in site selection could be the potential for either fouling or corrosion of the heat exchanger surfaces which would lower the efficiency past the point of economic viability. The University of Miami's Marine School has been asked to assemble the available related oceanographic data, review it, and make recommendations for obtaining additional information.

Five potential sites were selected for study based on proximity to the United States (including Territories), the available $\Delta T$ over the water column, and the bathymetry. They are:

Eastern Gulf of Mexico
Hawaii/Oahu
Guam
Straits of Florida
Puerto Rico/Virgin Islands

Twelve parameters were chosen for study because of their potential impact on heat exchanger corrosion and biofouling. These were divided among three categories:

| Physical | Chemical | Biological |
|---|---|---|
| temperature profile | pH | nutrients |
| salinity | dissolved oxygen | silicate |
| surface currents | trace metals | nitrate |
| current profile | dissolved $CO_2$ | phosphate |
| turbidity | $E_H$ | microbial cell count |

The primary source of this information is the NOAA Marine Library. The National Oceanic and Atmospheric Administration (NOAA) Environmental Data Index and the Oceanic and Atmospheric Scientific Information System (ENDEX/OASIS) were used to provide abstracts and data. Using Marsden square grid locators and appropriate keywords, searches were made of both services. The citations were assessed, original documents obtained and reviewed, along with the data.

A source book is in preparation incorporating the reviewed data, the bibliography from which it has been obtained, and sections containing recommendations on further work to fill gaps that were found. Site descriptions, parameter definition, a glossary, keywords, and sources are included.

## INTRODUCTION

To the untutored eye, the amount of available oceanographic data must appear as vast as the oceans themselves. Seafarers have been recording observations in their logbooks for as long as ships have been traversing the seas. It is as amazing as it is factual that some of the figures we have gathered for use in planning man's latest engineering challenge, the OTEC plant, were collected over a century ago by some skipper plying the Straits of Florida or skirting the shores of Puerto Rico. An example of this is the SCUDS file, a data bank typical of the sources available to the ocean engineer. The acronym "SCUDS" stands for Surface CUrrent Data System. The collection technique for SCUDS data represents a highly refined analog of the method Benjamin Franklin suggested to colonial ship captains, which was the use of water temperature measurements to detect the Gulf Stream. Presently, the captain records his ship track with respect to some fixed reference point or navigational aid and compares this to his planned ship track. The difference is calculated as the ships drift and is attributed to the surface currents. This information is relayed to the data bank where it is combined with the rest of the data for that particular area to await recall by some scientist or engineer.

Data retrieved from the SCUDS file is shown in Table 1. It was obtained originally in computer printout form from the National Ocean Data Center (NODC), a facility operated by the National Oceanic and Atmospheric Administration (NOAA), by specifying the latitude and longitude of the desired area. The finest scale on which data may be obtained is a 1/4 degree square.

## STATEMENT OF THE PROBLEM

At the University of Miami's Rosenstiel School of Marine and Atmospheric Science (RSMAS), the SCUDS file and others like it have been searched as part of a project to assemble and assess oceanographic data pertinent to the biofouling and corrosion behavior of OTEC heat exchangers. In addition to computerized data banks, the entire span of oceanographic literature has been tapped for potential sources. This concerted effort was initiated because of the rapidly approaching deadline for making firm engineering decisions with regard to OTEC heat exchanger design and plant siting.

Our techniques of searching the oceanographic literature, including computerized data banks, are presented in this paper. In general, following the determination of geographic site limits, the work flow pattern involves determining what to look for, where to look for it and how to look for it.

## SITING

The first step is to define the potential plant sites. The two major distinctions are 1) distance from the prospective user and, 2) a difference in temperature ($\Delta T$) between the warm surface water and the cold deep water.

Since the United States has recently claimed territorial fishing rights and established a 200-mile limit, it seems reasonable to look first for potential sites in these waters. (Figures 1 and 2). Considerations are the logistics of delivering the product, servicing the plant, and protection from interference by unauthorized parties.

The $\Delta T$ factor restricts potential sites to tropical locations where warm surface water overlies a cold bottom water. (Water at the ocean bottom, regardless of latitude, ranges from -1.9°C to 6°C). See Figures 1 and 2 for 20°C and 25°C isotherms during January.

From these and other considerations, particularly bathymetry, five potential OTEC sites were selected for investigation. They are:

1) Straits of Florida
2) Puerto Rico/Virgin Islands
3) Eastern Gulf of Mexico
4) Hawaii/Oahu
5) Guam

## WHAT TO LOOK FOR: PARAMETERS

Following siting, the problem was deciding which measurements are of significance in assessing the impact of the water masses on the biofouling and corrosion behavior of the materials used in OTEC plants. Twelve parameters were selected for cataloguing, divided among the three categories:

| Physical | Chemical | Biological |
|---|---|---|
| temperature profile | pH | nutrients |
| salinity | dissolved $O_2$ | silicate |
| surface currents | trace metals | nitrate |
| current profile | dissolved $CO_2$ | phosphate |
| turbidity | $E_H$ | microbial cell count |

Biofouling is dependent on each of these, ranging from the currents which distribute the spat and larvae to the microbial cells which represent the building blocks for organic growth. Corrosion is less sensitive, but trace metals can alter the form of attack; for example, from uniform film dissolution to pitting.

Another problem related to biofouling and corrosion is scale deposition. Surface seawater is supersaturated with respect to calcium carbonate due to the availability of dissolved carbon dioxide and wide fluctuations in temperature. Any source of nucleation will lead to growth of crystals which may degrade the heat transfer properties of the surfaces on which they form. The pH and dissolved $CO_2$ can be used to calculate the degree of supersaturation.

## WHERE TO LOOK FOR IT: DATA SOURCES

Data pertaining to each of the 12 parameters is distributed throughout the oceanographic literature. Searching it out requires thoroughness and dedication. Part of the problem is the changing nature of information science. Computers are now taking over the primary responsibility of data archiving, a job normally performed by atlases, reference books, journals, and monographs. At this time, NODC files contain an estimated 40 to 80% of the existing oceanographic data. The balance is divided among accounts in the open literature, unpublished reports, or even on magnetic tapes as yet unreduced to meaningful characters.

Since ERDA has been sponsoring an increasing number of OTEC-related studies, many recent reports have been forthcoming of immediate concern to this project. Obtaining data from each of these sources requires a different approach.

Take, for example, the NODC computer service Oceanic and Atmospheric Scientific Information System, or OASIS. Use of the magic key words unlocks the files and out pours citation after citation. Since most references are not site specific to the degree needed for this catalogue, the originals often have to be scanned by a trained searcher. Fortunately, the RSMAS Marine Library has about 75% of the items sought by our group, so only one in four has had to be ordered through NTIS, Interlibrary Loan Service, or through correspondence to the principal investigator.

Eight major abstracting services have been searched through the OASIS files:

| Name | Period | Citations |
|---|---|---|
| Biological Abstracts (BA) | 1972- | 850,000 |
| Biological Information Retrieval Services (BIRS) | 1955-74 | 25,000 |
| Chemical Abstract Condensates (CAC) | 1970- | 1,600,000 |
| Government Reports Announcements (GRA) | 1964- | 500,000 |
| Meteorological and Geoastrophysical Abstracts (MGA) | 1972- | 25,000 |
| Oceanic Abstracts (OA) | 1964- | 81,000 |
| Aquatic Sciences and Fisheries Abstracts (ASFA) | unknown | new |
| Smithsonian Science Information Exchange (SSIE) | 1974-76 | 200,000 |

Note the comparative newness of each of these in relation to a literature which extends back to 1876 (Challenger voyage) and beyond.

A second major source of information is ENDEX, Environmental Data Index. It has three major components: 1) Detailed inventories of large, commonly used files, 2) Descriptions of data files, and 3) Descriptions of data collection efforts.

Some of the data bases searched are:

NIMSCO - NODC Index for Instrument Measured Subsurface Current Observations, covering 1965 to the present, containing 2,200 records.

PIDS - Parameter Inventory Display System--Contains temperature, salinity, and/or transparency (Secchi disc), dating from 1893 to the present with more than 1,508,000 records.

ROSCOP - Report of Observations/Samples Collected by Oceanographic Programs--1974 to the present with over 1,000 inventories of data.

EDBD - Environmental Data Base Directory, from 1850 to the present with 3,500 data file descriptions.

SCUDS - Surface Current Data System--from 1850 through 1974, contains over 4,000,000 ships set and drift observations.

Using geographic locators, printouts are obtained which summarize all oceanographic station data within the specified area, including depth, temperature, salinity, and, when available, $O_2$, $CO_2$, $PO_4^{\equiv}$, $NO_3^-$ and transparency.

In addition to the above NODC computer services, both Enviroline/Environmental Abstracts and Comprehensive Dissertation Abstracts have been searched. The latter contains over 500,000 abstracts of U.S. and Canadian Doctoral Dissertations since 1861.

## HOW TO LOOK FOR IT: SEARCH METHODOLOGY

The initial step is to select the appropriate key words which identify the sites and parameters of interest. In some instances, a geographic term such as "Gulf of Mexico" is used, while some computer sources employ latitude and longitude descriptions, such as the Marsden square. (For example, see Figures 3 and 4). One problem is that the same parameter can masquerade under such diverse terms as turbidity, transparency, Secchi disc measurements, transmittance, light attenuation, light scattering coefficient, T.D. solids (total dissolved...), particulate matter, and probably a dozen more, given the ingenuity of the scientist interested in the phenomenon.

### Assemble Citations/Data (Refer to Figure 5)

A search of a selected abstract service or data file is then ordered. In a relatively short time, the typewriter begins to spill back the desired citations (known as hits) or tables of figures. Once in a while, when apparently inappropriate key words are used, it has happened that only a few hits, and none especially pertinent, are received from a service with over a half-million selections. Other times, large quantities of data are obtained, as when a one-degree square near Miami in the Florida Straits turned up over 400 profiles.

### Retrieve Data

Next, the actual information is located and ordered from the appropriate source, if not readily available at RSMAS. A variety of forms is generated: journal articles, reference books, atlases, monographs, charts, technical reports, microfiche, computer printouts, or magnetic tapes.

### Assess Documents/Data

After screening by the literature searcher, documents are sorted into six classifications: A through D and X. The latter type is discarded, usually for reasons such as noncompliance to site location, or parameter definition. The others provide an initial review based on timeliness and coverage.

## Review Data

At this stage, a decision must be made to assure the most relevant data is incorporated into the catalogue. A senior panel composed of a biological oceanographer, a physical oceanographer, and an ocean engineer has been assembled to perform this task.

## Final Stages

From the beginning our eye has been on the goal: a source book that will be convenient, informative, as complete as possible, and useful to the engineer who will employ the data. An outline has been prepared, reviewed, revised and established as the framework on which to hang our efforts. See Figure 6. The central section, naturally, will be composed of several hundred pages of carefully formatted data.

Among the peripheral sections will be discussions of biofouling, corrosion, search methods, sources, parameter definitions, site descriptions, key words, a glossary, and an index of symbols and units. A complete annotated bibliography will be included. All the available data will appear in an appendix consisting of documents, microfiche, printouts, and magnetic tapes.

## Tentative Results and Recommendations

Table 2 summarizes the citations and computerized data hits retrieved as of 17 March 1977. It is estimated that 90% of the data retrieval phase is complete.

Of the 687 citations, 250 were deemed relevant after preliminary review. The relevant citations are presently undergoing a second review by the Principal Investigator, after which will follow a final review, and then incorporation into the catalogue.

Table 3 gives a citation hit record (literature sources only) of preliminary results. It indicates that there is substantial physical data, with the possible exception of transparency. Dissolved $O_2$, trace metal, and nutrient data is sporadic; many of the better profiles have been from NODC Nansen Cast and STD printouts. Sources are sparse for dissolved $CO_2$, $E_H$, pH, and microbial cell count profiles measured in the five sites under consideration.

On a site basis, Hawaii (Bathen, 1975) and Puerto Rico (Atwood, 1976) have been the subject of recent OTEC-specific oceanographic field studies, as well as substantial oceanographic work in the past ten years by the University of Hawaii and the University of Puerto Rico. Thus, enough data may have been collected at these sites to substantiate engineering decisions regarding OTEC. The Florida Straits and the Eastern Gulf have also been extensively studied, especially by the University of Miami and Texas A & M University. Abundant chemical, biological, and especially physical data are available. However, because the data have been collected in random projects over a 25 year period, there is little cohesiveness from an OTEC viewpoint; that is, there is a lack of standardization of the data collection. It is time for the community of oceanographic scientists to further standardize data collection efforts.

Compared to the other sites, very little work has been done in Guam waters. An environmental impact study of a Guam-sited OTEC plant was made in 1975 (Corey). The work, however, did not involve any field measurements. It is our preliminary position that for Guam to be seriously considered as a potential site, more OTEC-specific oceanographic field studies are required.


## ACKNOWLEDGEMENTS

The authors wish to acknowledge the assistance of Marty Perlmutter and Steve Hess of RSMAS in this work.


## REFERENCES


1. Bathen, K. H., (1975), "An Evaluation of Oceanographic and Socio-Economic Aspects of a Nearshore Ocean Thermal Energy Conversion Pilot Plant in Subtropical Hawaiian Waters," Final Report prepared under NSF/RANN Grant GI-43768, ERDA Contract AER74-17521A01, 305 pp.

2. Atwood, D. K., P. Duncan, M. C. Stalcup, and M. J. Barcelona, (1976), "Ocean Thermal Energy Conversion: Resource Assessment and Environmental Impact for Proposed Puerto Rico Site," Final Report prepared under NSF Grant No. AER 75-00145, 103 pp.

3. Corey, R. R., (1975), "Suitability of Guam from an Environmental Aspect as a Potential Site for OTEC Plants," Final Report of the U.S. Naval Academy, 1 July 1974-1 Jan 1975 Energy-Environment Study Group Report USNA-EPRD-11, 14 pp.


TABLE 1

Surface Current Data (Ships Drift)

Site: Puerto Rico
10 Degree Square: 1008
1 Degree Square: 75
1/4 Degree Square: 1

| Month | Total Observ. | Number of Calms | North Comp. | East Comp. | Resultant Direction | Resultant Speed |
|---|---|---|---|---|---|---|
| 1 | 17 | 1 | -0.0 | -0.4 | 267 | 0.4 |
| 2 | 7 | 0 | -0.0 | -0.3 | 266 | 0.3 |
| 3 | 7 | 1 | 0.2 | -0.5 | 286 | 0.6 |
| 4 | 12 | 0 | 0.2 | -0.4 | 293 | 0.5 |
| 5 | 11 | 1 | 0.0 | -0.4 | 275 | 0.4 |
| 6 | 2 | 0 | 0.7 | -0.1 | 351 | 0.7 |
| 7 | 3 | 0 | 0.6 | -0.0 | 357 | 0.6 |
| 8 | 13 | 2 | 0.0 | -0.2 | 273 | 0.2 |
| 9 | 4 | 0 | 0.3 | -0.2 | 317 | 0.4 |
| 10 | 13 | 0 | 0.2 | -0.6 | 284 | 0.6 |
| 11 | 18 | 1 | 0.1 | -0.5 | 279 | 0.5 |
| 12 | 3 | 0 | 0.2 | -0.3 | 305 | 0.3 |

TABLE 2

A. Citations (including reprints, atlases, texts, journal articles, technical reports, computer references to publications and ongoing research)

Total Citations: 687 Relevant citations (after preliminary review): 250

B. Station Data (provided directly through computer services)

| | SCUDS (observations) | XBT (stations) | STD (stations) |
|---|---|---|---|
| Miami | 135 | 400 | 400 |
| Puerto Rico | 458 | 400 | 51 |
| Eastern Gulf of Mexico | 20,301 | 200 | 4,452 |
| Hawaii | 31 | 33 | 107 |
| Oahu | 658 | 400 | 107 |
| Guam | 243 | 50 | 18 |
| Totals | 21,826 | 1,483 | 5,135 |

| | Surface Temperature 1 | Temperature Profile 2 | Salinity 3 | Surface Current 4 | Current Profile 5 | Transparency 6 | pH 7 | Dissolved $O_2$ 8 | Trace Metals 9 | Dissolved $CO_2$ 10 | $E_H$ 11 | Nutrient 12 | Parameter Hits |
|---|---|---|---|---|---|---|---|---|---|---|---|---|---|
| Straits of Florida | 40 | 36 | 23 | 38 | 42 | 5 | 1 | 3 | 13 | -- | -- | 14 | 215 |
| Puerto Rico | 26 | 23 | 18 | 11 | 37 | 5 | 2 | 5 | 5 | 2 | -- | 7 | 141 |
| Eastern Gulf | 72 | 64 | 57 | 40 | 33 | 12 | 5 | 14 | 9 | 2 | 1 | 27 | 336 |
| Hawaii | 41 | 35 | 30 | 16 | 31 | -- | 9 | 13 | 4 | 1 | 1 | 20 | 201 |
| Guam | 13 | 3 | 5 | 2 | 3 | -- | -- | 2 | -- | 1 | -- | -- | 29 |
| | | | | | | | | | | | Total: | | 922 |

TABLE 3 - Parameter Hits by Site

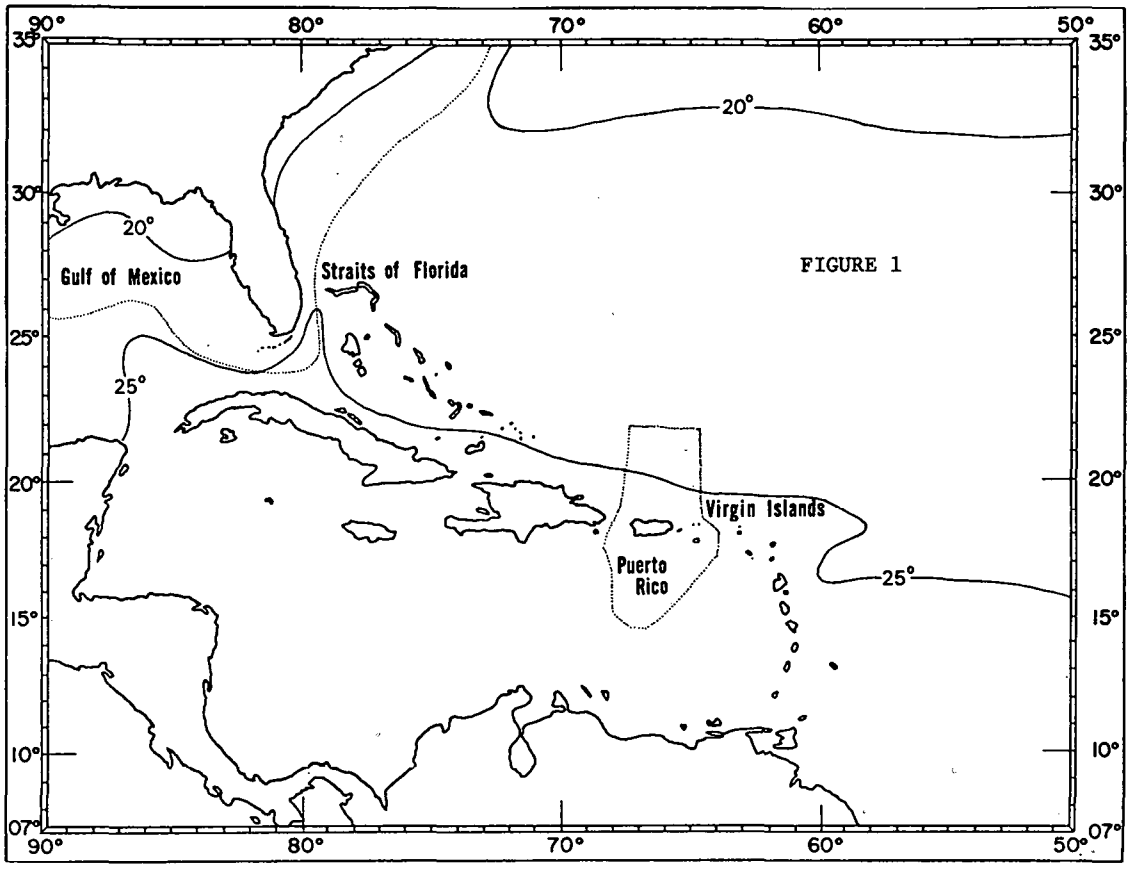



FIGURE 1

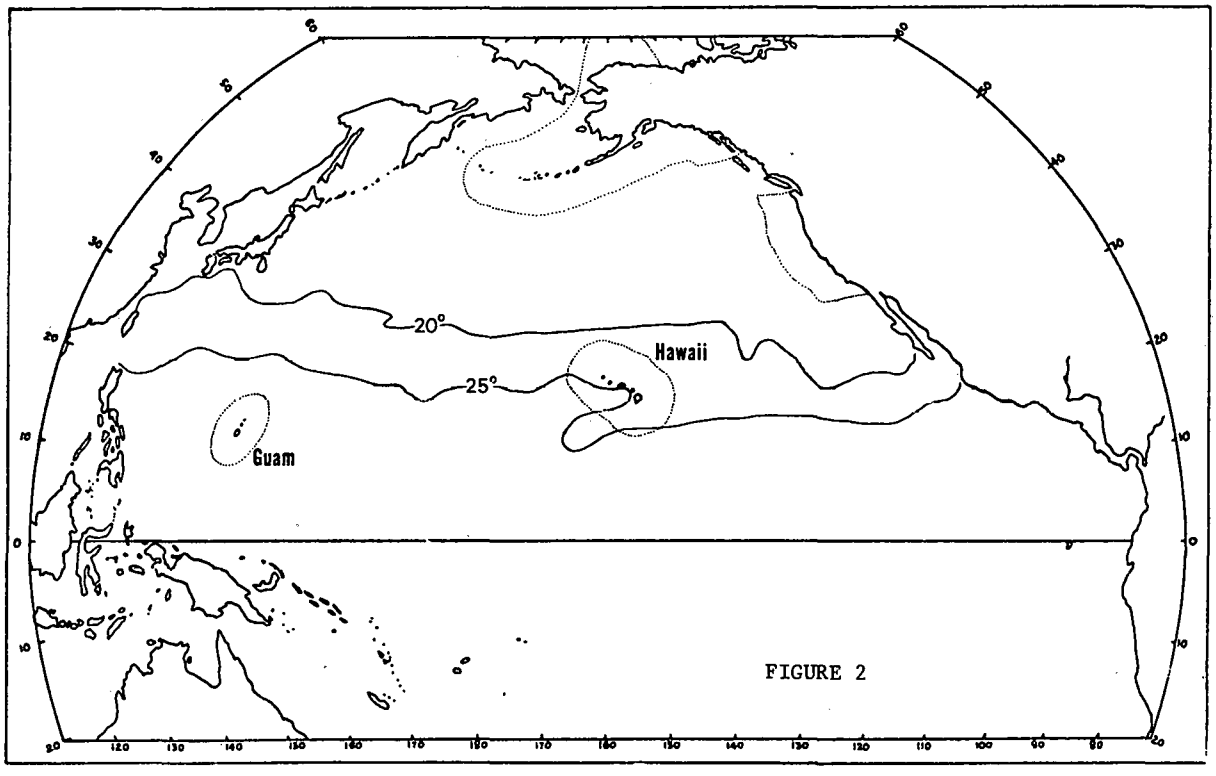



FIGURE 2

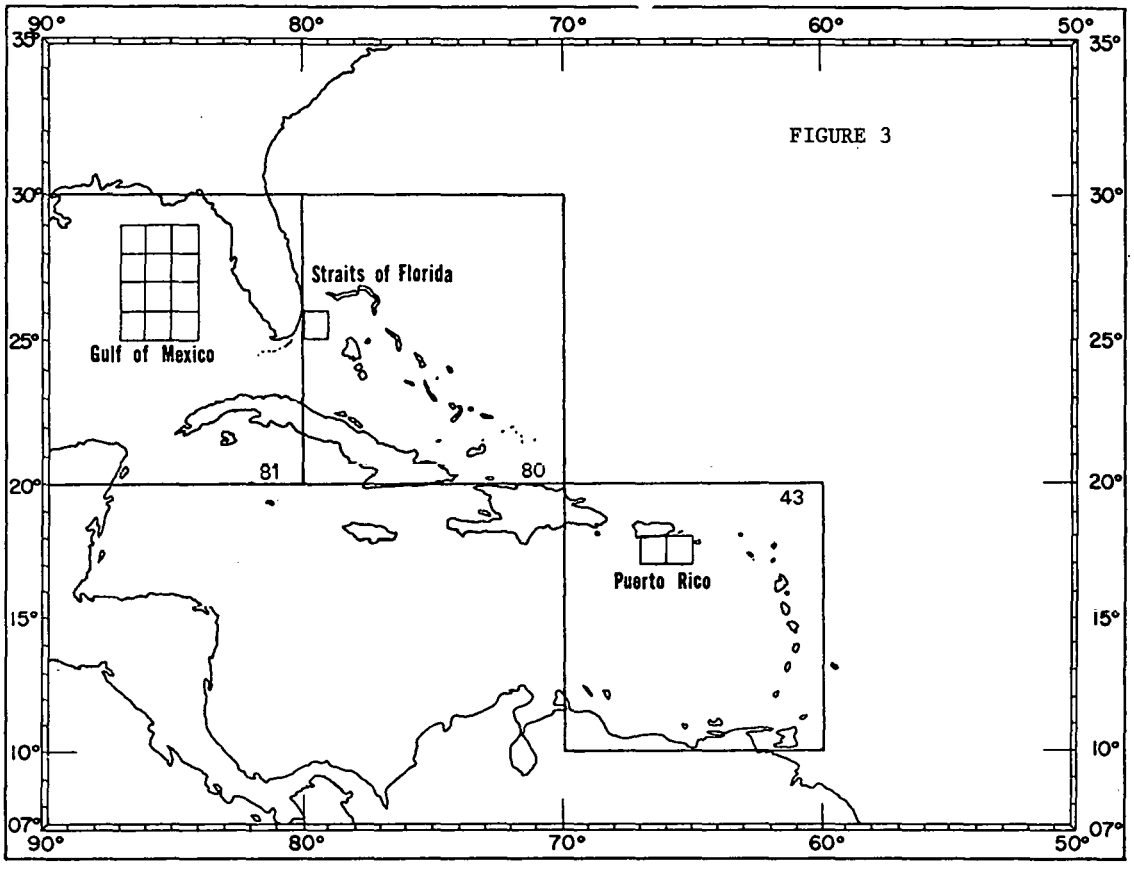



FIGURE 3

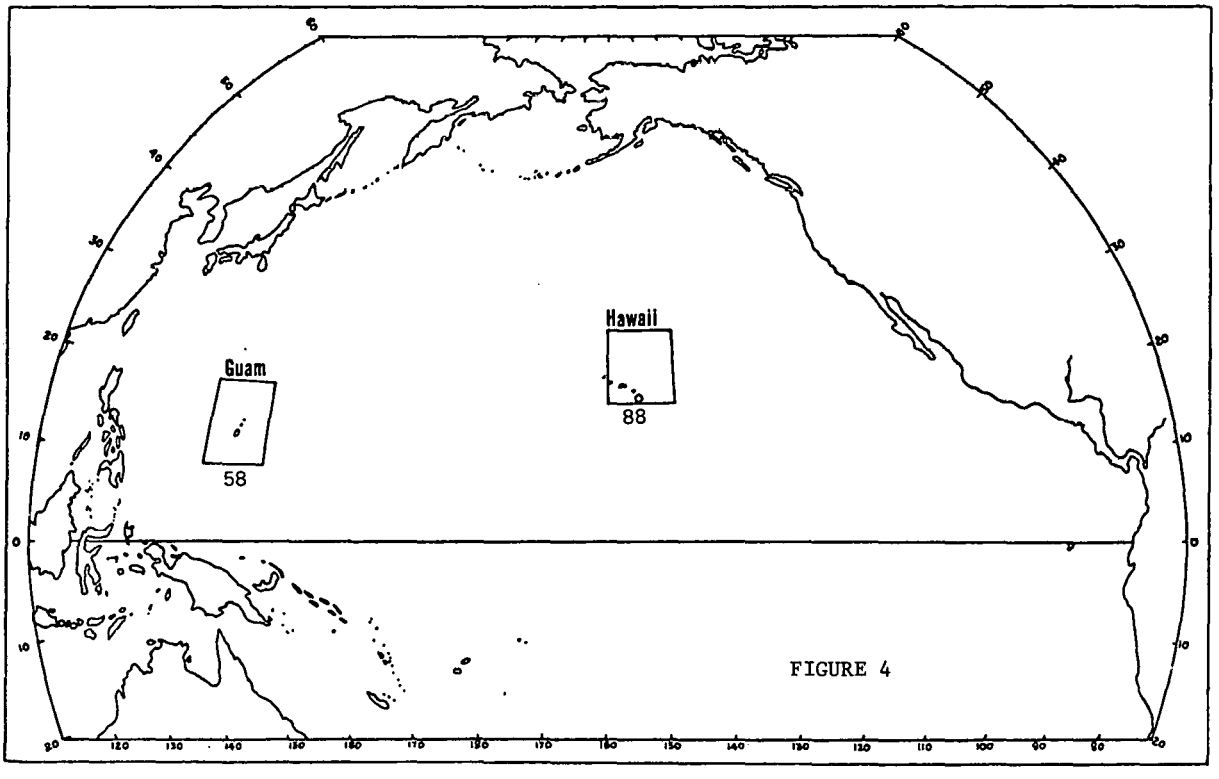
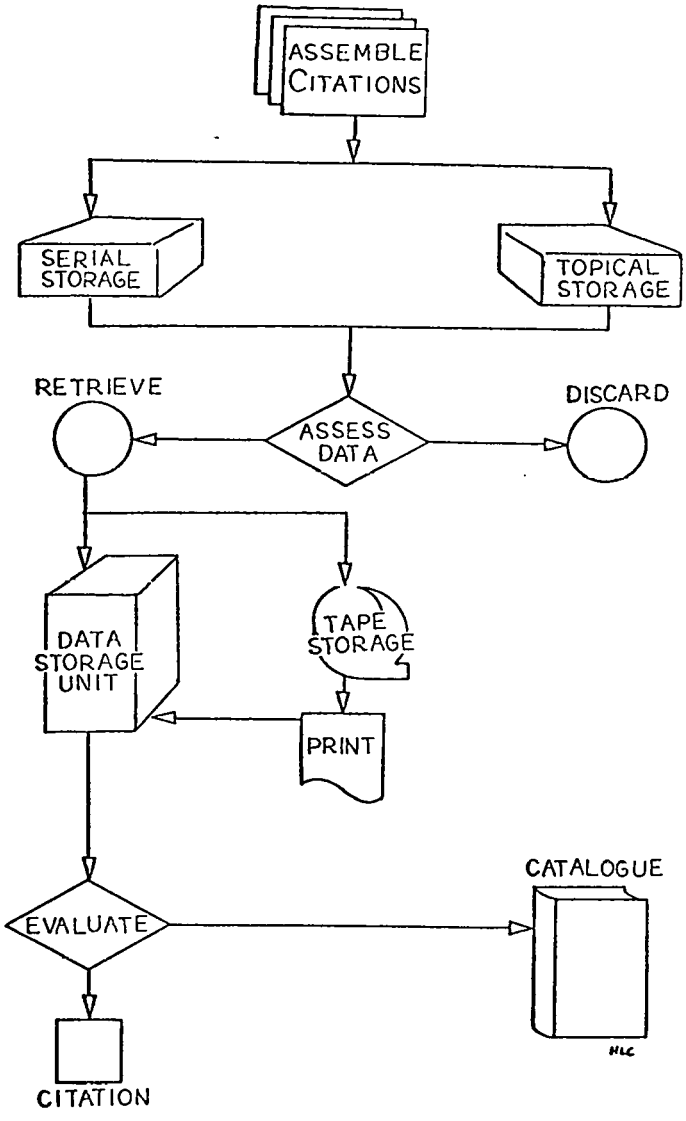



FIGURE 4

FIGURE 5




CATALOGUE FLOW CHART

FIGURE 6

RSMAS OTEC SOURCE BOOK

1.0 Executive Summary

2.0 Introduction
- 2.1 Site Selection
- 2.2 Parameter Section
  - 2.2.1 Corrosion
  - 2.2.2 Physical
  - 2.2.3 Biology
- 2.3 Procedures
- 2.4 References

3.0 Recommendations and Conclusions

4.0 Procedures
- 4.1 Justification for this search
- 4.2 Structure of the scientific literature
- 4.3 Organization of the search
- 4.4 Detailed procedures
- 4.5 Summary - Principles
- 4.6 Recommendations
- 4.7 References

5.0 Background on Parameters
- 5.1 Biofouling
- 5.2 Corrosion
- 5.3 Parameters
- 5.4 Glossary of Terms
- 5.5 Index of Symbols

6.0 Discussion (Data Compilation)
- 6.1 Named Site (i.e., Miami)
  - 6.1.1 Site description
  - 6.1.2 Recommendations for needed data
  - 6.1.3 Data by parameter

7.0 Annotated Bibliography
- 7.1 References cited in Source Book
- 7.2 References reviewed but not cited

8.0 Appendix
- 8.1 Inventory of Data
- 8.2 Data Parcels
  - 8.2.1 Reports, Reprints
  - 8.2.2 Microfiche
  - 8.2.3 Computer printouts
  - 8.2.4 Charts
  - 8.2.5 Magnetic tapes

# CORROSION AND BIOFOULING ON AN OCEAN THERMAL ENERGY CONVERSION POWER PLANT WHAT ARE THE QUESTIONS?

V. J. CASTELLI
*David W. Taylor Naval Ship R&D Center*
*Annapolis Laboratory*
*Annapolis, Maryland*

Abstract

Of the large number of problems which confront economical Ocean Thermal Energy Conversion (OTEC) plant construction and operation, both biofouling and corrosion are major items. Present antifouling coating systems are limited to a maximum three-year service life in temperate waters, and less in tropical waters. However, experience in fouling control systems for conventional power plants may be applicable in certain parts of the OTEC plant. In addition, some recent major advances in the long-term control of biofouling through coatings which have been sponsored by the Navy are in the development and testing phases. On the other hand, the development of long-term corrosion control systems has been more actively pursued for many years and successful solutions on previous applications can be transferred directly to OTEC Power Plants. Most problems in the area are expected to be associated with scale-up. Areas requiring accelerated short-term development and particular systems currently under advanced development will both be identified.

## Introduction

An Ocean Thermal Energy Conversion (OTEC) power plant must overcome many obstacles before it can be constructed and operated economically. Two particular operational problem areas that require control are corrosion and biofouling. Like many operational difficulties, their impact can be considerably blunted through enlightened design. The OTEC designer requires an authoritative, comprehensive set of criteria so that especially troublesome areas such as large-area, high fouling zones or galvanically incompatible couples are not designed into the plant. Many of these problem areas have been identified previously by the Navy and others who operate in the oceans, but often these data are scattered. A survey being conducted by the Navy will consolidate several decades of hard won information into a handy guide. However, in many areas a considerable lack of information will require the best of expert opinion to provide temporary guidance while actual experimental data is gathered.

## Biofouling

Fouling in the open ocean has been a mere scientific curiosity to date. Some investigations have been performed, (1-3) but the results have been scanty and few consistent trends have been documented. Some convincing evidence suggests that fouling severity decreases with distance from shore (4) as does the species diversity. Data for fouling as a function of depth is even more meager but the general consensus of experts is that fouling decreases very rapidly with depth (4,5). One point, also obvious in all of these studies is that biofouling in general is a poorly understood phenomenon and that the variability and diversity of fouling sometimes observed in open ocean fouling tests cannot be explained or predicted.

The problems associated with the accumulation of biofouling on an OTEC plant are many. The most obvious penalty is the increased mass associated with these attached macro-fouling organisms. This increased mass decreases the amount of reserve buoyancy which is available in the plant. If the fouling estimates are too low, this can cause a significant reduction in the emergency buoyancy available, and if the estimates of fouling are too high, this results in the design of excessive flotation for the module, hence increased capital costs. Another result of macro-fouling is the increased drag on the anchoring systems, which for an object the size of an OTEC plant is already of mammoth size and probably quite complex in its arrangement and deployment. Excessive fouling may subject the anchoring system to loads in excess of original design, with dire consequences. Macro-fouling also causes operation difficulties in many ways. These can be envisioned as causing difficulty by preventing effective mating when using the plant's built-in modular concept and aggravating the already difficult at sea maneuvers required. Another factor which is resultant from biofouling, both macro and micro, is related to the deterioration of the physical structure. Fouling organisms have been implicated in the accelerated corrosion of steel, aluminum and other alloys, concrete, and all types of organic materials (6,7).

## Biofouling Control and Removal

Current fouling control systems are based on many types of toxic chemicals: organics, copper salts, organometallics, etc. Much effort has been expended in developing methods for the effective utilization of these toxicants so as to prolong their effective service life to the maximum extent possible. The most sophisticated coatings systems that have been developed over the years have succeeded in producing maximum service life coatings of about three years. Organotin rubber sheeting is currently being marketed by one company

which offers the potential for at least a five year active service life. While some impetus for longer antifouling coatings has existed, research has hampered by a lack of available approaches. In addition, coating failures on ship bottoms could always be handled through drydocking and repainting even though it is rather expensive. However, the U.S. Navy has been sponsoring research aimed at developing long life antifouling systems. (8-11) Current expectations are that the service lives can be extended to five years for coatings and ten years for glass reinforced plastic structures. These predictions fall short of the desired 15 - 20 year protection sought for the mainframe of the OTEC plant. Such techniques, as well as others less exotic, may find utility for any demountable modules which are envisioned.

Another technique which warrants further study for its applicability to OTEC is underwater mechanical cleaning to remove fouling. This would be useful on the main housing which cannot have its surfaces refurbished otherwise for strictly logistical reasons. Many new cleaning techniques have surfaced in the past ten years with the primary purpose of ridding ship hulls of fouling growths. They capitalize on a wide variety of physical principles, are operated either by diver or remote control, and have varying degrees of success in their ability to remove differing types of fouling. This technology is progressing at a rapid pace and in the final analysis may be the only possible route to ensure fouling control on the main housing.

## Corrosion and Deterioration

To maintain the structural integrity of an OTEC plant sufficient regard must be given to the effects of metal corrosion and material deterioration. Corrosion is the gradual deterioration of a metal surface which is the result of chemical action. Different metals corrode at different rates, and even the same metal will corrode at varying rates depending on the environment. The sea presents a most aggressive environment to many materials, and as a result unretarded deterioration generally proceeds at a fast rate. The forms of corrosion encountered in seawater can be oxidative, as in the case of oxygen attack of an isolated steel structure, galvanic, which results when two metals of differing corrosion potentials are joined, or biological, which results from chemical attack by the secretions of living organisms. The metals of general construction for the OTEC plant will be carbon and low alloy steels, some bronzes, and possibly aluminum. All structures made from them will require active design effort to keep corrosion, and the effects of corrosion, to manageable levels.

Marine deterioration is not limited to metallic materials alone. The major material of construction for OTEC, reinforced concrete, suffers from accelerated decay as a consequence of its ocean deployment. This results from sulfate attack on the cement matrix, and permeation of ions from the seawater which accelerate the oxidation of the reinforcement rods. Another, possibly major, material of construction is fiber reinforced plastic (FRP). This has been proposed in design as the material of choice for the long cold water pipe. FRP, when constructed with glass fiber reinforcement, has proven itself to be very resistant to all manner of assault in the marine environment and will maintain its fine structural properties. Although it is quite expensive compared to a material such as steel, its inherent corrosion resistance may make it cost-effective.

## Corrosion and Deterioration Control

Active and passive protection of all components must be given high priority during initial design phases and not handled as an add-on at some later stages. Techniques such as impressed current cathodic protection and/or anticorrosive coatings are essential for all exposed ferrous metal, and may well be required for other metals, and metal combinations. These techniques have proven to be essential for marine structures and are credited with the capability of reduction corrosion to a negligible amount. However, such good results are possible only when such systems have been knowledgeably designed, for poor design can cause greatly accelerated general corrosion in addition to potentially more damaging localized corrosion in the form of pitting. Good design requires suitable electrode geometries to provide adequately throwing power to assure sufficient protection of all the surface. In addition, all areas being cathodically protected can benefit from the correct types of anti-corrosive coatings.

The deterioration of concrete in seawater can be significantly reduced through the correct choices of cement. These cements are quite effective at resisting the destructive effects of high sulfate concentration in the water. Further protection against sulfate attack can be granted by the judicious choice of coatings which effectively reduce the rate at which water and ions can enter the concrete. Essential requirements also dictate that the concrete mixes have low water/cement ratios to provide a considerably less porous matrix. This last item cannot be overemphasized, for no number of auxiliary techniques can prevent the damage resultant from improper concrete mix. The most obvious potential danger from a porous concrete exists for the steel reinforcement rods. The porous matrix allows relatively rapid influx of water and oxygen and causes accelerated corrosion. The tension present in the reinforcement rod also tends to accelerate this, leading to rod failure. Some techniques have been developed which mitigate this potentially dangerous condition.

## Conclusion

Some of the corrosion and fouling problems which are expected for the OTEC plant are solvable with existing technology. By far the vast majority of these deal with corrosion and deterioration, and their impact can be reduced substantially through knowledgeable design of an OTEC plant. Some of the corrosion problems will probably only be eliminated through advanced development of present laboratory demonstrated control methods.

The fouling problem, however, is less easy to solve. For the replaceable modules, state-of-the-art fouling control systems are probably capable of performing

satisfactorily in all but the most physically aggressive environments. The main housing can probably not benefit much from these products. Developmental antifouling products may hold some promise for these areas, but no present laboratory technique has demonstrated service effectiveness approaching the 15-20 years required. The main housing may therefore require either a fouling removal system or be designed with sufficient reserve bouyancy to support the fouling until a limiting fouling community size is eventually reached.

The opinions expressed in this paper are those of the author, and do not reflect official U.S. Navy position.

## References


1. Hartman, Patrick J., "Examination of Sea Lanes Mooring After Two Years on Station," National Data Bouy Center, Report # NDBCM-N 6222-2, Jul 1972.

2. Dexter, S. C., "Microbiological Fouling and Its Control in Coastal Waters and the Deep Ocean," Woods Hole Oceanographic Institute, Report #74-64, 1974.

3. Hoyt, J. W., P. R. Kenis, C. D. Runge and J. A. Beagles, "An Open Ocean Fouling Experiment." Naval Undersea Center, Report #TP-337, Mar 1973.

4. DePalma, J. R., "A Study of Deep-Ocean Fouling," 2nd International Congress on Marine Corrosion and Fouling," Athens, Greece, 20-24 Sep 1968.

5. "Fouling in Relation to Distance from Shore" in Marine Fouling and Its Prevention, Woods Hole Oceanographic Institute, p 107-115, 1952.

6. Muraoka, J. S., "The Effects of Marine Organisms on Engineering Materials for Deep Ocean Use," U.S. Naval Civil Engineering Laboratory, Report TR-R-182, 1962.

7. Muraoka, J. S., "Deep Ocean Biodeterioration of Materials. Part II. Six Months at 2340 ," U.S. Naval Civil Engineering Laboratory, Report TR-R-393, 1965.

8. Montemarano, J. A., S. A. Cohen, and E. C. Fischer, "Fouling, The Problem and Its Control by Polymeric Formulations," Proceedings of the International Controlled Release Pesticides Symposium, Wright State University, Dayton, Ohio, 1975.

9. Montemarano, J. A., and E. J. Dyckman, "Performance of Organometallic Polymers as Antifouling Materials," Proceedings of the Los Angeles Meeting of The American Chemical Society, Organic Coatings and Plastics Chemistry Division, Apr 1974.

10. Montemarano, J. A. and E. J. Dyckman, "Biologically Active Polymeric Materials Exhibiting Controlled Release Mechanisms for Fouling Prevention," Proceedings of the Controlled Release Pesticide Symposium, University of Akron, 1974.

11. Castelli, V. J. and W. L. Yeager, "Organometallic Polymers: Development of Controlled Release Polymeric Formulations, ACS Symposium Series 33, 197

# APPLICATION OF ALUMINUM ALLOYS

R. A. BONEWITZ
*Chemical Metallurgy Division*
*Alcoa Laboratories*
*Alcoa Technical Center*
*Alcoa Center, Pennsylvania*

ABSTRACT

The application of aluminum alloys to ocean thermal energy conversion (OTEC) depends on establishing their performance in both surface and deep sea water. A search of the existing literature and unpublished data on the corrosion performance of aluminum alloys in sea water is being conducted and quantitative data are being computer cataloged. Analysis of this data will establish relative alloy performance, effects of various exposure conditions on performance, and areas where additional information is required.

## INTRODUCTION

High costs associated with heat exchangers required for ocean thermal power plants may limit economic feasibility. Aluminum alloys afford the possibility of a wide variety of exchanger designs, such as fluted tubes for enhanced heat transfer, at reduced materials cost over other materials of construction.

Aluminum alloys have been used successfully with the proposed working fluid, ammonia, for many years. Their performance in anhydrous, or nearly anhydrous ammonia, is excellent as demonstrated by their application in anhydrous ammonia refrigeration systems. Aluminum alloys 1100, 3003, 5052, and 6063, which represent essentially unalloyed aluminum and Al-Mn, Al-Mg and Al-Mg-Si types, respectively, showed only mild etching after one year of exposure in liquid ammonia containing 5% water at 47 C (117 F)(1). The corrosion performance of aluminum alloys in solutions containing essentially 0% up to 100% ammonia has been described previously (2).

Because ammonia - sea water mixtures could exist in a leaking heat exchanger, an investigation was undertaken by Alcoa Laboratories under a subcontract to Carnegie-Mellon University (ERDA Contract No. E(11-1)-2641, CMU subcontract No. 1-53500) to determine the corrosion which could be expected as a result of the additional ions in sea water (3). These results are summarized in Figure 1 and indicate that conditions leading to rapid failure of an aluminum heat exchanger would not exist if a leak developed.

A primary consideration for using aluminum alloys for OTEC exchangers then is their performance in sea water. To establish this performance, the Chemical Metallurgy Division of Alcoa Laboratories, under a contract to Battelle Pacific Northwest Laboratories, is conducting a literature search and a computer compilation of published and unpublished corrosion data of applicable alloys in both surface and deep sea water.

## APPROACH

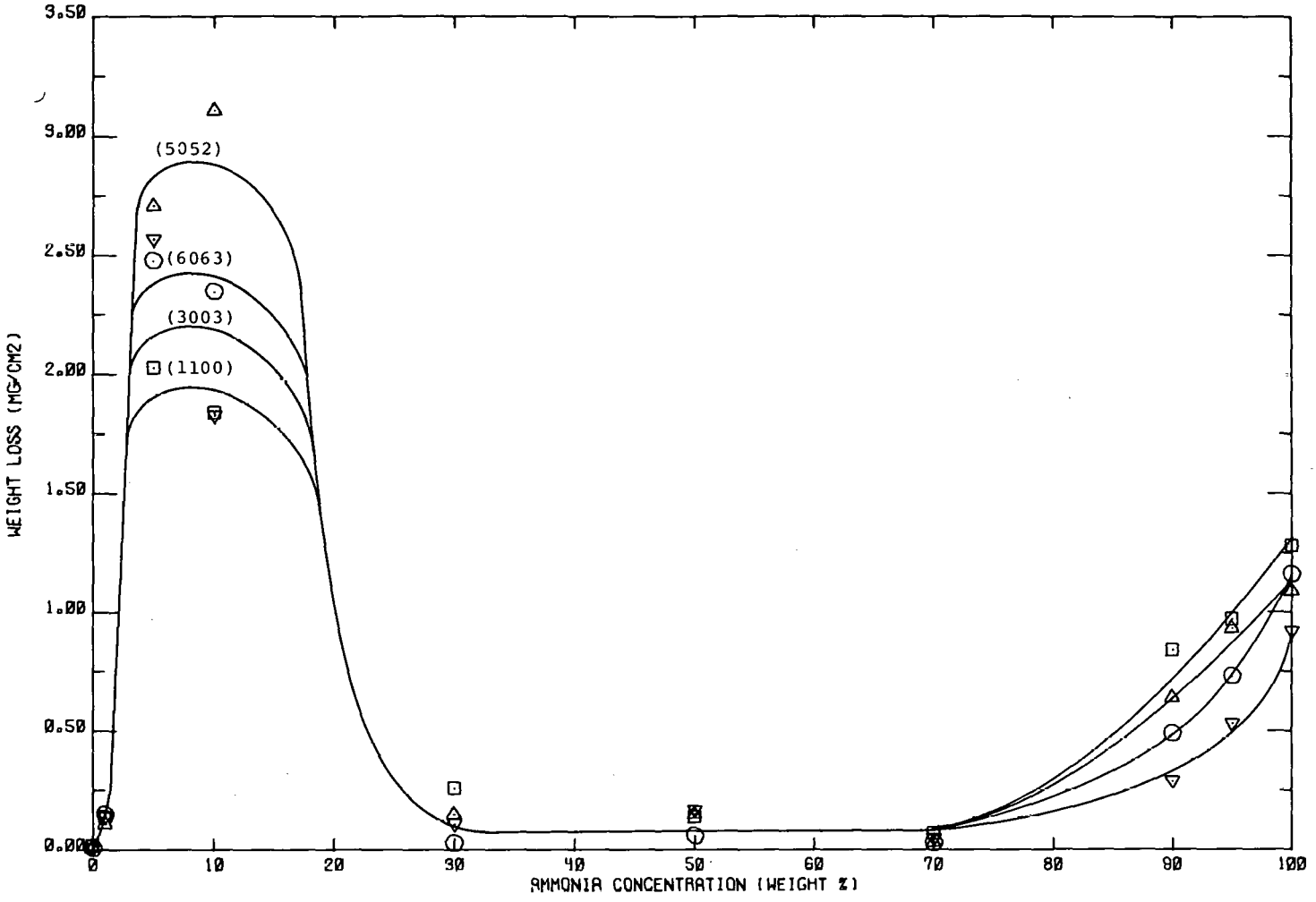
Literature resources reviewed included Chemical Abstracts (1927-1976), Corrosion Abstracts (1962-1975), Dissertation Abstracts (1861-1976), Engineering Index (1970-1976), Metals Abstracts (1944-1976), National Technical Information Service Database (1964-1976), Oceanic Abstracts (1968-1976) and World Aluminum Abstracts (1968-1976). In addition, unpublished Alcoa data have been included, and both private and government sources were requested to submit relevant data.

Only papers and reports giving quantitative data were computer cataloged. All information was cataloged using Data Processing Language (DPL) designed specifically for information storage and retrieval. After an initial screening of the literature and Alcoa reports, a list was established of the important variables describing the specimen, type of exposure, sea water composition, and various types of measurements relating corrosion performance. Because of the amount of information, two tables were required as shown in Figures 2 and 3.

Table I was set up to contain the information most frequently required. The first five columns describe the specimen including alloy and temper, the product evaluated, and specimen type and size. The column labeled specimen code indicates whether the specimen was (1) a single alloy, (2) an alloy welded to itself, or (3) an alloy welded to another alloy.

Columns 7-9 contain details of the exposure; location, depth and exposure time. Surface exposures are indicated as total immersion, meantide or tidewater and alternate immersion.

The final columns give the results of the examination. As shown in Figure 2,Several data lines may exist for each specimen describing each location examined; for example, for a welded specimen corrosion of the base alloy, heat affected zone, weld alloy and the other base alloy is indicated. For each location




**WEIGHT LOSSES FOR 1100 (□), 3003 (▽), 5052 (△) AND 6063 (○) ALLOYS EXPOSED ONE month IN 0 TO 100% AMMONIA-SEA WATER SOLUTIONS**

Figure 1

the type of attack, maximum and average depth of localized attack, and total weight loss expressed in inches/year are given.

Table II gives an additional description of the sample, miscellaneous corrosion information, sea water exposure conditions and a reference to the original source. The additional sample description includes, where possible, the manufacturer and the metal condition which includes such information as surface preparation and the presence of any anodic, conversion or inorganic or organic coatings.

A number of items were included under miscellaneous corrosion information. First was the depth of any crevice corrosion and pitting frequency. Stress corrosion data were given in terms of the stress level tested and the number of failures as compared to the total number of specimens exposed. Changes in mechanical properties expressed as the per cent change in tensile strength and elongation over an unexposed specimen are also given.

The method of measurement was included as an indication of the accuracy of the data. For example, a metallographic cross section of pit depth would be more accurate than the depth established by a pit depth gauge.

The final data section includes sea water exposure variables; velocity, pH, temperature, $O_2$ concentration, salinity, $CO_2$ and $CO_3$ concentrations and any indication of marine growth on the specimens.

To date, over 1300 individual specimens have been cataloged and additional data can be added as it

TABLE I

| IDENT. NUMBER | ALLOY AND TEMPER | PROD. | SC PO ED CE | TYPE OF SPECIMEN | SPECIMEN SIZE INCHES | DETAILS OF SPECIMEN EXPOSED: LOCATION | DEPTH-FT | MOS | RESULTS OF EXAMINATION: LOCATION EXAMINED | TYPE | DEPTH-INCHES: MAX. | DEPTH-INCHES: MEAN | GRAVI. DATA: RATE IN/YR |
|---|---|---|---|---|---|---|---|---|---|---|---|---|---|
| 258 | 5052-H34 | SHEET | 1 | | .05 T | HUENEME CAL | 2340 | 6 | BASE ALLOY | P | .0012 | | .0001 |
| 325 | 5052-0 | PLATE | 3 | PANEL | 3X9X.375 | MIAMI FLA | TOTAL | 60 | BASE ALLOY | P | .0013 | .0008 | |
| | | | | | | | | | HEAT AFFECTED ZONE | P | .0011 | .0005 | |
| | 5556 | | | | | | | | WELD BEAD | P | .0031 | .0013 | |
| | | | | | | | | | KNIFE LINE ATTACK | | NAA | | |
| | 5454-0 | | | | | | | | OTHER ALLOY BASE | P | .0047 | .0009 | |
| 328 | 5052-0 | PLATE | 2 | PANEL | 4X9X.375 | MIAMI FLA | TOTAL | 24 | BASE ALLOY | P | .0013 | .0007 | |
| | | | | | | | | | HEAT AFFECTED ZONE | P | .0017 | .0007 | |
| | 5554 | | | | | | | | WELD BEAD | P | .0013 | .0006 | |
| | | | | | | | | | KNIFE LINE ATTACK | | .0259 | | |

Figure 2

TABLE II

| IDENT. NUMBER | ADDITIONAL SAMPLE DESCRIPTION: ALLOY AND TEMPER | METAL CONDITION | MFGR | MISCELLANEOUS CORROSION INFORMATION: CREVICE ATTACK MAX DEPTH INCHES | FREQ PIT/SQCM | STRESS CORROSION: KSI | F/N | CHANGE IN PROPERTY: TS % | EL. % | METHOD USED TO MEASURE PITS | SEA WATER EXPOSURE CONDITION: FLOW FT/SEC | PH | TEMP (C) | O2 ML/L | SAL PPM | CO2 PPM | CO3 PPM | MARINE GROWTH | REFERENCE |
|---|---|---|---|---|---|---|---|---|---|---|---|---|---|---|---|---|---|---|---|
| 258 | 5052-H34 | | | 0 | | | | | | | 0.05 | 7.5 | 5.0 | 0.4 | 34360 | | | | LIT 263 |
| 325 | 5052-0 | MILL FINISH ALCOA | | | | | | | | X-SECT | | | | | | | | BARNAC | ALCOA |
| 328 | 5052-0 | MILL FINISH ALCOA | | | | | | | | X-SECT | | | | | | | | BARNAC | ALCOA |

Figure 3

becomes available. DPL permits this information to be grouped by any information in the columns, permitting rapid comparison of the data. For example, specimens can be grouped according to alloy, exposure site or depth of exposure and then listed in order of increasing exposure time. While it does not appear that the data available will lend itself to statistical prediction of service life, an attempt will be made to evaluate such factors as differences in exposure sites, and relative alloy performance.

In the course of this search, numerous articles were reviewed which contained no quantitative data. While such information could not be cataloged, it will be included in a complete discussion of the proper use and design with aluminum alloys for corrosion resistance. This discussion will include such factors as the effect of velocity, galvanic coupling, pollutants, and any relevant service experience with aluminum heat exchangers both with respect to corrosion and biofouling prevention.

REFERENCES

(1) J. R. Willard and R. B. Mears, "Aluminum in Refrigerating Equipment", Refrig. Eng., 40, 381 (1940).

(2) R. A. Bonewitz, "Corrosion of Aluminum in Ammonia-Water Mixtures", Alcoa Laboratories Report, March 15, 1973.

(3) R. A. Bonewitz, "Concurrent Studies of Enhanced Heat Trasnfer and Materials for Ocean Thermal Exchangers", Final Report Energy Research and Development Administration Contract No. E(11-1)-2641, February, 1977.

# CORROSION FATIGUE OF 5086-H34 ALUMINUM IN SEA WATER

STEVEN P. FLODDER AND WILLIAM H. HARTT
*Department of Ocean Engineering*
*Florida Atlantic University*
*Boca Raton, Florida*

## Abstract

Failure due to fatigue is often a significant problem in structural marine applications involving cyclic or time variable stresses. In OTEC Heat exchangers fatigue and corrosion fatigue of materials may well result from vibratory motion of the sea water and working fluid as these flow past or through metal components of the system. If the phenomenon of corrosion fatigue is not properly integrated into the materials selection and engineering design aspect of OTEC system development, then unexpected, premature failure of important components could result.

Aluminum alloys are prime candidates for the material of construction of OTEC heat exchange systems. While the corrosion properties of the 5xxx (aluminum-magnesium) alloys in sea water have been studied in some detail, the same is not true with regard to corrosion fatigue. Particularly lacking are corrosion fatigue data for aluminum alloys where a) the tests were performed in actual flowing sea water and b) where tests extended to the high cycle range. It was with these data gaps in mind that the present experiments were undertaken.

The present research involved corrosion fatigue crack growth rate determination for 0.500 inch thick, symmetrical center cracked plate specimens of 5086-H34 aluminum in both air and sea water. Limited experiments employing cathodic protection were also conducted. The data is presented as plots of crack growth rate as a function of stress intensity. Ranges of stress intensity where corrosion is most detrimental with regard to fatigue crack growth rate and where cathodic protection is most advantageous are made apparent. Importance of the experimental results with regard to OTEC systems is discussed.

## Introduction

Many comments have been made, and will continue to be made, concerning the importance of proper materials selection and proper design for corrosion prevention in Ocean Thermal Energy Conversion applications. Corrosion damage can occur in numerous forms, including uniform, galvanic, pitting, crevice, intergranular, dealloying, velocity and environmental cracking (1-3). The last of these (environmental cracking) can be particularly harmful in that the combined interaction of a tensile stress, either applied or residual, and a corrosive environment often results in brittle fracture under conditions where ductile behavior would otherwise be expected. An important form of environmental cracking is corrosion fatigue, and it is toward this topic that the present paper is directed.

The phenomenon of fatigue is a consequence of cyclic or time dependent stresses. Variables that are influential with regard to fatigue may, in general, be characterized as mechanical, material and environmental. These are tabulated in Table I along with the most important examples of each. Because it is not the objective of this paper to review and/or pursue these in detail, readers with such interests are referred to any of a number of comprehensive treatments which are available. (4-10).

There has historically been a great deal of research effort in the field of fatigue and corrosion fatigue, and this has resulted in a variety of experimental techniques and procedures. However, the types of test generally involve three specimen geometries: smooth, notched, and pre-cracked. Data for the first two is commonly presented as a plot of maximum stress per cycle (S) versus cycles to failure, N, (S-log N). A schematic representation of this is presented in Figure 1 for each of these two cases. Thus, cycles-to-failure increases with decreasing stress. For certain materials, such as ferrous alloys fatigued in air or a mildly corrosive electrolyte, an endurance or fatigue limit is reached below which failure does not occur irrespective of the number of cycles. No limiting stress is apparent, however, for

| Variable | Example |
|---|---|
| 1. Mechanical | a. Stress or stress intensity range |
| | b. Mean stress |
| | c. Frequency |
| | d. Stress wave form |
| 2. Material | a. Alloy chemistry |
| | b. Alloy microstructure |
| 3. Environment | a. Temperature of environment |
| | b. Phase make-up and chemistry of environment |

Table 1
Important Fatigue Variables with Examples of Each

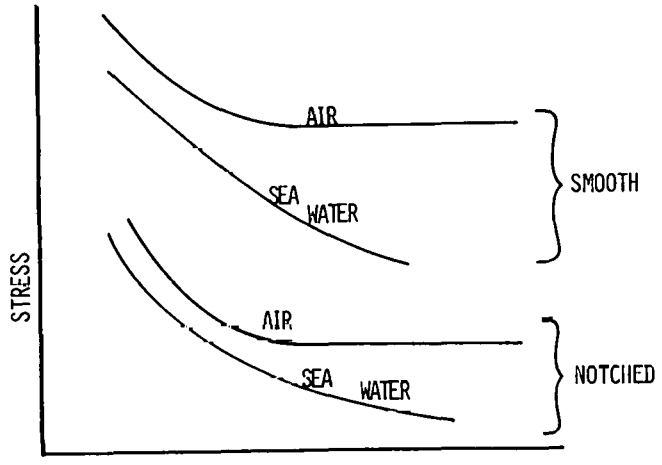



Figure 1
Schematic S-logN curves for smooth and notched specimens in both air and sea water

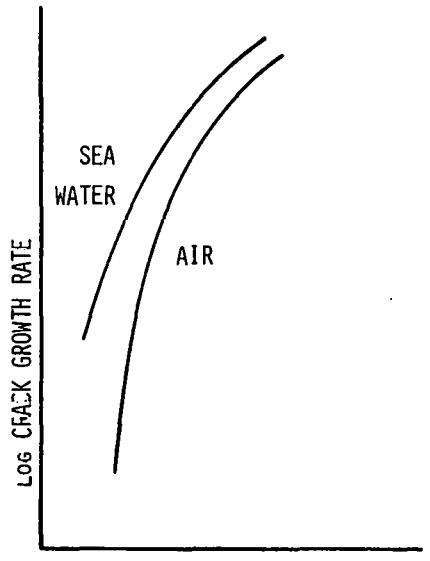



Figure 2
Schematic plot of fatigue crack growth rate versus stress intensity for air and sea water environments

more severe corrosion exposures such as would result in aerated sea water. (11,12). This situation also is shown in Figure 1. Most non-ferrous alloys, including aluminum (but not titanium), do not exhibit an endurance limit even in air.

An alternate approach to fatigue testing and research involves pre-cracked specimens. The test philosophy here considers that cracks or flaws are invariably present in commercial materials and that fatigue life simply involves the cycles required for these to grow to critical size (13, 14). A schematic illustration of how crack growth rate data is represented in this case is shown in Figure 2. Also indicated is that a corrosive environment generally accelerates crack growth rate relative to the air case. Numerous experiments involving smooth, notched and pre-cracked specimens have shown the influence of environment upon fatigue to increase with decreasing stress and with decreasing stressing rate.(15)

The present experiments were intended as an initial investigation of corrosion fatigue of an aluminum alloy in sea water. A procedure involving precracked specimens was selected because this permits obtaining considerable information from relatively few tests. Of particular interest was the range of low stress intensities where little data is presently available.

## Experimental Procedure

Fatigue tests were conducted using an MTS Model 812 servohydroaulic unit programmed for a positive sine wave and a frequency of 20 Hz. Center cracked specimens were sectioned and machined from a 0.500 inch (1.27 cm) thick plate of 5086-H34 aluminum to the final dimensions shown in Figure 3. Geometry of the initial center notch and starter crack conformed to criteria specified in the literature (16). This involved a jeweler's saw cut that was extended from the central hole normal to the rolling direction and a fatigue crack that was started from this by high amplitude cycling. As the crack extended, the load range was systematically reduced; and crack growth rate data was taken only after the total crack length, 2a, exceeded 1.000 inches (2.54 cm). Care was taken to ensure that the plastic zone size at the crack tip was indicative of the appropriate stress intensity range and not to a prior, higher stress cycling condition. Stress intensity range, $\Delta K$, was calculated according to the procedures of Tada et al, (16) and the R parameter ($K_{min}/K_{max}$) equaled 0.1 in all cases.

The specimen face was polished through 4/0 silicon carbide paper, and that region across which the crack was to propagate was scribed with reference lines 0.100 inches (0.254 cm) apart. Crack length as a function of the number of cycles was recorded by momentarily stopping the machine and viewing the specimen with a microscope and calibrated eyepiece at 30X.

Environment for tests in air was that common to the laboratory for which relative humidity ranged between 45 and 65 percent and temperature between 22 and 26° C. For the sea water tests a plexiglass bath was constructed and sealed about the specimen with General Electric silicone

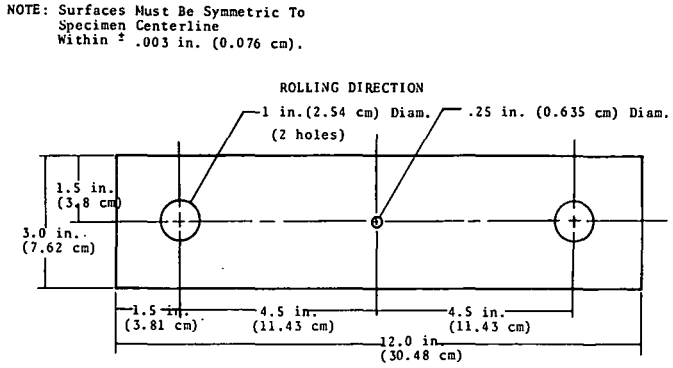



Figure 3
Geometry of center cracked plate specimens

A gravitational feed arrangement from a head tank provided a continuous, non-recirculating flow of approximately 1.3 liters per hour. The sea water was obtained from the FAU Marine Materials and Corrosion Laboratory which employs a wellpoint and all-plastic pump and delivery line. Thus, the water was filtered and virtually free of fouling organisms.

Corrosion potentials were measured with respect to a saturated calomel reference electrode (SCE). Constant potential tests involved a rectangular platinum counter electrode screen positioned on each side of the specimen and facing the fatigue crack. Selected potential values were achieved using a Wenking Model 68 FRO.5 potentiostat.

## Results and Discussion

The purpose of the present experiments was to establish the stress intensity dependence of fatigue and corrosion fatigue crack growth rate for the alloy in question. Figure 4 illustrates the resultant data for the case of tests in air. The trend that is apparent from this is typical of low stress intensity range fatigue, as illustrated above in conjunction with Figure 2. Since the data shown here is from three different specimens, it is apparent that experimental scatter from one specimen or test to the next is relatively small. An important aspect of the curve in Figure 4 is that any threshold stress intensity range apparently lies below 2.0 ksi $\sqrt{in}$ (1.8 MN·m$^{-3/2}$). Also evident is a slope change in the crack growth rate curve at a stress intensity range of approximately 10 ksi $\sqrt{in}$ (9 MN·m$^{-3/2}$).

In Figure 5 the air fatigue curve is reproduced in order to facilitate comparison with data from tests in sea water which are also shown. Thus, above a stress intensity range of approximately 4.5 ksi $\sqrt{in}$. (4.0 MN·m$^{-3/2}$) fatigue crack growth rates in air and sea water were the Below this value the two curves initially diverge

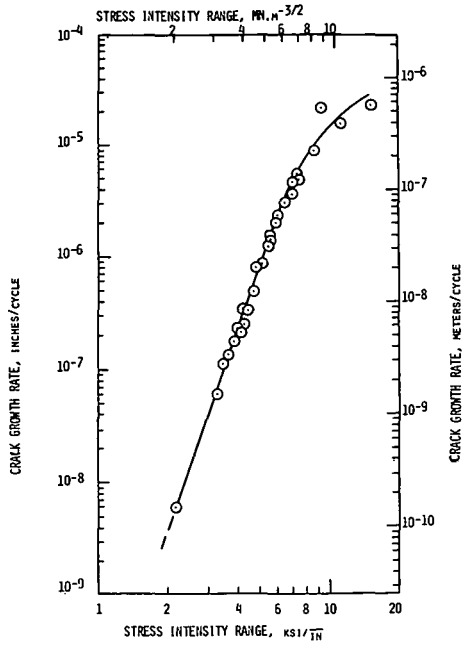



Figure 4
Fatigue crack growth rate versus stress intensity range for 5086-H34 aluminum in air

with a maximum enhancement of sea water fatigue crack growth rate relative to that in air by a factor of approximately 15 for a stress intensity range of 2.0-2.5 ksi $\sqrt{in}$. (1.8-2.25 MN·m$^{-3/2}$). Below this value the data suggests that the two curves again converge and possibly establish a threshold for fatigue crack propagation near 1.8 ksi $\sqrt{in}$. (1.6 MN·m$^{-3/2}$).

During the course of the above tests in sea water, corrosion potential was periodically measured with a digital voltmeter and saturated Calomel reference electrode. Values ranged from -0.70 volts when the specimen was first placed in the bath to near -0.90 volts as failure was approached. Thus, a generalized potential trend was evident, but no unique relationship between this parameter and stress intensity range or crack length could be established.

Experimental results for constant potential tests at -1.00 and -1.30 volts (SCE) are presented in Figure 6. Thus, cathodic polarization to the former value (-1.00 volts) reduced fatigue crack growth rate in sea water to the same values as for laboratory air. Even more distinct are the data for polarization to -1.30 volts. In this case an apparent threshold near 4.5 ksi $\sqrt{in}$ (4.0 MN·m$^{-3/2}$) is noted. As stress intensity range was increased to above this value, crack growth rate increased sharply and merged with the air curve. The data points with arrows indicate that no crack growth was detected during several million stress cycles for each of the indicated stress intensity ranges, and propagation rate was less than the value indicated. The order of testing for this specimen involved first fatiguing at a low stress inten-

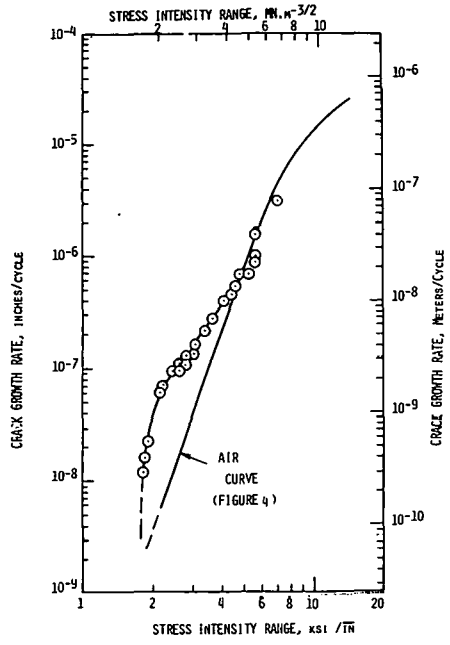



Figure 5
Fatigue crack growth rate versus stress intensity range for 5086-H34 aluminum freely corroding in sea water

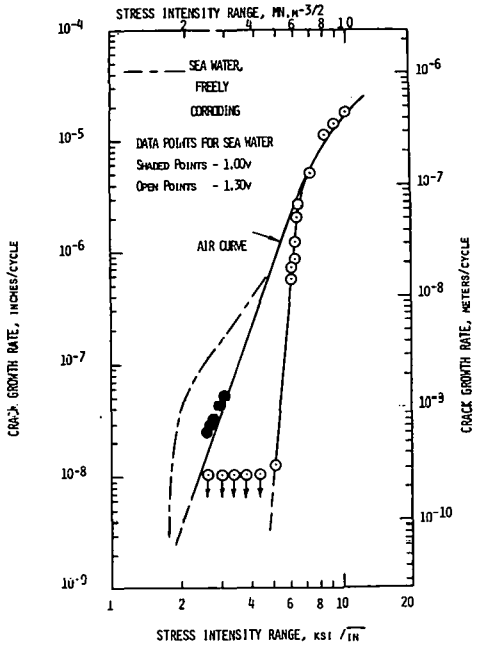



Figure 6
Fatigue crack growth rate versus stress intensity range for 5086-H34 aluminum in sea water at potentials of -1.00 and -1.30 volts, SCE

sity range while freely corroding and, second, polarizing to -1.30 volts followed by incremental increases in stress intensity range.

The relatively high threshold potential for fatigue crack propagation, at least compared to the value for this alloy in air, is indeed interesting and technological significant with regard to structural sea water applications involving 5086 aluminum. Specifically, the present data indicates that cathodic protection is an appropriate technique for halting propagation of corrosion fatigue cracks and thereby for mitigating this form of cracking. There is considerable potential usefulness of this point with regard to Ocean Thermal Energy Conversion systems. In particular, vibration of heat exchange tubes due to fluid flow and other causes can result in fatigue cracking and failure of the plant to properly perform its intended function. The data in Figure 6 suggests, however, that alcladding the sea water side of the tubing should contribute to prevention of such cracking; and, consequently, serious consideration should be given to this in the materials selection phase of the design process. Additional experiments are needed to more completely characterize the effectiveness of cathodic protection in mitigating corrosion fatigue.

## Bibliography


1. M. G. Fontana and N. D. Greene, Corrosion Engineering McGraw-Hill Co., New York, 1967.
2. H. H. Uhlig, Corrosion and Corrosion Control, 2nd Ed. J. Wiley and Sons, Inc., 1971.
3. F. L. LaQue, Marine Corrosion Causes and Prevention, J. Wiley and Sons, Inc., New York, 1975.
4. W. J. Plumbridge and D. A. Ryder, Metall. Rev., 136 (1967) 119.
5. J. C. Grosskreutz, Phys. Status Solidi(b), 47 (1971) 11.
6. J. C. Grosskreutz, Phys. Status Solidi(b), 47.(1971) 359.
7. Corrosion Fatigue: Chemistry, Mechanics and Microstructure, Nat. Assn. Cor. Engrs., Houston, 1972.
8. D. Walton and E. G. Ellison, Intl. Metall. Rev., 17, (1972) 100.
9. ASTM STP 520, Am. Soc. for Test. and Matls., Phila., 1973.
10. N. S. Stoloff and D. J. Duquette, ONR Tech. Rept. N00014-67-A-0117-0010, NR031-745 and N00014-67-A-0117-0012, NR036-093, August 30, 1974.
11. D. McAdam, Jr., Proc. ASTM, 26II(1926) 224; 27II (1927)102.
12. D.J. Duquette and H. H. Uhlig, Trans. ASM, 61, (1968) 449.
13. P.C. Paris, Proc. Tenth Sagamore Army Materials Res. Conf., Syracuse Univ. Press, 1965.

14. H. H. Johnson and P. C. Paris, J. Engr. Fr. Mech., 1 (1968) 1.
J. P. Gallagher, "Corrosion Fatigue Crack Growth Behavior Above and Below $K_{ISCC}$, NRL Rept. May 28, 1970.
16. H. Tada, P. Paris and G. Irwin, Stress Analysis of Cracks Handbook, Del Res. Corp., Hellertown, Pa. 1973, Section 19-9.

# COMPATIBILITY STUDIES FOR THE AMMONIA-TITANIUM-SEAWATER SYSTEM AS RELATED TO OCEAN THERMAL ENERGY CONVERSION

E. W. Saaski and P. C. Owzarski
*SIGMA RESEARCH, INC.*
*2950 George Washington Way*
*Richland, Washington*

Abstract

The objective of this project is to determine if titanium is susceptible to stress corrosion cracking (SCC) in ammonia-seawater environments. The scope involves slow tensile strain experiments until failure of titanium rods in pure liquid ammonia, ammonia-water (0.025-1.0%) and ammonia-seawater (0.025-1%) mixtures. Results will be quantified by percent elongation and area reduction at failure, galvanic voltage versus elongation and by microscopic analysis of SCC crack growth. Preliminary rapid strain experiments showed that the Ti specimens became highly anodic before failure and that repassivation occurred slowly, but at a somewhat faster rate in liquid ammonia-1½% seawater than in anhydrous ammonia. Small amounts of gas appeared on the Ti specimen under strain in anhydrous ammonia. White precipitate appeared in liquid ammonia (0.27-5%)-seawater mixtures and in seawater (1-5%)-ammonia mixtures. The nature and possible role in fouling and corrosion of these precipitates is addressed.

## Purpose, Objectives, Methodology

Materials for the heat exchangers in OTEC plants must be able to withstand a normally hostile marine environment on the seawater side and a nonaqueous working fluid on the evaporator side. Since titanium normally has shown outstanding corrosion resistance to seawater and since ammonia appears to be the chosen OTEC working fluid, serious consideration has to be given to the compatibility of titanium to the two environments and to combinations of the two: mixtures of seawater in ammonia and ammonia in seawater, both mixtures being possible because of heat exchanger leaks. Since a paucity of data exists for titanium corrosion in these mixtures, this project was initiated to fill part of the knowledge gap, i.e. to find out if titanium is susceptible to stress corrosion cracking (SCC) in ammonia and in ammonia containing small amounts of seawater.

If any single mechanism was solely responsible for SCC, it might be possible to predict a priori to any experiments whether SCC was likely in a given system. No single mechanism seems to explain all SCC phenomena and it is unlikely for one to be found for this controversial subject. Frequently failure occurs along grain boundaries (intergranular) and sometimes it occurs across grain structures (transgranular). In all cases, the material is under tensile stress. One explanation of SCC involves the rapid migration of hydrogen formed cathodically to the advancing edge of the crack. The hydrogen apparently embrittles the metal. Another suggests a self renewal of advancing fresh, highly anodic surface to propagate the crack with older passivated surfaces serving as a cathode. Because each metal environment situation can behave differently, only experimental tests or field failures will provide knowledge of SCC phenomena.

The general corrosion of titanium in either seawater or anhydrous ammonia is small due to its passive oxide coating but the possibility of insidious SCC could lead to catastrophic results in closed, high pressure systems containing liquid ammonia. Titanium alloys have a history of susceptibility to SCC in aqueous chloride solution and methanol, bromine, hydrogenated hydrocarbons and other organic liquids. Ammonia and methanol have similar solvent properties. For this reason, a systematic experimental approach was established to determine if SCC was possible in ammonia with small amounts of seawater present. The objectives of this experimental plan are to determine the effect of ammonia/water/seawater mixtures on titanium specimen tensile failure. This will be quantified in four ways:

1. percent elongation at failure
2. percentage reduction in area at fracture
3. electrode potential versus elongation
4. microscopic evidence of SCC crack growth in fractured samples.

The planned methodology incorporates a slow tensile strain rate of $10^{-6}$ mm/mm sec on a titanium rod immersed in ammonia solution. This rate is a compromise between a field situation of static strain and a reasonable test time. The SCC slow strain studies will include the following mixtures at 25 ±5°C:

1. high purity anhydrous liquid ammonia
2. 0.025, 0.06, 0.19 and 1.0 mol % distilled water in liquid ammonia
3. 0.025, 0.06, 0.19 and 1.0 mol % water as seawater in liquid ammonia

4. high purity anhydrous liquid ammonia with dissolved oxygen equivalent to an oxygen partial pressure of 1 atmosphere

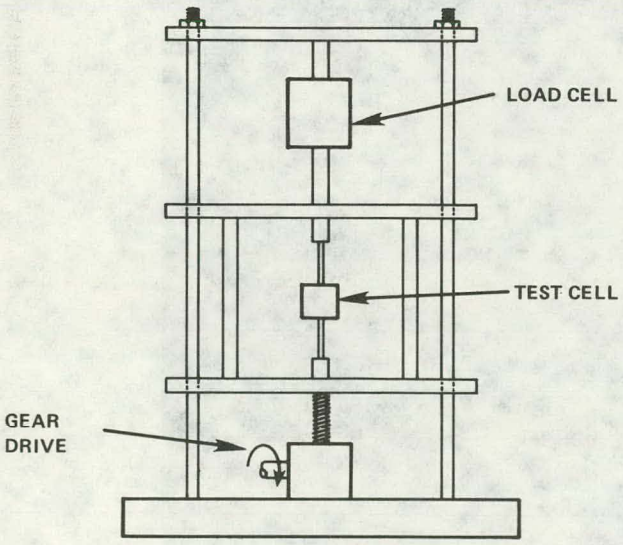
5. steel specimens in anhydrous ammonia to see if the well-known steel cracking in ammonia can be reproduced.

## Preliminary Results and Analysis

Several preliminary rapid strain experiments on titanium were carried out in anhydrous ammonia and in anhydrous ammonia-seawater mixtures. During these tests it was discovered that insoluble sea salt precipitates in liquid ammonia appeared when small amounts of seawater were added to liquid ammonia. Also confirmed was insoluble precipitate formation when small amounts of ammonia are added to seawater. During the rapid strain experiments the need was felt for a good reference potential in liquid ammonia. A $Cd/CdCl_2$(sat) electrode has given good results for this type of experiment.(1)

## Equipment Design

The slow strain experimental measurements are to be carried out at Electrochemical Technology Corporation, Seattle, under the direction of T. R. Beck. A schematic drawing of the constant strain-rate-mechanism is shown in Figure 1. The design and construction of that apparatus and the slow strain test cell are complete. The details of the latter are shown in Figure 2. The titanium test rod in the ammonia chamber is held in two Teflon sleeves and put under tensile stress until failure.




B. CONSTANT-STRAIN-RATE MECHANISM

FIGURE 1. CONSTANT SLOW STRAIN APPARATUS FOR STRESS CORROSION CRACKING AND HYDROGEN EMBRITTLEMENT STUDIES

7704-90.1

## Preliminary Rapid Strain Tests

Some preliminary rapid tensile strain tests were carried out in liquid ammonia and liquid ammonia containing small amounts of seawater to get approximate magnitudes of failure stresses, galvanic currents and potentials during and after the strain test and visual observations of failed specimens. Figure 3 shows a broken titanium specimen in anhydrous ammonia. The surprising appearance of gas bubbles on the specimen led to conjecture as to its nature. Either hydrogen or nitrogen formation are thermodynamically possible by the reactions:

$$3Ti + 2NH_3 \rightarrow 3TiH_2 + N_2$$

or

$$2Ti + 2NH_3 \rightarrow 2TiN + 3H_2$$

During the rapid strain, the titanium became fairly anodic (~1.0 volt with respect to a mild steel reference). This active state passivated slowly in anhydrous ammonia compared to repassivation in seawater, and somewhat more rapidly in liquid ammonia with 1½ wt.% seawater than in anhydrous ammonia (Figure 4). A plausible explanation for the difference is the presence of dissolved oxygen in seawater and a somewhat more conducting fluid with the seawater salts present. No microscopic evidence of SCC was seen on the failed rapid strain specimens.

## Precipitate Formation and Sea Salt Solubilities in $NH_3$-Seawater Solutions

Sigma Research has observed at room temperature that white precipitates formed in a solution of 1-5% ammonia in seawater and 0.27-5% seawater in liquid ammonia. Because these precipitates might influence corrosion rates by fouling surfaces and by changing the chemical composition of the solution, we have analyzed the potential precipitate causes at both ends of the seawater-ammonia solution spectrum. For the case of small amounts of seawater in ammonia, serious deficiencies exist in available solubility data and the chemical nature of the precipitate and the remaining solution are uncertain. Here $MgCl_2$ seems to be the most likely prevalent precipitate. At the other end of the spectrum, all solubility data seem quite adequate for analysis.

In air-free ammonia-seawater solutions, $Mg(OH)_2$ readily precipitates, and in aerated solutions, $MgCO_2$ and $CaCO_3$ are the expected precipitates. In both air-free and air-saturated cases, over 95% of the precipitating cations no longer are in solution at 1% $NH_3$ concentrations. This could potentially be a major fouling problem on the seawater side of OTEC heat exchangers. Below are more detailed technical discussions of the conditions for precipitate formation and the amounts of precipitates to be expected. It must be emphasized again that analysis of the situation where ammonia is the solvent is not possible at this time because the temperature-dependent solubilities of sea salts, and the dissociation characteristics of water in ammonia are

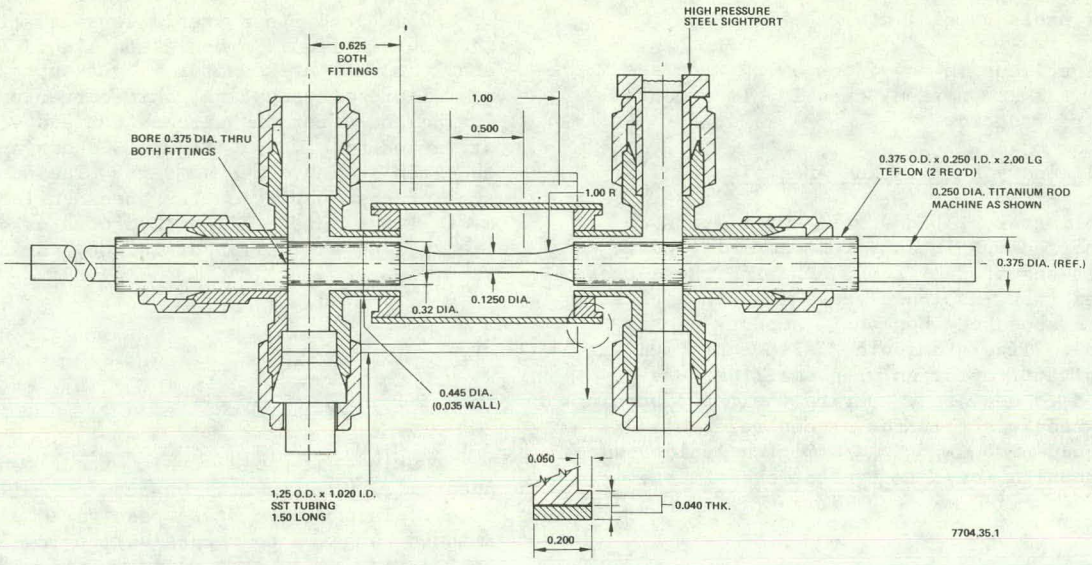



FIGURE 2. SLOW STRAIN TEST CELL

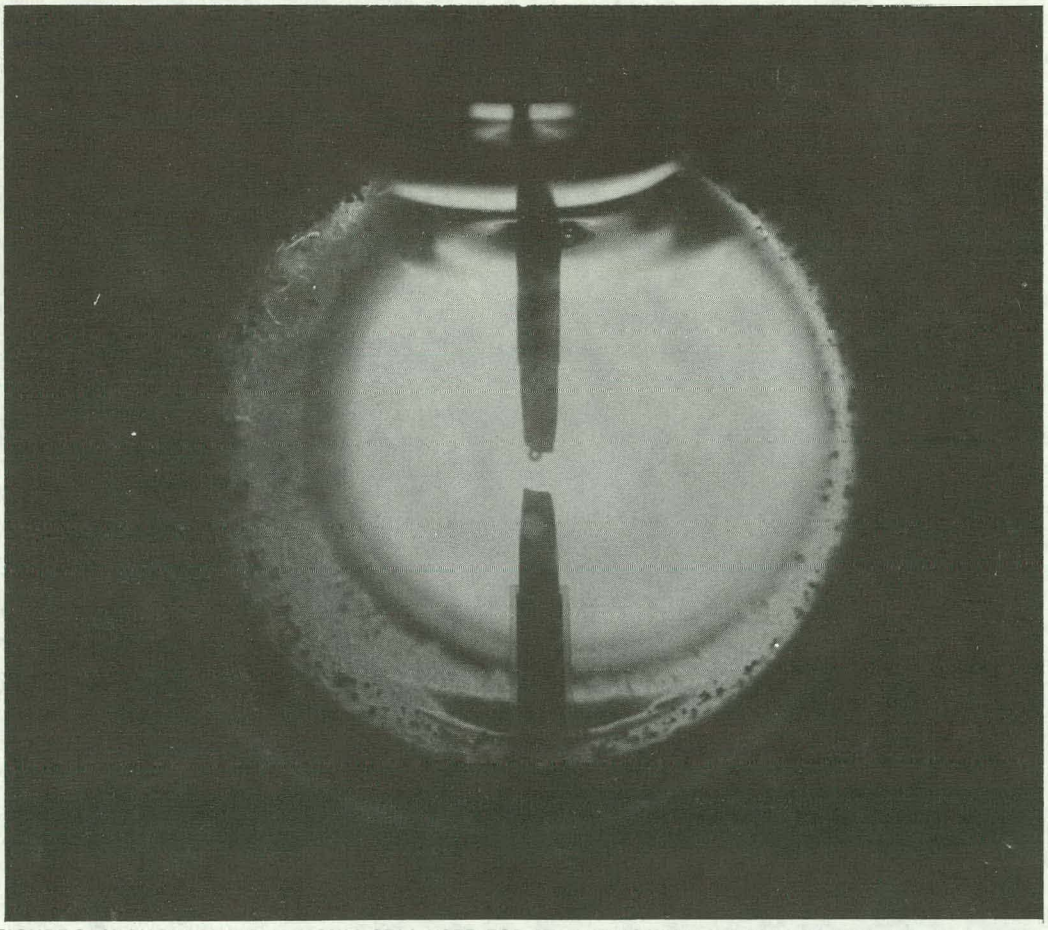


FIGURE 3. HIGH PRESSURE AMMONIA CELL USED FOR STRAINING WIRE SAMPLES TO FAILURE. CELL CONSTRUCTION ALLOWS CONCURRENT MEASUREMENT OF WIRE ELECTRODE POTENTIAL. NOTE GAS BUBBLE GENERATED BY STRAINING TITANIUM WIRE TO FAILURE.

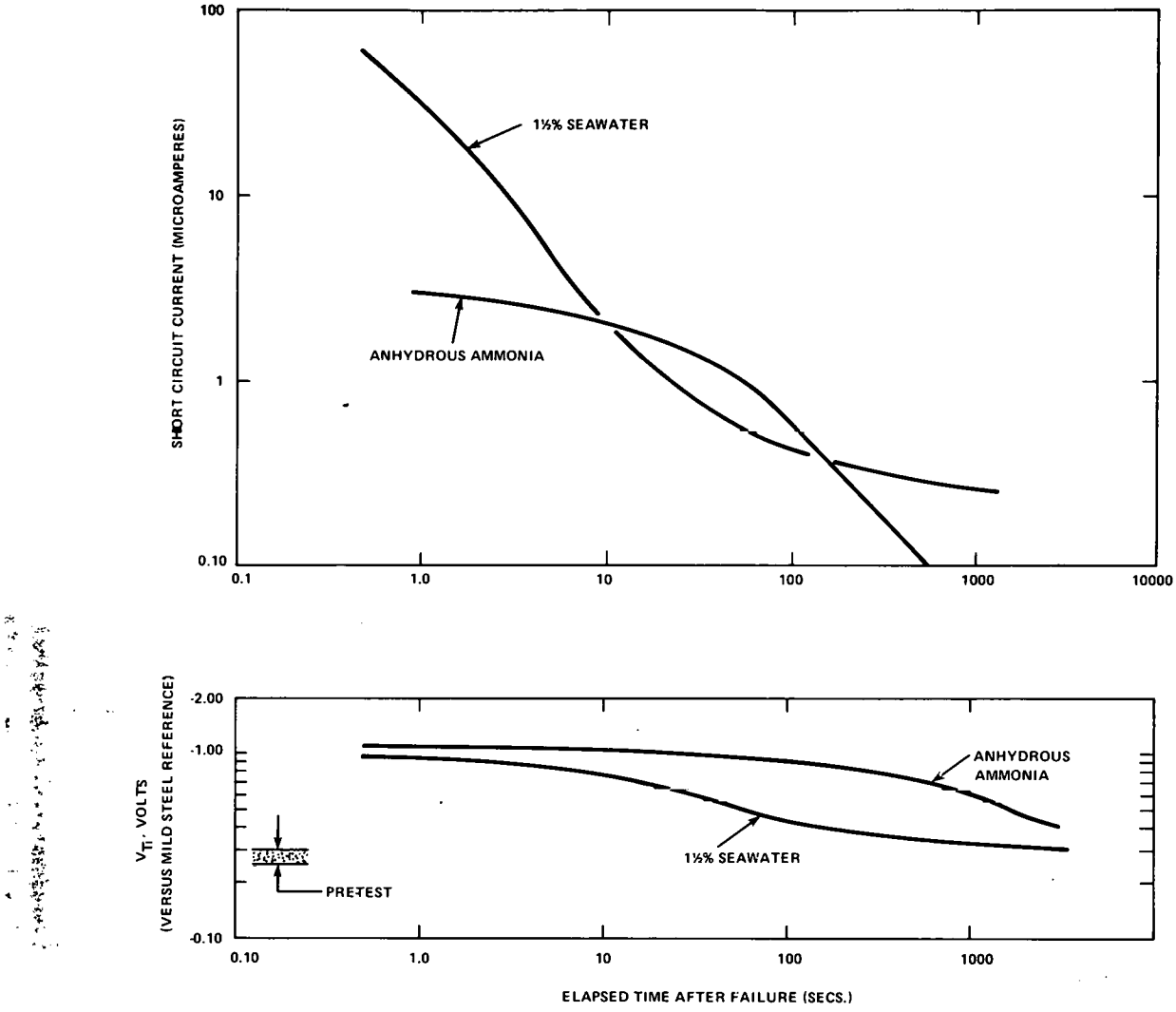



FIGURE 4. RE-PASSIVATION BEHAVIOR OF TITANIUM IN ANHYDROUS AMMONIA AND IN A SEAWATER-AMMONIA MIXTURE

7704-4.2

not known. Hence, the following discussions on seawater in ammonia are speculative.

Low Concentrations of Seawater in Ammonia

Seawater can be classified as a water solution of many inorganic ions. The principal cations and anions with concentrations greater than 10 ppm are listed in Table 1.

In $NH_3$ solutions, both $NH_4^+$ and $OH^-$ become important ions if water is present. The latter is particularly important since $Mg(OH)_2$, $Ca(OH)_2$, and $Sr(OH)_2$ can become precipitates.

From known solubility data in pure ammonia (data appears most frequently as "insoluble" without quantitative measurements) the observed precipitates appear to be one or more of the following shown in Table 2.

If one considers classes of compounds with similar chemical behavior, and limits an experimental matrix to those present in substantial quantity, or of importance in corrosion, then the salts of interest reduce to the following shorter list: $MgCl_2$, $MgSO_4$, $MgCO_3$, $Mg(OH)_2$, $Na_2SO_4$, $K_2SO_4$, and $CaCO_3$ and $Ca(OH)_2$. These must be investigated individually to get a picture of the composite precipitate. It is not possible to completely deduce the behavior of the eight compounds

Table 1. Principal Ionic Composition of Seawater

| Cation | g-mole/ℓ | eq./ℓ |
|---|---|---|
| $Na^+$ | 0.468 | 0.468 |
| $Mg^{++}$ | 0.0532 | 0.1065 |
| $Ca^{++}$ | 0.0102 | 0.0203 |
| $K^+$ | 0.00989 | 0.00989 |
| $Sr^{++}$ | 0.000151 | 0.00302 |
| | $\Sigma$ = | 0.608 |
| Anion | | |
| $Cl^-$ | 0.545 | 0.545 |
| S as $SO_4^=$ | 0.0532 | 0.1065 |
| C, inorganic | 0.00238 | 0.00475 as $CO_3^=$ |
| | $\Sigma$ = | 0.656 |

Table 2. Potential Precipitates From $NH_3$-Seawater Mixture

| | | |
|---|---|---|
| $MgCl_2$ | $Mg(OH)_2$ | $Ca,SrSO_4$ |
| $MgSO_4$ | $K_2SO_4$ | $Ca,SrCO_3$ |
| $MgCO_3$ | $Na_2SO_4$ | $Ca,Sr(OH)_2$ |

above from measurement of mixed precipitate components. If corrosion and fouling are likely to be influenced by precipitates on the ammonia side of the heat exchangers, it seems advisable that the nature of these precipitates should be determined in order to control them.

Low Concentrations of Ammonia in Seawater

Free ammonia dissolved in pure water significantly raises the pH (c.f. Figure 5). The free $OH^-$ formed is available to precipitate $Mg(OH)_2$ and to absorb $CO_2$ from the atmosphere. Thus the carbonates $CaCO_3$ and $MgCO_3$ are possible insoluble seawater components as well. Since the aqueous solubility products and equilibria of ammonia-water and carbon dioxide-water systems are fairly well understood, the results of an analysis of the pertinent equilibria follow.

Consider the carbon dioxide-water equilibria

$$CO_2 + H_2O \rightleftarrows HCO_3^- + H^+, \; K_1 = K_1' [CO_2] = \frac{[HCO_3^-][H^+]}{} \quad (1)$$

$$HCO_3^- \rightleftarrows CO_3^= + H^+, \quad K_2 \quad (2)$$

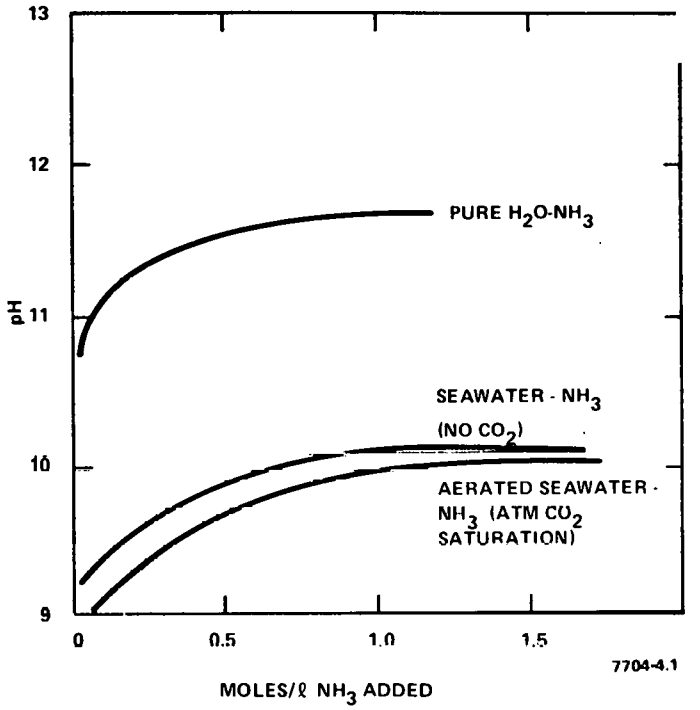



FIGURE 5. pH OF VARIOUS WATER, SEAWATER, $NH_3$ SOLUTIONS, 25°C

and the solubility of $CO_2$ in water as an equilibrium between molecular $CO_2$ in air and water related by a Henry's Law constant

$$[CO_2] = H\, p(CO_2) \quad (3)$$

On a total carbon basis Henry's Law does not hold, but the $CO_2$ activities in both phases must be equal ($[CO_2]$ = $CO_2$ concentration in the liquid phase and $p(CO_2)$ = partial pressure in the gas phase). The pertinent ammonia equilibrium is

$$NH_3 + H_2O \rightleftarrows NH_4^+ + OH^-, \quad K_4 \quad (4)$$

and water dissociation

$$H_2O \rightleftarrows H^+ + OH^-, \quad K_3 \quad (5)$$

The three solubility equilibria of interest are

$$Mg^{++} + 2OH^- \rightleftarrows Mg(OH)_2 \downarrow, \quad K_5 \quad (6)$$

or

$$Mg^{++} + CO_3^= \rightleftarrows CaCO_3 \downarrow, \quad K_6 \quad (7)$$

$$Ca^{++} + CO_3 \rightleftarrows CaCO_3 \downarrow, \quad K_7 \quad (8)$$

With an ion balance, eight equations and eight unas give a biquadratic equation for one of the varis, e.g. if we assign

a = initial concentration $Mg^{++}$, moles/ℓ

b = initial concentration $Ca^{++}$, moles/ℓ

c = total $NH_3$ and $NH_4^+$ present in seawater,

then, if $MgCO_3$ is the first of the magnesium salts to precipitate

$$c = \frac{(y + K_4)}{K_4}(2a + 2b) + y(1 + K_1/K_3) + \frac{2K_2K_1}{K_3^2}y^2 - \frac{K_3}{y} - \frac{2K_6K_3^2}{K_2K_1y^2} - \frac{2K_7K_3^2}{K_2K_1y^2} \quad (9)$$

where $y = [OH^-]$. If $Mg(OH)_2$ precipitates first, replace $2K_6K_3^2/K_2K_1$ by $2K_5$. All other concentrations can be calculated from the remaining equilibria in proper sequence. Using the following constants for 25°C[2-5]

$H = 3.35 \times 10^{-2}$ moles/ℓ atm

$p(CO_2) = 0.228$ torr (0.0003 atm)

$\therefore K_1 = [HCO_3^-][H^+] = 4.63 \times 10^{-12}$ $(mol/ℓ)^2$

($[CO_2]$ = constant for $p(CO_2)$ = constant)

$K_2 = 4.4 \times 10^{-11}$ mol/ℓ

$K_3 = 10^{-14}$ $(mol/ℓ)^2$

$K_4 = 1.86 \times 10^{-5}$ (mol/ℓ)

$K_5 = 1.6 \times 10^{-11}$ $(mol/ℓ)^3$

$K_6 = 1.0 \times 10^{-5}$ $(mol/ℓ)^2$

$K_7 = 4.8 \times 10^{-9}$ $(mol/ℓ)^2$

We can obtain the values of pH of seawater (Figure 5) for varying $NH_3$ present and also remaining dissolved $Mg^{++}$ and $Ca^{++}$ (Figure 6). For the values chosen, $MgCO_3$ is the controlling precipitate and no $Mg(OH)_2$ forms. The first figure compares the pH of pure $H_2O$-$NH_3$-saturated with atmospheric $CO_2$ and unaerated seawater. Both the atmospheric $CO_2$ saturated seawater and seawater alone serve as a buffer to the $NH_3$ in a complex manner tied to precipitate formation. Precipitates can form in both $CO_2$ free and aerated (saturated with atmospheric $CO_2$) seawater. In the $CO_2$ free system the $Mg^{++}$ ion is more insoluble than in the $CO_2$ saturated seawater for large amounts of $NH_3$ added. $Ca^{++}$ ion is more insoluble than the $Mg^{++}$ ion for the $CO_2$ system, since the $CaCO_3$ solubility product is 2000x smaller than that of $MgCO_3$.

It is necessary to calculate which magnesium compound ($Mg(OH)_2$ or $MgCO_3$) is at the solubility limit in the $CO_2$ system. For atmospheric $p(CO_2) = 9 \times 10^{-5}$ atm, or 30% of normal, $Mg(OH)_2$ is the saturated species. One would expect inorganic carbon to decrease at lower ocean depths, so both precipitates become important in the overall OTEC fouling analysis. Table 3 shows the concentration of precipitate controlling species in seawater solution of $NH_3$ saturated with atmospheric $CO_2$, as $NH_3$ is added. Alternately, if no carbon dioxide is present, the precipitate controlling concentrations are as shown in Table 4.

## Conclusion

The apparent conclusions from this equilibrium analysis are that precipitates readily form in seawater with $NH_3$ addition, with magnesium and calcium carbonates being the dominant species if the seawater is saturated with $CO_2$ at normal atmospheric concentrations and magnesium hydroxide if no $CO_2$ is present. Pytkowicz[6] provides interesting related information about the dynamics of precipitation of $CaCO_3$ supersaturated in seawater. $Mg^{++}$ apparently inhibits $CaCO_3$ precipitate growth rates. The analysis presented here is purely thermodynamic and not kinetic, so conclusions from his paper do not conflict with our conclusions. On the other hand, if our analysis were done on a closed system (i.e. finite $CO_2$ available), we would se $Mg^{++}$ and $Ca^{++}$ competing with each other available $CO_3^{=}$, and we could offer some thermodynamic support for his conclusions.

Although this statement is speculative, the insoluble crystalline precipitate in liquid ammonia after adding small amounts of seawater probably is primarily $MgCl_2$ with 11 other inorganic compounds as minor constituents.

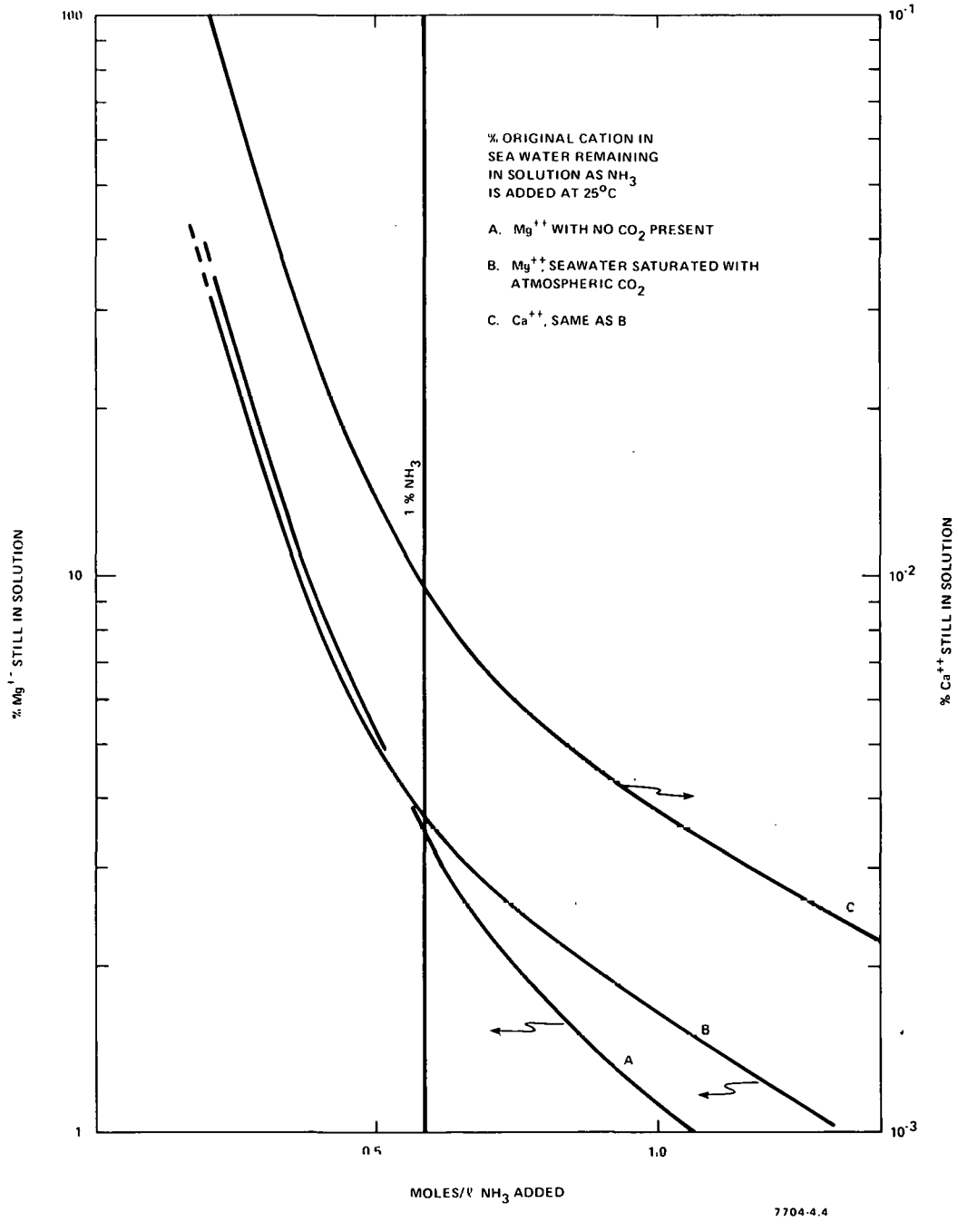



FIGURE 6. PERCENT ORIGINAL CATION IN SEAWATER REMAINING IN SOLUTION AS $NH_3$ IS ADDED AT 25°C

Table 3. Precipitate Controlling Species Remaining Soluble in Seawater as $NH_3$ is Added and Saturated with Atmospheric $CO_2$*

| pH | $NH_3$ Added | $NH_4^+$ | $OH^-$ | $M^{++}$ | $Ca^{++}$ | $HCO_3^-$ | $CO_2^=$ | $CO_2$ |
|---|---|---|---|---|---|---|---|---|
| 9.0 | 0.0447 | 0.0291 | $10^{-5}$ | $4.91 \times 10^{-2}$ | $2.36 \times 10^{-5}$ | $4.63 \times 10^{-3}$ | $2.04 \times 10^{-4}$ | $10^{-5}$ |
| 9.4 | 0.294 | 0.125 | $2.5 \times 10^{-5}$ | $7.81 \times 10^{-3}$ | $3.77 \times 10^{-6}$ | 0.0116 | $1.28 \times 10^{-3}$ | $10^{-5}$ |
| 9.7 | 0.576 | 0.156 | $5 \times 10^{-5}$ | $1.96 \times 10^{-3}$ | $9.42 \times 10^{-7}$ | 0.0332 | $5.10 \times 10^{-3}$ | $10^{-5}$ |
| 10.0 | 1.369 | 0.213 | $1 \times 10^{-4}$ | $4.91 \times 10^{-4}$ | $2.36 \times 10^{-7}$ | 0.0463 | $2.04 \times 10^{-2}$ | $10^{-5}$ |

*All concentrations in mol/ℓ.

Table 4. Precipitate Controlling Species Remaining Soluble in Seawater as $NH_3$ is Added - No $CO_2$ Present

| pH | $NH_3$ Added | $NH_4^+$ | $OH^-$ | $Mg^{++}$ |
|---|---|---|---|---|
| 7.8-8 | 0 | 0 | $10^{-6}$ | 0.0532 |
| 9.25 | 0.0447 | 0.025 | $1.8 \times 10^{-5}$ | 0.0415 |
| 9.65 | 0.294 | 0.089 | $4.5 \times 10^{-5}$ | $8.25 \times 10^{-3}$ |
| 9.9 | 0.576 | 0.102 | $7.9 \times 10^{-5}$ | $1.86 \times 10^{-3}$ |

*All concentrations in mol/ℓ.

References


1. D. A. Jones and B. E. Wilde, "Corrosion Performance of Some Metals and Alloys in Liquid Ammonia," Corrosion-NACE, 33, No. 2, p. 46-50, February 1977.

2. Handbook of Chemistry and Physics, 50th Ed., Chemical Rubber Co., Cleveland, 1969-70.

3. L. J. Curtman, Introduction to Semimicro Qualitative Analysis, McMillan, N.Y., 1950.

4. W. J. Blaedel and V. W. Meloche, Elementary Quantitative Analysis, Row, Peterson, Evanston, IL, 1957.

5. J. Chr. Gjalkback, Atca Chem. Scand., 1, p. 537-544 ($CO_2$ Solubility).

6. P. M. Pytkowicz, "Calcium Carbonate Retention in Supersaturated Seawater," Am. J. Sci., 273, p. 515-522.

# DESIGN FACTORS INFLUENCING BIOFOULING AND CORROSION OF OCEAN THERMAL ENERGY CONVERSION HEAT EXCHANGERS

J. F. JENKINS
*Civil Engineering Laboratory*
*Naval Construction Battalion Center*
*Port Hueneme, California*

ABSTRACT

The ability to obtain and maintain high levels of heat transfer efficiency is a major factor in the technical and economic feasibility of Ocean Thermal Energy Conversion (OTEC) power plants. A major factor in the efficiency of heat transfer through a material is the presence of surface films of low thermal conductivity. Nearly all materials will, when exposed to the ocean environment, quickly become covered with either a biological slime film, a corrosion product film, or both. Those initial films may be of sufficient thickness to severely limit the feasibility of OTEC plants. Also, if allowed to follow their natural course, these films will become thicker with time and further inhibit heat transfer.

While the nature of the metal surface has a primary influence on the formation of both biological and corrosion films other factors may also influence film formation. As the number of practical heat exchanger materials is limited by other factors to materials which are not inherently resistant to film formation, the inhibition of film formation must be accomplished by manipulation of those other factors.

The factors which can be manipulated to inhibit film formation fall into two broad catagories: Mechanical and Environmental. Mechanical factors include the geometry, orientation, layout, surface finish and location of the heat exchangers. Environmental factors include the chemical characteristics of the seawater, its velocity, flow regime, temperature and pressure.

This paper discusses the possible effects of these factors on biological and corrosion film formation on OTEC heat exchangers.

## Introduction

Heat exchangers are perhaps the most critical components of the Ocean Thermal Energy Conversion (OTEC) power plants using the closed cycle. These heat exchangers will be large, expensive and must maintain heat exchange capacity and leak resistance under difficult operating conditions. In many cases it has been assumed that the selection of a heat exchanger tube material is the final step in the corrosion and fouling control of a heat exchanger. Experience in corrosion and fouling control have shown that many factors other than material selection affect the ultimate performance of these systems. These factors can, when identified, often be controlled in the overall system design. These design factors are of two basic types: Mechanical and Environmental.

## Mechanical Design Factors

Typical mechanical design factors are: geometry, orientation, layout, surface finish and location. These, and other factors, may affect the corrosion of OTEC heat exchangers in two basic ways. They may either affect the amount or form of corrosive attack which occurs, or the effect of the corrosive attack on the performance of the heat exchangers. Ease of maintenance and repair are also design related factors which can influence the overall performance of the heat exchangers. An example of a mechanical design factor which may influence the corrosion of OTEC heat exchangers is geometry. It is well known that fluid turbulence adversely affects the performance of many heat exchanger materials. A good design promotes smooth flow conditions by avoiding sharp changes of flow direction or velocity. A poor design which results in turbulence may cause some heat exchanger materials to experience accelerated local attack.

Orientation may affect the corrosion of OTEC heat exchangers in many ways. For example, corrosion products or debris may collect on horizontal surfaces under stagnant or low velocity flow conditions. These accumulations may result in the accelerated corrosion of many materials due to concentration cell corrosion. Surface finish can affect both local turbulence and debris accumulation. Location primarily influences the maintainability of the heat exchangers.

Mechanical design factors can also affect biofouling by either affecting the type of biofouling which occurs, the rate of its accumulation or the case of its removal. For example, fouling organisms, usually tend (all factors being equal) to attach and grow on the upper side of horizontal surfaces in preference to vertical surfaces or on the lower side of horizontal surfaces. This should be taken into account in the design of the heat exchangers so that this heavier accumulation can be either tolerated or easily removed.

## Environmental Design Factors

Factors such as flow velocity, chemical composition, temperature, and pressure can be considered as envi

mental factors which can be controlled by design. These ors can also affect both the biofouling and corrosion TEC heat exchangers. Many materials show vastly ...erent corrosion behavior over the range of velocities being considered for OTEC heat exchangers. Some materials corrode more rapidly under conditions of high velocity flow whereas some materials corrode more rapidly under low flow conditions. The velocity of flow in the heat exchangers must be tailored to the tube materials. The chemical composition of seawater may vary significantly between various sites and between various depths. These variations in composition may significantly affect the corrosion of many materials. Chemical treatments such as chlorination to control fouling may also affect the corrosion of many materials. Temperature and pressure over the ranges expected for OTEC plants have not been shown to have gross effects on corrosion but should not be ignored as very subtle effects may significantly affect the overall corrosion performance of OTEC heat exchangers.

The effect of environmental design factors on biofouling may prove to be a very important factor in the performance of OTEC heat exchangers. There is known to be a wide difference between the types of fouling which are present in shallow ocean water and in deep ocean water. Fouling in shallow water consists of both plant and animal forms, is very prolific and is normally limited by the avalability of nutrients in the seawater. Both micro-fouling and macro-fouling are prevalent in shallow ocean environments. Micro-fouling organisms are the very small, simple organisms which form soft and thin films on nearly any surface soon after exposure to seawater. In ordinary applications, this "primary film" of micro-organisms is of little consequence except that it is the usual substrate for the attachment of the larger, thicker and often hard shelled organisms usually described as macro-fouling organisms. In OTEC heat exchangers however, this thin "primary film" may inhibit heat transfer to the extent that it must be prevented or removed.

In the deep ocean both micro and macro fouling organisms are present although they are much less prolific than their shallow ocean counterparts. Only animal life is active in the deep ocean and its growth is limited primarily by the availability of chemical energy in its food; primarily detritus from the shallow water above. Although macro-fouling is present, the deep ocean microfouling organisms are much more prevalent. It must not be assumed that the deep ocean is a sterile environment and that significant deterioration of heat exchanger efficiency will not occur due to the formation of biological films in these environments.

Velocity is another important factor in biofouling of OTEC heat exchangers. It is well known that a velocity which induces sufficient fluid shear stress at a surface can prevent the attachment of fouling organisms. If this velocity is maintained, then fouling can be prevented. However, if the velocity falls below this critical level for short periods, organisms can attach and survive subsequent high velocities.

Pressure, or rather pressure change, may have a pro- effect on biofouling of OTEC heat exchangers. It is possible that the sudden release of the pressure of the deep ocean as deep water is brought to the surface may inhibit the subsequent growth of the deep ocean fouling organisms.

## Conclusions

Many factors other than materials selection will markedly affect the biofouling and corrosion of OTEC heat exchangers and the effect of this biofouling and corrosion on OTEC plant efficiency. Optimum OTEC plant efficiency can only be attained if these factors are incorporated into the plant design.

# HYDRODYNAMIC CONTROL OF BIOFOULING IN OTEC HEAT EXCHANGERS

J. S. TENNANT AND M. A. WOOD
*Department of Ocean Engineering*
*Florida Atlantic University*
*Boca Raton, Florida*

## Abstract

The work described in this paper addresses an effort to determine the relationship between hydrodynamic boundary layer parameters and biofouling. Wall shear stress is shown to be an important parameter and its relationship to biofouling is examined in detail. Seawater flow parallel to a flat plate with a laminar boundary layer is used to insure that experimental conditions exist in which a known wall shear stress distribution has been established. The tests were conducted in a submerged water tunnel attached to a dock at Virginia Key in Miami, Florida. The results of the experiments clearly indicate a limiting value of wall shear stress exists, which effectively inhibits attachment of the macrofouler under study, the acorn barnacle (Balanus spp.). Reported growth rates from other studies are presented to substantiate these results. Recommendations for additional hydrodynamic investigations in dealing with biofouling are made.

## Introduction

The economic feasibility of Ocean Thermal Energy Conversion is dependent in large part on the design operation and maintenance of an efficient heat exchanger system (1). Quite obviously, like any system exposed to fouler-laden seawater, OTEC plans will be subjected to various degrees of biofouling, the magnitude of which will drastically effect the efficiency of the heat exchanger. In addition, any auxiliary components such as pumps, diffusers, seawater piping systems which will be exposed to the fouling environment will suffer various degrees of failure or losses of efficiency necessitating the use of backup systems to compensate for required off-line repair. The ability to control or eliminate this biofouling in critical areas will therefore greatly effect OTEC's ultimate success.

## Previous Work

Until recently biofouling has been examined primarily from a biological point of view. Much attention has been focused on the detailed growth cycle and mechanism of attachment, in order to assist in the development of anti-fouling coatings which may be applied to potential fouling surfaces, and toxins which may be injected into the fouling environment (2).

For years, biologists and mariners have observed that a relationship also existed between fouling growth rates and flow velocity. Historically, ships that spend most of their time at sea have less problems with fouling than those that remain in port. In seawater piping systems, pipes with higher velocities tend to foul less often than those with lower velocities. The documentation of this effect has usually been made by biologists as secondary observations to biological experiments. Several experimenters have tried to relate growth rate to fluid velocity, reasoning that if the drag force on the attaching organism exceeded its ability to grasp the surface, it would be unable to attach. Most of these experiments were carried out without regard to the more obvious boundary layer parameters such as wall shear stress. Of the few cases where boundary layer parameters were considered, limited control of the hydrodynamic environment and misapplication of basic hydrodynamic concepts leave doubts as to the accuracy of the results.

The most detailed investigation to date was conducted by D.J. Crisp in 1955 (3). He attempted to relate barnacle cyprid attachment to the velocity gradient that exists within the boundary layer. He used several methods to determine this relationship including: injections of fouler laden water between rotating discs, a flat plate immersed in a water trough subject to flows maintained by water jets, and finally the observation of isolated barnacle cyprids as they were injected into glass tubes of various diameters subject to various velocities. The first two experiments were such that the wall shear stresses could not be accurately correlated to other measurable quantities describing the experiment. The third experiment, although still subject to minor hydrodynamic inaccuracies, was the most realistic for relating growth rate to velocity gradient. Crisp's method of experimentation was to introduce individual cyprids, by means of a pipette, into a glass tube approximately 1.5 meters long in which it was assumed laminar flow conditions existed (a subcritical Reynolds number was maintained). Tube radii varied from 1.1 mm to 3.2 mm. Although this experiment was the most accurate hydrodynamically of those attempted by Crisp, it is subject to some doubt. It is quite possible that the tubes were not of sufficient length to insure a fully developed laminar flow. In addition, the ratio of the size of the cyprids to the radius of the tube was relatively large and may have increased local flow velocities resulting in invalid velocity gradient calculations.

The relationship developed by Crisp was expressed in terms of the percentage of cyprids which were able to attach to the tube walls versus the velocity gradient at the wall. At very low gradients, less than 75 $sec^{-1}$, the cyprids were rolled passively along the surface and

attachment rate was low. The rate increased to a maximum 10 sec $^{-1}$ at which point a sharp decline was indicated. A value of 400 sec$^{-1}$ inhibited most attachment. The low initial values at low velocities compare favorably with biological data which indicates that at low velocities, oxygen availability is too low to provide a suitable environment. Therefore, attachment and growth in general is low. At slightly higher velocities, oxygen availability increases and growth rate is stimulated. The sharp drop in growth rate found by Crisp at velocity gradient values in between 100 sec $^{-1}$ and 300 sec $^{-1}$ equate to shear stress values along the plate of 2.1 to 6.3 x 10 $^{-5}$ psi. The value of velocity gradient equal to 400 sec $^{-1}$ provides a shear stress value of 8.3 x 10 $^{-5}$ psi and indicates a definite maximum value which the cyprids could successfully resist.

## Experimental Approach

In order to examine a wide range of shear stresses simultaneously, and to illustrate the independence of biofouling growth rate and free stream velocity, an experiment was designed to examine a sharp edged flat plate subject to a parallel uniform flow. A flat plate submerged in a uniform flow is the most basic problem of boundary layer theory. A plate subject to such a flow will develop a boundary layer which separates the plate from the free stream flow (4). Initially the boundary layer is laminar; meaning that rapid random fluctuations in velocity are not present and a series of lamina or layers with gradually increasing velocities exist (velocities along the plate are zero and velocities at the outer edge of the boundary are equal to the free stream values). At some point downstream from the leading edge, the Reynold's number ($U_\infty X/\nu$), reaches a critical value (around 500,000) and the boundary layer becomes turbulent. Blasius first solved the flow situation in the laminar section of a flat plate in 1913, and his results are indicated in Figure 4C-4-1, where shear stress, $\tau_o$, at the boundary is related to velocity gradient by dynamic viscosity.

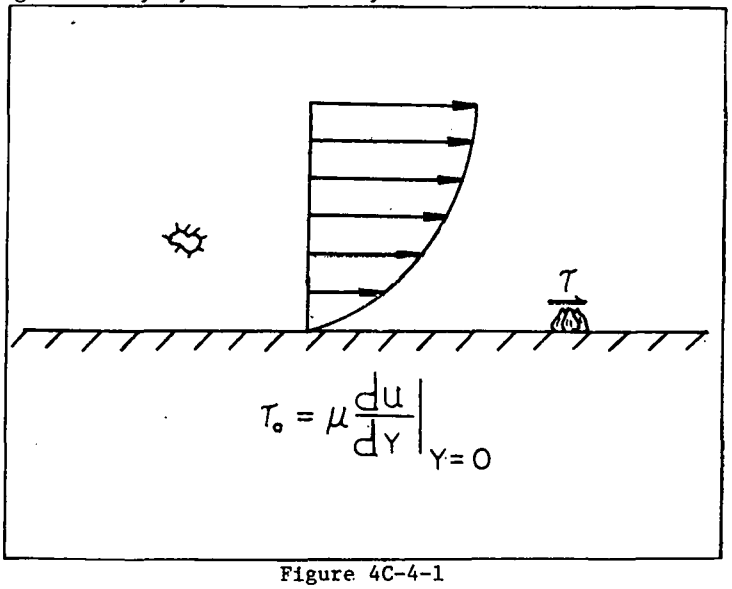



Figure 4C-4-1

A numerical value of wall shear stress can be calculated from the following relationship given by Blasius:

$$\tau_o = .332 \rho \nu^{1/2} U_\infty^{3/2} x^{-1/2}$$

where

$\rho$ - density of the fluid
$\nu$ - kinematic viscosity
$U_\infty$ - free stream velocity
x - distance from leading edge

Thus, if the free stream velocity is known and fluid properties are available, wall shear stress can be calculated for any position, x, along the plate. By measuring the growth rate at a specific location, from the leading edge of the plate (x), growth rate can be correlated to shear stress along the surface.

Looking at the variation of shear stress along the plate, in terms of a non-dimensionalized shear stress, $C_f$ (shear friction coefficient), versus a non-dimensionalized length, expressed in terms of Reynolds number (Figure 4C-4-2), we see that values adjacent to the leading edge are extremely high, with a gradual decline as Reynolds numbers increase to a point where the flow is no longer laminar. It would therefore be anticipated that a variation in growth rate inversely proportional to this relationship would exist. This concept of varying growth rates within a constant velocity flow is contrary to earlier beliefs that velocity magnitude alone regulated growth rates.

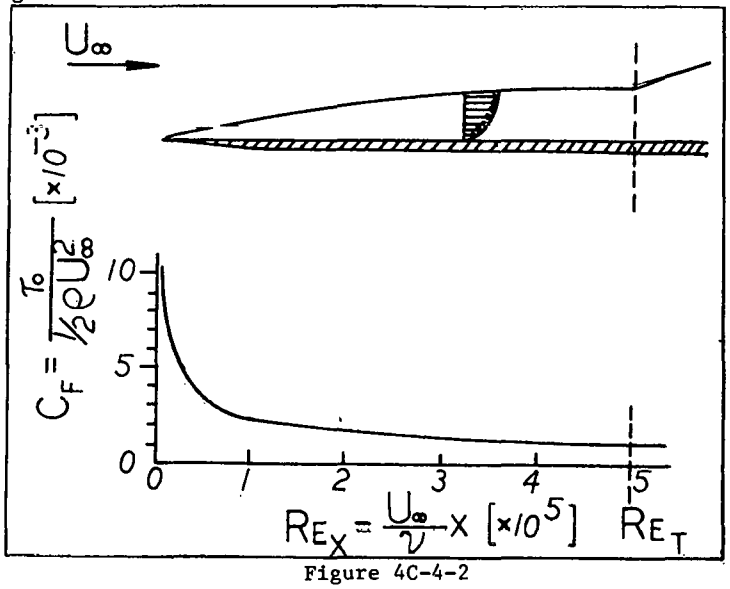



Figure 4C-4-2

In order to investigate the biofouling of a flat plate subject to a constant free stream velocity, a submersible water tunnel was designed to provide for: a) constant velocity across a flat plate variable from 1 ft/sec to 7 ft/sec, b) a test section which would allow tests of vertical or horizontal flat plates, c) isolation of the test section from external velocity sources such as tidal currents and wave action, and d) ease of access to facilitate frequent monitoring of

experiments and frequent change of experimental parameters. A schematic of the tunnel is shown in Figure 4C-4-3. A well defined intake provides for a uniform flow across a flat plate mounted in a Plexiglass test section. The intake and exhaust elements are designed to isolate the test section from tidal flows and the intake is covered with a mesh net to prevent debris from entering the tunnel. A Plexiglass test section allows for access of sunlight to the plate, which may be mounted either horizontally or vertically, to test for effects of plate orientation on growth magnitudes. The tunnel is powered by a 24 volt d.c. electric motor, which varies the free stream velocity by alteration of input voltage.

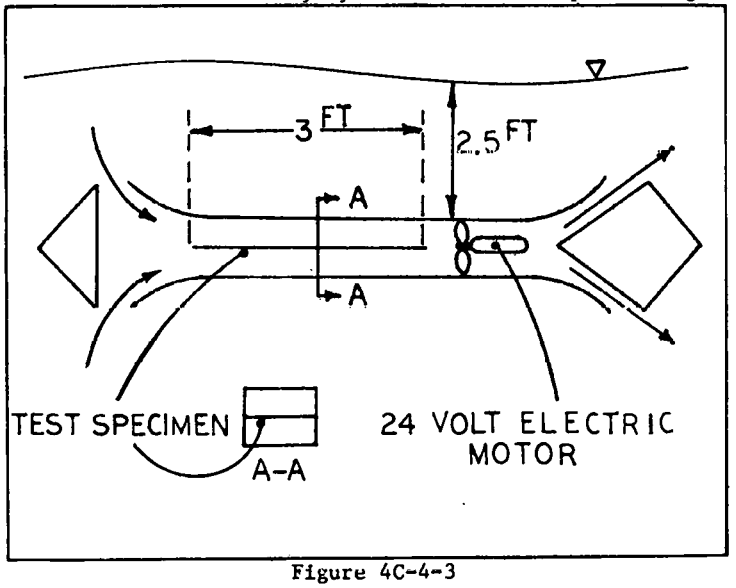



Figure 4C-4-3

The tunnel itself is mounted on a support swing which is suspended under a dock (Figure 4C-4-4). The depth of the tunnel below the free surface varies from 2.5 to 4.5 ft. depending on tidal conditions. Actual maintenance on the tunnel or changes to experiments may be performed by rotating the tunnel to a vertical position next to the dock. The dock to which the tunnel was attached is located at the NOAA Southeast Fisheries Laboratory, on Virginia Key in Miami, Florida (Figure 4C-4-5).

Experimentation was begun in mid-October, 1976. The first series of experiments used horizontal flat plates subject to free stream velocities varying from 2 ft/sec to 4 ft/sec. Initial tests in waters of about 80-85° F required exposure times of less than 4 days to insure organism sizes and quantities which could be identified and tabulated visually. As water temperature gradually dropped to 60° F by mid-January, exposure times of up to two weeks were required to obtain sufficient growth samples. The specific macrofouler being investigated is the Acorn Barnacle (Balanus spp.). It should be noted that in addition to their abundance, Acorn Barnacles were investigated, as opposed to microfoulers such as those found in slime films, because of the ease in identifying organisms and determining growth rates by visual means.

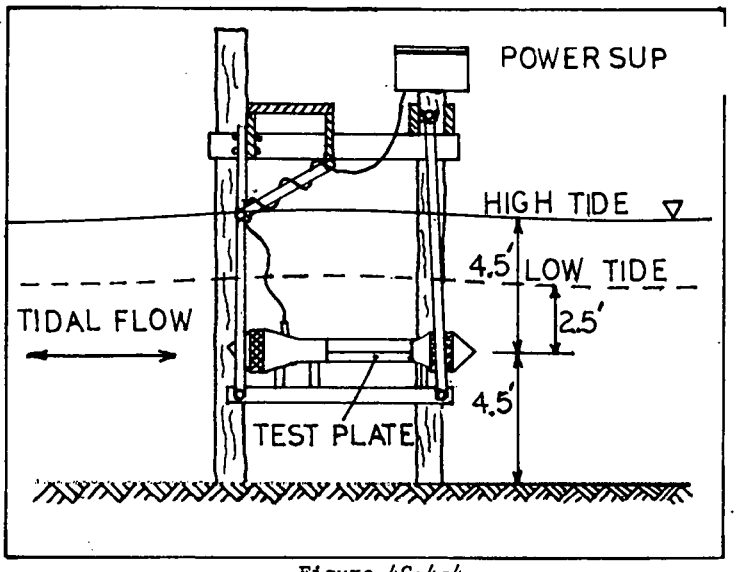



Figure 4C-4-4

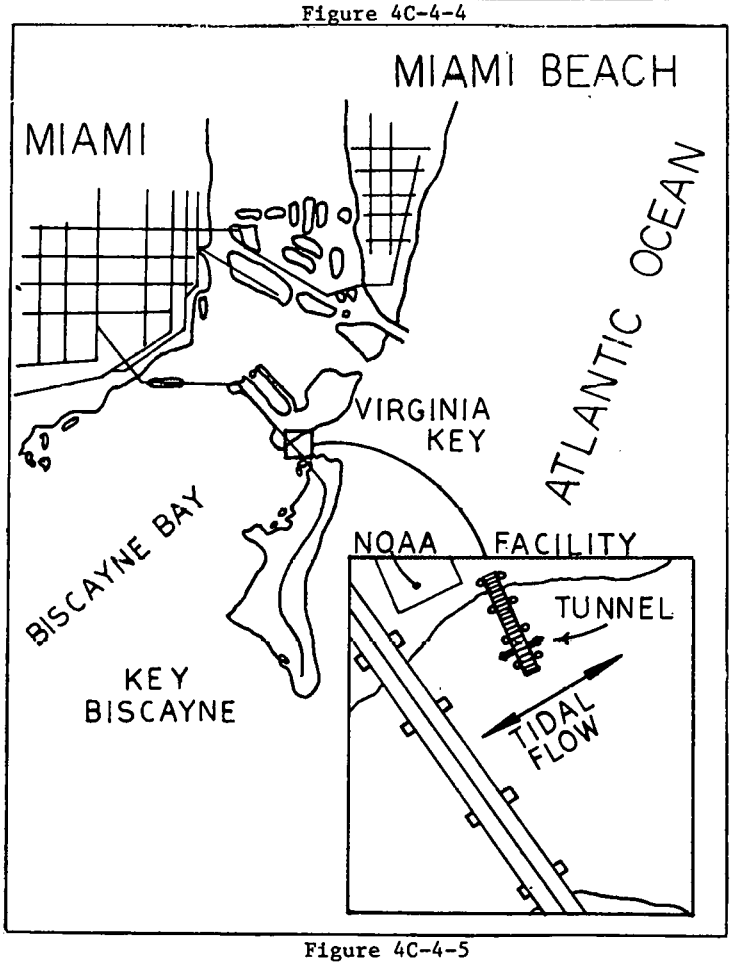



Figure 4C-4-5

## Results

Initial observation of exposed plates disclosed

minimum areas of growth near the leading edge. As distance away from the leading edge increased, the magnitude of attached barnacles increased. Calculations of barnacles/inch$^2$/day were made at regular intervals along the plate and values were plotted versus shear stresses present at the same locations. A representative data sample is shown in Figure 4C-4-6. Two plots are shown, one for the upper surface and one for the bottom surface. Both plots show a drastic drop in growth rate at a value of 3.0 to 4.0 x $10^{-5}$ psi with a maximum tolerable shear in the area of 8.0 x $10^{-5}$ psi. These values are consistent with the results of several tests and compare favorably with the data of Crisp, whose results equated to shear stress values from 2.1 to 6.3 x $10^{-5}$ psi with a maximum value of 8.3 x $10^{-5}$ psi. In addition, a difference is noted in relative growth magnitudes between the top and bottom of the plate. These differences were quite obvious upon visual inspection and show the effect due to gravity on the settlement of barnacles. It should be noted that gravity did not alter the shear stress cut off value, but did alter the magnitude of organisms able to attach. (More recent tests with vertical plates have growth rates quite similar in magnitude to the bottom surface of this experiment.)

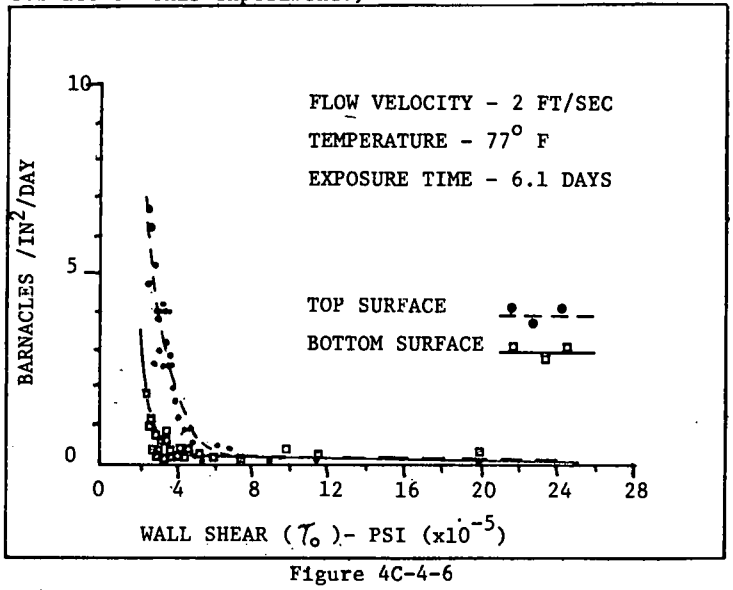


Figure 4C-4-6

In order to further confirm the relationship developed, other investigations were examined to see if sufficient data existed to relate reported growth rates to shear stress. Two such investigations were found. Both experiments involved fouling of piping systems. Since the authors provided pipe size and velocity, the shear stresses existing in their experiments could be determined and related to the reported fouling growth rates. In order to relate this experiment to flow through pipes, a plot of flow velocity versus pipe diameter for values of constant shear force was constructed (Figure 4C-4-7). The value of shear stress selected for the beginning of the transition area, 8.0 x $10^{-5}$ psi, is based on the data shown in Figure 4C-4-6. The upper value of the transition zone, 24.0 x $10^{-5}$ psi, is an arbitrary selection of 3 times the lower value, to provide for isolated growth areas which may occur. Therefore, values falling below the transition zone should foul heavily and those values above the transition zone should exhibit minimized fouling.

Data points A and D (Figure 4C-4-7) were determined from a study of a seawater intake system in Logy Bay, Newfoundland made by Sergy and Evans (5). Seawater was pumped into a reservoir through a 10 cm (4 inch) diameter pipe, at velocities varying from 4.7 to 6.8 ft/sec. The water was then removed from the reservoir through a 15 cm (6 inch) pipe at velocities varying from 1.2 to 2.0 ft/sec. The system was in continuous operation from the fall of 1967 to December, 1971, when sampling was completed. The 10 cm pipe (data point D) was found to be relatively free of fouling. Only a few spirorbid worms were discovered after direct examination of the pipe. Data point D falls within the area anticipated to have minimized fouling. The 15 cm pipe (data point A) was found to be heavily fouled, with a 2-3 cm thick build up of organisms primarily muscles (Mytilus edulis). Data point A falls within the area anticipated to have heavy fouling.

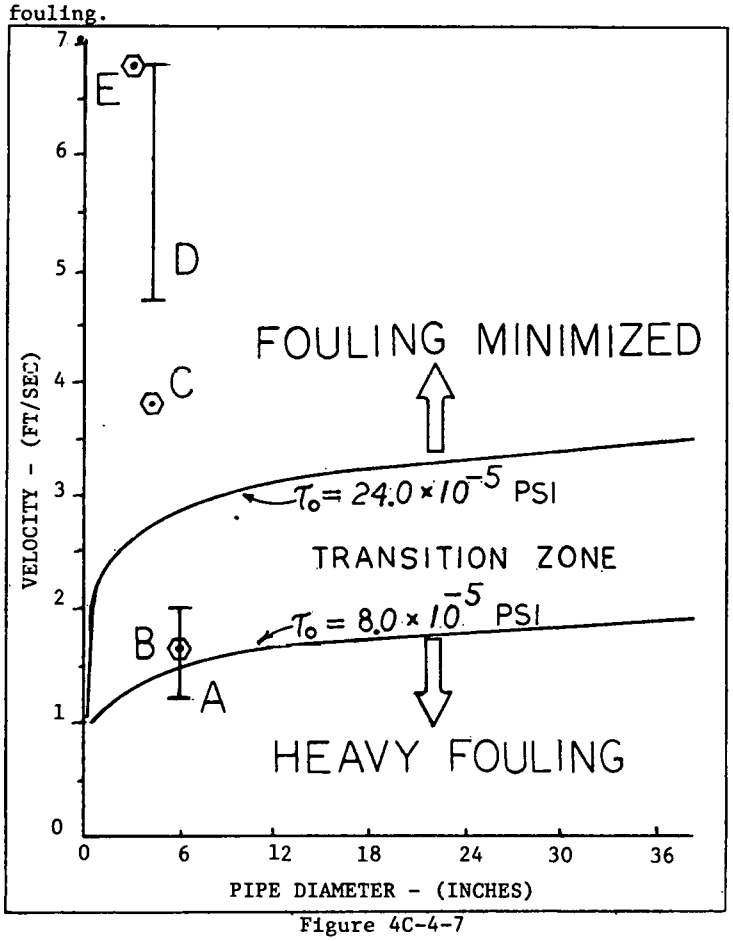


Figure 4C-4-7

Another situation investigated was the work of Mangum, Shepherd, and McIlhenny on the control of fouling of intake systems (data points B, C, and E, Figure 4C-4-7) (6). In their experiment seawater was pumped through a series of pipes of various diameters. Three situations

investigated were a 6 inch diameter pipe with a flow of 1.7 st/sec (data point B), a 4 inch diameter pipe with a flow of 3.8 ft/sec (data point C), and a 3 inch diameter pipe with a flow of 6.8 ft/sec (data point E). The 6 inch diameter pipe (data point B) was found to be heavily fouled after just one month. The interior was partially bare steel and partially lined with a layer of epoxy. Both sections fouled. Data point B falls within the transition area, towards the area anticipated to have heavy fouling. The 3 inch pipe (data point E) was partially bare steel and partially lined with Saran. Neither section fouled after 8 months. Data point E falls within the area of anticipated minimized fouling. The 4 inch pipe (data point C) was partially bare steel and partially lined with Saran. Very little fouling occurred in the lined portion of the pipe after 8 months. The unlined portion of the pipe remained free of fouling for several months, until the metal began to corrode. At this point, fouling began to occur. But it must be noted that as the corrosion product began to build up, the surface roughness of the pipe changed, disrupting the boundary layer and the shear forces. This change obviously had a detrimental effect on the fouling conditions. Data point C fell within the area of anticipated minimized fouling.

## Conclusions

It is apparent from the results presented that wall shear plays an important role in biofouling. The ability to maintain or induce high values of shear stress could significantly minimize biofouling problems in areas where flows can be manipulated such as in heat exchanger systems. Although the investigation as described in this paper has considered the macrofoulers, the same basic principles should apply to microfouling and similar experiments should be carried out to examine the hydrodynamic-microbiofouling relationship.

Many other hydrodynamic parameters may be worth consideration for hydrodynamic control. Turbulence intensity within the flow field may in fact give greater protection due to the high shear forces generated within a turbulent region. The study of multiphase interaction (flow which combines liquids and particulate matter, such as fouling organisms) of various systems has shown that certain conditions may exist in which the lift forces on specific particles may tend to move these particles either towards a surface or towards an equilibrium position closer to the center of a pipe. The potential implication of completely inhibiting organism movement to a surface surely deserves further investigation. The existence of secondary flows, generated by specific tube or pipe geometries has been studied extensively. The effects of these flows either detrimental or beneficial to biofouling control in unknown. Finally, the need for examination of the effect of surface roughness is illustrated by the Mangum experiment where the surface roughness due to corrosion initiated biofouling in an otherwise non-fouling hydrodynamic situation.

As new investigations are initiated into solving the biofouling problems associated with OTEC plants, more effort should be expended to fully understand the relationship between biofouling rates and the hydrodynamic flow field. The use of hydrodynamic control may prove to be a significant means for controlling biofouling in areas where favorable flow conditions can maintained. The adaptability of hydrodynamic contro. relatively minimum expense, in terms of additional hardware, may also make it a valuable addition to state of the art mechanical, coating or toxin systems, which may not in themselves be sufficient to deal with the biofouling problem.

## References


1. Ocean Thermal Energy Conversion (OTEC) Program Summary, October, 1976, ERDA 76-142, Energy Research and Development Administration, Washington, D. C. pp. 4-8.
2. Perkins, E. J., The Biology of Estuaries and Coastal Waters, Academic Press, New York, 1974, pp. 353-389.
3. Crisp, D. J., "The Behaviour of Barnacle Cyprids in Relation to Water Movement Over a Surface", Journal of Experimental Biology, Vol. 32, 1955, pp. 565-590.
4. Li, W. H. and Lam, S.H., Principles of Fluid Mechanics, Addison-Wesley, Reading, Mass., 1976, pp. 232-250.
5. Sergy, G.A., and Evans, J. W., "The Settlement and Distribution of Marine Organisms Fouling a Seawater Pipe System", The Veliger, California Malacozoological Society, Inc., Vol. 18, July 1975, pp. 87-92.
6. Mangum, D. C., Shepherd, B. P. and McIlhenny, W. T., "Intake Systems for Desalting Plants", Office of Saline Water Research and Development Report No. 678, April, 1971.

# AUTOMATIC TUBE CLEANING SYSTEM—BRUSH AND CAGE PRINCIPLE

E. DIETER NÜBEL
*American Man Corporation*
*1114 Avenue of the Americas*
*New York City, New York*

Abstract

The M.A.N. System uses flow reversal to move brushes which are permanently installed in each tube. Flow reversal is very quick and heat exchangers are cleaned one section at a time, so influence on load factor is negligable. The M.A.N. brush and basket system guarantees that each tube is cleaned on every cycle. It offers an effective and simple solution to the fouling problem. The M.A.N. System is completely automatic and requires no supporting equipment.

M.A.N., the initials by the way stand for Machinefactory Augsburg - Nuernberg, is a company which has a great deal to offer in the field of power generation. Worldwide M.A.N. offers complete powerplants on a turn-key basis or components for these ranging from stacker reclaimers to steamturbines, and from structural steel to inspection systems for the interior of pressurized water reactors. That M.A.N. was midwife to the Diesel engine and has ever since been a leading force in the development and application of it is hardly news to anyone. Research and Development activity by M.A.N. has covered such diverse subjects as dry cooling towers and helium driven gas turbines directly coupled to nuclear reactors.

If one can claim such a thing as "talent" for a company, it is certainly justified to state that M.A.N. has a knack for steel fabrication. Whether it be supporting structures for radiotelescopes, pressure containements for the most demanding service, offshore or hydro-construction projects or structural steel applications of any kind, our people time and again manage to come through where others despair. To illustrate my point, M.A.N. has built close to a thousand steel pedestals for turbine generators of varying size, nobody else has been able to profitably tackle the challenge of building such a very large steel table to the exacting tolerances demanded.

That such refinements as Automatic Tube Cleaning Systems often originate in Europe should neither amaze nor embarass us. After all, the European countries are much more densley populated and have for many more years been confronted with the problems of limited resources. For example, one of the things I personally found astonishing when I came from Holland eleven years ago was the large number of dead trees that are left to rot either standing up of fallen down. In Europe when a tree dies, for whatever reason, it is cut down and the lumber applied to useful purpose, whatever kind of wood it may be.

The principle of the M.A.N. Tube Cleaning System is simple: Each tube of the cooler or condenser is equipped with a permanently attached cylindrical basket at either end and one nylon bristled brush. Under normal operating conditions the brushes rest in the cages beyond the downstream tubesheet. Periodically the flow of the cooling water is reversed for a brief period. This causes the brushes to travel through the tubes to the opposite end where they are captured in the baskets, held briefly and, upon return to standard flow direction shuttled through the tubes again to resume their starting position. On their trip through the tubes and back the brushes effectively loosen all sediment and biofouling, which is flushed out ahead of the brushes since these are designed to move at about half the velocity of the water.

Backwashing a heatexchanger is a tried and true means to increase the effectiveness of chemical water-treatment and heattransfer efficiency. With the brush and cage cleaning system optimal cleanliness with all its inherent benefits can be maintained. The flow reversal operation itself takes only one to two minutes, even in the largest units. The effect of backwashing on the generation or chilling process is negligible: Case in point, in an 850 MW steam generating unit less than 1% of capacity is sacrificed for approximately 20 seconds per shift. Experience indicates that reversing of the cooling water flow and the resulting back and forth trip of the brushes, three times per 24 hours period suffices to maintain maximum heattransfer efficiency under average conditions. The

frequency of backwashing is easily tailored to meet requirements.

The credentials of the cleaning system are impressive: In practice established service of up to nine years without need of replacement parts under demanding conditions, saving up to 35% in power cost in chiller applications, effectiveness documented by University Research.

The very simplicity of the Brush and Cage Cleaning System is appealing. A proven technique, the backwashing of a condenser is teamed up with the universal cleaning tool, the brush. The combination of these two applied with the proper frequency will assure the best possible performance of your heat exchangers. The advantages of this system over others are numerous. Let me first mention a minor disadvantage: With a tubesheet full of the small retainers, it becomes impossible to use the old-time method of finding leaks that calls for sealing of the tubesheet with Saran Wrap or wet newspaper. In view of the fact that there are several other methods of leak-detection, faster and more accurate ones, this drawback carries little weight.

The positive points, however, are of indisputable value:

Since every tube receives and retains its own brush, one has absolute assurance that "ALL" the tubes will be cleaned. One does not have to rely on the random distribution of cleaning elements.

The life expectancy of the brushes is at least five years. Therefore, it is not necessary to weekly measure the size of the cleaning elements to insure they are still able to perform their function properly.

As it is impossible for the brushes to escape down the discharge or hide out in nooks and crannies in the water circuit, no counting of the number of cleaning elements, and frequent replacing of worn one, which is necessary with other cleaning systems, is required.

The above mentioned points lead to yet another plus:

The constant monitoring which is vital to ascertain satisfactory performance of other cleaning methods is eliminated!

It is really very hard to list all the advantages in order of importance. The following always seems to me like the greatest aspect of the M.A.N. System:

You don't need any supporting equipment! All it takes is the flow reversal capability, which can be easily had by adding a few standard valves. The valve maneuver which generates the flow reversal is simply and inexpensively automated by combining the valve operator controls with timers and relays in a control panel. The result is an effective cleaning system that requires virtually no attention from the operating personnel. A system, moreover, that gives you positive control at all times, it can be triggered manually whenever desire. In case of an upcoming outage, for example, one can run the brushes back and forth a couple times and the gentle, yet thorough cleaning action will insure that each and every tube is free of deposits that might cause corrosion problems while the condenser is dry. No other automatic tube cleaning system gives the operator this positive control.

Aside from its inherent advantages, the flow reversal feature gives us another plus: Should a cleaning element become lodged inside a tube, something we cannot discount with any cleaning method in open cycle applications, it will be freed when one returns to normal flow direction. With cleaning methods that do not employ the flow reversal, the chances of a cleaning element getting stuck are just as great, the chances of it becoming dislodged are marginal at best.

An advantage of the M.A.N. Tube Cleaning System that has taken on new significance in light of recent developments in the O T E C Project is the fact that it can be used with internally finned tubes. As a matter of fact, M.A.N.'s deep involvement in all aspects of power generation has led to the development by M.A.N. and Wieland Works, a German tube manufacturer, of a patented tube design which in its standard edition gives an internal surface enhancement of 1 to 1.42 at one inch O.D. The tubes are marketed in the United States by a subsidiary of the Wieland Company.

The Brush and Cage Cleaning method has been in service in heat-exchangers equipped with internally finned tubes for many years. One installation for example that I know of has been running in M.A.N. - Wieland type tubes since 1964. In February of 1971, after giving seven years of satisfactory service, the brushes were replaced. It is an open cycle system which uses riverwater.

In this installation, as well as many others with conventional tubes, our cleaning system maintains optimum heattransfer conditions by virtue of its gentle brushing action. In air conditioning and industrial process chiller applications in this country, we have held the fouling factor to levels of .0002 or less. In power stations, of course, conclusive measurements are much harder to come by, since the installations are so much larger and there are many more constantly varying parameters. Nevertheless, we have achieved convincing successes in steam applications. A typical example being a large generating station in Pennsylvania. During the first year of operation the circulating water of this closed cycle system was found to carry a relatively high positive Langelier index, which indicates a strong scaling tendency. Since this condition prevailed for the better part of the year, the tubes were scrutinized extra thoroughly during the annual inspection. They were found to be, as the independent expert stated in his report, exceptionally clean

In closing, let me briefly repeat the r advantages of the M.A.N. Tube Cleaning em:

_t is completely automatic and needs no attention beyond an occasional inspection. It can run for years without the need to measure, count and add cleaning elements. It is a major improvement over the random distribution of cleaning elements in the circulating water, since each tube retains its own brush. This gives positive assurance that all tubes will be kept clean. No supporting equipment is needed. This fact does away with the complex mechanisms other systems need and eliminates numerous sources of possible failure.

By virtue of the flow reversal feature, foreign objects that become lodged in the tubes will be freed when the condenser is backwashed. Over and above that, this capability can also serve to enhance the effectiveness of chemical water treatment. The brush and basket cleaning method gives the operating personnel positive control. Additional cleaning cycles can be triggered at any time, one push on the button and within minutes the entire tubebundle is gently but thoroughly freed of all deposits and biofouling.

The O T E C Project poses many challenges to science and technology. Even though there are still many people who doubt that it will ever lead to practical results, we believe it is a viable concept and we will be available at all times to help solve the many problems that are likely to come up.

# INCREASING HEAT EXCHANGER EFFICIENCY THROUGH CONTINUOUS MECHANICAL TUBE MAINTENANCE

W. I. KERN
*Amertap Corporation*
*Mineola, New York*

Abstract

The application of continuous mechanical tube cleaning through the recirculation of sponge rubber cleaning balls has been well established for large power plant condensers. In these power plant installations the economics of the mechanical tube cleaning equipment have been easily justified on the basis of improved performance and efficiency.

The technique of mechanical tube cleaning has been applied to several process industry condensers and heat exchangers and the results have been similar to the power plant experience, i.e., significant increases in the efficiency of heat transfer, and corresponding decreases in energy consumption and maintenance costs.

## Condenser And Heat Exchanger Fouling Affect Plant Performance

The heat exchanger and steam condenser have become focal points of attention in industry's efforts to obtain more efficient utilization of fuel and energy.

Because of the growing demand for energy, higher fuel costs, and shortages, environmentalist pressure, shrinking availability of sites and cooling media, it has become a critical necessity to obtain greater reliability and efficiency from surface condensers and heat exchangers.

And in the face of this requirement is the growing complexity and size of these units. Condensers for fossil-fueled turbine units continue to increase in surface area. Nuclear units now on line or planned for the future are a quantum jump larger in size. Moreover many more special functions have been imposed--reheating, regenerative preheating, multipressure units, by-passed steam--to add to the complexity of the condenser.

It has become evident that the designer and operator can no longer rest comfortably on assumptions and standards of performance prevalent a decade ago.

## Effect of Backpressure On Turbine Performance

The most effective way to improve heat rate is to improve turbine performance. And at the heart of better turbine performance is maintenance of design back pressure. But back pressure is a function of condenser efficiency. When the circulating cooling water produces an absolute pressure at the turbine flange that induces choking flow, the optimum heat rate is obtained. At a pressure above or below that point, there is a loss in heat rate. This is because at choking flow the steam passing through the turbine exit annulus has reached sonic velocity. When that occurs, no additional energy can be imparted to the turbine by further lowering the absolute pressure.1/

It is important to maintain the condenser back pressure as close as possible to this maximum energy level in order to operate at the best possible heat rate.

Improved heat rates can result in both increased generation capacity and reduced fuel requirements. For example, consider a 600 Mw generating unit. As little as 0.2" Hg absolute improvement in condenser back pressure can equal a 0.5 percent improvement in turbine heat rate. This is equal to approximately three additional megawatts of generating capacity. In addition significant fuel savings result. At a fuel cost of $0.40 per $10^6$ Btu, and a 60 percent loading factor for this unit, savings of over $60,000 per year can be realized ... by simply reducing back pressure 0.2" Hg.

In many areas of the country fuel costs have risen sharply and shortages exist. Thus it is becoming increasingly important to conserve fuel through more efficient heat rejection.

But maintenance of efficient heat rejection depends largely on the maintenance of a high state of cleanliness of the condenser tubes.

## Initial Installation Cost

For both condensers and heat exchangers if higher cleanliness factors can be utilized, less heat transfer surface is required. Savings in capital costs can be attained.

## Maintenance Cost

A condenser or heat exchanger that is kept free from corrosion, leakage, blockage, is a more reliable unit Costs for outages can run $100,000 a day for a mid-range turbine generating unit. Eliminating one unplanned outage can more than pay for measures taken to maintain cooling water tube cleanliness.

1/ R.J. Stoker and E.F. Seavey, "The Selection of Large Steam Surface Condensers", Combustion, September 1967.

In addition to the sheer cost of unnecessary fuel mption, plant outages, chemical treatment, ineffi- use of cooling media, there are the necessary rns that industry has for the environment and regulatory pressure. These are also very good reasons for maintaining the highest possible level of surface condenser and heat exchanger efficiency.

## Fouling Mechanisms in Plant Condensers

Deviations from the standard back pressure or operating point based on the guaranteed performance of the condenser or heat exchanger are caused by a number of variable factors, many of which can be controlled by the plant.

## Effect Of Water Velocity

Inlet temperature significantly affects back pressure of the condenser. If once-through cooling water is used, inlet temperature is not a factor that can be controlled. However, mechanical draft cooling towers can regulate the inlet temperature. Where once-through water is used, seasonal variations magnify the effects of increased back pressure. One study,2/ done in the early 1960's points up the seasonal effects of an increase as samll as 0.1" Hg absolute, occasioned by waterside deposits in the condenser of a 265 Mw generating unit. The curve (figure 1) shows increased operating costs that result from this fouling range as high as $1000 per month during periods of high inlet temperature. It should be noted that since this study was made, fuel costs have tripled in many areas.

An analysis of heat flow resistance in a condenser made by Lustenader and Staub3/ is shown graphically in figure 2. It should be noted that the effects of corrosion are not included in this analysis, which would further accentuate the role of waterside resistances.

Waterside resistance accounts for 72% of the total resistance to heat transfer of the tube. Note that there are two components to waterside resistance: the so-called laminar film of stagnant water next to the tube wall and the buildup of sedimentary deposits or scale, called "fouling".

The laminar film has insulating qualities and accounts for a significant 39 percent of the total heat transfer resistance of the condenser. In addition it isolates the turbulent water within the tube from the fouling buildup on the tube surface, which contributes to a fast rate of deposit.

Tests4/ have shown that there is a rapid decrease in heat transfer after a thorough manual cleaning of the condenser tube...as much as 15 to 20 percent after only ten hours of operation on a 90,000 $ft^2$ surface condenser. See figure 3.

If the laminar film is disrupted by continuous mechanical cleaning the heat transfer through the tube can be significantly increased and the rate of waterside fouling significantly reduced.

In addition to the rapid initial fouling that occurs during the first hours of operation, a steady long-range increase in fouling takes place in most condensers, owing to scaling or formation of corrosion products on the tube surface, which accounts for 33 percent of the resistance to heat transfer.

## Tube Material Considerations

Corrosion of brass tubing is relatively predictable based on water chemistry and known corrosion mechanism. This is not the case with deposits that form on brass and other metals. Among the many factors which affect the type of deposit are dissolved solids, pH, chlorination, bacteria, and water velocity. Much is yet to be learned of these mechanisms of fouling and at present many studies are being conducted including tests performed by Heat Transfer Research, Inc.

Deposits not only add to the heat resistance of the condenser, they contribute to corrosion, particularly of stainless steel tubing. Many authors have noted the effects of deposit formation in the presence of chlorides on corrosion pitting of stainless steel5,6,7/ and stressed the necessity of maintaining a high degree of cleanliness to avoid this.

The two most troublesome deposits in this respect6/ have been oxygen-excluding patches of calcium carbonate containing chlorides, and the soft, porous precipitate of a hydrous oxide of manganese found in seaboard locations. The mechanism for pitting on stainless steel is the creation of a small galvanically active area. Oxygen, which maintains the passive oxide surface of stainless steel, is severely reduced under the deposit. If there are chlorides present, a loss of passivity is encouraged. Thus the area becomes chemically active, surrounded by a large inert area and metal within the pit becomes anodic to the passive area.

---

2/ A. Heidrich, Jr.; J.J. Roosen, R.J. Kunkle "Calorimetric Evaluation of Heat Transfer by Admiralty Condenser Tubes", ASME Publication 65-WA/CT-2, presented at the Winter Annual Meeting of the American Society of Mechanical Engineers, Chicago, 7-11 Nov. 1965.

3/ E.L. Lustenader and F.W. Staub, "Development Contribution to Compact Condenser Design." INCO Power Conference, Wrightsville Beach, North Carolina, May 5, 1964.

4/ D.S. Detwiler "Improving Condenser Performance With Continuous In-Service Cleaning of Tubes", American Society for Testing Materials Publication STP 538.

5/ J.R. Maurer, "The Use of Stainless Steel Tubing in Condenser and Related Power Plant Equipment -- a Progress Report," Combustion July, 1967 (Prepared for the Southeastern Electric Exchange, Atlanta, Georgia, October 13, 1966).

6/ N.A. Long, "Recent Operating Experiences with Stainless Steel Tubes," Presented at the 1966 American Power Conference.

7/ "Experiences with Stainless Steel Tubes in Utility Condensers", Nickel Topics, Vol. 24, No. 5, 1971. (A publication of the International Nickel Company, Inc.)

It is stressed that the most effective way to prevent corrosion of stainless steel is by mechanical cleaning[6]. Besides discouraging the formation of pitting corrosion, mechanical cleaning can also retard the growth of existing pits. If the corrosion products within a pit are removed by cleaning, the area returns to the passive state.

Another source of fouling is organic nature. It varies from bacterial action that produces a heavy slime to the growth of marine organisms that thrive in the cooling media. Non-copper bearing metals are particularly susceptible to slime formation, which can reduce heat transfer. Marine organisms can promote localized pitting and erosion. The presence of bacteria can increase the manganese content of the cooling water. It has been noted that[6] though a river may contain no detectable concentration of manganese, once the water is impounded, the manganese content of the water may begin to increase as a result of biological activity ... to the detriment of stainless steel tubing.

## Water Type And Quality

Power plants and industrial facilities must rely more than ever on cooling water that is increasingly subjected to pollution in the form of manmade debris and industrial wastes. A large portion of this available cooling media is sea water or brackish water from estuaries that contains profuse marine life. All of this adds up to the ingestion of solids into the waterbox and tubing of the steam condenser or heat exchanger. Seaweed clogs tube sheets; mussel seeds penetrate the screens and thrive in the water mains, to eventually lodge in the tubes, along with plastic scraps, twigs, and other debris. The result is generally either outright plugging of the tube or perhaps more seriously, cause of localized erosion leaks. As the cooling water flows past the obstruction it must necessarily increase in velocity. Rapid erosion occurs in the vicinity. Copper bearing alloys are highly vulnerable to this; stainless steel, to some extent. Only titanium seems resistant to localized velocity increases[8].

The presence of silt - sand particles - in the cooling water is potentially deleterious to the condenser tubing. Particles can settle into the stagnant water layer and foul portions of the tube. This not only reduces heat transfer, but sets up conditions for corrosion; localized heating, reduced oxygenation, perhaps corrodents trapped in the silt. Only repeated thorough cleaning can prevent this. Sand particles in the water can also hasten localized erosion where there is ingested debris in the tube.

## Cleaning Methods Utilized To Combat Adverse Factors

A number of methods have been used by industry to combat adverse factors affecting condenser and heat exchanger efficiency. They range from cleaning techniques to new tube materials and cooling towers. The following is a brief review of the more significant methods.

Various chemicals, including acids and chlorine, have been used to reduce fouling and restore tube cleanliness. Acid cleaning presents the choice between strong acids which may be hazardous to the equipment and weaker acids, such as citric, formic, and sulfamic acids, which can be less effective and probably more expensive. Moreover, acid cleaning is limited to periods of a year or more. Between cleanings, foulding can severely affect condenser performance.

The use of chlorine is being cut back or eliminated in many regions by government regulation. Its effect is largely limited to organic fouling. Moreover the presence of chlorine can promote the corrosion of stainless steel. Chlorine is becoming less and less a viable choice to improve cooling efficiency.

Mechanical cleaning of condenser tubing seems to be assuming more of the burden of maintaining condenser back pressure. Mechanical cleaning can be either manual or automatic.

Manual methods include periodic cleanings with rubber plugs, nylon brushes, metal scrapers, or turbining tools. Where clean water conditions exist and the deposits are light, manual cleaning of tubes can be effective in reducing fouling deposits that account for 33 percent of the heat resistance.

However, manual cleaning is becoming increasingly more uneconomical as condensers and heat exchangers grow in size, as downtime becomes more expensive and unavailable, and qualified help becomes more scarce and hourly rates higher. Hourly rates are especially high during the prime overtime hours when shutdowns are feasible. Moreover it is difficult for manual cleaning to keep up with fouling and blockage where the available cooling water is highly aggressive, has high deposition, chlorides, and solid debris. One calorimetric test[2] indicates that even chemical cleaning is more effective in restoring heat transfer than manual mechanical cleaning. Figure 4.

The greatest drawback to manual cleaning, in addition to its high cost, is that it is highly intermittent. Between cleanings, fouling builds up rapidly and, as was pointed out in earlier paragraphs, heat transfer falls off rapidly.

---

6/ N.A. Long, "Recent Operating Experiences with Stainless Steel Tubes," Presented at the 1966 American Power Conference.

8/ N.G. Feige, "Titanium Tubing for Surface Condenser Heat Exchanger Service" Bulletin SC-1, Timet, Division of Titanium Metals Corporation of America, W. Caldwell, N.J.

2/ A. Heidrich, Jr.; J.J. Roosen, R. J. Kunkle "Calorimetric Evaluation of Heat Transfer by Admiralty Condenser Tubes", ASME Publication 65-WA/CT-2, presented at the Winter Annual Meeting of the American Society of Mechanical Engineers, Chicago, 7-11 Nov. 1965.

Automatic cleaning methods are especially economi- in those areas where deposition, pollutants, chlor- and other corrodents exist.

Automatic cleaning is continuous and is explained in greater detail later in this paper. It involves sponge rubber balls contained within the cooling water system. These distribute themselves at random through the condenser, passing through a given tube at an average of one every five minutes. Slightly larger in diameter than the tube, they effectively wipe the surface clean of fouling and deposits.

The importance of automatic cleaning, particularly continuous cleaning has been stressed frequently by authors in the field.[2,4,5,6,7,8,9,11,12]

In an effort to reduce solid debris ingestion, particularly in seawater locations, most facilities have employed one form or another of traveling or sliding screens. However, these have not proved to be entirely effective. As one utility manager stated it, "The screens sometimes act as handy conveyors for flotsam and jetsam right into the water mains." Some marine life, such as mussels and oysters penetrate the screens in spore form and thrive on the walls of the main. This is an ideal environment for mussels, for example: plenty of food, no competition, no predators. Mussel beds can grow to a density of 30,000 per square foot under these conditions. When they break off during the season, they are drawn directly into the waterbox, unless there is an additional filter in the system.

There have been several filters available for this purpose over the years, but until recently none could be flushed out on-line. A debris filter now is available that can be located adjacent to the waterbox and can be flushed without interrupting the flow of screened water to the condenser. This device is also described more fully later in this paper.

A number of new alloys have been formulated for condenser tubing. Latest developments have been summarized by two trade publications [9,10]. These include copper-nickel alloys. stainless steel, and titanium.

A thrust of these newer metals has been to provide greater resistance to the adverse conditions present in available cooling water. The selection of an alloy for a particular site is based on a complex set of conditions. In general, the stainless steels have shown a sharp increase in the past decade, although not as high as industry predictions. Titanium is a recent newcomer to the field and has been used full-scale by several utilities. It seems to show the greatest range of corrosion and erosion resistance of all the metals used in condenser systems.

It should be pointed out that condenser tubes made from these new alloys benefit from thorough cleaning despite their resistance. The stainless steels, in particular, are susceptible to pitting corrosion in adverse environments where there is a lack of cleaning.

Even though great corrosion resistance is reported for titanium[8], including immunity to seawater and resistance to higher velocities, it too benefits from cleaning. In particular, continuous mechanical cleaning, as described in this paper will remove silt and bacterial fouling and disturb the stagnant water layer. These are important components of resistance to heat flow in the condenser and heat exchanger tubes.

As good sites and once through cooling water becomes less available, and environmental and other considerations become more pressing, industry is turning more and more to cooling towers. However, these are not a panacea for condenser problems. Among the drawbacks, from the point of view of condenser efficiency, are a build up of dissolved solids and chloride concentrations. This is accentuated as plants strive for zero discharge.

As will be shown in later sections of this paper, thorough continuous cleaning of the condenser continues to play an important part in maintaining back pressure and tube life, where cooling towers and closed water-cycles are employed.

---

2/ A. Heidrich, Jr,; J.J. Roosen, R.J. Kunkle "Calorimetric Evaluation of Heat Transfer by Admiralty Condenser Tubes", ASME Publication 65-WA/CT-2, presented at the Winter Annual Meeting of the American Society of Mechanical Engineers, Chicago, 7-11 Nov. 1965.

4/D.S. Detwiler "Improving Condenser Performance with Continuous In-Service Cleaning of Tubes", American Society for Testing Materials Publication STP 538.

5/J.R. Maurer, "The Use of Stainless Steel Tubing in Condenser and Related Power Plant Equipment -- a Progress Report," Combustion July, 1967 (Prepared for the Southeastern Electric Exchange, Atlanta, Georgia, October 13, 1966).

6/N.A. Long, "Recent Operating Experiences with Stainless Steel Tubes," Presented at the 1966 American Power Conference.

7/"Experiences with Stainless Steel Tubes in Utility Condensers", Nickel Topics, Vol. 24, No. 5. 1971 (A publication of the International Nickel Company, Inc.)

8/N.G. Feige, "Titanium Tubing for Surface Condenser Heat Exchanger Service" Bulletin SC-1, Timet, Division of Titanium Metals Corporation of American, W. Caldwell, N.J.

9/J. Papamarcos, "Condenser Tube Design Directions," Power Engineering Volume 77, November 7, July 1963.

10/W. O'Keefe, "Better But Costlier Tube Metals Tackle Present and Future Condenser Problems", Power, Volume 117, Number 8, August 1973.

11/C.K. Kuester, C.E. Lynch, "Amertap at English Station", ASME publication 66-WA/CT-1, Contributed by the Research Committee on Condenser Tubes for Presentation at the Winter Annual Meeting and Energy Systems Exposition, New York, N.Y. November 27-December 1, 1966 to the American Society of Mechanical Engineers.

12/"Condenser Cleaning Improves Economics", Electrical World, December 15, 1969.

## Amertap Condenser Tube Cleaning And Filtering Systems

Amertap Systems are designed to provide continuous mechanical cleaning of condenser and heat exchanger tubes and filtering of cooling water, thus aiding significantly in maintaining condenser heat transfer efficiency.

The basic principal of the Amertap cleaning system is simple and logical. The object is to frequently wipe the inside of the tube clean while the unit is in operation.

This is accomplished by specially engineered rubber balls that constantly circulate throughout the unit. Since the balls are slightly larger in diameter than the tube, they are compressed as they travel the length of the tube. The constant rubbing action keeps the walls clean and virtually free from deposits of all types. Thus, suspended solids are kept moving, and not allowed to settle; bacterial fouling is wiped quickly away; pits are not allowed to form because deposits are prevented; the film of stagnant water is continuously interrupted.

The sponge rubber balls are selected to provide the maximum cleaning effect for the particular installation. Their specific gravity is nearly equal to that of the cooling media. Thus they tend to distribute themselves in a homogrenous fashion through the cooling media. When properly charged; i.e., the correct number of balls are inserted into the cycle, each tube receives a ball on the average of once every five minutes. The ball travels the length of the tube, forced partially by the pressure differential between the inlet and the outlet. The ball compresses slightly into an elongated shape, analogous to a piston, thus providing extended cleaning surface. The surface of the ball is designed to allow a certain amount of water to flow through the area of contact with the wall, flushing away accumulated deposits ahead of the ball. They are available in several degrees of resiliency, depending on the requirements.

An abrasive coated ball is also available for situations where the cooling water tubes have already been heavily fouled, prior to Amertap installation. The degree of abrasiveness can be varied to meet the degree of fouling. The effect is a gentle scouring of the tube, removing the scale slowly but steadily, until the tube is ready to be maintained by the normal sponge rubber ball. As will be shown, heat transfer efficiency climbs steadily throughout this treatment.

It should be noted that the cleaning or scouring action of the Amertap System is uniform over the tube wall.

The balls are circulated in closed loop, including the condenser or heat exchanger (figure 5). At the discharge end they are caught in a screening device installed directly in the line. They are then rerouted through a collector unit back to the condenser inlet ball injection nozzles. This insures that the balls are uniformly distributed over the pipe cross-section. Thus the cycle is repeated.

At the collector unit, the cycle can be interrupted at any time to count the balls, check sizes, or take them temporarily out of service. The number of balls required to make up a charge is a function of the number of cooling water tubes. Naturally there will be eventually some wear of the balls and reduction in size. When they reach a predetermined diameter, they should be replaced. This is done quickly and easily at the collector unit. Under certain conditions of badly scaled tubes from past, uncleaned usage, the balls will normally wear faster. Proper selection of ball type will correct this situation and restore the tube walls to a smooth, clean surface.

The labor required to count and check a charge is usually about one hour per week.

Amertap cleaning systems can be retrofitted into most existing condensers or heat exchangers. Naturally some modification of piping or unit design may be required to install the units. The most effective way to take advantage of the system's efficient cleaning technique is to provide for the installation of Amertap when the unit is being designed.

The Amertap Debris Filter is designed to prevent solid debris from entering the waterbox of the condenser or heat exchanger. It is located in the cooling water inlet, preferably adjacent to the waterbox and flushed as needed without shutting down or bypassing the filter. Figure 6.

## Case Histories Of Continuous Mechanical Tube Cleaning

There are approximately 200 installations of Amertap cleaning systems in Europe and we are approaching 200 in the U.S. They have achieved an outstanding record of success in maintaining condenser efficiency and reliability.

A typical case record is shown in the "before" and "after" graphs in figures 7 and 8. A 95 Mw unit was retubed in 1958 with stainless steel type 304. Data kept for the next five years showed an average 27 percent deterioration in cleanliness from the original 94 percent to 67 percent, despite 69 thorough manual cleanings. Figure 7.

In 1964 an Amertap system was installed in the same condenser. Figure 8 shows that the cleanliness approached 95 percent...attained within one week of operation with Amertap. This is the original cleanliness factor, which was never attained in five years of manual cleaning. Note that there is no indication of long range deterioration in figure 8. There is also evident a direct response of cleanliness factor to number of hours of ball circulation, an important consideration where peaking service is involved.

With continuous mechanical tube cleaning system it is possible to guarantee that condenser back pressure will be maintained to within 0.0285 psi of the best back pressure attained following a thorough cleaning of the condenser tubes by any method that does not attack t

tube surface.

A calorimetric evaluation of heat transfer after ation of a continuous tube cleaning system[2/] is shown in figure 9. A 3/4" admiralty tube in a badly fouled condition was removed from a condenser located on a large fresh water river. In the calorimeter it indicated a heat transfer coefficient of 325 Btu/hr/ft$^2$/°F at a cooling water velocity of 7.5 feet/second (curve number 1). This represented nearly 60 percent reduction in heat transfer, compared to a new tube.

Since the tube was badly fouled, it was first cleaned with abrasive coated sponge rubber balls. After 24 hours or approximately 300 passes with the abrasive balls, the heat transfer increased to 578 Btu/hr/ft/°F. (Curve number 2). Continued cleaning with slightly larger abrasive balls (curve number 3) brought the heat transfer coefficient to 613 Btu/hr/ft$^2$/°F, a recovery of 61 percent of the loss. After two weeks of circulation with the standard sponge rubber ball - no abrasive - a further increase in heat transfer was obtained, 638 Btu/hr/ft$^2$/°F. (Curve number 4). The added increment of efficiency is apparently due to the polishing action of the sponge rubber balls, following scouring action of the abrasive balls.

This test graphically charts the effectiveness of the abrasive balls. In actual practice, the use of abrasive balls has in many instances restored tubes that were heavily scaled, fouled, or pitted. It should be noted, however, that the use of this technique should strictly adhere to the manufacturer's guidelines in the selection of size, degree of abrasiveness, periods of use.

One of the most extensive studies ot continuous tube cleaning systems was conducted by United Illuminating at its English Station[11/] in brackish polluted water.

It was found that Amertap systems can effectively reduce fouling rate of new brass tubes by as much as 50 percent when compared with comparable tubes operated without continuous cleaning. The results on older, corroded brass tubes were limited, since there was no test of the abrasive balls to reduce scale.

The results of continuous cleaning of stainless steel tubing were even more significant. Amertap effectively maintained a cleanliness factor of 98 percent and a back pressure of 1.49" Hg. After 1800 hours of operation of the tube cleaning system it was taken out of service for test purposes. During a month of operation without cleaning the condenser back pressure climbed to 1.65" Hg and the cleanliness factor dropped from 98 to 81 percent. (Figure 10). At that point the tube cleaning system was restarted. Within ten days the original back pressure and cleanliness were recovered.

On the basis of this data, United Illuminating concludes that, in conjunction with stainless steel tubing, continuous cleaning systems can maintain original design back pressures, 98 to 100 percent of cleanliness, and that even after prolonged shutdown of the tube cleaning system, these original conditions can be recovered.

Virginia Electric Light and Power Company, Mount Storm, Virginia had a problem with hydrated manganese oxide deposits on stainless steel type 304 tubes in the condenser for a 544 Mw unit. The circulating water from a manmade lake had a pH of 4.5 and a manganese content of less than 1.0 parts per million. Nevertheless a rapid build up of deposit was found in the tubes during unit operation.

Periodic cleaning with nylon brushes failed to remedy the situation and condenser back pressure climbed. (Figure 11). In the middle of April continuous cleaning system started operation. Within a few weeks condenser cleanliness was restored and maintained; back pressures held within a narrow range, near original levels. The company came to the conclusion that the tube cleaning system would pay for itself in increased efficiency and perhaps, even more important, elimination of problems from manganese deposits.

Extensive documentation[12/] at the Tennessee Valley Authority Widows Creek Plant over a period of a year showed that the continuous cleaning system was highly economical and has superior performance over manual cleaning. They compared results from two nearly identical condensers, one maintained by Amertap the other by manual cleaning with brushes. The results are shown in figure 12.

Continuous cleaning by ball recirculation showed a 17 percent better performance over brush cleaning. This projected to an annual net savings of fuel (in 1969) of $20,000.

Economic evaluations showed that a gain of only 7.5 percent would offset the cost of the continuous tube cleaning equipment. Thus the system was economically justified.

The condensers were tubed with 7/8 in. BWG Admiralty tubes, 40 feet long. Condenser "B" was equipped with an Amertap system; Condenser "A" was cleaned periodically with brushes. TVA had used a tube cleanliness factor of

---

2/ A. Heidrich, Jr.; J.J. Roosen, R.J. Kunkle "Calorimetric Evaluation of Heat Transfer by Admiralty Condenser Tubes", ASME Publication 65-WA/CT-2, presented at the Winter Annual Meeting of the American Society of Mechanical Engineers, Chicago, 7-11 Nov. 1965.

11/ C.K. Kuester, C.E. Lynch, "Amertap at English Station", ASME publication 66-WA/CT-1, Contributed by the Research Committee on Condenser Tubes for Presentation at the Winter Annual Meeting and Energy Systems Exposition, New York, N.Y. November 27-December 1, 1966 to the American Society of Mechanical Engineers.

12/ "Condenser Cleaning Improves Economics," Electrical World, December 15, 1969

85 percent as a basis of condenser design; however condenser performance prior to the test, was below this optimum level.

Test results of the Amertap installation in Condenser "B" are shown.

Cleanliness rapidly rose to near design level and maintained an average of 81% over the next year. Various combinations of abrasive and normal balls were tried.

Condenser "A" cleaned by brushing showed an increase following cleaning but deteriorated rapidly.

Based on this test condenser tube cleaning systems were ordered for nuclear units at the Browns Ferry Nuclear Plant, at the Sequoya Nuclear Plant, and at the Watts Bar Nuclear Plant.

As has been previously mentioned, even though an element of control over the cooling media is possible in closed loop cooling tower systems, through inhibitors and other treatment, many factors harmful to condenser tubing still remain. These may include the source of the media, which is frequently reclaimed waste water or polluted brackish water, and a concentration of corrodents and minerals.

In addition, closed loop cooling tower systems pick up dirt, chemicals, and organic matter from exposure to atmosphere during the cooling cycle.

Continuous cleaning systems are creating a history of successful application in condensers cooled by closed loop cooling tower systems.

Example: Southwestern Public Service found that Amertap systems created annual fuel savings and increased reliability of its units in cooling tower operation.

In 1966 the Nichols Station, then in operation six years, found that the back pressures of Units 1 and 2 had raised to 0.7" Hg above a designed level of 1.5" Hg and that achieved cleanliness factors had dropped to 70%. It was assumed that the cause lay in the fouling of the admiralty brass tubing by the heavily chlorinated, treated sewage effluent used for cooling water make up. When Unit No. 3 (256 Mw) was erected, the utility decided to tube the condenser with stainless steel type 316 and install a condenser tube cleaning system. The ability of the sponge rubber cleaning balls to remove fouling deposits enabled the unit to run at design levels of back pressure.

Based on this success, tube cleaning systems were backfitted into Nichols Station 112.5 Mw Units 1 and 2, and installed in the C. B. Jones Station 256 Mw Units 1 and 2.

The backfit of Nichols No. 2 was economically justified as follows:

| | |
|---|---|
| Back pressure improvement | 0.7" Hg |
| Enthalpy Change | 16 Btu/lb |
| Steam Condensed | 535,000 lb/hr |
| Fuel cost | 28¢ / $10^6$ Btu |
| Annual Fuel Savings | $39,000 |

Analysis of Nichols 1 and 2 indicated a fuel and chlorine savings of $70,100 a year. After subtracting per annum capitalization for the Amertap system (operating costs were not considered significant) a net savings of $46,340 per year is returned to the utility as added profit on its investment in Amertap for these two units alone.

Tests performed on the Nichols Units 1 and 2, after installation of the Amertap systems, showed that back pressures were reduced from an average 2.2" Hg to design levels of 1.5" Hg. Terminal Difference (exhaust system temperature vs. outlet cooling water temperature - an excellent indication of tube cleanliness) dropped from 11F to 3.4F. Thus predictions for the effectiveness of the Amertap system were confirmed.

In summary, continuous cleaning and filtering systems effectively maintain a high level of cleanliness and, consequently, efficiency of surface condensers and other heat exchanger equipment.

Fuel savings. Specific examples have been named. There are many more available. Clean, unclogged, condenser tubing, maintained at design levels of cleanliness, will provide fuel economies for the power plant. In a period of rising fuel costs and shortages, and environmental considerations, fuel economy becomes more important than ever.

Fewer outages. Condenser tube cleaning systems eliminate unplanned outages that are caused by cooling water tube fouling, corrosion, leakage, or blockage. Such outages can cost $100,000 per day for a mid-range unit and up to $250,000 for a 1200 Mw nuclear unit.

Reduction or elimination of chemicals. Continuous cleaning of cooling water tubing greatly reduces the need for chemical treatment. In many cases it completely eliminates it. Governmental regulations and environmental considerations have made the use of strong chemicals in once-through cooling systems undesirable. In addition they cause an unnecessary expense. However, where chemical treatment is necessary, Amertap cleaning systems enable you to get optimum performance and safety.

Improved protective film. It has been found that in many instances injections of minute amounts of ferrous sulphate ($FeSO_4$) into the cooling water will provide complex oxide film on the interior of copper alloy tubes, such as admiralty bronze and 90-10 copper nickel. The film acts as a protective barrier against electrochemical attack on the copper alloy. Tests have shown that continuous cleaning systems actually improve the quality of the protective oxide film by providing a more uniform thickness and smoother surface. Moreover, should it become necessary to remove the film and replace it, cleaning systems provide a fast, efficient means to do so. First, abrasive balls are used to remove the film, uniformly and cleanly. The ferrous sulphate injections are renewed, simultaneously with standard sponge rubber ball injection. The protecti

film builds again smoothly and uniformly.

Eliminate labor costs. Continuous cleaning and filtering eliminates the cost of manually cleaning condenser and heat exchanger tubing and waterboxes. As hourly labor rates climb, as downtime becomes less available, manual cleaning becomes less attractive from an economic point of view as a means of maintaining condenser efficiency. Moreover, as pointed out in this paper, manual cleaning is not highly effective and is intermittent in nature. Between cleanings unit efficiency drops off rapidly.

Better cleanliness factors. Because the cleaning and filtering systems can maintain a condenser or heat exchanger at a high level of efficiency, the designer can plan on higher cleanliness factors - 95% to 100% in the case of stainless steel or titanium. Thus a smaller, more compact unit can be designed at a lower capital cost.

Longer life. By eliminating strong chemicals, solid debris ingestion, and corrosion from waterside deposits, cooling water tubing will last longer. Thus longer operating life from these highly expensive and vitally necessary units can be expected.

Can be completely automated. Both continuous condenser cleaning systems and Debris Filters are usually completely automated. However, their operation by manual means is simple and low in cost. The debris filter can be manually flushed by an operator in the normal course of his duties, taking up relatively few minutes in each shift. Or the units can be operated automatically, utilizing a manometer as a sensing device.

In the final analysis, only continuous cleaning and filtering systems are capable of maintaining the efficiency of the condenser or heat exchanger at its initial performance level.

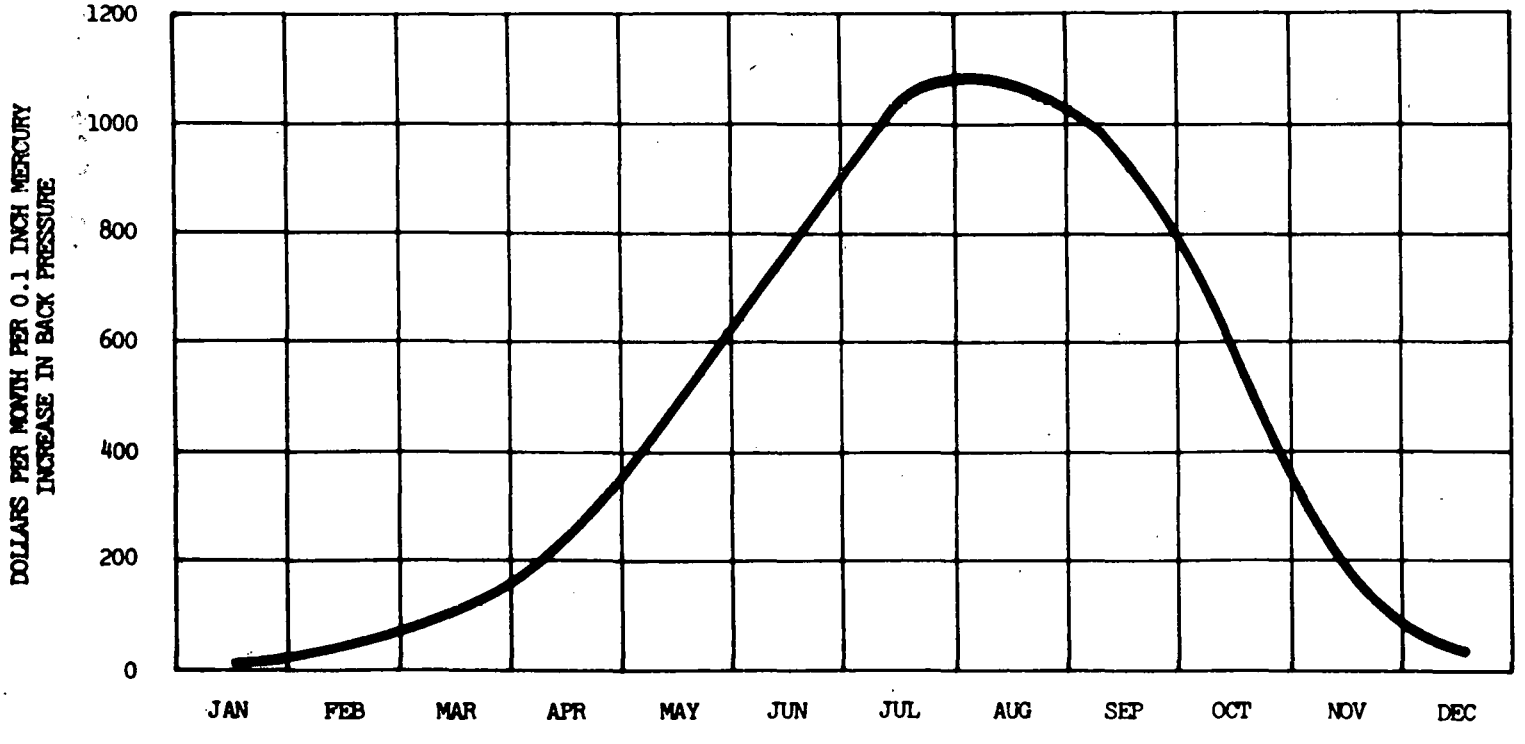



Fig. 1. Increase in operating costs resulting from a 0.1"Hg increase turbine back pressure for a 265 Mw unit.

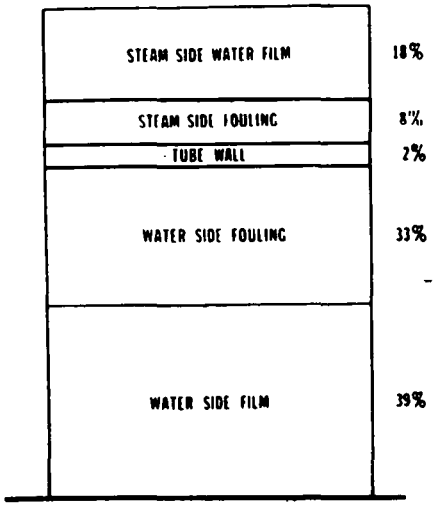



Fig. 2. Chart accounting for heat flow resistance in a condenser.

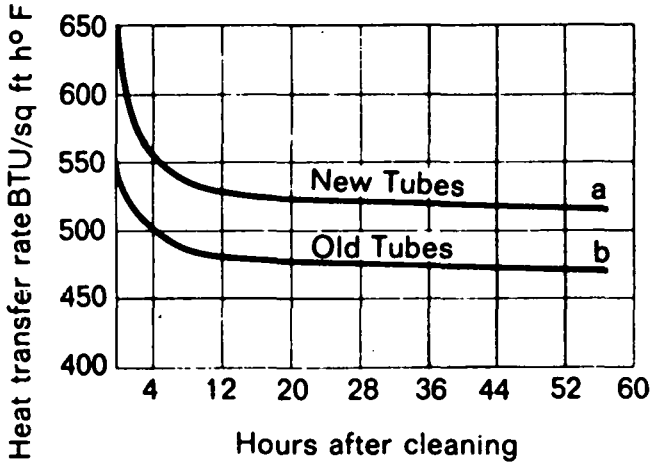



Fig. 3. Decrease in heat transfer rate vs. time.

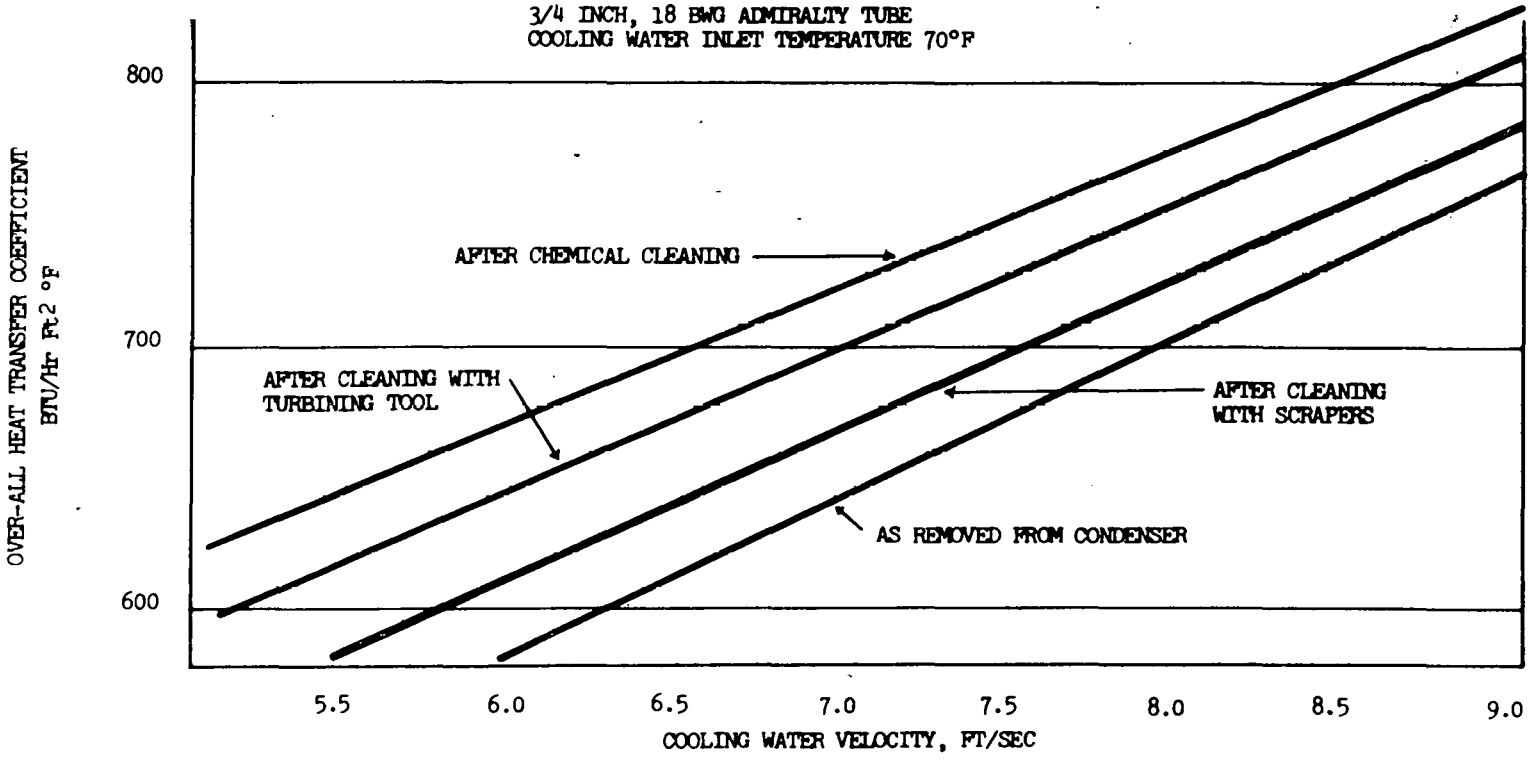



Fig. 4. Comparison of mechanical cleaning and chemical cleaning of Admiralty condenser tubes.

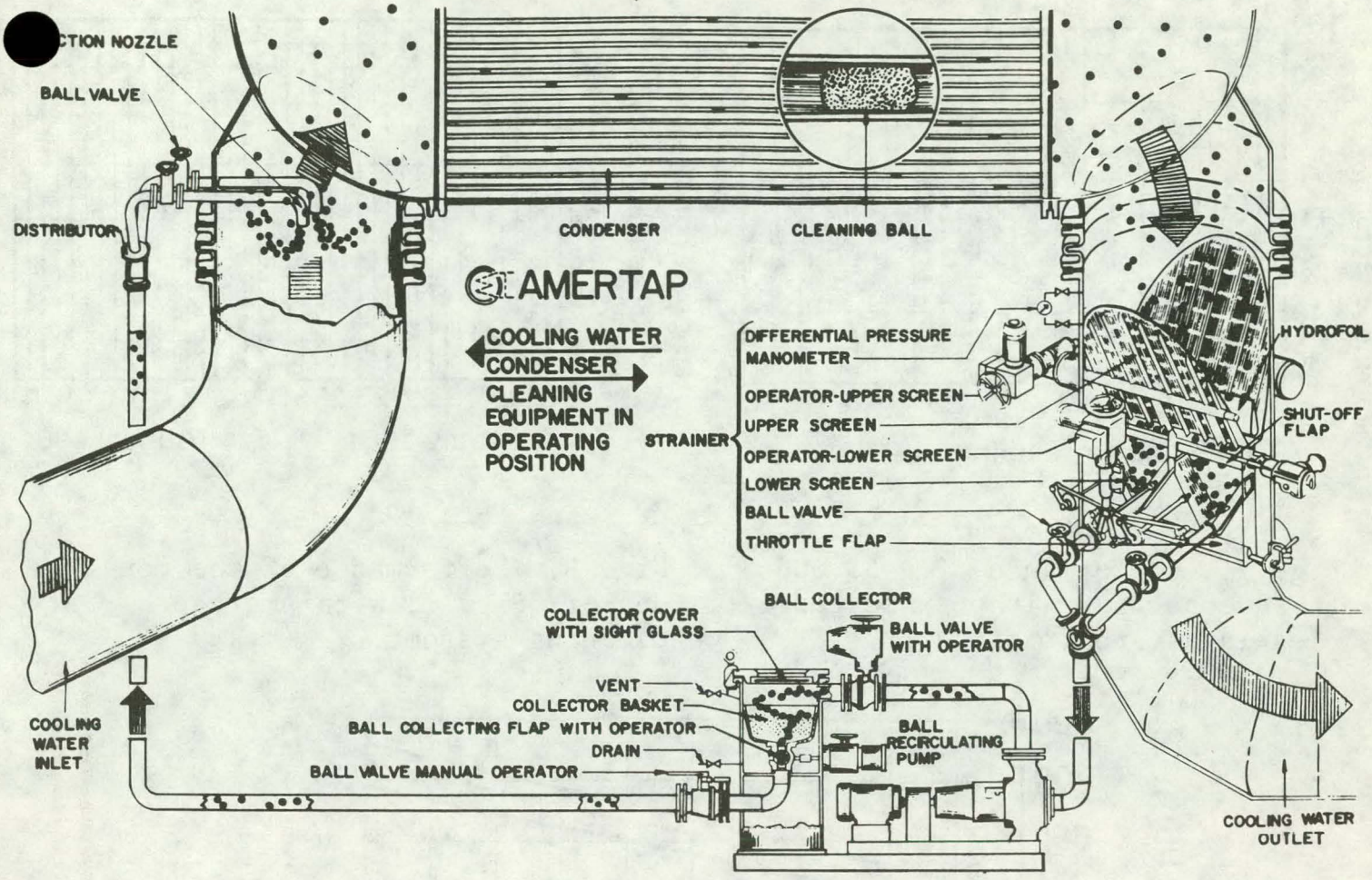



Fig. 5. Typical installation, Amertap Condenser Tube Cleaning System

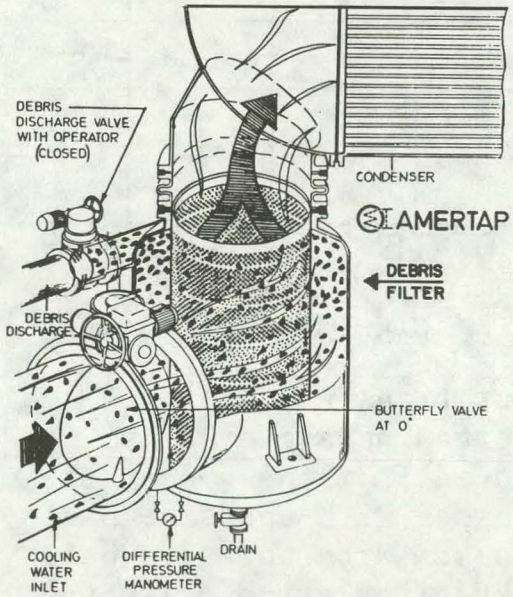



Fig. 6. Schematic of Amertap Debris Filter

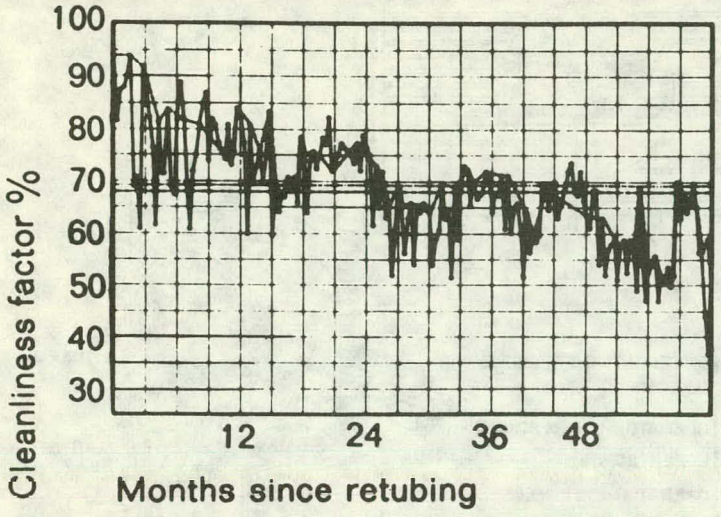



Fig. 7. Performance of a 55,000 ft-sq condenser without Amertap cleaning system.

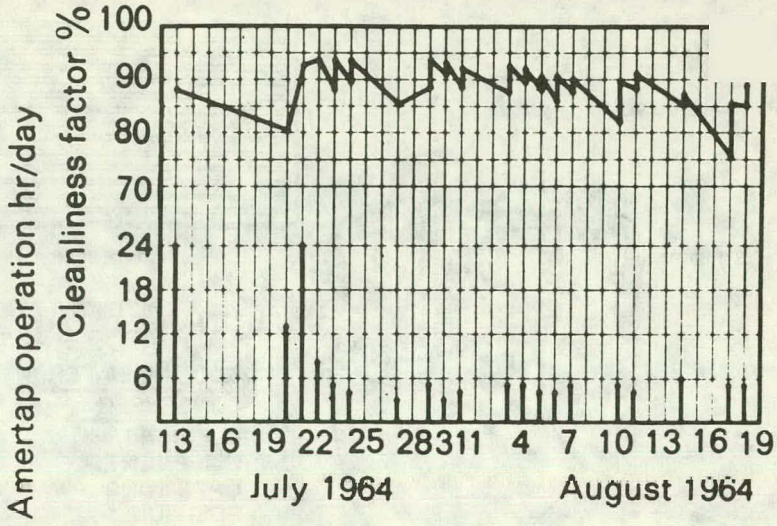



Fig. 8. Performance of the condenser, Fig. 7, with Amertap cleaning system.

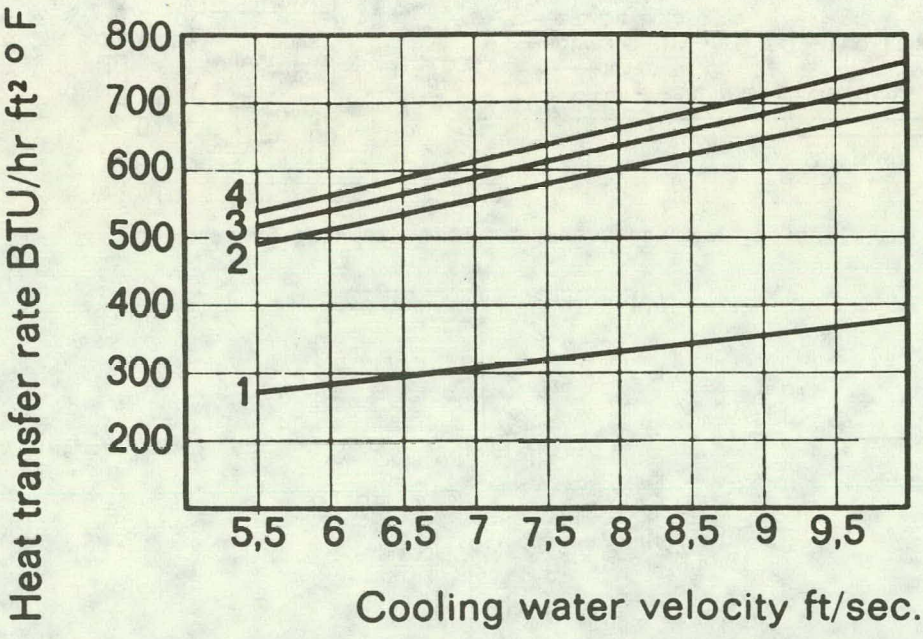



Fig. 9. Improvement of heat transfer rate of a scaled condenser tube through use of Amertap abrasive balls.

1) Tube as removed from the condenser
2) After 300 passes with abrasive balls
3) After 900 passes with abrasive balls
4) After 2 weeks circulation of sponge rubber balls

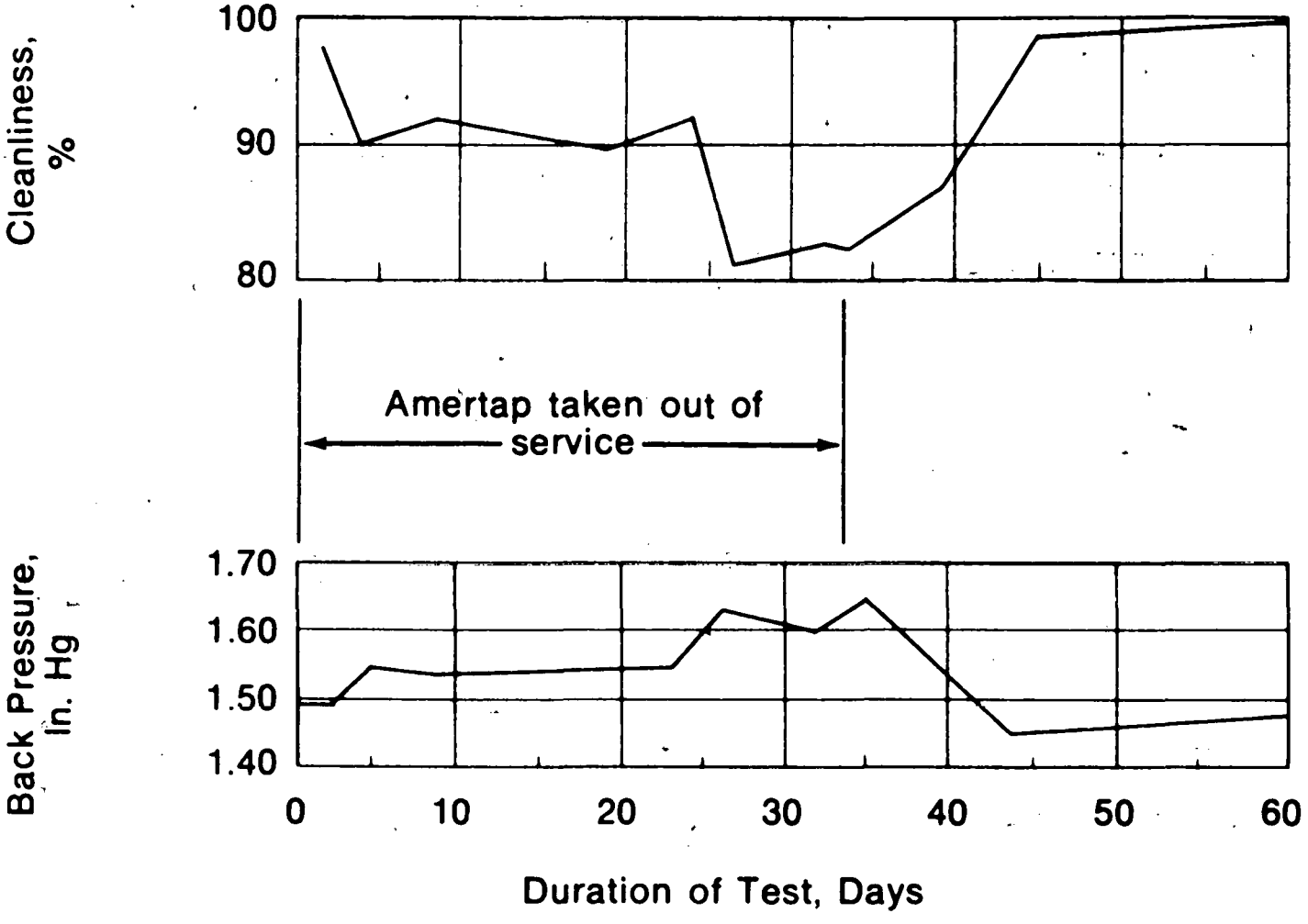



Fig. 10. Cleanliness and back pressure vs. time for stainless steel tubes, at English Station.

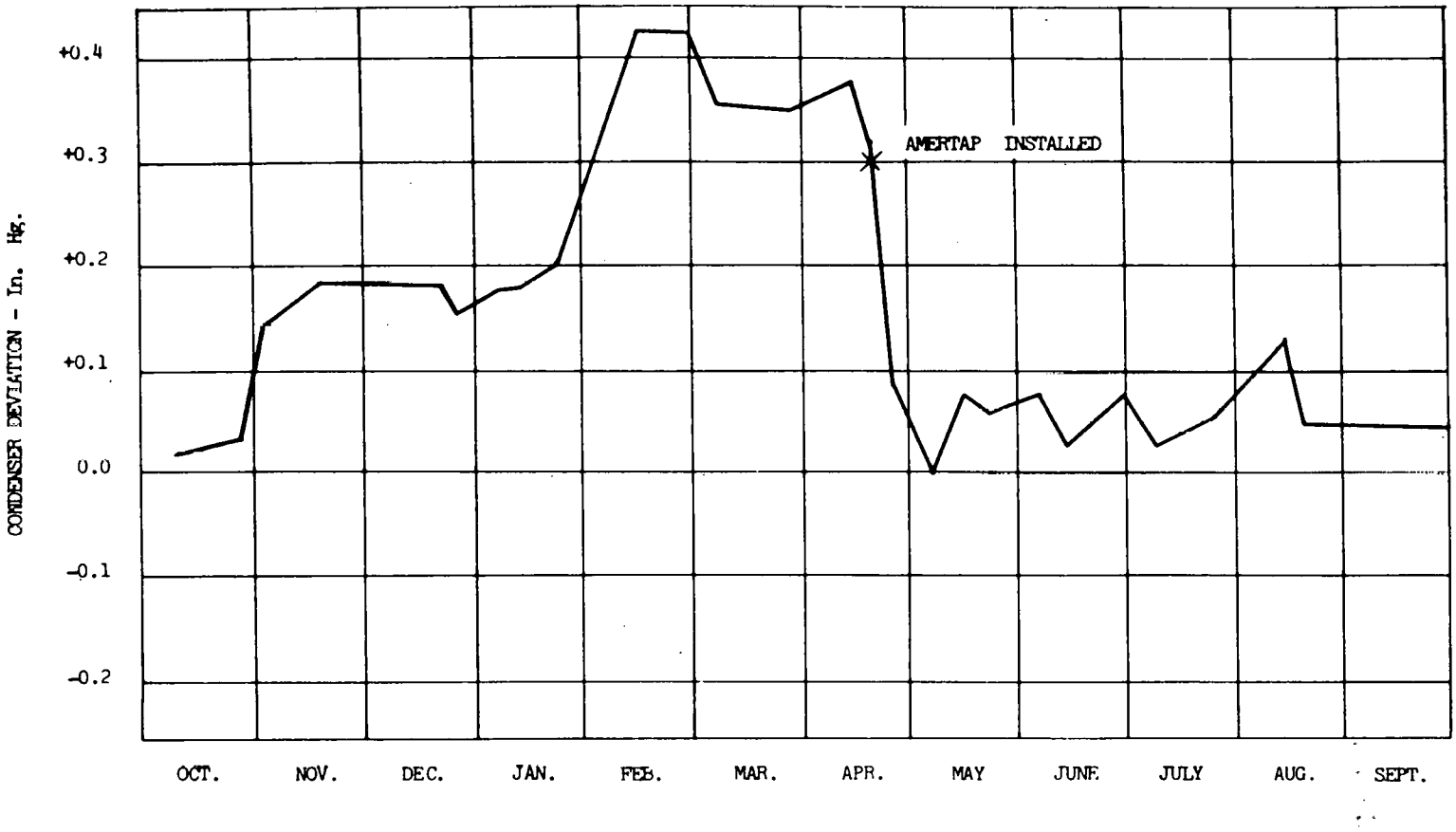



Fig. 11. CONDENSER PERFORMANCE, MT. STORM, UNIT NO. 1.

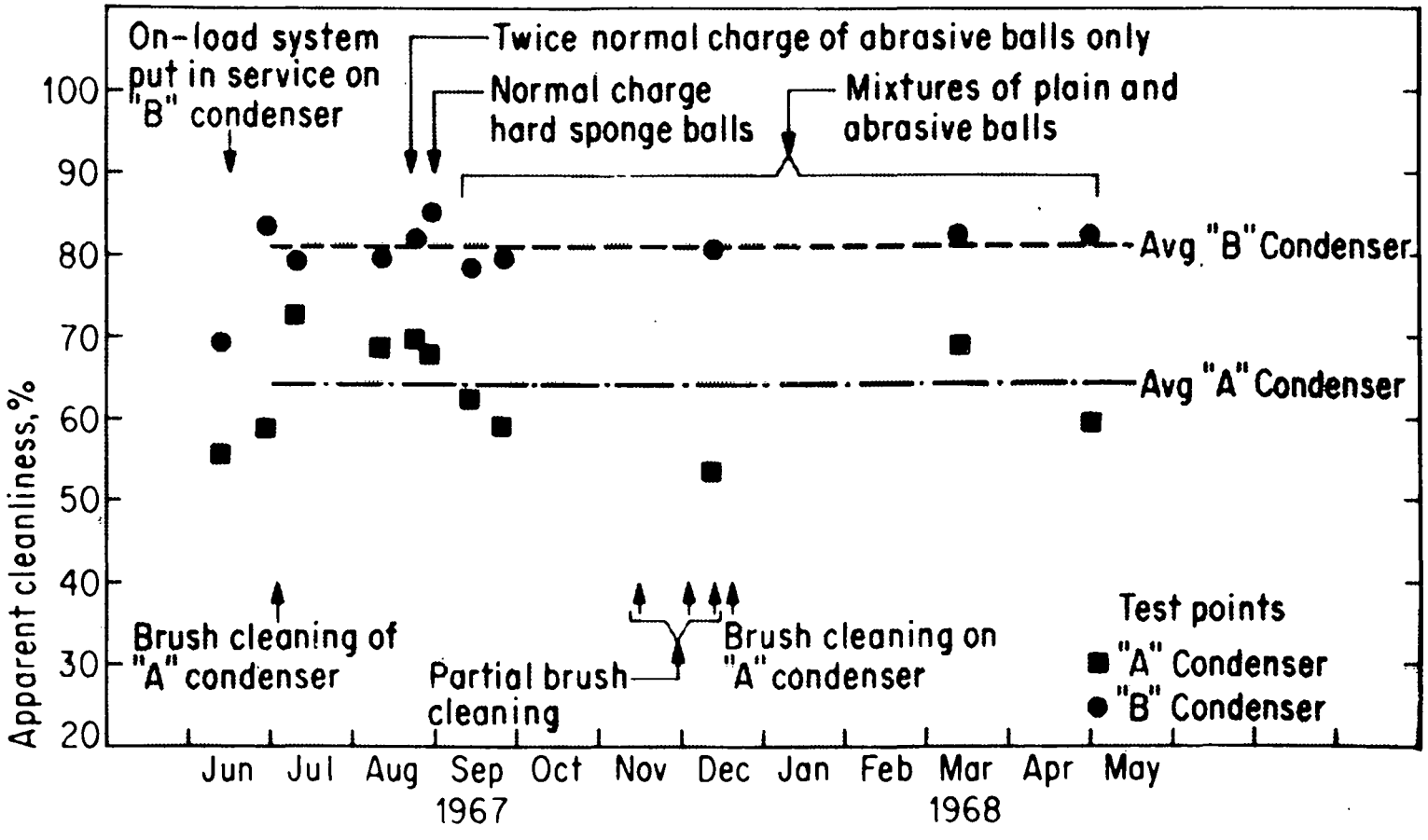



Fig. 12. Test experience at Tennessee Valley Authority's Widows Creek Plant with Amertap cleaning systems.

Table 1. Operating Conditions of Test Facility

| | Nominal Value | Range |
|---|---|---|
| Heat Duty of Test Units, $10^6$ Btu/hr<br>10 Btu/hr | 3.2 | 2.4 - 4.0 |
| Warm-Water Supply Temperature, °F | 80 | 75 - 85 |
| Cold-Water Supply Temperature, °F | | |
| Water-Temperature Change, °F | | |
| Log Mean Temperature Difference, °F | | |
| Water Flow Rate, gpm | | |

# VIII. ALTERNATIVE POWER CYCLES

GORDON L. DUGGER, CHAIRMAN
*Applied Physics Laboratory*
*The Johns Hopkins University*

THIS PAGE

WAS INTENTIONALLY

LEFT BLANK

# POTENTIAL OF OPEN CYCLE OTEC
# A GENERAL SURVEY

ARTHUR D. WATT, FRANK S. MATHEWS, AND ROBERT E. HATHAWAY

*Colorado School of Mines*
*Physics Department*
*Golden, Colorado*

ABSTRACT

The basic concept of converting the ocean thermal energy to mechanical power is straightforward. However, when one attempts a detailed system design, a number of complex problems are encountered. With OTEC plants, certain scale factors are involved which dictate the building of large size plants for efficient operation.

To gain an understanding of the problems involved, a barometric type open cycle plant is examined. It consists of three principal parts: a warm water loop, a turbogenerator, and a cold water loop. The low $\Delta T$ available leads to a low cycle efficiency, 3% or less. Hence, very large flow rates in both water loops are required. An examination of the pumping power versus head loss soon reveals the need of placing both evaporator and condenser close to the barometric level.

An important aspect of the open cycle is the amount of dissolved gases released in the evaporator and the effect of these gases on condenser performance. To maintain a high cycle efficiency, the condenser temperature must be kept low. This results in a very high specific volume for the steam and a large exit annulus area for the turbine.

In spite of the component sizes, a preliminary examination of potential costs indicates that a cost effective open cycle OTEC may be possible.

## Introduction

An interesting history of the early developments of thermal electric power conversion from the tropical seas was presented by Georges Claude in 1930 (1). Following earlier experiments at Ougree, Belgium, in 1929, he started work on a plant at Matamzas Bay, Cuba. Work on this plant was plagued by many construction problems; however, with much perseverance the plant was finally operated with a power output of 22 kilowatts. The inlet temperature was 27° C, and the cold water temperature 13° C. This early plant operating on the open cycle principle proved that electrical power could be produced from the thermal differences within the sea.

In the past decade, a resurgence of interest in OTEC has developed, based to a great extent upon the work of numerous persons working in this field, including: Anderson, Boot & McGowan, Brown & Wechsler, Heronemus, and Zener.

It has been well established that electrical power can be produced from the thermal differences of sea water and that there are vast amounts of energy to be tapped using only small portions of the ocean. The principal remaining questions are:

(1) What type and size of installations are likely to be most cost effective in producing useful energy from the sea,
(2) What are the near-term projections of energy costs, and
(3) What technological advances will contribute most to reducing the cost of energy produced by OTEC systems.

This investigation is limited strictly to open cycle systems and to the gathering of information relevant to the above questions.

In an open cycle system warm surface water is introduced into a low pressure chamber where it flashes to steam, passes through a turbine, and condenses in a low pressure chamber where the spent steam comes in direct contact with cold water from deep in the ocean. In order to sustain the operation of an open cycle system, the non-condensible gases from the ocean water which will accumulate in the condenser must be removed. This can be done either within the condenser itself, or in part by removing some of the non-condensibles at intermediate pressures before they enter the flashing and condensing chambers.

In examining the question of potential economic feasibility, a representative open cycle system is examined in terms of the water mass flow rates required

in the warm and cold water loops, and the steam flow rate through the turbine. Based on these rates, representative sizes of evaporator, turbine/generator and condenser are determined. It is found, for example, that there are certain physical limitations on the sizes of turbines which can be economically constructed at this time. There are other factors, such as multiple unit construction which make for a system with greater overall economy in that the start-up requirements for an isolated single large unit can be very expensive.

Structure sizes and material requirements for the evaporator, turbine/generator system, and condenser are examined and cost figures determined for each of these major components of the open cycle system. A computer program was developed in which the cost versus performance characteristics of each of the components are related in a system model. A comparison of major subsystem characteristics and costs is developed as the various input and operating parameters are varied.

The authors wish to acknowledge the valued assistance of Del Hoover, Dick Leyendecker and Ray Laub of the Westinghouse Electric Corporation in the areas of heat transfer and turbine design.

## System Layout

The general system layout for an open cycle OTEC plant is shown in Figure 1. This simplified diagram shows the system divided into 3 principal parts:

(1) the warm water loop,
(2) the turbine/generator, and
(3) the cold water loop.

The warm water loop on the left side consists of the inlet pipe, a degasifier/compressor, an evaporator and demister, and water pump/turbines in the warm water inlet and outfall to maintain efficiently a specified evaporator pressure even with head changes due to wave and tidal action. The steam out of the demister is fed as directly as possible into the turbine.

In the turbine, the steam is expanded through a set of fixed and rotating blades which are chosen to yield as large an efficiency as possible, while at the same time maintaining a high throughput of steam for a given turbine annulus area. The outlet of the turbine is fed to the condenser through a diffuser, so as to reduce the leaving losses to as low a level as possible.

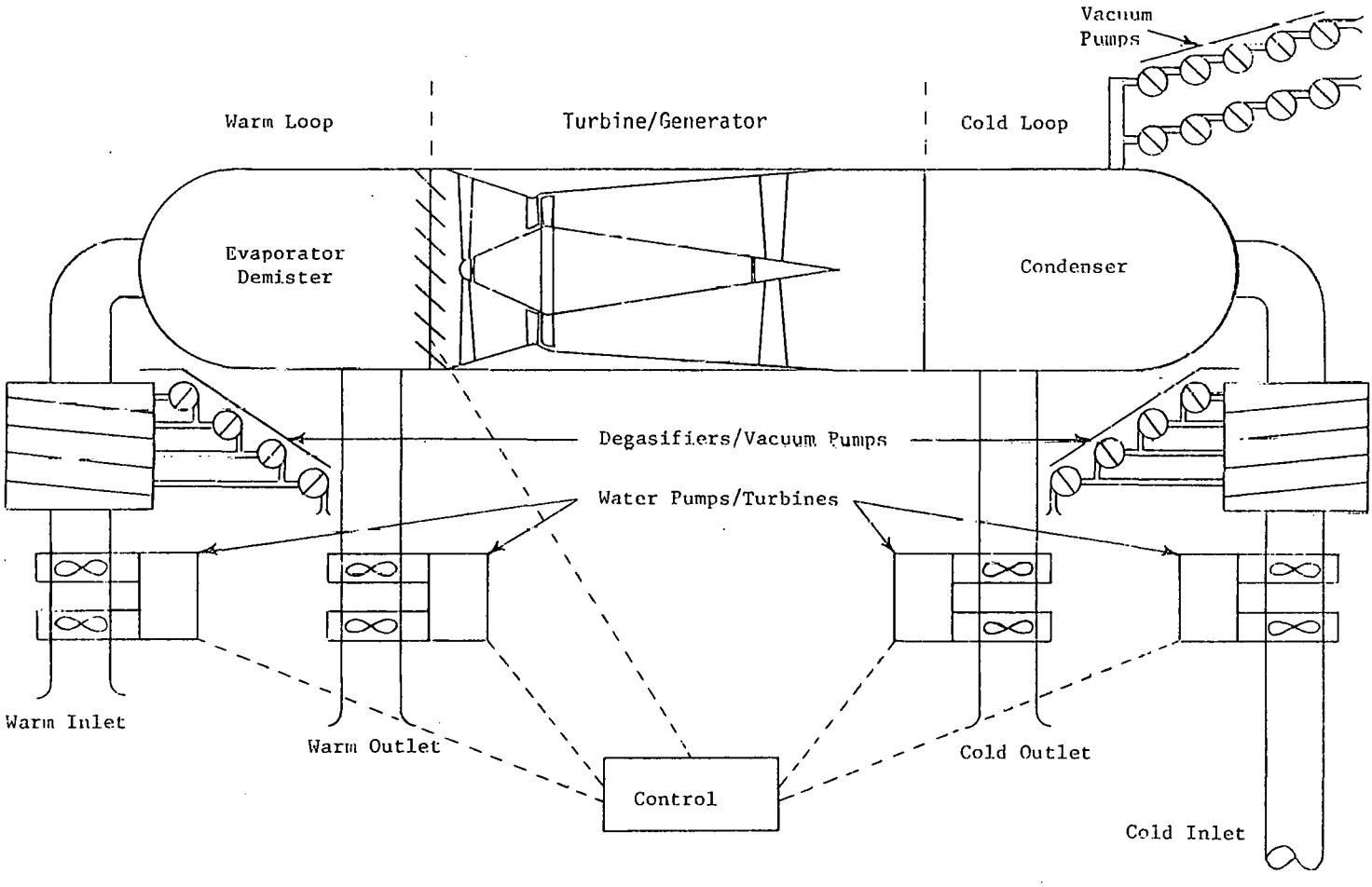



Fig. 1 General System Layout of an Open Cycle OTEC Plant.

The cold loop inlet comes from a depth on the order kilometer. The cold water passes through a pump/line and a degasifier, and is then introduced into the condenser. The water and condensed steam are removed from the condenser and pumped to the cold water outfall through another set of pumps. A degasifier shown on the condenser is used to remove non-condensibles released from the ocean water.

The general concept of a barometric plant is employed to the extent possible. The concept is to place the evaporator and condenser near the barometric level (10 meters above the water surface), so that there is not a great loss of effective head from water entering the evaporator and condenser. In designs of the size involved, where pipe diameters approaching 10 meters are needed, considerable care is required in both water loop designs. It is likely that, in order to maintain accurately the low pressures required in the evaporator and condensing chambers, carefully controlled pumps and hydraulic turbines will be necessary in both legs of each loop.

Some idea of the magnitude of the parameters involved is seen in Table 1. This summarizes the results of a first cut design for an open cycle OTEC plant with a turbine/generator output of 100 MW. The ocean parameters listed under item 1 are assumed for a desirable site, such as can be found in several locations. Item 2 gives the warm loop conditions for an assumed evaporator inlet temperature of 25° and outlet temperature of 21° C. For these and other associated conditions, the mass flow rate of the warm water will be on the order of 200,000 kilograms per second, or a volumetric flow rate of nearly 200 cubic meters per second. If a degasifier is used with staging and inter-cooling, 90% of the entrained gas can be removed with a required degasifier power of about 0.3 megawatt. The evaporator demister can operate with a steam temperature of 20° C and a steam mass flow rate of 1,400 kilograms per second. Because of the large specific volume of steam at this temperature, the volumetric flow rate of steam out of the evaporator is 84,000 cubic meters per second. The pumping power to account for some frictional loss and a total of 6 meters of freefall in the evaporator, demister and degasifiers, is on the order of 16MW.

Item 3 describes the basic turbine/generator parameters, including steam and condensing temperatures, the energy available for a kilogram of steam, and the Rankine cycle efficiency, along with an assumed turbine/generator efficiency of 83%. This assumption was for the first cut design. As we will see later, it appears that a somewhat lower efficiency would be a more cost effective choice. The turbine/generator output which was specified at 100 MW, requires a steam mass flow rate of 1,400 kilograms per second.

Cold loop parameters are shown in Item 4. In this case, an 8 meter head is assumed. About 1 meter of this is friction loss from the cold water pipe. Calculations were carried out to determine the temperature rise in various sizes of cold water inlet pipes. When large diameter pipes (on the order of 9 meters) such as would be required for a 100 MW installation are used, the rise is only 0.05°C. If smaller pipes are considered, such as a 1 meter diameter pipe, the water could rise by almost 2°C by the time it reached the surface. Such a loss in temperature difference would produce a serious decrease in the overall efficiency of an OTEC system. Because of this, it becomes apparent that small sized OTEC plants cannot be operated effectively unless insulation of the cold water inlet pipe is found to be feasible.

**Table 1**

**Parameters for First Cut Design of a Barometric Open Cycle OTEC Plant**

1. Ocean
   $T_{warm}$ = 25°C - gases 13/1000, Vol at STP
   $T_{cold}$ = 5°C - gases 15/1000, Vol at STP
   Salinity 35/1000

2. Warm Loop
   $T_{ei}$ = 25°C, evaporator inlet temperature
   $T_{eo}$ = 21°C, evaporator outlet temperature
   $\dot{m}_{ei}$ = $2.1 \times 10^5$ Kg/sec, mass flow rate
   $V'_{ei}$ = 205 $m^3$/sec, volumetric flow
   Degasifier, staged with intercooling
   $\dot{m}_{go}$ = 3.4 Kg/sec, 90% gas removed
   $P_{degas}$ ≃ .3 MW
   Evaporator & demister
   $T_s$ = 20°C, steam out
   $\dot{m}_s$ = $1.4 \times 10^3$, Kg/sec
   $V'_{so}$ ≃ $8.4 \times 10^4$, $m^3$/sec
   $P_{pump}$ = 16 MW (assumed 6 meter head)

3. Turbine/Generators
   $T_s$ = 20°C, inlet steam temperature
   $T_c$ = 10°C condenser
   $\eta_{cycle}$ ≃ .034 Rankine cycle eff.
   $\eta_{tg}$ = 0.83 (assumed)
   U/W = 20.1 Kcal/Kg available energy
   = $8.4 \times 10^4$ Watt sec/Kg
   Turbine/Generator output = 100 MW (specified)
   $\dot{m}_s$ = $1.4 \times 10^3$ Kg/sec

4. Cold Loop
   $T_{ci}$ = 5°C, condenser inlet temp.
   $T_{co}$ = 9°C, condenser outlet temp.
   $\dot{m}_{ci}$ = $2.06 \times 10^5$ Kg/sec, mass flow rate
   Degasifier, staged with intercooling
   $\dot{m}_{go}$ ≃ 4.6 Kg/sec, 90% gas removed
   $P_{degas}$ ≃ 0.4 MW staged
   (≃ 3.7 MW if not staged)
   Condenser
   $V'_{cwi}$ = 201 $m^3$/sec, cold water in
   $T_{sc}$ = 5°C, steam condensing temp.

Table 1, continued

Condenser

$\dot{m}_s$ = $1.4 \times 10^3$ Kg/sec, steam mass flow rate

$V'_{csi}$ = $1.5 \times 10^5$ $m^3$/sec, steam vol. flow rate

Pumping

$P_{pump}$ = 19 MW (assumed 8 meter head)

5. Power Available

| | | |
|---|---|---|
| Turbine Generator out | | 100 MW |
| Warm loop pumping | - | 16. |
| Warm loop degas. | - | 0.3 |
| Cold loop pumping | - | 19. |
| Cold loop degas. | - | 0.4 |
| Other auxiliaries | - | 4.0 |
| Net Output | | 60.3 |

After the "order-of-magnitude" flows and sizes were established in the first cut design, a revised computer simulation model was set up, permitting, for example, an analysis of the effect on other system parameters as certain key parameters were varied.

The manner in which the available temperature difference is divided up throughout the system can be seen in Figure 2. Starting with the warm water inlet temperature (25° in the example), the first drop is the "range" of the evaporator, i.e. inlet to outlet temperature difference of 4°C. The steam leaving the evaporator will be cooler than the leaving water by an amount referred to as the terminal temperature difference, (1°C in this example). This produces steam at a temperature of 20°C. The temperature drop through the turbine into the condenser is 10°, resulting in a condensing temperature of 10°C. When a terminal temperature difference in the condenser of 1° is employed, the cold loop inlet water temperature is 5°C. The cold water is warmed upto 9°C, yielding a range in the condenser of 4°.

Also shown in Figure 2 are representative losses of head for a revised system. The head losses are lower than for the first cut design, and can be varied in the model. The warm water inlet loss is close to 1 meter. Several meters of loss are assigned to the evaporator, and no warm loop degasifier is used. The cold water system has an additional 1 meter head loss because the cold water pipe is so much longer than the warm water inlet. In addition, because of the physical arrangement "most probably" required in the condenser, a somewhat greater head loss is also shown for this portion of the system.

In order to determine the probable sizes of piping required in various parts of the system, a program was developed to determine the optimum velocity and pipe diameters as a function of mass flow rates. For the initial design, we assumed the cost of fabricated steel at $2/kg, an amortization rate of .12 dollars per year per dollar, and a cost of electrical power of 3¢/kWh with a pump efficiency of 0.8 and a plant operation factor of 0.9. The results of this optimization are shown in Figure 3. It is realized that other types of pipe materials could be employed in the final design cold water pipe, and that the cost of electrical energy will have to be arrived at by iteration once the energy costs for the plant have been established.

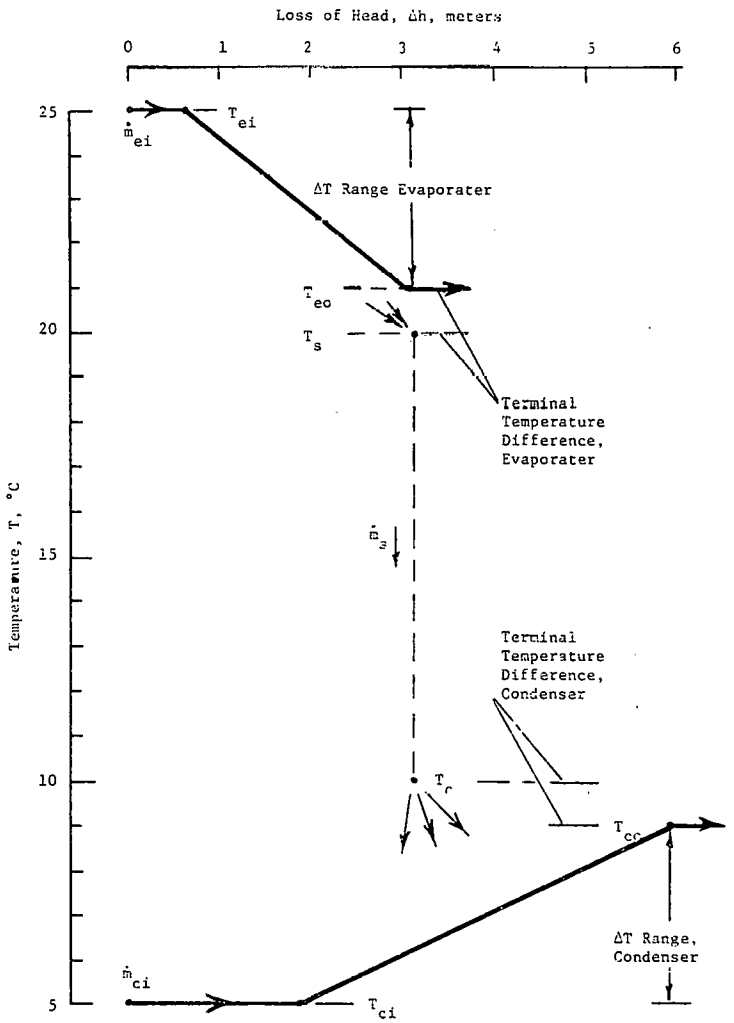



Fig. 2 Open Cycle OTEC Temperature, and Head Loss

Evaporator-Turbine/Generator-Condenser

Initial design considerations for the range of temperatures available for steam and condensing indicated a pressure ratio across the turbine on the order of 2. This is representative of the pressure ratio normally encountered across a single set of fixed and rotating blades. The pressure drop across this stage is, however, very small (on the order of 1/100 of an atmosphere).

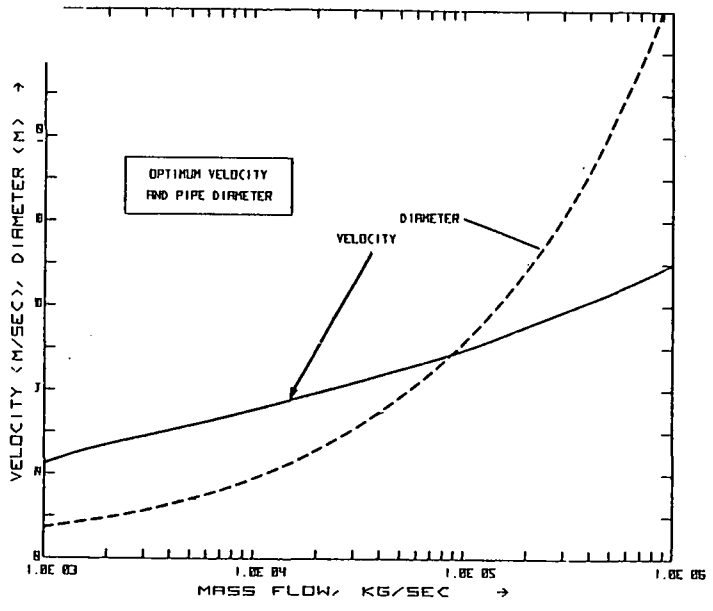



Fig. 3 Minimum Cost Water Velocity and Pipe Diameter - vs - Mass Flow Rate. (Steel at $2/kg, electrical energy 3¢/kWh.)

This, plus the consideration of the large specific volumes involved (on the order of 100 $m^3/kg$ at the exhaust) indicated that conventional turbine designs are not likely to be effective. An examination of centrifugal forces involved, and tip speeds, quickly led to the conclusion that the limiting factor will be tip velocity and not centrifugal force. In view of this, a range of materials is, in theory, available for blade construction. A range of operating speeds from 900 down to 300 rpm was examined and it appeared that a 300 rpm turbine with a 24 pole generator would probably be the best first-try choice.

The need to keep the entrance pressure drop as low as possible, in addition to preventing a buildup of back pressure at the exit of the turbine, soon led to the decision of building an integrated module of evaporator, turbine and condenser as shown in Figure 4. A number of other types of designs were considered, but it was finally concluded that, in order to keep the housing costs to a minimum, along with a minimum of pressure drop through the system, an in-line configuration contained within a large tubular structure with spherical ends would be the most cost effective. The questions remaining now were: what evaporator area and condenser volume are required and what turbine blade size and gauging angle are best?

Evaporator

The size of evaporator required is apparently determined by 2 factors:

(1) the allowable temperature drop; i.e., the range and terminal temperature difference described earlier, and
(2) the amount of moisture carryover permitted in the steam.

The first size constraint is based on a leaving velocity density defined in terms of $kg/sec/m^2$ of evaporator area. A log mean temperature difference expression similar to that used by Foot & McGowan (2) was employed. The size initially chosen was based on a 1° terminal temperature difference and a leaving flux density of .25 $kg/sec/m^2$. In the system simulation model, a relationship was established between leaving velocity and the log mean temperature difference. The second constraint is concerned with moisture carryover - vs - leaving flux density and is based on experimental performance of vacuum flashing equipment described by Ewoldsen et al (3). For the leaving flux density chosen,

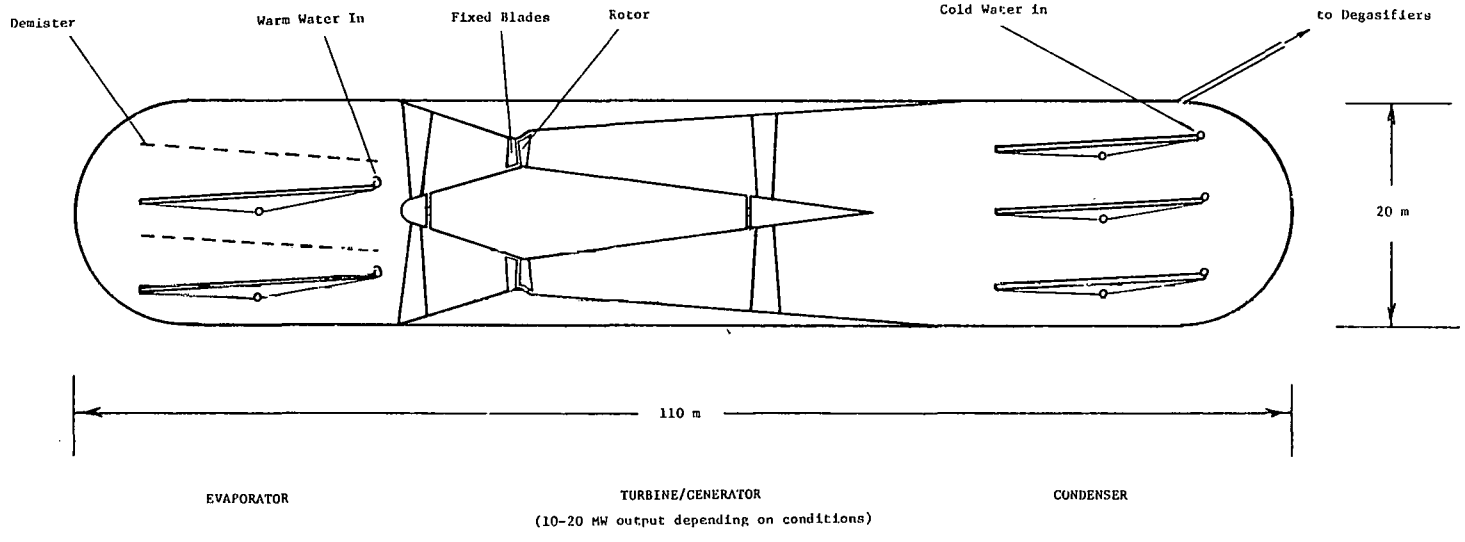



Fig. 4 Open Cycle OTEC Evaporator - Turbine/Generator - Condenser Module.

1 or 2% or even greater amounts of moisture could be carried over from open trays. In view of this, the cost calculations were based on placing demister screens above the evaporator trays. With these demisters a carryover on the order of a few tenths of a percent is expected.

Turbine-generator

An examination of the temperature entropy diagram for the steam expanding through a turbine/generator under these conditions shows that the outlet steam would contain on the order of 2% moisture. This is not expected to produce any serious problems in blade life or turbine efficiency loss. In the chamber construction, conservative ratings of stress in the steel were employed. In all cases, stress was kept below $7 \times 10^6$ kg/m$^2$, (equivalent to 10,000 psi.) The basic steel construction costs were assumed at $2/kg, with 100% add-on included later for installation, etc.

The turbine, operating at 300 rpm, has a set of fixed blades with a root diameter of 4 meters and a tip diameter of 6.5 meters. The rotor blades have a root diameter of 3.5 meters and a tip diameter of 7 meters, yielding a rotor blade length of 3.5 meters. For a turbine of this size the tip-to-casing clearance can be much larger than normal, since the annulus area is so large that the losses encountered around the tip will be negligible.

The static loading conditions can be met with a wide variety of materials. However, one of the major concerns is that we are still dealing with tip velocities which are just slightly subsonic and the blade lengths employed are much longer than have been used in conventional turbine design. The possibility of vibration and resulting fatigue is a real concern, and can only be resolved after a very detailed analysis is carried out. Preliminary considerations have led to the conclusion that blades of this length can be constructed and it may be possible, by employing special fabrication techniques, to arrive at vibrational frequencies which are not likely to be encountered in normal practice. For the initial costing, 96 fixed blades were considered, along with 109 blades in the rotor. The gauging angle was set up as a variable related to the effective annulus area, and expected turbine/generator efficiency. The effective annulus area controls permissible mass flow rate, or "swallowing capacity" of the turbine.

The electrical output available from each OTEC module of the sizes shown in this figure is expected to be in the range of from 10 to 20 MW, depending upon steam conditions and other parameters of the turbine.

Two of the major cost items in the turbine are the case and the rotor blades. Current costing rates for forged blades employed in conventional turbines run on the order of $22/lb installed. Rotor forgings are somewhat in excess of $3/lb and the rotor discs are around $5/lb. When costing rates of this nature are employed the cost of the turbine portion of the module using forged blades comes out on the order of $20,000,000 per module. Using a revised case design, and rotor blades of less costly materials, it appears that the cost would drop to $10,000,000 per unit, or less.

Condenser

The condenser is designed in such a manner as to locate the warmest water surface adjacent to the inlet steam. This counterflow principle was also used in the evaporator. The amount of condenser volume required is based on a relation where the volume is equal to the mass flow rate of steam divided by the log mean temperature difference and a volumetric density constant. This constant, k, appears to be on the order of .05 kg/sec/m$^3$°C. This amount of steam swallowing appears feasible based on the work of K.W. Coons (4).

In the condenser design it is essential that the water freefall be kept to a minimum, while at the same time exposing a maximum amount of water surface to the incoming steam. The conceptual design shown in the earlier figure indicates 3 trays, where each one is arranged in a separate sub loop such that the water flows to a catch basin with a freefall on the order of 3 meters. Preliminary evaluations have been made of the type and sizes of trays required and the slope necessary for the flow rates involved. Careful design is required to control velocity head loss at the water outlets as a function of pipe diameter and exiting velocity.

In order to arrive at preliminary estimates of the various cost components of an overall system, the initial calculations were based on the use of degasifiers at the condenser only. It was shown in Table 1 that this would require significantly greater electrical input to the degasifier. The reduction in freefall head loss by eliminating the in-line degasifiers, and the associated cost of the vacuum vessels, may more than offset the increased degasifier capital and operating costs. This determination remains to be made in a future more detailed analysis.

Preliminary Costing & System Optimization

The various input parameter selections and operating point determinations for the simulation model along with associated mass flow rates, power outputs and auxiliary power requirements, as well as the cost of the various subsystem components, are shown in Table 2. The OTEC system simulation model was arranged in such a manner that the steam and condensing temperatures could be arbitrarily chosen. The primary factor which was fixed in the calculations was that the combined turbine outputs would be 100 MW. The steam flow rates were calculated based on this requirement, along with the steam input and output conditions and the efficiency of the turbine. Turbine efficiency could also be selected as an input parameter which automatically determined the cost of the turbine based on the relationship between swallowing capacity and turbine/generator efficiency.

The various parameters in the system model are shown in Table 2. The cold water pipe length employed was 1100 meters, and the various temperatures used are shown in the first set of numbers. Next follow the mass flow rates, then the power outputs along with parasitic power requirements, and then the net output power available from the station. Costs in millions of dollars are then given for the various components of the whole system. These figures are then totaled and divided by the net output power to yield the station costing rate in $/kW of rated station capacity; i.e., related to the output after subtracting off the parasitic loads. The final line shows the cost of electrical energy in ¢/kWh based on ammortization of the capital costs of the com-

ponents listed at the .12 rate given earlier. Offshore m ; or on shore site costs are not included. Other f ; not included in this initial comparison are a ectural and engineering fees and interest during construction.

Table 2

Open Cycle OTEC System Comparisons

| | | | | |
|---|---|---|---|---|
| COLD WATER PIPE length = 1100 m | | | | |
| TEMPERATURES (°C) | | | | |
| evaporator in | 25 | 25 | 25 | 25 |
| evaporator out | 21 | 21 | 22 | 20 |
| steam | 20 | 20 | 21 | 19 |
| condensing | 7 | 10 | 10 | 10 |
| condenser in | 4.3 | 4.3 | 4.3 | 4.3 |
| condenser out | 6 | 9 | 9 | 9 |
| MASS FLOW RATES (kg/s) | | | | |
| warm water xE5 | 1.88 | 2.46 | 2.99 | 2.18 |
| steam xE3 | 1.29 | 1.68 | 1.54 | 1.86 |
| cold water xE5 | 4.42 | 1.92 | 1.73 | 2.15 |
| POWER (MW) eff = .7 | | | | |
| turbine out 100 | | | | |
| w.w. pump | 7.4 | 9.6 | 11.6 | 8.6 |
| c.w. pump | 31.7 | 14.6 | 13.3 | 16.3 |
| degasifier | 7.9 | 5.1 | 5.4 | 5.2 |
| start up | 6.9 | 4.7 | 4.8 | 4.7 |
| auxiliary | 5 | 5 | 5 | 5 |
| output | 47.9 | 65.6 | 64.6 | 65 |
| COSTS (M $) | | | | |
| w.w. pipe | 2.2 | 2.7 | 3.2 | 2.4 |
| w.w. pumps | .9 | 1.2 | 1.5 | 1.0 |
| evaporator | 20.7 | 27.1 | 28.4 | 26.7 |
| turbine/gen. | 61.7 | 65.4 | 59.5 | 72.7 |
| c.w. pipe | 48.3 | 24.2 | 22.2 | 26.6 |
| c.w. pumps | 3.9 | 1.8 | 1.7 | 2.0 |
| condenser | 30.5 | 25.1 | 22.8 | 27.7 |
| degasifiers | .8 | .5 | .5 | .5 |
| start up | .7 | .5 | .5 | .5 |
| aux & controls | 1 | 1 | 1 | 1 |
| total | 170.7 | 149.5 | 141.2 | 161.3 |
| Costing rate ($/kW) | 3564 | 2279 | 2187 | 2478 |
| Cost of energy (¢/kWh) (based on components listed) | 5.4 | 3.4 | 3.3 | 3.8 |

The first two columns show the effect of changing the condenser output temperature by 3°, while the last two columns show the effect of varying the evaporator output and steam temperatures for a fixed condensing temperature. The third column conditions yield the lowest relative cost of electrical energy. The results of carrying out this type of comparison for a wide range of conditions is shown in Figure 5. Changes in electrical power out and cost of energy with varying condenser temperatures are shown on the left. Taking the first minimum cost point on the left hand curve at a condensing temperature of 10°C, and then varying the steam inlet conditions, shown by the right hand curve, yields a lower minimum cost at a steam temperature of 21°C. The corresponding variations in output power are shown by the dashed lines. These were all carried out with a turbine/generator efficiency of 0.7.

The effect of turbine/generator efficiency (varied by changing the gauging angle and other factors affecting steam swallowing capacity) on the output power and the cost of electrical energy is shown in Figure 6. The resulting energy cost minimum occurs for a turbine/generator efficiency of 0.7 or slightly greater. This result was somewhat lower than had been anticipated when compared with conventional power plant practice where the turbine/generator efficiency is usually greater. An examination of the relative costs of the station, shown in Table 3, reveals that a large portion of the station cost is in the turbine/generator. The evaporator, cold water pipe and condenser are also seen to be large cost items. In a conventional power plant, the turbine generator cost is a small fraction of the total plant cost, so that the additional cost of making it very efficient is insignificant. Such is not the case with the open cycle OTEC turbine.

In view of these preliminary results, it appears that major efforts at cost reduction should be centered on the turbine/generator, evaporator-condenser and cold water pipe. The turbine/generator cost reduction will probably lie primarily in the choice of blade materials, the arrangement of blade mounting and generator coupling, and housing design.

It is known that others evaluating cold water pipe costs have arrived at costs which are probably somewhat lower employing materials other than steel. The next item likely to show a significant cost reduction is the evaporator. It is conceivable that somewhat higher leaving flux densities can be employed when proper demister arrangements are used. Condenser costs may also be reduced; however, at this point it is believed that they are probably the least flexible of the design factors.

Additional cost data obtained after the original model was set up indicate that although the degasifier power requirements are probably correct, the costing of degasifiers would be several times greater. This effect on the overall cost of energy is not likely to be noticed, however.

The costing procedures employed are believed to be representative of the types of costs encountered after about 10 units have been constructed. The use of modules whose output capacity is on the order of 1/4 to 1/8 of the total plant capacity appears desirable.

Because of the necessity of minimizing the amount of free fall head loss through the evaporator and con-

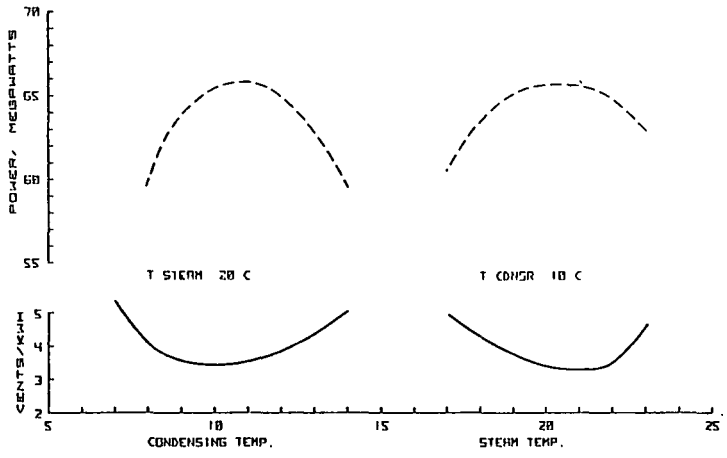



Fig. 5 Open Cycle OTEC. Power Output and Equipment Component of Energy Cost with Varying Steam and Condensing Temperatures.

denser, a number of different configurations have been examined. In the evaporator, it appears important to control the pressure drop in the feed lines to prevent flashing within the feed tubes before the water enters the evaporator trays or stand pipe arrangements. In any event, the placement and sizing of the outlet ports becomes extremely important. In view of the low free fall

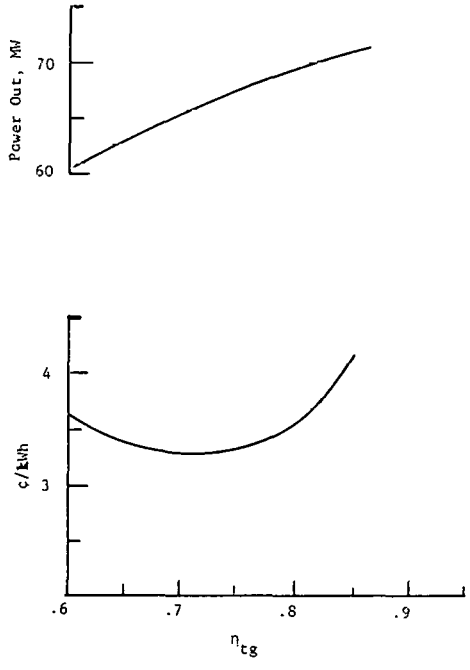



Fig. 6 Variation in Power Output and Cost of Electrical Energy with Turbine Efficiency

Table 3

Preliminary Cost Breakdown and System Parameters For A 65 MWe Output Open Cycle OTEC System

| | (Millions) |
|---|---|
| **WARM WATER LOOP** | |
| Inlet pipe - 100 m | $ 2.7 |
| Pumps - 7 MW, eff = 0.8 | $ 1.2 |
| Evaporator | $ 27.1 |
| $\dot{m}_{ei} = 2.4 \times 10^5$ Kg/sec | |
| TOTAL | $ 31.0 |
| **TURBINE GENERATORS** | |
| 6 to 8 units, 300 rpm | $ 65. |
| Dia = 20 m. Length = 50 m | |
| Rotor, $r_{tip} = 7$ m, $r_{root} = 3.5$ m | |
| Efficiency, $eff._{tg} = 0.65$ to 0.8 | |
| Power/module 10 - 20 MW, 100M total | |
| $T_{steam}$ 17 - 23°C | |
| $T_{cond.}$ 6 - 13°C | |
| $\dot{m}$ steam 150 to 250 kg/sec | |
| TOTAL | $ 65.0 |
| **COLD WATER LOOP** | |
| Condenser | $ 25.1 |
| $\dot{m}_{co} = 1.9 \times 10^5$ kg/sec | |
| Pumps 20 to 30 MW | $ 2 to 4 |
| Inlet pipe, 800 to 1200m | $ 24 |
| Degasifier | $ .5 |
| $\dot{m}_a$ 8 kg/sec | |
| Power 5 MW | |
| TOTAL | $ 53.6 |
| **AUXILIARY, ETC.** | |
| Start up (1/8) plant | $ .5 |
| Power 5 MW | |
| Controls & other | $ 1 |
| Power 5 MW | |
| TOTAL | $ 1.5 |
| **TOTAL** | $ 151.1 |

used, the system is sensitive to changes in platform orientation. Because of this, onshore siting for initial plants appears desirable.

Site parameters are very important in determining

the final cost of electrical energy. Each additional ... of available temperature difference will make a significant reduction in energy cost. Although the actual figures are not available as of this writing, they will be developed along with other system optimization criteria by selected sites during the remainder of this study and reported at a later date.

References


(1) Claude, Georges, Power from the Tropical Seas, Mechanical Engineering, Vol. 52, No. 12, Dec. 1930, p 1039-1044.

(2) Boot, J. L., and J. G. McGowan, Feasibility Study of a 100 MW Open Cycle Ocean Thermal Difference Power Plant, Report: NSF/RANN/SE/GI-34979/TR/74/3, August 1974.

(3) Ewoldsen, E. I., P. Dattani, A. F. Mills, E. M. Stocking, Sea Water Entrainment in Low Temperature Flash Evaporators, U. of California, Berkeley, Sea Water Conversion Lab. Report No. 64-3, Dec. 1964.

(4) Coons, K. W., Direct Condensers, Bulletin No. 3, Engineering Exp. Sta., Col. of Eng., U. of Alabama, June 1953.


## DISCUSSION

WECHSLER (Hydronautics, Inc.): We did a study of the open cycle system in 1975 in which we proposed a low cost approach for the turbines. What did you assume for the turbine design and cost?

WATT: Initially we are using steel forgings for the blades at a cost like $22 a pound. We also use disk costs of approximately $10 to $15 a pound as the upper bound which we feel we can stand behind and say, yes, you can build this using the existing technology. We also considered the possibility of using fabricated blades as opposed to forged blades which would be quite a bit less expensive. Turbine cost is a fairly large part of the total cost, although the pressure vessel is no insignificant part, as you know, I'm sure.

WECHSLER: Did you look at our paper [OTC #2254, Seventh Annual Offshore Technology Conference, Houston, May 6, 1975]?

WATT: Yes, some time ago; I don't remember whether you broke costs into these various parts.

Unidentified questioner: What design approach did you take for removing noncondensible gases?

WATT: Initially we considered taking the noncondensibles from the condenser directly, and we realized that at least five stages of recompression would be needed to go from the pressure in the condenser up to atmospheric pressure. In addition, it is essential to have intercooling between these stages to keep the power down. We estimate a power requirement of 5 to 8 $MW_e$, depending on the mass flow rate of the water through the system. A better approach, as was shown on one figure, would be to reduce the pressure on the water by stages and degasify at each stage, so that you do not have to pump all of the gas from this very low pressure up to atmospheric pressure; you may be able to reduce the power requirement by a factor of 10. However, the problem that concerns me most at this time, which I haven't had time to solve, is the size of degasifying vessels required, because you want to get that water through fast, but the rate of off-gasing is a function of the pressure differential between the equilibrium pressure and the pressure of that vessel. Thus, you have to find the optimum tradeoff between investment costs and pumping power costs. Since I didn't have time to do the detailed costing and other optimization prior to this meeting, I simply based the cost on what we knew we could do for the case of taking all of the noncondensibles from a single location.

Unidentified questioner: Did you consider the alternatives of a standard pump vs basically using the barometric head above sea level?

WATT: Yes, we have attempted to design this as close to a barometric system as we can. For a very idealized system it is simple to show the barometric system and say you balance out and recover all of your pumping differential except for the free fall in the evaporator and condenser. But, because of the problems associated with varying wave heights, very large masses of water, and large pipe diameters we felt it best to consider pumps both at the inlet and outlet and having these arranged so that in one case it's an economizer. It actually works as a hydraulic turbine if the wave action changes to try and regulate that.

# SEA THERMAL POWER CYCLES

LUDO VAN HEMELRYCK
*Port Aransas Marine Laboratory*
*The University of Texas Marine Science Institute*
*Port Aransas, Texas*

ABSTRACT

The limit of available energy per unit of "processed" seawater is established for a sea thermal power plant. Using the amount of power generated for a given deep-sea water flow as a criterion, methods to approach the theoretical limit are examined.

## INTRODUCTION

Proposals to build power plants which would use the temperature difference ($\Delta T$) between surface and subsurface waters in tropical and subtropical oceans have been around for awhile. Each of these proposals reflects a different perspective, depending on the background of their proponents.

While we may be identified mainly with the mariculture aspect of "artificial upwelling" (1), which uses the chemical nutrient content of deep-sea water, our interest from the onset covered also possible applications of its physical characteristics.

I want to focus on some aspects of the sea thermal power cycle as I understand it was approached by the Abidjan Project team.

## BACKGROUND

Although large masses of both warm and cold seawater are available in the ocean for free, their utilization for the production of power requires a power plant. The cost of the power produced is represented entirely by the amortization and operating costs of the plant. These costs, in turn, are related to the volume of seawater handled. The seawater processed by the plant is no longer free, but has acquired a "value" represented by those handling and equipment costs which are a function of the volume handled.

For power plants located at or near the surface, the unit costs associated with the deep-sea water flow are bound to be more significant than those related to the surface water flow. This has led us to consider the deep-sea water as the principal resource, which should be efficiently utilized.

It may be argued that the major cost items of a sea thermal power plant are the heat exchangers, and not the deep-sea water collector. As a consequence, optimal use of the deep-sea water would only have a minimal effect on overall plant economics. This opinion was not shared by earlier proponents of sea thermal power.

When evaluated on the basis of gross energy generated per $m^3$ of deep-sea water handled, the Abidjan Project (2) was expected to achieve 1125 $kW_e/m^3/sec$. A typical OTEC feasibility study (3) projects an output of 138.35 $kW_e/m^3/sec$. Both of these studies assumed a temperature differential between surface and deep-sea water of the order of 20°C.

Efficient use of the deep-sea water flow is reflected by the specific gross power generated, per unit of flow. We decided to investigate how the optimum operating point could be determined.

## AVAILABLE ENERGY

The amount of work produced by a thermodynamic process can be represented in terms of the quantity of heat (Q) involved, multiplied by the efficiency ($\eta$) of the process. A generalized expression reads:

$$\text{I.} \qquad W = \int \eta dQ$$

When a body with a given mass (M) undergoes a temperature change ($\Delta$) the heat released corresponds to:

$$\text{II.} \qquad Q = -kM\Delta$$

and:

$$\text{III.} \qquad \frac{dQ}{dT} = -kM$$

where k represents the specific heat of a unit of mass, in an appropriate energy unit. In further evaluations we have used the $m^3$ of seawater as our unit mass and adopted a value of:

$$\text{IV.} \qquad k = 4.187 \times 10^6 \text{ Joules } m^{-3} \, °K^{-1}$$

for deep-sea water within the range of temperatures of interest.

The efficiency of a "heat engine" used to transform thermal into mechanical energy cannot exceed the limit imposed by the second law of thermodynamics. Along an "ideal" process, entirely reversible, this upper limit is given by:

$$\text{V.} \qquad \eta_c = \frac{T_1 - T_2}{T_1}$$

where:

VI. a) $T_1$ = source temperature (°K)

b) $T_2$ = sink temperature (°K)

Introduction of this expression for $\eta$, and a change in variable of integration yields a maximum availab[illegible]

energy:

$$W_{max} = -kM \int \left( \frac{T_1 - T_2}{T_1} \right) dT$$

In the presence of an infinite heat sink at a temperature $T_h$, a mass of deep-sea water at a temperature of $T_c$ has an available energy limit of:

VIII. $$W_{max} = -kM \int_{T_c}^{T_h} \left( \frac{T - T_h}{T} \right) dT$$

which reduces to:

IX. a) $$W_{max} = -kM \left( T_h - T_c - T_h \ell n \frac{T_h}{T_c} \right) \quad *$$

and for $\frac{T_h}{T_c} \to 1$

b) $$W_{max} \approx kM \frac{(T_h - T_c)^2}{T_h + T_c} = kM \frac{(\Delta T)^2}{T_h + T_c} \quad *$$

Evaluation of this expression yields the theoretical limit of available energy as a function of the deep-sea water flow, assuming the surface water heat sink to be infinite.

Typically, for a cold source at 280°K and a warm sink at 300°K, the maximum available energy per $m^3$ of deep-sea water processed is:

X. $$W_{max}/m^3 \approx k \frac{(\Delta T)^2}{T_h + T_c} = 2.89 \times 10^6 \text{ Joules}$$

This available energy is equivalent to the potential energy of a 294.5-m high waterfall, carrying a flow identical to the cold water flow. Practical processes will generate a fraction of this available energy according to their effectiveness.

## THERMAL CYCLE OPTIMIZATION

Practical ocean thermal energy conversion plants are usually based on a Rankine cycle process. Such a Rankine cycle, within the applicable temperature span and for the working fluids under consideration, approaches the Carnot cycle efficiency.

It should be noted that the expression for the efficiency of an entirely reversible process (V.) can be applied as well to applications for which the source temperature is lower than the sink temperature. Because we have elected to reference our analysis to the cold water stream, we are using it that way. The resulting "negative" efficiencies are applied to the heat "rejected" by the process and may be larger than 1.

The process generally considered can be plotted onto a temperature/entropy field (Fig. 1). $T_h$ and $T_h'$ represent the temperatures at which the warm surface waters are introduced and released from the system. Similarly, $T_c$ and $T_c'$ indicate the cold water stream temperatures and the temperature change ($\Delta$) which the cold water undergoes within the process is:

XI. $$\Delta = T_c' - T_c$$

Because the cycle efficiency is low, the heat flow into the system on the warm side is almost equal to the heat extracted on the cold water side. Consequently, the temperature change in the warm water stream:

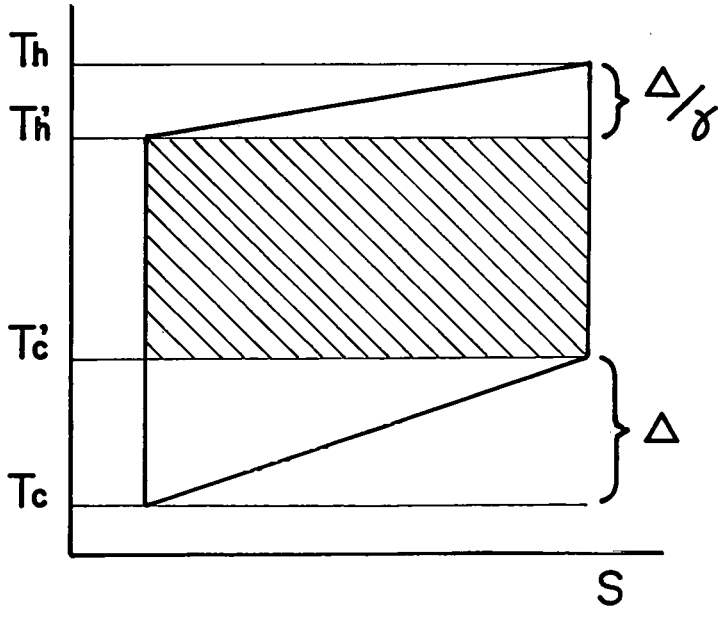
XII. $$T_h - T_h' = \Delta/\gamma$$

where $\gamma$ represents the ratio between warm and cold water flows.

The irreversible temperature drops due to finite heat-exchanger and/or condenser conductivity, are intentionally deleted from this graph. Their magnitude depends on an economic trade-off between the size of the exchangers and the effective $\Delta T$ which remains available to the thermal process.

The efficiency of the process represented in Figure 1 is expressed by:

XIII. $$\eta = \frac{T_c' - T_h'}{T_c'} = \frac{(T_c - T_h) + \Delta\left(1 + \frac{1}{\gamma}\right)}{T_c + \Delta}$$




$$\eta = \frac{T_c' - T_h'}{T_c'}$$

Figure 1. Temperature-entropy diagram for a single-stage ocean $\Delta T$ Rankine cycle power plant.

*Appendix 1.

and the power generated is obtained by applying this efficiency to the source heat flow (~kMΔ).

The thermodynamic efficiency is maximum for Δ = 0, but no energy is flowing through the system under this restriction. Conversely, if Δ is increased until $T_h' = T_c'$, η equals 0 and again no useful energy is produced. A plot of energy output (W) per $m^3$ of cold water versus the amount by which the cold water is warmed up (Δ) is shown in Figure 2 for three different values of the ratio of warm to cold water utilized.

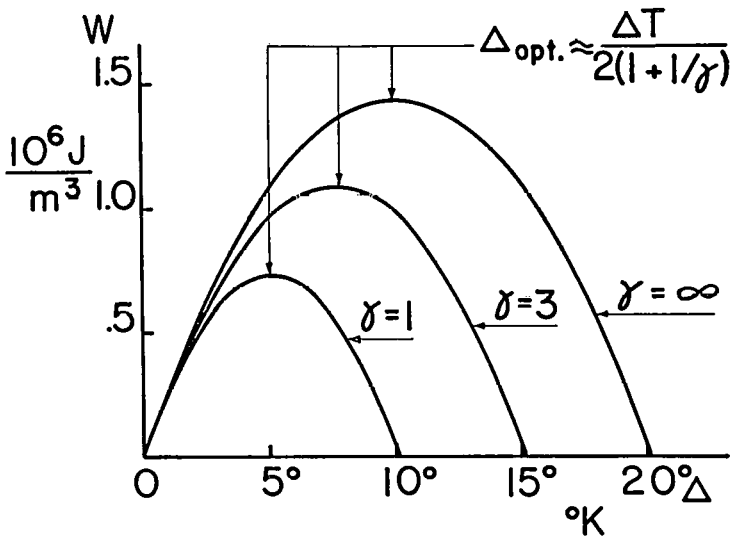



Figure 2. Energy available versus temperature increase of the cold water flow (Δ), for three different ratios of warm to cold water (γ).

The optimum operating point obtained by differentiating the expression for generated power indicates that:

XIV. $$\Delta_{opt} = T_c \left[ \sqrt{1 + \frac{(\Delta T)/T_c}{1 + 1/\gamma}} - 1 \right] \quad *$$

for: $\frac{\Delta T}{T_c} << 1$

XV. $$\Delta_{opt} \approx \frac{\Delta T}{2(1 + 1/\gamma)} \quad *$$

The value of the combined temperature drops in both the boiler and condenser circulation is:

XVI. $$\Delta_{opt}(1 + 1/\gamma) \approx \frac{\Delta T}{2}$$

and the energy produced by this process at this operating point is approximately 50% of the available energy.

I want to point out that this limitation results solely from the selection of a single stage Rankine cycle for the thermodynamic process. All unavoidable irreversible conductivity losses are as common to the ultimate available energy analysis as they are to t process just analyzed.

Frequently, the average temperature change of t deep or surface water flows is lumped together with conductivity losses in heat-exchanger evaluations. While this is an accepted practice, it masks the reversibility of a body's temperature change.

Although the distinction between the reversible and irreversible parts of a heat-exchanger temperature drop may usually be irrelevant, it becomes significant when 50% of the available energy is involved.

It should be noted that the inability to generate more than half of the available energy for a given deep-water flow is not due to the thermodynamic efficiency of the Rankine cycle, but caused by the limitation it imposes on the value of Δ. More than one approach is available to increase the fraction of available energy actually produced.

MULTIPLE STAGE CYCLE

In the study of a sea thermal power plant for Abidjan (Ivory Coast) by the "Energy des Mers" group, L. Nisolle (2) pointed out the potential merit of a multiple stage Rankine cycle plant. The power plant design which resulted from this study incorporated a cascade of three successive boiler/condenser stages, all coupled to a single turbine wheel. The proposed system is shown in Figure 3.

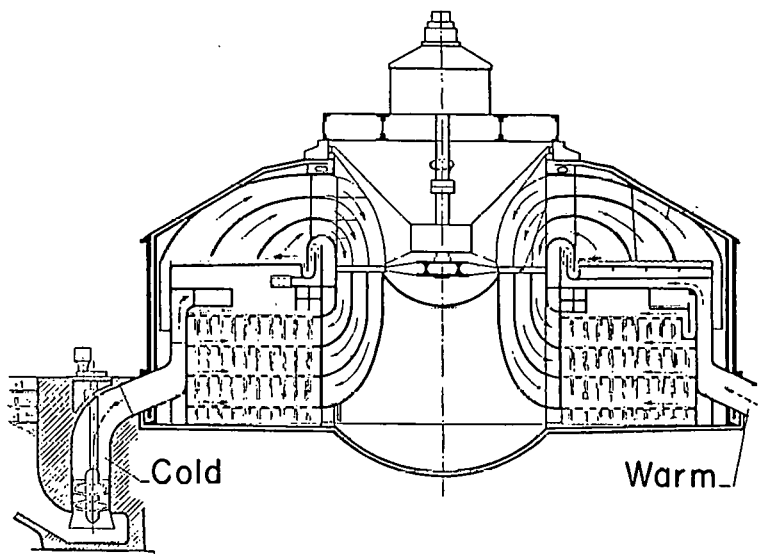



Figure 3. Schematic layout of the power generator proposed for Abidjan (Ivory Coast) during the 1950's.

Such a process can similarly be plotted on a temperature/entropy field (Figure 4). That an additional amount of energy, as compared with a single-stage process, is being produced is readily visible by superposition of both graphs (Figs. 1 and 4). This is, however, deceptive: a larger energy gain is derived from the fact that multiple-stage operation also increases the value of $\Delta_{opt}$, the temperature change to which the

*Appendix 2.

deep-sea water is subjected.

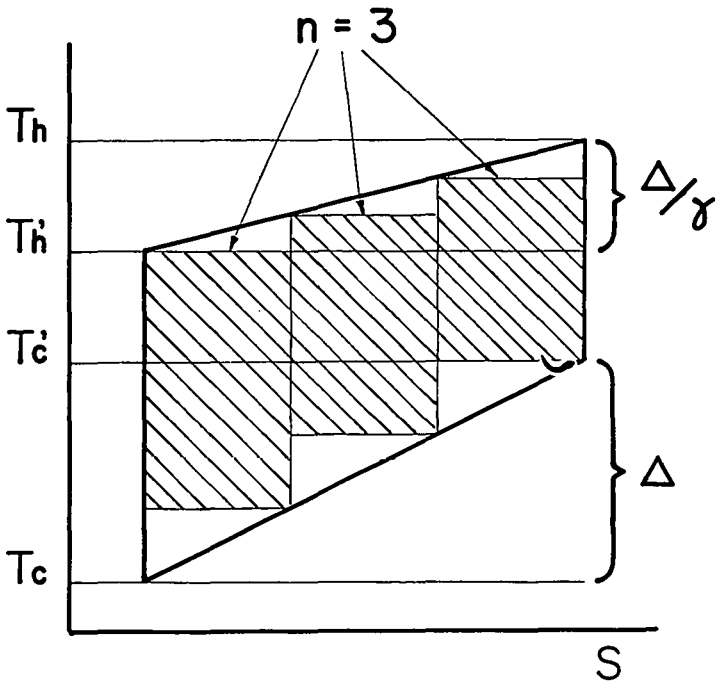



Figure 4. Temperature-entropy diagram for a three-stage ocean ΔT Rankine cycle power plant.

At the limit for an infinite number of stages and for $\frac{T_h}{T_c} \to 1$:

XVII. $$\eta \approx \frac{(T_c + T_c') - (T_h + T_h')}{T_c + T_c'}$$

and the maximum output is obtained for:

XVIII. $$\Delta_{opt} \approx 2\, T_c \left[\sqrt{1 + \frac{(\Delta T)/T_c}{1 + 1/\gamma}} - 1\right]$$

and for: $\frac{\Delta T}{T_c} \ll 1$

XIX. $$\Delta_{opt} \approx \frac{\Delta T}{1 + 1/\gamma}$$

The output of such a process would equal the available energy if operated with an infinite warm sink ($\gamma = \infty$). The value of the combined temperature drops in both the boiler and condenser would approach:

XX. $$\Delta_{opt}(1 + 1/\gamma) \approx \Delta T$$

which means that, except for heat-exchanger conductivity losses, both the surface and deep water discharges would be at the same temperature.

Most of the energy lost by a single-stage plant can be recuperated with a limited number of stages. The optimum operating conditions are dependent on the available ΔT and on the warm to cold water ratio ($\gamma$) entering the process. In Table I, both the temperature increase ($\Delta$) and the energy output per $m^3$ of cold water are listed for n = 1, 3 or 10 stages, for $\gamma$ = 1, 3 or 10 and for ΔT = 10°K or 20°K, centered around 290°K.

The outputs listed are the maximum achievable for each combination of operating conditions. They are to be compared to a maximum available energy of 720 kJ, for a ΔT of 10°K, to 2890 kJ, for a ΔT of 20°K.

Table I. Calculated energy output per $m^3$ of deep-sea water processed, for different values of ΔT, $\gamma$ and $\eta$.

| ΔT CENTERED ON 290°K | γ | n | Δ (°K) | OUTPUT (kJ $m^{-3}$) |
|---|---|---|---|---|
| 10°K | 1 | 1 | 2.49 | 182.04 |
| | | 3 | 3.73 | 273.06 |
| | | 10 | 4.53 | 330.99 |
| | 3 | 1 | 3.73 | 271.88 |
| | | 3 | 5.60 | 408.27 |
| | | 10 | 6.79 | 495.21 |
| | 10 | 1 | 4.51 | 328.65 |
| | | 3 | 6.79 | 494.04 |
| | | 10 | 8.24 | 599.65 |
| 20°K | 1 | 1 | 4.96 | 734.58 |
| | | 3 | 7.43 | 1101.93 |
| | | 10 | 9.81 | 1335.72 |
| | 3 | 1 | 7.40 | 1092.39 |
| | | 3 | 11.14 | 1642.22 |
| | | 10 | 13.53 | 1993.39 |
| | 10 | 1 | 8.95 | 1316.93 |
| | | 3 | 13.51 | 1983.87 |
| | | 10 | 16.44 | 2411.34 |

OTHER CYCLES

Instead of approximating a variable temperature heat transfer process with a series of Rankine stages, it may be worthwhile to investigate the application of other thermal cycles.

The Brayton cycle is an example of such a process. The large amount of compression work, relative to the net output, seems to make this approach impractical.

Another method consists in using a non-azeotropic binary working fluid. I made a suggestion to that effect in January 1974. A presentation on this subject was made by Drs. Iqbal and Starling (4) at the Third Workshop on Ocean Thermal Energy Conversion in Houston (May 1975).

The use of a mixture of two components instead of a pure compound, as a working fluid, allows both the boiler and the condenser to operate over a span of temperatures at a single working fluid pressure. In counter-flow boilers, the mixture evaporates its "lightest" fraction first, while in the condenser the "heaviest" fraction is liquefied at a temperature close to the cold seawater release temperature.

The full impact of the use of mixtures as working fluids in the OTEC cycles was not developed in the 1975 presentation. Rather than resulting in a slightly higher thermal efficiency, or in a reduction of the heat-exchanger size, it would, in my opinion, affect the optimum temperature ($\Delta_{opt}$) change in the deep water flow and, as a corollary, reduce the amount of deep water which has to be processed to produce a given amount of energy.

I also want to point out that the use of a Brayton or of a binary fluid cycle does not allow full utilization of the benefits which may result from an unequal surface and deep-sea water flow.

## CONCLUSIONS

— The application of thermal cycles which differ from the single-stage Rankine cycle may have a significant impact on the design and operating points of OTEC plants.

— The selection of operating points has to maximize the product of the amount of heat processed by the thermodynamic efficiency of the process and not the efficiency by itself. While certainly applicable in the design of heat exchangers, the use of a logarithmic mean temperature difference should not obscure the difference in reversibility between a conductive loss and the temperature change in both flows.

— Finally, operation of a plant in accordance with the principles developed, in addition to an economic benefit, would result in the release of deep-sea water at a temperature and density significantly closer to the surface-water temperatures. This affects both the fate of the discharge plume and surface fertilization evaluations.

## REFERENCES


(1) Roels, O.A., 1975. The economic contribution of Artificial Upwelling mariculture to sea-thermal power generation. Proc., Third Workshop on Ocean Thermal Energy Conversion, Applied Physics Lab./ Johns Hopkins University, APL/JHU-SR75-2: 128-130.

(2) Nizery, M.A., 1946. Etude sur les possibilitiés d'utilisation de l'énergie thermique des mers et de l'énergie solaire. Bulletin de l'Institut Oceanographique, No. 906.

(3) Lockheed Missiles & Space Company, 1975. Ocean thermal energy conversion (OTEC) power plant technical and economic feasibility. LMSC-D056566, Vols. I-II.

(4) Iqbal, K.Z. and K.E. Starling, 1975. Potential advantages of mixtures as working fluids in the OTEC cycles. Proc., Third Workshop on Ocean Thermal Energy Conversion, Applied Physics Lab./Johns Hopkins University, APL/JHU-SR75-2: 147-150.


## APPENDIX 1

$$W_{max} = -kM \int_{T_c}^{T_h} \left(\frac{T - T_h}{T}\right) dT$$

Integrated by parts:

$$= -kM \left[\int_{T_c}^{T_h} dT - T_h \int_{T_c}^{T_h} \frac{dT}{T}\right]$$

$$= -kM \left[\left(T_h - T_c\right) - T_h \left(\ell n T_h - \ell n T_c\right)\right]$$

$$= -kM \left(T_h - T_c - T_h \ell n \frac{T_h}{T_c}\right)$$

$$\ell n \frac{T_h}{T_c} = 2 \left[\left(\frac{\frac{T_h - T_c}{T_c}}{\frac{T_h + T_c}{T_c}}\right) + 1/3 \left(\frac{\frac{T_h - T_c}{T_c}}{\frac{T_h + T_c}{T_c}}\right)^3 + \cdots\right]$$

For $\frac{T_h}{T_c} \to 1$, only the first term of the expansion is significant.

Introducing: $T_h - T_c = \Delta T$

$$\ell n \frac{T_h}{T_c} \approx 2 \left(\frac{\frac{T_h - T_c}{T_c}}{\frac{T_h + T_c}{T_c}}\right) = \frac{2\Delta T}{T_h + T_c}$$

and:

$$W_{max} \approx -kM \left(\Delta T - \frac{2T_h \Delta T}{T_h + T_c}\right)$$

$$= -kM\Delta T \left(\frac{T_h + T_c - 2T_h}{T_h + T_c}\right)$$

$$= -kM\Delta T \left(\frac{T_c - T_h}{T_h + T_c}\right) = kM \frac{(\Delta T)^2}{T_h + T_c}$$

## APPENDIX 2

Combining II. and XIII. :

$$W = (-kM\Delta) \frac{(T_c - T_h) + \Delta(1 + 1/\gamma)}{T_c + \Delta}$$

$$= (kM\Delta) \frac{\Delta T - \Delta(1 + 1/\gamma)}{T_c + \Delta}$$

$$= (kM) \frac{(\Delta T)\Delta - (1 + 1/\gamma)\Delta^2}{T_c + \Delta}$$

$$\frac{dW}{d\Delta} =$$

$$(kM) \frac{(T_c + \Delta)[\Delta T - 2(1 + 1/\gamma)\Delta] - [(\Delta T)\Delta - (1 + 1/\gamma)\Delta^2]}{(T_c + \Delta)^2}$$

$\frac{dW}{d} = 0$ for:

$$(T_c + \Delta)[\Delta T - 2(1 + 1/\gamma)\Delta] - (\Delta T)\Delta + (1 + 1/\gamma)\Delta^2 = 0$$

$$= (\Delta T)T_c - 2(1 + 1/\gamma)T_c\Delta + (\Delta T)\Delta - 2(1 + 1/\gamma)\Delta^2 - (\Delta T)\Delta + (1 + 1/\gamma)\Delta^2$$

$$= -(1 + 1/\gamma)\Delta^2 - 2(1 + 1/\gamma)T_c\Delta + (\Delta T)T_c$$

$$= \Delta^2 + 2T_c\Delta - \frac{(\Delta T)T_c}{1 + 1/\gamma} = 0$$

for:

$$\Delta_{opt} = -T_c \pm \sqrt{T_c^2 + \frac{(\Delta T)T_c}{1 + 1/\gamma}}$$

or eliminating the negative root:

$$\Delta_{opt} = T_c\left[\sqrt{1 + \frac{(\Delta T)/T_c}{1 + 1/\gamma}} - 1\right]$$

Noting that for:

$$\frac{\Delta T}{T_c} << 1$$

$$1 + \frac{(\Delta T)/T_c}{1 + 1/\gamma} >> \left[\frac{(\Delta T)/T_c}{2(1 + 1/\gamma)}\right]^2 \to 0$$

Therefore:

$$1 + \frac{(\Delta T)/T_c}{1 + 1/\gamma} \approx 1 + \frac{2(\Delta T)/T_c}{2(1 + 1/\gamma)} + \left[\frac{(\Delta T)/T_c}{2(1 + 1/\gamma)}\right]^2$$

and:

$$\sqrt{1 + \frac{(\Delta T)/T_c}{1 + 1/\gamma}} \approx 1 + \frac{(\Delta T)/T_c}{2(1 + 1/\gamma)}$$

$$\Delta_{opt} \approx T_c\left[1 + \frac{(\Delta T)/T_c}{2(1 + 1/\gamma)} - 1\right]$$

$$\approx \frac{\Delta T}{2(1 + 1/\gamma)}$$

University of Texas Marine Science Institute Contribution #146. Supported by National Oceanic & Atmospheric Administration, U.S. Dept. Commerce, Sea Grant Number 04-6-158-44117.

## DISCUSSION

VAN HEMELRYCK [answering inaudible question]: I think the question is, would it be beneficial to apply multiple stages to a closed-cycle system using a binary mixture as a working fluid and to use multiple stages in addition to that, and I think the answer is negative. The interest in using a binary mixture is precisely to be able to have a working cycle which is using as much as possible of the available area on the T-S diagram.

Questioner: I think you've missed the point of my question. You illustrated a multiple-stage system for the open Rankine cycle, in which there would be a multiple stage holding system, with steam coming off at different pressures. Would multiple staging also be advantageous for a closed-cycle system using the same or possibly different working fluids in the different stages?

VAN HEMELRYCK: Yes. It is not farfetched to think in terms of multiple closed-cycle stages because most of the proposed plants are modular in nature, and instead of just putting the modules in parallel on both the deep and surface water flows, the cold water flow could very well go to a cascade in four modules, each achieving a bigger temperature drop and ratio of warm to cold water. The reason I am considering that a ratio of surface to deep water greater than unity would be used in the practical plant is the accessibility of surface water; there is less involved in pumping it and handling it.

[Inaudible questions followed regarding the treatment of heat sinks and work availability.]

WATT (Colorado School of Mines): In the case of multiple stages, do you take into account the terminal temperature difference between the water leaving and the vapor temperature for each stage?

VAN HEMELRYCK: This question falls in the area of tradeoff between the irreversible conductivity losses and the size of the device you are using, a tradeoff which is not part of the cycle selection but is related to the sizing of the equipment which is also competing for the $\Delta T$. That problem is at another level of analysis. I'm trying to pull out a little part of the problem artificially, but I hope I can justify it.

# STEAM LIFT CYCLE AT VERY LOW MIST DENSITIES

EARL J. BECK
*Design Services*
*998 Church Street #27*
*Ventura, California*

ABSTRACT

The proposed development of the steam driven version of the air lift pump presents some opportunities and some problems. The opportunities lie in simplicity and low cost. The problems as now understood result from the large steam volume when seawater is evaporated at, say, 27°C, the very low pressure difference available below the saturated pressure (0.03564 bar) and a reasonable condensing pressure of perhaps (0.02337 bar) at 22°C. Nevertheless, the particular mode of operation using a very small part of the warm water heat to elevate a greater mass of water promises to allow the development of large systems with moderate cost.

The nature of the air lift pump, the modification to make a steam lift pump, and the major modification to make a steam lift pump operating at low pressure are discussed.

In the lower section of the pump stable bubbles are formed but with decreasing pressure and the flashing of additional steam, the bubble will burst and the major pumping action will be dependent on successfully carrying these small drops of seawater to a useful hydraulic height.

The power required for providing the necessary condensing is discussed as well as the opportunity for eliminating air released in the nucleating and boiling processes by the use of a Taylor air compressor.

A short colored movie of an operating steam lift pump was shown at the meeting.

## INTRODUCTION

The Ocean Thermal Gradient Hydraulic Power Plant ( 1 ) proposes to avoid most of the problems associated with the closed or Rankine cycle plants under development. If it is capable of development at tropical ocean temperatures, it will indeed have produced a major step forward. Its conception resulted directly from (a) the inventor's perception of the problems in heat transfer in the closed cycle and (b) the closed cycle's recalcitrance in providing the designer with tools for cycle improvement such as have been so instrumental in improving high temperature steam plants. The remarkable potential for development of steam plants has resulted from ingenious use of superheaters, preheaters, etc. In the OTEC Rankine plant, it seems that the designer's best if not only approach is to pump as hard as he can and hope that the net power he can produce will be worth the trouble and cost. The OTGHPP and the concept's steam lift pump (SLP) in particular do not suffer these problems, but do present formidable and uncertain design problems in the low-temperature application. The potential and problems are the subject of this paper.

## BACKGROUND

The paradigm for the SLP is the air lift pump (ALP), which it resembles in many respects but not in others. A review of a large number of papers on the ALP revealed none that unequivocally named it for what it is -- primarily a hydraulic device, with limited thermodynamic traits. Both the ALP and the SLP are unquestionably static devices, depending upon the displacement of a low density mixture of the fluid pumped and a gas (ping pong balls or chunks of balsa would also provide the necessary 'voids' and so a reduced density) by a static pressure. In the ALP, Fig. 1, the force necessary to propel the mixture of air and water upward in the pump tube is provided by the water pressure at depth S. The more air used, the lighter the density in the tube, the greater the pumping effect. The general characteristics of an ALP are shown schematically in Fig. 2, adapted from (2). Note that no flow of water from the pump tube occurs until a minimum flow, $Q_o$, occurs; above this flow, water pumped rate, $Q_f$, increases very rapidly until eventually a maximum is reached above which $Q_f$ decreases, as would be expected as the air fraction becomes dominant and friction increases rapidly. On the same figure is shown the approximate head developed and the hydraulic pump power; this would be the equivalent of the maximum theoretical power from a OTGHPP, but the system curves might be quite different. Note that in the ALP, all points in the system are nominally above atmospheric pressure, unlike the SLP as discussed below.

While the ALP is a complex device considering all aspects of friction, bubble slip, etc., it appears to be capable of direct analysis on static basis using

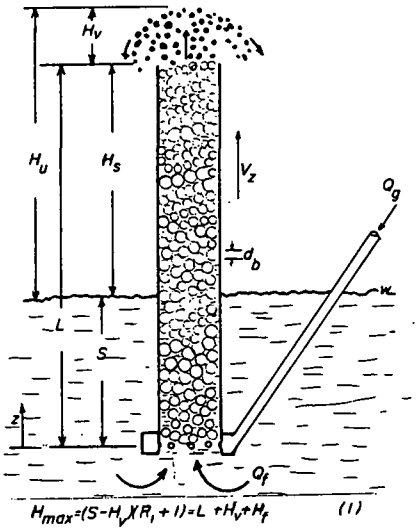



Fig. 1. Schematic of a basic air lift pump. (ALP)

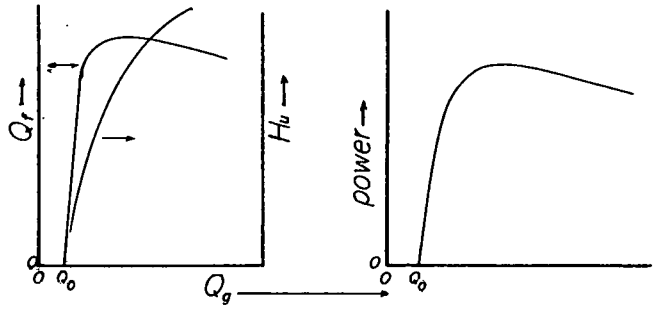



Fig. 2. General characteristics of the ALP, with flow, head and power as a function of gas flow. Note that no useful pumping can be done below $Q_o$.

well known hydraulic theory and empirical formulas except for the uncertainty in friction in two phase flow, complicated by the wide variations in the ratio of air to water flow. This also will be a complication in the SLP's development, but perhaps a minor one. The maximum theoretical pumping head that can be accomplished is shown in Eq. (1); the static head of interest in water pumping is appropriately reduced by the exiting velocity head, friction and an allowance for bubble slip. For high heads, the reduced density from the expansion of air must be taken into account as must such factors as bubble coalescence (causing the formation of slugs of air) and heat gain from the water to the expanding air; the expansion is essentially isothermal so at high pressure ratios of air inlet to discharge pressure, heat is supplied by the fluid pumped. At very high pumping heads, the bubbles may be expected to burst and above that the water must be carried by friction with the air. This will be the rule in ALP's operating at low, tropical ocean temperatures.

While the SLP is similar in many respects to the ALP, there are important differences. At high temperatures the SLP may operate at about the local boiling pressure and temperature, i.e., near 100C as in the small demonstration experiment, Civil Engineering Laboratory Demonstration Experiment, or CELDX, (3). This experiment (shown in a short color movie at the New Orleans conference) is shown schematically, Fig. 3, adapted from (3) with important dimensions added When

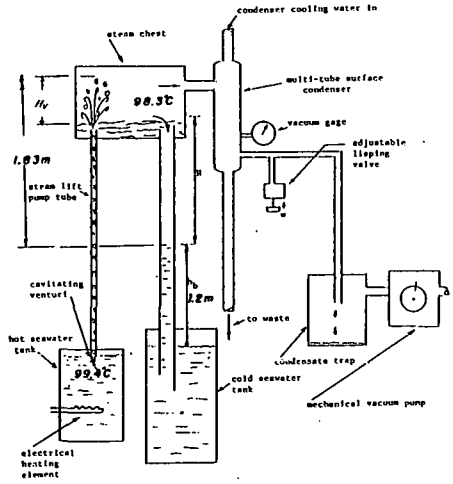



Fig. 3. Schematic of a small steam lift pump (SLP) from (3), with principle dimension added.

temperature at entry was just right, there was no large change in bubble dimensions, flow was smooth and bubbles appeared as a continuous froth. While very convincing, this first demonstration of the SLP is more relevant to possible high temperature applications, e.g., use of waste heat in water, than to the OTEC application.

The value of $$R_1 = \frac{Q_g}{Q_f} \qquad (2)$$

in this experiment was about 3 at the tube's bottom and probably slightly higher at the top. Instrumentation, or lack of, did not allow a complete analysis of the relationships shown in Eq. (1), but fair agreement was achieved with some estimates.

Before proceeding to the details of a low temperature SLP and other features of the OTGHPP at warm ocean temperatures, we should examine the conditions of bubble stability, size and growth as simply stated in the well known relationship:

$$P_b = P_a + \frac{4\sigma}{d_b} \qquad (3)$$

which has a comparable temperature form:

$$t_b = t_a + \Delta t_{sup} \qquad (4)$$
$$(sat)$$

The implications of (3) and (4) are considerable, and not obvious. First, the form of a plot of bubble diameter, $d_b$ against the pressure represented by the last term in (4) is a hyperbola and its temperature equivalent, $\Delta t_{sup}$ is also. Small bubbles require high superheats; with zero superheat, the theoretical

diameter $d_b$ approach infinity. A case with which we are all familiar is shown in Fig. 4, where a very small

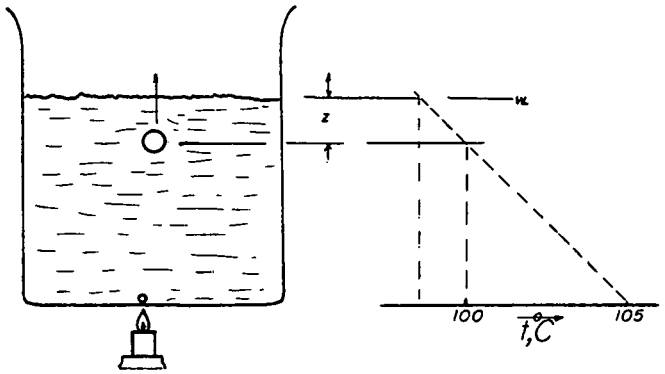



Fig. 4. Water boiling in a beaker, showing bubble growth as bubbles rise through increasingly cooler water, then collapse by condensation below 100C.

bubble is growing at the bottom of a beaker in hot water, superheated over the local saturation pressure. When it detaches and rises through the temperature gradient shown, it grows as the temperature of the water surrounding it decreases, and not as generally believed because the water head is decreasing; the head in this situation is trivial compared with the pressure in the bubble due to surface tension. The upper bubble is shown as it moves through a critical zone -- 100C water. Here, its upper half is condensing, its lower half attempting to grow by evaporation. As it moves higher under buoyancy, it will almost instantaneously condense and disappear. As heating and convection become more vigorous, the gradient as shown will be destroyed and bubbles can grow very large. Whether or not in any case part of the growth is accomplished by coalescence is moot, since coalescence is not needed for growth -- only an appropriate temperature regime.

At a water ambient temperature $t_a$ in which a bubble in equilibrium, heat transfer is extremely rapid and size adjustment is made almost instantaneously. This is seen in Fig. 5, adapted from (4). While at first

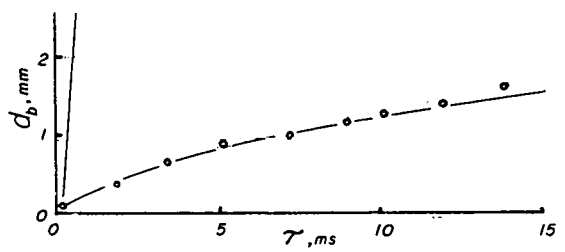



Fig. 5. Bubble growth rate in 103C water at one atmosphere. The upper curve is Rayleigh's prediction, the lower measured; growth is still very rapid.

glance it might appear that real growth rate, limited by inertia and thermal diffusion, is very small compared with Rayleigh's projections, it should be noted that the time for growth is still very short; in the SLP of the OTGHPP it may be expected to be much shorter, i.e., more nearly the theoretical than in Plesset's experiment because of the relatively fewer number of molecules of water which must evaporate to form a bubble of comparable size. The ratio of the specific volumes at the low (27C) temperature and higher (100C) of Plesset's work is about 40 to 1.673, or 24 while the ratio of latent heats of evaporation is about 2438 to 2260, or about 1.08. For transferring only a little more heat in evaporation, the volume of steam is increased many-fold at the lower temperature. Unfortunately, that is only part of the picture.

Returning to Eqs. (3) and (4), these provide a formidable design tool in designing an SLP until the bubble breaks, i.e., at $R_1$'s perhaps of the order of 8 to 12, to be determined. We can, by increasing the ambient pressure on a steam bubble according to Bernoulli's equation, reduce the superheat pressure/temperature and so cause the bubble to grow precipitously. This is exactly what was done in CELDX, in a venturi inserted into the pump tube's intake or lower end, see Fig. 15 of (3). The area ratio of the throat to the tube was 4, just right for $R_1$ of 3, for a density of $1/(R_1 + 1)$. An $R_1$ of 3 is an interesting case, that of approximately closest packing. Higher $R_1$'s are of non-spherical bubbles and the relevance of Equations (3) and (4) is not certain. Certainly at much higher $R_1$, the radii of the outside bubbles would control the bubbles pressure and so temperature.

But before growing and bursting bubbles at high steam volumes as will occur in the low-temperature SLP, we should consider how to grow a bubble from start, discussed in some detail in (3) but briefly here. In Fig. 6, at A' is seen a microscopic particle (usually a solid, as for example, a piece of fly ash) to which

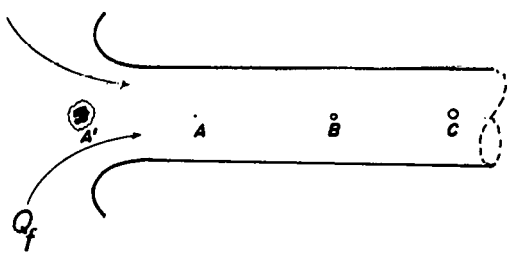



Fig. 6. A cavitating venturi as used for growth of micronuclei at A' to a small nucleus of air at B and a small air-steam bubble at C.

is adsorbed a layer of permanent (air) gases. There is no possibility to sufficient pressure to support a bubble, but when the particle initially at concentration equilibrium with the dissolved gas in the surrounding water is placed in a low pressure area in the venturi, gas migrates by diffusion and causes growth. When the correct combination of time, concentration gradient and pressure occur, the particle and its adherent gas cloud grow to a small bubble of air and low pressure steam, with surface tension dictating the size as in Eq. (3).

With the ambient water superheated as in (4), we are ----

in a position to dictate bubble growth as described ier.

high temperature SLP, e.g. CELDX (3), the designer can be fairly careless in his calculations and probably still pump water. This experiment had a total pressure drop of about 1.2 meters, as indicated by the barometric head, $H_b$, and this could have been much greater with more vigorous condensing; much more steam and so lower densities could have been produced. Not so in the low temperature SLP whch is, after all, a barometric device in limited respects similar to the pre-Watt steam engine of the 18th century. My concept of Watt's problem as he found it when he started to improve the steam engine is shown in Fig. 7 with a few embellishments for illustration. A large cylinder-

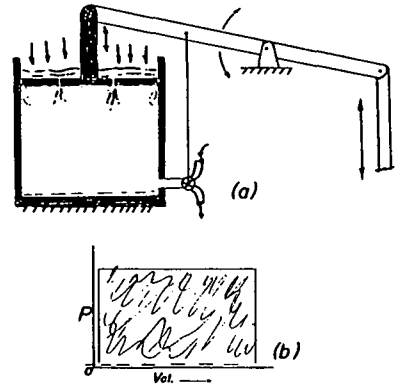



Fig. 7. Schematic of an atmospheric steam engine at (a), and its P-V diagram at (b). All the useful work is done by air pressure acting against a partial vacuum.

piston, reportedly very poorly fitting, is shown as used for pumping mines; in this application, no flywheel is needed as the weight of the water on the pump's piston would be sufficient to lift the engine's piston during steam admission -- which would be at 1 atmosphere or perhaps slightly less if necessary. When the piston reached the top dead center position as shown, the engine was flooded with cold water (perhaps from a bucket in early forms) and the water leaking into the cylinder would collapse the steam; atmospheric pressure forced the piston down and raised water in the pump. There is no danger from exploding boilers and no need for close machine work, as the water would make the seal. I've added orifices to facilitate spray condensing; these may not have been typical of early engines.

The indicator card (a pressure-volume diagram) for such an engine is shown at (b), a luxury of relatively high work output not to be enjoyed in the low-temperature SLP. But the pre-Watt engine shared one feature with the SLP -- the only force available to elevate the water is the atmosphere, and in the SLP a small portion of that, as no steam can be produced until the absolute pressure is reduced below the saturation pressure of the water, in the case of 27C seawater, about 0.0356 bar. And condensing with, say, 4.4C cooling water from ocean depths in a barometric condenser, a maximum backpressure (with infinite amount of cooling water) about 0.0085 bar gives a maximum usable pressure drop (approximately equivalent in purpose to the 1.2 m of CELDX, (3) ) of 0.027 bar, or the equivalent of 0.27 m of seawater. This may sound and is fairly small, but when the large volumes (so low density of the steam-water mixture) at low temperatures is considered, it appears very adequate. For instance, if it were possible (which it assuredly is not, unfortunately perhaps) to use steam bubbles with $R_1$'s approaching 400 (equivalent to a temperature drop for evaporation from 27C of about 5°C), then we might calculate maximum pumping heights of the order of, say, 400 x 0.25 or 100 meters, if the "card" for the SLP were a rectangle and perhaps 50 meters since it is not.

My concept of what a "card" for the SLP would look like, used here for discussion only, is shown in Fig. 8. When

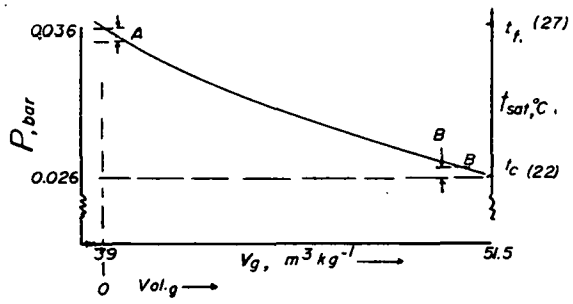



Fig. 8. A visualized P-V diagram for the SLP, with an initial pressure drop for bubble formation at A and a final pressure drop at B in the steam delivery tube to the condenser.

the bubbles burst, the first steam appears, and a pressure drop has already occurred. With further pressure drop, the specific volume of steam (and so $R_1$) increases, but the residual pressure also drops. Steam is still being produced after useful pumping has occurred, but this effect can probably be kept small if separation of drops and steam is good and the pressure drop in the steam conduit to the condenser kept small.

While the apparent "expansion" in Fig. 8 resembles that that would be expected in a steam engine with early cutoff, or in a steam turbine with expansion, the SLP is not an expansion engine. The increase in volume occurs solely because of a pressure drop and when friction's contribution to the total enthalpy is considered, there is an enthalpy increase in the fluid during its transit. The SLP is therefore a true hydraulic device, although its analysis is complicated by the change in specific and so total volume. The relevant equation, with a specific caveat, is the differential form of the Bernoulli equation:

$$v_g\, dP + d\frac{V^2}{2g} + dZ = 0 \qquad (5)$$

This equation would apply specifically only in the case of no slip; since there is a relative velocity between the drops and transporting steam after the bubbles burst, the first term must be evaluated numerically over the length of the SLP's tube, as discussed later.

In the real design world, it seems probable that steam bubbles with a steam volume/water volume (equivalent to $R_1$) of perhaps 10 may be expected to burst -- so we should plan on it, and plan to use the energy bound up in surface forces to our advantage. But before proceeding to the intricacies of SLP design (and they are many as now understood), let's look at the SLP's "card", Fig. 8. First, we can produce a small volume of steam and still have most of the available 0.27 msw pressure drop used for discussion, but it is more realistic to leave a little or a lot of temperature drop for the barometric condenser -- which also needs it. Without any pretense of stating that a 5°C temperature drop in the SLP is correct (if we knew that, we would not need to go further, we could probably build large machines), let's look at the 5°C case. We have then allocated our 27 - 4.4°C temperature drop, 5°C to the SLP and the remainder, 17.6°C is reserved for condensing. Since condensing is the critical function in producing a vacuum and also is the only power consuming device in the proposed system, we see that we should make every effort to reduce the total temperature (and pressure) drop through the SLP, and use as great a temperature drop as practicable in the condenser. This is seen in an index of performance:

$$R_2 = \frac{\text{Power generated in the hydraulic turbine}}{\text{Parasitic power absorbed in the condenser}} \quad (6)$$

This dimensionless index must be greater than one to produce power, and the cost of power produced should drop as $R_2$ increases, unless heroic and costly machinery must be built to increase it. It cannot be evaluated in any case until all important system parameters have been determined -- until a design of both the SLP and the barometric condenser has been made.

In approaching the problems in learning to design effective SLP with the low pressure drop but very high steam volumes available, we may well consider what an optimum warm surface water temperature might be, if we assume for argument that the lowest temperature of cooling water might be about 4°C. Assuming a minimum temperature of approach in the condenser of, say, 2°C, we can then define a temperature factor for the numerator in our FOM as $t_1-4-2= t_1-6$, °C. Since we need to produce large volumes of steam to either provide low densities in bubble-water mixtures or to transport water drops after the bubbles burst, we can place the specific volume/vg (evaluated for simplicity at $t_1$) in the numerator. In the denominator will be the latent heat of evaporation, $h_{fg}$. Finally, since we need an appreciable pressure drop, we place in the numerator $\Delta p/\Delta t$ at the surface temperature. We thus define a FOM for discussion purposes of:

$$FOM = \frac{V_g (t_f - 6)(\Delta p/\Delta t)}{h_{fg}} (1{,}000) \quad (7)$$

the factor 1,000 is arbitrarily applied to facilitate visibility, and plotting in Fig. 9 at A. The trend is what is expected based on classical thermodynamics,

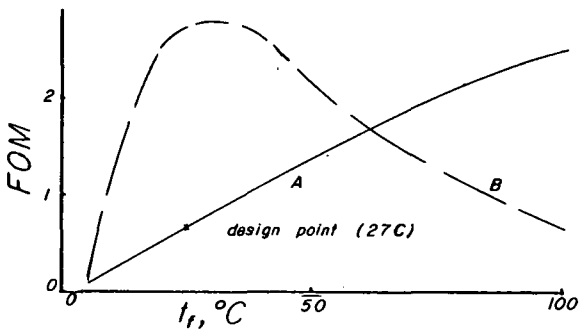



Fig. 9. A proposed figure of merit (FOM)A, for a SLP as discussed in the text. A similar FOM is shown, B, for the case in which the pressure drop/°C is ignored.

and predicts that we shall have to try hard to design a good system at low temperatures, while at higher temperatures, we might be more careless.

Fig. 1 is probably quite representative of the conditions where bubbles exist, as in the ALP, CELDX and for a short time in the low-temperature SLP, before the bubbles burst. After that, water drop transport is not dependent on density ratios, but on friction between the steam and the water drop, about which we will need to know a great deal to design a workable, efficient (in terms of equipment cost utilization but not necessarily thermal efficiency as we usually think of it) system. Unfortunately the engineering approaches to this problem tend to consider the friction loss in terms of head of the two-phase flow, as is typical of hydraulic practice. Referring to Fig. 10, a drop of water is shown being

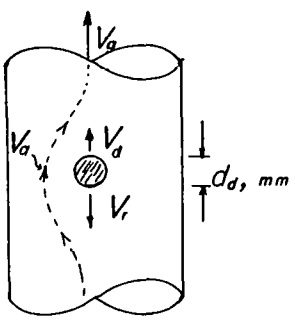



Fig. 10. A spherical drop being carried upward by a gas, while"falling" with respect to the gas at a terminal velocity, $V_r$; the repeated acceleration of the gas as it passes the drops is the source of pressure drop.

carried upward in a stream of low pressure steam, moving at a high velocity. Since the compressibility of the water is very small compared with that of the steam, there can be no pressure drop through the drop, but only in the steam around it. The support for the drop must be in the form of a relative velocity, $V_r$, which is the terminal velocity of a drop of that size falling i

the fluid, according to Stoke's work ( 5 ):

$$\frac{2}{3}(\rho_f - \rho_g) = \frac{4 \mu_g V_r}{d_d^2} \qquad (8)$$

For the case where the supporting fluid's density is trivial compared with that of the drop, and drop diameter is measured in mm, eq. (8) reduces to:

$$V_r = \frac{6.3 \times 10^6 \, d_d^2}{\mu_g} \qquad (8a)$$

This equation holds rigorously for Reynolds number, $N_{Re}$, of perhaps 2 or less, which would apply for drop diameters in 25C steam of 0.1 or less, but fairly well approximates the conditions with up to perhaps a 1mm drop. Rouse (5) attributes the deviations at higher $N_{Re}$'s because of drop deformation and so a change in form drag. This suggests that in the range of 0.1 to 1 mm drops, stripping of a drop may occur, controlling its size as has been reported for hailstones with water on the surface (6). Fortunately, the necessary experiments to resolve these points appear to be simple, relatively low in cost and usable in small experiment sizes. The important transport property of gas (steam) at low $N_{Re}$'s is viscosity, $\mu$, the absolute value of which for 25C steam is about 0.6 that for air at one atmosphere, while air is some 51.7 times more dense than the low pressure saturated steam.

Visualization of drop spacing for two values of $R_1$ is assisted by Fig. 11, which is to scale for 1 mm drops.

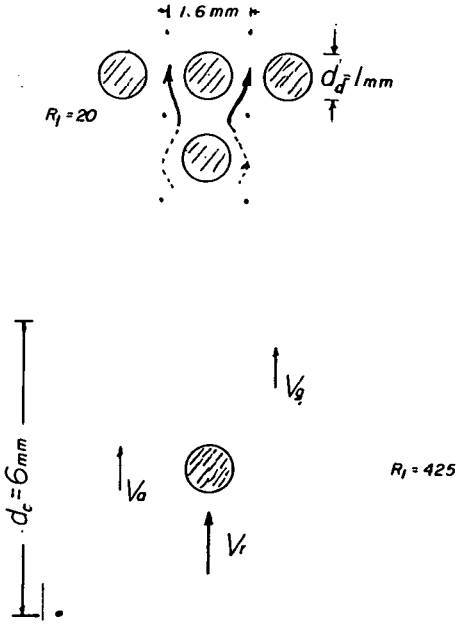



Fig. 11. Unit cells of steam-water drops for 1 mm water drops as in Fig 10, for two steam/water ratios.

Note that each time a change in area and velocity occurs as the steam passes between drops, shown for simplicity on a square grid, there is a sudden re-expansion and a loss in the difference in velocity heads in each cell. This loss was the basis for the friction loss calculations, which are summarized in Fig. 12. In making these calculations, average values of viscosity and specific volume were used, and deviations from Equation (7) were ignored for the large drop sizes. What we see from these curves is that small drops and large steam/water volumes are favored for low pressure drops. Note that the pressure drop is shown in meters of steam, as would be calculated in the applicable friction equations. In meters of water, the available drop in pressure is small but in meters of steam, impressively large.

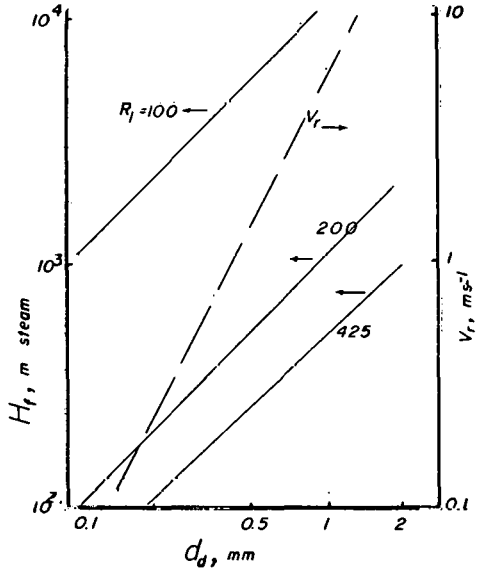



Fig. 12. Log-log plot of calculated pressure drops for saturated steam at about 25C; the terminal velocity of a drop in steam is also shown.

In Fig. 13 are plotted the important transport properties of low pressure steam in carrying small water drops. The relatively high and constant value of and large values of $V_g$ are both favorable to efficient drop transport if drops of an appropriate size can be generated and their size maintained or decreased during transit.

From the instant before the bubbles break, the design method appears to be on fairly solid ground. But from the instant of breaking upward, the discussion should be considered to be largely for experiment design and illustration, little more. Fig. 12 by no means presents a clear method for determining pressure drop (to these values, if appropriate, would be added the conventional duct friction losses), and the method must be tested by experiment.

Summarizing the basic reasoning for projecting the form of tube as shown in Fig. 14, we use the entry section for the growth of nuclei, the tripping section for sudden bubble growth, the section after that for rapid

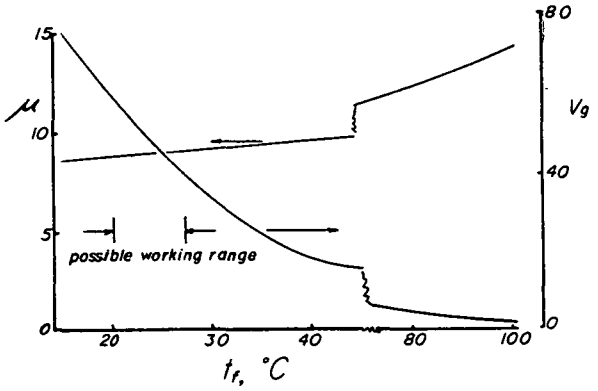



Fig. 13. Important transport properties of low pressure wet steam, plotted from (7). The viscosity is important in lifting water drops, the specific volume in achieving high velocities. Consider with Figures 10, 11 and 12.

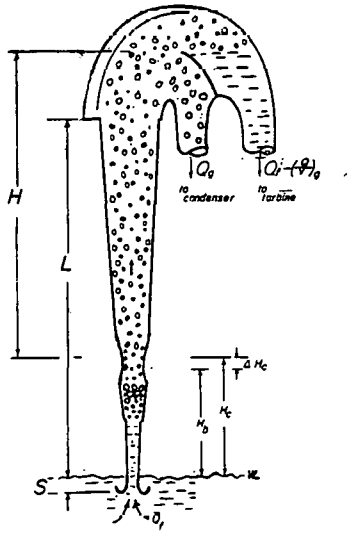



Fig. 14. A proposed SLP, with features as discussed in the text. No scale intended.

bubble growth and bursting, with hopefully small drops of water travelling in an upward direction at highest practicable velocity. Then, to further accelerate the drops and insure their efficient transport, we might introduce a modest venturi section which would provide the higher velocity, a <u>needed</u> pressure drop to increase the amount and specific volume of the transporting steam. Above the venturi's throat, area would be varied to produce the desired drop transport and/or acceleration until most of the available pressure drop has been used, at which level the section would be suddenly increased. Above that level the drops would decelerate under gravity to some usable height, $H_u$, at which they would still have sufficient velocity to allow their deflection into the hydraulic turbine's supply tube. While small bubbles appear to be desirable to this point, it would now be desirable that they be few and large, to facilitate complete separation. Fortunately, at the low relative velocities anticipated separation should be good even for small drops. From this point the main interest is in efficient delivery of steam and water to the condenser and turbine respectively and the efficient condensation of the steam in a system with minimum parasitic power loss.

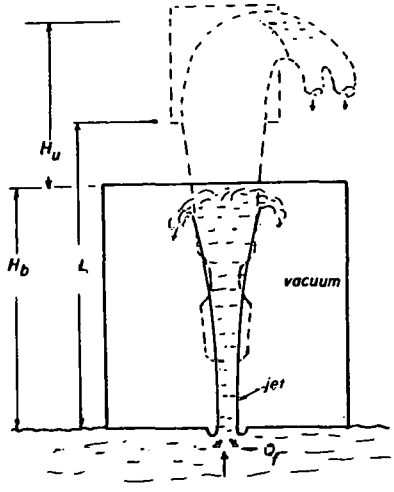



Fig. 15. Schematic of a free standing water jet as discussed in the text, with schematic of SLP tube superimposed, dotted.

To insure clarity of the nature of the pump system, Fig. 15 shows a free standing jet of seawater spouting into a vacuum chamber with an absolute pressure just under the water's saturation pressure, say 0.0357 bar for 27C water. Assume the water falling back after rising height $H_b$ is somehow removed and does not interfere with the jet's operation. The velocity in the stream is equal at any elevation z to the difference between $H_b$ and z, i.e., the velocity of a stream falling that distance under gravity. One approach, not useful, would be to let the stream decelerate until the maximum height has been reached, but this would require re-acceleration of the water, the formation of drops in a mechanical system, etc. Better to select some point for bubble formation based on the desired velocity and complete our design and construction as inferred in Fig. 11. The maximum velocity available with zero submergence is 13.8 m $sec^{-1}$, unless increased submergence or venturi with a diffuser is used. The first approach requires a longer tube length, L, for utilization. It is now apparent that while we have a lot of options for design, that the total picture in establishing a best design could be very complex. The known independent variables available will be listed later, and provide a formidable list.

A well-designed steam lift pump should provide large flows of water to optimum if not maximum heights. The maximum heights probably would not be desirable in a system exposed to tropical storms, and a more modest working head should be accepted (8, 9).

The previous discussion relates to the numerator of

equation (6), but the denominator is equally important, brief discussion of Barometric condensers, their ble improvement and an even briefer discussion of aylor air compressor seems appropriate.

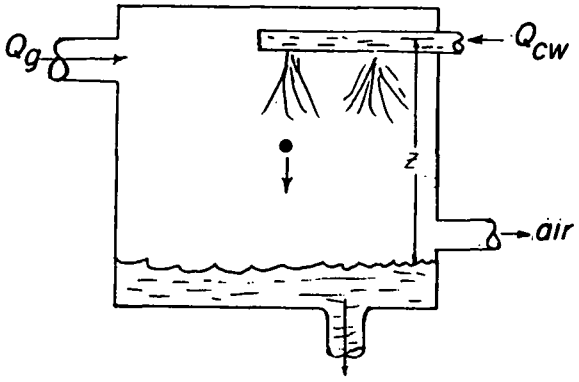



Fig. 16. Schematic of Claude's condenser (10), with high initial downward velocity, so short flight time.

Fig. 16 shows the approximate system used in a barometric condenser by Claude (10), in which water was sprayed from an overhead spray bar through nozzles. Non-condensables were removed to the atmosphere by a staged compressor with intercooling to remove the steam unavoidably removed with the gas.

This arrangement seems to have certain avoidable features, including a large vertical height, Z, a high spray nozzle pressure to produce small drops and a small residence time from the time the drop exits the spray nozzle and reaches the free water surface. The importance of these features can be understood if it is appreciated that a major part of the delivery pump's head would be in elevation to height Z and through the spray nozzle, and by examining the general heat transfer equation:

$$q = h_c(A\ \Delta t\ T), \qquad (9)$$

where q is the amount of heat removed in condensation per unit time, A is the total area of drops, $\Delta t$ the temperature difference between the steam and the drop; this decreases to a final, or "approach" temperature. All this must take place in a time, $T$, which in the barometric condenser is the time of flight of the drop. This picture is further complicated by the presence of non-condensable permanent gases which collect on the drops as the steam is condensed and so decrease the condensation coefficient, $h_c$ from a maximum at drop injection to a minimum at the water surface. This volume is substantial and at 1 atmosphere amounts typically to about 1/50th the volume of warm water, if degassification is complete. From Eq. (9), we see that an increase in area of drops (accomplished by breaking into smaller drops, which requires higher spray nozzle pressure drops or other techniques) decreases the thickness of the insulating layer of gases. The effective t can be increased by reducing the approach temperature difference but this requires pumping more water.

Finally, there seems to be considerable promise in increasing by the configuration (or others with similar purpose) shown in Fig. 17, by supporting a

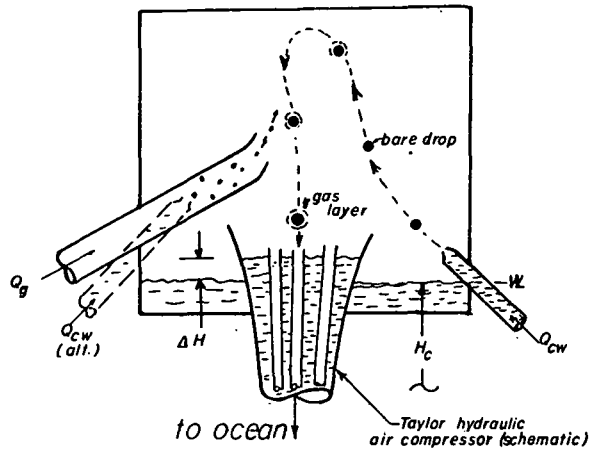



Fig. 17. Proposed improved barometric condenser as discussed in the text.

large drop projected upward from a minimum Z in the high velocity incoming steam; presumably, the drop's size can be reduced by 'stripping' from shear forces. A possible alternative is shown dotted, where the large drop is introduced with the steam, and so a minimum spray pressure but maximum Z and $T$ can be achieved with minimum pump power.

A final dimensionless ratio may be helpful in visualizing the total process; it bears directly on $R_2$:

$$R_3 = \frac{Q_f}{Q_{cw}} \qquad (10)$$

When the numerator and denominator are multiplied by the appropriate efficiencies and heads of turbine and pump, $R_2$ results.

The use of a Taylor compressor (11) to remove permanent gases which would otherwise accumulate in the condenser and 'break the vacuum' seems particularly appropriate here because of (a) its high reported efficiency (b) its simplicity (see (12) with reference to KISS in engineering design), and (c) its ability to directly condense the steam carried with the layer of permanent gases, which cause major power losses and complication in mechanical compressers. The probable efficacy and efficiency is not proven in this application; the effect on the system is to increase the apparent barometric height, $H_c$, by the losses in the Taylor compressor's venturi is indicated by the amount $\Delta H_c$ in Fig. 17.

A complete design analysis of a Steam Lift Cycle OTGHPP operating at ocean temperatures would require the selection of optimum values of a large number of variables, and inter-relating them through suitable equations, some of which have been listed. To summarize the scope of the needed work, the apparent independent variables which must be simultaneously considered as a function of elevation, Z, in the SLP,

Fig 14 and similar appropriate variables in the condenser, Fig. 17, are:

$R_1$, $R_2$
$V_z$, $P_z$
$H_f$, $H_c$ ($H_b$ is approximately established by ocean surface temperature)
$L$ , $D_z$, $Z_{tr}$ (height of first bubble formation, less than $H_b$)
$V_g$, $V_f$, $V_d$, $V_r$, $d_b$, $d_d$
$\Delta t_{app}$ (equals $t_c - t_d$, where $t_d$ is final temperature of drop in condenser)

A complete design procedure optimizing all of this list of variables will be very complex, and is not warranted pending proof of feasibility of (a) drop formation and size control and (b) elevation of drops in acceptable steam velocities and steam/water ratios (13).

## CONCLUSIONS

The feasibility of building SLP's at high temperatures has been demonstrated, and an approximate design method developed for the case in which steam/water ratios are such that stable bubbles can be maintained over most of the active length of the SLP.

The feasibility of low-temperature SLP's, while briefly explored, has not been demonstrated.

The immediate tasks in the development of large scale SLP's are the demonstration and quantification of design techniques to form drops of suitable size by breaking rapidly moving bubbles and to elevate them to a useful height in a high velocity, low-pressure temperature stream.

Following demonstration of the drop-support phases, a complete numerical method of SLP design, based on the best empirical design factors available at that time, will be needed.

## REFERENCES AND NOTES


1. Beck, E. J. US Patent 3,967,449 of 6 July 1976.
2. Stenning, A. H. and C. B. Martin, ASME Paper '67/WA/FE-1.
3. Beck, E. J. Civ.Engr.Lab Port Hueneme, Calif. 93043 Tech.Memo. M-80-76-77 (in publication).
4. Plesset, M. S. and S. A. Zwick, JourApplPhys 25, 4, pps 493-500, April 1954.
5. Rouse, H. "Fluid Mechs. for Hydr. Engrs." Dover, N.Y., 1938, 1961.
6. Loeb, L. B. in "Modern Physics for the Engr.", L. N. Ridenour, Ed. McGraw-Hill, New York 1954.
7. Schmidt, E. "Properties of Water and Steam in SI Units", Springer-Verlag, New York, 1969.
8. Beck, E. J., Science, 189,293 (1975).
9. _____, _____, 195,206 (1977).
10. Claude, G. Mechanical Engineering 52, 1039-44 (1930).
11. Marks, L. S. "Mechanical Engineers Handbook", 4th Ed. 1941, McGraw-Hill, New York. (Note: ref. to Taylor Hydr. Air Compr. omitted from current edition).
12. Shapley, D. Science 195, 1311-13. (1977).
13. For clarity and brevity, many details of the calculations and proposed experiments are omitted here but are available by direct correspondence with the author to interested parties.


## DISCUSSION

LYON (Consultant at ORNL): Earl, you said, I believe, that you had about 4 feet of pressure differential in your column in these tests to you were operating at about 13 psi at the top. Is that right? I gather what you have in mind ultimately is to have the pressure at the top below 1 psia.

BECK: The pressure has to go below 1/2 psia before you even make any steam, because that's the saturation point.

LYON: Was your temperature difference between the bottom and top comparable to what you expected?

BECK: Oh, no, this demonstrates the concept. Now in going to the low pressures there are some advantages because you get a lot of voids without evaporating much water; the low specific volume is a plus. But the limitation, the thing that makes it very difficult, and we're going to have to be good at designing, is that you only have about a third of a meter of sea water pressure equivalent to use, corresponding to a difference between the condensing temperature and the boiling temperature of, say, 5°C, and we have to use that judiciously. But it doesn't look bad; it looks very good. The densities of the steam water mixture are so very low that we can get considerable elevation in spite of that.

LYON: Do you think you will still stay in the regime where the water is continuous phase when you get down to these very large vapor fractions?

BECK: No, what happens is at a certain point you would want to make nice discrete bubbles, you're going to control their size, then you're going to control the growth, then you have to get drops at these low temperatures, and we want to design the system so the drops go almost as fast as the steam because you have considerable irreversibilities. Well, that's very optimistic. However, the steam, even though it's at very low pressure, has a density something like air and a 1-mm drop has a falling rate of 1.2 m/sec, so you don't really take a bad penalty. This is a complex problem which needs to be put on a very large computer, and Design Services is Earl Beck, and we don't own a large computer.

# THE FOAM OTEC SYSTEM: A PROPOSED ALTERNATIVE TO THE CLOSED CYCLE OTEC SYSTEM

CLARENCE ZENER
*Carnegie-Mellon University*
*Pittsburgh, Pennsylvania*

## Abstract

This paper discusses the many potential advantages of the Foam OTEC System (2) over the standard Closed Cycle OTEC System. These advantages include the absence of heat exchangers, the replacement of gas turbines by high head (over 600 ft) hydraulic turbines, the automatic elimination of the recirculation problem, more than 5 times greater power output per unit warm water intake, and hence 5 times greater power output per unit warm water intake, and hence 5 times greater power generated along the Louisiana Coast. The physical principles of foam, as well as of the foam system, will be discussed in detail.

## Introduction

After having worked on the OTEC program for four years, I have concluded that it may be on the wrong track. How it got on this track is an interesting story. Those of us who were first on the program grew accustomed to thinking of the warm upper layer as a heat reservoir, the cold deep layer as a heat sink. The standard way of taking advantage of the work potential latent in a heat reservoir is to interpose a heat engine between it and the heat sink. The term "heat engine" implies a device that absorbs heat from an external source, converts some of this heat into work, and rejects the remaining heat into the heat sink. We classified heat engines into two categories, the closed cycle engine of d'Arsonval, and the open cycle engine of Claude. As viewed from their inputs and outputs, however, both systems look almost identical (Top, Fig. 1). The input water gives up a small fraction of its heat, and is then rejected at a slightly lower temperature. The only input-output difference between the two systems is that in the closed cycle the output of slightly chilled water is identical to the cold water input. These identities are not applicable in the case of the open cycle system.

Reading the discussion of Earl Beck (1) jolted John Fetkovich and myself into recognizing a new type of heat engine. In this new type of heat engine the working medium is two-phase, rather than the single phase of the d'Arsonval closed cycle or the Claude open cycle. In the new system design, the input warm water, at least in principle, goes straight down the T-S diagram (Fig. 2) into the two-phase region. To the third significant figure, the work potential liberated by the warm water

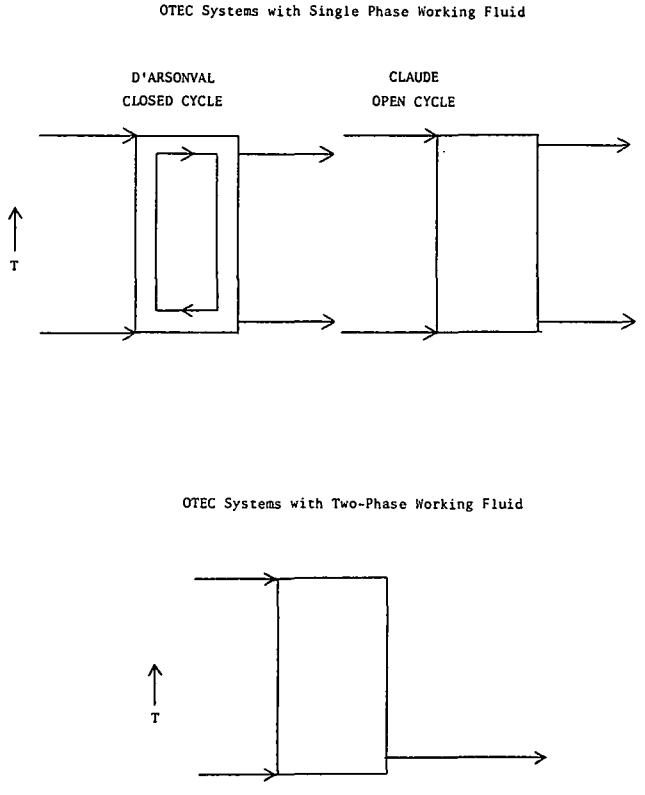



Fig. 1. Types of OTEC Systems

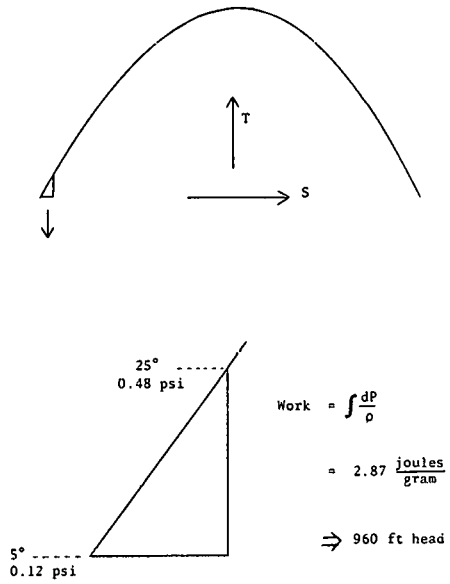



Fig. 2. Thermodynamics of Two-Phase OTEC System

input is just the area of the closed cycle, namely 2.87 joules/gram, corresponding to a head of 960 feet. In contrast to the single phase system of d'Arsonval and Claude, there is no warm water exhaust (Bottom, Fig. 1).

In order to minimize irreversible phenomena, two requirements are needed:

(1) The liquid component must be very thin in at least one direction. This requirement ensures that the heat for evaporation need travel only a very short distance, thereby maintaining the liquid and the surrounding vapor at essentially the same temperature. Loss of work potential by the flow of heat down a temperature gradient is made very small.

(2) The two-phase region must be so constituted that the motions of the liquid and vapor phase are closely coupled.

These two conditions can be satisfied by two extreme ways of distributing the liquid and gas phases: (1) a foam distribution, (2) a fine mist distribution. An OTEC system based upon a mist structure is described by Ridgeway at this session. Both systems have the same potential advantages discussed below.

## Potential Advantages of Two-Phase System

What are the advantages of two-phase systems?

Firstly: In common with all open cycles, they have no heat exchangers. Fouling problems are thereby mostly eliminated. A great cost reduction is hence possible. Whereas the Claude open cycle also has no heat exchangers, this advantage is compensated for by the requirement of having a large low pressure gas turbine. At least in the foam system, a high head hydraulic turbine may be used.

Secondly: We have no warm water exhaust. All recirculation problems are thereby automatically eli: ted. The plants may therefore be placed much closer together than in the case of the standard closed system OTEC plants.

Thirdly: For the same warm water input, from 5 to 10 times greater power output is obtained.

When we combine the second and third advantages, we see that a much greater power may be extracted from a limited area than in the case of the closed cycle.

This ability of having a high density of power generation within a limited area is especially advantageous when we transmit power to the mainland. Thus we can visualize a high density OTEC energy park within 100 miles off the Mississippi delta supplying a large fraction of the power needs of the Gulf states.

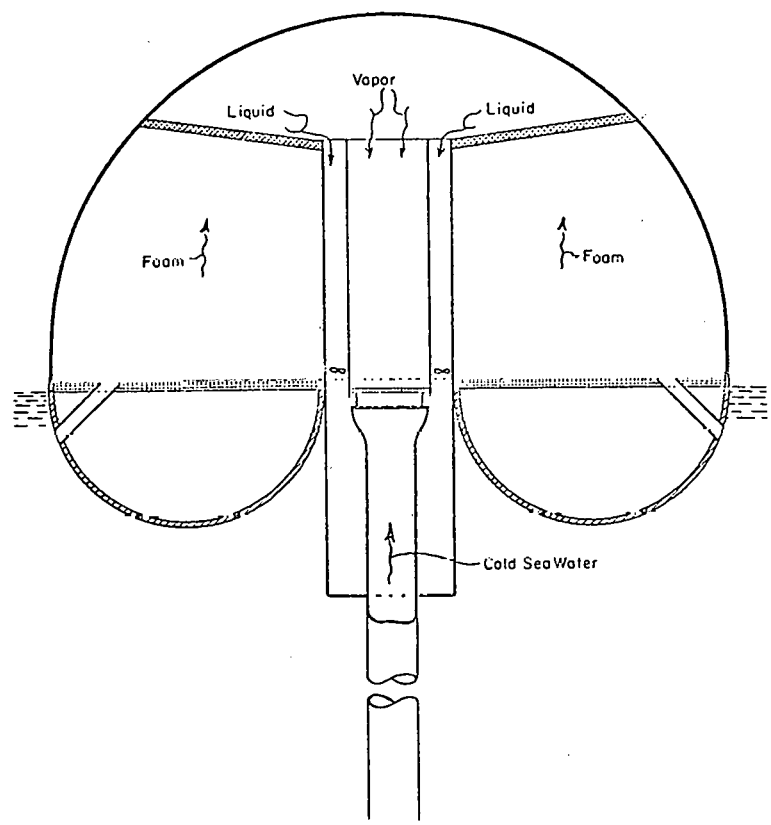



Fig. 3. Conceptual Foam OTEC System

After air evacuation, warm water is sucked in by the
ıl vacuum. After this water is foamed, it rises
han 600 ft past foam breakers. The vapor thereby
flows down the central pipe and is condensed by a spray of cold water which has been sucked up from the ocean depths. The liquid is collected in standing pipes which lead to hydraulic turbines.

The most striking visual feature of a foam OTEC plant is the large containing dome. In order to support the atmospheric pressure, the thickness of this dome must be 2 ft. The dome cost may be estimated by taking $500 per cubic yard, resulting in less than $100/kw.

The technically most challenging component of the foam OTEC system is the foam generator. One requirement of this generator is that the upward take-off foam velocity must be large compared to the downward bottom drainage velocity. Otherwise the liquid content of the foam would be much less than its theoretical value. This in turn implies a greater foam area per unit mass, and hence a large diversion of liberated work potential into surface energy.

When we first started we thought the requirement of a low cost surfactant would present a formidable problem. Thanks to the work of Sephton (3) and his colleagues at the University of California on sea water desalination, it appears that some currently used commercial surfactants may be fairly satisfactory, both in cost and in biodegradability. One such surfactant, Neodol 25-3A (Shell Chemical Company), reduces the surface tension of sea water from 74 to 55 dynes/cm$^2$ at a concentration of only 5 ppm. At 35¢/lb (in carload lots) we estimate this surfactant would cost less than 2 mills/kwh. This surfactant is biodegradable.

A most interesting scientific problem is to understand how a foam supports the liquid phase against the downward pull of gravity. Figure 4 shows the macro-stress system that supports the liquid at the foam corners. The mass density m per unit length gives a density

$$\rho = (m/\Delta x\, \Delta z) , \qquad (1)$$

where $\Delta x$ is related to the side length by

$$s \sin 60° = \Delta x . \qquad (2)$$

This density in turn gives rise to a pressure difference

$$\Delta P = \rho\, g\, dz \qquad (3)$$

between adjacent horizontal layers of foam. This pressure difference results in a curvature of the interfaces

$$\frac{1}{R} = \frac{\Delta P}{2\sigma} \qquad (4)$$

This curvature causes the angle between the upper two faces to decrease from 120° by the amount

$$2\,\delta\theta = \frac{s}{R} \qquad (5)$$

between the two lower faces to increase by the same amount. In both cases the resultant surface tension force acting upon each corner changes from zero to

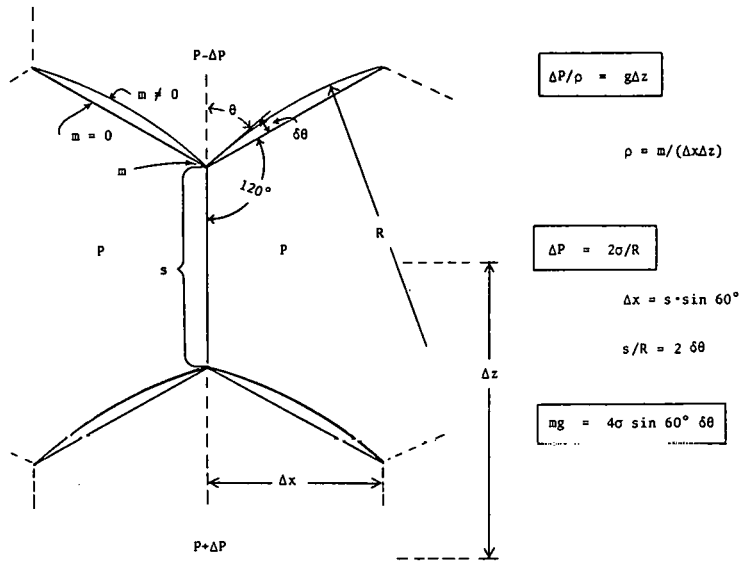



Fig. 4. Macro-stress Analysis of a Foam

a net upward surface tension force

$$\text{Net force} = 4\sigma\, \Delta\theta \sin 60° . \qquad (6)$$

Upon multiplying (6) by (1), (2), (3), (4) and (5), we obtain

$$\text{Net surface tension force per unit length of edge} = mg .$$

We thereby obtain a balancing of surface tension and gravity.

## Conclusion

The Foam OTEC System has been examined from the standpoints of both economics and technical feasibility. The extreme simplicity of the plant suggests the possibility of a very low cost. The most outstanding technical problems have been examined. None appear insoluble.

## References


1. E.J. Beck, Science 189, 293 (1975).
2. Clarence Zener and John Fetkovich, Science 189, 294 (1975).
3. H.H. Sephton et al., Desalination 16, 39 (1975); 16, 15 (1975).

# DISCUSSION

FISCHER (Gilbert Associates): Would you care to say a little bit about your foam maker and breaker and their costs?

ZENER: The way we are breaking our foam now is simply to have a cold water spray, which also serves the functions of condensing the water vapor and entraining the noncondensibles to take them out. This system would not be applicable to the commercial system that I depicted in the figure because in the commercial system the foam must be broken when it's, say, 600 feet high and we wouldn't want to take cold water that high. However, breaking the foam, I feel, is the least of our problems, since we need not have it more stable than to get it up that high. We are still troubled by the foam generator, but what we are doing at the present time is simply leaking air from the atmosphere into small tubes to form bubbles. I don't think it's a satisfactory way to proceed, and this is the major problem that we are working with now, namely, some other system to generate foam.

MAYER (U. of New Orleans): My question concerns the detergent. Clarence, you recall when you were here a couple of years ago, I suggested that the foam wouldn't be stable enough to go up to 600 feet with ordinary sea water and I think that I was right. Here's a subtle point. When you're talking about the market value for detergents, say, 1 mill/kWh, that detergent is presently made from petroleum, right? Petroleum is available at a market price of $2 to $3 per million Btu. Ultimately your plant is going to have to regenerate its own detergent, directly or indirectly, and somehow part of the energy is going to have to go into, say, the electrolysis of water and from hydrogen through carbon dioxide into synthetic organics and into the detergent. When you do that, what will be the energy input into the detergent relative to the energy output of the plant? Although I will concede that it will not be catastrophic, I think that it will be a significant factor.

ZENER: That's a very good question, David, that frankly I hadn't thought about, and next time I see you I'll have the answer.

FISCHER: Clarence, let me see if I can give you an answer. You don't have to make them out of petroleum. For example, Johnson's Baby Shampoo is made of sugar esters, and if we open trade with Cuba, we get a large supply of sugar near where we've got a large supply of warm and cold water. Detergents also can be made from corn sugars at a low cost in energy. There should be several ways to obtain non-petroleum detergents, especially since the foam system doesn't need a real good detergent, because you don't want a foam that you can not break.

# PRELIMINARY ANALYSIS OF THE EFFECTS OF SEA WATER LEAKAGE ON THE PERFORMANCE OF THE AMMONIA CYCLE

HAFEZ HAFEZZADAH, D. W. JOHNSON, AND K. E. STARLING
*School of Chemical Engineering and Materials Science*
*University of Oklahoma*
*Norman, Oklahoma 73069*

## Abstract

A preliminary investigation has been made into the effects of water contamination on an OTEC power plant utilizing ammonia as the working fluid. Both power cycles with and without recycle around the evaporator were studied. An optimized ammonia cycle plant was used as the basis for the study. The thermodynamic effects of increasing the water concentration were analyzed by utilizing the Han-Starling Generalized Correlation with appropriate parameters for ammonia-water mixtures. The results of this analysis placed upper limit bounds on the thermodynamically permissible amounts of water contamination. The actual power cycle degradation was studied using the OTEC simulator developed at the University of Oklahoma. In each case, it was assumed that an actual OTEC-ammonia plant was operating at an offshore location when the water contamination started. Thus, the major items of equipment, such as evaporator, condenser, turbine, cycle pump, hot and cold water pumps and cold water pipe were fixed. The preliminary results showed that a small amount of water could be tolerated without serious degradation in cycle performance. The amount of water which could be tolerated increased as the recycle ratio around the evaporator increased. Work is continuing in this area with three objectives: (1) further definition of the range of water concentrations which can be tolerated in OTEC plants, (2) optimization of an OTEC cycle with a water concentration attainable with available ammonia-water cleanup equipment, and (3) investigation of the effect of water concentrations on heat transfer in OTEC evaporators and condensers.

Ammonia appears to be the working fluid of choice for a closed cycle OTEC power plant. The superiority of ammonia over the other proposed working fluids (propane, freon, propane-butane mixtures) is due to two factors. First, ammonia has a much larger enthalpy change per unit mass in the expansion across the power turbine. This means that lower mass flows of ammonia are required to produce a given turbine output. This translates into lower parasitic pumping power and higher cycle efficiencies. Second, ammonia has a considerably higher liquid thermal conductivity than other working fluids. Since the viscosity of ammonia is close to the other working fluids, ammonia will have a higher liquid film heat transfer coefficient. This results in higher overall heat transfer coefficients for the ammonia cycle; thus, lower heat exchanger costs.

While ammonia has a decided advantage over the other potential OTEC working fluids, it has one major disadvantage: ammonia and water* are miscible in all proportions. This means that water leakage into an ammonia cycle can have disturbing effects on cycle performance. When we began this study, the effect of water leakage on an OTEC ammonia cycle was unknown. We feel that our preliminary results have provided a valuable insite into this area.

*For the present, we will assume that ammonia-water mixtures will represent the general behavior of ammonia-sea water mixtures.

## Why Does Water Affect the Ammonia Cycle?

Water affects the ammonia cycle because of its strong effect on the dew point temperature. For a pure fluid at constant pressure, the bubble and dew point temperatures are equal. Ammonia at 130 psia has a dew point of about 70.5°F and a bubble point of 70.5°F. However, a mixture of ammonia and water containing only 0.1% water has a dew point of 86.4°F and a bubble point of 70.5°F. This change in dew and bubble point temperature is shown in Figure 1.

The net result of the addition of water to ammonia is to increase the difference between the dew and bubble point temperatures. Figure 2 illustrates another aspect of this problem. This figure relates the percent of original liquid vaporized to the increase in temperature (over the bubble point) necessary to produce the effect. This is similar to determining the temperature required to boil away a given percentage of liquid in a pan. If the liquid in the pan were pure ammonia, a hot plate under the pan kept at 70.6°F would be sufficient to boil away all of the liquid. However, if the temperature was

set at 73.5°F, only 91% of a mixture of 99.5% ammonia and 0.5% water would boil off. If the initial water concentration was 5%, only 49% of the original liquid would boil away.

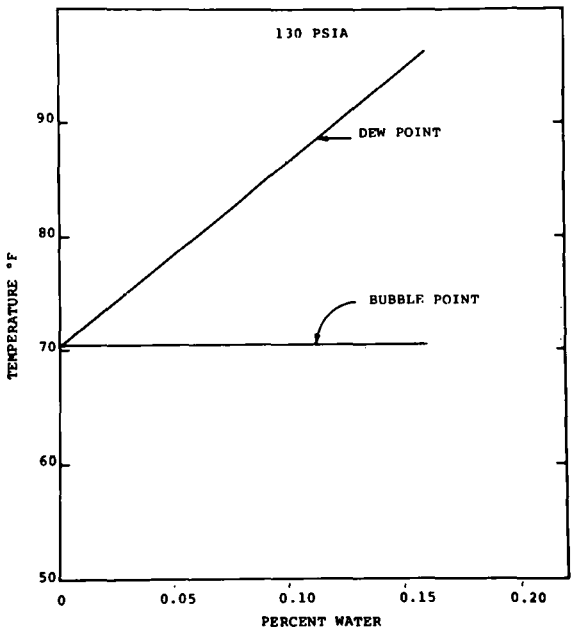



Figure 1. Effect of Water Concentration on Dew and Bubble Point.

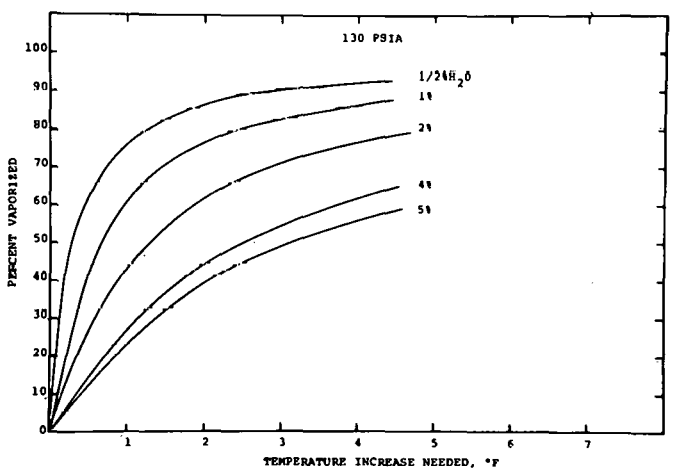



Figure 2. Temperature Increase Needed for Vaporization.

Since an OTEC evaporator cannot provide a boiling temperature above 79-80°F, it is obvious that at 130 psia, less than 0.1% water can be tolerated if 100% vaporization is required. Figure 3 shows this effect at 130 psia. The hot water line was constructed by using an energy balance, while the ammonia-water lines w obtained from flash calculations. The implication Figure 3 obvious, when the ammonia-water lines cross the hot water line, no heat transfer driving force is available (i.e., ΔT) and boiling would cease. The situation can be improved by lowering the pressure in the evaporator. Figure 4 shows the same effect at 110 psia. At 110 psia, more water can be tolerated than at 130 psia, but the amount is still very small. Sadly, the evaporator pressure cannot be lowered below about 70 psia since the condenser must operate above 40°F (the temperature of the deep ocean water).

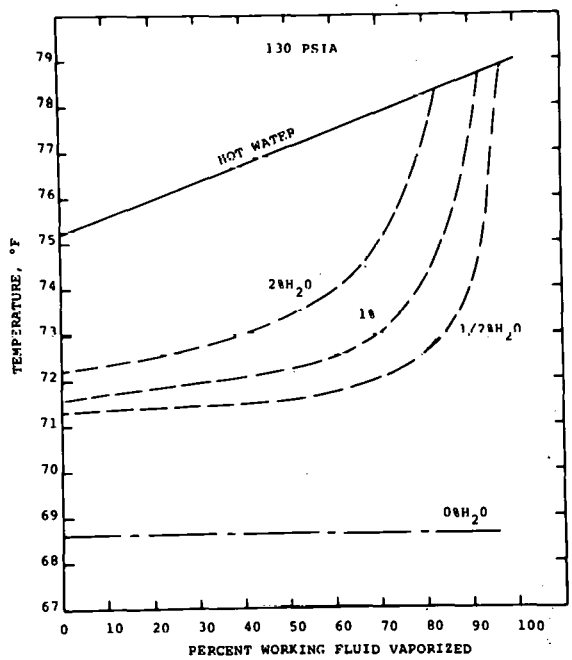



Figure 3. Effect of Water on Temperature Difference at 130 PSIA.

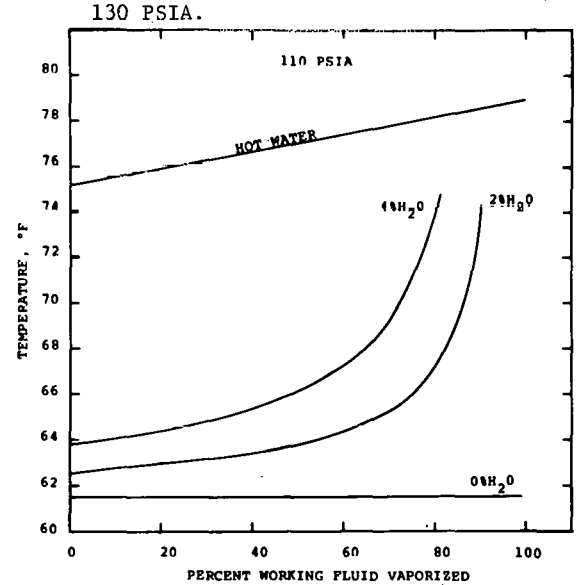



Figure 4. Effect of Water on Temperature Differenct at 110 PSIA.

## What can be Done to Minimize the Effect of Water?

nce an OTEC power plant with an evaporator pro-
di 100% vapor using ammonia as the working fluid could not tolerate water concentrations above 0.1% without a serious degradation in power production capability, it is obvious that OTEC evaporators going to 100% vaporization should not be considered. Fortunately, the use of an OTEC plant, as shown in Figure 5, in which the evaporator vaporizes only a fraction of the liquid feed has an excellent potential for use in situations where water leakage into the ammonia is possible. The vapor-liquid equilibrium for ammonia-water makes this procedure practical, since very little of the water will leave in the vapor stream. Figure 6 shows a typical VLE diagram for ammonia-water mixtures at 130 psia. For example, if the liquid entering the vapor-liquid separator contained 12% water, the vapor entering the turbine would contain only 0.036% water. By utilizing an ammonia evaporator which vaporizes less than 100% of its feed, an OTEC plant can be designed which minimizes the undesirable effects of water leakage.

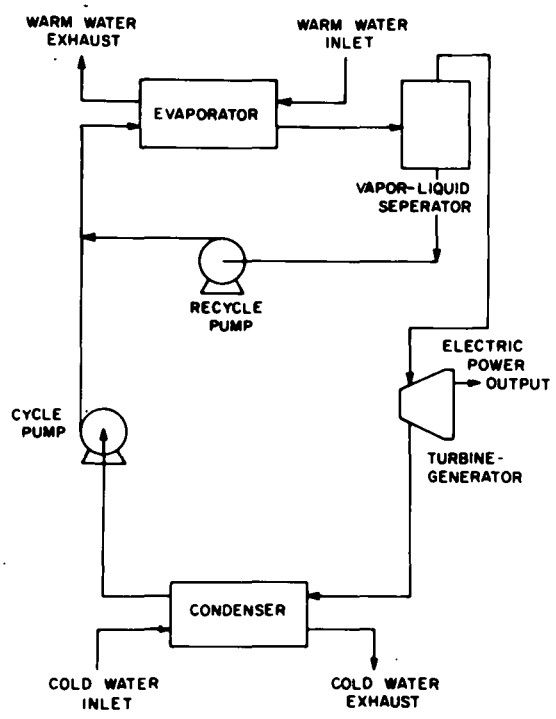



Figure 5. OTEC Plant with Recycle.

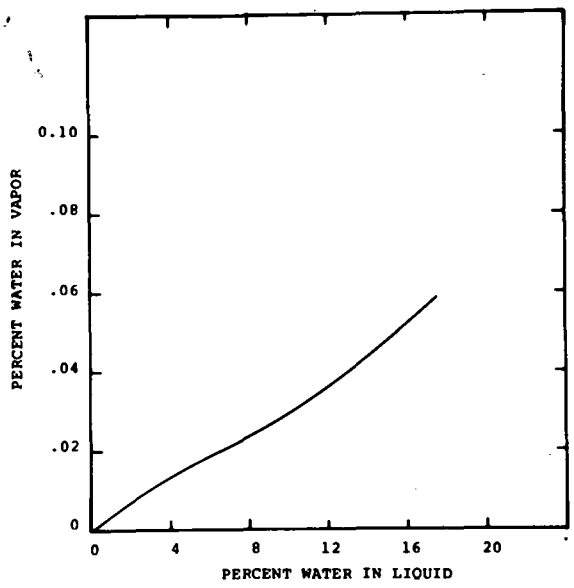



Figure 6. Vapor-Liquid-Equilibrium of Ammonia-Water Mixtures.

## How Can We Quantify the Effects of Water Leakage?

So far we have discussed the effects of sea water leakage in a qualitative way. This much is known: water leakage will degrade the cycle performance. How much degradation occurs for a given water concentration is the important question that we must answer.

At this point, a basis must be established for use in future computations. Our basis is an optimized operating OTEC plant with a net power output of 25 MW and utilizing pure ammonia as the working fluid. The plant will contain the major pieces of equipment as shown in Figure 5. Thus, the evaporator, condenser, turbine, generator, hot and cold water pumps, cycle pump, cold water pipe and hull are considered as non-exchangeable pieces of equipment. The vapor-liquid separator and recycle pump are assumed to be large enough to handle any amount of throughput. Other pertinent information is listed in Table I.

Table I
Base Case Parameters

I. Heat Exchangers:

Water on tube side
Ammonia on shell side
Evaporator and condenser tube OD = 1.000 inch
Evaporator and condenser tube ID = 0.960 inch
Minimum approach temperature = $2^{o}F$

II. Water Velocities:

Water velocity in evaporator = 5 ft/sec
Water velocity in condenser = 4.5 ft/sec
Water velocity in cold water pipe = 10 ft/sec

III. Other:

Length of cold water pipe = 3500 ft
Hot sea water inlet temperature = $79^{o}F$
Cold sea water inlet temperature = $40^{o}F$

The percent recycle is defined as the percent of the evaporator feed which enters the vapor-liquid separator as liquid. Thus, an evaporator vaporizing 75% of the feed would have 25% recycle. The water concentration in the cycle was taken as the water concentration entering the evaporator.

Before water leakage begins, the plant is assumed to be operating at steady state with minimum recycle. As water leaks into the cycle, the initial effect will be to lower the effective driving force for heat transfer in the evaporator (see Figure 3). The result is a drop in working fluid flow through the turbine and a decrease in power production. Two options are available for minimizing the power decrease: (1) lowering the evaporator pressure, thereby increasing the available temperature difference between hot sea water and working fluid and (2) increasing the amount of recycle to lower the percent of liquid vaporized in the evaporator. There will be an optimum pressure and recycle for each water concentration.

Within the limitations previously discussed, the OTEC simulator developed at the University of Oklahoma (1) was used to study a number of discrete water concentration levels, varying from 0 to 5% water. At each water concentration level, several values for the amount of recycle were utilized. The amount of recycle varied from 1 to 35%. At each value of water concentration and recycle, the evaporator pressure was allowed to seek an optimum value.

The results of many such OTEC cycle simulations are shown in Figure 7. Here, the percentage power loss, defined in the following manner

$$\% \text{ Loss} = 100(25\text{MW} - \text{Net Plant Output})/25\text{ MW}$$

is plotted versus the water concentration entering the evaporator with the amount of recycle as the third parameter. As Figure 6 shows, the amount of water which can be handled for a given power loss increases as the recycle increases. An interesting result of this study which is not readily observable in Figure 7 is that although increasing the amount of recycle (at a given water concentration) will lower the percentage of power lost, this decrease occurs at an ever slowing rate. Figure 8 illustrates this point very clearly. From the figure it is obvious that increasing the recycle above 40-50% will not provide much useful benefit in terms of minimizing the power loss.

The net result of our study so far is this: the amount of water that can be tolerated in an OTEC power plant utilizing ammonia as the working fluid will depend on the amount of net power loss which can be tolerated. This result is shown graphically in Figure 9 which relates the water concentrations which can be handled at the 10% and 33% power reduction levels to the amount of recycle.

Where Do We Go From Here?

Over the next half year, we will be pursuing our investigation of the effect of sea water leakage on the OTEC ammonia cycle in the following areas:

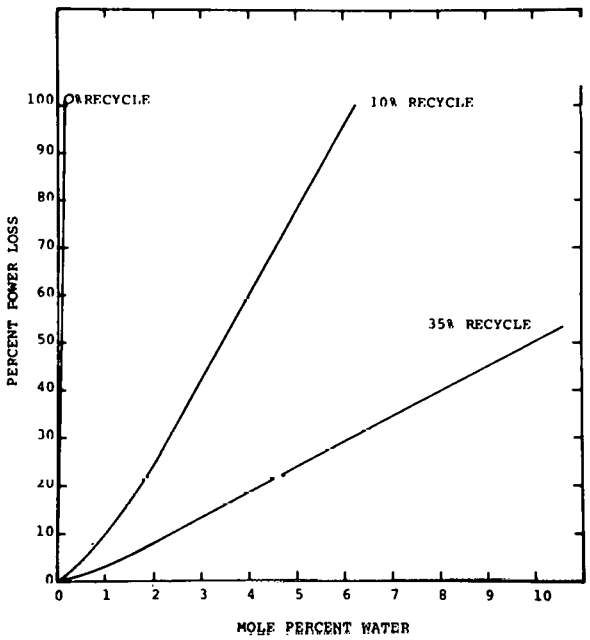



Figure 7. Effect of Water on Power Loss.

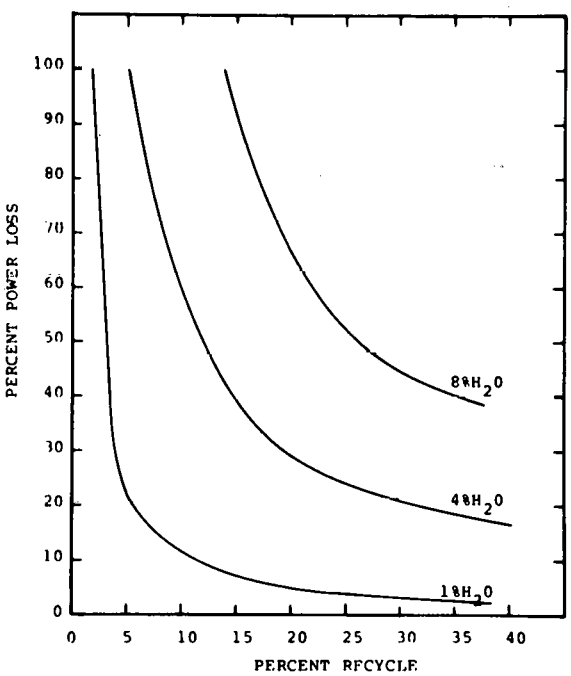



Figure 8. Effect of Recycle on Power Loss.

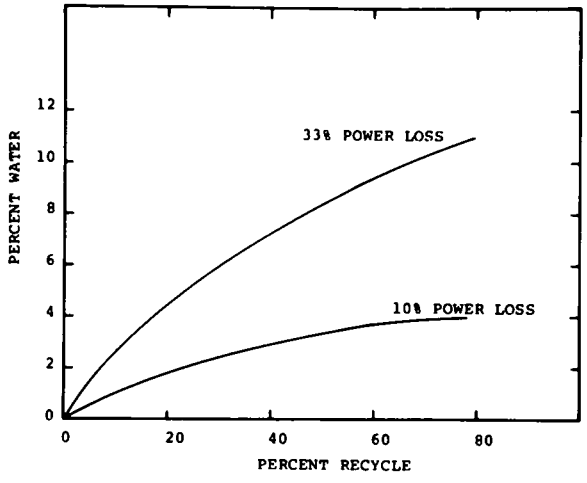



Figure 9. Amount of Water Tolerable at Given Power Loss.

1. Expand the range of water concentration and amount of recycle presently being studied.

2. Preliminary investigation of the effects of water on the heat transfer in an OTEC cycle.

3. Optimization of an OTEC plant with a water concentration equivalent to the output from a commercially available ammonia regeneration unit.

4. Correlation of the transport properties of ammonia-water mixtures in the range of OTEC operating conditions.

Potential future work will include a correlation of sea water-ammonia mixture properties, an investigation of the possibility of salt precipitation in ammonia-sea water mixtures and improving the present correlation of ammonia-water thermodynamic properties.

Acknowledgement

This work was supported by the Energy Research and Development Administration, Contract No. E-(40-1)-4918.

References

(1) Starling, K.E., et al., USE OF MIXTURES AS WORKING FLUIDS IN OCEAN THERMAL ENERGY CONVERSION CYCLES - PHASE I, FINAL REPORT - PHASE I, Report ORO-4918-9, August, 1976.

## DISCUSSION

DUGGER (APL/JHU): I have a comment. In the design of the closed-Rankine-cycle plant that APL proposes, the sea water is outside the tubes, and the maximum pressure it can have is about 35 psi, whereas the ammonia inside the tubes is 125 psi, so the leak would always be from inside out, and sea water will not get into the system.

JOHNSON: That's obviously the best way to handle it.

CONDON (U. of Calif., Irvine): I'm puzzled by what you've done here. I would expect that if there is a way for water to leak into the system, it will be a continuous leak, once it's started, and you'll want to be removing that water from the system, not just letting it recycle as you apparently assume. Yet you're going through an evaporation phase, which strikes me as a perfect way to separate out the water and pipe it off. Have you considered distillation--separation--to remove the water?

JOHNSON: Yes. As a matter of fact, some of the early studies done by TRW and Lockheed had a system in to clean up the ammonia. They had already anticipated water leakage, and we do want to get to an investigation of the questions: what could we buy today to remove water from ammonia? Will it produce a product that is 0.5%, 1%, or 2% water? Then we should optimize an OTEC plant around that, which would obviously have more favorable performance than the plant we've considered. We didn't consider a continuous leak because it was easier to assume fixed water concentrations and show their effects. We certainly wouldn't advise anybody to build an OTEC plant and say, let's just let it go to pot if water gets into the ammonia.

FISCHER (Gilbert Associates): Haven't any of you engineers ever run a plant? When you start up and you shut down, the ammonia pressure is substantially zero and the leak is going to be into the system, because it's under hydrostatic pressure. If you have an upset, I don't know which way the leak is going to go--it may go either way. Then the water content will not increase linearly; if you find and fix several leaks over a period of time, it will increase in what looks to you like steps in an intermittent process, and anything you can do, like the authors are doing, to tell us how bad this is, how soon we have to detect the leak and plug it, is a benefit in keeping down the operating cost and the repair and maintenance costs of these plants.

Post-session reply by DUGGER: The APL heat exchangers will be initially charged with the appropriate amounts of pure ammonia at substantial pressures before operation begins. The evaporator and the condenser will both be at some temperature near warm water temperature (say, 83°F) prior to startup of the water flows and hence would be at an internal pressure near 160 psia, with external water pressures varying from 18 psia (top pass) to 53 psia (bottom pass). During operation, the evaporator would have internal pressures above 125 psia (68°F); the condenser, above 86 psia (48°F). Sea water

could not leak in until essentially all of the ammonia had escaped through a leak. Before this could happen, substantial changes in operation would have been noted (e.g., reductions in ammonia sump level, pumping rate, and recycle from demister), and that module would have been shut down. You would not get water into the system and deliberately continue to operate. Because you can not get inside any proposed type of OTEC heat exchanger to repair a leak without interrupting its operation, another advantage of the APL approach is that there are eighty or more readily accessible modules of heat exchangers and a crane system to permit their removal one at a time for repair or replacement. The temporary loss of one or even several modules will have little affect on overall plant output.

# THE MIST FLOW OTEC PLANT

STUART L. RIDGWAY
*R & D Associates*
*Marina del Rey, California*

Abstract

The Mist Flow OTEC Plant uses the steam evaporated from a spray of very fine warm water droplets to lift these droplets to substantial heights. The used steam is condensed at the end of the lift by a cold water spray. Gravitational potential energy is removed from the warm water in a conventional hydraulic turbine to provide the desired power output. The large evacuated duct in which the upward mist flow takes place is the major ($360/kw) cost element of the system.

## Introduction

Faced with the present shortages of energy, and the prospect of even greater shortages in the future, the United States is engaged in an intensive program to develop new sources of energy. There is at present great government interest in the possibility of harnessing the heat in tropical oceans with heat engines that operate on the appreciable difference in temperature between the surface water and the deep water, which difference can be as much as 22°C. In the last century the French physicist D'Arsonval suggested using a refrigerant such as ammonia in a Rankine cycle heat engine. The ammonia would be boiled in a heat exchanger by the warm water at one pressure, and condensed in a second heat exchanger at a lower pressure by the cold water. The ammonia vapor flowing from the higher to the lower pressure would do work in a turbine. These closed cycle systems are presently favored, but the heat exchangers must be large, and represent a very significant fraction of their cost.

Another French physicist, Georges Claude, attempted to avoid the large heat exchangers by using the water itself as a working fluid. He built a plant off the coast of Cuba that operated briefly in the early thirties. Warm water was sprayed into one chamber that had been evacuated. Steam evaporated from the drops, went through a turbine to do work, and was condensed in a second chamber by a cold water spray. This type of system is an open cycle system. The very low density of the steam required a very large turbine to absorb the work from the steam. The size of the needed steam turbine has generally discouraged interest in this type of plant.

## The Mist Flow Concept

Inventors have searched for a way around the large cost and the mechanical design difficulties of the large steam turbine in open cycle systems. Beck (1) has suggested that the vapor generated from warm water be used to lift that water against gravity. Bubbles of steam would be nucleated in the water, and would lift the water in a manner similar to that which occurs in the air or gas lift pumps of the chemical industry and oil recovery practice. Zener and Fetkovich (2) have suggested that the two phase mixture of Beck have a foam structure. The energy would be extracted from the lifted water in a hydraulic turbine.

The new concept that we wish to introduce is an open cycle system in which a mist of water is lifted against gravity by the flow of steam from a higher pressure region to a lower pressure region. The warm water from the surface would first fall doing external work, made into a mist and then be lifted back to the surface of the ocean where it would be discharged. The general arrangement scaled for a 10 MW electrical power output is shown in Figure 1. The center of the system is the large duct proportioned to accommodate the vertical upward flow of the mist of small water droplets in steam. The bottom of the duct is appreciably below the ocean surface, and the top of the duct is somewhat above it. Warm water is taken from near the surface, filtered, and allowed to descend through a penstock. The water then passes through a hydraulic turbine, where most of the pressure energy is removed. By means of the pressure remaining, the water is sprayed in tiny jets into the bottom of the duct, where the ambient pressure is slightly below the saturation vapor pressure of the injected warm water. Some of the water evaporates to form steam, and this steam raises the water droplets to the top of the duct against the force of gravity. The droplets are small enough so that viscous friction is sufficient to enable the steam to carry them up. When the flow reaches the top, it is turned radially outward to the condenser. After condensing the steam the mixed waters are returned to the ocean. Electrical generators are connected to the hydraulic turbine to obtain the desired energy output. Basic to the concept is the successful generation of the steam water mist, and its survival for a few seconds.

The concept differs from those of Beck, and Zener in two respects. First in the position of the hydraulic turbine in the cycle, and second, in the type of two phase flow regime utilized. We place the hydraulic

turbine before the steam lift pump, which avoids the need for a vapor liquid separation step at the end of the lift. For both their systems and ours the gas to liquid ratio is determined by the thermodynamics of water.

Beck (1) starts with water in which vapor bubbles are to be nucleated, and as the lift and expansion of the mixture takes place the flow regime passes from bubbly flow to slug flow to annular mist flow. Zener proposes that the bubble regime be stabilized as a foam at very large gas to liquid ratios, either by natural detergency or by the addition of detergent. Our system bypasses the bubble and slug flow regimes characteristic of flows with moderate gas to liquid volume ratios by directly preparing the two phase mixture in the annular mist flow regime. The problem of vapor bubble nucleation is circumvented, and considerable control can be exercised over the properties of the two phase mixture.

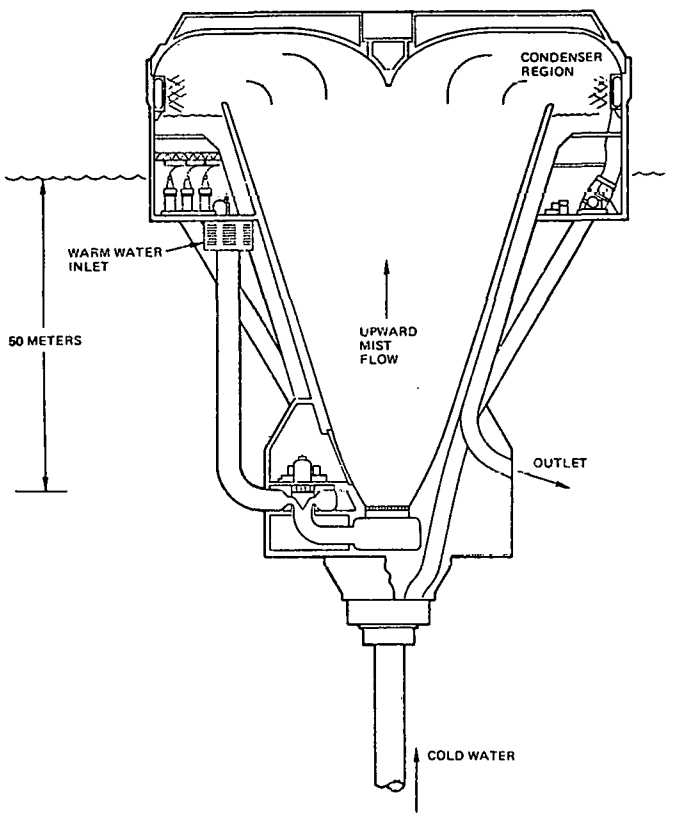



Figure 1. Ocean Thermal Energy Conversion Plant

## Thermodynamics

The steam-water mixture is lifted against gravity by the energy available as the result of the expansion of the mixture. The thermodynamic state of water that is expanded isentropically from saturated liquid water is given in Tables 1, 2 and 3, including the potential work available to lift against gravity, and the distance of such a lift. As the pressure on the mixture is reduced, some of the sensible heat of the water evaporates steam, which expands to do the work of the process. Initially only small amounts of work are available si there are only small amounts of steam to expand, but the amount of steam increases the amount of work available per degree temperature drop increases. Overall, the amount of work is quite closely quadratic with the temperature difference between the initial and final state; and is plotted in Figure 2.

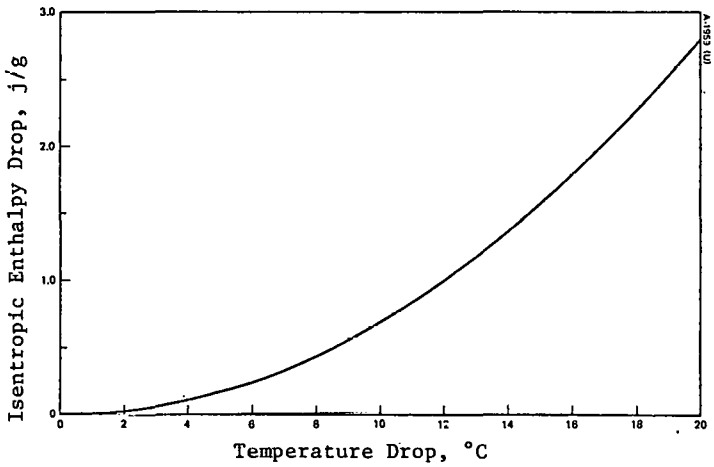



Figure 2.

Table 1. Isentrope of Saturated Water From 20°C to 7°C. Initial State 100% Liquid

| TEMPERATURE | MASS PERCENT STEAM | ENTHALPY DROP JOULES/GRAM | SPECIFIC VOLUME $CM^3/G$ | LIFT METERS |
|---|---|---|---|---|
| 20 | 0.0 | 0.0 | 1 | 0.0 |
| 19 | .170 | .00714 | 105 | 0.7 |
| 18 | .339 | .02863 | 221 | 2.92 |
| 17 | .51 | .0645 | 352 | 6.58 |
| 16 | .68 | .1149 | 495 | 11.7 |
| 15 | .84 | .1795 | 656 | 18.3 |
| 14 | 1.01 | .2588 | 836 | 26.4 |
| 13 | 1.17 | .353 | 1033 | 36.0 |
| 12 | 1.34 | .4616 | 1247 | 47.1 |
| 11 | 1.50 | .585 | 1500 | 59.7 |
| 10 | 1.66 | .723 | 1771 | 73.7 |
| 9 | 1.82 | .876 | 2070 | 89.3 |
| 8 | 1.99 | 1.043 | 2403 | 106.4 |
| 7 | 2.15 | 1.226 | 2771 | 125.1 |

Table 2. Isentrope of Saturated Water From 25°C to 7°C Initial State 100% Liquid

| TEMPERATURE °C | MASS PERCENT STEAM | ENTHALPY DROP j/g | SPECIFIC VOLUME $CM^3/G$ | LIFT, METERS |
|---|---|---|---|---|
| 25 | 0.0 | 0.0 | 1.0 | 0.0 |
| 24 | .17 | .007 | 79 | .7 |
| 23 | .34 | .028 | 166 | 2.9 |
| 22 | .51 | .063 | 263 | 6.4 |
| 21 | .68 | .1128 | 371 | 11.5 |
| 20 | .84 | .1765 | 492 | 18.0 |
| 19 | 1.01 | .2545 | 621 | 26.0 |
| 18 | 1.18 | .3468 | 767 | 35.4 |
| 17 | 1.34 | .4534 | 928 | 46.2 |
| 16 | 1.51 | .5745 | 1106 | 58.6 |
| 15 | 1.67 | .7101 | 1302 | 72.4 |
| 14 | 1.83 | .8602 | 1519 | 87.7 |
| 13 | 1.99 | 1.025 | 1758 | 104.6 |
| 12 | 2.15 | 1.204 | 2021 | 122.8 |
| 11 | 2.31 | 1.398 | 2312 | 142.6 |
| 10 | 2.47 | 1.607 | 2632 | 163.9 |
| 9 | 2.63 | 1.830 | 2984 | 186.7 |
| 8 | 2.79 | 2.069 | 3373 | 211.0 |
| 7 | 2.95 | 2.322 | 3801 | 236.8 |

Table 3. Isentrope of Saturated Water from 30°C to 7°C Initial State 100% Liquid

| TEMPERATURE °C | MASS PERCENT STEAM | ENTHALPY DROP j/g | SPECIFIC VOLUME $CM^3/G$ | LIFT, METERS |
|---|---|---|---|---|
| 30 | 0.0 | 0.0 | 1.0 | 0.0 |
| 29 | .17 | .0069 | 61 | .7 |
| 28 | .34 | .028 | 126 | 2.82 |
| 27 | .51 | .062 | 199 | 6.36 |
| 26 | .68 | .111 | 280 | 11.3 |
| 25 | .85 | .173 | 369 | 17.7 |
| 24 | 1.02 | .250 | 467 | 25.5 |
| 23 | 1.18 | .341 | 575 | 34.8 |
| 22 | 1.35 | .446 | 694 | 45.5 |
| 21 | 1.51 | .565 | 825 | 57.6 |
| 20 | 1.68 | .698 | 970 | 71.2 |
| 19 | 1.84 | .846 | 1128 | 86.3 |
| 18 | 2.00 | 1.008 | 1303 | 102.8 |
| 17 | 2.16 | 1.184 | 1494 | 120.8 |
| 16 | 2.32 | 1.375 | 1705 | 140.2 |
| 15 | 2.48 | 1.580 | 1935 | 161.2 |
| 14 | 2.64 | 1.800 | 2189 | 183.6 |
| 13 | 2.80 | 2.034 | 2467 | 207.5 |
| 12 | 2.96 | 2.283 | 2773 | 232.9 |
| 11 | 3.11 | 2.547 | 3109 | 259.8 |
| 10 | 3.27 | 2.825 | 3477 | 288.2 |
| 9 | 3.42 | 3.118 | 3880 | 318.0 |
| 8 | 3.58 | 3.426 | 4325 | 349.5 |
| 7 | 3.73 | 3.749 | 4812 | 382.4 |

There is obviously enough available energy to lift the warm water to interesting heights, even if its initial temperature is only 20°C (68°F) when 4°C (40°F) cold water is available to establish the final temperature. Figure 2 may also be read to give the temperature vs height relationship of the flow in the duct. Of particular interest is the fact that the first few degrees of temperature drop give very little lift. The practical consequence of this fact is that the first part of the expansion may be taken isenthalpically with very little loss in available energy for the purpose of quickly establishing a state with sufficient volume of steam to suspend and separate the water droplets, and to lift them against gravity.

The end state temperature is determined by the ratio of the flows of cold and warm water to the system, and is very nearly equal to the weighted mean temperature.

$$T_{end} = \frac{\dot{M}_{warm}\, T_{warm} + \dot{M}_{cold}\, T_{cold}}{\dot{M}_{warm} + \dot{M}_{cold}}$$

where $\dot{M}...$ is the corresponding mass flux. Lower end state temperatures give more lift, but require more cold water, and more duct exit area. Cold to warm ratios in the range of 1.0 to 2.0 seem to lead to reasonable designs.

## Mist Formation and Transport

At the bottom of the duct the water is injected as a mist of fine droplets. The spray head that forms this mist must be so designed that the droplets are sufficiently small to achieve good mechanical and thermal coupling with the steam without requiring excessive pressure drops for operation, or being too subject to clogging by the microscopic life that escapes the prefilter. Stokes law predicts that a .2 mm dia droplet will fall about 2m/sec in the low pressure steam, and the fall velocity decreases as the square with smaller diameters. If the upward steam velocity is chosen to be 20 m/s, a 2 m/s slip does not lead to excessive slip losses. For this application the most economical in energy method of preparing .2 mm diameter droplets is to have a set of orifices about .1 mm dia out of which jets of water issue. Rayleigh has shown that such a jet is always unstable, and the wavelength of maximum instability is about 4.5 diameters. Jet breakup with this wavelength implies a droplet radius about 1.9 times the radius of the jet. The theory agrees quite well with experiment (3). Small satellite drops also appear when the breakup of the stream is random. Nozzles have been vibrated to make the breakup of the jet regular, and the drops thus produced used in ink jet printers, microproportioners, and research on droplet combustion.

For the spray head of this power plant, we need a multiplicity of .01 cm dia orifices spaced on about .1 cm centers. The viscous friction in such a nozzle will not be too serious, corresponding to a loss of about 1 meter of water head at a jet velocity of 20 m/s.

The water is injected into the duct at an appreciable velocity, which might be the same as the exit velocity at the top of the duct. As the water emerges into the low pressure space it will evaporate steam from

its surface at a rate proportional to the amount the saturation temperature corresponding to the ambient pressure is below the water temperature and which will diminish as the droplet cools to the saturation temperature. A characteristic time, in which 77 percent of the possible heat flow takes place, for this process (for 0.02 cm dia water droplets) is .007 sec. If the ambient pressure corresponds to 18°C saturation temperature, and the injection temperature is 20°C, 200 volumes of steam are generated for each volume of injected water in .007 seconds, and this steam can fill the duct if its area is 1/10 the exit area. The distance progressed by the droplets is 14 cm before the duct is filled. In that initial region there will be some eddies set up around each entering jet but they will not absorb much energy from the jets. A rough calculation based on water jet driven convection cells in the stagnant steam next to the orifice plate with cylindrical Hagen-Poiseuille flow in each cell predicts an energy loss corresponding to about .04 meters of water gravity head. As the flow proceeds up the duct it diverges, with more steam evaporating from the droplets to lift them upward, and to keep them separate.

In order to achieve efficient operation, the sensible heat in the core of the droplet must flow rapidly to the surface to provide the necessary heat of evaporation without requiring a large temperature differential. Consider first a steady state in which the surface of the drop is being reduced in temperature at a constant rate and inquire what is the temperature difference between the center and the surface. The steady state assumption makes the rate of change of temperature the same throughout the volume, and the heat flow equation,

$$k\nabla^2 T = \rho c_p (\partial T/\partial t),$$

reduces to Poisson's equation with constant source strength throughout the spherical droplet. The solution is:

$$T - T_o = \frac{\dot{T}_s r^2}{6D}$$

where T is the temperature, $T_o$ the center temperature, $\dot{T}_s$ the rate of change of surface temperature, and D the diffusion coefficient for heat. For r = .01 cm, $D = 1.4 \times 10^{-3}$ cm$^2$/sec, and $\dot{T}_s = 4$°C/sec, $T - T_o = .05$°C, a negligible quantity. We also ask what the response to a sudden change in surface temperature will be, as will occur during the injection of the water into a lower pressure area.

The transient solution of the heat flow problem for a sphere given by Williamson and Adams, Phys. Rev., 14, 99 (1919), and quoted in Handbook of Physics, Condon and Odishaw, McGraw-Hill, New York, is plotted in Figure 3 for a .01 cm radius water droplet. The 7 millisecond distribution was integrated over the droplet, and it was learned that 77 percent of the initial heat had left the droplet. Thus if the droplets are small enough for good mechanical coupling, the heat transfer is extremely good.

Estimated performance of the system is given in Table 4 for several ocean surface temperatures. Reasonable allowances have been made for spray nozzle friction, duct exit loss, and the power needed to drive the cold water pump and the noncondensible pump.

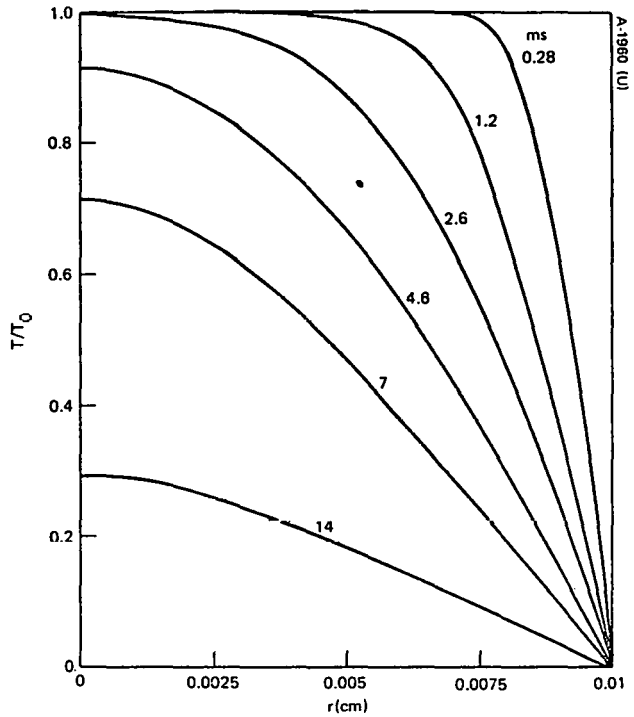



Figure 3. Cooling of a 0.01 cm Radius Water Droplet (Initial Temperature = $T_0$, Surface Temperature = 0)

Table 4. Overall Performance Predictions

| | | | |
|---|---|---|---|
| Initial Temperature | 20°C | 25°C | 30°C |
| Final Temperature | 8°C | 10.5°C | 12°C |
| Theoretical Head (m) | 89.3 | 153 | 232 |
| Losses: (m) | | | |
| a) Droplet Slip | 8.9 | 15 | 23 |
| b) Exit Kinetic Energy (m) | 20 | 20 | 20 |
| c) Cold Water Pump (m) | 10 | 10 | 10 |
| d) Nozzle Friction (m) | 2 | 2 | 2 |
| e) Noncondensible Pump (m) | 4 | 4 | 4 |
| Net Head Available for Turbine | 44 | 102 | 173 |
| X .85 Turbine Efficiency (m) | 37 | 87 | 147 |
| Power/Unit Exit Area (kW/m$^2$) | 3.32 | 6.6 | 9.9 |
| Exit Diameter (10MW)(m) | 62 | 44 | 36 |
| Warm Water Flow (M$^3$/sec) | 27.6 | 11.7 | 6.9 |
| Cold Water Flow (M$^3$/sec) | 59.4 | 25.7 | 15.1 |

Bibliography

1. rl J. Beck, "Ocean Thermal Gradient Hydraulic wer Plant," Science, 189, 293, July 25, 1975.

2. Clarence Zener and John Fetkovich, "Foam Solar Sea Power Plant," Science, 189, 294, July 25, 1975.

3. Charles D. Hendricks, "Micron and Submicron Particle Production," IEEE Transactions on Industry Applications, IA-10, 4, 1974.

## DISCUSSION

ALEXIOU (Office of Sea Grant): The small holes through which you create the jets look like a nice place for fouling. Have you given any thought to a method for keeping those clean?

RIDGWAY: Yes. Our intention was to provide, upstream of these holes, a sand-type filter as is used in municipal water supplies, so that the things that would cause fouling and the obstruction of the hole would be removed beforehand, and this filter would be flushed and/or replaced on a regular basis. We would also expect that the nozzles would erode and get bigger, and provisions would have to be made for their replacement or repair.

DUGGER (APL/JHU): What about the pressure drop and the power required to drive this system with the sand filter and all?

RIDGWAY: The pressure drop seems to be equivalent to two or three meters head of warm water and we have, at least for the 25°C case, approximately 100 meters of head to play with.

THIS PAGE

WAS INTENTIONALLY

LEFT BLANK

# IX. WORKING GROUP REPORTS

THIS PAGE

WAS INTENTIONALLY

LEFT BLANK

# REPORT OF THE WORKING GROUP ON TOTAL SYSTEMS

ABRAHIM LAVI, CHAIRMAN

During the discussion period the meeting was chaired by Dr. Abrahim Lavi. The meeting was then turned over to Dr. Bennett Silverstein who chaired the meeting during the preparation of the recommendations.

The major concern of the working group was that the OTEC program was insufficiently systems oriented. From the program inception several years ago it has consisted primarily of theoretical studies of the OTEC plant and research on specific components. This approach was adequate then. However, now that the program has gained greater acceptance and is starting to expand more rapidly, increased emphasis on management of the total system will be required. The OTEC office has been and continues to be woefully understaffed, with inadequate inhouse capability.

It was agreed that OTEC has great promise for the future. It is a complex system and it has not as yet been proven that OTEC will provide an economical source of renewable energy. The presently outlined pilot plant demonstration programs should have the objective of providing that proof.

The following recommendations were made:

o ERDA should establish an OTEC project office, with a strong staff to properly manage the technical and programmatical aspects of the program.

o Prepare a meaningful long range plan for the orderly commercial development of OTEC systems. It should have considerable detail for the near term and include clear cut objectives and goals, go no-go criteria, financial budgets, and planned involvement of industry.

o A special effort should be made to encourage the involvement of private industry at an early date with emphasis on gaining program acceptance from the ultimate users of OTEC energy.

o As the program moves into the phase where builders of platforms and manufacturers of equipment are drawn in, it becomes a matter of major importance that these many efforts are properly coordinated. One method of achieving this is by placing responsibility for major systems development in the hands of a few contractors, whose efforts will be controlled and directed by a strong ERDA program office.

o ERDA should ensure that all the right questions have been asked, and answers obtained. This is necessary to establish program credibility.

o Concentrate greater resources on the evaluation of the open cycle OTEC plant.

# REPORT OF THE WORKING GROUP ON MISSION ANALYSIS

ROBERT COHEN, CHAIRMAN

The working group agreed to limit their deliberations to issues, conclusions and recommendations related to OTEC missions. It was subsequently agreed that the conclusions and associated recommendations of the working group be presented to the full OTEC workshop without specific ranking as to priority or importance. There were no minority reports, although specific conclusions and recommendations received differing degrees of support. All of the conclusions and recommendations, therefore, reflect the consensus of the full working group on Mission Analysis.

Conclusions

o Parallel paths of OTEC development will significantly increase the probability of success and decrease the possibility the program will fail.

o Parallel paths with a diversity of applications are extremely important if the OTEC program is to be a commercial success in this century.

o There are insufficient funds in the ERDA FY '78 Budget Request.

o There is an urgent need to clarify the legal status of OTEC systems.

o The OTEC mission is to create a "substantial impact" in new energy production, yet the ERDA/OTEC plan ends with a 100 $MW_e$ demonstration.

o There is insufficient published information on OTEC market potential to attract commercial interests.

o Lack of Federal Agency interactions has hampered successful total exploration of OTEC technological potential.

o The public does not adequately understand OTEC.

o In the absence of an OTEC systems integrator, many institutional constraints may not be addressed adequately.

o Inadequate attention has been given to the international applications of OTEC.

o A sufficiently rigorous risk-benefit analysis does not exist.

Recommendations

o Increased funding for OTEC to permit parallel paths development consistent with risk-benefit criteria.

o The OTEC FY '78 budget authority should be at a level to contract for parallel application pilot plants.

o The status of OTEC platforms as vessels should be established.

o The ERDA/OTEC planning process should incorporate the needs of commercialization to achieve a "substantial impact" in new energy production.

o Market analysis should be strengthened and should specifically include parallel applications, product options, and an "OTEC energy island" concept.

o Strong interagency and intraagency liaison be established to support full development of OTEC potential.

o Strengthening of OTEC public information transfer through films, brochures, displays, etc., as soon as possible.

o The OTEC program should obtain a systems

integrator now.

o ERDA obtain and disseminate information on international applications of OTEC.

o ERDA should support risk-benefit analysis of OTEC options.

# REPORT OF THE WORKING GROUP ON ENVIRONMENTAL AND SITING CONSIDERATIONS

LLOYD LEWIS, CHAIRMAN

The discussion of the working group focused mainly on four issues. Recommendations to ERDA were made in each area.

1. Design

o Further conceptual design study of 100 MWe size units is needed in consideration of more detailed environmental data.

o It is premature to plan site specific environmental measurements in light of present plant design uncertainties.

o There is need for actual design engineer's (i.e., system contractor's) oceanographic data requirements in order to focus expensive environmental measurement programs.

o The far-field environmental effects of the potential deployment of large number of commercial OTEC's in a basin like the Gulf of Mexico should not be overlooked (i.e., more effort on far-field models).

o Serious consideration should be given to instrumenting EOTP-1 (and EOTP-5) for environmental and effects measurements (e.g., temperature, currents, biological, weather, etc.).

o ERDA should examine the possibility of evaluating the marine biota entrainment problem during EOTP-1 (and EOTP-5) exercises.

o ERDA should ensure that EOTP-1 (and EOTP-5) has meteorological station on board during operations.

2. Siting

o ERDA should reach a site selection decision on EOTP-1 as soon as possible so that appropriate site dependent design issues can be resolved.

o Resolution of the Law-of-the-Sea issue is required with regard to near term OTEC supported marine measurements/research and placement.

o A site selection committee with technical, economic, environmental, and political input is preferred to site selection based on political considerations only.

3. Data Files

o Recently acquired oceanographic data not now in the NOAA archives should be collected and cataloged.

o ERDA might be better off studying the entire (deep water) Gulf of Mexico rather than those track lines indicated to obtain a comprehensive data base.

o Some duplication of effort is evident in ERDA's thermal resource data file assembly.

o ERDA should solicit the requirements of OTEC data users in defining the format and content of its OTEC data files.

o Consideration should be given to establishing a data file for engineering, biofouling, corrosion, etc., study and measurement results.

4. Measurement

o Early emphasis to the acquisition of ocean current data is justified.

o ERDA should augment any currents measurement program with hydrodynamical numerical

modeling to reduce costs and improve reliability of

t ogram.

o The usefulness of additional "paper studies" of thermal resource is questioned. It is better to proceed with actual measurements immediately.

# REPORT OF THE WORKING GROUP ON OCEAN ENGINEERING

EUGENE SILVA, CHAIRMAN

The following topics were discussed during this session:

- o Platform Selection
- o Cold Water Pipes
- o Positioning
- o Internal Flow
- o Transmission
- o Siting Considerations
- o Other Ocean Engineering Matters

As a result of these deliberations, the following conclusions and recommendations were formulated by the Ocean Engineering Working Group.

OTEC Program: The working group participants found that the OTEC Program approach to ocean engineering was acceptable.

Mission and Timing: There is a need for guidance on OTEC component sizes and missions as a function of time or Program phasing. As component size and reliability demands increase, engineering approaches and data requirements will have to be varied.

Platform Selection: Platform options should be limited as soon as possible. Early hull selection is required to allow sufficient time for platform performance optimization. The Working Group agreed that platform selection should be made by considering the platform and cold water pipe (CWP) as a system. Isolated selection of either these components could lead to poor composite performance.

Site Information: There is a need for definitive site data. The criteria produced by considering "a region around the world between 20°N and 20°S" are reaching the limits of their utility. Site specific environmental data should include, as a minimum, current profiles, water chemistry information, diurnal/seasonal variations, biological threats, and seafloor characteristics.

New or Improved Design Methodology: With only two exceptions, it was the opinion of the group that existing or soon to be available ocean engineering design methods are sufficient for OTEC design. The exceptions were: (1) umbilical and transmission cable design, and (2) some of the dynamic aspects of cold water pipe and internal flow interaction.

Experiments: Anchor and mooring model tests are required. Large scale tests will be required to ensure the applicability of existing results to OTEC-sized applications. OTEC-1 is recommended as a mooring experiment platform.

There is also a need for experiments dealing with flow behavior in cold water pipes with pronounced elastic properties. Spirited discussion among the Working Group members indicated a need for empirical resolution of some of the controversial items.

Area Studies: The following areas were identified as requiring early study:

OTEC as a vessel class: In the opinion of the legal advisors, should OTEC platforms be "ships" or "facilities"? This will have a direct bearing on the ocean engineering design approach.

Mooring lines and termination: The need for ng lines and terminations designed to withstand OTEC plant loads was identified. Specialized deck machinery is considered a part of this area.

Intake shapes: As an early part of OTEC internal flow investigations. Is it considered important that intake designs be evolved. The shape and size of the intakes could have a major impact on CWP handling system design and hull configuration.

Seawater materials performance data: If nonmetallics are to be used for OTEC construction, there is a need for long term performance data on these materials in seawater environments. The body of data on materials such as plastics or lightweight concrete for long term service at depth is not comparable with information on metal performance.

# REPORT OF THE WORKING GROUP ON HEAT EXCHANGERS

NORMAN SATHER, CHAIRMAN

The Working Group on Heat Exchangers met to discuss the ERDA-sponsored program for development of heat exchangers for OTEC power plants. A wide range of topics was covered, most of which had to do with ways of improving the effectiveness of the current effort. At the close of the meeting an ad hoc committee was formed to set down in writing the various recommendations that came forth during the discussion. A statement of these recommendations follows:

o Future ERDA-OTEC RFP's should be more clear in specifying objectives and requirements of work to be done than has been the case for RFP's recently issued. Furthermore, the evaluation of proposals submitted should be made on the basis of responsiveness to these objectives and requirements. The Source Evaluation Board should be briefed on RFP objectives and requirements, and their concurrence should be obtained prior to issuing RFP's.

o The reasons for the program to procure 1 MWe heat exchangers should be clarified, and the 1 MWe heat exchanger test program objectives should be defined more explicitly.

o An effort should be made to more closely coordinate the heat exchanger development and biofouling and corrosion programs, and a procedure for timely exchange of results should be established to promote better coordination. It is further recommended that future OTEC meetings not have concurrent sessions on heat transfer and biofouling/corrosion, so that interested persons can participate in sessions in both areas. It is also recommended that a session on the effects of biofouling on methods for water-side heat-transfer enhancement should be held at the Biofouling/Corrosion Conference in the Fall of 1977.

o The structural and fabrication aspects of heat exchanger and system design should be examined as soon as possible in order to ensure that cost, safety and vessel (hull) certification requirements can be met in future OTEC plant designs.

o The effects of platform/sea interactions on heat exchanger performance should be investigated. The heat exchanger development program should then be modified, as appropriate, to reflect the results of this investigation. Land-based test programs should be designed to investigate effects of heat exchanger orientation on performance.

o More complete dissemination of heat exchanger design information should be encouraged.

o The experience of the Office of Saline Water should be reexamined for useful information on the cost effectiveness of enhanced vs. non-enhanced heat transfer surfaces.

# REPORT OF THE WORKING GROUP ON BIOFOULING AND CORROSION

LYLE PERRIGO, CHAIRMAN

Working Group 4 divided its time between discussion of mechanical cleaning of OTEC heat exchangers and identification of needed future research and emphasis in biofouling and corrosion. The discussion of mechanical cleaning was an outgrowth of presentations, questions and comments during the previous day's technical sessions on biofouling and corrosion problems, projects and plans.

Mechanical Cleaning - Most of the audience of over 50 people were involved in discussing the pros and cons of two mechanical cleaning processes. Of substantial benefit to the discussions were the questions raised by Dr. A. F. Conn, Hydronautics Corporation. The questions were an outgrowth of Dr. Conn's ERDA sponsored project on mechanical and chemical cleaning of OTEC heat exchangers. Representatives from two organizations that manufacture and market mechanical cleaning systems participated in the discussions and provided additional background information on cleaning processes. Major points of discussion included:

o The need with both cleaning processes for efficient screening for process effectiveness.

o The possibility that repetitive mechanical cleaning might remove protective oxide films from tubing materials, especially aluminum. Many in the group believed that this would not be a problem.

o The pressure drop penalties that would result from use of either process as now designed. However, design modification might overcome the problem.

o The need for more seawater experience with both cleaning processes.

o The need to modify or adjust both processes to clean heat exchangers with enhanced surfaces.

Other Points of Discussion - Other major points of discussion were:

o The need to acquire biofouling and corrosion data in cold deep water that will be used to condense the OTEC working fluid. Some participants believed there would be biofouling problems while others indicated the problem would be minimal or nonexistent. The possibilities of calcareous deposits and increased corrosion of aluminum were raised. There was general consensus that little was known about the cold water environment that will be encountered in OTEC and that work in this area should be emphasized.

o The desirability of having a modular heat exchanger on OTEC-1 (EOTP/HMB-1) so different materials and cleaning conditions could be evaluated rapidly. This might be possible with separate water boxes on the same heat exchanger.

o The need for better communications with other parts of the OTEC community was mentioned on several occasions by people involved in biofouling and corrosion work and by those with primary interests in other OTEC areas. Each area must know of progress and problems in other areas so that realistic planning and development work can be undertaken.

General Comments - Focusing on definite technical problems was a useful method of:
(1) broadening the understanding of the biofouling

and corrosion effort, and (2) eliciting valuable inputs that can have a beneficial impact on the program.

# REPORT OF THE WORKING GROUP ON MODELING AND OPTIMIZATION

RICHARD LYON, CHAIRMAN

The session started with a discussion of the bounds to be covered by the model or models. Some participants believed that separate models should be developed for the individual components, since this would reduce the number of variables in any optimization. Others argued that since the criterion should be the delivered cost of the product, realistic optimization would only be possible if the entire system was included in the model used for that optimization. Still others, while agreeing with the latter point of view, believed that there would probably be little interaction between the method of power generation and the system for product modification (conversion for AC to DC or vice versa, or production of some energy-intensive product) and product delivery and, therefore, separate models could be developed for these two systems. At least one participant argued against the need and usefulness of an optimizing program.

It ultimately became clear that thinking on the scope of the model, and on just what optimization consists of, would not coalesce into one or two opinions in the time available to the working group. The subject was then shifted to the types of information needed in modeling and to the need for adequate dissemination.

Without obvious dissent, the group concluded that a Data Book is needed to reduce duplication and to provide a better understanding by participants in the OTEC program on the milieu into which their work fits.

After some discussion, it was agreed that the Data Book could be divided into four general sections: Disciplines, Concepts or Systems, Components and Processes, and Safety.

I. DISCIPLINES

- o Heat Transfer
- o Fluid Mechanics
- o Corrosion
- o Biofouling
- o Thermodynamics
- o Instrumentation and Control
- o Properties of Materials, Seawater, and Working Fluids
- o Techniques for Optimization (including subroutines)

II. CONCEPTS AND SYSTEMS

A. Power Production

Claude, closed Rankine, vapor-lift, etc.

B. Ocean Systems

Hulls, anchoring or positioning systems, seawater delivery and disposal systems

C. Product Modification and Delivery

Electricity, hydrogen, ammonia, aluminum, U-235, etc.

The current variations of each concept would be described in enough detail to show its basic principles, obvious merits, constraints and restrictions on other systems (e.g., hull-power system interrelationships), and other recognized difficulties (components needing development, needed data, etc.).

This section would also include a description

and subroutines, if available, of mathematical models for concepts and systems of combined concepts, and it would present published capital and power cost estimates if available.

III. COMPONENTS AND PROCESSES

- o Evaporators
- o condensers
- o pumps
- o turbines
- o hulls (construction, as opposed to shape)
- o screens and filters
- o piping

In each case, the description would include:

Function

Design Approaches

Mathematical Models, and available Subroutines

Optimization Methods

Construction Methods

Transportation, Installation or Deployment

Quality Control

Reliability

Maintenance and Cleaning

Costs (construction, transportation, and installation)

IV. SAFETY

This subject was not discussed in any detail, but it was believed to be important enough to be a separate section in the Data Book. Presumably, it would cover both marine safety and plant safety problems.

Environmental problems were not discussed, perhaps because of the concurrent Environmental and Siting Workshop. Somewhere also the Data Book should include personnel maintenance.

The group agreed that an effective way to implement the development of the Data Book would be to establish a Central Working Committee and a broader Advisory Panel. Broad representation on the Committee and the Panel, both in discipline and from among active OTEC groups, will promote cooperation in acquiring input and will assist acceptance of the data in the book. The Central Committee or at least its Chairman should not be related to groups that champion particular concepts.

It was suggested and agreed that the Data Book be in loose-leaf form for easy piecemeal updating and expansion.

It was also agreed that the Data Book need not be complete at its first issue, but should be small at first in order to expedite its issuance. It would then expand as it was updated.

ERDA's Technical Information Center, which is in Oak Ridge, appears to be the logical agency for producing and distributing the Data Book and the updating material.

Gilbert, in its coordinating function for OTEC, appears to be a reasonable point for receiving input for the Data Book, if such a point is needed in addition to the Central Committee, its Chairman, and its Editor (who might be the Chairman).

# REPORT OF THE WORKING GROUP ON REPORTING AND INFORMATION DISSEMINATION

STEVE GRIFFITH, CHAIRMAN

The working group decided to limit the discussion to two items: Contractor Reporting Requirements and Information Dissemination.

A general discussion was held on the types and availability of printed material that deal with the OTEC Program. A display of various reports and brochures was presented to acquaint the participants with the current material. A handout was also provided to allow interested persons to be placed on the OTEC mailing list and receive the OTEC Program Summary Report.

Mr. Griffith made a brief presentation on the new ERDA Contractor Reporting Requirements currently being developed. This consisted of a review of the development of the OTEC Program from NSF days, a discussion of the current reporting requirements and plans for the future.

During the presentation, questions were answered and comments noted. After the presentation, a general discussion was held. This discussion addressed the current problems which the OTEC Program is facing in the way of information dissemination. As a result of the discussion, the following recommendations were drafted by the working group.

- o Trying to obtain information and/or reports through NTIS and TIC is a lengthy process. There is a need to standardize and implement report dissemination procedures to allow for the distribution of technical and programmatic information to ERDA contractors and the general interest groups.
- o In order to provide information of a general nature about the OTEC Program and to attempt to keep interest at a high peak, the possibility of an OTEC Newsletter should be explored. The implementation of a newsletter could be handled in several ways:
  - o Management and control by in-house resources at the ERDA Solar Division or OTEC Branch level.
  - o Management and control by a private resource or other government agency in conjunction with ERDA personnel. Support in the form of a grant to be provided from the ERDA Solar budget.
  - o Management and control by a private resource or government agency on a volunteer basis.
- o There is a need to begin development of a data-base for the OTEC Program. Currently, no basis exists which enables OTEC personnel to make comparisons between material which has been or is being developed by OTEC contractors. This data base would provide a valuable tool to assist OTEC managers and planners in directing and controlling the Program. (Editor: See Report of the Working Group on Modeling & Optimization.)

# LIST OF ATTENDEES

# FOURTH OTEC CONFERENCE

COORDINATORS

David F. Mayer
Department of Mathematics
University of New Orleans
New Orleans, La. 70122
(504) 283-0331

George E. Ioup
Department of Physics
University of New Orleans
New Orleans, La. 70122
(504) 283-0341

---

James H. Abbott
Dept. of Mathematics
University of New Orleans
New Orleans, La. 70122
(504) 283-0331

Arthur G. Alexiou
DOC/NOAA
Office of Sea Grant
3300 Whitehaven, N. W.
Washington, D. C. 20235

James H. Allender
Energy & Environmental Systems Div.
Argonne National Laboratory
9700 S. Cass Avenue
Argonne, Ill. 60439

Julie Ambler
Dept. of Oceanography
Oregon State University
Corvallis, OR. 97331

James H. Anderson, Jr.
Sea Solar Power, Inc.
2422 S. Queen Street
York, PA. 17402
(717) 741-0884

David Aronson
D. Aronson Associates
9 Riverview Drive West
Upper Montclair, N. J. 07043

J. Michael Atturio
Civil Engineering Lab.
U.S. Naval Construction Battalion Center
Port Hueneme, CA. 93043

Donald K. Atwood
NOAA/AOML
15 Rickenbacker Cswy.
Miami, FL. 33149

William H. Avery
Applied Physics Lab.
The Johns Hopkins University
Johns Hopkins Road
Laurel, MD. 20810

J. M. Ballinger
Sun Shipbuilding & Dry Dock Co.
Foot of Morton Avenue
Chester, PA. 19013
(215) 876-9121

David Bankston, Jr.
School of Engineering
University of New Orleans
New Orleans, La. 70122
(504) 283-0327

E. F. Barkman
Reynolds Metal Company
4th & Canal Streets
Richmond, VA. 23261

Roderick Barr
Hydronautics, Inc.
7210 Pindell School Road
Laurel, MD. 20810
(301) 776-7454

Robert Barratt
Foster Wheeler
15 Slope Drive
Cedar Knolls, N. J. 07927

Gregory B. Barthold
Alcoa
1200 18th Street, N. W.
Washington, D. C. 20036

Nedret S. Basar
M. Rosenblatt & Son, Inc.
350 Broadway
New York, N. Y. 10013

Karl H. Bathen
343 Mamaki Street
Honolulu, HI. 96821

Earl J. Beck
Design Services
998 Church Street No.27
Ventura, CA. 93001

E. L. Beeson
Dept. of Physics
University of New Orleans
New Orleans, La. 70122
(504) 283-0341

Kenneth J. Bell
Oklahoma State University
Stillwater, Okla. 74074

Bryn Beorse
Sea Water Conversion Lab.
University of California
1301 S. 46th Street
Richmond, CA. 94804

Ronald Berg
Gilbert Associates
1828 L Street, N.W., No.1201
Washington, D. C. 20036

N. Neil Berger
Lockheed Missiles & Space Co.
B/150 0/57-28
P. O. Box 504
Sunnyvale, CA. 94088

Clyde J. Bergeron, Jr.
Dept. of Physics
University of New Orleans
New Orleans, La. 70122
(504) 283-0341

Arthur Bergles
Dept. of Mechanical Engineering
Iowa State University
Ames, Iowa 50011

James Bernhisel
2127 Hyde Street
San Francisco, CA. 94109

L. F. Berridge
Dept. of Physics
Carnegie-Mellon University
Box 176
Pittsburgh, PA. 15213

Robert A. Bonewitz
Alcoa Laboratories
Alcoa Center, PA. 15232

Juan Bonnet
Puerto Rico Water Resources Authority
Box 4267
San Juan, P. R. 00936

Jack M. Booth
[illegible] Enterprises
[illegible] Avenue of the Americas
New York, N. Y. 10020
(212) 398-3754

John Braswell
Naval Coastal Systems Lab.
Panama City, Fla. 32407

Charles L Bretschneider
Dept. of Ocean Engineering
University of Hawaii
2565 The Mall
Honolulu, HI. 96822
(808) 533-6412

Edward M. Briggs
Southwest Research Institute
8500 Culebra Road
San Antonio, Tx. 78284

Dennis Brining
Lockheed Center for Marine Research
6350 Yarrow Drive
Carlsbad, CA. 92008

A. F. Brown
Route 4, Box 90W
Folsom, La. 70437

Denny F. Brown
Lorelei Corp.
P. O. Box 861
Gaitherburg, MD. 20760
(301) 840-1180

M. J. Brunner
General Electric Co.
1247 Berwyn Paoli Road
Berwyn, PA. 19312

Jon Buck
Giannotti & Buck Associates, Inc.
5711 Sarvice Ave., Suite 402
Riverdale, MD. 20852

David C. Burton
Gilbert/Commonwealth Companies
P. O. Box 1498
Reading, PA. 19603

V. J. Castelli
David W. Taylor Naval Ship R&D Center
Annapolis Laboratory
Annapolis, MD. 21462

Franklin K. H. Ching
Vought Corporation
P. O. Box 38
Moffett Field, CA. 94035

Ivan Chow
University of Florida
280-3 Corry Village
Gainesville, Fla. 32603

Philip Chow
Ty Lin International
315 Bay Street
San Francisco, CA. 94133

James Churgin
U.S. Dept. of Commerce
NOAA/Environmental Data Service
Washington, D.C. 20235

R. Michael Clancy
Science Applications, Inc.
8400 W. Park Avenue
McLean, VA. 22101

H. W. Clark
Honeywell, Inc.
5303 Shilshole Avenue
Seattle, WA. 98107

Joseph G. Cocchiara, Jr.
La. Offshore Terminal Authority
1130 ITM Bldg.
New Orleans, La. 70130
(504) 568-4678

Robert Cohen
ERDA
20 Massachusetts Ave. N.W.
Washington, D. C. 20545

Heyward H. Coleman
Southern Natural Gas Co.
P. O. Box 2563
Birmingham, AL. 35202

Melvin Colen
Avondale Shipyards
P. O. Box 50280
New Orleans, La. 70150

Paul E. Condon
University of California,Irvine
Dept. of Physics
Irvine, Calif. 92717

Andrew F. Conn
Hydronautics, Inc.
Pindell School Road
Laurel, MD. 20810

Raul J. Conti
Lockheed
3251 Hanover Street
Palo Alto, Calif. 94304

H. Lee Craig, Jr.
University of Miami
4600 Rickenbacker Cswy.
Miami, FL. 33149

James E. Crews
Florida Power Corp.
P. O. Box 14042
St. Petersburg, FL. 33733

Michael Cuming
Meteorology International, Inc.
205 Montecito Avenue
Monterey, CA. 93940

George Cypher
INCRA
825 Third Avenue
New York, N. Y. 10022

A. M. Czikk
Linde Division
Union Carbide Corporation
P. O. Box 44
Tonawanda, N. Y. 14150
(716) 877-1600

Caleb F. Davis
School of Engineering
University of New Orleans
New Orleans, La. 70122
(504) 283-0327

F. H. Davis
Globe Engineering Company
222 No. Dearborn Street
Chicago, ILL. 60601

Ralph M. Davison
Climax Molybdenum Company
3072 One Oliver Plaza
Pittsburgh, PA. 15222

Bruce E. Dawson
Foster Wheeler Corporation
110 South Orange Avenue
Livingston, N. J. 07039

John DePalma
U.S. Naval Oceanographic Office
2408 Shadyside Lane
Picayune, MS. 39466

Vito A. DePalma
Calspan Corporation
P. O. Box 235
Buffalo, N. Y. 14221

John D. Ditmars
Energy & Environmental Systems Div.
Argonne National Laboratory
9700 S. Cass Avenue
Argonne, ILL. 60439

L. K. Donovan
NAVFACENGCOM
8709 Prudence Drive
Annandale, VA. 22003
(202) 325-0505

R. H. Douglass
TRW DSSG
One Space Park R4/1198
Redondo Beach, CA. 90278
(213) 535-2446

Sue Dube
New Orleans City Planning Commission
City Hall Room 9W
New Orleans, La. 70112

G. L. Dugger
APL/Johns Hopkins University
Johns Hopkins Road
Laurel, MD. 20810
(301) 953-7100

Wilfred M. Dukes
Bell Aerospace Textron
P. O. Box 29307
New Orleans, La. 70189

Nancy Dunn
Dept. of Mathematics
University of New Orleans
New Orleans, La. 70122
(504) 283-0331

Harry Efferen
General Dynamics
Quincy Shipbuilding Division
97 E. Howard Street
Quincy, Mass. 02169

Gary G. Erickson
Ship Systems, Inc.
11750 Sorrento Valley Road
San Diego, CA. 92121

Orde R. Evans
ERDA
20 Massachusetts Ave., N.W.
Washington, D. C. 20545

R. W. Falconer
Mechanics Research, Inc.
2500 Colorado Ave.
Santa Monica, CA. 90406

Raymond D. Feldwick
Teledyne Energy Systems
110 W. Timonium Road
Timonium, MD. 21097
(301) 252-8220

John G. Fetkovich
Dept. of Physics
Carnegie-Mellon University
Schenley Park
Pittsburgh, PA. 15213

William H. Fischer
Gilbert Associates, Inc.
P. O. Box 1498
Reading, PA. 19603

Bryant Fitch
Carnegie-Mellon University
Schenley Park
Pittsburgh, PA. 15213

Joe R. Foote
Dept. of Mathematics
University of New Orleans
New Orleans, La. 70122
(504) 283-0331

E. J. Francis
APL/Johns Hopkins University
Johns Hopkins Road
Laurel, MD. 20810

Ivan A. Franson
TIMET
P. O. Box 2824
Pittsburgh, PA. 15230

Charles A. Frenzel
Coastal Science Associates
6900 Canal Blvd.
New Orleans, La. 70124

Lydia M. Frenzel
Dept. of Chemistry
University of New Orleans
New Orleans, La. 70122
(504) 283-0311

H. D. Fricke
Linde Division
Union Carbide Corporation
P. O. Box 44
Tonawanda, N. Y. 14150

Allen B. Fritsch
David Taylor Naval Ship R&D Center
Code 2745
Annapolis, MD. 21042

Roger Fuller
Lockheed Missiles & Space Co.
P. O. Box 504
Sunnyvale, CA. 94088

E. Ganic
Linde Division
Union Carbide Corporation
P. O. Box 44
Tonawanda, N. Y. 14150

C. J. Garrison
Naval Postgraduate School
Monterey, CA. 93940

George Giangrande
AC Transformer Corporation
89 Madison Street
Newark, N. J. 07105

Steven Giannino
F. R. Harris, Inc.
1828 L Street, N.W.
Washington, D. C. 20036

W. W. Goode, Jr.
Florida Energy Office
108 Collins Building
Tallahassee, FL. 32304

Chris Gottzmann
Union Carbide Corporation
P. O. Box 44
Tonawanda, N. Y. 14150

Robert H. Gray
Battelle, Pacific Northwest Labs.
Battelle Blvd.
Richland, WA. 99352

Larry Green
McDermott-Hudson Engineering
Box 36100
Houston, TX. 77036
(713) 782-4400

Derek P. Gregory
Institute of Gas Technology
3424 S. State Street
Chicago, ILL. 60616

Leroy Gresham
Chromalloy Natural Resources Corp.
P. O. Box 7036
Houma, La. 70361

Steven K. Griffith
Gilbert Associates
1828 L Street, N.W. Suite 1201
Washington, D. C. 20036
(202) 331-0252

Sigmund Gronich
ERDA, Division of Solar Energy
20 Massachusetts Avenue, N.W.
Washington, D. C. 20545

R. J. Haberski
Curtiss-Wright
One Passaic Street
Wood-Ridge, N. J. 07075

E. C. Haderlie
Dept. of Oceanography
Naval Postgraduate School
Monterey, CA. 93940

Hafez Haffezzadeh
University of Oklahoma
202 West Boyd
Norman, Okla. 73019

Dahlia Hagel
Hydronautics, Inc.
7210 Pindell School Road
Laurel, MD. 20810

George Hager
Times-Picayune Publishing Co.
3800 Howard Avenue
New Orleans, La. 70140

[illegible]am C. Hale, III
[illegible]rsity of Pennslyvania
[illegible]nergy Center
3221 Walnut Street
Philadelphia, PA. 19104

John Harding
NORDA/NSTL
Bay St. Louis, MS. 39520

Philip C. Hargraves
General Electric Company
777 14th Street, N.W.
Washington, D. C. 20005

Geoffrey K. Hart
DSS Engineers, Incorporated
7483 N.W. 4th Street
Ft. Lauderdale, FL. 33317

William Hartt
Florida Atlantic University
Boca Raton, FL. 33431

R. E. Hathaway
Colorado School of Mines
7630 Spring Drive
Boulder, Colo. 80303

L. G. Hauser
Westinghouse
Gateway Center
Pittsburgh, PA. 15668
(412) 255-3953

R. T. Hawley
Western Gear Corporation
2100 Norton Avenue
Everett, WA. 98202

Earl J. Hedrick
Urban Studies Institute
University of New Orleans
New Orleans, La. 70122
(504) 283-0277

Steve Hess
University of Miami
4600 Rickenbacker Cswy.
Miami, FL. 33149

Steven A. Hetyei
Carnegie-Mellon University
5819 Kentucky Avenue
Pittsburgh, PA. 15232

George Higgins
Dow Chemical
Building 566
Midland, Mich. 48640

Jules Hirshman
Tracor Marine, Inc.
P. O. Box 13114
Port Everglades, FL. 33316

John Hollett
Global Marine
4100 MacArthur
Newport Beach, CA. 92663

Duane T. Hove
Science Applications, Inc.
101 Continental Blvd.
El Segundo, CA. 90245
(213) 640-0480

H. E. Hurlburt
Jaycor
205 S. Whiting St., Suite 500
Alexandria, VA. 22304

Charles W. Hurter
Applied Physics Lab.
University of Washington
1013 N. E. 40th
Seattle, WA. 98105

Juliette Ioup
Physics Department
Xavier University
New Orleans, La. 70125

Al Isaacson
M. Rosenblatt & Son, Inc.
350 Broadway
New York, N. Y. 10013

Eva C. Jedruch
Dravo Corporation
One Oliver Plaza
Pittsburgh, PA. 15222
(412) 566-4975

Roy M. Jenevein
Computer Research Center
University of New Orleans
New Orleans, La. 70122
(504) 283-0347

James F. Jenkins
USN Civil Engineering Lab.
Port Hueneme, CA. 93043

Gerhard Jirka
Massachusetts Institute of Technology
MIT 48-315
Cambridge, Mass. 02139
(617) 253-1000

Alan Johnson
Dept. of Physics
University of New Orleans
New Orleans, La. 70122
(504) 283-0341

David W. Johnson
University of Oklahoma
202 West Boyd
Norman, Okla. 73019

James H. Jones
Natural Energy Laboratory of Hawaii
2540 Dole Street
Honolulu, HA. 96822
(808) 948-8745

David G. Jopling
Florida Power & Light Company
P. O. Box 013100
Miami, FL. 33133

C. T. Joy, Jr.
Lockheed Missiles & Space Company
P. O. Box 504, Bldg. 150,Dept.50-20
Sunnyvale, CA. 94088

David Juran
Van Houten Associates, Inc.
420 Lexington Ave.
New York, N. Y. 10017

John R. Justus
Congressional Research Service
Library of Congress
Washington, D. C. 20540

James A. Kelley
Kaiser Engineers
1844 ITM Building
New Orleans, La. 70130
(504) 523-4572

William Kern
Amertap Corporation
1501 Franklin Avenue
Mineola, N. Y. 11501

Edmund Kerut
NOAA Data Bouy Office
National Space Technology Labs.
Bay St. Louis, MS. 39529

G. M. Kikin
TRW DSSG
One Space Park R4/1198
Redondo Beach, CA. 90278

John Klein
Burns & Roe
185 Crossways Park Drive
Woodbury, N. Y. 11797

B. M. Klug
General Dynamics
7733 Forsyth
St. Louis, MO. 63105

H. Gary Knight
Louisiana State Univ. Law Center
Louisiana State University
Baton Rouge, La. 70803

James G. Knudsen
Office of Energy Research & Dev.
Oregon State University
Corvallis, OR. 97331

Alex Konopka
Institute of Gas Technology
3424 S. State Street
Chicago, ILL. 60616
(312) 567-3957

Prem K. Kulshrestha
Dept. of Mathematics
University of New Orleans
New Orleans, La. 70122
(504) 283-0331

Andy Kurtz
U. S. Navy
3312 Ardley Court
Falls Church, VA. 22041

Francis LaQue
Claridge House, Apt. 803
Claridge Drive
Verona, N. J. 07044

Clyde A. Laughlin
Honeywell, Inc.
5303 Shilshole Ave., N.W.
Seattle, WA. 98107

Abrahim Lavi
Division of Solar Energy
ERDA
20 Massachusetts Avenue, N.W.
Washington, D. C. 20545

Gay Heit Lavi
Carneigie-Mellon University
Pittsburgh, PA. 15213

C. D. Leedham
General Motors (Delco)
6767 Hollister Avenue
Goleta, CA. 93017

Donald Leonard
Computer Genetics Corporation
18 Lakeside Office Park
Wakefield, Mass. 01880

Robert D. Lessard
United Technologies Research Center
Silver Lane
E. Hartford, CT. 06108

John Lewis
Interstate Electronics
P. O. Box 3117
Anaheim, CA. 92803

Lloyd F. Lewis
ERDA/SOLAR
20 Massachusetts Avenue, N.W.
Washington, D. C. 20545

R. R. Leyendecker
Westinghouse Electric Corp.
Lester Branch,P.O.Box 9175
Philadelphis, PA. 19113

L. B. Lin
Jaycor
205 S. Whiting St.,Suite 500
Alexandria, VA. 22304

Baldur Lindal
DSS Engineers, Inc.
7483 Northwest 4th Street
Ft. Lauderdale, FL. 33317

Ray I. Lindberg
Reynolds Metals
Fourth & Canal Streets
Richmond, VA. 23261

Guy Linkous
Teledyne Energy Systems
110 Timonium Road
Timonium, MD. 21093

Mario V. Lipari
Value Engineering Co.
2550 Huntington Avenue
Alexandria, VA. 22303

Thomas E. Little
Westinghouse Electric Corp.
P. O. Box 1488
Annapolis, MD. 21404

Han Liu
Burns & Roe, Inc.
185 Crossway Park Drive
Woodbury, N. Y. 11797

James Lorenz
Argonne National Lab. Bldg.308
9700 S. Cass Avenue
Argonne, ILL. 60439

Jack Y. K. Lou
Ocean Engineering Program
Texas A & M University
College Station, TX. 77843

Richard Lyon
Oak Ridge National Laboratory
Box Y
Oak Ridge, Tenn. 37830

David Mager
Pacific Power & Protein, Inc.
1 Lincoln Plaza
New York, N. Y. 10023

L. M. Mahalingam
Carnegie Mellon University
Box 176
Pittsburgh, Pa. 15213

Ambrose F. Manikowski
Lockheed Missiles & Space Co.
P. O. Box 504, Dept.57-22, Bldg.150
Sunnyvale, Calif. 95014
(408) 742-2684

Jerold F. Mann
Sperry Systems Management
Great Neck, N. Y. 11020

Henry E. Markel, Jr.
New Orleans Public Service, Inc.
317 Baronne Street
New Orleans, La. 70112

Gregg Marland
Institute for Energy Analysis
Box 117
Oak Ridge, TN. 37830

Paul J. Martin
Science Applications, Inc.
8400 Westpark Drive
McLean, VA. 22101
(703) 821-4549

Paul J. Martineau
Ingalls Shipbuilding
P. O. Box 149
Pascagoula, MS. 39567

Rudy Martinez
Weed Instrument Co., Inc.
P. O. Box 549
Elgin, TX. 78621

Henry H. Marvin
Division of Solar Energy
ERDA
20 Massachusetts Avenue, N.W.
Washington, D. C. 20545

Frank S. Mathews
Colorado School of Mines
Dept. of Physics
Golden, Colo. 80401

James W. Mavor, Jr.
Woods Hole Oceanographic Institution
Woods Hole, Mass. 02543

George May
Sea Solar Power, Inc.
2422 S. Queen Street
York, PA. 17402

John McAuley
Science & Technology Department
British Embassy
3100 Massachusetts Ave., N.W.
Washington, D. C. 20008

Ross McCluney
Florida Solar Energy Center
300 State Rd. 401
Cape Canaveral, FL. 32920

Robert McCollom
Dames and Moore
1100 Glendon
Los Angeles, CA. 90024

Jon G. McGowan
of Mechanical Engineering
rsity of Massachusetts
Amherst, Mass. 01003

George C. McKoy
The Aerospace Corp.
2350 E. El Segundo Blvd.
El Segundo,CA. 90245
(213) 648-6406

David McMillan
Westinghouse Electric Corp.
700 Braddock Avenue
E. Pittsburgh, PA. 15112

Troy McQueen
Louisiana State University
Baton Rouge, La. 70803

Elena M. Medina
Dept. of Mathematics
University of New Orleans
New Orleans, La. 70122

G. Mehta
Hydronautics, Inc.
7210 Pindell School Road
Laurel, MD. 20810

Bernard Messinger
Lockheed Missiles & Space Co.
Dept. 5702, Bldg. 150
P. O. Box 504
Sunnyvale, CA. 94088
(408)742-4321

Richard Meyer
Popular Products, Inc.
1910 N. Elston Avenue
Chicago, ILL. 60622

John W. Michel
Oak Ridge National Laboratory
P. O. Box Y
Oak Ridge, TN. 37830

L. J. Milberger
FMC Corporation
5625 FM, 1960 W
Houston, TX. 77069

C. W. Miller
University of California
Dept. of Mechanical Engineering
Berkeley, CA. 94720

Stan Miller
Environmental Science & Technology
1155 16th Street
Washington, D. C. 20036

W. E. Miller
Chrysler Corporation
P. O. Box 29200
New Orleeans, La. 70189

Roy Moffett
Maritime Administration
ITM Building, Room 2828
2 Canal Street
New Orleans, La. 70130
(504) 589-6912

Robert L. Molinari
NOAA/AOML
15 Rickenbacker Cswy.
Miami, Fla. 33149
(305) 361-3361 (ext. 326)

Kenneth L. Money
The International Nickel Co.,Inc.
P. O. Box 656
Wrightsville Beach, N. C. 28480

Paul Morris
Weed Instrument Co., Inc.
P. O. Box 549
Elgin, TX. 78621

John W. Morse
University of Miami
4600 Rickenbacker Cswy.
Miami, FL. 33149

Ed Moyer
Gilbert Associates
1828 L Street, N.W. No. 1201
Washington, D. C. 20036

Anthony J. Mumphrey, Jr.
Urban Studies Institute
University of New Orleans
New Orleans, La. 70122
(504) 283-0277

F. C. Munchmeyer
University of Hawaii
4316 Koae Place
Honolulu, HI. 96816

Rob Munier
University of Miami
4600 Rickenbacker Cswy.
Miami, FL. 33149

Carlos Murawczyk
United Engineers & Constructors
30 South 17th Street
Philadelphia, PA. 19101
(215)422-3861

Frederick E. Naef
Lockheed
900 17th Street, N.W.
Washington, D. C. 20006
(202) 872-5947

John H. Nath
Dept. of Mechanical Engineering
Oregon State University
Corvallis, OR. 97331

Eric T. Nelson
Gilbert/Commonwealth Companies
P. O. Box 1498
Reading, PA. 19603
(215) 775-2600

Charles P. Neuman
Carnegie-Mellon University
Pittsburgh, PA. 15213

Frank Notaro
Linde Division
Union Carbide
P. O. Box 44
Tonawanda, N. Y. 14150

Dieter Nubel
American M.A.N. Corporation
1114 Avenue of the Americas
New York, N. Y. 10036

S. Richard Nusbaum
Pennslyvania Engineering Company
1107-21 N. Howard Street
Philadelphia, PA. 19123

P. S. O'Neill
Linde Division
Union Carbide Corporation
P. O. Box 44
Tonawanda, N. Y. 14150

Keith M. Overdyke
La. State Office of Conservation
P. O. Box 44156, CS
Baton Rouge, La. 70804

Robert A. Paddock
Energy & Environmental System Div.
Argonne National Laboratory
9700 S. Cass Ave.
Argonne, Ill. 60439

Katherine J. Padley
Urban Transportation & Planning
Associates
411 Frenchmen Street
New Orleans, La. 70116
(504) 944-7423

C. B. Panchal
Oklahoma State University
Stillwater, Okla. 74074

Peter P. Pandolfini
Johns Hopkins University
Applied Physics Lab.
Johns Hopkins Road
Laurel, MD. 20810

David F. Paskausky
NORDA/ONR
NSTL Code 410
Bay St. Louis, MS. 39529

Denzil C. Pauli
National Academy of Sciences
2101 Constitution Avenue
Washington, D. C. 20418

Fernando Perez
Puerto Rico Water Resources Authority
Box 4267
San Juan, P. R. 00936
(809) 725-8156

Robert W. Perkins
Spiral Tubing Corporation
533 Downey Drive
New Britain, Conn. 06051

Martin A. Perlmutter
University of Miami
4600 Rickenbacker Cswy.
Miami, FL. 33149

Lyle D. Perrigo
Battelle, Pacific Northwest Labs.
Battelle Blvd.
Richland, WA. 99352

Steve A. Piacsek
NORDA, Code 322
NSTL, Building 1100
Bay St. Louis, MS. 39529

Charles A. Pieroni
Simplex Wire & Cable
P. O. Box 479
Portsmouth, N. H. 03801

H. F. Poppendiek
Geoscience, Ltd.
410 S. Cedros Avenue
Solana Beach, CA. 92075

Robert C. Porter
ERDA
20 Massachusetts Ave., N.W.
Washington, D. C. 20545

Greg Powell
University of Florida
710 N. W. 16th Avenue No. 16
Gainesville, FL. 32601

Robert G. Quayle
National Climatic Center
Federal Building
Asheville, N. C. 28801

Robert Rail
Civil Engineering Laboratory
U.S. Naval Construction Battalion
Center
Port Hueneme, CA. 93043
(805) 982-4362

Edgar A. Rawls
Chrysler-Defense/Space Division
P. O. Box 29200
New Orleans, La. 70189

Charles Rees
Department of Mathematics
University of New Orleans
New Orleans, La. 70122
(504) 283-0331

Robert W. Reid, Jr.
The Aerospace Corporation
2350 E. El Segundo Blvd.
El Segundo, CA. 90009

H. H. Reizenstein
Economic Development Administration
U.S. Department of Commerce
Washington, D. C.
(202) 377-2814

Frank Remond
Sperry Corporation
NSTL
Bay St. Louis, MS. 39520

Mark S. Rice
Hydronautics, Inc.
7210 Pindell School Road
Laurel, MD. 20810

Stuart L. Ridgway
R & D Associates
P. O. Box 9695
Marina Del Rey, CA. 90291
(213) 822-1715

Robert Riggs
Friede & Goldman, Ltd.
225 Baronne Street, Suite 1414
New Orleans, La. 70112

Glyn O. Roberts
Science Applications, Inc.
8400 Westpark Drive
McLean, VA. 22101
(703) 821-4549

Ralph Roberts
The Mitre Corporation
Westgate Research Park
McLean, VA. 22101
(703) 790-6000

Oswald A. Roels
Port Aransas Marine Lab.
University of Texas
Port Aransas, TX. 78373
(512) 749-6711

Barry Roth
Chicago Bridge & Iron Company
800 Jorie Blvd.
Oak Brook, ILL. 60521

R. R. Rothfus
Carnegie-Mellon University
Schenley Park
Pittsburgh, PA. 15213
(412) 621-2600 (ext. 325)

E. P. Russo
School of Engineering
University of New Orleans
New Orleans, La. 70122
(504) 283-0327

Elric W. Saaski
Sigma Research, Inc.
2950 George Washington Way
Richland, WA. 99352
(509) 946-0663

Cullen M. Sabin
Geoscience, Ltd.
410 S. Cedros Avenue
Solana Beach, CA. 92075
(714) 755-9396

Edmund Sambuco
Hydronautics, Inc.
7210 Pindell School Road
Laurel, MD. 20810

Donald S. Sasscer
Center for Energy & Env. Research
University of Puerto Rico
College Station
Mayaguez, P. R. 00708

Norman F. Sather
Argonne National Laboratory
9700 S. Cass Avenue
Argonne, IL. 60439
(312) 739-7711

Kim David Saunders
Argonne National Laboratory
9700 S. Cass Avenue
Argonne, IL. 60439

Philip P. Sayre
Dept. of Health, Educ. & Welfare
Region IV
50 Seventh Street, N.E.
Atlanta, GA. 30323

M. Peter Scofield
E.G. & G., Idaho, Inc.
P. O. Box 1625
Idaho Falls, Idaho 83401

Hal Scowbo
Tetra Tech, Inc.
630 N. Rosemead Blvd.
Pasadena, CA. 91107
(213) 449-6400

J. F. Sebald
:t Associates
ills Office
g, PA. 19603

J. H. Seelinger
Maritime Administration
5367 28th Street, N.W.
Washington, D. C. 20015

David Shapiro
Tracor
1911 N. Fort Meyer
Arlington, VA. 22209

Herman E. Sheets
Ocean Engineering Department
University of Rhode Island
201 Lippitt Hall
Kingston, R. I. 02881

D. Max Sheppard
University of Florida
Gainesville, FL. 32611

W. C. L. Shih
S.A.I.
101 Continental Bldg.
El Segundo, CA. 90245

Paul H. Sidles
Ames Laboratory, ERDA
Iowa State University
Ames, Iowa 50011

E. A. Silva
Naval Facilities Command
Department of the Navy
200 Stovall Street
Alexandria, VA. 22332

Bennett Silverstein
Office of Technology Assessment-
Oceans Program
U.S. Congress
Washington, D. C. 20510

M. J. Smith
Mechanics Research, Inc.
2500 Colorado Avenue
Santa Monica, CA. 90406

Peter F. Sokolowski
Westinghouse Electric Corp.
P. O. Box 9175
Lester, PA. 19113

Richard M. Spath
Lockheed Missiles & Space Co.
Orgn. 57-02/Bldg. 150
P. O. Box 504
Sunnyvale, CA. 94088

Frank A. Spiehler
NOAA Data Buoy Office
NSTL
Bay St. Souis, MS. 39529

Kenneth E. Starling
University of Oklahoma
202 West Boyd
Norman, Okla. 73019

A. Steinbruchel
Aqua-Chem, Inc.
P. O. Box 421
Milwaukee, Wis. 53201

T. R. Sundaram
Hydronautics, Inc.
7210 Pindell School Road
Laurel, MD. 20810

W. J. Tallon
TRW DSSG
One Space Park R4/1198
Redondo Beach, CA. 90278

Barrie F. Taylor
University of Miami
4600 Rickenbacker Cswy.
Miami, FL. 33149

Donald M. Taylor
Ocean Industry Magazine
Box 2608
Houston, TX. 77001

C. Clark Tefft
Tefft, Kelly and Motley
1225 Connecticut Avenue, N.W.
Washington, D. C. 20036

Jeffery S. Tennant
Florida Atlantic University
Boca Raton, FL. 33431

W. Thielbahr
U. S. Naval Weapons Center
Code 3161
China Lake, CA. 93555

David L Thomas
Ichthyological Associates
West Brooklane
Absecon, N. J. 08201

J. Dana Thompson
Jaycor Suite 500
205 S. Whiting Street
Alexandria, VA. 22304

Nelson Tolar
P & T Pipe Testing Co., Inc.
2000 E. Park Ave., P. O. Box 1697
Houma, La. 70361

R. M. Troy, Jr.
Department of Justice
234 Loyola Avenue
New Orleans, La. 70112

Walter Trzaskoma
Gilbert Associates
1828 L Street, N. W., No.1201
Washington, D. C. 20036

Edward J. Tschupp
TEMPO-General Electric Company
777 14th Street, N. W.
Washington, D.C. 20005

Joseph R. Vadus
NOAA
Office of Ocean Engineering
Rockville, MD. 20850

Ludo Van Hemelrijck
Port Aransas Marine Laboratory
University of Texas
Port Aransas, TX. 78373

John vanSummern
Gilbert Associates
1828 L Street, N.W., No.1201
Washington, D. C. 20036

T. Nejat Veziroglu
School of Engineering
University of Miami
Box 8294
Coral Gables, FL. 33124

Robert J. Vincent
Burns & Roe, Inc.
550 Kinderkamack Road
Oradell, N. J. 07649

Peter J. Vogelberger
Teledyne Energy Systems
110 W. Timonium Road
Timonium, MD. 21057

Fred Vukovich
Research Triangle Institute
Research Triangle Park, N. C. 27709

W. Wagner
Rocketdyne/Rockwell
6633 Canoga Avenue
Canoga Park, CA. 91304

Terry E. Walsh
Bechtel Corporation, 301/3/B5
P. O. Box 3965
San Francisco, CA. 94119

Alex C. Warn-Varnas
Dept. of the Navy
Naval Ocean Research & Dev. Activity
NSTL Station, MS. 39529

Byron J. Washom
Off. of Interdisciplinary Prog.Dev.
Administration Bldg., Room 259
University of Southern California
Los Angeles, CA. 90007

Arthur D. Watt
Watt Engineering, Ltd.
Route 1 - Box 183
Cedaredge, Colo. 81413

Joe L. Weber
Ebasco Services
145 Technology Park
Norcross/Atlanta, GA. 30092

Laskar Wechsler
Hydronautics, Inc.
7210 Pindell School Road
Laurel, MD. 20810

Tom Whalen
Urban Studies Institute
University of New Orleans
New Orleans, La. 70122

Pat Wilde
University of California
438 Hearst Mining Building
Berkeley, CA. 94720

Charles A. Willingham
Battelle
Marine Biology Department
Drawer AH
Duxbury, Mass. 02332

L. A. Wilson
Middle South Services
225 Baronne Street
P. O. Box 61000
New Orleans, La. 70161

Bette M. Winer
Arthur D. Little, Inc.
Acorn Park
Cambridge, Mass. 02140
(617) 864-5770

James G. Withers
Wolverine Tube
P. O. Box 2202
Decatur, AL. 35601

Robert Wolf
Interstate Electronics Corp.
P. O. Box 3117
Anaheim, CA. 92803

Paul Wolff
Ocean Data Systems, Inc.
2400 Garden Road
Monterey, CA. 93940

M. A. Wood
Florida Atlantic University
N. W. 20th Street
Boca Raton, FL. 33432

Donald Woodford
Dames & Moore
199 Lennox Court
New Orleans, La. 70114

Edgar 'D' Wragge, Jr.
5371 Franklin Avenue
New Orleans, La. 70122

David Wright
Rocketdyne/Rockwell
6633 Canoga Park
Canoga Park, CA. 91304

B. Diane Wyble
Westinghouse
1801 K Street, N.W.
Washington, D. C. 20006

Charles S. Yentsch
Bigelow Laboratory for Ocean Sciences
McKown Point
West Boothbay Harbor, Maine 04575

John M. Zeigler
Virgina Institute of Marine Science
Gloucester Point, VA. 23062

M. W. Zembal
Dow Chemical
Drawer K
Freeport, TX. 77541

Clarence Zener
Carnegie-Mellon University
Pittsburgh, PA. 15213